近畿大学医学部消化器内科学教室

平成 26 年度　年報

Kinki University School of Medicine

Department of Gastroenterology and Hepatology

Annual Report-2014-

近畿大学医学部　消化器内科学
近畿大学医学部附属病院　光学治療センター
近畿大学医学部附属病院　中央超音波診断・治療室
近畿大学医学部堺病院　消化器内科
近畿大学医学部奈良病院　消化器・内分泌内科

年報 Annual Report 2014

近畿大学医学部消化器内科学教室

医局員集合写真

第9回 Kinki GUT Club 平成27年2月22日

目　　次

１．　2014 年 Annual Report の発刊にあたって

・・・・・・・・・・・・　1

２．　消化器内科学業績抜粋　・・・・・・・・・・・・　22

３．　消化器内科診療実績　・・・・・・・・・・・・　25

４．　近畿大学消化器内科学教室医局員　・・・・・・・・・・・・　33

５．　医局員の略歴および近況　・・・・・・・・・・・・　37

６．　消化器内科学教室業績一覧（2014 年）

英文論文（著書、分担執筆）　・・・・・・・・・・・・　49
英文論文　・・・・・・・・・・・・　49
和文論文（著書、分担執筆）　・・・・・・・・・・・・　54
和文論文　・・・・・・・・・・・・　54
招待講演・特別講演（海外）　・・・・・・・・・・・・　56
招待講演・特別講演（国内）　・・・・・・・・・・・・　58
学会発表（海外シンポジウム）　・・・・・・・・・・・・　61
学会発表（海外一般演題）　・・・・・・・・・・・・　62
学会発表（国内シンポジウム・パネルディスカッション・ワークショップ）
・・・・・・・・・・・・　68
学会発表（国内一般演題）　・・・・・・・・・・・・　72

７．　別刷、新聞・雑誌・報道等　・・・・・・・・・・・・　79

８．　近畿大学医学部消化器内科学教室同門会名簿
・・・・・・・・・・・・528

９．　近畿大学医学部消化器内科学教室同門会役員
・・・・・・・・・・・・529

１０．近畿大学医学部消化器内科学教室同門会会則　・・・・・・・　530

１１．編集後記　・・・・・・・・・・・・532

2014年Annual Reportの発刊にあたって

近畿大学消化器内科学教室主任教授　工藤正俊

1.はじめに

2014年の教育、研究、診療の実績をお届けします。近畿大学医学部に消化器内科学教室が新設されたのは平成11年4月であります。従って平成26年3月で区切りの15年が経過したことになります。開設当初は医局のスペースも2部屋のみでスタッフ8名、研修医6名、計14名での出発でありました。現在では狭山の本院に籍を置くスタッフは約40名、また堺病院や奈良病院もそれなりに人材・設備共に整いつつあります。

しかしながら、私立医大の宿命かもしれませんが、2004年より始まった新臨床研修医制度の余波をまともに受けて消化器内科も毎年5～6人から12～13人入局していた入局者数が最近では激減し、また次第に開業あるいは結婚退職、郷里へのUターンなどの退職者も増え、現在なお厳しい状況に置かれているというのが現状です。ただし、ここ数年は2～4人の入局がコンスタントに続いており、良い傾向が見え始めました。今後の更なる消化器内科学教室の発展のために医局員一同が一致団結して診療、研究、教育活動に専念していかなければならない重要な時期であると考えております。

2.診療活動

別添えの資料をご覧頂ければ一目瞭然でありますが、消化器内科の年間の入院及び外来収入、及びそれを合計した総収入は平成11年の開設初年度は約8億程度でありましたが、平成26年には34億円を超える収入となっており、病院経営にも多大の貢献をしております。また一日平均入院患者数も年間を通して80人前後、平均在院日数も7日前後であり極めて多忙な診療活動を行っていることがおわかり頂けると思います。腹部超音波検査の件数も確実に右肩上がりであり、内視鏡の件数も総件数が平成26年度は19,196例と着実に上昇を示しております。また、肝癌に対するラジオ波治療（RFA）の総件数も多く、日経新聞や朝日新聞、読売新聞、週刊朝日等にも度々取り上げられ、総件数としては連続9年以上、日本国内の2位もしくは3位（内科と外科の件数、及び転移性肝癌を含めて）に位置づけられるという実績を残しております。ラジオ波は

平成 11 年 6 月より開始し、平成 25 年 12 月末の時点で総件数 4,500 例に達しており、5 年生存率は 70%強と、手術とほぼ同等の治療成績が得られております。現在、C 型肝炎治療を積極的に行っており、大阪南部から C 型肝炎・肝癌を根絶したいと願っています。平成 26 年からはいよいよ IFN free の経口剤（DAA）のみによる治療が開始されました。難治性の Ib 型高ウイルス検査の SRV 率もほぼ 100%となることが見込まれています。B 型肝炎も核酸アナログで制御されるようになっている現在益々、肝癌の治療が重要になってくるものと思われます。

平成 15 年度に導入した早期胃癌に対する内視鏡的粘膜下層切開剥離術（ESD）も確実に症例数が増え、今後も益々増え続けていくものと考えております。もちろん、ESD 関連の研究論文も少しずつ増えていっております。また、大腸 ESD も平成 22 年より開始され、症例も増加しています。また従来より行っていた胆膵グループによる超音波内視鏡検査の件数も増加しています。平成 23 年度には内視鏡室が光学治療センターに格上げとなり、スペースも拡充されました。平成 23 年 11 月 27 日に第 1 回目を行った関西消化器内視鏡ライブコースも第 2 回目を平成 24 年 11 月 25 日に行われ、第 3 回目は平成 26 年 2 月 9 日に行い、約 300 人の参加者を得て成功裏に終わりました。

御承知のように大和川以南は一般に「南大阪」と呼ばれておりますが、その南大阪の人口は約 240 万にも達しております。その 240 万人の医療圏の中で特定機能病院大学医学部は近畿大学のみであります。その意味でこの 240 万人の方々の健康を守るのが我々に課せられた使命であります。さらには、平成 35 年には医学部・病院が泉ヶ丘の駅の隣接した地に新築移転する計画が発表されました。消化器内科も含めた近畿大学医学部の発展がさらに期待されます。

3. 教育活動

教育は当然のことながら大学医学部の役割の極めて根幹を占める重要な部分であります。消化器内科学は消化器コースの内の肝臓の責任科であり、肝臓のユニットを 1 週間担当している他、上部消化管、下部消化管、胆膵のユニットや臨床腫瘍コースならびに画像診断のコースでも講義を担当しております。更には病因・病態のコースの 3 週間のうち 1 週間の責任科として大変多忙な教育活動を行っております。5 年生 6 年生のクリニカルクラークシップも例年 6 年生を常時 6 人程度受け入れており、講義や総括など充実した bed side 教育となるよう全力を尽くしております。国家試験の成績も是非とも向上させなければ

なりません。

平成 20 年 10 月から病院長に任ぜられ、3 期目となりましたが無事平成 26 年 9 月には任期満了により退任いたしました。その間は公務のために教育活動の多くの部分を北野准教授、松井講師はじめ多くの先生方にご負担をおかけすることになってしまい、申し訳なく思っております。消化器コース及び病因・病態コースあるいは日々のクリニカルクラークシップ等の教育活動では決して手を抜かず積極的に行っていくつもりですので何卒ご容赦下さい。この紙面をお借りして感謝とお詫びを申し上げたいと思います。

3. 研究活動

(1) 論文業績

英文論文の発表は 1999 年消化器内科の設立当初は一桁台でありましたが、年と共に確実に増加し、3 年目からは平均 20 編以上の英文論文がコンスタントに出るようになりました。2010 年の英文論文数は 51 編に達しました。残念ながら 2011 年は 48 編、2012 年は 44 編にとどまりました。しかし、2014 年からは再び 56 編と 50 編の大台に回復しました。また 16 年間の総インパクトファクターは 1635.304 点であり英文総論文数は 466 編ですので、近畿大学消化器内科のような小さな所帯の教室としてはまずまずの結果を残せているのではないかと思っております。来年以降は最低、英文原著論文は 60 編以上を目標に頑張っていきたいと考えておりますので教室員の皆様の自覚と更なる奮闘を期待致しております。

(2) 厚生労働省科学研究費補助金事業研究班の活動

平成 22 年度に採択された厚労科研（がん臨床部門）**「進行・再発肝細胞癌に対する動注化学療法と分子標的薬併用による新規治療法の確立を目指した臨床試験（Phase III）ならびに効果を予測する biomarker の探索研究」**（工藤班）の主任研究者として日本発のエビデンスを創出すべく、努力していまいりました（平成 22－24 年)。また平成 23 年度には厚労科研（難病･がん等の疾患分野の医療の実用化部門）**「慢性ウイルス性肝疾患の非侵襲的線化評価法の開発と臨床的有用性の確立」**（工藤班）の主任研究者としても採択され、多くの大学との協同研究を行いました（平成 23－25 年)。平成 26 年度には厚生労働科学研究委託費（肝炎等克服実用化研究事業（肝炎等克服緊急対策研究事業))「慢性ウイル

ス性肝炎の病態把握（重症度・治療介入時期・治療効果判定・予後予測）のための非侵襲的病態診断アルゴリズムの確立」という課題が採択となり、更に 3 年間新しいエビデンスを創出すべく頑張りたいと思っております。平成 26 年度には平成 27 年度日本医療研究開発機構（AMED）の委託費となり現在研究が進行中です。またその他にも下記の厚労科研の分担研究者として教室の先生方に実務を担当して頂いております。この場をお借りして感謝申し上げます。

① 「抗悪性腫瘍薬による肝炎ウイルス再活性化の調査とその対応に関する研究」（池田班）（国立がん研究センターがん研究補助金）
② 「初発肝細胞癌に対する肝切除とラジオ波焼灼両方の有効性に関する多施設共同研究」（國土班）（厚労科研）
③ 「進行肝胆膵がんの治療法の開発に関する研究」（奥坂班）（国立がん研究センターがん研究補助金）

(3) 今後の研究の方向性

今年の消化器内科の論文も一覧するとやはりまだまだ Impact factor の高い雑誌に掲載されているのは少ないようです。やはり Impact factor 15 点以上の雑誌を目指すには prospective な比較試験など中・長期的な視野に立った研究計画を組んで質の高い臨床研究を進めて行くことが現時点での我々に課せられた最も大きな課題と考えております。臨床試験については 2008 年 9 月 11 日に大阪府より認証を受けた NPO 法人「日本肝がん臨床研究機構（JLOG)」を中心に現在 7 つの prospective study が走っております。なかでも SELECTED study は H24 年 10 月に終了し、ポジティブな結果が得られたため平成 25 年の AASLD で oral 発表すると共に、NEJM にも投稿予定です。来年中には SILIUS 試験の結果も出る予定です。これからも世界へ向けて発信できるような成果を出して行くつもりでおります。もちろん、retrospective な解析研究で新しいデータを publish していくという努力も今後も続けていかなければなりません。

また基礎研究の分野でも西田直生志准教授、櫻井俊治講師、萩原智講師を中心に積極的に研究を進めて頂いており、今後の publication を期待しております。

もう一つの重要な点は私が常日頃申し上げておりますように症例観察の重要性であります。臨床においては一例一例がたとえ同じ病名であったとして

も一例として同じ症例はありません。同じ病気でも一つとして全く同一であるということはなく、何か異なるメッセージを発信しているのです。そのことを的確にキャッチすることにこそ意味があるという目で一例一例の患者さんを注意深く診療し観察していくことこそが最も大事であると考えています。そのような注意深い観察から新しい臨床的な発見も生まれてきますし、また逆にそのような観察眼が生まれる素地としては臨床家として真面目に臨床と向き合って最高の level に到達している必要があります。そのような点で日々の臨床の現場には”clinical pearl”とでも言うべきものがあちこちに転がっている、まさに宝の山であります。そのような理由で症例観察に基づいたケースレポートを書くということも極めて、その本人の勉強になることはもちろんのこと、今後の新しい疾患概念の確立、新しい治療法の着想などに結びつき得る重要な姿勢であると思われます。残念ながら、ケースレポートは最近の Impact factor 重視主義の多くの Journal から採用されない傾向にはありますが、それでも short report や Letter to the Editor などとしては採用されますので業績をあげるという目的ではなく、症例をキチンと観察・整理して document していくという姿勢に立つことは重要であります。すなわち症例の観察研究を報告することは我々、アカデミアに籍を置く者に課せられた使命であると自覚すべきと考えております。

大規模な前向きな比較試験を行うべきということと症例の観察研究とでは全く正反対の次元の違うことを述べているように思われるかもしれません。しかしこの 2 つは臨床を知り尽くし、かつ、臨床をじっくり真面目にやっている医師にしかできないことであるという点で共通していることであります。基礎研究あるいは臨床に結びつくかもしれない基礎研究までは MD ではなくとも PhD でも実行可能なことであり、その field ではしばしば PhD の方が quality の高い研究成果を上げ得るかも知れません。しかしながら、臨床の疑問点にもとづいた基礎研究もしくは本当に臨床に直結するような基礎研究や症例の観察研究、および大規模臨床試験などはその価値を知り得る MD にしかできないことであることは間違いありませんし、それらを遂行し得るのは患者さんと日々正面から向き合っている最高水準の医師にしかできない研究であります。そのような点でこの二つは決して矛盾するものではありませんし、両方ともに臨床家こそがやるべき研究であります。

以上、述べた 2 つの異なったアプローチは、我々の教室の研究の方向性

として今後も積極的に実行して行きたいと思っております。繰り返しになりますが、臨床的な発想に基づく、あるいは臨床に本当に必要な基礎的データを抑えるという研究は、大変重要ですのでそれらは引き続き継続していかなくてはなりません。

2009年に私が立ち上げた日本肝がん分子標的治療研究会（第1回研究会：2010年1月16日、参加者450人）は年2回開かれております。これからはC型肝炎もB型肝炎も、ほとんどが経口剤だけで容易に治癒して行く時代になりますので、相対的に肝癌治療の重要性が増してゆきます。また肝癌はこれからは分子標的治療が大変重要な治療のひとつとなる時代ですのでゲノム生物学教室（西尾和人教授）との共同研究は今後も継続していきたいと思っています。特許も出願することが出来ましたし、Impact Factorが7以上の雑誌にもこの分野で2-3編通りました。臨床的ニーズに基づいた基礎研究で成果を上げることほどエキサイティングなことはありません。是非とも近畿大学から肝癌に関して臨床に貢献できる基礎的エビデンスを次々と発信して行きたいと心から願っています。

(4) Research Conference

現在消化器内科では定期の各グループの臨床カンファレンスに加え、毎週火曜日の早朝の1時間みっちりとResearch Conferenceを行っております。このカンファレンスでは全て英語でPresentationからDiscussionまでを行っております。ほとんど1年を通じて海外からの留学生がおりますし、特筆すべき点としてこれまではアジアの留学生が中心でしたが平成22年はイタリア人のDr. Lorenzoがapplyしてできたことです。これも日本における肝細胞癌研究のleading centerとしてヨーロッパの国からも認知され始めている証拠であると思いますので大変喜ばしいと思っております。平成23年には世界で最も古い歴史のあるイタリアボローニャ大学のProf. Bolondiの教室からDr. Albertoがやってきて3か月の研修を終えて帰りました。そのような留学生にも配慮してResearch Conferenceは英語で行っておりますが、やはりこのEnglish Research Conferenceというのが消化器内科が行っているカンファレンスの中でも最も重要であると考えております。もちろん、このカンファレンスへの出席は本人の自発的意欲に基づくものではありますが、毎週多くの教室員に参加して頂いております。以下にこの数年の出席率を示しますが、出席率の高い医局員ほどや

はり研究に対するactivityが高い傾向にあると感じておりますので今後も引き続き積極的に参加して頂きたいと思っております。

副次的な効果としてこのカンファレンスを通じて海外で英語でDiscussionできる英語力や自信も自然と磨かれるものと確信しております。

English Reseach Conference 出席状況

教室員	2008		2009		2010		2011		2012		2013		2014	
	出席回数	出席率	出席回数	出席率	出席回数	出席率	出席回数	出席率	出席回数	出席率	出席回数	出席率	出席回数	出席率
工藤	27/27	100%	20/20	100%	29/29	100%	23/23	100%	32/32	100%	25/25	100%	22/22	100%
樫田	−	−	−	−	12/19	63%	20/23	87%	27/32	84%	19/25	76%	20/22	91%
西田							5/5	100%	24/32	75%	10/25	40%	4/22	18%
北野	25/27	93%	16/20	80%	21/29	72%	21/23	91%	25/32	78%	21/25	84%	12/22	55%
松井	22/27	81%	18/20	90%	23/29	79%	23/23	100%	30/32	94%	23/25	92%	20/22	91%
上嶋	6/27	22%	3/20	15%	12/29	41%	7/23	30%	9/32	28%	6/25	24%	5/22	23%
櫻井	−	−	−	−	17/19	89%	20/23	87%	25/32	78%	15/25	60%	15/22	68%
南	19/24	79%	1/2	50%	−	−	13/14	93%	31/32	97%	22/25	88%	19/22	86%
萩原	11/24	46%	5/20	25%	9/29	31%	11/23	48%	10/32	31%	9/25	36%	4/22	18%
井上	17/25	68%	16/20	80%	25/29	86%	21/23	91%	23/32	72%	17/25	68%	5/22	23%
矢田	7/11	64%	14/19	74%	26/29	90%	14/23	61%	9/32	28%	15/25	60%	3/22	14%
坂本	19/27	70%	1/2	50%	12/19	63%	11/23	48%	20/32	63%	15/25	60%	5/22	23%
北井	15/27	56%	8/20	40%	15/29	52%	13/23	57%	20/32	63%	16/25	64%	13/22	59%
朝隈	16/27	59%	12/20	60%	11/29	38%	15/23	65%	15/32	47%	15/25	60%	15/22	68%
米田	−	−	−	−	−	−	−	−	−	−	−	−	22/22	100%
永井	18/19	95%	17/20	85%	14/29	48%	12.5/23	54%	23/32	72%	14/25	56%	−	−
川崎	23/27	85%	6/20	30%	4/29	14%	6/23	26%	4/32	13%	2/25	8%	−	−
田北	1/2	50%	13/20	65%	15/29	52%	7/23	30%	9/23	39%	12/25	48%	4/22	18%
早石	10/19	53%	9/19	47%	5/29	17%	8/23	35%	9/23	39%	−	−	−	−
田中	−	−	−	−	−	−	−	−	24/27	89%	18/25	72%	5/22	23%
山田	−	−	−	−	−	−	−	−	23/25	92%	15/25	60%	6/22	27%
山雄	−	−	−	−	−	−	−	−	−	−	14/25	56%	19/22	86%
永田	−	−	13/15	87%	16/29	55%	12/23	52%	11/32	34%	2/25	8%	−	−

今井	-	-	9/15	60%	18/29	62%	10/23	43%	13/32	41%	7/25	28%	8/22	36%
岡崎	-	-	-	-	-	-	-	-	-	-	-	-	15/22	68%
有住	-	-	7/15	47%	15/29	52%	17/23	74%	26/32	81%	18/25	72%	19/22	86%
鎌田	-	-	11/15	73%	15/29	52%	10/23	43%	16/32	50%	9/25	36%	6/22	27%
高山	-	-	4/7	57%	-	-	13/14	93%	16/32	50%	16/25	64%	4/22	18%
宮田	-	-	9/15	60%	16/29	55%	14.5/23	63%	22/32	69%	15/25	60%	17/22	77%
岡元	-	-	-	-	-	-	-	-	-	-	12/25	48%	18/22	82%
河野	-	-	-	-	-	-	-	-	-	-	-	-	20/22	91%
峯	-	-	9/15	60%	17/29	59%	17/23	74%	19/32	59%	19/25	76%	4/22	18%
足立	-	-	-	-	-	-	8/14	57%	22/32	69%	17/25	68%	16/22	73%
大本	-	-	-	-	-	-	12/14	86%	29/32	91%	19/25	76%	18/22	82%
門阪	-	-	-	-	-	-	12/14	86%	22/32	69%	16/25	64%	9/22	41%
千品	-	-	-	-	-	-	-	-	29/32	91%	22/25	88%	17/22	77%
南(知)	-	-	-	-	-	-	-	-	-	-	21/25	84%	19/22	86%

4. 学会活動および海外における活動

2014 年における国内の学会発表については 69 演題、国際学会の発表については 40 演題、海外特別講演は 16、国内特別講演は 13 でありました。私自身の海外出張は 2014 年は 12 回とこれは例年よりやや少ない回数となりました。

2014 年

1. 1 月 16 日 - 1 月 17 日　アメリカ臨床腫瘍学会消化器癌シンポジウム（ASCO GI）(USA, San Francisco)
   RAD-001 共同演者
   GIDEON の運営委員会へ出席
2. 1 月 30 日 - 2 月 4 日　世界超音波医学会（WFUMB）理事会へ出席(MEXICO, Cabo San Lucas)
3. 2 月 27 日 - 2 月 28 日　1st Asia Bayer Clinical Day(ABCD)へ出席（CHINA, Shanghai）
4. 3 月 1 日 - 3 月 2 日　アジア超音波医学会（AFSUMB）ワークショップ（NEPAL, Kathmandu）

5.	3月13日－3月15日	Lilly TGFb HCC Advisory Board Meetingへ出席（UK, London）
6.	3月26日－3月27日	国際肝胆膵学会（IHPBA）にて講演(KOREA, Seoul)
7.	4月8日－4月12日	ヨーロッパ肝臓学会（EASL）へ出席・発表（UK, London）
8.	5月3日－5月5日	1st Asian Conference on Tumor AblationAsianへ出席（TAIWAN, Taipei）
9.	6月9日－6月14日	世界超音波医学会理事会(WFUMB)へ出席（ITALIA, Rome）
10.	10月10日－10月14日	アジア太平洋肝癌専門家会議(APPLE)(TAIWAN, Taipei)
11.	10月28日－11月1日	アジア超音波医学会（AFSUMB）にて講演（MALAYSIA, Kuala Lumpur）
12.	11月5日－11月12日	米国肝臓学会（AASLD）へ出席（USA, Boston）

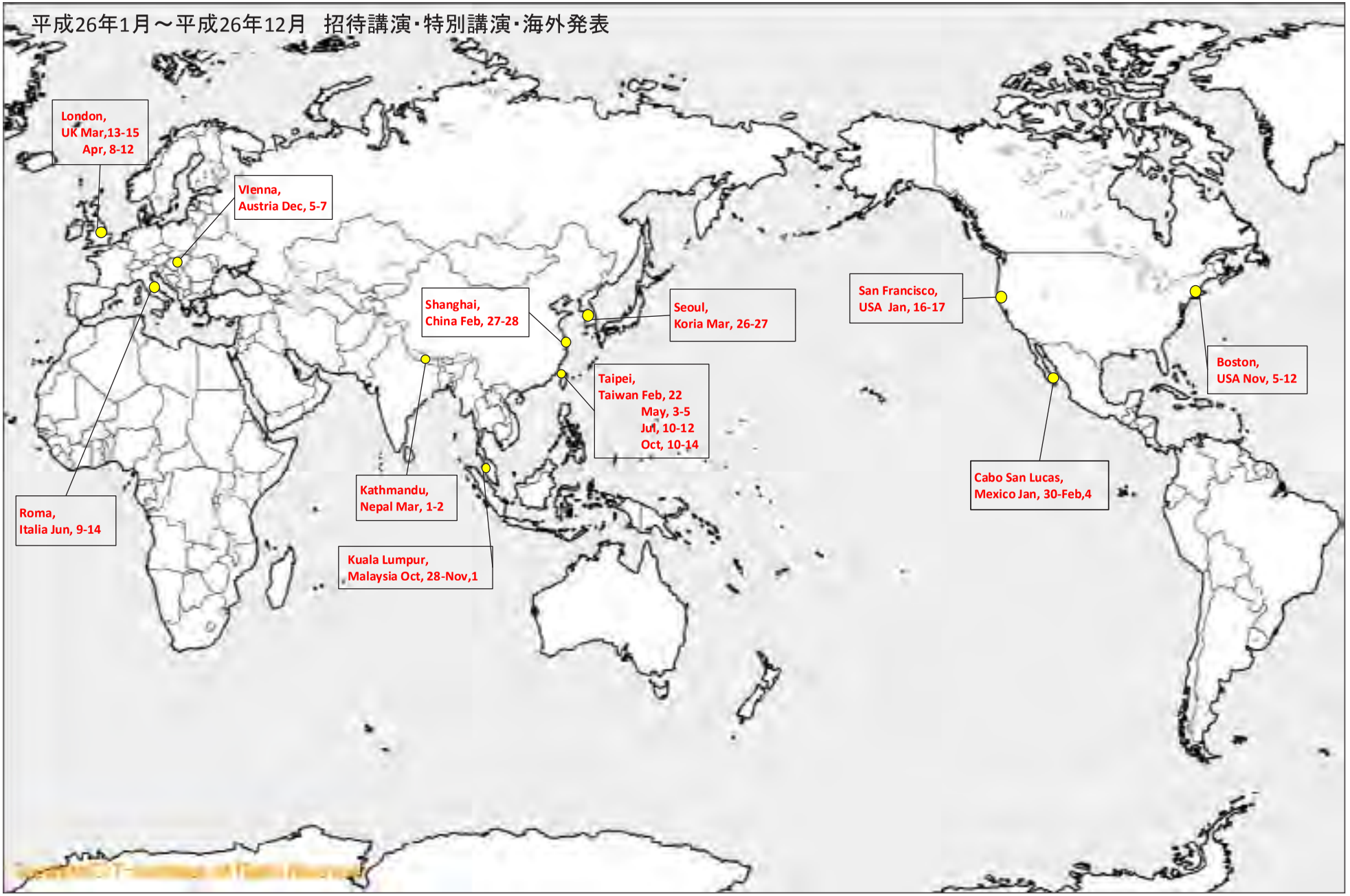
平成26年1月～平成26年12月　招待講演・特別講演・海外発表
London,
UK Mar,13-15
Apr, 8-12
Vienna,
Austria Dec, 5-7
Roma,
Italia Jun, 9-14
Kathmandu,
Nepal Mar, 1-2
Kuala Lumpur,
Malaysia Oct, 28-Nov,1
Shanghai,
China Feb, 27-28
Seoul,
Koria Mar, 26-27
Taipei,
Taiwan Feb, 22
May, 3-5
Jul, 10-12
Oct, 10-14
San Francisco,
USA Jan, 16-17
Cabo San Lucas,
Mexico Jan, 30-Feb,4
Boston,
USA Nov, 5-12

平成26年1月～平成26年12月　招待講演・特別講演

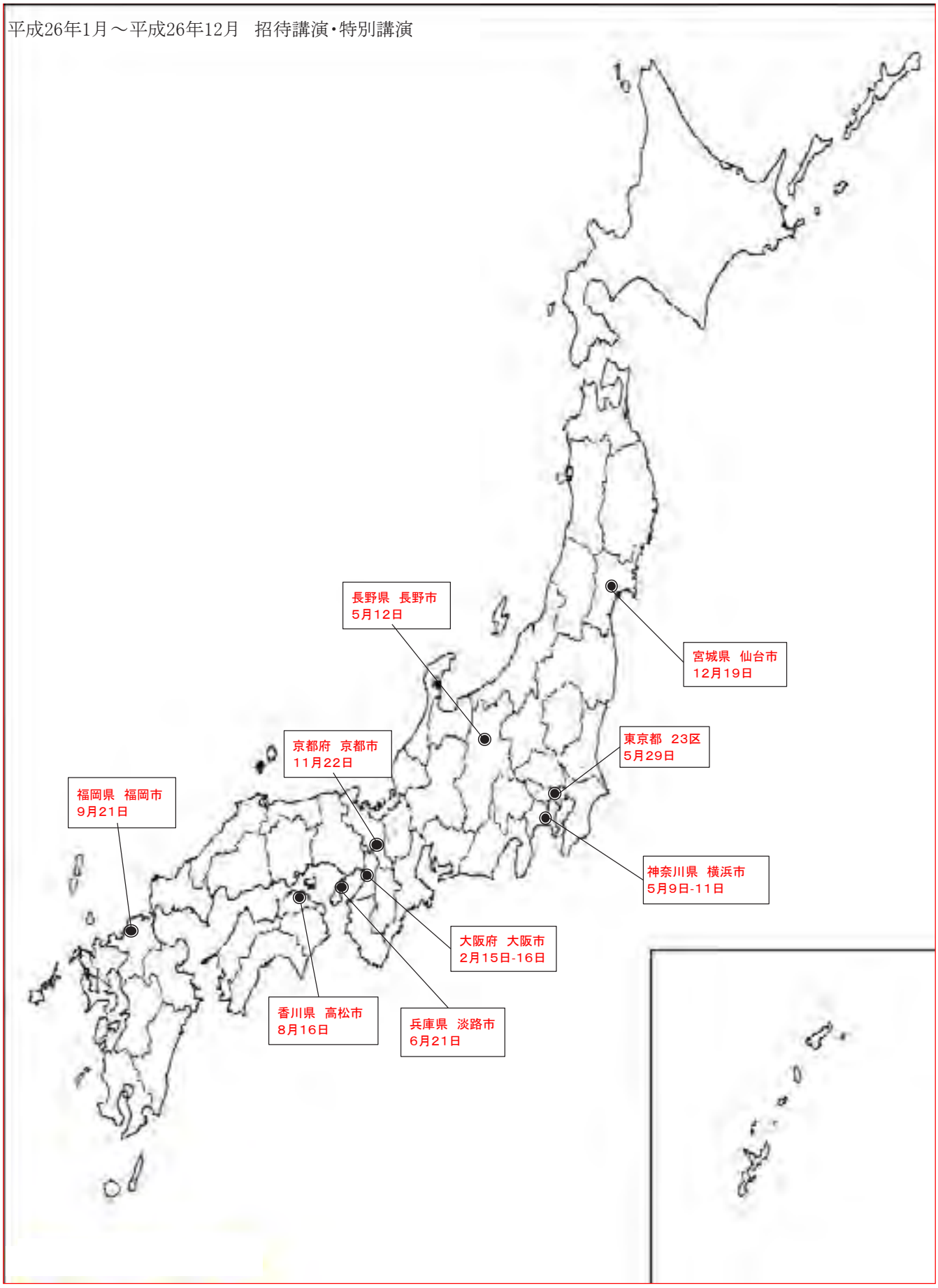

5. 留学生受け入れ

留学生の受け入れですが、1999年から2000年にかけて中国上海からDing Hong先生（丁　紅）（上海医科大学)、2001年には中国広州からWen YL先生（文艶玲）（中山医科大学)、2002年には中国広州からZheng RQ先生（鄭　栄琴）（中山医科大学)、2003年には中国重慶よりZhou Pei（周　佩）（人民解放軍重慶病院)、2004年にはカンボジアよりLy Sokhey先生、2005年にはタイからWorawan Chinamnan先生、同じく2005年に若干時期を違えてインドからKaushal Madan先生（All India Institute of Medical Science: AIIMS)、2007年Kunal Das先生を受け入れました。2008年 Yu Xia(北京、中国)、2009年　Md. Nadiruzzaman（バングラディシュ)、2010年Lorenzo Andreana（イタリア）が来ていました。またエジプトからAlshimaa先生も来られました。2011年にはマレーシアからHadzri先生が来られましたし、またイタリア　ボローニャ大学からもAlberto先生が来られました。2012年7月には中国からZhang Shuo先生、2013年10月にはマレーシアからChai Soon Ngiu先生、2014年9月にはインドからHarwani Yogesh Purshottam先生が来られました。このように毎年、留学生が日中友好協会、笹川財団や日本消化器病学会、日本超音波医学会のフェローシップ留学生あるいは自国でのfundをもって私どもの教室を希望して頂き、受け入れてきました。また来年度以降も先生方にはご迷惑をお掛けするかと思いますが、これも国際交流、アジアや世界への日本の貢献、各々の英語力に磨きをかけるという意味で有益と思いますので何卒御理解・御協力のほどお願い申し上げます。

6. 人事について

冒頭でも述べましたが、2003年までの入局者は毎年5、6名～12、13名と大学内でも最も多くの入局者がおりましたが、2004年に新臨床研修医制度が開始されてからの入局者、すなわち2006年の入局者は2名に留まり、2007年の入局者も1名に留まりました。2008年には8名もの入局者が入って来られました。2011年は3名の研修医が入局し、2012年にも3名が入局しました。反面、2-3人の方が医局を離れました。2014年度におきましては3名の入局と2名の退職があり、依然として医局の体制は大変厳しい状況にあります。このような状況の中で南大阪では大阪大学や大阪市大、和医大、奈良医大などがそれぞれの大学に人を引き上げているという状況のため、消化器内科医が激減し、南大阪の多くの公的病院では消化器内科医がほとんどゼロの状態が続いております。

そのあおりで近医からの紹介患者や外来患者数は激増し、消化器内科の診療にも大きな負担がかかっております。しばらくはこのような状況が続くものと思われるますので、本学ならびに分院の奈良病院、堺病院ともに結束して一人でも多くの人に入局して頂き、教育・研究・診療を円滑に行っていきたいと考えております。

7. NPO法人「日本肝がん臨床研究機構(Japan Liver Oncology Group)」の活動

1. JLOG 0801 trial「肝癌早期診断のための多施設共同無作為化比較試験（Sonazoid-Enhanced LivEr Cancer Trial for Early Detection (SELECTED Study))」

→2012年10月終了、現在データ解析中、論文発表予定

2. JLOG 0901 trial 「進行・再発肝細胞癌に対する動注化学療法と分子標的薬併用による新規治療法の確立を目指した臨床試験（Phase III）ならびに効果を予測するbiomarkerの探索研究（Randomized Controlled Trial Comparing Efficacy of Sorafenib versus Sorafenib In combination with Low dose cisplatin/fluorouracil hepatic arterial InfUSion chemotherapy in Patients with Advanced Hepatocellular Carcinoma And Explolatory Study of Biomarker Predicting Its Efficacy (SILIUS Phase III trial))」

→2010年より厚労科研に移行（厚生労働省科学研究費補助金　厚生労働省科学研究費補助金事業研究班（がん臨床部門）平成23年度「進行・再発肝細胞癌に対する動注化学療法と分子標的薬併用による新規治療法の確立を目指した臨床試験（Phase III）ならびに効果を予測するbiomarkerの探索研究」（工藤班)）→2013年で終了、試験自体は2015年6月終了予定。

3. JLOG 0902 trial「早期肝癌診断におけるEOB-MRIの有用性に関する多施設共同研究（Diagnosis of Early LIver Cancer Through EOB-MRI(DELICATE Study))」

4. JLOG 1001 trial 「切除不能肝細胞癌に対する肝動脈化学塞栓療法（TACE）とソラフェニブの併用療法第II相臨床試験（Phase II study: Transcatheter Arterial Chemoembolization Therapy In Combination with Sorafenib (TACTICS Study))」

5. JLOG 1002 trial「慢性肝疾患における非侵襲的弾性検査法を用いた肝線維化評価予測に関する研究(Assessment of Liver FIBROsis by Real-time Tissue

ELASTography in Chronic Liver Disease (FIBROELAST Study))」

→**2011 年より厚労科研に移行**（厚生労働省科学研究費補助金事業研究班（難病・がん等の疾患分野の医療の実用化部門）平成 23 年度「慢性ウイルス性肝疾患の非侵襲的線化評価法の開発と臨床的有用性の確立」（工藤班））

6. **JLOG 1003 trial**「非侵襲的弾性検査法を用いた肝線維化度評価によるウイルス性肝炎患者における肝発癌・門脈圧亢進症の発現予測（Prediction of Incidence of Liver Cancer or porTal Hypertension in Patients with Viral Hepatitis by Use of Real-time Tissue Elastography (PICTURE Study))」

→**2011 年より厚労科研に移行**（厚生労働省科学研究費補助金事業研究班（難病・がん等の疾患分野の医療の実用化部門）平成 23 年度「慢性ウイルス性肝疾患の非侵襲的線化評価法の開発と臨床的有用性の確立」（工藤班））

7. **JLOG 1004 trial**「インスリン抵抗性を合併する C 型代償性肝硬変患者を対象とした BCAA 顆粒製剤の肝細胞癌抑制効果に関する第 III 相臨床試験（BCAA Granule for patients with Hepatitis C-related Liver Cirrhosis and Insulin Resistance On the Effect of Reduction of Carcinogenic RisK in the Liver(Phase III study)(BLOCK Study))」

8. **厚生科学研究委託事業**（肝炎等克服実用化研究事業（肝炎等克服緊急対策研究事業))「慢性ウイルス性肝炎の病態把握（重症度・治療介入時期・治療効果判定・予後予測）のための非侵襲的病態診断アルゴリズムの確立」

8. おわりに

この年報を作成にあたりましては例年の如く、教授秘書、医局秘書の秘書連合軍の 14 名の皆様に全面的に編集をして頂き大変感謝を致しております。また、医局員の皆様にも大変この一年お世話になりました。この一年間も大変なハードワークではありましたが、無事皆様の頑張りにより乗り切ることができました。この場をお借りして深く感謝申し上げます。2010 年には念願の一病棟まるまる消化器内科が占めるという状態が実現しましたし、腹部超音波室も拡充されました。2014 年 12 月には救急災害棟も完成いたしました。光学治療センターの拡充も終了しましたので何卒昨年以上にモチベーションを上げて頂いて日本一、あるいは世界一の消化器内科学教室へ育つようにご尽力頂きたいと思います。2014 年も教育・診療・研究において、特に英文論文、新しい研究の立ち上げということについては例年以上に積極的に取り組んでいきたいと考え

ておりますので医局員全員が共通の価値観と消化器内科の将来の方向性に対するベクトルを共有し、心を一つにして邁進して頂きたいと祈念・期待しております。

2015 年 12 月　大阪狭山にて

2014 年度表彰式一覧

- **Highest Impact Factor Award 2014（最高インパクトファクター賞）**

  1 位　櫻井俊治　　9.284（Cancer Res）
  2 位　北野雅之　　5.196（Endoscopy）
  2 位　鎌田　研　　5.196（Endoscopy）

  ※　4 位　有住忠晃　4.020（J Gastroenterol）
  ※　工藤正俊　11.190（Hepatology）

- **Most Numbers of Paper Award 2014（最多英文論文発表賞）**

  1 位　西田直生志　4 本（Digest Dis × 3, LiverCancer × 1）
  1 位　有住忠晃　　4 本（J Gastroenterol × 1, Oncology-Basel × 1, Digest Dis × 2）

  ※　3 位　北野雅之　3 本（Digest Endosc × 2, Endoscopy）
  ※　3 位　南　康範　3 本（Liver Cancer × 1, World J Gastroenterol × 1, Digest Dis × 1）
  ※　工藤正俊　10 本

- **Total Highest Impact Factor Award 2014（累積最高インパクトファクター賞）**

  1 位　有住忠晃　10.297（4 本）
  2 位　北野雅之　 9.174（3 本）

  ※　3 位　西田直生志　5.496（4 本）
  ※　工藤正俊　32.051（10 本）

- **最多入院受持患者賞**

  1 位　今井　元　228 人
  2 位　足立哲平　217 人

  ※　3 位　大本俊介　206 人

- **最多緊急内視鏡賞**

  1 位　今井　元　88 件
  2 位　門阪薫平　72 件

  ※　3 位　大本俊介　71 件

- **最多外来患者診療賞**

  1 位　萩原　智　3,414 人
  2 位　上嶋一臣　3,197 人

  ※ 3 位　松井繁長　2,905 人
  ※ 工藤正俊　2,221 人

工藤正俊（くどうまさとし）

（平成 27 年 12 月更新）



昭和 29 年	愛媛県西条市生まれ
昭和 53 年	京都大学医学部 卒業
同	京都大学医学部附属病院 勤務（研修医）
昭和 54 年	神戸市立中央市民病院内科　勤務（研修医）
昭和 55 年	同　消化器内科　医員
昭和 60 年	同　消化器内科　副医長
昭和 62 年	カリフォルニア大学留学（デービスメデイカルセンター）
平成元年	神戸市立中央市民病院消化器内科　副医長　復職
平成　4 年	同　消化器内科　医長
平成　9 年	近畿大学医学部第２内科学　助教授
平成 11 年	近畿大学医学部消化器内科学 教授　現在に至る
平成 20 年	近畿大学医学部附属病院病院長（平成 20 年 10 月～平成 26 年 9 月）
	近畿大学医学部高度先端医療センター長（平成 20 年 10 月～平成 26 年 9 月）
	近畿大学医学部光学治療センター長（平成 20 年 10 月～平成 27 年 9 月）
	近畿大学医学部附属病院救急災害センター長（平成 25 年 9 月 1 日～平成 26 年 9 月）
平成 27 年	学校法人近畿大学理事
（現在の併任）	近畿大学医学部奈良病院消化器・内分泌内科 教授（兼務）
	近畿大学医学部堺病院消化器科 教授（兼務）
	神戸市立中央市民病院消化器内科 顧問（兼務）

主な所属学会

日本消化器病学会（財団評議員・指導医・専門医）、日本肝臓学会（理事・指導医・専門医・国際委員会委員長）、日本消化器内視鏡学会（社団評議員・指導医・専門医・ネットワーク委員会委員）、日本超音波医学会（理事長・指導医・専門医・国際交流委員会委員長）、日本内科学会(評議員・認定内科医)、日本高齢消化器病学会（理事），日本核医学会(評議員・専門医)、日本肝癌研究会（常任幹事・追跡調査委員長・取扱規約委員・肝癌治療効果判定基準作成委員会委員長・事務局代表)、日本肝移植研究会（世話人)、肝血流動態イメージ研究会（幹事)、日本腹部造影エコー・ドプラ診断研究会（事務局・代表世話人)、肝癌治療シミュレーション研究会（副代表幹事・企画委員)、超音波治療研究会（常任世話人)、日本肝がん分子標的治療研究会（代表世話人・事務局代表)、日本消化器内視鏡財団（評議員)、日本臨床腫瘍学会（評議員・保険委員会委員（2013 年 4 月－現在))、日本癌学会（評議員)、米国肝臓学会（AASLD)(肝癌部門企画運営委員：Steering Committee of hepatobiliary malignancy)、米国消化器病学会（AGA)、世界肝臓学会　(IASL)、欧州肝臓学会（EASL）、米国消化器内視鏡学会（ASGE)など

委員・資格など

- 世界超音波医学会（WFUMB）,Immediate Past President（前理事長）
- アジア超音波医学会（AFSUMB）Secretary（庶務担当理事）
- 国際肝癌学会（ILCA）理事（Founding Board Member, Governing Board Council Member）
- 米国肝臓学会（AASLD）肝癌部門運営委員会委員（Steering Committee Member）
- 日本肝がん臨床研究機構（JLOG）（理事長）
- 世界保健機構（WHO）Blue Book「Classification of the Tumor」改訂委員（平成 21 年 5 月 1 日）
- ウイルス肝炎研究財団　日米医学協力研究会肝炎専門部会研究員
- International Liver Thought Leadership Study (ILCS), Council member
- アジア太平洋肝癌専門家会議（APPLE）理事長（President）
- Editor-in-Chief: Liver Cancer (Karger, Basel)

受賞

- 米国核医学会 Berson-Yalow Award 受賞（平成元年 6 月）
- 日本対がん協会がん研究助成奨励賞 受賞（平成 4 年 3 月）

- 日本消化器病学会奨励賞 受賞（平成4年4月）
- 日本核医学会賞 受賞（平成5年10月）
- 米国超音波医学会（AIUM）学会賞受賞（平成15年6月4日）
- ボローニャ大学医学部医学会名誉会員賞（平成18年9月15日）
- フィリピン超音波医学会名誉会員（Honorary Member of PSUCMI）（平成20年3月19日）
- アジア太平洋消化器病学会（APDW）OKUDA Award受賞（平成20年9月13日）
- 北米放射線学会 Certificate of Merit受賞（平成20年）
- インド肝臓学会 Madangopalan Award受賞（平成21年3月28日）
- 北米放射線学会 Cum Laude賞受賞（平成21年12月）（7000編の論文中上位10編に採択）
- 日本肝臓学会「日本肝臓学会機関誌 Highest Citation賞」受賞（平成22年6月）
- JISAN Lecture Award Presented by Korean Society of Ultrasound in Medicine（平成22年5月）
- 米国超音波医学会名誉会員賞（AIUM Honorary Member Award）受賞（平成23年4月）
- 韓国超音波医学会名誉会員賞（KSUM honorary Award）受賞（平成23年5月）
- 日本肝臓学会「日本肝臓学会機関誌 Highest Citation賞」受賞（平成23年6月）（2回目）
- Romanian Society of Ultrasound in Medicine and Biology（SRUMB）Honorary Award受賞（平成23　年6月）
- 北米放射線学会 Certificate of Merit受賞（平成23年11月）（2回目）
- USE論文賞（応用物理学会論文賞）」受賞（平成24年11月）
- Lorenzo Capussotti Award受賞（from IASGO）（平成26年12月）

著書（単著）

- Contrast Harmonic Imaging in the Diagnosis and Treatment of Liver Tumors（Springer-Verlag　2003）
- 肝腫瘍における造影ハーモニックイメージング（医学書院　2001）

編集

- 松井　修，**工藤正俊**,編集：消化器疾患の造影エコーUp Date．南江堂，東京，2003.
- **工藤正俊**，編集：肝細胞癌治療の最近の進歩，消化器病セミナー97，へるす出版，東京，2004.
- 河田純男，白鳥康史，**工藤正俊**，榎本信幸，編集，小俣政男，監修：肝疾患Review 2004，日本メディカルセンター，東京，2004.
- 河田純男，白鳥康史，**工藤正俊**，榎本信幸，編集，小俣政男，監修：肝疾患Review 2006-2007,日本メディカルセンター，東京，2006.
- 河田純男，横須賀收，**工藤正俊**，榎本信幸，編集，小俣政男，監修：肝疾患Review 2008-2009，日本メディカルセンター，東京，2008.
- 河田純男，横須賀收，**工藤正俊**，榎本信幸，編集，小俣政男，監修：肝疾患Review 2010-2011，日本メディカルセンター，東京，2010.
- 幕内雅敏，菅野健太郎，**工藤正俊**，編集：今日の消化器疾患治療指針　第3版，医学書院，東京，2010.
- **工藤正俊**，泉　並木，編集：症例から学ぶ ウイルス肝炎の治療戦略．　（株）診断と治療社，東京，2010.
- **工藤正俊**，編集：肝細胞癌の分子標的治療，アークメディア，東京，2010.
- 山雄健次，**工藤正俊**，編集：見逃し、誤りを防ぐ!肝・胆・膵癌画像診断アトラス，羊土社，東京，2010.
- **工藤正俊**，編集：医学のあゆみ「肝癌の分子標的治療」，医歯薬出版株式会社，東京，2011.
- **工藤正俊**，編集：「肝細胞がん診療の進歩：Up-To-Data」,最新医学社，大阪，2011.
- **工藤正俊**，編集：朝倉内科学，矢崎義雄，「総編集」，朝倉書店，東京，2013.
- **工藤正俊**,國分茂博,編集：EOB-MRI/ソナゾイド造影超音波による肝癌の診断と治療,医学書院,東京,2013

EDITER-IN－CHIEF: Liver Cancer（Basel）

Associate Editor: Journal of Oncology（Germany),肝胆膵（アークメディア））

EDITORIAL BOARD:

国際学術雑誌: International Journal of Clinical Oncology（Tokyo）Ultrasound in Medicine and Biology（ELSEVIER, New York）Hepatology International（Springer, New York）Liver International（Blackwell, UK）World Journal of Gastroneterology Liver Cancer Review Letters

国内学術雑誌: 肝胆膵、その他の学会誌（3）

論文査読委員

J Clin Oncol(18.832)，Lancet Oncol（22.589），Gastroenterology(11.675)，Hepatology(11.665)，J Hepatol(9.264)，Oncologist(3.910)，Am J Gastroenterol(7.282)，Endoscopy(5.210)，Clin Exp Metastas(4.113)，Cancer Sci(3.846)，Expert Rev Mol Diagn(4.652)，Eur Radiol(3.594)，Liver Int(3.840)，J Gastroenterol(4.160)，Eur J Clin Invest(2.736)，J Nucl Med(6.381)，J Gastroen Hepatol(2.410)，Oncology-Basel（International Journal of Cancer Research and Treatment)(2.538)，Ultrasound Med Biol(2.493)，Acta Paediatr(1.955)，Hepatol Int(2.963)，Eur J Gastroen Hepat（1.598），J Hepato-Bil-Pan Scu（1.963)，Hepatol Res(1.857)，Int J Clin Oncol(1.437)，Jpn J Clin Oncol(1.856)，Internal Med(1.037)，J Clin Ultrasound(0.808)，Biomark Med(1.247)，Hepato-Gastroenterol(0.677)，Ann Nucl Med(1.386)，Expert Review of Anticancer Treatment(0)，J Cancer Res Ther（0.825)，CSR National Registry(0)，J Gastrointest Liver（1.434)，Cancer Informatics(0)，Expert Review of Proteomics and Future Oncology(0)

SIENTIFIC PAPER PUBLICATION:

学術論文	英文論文: 596（IF: 2048.072）	
	和文論文: 841	
教科書（単著）	英文: 2	和文: 6
分担執筆	英文: 21	和文: 264

特別講演・招待講演・教育講演:

国際学会: 330
国内学会: 637

科学研究費等外部資金の獲得状況

- 文部科学省科学研究費補助金　基盤研究(A)　2 件（総額 1,100 万円）
  基盤研究(B)　6 件（総額 2,311 万円）
  基盤研究(C)　12 件（総額 1,240 万円）
  挑戦的萌芽研究　3 件（総額　310 万円）
  （主任研究者）（　260 万円）
  「肝細胞癌の発癌・進展の分子機序: 造影超音波クッパー相と遺伝子発現を用いた融合解析」
  （分担研究者）（　50 万円）
  「肝細胞癌のソラフェニブ著効例における感受性規定遺伝子変異の探索」（主任研究者　西尾和人）
- 知的クラスター創生事業（がんペプチドワクチン）　1 件（総額　10 万円）
- 車両財団がん研究助成金　1 件（総額　100 万円）
- 学会奨励研究補助金　6 件（総額　530 万円）
- 医師会・民間医学振興財団等研究補助金　32 件（総額 2,089 万 5 千円）
- 国立がん研究センターがん研究開発費（分担研究者）（　245 万円）
  「抗悪性腫瘍薬による肝炎ウイルス再活性化の調査とその対応に関する研究」（班長　池田公史）
- 国立がん研究センターがん研究開発費（分担研究者）（　12 万円）
  「進行肝胆膵がんの治療法の開発に関する研究」（班長　奥坂拓志）

- **厚生労働省科学研究費**　主任研究者　3 件（総額 3 億 825 万円）
  1.（がん臨床研究事業）
  「進行・再発肝細胞癌に対する動注化学療法と分子標的薬併用による新規治療法の確立を目指した臨床試験（Phase III）ならびに効果を予測する biomarker の探索研究」（平成 22 年 - 24 年度）
  2.（難病・がん等の疾患分野の医療の実用化研究事業）
  「慢性ウイルス性肝疾患の非侵襲的線化評価法の開発と臨床的有用性の確立」（23 年-25 年度）
  3. 平成 27 年度日本医療研究開発機構委託研究開発費(AMED)
  （肝炎等克服実用化研究事業（肝炎等克服緊急対策研究事業））「慢性ウイルス性肝炎の病態把握（重症度・治療介入時期・治療効果判定・予後予測）のための非侵襲的病態診断アルゴリズムの確立」（26 年-現在）

- **厚生労働省科学研究費**　分担研究者　29 件（総額 3,325 万円）
  1.（肝炎等克服緊急対策研究事業）
  「血小板低値例へのインターフェロン治療法の確立を目指した基礎および臨床的研究」（班長　西口修平）
  2.（がん臨床研究事業）
  「初発肝細胞癌に対する肝切除とラジオ波焼灼両方の有効性に関する多施設共同研究」（班長　國土典宏）
  3.（肝炎等克服緊急対策研究事業）
  「肝がんの新規治療法に関する研究」（班長　本多政夫）
  4.（難治性疾患克服研究事業）
  「多発肝のう胞症に対する治療ガイドライン作成と試料バンクの構築」（班長　大河内信弘）
  5.（難病・がん等の疾患分野の医療の実用化研究事業）
  「慢性ウイルス性肝疾患患者の情報収集の在り方等に関する研究」（班長　相崎英樹）

ガイドライン策定委員会委員

- 「科学的根拠に基づく肝癌診療ガイドライン」（日本肝臓学会編），金原出版
- 「「慢性肝炎の治療ガイドライン」（日本肝臓学会編），文光堂
- 「肝癌診療マニュアル」（日本肝臓学会編），医学書院
- 「肝癌治療効果判定基準」（日本肝癌研究会取扱い規約委員会編），肝臓
- 臨床病理「肝癌取り扱い規約」（日本肝癌研究会編）
- Clinical Practice Guidelines for Hepatocellular Carcinoma, Japan Society of Hepatology, Hepatology Research
- General Rules for the Clinical and Pathological Study of Primary Liver Cancer, 3rd English Version, Liver Cancer Study Group of Japan, Kanehara, Tokyo, 2010
- Response Evaluation criteria in the Cancer of the Liver (RECICL), Liver Cancer Study Group of Japan, Hepatology Research
- 「多発肝のう胞症に対する治療ガイドライン」
- RECICL 2014 update 版, Hepatology Research

特許取得

発明の名称：　ソラフェニブの効果予測方法
出願番号：　特願 2011-104275
出願日：　2011 年 5 月 9 日
発明者：　荒尾徳三、松本和子、西尾和人、工藤正俊
出願人：　学校法人近畿大学

発明の名称：　N 型糖鎖を利用した膵臓癌の診断方法
公開番号：　特許公開 2009-270996
公開日：　2009 年 11 月 19 日
発明者：　荒尾徳三、松本和子、西尾和人、坂本洋城、北野雅之、工藤正俊
出願人：　住友ベークライト株式会社

全国規模の学会・研究会事務局

- 日本肝癌研究会（**事務局・追跡調査委員長・常任幹事**）
- 日本腹部造影エコー・ドプラ診断研究会（**代表世話人・事務局**）
- NPO 法人日本肝がん臨床研究機構（**理事長・事務局**）
- 日本肝がん分子標的治療研究会（**代表世話人・事務局**）

全国規模の研究会世話人・役員

平成 6 年 4 月–8 年 3 月　日本超音波医学会腹部造影エコー研究部会幹事
平成 7 年 11 月–現在　肝血流動態イメージ研究会世話人
平成 8 年 4 月–現在　日本腹部造影エコー・ドプラ造影研究会世話人（事務局兼務)(平成 25 年より**代表世話人**)
平成 9 年 7 月–現在　肝動脈塞栓療法研究会世話人
平成 10 年–現在　国際造影超音波研究会（現、Asia Contrast Ultrasound Imaging Society）世話人
平成 11 年 10 月–現在　臨床消化器病研究会世話人
平成 11 年 7 月–現在　西日本肝臓研究会世話人
平成 13 年 5 月–現在　肝疾患フォーラム世話人
平成 14 年 4 月–現在　犬山シンポジウム会員
平成 14 年 9 月–現在　日本消化器画像診断研究会世話人
平成 16 年–現在　Liver Forum in Kyoto 世話人
平成 18 年–現在　肝癌治療シミュレーション研究会副代表幹事
平成 19 年 11 月–現在　日本超音波治療研究会常任世話人
平成 20 年–現在　日本肝がん分子標的治療研究会（**代表世話人**）

関西地区研究会代表世話人

- 平成 11 年–平成 19 年　関西造影超音波研究会（**代表世話人**）
- 平成 13 年–現在　関西 B 型肝炎研究会（**代表世話人**）
- 平成 14 年–現在　肝癌局所治療研究会（**代表世話人**）
- 平成 14 年–現在　大阪消化器化学療法懇話会（**代表世話人**）
- 平成 15 年–現在　臨床消化器病フォーラム（**代表世話人**）
- 平成 18 年–平成 22 年　Bay Area Gut Club（**代表世話人**）
- 平成 18 年–平成 22 年　South Osaka Liver Club（**代表世話人**）
- 平成 19 年–現在　関西肝血流動態イメージ研究会（**代表世話人**）
- 平成 20 年–現在　Kinki Liver Club（**代表世話人**）
- 平成 21 年–現在　南大阪肝疾患研究会（**代表世話人**）
- 平成 21 年–現在　南大阪肝胆膵疾患研究会（**代表世話人**）

関西地区研究会世話人

- 平成 2 年–現在　大阪肝穿刺生検治療研究会世話人
- 平成 6 年–現在　兵庫インターベンショナルラディオロジー研究会世話人
- 平成 8 年–現在　肝胆膵治療フォーラム・神戸世話人
- 平成 9 年–現在　京都肝疾患懇話会世話人
- 平成 9 年–現在　肝臓分子生物学研究会
- 平成 11 年–平成 18 年　肝代謝コロキウム世話人
- 平成 11 年–現在　大阪肝胆膵懇話会世話人
- 平成 11 年–現在　南大阪肝胆膵疾患研究会世話人
- 平成 11 年–現在　南大阪消化器病懇話会世話人
- 平成 11 年–現在　南大阪肝疾患研究会世話人
- 平成 11 年–平成 24 年　消化器ラウンドテーブルディスカッション世話人

- 平成 11 年–平成 18 年　泉州肝臓病研究会世話人
- 平成 11 年–平成 18 年　大阪肝炎ミーティング世話人
- 平成 12 年–現在　大阪肝臓病談話会世話人
- 平成 12 年–現在　関西経皮内視鏡的胃瘻造設術研究会世話人
- 平成 12 年–現在　肝疾患座談会 in Kyoto 世話人
- 平成 12 年–現在　近畿肝癌談話会常任幹事
- 平成 13 年–現在　関西肝血流動態イメージ研究会世話人
- 平成 16 年–平成 23 年　あおい肝臓研究会世話人
- 平成 18 年–現在　大阪肝臓ミーティング世話人
- 平成 19 年–現在　近畿・超音波内視鏡研究会顧問

全国規模の国内研究会主催（会長）

- 1997 年 2 月　第 3 回肝血流動態イメージ研究会（神戸）
- 1996 年 10 月　第 1 回日本造影エコー・ドプラ診断研究会（神戸）
- 2005 年 2 月　第 11 回肝血流動態イメージ研究会（横浜）
- 2007 年 9 月　第 2 回肝癌治療シミュレーション研究会（大阪）
- 2008 年 9 月　第 49 回日本消化器画像診断研究会（大阪）
- 2010 年 1 月　第 1 回日本肝癌分子標的治療研究会（神戸）
- 2014 年 2 月　第 20 回肝血流動態・機能イメージ研究会（大阪）

国内学会主催（会長）

- 第 45 回日本肝臓学会総会（2009 年 6 月）, 神戸
- 第 83 回日本超音波医学会学術集会（2010 年 5 月）, 京都
- 第 50 回日本肝癌研究会（2014 年 6 月）, 京都
- 第 89 回日本超音波医学会学術集会（2016 年 5 月）, 京都（予定）

近畿地区学会主催（会長）

- 第 82 回日本消化器内視鏡学会近畿支部例会（2009 年 8 月）
- 第 95 回日本消化器病学会近畿支部例会（2011 年 8 月）

国際学会主催（会長）

- JSH Single Topic Conference on HCC (2005年), Awaji-shima
- The 3rd International Kobe Liver Cancer Symposium on HCC (IKLS) (2009年6月), Kobe
- The 2nd Asia Pacific Primary Liver Cancer Expert Meeting (APPLE)(2011年7月), Osaka
- The 14th WFUMB 2013 (世界超音波医学会) (2013年5月), Sao Paulo (Co-President with Leandro Fernandez and Giovanni Guido Cerri)
- The 4th International Kyoto Liver Cancer Symposium(IKLS) (2014年6月6-7日),Kyoto
- the 8th International Liver Cancer Association (ILCA) (国際肝癌学会) (2014年9月5日-7日),Kyoto (Co-President with Peter Galle)
- The 6th Asia Pacific Primary Liver Cancer Expert Meeting (APPLE)(2015年7月),Osaka(予定)
- AFSUMB 2016 (アジア超音波医学会) (2016年5月),Kyoto (予定)
- ACUCI (アジア造影超音波医学会) (2016年5月),Kyoto (予定)

消化器内科学教室業績抜粋

	1999	2000	2001	2002	2003	2004	2005	2006	2007	2008	2009	2010	2011	2012	2013	2014	2015	計
英文論文 (Impact Factor)	7 44.978	5 25.818	19 60.598	13 22.967	21 59.994	20 78.461	19 54.801	15 46.834	31 108.649	41 157.194	26 102.991	59 128.992	47 153.682	43 170.422	54 206.820	56 212.103	64 245.559	540 1880.863
和文論文 （著書・分担執筆を含む）	37	41	43	34	31	54	45	39	45	74	81	126	59	54	17	21	50	851
海外学会発表	2	9	4	6	24	23	14	14	17	26	20	34	64	52	35	40	31	415
国内学会発表	46	56	71	113	105	79	69	52	79	87	65	96	100	118	117	110	98	1461
海外特別講演	0	11	4	11	8	18	16	25	18	36	34	42	28	34	33	20	31	369
国内特別講演	37	40	40	52	37	38	39	27	36	39	62	94	75	59	43	30	39	787
単著教科書			1		1 （英文）													2

近畿大学医学部消化器内科　英文論文総数（530編）

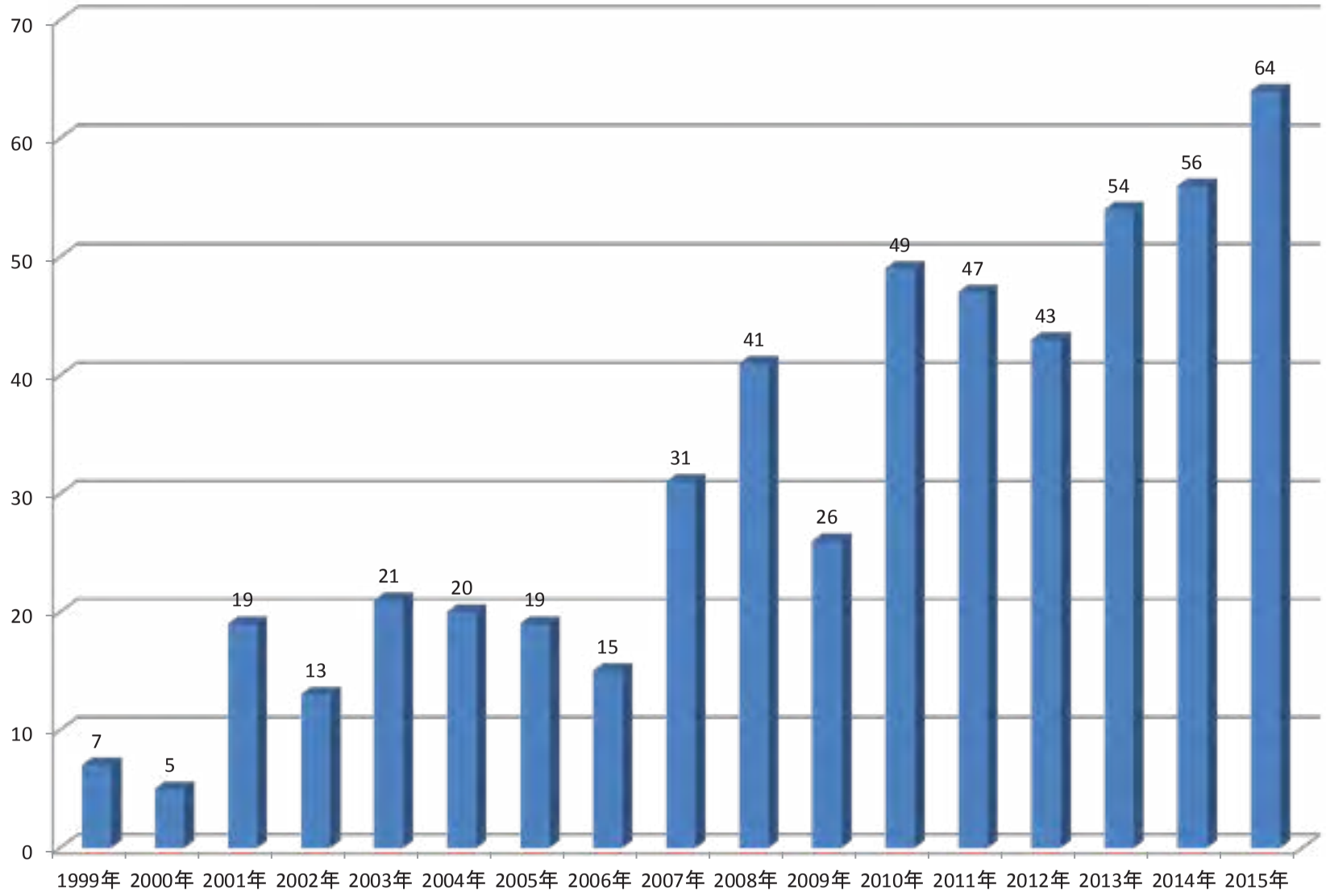

近畿大学医学部消化器内科　英文論文　Impact Factor総数
（IF=1880.863)

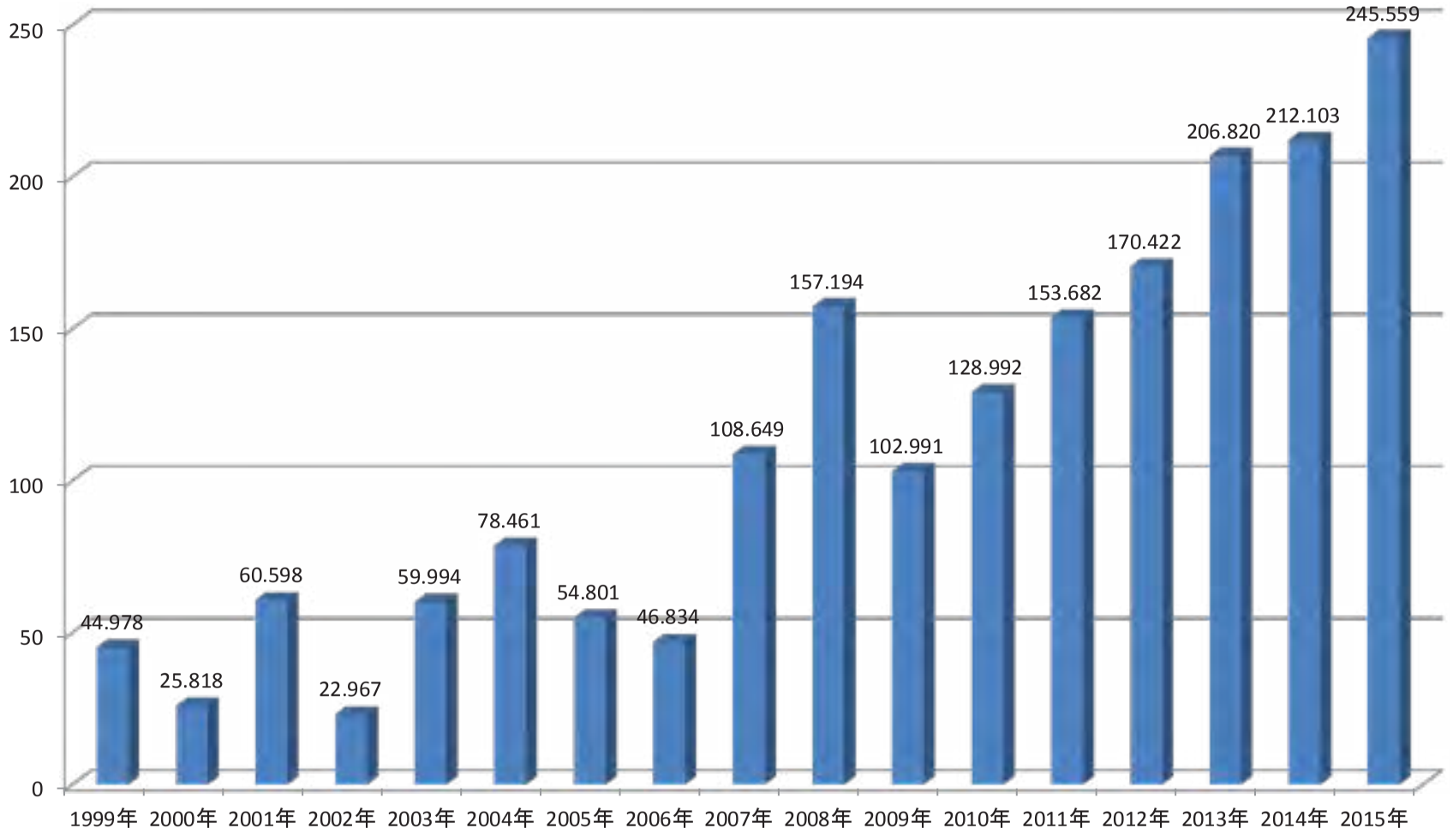

消化器内科年度別診療実績

	H11	H12	H13	H14	H15	H16	H17	H18	H19	H20	H21	H22	H23	H24	H25	H26	H27
稼働床	40	44	44	44	60	78	78	77	76	73	85	84	84	84	80	80	80
稼働率	107.2%	98.5%	126.7%	148.2%	121.0%	89.5%	95.3%	89.2%	94.7%	96.3%	91.8%	89.9%	85.8%	89.0%	91.0%	93.9%	98.2%
日平均入院患者数	40.0	43.3	55.8	65.2	72.6	69.8	74.4	68.7	72.0	70.3	70.3	76.1	72.0	74.7	77.0	75.1	78.6
平均在院日数	31.1	25.6	21.4	18.6	15.4	14.7	12.8	10.7	10.5	9.6	9	8.6	7.9	7.2	7.2	6.7	7.0
年間入院収入	501,570,188	570,616,464	801,199,124	923,171,333	1,065,481,449	1,023,271,279	1,152,778,111	1,106,484,453	1,224,122,968	1,244,806,271	1,312,812,506	1,516,925,835	1,417,104,402	1,535,069,456	1,575,321,748	1,621,531,082	1,697,023,084
年間外来収入	314,641,639	334,517,979	386,084,329	530,035,297	635,562,806	649,876,475	818,049,485	966,247,389	1,013,910,559	1,257,804,553	1,432,350,698	1,464,645,183	1,529,385,181	1,610,826,432	1,586,645,573	1,771,578,798	2,449,084,225
消化器内科年間収入	816,211,827	905,134,443	1,187,283,453	1,453,206,630	1,701,044,255	1,673,147,754	1,970,827,596	2,072,731,842	2,238,033,527	2,502,610,824	2,745,163,204	2,981,571,018	2,946,489,583	3,145,895,888	3,161,967,321	3,393,109,880	4,146,107,309

消化器内科年間外来収入

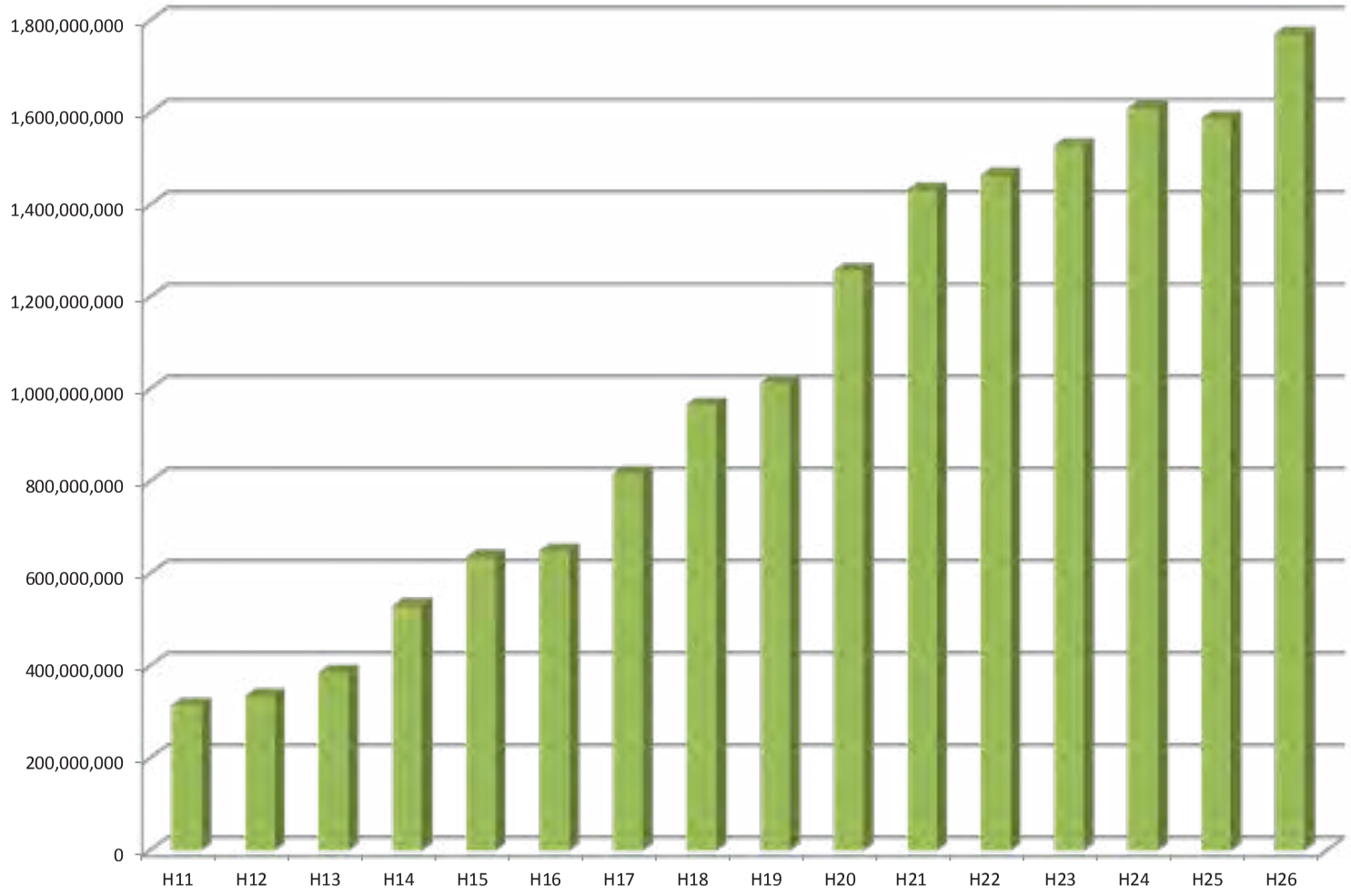

消化器内科年間入院収入

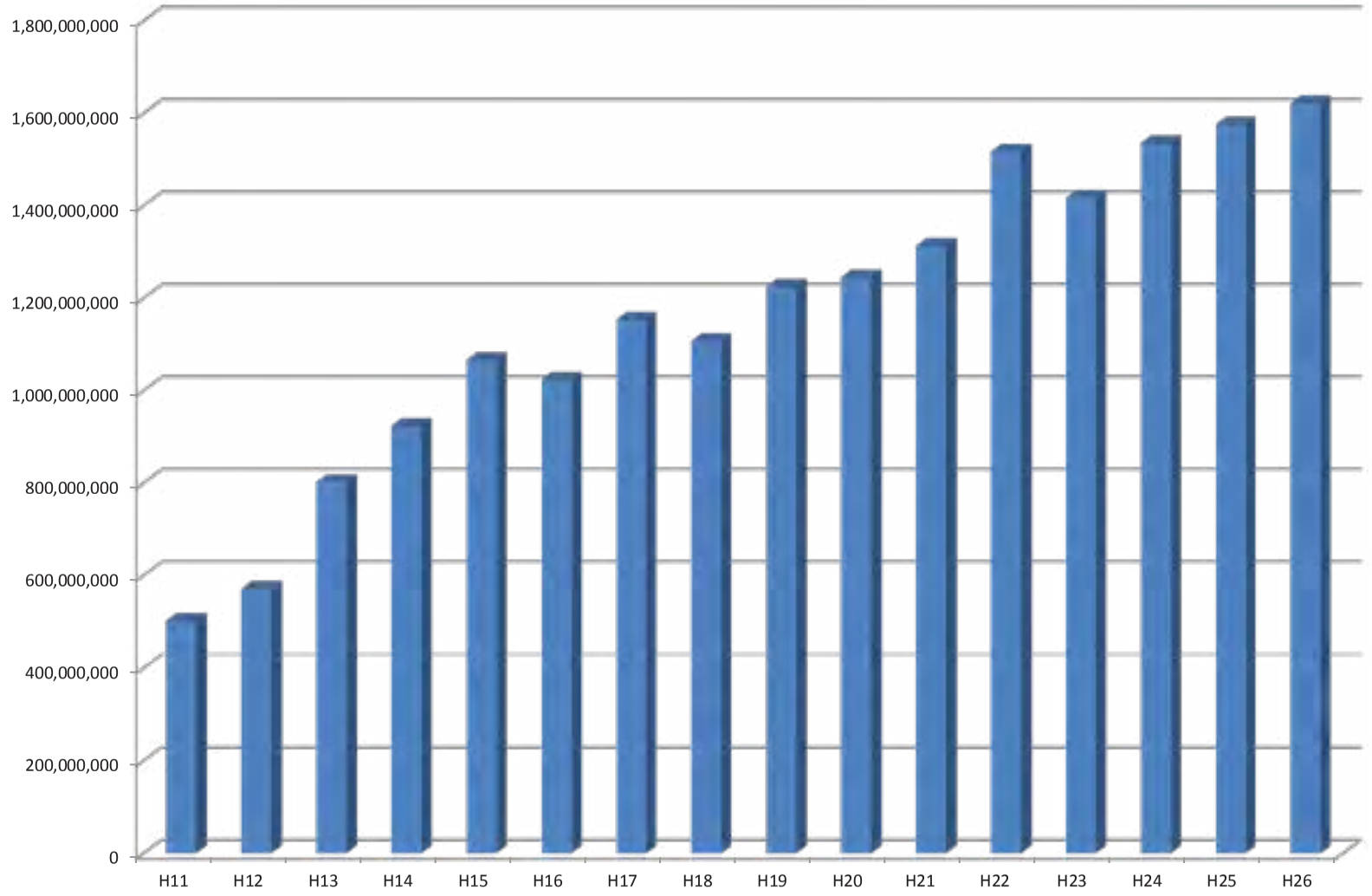

消化器内科年間総収入

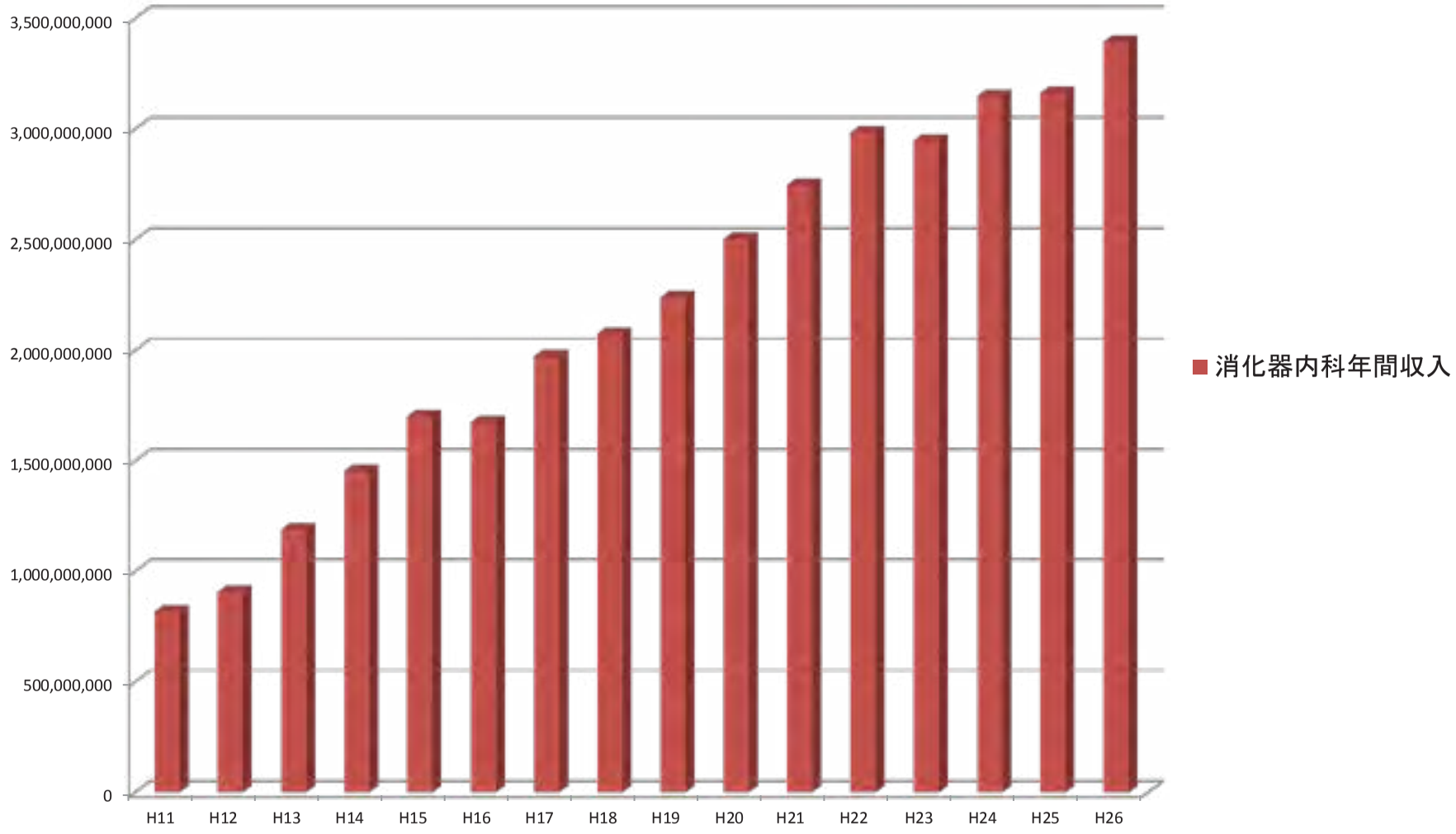
3,500,000,000
3,000,000,000
2,500,000,000
2,000,000,000
1,500,000,000
1,000,000,000
500,000,000
0
H11
H12
H13
H14
H15
H16
H17
H18
H19
H20
H21
H22
H23
H24
H25
H26
消化器内科年間収入

消化器内科入院診療実績

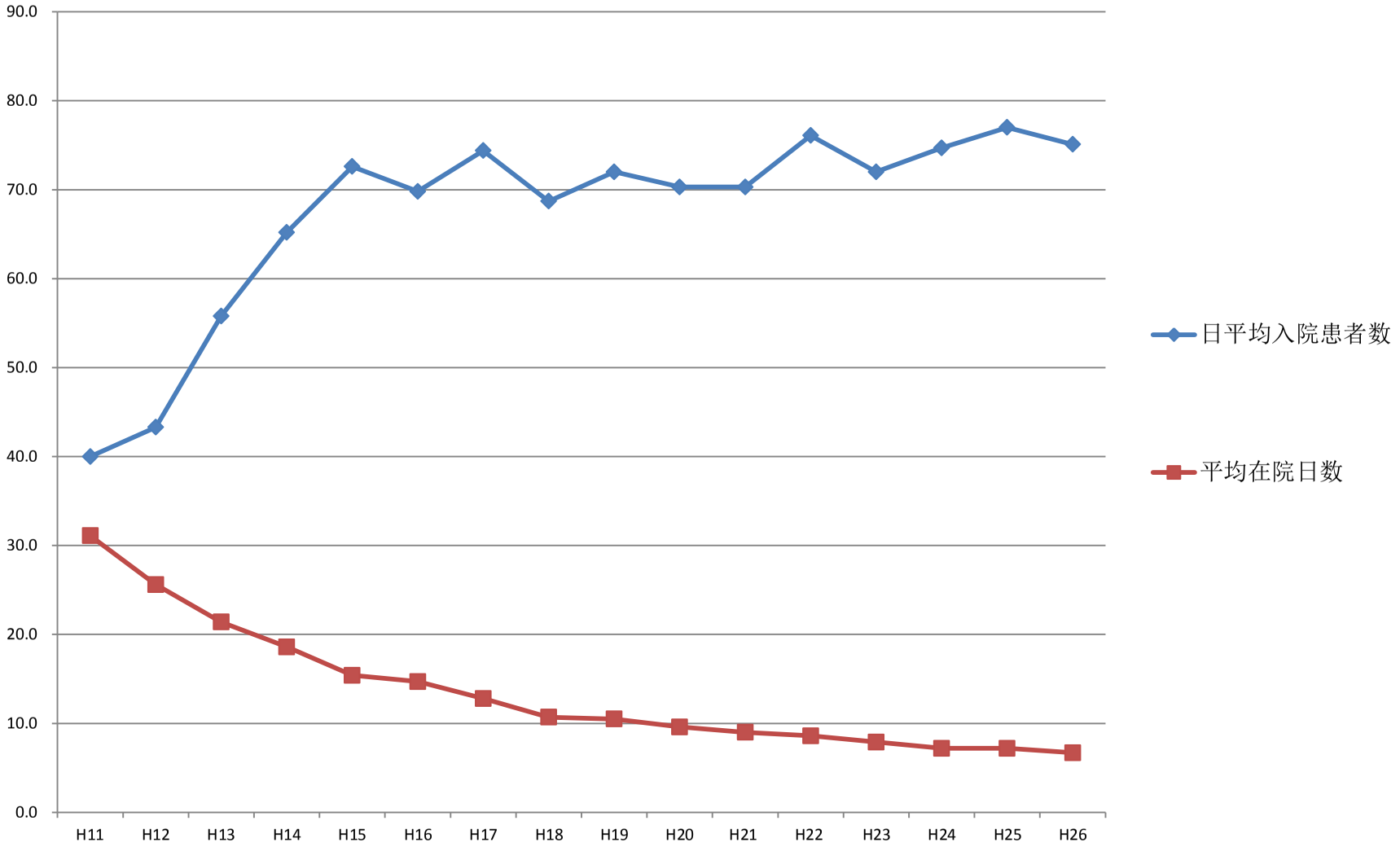

内視鏡部年報

	H26	H27(1～12月)
胃・十二指腸　球部	9046	8993
小腸	108	125
カプセル内視鏡	33	17
大腸	3873	3928
ERCP	588	627
気管支	520	542
計(スクリーニング)	14168	14232
緊急内視鏡検査	1158	1101
止血術	191	214
食道静脈瘤結紮術（EVL）	61	63
硬化療法（EIS）	3	7
EISL	30	25
ESD（食道）	46	49
ESD（胃）	136	147
EMR（胃）	32	40
胃ポリペクトミー	4	3
大腸ポリペクトミー	197	109
EMR（大腸）	456	521
ESD（大腸）	99	99
異物除去	28	25
食道ブジー	158	153
ステント留置（食道）	8	11
ステント留置（胃・十二指腸）	27	38
ステント留置（大腸）	–	–
経皮内視鏡的胃瘻造設術（PEG）	75	68
胆道ドレナージ	290	349
乳頭切開	122	127
乳頭バルーン拡張術	2	1
結石除去	136	166
超音波内視鏡（食道・胃）	47	53
超音波内視鏡（大腸）	11	10
超音波内視鏡（胆膵）	1711	1817
計	5028	5196

経皮的局所治療･肝生検総件数

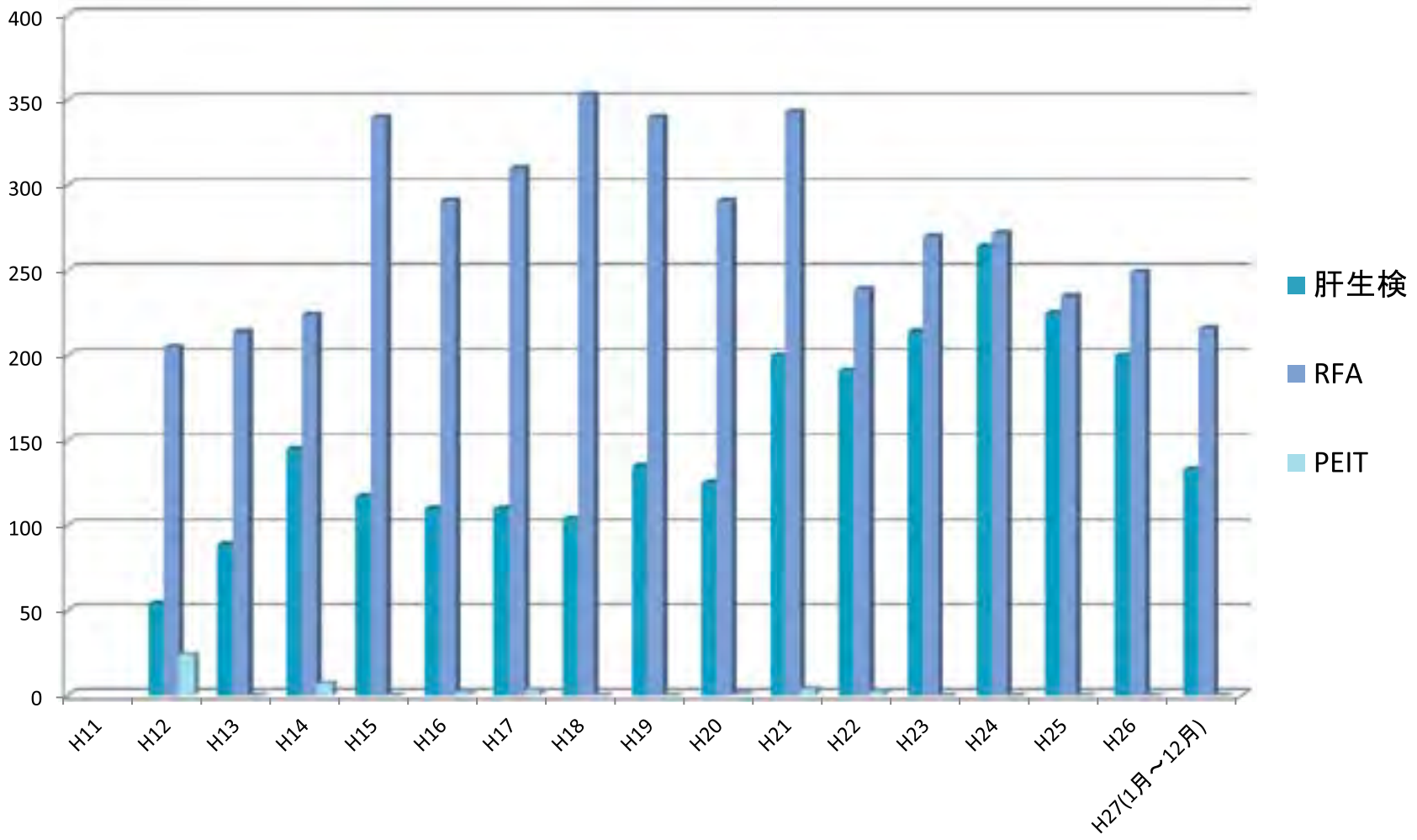

腹部造影エコー検査

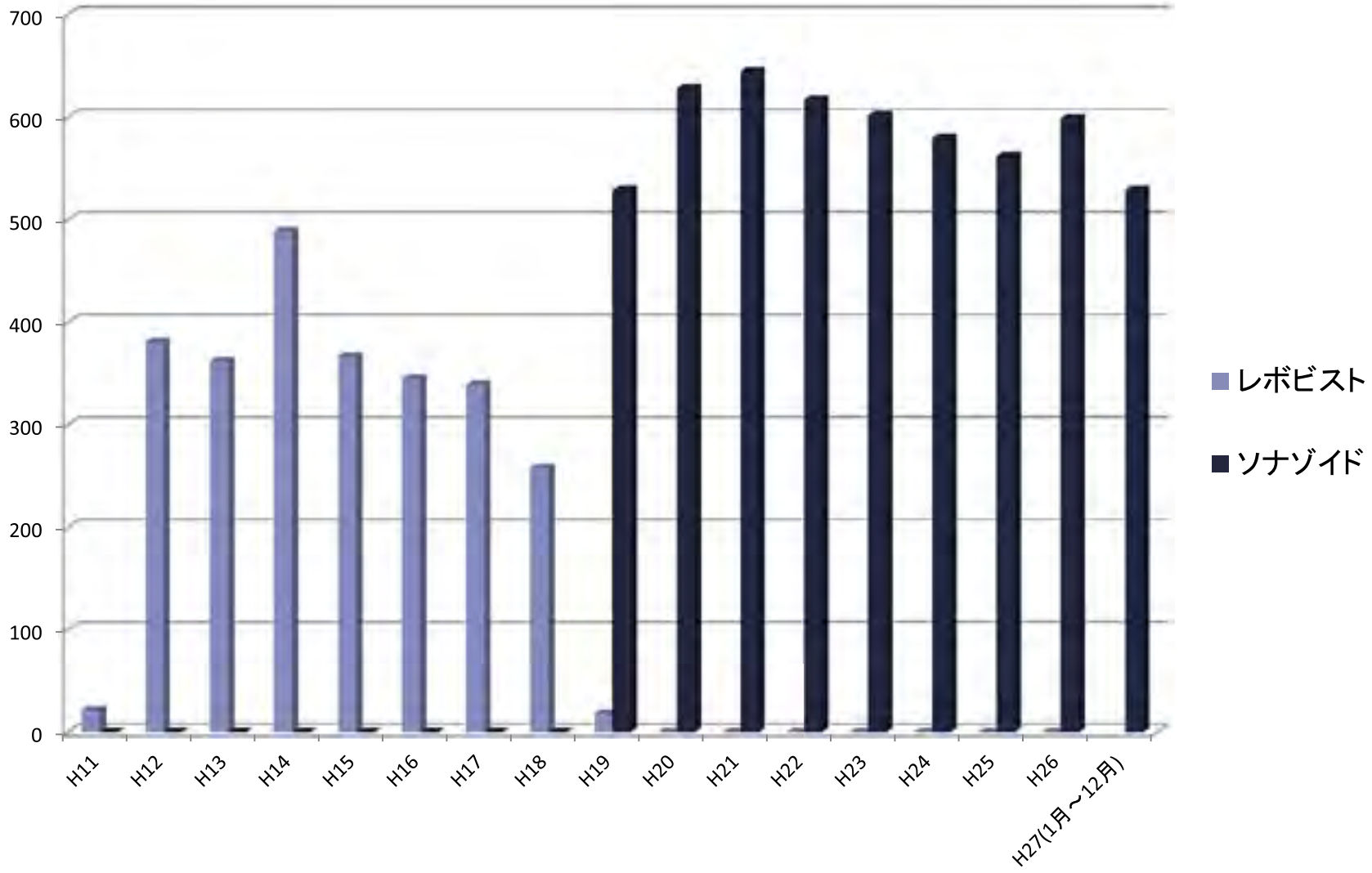
700
600
500
400
300
200
100
0
H11
H12
H13
H14
H15
H16
H17
H18
H19
H20
H21
H22
H23
H24
H25
H26
H27(1月～12月)
レボビスト
ソナゾイド

近畿大学　消化器内科学教室医局員

（平成 28 年 2 月現在）

主任教授	工藤正俊	S53	肝臓・消化器・肝癌の診断と治療
教授（内視鏡部）	樫田博史	S58	下部消化管
准教授	汐見幹夫	S55	上部・胆膵内視鏡（関空クリニック所長・教授兼務）
	西田直生志	S60	肝臓病学・肝癌の分子生物学
	北野雅之	H2	消化管全般・胆膵疾患
講師	松井繁長	H3	食道静脈瘤止血・上部消化管
	(医局長)		
医学部講師	上嶋一臣	H7	慢性肝炎・肝癌の治療
	(病棟医長)		
	櫻井俊治	H7	上部消化管・分子生物学
	(外来医長)		
	依田　広	H8	肝疾患・消化器一般
	南　康範	H9	肝疾患・消化器一般
	萩原　智	H10	肝疾患・消化器一般
	矢田典久	H11	肝疾患・消化器一般
	朝隈　豊	H14	上部消化管・消化器一般
	田北雅弘	H15	肝疾患・消化器一般
医学部助教	米田頼晃	H13	消化器一般
	岡崎能久	H13	消化器一般
	永井知行	H16	消化器一般
	今井　元	H17	胆膵疾患・消化器一般
	山雄健太郎	H18	胆膵疾患・消化器一般
	山田光成	H18	消化器一般
	有住忠晃	H19	肝疾患・消化器一般
	鎌田　研	H19	胆膵疾患・消化器一般
	峯　宏昌	H19	消化器一般
	宮田　剛	H19	胆膵疾患・消化器一般
	三長孝輔	H19	胆膵疾患・消化器一般
	松田友彦	H19	胆膵疾患・消化器一般
	足立哲平	H20	肝疾患・消化器一般
	大本俊介	H20	消化器一般
	門阪薫平	H20	胆膵疾患・消化器一般
	田中梨絵	H22	消化器一般
	千品寛和	H22	消化器一般
	河野匡志	H22	消化器一般
	南　知宏	H23	消化器一般
	岡元寿樹	H23	消化器一般
	岩西美奈	H25	消化器一般

非常勤	仲谷達也	H3	仲谷クリニック
	中岡良介	H8	山本病院　消化器内科部門
	福田信宏	H10	朝日大学附属村上記念病院　消化器内科
	市川　勉	H13	内海町いちかわ診療所
	黒木恵美	H12	PL 病院　消化器内科
	柴田千栄	H15	肝疾患・消化器一般
	上田泰輔	H15	上田内科　内科
	井上達夫	H11	井上医院　内科
	坂本洋城	H12	葛城病院　内科・消化器内科
	北井　聡	H14	北井整形外科
	大﨑往夫		大阪赤十字病院　消化器内科
	渡邉智裕		京都大学大学院医学研究科　消化器内科学
	徳永行彦		京都逓信病院　外科
	中野智景		兵庫医科大学病院　超音波センター
	滝原浩守		岸和田徳洲会病院　消化器内科
	松浦貴嶺		消化器一般
	木下真樹子		南和歌山医療センター　消化器

大学院 3 年	千品寛和	H22	消化器一般
	南　知宏	H23	消化器一般
大学院 2 年	河野匡志	H22	消化器一般
	山雄健太郎	H18	胆膵疾患・消化器一般
大学院 1 年	米田頼晃	H13	消化器一般
	山田光成	H18	消化器一般
	三長孝輔	H19	胆膵疾患・消化器一般
	岡元寿樹	H23	消化器一般

実験助手	鏡　郁子
	久々彩香
臨床研究補助	弓削公子
	濱田恵里
教授秘書	田中真紀
	村橋亜季
	本廣佳香
	和田千尋
日本肝癌研究会	田村利恵
	前原なつみ
	上妻智子
医局秘書	胡桃由佳
	朝隈　智
	浦田亜樹

分院勤務

堺病院	辻　直子	S60	近畿大学堺病院　准教授・科長
	川崎正憲	H15	近畿大学堺病院　診療講師
	高場雄久		近畿大学堺病院　医学部助教
	松本　望		近畿大学堺病院　医学部助教
	尾崎信人		近畿大学堺病院　医学部助教
奈良病院	川崎俊彦	S58	近畿大学奈良病院消化器内科　教授・部長
	茂山朋広	H17	近畿大学奈良病院消化器内科　診療助教
	奥田英之	H19	近畿大学奈良病院消化器内科　診療助教
	木下大輔	H20	近畿大学奈良病院消化器内科　診療助教
	秦　康倫	H21	近畿大学奈良病院消化器内科　診療助教
	高山政樹	H19	近畿大学奈良病院消化器内科　医学部助教
他病院勤務	山本健二		岡本クリニック
	林　道友		医療法人恵和会　林内科クリニック　院長
	中里　勝		上ヶ原病院
	南野達夫	S55	なんの医院
	水野成人	S61	神戸薬科大学　医療薬学研究室
			近畿大学奈良病院消化器内分泌内科　非常勤医師
	鍋島紀滋	S61	三菱京都病院消化器内科
	由谷逸朗	S62	富田林病院
	川端一史	H1	川端内科クリニック
	米田　円	H1	米田内科胃腸科
	渡邉和彦	H3	結核予防会大阪府支部相談診療所
	森村正嗣	H3	森村医院
	仲谷達也	H3	仲谷クリニック
	福永豊和	H4	北野病院　消化器内科
	遠田弘一	H7	慈温堂遠田医院　院長
	遠田由紀		
	亀山千晴	H7	しあわせクリニック
	小牧孝充	H7	富田林病院消化器内科
	鄭　浩柄	H8	神戸市医療センター中央市民病院
	中岡良介	H8	山本病院内科
	末冨洋一郎	H8	末冨内科クリニック

福田信宏	H10	朝日大学歯学部附属村上記念病院　消化器内科
小川　力	H11	高松赤十字病院　消化器内科
坂口康浩	H11	坂口クリニック
梅原　泰	H11	辻　腎太郎クリニック
加藤玲明	H11	かとう内科眼科クリニック
宮本容子	H12	
梅原康湖	H12	JR 大阪鉄道病院　非常勤医師
永島美樹	H12	桃坂クリニック
乾　可苗	H12	乾医院
市川　勉	H13	内海町いちかわ診療所
冨田崇文	H14	冨田病院
齊藤佳寿	H14	
高橋俊介	H14	堺市立総合医療センター
西尾　健	H14	阪南市民病院　内科　非常勤医師
坂本康明	H15	（医）坂本クリニック
早石宗右	H18	医療法人早石会　早石病院
山本典雄	H19	大阪市立大学医学部附属病院　呼吸器内科

医局員の略歴
および近況

BAR

難波に学生時代から、２、３年に１回くらい訪れている老舗 BAR があります。

移転後の現在は寂れたビルの地下にあるカウンター席とテーブル席１つの、いわゆるオーセンティックバーです。バーテンダーであるマスターの某医大に通われていたご子息と近大の同級生がバンド仲間であった縁で通うようになってもう 40 年ほどになります。マスターはハーレーダビットソンを乗り回し、毎年筆書きの達筆な年賀状をくださる洒落た紳士です。さすがにご高齢なのでもうハーレーは卒業されていると思いますが・・・

学生時代、お酒の呑み方や作法のイロハ、いろいろなカクテルを「超学割」で教えていただきました。中でも７種類、７色のお酒で作る「レインボー」というカクテルは比重の違うお酒が混ざらないように細心の注意を払いながら、時間をかけて集中して注がないと成功しないそうです。最近はお忙しいのか、多少の振戦？のためか作られることはなく、まさに幻のカクテルです。

良いバーテンダーには酒に関する豊富な知識とそれらを調合する技術の他に、他人に対する優しさ、心配りと hospitality が求められます。tender には看護人や世話する人という意味があることからもおわかりのように、客の話を聴いたり、その日の体調に合わせたレシピのカクテルを作ったりすることが重要です。これは、多くの薬剤の中から患者さんの話をよく聞いて、その時々に応じた処方をする我々医師にも通じるところがあると思います。

もちろん飲み過ぎが良くないことは多くの患者さんが教えてくれていますが、上手にたしなめばお酒は人生を豊かにし、疲れや悲しみを癒やしてくれます。今、「マッサン」でウヰスキーがブームになっていますが、ハイボールもソーダの注ぎ方、混ぜ方などでまったく違ったものになるはずです。一度、BAR の重厚な扉を開けてみられたらいかがでしょうか。

汐見　幹夫

まつい　しげなが
松井　　繁長
平成 3 年　　近畿大学医学部卒業
平成 3 年　　近畿大学第二内科入局
平成 11 年　近畿大学消化器内科助手
平成 14 年　近畿大学消化器内科講師
平成 18 年　近畿大学消化器内科医局長

専門領域
消化器病、消化器内視鏡、門脈圧亢進症、食道、胃静脈瘤
早期食道・胃癌の内視鏡診断と治療

所属学会
日本内科学会、日本消化器病学会、日本消化器内視鏡学会
日本門脈圧亢進症学会、日本消化管学会
資格
日本内科学会認定医
日本消化器病学会（専門医、学会評議員）
日本消化器内視鏡学会（指導医、学術評議員）
日本門脈圧亢進症学会　（評議員、内視鏡技術認定取得医）
日本消化管学会胃腸科認定医
近畿大学医学博士

去年の反省：毎日が反省
今年の目標：一日一善

櫻井　俊治

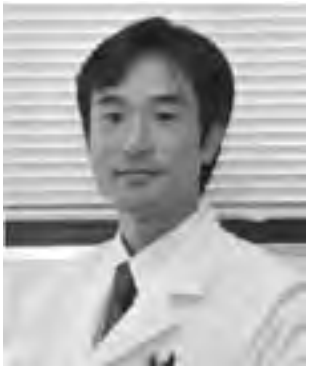

1995 年 3 月　京都大学　医学部　卒業
1995 年 5 月　神戸市立中央市民病院　医師
1997 年 4 月　天理よろづ病院　医師
2004 年 3 月　京都大学大学院　博士課程修了
2004 年 9 月　京都大学　医学部　助手
2008 年 4 月　カリフォルニア大学サンディエゴ校　客員研究員
2010 年 4 月　近畿大学　医学部　講師
現在に至る

診療内容：消化管早期癌、炎症性腸疾患の診断と治療
研究内容：炎症から発癌の分子機序の解明と新規治療・診断法の開発

近大に赴任して 5 年がたち、内視鏡治療と炎症性腸疾患の診断と治療においてすこしずつではありますが、近大消化器内科の知名度を高まっているのではないかと感じています。当院での早期消化管癌や潰瘍性大腸炎・クローン病の患者さんの数は増加傾向にあります。その評価の一端として、消化管グループでは初めてとなる治験を任されることとなりました。潰瘍性大腸炎を対象にした経口分子標的薬 AJM300（インテグリン阻害剤）の第 III 相試験が 2015 年 5 月から始まります。今後より多くの治験に参加できるよう、肝臓、胆膵だけでなく消化管領域での近大の知名度はさらに高めるよう頑張らなければいけないと思います。

学術的には、炎症性腸疾患と大腸発癌についての論文を２つ、学術雑誌 Cancer Research と Inflammatory Bowel Diseases に寄稿させていただきました。後者は足立先生の学位論文になりました。慢性炎症によるストレスが治療抵抗性を惹起し、更なる慢性炎症と大腸発癌を引き起こす、という内容です。内視鏡を用いて腸管のうけるストレスを定量化することによって、治療抵抗性や発癌リスクの予測が可能になると思われます。今後新しい治療薬の開発につながる可能性も示唆されました。この成果につきましては、2015 年 5 月にワシントン開かれます DDW2015 米国消化器病週間のプレナリーセッションでの発表の機会をいただくこととなりました。工藤正俊教授、樫田博史教授および皆様のご指導・ご協力のもと臨床と研究においてますます精進していきたいと思います。ご指導、ご鞭撻のほどよろしくお願いいたします。

「飛躍の午年」

南　康範

古くから「午年は飛躍の年」と言われますが、私にとっても正に飛躍の年でした。

具体的には、年間の発表回数が 19 回（自身過去最高)、5 本の論文作成（共著も含む）に携わる、外科指導医の資格取得、等です。特に飛躍の象徴的事柄だったのが、5 月に台湾で開催された ACTA 2014（The 1st Asia Conference on Tumor Ablation）で大満足なスピーチができたことです。それまで国際学会での oral presentation の経験はありましたが、正直に言ってたどたどしい発表ばかりでした。しかし、今回は初めての海外招待講演であることから、しっかりスライドを作り込んだうえで予行演習を十分にして臨みました。

この国際研究会は 2 日間開催で、私の発表は初日早朝のセッション「Pre-conference Training Course」の 2 番目で「How to do US-guided RFA?」のテーマを与えられました。しかし、専門家が集まる研究会であまりにも初心者向けのようなテーマであることから、最初はスライドをどのように作るか悩みました。

私の発表はいわゆる前座のセッションですし、「RFA 初心者向けに一般論を述べる」という形でも「あり」だったでしょう。しかし、大げさかも知れませんが「日本代表」である近畿大学からの発表として、何かの形でプレゼンスを示さなくてはならない！と考えました。そこで、一般論を語るのではなく、聴衆が感心を持つように「具体性」を発表に盛り込むことにしました。ご存じの通り B モード描出困難な状況下で RFA 治療することには技術的困難さを伴うのですが、講演前半ではそれら困難な状況を具体的に取り上げ、「どのような解決法があるか？」と聴衆に問いかけることで臨場感を演出することにしました。また、私のことを知らない海外のドクターが多いでしょうし、舐められないように「我々（もしくは、筆頭著者である私）は治療実績をしっかり論文化してきた」ことをアピールするようにスライドを作りました。さらに、英語が流暢ではない私なので、発表においては「1 スライド、1 メッセージ」の構成にして私の伝えたいことを明確化するよう心懸けました。

講演後半は「RFA vs. Surgical resection」と少し刺激的なテーマを取り上げました。2 本の RCT 論文を取り上げて、生存率について「有意差なし」と「外科切除が良い」とそれぞれで異なる結論を紹介した後に、「Once Again! Which is better treatment for early stage HCC, RFA or surgical resection?」のスライド

を見せました。その時、聴衆の注目を一手に集めていることを自覚しつつ、少し間を置いてから「Still controversial」を表示すると一気に会場内で笑いがあふれて「してやったり」でした。

講演が終わって壇上から降りると韓国ドクター数名から「お前のことは論文を読んで知っている」と言われて、論文を書いてきた苦労が本当に報われた思いでした。また、会長の Shi-Ming Lin 先生から繰り返し「Nice presentation!」と声を掛けて下さり本当に自信になりました。

今年は福岡で ACTA 2015 が開催予定で、会長の田中正俊先生から「発表たのむな！」と依頼されています。「日本代表」との意気込みを持ちつつ、さらに良い発表ができるように頑張ります。

略歴：

平成 9 年 3 月　近畿大学医学部卒業
平成 9 年 4 月　近畿大学医学部旧第 1 外科入局
平成 10 年 7 月　八尾徳洲会病院外科
平成 11 年 4 月　近畿大学医学部大学院（外科学）入学
平成 12 年 7 月　旧第 1 外科から消化器内科へ出向
平成 15 年 3 月　近畿大学医学部大学院（外科学）卒業
平成 15 年 4 月　近畿大学医学部消化器内科助手
平成 18 年 5 月　近畿大学医学部消化器内科講師
平成 20 年 12 月～平成 21 年 3 月　University California, San Diego (UCSD) の Department of Radiology に Visiting fellow として短期留学
平成 21 年 4 月　近畿大学医学部堺病院
平成 23 年 4 月　近畿大学医学部消化器内科

資格：外科専門医・指導医、肝臓専門医、消化器病専門医、
消化器内視鏡専門医、超音波専門医・指導医

評議員：日本消化器病学会　近畿支部評議員
日本肝臓学会　西部肝評議員

Editorial Board / 論文査読委員：

World Journal of Radiology, an Editorial Board Member (2009~)
日本超音波医学会 論文査読委員（2013~）
Liver Cancer, an Editorial Board Member (2015~)

米田　頼晃(こめだ　よりあき)　奈良県出身

略歴

平成１３年３月　北里大学医学部医学科　卒業
平成１３年４月　奈良医大第３内科(消化器・内分泌代謝・心療内科)　入局
　　奈良医大附属病院・関連病院(ベルランド総合病院)　研修
平成１９年４月　佐久総合病院胃腸科　専修医(ESD 研修)
平成２０年４月　若草第一病院消化器内科
平成２３年１月　イギリス　セントマークス病院内視鏡科　留学
平成２４年３月　オランダ　エラスムス大学医療センター消化器内科　留学
平成２４年９月　若草第一病院消化器内科　復職
平成２６年４月　近畿大学消化器内科入局　助教
現在に至る

専門領域・研究領域
早期消化管癌の内視鏡診断と治療　炎症性腸疾患の診断と治療

2014 年の反省と 2015 年の抱負

欧州留学から帰国後、近畿大学の内視鏡ライブセミナーに参加して精度の高い内視鏡手技に感銘をうけ 2014 年 4 月に入局させて頂きました。

2014 年の学術活動としては近畿支部例会のシンポジウム発表２題、内視鏡ライブセミナーの大腸 ESD の介助、ギリシャでの内視鏡ハンズオンセミナーに講師として参加しました。また大阪胃研究会の読影委員にご推薦を頂きました。

2015 年の抱負は念願の？大学院に 10 年遅く入学させて頂きましたので、早く卒業できるように頑張りたいと思います。(合格できてよかったです)

工藤正俊教授、樫田博史教授、松井繁長先生のご指導のもと臨床・研究に邁進していきたいと思います。ご指導のほどよろしくお願い致します。

2014 年の反省と 2015 年の抱負

２０１４年１０月よりくしもと町立病院に半年間出向となりました。このエッセイも、くしもと町立病院の医局で綴っています。

２００７年度より近畿大学医学部付属病院で臨床研修をはじめ、２００９年に近畿大学医学部消化器内科に入局してから、今まで近畿大学医学部で純正培養されてきました。本来３ヶ月ごとの出向を、自分の希望で半年間に延長させていただいたのも、今回初めて市中病院で勤務する機会を得て、自分の技量がどれほどのものか試してみたいという思いがあったからです。

出向の半年間を終えるにあたり、この半年間で見えてきた自分の長所短所をまとめたいと思います。

長所

- やっぱり内視鏡が好きでした（週二日の検査日で半年で５１４件、増やしすぎて串本の内視鏡の看護師さんに怒られました）
- 意外と研修医時代の手技は身についてました（PTGBA、肝生検、腹水穿刺 etc）
- 意外とできた ERCP(大学と外勤の山本 HP でのご指導のおかげです)
- やたらと高齢者にモテる（特に８０歳以上のおばあちゃんに絶大な人気！若人にはさっぱりです）

短所

- 指示が抜ける、処方忘れるはどこに行っても同じでした（大学戻ったら気をつけます）
- やっぱり ERCP、ESD は難しい
- 乗り物酔いが激しい（串本で救急搬送中、車内挿管中に嘔吐しかけました）
- 子供よりも早く寝てしまう（２２時前就寝、６時起床の健全な生活は大学でも維持できるでしょうか笑）
- お酒はいくら練習しても飲めるようにはなりませんでした。

大学に戻って、少しでも長所を伸ばせるよう、少しでも短所を少なくできるよう、これからもご指導ご鞭撻のほどよろしくお願いします。

近畿大学医学部奈良病院　消化器・内分泌内科　2014 年年報（1～12 月）

１．スタッフ

教授	川崎俊彦（昭和 58 年卒）
講師	岸谷　譲（昭和 62 年卒）
助教 B	永田嘉明（平成 16 年卒）（5 月退職）
助教 A	永井知行（平成 16 年卒）（6 月より赴任）
診療助教	奥田英之（平成 19 年卒）
診療助教	木下大輔（平成 20 年卒）
診療助教	秦　康倫（平成 21 年卒）
助教 B	貫戸幸星（平成 21 年卒）（9 月より赴任）
非常勤医師	水野成人
非常勤医師	茂山朋広

２．臨床業績

1 日平均外来患者	83.8 人
1 日平均在院患者	23.2 人
平均在院日数	7.9 日
上部内視鏡検査	3005 件（含 ESD 58 件（食道 4 件,胃 54 件））
下部内視鏡検査	1693 件（含 EMR 340 件+ESD5 件）
ERCP	124 件
超音波内視鏡	22 件（含 EUS-FNA 9 件）
腹部超音波	2131 件
腹部血管造影	83 件
ラジオ波治療	37 件

３．論文業績

（１）「７０歳以上の高齢者 C 型肝炎における瀉血療法とインターフェロンベース治療の比較検討：肝発癌と生存成績，多施設共同」
（京都医療センター消化器科）勝島慎二、（関西電力病院消化器内科）中村武史、（市立奈良病院消化器肝臓病センター）角田圭雄、田中斉祐（宇治徳洲会病院消化器科）小畑達郎、（天理よろづ相談所病院消化器内科）鍋島紀滋、岡野明浩、（星ヶ丘厚生年金病院消化器病センター）山東剛裕、

（近畿大学医学部奈良病院消化器・内分泌内科）川崎俊彦、（奈良社会保険病院消化器内科）藤村和代、（松下記念病院消化器科）長尾泰孝、（公立山城病院消化器科）新井正弘、（京都きづ川病院消化器内科）辻和宏
肝臓　５５（６）：３３５−３４８，２０１４

（２）「食道 PTP 異物と診断したら，軟性内視鏡下での摘出が最良？」
（近畿大学医学部奈良病院耳鼻咽喉科）家根旦有（同　消化器・内分泌内科）奥田英之，宮部欽生
JOHNS　３０（９）：１３０９−１３１１，２０１４

（３）「Effect of alogliptin, a DPP-4 inhibitor, on markers of lipid in type 2 diabetic patients.」
Kishitani Y, Okuda H, Kinoshita D, Hata K, Kawasaki T.
Int J Diabetes Clin Res 1:017, 2014

４．学会業績

（１）第 87 回日本内分泌学会学術総会
「Marine-Lenhart 症候群の１例」
（近畿大学医学部奈良病院消化器・内分泌内科）岸谷　譲，奥田英之，秦　康倫，木下大輔，永田嘉昭，川崎俊彦（同　耳鼻咽喉科）金澤成典，家根旦有（同　臨床検査部）太田善夫（近畿大学医学部堺病院内分泌・代謝・糖尿病内科）大野恭裕

（２）第 92 回日本消化器内視鏡学会近畿支部例会
「術前診断が可能であった胆管原発悪性リンパ腫の 1 例」
（近畿大学医学部奈良病院消化器・内分泌内科）秦　康倫，木下大輔，奥田英之，永田嘉昭，岸谷　譲，川崎俊彦（同　外科）原　譲次，辻江正徳，井上雅智（同　臨床検査部）若狭朋子，太田善夫（近畿大学医学部附属病院消化器内科）工藤正俊

（３）第 97 回日本消化器病学会近畿支部例会
「EUS-FNA で診断可能であった，腎癌膵転移の 1 例」
（近畿大学医学部奈良病院消化器・内分泌内科）濱田隆介，木下大輔，秦　康倫，奥田英之，永井知行，岸谷　譲，川崎俊彦（同　臨床検査部）若狭朋子，太田善夫（同　附属病院消化器内科）工藤正俊

（４）第 93 回日本消化器内視鏡学会近畿支部例会
「ステロイドが奏効した Cronkhite-Canada 症候群の 1 例」
（近畿大学医学部奈良病院消化器・内分泌内科）長原　大，奥田英之，秦　康倫，木下大輔，永井知行，岸谷　譲，川崎俊彦（同　臨床検査部）若狭朋子，太田善夫（近畿大学医学部附属病院消化器内科）工藤正俊

５．学会業績（研究会）

（１）肝臓病医療講演会

「最近の肝疾患診療の話題」

（近畿大学医学部奈良病院消化器・内分泌内科）川崎俊彦

（２）第 13 回北和肝疾患病診連携勉強会

「C 型慢性肝炎に対する 3 剤併用療法の当院における現況」

（近畿大学医学部奈良病院消化器・内分泌内科）川崎俊彦，秦　康倫，木下大輔，奥田英之，永井知行，岸谷　譲，

川崎俊彦

略歴

昭和 58 年	京都大学医学部医学科専門課程卒業
昭和 58 年	京都大学医学部附属病院（研修医）
昭和 59 年	大阪府済生会野江病院（内科医員）
昭和 61 年	京都大学医学部附属病院（第一内科医員）
平成２年	京都桂病院（内科医員）
平成５年	Diagnostic Radiology, Yale University School of Medicine, (Visiting Scientist)
平成６年	神戸中央市民病院（内科副医長）
平成６年	西神戸医療センター（内科副医長）
平成９年	西神戸医療センター（内科医長）に昇進
平成 12 年	近畿大学医学部附属病院（講師）
平成 16 年	大阪北逓信病院第１内科（部長）
平成 22 年	近畿大学医学部奈良病院消化器・内分泌内科（准教授）
平成 25 年	近畿大学医学部奈良病院消化器・内分泌内科（教授）

2014 年の反省と 2015 年の抱負。

2014 年は当初より，2 人欠員状態で開始し，5 月末に永田医師が開業の為に退職し，その代わりに永井先生が近大本学から赴任してくれました。この為，1 年を通して 2 人欠員状態で終始しました。一方，内分泌・代謝部門は長らく岸谷先生が一人でやって来たのが，9 月から近大本学から貫戸先生が半年間の約束で赴任してこられ，その後も半年から 1 年交代で誰かが赴任されるということですので，岸谷先生の負担もかなり軽減したと思います。消化器部門も，そういう形の 1 年交代でも良いので，もう一人の赴任をお願いしたいと切実に思います。

このため，学会活動は、昨年に続き地方会 4 題，研究会 2 題とほぼ休眠状態だったのは，臨床優先のため仕方がなかったと思います。

2015 年は４月から，以前准教授奈良病院で働いていて，長らく非常勤としてお手伝いして頂いた，水野先生が内視鏡部の教授として赴任することが決定しており，暫く続いた内視鏡部の衰退傾向に終止符が打てるのではないかと期待しています。

消化器内科学業績一覧(2014 年)

Ⅰ. 英文論文

1. 2014 Hasegawa K, Makuuchi M, Kokudo N, Izumi N, Ichida T, **Kudo M**, Ku Y, Sakamoto M, Nakashima M, Matsui O, Matsuyama Y, for the Liver Cancer Study Group of Japan: Impact of histologically confirmed lymph node metastases on the patient survival after surgical resection for hepatocellular carcinoma: report of a Japanese nationwide survey. **Ann Surg** 259:166-170, 2014. (IF:8.327)

2. 2014 Kamata K, Kitano M, **Kudo M**, Sakamoto H, Kadosaka K, Miyata T, Imai H, Maekawa K, Chikugo T, Kumano M, Hyodo T, Murakami T, Chiba Y, Takeyama Y: Value of EUS in early detection of pancreatic ductal adenocarcinomas in patients with intraductal papillary mucinous n eoplasms. **Endoscopy** 46: 22-29, 2014. (IF:5.053)

3. 2014 Utsunomiya T, Shimada M, **Kudo M**, Ichida T, Matsui O, Izumi N, Matsuyama Y, Sakamoto M, Nakashima O, Ku Y, Kokudo N, Makuuchi M for the Liver Cancer Study Group of Japan: Nationwide study of 4741 patients with non-B non-C hepatocellular carcinoma with special reference to the therapeutic impact. **Ann Surg** 259:336-345, 2014. (IF:8.327)

4. 2014 Cheng AL, Amarapurkar D, Chao Y, Chen PJ, Geschwind JF, Goh KL, Han KH, **Kudo M**, Lee HC, Lee RC, Lesmana LA, Lim HY, Paik SW, Poon RT, Tan CK, Tanwandee T, Teng G, Park JW: Re-evaluating transarterial chemoembolization for the treatment of hepatocellular carcinoma: consensus recommendations and review by an international expert panel. **Liver Int** 34:174-183, 2014. (IF:4.850)

5. 2014 Kitano M, Sakamorto H, **Kudo M**: Contrast-enhanced endoscopic ultrasound. **Digest Endosc** 26:79-85, 2014. (IF:2.058)

6. 2014 **Kudo M***: Prediction of incidence risk of hepatocellular carcinoma by ultrasound elastography. **Liver Cancer** 3:1-5, 2014.(IF:0.0)

7. 2014 Kitano M, Kamata K, **Kudo M**: Reply to Kadayifci and brugge. **Endoscopy** 46:358, 2014. (IF:5.053)

8. 2014 Kawanaka M, Nishio K, Nakamura J, Oka T, Urata N, Goto D, Suehiro M, Kawamoto H, **Kudo M**, Yamada G: Quantitative levels of hepatitis B virus DNA and surface antigen and the risk of hepatocellular carcinoma in patients with hepatitis B receiving long-term nucleos(t)ide analogue therapy. **Liver Cancer** 3:41-52, 2014. (IF:0.0)

9. 2014 Minami Y, Yagyu Y, Murakami T, **Kudo M**: Tracking Navigation Imaging of Transcatheter Arterial Chemoembolization for Hepatocellular Carcinoma using Three-Dimensional Cone-Beam CT Angiography. **Liver Cancer** 3:53-61, 2014. (IF:0.0)

10. 2014 Minami Y, Nishida N, **Kudo M**: Therapeutic Response Assessment of RFA

for HCC: Contrast-enhanced US, CT and MRI. **World J Gastroenterol**20:4160-4166, 2014. (IF:2.369)

11. 2014 Nishiguchi S, Enomoto H, Aizawa N, Nishikawa H, Osaki Y, Tsuda Y, Higuchi K, Okazaki K, Seki T, Kim SR, Hongo Y, Jyomura H, Nishida N, **Kudo M**: Relevance of the core 70 and IL-28B polymorphism and response-guided therapy of peginterferon alfa-2a± ribavirin for chronic hepatitis C of genotype 1b: A multicenter randomized trial, ReGIT-J study. **J Gastroenterol** 49:492-501, 2014. (IF:4.523)

12. 2014 Hatanaka K, Minami Y, **Kudo M***, Inoue T, Chung H, Haji S: The gross classification of hepatocellular carcinoma: usefulness of contrast-enhanced US. **J Clin Ultrasound** 42:1-8, 2014. (IF:0.691)

13. 2014 Lencioni R, **Kudo M**, Ye SL, Bronowicki JP, Chen XP, Dagher L, FuruseJ, Geschwind JF, de Guevara LL, Papandreou C, Takayama T, Yoon SK, Nakajima K, Lehr R, Heldner S, Sanyal AJ: GIDEON (Global Investigation of therapeutic DEcisions in hepatocellular carcinoma and Of its treatment with sorafeNib): second interim analysis. **Int J Clin Pract** 68:609-617, 2014. (IF:2.566)

14. 2014 **Kudo M***, Arizumi T, Ueshima K: ART score for repeated transarterial chemoembolization in patients with hepatocellular carcinoma. **Hepatology** 59:2424-2425, 2014. (IF:11.055)

15. 2014 **Kudo M**: Recent advances in Bioinformatics reveal the molecular heterogeneity of hepatocellular carcinoma. **Liver Cancer** 3:68-70, 2014. (IF:0.0)

16. 2014 Togashi Y, Sakamoto H, Hayashi H, Terashima M, Velasco MA, Fujita Y, Kodera Y, Sakai K, Tomida S, Kitano M, **Kudo M**, Nishio K: Homozygous deletion of the activin A receptor, type IB gene is associated with an aggressive cancer phenotype in pancreatic cancer. **Mol Cancer** 13:126, 2014. (IF:4.257)

17. 2014 Zhu AX, **Kudo M**, Assenat E, Cattan S, Kang YK, Lim HY, Poon RTP, Blanc JF, Vogel A, Chen CL, Dorval E, Radosavljevic MPR, Santoro A, Daniele B, Furuse J, Jappe A, Perraud K, Anak O, Sellami DB, Chen LT: Effect of everolimus on survival in advanced hepatocellular carcinoma after failure of sorafenib: The EVOLVE-1 randomized clinical trial. **J Am Med Assoc (JAMA)** 312:57-67, 2014. (IF:35.289)

18. 2014 Ikeda N, Imanishi H, Aizawa N, Tanaka H, Iwata Y, Enomoto H, Siato M, Iijima H, Iimuro Y, Fujimoto J, Yamamoto S, Hirota S, **Kudo M**, Arii S, Nishiguchi S: Nationwide survey in Japan regarding splenectomy/partial splenic embolization for interferon treatment targeting hepatitis C virus-related chronic liver disease in patients with low platelet count. **Hepato Res** 44:829-836, 2014. (IF:2.735)

19. 2014 Kim SR, Kondo F, Otono Y, Imoto S, Ando K, Hirakawa M, Fukuda K, Sakaki M, Kim SK, Komaki T, Tsuchida S, Kobayashi S, Matsuoka T, **Kudo M**: Serum amyloid A and C-reactive protein positive nodule in alcoholic liver cirrhosis, hard to make definite diagnosis. **Hepatol Res** 44:584-590,

2014. (IF:2.735)

20. 2014 Aoki T, Kokudo N, Matsuyama Y, Izumi N, Ichida T, **Kudo M**, Ku Y, Sakamoto M, Nakashima O, Matsui O, Makuuchi M, for the Liver Cancer Study Group of Japan: Prognostic imapct of spontaneous tumor rupture in patients with hepatocellular carcinoma: an analysis of 1,160 cases from a nationwide survey. **Ann Surg** 259:532-542, 2014. (IF:8.327)

21. 2014 Kitano M, Kamata K, **Kudo M**: Endoscopic ultrasonography-guided gallbladder drainage procedures: is the glass half-full or half-empty? **Digest Endosc** 26:636-637, 2014. (IF:2.058)

22. 2014 Ogawa K, Fukunaga K, Takeuchi T, Kawagishi N, Ubara Y, **Kudo M**, Ohkohchi N: Current treatment status of polycystic liver disease in Japan. **Hepatol Res** 44:1110-1118, 2014. (IF:2.735)

23. 2014 **Kudo M***: Biomarkers and personalized sorafenib therapy. **Liver Cancer** 3:399-404, 2014. (IF:0.0)

24. 2014 Nishida N, **Kudo M**: Alteration of epigenetic profile in human hepatocellular carcinoma and its clinical implications. **Liver Cancer** 3:417-427, 2014. (IF:0.0)

25. 2014 **Kudo M***, Matsui O, Izumi N, Iijima H, Kadoya M, Imai Y, Okusaka T, Miyayama S, Tsuchiya K, Ueshima K, Hiraoka A, Ikeda M, Ogasawara S, Yamashita T, Minami T, Yamakado K, on behalf of the Liver Cancer Study Group of Japan: JSH cnsensus-based clinical practice guidelines for the management of hepatocellular carcinoma: 2014 update by the Liver Cancer Study Group of Japan. **Liver Cancer** 3:458-468, 2014. (IF:0.0)

26. 2014 **Kudo M***: Emerging strategies for the management of hepatocellular carcinoma. **Digest Dis** 32:655-657, 2014. (IF: 2.181)

27. 2014 Nishida N, Nishimura T, Nakai T, Chishina H, Arizumi T, Takita M, Kitai S, Yada N, Hagiwara S, Inoue T, Minami Y, Ueshima K, Sakurai T, **Kudo M**: Genome-wide profiling of DNA methylation and tumor progression in human hepatocellular carcinoma. **Digest Dis** 32:658-663, 2014. (IF: 2.181)

28. 2014 Kono M, Inoue T, **Kudo M***, Chishina H, Arizumi T, Takita M, Kitai S, Yada N, Hagiwara S, Minami Y, Ueshima K, Nishida N, Murakami T: Radiofrequency ablation for hepatocellular carcinoma measuring 2 cm or smaller: Results and risk factors for local recurrence. **Digest Dis** 32:670-677, 2014. (IF: 2.181)

29. 2014 Minami Y, **Kudo M**: Ultrasound fusion imaging of hepatocellular carcinoma: a review of current evidence. **Diegst Dis** 32:690-695, 2014. (IF: 2.181)

30. 2014 Arizumi T, Ueshima K, Chishina H, Kono M, Takita M, Kitai S, Inoue T, Yada N, Hagiwara S, Minami Y, Sakurai T, Nishida N, **Kudo M***: Duration of stable disease is associated with overall survival in patients with advanced hepatocellular carcinoma treated with sorafenib. **Digest Dis** 32:705-710, 2014. (IF: 2.181)

31. 2014 Kitai S, **Kudo M***, Izumi N, Kaneko S, Ku Y, Kokudo N, Sakamoto M, Takayama T, Nakashima O, Kadoya M, Matsuyama Y, Matsunaga T, for the Liver Cancer Study Group of Japan: Validation of three staging systems for hepatocellular carcinoma (JIS score, biomarker-combined JIS score, and BCLC system) in 4,649 cases from a Japanese nationwide survey. **Digest Dis** 32:717-724, 2014. (IF: 2.181)

32. 2014 Arizumi T, Ueshima K, Chishina H, Kono M, Takita M, Kitai S, Inoue T, Yada N, Hagiwara S, Minami Y, Sakurai T, Nishida N, **Kudo M***: Decreased blood flow after sorafenib administration is an imaging biomarker to predict overall survival in patients with advanced hepatocellular carcinoma. **Digest Dis** 32:733-739, 2014. (IF: 2.181)

33. 2014 Nishida N, Chishina H, Arizumi T, Takita M, Kitai S, Yada N, Hagiwara S, Inoue T, Minami Y, Ueshima K, Sakurai T, **Kudo M**: Identification of epigenetically inactivated genes in human hepatocellular carcinoma by integrative analyses of methylation profiling and pharmacological unmasking. **Digest Dis** 32:740-746, 2014. (IF: 2.181)

34. 2014 Nishida N, **Kudo M**: Clinical features of vascular disorders associated with chronic hepatitis virus infection. **Digest Dis** 32:786-790, 2014.

35. 2014 Wu T, Ren J, Cong SZ, Meng FK, Yang H, Luo Y, Lin HJ, Sun Y, Wang XY, Pei SF, Zheng Y, He Y, Chen Y, Hu Y, Yang N, Li P, **Kudo M**, Zheng RQ: Accuracy of real-time tissue elastography for the evaluation of hepatic fibrosis in patients with chronic hepatitis B: a prospective multicenter study. **Digest Dis** 32:791-799, 2014. (IF: 2.181)

36. 2014 **Kudo M***: Breakthroughs in the management of hepatocellular carcinoma: celebrationg 50 years of the Liver Cancer Study Group of Japan. **Oncology** 87:1-6, 2014. (IF: 2.422)

37. 2014 **Kudo M***, Matsui O, Izumi N, Iijima H, Kadoya M, Imai Y, on behalf of the Liver Cancer Study Group of Japan: Surveillance and diagnostic algorithm for hepatocellular carcinoma proposed by the Liver Cancer Study Group of Japan: 2014 update. **Oncology** 87:7-21, 2014. (IF: 2.422)

38. 2014 **Kudo M***, Matsui O, Izumi N, Kadoya M, Okusaka T, Miyayama S, Yamakado K, Tsuchiya K, Ueshima K, Hiraoka A, Ikeda M, Ogasawara S, Yamashita T, Minami T, on behalf of the Liver Cancer Study Group of Japan: Transarterial chemoembolization failure/refractoriness: JSH-LCSGJ criteria 2014 update. **Oncology** 87:22-31, 2014. (IF: 2.422)

39. 2014 Arizumi T, Ueshima K, Chishina H, Kono M, Takita M, Kitai S, Inoue T, Yada N, Hagiwara S, Minami Y, Sakurai T, Nishida N, **Kudo M***: Validation of the criteria of transcatheter arterial chemoembolization failure or refractoriness in patients with advanced hepatocellular carcinoma proposed by LCSGJ. **Oncology** 87:32-36, 2014. (IF: 2.422)

40. 2014 Kondo F, Fukusato T, **Kudo M**: Pathological diagnosis of benign hepatocellular nodular lesions based on the new world health organization classification. **Oncology** 87:37-49, 2014. (IF: 2.422)

41. 2014 Ogawa C, Minami Y, Morioka Y, Noda A, Arasawa S, Izuta M, Kubo A, Matsunaka T, Tamaki N, Shibatouge M, **Kudo M***: Virtual sonography for novice sonographer: usefulness of synapse vincent® with pre-check imaging of tumor location. **Oncology** 87:50-54, 2014. (IF: 2.422)

42. 2014 Minami T, Minami Y, Chishina H, Arizumi T, Takita M, Kitai S, Yada N, Inoue T, Hagiwara S, Ueshima K, Nishida N, **Kudo M***: Combination guidance of contrast-enhanced US and fusion imaging in radiofrequency ablation for hepatocellular carcinoma with poor conspicuity on contrast-enhanced US/fusion imaging. **Oncology** 87:55-62, 2014. (IF: 2.422)

43. 2014 Yada N, **Kudo M***, Kawada N, Sato S, Osaki Y, Ishikawa A, Miyoshi H, Sakamoto M, Kage M, Nakashima O, Tonomura A: Noninvasive diagnosis of liver fibrosis: utility of data mining of both ultrasound elastography and serological findings to construct a decision tree. **Oncology** 87:63-72, 2014. (IF: 2.422)

44. 2014 Ikeda K, Osaki Y, Nakanishi H, Nasu A, Kawamura Y, Jyoko K, Sano T, Sunakozaka H, Uchino Y, Minami Y, Saito Y, Nagai K, Inokuchi R, Kokubu S, **Kudo M**: Recent progress in radiofrequency ablation therapy for hepatocellular carcinoma. **Oncology** 87:73-77, 2014. (IF: 2.422)

45. 2014 Yamakado K, **Kudo M**: Treatment strategies of Intermediate-stage hepatocellular carcinomas in Japan (Barcelona clinic liver cancer stage B). **Oncology** 87:78-81, 2014. (IF: 2.422)

46. 2014 Nouso K, Kokudo N, Tanaka M, Kuromatsu R, Nishikawa H, Toyoda H, Oishi N, Kuwaki K, Kusanaga M, Sakaguchi T, Morise Z, Kitai S, **Kudo M**: Treatment of hepatocellular carcinoma with Child-Pugh C cirrhosis. **Oncology** 87:99-103, 2014. (IF: 2.422)

47. 2014 Tanaka K, Shimada M, **Kudo M**: Characteristics of long-term survivors following sorafenib treatment for advanced hepatocellular carcinoma: report of a workshop at the 50th annual meeting of the Liver Cancer Study Group of Japan. **Oncology** 87:104-109, 2014. (IF: 2.422)

48. 2014 Takita M, Hagiwara S, **Kudo M***, Kono M, Chishina H, Arizumi T, Kitai S, Yada N, Inoue T, Minami Y, Ueshima K: Efficacy and safety of Telaprevir-based antiviral treatment for elderly patients with hepatitis C virus. **Oncology** 87:110-117, 2014. (IF: 2.422)

49. 2014 Yada N, Sakurai T, Minami T, Arizumi T, Takita M, Inoue T, Hagiwara S, Ueshima K, Nishida N, **Kudo M***: Ultrasound elastography correlates treatment response by antiviral therapy in patients with chronic hepatitis C. **Oncology** 87:118-123, 2014. (IF: 2.422)

50. 2014 **Kudo M***, Han G, Finn RS, Poon RTP, Blanc JF, Yan L, Yang J, Lu L, Tak WY, Yu X, Lee JH, Lin SM, Wu C, Tanwandee T, Shao G, Walters IB, Cruz CD, poulart V, Wang JH: Brivanib as adjuvant therapy to transarterial chemoembolization in patients with hepatocellular carcinoma: a randomized phase 3 trial. **Hepatology** 60:1697-1707, 2014. (IF:11.055)

51. 2014 Ashida R, Yasukawa S, Yanagisawa A, Kamata K, **Kudo M**, Ogura T, Higuchi K, Fukutake N, Nebiki H, Hirose S, Hoki N, Asada M, Yazumi S, Takaoka M, Okazaki K, Matsuda F, Okabe Y, Kitano M: Prospective Multicenter Randomized Controlled Trial of Histological Diagnostic Yield Comparing 25G EUS-FNA Needles With and Without a Core Trap in Patients With Solid Pancreatic Masses. **Gastrointest Endosc** 79:AB111, 2014. (IF: 5.369)

52. 2014 Pinato DJ, Karamanakos G, Arizumi T, Adjogatse D, Kim YW, **Kudo M**, Jang JW, Sharma R: Dynamic changes of the inflammation based index (IBI) predict mortality following chemoembolization for hepatocellular carcinoma: a prospective study. **Aliment Pharm Ther** 40:1270-1281, 2014. (IF:5.727)

53. 2014 Sakurai T, Kashida H, Watanabe T, Hagiwara S, Mizushima T, Iijima H, Nishida N, Higashitsuji H, Fujita J, **Kudo M**: Stress response protein Cirp links inflammation and tumorigenesis in colitis-associated cancer. **Cancer Res** 74:6119-6128, 2014. (IF: 9.329)

54. 2014 Watanabe T, Asano N, Meng G, Yamashita K, Arai Y, Sakurai T, **Kudo M**, Fuss IJ, Kitani A, Shimosegawa T, Chiba T, Strober W: NOD2 Down-regulates colonic inflammation by IRF4-mediated inhibition of K63-linked polyubiquitination of RICK and TRAF6. **Mucosal Immunol** 7:1312-1325, 2014. (IF:7.374)

55. 2014 Arizumi T, Ueshima K, Takeda H, Osaki Y, Takita M, Inoue T, Kitai S, Yada N, Hagiwara S, Minami Y, Sakurai T, Nishida N, **Kudo M***: Comparison of systems for assessment of post-therapeutic response to sorafenib for hepatocellular carcinoma. **J Gastroenterol** 49:1578-1587, 2014. (IF:4.523)

56. 2014 Taki H, Taki K, Yamakawa M, Shiina T, **Kudo M**, Sato T: Stabilization technique for real-time high-resolution vascular ultrasound using frequency domain interferometry. **Conf Proc IEEE Eng Med Biol Soc** 5085-5088, 2014. (IF:0.0)

57. 2014 Ogura T, Imoto A, Masuda D, Sano T, Onda S, Yamamoto K, Kitano M, Takeuchi T, Inoue T, Higuchi K: Antegrade biopsy by using a trans-catheter technique through EUS-guided hepaticojejunostomy. **Gastrointest Endosc** 81: **1007-8**, 2014. (IF:5.369)

Ⅲ. 和文論文

1. 2014 北野雅之, 工藤正俊: 教室・施設紹介「近畿大学医学部消化器内科」. 膵臓 29:112-115, 2014.

2. 2014 上嶋一臣, 工藤正俊: 臓器癌と mTOR: 肝癌. 特集「mTOR と悪性腫瘍」, 医学のあゆみ 248: 138-140, 2014.

3. 2014 井上達夫, 工藤正俊: ナーシングプロセス: 肝がん, 疾患の理解編. 特集「国試に出る！統計と法律」クリニカルスタディ 35: 9-16, 2014.

4. 2014 北野雅之, 坂本洋城, 工藤正俊: 膵充実性腫瘤の造影超音波内視鏡分類. 特集「内視鏡分類 update」, 消化器内視鏡 26: 145-147, 2014.

5. 2014 北野雅之, 工藤正俊: 胆膵疾患における Interventional EUS. 最新医学 69:130-138, 2014.

6. 2014 山雄健太郎, 北野雅之, 工藤正俊: 膵腫瘍性病変診断における造影ハーモニック EUS 検査の有用性. 超音波 TECHNO 26:76-78, 2014.

7. 2014 北野雅之, 今井 元, 工藤正俊: 悪性中下部胆道狭窄に対するステンティング. 特集「悪性胆道狭窄に対する診断・治療の進歩」, 臨床消化器内科 29:1231-1240, 2014.

8. 2014 井上達夫, 前川 清, 工藤正俊: 肝造影超音波診断. 特集「肝造影検査 Update 2014」, 画像診断 34:761-770, 2014.

9. 2014 北野雅之, 坂本洋城, 工藤正俊: コンベックス型超音波内視鏡による胆膵疾患スクリーニングのコツ. Gastroenterol Endosc 56:296-308, 2014.

10. 2014 井本真由美, 松村 到, 船内正憲, 中川和彦, 鮫島謙一, 前田裕弘, 森嶋祥之, 中江健市, 上硲俊法, 工藤正俊, 櫻林郁之助: 尿タンパク試験紙に Bence Jones タンパクが反応することの検証. 臨床化学 43:217-225, 2014.

11. 2014 鎌田 研, 北野雅之, 工藤正俊, 山雄健太郎, 今井 元, 坂本洋城: IPMN 診療における EUS の有用性. 特集「膵管内乳頭粘液性腫瘍 (IPMN) の診療の現況」, 臨床消化器内科 29:1709-1716, 2014.

12. 2014 宮田 剛, 北野雅之, 工藤正俊:超音波内視鏡下腹腔神経叢融解術 (EUS-CPN) の実際. 膵・胆道癌 FRONTIER 4(2):82-86, 2014.

13. 2014 宮田 剛, 北野雅之, 大本俊介, 門阪薫平, 鎌田 研, 山雄健太郎, 今井 元, 坂本洋城, 工藤正俊:造影ハーモニック EUS による胆・膵疾患の診断 - 造影 CT との違いは? 胆と膵 35(8):707-713, 2014.

14. 2014 宮田 剛, 北野雅之, 大本俊介, 門阪薫平, 鎌田 研, 山雄健太郎, 今井 元, 坂本洋城, 工藤正俊: 慢性膵炎の経消化管的治療. 胆と膵 35(5):455-461, 2014.

15. 2014 松井繁長, 樫田博史, 工藤正俊: 発赤調で粘液の付着を伴う胃粘膜下腫瘍様病変. 消化器内視鏡 26(7):1009-1010, 2014.

16. 2014 松井繁長，樫田博史，高山政樹，峯　宏昌，足立哲平，永井知行，川崎正憲，朝隈　豊，櫻井俊治，工藤正俊，筑後孝章：胃癌類似形態を呈した胃限局性ATTRアミロイドーシスの1例．胃と腸 49(3):377-384，2014.

17. 2014 松井繁長，樫田博史，工藤正俊：食道疣状扁平上皮癌．消化器内視鏡 26(10):1606-1607，2014.

18. 2014 鎌田　研，北野雅之：ERCPとEUS-FNAの使い分けを教えてください．これだけは知っておきたい膵疾患診療の手引き「第7章予後改善のために！膵癌」，編著　花田敬士，中外医学社，p215-220，2014.

19. 2014 北野雅之，菅野　敦：腺房細胞癌．画像で見ぬく消化器疾患　胆道・膵臓，糸井隆夫編，医学出版，p197-198，2014.

Ⅳ．招待講演・特別講演（海外）

1. Kudo M：Invited Lecture “Lessons from other TKI trials combined with TACE”，3rd Investigators Meeting for ORIENTAL, Taipei, Taiwan, February 22, 2014.

2. Kudo M：Invited Lecture “Current evidence and future perspective of molecular targeted therapies in HCC”，The 11th World Congress of the International Hepato-Pancreato-Biliary Association (IHPBA World Congress 2014), Seoul, Korea, March 22-27, 2014.

3. Kudo M：Special Lecture “Emerging role of CEUS”，The 4th International Kyoto Liver Cancer Symposium (IKLS), Kyoto International Conference Center, Kyoto, July 7-8, 2014.

4. Kudo M：Special Lecture “GIDEON final analysis data：regional difference”，The 4th International Kyoto Liver Cancer Symposium (IKLS), Kyoto International Conference Center, Kyoto, July 7-8, 2014.

5. Kudo M：Special Lecture “LCSGJ consensus”，The 4th International Kyoto Liver Cancer Symposium (IKLS), Kyoto International Conference Center, Kyoto, July 7-8, 2014.

6. Kudo M：Invited Lecture “Case-study sharing：sorafenib use in intermediate HCC”，Expert Panel Opinion on Interventions in Hepatocellular Carcinoma (EPOIHCC), The Grand Hotel Taipei, Taiwan, July 10, 2014.

7. Kudo M：Invited Lecture “HCC guidelines in the region：an update-Japan”，Expert

Panel Opinion on Interventions in Hepatocellular Carcinoma (EPOIHCC), The Grand Hotel Taipei, Taiwan, July 10, 2014.

8. Kudo M: Invited Lecture “Lessons from the TACE trials”, The 5th Asia-Pacific Primary Liver Cancer Expert Meeting (APPLE), The Grand Hotel, Taipei, Taiwan, July 12, 2014.

9. Kudo M: Invited Lecture “Surveillance, treatment and outcome of HCC in Japan”, ILCA Symposium 3 “Noevel opportunities for treatment in HCC”, The 8th Annual Conference, International Liver Cancer Association (ILCA), Hotel Granvia Kyoto, Japan, September 5-7, 2014.

10. Kudo M: Invited Lecture “Fusion imaging for treatment guidance of hepatic tumours”, The 11the Congress of the Asian Federation of Societies for Ultrasound and Biology (AFSUMB 2014), Kuala Lumpur, Malaysia, October 29-November 1, 2014.

11. Kudo M: Invited Lecture “Interventaional and contrast EUS for pancreatobiliary disease”, The 11the Congress of the Asian Federation of Societies for Ultrasound and Biology (AFSUMB 2014), Kuala Lumpur, Malaysia, October 29-November 1, 2014.

12. Kudo M: Invited Lecture “Molecular targeted therapy for HCC: Past, present and future perspective”, 24th World Congress of the International Association of Surgeons, Gastroenterologists and Oncologists (IASGO 2014), Vienna, Austria, December 5-7, 2014.

13. Kitano M: Invited Lecture “Introduction to the meeting”. The 2nd European Workshop on CH-EUS and EUS Image Enhancement Techniques, June 29-July 1, Imola, Italy.

14. Kitano M: Invited Lecture “CH-EUS: the invention of a new technique and how to get the best results out of it (setting the equipment, different presets, qualitative and quantitative techniques)”. The 2nd European Workshop on CH-EUS and EUS Image Enhancement Techniques, June 29-July 1, Imola, Italy.

15. Kitano M: Invited Lecture “Live EUS”, Third Session “Live EUS”. The 2nd European Workshop on CH-EUS and EUS Image Enhancement Techniques, June 29-July 1, Imola, Italy.

16. Kitano M: Invited Lecture “Innovative applications: prediction and evaluation of response to chemotherapy, vascular lesions, guidance for EUS interventions, and other”. The 2nd European Workshop on CH-EUS and EUS Image Enhancement

Techniques, June 29-July 1, Imola, Italy.

17. Kitano M: Best evidence-based techniques for performing EUS-guided FNA. 19th International Symposium on Endoscopic Ultrasonography (EUS2014), Chennai, India, September 18-20, 2014.

18. Larghi A, Kitano M, Deprez P: EUS-guided tissue acquisition. “Basic Training and Tutorials”, 19th International Symposium on Endoscopic Ultrasonography (EUS2014), Chennai, India, September 18-20, 2014.

19. Kitano M: How to manage mild dilation of pancreatic duct with elevated CA19-9. 19th EUS and 16th Early GI Cancer Conference of Taiwan, National Taiwan University College of Medicine, Taiwan, December 21, 2014.

20. Kitano M: Update of EUS elastography and contrast EUS. 19th EUS and 16th Early GI Cancer Conference of Taiwan, National Taiwan University College of Medicine, Taiwan, December 21, 2014.

Ⅴ. 招待講演・特別講演（国内）

1. 工藤正俊: 「肝血流動態・機能イメージ研究会 20 年の歩み」, 第 20 回肝血流動態・機能イメージ研究会, 平成 26 年 2 月 15 日-16 日, 大阪国際交流センター「大ホール」, 大阪.

2. 工藤正俊: シンポジウム「5. 肝細胞腺腫は悪性転化するか？ 2）臨床の立場より（文献的考察・アンケート・一般演題の結果を踏まえて」, シンポジウム 2「肝細胞腺腫の亜分類の新しい考え方」, 第 20 回肝血流動態・機能イメージ研究会, 平成 26 年 2 月 15 日-16 日, 大阪国際交流センター「大ホール」, 大阪.

3. 工藤正俊: シンポジウム「組織弾性評価手法の世界的動向と消化器領域への展開」, シンポジウム領域横断 2「組織弾性評価手法の現状と将来動向」, 日本超音波医学会第 87 回学術集会, 平成 26 年 5 月 9 日, パシフィコ横浜, 神奈川.

4. 工藤正俊: ランチョンセミナー3「肝線維化診断における Real-time Tissue Elastography の有用性」, 日本超音波医学会第 87 回学術集会, 平成 26 年 5 月 9 日-11 日, パシフィコ横浜, 神奈川.

5. 工藤正俊: ランチョンセミナー17「ソナゾイド造影超音波の新たな展開～肝癌スクリーニングと肉眼形態診断への応用～」, 日本超音波医学会第 87 回学術集会, 平成 26 年 5 月 9 日-11 日, パシフィコ横浜, 神奈川.

6. 工藤正俊: 特別講演「ソナゾイド造影超音波の新たな展開～肝癌スクリーニングと肉眼形態診断への応用～」, 北信消化器画像セミナー, 平成 26 年 5 月 12 日, ホテル国際 21, 長野.

7. 工藤正俊：特別講演「今後の展望」,第 50 回日本肝臓学会総会，平成 26 年 5 月 29 日，ホテルニューオータニ，東京.

8. 工藤正俊：総括発言「新規分子標的薬剤の動向と展望」，第 10 回肝がん分子標的治療研究会共催シンポジウム，平成 26 年 6 月 21 日，淡路夢舞台国際会議場，兵庫.

9. 工藤正俊：特別講演「肝細胞癌の分子標的治療：現状と今後の課題」，TACE Refractory Focus Expert Meeting，平成 26 年 8 月 16 日，JR クレメントホテル高松，香川.

10. 工藤正俊：招待講演「造影超音波の新しい展開：肝癌スクリーニングと肉眼形態診断への応用」，日本超音波医学会第 24 回九州地方会学術集会，平成 26 年 9 月 21 日，福岡国際会議場，福岡.

11. 工藤正俊：特別講演「Liver」，日本超音波医学会第 41 回関西地方会学術集会，平成 26 年 11 月 22 日，ホテルグランヴィア京都，京都.

12. 工藤正俊：特別講演「びまん性肝疾患診療における Real-time Tissue Elastography の役割」，日本超音波医学会第 41 回関西地方会学術集会，平成 26 年 11 月 22 日，ホテルグランヴィア京都，京都.

13. 工藤正俊：特別講演「肝癌に対する分子標的治療：現状と今後の展望」，第 1 回東北肝癌分子標的治療セミナー，平成 26 年 12 月 19 日，TKP 仙台カンファレンスセンター3F，仙台，宮城.

14. 上嶋一臣：教育講演「既存治療との組み合わせと今後の新薬開発状況について」．第 9 回日本肝がん分子標的治療研究会，平成 26 年 1 月 25 日，海運クラブ，東京.

15. 北野雅之：特別講演「膵疾患診断における超音波の役割～拾い上げから確定診断まで～」．第 177 回大阪腹部超音波研究会，平成 26 年 3 月 6 日，薬業年金会館，大阪.

16. 北野雅之：特別講演「切除不能膵癌に対するステント治療」．ボストン・サイエンティフィックジャパン株式会社宮崎テクノロジー＆教育センター（2014 BSJ Endoscopy Dealer Training），平成 26 年 4 月 18 日，インスティテュート宮崎，宮崎.

17. 北野雅之：ランチョンセミナー「EUS-FNA の臨床的意義と診断精度向上のための工夫-内視鏡医からのメッセージ-」，第 103 回日本病理学会総会，平成 26 年 4 月 24-26 日，広島国際会議場，広島.

18. 北野雅之：サテライトシンポジウム「EUS 画像診断の最先端」，サテライトシンポジウム 3「EUS 診断・治療 A to Z」，第 87 回日本消化器内視鏡学会総会，平成 26 年 5

月 16 日，福岡国際会議場，福岡.

19. 北野雅之：腹腔神経叢ブロック．第 1 回超音波内視鏡下穿刺術の手技標準化に関する研究会，平成 26 年 5 月 17 日，福岡国際会議場，福岡.

20. 松井繁長：教育講演「内視鏡的静脈瘤硬化療法における実際の手技」，第 23 回近畿食道・胃静脈瘤研究会，平成 26 年 6 月 14 日，大阪薬業年金会館，大阪.

21. 北野雅之：特別講演「日常診療で見落としやすい膵疾患」．第 4 回泉北消化器セミナー，平成 26 年 7 月 5 日，近畿大学医学部堺病院，大阪.

22. 南　康範：RFA. Debates session「大腸がん肝転移の治療戦略を如何に組み立てるか？」，第 14 回肝血流動態・機能イメージ研究会，平成 26 年 7 月 5 日，オーバルホール，大阪.

23. 北野雅之：特別講演「非切除悪性胆道ドレナージ術の変遷」．第 15 回関東胆・膵治療懇話会「Biliary Drainage Update」，平成 26 年 7 月 19 日，野村カンファレンスプラザ日本橋，東京.

23. 北野雅之：特別講演「“膵外分泌機能不全“の早期診断とは？」．リパクレオン発売 3 周年記念講演会，平成 26 年 7 月 26 日，グランドプリンスホテル新高輪，東京.

24. 北野雅之：特別講演「膵疾患診断における超音波の役割～拾い上げから確定診断まで～」．日本超音波医学会第 50 回中国地方会学術集会ランチョンセミナー2，平成 26 年 9 月 6 日，岡山コンベンションセンター，岡山.

25. 北野雅之：特別講演「EUS による胆膵疾患診療―基礎から最先端治療まで―」．第 5 回神奈川県胆膵内視鏡レクチャー，平成 26 年 9 月 12 日，崎陽軒本店，神奈川.

26. 松井繁長：特別講演「低用量アスピリンによる消化管粘膜傷害の現状と治療～ピロリ菌除菌も含めて～」，平成 26 年 9 月 13 日，橿原ロイヤルホテル，奈良.

27. 北野雅之：診断精度向上の工夫で見えてきたこと．ブレックファーストセミナー27「EUS-FNA 最前線」，第 22 回日本消化器関連学会週間 JDDW2014（第 88 回日本消化器内視鏡学会総会，第 56 回日本消化器病学会大会，第 18 回日本肝臓学会大会，第 12 回日本消化器外科学会大会，第 52 回日本消化器がん検診学会大会），平成 26 年 10 月 23-26 日，神戸国際展示場・ポートピアホテル・神戸国際会議場，神戸.

28. 北野雅之：胆膵超音波内視鏡の応用～造影 EUS から Therapeutic EUS まで～．第 2 回新潟胆膵内視鏡セミナー，平成 26 年 11 月 8 日，新潟大学医歯学総合病院，新潟.

29. 萩原　智：ダクラタスビル・アスナプレビル併用療法を用いた HCV の治療戦略．南大

阪 HCV 治療懇話会，平成 26 年 12 月 11 日，アゴーラ・リージェンシー堺，大阪.

30. 松井繁長：当科における H. pylori 除菌の現状．ヘリコバクター・ピロリ感染症の除菌療法を考える会，平成 26 年 3 月 6 日，ホテル・アゴーラリージェンシー堺，大阪.

31. 森　秀明，畠　二郎，樫田博史，関根智紀，西田　睦，西川かおり，長谷川雄一，藤井康友，本田伸行，宮本幸夫，山田博康：消化管診断基準小委員会からの報告．シンポジウム消化器 4「消化管超音波診断の進歩」，日本超音波医学会第 87 回学術集会，平成 26 年 5 月 9 日-11 日，パシフィコ横浜，神奈川.

32. 朝隈　豊，松井繁長，樫田博史：（追加発言 2）当院における食道 ESD のストラテジー，ビデオワークショップ 1「ESD の工夫―安全性と効率の両立を目指して」，日本消化器内視鏡学会近畿支部第 92 回支部例会，平成 26 年 6 月 21 日，大阪国際交流センター，大阪.

34. 汐見幹夫：関西地区でのアンケート報告からみた PEG の現況-平成 14 年と平成 25 年の比較-．第 19 回 PEG・在宅医療研究会学術集会，平成 26 年 9 月 13 日，ステーションコンファレンス東京，東京．2014　山田光成，松井繁長，樫田博史：緊急内視鏡検査における体制と問題点．ワークショップ 1「緊急内視鏡の現状とマネージメント」，日本消化器内視鏡学会近畿支部第 93 回支部例会，平成 26 年 11 月 15 日，大阪国際交流センター，大阪.

35. 北野雅之：胆道疾患に対する EUS 治療．Next TV Symposium 2014 EUS-応用編-，平成 26 年 12 月 2 日，近畿大学，大阪.

36. 櫻井俊治：肝発癌におけるストレス応答蛋白 Cirp の役割．第 14 回肝疾患フォーラム学術集会，平成 26 年 12 月 6 日，梅田スカイビルタワーウエスト 23 階，大阪.

VI. 学会発表（海外シンポジウム）

1. Kitano M, Sakamoto H, Kudo M: Predictive factors for pain relief after EUS-guided neurolysis in patietnts suffering from upper abdominal cancer pain. International Session (Symposium) 6 “EUS-guided therapy: current status and future directions”, Japan Digestive Disease Week 2014 (JDDW). Kobe, Japan, October 23-26, 2014.

2. Sakurai T, Kashida H, Kudo M: Involvement of stress response protein crip in refractory inflammatory bowel diseases and colitis-associated cancer. Symposium 1 “Cancer prevention and early diagnosis”, The 25th Annual Meeting of the Japanese Society for Gastroenterological Carcinogenesis, ホテル日航福岡，九州，November 13-14, 2014.

Ⅶ. 学会発表（海外一般演題）

1. Furuse J, Ye SL, Marrero J, Lencioni R, Venook A, Nakajima K, Kudo M: Final analysis of GIDEON (global investigation of therapeutic decisions in hepatocellular carcinoma and of its treatment with sorafenib): treatment practices, safety and outcomes by race. Asian Pacific Association for the Study of the Liver (APASL 2014), Brisbane, Australia, March 12-15, 2014.

2. Izumi N, Tateishi R, Seike M, Kudo M, Tamai H, Kawazoe S, Tanaka K, Kurokawa M, Osaki Y, Yamamoto K, Imawari M: Once-daily oral lusutrombopag, alternative to platelet transfusion in thrombocytopenic patients with chronic liver disease undergoing radiofrequency ablation: results from a phase 2B, randomized, double-blind study. 49th Annual Meeting of the European Association for the Study of the Liver (EASL), London, United Kingdom, April 9-13, 2014.

3. Bronowicki JP, Venook A, Kudo M, Marrero J, Ye SL, Nakajima K, Lencioni R: Final analysis of GIDEON (global investigation of therapeutic decisions in hepatocellular carcinoma [HCC] and of its treatment with sorafenib): factors influencing treatment duration and outcomes. 49th Annual Meeting of the European Association for the Study of the Liver (EASL), London, United Kingdom, April 9-13, 2014.

4. Bruix J, Finn RS, Kudo M, Llovet JM, Qin S, Le Berre MA, Wagner A, Cheng AL: Regorafenib in patients with hepatocellular carcinoma (HCC) progressing following sorafenib: an ongoing randomized, double-blind, phase III trial. American Society of Clinical Oncology (ASCO) 50th Annual Meeting, Chicago, USA, May 30-June 3, 2014.

5. Vergote I, Ball D, Kudo M, Sachdev P, Matijevic M, Kadowaki T, Funahashi Y, Flaherty K: Prognostic and predictive role of circulating angiopoietin-2 in multiple solid tumors: An analysis of approximately 500 patients treated with lenvatinib across tumor types. American Society of Clinical Oncology (ASCO) 50th Annual Meeting, Chicago, USA, May 30-June 3, 2014.

6. Finn RS, Cheng AL, Ikeda K, Kudo M, Tamai T, Dutcus C, Younger S, Han KH, Qin S, Raymond E: A multicenter, open-label, phase 3 trial to compare the efficacy and safety of Lenvatinib (E7080) versus Sorafenib in first-line treatment of patients with unresectable hepatocellular carcinoma. American Society of Clinical Oncology (ASCO) 50th Annual Meeting, Chicago, USA, May 30-June 3, 2014.

7. Kondo S, Ikeda M, Kudo M, Nadano S, Furuse J, Osaki Y, Kumada T, Ohkawa K, Mizokami M: Multicenter observational study of reactivation of hepatitis B virus caused by chemotherapy for solid tumors. American Society of Clinical Oncology (ASCO) 50th Annual Meeting, Chicago, USA, May 30-June 3, 2014.

8. Bruix J, Takayama T, Mazzaferro V, Chau GY, Yang J, Kudo M, Cai J, Poon RT, Han KH, Tak WY, Lee HC, Song T, Roayaie S, Bolondi L, Lee KS, Makuuchi M, Souza F, Le Berree MA, Meinhardt G, Llovet JM on behalf of the STORM Investigators: STORM: a phase III, randomized, double-blind, placebo-controlled trial of adjuvant sorafenib after resection or ablation to prevent recurrence of hepatocellular carcinoma. American Society of Clinical Oncology (ASCO) 50th Annual Meeting, Chicago, USA, May 30-June 3, 2014.

9. Peck-Radosavljevic M, Raoul JL, Lee HC, Kudo M, Nakajima K, Cheng AL, on behalf of the OPTIMIS Investigators: OPTIMIS: an International observational study to assess the use of sorafenib after transarterial chemoembolization in patients with hepatocellular carcinoma. American Society of Clinical Oncology (ASCO) 50th Annual Meeting, Chicago, USA, May 30-June 3, 2014.

10. Yen CJ, Daniele B, Kudo M, Merle P, Park JW, Ross P, Peron JM, Ebert O, Chan S, Poon TP, Colombo M, Okusaka T, Ryoo BY, Minguez B, Tanaka T, Ohtomo T, Rutman O, Chen YC, Lee R, Abou-Alfa GK: Randomized phase II trial of intravenous RO5137382/GC33 at 1600 mg every other week and placebo in previously treated patients with unresectable advanced hepatocellular carcinoma (HCC) (NCT01507168). American Society of Clinical Oncology (ASCO) 50th Annual Meeting, Chicago, USA, May 30-June 3, 2014.

11. Minami Y, Kudo M, Yagyu Y, Murakami T: Early response prediction of hepatocellular carcinoma to transcatheter therapies using intraprocedual plain cone-beam CT. Computer Assisted Radiology and Surgery (CARS 2014), 28th International Congress and Exhibition, Fukuoka, Japan, June 25-28, 2014.

12. Kamata K, Kitano M, Kudo M: Value of semi-annual follow-up of EUS in patients with IPMN. International Teleconference 2 “Intraductal papillary mucinous neoplasm of the pancreas: clinical experiences in Asian countries”, the 45th Annual Meeting of the Japan Pancreas Society, Kitakyushu International Conference Center, Japan, July 11-12, 2014.

13. Ye SL, Lencioni R, Marrero JA, Venook AP, Nakajima K, Kudo M: Treatment patterns in >3000 sorafenib-treated patients: final analysis of GIDEON (Global investigation of therapeutic decisions in hepatocellular carcinoma and of its treatment with sorafenib). The 5th Asia-Pacific Primary Liver Cancer Expert Meeting (APPLE), Taipei, Taiwan, July 11-13, 2014.

14. Kudo M, Yen CJ, Daniele B, Merle P, Park JW, Ross P, Peron JM, Ebert O, Chan S, Poon TP, Colombo M, Okusaka T, Ryoo BY, Minguez B, Tanaka T, Ohtomo T, Rutman O, Chen YC, Lee R, Abou-Alfa GK: Randomized phase II trial of intravenous RO5137382/GC33 at 1600 mg every other week and placebo in previously treated patients with unresectable advanced hepatocellular carcinoma (HCC) (NCT01507168). 8th Annual Conference, International Liver Cancer Association (ILCA 2014), Hotel Granvia Kyoto, Japan, September 5-7, 2014.

15. Kudo M, Marrero J, Lencioni R, Nakajima K, Ye SL: Tumor response to transarterial chemoembolization in unresectable hepatocellular carcinoma patients in clinical practice: findings from the GIDEON database. 8th Annual Conference, International Liver Cancer Association (ILCA 2014), Hotel Granvia Kyoto, Japan, September 5-7, 2014.

16. Roayaie S, Jibara G, Tabrizian P, Park JW, Yang J, Yan L, Han G, Izzo F, Chen M, Blanc JF, Johnson P, Kudo M, Roberts LR, Sherman M: How is BCLC stage C HCC treated in real-word practice and what outcomes are obtained? Answers from the Bridge database. 8th Annual Conference, International Liver Cancer Association (ILCA 2014), Hotel Granvia Kyoto, Japan, September 5-7, 2014.

17. Kudo M, Ueshima K, Osaki Y, Hirooka M, Imai Y, Aso K, Numata K, Ichinose M, Kumada T, Izumi N, Sumino Y, Akazawa K: B-mode ultrasonography versus contrast-enhanced ultrasonography for surveillance of hepatocellular carcinoma: a prospective multicenter randomized controlled trial (Nct01507168). 8th Annual Conference, International Liver Cancer Association (ILCA 2014), Hotel Granvia Kyoto, Japan, September 5-7, 2014.

18. Minami Y, Murakami T, Kudo M: Early response prediction of hepatocellular carcinoma to conventional transcatheter chemoembolization using intraprocedual plain cone-beam CT. 8th Annual Conference, International Liver Cancer Association (ILCA 2014), Hotel Granvia Kyoto, Japan, September 5-7, 2014.

19. Llovet JM, Takayama T, Mazzaferro V, Chau GY, Yang J, Kudo M, Cai J, Poon RT, Han KH, Tak WY, Lee HC, Song T, Roaayaie S, Bolondi L, Lee KS, Makuuchi M, Souza F, Le Berre MA, Meinhardt G, Bruix J, on behalf of the STORM investigators: STORM: A phase III, randomized, double-blind, placebo-controlled trial of adjuvant sorafenib after resection or ablation to prevent recurrence of hepatocellular carcinoma. 8th Annual Conference, International Liver Cancer Association (ILCA 2014), Hotel Granvia Kyoto, Japan, September 5-7, 2014.

20. Sakamoto Y, Kokudo N, Matsuyama Y, Izumi N, Ichida T, Ku Y, Kudo M, Sakamoto M, Takayama T, Nakashima O, Matsui O: Proposals for improvement of the AJCC/UICC and Japanese staging systems for intrahepatic cholangiocarcinoma in review of the Japanese nationwide database. 8th Annual Conference, International Liver Cancer Association (ILCA 2014), Hotel Granvia Kyoto, September 5-7, 2014.

21. Ogawa C, Kudo M: Newly simulated virtual ultrasound sonography software before RFA. 8th Annual Conference, International Liver Cancer Association (ILCA 2014), Hotel Granvia Kyoto, September 5-7, 2014.

22. Sakurai T, Kudo M, Nishida N, Fujita J, Kashida H: Stress response protein Cirp links inflammation and tumorigenesis in colitis-associated cancer. The 73rd Annual Meeting of the Japanese Cancer Association, Pacifico Yokohama, September 25-27, 2014.

23. Kang YK, Yau T, Park JW, Boucher E, Lim HY, Poon RTP, Lee TY, Obi S, Chan SL, Qin SK, Kim RD, Tang J, Valota O, Chakrabarti D, Kudo M: Randomised study of axitinib (Axi) plus best supportive care (BSC) versus placebo (Pbo) plus BSC in patients with advanced hepatocellular carcinoma (HCC) following prior antiangiogenic therapy. European Society for Medical Oncology Congress (ESMO 2014), Madrid, Spain, September 26-30, 2014.

24. Raoul JL, Peck-Radosavljevic M, Lee HC, Kudo M, Nakajima K, Cheng AL, on behalf of the OPTIMIS investigators: An International observational study to assess the use of sorafenib following TACE: design and rationale for OPTIMIS. European Society for Medical Oncology Congress (ESMO 2014), Madrid, Spain, September 26-30, 2014.

25. Peck-Radosavljevic M, Raoul JL, Lee HC, Kudo M, Nakajima K, Cheng AL, on behalf of the OPTIMIS Investigators: OPTIMIS: an International observational study to

assess the use of sorafenib after transarterial chemoembolization in patients with hepatocellular carcinoma. European Society for Medical Oncology Congress (ESMO 2014), Madrid, Spain, September 26-30, 2014.

26. Zhu A, Ryoo BY, Yen CJ, Kudo M, Poon R, Pastorelli D, Blanc JF, Chung H, Baron A, Pfiffer T, Okusaka T, Kubackova K, Trojan J, Sastre J, Chau I, Chang SC, Abada P, Yang L, Schwartz J, Park J: Ramucirumab (RAM; IMC-1121B) as second-line treatment in patients with advanced hepatocellular carcinoma following first-line therapy with sorafenib: results from the randomized phase III REACH study. European Society for Medical Oncology Congress (ESMO 2014), Madrid, Spain, September 26-30, 2014.

27. Kitai S, Kudo M, Nishida N, Izumi N, Sakamoto M, Matsuyama Y, Ichida T, Nakashima O, Matsui O, Ku Y, Kokudo N, Makuuchi M, and Liver Cancer Study Group of Japan: Validation of staging systems for hepatocellular carcinoma: a comparison of the BM-JIS score, the JIS score and the BCLC staging. United European Gastroenterology Week (UEGW 2014), Vienna, Austria, October 18-22, 2014.

28. Nebiki H, Yanagisawa A, Yasukawa S, Kamata K, Kudo M, Ogura T, Higuchi K, Fukutake N, Ashida R, Yamasaki T, Hirose S, Hoki N, Asada M, Yazumi S, Takaoka M, Okazaki K, Matsuda F, Okabe Y, Kitano M: Prospective multicenter randomized controlled trial of histological diagnostic yield comparing 25G EUG-FNA needles with and without a core trap in solid pancreatic masses: analysis of factors affecting tissue acquisition and diagnostic accuracy. United European Gastroenterology Week (UEGW 2014), Vienna, Austria, October 18-22, 2014.

29. Roayaie S, Jibara G, Tabrizian P, Park JW, Yang J, Yan L, Han G, Izzo F, Chen M, Blanc JF, Johnson P, Kudo M, Roberts LR, Sherman M: How is BCLC stage C HCC treated in real-word practice and what outcomes are obtained? 65th Annual Meeting, American Association for the Study of Liver Diseases (AASLD2014), Boston, USA, November 7-11, 2014.

30. Nishida N, Yada N, Chishina H, Arizumi T, Takita M, Kitai S, Inoue T, Hagiwara S, Minami Y, Ueshima K, Sakurai T, Kudo M: Pathological feature, oxidative DNA damage and epigenetic alteration of tumor suppressor genes in nonalcoholic fatty liver disease. 65th Annual Meeting, American Association for the Study of Liver Diseases (AASLD2014), Boston, USA, November 7-11, 2014.

31. Minami Y, Kudo M: Early response prediction of hepatocellular carcinoma to conventional transcatheter chemoembolization using intraprocedual plain cone-beam CT. 65th Annual Meeting, American Association for the Study of Liver Diseases (AASLD2014), Boston, USA, November 7-11, 2014.

32. Adachi T, Tanaka R, Yamada M, Takayama M, Mine H, Nagai T, Kawasaki M, Asakuma Y, Okazaki Y, Komeda Y, Sakurai T, Matsui S, Kashida H, Kudo M: The usefulness of single-balloon endoscopy for the small bowel lesions. Asian Pacific Digetive Week (APDW 2014), Bali, Indonesia, November 22-25, 2014.

33. Adachi T, Tanaka R, Yamada M, Takayama M, Mine H, Nagai T, Kawasaki M, Asakuma Y, Okazaki Y, Komeda Y, Sakurai T, Matsui S, Kashida H, Kudo M: Comparison of Japanese primary and secondary regimen of Helicobacter pylori eradication. Asian Pacific Digetive Week (APDW 2014), Bali, Indonesia, November 22-25, 2014.

34. Kashida H, Adachi T, Komeda Y, Sakurai T, Asakuma Y, Takayama M, Mine H, Kudo M: Colorectal endoscopic submucosal dissection is useful and safe. Asian Pacific Digetive Week (APDW 2014), Bali, Indonesia, November 22-25, 2014.

35. Matsui S, Kashida H, Okamoto K, Asakuma Y, Sakurai T, Kudo M: Two cases of gastric amyloidosis. Asian Pacific Digetive Week (APDW 2014), Bali, Indonesia, November 22-25, 2014.

36. Matsui S, Kashida H, Kawasaki M, Asakuma Y, Sakurai T, Kudo M: The clinical characteristics and treatment of eosinophilic esophagitis. Asian Pacific Digetive Week (APDW 2014), Bali, Indonesia, November 22-25, 2014.

37. Nagai T, Tanaka R, Yamada M, Adachi T, Takayama M, Mine H, Okazaki Y, Komeda Y, Asakuma Y, Sakurai T, Matsui S, Kashida H, Kudo M: Small-intestinal mucosal injury induced by non-steroidal anti-inflammatory drugs or antiplatelet agents in our hospital. Asian Pacific Digetive Week (APDW 2014), Bali, Indonesia, November 22-25, 2014.

38. Yamada M, Kashida H, Tanaka R, Adachi T, Mine H, Takayama M, Okazaki Y, Nagata Y, Nagai T, Kawasaki M, Komeda N, Asakuma Y, Sakurai T, Matsui S, Kudo M: Endoscopic resection for rectal nets (neuroendocrine tumors): EMR-C (EMR using a cap), EMR-L (EMR with a ligation device), or conventional EMR. Asian Pacific Digetive Week (APDW 2014), Bali, Indonesia, November 22-25, 2014.

Ⅷ. 学会発表（国内シンポジウム・パネルディスカッション・ワークショップ）

1. 坂本洋城，北野雅之，工藤正俊：癌性疼痛に対するEUS下腹腔内神経叢融解術の有用性とその適応．シンポジウム9「膵胆道疾患におけるInterventional EUSの有用性と問題点」，第100回日本消化器病学会総会，平成26年4月23日-26日，東京国際フォーラム，東京．

2. 門阪薫平，北野雅之，工藤正俊：機能性ディスペプシアと早期慢性膵炎との関係性について．パネルディスカッション4「FDの亜分類と治療選択」，第100回日本消化器病学会総会，平成26年4月23日-26日，東京国際フォーラム，東京．

3. 鎌田　研，北野雅之，工藤正俊：分枝型IPMNの経過観察例からみた2012年国際診療ガイドラインの妥当性の検証．パネルディスカッション11「IPMNの経過観察，治療のタイミングと予後」，第100回日本消化器病学会総会，平成26年4月23日-26日，東京国際フォーラム，東京．

4. 坂本洋城，北野雅之，工藤正俊：EUS下腹腔内神経叢融解術の偶発症とその対策．パネルディスカッション3「胆膵インターベンショナルEUSの偶発症とその対策」，第87回日本消化器内視鏡学会総会，平成26年5月15日-17日，福岡国際会議場，福岡．

5. 今井　元，北野雅之，工藤正俊：EUSガイド下胆道ドレナージ術におけるコツとトラブルシューティング．パネルディスカッション3「胆膵インターベンショナルEUSの偶発症とその対策」，第87回日本消化器内視鏡学会総会，平成26年5月15日-17日，福岡国際会議場，福岡．

6. 坂本洋城，北野雅之，工藤正俊：当院におけるEUS-FNAのラーニングカーブについての検討：EUS-FNAの診断率．ワークショップ8「胆膵内視鏡における質の高い技術習得を目指した指導法の工夫」，第87回日本消化器内視鏡学会総会，平成26年5月15日-17日，福岡国際会議場，福岡．

7. 山雄健太郎，北野雅之，工藤正俊：悪性胃十二指腸狭窄に対する治療戦略～胆道狭窄合併例に対するEUS下胆道ドレナージ術も含めて～，ワークショップ16「消化管狭窄の内視鏡治療上部」，第87回日本消化器内視鏡学会総会，平成26年5月15日-17日，福岡国際会議場，福岡．

8. 鎌田　研，北野雅之，工藤正俊：EUSを主としたIPMNの診断および経過観察の成績～IPMN国際診療ガイドライン2012年度版の妥当性の検証～．シンポジウム6「分枝型膵IPMNの診断・悪性度の評価における内視鏡の役割」，第87回日本消化器内視鏡学会総会，平成26年5月15日-17日，福岡国際会議場，福岡．

9. 矢田典久，工藤正俊：超音波エラストグラフィによる肝線維化・炎症の評価．ワークショップ8「肝臓病理に画像診断はどこまで迫れたか」，第50回日本肝臓学会総会，平成26年5月29-30日，ホテルニューオータニ，東京．

10. 南　康範，村上卓道，工藤正俊：plain cone-beam CTによる肝動脈塞栓術の定量的治療効果予測．ワークショップ13「肝癌に対する肝動脈塞栓療法の新展開」，第50回日本肝臓学会総会，平成26年5月29-30日，ホテルニューオータニ，東京．

11. 兵頭朋子，矢田典久，前西　修，工藤正幸，朝戸信行，柳生行伸，鶴崎正勝，松木充，足利竜一朗，石井一成，工藤正俊，村上卓道：Dual-energy CT を用いた肝脂肪定量．パネルディスカッション1「肝画像診断のイノベーション」，第50回日本肝癌研究会，平成26年6月5日-6日，国立京都国際会館，京都．

12. 萩原　智，西田直生志，工藤正俊：ヒト肝発癌における酸化ストレスとエピゲノム変異の関連．パネルディスカッション2「ゲノム・エピゲノム解析に基づく肝癌診療の将来展望」，第50回日本肝癌研究会，平成26年6月5日-6日，国立京都国際会館，京都．

13. 有住忠晃，上嶋一臣，工藤正俊：進行肝細胞癌に対するソラフェニブ+TACE 併用療法．パネルディスカッション3「肝癌における分子標的治療の近未来展望」，第50回日本肝癌研究会，平成26年6月5日-6日，国立京都国際会館，京都．

14. 清水　怜，池田公史，森本　学，加藤弥菜，河田則文，工藤正俊，中森正二，金子周一，杉本理恵，古瀬純司，奥坂拓志：進行肝細胞癌を対象としたソラフェニブとシスプラチン肝動注の併用療法．パネルディスカッション3「肝癌における分子標的治療の近未来展望」，第50回日本肝癌研究会，平成26年6月5日-6日，国立京都国際会館，京都．

15. 北井　聡，工藤正俊，西田直生志，泉　並木，坂元亨宇，松山　裕，市田隆文，中島収，松井　修，具　英成，國土典宏，幕内雅敏：肝細胞癌(HCC)合併の非代償性肝硬変患者に対する局所治療の有用性についての検討．ワークショップ1「Child-Pugh C 肝癌に対する治療」，第50回日本肝癌研究会，平成26年6月5日-6日，国立京都国際会館，京都．

16. 上嶋一臣，有住忠晃，工藤正俊：ソラフェニブ開始後3年以上の長期生存例の臨床的特徴に関する検討．ワークショップ4「進行肝細胞癌に対する分子標的治療開始後の長期生存例（3年以上)」，第50回日本肝癌研究会，平成26年6月5日-6日，国立京都国際会館，京都．

17. 阪本良弘，國土典宏，松山　裕，泉　並木，市田隆文，具　英成，工藤正俊，坂元亨宇，高山忠利，中島　収，松井　修：全国原発性肝癌追跡調査データからみた第5版取扱規約における肝内胆管癌の病期分類の問題点について．ワークショップ5「肝内胆管癌に対する治療戦略」，第50回日本肝癌研究会，平成26年6月5日-6日，国立京都国際会館，京都．

18. 門阪薫平，北野雅之，工藤正俊：当院における EUS 下胆道ドレナージの工夫と成績．ビデオワークショップ2「閉塞性黄疸の治療戦略」，日本消化器内視鏡学会近畿支部第92回支部例会，平成26年6月21日，大阪国際交流センター，大阪．

19. 足立哲平，樫田博史，工藤正俊：大腸 ESD 後潰瘍の縫縮における小切開法の導入，ビデオワークショップ1「ESD の工夫―安全性と効率の両立を目指して」，日本消化器内視鏡学会近畿支部第92回支部例会，平成26年6月21日，大阪国際交流センター，大阪

20. 高山政樹，松井繁長，工藤正俊：当院で内視鏡治療を施行した表在型バレット食道腺癌の検討．シンポジウム「GERD～バレット食道癌の現状」，日本消化器内視鏡学会近畿支部第92回支部例会，平成26年6月21日，大阪国際交流センター，大阪．

21. 小川　力，荒澤壮一，柴峠光成，馬場伸介，妹尾知典，永野拓也，高口浩一，谷　丈二，三好久昭，米山弘人，正木　勉，守屋昭男，安東正晴，出口章広，國土泰孝，工藤正俊：香川県下におけるソラフェニブの使用経験～開始容量，肝機能，副作用の検討～．ワークショップ「分子標的薬に関する多施設共同研究から得られた知見」，第10

回日本肝がん分子標的治療研究会，平成26年6月21日，淡路夢舞台国際会議場，兵庫.

22. 坂本洋城，北野雅之，工藤正俊：非切除膵癌の癌性疼痛に対するEUS下腹腔内神経叢融解術の治療戦略．シンポジウム2「膵癌に対する新たな治療戦略-非切除膵癌」，第45回日本膵臓学会大会，平成26年7月11-12日，北九州国際会議場，北九州.

23. 今井　元，北野雅之，工藤正俊：膵神経内分泌腫瘍に対するEUSの有用性の検討．パネルディスカッション1「PNET診療ガイドラインをめぐって」，第45回日本膵臓学会大会，平成26年7月11-12日，北九州国際会議場，北九州.

24. 門阪薫平，北野雅之，工藤正俊：早期慢性膵炎画像所見と臨床症状との関係．ワークショップ1「早期慢性膵炎の現状」，第45回日本膵臓学会大会，平成26年7月11-12日，北九州国際会議場，北九州.

25. 宮田　剛，北野雅之，工藤正俊，竹山宜典：当院におけるStage 0/I膵癌の特徴～膵癌早期診断ストラテジーの標準化にむけて～，パネルディスカッション2「膵癌早期診断を目指して」，第45回日本膵臓学会大会，平成26年7月11-12日，北九州国際会議場，北九州.

26. 山雄健太郎，北野雅之，工藤正俊，竹山宜典：膵液瘻に対するEUS下ドレナージ術の有用性．ミニシンポジウム3「膵空腸吻合の工夫と術後管理」，第45回日本膵臓学会大会，平成26年7月11-12日，北九州国際会議場，北九州.

27. 小川　力，荒澤壮一，出田雅子，柴峠光成，工藤正俊：VINCENTの仮想超音波とAWを併用した経皮的RFAのシミュレーション．シンポジウム2「経皮的治療もしくはInterventional Radiologyにおけるシミュレーション・ナビゲーション技術の最近の工夫」，第9回肝癌治療シミュレーション研究会，平成26年9月27日，大阪国際会議場，大阪.

28. 永井知行，樫田博史，工藤正俊：当院におけるNSAIDs/LDAによる小腸粘膜傷害の現況．シンポジウム1「NSAIDs/LDAによる薬剤性消化管障害」，日本消化器病学会近畿支部第101回例会，平成26年10月4日，大阪国際交流センター，大阪.

29. 今井　元，北野雅之，工藤正俊：EUS下胆嚢ドレナージ術の有用性．ワークショップ2「肝胆膵疾患の診断と治療の進歩」，日本消化器病学会近畿支部第101回例会，平成26年10月4日，大阪国際交流センター，大阪.

30. 田中梨絵，櫻井俊治，樫田博史，工藤正俊：潰瘍性大腸炎における腸管感染症の合併．ワークショップ3「急性消化管感染症の臨床」，日本消化器病学会近畿支部第101回例会，平成26年10月4日，大阪国際交流センター，大阪.

31. 米田頼晃，樫田博史，櫻井俊治，工藤正俊：大腸表在癌・腺腫に対する大腸ESDの現況について．ワークショップ1「消化管表在癌に対する内視鏡的治療の現況と位置づけ」，日本消化器病学会近畿支部第101回例会，平成26年10月4日，大阪国際交流センター，大阪.

32. 大本俊介，北野雅之，工藤正俊：急性膵炎の病態把握におけるプロカルシトニンの有用性について．シンポジウム2「重症急性膵炎の病態と有効な初期治療をめざして」，第22回日本消化器関連学会週間JDDW2014（第88回日本消化器内視鏡学会総会，第56回日本消化器病学会大会，第18回日本肝臓学会大会，第12回日本消化器外科学会大会，第52回日本消化器がん検診学会大会），平成26年10月23-26日，神戸国際展示場・ポートピアホテル・神戸国際会議場，兵庫.

33. 西田直生志，工藤正俊：NBNC 肝癌の背景肝におけるメチル化プロファイルと加齢および糖尿病の影響．シンポジウム 14「NBNC 肝がんの諸問題」，第 22 回日本消化器関連学会週間 JDDW2014（第 88 回日本消化器内視鏡学会総会，第 56 回日本消化器病学会大会，第 18 回日本肝臓学会大会，第 12 回日本消化器外科学会大会，第 52 回日本消化器がん検診学会大会），平成 26 年 10 月 23-26 日，神戸国際展示場・ポートピアホテル・神戸国際会議場，兵庫．

34. 櫻井俊治，樫田博史，工藤正俊：Colitc cancer におけるストレス応答蛋白の役割．パネルディスカッション 5「消化管とがん幹細胞」，第 22 回日本消化器関連学会週間 JDDW2014（第 88 回日本消化器内視鏡学会総会，第 56 回日本消化器病学会大会，第 18 回日本肝臓学会大会，第 12 回日本消化器外科学会大会，第 52 回日本消化器がん検診学会大会），平成 26 年 10 月 23-26 日，神戸国際展示場・ポートピアホテル・神戸国際会議場，兵庫．

35. 矢田典久，河田則文，工藤正俊：背景肝による Real-time Tissue Elastography 画像の違い-HBV と HCV との比較-．パネルディスカッション 8「画像診断を駆使した肝疾患治療の最前線」，第 22 回日本消化器関連学会週間 JDDW2014（第 88 回日本消化器内視鏡学会総会，第 56 回日本消化器病学会大会，第 18 回日本肝臓学会大会，第 12 回日本消化器外科学会大会，第 52 回日本消化器がん検診学会大会），平成 26 年 10 月 23-26 日，神戸国際展示場・ポートピアホテル・神戸国際会議場，兵庫．

36. 今井　元，北野雅之，工藤正俊：EUS ガイド下胆道ドレナージ術における金属ステントの有用性．パネルディスカッション 17「悪性消化管・胆管閉塞に対する内視鏡的金属ステント治療の進歩」，第 22 回日本消化器関連学会週間 JDDW2014（第 88 回日本消化器内視鏡学会総会，第 56 回日本消化器病学会大会，第 18 回日本肝臓学会大会，第 12 回日本消化器外科学会大会，第 52 回日本消化器がん検診学会大会），平成 26 年 10 月 23-26 日，神戸国際展示場・ポートピアホテル・神戸国際会議場，兵庫．

37. 櫻井俊治，足立哲平，工藤正俊：腸粘膜防御機構におけるストレス応答蛋白の役割．ワークショップ 1「腸粘膜防御機構の維持と再生をめざして」，第 22 回日本消化器関連学会週間 JDDW2014(第 88 回日本消化器内視鏡学会総会，第 56 回日本消化器病学会大会，第 18 回日本肝臓学会大会，第 12 回日本消化器外科学会大会，第 52 回日本消化器がん検診学会大会），平成 26 年 10 月 23-26 日，神戸国際展示場・ポートピアホテル・神戸国際会議場，兵庫．

38. 櫻井俊治，樫田博史，工藤正俊：ピロリ菌感染に対する胃粘膜防御機構．ワークショップ 4「胃/十二指腸粘膜防御とその破綻-revisited」，第 22 回日本消化器関連学会週間 JDDW2014（第 88 回日本消化器内視鏡学会総会，第 56 回日本消化器病学会大会，第 18 回日本肝臓学会大会，第 12 回日本消化器外科学会大会，第 52 回日本消化器がん検診学会大会），平成 26 年 10 月 23-26 日，神戸国際展示場・ポートピアホテル・神戸国際会議場，兵庫．

39. 山雄健太郎，北野雅之，工藤正俊：胆膵良性疾患の救命救急における EUS 下ドレナージ術の位置づけ．ワークショップ 13「Life saving endoscopy」，第 22 回日本消化器関連学会週間 JDDW2014(第 88 回日本消化器内視鏡学会総会，第 56 回日本消化器病学会大会，第 18 回日本肝臓学会大会，第 12 回日本消化器外科学会大会，第 52 回日本消化器がん検診学会大会），平成 26 年 10 月 23-26 日，神戸国際展示場・ポートピアホテル・神戸国際会議場，兵庫．

40. 門阪薫平，北野雅之，工藤正俊：早期慢性膵炎における EUS 画像所見と臨床的意義の検討．ワークショップ 14「慢性膵炎とその進展予防」，第 22 回日本消化器関連学会週間

JDDW2014（第 88 回日本消化器内視鏡学会総会，第 56 回日本消化器病学会大会，第 18 回日本肝臓学会大会，第 12 回日本消化器外科学会大会，第 52 回日本消化器がん検診学会大会），平成 26 年 10 月 23-26 日，神戸国際展示場・ポートピアホテル・神戸国際会議場，兵庫.

41. 山雄健太郎，北野雅之，工藤正俊：経乳頭処置困難総胆管結石に対する rendezvous 法の手技と成績．ワークショップ 21「胆管結石治療困難例への戦略《ビデオ》」，第 22 回日本消化器関連学会週間 JDDW2014（第 88 回日本消化器内視鏡学会総会，第 56 回日本消化器病学会大会，第 18 回日本肝臓学会大会，第 12 回日本消化器外科学会大会，第 52 回日本消化器がん検診学会大会），平成 26 年 10 月 23-26 日，神戸国際展示場・ポートピアホテル・神戸国際会議場，兵庫.

42. 宮田　剛，北野雅之，工藤正俊：腫瘍径 1cm 以内の膵癌の特徴と診断ストラテジー．ワークショップ 15「微小膵癌発見のための検査・診断法」，第 22 回日本消化器関連学会週間 JDDW2014（第 88 回日本消化器内視鏡学会総会，第 56 回日本消化器病学会大会，第 18 回日本肝臓学会大会，第 12 回日本消化器外科学会大会，第 52 回日本消化器がん検診学会大会），平成 26 年 10 月 23-26 日，神戸国際展示場・ポートピアホテル・神戸国際会議場，兵庫.

43. 足立哲平，樫田博史，工藤正俊：大腸 ESD 施行時の出血のリスクについての検討．パネルディスカッション 1「内視鏡治療における偶発症の予防と対処法」，日本消化器内視鏡学会近畿支部第 93 回支部例会，平成 26 年 11 月 15 日，大阪国際交流センター，大阪.

44. 山雄健太郎，北野雅之，工藤正俊：当院における EUS-BD の成績．パネルディスカッション 2「胆膵疾患における診断と治療」，日本消化器内視鏡学会近畿支部第 93 回支部例会，平成 26 年 11 月 15 日，大阪国際交流センター，大阪.

45. 岡﨑能久，樫田博史，工藤正俊：小腸内視鏡から見た overtOGIB の特徴．ワークショップ 2「カプセル内視鏡とバルーン内視鏡の現状と展望」，日本消化器内視鏡学会近畿支部第 93 回支部例会，平成 26 年 11 月 15 日，大阪国際交流センター，大阪.

46. 門阪薫平，北野雅之，工藤正俊：高齢者または手術不能の急性胆嚢炎に対する EUS 下胆嚢ドレナージ術．ワークショップ 1「緊急内視鏡の現状とマネージメント」，日本消化器内視鏡学会近畿支部第 93 回支部例会，平成 26 年 11 月 15 日，大阪国際交流センター，大阪.

Ⅸ. 学会発表（国内一般演題）

1. 有住忠晃，上嶋一臣，千品寛和，田北雅弘，北井　聡，井上達夫，矢田典久，萩原智，南　康範，櫻井俊治，西田直生志，工藤正俊：TACE 不応の進行肝細胞癌に対するソラフェニブ開始時期の検討．第 9 回日本肝がん分子標的治療研究会，平成 26 年 1 月 25 日，海運クラブ，東京.

2. 峯　宏昌，足立哲平，高山政樹，永井知行，川崎正憲，朝隈　豊，松井繁長，樫田博史，工藤正俊：NST 介入患者における胃瘻と半固形栄養剤の有用性について．第 10 回日本消化管学会総会学術集会，平成 26 年 2 月 14 日-15 日，ホテル福島グリーンパレス，福島.

3. 高山政樹，足立哲平，峯　宏昌，永井知行，川崎正憲，朝隈　豊，櫻井俊治，　松井繁長，樫田博史，工藤正俊：当院において OGIB と診断され、シングルバルーン小腸内視鏡検査を施工した高齢者症例の臨床的検討．第 10 回日本消化管学会総会学術集会，平成 26 年 2 月 14 日-15 日，ホテル福島グリーンパレス，福島.

4. 岡本寿樹，高山政樹，峯　宏昌，山田光成，足立哲平，永井知行，川崎正憲，朝隈豊，櫻井俊治，松井繁長，樫田博史，工藤正俊：興味のある経過を示した胃アミロイドーシスの1例．第10回日本消化管学会総会学術集会，平成26年2月14日-15日，クラッセふくしま，福島．

5. 朝戸信行，鶴崎正勝，兵頭朋子，工藤正幸，福井秀行，任　誠雲，柳生行伸，岡田真広，今岡いずみ，松木　充，足利竜一朗，矢田典久，前西　修，工藤正俊：Dual energy CTを用いたdynamicCTによる肝線維化の評価．第20回肝血流動態・機能イメージ研究会，平成26年2月15日-16日，大阪国際交流センター「大ホール」，大阪．

6. 南　康範，南　知宏，有住忠晃，田北雅弘，北井　聡，矢田典久，井上達夫，萩原智，上嶋一臣，西田直生志，工藤正俊，柳生行伸，村上卓道：plain cone-beam CTによる肝動脈塞栓術の定量的治療効果予測．第20回肝血流動態・機能イメージ研究会，平成26年2月15日-16日，大阪国際交流センター「大ホール」，大阪．

7. 井上達夫，兵頭朋子，千品寛和，有住忠晃，田北雅弘，北井　聡，矢田典久，萩原智，上嶋一臣，西田直生志，村上卓道，工藤正俊：EOB-MRIと造影超音波検査により乏血性結節の多血化因子の検討．第20回肝血流動態・機能イメージ研究会，平成26年2月15日-16日，大阪国際交流センター「大ホール」，大阪．

8. 出田雅子，小川　力，野田晃世，森岡弓子，荒澤壮一，宮本由貴子，石川哲朗，松中寿浩，玉置敬之，柴峠光成，石川順英，廣瀬哲朗，島田俊秀，荻野哲朗，工藤正俊：肝細胞癌との鑑別が困難であった肝内副副腎腺種の一例．第20回肝血流動態・機能イメージ研究会，平成26年2月15日-16日，大阪国際交流センター「大ホール」，大阪．

9. 小川　力，森岡弓子，野田晃世，荒澤壮一，出田雅子，宮本由貴子，石川哲朗，松中寿浩，玉置敬之，柴峠光成，嶋田俊秀，荻野哲朗，隈部　力，中島　収，工藤正俊：病理学的にはFNH of FHN like noduleが疑われたが肝静脈、門脈の腫瘍内の貫通を認めた肝腫瘍の1例．第20回肝血流動態・機能イメージ研究会，平成26年2月15日-16日，大阪国際交流センター「大ホール」，大阪．

10. 伊藤貴嶺，北野雅之，門阪薫平，大本俊介，鎌田　研，宮田　剛，山雄健太郎，今井元，坂本洋城，工藤正俊：分岐型IPMNに対する造影EUSのフォローによりIPMN由来癌を早期診断した1例．日本消化器病学会近畿支部第100回例会，平成26年2月22日，大阪国際交流センター，大阪．

11. 南　知宏，南　康範，千品寛和，有住忠晃，田北雅弘，北井　聡，矢田典久，井上達夫，　萩原　智，上嶋一臣，西田直生志，工藤正俊：TS-1+ Interferon 併用療法が奏効した巨大な肝細胞癌の一例．日本消化器病学会近畿支部第100回例会，平成26年2月22日，大阪国際交流センター，大阪．

12. 門阪薫平，北野雅之，大本俊介，鎌田　研，宮田　剛，山雄健太郎，今井　元，坂本洋城，工藤正俊：機能性ディスペプシアと早期慢性膵炎の鑑別について．日本消化器病学会近畿支部第100回例会，平成26年2月22日，大阪国際交流センター，大阪．

13. 岡元寿樹，永井知行，山田光成，足立哲平，高山政樹，峯　宏昌，川崎正憲，朝隈豊，櫻井俊治，松井繁長，樫田博史，工藤正俊，田中裕美子，石川　原，竹山宜典：診断に難渋した十二指腸隆起性潰瘍性病変の一例．日本消化器病学会近畿支部第100回例会，平成26年2月22日，大阪国際交流センター，大阪．

14. 大本俊介，北野雅之，門阪薫平，宮田　剛，鎌田　研，山雄健太郎，今井　元，坂本

洋城，工藤正俊：Time intensity curve（TIC）を用いた造影ハーモニック EUS による膵腫瘍血流評価の検討．日本消化器病学会近畿支部第100回例会，平成26年2月22日，大阪国際交流センター，大阪．

15. 千品寛和，峯　宏昌，南　知宏，田中梨絵，山田光成，足立哲平，高山政樹，永井知行，川崎正憲，朝隈　豊，櫻井俊治，松井繁長，樫田博史，工藤正俊，杉浦史哲，上田和毅，奥野清隆，筑後孝章，佐藤隆夫：上行結腸動静脈奇形の1例．日本消化器病学会近畿支部第100回例会，平成26年2月22日，大阪国際交流センター，大阪．

16. 南　知宏，千品寛和，有住忠晃，田北雅弘，北井　聡，矢田典久，萩原　智，井上達夫，南　康範，上嶋一臣，西田直生志，工藤正俊：B-mode で描出困難な肝癌に対する Fusion image+造影 US ガイドでのラジオ波焼灼術の有用性．第 27 回日本腹部造影エコー・ドプラ診断研究会，平成26年4月5日，はまぎんホールヴィアマーレ，横浜．

17. 横川美加，前野知子，前川　清，北井　聡，井上達夫，南　康範，工藤正俊，川崎俊彦：肝炎に続発した肝内多発輪状結節の 1 例．第 27 回日本腹部造影エコー・ドプラ診断研究会，平成26年4月5日，はまぎんホールヴィアマーレ，横浜．

18. 井上達夫，兵頭朋子，千品寛和，有住忠晃，田北雅弘，北井　聡，矢田典久，萩原智，上嶋一臣，西田直生志，村上卓道，工藤正俊：EOB-MRI と造影超音波検査による乏血性結節の多血化因子の検討．第 27 回日本腹部造影エコー・ドプラ診断研究会，平成26年4月5日，はまぎんホールヴィアマーレ，横浜．

19. 松井繁長，樫田博史，工藤正俊，川崎正憲，朝隈　豊，永井知行，櫻井俊治：当院における好酸球性食道炎の検討．第100回日本消化器病学会総会，平成26年4月23日-26日，東京国際フォーラム，東京．

20. 永井知行，高山政樹，岡元寿樹，千品寛和，山田光成，足立哲平，峯　宏昌，川崎正憲，朝隈　豊，櫻井俊治，松井繁長，樫田博史，工藤正俊：当院における NSAIDs・抗血小板薬起因性の小腸粘膜傷害の検討．第 100 回日本消化器病学会総会，平成 26 年 4 月 23 日-26 日，東京国際フォーラム，東京．

21. 南　康範，南　知宏，有住忠晃，田北雅弘，北井　聡，矢田典久，井上達夫，萩原智，上嶋一臣，西田直生志，工藤正俊，柳生行伸，村上卓道：Plain cone-beam CT による肝動脈塞栓術の定量的治療効果予測．第 100 回日本消化器病学会総会，平成 26 年 4 月 23 日-26 日，東京国際フォーラム，東京．

22. 矢田典久，萩原　智，工藤正俊：超音波エラストグラフィによる非アルコール性脂肪性肝疾患患者の意識改革．第100回日本消化器病学会総会，平成26年4月23日-26日，東京国際フォーラム，東京．

23. 北野雅之，工藤正俊：EUS 下膵管ドレナージ術．日本消化器内視鏡学会附置研究会超音波内視鏡下治療研究会共同企画「消化器領域における EUS-FNA の現在とこれから」，日本超音波医学会第87回学術集会，平成26年5月9日-11日，パシフィコ横浜，神奈川．

24. 矢田典久，工藤正俊：エラストグラフィと肝血清マーカーを用いた肝線維化診断-臨床応用に向けて-．日本超音波医学会第 87 回学術集会，平成 26 年 5 月 9 日-11 日，パシフィコ横浜，神奈川．

25. 大本俊介，田中梨絵，門阪薫平，鎌田　研，宮田　剛，山雄健太郎，今井　元，坂本洋城，北野雅之，工藤正俊：造影ハーモニック EUS（CH-EUS）における膵腫瘍の血流評価の有用性について．超音波 Week2014，平成26年5月9日-11日，パシフィコ横浜，神

奈川.

26. 前野知子，横川美加，辻　裕美子，塩見香織，前川　清，工藤正俊，八木　誠，上杉忠雄，筑後孝章，佐藤隆夫：超音波検査で観察し得た新生児 chest wall hamartoma の一例．超音波 Week2014，平成 26 年 5 月 9 日-11 日，パシフィコ横浜，神奈川.

27. 北野雅之，工藤正俊：胆膵疾患における超音波内視鏡による造影超音波診断．第 6 回アジア造影超音波会議，平成 26 年 5 月 10 日，パシフィコ横浜，神奈川.

28. 門阪薫平，北野雅之，工藤正俊：急性胆嚢炎および胆管炎例に対する EUS 下胆嚢ドレナージ術の有用性．第 87 回日本消化器内視鏡学会総会，平成 26 年 5 月 15 日-17 日，福岡国際会議場，福岡.

29. 今井　元，北野雅之，工藤正俊，大本俊介，門阪薫平，宮田　剛，鎌田　研，山雄健太郎，坂本洋城：膵神経内分泌腫瘍に対する EUS の有用性．第 87 回日本消化器内視鏡学会総会，平成 26 年 5 月 15 日-17 日，福岡国際会議場，福岡.

30. 山田光成，樫田博史，南　知宏，田中梨絵，足立哲平，高山政樹，峯　宏昌，永井知行，川崎正憲，朝隈　豊，櫻井俊治，松井繁長，工藤正俊：当院における直腸内分泌腫瘍（NET）の診断と治療成績．第 87 回日本消化器内視鏡学会総会，平成 26 年 5 月 15 日-17 日，福岡国際会議場，福岡.

31. 永井知行，樫田博史，工藤正俊，南　知宏，田中梨絵，山田光成，足立哲平，峯　宏昌，高山政樹，川崎正憲，朝隈　豊，櫻井俊治，松井繁長：当院における超高齢者（85 歳以上）の下部内視鏡検査・治療の現況．第 87 回日本消化器内視鏡学会総会，平成 26 年 5 月 15 日-17 日，福岡国際会議場，福岡.

32. 岡元寿樹，高山政樹，峯　宏昌，山田光成，足立哲平，永井知行，川崎正憲，櫻井俊治，松井繁長，樫田博史，工藤正俊：胃アミロイドーシスの 2 例．第 87 回日本消化器内視鏡学会総会，平成 26 年 5 月 15 日-17 日，福岡国際会議場，福岡.

33. 西田直生志，中居卓也，工藤正俊：肝外再発例の肝癌 DNA メチル化プロファイルを用いた治癒切除後の早期再発予測．第 50 回日本肝臓学会総会，平成 26 年 5 月 29-30 日，ホテルニューオータニ，東京.

34. 西川浩樹，榎本平之，斎藤正紀，絵澤信弘，津田泰宏，樋口和秀，岡崎和一，関　寿人，金　守良，本合　泰，城村尚登，西田直生志，工藤正俊，大﨑往夫，西口修平：高齢者 Genotype 1b 高ウイルス量の C 型慢性肝炎患者における治療効果と安全性～ReGIT-J 試験の層別解析～．第 50 回日本肝臓学会総会，平成 26 年 5 月 29-30 日，ホテルニューオータニ，東京.

35. 小川　力，柴峠光成，工藤正俊：VINCENT の仮想超音波システムを用いた簡便な腫瘍，走行血管の描出と安全な穿刺ラインの同定方法．第 50 回日本肝臓学会総会，平成 26 年 5 月 29-30 日，ホテルニューオータニ，東京.

36. 上嶋一臣，有住忠晃，工藤正俊：現行の TACE 不応基準の妥当性の検証．コンセンサスミーティング 2「TACE 不応の定義をめぐって」，第 50 回日本肝癌研究会，平成 26 年 6 月 5 日-6 日，国立京都国際会館，京都.

37. 尾崎信人，松本　望，高場雄久，川崎正憲，冨田崇文，梅原康湖，森村正嗣，米田円，山田　哲，辻　直子，落合　健，前倉俊治，工藤正俊：プロトンポンプ阻害剤長期投与により胃底腺ポリープが増大したと思われる 1 例．日本消化器内視鏡学会近畿支

部第 92 回支部例会，平成 26 年 6 月 21 日，大阪国際交流センター，大阪.

38. 池田　守，足立哲平，南　知宏，田中梨絵，山田光成，高山政樹，峯　宏昌，永井知行，朝隈　豊，櫻井俊治，松井繁長，樫田博史，工藤正俊：急性壊死性食道炎の 1 例．日本消化器内視鏡学会近畿支部第 92 回支部例会，平成 26 年 6 月 21 日，大阪国際交流センター，大阪.

39. 秦　康倫，木下大輔，奥田英之，永田嘉昭，岸谷　譲，川崎俊彦，原　譲次，辻江正徳，井上雅智，若狭朋子，太田善夫，工藤正俊：術前診断が可能であった胆管原発悪性リンパ腫の 1 例．日本消化器内視鏡学会近畿支部第 92 回支部例会，平成 26 年 6 月 21 日，大阪国際交流センター，大阪.

40. 有住忠晃，上嶋一臣，千品寛和，田北雅弘，北井　聡，井上達夫，矢田典久，萩原智，南　康範，櫻井俊治，西田直生志，工藤正俊：ソラフェニブ投与にて PD 判定であった進行肝細胞癌患者の検討．第 10 回日本肝がん分子標的治療研究会，平成 26 年 6 月 21 日，淡路夢舞台国際会議場，兵庫.

41. 千品寛和，田北雅弘，有住忠晃，北井　聡，井上達夫，矢田典久，南　康範，萩原智，上嶋一臣，西田直生志，朝戸信行，任　誠雲，柳生行伸，松木　充，鶴﨑正勝，村上卓道，工藤正俊：当院におけるマイクロバルーン閉塞下肝動脈化学塞栓療法（B-TACE）導入後の検討．第 14 回肝血流動態・機能イメージ研究会，平成 26 年 7 月 5 日，オーバルホール，大阪.

42. 渡口真史，鶴﨑正勝，柳生行伸，沼本勲男，朝戸信行，山川美帆，任　誠雲，松木充，村上卓道，井上達夫，萩原　智，南　康範，上嶋一臣，工藤正俊：当院における肝細胞癌に対するディーシービーズ®を用いた TACE の初期経験．第 14 回肝血流動態・機能イメージ研究会，平成 26 年 7 月 5 日，オーバルホール，大阪.

43. 南　知宏，南　康範，工藤正俊：B-mode で描出困難な肝細胞癌に対する Fusion-imaging+造影 US ガイドでのラジオ波焼灼術．第 14 回肝血流動態・機能イメージ研究会，平成 26 年 7 月 5 日，オーバルホール，大阪.

44. 北野雅之，鎌田　研，工藤正俊：膵癌早期診断における EUS の位置づけ．第 45 回日本膵臓学会大会，平成 26 年 7 月 11-12 日，北九州国際会議場，北九州.

45. 大本俊介，北野雅之，門阪薫平，宮田　剛，鎌田　研，山雄健太郎，今井　元，坂本洋城，工藤正俊：自己免疫性膵炎の診断，治療における EUS の役割．第 45 回日本膵臓学会大会，平成 26 年 7 月 11-12 日，北九州国際会議場，北九州.

46. 濱田隆介，木下大輔，秦　康倫，奥田英之，永井知行，岸谷　譲，川崎俊彦，若狭朋子，太田善夫，工藤正俊：EUS-FNA にて診断可能であった、腎癌膵転移の 1 例．日本消化器病学会近畿支部第 101 回例会，平成 26 年 10 月 4 日，大阪国際交流センター，大阪.

47. 加藤　寛，宮田　剛，北野雅之，大本俊介，門阪薫平，鎌田　研，山雄健太郎，今井元，坂本洋城，工藤正俊：肝左葉切除後の肝門部胆管閉塞に対し超音波内視鏡下胆管胃吻合術（EUS-HGS）が奏効した一例．日本消化器病学会近畿支部第 101 回例会，平成 26 年 10 月 4 日，大阪国際交流センター，大阪.

48. 山本貴子，萩原　智，千品寛和，河野匡志，有住忠晃，田北雅弘，北井　聡，井上達夫，矢田典久，南　康範，櫻井俊治，上嶋一臣，西田直生志，工藤正俊，庭野史丸，池上博司：甲状腺クリーゼを契機に急性肝不全を発症した 1 例．日本消化器病学会近畿支部第 101 回例会，平成 26 年 10 月 4 日，大阪国際交流センター，大阪.

49. 山雄健太郎，北野雅之，工藤正俊：悪性消化管、胆道狭窄に対する治療戦略～EUS 下胆道ドレナージと消化管ステントによる double stenting の有用性～．第 63 回近畿膵疾患談話会，平成 26 年 10 月 18 日，エーザイ株式会社大阪コミュニケーションオフィス，大阪．

50. 鎌田　研，北野雅之，工藤正俊：嚢胞性膵疾患の鑑別診断および経過観察における EUS の有用性～造影法を含めて～．第 22 回日本消化器関連学会週間 JDDW2014（第 88 回日本消化器内視鏡学会総会，第 56 回日本消化器病学会大会，第 18 回日本肝臓学会大会，第 12 回日本消化器外科学会大会，第 52 回日本消化器がん検診学会大会），平成 26 年 10 月 23-26 日，神戸国際展示場・ポートピアホテル・神戸国際会議場，兵庫．

51. 南　知宏，南　康範，千品寛和，有住忠晃，田北雅弘，北井　聡，矢田典久，井上達夫，萩原　智，上嶋一臣，西田直生志，工藤正俊：B-mode で描出困難な肝癌に対する Fusion imaging+造影 US ガイドでのラジオ波焼灼術．第 22 回日本消化器関連学会週間 JDDW2014（第 88 回日本消化器内視鏡学会総会，第 56 回日本消化器病学会大会，第 18 回日本肝臓学会大会，第 12 回日本消化器外科学会大会，第 52 回日本消化器がん検診学会大会），平成 26 年 10 月 23-26 日，神戸国際展示場・ポートピアホテル・神戸国際会議場，兵庫．

52. 小川　力，森岡弓子，野田晃世，荒澤壮一，出田雅子，久保敦司，松中寿浩，玉置敬之，柴峠光成，工藤正俊：VINCENT の仮想超音波システムと GE 社のワークステーション AW を用いた RFA 前のシミュレーション．第 22 回日本消化器関連学会週間 JDDW2014（第 88 回日本消化器内視鏡学会総会，第 56 回日本消化器病学会大会，第 18 回日本肝臓学会大会，第 12 回日本消化器外科学会大会，第 52 回日本消化器がん検診学会大会），平成 26 年 10 月 23-26 日，神戸国際展示場・ポートピアホテル・神戸国際会議場，兵庫．

53. 南　康範，中居卓也，工藤正俊：当院における肝転移に対する経皮的ラジオ波焼灼術．第 22 回日本消化器関連学会週間 JDDW2014（第 88 回日本消化器内視鏡学会総会，第 56 回日本消化器病学会大会，第 18 回日本肝臓学会大会，第 12 回日本消化器外科学会大会，第 52 回日本消化器がん検診学会大会），平成 26 年 10 月 23-26 日，神戸国際展示場・ポートピアホテル・神戸国際会議場，兵庫．

54. 朝隈　豊，松井繁長，南　知行，山田光成，田中梨絵，足立哲平，高山政樹，峯　宏昌，永井知行，櫻井俊治，樫田博史，工藤正俊，白石　治，安田卓司：当院における食道表在癌の日本食道学会拡大内視鏡分類による深達度診断の検討．第 22 回日本消化器関連学会週間 JDDW2014（第 88 回日本消化器内視鏡学会総会，第 56 回日本消化器病学会大会，第 18 回日本肝臓学会大会，第 12 回日本消化器外科学会大会，第 52 回日本消化器がん検診学会大会），平成 26 年 10 月 23-26 日，神戸国際展示場・ポートピアホテル・神戸国際会議場，兵庫．

55. 河野　匡，梅原康湖，辻　直子，尾崎信人，松本　望，高場雄久，川崎正憲，冨田崇文，森村正嗣，山田　哲，米田　円，落合　健，前倉俊治，工藤正俊：PPI 内服による胃底腺ポリープの変化．第 22 回日本消化器関連学会週間 JDDW2014（第 88 回日本消化器内視鏡学会総会，第 56 回日本消化器病学会大会，第 18 回日本肝臓学会大会，第 12 回日本消化器外科学会大会，第 52 回日本消化器がん検診学会大会），平成 26 年 10 月 23-26 日，神戸国際展示場・ポートピアホテル・神戸国際会議場，兵庫．

56. 辻　直子，尾崎信人，松本　望，高場雄久，川崎正憲，冨田崇文，梅原康湖，谷池聡子，森村正嗣，米田　円，山田　哲，落合　健，前倉俊治，工藤正俊：H. Pylori 陰性 C-0 胃症例のたこいぼびらんに認めた腸上皮化生についての検討．第 22 回日本消化器関連学会週間 JDDW2014（第 88 回日本消化器内視鏡学会総会，第 56 回日本消化器病学会大

会，第 18 回日本肝臓学会大会，第 12 回日本消化器外科学会大会，第 52 回日本消化器がん検診学会大会），平成 26 年 10 月 23-26 日，神戸国際展示場・ポートピアホテル・神戸国際会議場，兵庫.

57. 足立哲平，南　知行，田中梨絵，山田光成，高山政樹，峯　宏昌，永井知行，朝隈豊，櫻井俊治，松井繁長，樫田博史，工藤正俊：当院におけるヘリコバクターピロリ除菌の治療成績の検討．第 22 回日本消化器関連学会週間 JDDW2014（第 88 回日本消化器内視鏡学会総会，第 56 回日本消化器病学会大会，第 18 回日本肝臓学会大会，第 12 回日本消化器外科学会大会，第52回日本消化器がん検診学会大会），平成26年10月23-26日，神戸国際展示場・ポートピアホテル・神戸国際会議場，兵庫.

58. 南　康範，大本俊介，松井繁長，北野雅之，樫田博史，工藤正俊：肝硬変を合併した限局性強皮症における難治性上部消化管出血にアルゴンプラズマ凝固法が有効であった一例．日本消化器内視鏡学会近畿支部第 93 回支部例会，平成 26 年 11 月 15 日，大阪国際交流センター，大阪.

59. 高場雄久，尾崎信人，松本　望，川崎正憲，冨田崇文，梅原康湖，森村正嗣，米田円，山田　哲，辻　直子，落合　健，前倉俊治，工藤正俊：ESD にて切除しえた胃底腺型胃癌の一例．日本消化器内視鏡学会近畿支部第93回支部例会，平成26年11月15日，大阪国際交流センター，大阪.

60. 長原　大，奥田英之，秦　康倫，木下大輔，永井知行，岸谷　譲，川崎俊彦，若狭朋子，太田善夫，工藤正俊：ステロイドが奏効した Cronkhite-Canada 症候群の 1 例．日本消化器内視鏡学会近畿支部第 93 回支部例会，平成 26 年 11 月 15 日，大阪国際交流センター，大阪.

61. 中尾剛幸，樫田博史，米田頼晃，山田光成，田中梨絵，足立哲平，峯　宏昌，高山政樹，岡崎能久，朝隈　豊，櫻井俊治，松井繁長，工藤正俊，佐野博幸，前西　修，佐藤隆夫：腸結核の 4 例．日本消化器内視鏡学会近畿支部第 93 回支部例会，平成 26 年 11 月 15 日，大阪国際交流センター，大阪.

62. 古川健太郎，北野雅之，大本俊介，門阪薫平，宮田　剛，鎌田　研，山雄健太郎，今井　元，坂本洋城，工藤正俊：Walled-off necrosis に対してリタリックステントを用いた EUS 下ドレナージ術が有用であった 1 例．日本消化器内視鏡学会近畿支部第 93 回支部例会，平成 26 年 11 月 15 日，大阪国際交流センター，大阪.

63. 前川　清，横川美加，前野知子，塩見香織，井上達夫，南　康範，工藤正俊：低音圧 Tissue Harmonic Imaging による造影下穿刺治療画面の提案．日本消化器内視鏡学会近畿支部第 93 回支部例会，平成 26 年 11 月 15 日，大阪国際交流センター，大阪.

別刷
新聞・雑誌・報道等

Impact of Histologically Confirmed Lymph Node Metastases on Patient Survival After Surgical Resection for Hepatocellular Carcinoma

Report of a Japanese Nationwide Survey

Kiyoshi Hasegawa, MD, Masatoshi Makuuchi, MD,† Norihiro Kokudo, MD, PhD,* Namiki Izumi, MD,‡ Takafumi Ichida, MD,§ Masatoshi Kudo, MD,¶ Yonson Ku, MD,|| Michiie Sakamoto, MD,** Osamu Nakashima, MD,†† Osamu Matsui, MD,‡‡ and Yutaka Matsuyama, PhD§§; on behalf of for the Liver Cancer Study Group of Japan*

Objective: To clarify the clinical significance of resection of lymph node metastases in patients' hepatocellular carcinoma (HCC).

Background: Although the presence of lymph node metastasis form HCC has been considered as a systemic disease, prognosis after resection of them remains unknown.

Methods: From the database of a Japanese nationwide survey, 14,872 patients of HCC treated by surgical resection between 2000 and 2005 were enrolled. We modified the current Japanese staging system for HCC, by further dividing stage IVA into stage IVAnon-n1 and stage n1, according to the absence or presence of pathologically proven lymph node metastasis. Thus, the patients classified into 6 disease stages, that is, I (n = 1494), II (n = 8056), III (n = 4243), IVAnon-n1 (n = 701), n1 (n = 112), and IVB (n = 266), and their long-term outcomes were compared.

Results: The median follow-up period was 20.6 months. The 3-year overall survival rates of the patients with stage IVAnon-n1, stage n1, and stage IVB were 51.6%, 38.9% and 27.2%, respectively. A multivariate analysis showed that stage IVAnon-n1 would have a similar impact on the survival as stage n1 (hazard ratio: 0.88, 95% confidence interval: 0.59–1.33, $P = 0.555$), and that stage n1 still represented one class less advanced than stage IVB (hazard ratio: 0.52, 95% confidence interval: 0.34–0.80, $P = 0.003$).

Conclusions: The prognosis of patients with histologically node-positive HCC was similar to that of patients with locally advanced HCC (stage IVA), which supports the validity of the current Japanese staging system and also partially validates the system proposed by the UICC/AJCC.

From the *Hepato-Biliary-Pancreatic Surgery Division, Department of Surgery, Graduate School of Medicine, University of Tokyo; †Japanese Red Cross Medical Center; ‡Department of Gastroenterology, Musashino Red Cross Hospital; §Department of Gastroenterology, Juntendo University Shizuoka Hospital; ¶Department of Gastroenterology and Hepatology, Kinki University School of Medicine; ||Division of Hepato-Biliary-Pancreatic Surgery, Kobe University Graduate School of Medicine; **Department of Pathology, Keio University School of Medicine; ††Department of Clinical Laboratory Medicine, Kurume University Hospital; ‡‡Department of Radiology, Kanazawa University Graduate School of Medical Science; and §§Department of Biostatics, School of Public Health University of Tokyo.

All the authors are members of the Liver Cancer Study Group of Japan.

Disclosure: The authors declare no conflicts of interest. This study was supported by the Liver Cancer Study Group of Japan. There were no other sources of funding for any authors. The authors declare no conflicts of interest.

Reprints: Norihiro Kokudo, MD, PhD, Hepato-Biliary-Pancreatic Surgery Division, Department of Surgery, Graduate School of Medicine, University of Tokyo, 7–3–1 Hongo Bunkyo-ku, Tokyo 113–0033. E-mail: KOKUDO-2SU@h.u-tokyo.ac.jp.

ISSN: 0003-4932/13/25901-0166
DOI: 10.1097/SLA.0b013e31828d4960

Keywords: hepatocellular carcinoma, lymph node metastasis, the UICC/AJCC staging system

(*Ann Surg* 2014;259:166–170)

Although hepatocellular carcinoma (HCC) with lymph node metastasis has been considered as a systemic disease with a dismal prognosis, the actual impact of the node status on the patient outcome has never been thoroughly investigated. According to both the current Japanese (Table 1)[1] and UICC/AJCC staging systems (Table 2),[2,3] N1 (lymph node metastasis macroscopically suspected) with any T factor is classified as stage IVA, which represents the second worst stage of the disease. However, there have been few concrete data supporting the validity of these staging systems.

In patients with HCC, detection of enlarged lymph nodes around the liver is not rare, because accompanying liver inflammation (viral hepatitis, alcoholic hepatitis, steatohepatitis, etc) frequently induces reactive lymph node swelling.[4,5] It is often difficult to distinguish between benign reactive lymph node swelling and metastatic lymph node enlargement preoperatively, despite the recent remarkable advances in imaging technologies.[5,6] In addition, sampling of the hepatic hilar lymph nodes is avoided during surgery for HCC, because it has been known to increase the risk of postoperative refractory ascites.[7,8] Thus, the actual impact of resection of histologically proven lymph node metastases remains unknown.

Since 1965, the Liver Cancer Study Group of Japan has been conducting biannual nationwide surveys of patients with HCC; however, no data concerning HCC patients with histologically proven lymph node metastases have been accumulated. Therefore, we added several items related to the histological lymph node status to the questionnaire of the registry system in 2000. Because sufficient clinical data have been obtained over the 6 years since 2000, we conducted this retrospective study, based on prospectively gathered data, in the latest Japanese survey.

PATIENTS AND METHODS

With the cooperation of 795 institutions in Japan, patients with primary liver cancer are registered every 2 years and followed up prospectively in a nationwide survey conducted by the Liver Cancer Study Group of Japan. HCC is diagnosed on the basis of imaging studies, clinical data, and/or histopathological studies at each institution. Among the 57,444 patients with HCC who were newly registered with the survey between 2000 and 2005, a total of 14,872 patients who underwent surgical resection for HCC and for whom complete information concerning the disease stage, liver function, and prognosis was available were entered into this study. Then, the patients were

TABLE 1. The Japanese Staging System for HCC

Stages	T Factor	N Factor	M Factor
Stage I	T1	N0	M0
Stage II	T2	N0	M0
Stage III	T3	N0	M0
Stage IVA	T4	N0	M0
Stage IVA	Any T	N1	M0
Stage IVB	Any T	Any N	M1

TABLE 2. The UICC/AJCC Staging System for HCC

Stages	T Factor	N Factor	M Factor
Stage I	T1	N0	M0
Stage II	T2	N0	M0
Stage IIIA	T3a	N0	M0
Stage IIIB	T3b	N0	M0
Stage IIIC	T4	N0	M0
Stage IVA	Any T	N1	M0
Stage IVB	Any T	Any N	M1

prospectively followed up at each institution. Although no definitive follow-up protocol was set, most liver surgeons observed the protocol shown in "Clinical Practice Guidelines for Hepatocellular Carcinoma,"[9] which recommends ultrasonography and serum tumor marker measurements every 3 or 4 months, and enhanced computed tomography or magnetic resonance imaging every 6 or 12 months. Although this study protocol was not submitted to the institutional review board of each institution participating in the nationwide survey, collection of the data and registering patients with HCC were conducted with the approval of each institution.

According to the fifth version of the General Rules for the Clinical and Pathological Study of Primary Liver Cancer, patients with histologically confirmed lymph node metastasis (labeled n1) in the absence of distant metastasis are classified as having stage IVA disease (Table 1)[1]; however, for this study, we further classified patients with stage IVA disease into stage IVAnon-n1 and stage n1 groups, to clarify the clinical significance of n1 (Table 3). Thus, on the basis of the disease stage, the study population (14,872 patients) was classified into 6 groups: stage I (n = 1,494), stage II (n = 8,056), stage III (n = 4,243), stage IVAnon-n1 (n = 701), stage n1 (n = 112), and stage IVB (n = 266). In this study, all patients classified as having stage n1 disease were treated by hepatic resection for HCC simultaneously.

Table 4 summarizes the baseline characteristics of the 6 groups. To clarify the differences among stages III, IVAnon-n1, n1, and IVB, pairwise *P* values are shown in Table 5. Table 6 shows the number and percentage of cases with n1 for each T factor, which indicates that even patients with T1 and T2 tumors, who would be classified as having stage I and stage II disease, respectively, in the absence of lymph node metastasis, could include several n1 cases.

The overall survival curves were plotted by the Kaplan-Meier method and compared by the log-rank test. In this study, recurrence-related data were not analyzed, because surgery performed in patients with stage n1 and stage IVB disease cannot be regarded as curative. The differences in the impact of each stage on the survival were estimated using a Cox proportional-hazards model including the following 10 covariates: age, gender, type of background hepatitis, platelet count ($<$ or $\geq 10 \times 10^4$ per μL), serum albumin level, serum total bilirubin level, indocyanine green retention rate at 15 minute ($<$ or $\geq$20%), serum alpha-fetoprotein level ($<$ or $\geq$20 ng/mL), serum des-γ-carboxy prothrombin level ($<$ or $\geq$40 AU/mL), and pathological differentiation grade of the tumor. The 10 covariates were chosen among the available factors in our database, because we regarded them as clinically important on the basis of previously published reports. The results of the multivariate analysis are expressed as hazard ratios calculated between consecutive stages with 95% confidence intervals. *P* values of less than 0.05 were considered to indicate statistical significance.

TABLE 3. The Classification Used in This Study

Stages	T Factor	N Factor	M Factor
Stage I	T1	N0	M0
Stage II	T2	N0	M0
Stage III	T3	N0	M0
Stage IVAnon-nl	T4	N0	M0
Stage nl	Any T	n1	M0
Stage IVB	Any T	Any N	M1

n1; patologocally proven lymph node metastasis

RESULTS

The median follow-up period after treatment was 20.6 months, and the 25th and 75th percentiles were 8.7 and 38.1 months, respectively. The overall 3-/5-year survival rates of the patients with stage I, II, III, IVAnon-n1, n1, and IVB disease were 90.4%/77.8%, 80.8%/66.6%, 66.6%/49.5%, 51.6%/37.0%, 38.9%/29.5%, and 27.2%/22.0%, respectively (Fig. 1).

The multivariate analysis (Table 7) showed that the hazard ratio for survival of patients with stage IVAnon-n1 relative to patients with stage n1 disease was 0.88 (95% confidence interval: 0.59–1.33, $P = 0.555$), although that of patients with stage n1 disease relative to those with stage IVB disease was statistically significantly higher (0.52, 95% confidence interval: 0.34–0.80, $P = 0.003$). Except for the situations mentioned earlier, the hazard ratio for survival of patients with each disease stage relative to that of patients with one level higher disease stage was significantly low in all combinations, which indicated that the clinical impact of the stage factor on death increased in the order of the disease stage.

DISCUSSION

The results of this study indicate that the prognosis after resection of lymph node metastasis in patients with HCC, irrespective of the T factor in the TNM classification, would be equivalent to that of stage IVAnon-n1, and inferior to that of the prognosis associated with stages I to III. Our analysis also suggests that extrahepatic spread other than to the lymph nodes is associated with a significantly poorer prognosis than metastasis to the lymph nodes alone.

According to autopsy studies of HCC, the estimated incidence of lymph node metastasis in HCC patients, overall, is 30.3%,[10] whereas that in patients undergoing surgery is only 1% to 2%.[7,10,11] Although, until date, there have been few data on the clinical impact of lymph node metastasis in patients with HCC, on the basis of the results of small retrospective studies and clinical experience, it has been suspected that lymph node metastasis may be one of the worst prognostic factors in these patients. Uenishi et al[7] reported that of 504 patients, all 6 with lymph node metastasis died within 14 months of surgery. According to Sun et al[12] and Kobayashi et al,[13] the 3-year overall survival rates were 31% and 25.9%, respectively, in 49 and 21 HCC patients with lymph node metastasis. In this study, the 3-year survival rate of patients with lymph node metastasis of 38.9% was consistent with the 2 reports mentioned earlier.

TABLE 4. Baseline Characteristics

Variables	I n = 1494	II n = 8056	III n = 4243	IVAnon-n1 n = 701	n1 n = 112	IVB n = 266
Age, Median (interquartile range), yrs	66 (12)	67 (12)	67 (13)	65 (14)	66 (13.5)	62 (17)
Gender, No. (%)						
Male	1078 (72.2)	6143 (76.3)	3415 (80.5)	572 (81.6)	88 (78.6)	206 (77.4)
Female	416 (27.8)	1913 (23.7)	828 (19.5)	129 (19.5)	24 (21.4)	60 (22.6)
Hepatitis virus infection, No. (%)						
HBsAg(+)/HCV-Ab(−)	248 (16.6)	1320 (16.4)	776 (18.3)	165 (23.5)	19 (20.0)	72 (27.1)
HBsAg(−)/HCV-Ab(+)	969 (64.9)	4459 (55.4)	2314 (54.5)	346 (49.4)	56 (50.0)	96 (36.1)
HBsAg(+)/HCV-Ab(+)	29 (1.9)	143 (1.8)	71(1.7)	18 (2.6)	2(1.8)	6 (2.3)
HBsAg(−)/HCV-Ab(−)	189 (12.7)	1808 (22.4)	903 (21.3)	146 (20.8)	33 (32.4)	76 (28.6)
Unknown	59 (3.9)	326 (4.0)	179 (4.2)	26 (3.7)	2(1.8)	16 (6.0)
Serum albumin, g/dL*	3.9 (0.6)	3.9 (0.6)	3.9 (0.6)	3.9 (0.7)	3.8 (0.6)	3.8 (0.7)
Serum total bilirubin, mg/dL*	0.8 (0.4)	0.7 (0.4)	0.8 (0.4)	0.7 (0.4)	0.8 (0.4)	0.7(0.3)
Platelet count, No. (%)						
$\geq 10 \times 10$ per μL	961 (64.3)	5971 (74.1)	3208 (75.6)	564 (80.5)	91 (81.2)	226 (85.0)
$< 10 \times 10^4$ per μL	468 (31.3)	1814 (22.5)	890 (21.0)	118 (16.8)	16 (14.3)	29 (10.9)
Unknown,	65 (4.4)	271 (3.4)	145 (3.4)	19 (2.7)	5 (4.5)	11 (4.1)
ICG R15, No. (%)						
≥20%	467 (31.2)	2111 (26.2)	1128 (26.6)	157 (22.4)	26 (23.2)	56 (21.1)
<20% L	896 (60.0)	5190 (64.4)	2716 (64.0)	479 (68.3)	76 (67.9)	174 (65.4)
Unknown	131 (8.8)	755 (9.4)	399 (9.4)	65 (9.3)	10 (8.9)	36 (13.5)
Alpha-fetoprotein, No. (%)						
≥20 ng/mL	623 (41.7)	3645 (45.2)	2414 (56.9)	468 (66.7)	63 (56.2)	186 (69.9)
<20 ng/mL	795 (53.2)	4034 (50.1)	1619 (38.2)	203 (29.0)	42 (37.5)	66 (24.8)
Unknown	76 (5.1)	377 (4.7)	210 (4.9)	30 (4.3)	7(6.3)	14 (5.3)
Des-y-carboxy prothrombin, No. (%)						
≥40 AU/mL	401 (26.8)	3645 (45.2)	2414 (56.9)	468 (66.8)	63 (56.3)	186 (69.9)
<40 AU/mL	795 (53.2)	4034 (50.1)	1619 (38.2)	203 (28.9)	42 (37.5)	66 (24.8)
Unknown	298 (20.0)	357 (4.7)	210 (4.9)	30 (4.3)	7 (6.2)	14 (5.3)
Tumor differentiation grade, No. (%)						
Well	483 (32.3)	1668 (20.7)	612 (14.4)	53 (7.6)	2(1.8)	18 (6.8)
Moderate	731 (48.9)	4748 (58.9)	2537 (59.8)	416 (59.3)	54 (48.2)	134 (50.4)
Poor	101 (6.8)	668 (8.3)	529 (12.5)	139 (19.8)	34 (30.4)	62 (23.3)
Unknown	179 (12.0)	972(12.1)	565 (13.3)	93 (13.3)	22 (19.6)	52 (19.5)

HBsAg indicates hepatitis B virus antigen; HCV-Ab, hepatitis C virus antibody;
ICG R15, indocyanine green retention rate at 15 minutes.

TABLE 5. Pairwise P Value Among Stages III, IVA non-n1, n1, and IVB

Variable	III vs IVAnon-n1	IVAnon-n1 vs n1	n1 vs IVB
Age*	0.009	0.457	0.002
Gender†	0.490	0.447	0.810
Virus infection†	0.002	0.154	0.073
Serum albumin*	0.169	0.062	0.916
Serum bilirubin*	0.612	0.586	0.318
Platelet count†	0.009	0.547	0.346
ICG R15†	0.016	0.861	0.824
Alpha-fetoprotein†	0.000	0.046	0.010
Des-gamma-carboxy prothrombin†	0.000	0.002	0.000
Tumor differentiation grade‡	0.006	0.016	0.323

*t test.
†χ^2 test.
‡Mantel trend test.

TABLE 6. Association Between T and n Factors

	T1 n = 1426	T2 n = 7663	T3 n = 4110	T4 n = 709
n0, No. (%)	971 (68.1)	5275 (68.8)	2759 (67.1)	468 (66.0)
Unknown, No. (%)	450 (31.6)	2353 (30.7)	1295 (31.5)	219 (30.9)
n1, No. (%)	5 (0.3)	35 (0.5)	56 (1.4)	22 (3.1)

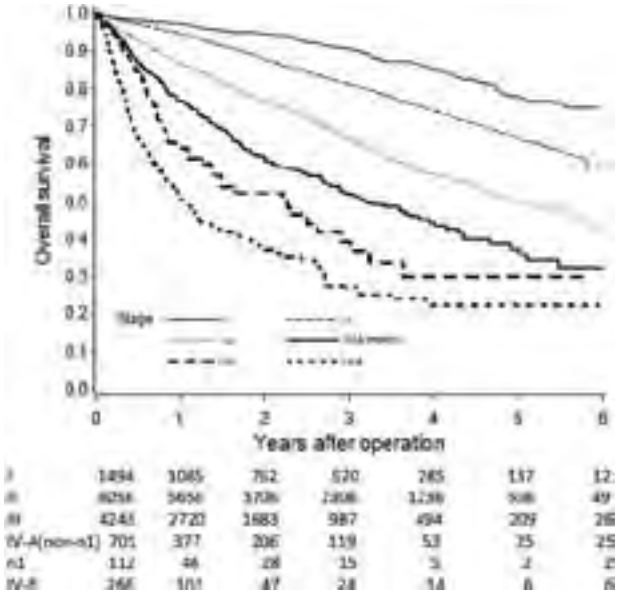

FIGURE 1. Overall survival curves after surgery for hepatocellular carcinoma in patients with stage I, II, III, IVAnon-n1, n1, and IVB disease are demonstrated.

TABLE 7. Hazard Ratios

	Hazard Ratio	95% Confidence Interval	*P*
Stage I (vs II)	0.61	0.49–0.76	<0.001
Stage II (vs III)	0.56	0.51–0.62	<0.001
Stage III (vs IVAnon-n1)	0.69	0.58–0.81	<0.001
Stage IVAnon-n1 (vs n1)	0.88	0.59–1.33	0.555
Stage n1 (vs IVB)	0.52	0.34–0.80	0.003

Our data indicate that extrahepatic spread other than to lymph nodes is associated with an even poorer prognosis than spread to the lymph nodes alone. In both the Japanese and UICC/AJCC staging systems,[1–3] cases of M1 (meaning extrahepatic spread) are classified into the worst disease stage (IVB), irrespective of the T and N factors. The results of this study clearly supported the validity of separating lymph node metastasis from extrahepatic spread in the 2 currently used staging systems.

On the contrary, there was no significant difference in the prognosis between stage IVAnon-n1 and stage n1 in this study, which suggested that the outcome of patients with T4 (denoting multiple tumors, maximum tumor diameter >2 cm, and presence of vascular invasion) classified according to the Japanese system would be equivalent to those of patients with lymph node metastasis, irrespective of the T factor. On this point, the results of this study did not support the UICC/AJCC system, in which T4 cases without N1 or M1 are classified as stage IIIC, a disease stage lower than stage IVA.

One of the most important points of this study is that lymph node metastasis was microscopically confirmed in the resected specimens in all cases. This overcame the major problem of some previous studies in which pathological information was lacking,[11,13] as it is quite difficult to macroscopically distinguish true metastasis from reactive lymph node swelling. Because our study had the largest number of cases (>100) to date, with pathological confirmation, we expect that our results would be useful for estimating the true impact of lymph node metastasis on the prognosis.

On the contrary, the above advantage could be weighed down by several biases, which should be taken into consideration while interpreting our data. For example, there could have been a bias toward cases with good liver function in the study population, because liver resection could be performed in the patients. The impact of lymph node metastasis may be different in patients with moderate or poor liver function, which needs further study.

Caution should also be exercised while interpreting our data from the aspect that there were no clear criteria for dissection of lymph nodes during the operation in our series. Because of the difficulty in macroscopically distinguishing between benign and malignant lymph nodes, several cases with microscopic lymph node metastasis might have been misclassified into stages I, II, III, and IVAnon-n1 in this study. Some cases from the study populations, in which lymph node metastasis was found by intraoperative pathological examination on frozen sections and hepatic resection was abandoned, might have been dropped from the analysis. These limitations make it difficult to arrive at a definitive conclusion. To strictly evaluate the significance of the presence of lymph node metastasis in HCC patients, routine sampling of lymph nodes would, theoretically, be a suitable strategy. However, this would be unacceptable from the ethical standpoint, because routine sampling would place the patients at risk for refractory ascites and liver failure after surgery. Positron emission tomography using ^{18}F-fluorodeoxy glucose, which was developed recently, is also not very sensitive for differentiating between metastatic and inflammatory swelling of the lymph nodes, although it has been found to be useful to detect systemic metastases from cancer.

The clinical significance of resection of lymph node metastases in patients with HCC remains under debate.[12,14,15] It would also be difficult to arrive at a solution to this problem on the basis of the current data, because there was no uniform strategy to cope with swollen lymph nodes in this study. Another prospective investigation is therefore warranted.

In this study, the follow-up period and number of study were probably insufficient, because the interval between the change of the registry form and the collection of data was 6 years. However, at least, we are able to show the outcomes of surgical resection of HCC in more than 100 cases of pathologically confirmed lymph node metastases. Although further investigation would be useful, however, our results may also hold importance in the current situation.

CONCLUSIONS

In conclusion, the results of this study support the current staging system used in Japan, in which patients with lymph node metastasis, irrespective of the T stage, are classified as having stage IVA disease, a stage lower than M1 (extrahepatic spread). Our results provide only partial validation of the UICC/AJCC staging system.

ACKNOWLEDGMENTS

The authors thank Mr Tomohiro Shinozaki, PhD, for his valuable contribution to the preparation of the data for statistical analyses. The roles of authors were as follows: Conception and design (K.H., N.K.), acquisition of data (all authors), analysis and interpretation (N.K., M.M., Y.M.), drafting (K.H.), critical revision (N.I., T.I., M.K., Y.K., M.S., O.N., O.M.), and final approval (N.K., M.M.).

REFERENCES

1. The Liver Cancer Study Group of Japan. *The General Rules for the Clinical and Pathological Study of Primary Liver Cancer*. 5th ed. Tokyo, Japan: Kanehara & Co, Ltd; 2009.
2. Vauthey JN, Lauwers GY, Esnaola NF, et al. Simplified staging for hepatocellular carcinoma. *J Clin Oncol*. 2002;20:1527–1536.

3. American Joint Committee on Cancer. *AJCC Cancer Staging Manual*. 7th ed. New York, NY: Springer; 2010.
4. Dodd GD, Baron RL, Oliver JH, III, et al. Enlarged abdominal lymph nodes in endstage cirrhosis: CT-histopathologic correlation in 507 patients. *Radiology*. 1997;203:127–130.
5. Grobmyer SR, Wang L, Gonen M, et al. Perihepatic lymph node assessment in patients undergoing partial hepatectomy for malignancy. *Ann Surg*. 2006;244:260–264.
6. Katyal S, Oliver JH III, Peterson MS, et al. Extrahepatic metastases of hepatocellular carcinoma. *Radiology*. 2000;216:698–703.
7. Uenishi T, Hirohashi K, Shuto T, et al. The clinical significance of lymph node metastases in patients undergoing surgery for hepatocellular carcinoma. *Surg Today*. 2000;30:892–895.
8. Ercolani G, Grazi GL, Ravaioli M, et al. The role of lymphadenectomy for liver tumors. Further considerations on the appropriateness of treatment strategy. *Ann Surg*. 2004;239:202–209.
9. Makuuchi M, Kokudo N. Clinical practice guidelines for hepatocellular carcinoma: the first evidence based guidelines from Japan. *World J Gastroenterol*. 2006;12:828–829.
10. The Liver Cancer Study Group of Japan. Primary liver cancer of Japan: clinicopathological features and results of surgical treatment. *Ann Surg*. 1990;211:277–287.
11. Lee CW, Chan KM, Lee CF, et al. Hepatic resection for hepatocellular carcinoma with lymph node metastasis: clinicopathological analysis and survival outcome. *Asian J Surg*. 2011;34:53–62.
12. Sun HC, Zhuang PY, Qin LX, et al. Incidence and prognostic values of lymph node metastasis in operable hepatocellular carcinoma and evaluation of routine complete lymphadenectomy. *J Surg Oncol*. 2007;96:37–45.
13. Kobayashi S, Takahashi S, Kato Y, et al. Surgical treatment of lymph node metastases from hepatocellular carcinoma. *J Hepatobiliary Pancreat Sci*. 2011;18:559–566.
14. Natsuizaka M, Omura T, Akaike T, et al. Clinical features of hepatocellular carcinoma with extrahepatic metastases. *J Gastroenterol Hepatol*. 2005;20:1781–1787.
15. Xiaohong S, Huikai L, Feng W, et al. Clinical significance of lymph node metastasis in patients undergoing partial hepatectomy for hepatocellular carcinoma. *World J Surg*. 2010;34:1028–1033.

Value of EUS in early detection of pancreatic ductal adenocarcinomas in patients with intraductal papillary mucinous neoplasms

Authors Ken Kamata[1], Masayuki Kitano[1], Masatoshi Kudo[1], Hiroki Sakamoto[1], Kumpei Kadosaka[1], Takeshi Miyata[1], Hajime Imai[1], Kiyoshi Maekawa[2], Takaaki Chikugo[3], Masashi Kumano[4], Tomoko Hyodo[4], Takamichi Murakami[4], Yasutaka Chiba[5], Yoshifumi Takeyama[6]

Institutions Institutions are listed at the end of article.

submitted
26. December 2012
accepted after revision
18. September 2013

Bibliography
DOI http://dx.doi.org/10.1055/s-0033-1353603
Published online: 11.11.2013
Endoscopy 2014; 46: 22–29

ISSN 0013-726X

Corresponding author
Masayuki Kitano, MD, PhD
Department of Gastroenterology and Hepatology
Kinki University Faculty of Medicine
377-2 Ohno-higashi
Osaka-sayama 589-8511
Japan
Fax: +81-72-3672880
m-kitano@med.kindai.ac.jp

Background and study aims: Pancreatic ductal adenocarcinomas (PDAC) sometimes arise in patients with intraductal papillary mucinous neoplasms (IPMNs). This study examined the incidence of PDACs concomitant to or derived from branch duct IPMNs. The usefulness of endoscopic ultrasonography (EUS) relative to other imaging methods for detecting these tumors was also assessed.

Patients and methods: This retrospective study used data from clinical records and imaging studies that were collected prospectively. During 2001–2009, 167 consecutive patients with IPMNs underwent EUS, ultrasonography, computed tomography (CT), and magnetic resonance imaging (MRI). The 102 patients whose branch duct IPMNs lacked mural nodules/symptoms and thus did not qualify for resection were followed up by semiannual EUS and annual ultrasonography, CT, and MRI. The sensitivity and specificity with which the four modalities detected IPMN-derived and -concomitant PDACs at the first examination and throughout the study period were evaluated. The rate of PDAC development during follow-up was analyzed by the Kaplan–Meier method.

Results: A total of 17 IPMN-derived and 11 IPMN-concomitant PDACs were diagnosed at the first examination. Lesions that did not qualify for resection or chemotherapy were followed up for a median of 42 months. Seven IPMN-concomitant PDACs and no IPMN-derived PDACs were detected during follow-up. The 3- and 5-year rates of IPMN-concomitant PDAC development were 4.0 % and 8.8 %, respectively. At the first examination, EUS was superior to other imaging modalities in terms of IPMN-derived and -concomitant PDAC detection. Throughout the study period, including follow-up, EUS was significantly better at detecting IPMN-concomitant PDACs than the other modalities.

Conclusions: IPMN-concomitant PDACs are quite often found at diagnosis and during follow-up. EUS examination of the whole pancreas plays an important role in the management of IPMNs as it allows the early detection of these small invasive carcinomas.

Introduction

Intraductal papillary mucinous neoplasms (IPMN) of the pancreas develop from epithelial cells in the main pancreatic duct (MPD) or branch duct [1–4]. Histologically, these lesions can be classified into benign IPMNs (hyperplasia, adenoma, and borderline neoplasm) or malignant IPMNs (noninvasive, minimally invasive, and invasive carcinomas) [5–7]. Although the natural history of IPMNs is still poorly understood, all of these lesions are considered to be premalignant because even benign lesions such as hyperplasias or adenomas can progress to invasive carcinomas. Thus, even benign IPMNs may have to be surgically resected to prevent malignant transformation [8]. However, the risk associated with the surgical procedures should be balanced against the risk of malignant transformation [7]. Thus, to facilitate decision making it is necessary to understand the natural history of IPMNs and to identify the IPMN features that are associated with a high potential for malignancy.

The features of IPMNs usually differ from those of ordinary pancreatic ductal adenocarcinomas (PDAC) [9–11]. However, several reports have shown that relative to the incidence of PDACs in the general population, PDACs occur at higher rates in patients with IPMNs; they are also frequently discovered at an unresectable stage [12–16]. There are two types of IPMN-related PDACs, namely, those that infiltrate the IPMN (designated here as IPMN-derived PDAC) and those that are

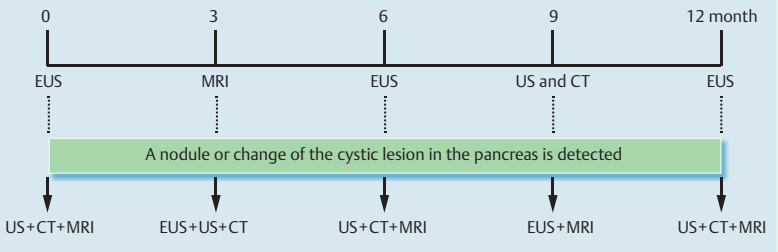

Fig. 1 The diagnostic and follow-up strategy with endosonography (EUS), ultrasonography (US), computed tomography (CT), and magnetic resonance imaging (MRI).

histologically distinct from the IPMN (designated here as IPMN-concomitant PDAC).

In recent times, it has become possible to diagnose IPMNs with a variety of imaging tools. Endoscopic ultrasonography (EUS) is superior to the other available imaging methods in terms of spatial resolution [17–20]. The present study had two main aims. The first was to investigate the natural course of branch duct IPMNs by using four imaging modalities: EUS, ultrasonography, computed tomography (CT), and magnetic resonance imaging (MRI). In particular, the frequencies of cystic lesion changes and IPMN-derived and -concomitant PDAC development during follow-up were determined. The second aim was to compare the diagnostic accuracy of the four imaging modalities in terms of the detection of IPMN-derived and -concomitant PDACs.

Patients and methods

Study design

This study was approved by the Institutional Review Board of Kinki University School of Medicine. It was a retrospective study that used a database created after the clinical record and imaging examination data were collected prospectively. The surgical indications and follow-up method were unified during the study period. Outcomes were reviewed retrospectively.

Patients

Between April 2001 and March 2009, 167 consecutive patients who were suspected to have an IPMN had their first examinations with EUS, ultrasonography, CT, and magnetic resonance cholangiopancreatography (MRCP/MRI) at the Kinki University Hospital. All four imaging methods were performed within 1 month.

Diagnosis of IPMNs

With all of the imaging modalities, IPMN was defined as a dilation of the MPD or its branches. To exclude simple cysts, a lesion was suspected to be an IPMN if it was more than 5 mm in diameter. IPMN was classified from imaging studies as either main duct or branch duct IPMN according to the new Fukuoka criteria [21]. Thus, if the MPD was ≥ 6 mm, the lesion was defined as main duct IPMN. However, if the branch duct was dilated and communicated with the pancreatic duct without MPD dilation, the lesion was defined as branch duct IPMN. The lesions were also examined for the presence of mural nodules.

Distinction between IPMN-derived and -concomitant PDACs

IPMN-derived PDACs were distinguished from IPMN-concomitant PDACs on the basis of radiological images and macroscopic or microscopic findings of the resected specimens. A pathologist examined these specimens carefully for the presence of non-neoplastic ducts between the IPMN and PDAC: if intervening normal ducts were observed, the PDAC was defined as an IPMN-concomitant PDAC. If a histological transition between the IPMN and PDAC was observed, the PDAC was defined as an IPMN-derived PDAC [22].

Indications for surgery and follow-up strategy

All main duct IPMNs and the branch duct IPMNs with nodules or symptoms were surgically resected. The remaining branch duct IPMNs, which lacked nodules/symptoms, were not surgically resected; instead, the patients underwent periodic follow-up with EUS, ultrasonography, CT, and MRI as outpatients (**Fig. 1**). Thus, EUS was performed semiannually and the ultrasonography, CT, and MRI examinations were performed annually between the two EUS examinations: the MRI was performed 2–4 months after the first EUS examination, and both ultrasonography and CT were performed 2–4 months after the next semiannual EUS examination, after which the cycle was repeated. If one of the four modalities showed during follow-up that the cystic lesion had changed (dilation of cystic lesion ≥ 10 mm) or a nodule had appeared, the other three modalities were performed within the following month so that the detection abilities of the four modalities could be compared.

Imaging techniques

All imaging techniques, both at the first examination and during follow-up, were performed in a blinded manner: the endosonographers, the ultrasonographer, and the radiologists were all unaware of the results of the other imaging investigations.

EUS

The electronic convex echoendscope (GF-UC240P-AL5; Olympus, Tokyo, Japan) was employed for EUS. All EUS observations of the pancreas were performed by the same two endosonographers (M.K. and H.S.), who were qualified by the Japan Gastroenterological Endoscopic Society and were experienced in EUS, having performed more than 3000 EUS examinations each.

US

A GE LOGIQ9 or 700 MR EXPERT Series unit (General Electric Medical Systems, Milwaukee, Wisconsin, USA) with a 2–4-MHz curved-array wide-band transducer was used for abdominal ultrasound. All ultrasound observations of the pancreas were performed by the same ultrasonographer (K.M.), who had 20 years of experience in gastrointestinal ultrasonography.

CT

Intravenous contrast-enhanced CT imaging was performed by using two-phase CT (Toshiba X-vigor; Toshiba Medical System, Tokyo, Japan) or a 64-channel multidetector CT scanner (Light

Table 1 Clinical characteristic of the 167 patients with intraductal papillary mucinous neoplasms.

Characteristic	Total	Follow-up group*
Number of patients	167	102
Age, mean (range), years	69 (33 – 88)	71 (33 – 86)
Sex, M:F, n	110 : 57	61 : 41
Type of IPMN		
Main duct	19	0
Branch duct	148	102
Site of IPMN		
Head	114	64
Body/tail	53	38

IPMN, intraductal papillary mucinous neoplasm.

* In total, 114 of the 167 IPMN lesions were branch duct IPMNs without mural nodules or symptoms. None of these cases underwent resection and were to be followed-up by the four imaging modalities for at least 12 months. In 12 cases, this follow-up did not occur and these cases were excluded from the remaining analyses, leaving 102 cases that were followed up according to the study protocol.

Speed VCT Vision: GE Healthcare, Milwaukee, Wisconsin, USA) with a 5.0 mm image thickness. In the former modality, 100 mL of Iopamiron (iopamidol; Nihon Schering, Osaka, Japan) with an iodine concentration of 370 mg/mL was injected. Dynamic acquisition in the early arterial phase (30 seconds) and portal phase (60 seconds) was performed. In the latter modality, after the unenhanced images were acquired, 510 mg iodine per kg of iodinated contrast material was administered intravenously at a rate of 3 – 4 mL/s. Scanning was performed during the pancreatic parenchymal phase (at 40 seconds) with the liver phase being obtained at 70 seconds. The images were evaluated by two radiologists (T.H. and M.K.), who had 15 and 20 years of experience in gastrointestinal radiology, respectively. The two readers first read the data independently. If either of them suspected that there was a solid tumor as well as the cystic lesions, the two readers re-assessed the images together until an agreement was obtained.

MRI

MRI studies were performed by using a 3.0 T system (Achieva: Philips Medical Systems, Best, The Netherlands) or either of two 1.5 T systems (Signa Excite HDxt, GE Healthcare; and Gyroscan Intera Nova, Philips Medical Systems). Axial and coronal breath-hold single-shot fast spin-echo (SSFSE) or half-Fourier acquisition SSFSE T2-weighted, 2 D thick-slab SSFSE MRCP, 3 D MRCP, T1-weighted dual-echo, b800 diffusion-weighted images, and T2-weighted image acquired with fat-suppressed turbo spin-echo sequence were obtained. The MRI and MRCP images were analyzed independently by the same radiologists (T.H. and M.K.) who performed the CT studies. As with the CT analyses, the two readers first read the data independently. If either of them suspected that there was a solid tumor as well as the cystic lesions, the two readers re-assessed the images together until an agreement was obtained.

Gold standard of PDAC diagnosis

The gold standard for the diagnosis of PDAC was histopathology of surgically resected specimens and/or EUS-guided fine-needle aspiration (FNA) specimens plus follow-up with the four modalities every 3 months for at least 12 months (**Fig. 1**). In the cases where a PDAC was not suspected on the basis of the imaging studies, the final diagnoses were confirmed by follow-up (**Fig. 1**).

Variables

The following outcomes were calculated: (i) the frequencies of main duct IPMN, branch duct IPMN with or without mural nodules/symptoms, and IPMN-derived and IPMN-concomitant PDACs at the first examination; (ii) frequencies of changes in the followed up (unresected) IPMNs and the new development of IPMN-derived and IPMN-concomitant PDACs during follow-up; (iii) the relative sensitivity and specificity with which each imaging modality detected PDAC at the first examination (to calculate these values, PDACs detected during follow-up were defined to be occult lesions that had not been detected at the first examination); and (iv) the relative sensitivity and specificity with which each imaging modality detected PDAC throughout the study period (to calculate these values, the latest examination during the study period was used). For (iv), the modality that detected the PDAC at the first examination or during follow-up was compared with the other three modalities that were performed within 1 month of the PDAC detection.

Statistical analysis

All analyses were performed using the statistical software SAS 9.1.3 (SAS Institute Inc., Cary, North Carolina, USA). The patients with IPMN-concomitant PDACs that were detected at the first examination were compared with the patients with new IPMN-concomitant PDACs in terms of their clinicopathological data by using Student's *t* test and Fisher's exact test. The McNemar test was applied to evaluate the differences between EUS, ultrasonography, CT, and MRI in terms of detecting PDACs. Differences were considered to be significant when P was <0.05. The development of IPMN-concomitant PDACs was analyzed by the Kaplan–Meier method.

Results

Clinical characteristics of patients

Table 1 shows the clinical characteristics of the 167 patients with IPMNs. The mean age was 69 years and the ratio of males to females was approximately 2 : 1. The IPMNs occurred twice as frequently in the pancreas head as in the body or tail. The flow chart (**Fig. 2**) shows that 11 of the 167 patients (7 %) were found incidentally to have IPMN-concomitant PDACs. This diagnosis was confirmed by EUS–FNA, after which seven of these patients underwent surgery. The remaining four patients with PDAC received chemotherapy because their PDAC lesions were at an inoperable stage. With regard to the remaining cohort of 156 patients without IPMN-concomitant PDACs, the 42 patients who had a main duct IPMN (n = 19) or a branch duct IPMN with mural nodules (n = 19) or symptoms (n = 4) underwent surgical resection. The histological diagnoses of all resected IPMN specimens (both main and branch duct IPMNs) were hyperplasia (n = 1), adenoma (n = 24), noninvasive carcinoma (n = 6), minimally invasive carcinoma (n = 7), and invasive carcinoma (n = 4). Seven of the 23 (30 %) resected branch duct IPMNs and 10 of the 19 (53 %) main duct IPMNs were carcinomas.

Of the remaining 114 patients who did not undergo surgical resection or chemotherapy, 102 were followed up for 12 months or longer. The other 12 patients who did not undergo periodic follow-up were excluded from this study. There was no further loss to follow-up. A total of 59 patients were continuously followed-up until the last date of the study (31 March 2010). The other 43 patients were censored after a follow-up of 12 months or longer

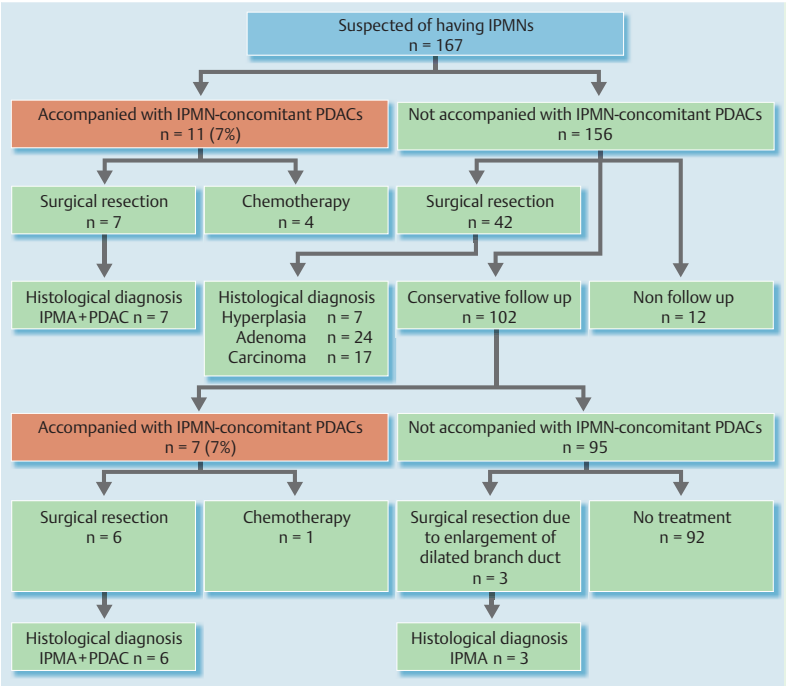

Fig. 2 Flow chart summarizing the passage of the 167 patients with intraductal papillary mucinous neoplasm (IPMN) during the study period. IPMA, intraductal papillary mucinous adenomas; PDAC, pancreatic ductal adenocarcinoma.

because follow-up was no longer possible due to the occurrence of other serious diseases, namely, gastric cancers (n=4), colon cancers (n=2), and benign diseases (n=37). The median duration of follow-up was 42 months (range 12–122). **Table 1** summarizes the characteristics of the 102 patients in the follow-up group. Their mean age was 71 years and the male:female ratio was 3:2. Similar to the whole cohort, their IPMNs occurred twice as frequently in the pancreas head as in the body or tail.

Outcomes of imaging examinations during follow-up period

In 3 of the 102 followed-up patients, the diameter of the dilated branch ducts increased during follow-up (**Fig. 2**). In all cases, all four imaging modalities detected this change. All three patients underwent surgical resection, but the histological diagnoses of the surgical specimens revealed that they had intraductal papillary mucinous adenomas (IPMAs). Mural nodules did not develop in any of the followed-up branch duct IPMNs. Thus, new IPMN-derived carcinomas did not arise from the branch duct IPMNs themselves during follow-up. However, seven (7%) IPMN-concomitant PDACs were detected in the follow-up period between 12 and 74 months after the initial diagnosis of IPMN (**Figs. 3, 4**). Thus, the 3- and 5-year rates of IPMN-concomitant PDAC development were 4.0% (95%CI 0.1–7.9) and 8.8% (95%CI 1.2–16.4), respectively. All lesions were detected at an operable stage, but one patient rejected surgical resection because of his advanced age and underwent chemotherapy instead.

Outcomes of surgical resection and histopathological examinations

Over the course of the study, surgery was performed in 58 patients because the IPMN was accompanied by a concomitant PDAC (n=13), the IPMN was a main duct IPMN or a branch duct IPMN with mural nodules/symptoms (i.e. the IPMN met the IPMN surgical resection indications, n=42), or the cystic lesion

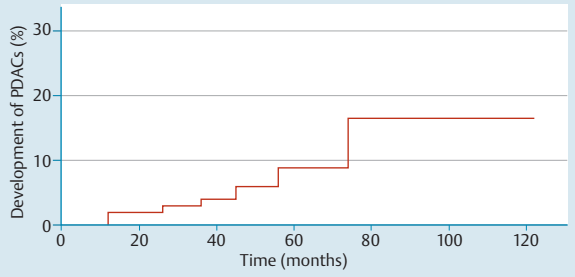

Fig. 3 Rate of intraductal papillary mucinous neoplasm (IPMN)-concomitant pancreatic ductal adenocarcinomas (PDAC) development during the follow-up of branch duct IPMNs, as analyzed by the Kaplan–Meier method.

became enlarged during the follow-up period (n=3). Pathological analysis of the resected lesions revealed that all had been correctly diagnosed as IPMNs by the preoperative studies.

In the 17 IPMN-derived PDACs detected at the first examination, all of which were resected immediately, histology revealed clear interconnections between the PDAC and the IPMN. Of the 18 IPMN-concomitant PDACs that were detected at the first examination or during follow-up, 13 were resected and histology revealed that all of these IPMNs were clearly divided from the PDAC by normal pancreatic duct.

Characteristics of patients with IPMN-concomitant PDACs

Table 2 summarizes the clinicopathological features of the 11 patients with IPMN-concomitant PDACs that were detected at the first examination and the seven patients with IPMN-concomitant PDACs that were detected during follow-up. Whereas two-thirds of the IPMNs of all of these cases were located in the pancreatic head, the PDACs showed the opposite orientation, with

Characteristic	Total (n = 18)	First examination (n = 11)	During follow-up (n = 7)	*P* value*
Age, mean (range), years	68 (59 – 88)	69 (60 – 80)	67 (59 – 72)	0.477
MPD size, mean (range), mm	3 (2 – 5)	3 (2 – 5)	4 (2 – 5)	0.218
Branch duct size, mean (range), mm	14 (8 – 28)	15 (8 – 28)	13 (10 – 18)	0.285
Mural nodule size, mean (range), mm	1 (0 – 11)	1 (0 – 11)	0	0.422
PDAC size, mean (range), mm	19 (7 – 50)	24 (15 – 50)	16 (7 – 30)	0.085
Location of IPMN				0.572
Head	12	7	5	
Body/tail	6	4	2	
Location of PDAC				0.324
Head	5	4	1	
Body/tail	13	7	6	

IPMN, intraductal papillary mucinous neoplasm; MPD, main pancreatic duct; PDAC, pancreatic ductal adenocarcinoma.
* Comparison of the group with concomitant PDACs at the first examination to the group with concomitant PDACs discovered during follow-up.

Table 2 Clinicopathological features of the 18 patients with intraductal papillary mucinous neoplasms-concomitant pancreatic ductal adenocarcinoma that were either detected by the first examinations or during follow-up.

two-thirds or more detected in the body or tail. This tendency was particularly pronounced in the seven PDACs discovered during follow-up: six were located in the body or tail. All concomitant IPMNs were branch duct IPMNs without mural nodules. The concomitant PDACs that were detected at the first examination had a mean (±SD) size of 24±10.6 mm. By contrast, the concomitant PDACs of the follow-up group were smaller (16±7.5 mm), although this difference did not achieve statistical significance (P=0.085). In the seven patients whose PDACs were detected during follow-up, the longest diameter of the dilated branch duct and the width of the pancreatic duct at the first examination were 13±3 mm and 4±1 mm, respectively. These duct dimensions did not increase during follow-up.

Sensitivity and specificity of imaging modalities to detect IPMN-derived and -concomitant PDACs

Table 3 summarizes the sensitivity and specificity with which the four modalities diagnosed IPMN-derived and -concomitant PDACs at the first examination and throughout the study period. For the calculations regarding the first examination, the seven IPMN-concomitant PDACs that were discovered during follow-up were considered to be occult lesions that had not been detected by any of the imaging modalities at the first examination. At the first examinations, EUS seemed to be superior to the other imaging modalities in detecting both IPMN-derived and -concomitant PDACs, although only the difference between EUS and ultrasonography achieved statistical significance. During follow-up, six of seven new PDACs were first detected by EUS despite the fact that ultrasonography, CT, and MRI had been performed between 2 and 10 months earlier (**Fig. 4**). The other three modalities were then performed within 1 month of the PDAC-detecting EUS. For IPMN-concomitant PDAC that was detected during follow-up, EUS, ultrasonography, CT, and MRI detected 100% (7/7), 0% (0/7), 43% (3/7), and 43% (3/7), respectively. Thus, EUS was still superior to ultrasonography, CT, and MRI in detecting these PDACs. When calculating sensitivity and specificity of the four modalities to detect IPMN-concomitant PDACs at the latest examination throughout the study period including follow-up, EUS was significantly better than the other three imaging modalities (**Table 3**).

Table 3 Sensitivity and specificity with which endosonography, ultrasonography, computed tomography, and magnetic resonance imaging detected intraductal papillary mucinous neoplasm-derived and -concomitant pancreatic ductal adenocarcinoma.

Modality	IPMN-derived PDACs (n = 17)			IPMN-concomitant PDACs (n = 18)					
	At the first examination			At the first examination			Throughout the study period		
	Sensitivity, % [95%CI]	Specificity, % [95%CI]	*P* value* vs. EUS	Sensitivity, % [95%CI]	Specificity, % [95%CI]	*P* value* vs. EUS	Sensitivity [95%CI]	Specificity [95%CI]	*P* value* vs. EUS
EUS	100 [0.83 – 1.00]	85 [0.83 – 0.85]	–	61 [0.48 – 0.61]	100 [0.98 – 1.00]	–	100 [0.90 – 1.00]	100 [0.99 – 1.00]	–
Ultrasound	47 [0.31 – 0.55]	99 [0.97 – 1.00]	0.089	39 [0.24 – 0.47]	99 [0.97 – 1.00]	0.041	39 [0.25 – 0.43]	99 [0.97 – 1.00]	0.001
CT	53 [0.35 – 0.66]	97 [0.95 – 0.99]	0.110	39 [0.26 – 0.39]	100 [0.98 – 1.00]	0.134	56 [0.42 – 0.56]	100 [0.98 – 1.00]	0.013
MRI	53 [0.35 – 0.71]	92 [0.90 – 0.94]	0.814	33 [0.21 – 0.33]	100 [0.98 – 1.00]	0.074	50 [0.37 – 0.50]	100 [0.98 – 1.00]	0.008

CI, confidence interval; CT, computed tomography; EUS, endosonography; IPMN, intraductal papillary mucinous neoplasm; MRI, magnetic resonance imaging; PDAC, pancreatic ductal adenocarcinoma.
During follow-up, IPMN-derived PDACs were not detected, but IPMN-concomitant PDACs were detected in seven patients. When comparing the imaging methods at the first examination, the seven PDACs that were detected during follow-up were considered to be occult lesions that had not been detected by any of the imaging modalities. When comparing the imaging methods throughout the study period, the latest examination during study period was used.
* McNemar test

Discussion

When IPMN lesions are examined by imaging, it is necessary to check for mural nodules and to determine whether the lesion communicates with the MPD. EUS has better spatial resolution than ultrasonography and CT and can therefore more clearly visualize the internal structure of cystic tumors of the pancreas [20]. For this reason, EUS is often used to follow-up IPMNs in order to assess whether changes in the cystic lesions have occurred. In the present study, EUS was also useful for detecting IPMN-concomitant PDACs both at the first examination and during follow-up.

IPMN is a cystic tumor that has a marked potential to progress to a malignant state. Several studies indicate that 60 % – 100 % of resected main duct IPMNs are malignant [4, 23 – 26]. Therefore, in patients with good life expectancy, main duct IPMNs should be resected. By contrast, branch duct IPMNs are associated with a lower risk of malignancy [4, 23 – 26]. However, the 2012 international consensus guidelines recommend that branch duct IPMNs that have a higher likelihood of malignancy should be surgically resected. Predictors of malignancy in these IPMNs are the presence of large branch ducts (> 30, 35, 40 or 50 mm) and a particular height of mural nodules (> 5 or 10 mm) [25, 27 – 30]. However, the natural history of branch duct IPMNs is poorly understood. In the present study, all branch duct IPMNs with mural nodules and/or symptoms were resected regardless of the dilated branch duct and mural nodule size, whereas the patients with branch duct IPMNs without mural nodules or symptoms were followed up by EUS (and other imaging modalities) to check the IPMN growth and to judge whether the patients with these IPMNs should undergo surgery. Although mural nodules never arose during follow-up, the cystic lesions in three (3 %) patients grew in size during follow-up and were resected. Histology revealed that all three were IPMAs. Thus, IPMN-derived carcinomas were not detected during follow-up in the present study. These observations are consistent with an increasing body of evidence that suggests that most branch duct IPMNs can be followed up [4, 26 – 31]. For example, when Salvia et al. prospectively evaluated the effectiveness of follow-up for a median of 32 months in 89 asymptomatic patients with branch duct IPMNs (< 3.5 cm) without mural nodules, only five (5.6 %) exhibited an increase in lesion size and were resected [26]. Histological examination of those resected specimens revealed that none were malignant. Another prospective study found that in 69 of 82 patients (84.1 %) with branch duct IPMNs without mural nodules, the lesions did not change during a median follow-up period of 61 months [31]. These reports suggest that branch duct IPMNs without mural nodules rarely progress to cancer over short periods of follow-up. Nevertheless, more follow-up data are needed to improve our understanding of the natural history of branch duct IPMNs without mural nodules.

In the present study, 11 IPMN-concomitant PDACs (7 % of all IPMNs) were incidentally detected by several imaging methods at the first examination for IPMNs. Several studies have also shown that IPMNs are frequently accompanied by carcinomas that are distinct from IPMNs, both at the first medical examination and during IPMN follow-up [12, 15, 16]. Uehara et al. [15] reported that the 5-year rate of ductal carcinoma development in 60 patients with branch duct IPMNs was 6.9 %, and Tada et al. [16] reported that 5 % of patients with IPMN developed PDAC during a 3.8-year follow-up. Similarly, Yamaguchi et al. [22] showed that 4.1 % of patients diagnosed with IPMN also had an IPMN-derived or -concomitant PDAC. The 5-year rate of IPMN-concomitant PDAC in the present study was 8.8 %, which is higher than the rates of the latter studies, although it should be noted that the studies differed in terms of median follow-up period and cohort size. The higher rate in the present study may relate to the strict periodic follow-up with several modalities and the fact that EUS was used. These factors may have been responsible for the detection of the other seven PDACs during follow-up, which increased the 5-year rate.

The use of EUS together with the periodic follow-up probably also allowed the detection of these seven PDACs at an early stage. These PDACs may be indolent and thus would not have manifested as clinical cases had they been left in place. Uehara et al. reported that the IPMN-concomitant PDACs that were detected during follow-up, largely by transabdominal ultrasonography, were found in an advanced state, even though the patients were examined at 6-month intervals [15]. By contrast, in the present study, all of the PDACs that were detected during follow-up could still be resected. During follow-up, six of the seven IPMN-concomitant PDACs were first detected by EUS despite the fact that ultrasonography, CT, and MRI had been performed between 2 and 10 months earlier.

The utility of EUS for the follow-up of IPMNs is also indicated by the fact that, when comparing the four modalities after one modality detected a PDAC, EUS detected all of these seven PDACs, whereas CT and MRI only detected 43 % of these lesions and ultrasonography could not detect any. Accordingly, EUS detected PDACs significantly better than the other modalities throughout the study period including follow-up. Thus, EUS appears to be more useful than ultrasonography, CT, and MRI for the early detection of PDACs. However, it should be noted that there was some methodological bias because EUS was performed semiannually whereas the other modalities were only performed once per year. This may have increased the sensitivity of EUS. However, although it would have been preferable to follow the patients up with all four modalities during the same visit, this was not done because it would have placed an undue burden on the patients.

To our knowledge, this study is the first to employ EUS for the follow-up of branch duct IPMNs. This observation suggests that, in cases of partial surgical resection, the in situ gland should be subjected to close surveillance. This approach would also aid the early detection of PDACs. Moreover, considering the malignant potential of the in situ gland, total pancreatectomy may be indicated in some cases of IPMN. However, in these cases, the complications associated with total pancreatectomy, such as diabetes and indigestion, should be balanced against the risk of malignant transformation. Moreover, Yamaguchi et al. have reported that IPMN-concomitant PDACs are significantly smaller, less invasive, and less extensive than ordinary PDACs [22]. These factors should be considered when deciding the extent of resection particularly in elderly patients. The relatively high frequency of IPMN-associated PDACs also indicates that it is important to carefully survey the entire pancreas in patients with an IPMN rather than focusing only on the cysts, as this allows concomitant carcinoma to be detected. Moreover, unresected IPMNs should be subjected to periodic follow-up with EUS to ensure that IPMN-concomitant PDACs are detected early, although the optimal interval between follow-up examinations of branch type IPMNs is not yet clear.

A recent report from Japan that analyzed radiological images and macroscopic or microscopic findings showed clearly for the first time that some PDACs exist concomitantly with IPMNs rather

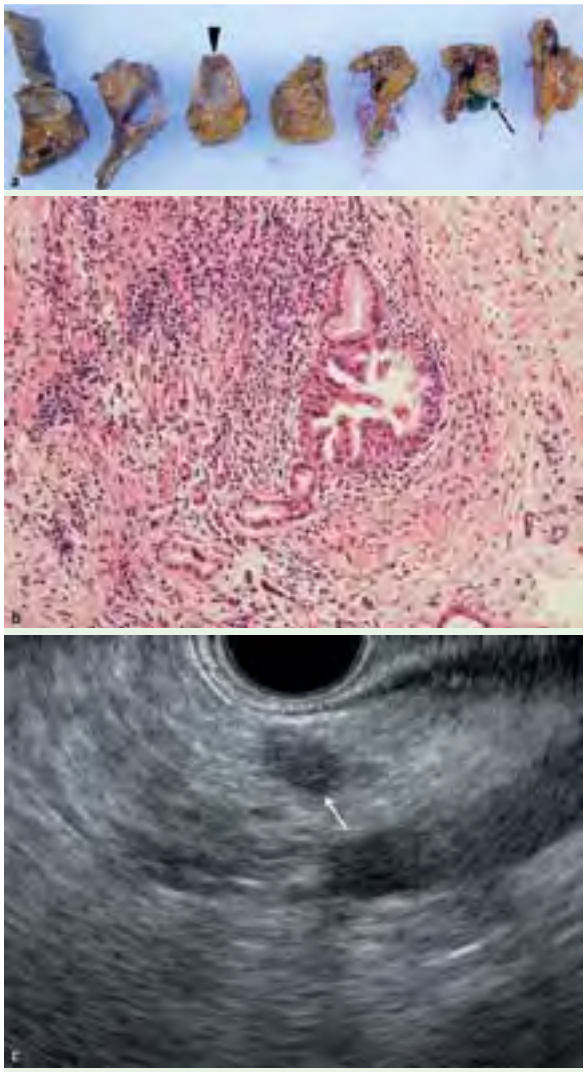

Fig. 4 Specimens, histology, and imaging data of a patient with a branch duct intraductal papillary mucinous neoplasm (IPMN) who developed a concomitant pancreatic ductal adenocarcinoma (PDAC) during follow-up. **a** Resected specimen. The surgical findings revealed that the pancreatic tumor (arrow) exited from the pancreatic body and was distinct from the cystic lesion (arrowhead). **b** Histology of the tumor (hematoxylin and eosin staining). Pathological examination of the resected specimen revealed a PDAC in the pancreas body. **c** Endoscopic ultrasonography imaging revealed a hypoechoic area (arrow) in the pancreas body that was 7 mm in diameter.

than deriving from them [22]. By contrast, several reports on IPMNs in Western countries [26, 32–34] did not report cases of such concomitant PDACs. This discrepancy may reflect the fact that such IPMN-concomitant PDACs were not sought in the latter studies. Alternatively, or in addition, it may also reflect differences between races in terms of PDAC pathogenesis.

In conclusion, when diagnosing and treating IPMNs, it is necessary to search for concomitant carcinomas, as the present study showed that 7% of these lesions were accompanied by carcinomas elsewhere in the pancreas. EUS is expected to play the prominent role in detecting these carcinomas at IPMN diagnosis. Moreover, in a substantial proportion of cases with branch duct IPMNs without mural nodules, concomitant carcinomas will appear during follow-up: the present study showed 3- and 5-year rates of IPMN-concomitant PDAC development of 4.0% and 8.8%, respectively. Performing EUS at regular follow-up visits will help to detect these new carcinomas early. Moreover, it may be necessary to consider resecting branch duct IPMNs without mural nodules although this option should be balanced against surgical complications.

Competing interests: None

Institutions

[1] Department of Gastroenterology and Hepatology, Kinki University Faculty of Medicine, Osaka-sayama, Japan
[2] Section of Abdominal Ultrasound, Kinki University Faculty of Medicine, Osaka-sayama, Japan
[3] Department of Pathology, Kinki University Faculty of Medicine, Osaka-sayama, Japan
[4] Department of Radiology, Kinki University Faculty of Medicine, Osaka-sayama, Japan
[5] Division of Biostatistics, Clinical Research Center, Kinki University Faculty of Medicine, Osaka-sayama, Japan
[6] Department of Surgery, Kinki University Faculty of Medicine, Osaka-sayama, Japan

References

1 *Seki M, Yanagisawa A, Ohta H* et al. Surgical treatment of intraductal papillary mucinous tumor (IPMT) of the pancreas: operative indications based on surgico-pathologic study focusing on invasive carcinoma derived from IPMT. J Hepatobiliary Pancreat Surg 2003; 10: 147–155
2 *Kloppel G, Kosmahl M*. Cystic lesions and neoplasm of the pancreas: the features are becoming clearer. Pancreatology 2001; 1: 648–655
3 *Baumgaertner I, Corcos O, Couvelard A* et al. Prevalence of extrapancreatic cancers in patients with histologically proven intraductal papillary mucinous neoplasms of the pancreas: a case–control study. Am J Gastroenterol 2008; 103: 2878–2882
4 *Nagai K, Doi R, Ito T* et al. Single-institution validation of the international consensus guidelines for treatment of branch duct intraductal papillary mucinous neoplasms of the pancreas. J Hepatobiliary Pancreat Surg 2009; 16: 353–358
5 *Kloppel G, Solcia E, Longnecker DS* et al. World Health Organization international histological classification of tumors. Histological typing of tumors of the exocrine pancreas. 2nd edn. Springer; Berlin: 1996: 1–61
6 *Kloppel G*. Clinicopathologic view of intraductal papillary-mucinous tumor of the pancreas. Hepatogastroenterology 1998; 45: 1981–1985
7 *Bournet B, Kirzin S, Carrere N* et al. Clinical fate of branch duct and mixed forms of intraductal papillary mucinous neoplasia of the pancreas. J Gastroenterol Hepatol 2009; 24: 1211–1217
8 *Tanaka M, Chari S, Adsay V* et al. International Association of Pancreatology. International consensus guidelines for management of intraductal papillary mucinous neoplasm and mucinous cystic neoplasms of the pancreas . Pancreatology 2006; 6: 17–32
9 *Sohn TA, Yeo CJ, Cameron JL* et al. Intraductal papillary mucinous neoplasms of the pancreas: an increasingly recognized clinicopathologic entity. Ann Surg 2001; 234: 313–321
10 *Maire F, Hammel P, Terris B* et al. Prognosis of malignant intraductal papillary mucinous tumors of the pancreas after surgical resection. Comparison with pancreatic ductal adenocarcinoma. Gut 2002; 51: 717–722
11 *Woo SM, Ryu JK, Lee SH* et al. Survival and prognosis of invasive intraductal papillary mucinous neoplasms of the pancreas: comparison with pancreatic ductal adenocarcinoma. Pancreas 2008; 36: 50–55
12 *Komori T, Ishikawa O, Ohigashi H* et al. Invasive ductal adenocarcinoma of the remnant pancreatic body 9 years after resection of an intraductal papillary-mucinous carcinoma of the pancreatic head: a case report and comparison of DNA sequence in K-ras gene mutation. Jpn J Clin Oncol 2002; 32: 146–151
13 *Yamaguchi k, Ohuchida J, Ohtsuka T* et al. Intraductal papillary-mucinous tumor of the pancreas concomitant with ductal carcinoma of the pancreas. Pancreatology 2002; 2: 484–490

14 *Kamisawa T*, *Tu Y*, *Egawa N* et al. Malignancies associated with intraductal papillary mucinous neoplasm of the pancreas. World J Gastroenterol 2005; 11: 5688 – 5690
15 *Uehara H*, *Nakaizumi A*, *Ishikawa O* et al. Development of ductal carcinoma of the pancreas during follow-up of branch duct intraductal papillary mucinous neoplasm of the pancreas. Gut 2008; 57: 1561 – 1565
16 *Tada M*, *Kawabe T*, *Arizumi M* et al. Pancreatic cancer in patients with pancreatic cystic lesions: a prospective study in 197 patients. Clin Gastroenterol Hepatol 2006; 4: 1265 – 1270
17 *Koito K*, *Namieno T*, *Nagakawa T* et al. Solitary cystic tumor of the pancreas: EUS-pathologic correlation. Gastrointest Endosc 1997; 45: 268 – 276
18 *Yamaguchi K*, *Tanaka M*. Radiologic imagings of cystic neoplasms of the pancreas. Pancreatology 2001; 1: 633 – 636
19 *Ahmad NA*, *Kochman ML*, *Lewis JD* et al. Can EUS alone differentiate between malignant and benign cystic lesions of the pancreas? Am J Gastroenterol 2001; 96: 3295 – 3300
20 *Kubo H*, *Nakamura K*, *Itaba S* et al. Differential diagnosis of cystic tumors of the pancreas by endoscopic ultrasonography. Endoscopy 2009; 41: 684 – 689
21 *Tanaka M*, *Fernández-del Castillo C*, *Adsay V* et al. International consensus guidelines 2012 for the management of IPMN and MCN of the pancreas. Pancreatology 2012; 12: 183 – 197
22 *Yamaguchi K*, *Kanemitsu S*, *Hatori T* et al. Pancreatic ductal adenocarcinoma derived from IPMN and pancreatic ductal adenocarcinoma concomitant with IPMN. Pancreas 2011; 40: 571 – 580
23 *Kobari M*, *Egawa S*, *Shibuya K* et al. Intraductal papillary mucinous tumors of the pancreas comprise 2 clinical subtypes: differences in clinical characteristics and surgical management. Arch Surg 1999; 134: 1131 – 1136
24 *Matsumoto T*, *Aramaki M*, *Yada K* et al. Optimal management of the branch duct type intraductal papillary mucinous neoplasms of the pancreas. J Clin Gastroenterol 2003; 36: 261 – 265
25 *Sugiyama M*, *Izumisato Y*, *Abe N* et al. Predictive factors for malignancy in intraductal papillary mucinous tumors of the pancreas. Br J Surg 2003; 90: 1244 – 1249
26 *Salvia R*, *Femandez-del Castillo C*, *Bassi C* et al. Main-duct intraductal papillary mucinous neoplasms of the pancreas: clinical predictors of malignancy and long-term survival following resection. Ann Surg 2004; 239: 678 – 685
27 *Shima Y*, *Mori M*, *Takakura N* et al. Diagnosis and management of cystic pancreatic tumors with mucin production. Br J Surg 2000; 87: 1041 – 1047
28 *Rodriguez JR*, *Salvia R*, *Crippa S* et al. Branch-duct intraductal papillary mucinous neoplasms: observations in 145 patients who underwent resection. Gastroenterology 2007; 133: 72 – 79
29 *Salvia R*, *Crippa S*, *Falconi M* et al. Branch-duct intraductal papillary mucinous neoplasms of the pancreas: to operate or not to operate? Gut 2007; 56: 1086 – 1090
30 *Schmidt CM*, *White PB*, *Waters JA* et al. intraductal papillary mucinous neoplasms: predictors of malignant and invasive pathology. Ann Surg 2007; 246: 644 – 654
31 *Tanno S*, *Nakano Y*, *Nishikawa T* et al. Natural history of branch duct intraductal papillary-mucinous neoplasms of the pancreas without mural nodules: long-term follow-up results. Gut 2008; 57: 339 – 343
32 *Chari ST*, *Yadav D*, *Smyrk TC* et al. Study of recurrence after surgical resection of intraductal papillary mucinous neoplasm of the pancreas. Gastroenterology 2002; 123: 1500 – 1507
33 *Sohn TA*, *Yeo CJ*, *Cameron JL* et al. Intraductal papillary mucinous neoplasms of the pancreas: an updated experience. Ann Surg 2004; 239: 788 – 797
34 *D'Angelica M*, *Brennan MF*, *Suriawinata AA* et al. Intraductal papillary mucinous neoplasms of the pancreas: an analysis of clinicopathologic features and outcome. Ann Sur 2004; 239: 400 – 408

Nationwide Study of 4741 Patients With Non-B Non-C Hepatocellular Carcinoma With Special Reference to the Therapeutic Impact

Tohru Utsunomiya, MD, PhD, Mitsuo Shimada, MD, PhD,* Masatoshi Kudo, MD, PhD,† Takafumi Ichida, MD, PhD,‡ Osamu Matsui, MD, PhD,§ Namiki Izumi, MD, PhD,¶ Yutaka Matsuyama, MD, PhD,‖ Michiie Sakamoto, MD, PhD,** Osamu Nakashima, MD, PhD,†† Yonson Ku, MD, PhD,‡‡ Norihiro Kokudo, MD, PhD,§§ and Masatoshi Makuuchi, MD, PhD¶¶; Liver Cancer Study Group of Japan*

Objective: To examine the prognostic factors and outcomes after several types of treatments in patients with hepatocellular carcinoma (HCC) negative for hepatitis B surface antigen and hepatitis C antibody, so-called "non-B non-C HCC" using the data of a nationwide survey.

Background: The proportion of non-B non-C HCC is rapidly increasing in Japan.

Methods: A total of 4741 patients with non-B non-C HCC, who underwent hepatic resection (HR, n = 2872), radiofrequency ablation (RFA, n = 432), and transcatheter arterial chemoembolization (TACE, n = 1437) as the initial treatment, were enrolled in this study. The exclusion criteria included extrahepatic metastases and/or Child-Pugh C. Significant prognostic variables determined by a univariate analysis were subjected to a multivariate analysis using a Cox proportional hazard regression model.

Results: The degree of liver damage in the HR group was significantly lower than that in the RFA and TACE groups. The HR and TACE groups had significantly more advanced HCC than the RFA group. The 5-year survival rates after HR, RFA, and TACE were 66%, 49%, and 32%, respectively. Stratifying the survival rates, according to the TNM stage and the Japan Integrated Staging (JIS) score, showed the HR group to have a significantly better prognosis than the RFA group in the stage II and in the JIS scores "1" and "2." The multivariate analysis showed 12 independent prognostic factors. HR offers significant prognostic advantages over TACE and RFA.

Conclusions: The findings of this large prospective cohort study indicated that HR may be recommended, especially in patients with TNM stage II and JIS scores "1" and "2" of non-B non-C HCC.

From the *Department of Surgery, The University of Tokushima, Japan; †Department of Gastroenterology and Hepatology, Kinki University School of Medicine, Japan; ‡Department of Hepatology and Gastroenterology, Juntendo Shizuoka Hospital, Japan; §Department of Radiology, Kanazawa University Graduate School of Medical Science, Japan; ¶Department of Gastroenterology and Hepatology, Musashino Red Cross Hospital, Japan; ‖Department of Biostatistics, School of Public Health, University of Tokyo, Japan; **Department of Pathology, Keio University School of Medicine, Japan; ††Department of Clinical Laboratory Medicine, Kurume University Hospital, Japan; ‡‡Department of Surgery, Kobe University Graduate School of Medicine, Japan; §§Department of Hepatobiliary and Pancreatic Surgery, University of Tokyo Graduate School of Medicine, Japan; and ¶¶Department of Surgery, Japanese Red Cross Medical Center, Japan.

Disclosure: This work was supported in part by Grants-in-Aid for Scientific Research (C) (24592003) and Grant-in-Aid for Challenging Exploratory Research (22659233), Japan Society for the Promotion of Science. The authors who have taken part in this study declared that they do not have anything to disclose regarding funding or conflict of interest with respect to this manuscript.

Supplemental digital content is available for this article. Direct URL citations appear in the printed text and are provided in the HTML and PDF versions of this article on the journal's Web site (www.annalsofsurgery.com).

Reprint: Tohru Utsunomiya, MD, PhD, Department of Surgery, The University of Tokushima, 3-18-15 Kuramoto, Tokushima 770-8503, JAPAN. E-mail: utsunomiya@clin.med.tokushima-u.ac.jp.

ISSN: 0003-4932/13/00000-0001
DOI: 10.1097/SLA.0b013e31829291e9

Keywords: hepatectomy, nationwide survey, non-B non-C, prognostic factor, radiofrequency ablation, transarterial chemoembolization

(*Ann Surg* 2013;00: 1–10)

Hepatocellular carcinoma (HCC) is the third leading cause of cancer-related deaths and fifth most common cancer worldwide.[1,2] Moreover, the incidence and mortality rate have been increasing in the United States and other countries.[3,4] The prominent etiological factors associated with HCC include chronic infection of hepatitis B virus (HBV) and hepatitis C virus (HCV), and chronic alcohol consumption. Although HCV-related HCC is responsible for the greatest proportion of HCC patients in Japan,[5,6] many hepatologists note that the proportion of HCC negative for hepatitis B surface antigen (HBsAg) and hepatitis C antibody (HCVAb), so-called "non-B non-C HCC," is rapidly increasing.[7,8] Indeed, a nationwide follow-up survey by the Liver Cancer Study Group of Japan (LCSGJ) found the proportions of HBV- and HCV-related HCC to have decreased over the previous decade, possibly thanks to the promotion of antiviral therapy, whereas the number of other HCC patients (mostly non-B non-C HCC) have more than doubled during the same period from 6.8% to 17.3%.[9] The exact background or molecular mechanisms for such a sharp increase in the incidence of non-B non-C HCC remain unclear at this point; however, nonalcoholic steatohepatitis (NASH) and metabolic syndrome are suggested to be important risk factors.[10] Nonetheless, it is crucial to elucidate clinicopathological characteristics including the prognostic factors of such patients with non-B non-C HCC at this moment.

Several studies, most of which enrolled around 100 patients or less, have investigated the clinical features of non-B non-C HCC to date.[11–16] However, the impact of the treatment, such as surgical treatment, local ablative therapy, and hepatic arterial embolization, for these patients has not been thoroughly examined. On the contrary, many studies have compared the outcomes after several therapeutic modalities for patients with HCC, and the results have been controversial because of the different therapeutic designs and small sample sizes.[17–21] All these findings prompted a study, clarifying the prognostic factors and the therapeutic impact of several types of treatment for the patients with non-B non-C HCC based on the data of the nationwide follow-up survey by the LCSGJ.

METHODS

A total of 62,321 patients with primary liver cancer were prospectively registered biannually from January 2000 to December 2005 by the LCSGJ using a registration/questionnaire sheet with more than 180 questions. They included 57,450 patients who were clinically diagnosed with HCC using multiple imaging modalities, clinical data, such as tumor markers, and/or histopathological

studies at each institution. Radiofrequency ablation (RFA) began to be more widely used in Japan in 2000. In addition, the data of the Child-Pugh class were requested on the form from the 16th survey. Therefore, the current study used the data from 2000 (16th survey) to 2005 (the latest 18th survey). In this study, 3447 patients for whom the data of hepatitis viral infection status of HBsAg and HCVAb were not available were excluded (Fig. 1), and 9307 of the remaining 54,003 patients with HCC (17.2%) were negative for both HBsAg and HCVAb (defined as "non-B non-C HCC").

The main purpose of this study was to compare the outcomes after hepatic resection (HR), RFA, and transcatheter arterial chemoembolization (TACE) in the non-B non-C HCC patients. The treatment algorithm for HCC proposed by Japanese guideline[22] indicates these 3 types of therapeutic modalities for patients without extrahepatic metastasis in the degree of liver damage A or B. The treatment algorithm[22] is based on 3 factors: "degree of liver damage" defined by the LCSGJ,[23] "number of tumors," and "tumor diameter." However, Child-Pugh class was adopted instead of the degree of liver damage because the former is globally used to evaluate liver function. Accordingly, the patients with extrahepatic metastasis (n = 944) and those in Child-Pugh C (n = 1028) were excluded. The study also excluded the 2192 patients who underwent the treatment other than the 3 types of therapeutic modalities described earlier. In addition, patients lacking outcome data were excluded (n = 402). Finally, 4741 non-B non-C HCC patients were selected in the current cohort study (Fig. 1) and classified according to the primary treatment into the HR group (n = 2,872), the RFA group (n = 432), and the TACE group (n = 1,437). In fact, the majority of Japanese patients with HCC are treated with 1 of the 3 types of treatment modalities, including surgical treatment, local ablative therapy, and hepatic arterial embolization. The questionnaire sheet of LCSGJ subclassified "Surgical treatment" into HR, liver transplantation, and others. "Local ablative therapy" includes RFA, ethanol injection therapy, microwave coagulation therapy, and others. "Hepatic arterial embolization" is subdivided into TACE (anticancer agents and lipiodol followed by gelatin sponge particles; this method was defined as "TACE" in this study), anticancer agents and lipiodol alone, anticancer agents and gelatin sponge particles alone, and others. The current investigation strictly selected HR, RFA, and TACE as the most frequently adopted and well-standardized therapeutic strategy from each type of treatment modality in Japan. Indeed, the 18th survey of LCSGJ found that approximately 97% of "Surgical treatment" was HR, 72% of "Local ablative therapy" was RFA, and 76% of "Hepatic arterial embolization" was TACE.

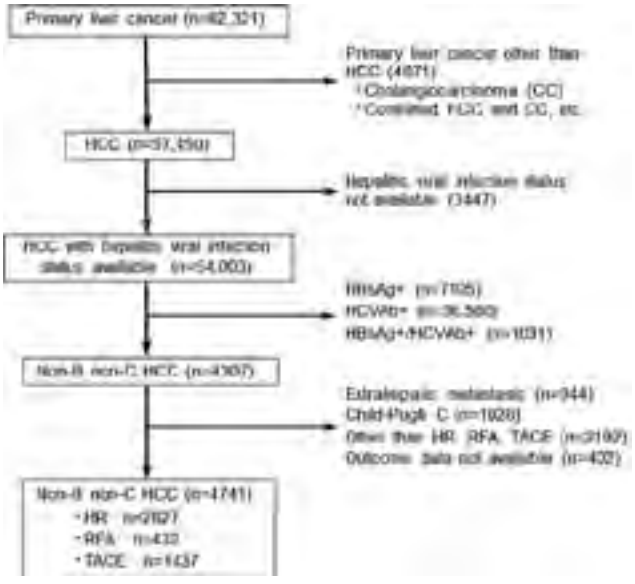

FIGURE 1. Flow chart of the patients with non-B non-C hepatocellular carcinoma (HCC) analyzed in this study.

The patients were prospectively followed up at each institution. Most of the patients have been traditionally observed according to the protocol, similar to the Japanese guidelines,[22] in which ultrasonography and measurement of the tumor markers every 3 or 4 months and enhanced computed tomography or magnetic resonance imaging every 6 or 12 months is recommended. The final prognosis of these registered patients was followed until confirmation of death at every survey.

The clinical characteristics among the 3 treatment groups were summarized in Table 1. All of the 19 variables were significantly different among the groups. Particularly, for the patients in the HR group, the positive percent of habitual alcohol consumption, defined as 86 g or more of ethanol per day over a 10-year period, was significantly lower than that in the RFA and TACE groups. The results of liver function tests, such as indocyanine green retention rate at 15 minutes (ICGR15) and prothrombin activity in this group, were significantly better than those in the RFA and TACE groups. These findings were well coordinated with the status of Child-Pugh class among the 3 groups. On the contrary, the HR and TACE groups had significantly more advanced HCC based on the most of tumor factors, such as the tumor size, tumor markers, and portal venous invasion, than the RFA group. However, the number of tumors in the HR group was the smallest, whereas that in the TACE group was largest. Liver-related deaths, such as those due to liver failure, in the RFA group were more frequently observed, whereas HCC-related deaths were more common in the HR and TACE groups (Table 1).

Statistical Analysis

The clinical characteristics among the 3 treatment groups were compared by either the chi-square test or the Kraskul-Wallis test. The survival rate after each treatment was calculated by the Kaplan–Meier method and then was compared by the log-rank test. The Bonferroni correction was applied for the multiple comparisons. Nineteen clinical variables, including type of treatment were evaluated by univariate analysis using a log-rank test to determine the prognostic factors in the patients with non-B non-C HCC. The survival rates after each treatment were stratified according to the TNM staging system defined by the LCSGJ (Table 2 and Table 3)[23] and the Japan Integrated Staging (JIS) score (Table 4).[24] Because the patients in Child-Pugh C were excluded in this study, JIS score "2" indicated either Child-Pugh class A/stage III or Child-Pugh class B/stage II, JIS score "3" indicated either Child-Pugh class A/stage IVA or Child-Pugh class B/stage III, and JIS core "4" indicated Child-Pugh class B/stage IVA.

Continuous variables were divided into 2 groups according to the median value. Significant variables with a *P* value less than 0.05 by the univariate analysis were subjected to multivariate analysis using a Cox proportional hazard regression model with backward elimination method.[25] All significance tests were 2-tailed, and a *P* value less than 0.05 was considered statistically significant. All statistical analyses were performed with the Statistical Analysis System (SAS) version 9.1.3 (SAS Inc, Cary, NC).

RESULTS

The follow-up periods after the treatment of HR, RFA, and TACE were 1.9 ± 1.6 years, 2.3 ± 1.4 years, and 1.5 ± 1.4 years, respectively. The 1-, 3-, and 5-year survival rates of the 4741 patients with non-B non-C HCC were 89%, 70%, and 55%, respectively.

TABLE 1. Clinical Characteristics in the Non-B Non-C HCC Patients Who Underwent 3 Types of Therapeutic Strategies

Variables	HR (n = 2872)	RFA (n = 432)	TACE (n = 1437)	*P*
Age (yr)	67 (50, 79)	68 (53, 81)	69 (53, 83)	<0.001
Gender				<0.001
Male	2332 (81%)	315 (73%)	1124 (78%)	
Female	540 (19%)	117 (27%)	313 (22%)	
Alcohol				<0.001
None	1,652 (58%)	209 (48%)	689 (48%)	
Positive*	874 (30%)	178 (41%)	619 (43%)	
Unknown	346 (12%)	45 (10%)	129 (9%)	
Serum albumin (g/dL)	4.0 (3.2, 4.7)	3.8 (2.9, 4.6)	3.7 (2.8, 4.5)	<0.001
Serum total bilirubin (mg/dL)	0.8 (0.4, 1.5)	1.1 (0.4, 2.4)	1.1 (0.4, 2.3)	<0.001
ICG R15 (%)	15 (4, 32)	26 (8, 52)	25 (5, 56)	<0.001
Prothrombin activity (%)	89 (65, 114)	80 (54, 104)	82 (55, 106)	< 0.001
Esophageal varices				<0.001
None	2231 (78%)	195 (45%)	740 (52%)	
Positive	276 (10%)	152 (35%)	489 (34%)	
Unknown	365 (13%)	85 (20%)	208 (15%)	
Degree of liver damage†				<0.001
A	2368 (83%)	224 (52%)	808 (56%)	
B	409 (14%)	132 (31%)	399 (28%)	
C	10 (0.3%)	14 (3%)	39 (3%)	
Unknown	85 (3%)	62 (14%)	191 (13%)	
Child-Pugh class				<0.001
A	2679 (93%)	316 (73%)	1068 (74%)	
B	193 (7%)	116 (27%)	369 (26%)	
Alpha-fetoprotein (ng/mL)	3491 (15, 16368)	215 (15, 927)	3177 (15, 13605)	<0.001
PIVKA-II (AU/mL)‡	2198 (40, 10000)	501 (40, 10000)	1905 (40, 10000)	<0.001
Tumor number				<0.001
1	2193 (76%)	293 (68%)	679 (47%)	
2	323 (11%)	85 (20%)	256 (18%)	
>3	126 (4%)	28 (7%)	126 (9%)	
Tumor size (mm)	5.8 (1.8, 14)	3.0 (1.1, 6)	5.0 (1.4, 13)	<0.001
Gross classification§				<0.001
Type 1	2362 (82%)	407 (94%)	1181 (82%)	
Type 2	199 (7%)	9 (2%)	160 (11%)	
Type 3	21 (0.7%)	2 (0.5%)	39 (3%)	
Unknown	290 (10%)	14 (3%)	57 (4%)	
Portal venous invasion				<0.001
Negative	2336 (81%)	403 (93%)	1218 (85%)	
Positive	342 (12%)	8 (2%)	179 (10%)	
Unknown	194 (7%)	21 (5%)	76 (5%)	
TNM stage†				<0.001
I	251 (9%)	119 (28%)	160 (11%)	
II	1489 (52%)	189 (44%)	550 (38%)	
III	707 (25%)	75 (17%)	517 (36%)	
IVA	321 (11%)	4 (1%)	74 (5%)	
Unknown	85 (3%)	45 (10%)	136 (10%)	
JIS score				<0.001
0	233 (8%)	87 (20%)	116 (8%)	
1	1423 (50%)	173 (40%)	466 (32%)	
2	732 (26%)	103 (24%)	514 (36%)	
3	374 (13%)	23 (5%)	184 (13%)	
4	25 (1%)	1 (0.2%)	21 (2%)	
Unknown	85 (3%)	45 (10%)	136 (10%)	
Cause of death				<0.001
HCC-related	302 (63%)	41 (38%)	271 (62%)	
Liver-related	69 (14%)	31 (29%)	94 (22%)	
Treatment-related	15 (3%)	2 (2%)	1 (0.2%)	
Others	96 (20%)	34 (32%)	68 (16%)	
Median follow-up period (yr)	1.9 (0.1, 5.1)	2.3 (0.1, 4.7)	1.5 (0.1, 4.3)	<0.001

Data are shown as the median (5 percentile, 95 percentile) unless specified.
*Eighty-six gram of alcohol daily for more than 10 years.
†By the Liver Cancer Study Group of Japan.
‡Questionnaire sheet requested the actual value when it was between 40 and 10,000 AU/mL.
§Type 1, simple nodular type; Type 2, simple nodular type with extranodular growth; Type 3, confluent multinodular type.

TABLE 2. TNM Stage by the Liver Cancer Study Group of Japan

	T Category	N Category	M Category
Stage I	T1	N0	M0
Stage II	T2	N0	M0
Stage III	T3	N0	M0
Stage IVA	T4	N0	M0
	T1, T2, T3, T4	N1	M0
Stage IVB	T1, T2, T3, T4	N0, N1	M1

The grade for each category is determined individually, and the staging of the disease is determined according to the aforementioned chart.

M1 indicates presence of distant metastasis; N1: presence of lymph node metastasis.

TABLE 3. T Category of the TNM Stage by the Liver Cancer Study Group of Japan

	T1		T2		T3		T4	
No. tumor: multiple	−	+	−	−	+	+	−	+
Tumor diameter: >2 cm	−	−	+	−	+	−	+	+
Vascular and/or bile duct invasion	−	−	−	+	−	+	+	+

The T category is determined on the basis of the "number," "size," and "vascular and/or bile duct invasion" by the tumor. All multiple tumors, including multicentric tumors and intrahepatic metastatic tumors, are counted.

TABLE 4. Definition and Criteria for the JIS Score

	0	1	2	3
Child-Pugh class	A	B	C	
TNM stage*	I	II	III	IV

JIS score = Child-Pugh class + TNM stage.

*By the Liver Cancer Study Group of Japan.

Prognostic Factors and Survival Rates

Nineteen clinical variables were screened as prognostic factors using a univariate analysis (Table 5). Gender and habitual alcohol intake were not selected as prognostic factors, whereas the remaining 17 variables, including age, serum albumin, serum total bilirubin, ICGR15, prothrombin activity, esophageal varices, degree of liver damage, Child-Pugh class, alpha-fetoprotein, protein induced by Vitamin K absence-II (PIVKA-II), tumor number, tumor size, gross classification, portal venous invasion, TNM stage, JIS score, and type of treatment, were significant prognostic factors. With the Child-Pugh class, 5-year survival rates of grades A and B were 58% and 31%, respectively, with statistical significance ($P < 0.001$; Fig. 2A). The TNM staging system by the LCSGJ[23] revealed that 5-year survival rates in stages I, II, III, and IVA were 66%, 64%, 46%, and 19%, respectively. A good separation, except stage I vs II, was observed (Fig. 2B). The 5-year survival rates based on a JIS score of 0, 1, 2, 3, and 4 were 70%, 67%, 44%, 23%, and 0%, respectively. There was a good separation, except JIS score "0" vs "1" (Fig. 2C). The 5-year survival rates after HR, RFA, and TACE were 66%, 49%, and 32%, respectively (Fig. 2D). There was no significant difference between the HR group and the RFA group ($P = 0.101$).

However, when the survival rates were stratified according to the TNM staging system (Fig. 3), the HR group showed a significantly better prognosis than the TACE group in all 4 stages (stage I to IVA). The RFA group had a significantly better prognosis than the TACE group only in the stage II and III. A comparison between the HR group and the RFA group showed that the HR group had a significantly better prognosis than the RFA group in stage II (Fig. 3B). However, there were no statistically significant differences between the 2 groups in stages I, III, and IVA. The survival rates in the stage II patients were further stratified according to each T category (Table 3) on the basis of the "number of tumors: multiple," "tumor diameter > 2 cm," and "vascular and/or bile duct invasion" by the tumor (Fig. 4). The HR group had a significantly better prognosis than the RFA group in all 3 T categories. The effectiveness of RFA was almost identical to that of TACE in the stage II patients with multiple tumors (Fig. 4A) and only HR could provide long-term survival in the stage II patients with vascular and/or bile duct invasion (Fig. 4C).

Similarly, stratifying survival rates according to the JIS score (Fig. 5) showed that the HR group had a significantly better prognosis than the TACE group in all the 4 scores (JIS score "0" to "3"). The RFA group had a significantly better prognosis than the TACE group only in the JIS score "1" and "3." A comparison between the HR group and the RFA group revealed that the former had a significantly better prognosis than the later in the JIS scores "1" and "2" (Figs. 5B, C). In contrast, the RFA group had an even better prognosis than the HR group in the JIS score "3" (Fig. 5D). The survival rates in the JIS scores "1," "2," and "3" were further stratified according to each criterion (Table 4) on the basis of the "Child-Pugh class" and "TNM stage" (Supplemental Figs 1–3, available at http://links.lww.com/SLA/A388, http://links.lww.com/SLA/A389, and http://links.lww.com/SLA/A390).

Analysis of the Factors Independently Affecting the Survival of Patients

The multivariate initial model provided 11 variables as independent prognostic factors: age, serum albumin, ICGR15, esophageal varices, Child-Pugh class, alpha-fetoprotein, PIVKA-II, tumor size, gross classification, TNM stage, and type of treatment (Supplemental Table 1, available at http://links.lww.com/SLA/A387). Consequently, the multivariate final model showed 12 variables as independent prognostic factors: the 11 variables described earlier and portal venous invasion (Table 6). The stage IVA and gross classification type 3 (confluent multinodular type) had the highest hazard ratio of 3.83 and 2.86, respectively. In particular, the univariate analysis showed no significant difference between the HR group and the RFA group (Table 5), but the multivariate analysis revealed a statistically significant difference (hazard ratio: 1.54, $P = 0.014$) between the 2 groups.

DISCUSSION

In general, it is theoretically difficult to clarify the prognostic factors and therapeutic outcomes after treatments for patients with HCC due to the diversities of tumor stage, degree of chronic liver damage, and therapeutic design, as well as variable etiologic factors of HCC. The present study focused on a relatively small proportion of patients with non-B non-C HCC in Japan, which were further restricted to the patients without extrahepatic metastasis in the Child-Pugh A or B, and which principally met the indications for HR, RFA, and TACE based on the treatment guideline.[22] It was obvious that such strict selection of patients requires huge number of patients to be analyzed. Therefore, the present study used the data of a nationwide follow-up survey by the LCSGJ.

The study first compared the clinical backgrounds among the patients who underwent HR, RFA, or TACE as the initial therapy (Table 1). The degree of liver damage in the HR group was significantly lower than those in the RFA and TACE groups. On the contrary, the HR and TACE groups had significantly more advanced HCC than the RFA group. These findings seem to be consistent with

TABLE 5. Prognostic Factors Determined by the Univariate Analysis in the Patients with Non-B Non-C Hepatocellular Carcinoma

		Survivals (%)			
Variables	**No. Patient**	**1-yr**	**3-yr**	**5-yr**	***P***
All	4741	89	70	55	
Age (yr)					
<69	2289	88	72	58	Reference
≥69	2438	90	69	50	0.046
Gender					
Male	3771	88	71	56	Reference
Female	970	91	66	51	0.312
Alcohol					
None	2550	89	69	56	Reference
Positive*	1671	89	72	52	0.907
Serum albumin (g/dL)					
<3.9	2004	85	61	42	Reference
≥3.9	2645	92	76	63	<0.001
Serum total bilirubin (mg/dL)					
<0.8	2004	90	74	61	Reference
≥0.8	2645	88	67	48	<0.001
ICGR15 (%)					
<14	1809	90	75	75	Reference
≥14	1896	89	68	68	<0.001
Prothrombin activity (%)					
<87	2177	88	66	48	Reference
≥87	2239	89	73	61	<0.001
Esophageal varices					
None	3166	90	74	60	Reference
Positive	917	85	58	32	<0.001
Degree of liver damage†					
A	3400	90	90	60	Reference
B	940	85	85	39	<0.001
C	63	68	68	–	<0.001
Child-Pugh class					
A	4063	90	73	58	Reference
B	678	81	51	31	<0.001
Alpha-fetoprotein (ng/mL)					
<15	2638	95	80	63	Reference
≥15	1915	81	57	43	<0.001
PIVKA-II (AU/mL)					
<148	2069	94	79	66	Reference
≥148	2074	84	62	45	<0.001
Tumor number					
1	3165	91	76	62	Reference
>2	1461	84	56	38	<0.001
Tumor size (mm)					
<40	2128	94	77	58	Reference
≥40	2455	85	65	53	<0.001
Gross classification‡					
Type 1	3950	91	73	57	Reference
Type 2	368	70	41	32	<0.001
Type 3	62	55	32	0	<0.001
Portal venous invasion					
Negative	3957	91	73	57	Reference
Positive	493	67	41	24	<0.001
TNM stage†					
I	530	96	83	66	Reference
II	2228	93	78	64	0.121
III	1299	87	62	46	<0.001
IVA	399	64	35	19	<0.001
JIS score					
0	436	97	85	70	Reference
1	2062	94	81	67	0.208
2	1349	87	62	44	<0.001
3	581	71	41	23	<0.001
4	47	49	9	0	<0.001
Type of treatment					
HR	2872	91	77	66	Reference
RFA	432	93	73	49	0.101
TACE	1437	83	55	32	<0.001

*Eighty-six gram of alcohol daily for more than 10 yrs.
†By the Liver Cancer Study Group of Japan.
‡Type 1, simple nodular type; Type 2, simple nodular type with extranodular growth; Type 3, confluent multinodular type.

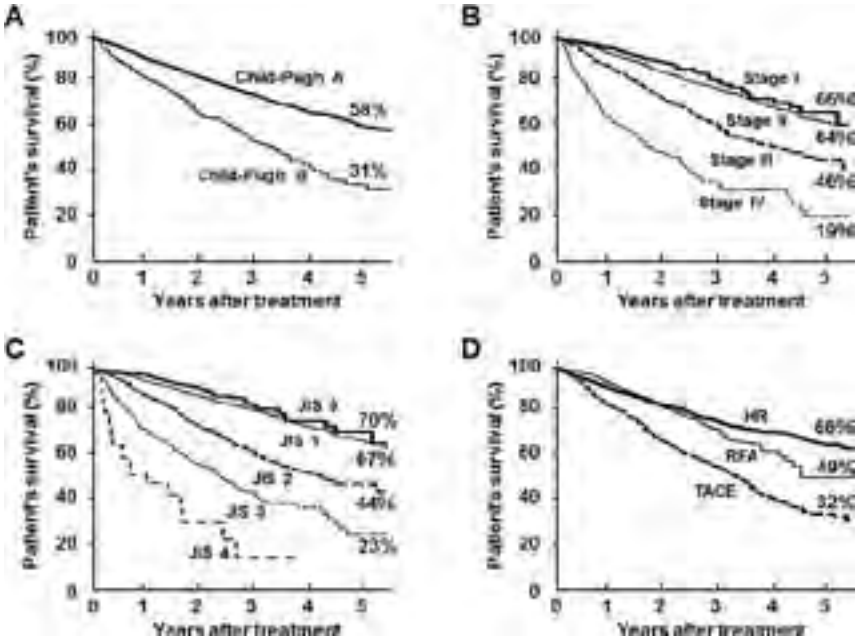

FIGURE 2. Comparisons of the survival rates among liver function, tumor stage, and type of treatment. Survival rates stratified by Child-Pugh A and B (A), staging system according to the Liver Cancer Study Group of Japan (B), JIS score (C), and type of treatment (D). HR vs RFA, $P = 0.30$; HR vs TACE, $P < 0.001$; RFA vs TACE, $P < 0.001$. All comparisons were made the log-rank test with Bonferroni correction.[24]

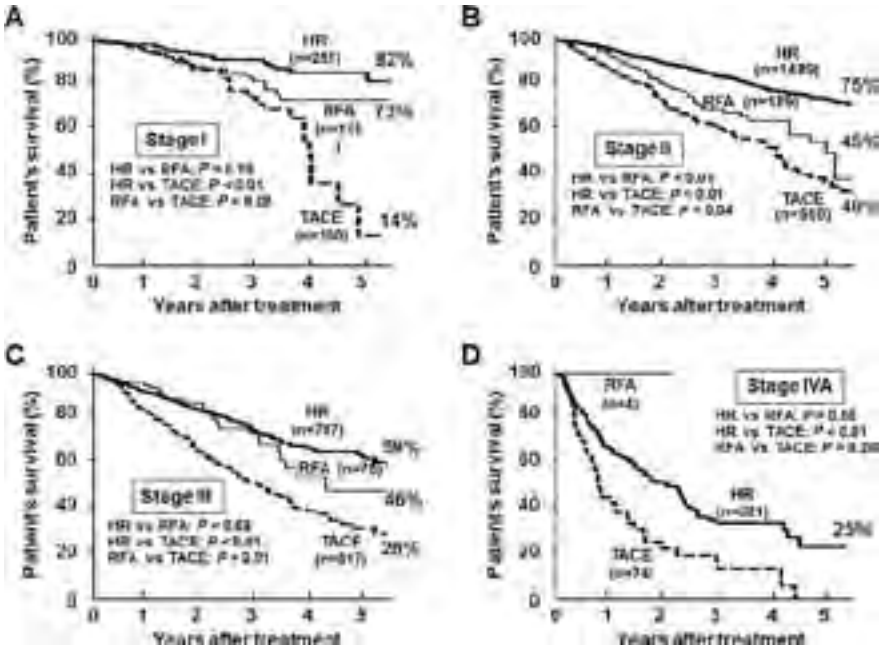

FIGURE 3. Comparisons of the survival rates among the type of treatment. Survival rates were stratified by stage I (A), stage II (B), stage III (C), and stage IVA (D). All comparisons were made by the log-rank test with Bonferroni correction.

those in other studies that included the patients with HCC of varied etiologies of liver disease. However, none of the previous studies have compared the prognostic factors and therapeutic outcomes after the 3 types of treatment modalities with taking such differences in the clinical backgrounds into consideration, possibly due to the limited number of patients.

The study then analyzed the prognostic factors and found that 17 variables, including types of treatment, were significant prognostic factors. Gender and alcohol abuse were not selected as prognostic factors. Although the synergic action of alcohol and HCV infection on hepatocarcinogenesis has been suggested,[26] alcohol consumption alone may not always affect the progression of HCC. The 5-year survival rate in the TACE group (32%) was significantly poorer, whereas there was no significant difference between the RFA group (49%) and the HR group (66%) in the univariate analysis. The 5-year survival rate after TACE in this series (32%) was almost identical to that (34%) based on the data of same nationwide survey (LCSGJ) during the same periods (January 2000–December 2005) but not restricted to the patients with non-B non-C HCC.[27] Hasegawa et al[18] also used the data of the nationwide survey by LCSGJ and compared the prognosis after surgical resection, RFA, and percutaneous ethanol injection. Their evaluation of more than 7000 HCC patients revealed that the time-to-recurrence rate of surgical resection was significantly better than that of RFA or percutaneous ethanol injection. However, the median follow-up period was only 10.4 months, and they did not provide the 5-year survival rate in their study.

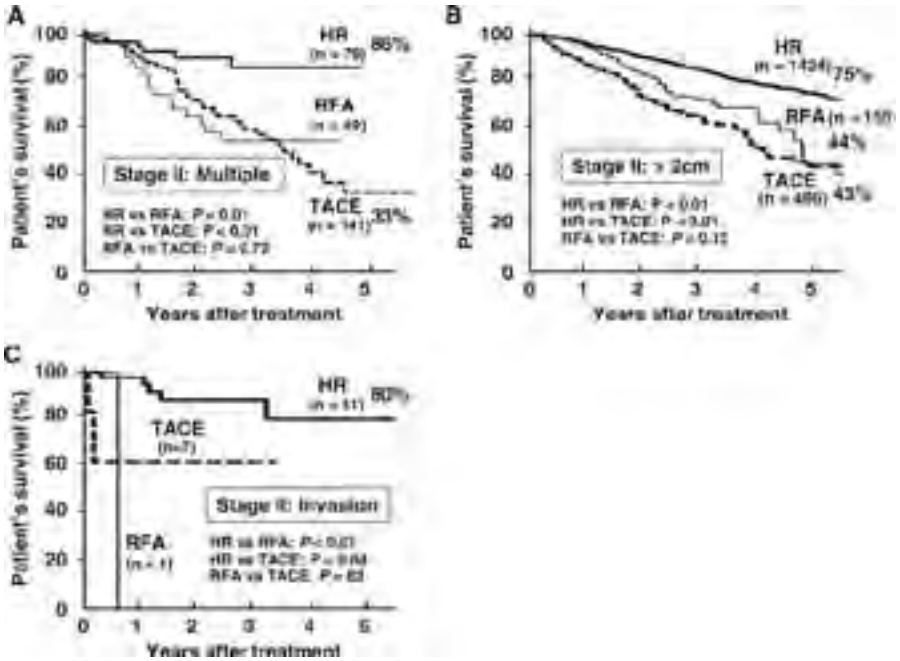

FIGURE 4. Comparisons of the survival rates based on the type of treatment. The survival rates in the stage II were further stratified by number of tumor (A), tumor size (B), and vascular and/or bile duct invasion (C). All comparisons were made by the log-rank test with Bonferroni correction.

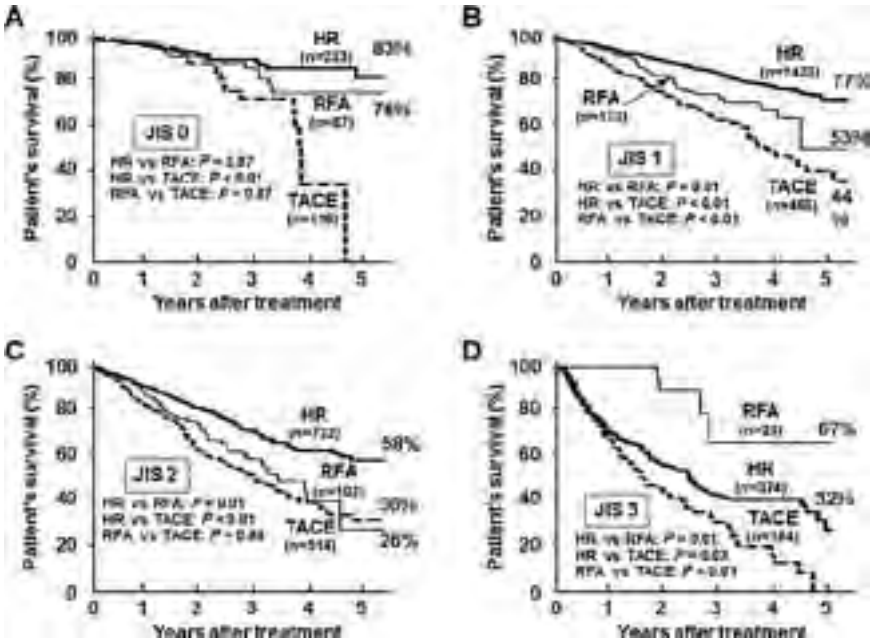

FIGURE 5. Comparisons of the survival rates among the type of treatment. Survival rates were stratified by JIS score "0" (A), JIS score "1" (B), JIS score "2" (C), and JIS score "3" (D). All comparisons were made by log-rank test with Bonferroni correction. [24]

The patients in the TACE group had poorer liver functional reserve and more advanced stage of HCC, thus it would be quite natural that overall survival rate in this group had a poorer prognosis. Because the degree of chronic liver damage and the tumor stage were markedly different among the HR, RFA, and TACE groups, the patients were stratified according to the TNM stage. The study also stratified the patients on the basis of the JIS score.[24] Particularly, the HR group had a significantly better prognosis than the TACE group in all 4 stages and the 4 JIS scores even after the stratifications. On the contrary, the prognosis for the patients in the RFA group did not differ significantly in comparison with those in the TACE group in stages I and IVA and JIS scores "0 and 2." The comparison between the HR group and the RFA group showed the HR group to have a significantly better prognosis than the RFA group only in stage II and in JIS scores "1" and "2." These findings suggest that the HR may not offer prognostic advantages over RFA in the early or far advanced stage of non-B non-C HCC patients. Because the stage II patients included the 3 different types of T categories (Table 3), the survival rates were further stratified on the basis of the T categories (Fig. 4). The HR group had a significantly better prognosis than the RFA group, especially for the patients with multiple tumors and with vascular and/or bile duct invasion. Long-term survival could be expected only after HR in the stage II patients with vascular and/or bile duct invasion (Fig. 4C). Similarly, the survival rates in the

TABLE 6. Independent Prognostic Factors Determined by the Cox Proportional Hazard Regression Analysis With the Backward Elimination Method (Multivariate Final Model)

Variables	No. Patient	Hazard Ratio (95% CI)	*P*
Age (yr)			
<69	1125	Reference	—
≥69	1174	1.37 (1.13, 1.66)	0.001
Serum albumin (g/dL)			
<3.9	939	Reference	—
≥3.9	1360	0.81 (0.66, 0.99)	0.047
ICGR15 (%)			
<14	1129	Reference	—
≥14	1170	1.29 (1.04, 1.59)	0.021
Esophageal varices			
None	1844	Reference	—
Positive	455	1.71 (1.34, 2.17)	<0.001
Child-Pugh class			
A	2032	Reference	—
B	267	1.46 (1.10, 1.92)	0.008
Alpha-fetoprotein (ng/mL)			
<15	1354	Reference	—
≥15	945	1.46 (1.20, 1.79)	<0.001
PIVKA-II (AU/mL)			
<148	1149	Reference	—
≥148	1150	1.60 (1.28, 1.99)	<0.001
Tumor size (mm)			
<40	1015	Reference	—
≥40	1284	1.36 (1.07, 1.74)	0.013
Gross classification*			
Type 1	2105	Reference	—
Type 2	171	1.59 (1.18, 2.12)	0.002
Type 3	23	2.86 (1.48, 5.51)	0.002
Portal venous invasion			
Negative	2068	Reference	—
Positive	231	1.41 (1.04, 1.91)	0.025
TNM stage†			
I	257	Reference	—
II	1168	1.51 (0.97, 2.33)	0.062
III	677	1.96 (1.25, 3.05)	0.003
IVA	197	3.83 (2.27, 6.47)	<0.001
Type of treatment			
HR	1644	Reference	—
RFA	167	1.54 (1.09, 2.19)	0.014
TACE	488	1.56 (1.23, 1.97)	< 0.001

*Type 1, simple nodular type; Type 2, simple nodular type with extranodular growth; Type 3, confluent multinodular type.
†By the Liver Cancer Study Group of Japan.

patients with JIS scores of "1" and "2" were further stratified (Supplemental Figs. 1, 2, available at http://links.lww.com/SLA/A388 and http://links.lww.com/SLA/A389). The effect of HR was observed only in the patients with Child-Pugh class A. Interestingly, the patients in the RFA group (n = 23) in the JIS score "3" subgroup had a significantly better prognosis than the HR group (n = 374). However, after further stratification (Supplemental Fig. 3, available at http://links.lww.com/SLA/A390), there was no statistically significant difference between the 2 groups, possibly because of the small number of patients. A possible therapeutic advantage of RFA in the JIS score "3" patients remains to be confirmed.

Surgical hepatectomy provides better survival and lower recurrence rates than RFA for patients with HCC conforming to the Milan criteria in a randomized clinical trial.[19] The authors considered that segment-based anatomic hepatectomy with at least 1 cm of the rim of nontumor parenchyma eradicates both the primary tumor and intrahepatic micrometastasis. There are 2 types of HCC recurrence; one is "early recurrence" due to intrahepatic metastasis and the other is "late recurrence" due to multicentric hepatocarcinogenesis.[28] Recurrence in non-B non-C HCC are mainly dependent on the advanced tumor factors, such as lager tumor size and portal venous invasion, and thus local control of microscopic intrahepatic metastases is required.[29] The importance of an adequate surgical margin for the non-B non-C HCC has also been reported.[14] Therefore, HR, if a segment-based anatomic hepatectomy is deemed to be possible, should be recommended especially for the patients with stage II or the JIS scores "1" and "2" of non-B non-C HCC. Anatomic hepatectomy with adequate surgical margin may decrease the risk of "early recurrence" of non-B non-C HCC due to intrahepatic metastasis. However, the prediction and prevention of "late recurrence" of non-B non-C HCC due to de novo hepatocarcinogenesis may be difficult, because the background liver diseases can be multifactorial and non-B non-C HCC may develop without displaying any features of severe underlying fibrosis.[29–32] In fact, 13,572 patients underwent HR among the 54,003 total patients for whom the data regarding the hepatitis viral infection status were available (Fig. 1). The incidence of liver cirrhosis based on

the histological examination of resected specimens was 1130 of 2495 patients (45%) with HBV-related HCC, 3666 of 7783 patients (47%) with HCV-related HCC, and 788 of 3040 patients (26%) with non-B non-C HCC, indicating that there was a markedly lower incidence of cirrhosis in the non-B non-C HCC patients. Information regarding the possible etiologies of non-B non-C HCC, such as NASH, diabetes mellitus, autoimmune hepatitis, primary biliary cirrhosis, aflatoxin-B1-contaminated food consumption, and hemochromatosis was not available because of lack of inclusion in the questionnaire sheet of this survey. However, according to the reports describing the recent trend of clinical features in Japanese patients with HCC,[10,33] it is conceivable that a nonnegligible proportion of patients in this study met the criteria for the metabolic syndrome. Potential carcinogenic mediators related to NASH in metabolic syndrome are insulin, lipid peroxidation, free radical oxidative stress, and proinflammatory cytokines.[34–36] Because HCC associated with metabolic syndrome can often develop without significant liver fibrosis,[31,32] metabolic syndrome per se may have a direct oncogenic effect, and it may follow a specific molecular pathway of tumorigenesis different from the usual multistep process: fibrosis-cirrhosis-HCC.[31] In this context, specific strategies for screening "late recurrence" may be required for patients with HCC related to metabolic syndrome, even when underlying chronic liver damage is only minimal.

The molecular mechanisms underlying the individual predisposition to non-B non-C HCC may be different, and a better understanding of these mechanisms will lead to improvements in the prevention and early diagnosis of "late recurrence."[9] Because the number of patients with each etiology is limited, a prospective accumulation of non-B non-C HCC patients including information regarding the possible etiologies is essential, and a nationwide multi-institutional study would be desirable.

Finally, 12 independent prognostic factors, including the type of treatment, were identified by using the Cox proportional hazard regression analysis. There was a significant prognostic advantage of HR not only to TACE but also to RFA. Many studies have compared the outcomes after several therapeutic modalities for patients with HCC,[17–21] most of which compared HR versus RFA, whereas a few studies compared HR versus TACE or RFA versus TACE. This is the first study to compare the prognostic factors and outcomes after 3 types of therapeutic modalities at once. All these findings regarding the non-B non-C HCC patients in Japan may be applicable to the HCC patients in the United States and Western countries where the prominent etiological factors are NASH and metabolic syndrome rather than chronic infection of hepatitis viruses.

Limitations of this study include that the data of TNM staging system of the American Joint Committee on Cancer (AJCC)/International Union Against Cancer (UICC) were not available to directly apply the current data to the HCC patients in other countries. However, both the TNM stage by the LCSGJ and the AJCC/UICC were developed on the basis of a survival analysis of patients who underwent HR. Therefore, the applicability of these surgical staging systems to other therapies, such as RFA and TACE, has been a matter of controversy.[37] Comparisons of clinicopathological features and prognostic factors between the non-B non-C HCC and HCC caused by other etiological factors, such as HBV- and HCV-related HCC, are beyond the scope of this study. Because the current study was not prospectively randomized, the treatment polices were not regulated and the effectiveness of each treatment might not be comparable among the different institutions. In addition, although this study used a multivariate analysis to assess the impact of diverse background on outcomes, there are limits to such a statistical approach.

CONCLUSIONS

This large prospective study based on data derived from a nationwide follow-up survey suggested that HR offers prognostic advantage over RFA and TACE although such advantage may depend upon the degrees of chronic liver damage and the tumor stage.

REFERENCES

1. Llovet JM, Burroughs A, Bruix J. Hepatocellular carcinoma. *Lancet*. 2003;362:1907–1917.
2. Jemal A, Siegel R, Xu J, et al. Cancer statistics, 2010. *CA Cancer J Clin.* 2010;60:277–300.
3. El-Serag HB, Mason AC. Rising incidence of hepatocellular carcinoma in the United States. *N Engl J Med.* 1999;340:745–750.
4. Altekruse SF, McGlynn KA, Reichman ME. Hepatocellular carcinoma incidence, mortality, and survival trends in the United States from 1975 to 2005. *J Clin Oncol.* 2009;27:1485–1491.
5. Ikai I, Arii S, Okazaki M, et al. Report of the 17th nationwide follow-up survey of primary liver cancer in Japan. *Hepatol Res.* 2007;37:676–691.
6. Namiki I, Nishiguchi S, Hino K, et al. Management of hepatitis C: report of the consensus meeting at the 45th annual meeting of the Japan Society of Hepatology (2009). *Hepatol Res.* 2010;40:347–368.
7. Umemura T, Kiyosawa K. Epidemiology of hepatocellular carcinoma in Japan. *Hepatol Res.* 2007;37(suppl 2):S95–S100.
8. Tanaka H, Imai Y, Hiramatsu N, et al. Declining incidence of hepatocellular carcinoma in Osaka, Japan, from 1990 to 2003. *Ann Intern Med.* 2008;148:820–826.
9. Utsunomiya T, Shimada M. Molecular characteristics of non-cancerous liver tissue in non-B non-C hepatocellular carcinoma. *Hepatol Res.* 2011;41:711–721.
10. Nagaoki Y, Hyogo H, Aikata H, et al. Recent trend of clinical features in patients with hepatocellular carcinoma. *Hepatol Res.* 2012;42:368–375.
11. Hatanaka K, Kudo M, Fukunaga T, et al. Clinical characteristics of NonB NonC-HCC: comparison with HBV and HCV related HCC. *Intervirology.* 2007;50:24–31.
12. Abe H, Yoshizawa K, Kitahara T, et al. Etiology of non-B non-C hepatocellular carcinoma in the eastern district of Tokyo. *J Gastroenterol.* 2008;43:967–974.
13. Ikeda K, Kobayashi M, Someya T, et al. Occult hepatitis B virus infection increases hepatocellular carcinogenesis by eight times in patients with non-B, non-C liver cirrhosis: a cohort study. *J Viral Hepat.* 2009;16:437–443.
14. Shinkawa H, Uenishi T, Takemura S, et al. Risk factors for postoperative recurrence of non-B non-C hepatocellular carcinoma. *J Hepatobiliary Pancreat Sci.* 2010;17:291–295.
15. Kim SK, Marusawa H, Eso Y, et al. Clinical characteristics of non-B non-C hepatocellular carcinoma: a single-center retrospective study. *Digestion.* 2011;84(suppl 1):43–49.
16. Nakajima T, Nakashima T, Yamaoka J, et al. Greater age and hepatocellular aging are independent risk factors for hepatocellular carcinoma arising from non-B non-C non-alcoholic chronic liver disease. *Pathol Int.* 2011;61:572–576.
17. Chok KS, Ng KK, Poon RT, et al. Comparable survival in patients with unresectable hepatocellular carcinoma treated by radiofrequency ablation or transarterial chemoembolization. *Arch Surg.* 2006;141:1231–1236.
18. Hasegawa K, Makuuchi M, Takayama T, et al. Surgical resection vs. percutaneous ablation for hepatocellular carcinoma: a preliminary report of the Japanese nationwide survey. *J Hepatol.* 2008;49:589–594.
19. Huang J, Yan L, Cheng Z, et al. A randomized trial comparing radiofrequency ablation and surgical resection for HCC conforming to the Milan criteria. *Ann Surg.* 2010;252:903–912.
20. Cho YK, Kim JK, Kim WT, et al. Hepatic resection versus radiofrequency ablation for very early stage hepatocellular carcinoma: a Markov model analysis. *Hepatology.* 2010;51:1284–1290.
21. Luo J, Peng ZW, Guo RP, et al. Hepatic resection versus transarterial lipiodol chemoembolization as the initial treatment for large, multiple, and resectable hepatocellular carcinomas: a prospective nonrandomized analysis. *Radiology.* 2011;259:286–295.
22. Makuuchi M, Kokudo N, Arii S, et al. Development of evidence-based clinical guidelines for the diagnosis and treatment of hepatocellular carcinoma in Japan. *Hepatol Res.* 2008;38:37–51.
23. The Liver Cancer Study Group of Japan. The general rules for the clinical and pathological study of primary liver cancer. 2nd English ed. Tokyo, Japan: Kanehara & Co, Ltd; 2003.

24. Kudo M, Chung H, Haji S, et al. Validation of a new prognostic staging system for hepatocellular carcinoma: the JIS score compared with the CLIP score. *Hepatology.* 2004;40:1396–1405.
25. Schneider HJ, Wallaschofski H, Völzke H, et al. Incremental effects of endocrine and metabolic biomarkers and abdominal obesity on cardiovascular mortality prediction. *PLoS One.* 2012;7:e33084.
26. Alisi A, Ghidinelli M, Zerbini A, et al. Hepatitis C virus and alcohol: same mitotic targets but different signaling pathways. *J Hepatol.* 2011;54:956–963.
27. Takayasu K, Arii S, Kudo M, et al. Superselective transarterial chemoembolization for hepatocellular carcinoma. Validation of treatment algorithm proposed by Japanese guidelines. *J Hepatol.* 2012;56:886–892.
28. Utsunomiya T, Shimada M, Imura S, et al. Molecular signatures of noncancerous liver tissue can predict the risk for late recurrence of hepatocellular carcinoma. *J Gastroenterol.* 2010;45:146–152.
29. Wakai T, Shirai Y, Yokoyama N, et al. Hepatitis viral status affects the pattern of intrahepatic recurrence after resection for hepatocellular carcinoma. *Eur J Surg Oncol.* 2003;29:266–271.
30. Kondo K, Chijiiwa K, Funagayama M, et al. Differences in long-term outcome and prognostic factors according to viral status in patients with hepatocellular carcinoma treated by surgery. *J Gastrointest Surg.* 2008;12:468–476.
31. Paradis V, Zalinski S, Chelbi E, et al. Hepatocellular carcinomas in patients with metabolic syndrome often develop without significant liver fibrosis: a pathological analysis. *Hepatology.* 2009;49:851–859.
32. Reddy SK, Steel JL, Chen HW, et al. Outcomes of curative treatment for hepatocellular cancer in nonalcoholic steatohepatitis versus hepatitis C and alcoholic liver disease. *Hepatology.* 2012;55:1809–1819.
33. Okanoue T, Umemura A, Yasui K, et al. Nonalcoholic fatty liver disease and nonalcoholic steatohepatitis in Japan. *J Gastroenterol Hepatol.* 2011;26:153–162.
34. Eckel RH, Grundy SM, Zimmet PZ. The metabolic syndrome. *Lancet.* 2005;365:1415–1428.
35. Siegel AB, Zhu AX. Metabolic syndrome and hepatocellular carcinoma: two growing epidemics with a potential link. *Cancer.* 2009;115:5651–5661.
36. Starley BQ, Calcagno CJ, Harrison SA. Nonalcoholic fatty liver disease and hepatocellular carcinoma: a weighty connection. *Hepatology.* 2010;51:1820–1832.
37. Minagawa M, Ikai I, Matsuyama Y, et al. Staging of hepatocellular carcinoma assessment of the Japanese TNM and AJCC/UICC TNM systems in a cohort of 13,772 patients in Japan. *Ann Surg.* 2007;245:909–922.

Liver INTERNATIONAL
OFFICIAL JOURNAL OF THE INTERNATIONAL ASSOCIATION FOR THE STUDY OF THE LIVER

Liver International ISSN 1478-3223

REVIEW ARTICLE

Re-evaluating transarterial chemoembolization for the treatment of Hepatocellular Carcinoma: Consensus recommendations and review by an International Expert Panel

Ann Lii Cheng[1], Deepak Amarapurkar[2], Yee Chao[3], Pei-Jer Chen[4], Jean-François Geschwind[5], Khean L. Goh[6], Kwang-Hyub Han[7], Masatoshi Kudo[8], Han Chu Lee[9], Rheun-Chuan Lee[10], Laurentius A. Lesmana[11], Ho Yeong Lim[12], Seung Woon Paik[13], Ronnie T. Poon[14], Chee-Kiat Tan[15], Tawesak Tanwandee[16], Gaojun Teng[17] and Joong-Won Park[18]

1 Department of Oncology and Internal Medicine, National Taiwan University Hospital, Taipei, Taiwan
2 Department of Gastroenterology, Bombay Hospital and Medical Research Centre, Mumbai, India
3 Division of Chemoradiotherapy, Cancer Centre Taipei Veterans General Hospital, Taipei, Taiwan
4 Graduate Institute of Clinical Medicine, College of Medicine, Taiwan National University, Taipei, Taiwan
5 Johns Hopkins University School of Medicine, Baltimore, Maryland, USA
6 Division of Gastroenterology, Department of Medicine, University of Malaya, Kuala Lumpur, Malaysia
7 Department of Internal Medicine, Yonsei University College of Medicine, Seoul, Korea
8 Department of Hepatology and Gastroenterology, Kinki University School of Medicine, Ohnohigashi, Osaka-Sayama, Japan
9 Department of Internal Medicine, Asan Medical Center, University of Ulsan College of Medicine, Seoul, Korea
10 Department of Radiology, Taipei Veterans General Hospital, Taipei, Taiwan
11 Hepatology Section, Department of Internal Medicine, Faculty of Medicine, University of Indonesia, Jakarta, Indonesia
12 Division of Hematology-Oncology, Department of Medicine, Samsung Medical Center, Seoul, Korea
13 Department of Medicine, Samsung Medical Center, Sungkyunkwan University School of Medicine, Seoul, Korea
14 Department of Surgery, Queen Mary Hospital, University of Hong Kong, Pokfulam, Hong Kong
15 Department of Gastroenterology and Hepatology, Singapore General Hospital, Singapore
16 Division of Gastroenterology, Department of Medicine, Siriraj Hospital, Mahidol University, Bangkok, Thailand
17 Department of Radiology, Zhong-Da Hospital, Southeast University, Nanjing, China
18 Centre for Liver Cancer, National Cancer Center Hospital, Goyang, Korea

Keywords
combination therapy – hepatocellular carcinoma – sorafenib – TACE

Correspondence
Joong-Won Park
Center for Liver Cancer, National Cancer Center 323 Ilsan-ro, Ilsan dong-gu, Goyang-si, Gyeonggi-do, 410-769, South Korea
Tel: +82 31 920 1605
Fax: +82 31 920 1520
e-mail: jwpark@ncc.re.kr

Received 18 December 2012
Accepted 29 August 2013

DOI:10.1111/liv.12314
Liver Int. 2014: 34: 174–183

Abstract

Patients with unresectable hepatocellular carcinoma (HCC) usually receive transarterial chemoembolization (TACE) or systemic therapies with intermediate and advanced-stage disease. However, intermediate-stage HCC patients often have unsatisfactory clinical outcomes with repeated TACE and there is considerable uncertainty surrounding the criteria for repeating or stopping TACE treatment. In July 2012, an Expert Panel Opinion on Interventions in Hepatocellular Carcinoma (EPOIHCC) was re-convened in Shanghai in an attempt to provide a consensus on the practice of TACE, particularly in regard to evaluating TACE 'failure'. To that end, current clinical practice throughout Asia was reviewed in detail including safety and efficacy data on TACE alone as well as in combination with targeted systemic therapies for intermediate HCC. This review summarizes the evidence discussed at the meeting and provides expert recommendations regarding the use of TACE for unresectable intermediate-stage HCC. A key consensus of the Expert Panel was that the current definitions of TACE failure are not useful in differentiating between situations where TACE is no longer effective in controlling disease locally vs. systemically. By redefining these concepts, it may be possible to provide a clearer indication of when TACE should be repeated and more importantly, when TACE should be discontinued.

The preferred curative treatments for hepatocellular carcinoma (HCC) include liver transplantation, surgical resection or local ablation. These treatments offer the best survival advantages but in practice, most patients either present when the tumour is in an advanced stage or the degree of underlying liver disease precludes these options. Subsequently, treatment algorithms recommend treatment stratification based on the stage of disease. For intermediate-stage patients (1) with unresectable, large/multifocal HCC, most guidelines recommend TACE as a first-line treatment (2–6) whereas for patients with advanced-stage HCC (1)

systemic therapies are the treatment of choice (2). In addition to TACE, there are numerous loco-regional therapies available for unresectable HCC treatment. Potentially curative treatments include percutaneous ethanol injection (PEI) and radiofrequency ablation (RFA), whereas other non-curative treatments include radioembolization and drug-eluting microspheres. Although some of these therapies have been shown to provide benefits in controlled clinical studies, survival benefits have not been proven. These have been reviewed in detail elsewhere and will not be discussed here (7, 8). The only non-curative treatments that improve survival are TACE and sorafenib (9–11).

The widely accepted classification for staging and treatment proposed by the Barcelona Clinic Liver Cancer (BCLC) considers TACE to be the standard of care for intermediate-stage HCC (1). Although this and other guidelines provide clear definitions of when TACE is contraindicated, there is considerable uncertainty around when TACE should be repeated given the variable nature of clinical responses. An additional complication is that compliance for performing TACE according to specific criteria in the various guidelines under well-controlled conditions such as a clinical trial is quite different from that occurring in standard clinical practice.

Expert panel meeting

In July, 2012, the Expert Panel Opinion on Interventions in Hepatocellular Carcinoma (EPOIHCC) meeting was convened in Shanghai bringing together 17 experts from Asia-Pacific. The panel was intended to provide a multidisciplinary approach to optimizing HCC management incorporating input from specialists in gastroenterology, hepatology, surgery, transplant surgery, interventional and diagnostic radiology, medical oncology, radiation oncology and nuclear medicine. The objectives for the meeting were to review current clinical practice with TACE in Asia with respect to clarifying uncertainties around patient selection, scheduling of TACE, evaluation of response, the definition of TACE failure and the evidence for TACE combination therapy from current clinical trials. This is intended to assist clinicians determine the most appropriate treatment strategy in cases where TACE is no longer effective, for whatever reason. To assist with these discussions and to provide a snapshot of current clinical practice in Asia, a premeeting survey was completed by 15 of the expert panel members (Table 1).

Conventional vs. DEB-TACE

Conventional TACE is the primary treatment used most frequently for unresectable HCC and involves embolization of the hepatic artery with the aim of inducing necrosis in large vascularized HCC (7). A chemotherapy agent (most commonly doxorubicin) is mixed into an emulsion with lipiodol and selectively infused via the transarterial route into the tumour, usually in combination with an embolizing agent (most commonly a gelatin sponge or polyvinyl particles). This combination of vessel obstruction and chemotherapeutic agent results in increased exposure of the tumour to the chemotherapeutic agent (12). Using this approach, the lipiodol is selectively retained within the tumour and is thought to magnify the exposure of the neoplastic cells to chemotherapy with additional benefits conferred by obstruction of the feeding arteries. However, tumour response to TACE can be variable and it is considered a non-curative treatment as complete tumour necrosis is difficult to achieve, even with repeated TACE treatments (2, 13). In addition to the highly heterogeneous nature of intermediate HCC, there is also no standard regimen regarding patient selection, treatment schedule or re-treatment strategy, type of chemotherapy or embolizing agent. Efficacy of TACE is most likely related to drug exposure but may also depend on the degree of ischaemia induced. Subsequently, technical proficiency is key in achieving optimal responses to TACE and for preventing complications. Despite this, even with technically perfect TACE procedures, responses are not 100% indicating the paramount importance of tumour-related factors. These include vascularization type, features of the disease and tumour aggressiveness. Superselective TACE may provide benefits in minimizing damage to non-tumourous areas using a microcatheter to selectively (or superselectively) catheterize the hepatic segmental or subsegmental arteries nourishing the tumour (14).

The recently developed TACE with drug-eluting beads (DEB) offers the possibility of more targeted chemotherapeutic delivery with potentially less side effects. The bead's high affinity for the drug results in a gradual release of doxorubicin into the tumour, allowing a longer intratumoural exposure and less systemic exposure of the drug, reducing toxicity (7). A number of recent studies have demonstrated higher tumour concentrations and lower systemic concentrations of doxorubicin compared with intra-arterial doxorubicin used in conventional TACE [reviewed in (7)]. Precision-V, a randomized controlled trial comparing DEB-TACE with conventional TACE recently reported similar tumour response rates but slightly better objective response rates and disease control rates in the DEB-TACE arm, although these were not statistically significant (15). Treatment-related serious adverse events were similar for both groups, but the secondary safety outcomes (incidence and severity of adverse events, liver function parameters and cardiac function) were significantly better in the DEB-TACE group (15). Similarly, a recent retrospective comparison of conventional and DEB-TACE demonstrated significantly better objective response rates (81.6% vs 49.4%) and time to progression (11.7 vs 7.6 months) for the DEB-TACE group (16). There was no statistically significant difference in liver toxicity between groups. Despite these promising results, DEB-TACE uptake in Asia is relatively low compared with

Table 1. EPOIHCC premeeting survey questions and summary of responses

Question	No. of responses
Q1. Do you rely on specific guidelines to advise the use of TACE in HCC?	
Yes	12
No	3
Local/Hospital guidelines	7
AASLD HCC Practice Guidelines	4
NCCN Guidelines	2
APASL Guidelines	4
EASL Guidelines	1
JSH Guidelines	2
KLCSG-NCC Guidelines	3
Other	
Q2. Which TACE regimen do you use routinely in clinical practice?	
DC Beads	5
cTACE-Doxorubicin	13
cTACE-Cisplatin	5
cTACE-Mitomycin	3
Other	
Q3. In your experience, what is the optimal number of TACE procedures required in the treatment of intermediate HCC patients? Please specify average in your practice.	
Q4. How do measure patient response to TACE in clinical practice?	
Response Evaluation Criteria in Solid Tumours (RECIST)	5
Modified RECIST (mRECIST)	11
WHO	0
EASL	1
Other (specify)	
Q5. What is the greatest challenge faced in the application of TACE in intermediate HCC patients?	
Liver Function	12
Vascular Access	7
Tumour Size	5
Tumour Number	5
Evidence	0
Other (specify)	0
Q6. In your opinion, would improved patient outcomes with TACE, mean less procedures and preserve liver function?	
Yes	13
No	2
Q7. For the case of poor response or refractory TACE, would you consider these options?	
Yt-90	8
RFA	3
External beam radiotherapy	5
Other (specify)	5
Q8. Which patients are unsuitable for TACE, what treatment options would you consider in these cases?	
Technical issues	13
Tumour size	12
Liver function	12
In your opinion, there is insufficient evidence to support alternatives	2
Q9. In your opinion, which intermediate-stage HCC patients would potentially benefit from molecular-targeted therapy?	
Patients with tumour >10 cm	6
Patients with vascular invasion	10
Patients who have undergone ≥2 TACE procedures, without satisfactory response	11
Other (specify	4
Q10. In your opinion, is there sufficient evidence to support the use of sorafenib and TACE in combination therapy?	
I do use it in clinical practice currently	3
I do use it but only in special patient populations	10
I do not use it in clinical practice	4

the USA or Europe. Our survey of the EPOIHCC revealed that only 5 of 16 (31%) panellists routinely use DEB-TACE in clinical practice in Asia. This is increased slightly from a 2011 survey of the same Expert Panel where 25% routinely used DEB-TACE.

TACE in Asia

The usage of TACE varies considerably throughout the world as demonstrated by the ongoing GIDEON study. Compared with the USA (44%), Europe (49%) and

Latin America (29%), rates of prior use of TACE in HCC patients are considerably higher in Asia-Pacific (69%) with a reported 84% of Japanese patients receiving TACE prior to the analysed period (17). The number of patients receiving at least 3 TACE treatments prior to this study was also higher in Asia-Pacific and Japan than in other regions. Observations of HCC management patterns from the global BRIDGE study reported that TACE is the most frequently used first recorded treatment in Asia and North America (18). There is now good evidence that TACE prolongs survival compared with best supportive care (19, 20); however, conventional TACE has a wide range of survival rates between clinical series reflecting variations in patient selection and differences in chemoembolization techniques (21–24). Only a limited number of studies report 5-year survival rates for conventional TACE, but these are consistently poorer in Western patients (1–13%) (24, 25) than in Asian patients (24%) (21). A recent systematic review noted a trend since 2000 of studies reporting better survival rates compared with those before 2000, mainly because of better selection of patients (21). Some of the highest survival rates observed are in studies from Japan, which have reported rates of 26% in 2006 (26) and 34% in 2012 (14) primarily through improved patient selection. A recent report on the 5-year overall survival of HCC patients treated with DEB-TACE reported overall survival at 3 and 5 years of 62 and 22.5% respectively (27).

Objectively evaluating treatment response

To objectively evaluate the response to loco-regional therapy, the Response Evaluation Criteria in Solid Tumors (RECIST) (28, 29) and the European Association for the Study of the Liver Criteria (EASL) (30) have been developed. These have gained widespread use internationally despite inherent limitations. RECIST may evaluate unidimensional tumour measurements and does not capture the efficacy of loco-regional therapies in inducing tumour necrosis (31). Although EASL criteria do evaluate response by measuring the extent of tumour necrosis, there is a lack of data supporting correlations with improving survival (7). In 2010, a modification in RECIST (mRECIST) with criteria similar to RECIST was proposed, which includes an assessment of the disappearance or decrease in the intratumoural arterial enhancement in the target lesion (32). Although many clinicians around the world have moved towards mRECIST, the assessment of intratumoural arterial enhancement is relatively subjective and requires validation and correlation with survival. Our survey of the EPOIHCC revealed that 5 of 15 (33%) panellists use RECIST in clinical practice in Asia, whereas 13 of 15 (86%) use mRECIST. Only one respondent indicated that they use EASL criteria. In our 2011 survey, equal numbers of respondents used RECIST and mRECIST. Given the limitations in both criteria, the panel believes that RECIST is still essential for objective assessment. In the months following the EPOIHCC meeting in Shanghai, several publications have considered this controversy in detail. Sato *et al.* directly compared response rates following TACE reported using RECIST and mRECIST in addition to evaluating their variability (33). The CR rate and the response rate obtained using mRECIST (56.9% and 79.7%) were higher than those obtained using RECIST version 1.1 (9.2% and 43.1%) while mRECIST exhibited almost perfect agreement in inter- and intra-observer reproducibility. RECIST version 1.1 exhibited substantial agreement in reproducibility. The authors suggest that mRECIST may be more suitable for tumour response criteria in clinical trials of TACE for HCC as it exhibits higher inter- and intra-observer reproducibility. Although not compared directly to mRECIST, Muenzel *et al.* demonstrated low intra- and inter-observer variabilities for measurements of single target lesions using RECIST, but the high variability in change in Δ sum LD reveals the potential for misclassification of the overall response according to the RECIST guidelines (34). The authors suggest that reproducibility of RECIST reporting can be improved for the case assessment by a single reader and mean results of multiple readers. Shim *et al.* reported good intercriterion agreement between mRECIST and EASL guidelines while a poor correlation was observed between RECIST and mRECIST (35). This study also suggested that mRECIST could more reliably help predict long-term survival in HCC patients treated with TACE than other size-based imaging guidelines. Similarly, a comparison of RECIST1.1, mRECIST, EASL and WHO guidelines suggests that mRECIST provides the highest correlation with survival in HCC patients treated with DEB-TACE while RECIST1.1 is the least useful in predicting survival in these patients (36). An additional study comparing RECIST with mRECIST specifically in patients who received Sorafenib for advanced HCC reported that the majority of patients who had SD according to RECIST had a different prognosis according to mRECIST (37). The authors go on to suggest that for patients with HCC, mRECIST should be used for the standard assessment of treatment efficacy, particularly in patients who are receiving antiangiogenic drugs.

Taking these recent studies into consideration, we acknowledge that mRECIST is widely used in other parts of the world; however, uptake rates are lower in Asia, necessitating an evidence-based assessment of RECIST vs mRECIST prior to widespread incorporation into local practice. Although these recent studies will assist with partial validation of mRECIST as a viable, and potentially, superior response criteria, further prospective evaluation is still necessary. For this reason, we recommend that mRECIST be used in combination with RECIST, wherever possible.

Consensus #1. The panel believes that RECIST is still valuable for objective assessment. We acknowledge that mRECIST is widely used and recent studies are

beginning to address its validation. However, given the continued usage of RECIST in Asia, mRECIST should be used in combination with RECIST wherever possible. Before mRECIST can be widely incorporated for generalized use, EPOIHCC recommends that mRECIST should be more intensively and prospectively studied.

Standardizing TACE protocols

The inherent variability associated with TACE outcomes is primarily related to the heterogenous patient population undergoing treatment; however, variations in the time intervals between treatments and the number of cycles of TACE performed are also likely to be important prognostic factors. Even in the absence of conclusive, predictive biomarkers, it is becoming clearer that the best candidates for TACE are largely asymptomatic patients with preserved liver function without vascular invasion or extrahepatic tumour spread. (38) There are a number of HCC treatment algorithms, which have been proposed as the most widely accepted being the BCLC staging system (1). Recent comparisons of the BCLC and Japanese Society of Hepatology (JSH) guidelines (39) have concluded that they are essentially quite similar in terms of inclusion criteria for TACE and in their absolute contraindications to TACE (40, 41). The EPOIHCC generally supports the use of these criteria. However, we believe that the limitation of TACE to strictly BCLC B patients should be further evaluated. TACE has demonstrated efficacy in patients prior to transplantation (BCLC A), particularly if the waiting time is likely to be more than 6 months (42, 43).

Response to TACE may also be used as a predictor of tumour biology in patients awaiting transplantation (44). TACE also appears to be a safe and effective option in patients clinically excluded from transplantation and who are unfit for surgery or percutaneous ablation (45). At the other end of the TACE spectrum, BCLC C patients with acceptable PS or only partial PVT may also benefit from selective or DEB-TACE treatment. While PVT has been widely accepted as a relative contraindication for TACE, studies have demonstrated little negative impact on hepatic function in cases of PVT and TACE can be safely performed if hepatopedal collateral flow is present (46, 47). In these patients, a superselective approach as well as an adjustment of the chemotherapeutic dosage may minimize liver damage (48). An important recognition is that although the BCLC recommendations are clear, not everybody follows them. In Asia and most of North America, patients with BCLC A-C would probably be considered for TACE. This does not mean that TACE has been recognized as the treatment of choice for those patients, but rather for patients with BCLC A who do not meet the Milan selection criteria for transplantation, and who are unsuitable for resection or local ablation owing to tumour location, TACE remains the only treatment strategy (45). Similarly, patients with ECOG 1 who would be BCLC C could benefit from TACE provided appropriate measures are taken to minimize liver damage.

Consensus #2. Suitable patients for TACE are those that are BCLC A, B or C, ECOG PS <2, Child-Pugh <C. For cases with vascular invasion or metastasis, combination therapy with sorafenib may be tried in practice, but solid evidence from controlled prospective studies is still required to evaluate this approach.

Although most guidelines indicate that the presence of extrahepatic metastases is an absolute contraindication for TACE, in clinical practice, there may be specific situations where patients have extrahepatic progression, but the bulk of disease is within the liver. This will be case specific but if the clinician concludes that the patient is most likely to die from liver disease, in these patients, there may still be a role for TACE, making extrahepatic metastases a relative contraindication only.

Consensus #3. Absolute contraindications for TACE include Child C and poor ECOG status while relative contraindications include extrahepatic disease depending on how extensive.

Multiple TACE cycles can be performed either at regular intervals or based on tumour response (on demand), when there is evidence of insufficient tumour response, tumour recurrence or disease progression. Although it is generally accepted that chemoembolization achieves maximal tumour response when repeated multiple times (49) it is not yet clear whether this results in better survival. In addition, it is also unknown if on demand TACE is preferable to fixed interval TACE. On one hand, TACE repeated at a fixed time, until the planned number of courses has been reached, should provide the greatest opportunity for persistent tumour necrosis. However, repeated chemotherapy insults may cause progressive liver atrophy and vascular damage (50, 51). Alternatively, TACE performed on demand, on the basis of tumour response and patient tolerance, is likely to reduce the degree of liver damage and complications and it allows a proper patient selection at each cycle of TACE (51) but may potentially result in undertreating the tumour. A recent study assessed the clinical impact of TACE repeated on demand on HCC outcome (52). The number of patients submitted to a second and third TACE declined substantially from those initially enrolled; however, similar CR and recurrence rates were observed after the first, second and third TACE procedures. This not only demonstrates the efficacy of repeated on demand TACE procedures but also highlights the declining patient population suitable for repeated TACE. A comparative trial performed conventional TACE in 80 patients from 1986 to 1993 using a fixed schedule of at least three times at 2-month intervals. On demand TACE was performed in a second group of 80 patients from 1993 to 1996, where TACE was used selectively and repeated only when necessary on the basis of follow-up CT or MR imaging (51). Complications of TACE occurred in 19 patients from group 1 and six patients from group 2 ($P < 0.001$) potentially

reflecting the greater number of TACE cycles performed. Similarly, the mean time between the first and the third TACE cycle was significantly different between group 1 (4 months) and group 2 (14 months) ($P < 0.001$). Of note, the 1-year, 2-year and 3-year survival rates were significantly different between the two groups of patients graded as Okuda stage 1: 58, 28, 11% for fixed schedule TACE and 89, 68, 39%, respectively, for on demand TACE ($P < 0.001$). This observation clearly demonstrates the efficacy and tolerability of TACE increase when it is used selectively and repeated on demand (51). A recent systematic review noted that in 63% of studies assessed (reported by 54 studies), TACE was repeated at fixed time intervals until the planned number of courses was reached or death occurred, while on demand TACE was only performed in 27% of studies when there was evidence of unsatisfactory response or recurrence of the tumour (21). Unfortunately, this analysis made no attempt to compare patient outcomes in these two populations.

Consensus #4. TACE should be performed on demand. The decision to repeat TACE should be based not only on tumour response or progression but also on patients' clinical conditions and tolerance, which should be assessed before each new cycle of TACE.

Redefining TACE failure

Key areas of uncertainty not sufficiently addressed by existing guidelines include the criteria for repeating TACE and recommendations about the number of TACE cycles to be repeated before switching to another or no treatment. This latter point relates to the criteria used to determine when to stop TACE treatments, either because TACE is now contraindicated, or because TACE is no longer effective in controlling the disease, referred to generally as TACE failure. The JSH defines TACE failure as the development of an intrahepatic lesion, the appearance of vascular invasion, the appearance of extrahepatic spread or a continuous elevation of tumour markers even though right after TACE (41). In clinical practice, less formal definitions include the treatment of all visible disease in liver without response, being unable to prevent tumour growth and significant toxicities. We believe that an important distinction to make regarding the efficacy of TACE is whether disease progression is characterized by intra or extrahepatic spread. If there is any progression at all, it is clear that TACE is not effective in controlling the disease, but this does not necessarily indicate TACE failure. Technically, the TACE procedure may have been successful, in terms of lipiodol deposition and local tumour necrosis, etc., but patients may still go on to develop metastases. Describing this scenario simply as TACE failure is misleading and scientifically inaccurate. As TACE is a loco-regional therapy, TACE failure should refer to the specific control of the tumour that was planned for treatment. The appearance of subsequent disease is progression of disease and this may, or may not, be caused by TACE failure. This view has recently been proposed by others citing 'progression itself does not seem necessarily to imply the failure of TACE' (53). Untreatable progression, in terms of TACE therapy, may correspond to the development of portal vein thrombosis, extrahepatic metastases or worsening of liver function, for example, despite a clear control of the lesion targeted for TACE.

Consensus #5. As a loco-regional therapy, TACE failure should refer to the specific control of the tumour that was planned for treatment and, therefore, may not be useful in evaluating TACE effectiveness in patients with extrahepatic metastases.

The recent proposal of 'stage progression' from Korea is potentially a useful concept and may provide a surrogate end-point for TACE refractoriness (53). By evaluating 264 patients with intermediate-stage HCC who underwent TACE and designating the development of vascular invasion or extrahepatic spread during follow-up as stage progression (SP), the authors classified the patients according to disease course as: no progressive disease, PD without SP, PD followed by SP, and simultaneous PD and SP. Patients without SP (including both patients with no PD and those with PD but no SP) showed no difference in overall survival (36.6 and 35.8 months, respectively), patients with PD followed by SP had intermediate overall survival (23.9 months) and patients with simultaneous PD and SP had the worst overall survival (12 months). Multivariate analyses of OS indicated corresponding hazard ratios for each patient group. By classifying SP as new vascular invasion or extrahepatic spread, which includes radiological progression of stage from BCLC stage B to stage C, the time from initial treatment to this point can be referred to as 'time-to-stage progression' (TTSP). A further variation in this concept to accommodate the increasing number of cases of SP that develop as the duration of follow-up increases has been proposed as 'SP-free survival' (53). The authors contend that this provides a composite end-point instead of TTSP, which may indicate TACE-refractory HCC. Subsequent analysis indicated that both the development of progression during the first 6 months from the initial TACE and the need for three sessions of TACE during the first 6 months were associated with shorter SP-free survival and thus, TACE-refractory HCC (53).

Consensus #6. Stage progression, defined as the development of vascular invasion or extrahepatic spread during follow-up, may provide a useful surrogate measure of TACE refractoriness, although there are currently limited data regarding this.

Taking this current proposal into consideration along with existing guidelines and the collective clinical experience of the EPOIHCC, the panel agrees that three sessions of TACE in clinical practice (within 6 months) should be adequate for effective tumour control. Sorafenib is recommended for those who have failed TACE or for TACE-refractory patients. By defining TACE

refractoriness more clearly using SP, in intermediate-stage HCC patients who are not eligible for, or who have demonstrated SP after TACE, a switch to sorafenib might be a considered. It should also be noted that TACE, particularly repeated TACE, can result in liver toxicity and chemotherapy-related side effects (50, 51), which may influence retreatment decisions. Recent advances aimed at minimizing the injury to non-tumoural liver tissue include selective (or superselective) TACE (14, 54) and DEB-TACE (15).

Consensus #7. Three sessions of TACE in clinical practice (within 6 months) should be adequate for effective tumour control.

TACE in combination with sorafenib

Transarterial chemoembolization is associated with disturbances of the tumour microenvironment, which result in increased hypoxia, leading to an upregulation in hypoxia-inducible factor-1a, which in turn upregulates vascular endothelial growth factor (VEGF) and platelet-derived growth factor receptor (PDGFR) and increases tumour angiogenesis (55–57). Increased angiogenesis may in turn result in tumour-promoting effects and elevations in serum VEGF are a poor prognostic indicator in patients with HCC (58–60). Combining antiangiogenic-targeted agents with TACE to decrease post-TACE angiogenesis may improve the efficacy of TACE therapy as well as improving long-term outcomes. Sorafenib is a potent multikinase inhibitor with antiangiogenic and antiproliferative properties that targets the Raf/MEK/ERK pathway (61) as well as VEGFR-1/2/3, PDGFR-β, KIT, Flt-3 and RET (62). Two landmark phase III trials comparing sorafenib with placebo in patients with advanced HCC reported significant improvements in overall survival establishing sorafenib as the standard of care in advanced HCC patients (10, 11).

Given the success of sorafenib in advanced HCC and the theoretical advantages of combining TACE with sorafenib, a number of ongoing trials are evaluating this combination in intermediate-stage HCC patients. In theory, additional support for either on demand TACE schedules or fixed TACE schedules should be available from recent combination trials of TACE and sorafenib. However, most combination trials have utilized an on demand TACE schedule with only the recent phase II Johns Hopkins University (JHU) and SPACE trials incorporating a fixed schedule of DEB-TACE with concurrent continuous sorafenib administration (63, 64). The JHU trial was a small Phase II study in 35 patients in which DEB-TACE was performed with concurrent continuous sorafenib and reported a disease control rate as evaluated per lesion of 92 to 100%, with an objective response rate of 58% (64). The SPACE trial enrolled 307 patients with intermediate-stage HCC reporting a median treatment duration in the treatment and placebo groups of 4.8 and 6.3 months, respectively, and a HR for TTP of 0.797 (63). Although median TTP reported was similar for both groups, there were considerable differences in TTP at the 25th and 75th percentiles and this study met its primary end-point of improving TTP when sorafenib was added to a regimen of DEB-TACE, compared with DEB-TACE. To eliminate variations in sorafenib administration and type of TACE performed, there is only a single recent European study appropriate for direct comparison. In a small group of patients, this study incorporated a continuous sorafenib schedule with on demand TACE but was stopped prematurely because of safety concerns (65). There are three ways to combine TACE and sorafenib. An interrupted design where sorafenib is stopped around the time of TACE (e.g. START) (66) sequential where several cycles of TACE are performed first and then sorafenib is started (67) or continuous, where both are applied together (e.g. COTSUN, JHU and SPACE) (63, 64, 68). There are currently a substantial number of clinical trials assessing the various combinations of TACE with sorafenib and these have been reviewed elsewhere (8). The outcomes of these combination trials are eagerly awaited and are likely to change the treatment landscape for intermediate HCC patients.

Consensus #8. The combination of sorafenib and TACE may improve the efficacy of TACE therapy as well as improving long-term patient outcomes. However, despite promising initial data, the successful completion of several clinical trials in progress will be essential before recommending the combination of sorafenib plus TACE for patients with intermediate-stage HCC.

Summary

This expert panel meeting was convened to address unresolved issues surrounding the use of TACE in clinical practice in Asia. The palliative nature of TACE frequently necessitates repeated TACE treatments; however, there is still considerable ambiguity surrounding the criteria for repeating TACE, how long TACE should be repeated for, and when it should be stopped and replaced with alternate therapy (or no treatment). The EPOIHCC recommends that a maximum of three sessions of on demand TACE within a period of 6 months should be sufficient for successful treatment. Disease progression during this time may indicate TACE refractoriness and a change in treatment strategy should be considered. By refocusing clinicians on identifying TACE refractoriness rather than the ambiguous concept of TACE failure, patient selection for repeated TACE can be improved leading to important survival advantages.

Acknowledgements

All authors received honoraria for participation in the expert panel meeting, but received no compensation for their authorship of this manuscript. The authors would also like to acknowledge Bruce Mungall BSc, PhD from

UBM Medica Pte Ltd Singapore for providing editorial and writing support, which was supported by an educational grant from Bayer (South East Asia) Pte Ltd.

Conflict of interest: The authors do not have any disclosures to report.

References

1. Llovet JM, Bru C, Bruix J. Prognosis of hepatocellular carcinoma: the BCLC staging classification. *Semin Liver Dis* 1999; **19**: 329–38.
2. Bruix J, Sherman M. Management of hepatocellular carcinoma: an update. *Hepatology* 2011; **53**: 1020–2.
3. Benson AB 3rd, Abrams TA, Ben-Josef E, *et al.* NCCN clinical practice guidelines in oncology: hepatobiliary cancers. *J Natl Compr Canc Netw* 2009; **7**: 350–91.
4. Omata M, Lesmana LA, Tateishi R, *et al.* Asian Pacific Association for the Study of the Liver consensus recommendations on hepatocellular carcinoma. *Hepatol Int* 2010; **4**: 439–74.
5. Arii S, Sata M, Sakamoto M, *et al.* Management of hepatocellular carcinoma: Report of Consensus Meeting in the 45th Annual Meeting of the Japan Society of Hepatology (2009). *Hepatol Res* 2010; **40**: 667–85.
6. Nilsson SE, Fransson E, Brismar K. Relationship between serum progesterone concentrations and cardiovascular disease, diabetes, and mortality in elderly Swedish men and women: An 8-year prospective study. *Gend Med* 2009; **6**: 433–43.
7. Meza-Junco J, Montano-Loza AJ, Liu DM, *et al.* Locoregional radiological treatment for hepatocellular carcinoma; Which, when and how? *Cancer Treat Rev* 2011; **38**: 54–62.
8. Park JW, Amarapurkar D, Chao Y, *et al.* Consensus recommendations of an Expert Panel on Interventions in Hepatocellular Carcinoma (EPOIHCC). *Liver Int* 2013; **33**: 327–37.
9. Llovet JM, Bruix J. Systematic review of randomized trials for unresectable hepatocellular carcinoma: Chemoembolization improves survival. *Hepatology* 2003; **37**: 429–42.
10. Llovet JM, Ricci S, Mazzaferro V, *et al.* Sorafenib in advanced hepatocellular carcinoma. *N Engl J Med* 2008; **359**: 378–90.
11. Cheng AL, Kang YK, Chen Z, *et al.* Efficacy and safety of sorafenib in patients in the Asia-Pacific region with advanced hepatocellular carcinoma: a phase III randomised, double-blind, placebo-controlled trial. *Lancet Oncol* 2009; **10**: 25–34.
12. Brown DB, Geschwind JF, Soulen MC, Millward SF, Sacks D. Society of Interventional Radiology position statement on chemoembolization of hepatic malignancies. *J Vasc Interv Radiol* 2009; **20**: S317–23.
13. Alba E, Valls C, Dominguez J, *et al.* Transcatheter arterial chemoembolization in patients with hepatocellular carcinoma on the waiting list for orthotopic liver transplantation. *AJR Am J Roentgenol* 2008; **190**: 1341–8.
14. Takayasu K, Arii S, Kudo M, *et al.* Superselective transarterial chemoembolization for hepatocellular carcinoma. Validation of treatment algorithm proposed by Japanese guidelines. *J Hepatol* 2012; **56**: 886–92.
15. Lammer J, Malagari K, Vogl T, *et al.* Prospective randomized study of doxorubicin-eluting-bead embolization in the treatment of hepatocellular carcinoma: results of the PRECISION V study. *Cardiovasc Intervent Radiol* 2010; **33**: 41–52.
16. Song MJ, Chun HJ, Song DS, *et al.* Comparative study between doxorubicin-eluting beads and conventional transarterial chemoembolization for treatment of hepatocellular carcinoma. *J Hepatol* 2012; **57**: 1244–50.
17. Geschwind JF, Lencioni R, Marrero JA, *et al.* (2012) Worldwide trends in locoregional therapy for hepatocellular carcinoma (HCC): Second interim analysis of the Global Investigation of Therapeutic Decisions in HCC and of Its Treatment with Sorafenib (GIDEON) study. *J Clin Oncol* **30** (Suppl 4; abstr 317).
18. Park JW, Sherman M, Colombo M, *et al.* (2012) Observations of hepatocellular carcinoma (HCC) management patterns from the global HCC bridge study: First characterization of the full study population. *J Clin Oncol* **30** (Suppl; abstr 4033).
19. Lo CM, Ngan H, Tso WK, *et al.* Randomized controlled trial of transarterial lipiodol chemoembolization for unresectable hepatocellular carcinoma. *Hepatology* 2002; **35**: 1164–71.
20. Llovet JM, Real MI, Montana X, *et al.* Arterial embolisation or chemoembolisation versus symptomatic treatment in patients with unresectable hepatocellular carcinoma: a randomised controlled trial. *Lancet* 2002; **359**: 1734–9.
21. Marelli L, Stigliano R, Triantos C, *et al.* Transarterial therapy for hepatocellular carcinoma: which technique is more effective? A systematic review of cohort and randomized studies. *Cardiovasc Intervent Radiol* 2007; **30**: 6–25.
22. Vogl TJ, Naguib NN, Nour-Eldin NE, *et al.* Review on transarterial chemoembolization in hepatocellular carcinoma: palliative, combined, neoadjuvant, bridging, and symptomatic indications. *Eur J Radiol* 2009; **72**: 505–16.
23. Bruix J, Llovet JM. Major achievements in hepatocellular carcinoma. *Lancet* 2009; **373**: 614–6.
24. Raoul JL, Sangro B, Forner A, *et al.* Evolving strategies for the management of intermediate-stage hepatocellular carcinoma: available evidence and expert opinion on the use of transarterial chemoembolization. *Cancer Treat Rev* 2011; **37**: 212–20.
25. O'Suilleabhain CB, Poon RT, Yong JL, *et al.* Factors predictive of 5-year survival after transarterial chemoembolization for inoperable hepatocellular carcinoma. *Br J Surg* 2003; **90**: 325–31.
26. Takayasu K, Arii S, Ikai I, *et al.* Prospective cohort study of transarterial chemoembolization for unresectable hepatocellular carcinoma in 8510 patients. *Gastroenterology* 2006; **131**: 461–9.
27. Malagari K, Pomoni M, Moschouris H, *et al.* Chemoembolization with Doxorubicin-eluting beads for unresectable hepatocellular carcinoma: five-year survival analysis. *Cardiovasc Intervent Radiol* 2012; **35**: 1119–28.
28. Therasse P, Arbuck SG, Eisenhauer EA, *et al.* New guidelines to evaluate the response to treatment in solid tumors. European Organization for Research and Treatment of Cancer, National Cancer Institute of the United States, National Cancer Institute of Canada. *J Natl Cancer Inst* 2000; **92**: 205–16.
29. Therasse P, Eisenhauer EA, Verweij J. RECIST revisited: a review of validation studies on tumour assessment. *Eur J Cancer* 2006; **42**: 1031–9.

30. Bruix J, Sherman M, Llovet JM, *et al.* Clinical management of hepatocellular carcinoma. Conclusions of the Barcelona-2000 EASL conference. European Association for the Study of the Liver. *J Hepatol* 2001; **35**: 421–30.
31. Forner A, Ayuso C, Varela M, *et al.* Evaluation of tumor response after locoregional therapies in hepatocellular carcinoma: are response evaluation criteria in solid tumors reliable? *Cancer* 2009; **115**: 616–23.
32. Lencioni R, Llovet JM. Modified RECIST (mRECIST) assessment for hepatocellular carcinoma. *Semin Liver Dis* 2010; **30**: 52–60.
33. Sato Y, Watanabe H, Sone M, *et al.* Tumor response evaluation criteria for HCC (hepatocellular carcinoma) treated using TACE (transcatheter arterial chemoembolization): RECIST (response evaluation criteria in solid tumors) version 1.1 and mRECIST (modified RECIST): JIVROSG-0602. *Ups J Med Sci* 2013; **118**: 16–22.
34. Muenzel D, Engels HP, Bruegel M, *et al.* Intra- and inter-observer variability in measurement of target lesions: implication on response evaluation according to RECIST 1.1. *Radiol Oncol* 2012; **46**: 8–18.
35. Shim JH, Lee HC, Kim SO, *et al.* Which response criteria best help predict survival of patients with hepatocellular carcinoma following chemoembolization? A validation study of old and new models. *Radiology* 2012; **262**: 708–18.
36. Prajapati HJ, Spivey JR, Hanish SI, *et al.* (2012) mRECIST and EASL responses at early time point by contrast-enhanced dynamic MRI predict survival in patients with unresectable hepatocellular carcinoma (HCC) treated by doxorubicin drug-eluting beads transarterial chemoembolization (DEB-TACE). *Ann Oncol* **24**, 965–73.
37. Edeline J, Boucher E, Rolland Y, *et al.* Comparison of tumor response by Response Evaluation Criteria in Solid Tumors (RECIST) and modified RECIST in patients treated with sorafenib for hepatocellular carcinoma. *Cancer* 2012; **118**: 147–56.
38. Bruix J, Sala M, Llovet JM. Chemoembolization for hepatocellular carcinoma. *Gastroenterology* 2004; **127**: S179–88.
39. Makuuchi M, Kokudo N, Arii S, *et al.* Development of evidence-based clinical guidelines for the diagnosis and treatment of hepatocellular carcinoma in Japan. *Hepatol Res* 2008; **38**: 37–51.
40. Takayasu K. Transarterial chemoembolization for hepatocellular carcinoma over three decades: current progress and perspective. *Jpn J Clin Oncol* 2012; **42**: 247–55.
41. Kudo M, Izumi N, Kokudo N, *et al.* Management of hepatocellular carcinoma in Japan: Consensus-Based Clinical Practice Guidelines proposed by the Japan Society of Hepatology (JSH) 2010 updated version. *Dig Dis* 2011; **29**: 339–64.
42. Graziadei IW, Sandmueller H, Waldenberger P, *et al.* Chemoembolization followed by liver transplantation for hepatocellular carcinoma impedes tumor progression while on the waiting list and leads to excellent outcome. *Liver Transpl* 2003; **9**: 557–63.
43. Otto G, Heise M, Moench C, *et al.* Transarterial chemoembolization before liver transplantation in 60 patients with hepatocellular carcinoma. *Transplant Proc* 2007; **39**: 537–9.
44. Otto G, Herber S, Heise M, *et al.* Response to transarterial chemoembolization as a biological selection criterion for liver transplantation in hepatocellular carcinoma. *Liver Transpl* 2006; **12**: 1260–7.
45. Bargellini I, Sacco R, Bozzi E, *et al.* (2011) Transarterial chemoembolization in very early and early-stage hepatocellular carcinoma patients excluded from curative treatment: A prospective cohort study. *Eur J Radiol* 2012; **81**: 1173–8.
46. Georgiades CS, Hong K, D'Angelo M, Geschwind JF. Safety and efficacy of transarterial chemoembolization in patients with unresectable hepatocellular carcinoma and portal vein thrombosis. *J Vasc Interv Radiol* 2005; **16**: 1653–9.
47. Chung JW, Park JH, Han JK, Choi BI, Han MC. Hepatocellular carcinoma and portal vein invasion: results of treatment with transcatheter oily chemoembolization. *AJR Am J Roentgenol* 1995; **165**: 315–21.
48. Liapi E, Georgiades CC, Hong K, Geschwind JF. Transcatheter arterial chemoembolization: current technique and future promise. *Tech Vasc Interv Radiol* 2007; **10**: 2–11.
49. Jaeger HJ, Mehring UM, Castaneda F, *et al.* Sequential transarterial chemoembolization for unresectable advanced hepatocellular carcinoma. *Cardiovasc Intervent Radiol* 1996; **19**: 388–96.
50. Yamashita Y, Torashima M, Oguni T, *et al.* Liver parenchymal changes after transcatheter arterial embolization therapy for hepatoma: CT evaluation. *Abdom Imaging* 1993; **18**: 352–6.
51. Ernst O, Sergent G, Mizrahi D, *et al.* Treatment of hepatocellular carcinoma by transcatheter arterial chemoembolization: comparison of planned periodic chemoembolization and chemoembolization based on tumor response. *AJR Am J Roentgenol* 1999; **172**: 59–64.
52. Terzi E, Golfieri R, Piscaglia F, *et al.* Response rate and clinical outcome of HCC after first and repeated cTACE performed "on demand". *J Hepatol* 2012; **57**: 1258–67.
53. Kim HY, Park JW, Joo J, *et al.* Severity and Timing of Progression Predict Refractoriness to Transarterial Chemoembolization in Hepatocellular Carcinoma. *J Gastroenterol Hepatol* 2011; **27**: 1051–6.
54. Sacco R, Bertini M, Petruzzi P, *et al.* Clinical impact of selective transarterial chemoembolization on hepatocellular carcinoma: a cohort study. *World J Gastroenterol* 2009; **15**: 1843–8.
55. Li X, Feng GS, Zheng CS, Zhuo CK, Liu X. Expression of plasma vascular endothelial growth factor in patients with hepatocellular carcinoma and effect of transcatheter arterial chemoembolization therapy on plasma vascular endothelial growth factor level. *World J Gastroenterol* 2004; **10**: 2878–82.
56. Wang B, Xu H, Gao ZQ, *et al.* Increased expression of vascular endothelial growth factor in hepatocellular carcinoma after transcatheter arterial chemoembolization. *Acta Radiol* 2008; **49**: 523–9.
57. Carmeliet P, Jain RK. Angiogenesis in cancer and other diseases. *Nature* 2000; **407**: 249–57.
58. Yao DF, Wu XH, Zhu Y, *et al.* Quantitative analysis of vascular endothelial growth factor, microvascular density and their clinicopathologic features in human hepatocellular carcinoma. *Hepatobiliary Pancreat Dis Int* 2005; **4**: 220–6.
59. Kaseb AO, Hassan MM, Lin E, *et al.* V-CLIP: Integrating plasma vascular endothelial growth factor into a new scoring system to stratify patients with advanced hepatocellu-

lar carcinoma for clinical trials. *Cancer* 2010; **117**: 2478–88.
60. Tseng CS, Lo HW, Chen PH, *et al.* Clinical significance of plasma D-dimer levels and serum VEGF levels in patients with hepatocellular carcinoma. *Hepatogastroenterology* 2004; **51**: 1454–8.
61. Wilhelm S, Chien DS. BAY 43-9006: preclinical data. *Curr Pharm Des* 2002; **8**: 2255–7.
62. Carlomagno F, Anaganti S, Guida T, *et al.* BAY 43-9006 inhibition of oncogenic RET mutants. *J Natl Cancer Inst* 2006; **98**: 326–34.
63. Lencioni R, Llovet JM, Han G, *et al.* (2012) Sorafenib or placebo in combination with transarterial chemoembolization (TACE) with doxorubicin-eluting beads (DEBDOX) for intermediate-stage hepatocellular carcinoma (HCC): Phase II, randomized, double-blind SPACE trial. *J Clin Oncol* **30**, (Suppl 4; abstr LBA154).
64. Pawlik TM, Reyes DK, Cosgrove D, *et al.* Phase II Trial of Sorafenib Combined With Concurrent Transarterial Chemoembolization With Drug-Eluting Beads for Hepatocellular Carcinoma. *J Clin Oncol* 2011; **29**: 3960–7.
65. Sieghart W, Pinter M, Reisegger M, *et al.* Conventional transarterial chemoembolisation in combination with sorafenib for patients with hepatocellular carcinoma: a pilot study. *Eur Radiol* 2012; **22**: 1214–23.
66. Chung YH, Han G, Yoon JH, *et al.* Interim analysis of START: Study in asia of the combination of TACE (Transcatheter arterial chemoembolization) with sorafenib in patients with hepatocellular carcinoma trial. *Int J Cancer* 2013; **132**: 2448–58.
67. Kudo M, Imanaka K, Chida N, *et al.* Phase III study of sorafenib after transarterial chemoembolisation in Japanese and Korean patients with unresectable hepatocellular carcinoma. *Eur J Cancer* 2011; **47**: 2117–27.
68. Park JW, Koh YH, Kim HB, *et al.* Phase II study of concurrent transarterial chemoembolization and sorafenib in patients with unresectable hepatocellular carcinoma. *J Hepatol* 2012; **56**: 1336–42.

Digestive Endoscopy 2014; **26** (Suppl. 1): 79–85 doi: 10.1111/den.12179

Review

Contrast-enhanced endoscopic ultrasound

Masayuki Kitano, Hiroki Sakamoto and Masatoshi Kudo

Department of Gastroenterology and Hepatology, Faculty of Medicine, Kinki University, Osaka-sayama, Japan

Compared to other imaging modalities, endoscopic ultrasound (EUS) has limitations in terms of image enhancement. However, with the availability of contrast agents in ultrasonography, EUS has evolved. Contrast-enhanced Doppler EUS (CD-EUS) enhances Doppler signals from vessels and is useful for characterizing lesions detected by EUS. Moreover, contrast-enhanced harmonic EUS (CH-EUS) with second-generation ultrasound contrast agents and a broad band transducer allows microvessels and parenchymal perfusion to be visualized. Vascularity can also be quantitatively analyzed during CH-EUS by generating a time-intensity curve. CE-EUS is useful for characterizing pancreatic lesions and can detect pancreatic adenocarcinomas with a sensitivity of 94% and a specificity of 89% as a result of the hypo-enhancement of these lesions. Indeed, CH-EUS is superior to multiple detector-computed tomography in terms of the differential diagnosis of small lesions that are ≤2 cm. CH-EUS complements EUS-guided fine-needle aspiration (EUS-FNA) as it identifies the EUS-FNA target and lesions with false-negative EUS-FNA findings. CH-EUS is also used to estimate the malignant potential of gastrointestinal stromal tumors and helps to differentiate between malignant and benign lymphadenopathy.

Key words: contrast-enhanced endoscopic ultrasound, endoscopic ultrasound, ultrasound contrast

DEVELOPMENT OF CONTRAST-ENHANCED ENDOSCOPIC ULTRASOUND

ENDOSCOPIC ULTRASOUND (EUS) imaging has been evolving since the first report on its utility in the diagnosis of digestive diseases.[1–3] Its development includes color and power Doppler, 3D imaging and electronic scanning, tissue harmonic, elastography and contrast enhancement.[4] However, compared to other imaging modalities such as computed tomography (CT) and magnetic resonance imaging (MRI), EUS is limited in terms of characterizing lesions with contrast enhancement.

Hemodynamics of any area, both pathological and normal, needs to be evaluated for both blood flow in small vessels (2 or 3 mm in minimum diameter) and parenchymal microvasculature.[5] Contrast-enhanced endoscopic ultrasound (CE-EUS) was first reported by Kato *et al*., who used fundamental EUS with carbon dioxide gas.[6] The infusion of carbon dioxide gas through a catheter implanted into the celiac or superior mesenteric artery allowed vascularity to be depicted in EUS images. However, this technique was limited by the fact that the EUS had to be carried out during angiography examinations. EUS was then equipped with color and power Doppler mode to identify large vessels; this was particularly useful for avoiding vessels during EUS-guided fine-needle aspiration (EUS-FNA). However, whereas Doppler EUS can be used to assess whether target lesions have large vessels, it detects vessels with slow flow with poor sensitivity and cannot depict parenchymal perfusion.

The subsequent development of i.v. ultrasound contrast agents composed of microbubbles enabled us to carry out CE-EUS without having to carry out angiography.[7–9] Contrast-enhanced Doppler EUS increases the sensitivity to signals from vessels by generating pseudo-Doppler signals from microbubbles.[7–12] However, contrast-enhanced Doppler EUS suffers from artifacts such as blooming, in which vessels appear to be larger than they really are.[8–10] Recently, technological innovations in contrast-enhanced harmonic imaging have allowed microvessels and parenchymal perfusion to be visualized.[13,14] This allows lesions to be characterized more accurately.

INTRAVENOUS ULTRASOUND CONTRAST AGENTS

ULTRASOUND CONTRAST AGENTS consist of microbubbles of approximately 2–5 μm in diameter.[9,15] In addition to the back-scattering of the ultrasound signal, contrast microbubbles oscillate to sound pressure and have a

Corresponding: Masayuki Kitano, Department of Gastroenterology and Hepatology, Kinki University Faculty of Medicine, 377-2 Ohno-higashi, Osaka-sayama 589-8511, Japan. Email: m-kitano@med.kindai.ac.jp
Received 29 May 2013; accepted 21 August 2013.

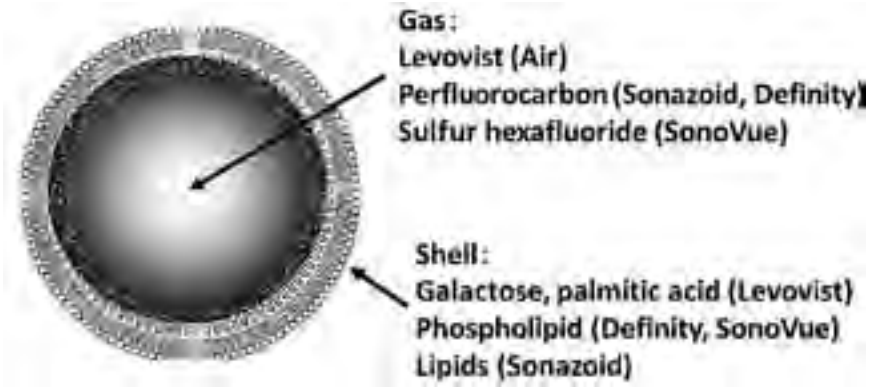

Figure 1 Ultrasound contrast agents. First-generation ultrasound contrast agent (Levovist; Bayer Schering Pharma, Berlin, Germany) is composed of air, whereas second-generation ultrasound contrast agents (SonoVue [Bracco SpA, Milan, Italy], Sonazoid [Daiichi-Sankyo, Tokyo, Japan; GE Healthcare Milwaukee, WI, USA, and Definity [Lantheus Medical Imaging, Billerica, MA, USA]) are composed of other gasses.

variable asymmetrical diameter of between 2 and 10 μm.[15,16] As the microbubbles are given through a large peripheral vein, they do not leave the vascular system and pass through the lung circulation inducing contrast enhancement of the whole vascular system.[15,16] The first ultrasound contrast agent was Levovist (Bayer Schering Pharma, Berlin, Germany), which consists of microbubbles of air that are covered by galactose and palmitic acid (Fig. 1).[15] When used during transabdominal ultrasonography, Levovist depicts harmonic signals from microbubbles, thus allowing contrast-enhanced harmonic imaging.[17–20] However, contrast-enhanced harmonic imaging requires high acoustic power to oscillate or break the Levovist microbubbles. EUS is equipped with only a small transducer and the transmission signals from this transducer are too low to oscillate or break Levovist microbubbles. By contrast, second-generation ultrasound contrast agents, such as SonoVue (Bracco SpA, Milan, Italy), Sonazoid (Daiichi-Sankyo, Tokyo, Japan; GE Healthcare Milwaukee, WI, USA) and Definity (Lantheus Medical Imaging, Billerica, MA, USA) (which consists of microbubbles of gases other than air) (Fig. 1), can be oscillated or broken by lower acoustic power.[9,10,13,21] The development of the latter microbubbles thus promoted contrast-enhanced harmonic imaging in the field of EUS.[13,14,16,22,23]

CONTRAST-ENHANCED DOPPLER EUS

UNTIL RECENTLY, POWER Doppler and color Doppler were used for CE-EUS.[7,8,21,24–27] All types of ultrasound contrast agents induce phase shift (pseudo-Doppler signals), which enhances the Doppler signals from the vessels. Thus, infusing a contrast agent increases the sensitivity with which color and power Doppler imaging depicts Doppler signals from vessels.[10,11] However, contrast-enhanced Doppler EUS suffers from Doppler-related artifacts such as blooming. Recently, a novel type of directional power Doppler method called Directional eFLOW (Aloka Co., Ltd, Tokyo, Japan) was developed.[28] This method permits blood flow in minute vessels to be detected in more detail than can be achieved with conventional power or color Doppler (Fig. 2). In the directional eFLOW mode, fewer blooming artifacts are observed because broadband transmission is optimized and the real repeating frequency is increased.

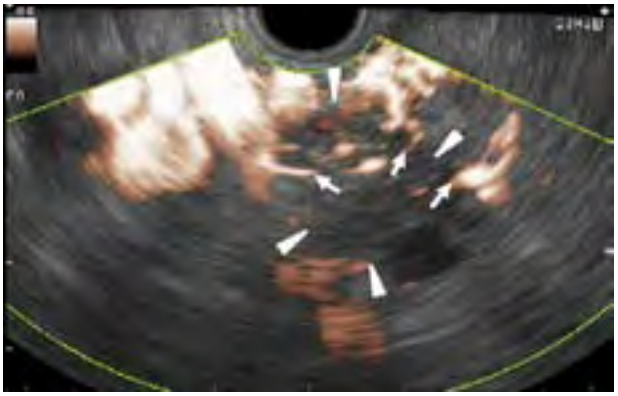

Figure 2 Contrast-enhanced directional eFLOW imaging in a pancreatic carcinoma. Endoscopic ultrasound with contrast-enhanced directional eFLOW imaging shows a hypoechoic tumor (arrowheads) at the pancreas head. Irregular vessels (arrows) are observed at the periphery of the tumor with fewer blooming artefacts. Color signals are fewer in the center of the tumor than in the periphery.

CONTRAST-ENHANCED HARMONIC EUS

WHEN THE ULTRASOUND contrast agents receive a certain range of acoustic power, they produce a second harmonic component.[10,11,29,30] The second harmonic component from microbubbles is much higher than that from

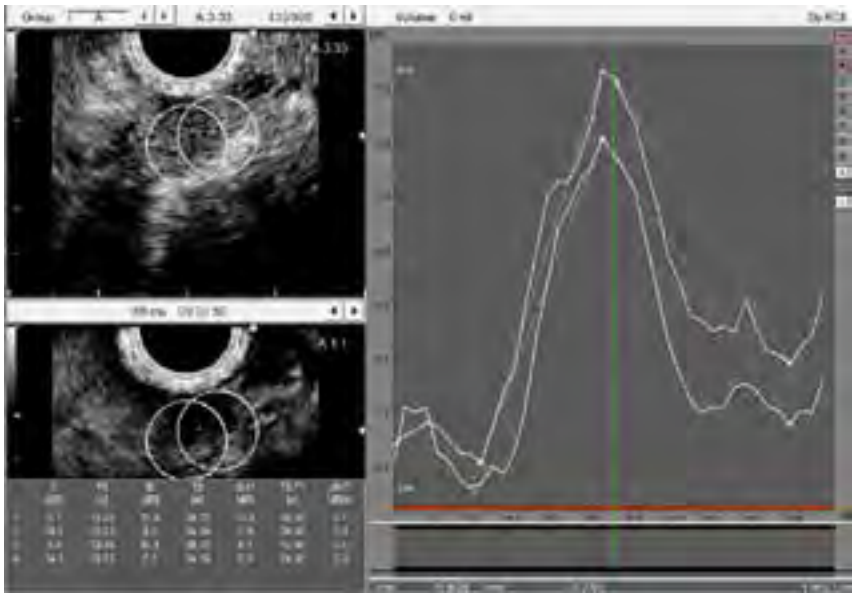

Figure 3 Time–intensity curve of echo intensity in a pancreatic carcinoma. Time-course of the echo intensity in the colored circle is measured.

the tissue. Contrast-enhanced harmonic EUS selectively depicts the second harmonic component, which results in selective visualization of microbubbles.[10,11,29,30] Compared to Doppler imaging, which depicts vessel flow, contrast-enhanced harmonic imaging depicts the microbubbles themselves.[10,11,14] Thus, contrast-enhanced harmonic imaging can visualize fine vessels with slow flow. This technology allows microvessels to be visualized as well as parenchymal perfusion.[14] Moreover, by measuring the time-course of echogenicity intensity (time–intensity curve), vascularity can be quantitatively analyzed (Fig. 3).[5,31–34]

CE-EUS FOR PANCREATIC DISEASES

ENDOSCOPIC ULTRASOUND HAS an advantage over other imaging methods in obtaining high-resolution images of the pancreas, which is a highly sensitive method for the diagnosis of pancreatic tumors.[35–37] However, EUS has been limited in the characterization of some lesions in the pancreas. Evaluation of vascularity using contrast agents is one of the candidates to improve the ability to characterize pancreatic lesions depicted by EUS.[5,9,16,22,30] The finding of a hypoenhancing mass was a sensitive and accurate identifier of patients with adenocarcinoma, which was more accurate in the diagnosis than finding a hypoechoic lesion using standard EUS ($P < 0.001$).[38] A recent meta-analysis on CE-EUS that analyzed reports on both contrast-enhanced Doppler and contrast-enhanced harmonic EUS showed that this method differentially diagnoses pancreatic adenocarcinomas with a pooled sensitivity and specificity of 94% and 89%, respectively.[39] This article also showed that the detection of a hypoenhanced lesion is an accurate predictor of pancreatic adenocarcinoma. However, this article included results of both CD-EUS and CH-EUS.[39] As described previously, CD-EUS has a limitation in the depiction of small vessels with slow flow and depicts artifacts such as blooming. Therefore, CD-EUS fails to evaluate the vascularity of some tumors, such as those of small size and adjacent to large vessels. In contrast, CH-EUS allows visualization of microvasculature, which results in detailed observation of intratumoral structure and characterization of difficult cases (Fig. 4).[14,40] Indeed, hypovascularity as a sign of ductal carcinomas in CH-EUS obtained a sensitivity of 89–95% and a specificity of 64–89%.[38,40,41] Particularly, CH-EUS was significantly more accurate than CT in diagnosing small ductal carcinomas of ≤2 cm ($P < 0.034$).[41] The sensitivity and specificity in diagnosing pancreatic carcinomas with EUS are 91% and 94%, respectively, whereas those values with CT are 71% and 92%, respectively.[41]

With respect to pancreatic neuroendocrine tumors, most heterogeneous hypoechoic areas and anechoic areas corresponded to hemorrhage or necrosis on pathological examination, which was the most significant factor for malignancy. They were identified as filling defects in CD-EUS and were more clearly recognized than in conventional EUS.[26] Recent articles on quantitative analyses using a time–intensity curve with CH-EUS revealed that the values of maximum intensity,[33] accumulated intensity during observation,[34] intensity reduction rate,[32] and the ratio between the uptake inside the mass and the uptake of the surrounding parenchyma[31] are

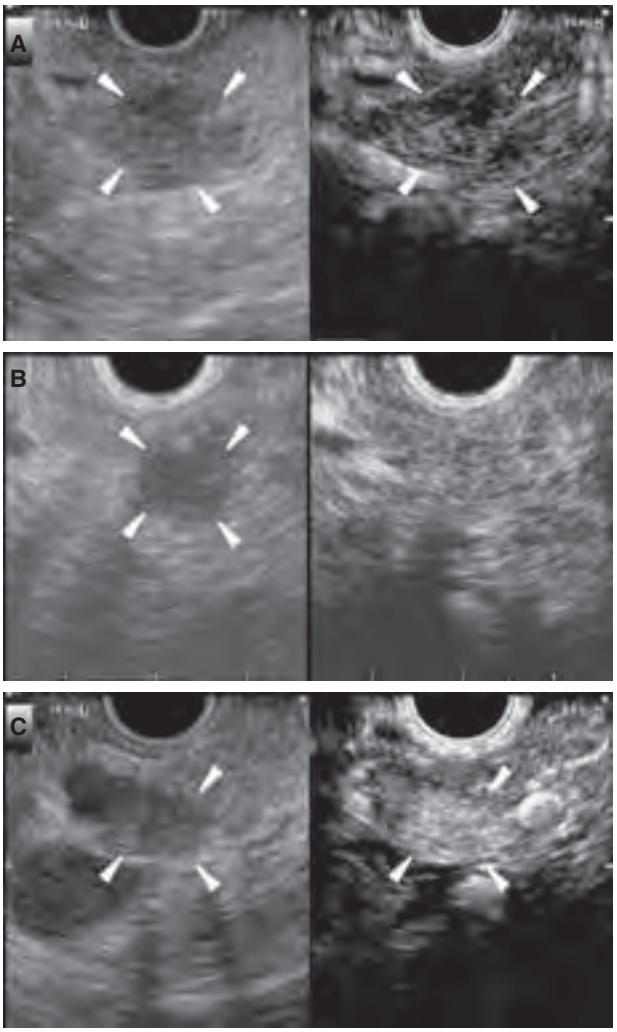

Figure 4 Typical contrast-enhanced harmonic endoscopic ultrasound (CH-EUS) images of pancreatic tumors. (a) Ductal carcinoma with hypoenhancement. Conventional EUS (left) shows a hypoechoic area (arrowheads) of 15 mm in diameter at the pancreas tail. CH-EUS (right) indicates that the area has hypoenhancement (arrowheads) compared with the surrounding tissue. (b) Inflammatory pseudotumor with isoenhancement. Conventional EUS (left) shows a hypoechoic area (arrowheads) of 9 mm at the pancreas body. CH-EUS (right) indicates homogeneous enhancement in this area similar to the surrounding tissue; a margin is not observed. (c) Neuroendocrine tumor with hyperenhancement. Conventional EUS (left) shows a hypoechoic mass (arrowheads) of 9 mm in diameter at the pancreas body. CH-EUS (right) indicates that enhancement (arrowheads) in the mass is higher than in the surrounding tissue.

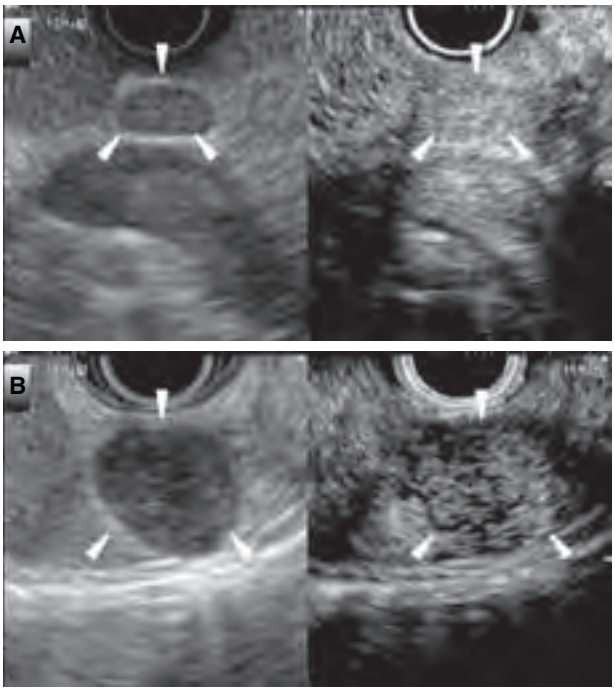

Figure 5 Typical contrast-enhanced harmonic endoscopic ultrasound (CH-EUS) images of lymphadenopathy. (a) Reactive lymphadenopathy with homogeneous enhancement. Conventional EUS (left) shows a lymph node of 10 mm in diameter (arrowheads). CH-EUS (right) indicates that the lymph node has homogeneous enhancement (arrowheads). (b) Metastatic lymphadenopathy with heterogeneous enhancement. Conventional EUS (left) shows a lymph node of 15 mm in diameter (arrowheads). CH-EUS (right) indicates that the lymph node has heterogeneous enhancement (arrowheads).

useful for discrimination of carcinomas from autoimmune pancreatitis, pseudotumors and neuroendocrine tumors. CH-EUS is also used for T staging of pancreatobiliary carcinomas. CH-EUS is superior to tissue harmonic EUS without contrast enhancement in T staging.[42] In particular, CH-EUS more clearly depicts invasion of the portal vein.

CE-EUS FOR DIGESTIVE TRACT DISEASES

WHEN CH-EUS WAS carried out in subepithelial tumors, the time–intensity curve revealed that echo intensity in gastrointestinal stromal tumors (GIST) was significantly higher than that in benign tumors such as lipomas.[43] In addition, CH-EUS allows visualization of vessels flowing from the periphery to the center of GIST (Fig. 5).[43,44] All high-grade malignancy GIST possess these irregular vessels.[44] CH-EUS depicted these irregular vessels in all high-grade malignancy GIST, whereas CT depicted

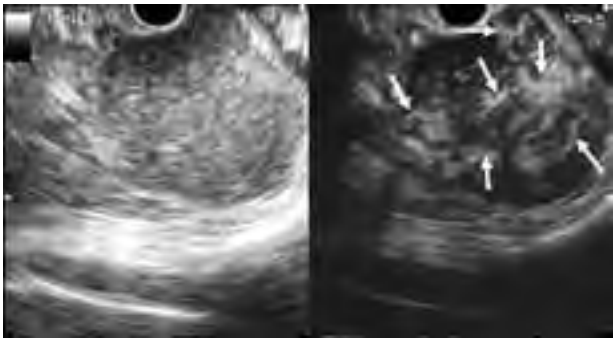

Figure 6 Typical contrast-enhanced harmonic endoscopic ultrasound (CH-EUS) image of gastrointestinal stromal tumor with high-grade malignancy. Conventional EUS (left) shows a submucosal tumor of 50 mm in diameter. CH-EUS (right) indicates that the tumor has irregular vessels (arrows).

Figure 7 Fine-needle aspiration (FNA) guided by contrast-enhanced harmonic endoscopic ultrasound (CH-EUS). CH-EUS (right) reveals a tumor with hypoenhancement (arrowheads), whereas conventional EUS does not (left). FNA can be carried out under the guidance of CH-EUS. Arrows indicate a needle.

them in only 31%.[44] These results suggest that CH-EUS can be applied for estimation of the malignant potential of GIST.[44]

Differential diagnosis of malignant from benign lymphadenopathy is challenging for radiologists and gastroenterologists. CD-EUS is reported to be useful for differential diagnosis of malignant from benign lymphadenopathy. On CD-EUS, filling defect is a typical feature of malignant lymphadenopathy with a sensitivity of 100% and a specificity of 86.4%.[27] When CH-EUS was used for the diagnosis of intra-abdominal lesions of undetermined origin, 96.3% of malignant lesions exhibited heterogeneous enhancement, whereas 75% of benign lesions exhibited homogeneous enhancement (Fig. 6).[45] Thus, these techniques can be applied for N staging of digestive tumors.

CE-EUS FOR EUS-FNA

CONVENTIONAL EUS SOMETIMES fails to depict pancreatic tumors in cases with chronic pancreatitis, diffusely infiltrating carcinoma or a recent episode of acute pancreatitis.[46] In such cases, the target of EUS-FNA cannot be identified. Because contrast-enhanced harmonic EUS clearly depicts subtle lesions that conventional EUS cannot identify, it can be used to identify the target of EUS-FNA (Fig. 7).[38,41,47] It can also be used to identify a specific site within an otherwise clearly visible lesion that would be more suitable than other sites for EUS-FNA.[48] Identification and avoidance of an avascular site in a lesion may help avoid sampling necrotic areas (Fig. 8).

Two articles have reported that contrast-enhanced harmonic EUS is as sensitive as EUS-FNA and thus may be complementary to EUS-FNA, particularly with respect to the

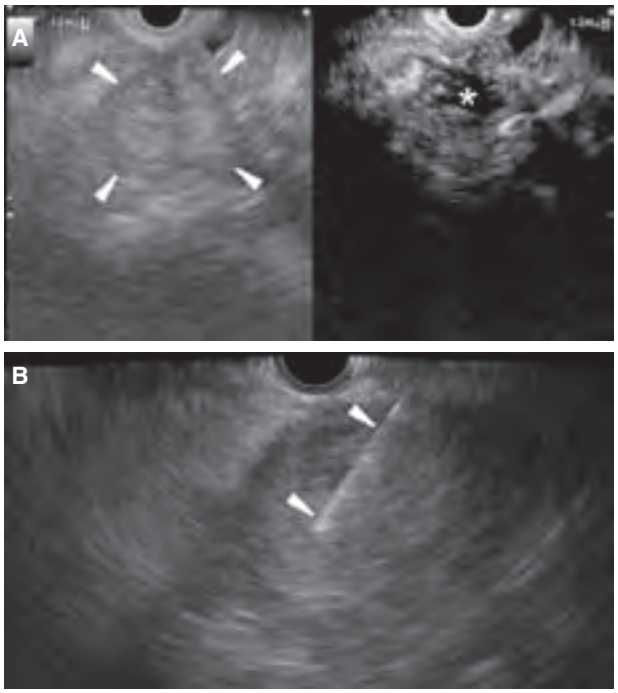

Figure 8 Contrast-enhanced harmonic endoscopic ultrasound (CH-EUS) images of pancreatic carcinoma with a necrotic area. (a) Conventional EUS (left) shows a tumor of 35 mm in diameter (arrowheads) at the pancreas head. CH-EUS (right) identifies an avascular site (asterisk) at the center of the tumor. (b) EUS-fine-needle aspiration is carried out at the periphery of the tumor. Arrowheads indicate a needle.

identification of pancreatic adenocarcinomas with false-negative EUS-FNA findings.[40,41] EUS-FNA is sometimes difficult to carry out because of intervening vessels or anticoagulation treatment. In such cases, CE-EUS could be a

useful substitute.[49] CE-EUS might also help assess lymph nodes that cannot be accessed by EUS-FNA because of an intervening tumor or help eliminate the waste of time and risk in carrying out EUS-FNA at a second site.[49]

CONCLUSIONS

CONTRAST-ENHANCED EUS IS useful for characterization of tumors in the digestive organs. By elimination of Doppler-related artifacts, contrast enhanced harmonic EUS allows visualization of microvasculature and parenchymal perfusion, which leads not only to improved characterization of EUS-detected lesions, but also to identification of small tumors, estimation of malignant potential, as well as tumor staging. Contrast-enhanced harmonic EUS also complements EUS-FNA as it clearly depicts the target of EUS-FNA and identifies tumors with false-negative EUS-FNA findings.

CONFLICT OF INTERESTS

AUTHORS DECLARE NO conflict of interests for this article.

REFERENCES

1 DiMagno EP, Baxton JL, Regan PT *et al*. Ultrasonic endoscope. *Lancet* 1980; **i**: 629–31.
2 Strohm WD, Phillip J, Classen M *et al*. Ultrasonic tomography by means of an ultrasonic fiberendoscope. *Endoscopy* 1980; **12**: 241–4.
3 Kitano M, Kudo M, Sakamoto H *et al*. Endoscopic ultrasonography and contrast-enhanced endoscopic ultrasonography. *Pancreatology* 2011; **11** (Suppl 2): 28–33.
4 Fusaroli P, Saftoiu A, Mancino MG, Caletti G Eloubeidi MA. Techniques of image enhancement in EUS (with videos). *Gastrointest. Endosc.* 2011; **74**: 645–55.
5 Hirooka Y, Itoh A, Kawashima H *et al*. Contrast-enhanced endoscopic ultrasonography in digestive diseases. *J. Gastroenterol.* 2012; **47**: 1063–72.
6 Kato T, Tsukamoto Y, Naitoh Y *et al*. Ultrasonographic and endoscopic ultrasonographic angiography in pancreatic mass lesions. *Acta Radiol.* 1995; **36**: 381–7.
7 Hocke M, Schulze E, Gottschalk P *et al*. Contrast-enhanced endoscopic ultrasound in discrimination between focal pancreatitis and pancreatic cancer. *World J. Gastroenterol.* 2006; **12**: 246–50.
8 Sakamoto H, Kitano M, Suetomi Y *et al*. Utility of contrast-enhanced endoscopic ultrasonography for diagnosis of small pancreatic carcinomas. *Ultrasound Med. Biol.* 2008; **34**: 525–32.
9 Sanchez MV, Varadarajulu S, Napoleon B. EUS contrast agents: What is available, how do they work, and are they effective? *Gastrointest. Endosc.* 2009; **69**: 571–7.
10 Kudo M. Various contrast-enhanced imaging modes after administration of Levovist. In: Kudo M (ed.). *Contrast Harmonic Imaging in the Diagnosis and Treatment of Hepatic Tumors*. Tokyo: Springer, 2003; 22–30.
11 Kitano M, Sakamoto H, Kudo M. Endoscopic ultrasound: Contrast enhancement. *Gastrointest. Endosc. Clin. N. Am.* 2012; **22**: 349–58.
12 Bhutani MS, Hoffman BJ, van Velse A *et al*. Contrast-enhanced endoscopic ultrasonography with galactose microparticles: SHU508A (Levovist). *Endoscopy* 1997; **29**: 635–9.
13 Kitano M, Kudo M, Sakamoto H *et al*. Preliminary study of contrast-enhanced harmonic endosonography with second-generation contrast agents. *J. Med. Ultrason.* 2008; **35**: 11–8.
14 Kitano M, Sakamoto H, Matsui U *et al*. A novel perfusion imaging technique of the pancreas: Contrast-enhanced harmonic EUS (with video). *Gastrointest. Endosc.* 2008; **67**: 141–50.
15 Quaia E. Classification and safety of microbubble-based contrast agents. In: Quaia E (ed.). *Contrast Media in Ultrasonography. Basic Principles and Clinical Applications*. Berlin: Springer, 2005; 1–14.
16 Săftoiu A, Dietrich CF, Vilmann P. Contrast-enhanced harmonic endoscopic ultrasound. *Endoscopy* 2012; **44**: 612–7.
17 Oshikawa O, Tanaka S, Ioka T *et al*. Dynamic sonography of pancreatic tumors: Comparison with dynamic CT. *Am. J. Roentgenol.* 2002; **178**: 1133–7.
18 Kitano M, Kudo M, Maekawa K *et al*. Dynamic imaging of pancreatic diseases by contrast enhanced coded phase inversion harmonic ultrasonography. *Gut* 2004; **53**: 854–9.
19 Fukuta N, Kitano M, Maekawa K *et al*. Estimation of the malignant potential of gastrointestinal stromal tumors: The value of contrast enhanced coded phase-inversion harmonic US. *J. Gastroenterol.* 2005; **40**: 247–55.
20 Sofuni A, Iijima H, Moriyasu F *et al*. Differential diagnosis of pancreatic tumors using contrast imaging. *J. Gastroenterol.* 2005; **40**: 518–25.
21 Becker D, Strobel D, Bernatik T *et al*. Echo-enhanced color- and power-Doppler EUS for the discrimination between focal pancreatitis and pancreatic carcinoma. *Gastrointest. Endosc.* 2001; **53**: 784–9.
22 Reddy NK, Ioncică AM, Săftoiu A *et al*. Contrast-enhanced endoscopic ultrasonography. *World J. Gastroenterol.* 2011; **17**: 42–8.
23 Dietrich CF, Ignee A, Frey H. Contrast-enhanced endoscopic ultrasound with low mechanical index: A new technique. *Z. Gastroenterol.* 2005; **43**: 1219–23.
24 Saftoiu A, Iordache SA, Gheonea DI *et al*. Combined contrast-enhanced power Doppler and real-time sonoelastography performed during EUS, used in the differential diagnosis of focal pancreatic masses (with videos). *Gastrointest. Endosc.* 2010; **72**: 739–47.

25 Dietrich CF, Ignee A, Braden B *et al*. Improved differentiation of pancreatic tumors using contrast-enhanced endoscopic ultrasound. *Clin. Gastroenterol. Hepatol.* 2008; **6**: 590–7.
26 Ishikawa T, Itoh A, Kawashima H *et al*. Usefulness of EUS combined with contrast-enhancement in the differential diagnosis of malignant versus benign and preoperative localization of pancreatic endocrine tumors. *Gastrointest. Endosc.* 2010; **71**: 951–9.
27 Kanamori A, Hirooka Y, Itoh A *et al*. Usefulness of contrast-enhanced endoscopic ultrasonography in the differentiation between malignant and benign lymphadenopathy. *Am. J. Gastroenterol.* 2006; **101**: 45–51.
28 Das K, Kudo M, Kitano M *et al*. Diagnostic value of endoscopic ultrasound-guided directional eFLOW in solid pancreatic lesions. *J. Med. Ultrason.* 2013; **40**: 211–18.
29 Whittingham TA. Contrast-specific imaging techniques; technical perspective. In: Quaia E (ed.). *Contrast Media in Ultrasonography. Basic Principles and Clinical Applications*. Berlin: Springer, 2005; 43–84.
30 Kitano M, Sakamoto H, Komaki T, Kudo M. New techniques and future perspective of EUS for the differential diagnosis of pancreatic malignancies; Contrast harmonic imaging. *Dig. Endosc.* 2011; **23** (Suppl 1): 46–50.
31 Seicean A, Badea R, Stan-Iuga R, Mocan T, Gulei I, Pascu O. Quantitative contrast-enhanced harmonic endoscopic ultrasonography for the discrimination of solid pancreatic masses. *Ultraschall. Med.* 2010; **31**: 571–6.
32 Matsubara H, Itoh A, Kawashima H *et al*. Dynamic quantitative evaluation of contrast enhanced endoscopic ultrasonography in the diagnosis of pancreatic diseases. *Pancreas* 2011; **40**: 1073–9.
33 Imazu H, Kanazawa K, Mori N *et al*. Novel quantitative perfusion analysis with contrast-enhanced harmonic EUS for differentiation of autoimmune pancreatitis from pancreatic carcinoma. *Scand. J. Gastroenterol.* 2012; **47**: 853–60.
34 Gheonea DI, Streba CT, Ciurea T Săftoiu A. Quantitative low mechanical index contrast enhanced endoscopic ultrasound for the differential diagnosis of chronic pseudotumoral pancreatitis and pancreatic cancer. *BMC Gastroenterol.* 2013; **13**: 2.
35 Rösch T, Lightdale CJ, Botet JF *et al*. Localization of pancreatic endocrine tumors by endoscopic ultrasonography. *N. Engl. J. Med.* 1992; **326**: 1721–6.
36 DeWitt J, Devereaux B, Chriswell M *et al*. Comparison of endoscopic ultrasonography and multidetector computed tomography for detecting and staging pancreatic cancer. *Ann. Intern. Med.* 2004; **141**: 753–63.
37 Khashab MA, Yong E, Lennon AM *et al*. EUS is still superior to multidetector computed tomography for detection of pancreatic neuroendocrine tumors. *Gastrointest. Endosc.* 2011; **73**: 691–6.
38 Fusaroli P, Spada A, Mancino MG *et al*. Contrast harmonic echo-endoscopic ultrasound improves accuracy in diagnosis of solid pancreatic masses. *Clin. Gastroenterol. Hepatol.* 2010; **8**: 629–34.
39 Gong TT, Hu DM, Zhu Q. Contrast-enhanced EUS for differential diagnosis of pancreatic mass lesions: A meta-analysis. *Gastrointest. Endosc.* 2012; **76**: 301–9.
40 Napoleon B, Alvarez-Sanchez MV, Gincoul R *et al*. Contrast-enhanced harmonic endoscopic ultrasound in solid lesions of the pancreas: Results of a pilot study. *Endoscopy* 2010; **42**: 564–70.
41 Kitano M, Kudo M, Yamao K *et al*. Characterization of small solid tumors in the pancreas: Contrast: The value of contrast-enhanced harmonic endoscopic ultrasonography. *Am. J. Gastroenterol.* 2012; **107**: 303–10.
42 Imazu H, Uchiyama Y, Matsunaga K *et al*. Contrast-enhanced harmonic EUS with novel ultrasonographic contrast (Sonazoid) in the preoperative T-staging for pancreaticobiliary malignancies. *Scand. J. Gastroenterol.* 2010; **45**: 732–8.
43 Kannengiesser K, Mahlke1 R, Petersen F *et al*. Contrast-enhanced harmonic endoscopic ultrasound is able to discriminate benign submucosal lesions from gastrointestinal stromal tumors. *Scand. J. Gastroenterol.* 2012; **47**: 1515–20.
44 Sakamoto H, Kitano M, Matsui S *et al*. Estimation of malignant potential of GIST by contrast-enhanced harmonic EUS (with video). *Gastrointest. Endosc.* 2011; **73**: 27–237.
45 Xia Y, Kitano M, Kudo M *et al*. Characterization of intra-abdominal lesions of undetermined origin by contrast-enhanced harmonic EUS (with videos). *Gastrointest. Endosc.* 2010; **72**: 637–42.
46 Bhutani MS, Gress FG, Giovannini M *et al*. The no endosonographic detection of tumor (NEST) study: A case series of pancreatic cancers missed on endoscopic ultrasonography. *Endoscopy* 2004; **36**: 385–9.
47 Romagnuolo J, Hoffman B, Vela S *et al*. Accuracy of contrast-enhanced harmonic EUS with a second-generation perflutren lipid microsphere contrast agent (with video). *Gastrointest. Endosc.* 2011; **73**: 52–63.
48 Kitano M, Sakamoto H, Komaki T *et al*. FNA guided by contrast-enhanced harmonic EUS in pancreatic tumors. *Gastrointest. Endosc.* 2009; **69**: A328–A329.
49 Romagnuolo J. Flow, firmness, or FNA? Is enhanced EUS fantastic or just fancy? *Gastrointest. Endosc.* 2012; **76**: 310–2.

Liver Cancer

Liver Cancer 2014;3:1–5
DOI: 10.1159/000343859
Published online: February 28, 2014

2235-1795/14/0031-0001$39.50/0
www.karger.com/lic

Editorial

Prediction of Hepatocellular Carcinoma Incidence Risk by Ultrasound Elastography

Prof. M. Kudo

Editor *Liver Cancer*

In patients with chronic hepatitis and continuous inflammation of the liver, fibrosis develops during the course of wound healing, and with recurrent accumulation of scar tissue and regenerative nodular formation, chronic hepatitis progresses to cirrhosis. In untreated patients with chronic hepatitis C infection, which is a leading cause of hepatocellular carcinoma (HCC), the Metavir liver fibrosis stage (F0, no fibrosis; F4, cirrhosis)[1] increases at an annual rate of F0.1 [2], with a concurrent increase in the incidence of HCC [3]. Therefore, it is extremely important to evaluate the liver fibrosis stage during follow up of chronic hepatitis C so as to understand the HCC risk. However, liver biopsy, the gold standard for diagnosing liver fibrosis, is susceptible to sampling variability [4] and diagnostic variability among pathologists. In addition, repeat biopsy is not recommended because of its invasiveness, the associated pain and risk of hemorrhage. Although serum fibrosis marker and hematology-based prediction algorithms have been widely reported for evaluating liver fibrosis, the results obtained with these methods may be affected by fibrotic conditions in other organs.

Ultrasound elastography emerged as an imaging modality around 2010 and has been found in many studies to be diagnostically useful for liver fibrosis. The word “elastography” (“elasticity” + “graphy”), a collective term for the graphical display of tissue elasticity, was first used in 1991 to describe the technique of strain elastography proposed by Dr. Ophir at the University of Texas. Another term, “tissue elasticity imaging,” is used to define the graphic technology used to capture tissue elasticity over a wider area. However, the terms “elastography” and “tissue elasticity imaging” are now often used interchangeably and are even applied to non-graphic quantitative measurement methods such as that employed by FibroScan.

Ultrasound elastography is classified into two major types based on the measurement principles adopted: strain elastography, which displays differences in tissue strain and is used in real-time tissue elastography (RTE), which is the first commercially available machine in the world launched in 2003 and shear wave elastography, which measures the speed of propagating waves and is used in FibroScan and Virtual Touch tissue quantification (VTQ) [5](table 1). While strain elastography enables the measurement (display) of liver fibrosis,

Liver Cancer 2014;3:1–5
DOI: 10.1159/000343859
Published online: February 28, 2014

Table 1. Classification of various elastography methods. Reproduced with permission from Shiina T et al.[5].

Elastography method / Excitation methods	Strain imaging a)Strain (displacement) b)Geometric measures -Strain ratio -E/B size ratio	Shear wave imaging a)Shear wave speed b)Shear wave speed, Young's modulus
(A)Manual compression -Palpation, -Cardiovascular pulsation	Strain elastography -Real-time tissue elastography™ (Hitachi Aloka) -Elastography (GE, Philips, Toshiba) -ElastoScan™ (Samsung) -eSie Touch™ Elasticity Imaging (Siemens)	
(B)Acoustic radiation force impulse	ARFI imaging -Virtual Touch™ Imaging (Siemens)	Shear wave elastography -ShearWave™ Elastography: SWE (SSI) -Virtual Touch™ IQ: VTIQ (Siemens) -Virtual Touch™ Quantification: VTQ (Siemens) -ElastPQ™ (Philips)
(C)Mechanical vibration and impulse		Transient elastography -FibroScan™ (Echosens)

E/B size ratio=the ratio of the size of a lesion in a stain image to its size in a B-mode image; ARFI=acoustic radiation force impulse.

measurement values in shear wave elastography are affected by inflammation, jaundice, and congestion in addition to fibrosis [6–9]. In other words, measurement values with the latter technique increase as fibrosis, inflammation, jaundice, and congestion exacerbate, and vice versa, presumably because these pathological conditions alter the density, and thereby the elasticity and viscosity, of liver tissue [10].

In 2003, the French company Echosens launched FibroScan. This device calculates the degree of liver stiffness (in kPa) by sending acoustic push pulses from the body surface to the liver and following the waves by ultrasound to measure the shear wave speed. The propagation velocity of shear waves correlates with tissue stiffness, with waves traveling faster in harder tissues. FibroScan has several advantages: (1) it is a non-invasive and painless technique, (2) it provides immediate results (within 30 s of measurement), (3) the results are highly reproducible, (4) the measurement area is as wide as ~1/500th of the total liver mass (the size of a biopsy specimen is ~1/50,000th of the total liver mass), and (5) it can be safely repeated for follow up. On the down side, measurement reproducibility and even the measurement itself can be adversely affected by ascites (push pulses do not travel through fluids) and by thick layers of subcutaneous fat, narrow intercostal spaces, and severe liver atrophy.

In a meta-analysis of studies assessing the stage of liver fibrosis using FibroScan, Friedrich-Rust et al. found that the cut-off level for a diagnosis of F2 or higher was 7.65 kPa [area under receiver operating characteristic (AUROC) curve, 0.84] and for a diagnosis of F4, the cut-off level was 13.01 kPa (AUROC, 0.94) [11], demonstrating that fibrosis staging by FibroScan has high accuracy. However, the stages of fibrosis diagnosed based on liver stiffness do not always match the pathological stage established by liver biopsy. In a study conducted

Liver Cancer

Liver Cancer 2014;3:1–5

DOI: 10.1159/000343859
Published online: February 28, 2014

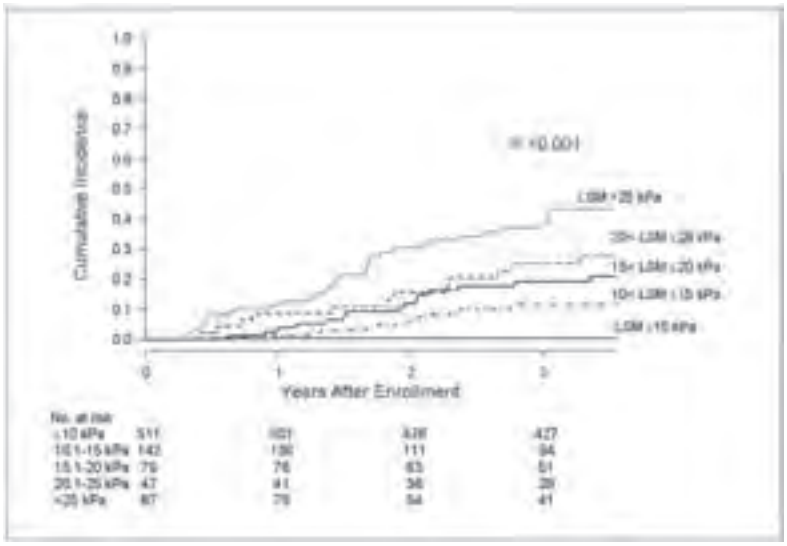

Fig. 1. Cumulative incidence of HCC development stratified based on liver stiffness measurement (LSM, n = 866) in patients with hepatitis C. Reproduced with permission from Masuzaki R et al.[13].

by Ichino et al., 17 (40%) of 42 patients with F2 fibrosis determined by liver biopsy were diagnosed with F0–F1 fibrosis by FibroScan, even though an AUROC of 0.88 was taken to be F2 or higher liver fibrosis, with 81% sensitivity and 80% specificity [12].

Many studies have reported staging differences in liver fibrosis between liver stiffness-based diagnoses and biopsy findings. During the acute phase of acute hepatitis, the liver becomes as stiff as cirrhotic liver, although the stiffness returns to normal as hepatitis improves. Moreover, even among patients with the same fibrosis stage, those with high alanine aminotransferase (ALT) levels resulting from hepatitis B virus (HBV)- or HCV-induced chronic hepatitis have a high degree of liver stiffness compared with patients with normal ALT levels owing to antiviral treatment or the natural course. This suggests that liver stiffness is affected by the severity of inflammation as well as by liver fibrosis, leading to an overestimation of liver stiffness when inflammation is present. Therefore, when staging liver fibrosis based on liver stiffness in patients with high ALT levels, it is important to keep in mind that the actual fibrosis stage might be lower. Note that strain elastography, however, is not affected by inflammation in the liver.

In a study by Masuzaki et al. investigating the relationship between cirrhosis and the incidence of HCC in 866 patients with hepatitis C, HCC developed in 77 patients over the 3-year follow-up period [13]. When patients were classified based on liver stiffness at the initial FibroScan examination, patients with a high degree of liver stiffness subsequently had a high incidence of HCC (fig. 1), and on multivariate analysis, in addition to age, sex, and albumin level, liver stiffness was an independent risk factor associated with HCC incidence [13]. Similarly, in a study by Jung et al. investigating the association between liver stiffness and the incidence of HCC in patients with hepatitis B [14], HCC developed in 57 of 1130 patients after a median follow up of 31 months (fig. 2). Multivariate analysis extracted liver stiffness at initial examination, together with age, sex, alcohol consumption, albumin level, and HB e-antigen positivity, as risk factors associated with HCC incidence.

Because liver stiffness is correlated with the stage of liver fibrosis, it is reasonable to assume that liver with a high degree of stiffness indicates advanced liver fibrosis. This strong correlation between liver stiffness and HCC risk also applies to cirrhotic patients, who have

Liver Cancer 2014;3:1–5
DOI: 10.1159/000343859
Published online: February 28, 2014

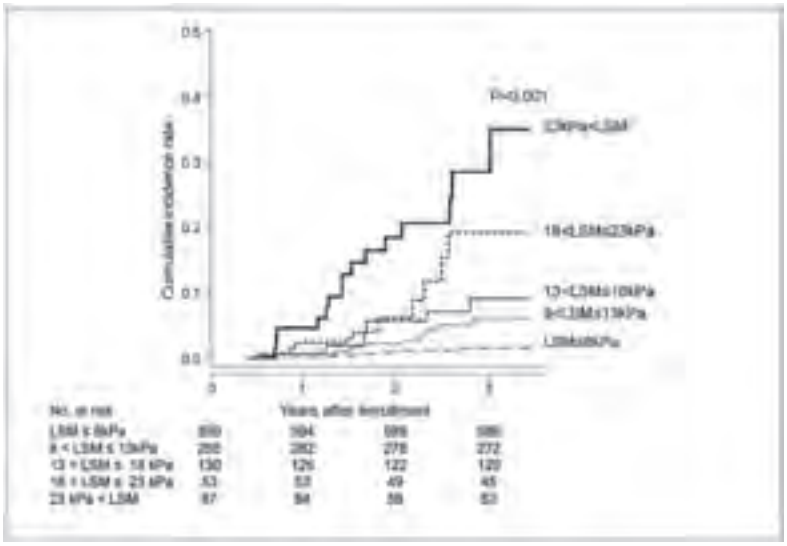

Fig. 2. Cumulative incidence rates of HCC based on stratified LSM (Kaplan-Meier plot) in patients with hepatitis B. The cumulative incidence rates increased significantly in association with higher LSM (log-rank test, $p < 0.0001$, $n = 1130$). Reproduced with permission from Jung KS et al.[14].

a high degree of liver stiffness, suggesting that liver stiffness is a useful clinical indicator to classify patients at high risk of HCC.

In summary, recent advances in ultrasound elastographic technology allow us to predict the occurrence of HCC more accurately. Conventionally, serum fibrosis markers, platelet count, and imaging findings are used to diagnose cirrhosis and the potential risk for HCC. In contrast, ultrasound elastography is a simple, non-invasive, and highly accurate method for predicting the occurrence of HCC. We recommend the proactive use of not only FibroScan, but also VTQ and RTE (table 1), in clinical settings because they are all useful in predicting the risk of a patient developing HCC.

References

1 Bedossa P, Poynard T for the METAVIR cooperative study group: An algorithm for the grading of activity in chronic hepatitis C. The METAVIR Cooperative Study Group. Hepatology 1996;24:289–293.
2 Shiratori Y, Imazeki F, Moriyama M, Yano M, Arakawa Y, Yokosuka O, Kuroki T, Nishiguchi S, Sata M, Yamada G, Fujiyama S, Yoshida H, Omata M: Histologic improvement of fibrosis in patients with hepatitis C who have sustained response to interferon therapy. Ann Intern Med 2000;132:517–524.
3 Yoshida H, Shiratori Y, Moriyama M, Arakawa Y, Ide T, Sata M, Inoue O, Yano M, Tanaka M, Fujiyama S, Nishiguchi S, Kuroki T, Imazeki F, Yokosuka O, Kinoyama S, Yamada G, Omata M: Interferon therapy reduces the risk for hepatocellular carcinoma: national surveillance program of cirrhotic and noncirrhotic patients with chronic hepatitis C in Japan. IHIT Study Group. Inhibition of Hepatocarcinogenesis by Interferon Therapy. Ann Intern Med 1999;131:174–181.
4 Bedossa P, Dargère D, Paradis V: Sampling variability of liver fibrosis in chronic hepatitis C. Hepatology 2003;38:1449–1457.
5 Shiina T: JSUM ultrasound elastography practice guidelines: basics and terminology. J Med Ultrasonics 2013;40:309–323.
6 Arena U, Vizzutti F, Corti G, Ambu S, Stasi C, Bresci S, Moscarella S, Boddi V, Petrarca A, Laffi G, Marra F, Pinzani M: Acute viral hepatitis increases liver stiffness values measured by transient elastography. Hepatology 2008;47:380–384.
7 Millonig G, Reimann FM, Friedrich S, Fonouni H, Mehrabi A, Büchler MW, Seitz HK, Mueller S: Extrahepatic cholestasis increases liver stiffness (FibroScan) irrespective of fibrosis. Hepatology 2008;48:1718–1723.

Liver Cancer 2014;3:1–5
DOI: 10.1159/000343859
Published online: February 28, 2014

8 Sagir A, Erhardt A, Schmitt M, Häussinger D: Transient elastography is unreliable for detection of cirrhosis in patients with acute liver damage. Hepatology 2008;47:592–595.
9 Colli A, Pozzoni P, Berzuini A, Gerosa A, Canovi C, Molteni EE, Barbarini M, Bonino F, Prati D: Decompensated chronic heart failure: increased liver stiffness measured by means of transient elastography. Radiology 2010;257:872–878.
10 Kudo M, Shiina T, Moriyasu F, Iijima H, Tateishi R, Yada N, et al: JSUM ultrasound elastography practice guidelines: liver. J Med Ultrasonics 2013;40:325–357.
11 Friedrich-Rust M, Ong MF, Martens S, Sarrazin C, Bojunga J, Zeuzem S, Herrmann E: Performance of transient elastography for the staging of liver fibrosis: a meta-analysis. Gastroenterology 2008;134:960–974.
12 Ichino N, Osakabe K, Nishikawa T, Sugiyama H, Kato M, Kitahara S, Hashimoto S, Kawabe N, Harata M, Nitta Y, Murao M, Nakano T, Arima Y, Shimazaki H, Suzuki K, Yoshioka K: A new index for non-invasive assessment of liver fibrosis. World J Gastroenterol 2010;16:4809–4816.
13 Masuzaki R, Tateishi R, Yoshida H, Goto E, Sato T, Ohki T, Imamura J, Goto T, Kanai F, Kato N, Ikeda H, Shiina S, Kawabe T, Omata M: Prospective risk assessment for hepatocellular carcinoma development in patients with chronic hepatitis C by transient elastography. Hepatology 2009;49:1954–1961.
14 Jung KS, Kim SU, Ahn SH, Park YN, Kim do Y, Park JY, Chon CY, Choi EH, Han KH: Risk assessment of hepatitis B virus-related hepatocellular carcinoma development using liver stiffness measurement (FibroScan). Hepatology 2011;53:885–894.

Reply to Kadayifci and Brugge

Masayuki Kitano, Ken Kamata, Masatoshi Kudo

We thank Drs. Kadayifci and Brugge for their valuable comments. They discussed the utility of performing endosonography-guided fine-needle aspiration (EUS-FNA) for the differential diagnosis of cystic lesions in the pancreas. We agree that the differential diagnosis of pancreatic cystic lesions can be aided by analyzing fluids for carcinoembryonic antigen and amylase levels, and by performing cytology, *GNAS* mutation analysis, and confocal endomicroscopy [1–3]. In our study [4], patients with branch duct intraductal papillary mucinous neoplasms (IPMNs; cystic lesions connected to the pancreatic duct) underwent surgery because they had symptoms, mural nodules, or concomitant pancreatic ductal adenocarcinomas (PDACs). Pathological diagnosis of all of the resected cystic lesions connected to the pancreatic duct showed that they were branch duct IPMNs. During the same study period, some patients who had pancreatic cystic lesions that were not connected to the pancreatic duct underwent surgery; however, in these cases, the cystic lesions consisted of serous cystic neoplasms, mucinous cystic neoplasms, branch duct IPMNs, and other types of cystic lesions. In other words, the differential diagnosis of cystic lesions that are not connected to the pancreatic duct is difficult and sometimes requires interventional diagnostic methods [1–3], as mentioned by Drs. Kadayifci and Brugge.

The diagnostic criteria employed in our study [4], which depended on the detection of a connection between the lesion and the pancreatic duct, and of mural nodules, were limited by the fact that pathological diagnoses of the resected branch duct IPMNs in 25 of 42 patients revealed them to be benign. As suggested, it is important to avoid unnecessary surgery; thus, EUS-FNA, including cytology and cyst fluid analysis, to predict malignancy can help in this regard [2, 5, 6].

With respect to the surveillance of branch duct IPMN according to size stratification [7], patients were followed at fixed intervals with semiannual EUS, and annual EUS, computed tomography, and magnetic resonance imaging, irrespective of the cyst size [4]. The aim of our study was to investigate the role of follow-up with EUS for the detection of IPMN-derived and IPMN-concomitant PDACs [4]. Therefore, we needed to use a unified interval period for follow-up (semiannual EUS). The results showed that IPMN-concomitant PDACs occurred during follow-up in patients with branch duct IPMNs of 20 mm or less (see Table 2 in our study) [4]. This means that size stratification may not be useful for the detection of IPMN-concomitant PDACs [4].

Competing interests: None

References

1 *Brugge WR, Lewandrowski K, Lee-Lewandrowski E* et al. Diagnosis of pancreatic cystic neoplasms: a report of the cooperative pancreatic cyst study. Gastroenterology 2004; 126: 1330–1336

2 *Dal Molin M, Matthaei H, Wu J* et al. Clinicopathological correlates of activating GNAS mutations in intraductal papillary mucinous neoplasm (IPMN) of the pancreas. Ann Surg Oncol 2013; 20: 3802–3808

3 *Konda VJ, Meining A, Jamil LH* et al. A pilot study of in vivo identification of pancreatic cystic neoplasms with needle-based confocal laser endomicroscopy under endosonographic guidance. Endoscopy 2013; 45: 1006–1013

4 *Kamata K, Kitano M, Kudo M* et al. Value of EUS in early detection of pancreatic ductal adenocarcinomas in patients with intraductal papillary mucinous neoplasms. Endoscopy 2014; 46: 22–29

5 *Pitman MB, Genevay M, Yaeger K* et al. High-grade atypical epithelial cells in pancreatic mucinous cysts are a more accurate predictor of malignancy than "positive" cytology. Cancer Cytopathol 2010; 118: 434–440

6 *Genevay M, Mino-Kenudson M, Yaeger K* et al. Cytology adds value to imaging studies for risk assessment of malignancy in pancreatic mucinous cysts. Ann Surg 2011; 254: 977–983

7 *Tanaka M, Fernandez-del Castillo C, Adsay V* et al. International consensus guidelines 2012 for the management of IPMN and MCN of the pancreas. Pancreatology 2012; 12: 183–197

Masayuki Kitano, MD, PhD
Department of Gastroenterology and Hepatology
Kinki University Faculty of Medicine
377-2 Ohno-higashi
Osaka-sayama
589-8511 Japan
Fax: +81-72-3672880
m-kitano@med.kindai.ac.jp

Correction

Kamata K et al. Value of EUS in early detection of pancreatic ductal adenocarcinomas in patients with intraductal papillary mucinous neoplasms. Endoscopy 2014; 46: 22–29

Figure 2 in the abovementioned article was inadvertently published recording the number of patients with hyperplasia as n = 7. This number is incorrect and the number of patients with hyperplasia should be recorded as n = 1.

Liver Cancer

Liver Cancer 2014;3:41–52
DOI: 10.1159/000343857
Published online: March 10, 2014

2235-1795/14/0031-0041$39.50/0
www.karger.com/lic

Original Paper

Quantitative Levels of Hepatitis B Virus DNA and Surface Antigen and the Risk of Hepatocellular Carcinoma in Patients with Hepatitis B Receiving Long-Term Nucleos(t)ide Analogue Therapy

Miwa Kawanaka[a] Ken Nishino[a] Jun Nakamura[a] Takahito Oka[a]
Noriyo Urata[a] Daisuke Goto[a] Mitsuhiko Suehiro[a]
Hirofumi Kawamoto[a] Masatoshi Kudo[b] Gotaro Yamada[a]

[a]Department of General Internal Medicine 2, Kawasaki Hospital, Kawasaki Medical School, Okayama,
[b]Department of Gastroenterology and Hepatology, Kinki University School of Medicine,
Osaka, Japan

Key Words
HBV DNA · Hepatitis B surface antigen · Hepatitis B virus · Hepatocellular carcinoma · Nucleos(t)ide analogues

Abstract
Background: Serum levels of hepatitis B virus (HBV) DNA are an important predictor of the risk of hepatocellular carcinoma (HCC) in patients with chronic HBV infection. However, little is known about whether high levels of hepatitis B surface antigen (HBsAg) increase the risk for HCC. ***Methods:*** We investigated 167 patients who were treated with nucleos(t)ide analogues (NA) for at least 2 years (median: 5.8 years, range: 2–13.1 years). Relationships between reduced levels of HBsAg and various factors were evaluated. In addition, we evaluated the usefulness of quantitative serum levels of HBV DNA and HBsAg as predictors of HCC development in patients receiving long-term NA therapy. ***Results:*** HCC developed in 9 of the 167 NA-treated patients. In the 9 patients with HCC, HBV DNA was undetectable (<2.1 log copies/mL), but HBsAg levels were ≥2000 C.O.I. in 7 patients. No maternal transmission, long NA treatment period, HBV DNA levels <3.0 log copies/mL, and reduced hepatitis B e antigen levels during the first 24 weeks of treatment were a significant factor of HBsAg levels <2000 C.O.I.. ***Conclusions:*** Hepatocarcinogenesis was observed in patients with high HBsAg levels,

Miwa Kawanaka, MD, PhD

Department of General Internal Medicine 2, Kawasaki Hospital,
Kawasaki Medical School
2-1-80 Nakasange, Kita-ku, Okayama City, Okayama 700-8505 (Japan)
Tel. +81 86 225 2111, E-Mail m.kawanaka@med.kawasaki-m.ac.jp

Liver Cancer

Liver Cancer 2014;3:41–52
DOI: 10.1159/000343857
Published online: March 10, 2014

despite the negative conversion of HBV DNA as a result of long-term NA therapy. Therefore, to suppress hepatocarcinogenesis, it is important to control not only HBV DNA levels but also HBsAg levels.

Introduction

Globally, approximately 400 million people are infected with the hepatitis B virus (HBV). Among them, half a million people develop cirrhosis or hepatocellular carcinoma (HCC) annually [1, 2]. Approximately 1 million people die annually from hepatitis B-induced HCC, underlining the fact that this is an important problem [3]. In Japan, HBV infection accounts for approximately 6% of HCC cases [4]. For this reason, patients with persistent hepatitis require antiviral interferon (IFN) or nucleos(t)ide analogue (NA) therapy. Anti-HBV therapy aims to suppress hepatitis through the continuous suppression of HBV. Additionally, the ultimate therapeutic goal is to improve vital prognosis through arrested cirrhosis or HCC development.

The risk of progression from chronic hepatitis B to cirrhosis is significantly affected by blood levels of HBV DNA. When the levels of HBV DNA are less than 4.0 log copies/mL, the risk of progression to cirrhosis is low. However, the risk of cirrhosis is reported to increase with an increase in the levels of HBV DNA above 4.0 log copies/mL [5]. Similarly, HBV DNA levels at the start of observation are thought to be associated with hepatocarcinogenesis. Because the risk of hepatocarcinoma increases as the HBV DNA level increases above 4.0 log copies/mL, therapies that control HBV DNA levels are important [6]. NAs are therapeutic agents that strongly control HBV DNA levels and also reduce alanine aminotransferase (ALT) levels. NA therapy is an epoch-making therapy that suppresses both hepatitis [7] and the onset of hepatocarcinoma [7–10].

Recently, the levels of hepatitis B surface antigen (HBsAg), in addition to levels of HBV DNA, were linked with the risk of hepatocarcinogenesis in untreated hepatitis B patients [11]. Quantified HBsAg levels are increasingly recognized as a marker with which to evaluate the host immunological control of HBV replication and infection [12–14]. Low HBsAg levels in patients with HBV genotype B or C are considered to indicate a high likelihood of HBV clearance and lower hepatitis activity [13–15]. Studies of HBV genotype D have also defined patients with less than 1000 IU/mL of HBsAg as inactive virus carriers.

From the clinical perspective, we were interested in whether the incidence of HCC might vary in an HBsAg level-dependent manner in Japanese patients of genotype C in whom HBV DNA is controlled by long-term NA therapy. To address this interesting question, we enrolled 167 hepatitis B patients to whom we had administered NA therapy in our hospital for more 2 years. This study aimed to identify the predictors of HBsAg level reduction in the context of long-term NA administration. In addition, hepatocarcinogenesis during long-term NA administration about whether related to the amount of HBsAg, we investigated for the first time in Japan.

Patients and Methods

Patients

The subjects were 167 patients who had received NA therapy for more than 2 years and were selected from the hepatitis B patients with ALT levels ≥31 U/L and HBV DNA levels ≥4.0 log copies/mL who visited

Liver Cancer

Liver Cancer 2014;3:41–52

DOI: 10.1159/000343857
Published online: March 10, 2014

Table 1. Characteristics of patients before and after NA treatment

NA treatment duration (years), n=167	5.8 ± 2.8	
ETV, n=72	4.4± 1.9	
LMV only, n=57	6.5± 3.1	
LMV plus ADV, n=38	7.3± 2.8	
	Before NA treatment	After NA treatment
Age (years)	49.2 ± 11.1	56.7 ± 25.4
Gender (male/ female)	112/55	—
Chronic hepatitis/liver cirrhosis	126/41	—
HBV DNA (log copies/ml)	6.8 ± 1.3	1.6 ± 1.5
HBV genotype (A/B/C/ND)	3/4/144/16	—
HBeAg positive	81 (50.9%)	42 (25.6%)
HBsAg (< 2000/ ≥ 2000 C.O.I.)	8/159	28/139

Values are mean±standard deviation (SD). ND=no data; C.O.I.=cut off index.

Kawasaki Hospital, Kawasaki Medical School, between 1999 and 2010. Seventy-two patients received 0.5 mg/day of entecavir (ETV), 57 patients received 100 mg/day of lamivudine (LMV), and 37 patients received adefovir dipivoxil (ADV) in addition to LMV to treat LMV-resistant virus. The median administration period of NA was 5.8 ± 2.8 years. The average age at the start of therapy, the male to female ratio, and the ratio of subjects with chronic hepatitis to those with cirrhosis were 49.2 ± 11.1 years, 112/55, and 126/41, respectively. The average HBV DNA level at the start of therapy was 6.8 ± 1.3 log copies/mL. Among the subjects, 3, 4, 144, and 16 carried A, B, C, and unknown HBV genotypes, respectively; thus, the majority of infections were of genotype C. Eighty-one patients (50.9%) were positive for the hepatitis B e antigen (HBeAg). The HBsAg levels were below 2000 C.O.I in 8 (4.7%) subjects and above 2000 C.O.I. in 159 (95.3%) subjects (table 1).

Methods

Data were collected to measure the negative conversion rate of HBsAg, the negative conversion and seroconversion rates of HBeAg, the alanine aminotransferase (ALT) normalization (<30 IU/L) rate, and the negative conversion (<3.0 log copies/mL) rate of HBV DNA during the final evaluations of therapeutic effects in 167 patients with hepatitis B who had received NA for more than 2 years. Additionally, we verified the relationships of various factors (age, sex, chronic hepatitis/cirrhosis, HBV DNA level, HBV genotype, initial HBeAg level, initial HBsAg level, initial ALT value, IFN therapy history, the presence or absence of mother-to-child transmission, NA administration period, and HBV DNA and HBsAg levels at 24 weeks after the start of NA administration) with reduced HBsAg levels. Furthermore, we investigated the relationships between HCC incidence and the levels of HBV DNA and HBsAg at the final observation.

HBV Marker Assay

Serum HBsAg and anti-HBs antibody levels were measured by chemiluminescent enzyme immunoassay (CLEIA, Lumipulse System; Fujirebio, Tokyo, Japan). HBeAg and anti-HBe antibody levels were determined using commercially available enzyme-linked immunosorbent assay kits (EIA, Abbot Japan, Tokyo, Japan). HBV DNA was assayed using the COBAS Amplicor HBV Monitor Test (Roche Diagnostics, Tokyo, Japan), which has a dynamic range of 2.6 to 7.6 log copies/mL, or the COBAS TaqMan HBV Test, version 2.0 (Roche Diagnostics, Tokyo, Japan), which has a dynamic range of 2.1 to 9.0 log copies/mL.

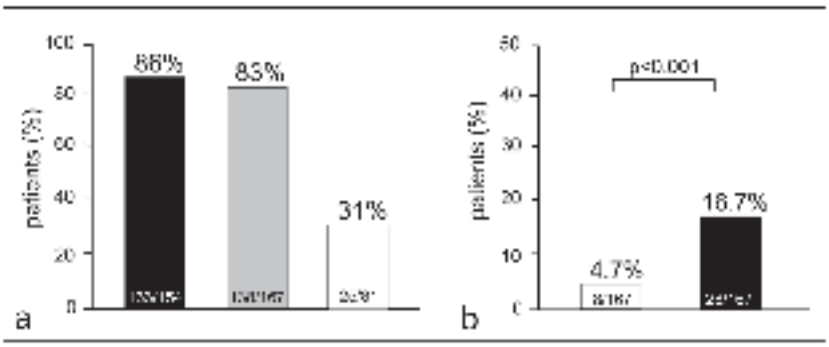

Fig. 1. (**a**) Virological and biochemical outcomes after long-term NA therapy. ■: undetectable HBV DNA (<3.0 log copies/mL); ▨: normalization of ALT (<30 IU/L); □: HBe seroconversion of hepatitis B e antigen-positive patients. (**b**) Percentages of patients with serum HBsAg levels <2000 C.O.I. before/after long-term NA therapy. □: HBsAg <2000 C.O.I. before NA treatment; ■: HBsAg <2000 C.O.I. after NA treatment.

Statistical Analysis

Statistical analyses were performed using the SAS statistical software package, version 9 (Cary, NC, USA). We used the Wilcoxon test, chi-square test, and Fisher's exact test for univariate analyses. Cumulative HCC incidence rates were analyzed according to the Kaplan–Meier method. We compared the cumulative incidence of HCC using the log-rank test. Significance was defined as $p < 0.05$ for all two-tailed tests.

Ethical Considerations

Informed consent was obtained from all participants. The study protocol complied with the ethical guidelines of the Declaration of Helsinki of 1975 (2004 revision) and was approved by the Ethics Committee of Kawasaki Hospital, Kawasaki Medical School.

Results

Virological and Biochemical Outcomes after Long-Term NA Therapy

After long-term (median: 5.8 years, range: 2–13.1 years) of NA therapy, the ALT normalization (<30 IU/L) rate was 83% (138/167). The proportion of subjects in whom the HBV DNA level decreased below 3.0 log copies/mL was 86% (143/167). The seroconversion rate was 31% (25/81) (fig. 1a).

Percentage of Patients with Low HBsAg Levels before/after Long-Term NA Therapy

The proportion of patients with low HBsAg levels (<2000 C.O.I.) was 4.7% (8/167) prior to NA administration. However, after long-term NA administration, a significant increase to 16.7% (28/167) in the proportion of patients with low HBsAg levels was observed ($p < 0.001$) (fig. 1b).

Factors Related to Reduced HBsAg Levels

The 28 patients with low HBsAg values (<2000 C.O.I.) were compared with the 139 patients with high HBsAg values (≥2000 C.O.I.) at the observation after at least 2 years of long-term NA therapy (table 2). A long period of NA therapy (7.0 years vs. 5.5 years, $p = 0.010$)

Liver Cancer

Liver Cancer 2014;3:41–52

DOI: 10.1159/000343857
Published online: March 10, 2014

Table 2. Characteristics of patients with HBsAg <2000 C.O.I. and HBsAg ≥2000 C.O.I. after long-term NA therapy

	HBsAg <2000 C.O.I. (n=28)	HBsAg ≥2000 C.O.I. (n=139)	p value
Age (years)	49.1 ± 12.9	49.8 ± 12.4	0.630
Gender (male/female)	20/8	92/47	0.587
Chronic hepatitis/liver cirrhosis	17/11	109/30	0.057
HBV DNA (log copies/ml)	6.8 ± 1.3	6.6 ± 1.4	0.480
HBV genotype C (%)	96	95	0.826
HBeAg positive (%)	35	54	0.156
ALT (IU/L)	155 ± 190	134 ± 156	0.343
Previous IFN treatment (%)	37	24	0.175
Maternal transmission (%)	66	74	0.042
Period of NA treatment (years)	7.0 ± 3.1	5.5 ± 2.8	0.010
At 24 weeks; HBV DNA < 3.0 log copies/ml (%)	88	67	0.031
HBeAg negative (%)	81	52	0.005

Values are mean±standard deviation (SD).

and non-mother-to-child transmission (66% vs. 74%, p = 0.042) were extracted as significant factors.

Additionally, an evaluation of viral dynamics during therapy revealed that HBsAg levels decreased significantly both in patients with low HBV DNA levels (<3.0 log copies/mL; 87.5% vs. 66.9%, p = 0.031) and in HBeAg-negative patients (81% vs. 52%, p = 0.005) at 24 weeks after the start of NA therapy. Cirrhosis or a history of IFN therapy was more frequently noted, with marginal significance, in patients with HBsAg levels below 2000 C.O.I. On the other hand, no significant differences were observed with regard to age; sex; genotype; or levels of HBV DNA, HBeAg, or ALT before therapy.

Factors Related to Liver Carcinogenesis

Comparison of background factors was conducted for the 9 patients who developed HCC during long-term NA therapy and for the 158 patients who did not develop liver cancer during the treatment period. Among the factors that were present before NA therapy, being male (p = 0.03) and the presence of hepatic cirrhosis (p = 0.04) were significant factors for the development of HCC. However, the ALT level normalization, low HBsAg level, and HBV-DNA negativation at the last observation at the end of the long-term NA therapy were not found to be significant factors for the development of HCC (table 3).

Table 3. Characteristics of patients with HCC and without HCC after long-term NA therapy

	Without HCC (n=158)	With HCC (n=9)	p value
Before NA treatment			
Age (years)	48.9	54.8	0.115
Gender (male/female)	104/54	9/0	0.033
Chronic hepatitis/liver cirrhosis	122/36	4/5	0.040
HBV DNA (log copies/ml)	6.7	7.1	0.840
HBV genotype C (%)	96	88	0.358
HBeAg positive (%)	22	52	0.180
ALT (IU/L)	142	72	0.675
Previous IFN treatment (%)	26	33	0.627
Maternal transmission (%)	50	71	0.306
Period of NA treatment (years)	5.7	6.8	0.213
At HCC			
HBV DNA < 2.1 log copies/ml (%)	69	78	0.552
HBsAg < 2000 C.O.I. (%)	16	11	0.652
ALT < 40 (IU/L)	91	100	0.500

Incidence of HCC in Relation to HBV DNA and HBsAg Levels

HCC was observed in 9 of 167 patients (5.3%) who received long-term NA therapy; of these, 2 patients were positive for HBV DNA (>2.1 log copies/mL) at the onset of HCC. However, the remaining 7 patients developed HCC despite a negative conversion of HBV DNA (<2.1 log copies/mL) and all of these 7 patients had high HBsAg levels (>2000 C.O.I.). Patients who had low levels of both HBV DNA and HBsAg did not develop HCC (figs. 2, 3, 4 and 5).

Discussion

HBV DNA levels have been considered an important factor related to hepatitis B-induced carcinogenesis. The rate of carcinogenesis is known to increase proportionally with increased HBV DNA levels [6]. NAs are epoch-making hepatitis B therapeutic agents because they reduce HBV DNA and ALT levels, resulting in the suppression of hepatitis [7]. Moreover, NAs have been shown to significantly reduce hepatocarcinogenesis [8, 9]. In a matched control study of patients receiving long-term ETV administration versus untreated controls, the 5-year carcinogenic rates were 3.7% and 13.7%, respectively, indicating a significant suppression of carcinogenesis in the ETV group [10].

Liver Cancer

Liver Cancer 2014;3:41–52

DOI: 10.1159/000343857
Published online: March 10, 2014

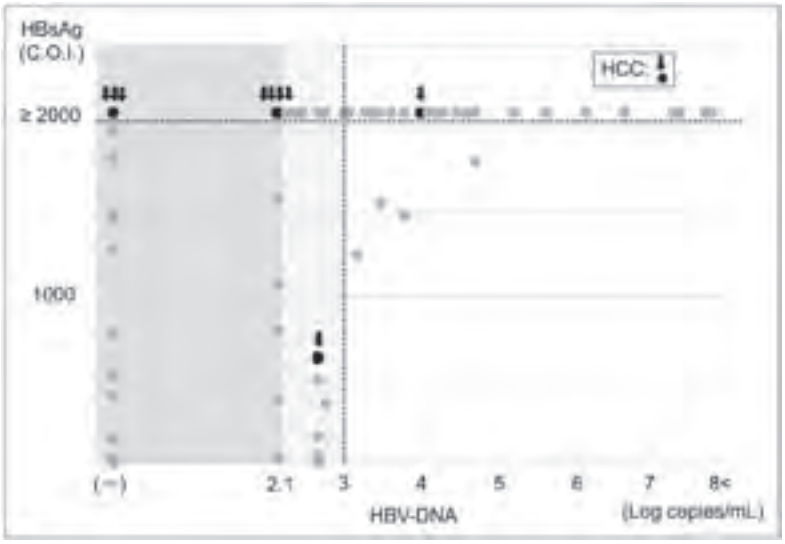

Fig. 2. HCC risk and levels of HBV DNA and HBsAg after long-term NA therapy (scatter plot). Among patients with low viral loads under long-term NA therapy, HCC were frequently observed in patients with hight HBsAg levels. ●: hepatocarcinogenesis; ●: no hepatocarcinogenesis.

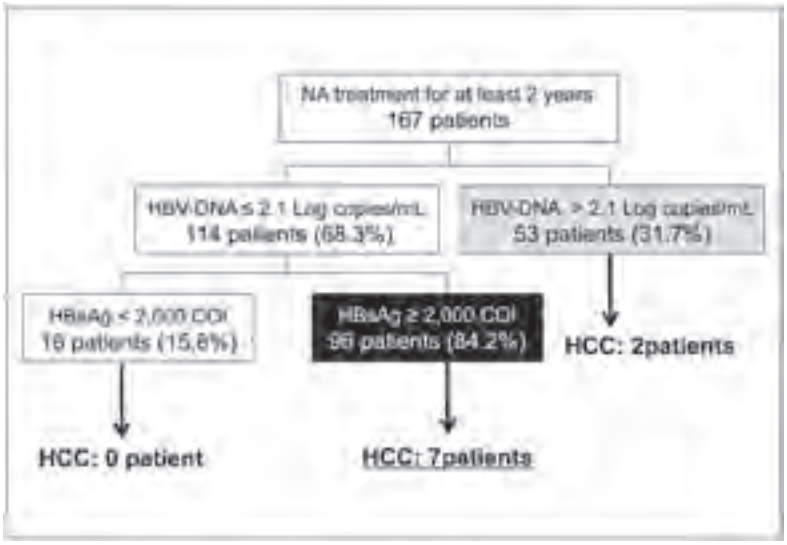

Fig. 3. HCC risk and levels of HBV DNA and HBsAg after long-term NA therapy (flowchart). HCC developed in 9 of 167 patients who were treated with NA. In 7 of the 9 HCC patients, HBV DNA levels were below 2.1 log copies/mL, although HBsAg levels were >2000 C.O.I.

On the other hand, HBsAg levels, in addition to HBV DNA levels, were recently reported to be related to the carcinogenic risk. Tseng et al. [11] observed the natural courses of 2688 cases of chronic hepatitis B, excluding those with cirrhosis, for an average of 14.7 years and reported that male sex, old age, a high serum ALT level, HBeAg positivity, genotype C, an HBV DNA level ≥ 2000 IU/mL, and an HBsAg level ≥ 1000 IU/mL are significant predictors of

Liver Cancer 2014;3:41–52
DOI: 10.1159/000343857
Published online: March 10, 2014

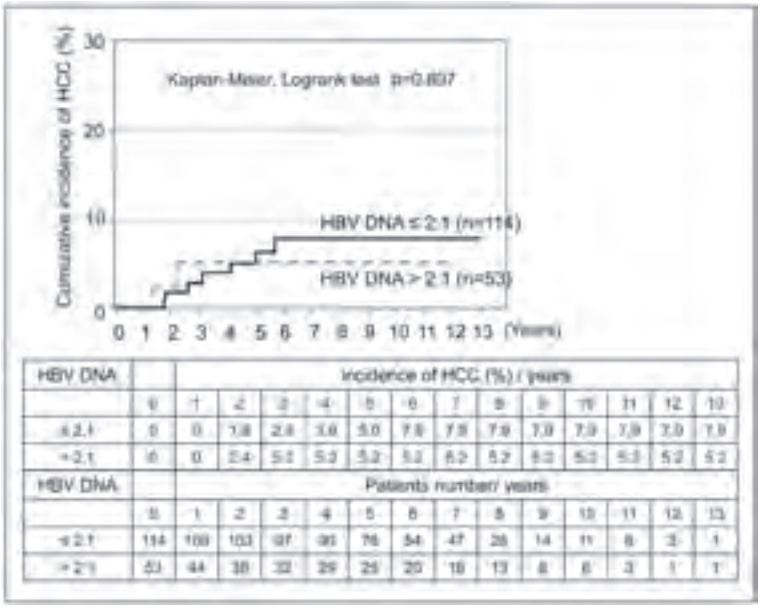

Fig. 4. HCC risk of HBV DNA levels after long-term NA therapy. ——: HBV DNA ≤2.1 log copies/mL; – –: HBV DNA >2.1 log copies/mL.

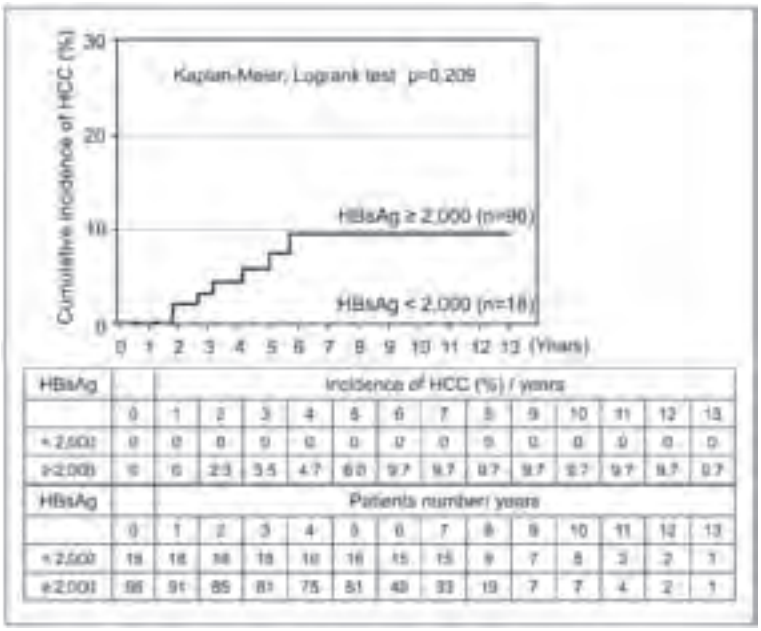

Fig. 5. HCC risk and HBsAg levels in patients with HBV DNA levels ≤2.1 log copies/mL after long-term NA therapy. ——: HBsAg ≥2000 C.O.I. and HBV DNA ≤2.1 log copies/mL; – –: HBsAg < 2000 C.O.I. and HBV DNA ≤ 2.1 log copies/mL.

hepatocarcinogenesis. In an analysis stratified by HBV DNA levels, the HBV DNA level was not extracted as a factor related to carcinogenesis in patients with HBV DNA levels below 2000 IU/mL. On the other hand, the researchers reported the importance of the HBsAg level as a hepatocarcinogenesis-related factor because old age, a high ALT value, and an HBsAg level >1000 IU/mL were significantly related to hepatocarcinogenesis. Additionally, of a total of 5055 hepatitis B cases with natural progression or intervention, only 2 patients of 231 patients with negative conversion of HBsAg developed hepatic carcinoma, indicating that HBsAg could be predictive of hepatocarcinogenesis [16].

HBsAg was first discovered in 1965 as the "Australia antigen" from the sera of Aboriginal people by Blumberg et al. [17]. In 1968, Okochi et al. reported relationships between the Australia antigen and hepatitis [18]. HBsAg is produced via multiple pathways in the lifecycle of HBV and uses cccDNA as a template. Therefore, HBsAg levels are reported to correlate with cccDNA levels [19–22]. Indeed, hepatitis B patients with HBsAg levels below 1–2 × 10^3 IU/mL and HBV DNA levels below 2 × 10^3 IU/mL have a low risk of hepatitis recrudescence. Because the HBsAg level reflects HBV replication, it appears necessary to focus on HBsAg as well as on HBV DNA in hepatocarcinogenesis [23–25]. Additionally, it was reported that HBV DNA levels above 3 log copies/mL at the termination of NA therapy are likely to lead to recrudescence and that, despite the negative conversion of HBV DNA, high HBsAg and HBeAg levels are likely to lead to recrudescence in patients who received NA [26]. Therefore, the HBsAg level is an important indicator of both hepatocarcinogenesis and hepatitis recrudescence.

Moreover, the therapeutic goals for chronic hepatitis B put forth in the guidelines of the American Association for the Study of Liver Diseases, the European Association for the Study of the Liver, and the Asian Pacific Association for the Study of the Liver are improvements in the quality of life and survival rates through the prevention of hepatic cirrhosis, decompensated cirrhosis, end-stage liver diseases, HCC, and progression to death. Furthermore, the guidelines mention that the ideal endpoint is the "disappearance of HBsAg" [27–29].

The disappearance rate of HBsAg during the natural course of infection has been reported in several studies as 0.5–3.0% per year [27–29]. In our previous study, the disappearance rate of HBsAg in cirrhosis patients was 0.9% per year [30]. The significant factors that led to the disappearance of HBsAg within 3 years were reported to be HBsAg levels <2000 IU/mL or a decrease in HBsAg levels at an annual rate of 0.5 log IU/mL [31]. However, because the annual disappearance rate of HBsAg was the lowest in patients infected with HBV genotype C in our present study [32], the HBV subgenotype C2/Ce observed in many Japanese is an independent risk factor for HCC [33]. Therefore, we consider it necessary to reduce HBsAg levels as much as possible through antiviral therapy to suppress hepatocarcinogenesis.

The negative conversion rates of HBsAg after a year of NA therapy were reported to be 2, 0–1, and 0% in ETV-, LAM-, and ADV-treated patients, respectively [7, 34–39]. In our study, HBsAg levels decreased to below 2000 C.O.I. in 16.7% of all patients who received long term NA therapy over 2 years; these proportions were 4.2 and 26.3% in ETV- and LMV (with or without ADV)-treated patients, respectively. However, among all patients, this level of reduction was seen in only four patients (2.3%) with a negative conversion of HBsAg. The significant factors that led to reductions of HBsAg levels below 2000 C.O.I during long-term NA therapy were a long period of NA therapy, non-mother-to-child transmission, a low HBV DNA level at 24 weeks after the start of NA therapy, and HBeAg negativity at 24 weeks after the start of NA therapy. These patients were expected to have reduced HBsAg levels, although they accounted for no more than 16.7% of the total number of patients.

In the present study, hepatocarcinogenesis was observed in 9 of 167 patients (5.3%) who received long-term NA therapy, and 2 of these patients showed a positive conversion of HBV DNA. However, all 7 remaining patients had HBsAg levels above 2000 C.O.I., despite the negative conversion of HBV DNA. This indicates that patients with high HBsAg levels should be

observed for hepatocarcinogenesis even in cases with successful negative conversion of HBV DNA during NA therapy. On the basis of the above results, we consider that both HBV DNA and HBsAg levels are important in hepatocarcinogenesis.

NA are reported low effective in the reduction of HBsAg levels because of difficulties in elimination of cccDNA, although NA strongly reduces HBV DNA levels by inhibiting HBV replication through reverse transcription [19]. On the other hand, after reviewing reductions in HBsAg levels in response to NA therapy and IFN therapy in 11 studies, Liaw reported that IFN therapy reduced HBsAg levels more efficiently than NA therapy did [40]. Furthermore, other reports state that the negative conversion rate of HBsAg after 48 weeks of pegylated-IFN administration is 3–7%, which is higher than the 0–2% rate reported for NA therapy [34, 41]. Moreover, a 5-year follow-up after the termination of pegylated-IFN therapy showed that the negative conversion rate of HBsAg was further elevated in a time-dependent manner, achieving a rate of 12% at 5 years [42, 43]. Similarly, a study in Japan, where genotype C accounts for the majority of hepatitis B infections, also demonstrated that the negative conversion rate of HBsAg was elevated in a time-dependent manner, although not as markedly in genotype C as in genotypes A and B; this elevation resulted in a negative conversion rate of 11% at 10 years [44].

Our present study revealed that 8 of 9 patients who developed HCC had high HBsAg levels during long-term NA therapy. Therefore, to achieve the suppression of hepatocarcinogenesis, it may be important to reduce HBsAg levels not only by NA therapy, but also by combining NA with IFN. This is the goal of hepatitis B therapy, as the suppressive effects of IFN therapy on carcinogenesis have been previously reported [45, 46].

In conclusion, despite the negative conversion of HBV DNA during long-term NA therapy, hepatocarcinogenesis was observed in patients with high HBsAg levels. Therefore, the control of both HBV DNA and HBsAg levels is important for the suppression of hepatocarcinogenesis.

Conflict of Interest

All authors declare that they have no conflicts of interest.

References

▶1 Sorrell MF, Belongia EA, Costa J, Gareen IF, Grem JL, Inadomi JM, Kern ER, McHugh JA, Petersen GM, Rein MF, Strader DB, Trotter HT: National Institutes of Health consensus development conference statement: management of hepatitis B. Hepatology 2009;49(Suppl):S4–S12.
▶2 Kim DY, Han KH: Epidemiology and surveillance of hepatocellular carcinoma. Liver Cancer 2012;1:2–14.
▶3 Fontana RJ: Management of patients with decompensated HBV cirrhosis. Semin Liver Dis 2003;23:89–100.
▶4 Nissen NN, Martin P: Hepatocellular carcinoma: the high-risk patient. J Clin Gastroenterol 2002;35(Suppl 2):S79–S85.
▶5 Iloeje UH, Yang HI, Su J, Jen CL, You SL, Chen CJ, Risk Evaluation of Viral Load Elevation and Associated Liver Disease/Cancer-In HBV (the REVEAL-HBV) Study Group: Predicting cirrhosis risk based on the level of circulating hepatitis B viral load. Gastroenterology 2006;130:678–686.
▶6 Chen CJ, Yang HI, Su J, Jen CL, You SL, Lu SN, Huang GT, Iloeje UH, REVEAL-HBV Study Group: Risk of hepatocellular carcinoma across a biological gradient of serum hepatitis B virus DNA level. JAMA 2006;295:65–73.
▶7 Lai CL, Chien RN, Leung NW, Chang TT, Guan R, Tai DI, Ng KY, Wu PC, Dent JC, Barber J, Stephenson SL, Gray DF, Asia Hepatitis Lamivudine Study Group: A one-year trial of lamivudine for chronic hepatitis B. N Engl J Med 1998;339:61–68.

8 Liaw YF, Sung JJ, Chow WC, Farrell G, Lee CZ, Yuen H, Tanwandee T, Tao QM, Shue K, Keene ON, Dixon JS, Gray DF, Sabbat J, Cirrhosis Asian Lamivudine Multicentre Study Group: Lamivudine for patients with chronic hepatitis B and advanced liver disease. N Engl J Med 2004;351:1521–1531.
9 Matsumoto A, Tanaka E, Rokuhara A, Kiyosawa K, Kumada H, Omata M, Okita K, Hayashi N, Okanoue T, Iino S, Tanikawa K, Inuyama Hepatitis Study Group: Efficacy of lamivudine for preventing hepatocellular carcinoma in chronic hepatitis B: A multicenter retrospective study of 2795 patients. Hepatol Res 2005;32:173–184.
10 Hosaka T, Suzuki F, Kobayashi M, et al: Long-term entecavir treatment reduces hepatocellular carcinoma incidence in patients with hepatitis B virus infection. Hepatology 2013;58:98–107.
11 Tseng TC, Liu CJ, Yang HC, Su TH, Wang CC, Chen CL, Kuo SF, Liu CH, Chen PJ, Chen DS, Kao JH: High levels of hepatitis B surface antigen increase risk of hepatocellular carcinoma in patients with low HBV load. Gastroenterology 2012;142:1140–1149, e3, quiz e13–e14.
12 Chan HL, Wong VW, Wong GL, Tse CH, Chan HY, Sung JJ: A longitudinal study on the natural history of serum hepatitis B surface antigen changes in chronic hepatitis B. Hepatology 2010;52:1232–1241.
13 Tseng TC, Liu CJ, Su TH, et al. Serum hepatitis B surface antigen levels predict surface antigen loss in hepatitis B e antigen seroconverters. Gastroenterology 2011;141:517–525 e2.
14 Tseng TC, Liu CJ, Yang HC, Su TH, Wang CC, Chen CL, Kuo SF, Liu CH, Chen PJ, Chen DS, Kao JH: Determinants of spontaneous surface antigen loss in hepatitis B e antigen-negative patients with a low viral load. Hepatology 2012;55:68–76.
15 Chan HL, Wong GL, Tse CH, Chan HY, Wong VW: Viral determinants of hepatitis B surface antigen seroclearance in hepatitis B e antigen-negative chronic hepatitis B patients. J Infect Dis 2011;204:408–414.
16 Arase Y, Ikeda K, Suzuki F, et al. Long-term outcome after hepatitis B surface antigen seroclearance in patients with chronic hepatitis B. Am J Med 2006;119:e9–71.e16.
17 Blumberg BS, Alter HJ, Visnich S: A "new" antigen in leukemia sera. JAMA 1965;191:541–546.
18 Okochi K, Murakami S: Observations on Australia antigen in Japanese. Vox Sang 1968;15:374–385.
19 Werle-Lapostolle B, Bowden S, Locarnini S, Wursthorn K, Petersen J, Lau G, Trepo C, Marcellin P, Goodman Z, Delaney WE 4th, Xiong S, Brosgart CL, Chen SS, Gibbs CS, Zoulim F: Persistence of cccDNA during the natural history of chronic hepatitis B and decline during adefovir dipivoxil therapy. Gastroenterology 2004;126:1750–1758.
20 Volz T, Lutgehetmann M, Wachtler P, Jacob A, Quaas A, Murray JM, Dandri M, Petersen J: Impaired intrahepatic hepatitis B virus productivity contributes to low viremia in most HBeAg-negative patients. Gastroenterology 2007;133:843–852.
21 Chan HL, Wong VW, Tse AM, Tse CH, Chim AM, Chan HY, Wong GL, Sung JJ: Serum hepatitis B surface antigen quantitation can reflect hepatitis B virus in the liver and predict treatment response. Clin Gastroenterol Hepatol 2007;5:1462–1468.
22 Brunetto MR: A new role for an old marker, HBsAg. J Hepatol 2010;52:475–477.
23 Chen CH, Lee CM, Wang JH, Tung HD, Hung CH, Lu SN: Correlation of quantitative assay of hepatitis B surface antigen and HBV DNA levels in asymptomatic hepatitis B virus carriers. Eur J Gastroenterol Hepatol 2004;16:1213–1218.
24 Brunetto MR, Oliveri F, Colombatto P, Moriconi F, Ciccorossi P, Coco B, Romagnoli V, Cherubini B, Moscato G, Maina AM, Cavallone D, Bonino F: Hepatitis B surface antigen serum levels help to distinguish active from inactive hepatitis B virus genotype D carriers. Gastroenterology 2010;139:483–490.
25 Jaroszewicz J, Calle Serrano B, Wursthorn K, Deterding K, Schlue J, Raupach R, Flisiak R, Bock CT, Manns MP, Wedemeyer H, Cornberg M: Hepatitis B surface antigen (HBsAg) levels in the natural history of hepatitis B virus (HBV)-infection: a European perspective. J Hepatol 2010;52:514–522.
26 Matsumoto A, Tanaka E, Suzuki Y, Kobayashi M, Tanaka Y, Shinkai N, Hige S, Yatsuhashi H, Nagaoka S, Chayama K, Tsuge M, Yokosuka O, Imazeki F, Nishiguchi S, Saito M, Fujiwara K, Torii N, Hiramatsu N, Karino Y, Kumada H: Combination of hepatitis B viral antigens and DNA for prediction of relapse after discontinuation of nucleos(t)ide analogs in patients with chronic hepatitis B. Hepatol Res 2012;42:139–149.
27 Lok AS, McMahon BJ: Chronic hepatitis B: update 2009. Hepatology 2009;50:661–662.
28 European Association For The Study Of The Liver: EASL clinical practice guidelines: Management of chronic hepatitis B virus infection. J Hepatol 2012;57:167–185.
29 Liaw YF, Kao JH, Piratvisuth T, et al: Asian-Pacific consensus statement on the management of chronic hepatitis B: a 2012 update. Hepatol Int. 2012;6:531–561.
30 Mahmood S, Niiyama G, Kamei A, Izumi A, Nakata K, Ikeda H, Suehiro M, Kawanaka M, Togawa K, Yamada G: Influence of viral load and genotype in the progression of Hepatitis B-associated liver cirrhosis to hepatocellular carcinoma. Liver Int 2005;25:220–225.
31 Seto WK, Wong DK, Fung J, Hung IF, Fong DY, Yuen JC, Tong T, Lai CL, Yuen MF: A large case-control study on the predictability of hepatitis B surface antigen levels three years before hepatitis B surface antigen seroclearance. Hepatology 2012;56:812–819.
32 Simonetti J, Bulkow L, McMahon BJ, Homan C, Snowball M, Negus S, Williams J, Livingston SE: Clearance of hepatitis B surface antigen and risk of hepatocellular carcinoma in a cohort chronically infected with hepatitis B virus. Hepatology 2010;51:1531–1537.
33 Tanaka Y, Mukaide M, Orito E, Yuen MF, Ito K, Kurbanov F, Sugauchi F, Asahina Y, Izumi N, Kato M, Lai CL, Ueda R, Mizokami M: Specific mutations in enhancer II/core promoter of hepatitis B virus subgenotypes C1/C2 increase the risk of hepatocellular carcinoma. J Hepatol 2006;45:646–653.

34 Lau GK, Piratvisuth T, Luo KX, Marcellin P, Thongsawat S, Cooksley G, Gane E, Fried MW, Chow WC, Paik SW, Chang WY, Berg T, Flisiak R, McCloud P, Pluck N, Peginterferon Alfa-2a HBeAg-Positive Chronic Hepatitis B Study Group: Peginterferon Alfa-2a, lamivudine, and the combination for HBeAg-positive chronic hepatitis B. N Engl J Med 2005;352:2682–2695.
35 Dienstag JL, Schiff ER, Wright TL, Perrillo RP, Hann HW, Goodman Z, Crowther L, Condreay LD, Woessner M, Rubin M, Brown NA: Lamivudine as initial treatment for chronic hepatitis B in the United States. N Engl J Med 1999;341:1256–1263.
36 Chang TT, Gish RG, de Man R, Gadano A, Sollano J, Chao YC, Lok AS, Han KH, Goodman Z, Zhu J, Cross A, DeHertogh D, Wilber R, Colonno R, Apelian D, BEHoLD AI463022 Study Group: A comparison of entecavir and lamivudine for HBeAg-positive chronic hepatitis B. N Engl J Med 2006;354:1001–1010.
37 Lai CL, Gane E, Liaw YF, Hsu CW, Thongsawat S, Wang Y, Chen Y, Heathcote EJ, Rasenack J, Bzowej N, Naoumov NV, Di Bisceglie AM, Zeuzem S, Moon YM, Goodman Z, Chao G, Constance BF, Brown NA, Globe Study Group: Telbivudine versus lamivudine in patients with chronic hepatitis B. N Engl J Med 2007;357:2576–2588.
38 Marcellin P, Chang TT, Lim SG, Tong MJ, Sievert W, Shiffman ML, Jeffers L, Goodman Z, Wulfsohn MS, Xiong S, Fry J, Brosgart CL, Adefovir Dipivoxil 437 Study Group: Adefovir dipivoxil for the treatment of hepatitis B e antigen-positive chronic hepatitis B. N Engl J Med 2003;348:808–816.
39 Marcellin P, Heathcote EJ, Buti M, Gane E, de Man RA, Krastev Z, Germanidis G, Lee SS, Flisiak R, Kaita K, Manns M, Kotzev I, Tchernev K, Buggisch P, Weilert F, Kurdas OO, Shiffman ML, Trinh H, Washington MK, Sorbel J, Anderson J, Snow-Lampart A, Mondou E, Quinn J, Rousseau F: Tenofovir disoproxil fumarate versus adefovir dipivoxil for chronic hepatitis B. N Engl J Med 2008;359:2442–2455.
40 Liaw YF: Clinical utility of hepatitis B surface antigen quantitation in patients with chronic hepatitis B: a review. Hepatology 2011;54:E1–E9.
41 Janssen HL, van Zonneveld M, Senturk H, Zeuzem S, Akarca US, Cakaloglu Y, Simon C, So TM, Gerken G, de Man RA, Niesters HG, Zondervan P, Hansen B, Schalm SW, HBV 99-01 Study Group Rotterdam Foundation for Liver Research: Pegylated interferon alfa-2b alone or in combination with lamivudine for HBeAg-positive chronic hepatitis B: a randomised trial. Lancet 2005;365:123–129.
42 Lampertico P, Viganò M, Colombo M: Treatment of HBeAg-negative chronic hepatitis B with pegylated interferon. Liver Int 2011;31(Suppl 1):90–94.
43 Keating GM: Peginterferon-α-2a (40 kD): A review of its use in chronic hepatitis B. Drugs 2009;69:2633–2660.
44 Suzuki F, Arase Y, Suzuki Y, Akuta N, Sezaki H, Seko Y, Kawamura Y, Hosaka T, Kobayashi M, Saito S, Ikeda K, Kobayashi M, Kumada H: Long-term efficacy of interferon therapy in patients with chronic hepatitis B virus infection in Japan. J Gastroenterol 2012;47:814–822.
45 Lin SM, Yu ML, Lee CM, Chien RN, Sheen IS, Chu CM, Liaw YF: Interferon therapy in HBeAg positive chronic hepatitis reduces progression to cirrhosis and hepatocellular carcinoma. J Hepatol 2007;46:45–52.
46 Yang YF, Zhao W, Zhong YD, Xia HM, Shen L, Zhang N: Interferon therapy in chronic hepatitis B reduces progression to cirrhosis and hepatocellular carcinoma: a meta-analysis. J Viral Hepat 2009;16:265–271.

Liver Cancer

Liver Cancer 2014;3:53–61
DOI: 10.1159/000343858
Published online: March 10, 2014

2235-1795/14/0031-0053$39.50/0
www.karger.com/lic

Original Paper

Tracking Navigation Imaging of Transcatheter Arterial Chemoembolization for Hepatocellular Carcinoma Using Three-Dimensional Cone-Beam CT Angiography

Yasunori Minami[a] Yukinobu Yagyu[b] Takamichi Murakami[b]
Masatoshi Kudo[a]

[a]Department of Gastroenterology and Hepatology, and [b]Department of Diagnostic Radiology, Kinki University Faculty of Medicine, Osaka, Japan

Key Words
Feeding arteries · Hepatocellular carcinoma · Three-dimensional cone-beam CT angiography · Tracking navigation imaging · Transcatheter arterial chemoembolization

Abstract
Purpose: New tracking navigation imaging software was used to evaluate the usefulness of three dimensional (3D) CT angiography for transcatheter arterial chemoembolization (TACE) in patients with hepatocellular carcinoma (HCC). ***Materials and Methods:*** Fifty-two patients with 73 HCCs were enrolled in this study retrospectively. Rotational angiography was performed from the hepatic artery for evaluation of the tumor feeding vessels. Arteries feeding the tumor were traced automatically by adjusting the region of interest around the targeted tumor on axial and coronal images using tracking navigation imaging with 3D cone-beam CT angiography. ***Results:*** Using final selective angiographic findings as the gold standard, the detection of feeding vessels was 90.4% (66/73) for tracking navigation imaging and 50.7% (37/73) for celiac trunk angiography. This difference was statistically significant (Wilcoxon rank sum test, $p < 0.001$). The sensitivity, specificity, positive predictive value, and negative predictive value for the detection of feeding arteries were 97.1% (66/68), 80.0% (4/5), 98.5% (66/67), and 66.7% (4/6), respectively. The kappa coefficient had a value of 0.638 (95% CI: 0.471–0.805), which is considered to indicate a good degree of agreement. With the as-

Yasunori Minami, MD, PhD
Department of Gastroenterology and Hepatology,
Kinki University Faculty of Medicine
377-2 Ohno-Higashi, Osaka-Sayama, Osaka 589-8511 (Japan)
Tel. +81 72 366 0221 (Ext. 3149), E-Mail minkun@med.kindai.ac.jp

KARGER

Liver Cancer

Liver Cancer 2014;3:53–61
DOI: 10.1159/000343858
Published online: March 10, 2014

sistance of tracking navigation imaging, the disease control rate of TACE for HCC was 67.3% (35/52) according to the modified Response Evaluation Criteria in Solid Tumors. During follow-up periods of 1–11 months, 10 patients (19.2%) remained cancer-free after TACE. ***Conclusion:*** Tracking navigation imaging with 3D cone-beam CT angiography should be useful for TACE in HCC patients with complicated feeding arteries.

Introduction

Transcatheter arterial chemoembolization (TACE) is used widely in the treatment of hepatocellular carcinomas (HCC) that are not amenable to surgical resection or to percutaneous ablation therapies [1–8]. Usually, visualization of the liver arterial branch during TACE is guided by two-dimensional (2D) angiography [9–11]. Detailed information of the feeding vessels of HCC is essential for successful catheterization and sufficient TACE [7, 12]. However, it is sometimes difficult to identify some arteries feeding HCCs on 2D angiographic images because of overlapping vessels. CT during hepatic arteriography is very useful for detecting hypervascular HCC and identifying the feeding vessels [13–15]. The unified angiography/CT system allows angiography and CT to be conducted with the patient on the same bed, thus minimizing the risk of catheter dislodgment [16, 17]. However, such systems are only found in a limited number of hospitals because they are rather expensive and take up a great deal of space. In many hospitals, patients must be transferred from the angiography room to a separate CT room for CT hepatic angiography.

Recently, three-dimensional (3D) cone-beam CT technology using a flat-panel detector has provided good 3D angiography and cross-sectional soft tissue imaging as party of an angiography system [18]. Cone-beam CT is a technique that permits assessment of the complex vascular anatomy of the liver [19–22], and, compared with a unified angiography/CT system, cone-beam CT is inexpensive and does not require a great deal of space. Several studies have shown that cone-beam CT angiography can be helpful during TACE, especially in patients with complex hepatic arterial anatomy [23–25]. In addition, recent software developments have enabled automatic identification of the feeding vessels on 3D angiography. The TACE procedure can be carried out with less chance of going astray in patients with complicated vessels of the liver by virtually color-coding the feeding vessels. The purpose of this study was to evaluate the usefulness of new tracking navigation imaging software for cone-beam CT angiography in patients with HCC undergoing treatment with TACE.

Materials and Methods

Patients

Approval for this retrospective study was obtained from the local ethical review board. Between May 2011 and April 2012, 52 patients with 73 HCCs were enrolled in this retrospective study. The patient population included 34 men and 18 women (age range, 54–90 years; mean ± SD, 73.9 ± 7.9 years). The maximal diameter of the tumors ranged from 1.5 to 10 cm (mean ± SD, 2.6 ± 1.4 cm) on dynamic CT. Thirty-six patients had liver cirrhosis of Child-Pugh class A and the remaining 16 had Child-Pugh class B cirrhosis.

All patients met the following inclusion criteria: multiple hypervascular HCCs or HCCs larger than 3 cm in diameter, some overlapping arteries to the tumor depicted on celiac angiography, absence of portal venous and extrahepatic metastasis, prothrombin time-international normalized ratio less than 1.7, total bilirubin less than 3.0 mg/dl, and platelet count greater than 50,000/μl. We diagnosed HCC based

on the findings of three-phase contrast-enhanced CT. HCCs were positively enhanced in the arterial phase and washed out in the portal-venous and/or equilibrium phase of contrast-enhanced CT. All patients underwent contrast-enhanced CT 1 month before TACE.

Cone-Beam CT and Tracking Navigation Imaging

C-arm cone-beam CT angiography was performed using an Innova 4100^{IQ} pro angiographic unit (GE Healthcare, Amersham, UK). Patients did not need to elevate their arms above their heads for the rotation. After breathing was suspended, there was a 5-s delay for contrast filling of the vessels and tumors prior to C-arm rotation. Contrast medium (Omnipaque 300 mg/ml; GE Healthcare) was injected at a flow rate of 1.5–2.0 ml/s through a microcatheter in the common hepatic artery, the proper hepatic artery, or the replaced hepatic artery. The total volume of contrast used for the rotation was 15–20 ml. Cone-beam CT images were acquired using the following parameters: total scanning angle, 200°; rotation speed, 20° or 40°/s; acquisition time, 5 or 10 s; matrix size, 1500 ×1500; isotropic voxel size, 0.2 mm; and effective field-of-view, 18 cm^2. During rotation, 300 images were obtained at a frame rate of 30 frames/s. Acquired images were then transferred to an external workstation (Advantage Workstation 4.2; GE Healthcare) where a volume data set was reconstructed in a CT-type data set consisting of many sections with the thickness of the voxel size and visualized with a volume-rendering technique. The reconstructed 3D field of view was 40 × 40 cm and the image matrix size was 512 × 512 × 512 voxels.

The tracking navigation software is an advanced vascular 3D clinical analysis tool using data from cone-beam CT angiography [26]. In the first step, we set the cross at the tip of the microcatheter on axial and coronal images. In the second step, a spherical region of interest (ROI) was adjusted around the targeted tumor on axial and coronal images. The three-dimensional positions of the starting point and the target were thereby fixed. The 3D navigation software could then automatically depict all vessels in the vicinity of the target as being feeding arteries (figs. 1,2). The vicinity was automatically determined by geometric considerations and could be displayed on the angiography room monitor in approximately 20 s after the cone-beam CT angiography procedure. This tracking navigation imaging was able to highlight all vessels (from the tip of the microcatheter to the tumor) that appeared to feed the tumor by coming into close geometric proximity with the ROI. The total time required to create the tracking navigation images per patient study was approximately 30 s. Moreover, virtual "3D roadmap" imaging can superimpose the live fluoroscopic images with the 3D reconstruction. This 3D roadmap is automatically adjusted in real time for all changes in C-arm angulations, field of view, and table positions.

The TACE Technique

The right femoral artery was accessed with an 18-gauge Seldinger needle and a 4-Fr sheath was inserted. The celiac artery was selectively catheterized using a 4.2-Fr catheter. A 2.2-Fr microcatheter (Shirabe; Piolax, Yokohama, Japan) was advanced coaxially through the catheter into the common or proper hepatic artery. Rotational angiography was performed to evaluate the feeding vessels and to reveal hypervascular tumors in the liver. The tip of the catheter was selectively placed into the segmental and subsegmental arteries feeding the tumor in reference to selective hepatic angiography and/or the tracking navigation imaging findings. Chemoembolization was performed using 10–30 mg of epirubicin (Epirubicin; Nippon Kayaku, Tokyo, Japan) dissolved in 1–3 ml of distilled water and emulsified with 2 ml of iodized oil (Lipiodol Ultra-Fluid; Guerbet, Paris, France) and gelatin sponge particles (Gelpart; Nippon Kayaku). The volume of the emulsion to be injected was determined by the tumor volume (maximal volume of emulsion, 8 ml).

Imaging Data Evaluation and Follow-Up

The cone-beam CT scans and the tracking navigation images were prospectively recorded and retrospectively evaluated. The primary objective of this study was, using final selective angiographic findings as the gold standard, to evaluate the diagnostic performance of the tracking navigation imaging system using 3D rotational common/proper hepatic arteriography compared with 2D celiac angiography for identifying the tumor feeding arteries. Overall, interpretation of celiac angiography, cone-beam CT, the tracking navigation imaging, and selective hepatic angiography was performed in a nonblinded manner.

The secondary objective was the TACE treatment response. The treatment response was assessed 1 or 2 months after TACE using the modified Response Evaluation Criteria in Solid Tumors (mRECIST) guideline proposed by the American Association for the Study of Liver Diseases–Journal of the National Cancer Institute [27]. If the follow-up CT images indicated successful TACE and the absence of new tumors, three-phase dynamic CT scans were repeated at 3-month intervals. Any complications were recorded.

Liver Cancer 2014;3:53–61
DOI: 10.1159/000343858
Published online: March 10, 2014

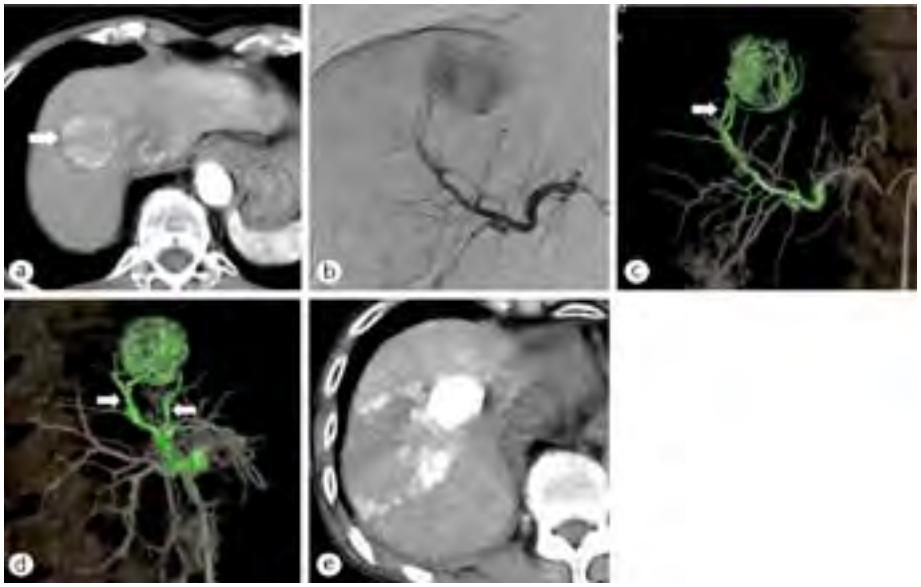

Fig. 1. The patient was a 77-year-old man with an HCC of 4.0 cm diameter. (**a**) Early-phase dynamic CT scan shows naive HCC as enhanced lesion in segment 8 of liver. (**b**) 2D angiography shows HCC as an enhanced lesion complicated with right anterio/posterior hepatic arteries. (**c**) Two main feeder vessels (arrow) are highlighted from the right anterior hepatic artery by anteroposterior view on tracking navigation imaging. (**d**) Two main arteries feeding from A8 (arrows) were clearly shown on the right posterior oblique view on tracking navigation imaging. (**e**) Plain CT scan obtained 1 month after TACE shows well-accumulated lipiodol in the tumor.

Fig. 2. The patient was a 70-year-old man with an HCC of 3.0 cm diameter. (**a**) 2D angiography shows HCC as an enhanced lesion (arrow) complicated with right anterior/posterior hepatic arteries. (**b**) The green vessel indicates a tumor-feeding artery from the right anterior hepatic artery to the tumor (circle) according to the tracking navigation imaging system. (**c**) Well-accumulated lipiodol in the tumor is shown on an axial plain 3D cone-beam CT image immediately after TACE.

Statistical Analysis

Data are expressed as mean ± SD. Significant differences were calculated using the Wilcoxon rank sum test in detection of the feeding vessels between the tracking navigation imaging group and the celiac angiography group. A p value of less than 0.05 was considered statistically significant. The agreement of the tracking navigation imaging versus the results of selective angiography was measured using the kappa coefficient. Data were analyzed using statistical software (SPSS 11.5, Statistical Package for the Social Sciences, Chicago, IL, USA). The 95% confidence intervals were calculated according to the binomial distribution. A kappa statistic of 0.41–0.60 was considered to indicate moderate agreement, a weighted kappa statistic of 0.61–0.80 was considered to indicate good agreement, and a weighted kappa statistic of 0.81–1.00 was considered to indicate excellent agreement [28].

Table 1. Sensitivity, specificity, positive and negative predictive values, and accuracy of 3D tracking navigation imaging and 2D celiac angiography in identifying feeder arteries of HCC

	Sensitivity [%]	Specificity [%]	PPV [%]	NPV [%]	Accuracy [%]
3D tracking navigation imaging	97.1	80.0	98.5	66.7	90.4
2D celiac angiography	54.4	60.0	94.9	8.8	50.7

NPV = negative predictive value; PPV = positive predictive value.

Results

Two hundred ninety-four patients were treated by TACE or transcatheter arterial infusion chemotherapy at our hospital between May 2011 and April 2012. HCC patients who received TACE using the tracking navigation imaging system accounted for 17.7% (n = 52) of the total patients treated with therapeutic angiography. Among the 73 HCC nodules in these 52 patients, 62 tumors (84.9%) were diagnosed as naive HCCs, 8 tumors (11.0%) as local recurrences around the lipiodol deposit, and 3 tumors (4.1%) as residual HCCs without accumulation of lipiodol. Transfemoral TACE was carried out in 52 TACE sessions and was performed for 35 subsegmental arteries and 17 segmental arteries. Complete devascularization of postembolization angiography was achieved in all 52 (100%) procedures.

The detection of feeding vessels was 90.4% (66/73) for tracking navigation imaging and 50.7% (37/73) for celiac trunk angiography. This difference was statistically significant (Wilcoxon rank sum test, $p < 0.001$). Tracking navigation imaging could not depict the feeding vessels in HCC patients with weak enhancement of tumor stain (voxel value from cone-beam CT: median 16.51; range: −59.64 to 120.76). However, celiac trunk angiography failed to confirm the feeding vessels not only because of weak enhancement of HCC, but also because of crossing and overlapping arteries of the liver. Using final selective angiographic findings as the gold standard, the sensitivity, specificity, positive predictive value, and negative predictive value for the detection of feeding arteries were 97.1% (66/68), 80.0% (4/5), 98.5% (66/67), and 66.7% (4/6), respectively (table 1). The kappa coefficient had a value of 0.638 (95% CI: 0.471–0.805).

According to mRECIST, 17 of 52 (32.7%) individuals had a complete response, 8 (15.4%) had a partial response, 10 (19.2%) had stable disease, and 17 (32.7%) had progressive disease. Thus, the disease control rate, defined as a complete response, partial response, or stable disease, was 67.3%. Development of new lesions was the sole reason for progression in all patients with progressive disease. The follow-up period ranged from 1 to 11 months (mean ± SD, 6.1 ± 4.2 months). During follow-up, 10 patients (19.2%) remained cancer-free after TACE, 31 patients (59.6%) received or were scheduled for additional TACE, 3 patients (5.8%) received sorafenib, 3 patients (5.8%) received radiofrequency ablation, and 5 patients (9.6%) received best supportive care. No serious side effects or procedure-related complications (e.g., hemorrhage, infection, hepatic failure, or death) occurred.

Liver Cancer

Liver Cancer 2014;3:53–61
DOI: 10.1159/000343858
Published online: March 10, 2014

Discussion

Among the many techniques for 3D image manipulation, maximum intensity projection (MIP) and volume rendering are widely used for 3D vascular imaging [13–17]. MIP is a specific type of rendering in which the brightest voxel is projected into the 3D image. Unlike MIP, which displays only a small fraction of the available data, volume rendering can display a volume of data in its entirety. This property allows volume-rendered CT angiograms to provide vessel "depth," to display multiple overlapping vessels much more clearly, and to exclude surrounding structures [29–31]. Recently, the medical imaging community has embraced volume rendering for a wide variety of 3D imaging applications including navigation imaging based on cone-beam CT.

The new 3D navigation imaging software successfully traced feeding arteries in the vicinity of the target. In this study, 3D navigation imaging was found to be significantly better for accurate detection of feeding arteries than 2D celiac angiography was ($p < 0.001$). A good degree of agreement was achieved between 3D navigation imaging and the final angiographic findings (kappa = 0.638). Our results indicate that this tracking navigation imaging system could contribute to selection of the feeding arteries and could assist with therapeutic angiography for unresectable HCC, especially in patients with complicated feeding anatomies. In the 52 patients who underwent TACE using the tracking navigation imaging system, the disease control rate by TACE was 67.3%, according to selective angiography. During follow-up (mean, 6.1 months; range, 1–11 months), 19.2% remained recurrence-free in this study.

This new tracking navigation imaging system with cone-beam CT has three important features for clinical application as part of TACE. The first is speed. The tracking image can be displayed on the angiography room monitor approximately 30 s after completion of the cone-beam CT angiography procedure, and the operator can get feedback to advance the catheter. The second feature is high resolution: clear images of intrahepatic arterial branches can be obtained without patients having to raise their arms. The third feature is multifunctionality. Not only a 3D rotational view but also a 3D roadmap can help the operator position the catheter using less x-ray dye and in a shorter time. Modern vessel identification software that uses cone-beam CT data has been developed. Wang et al. reported that the 3D vessel tracking system has advantages over conventional 2D hepatic angiography in revealing the cystic artery ($p < 0.001$) [32]. Miyayama et al. found the usefulness of automatic feeder vessel detection software with a true-positive ratio with 88% in the identification of the tumor-feeding artery [33]. Iwazawa et al. also showed that the sensitivity in detecting tumor feeders was 87.7% [34]. They reported that the software improved the sensitivity of tumor feeder detection with a shorter processing time than manual assessment angiography.

In the present study, in four HCCs in four patients, neither this tracking imaging method nor selective angiography could display the feeding arteries; this shortcoming might be the result of poor enhancement of the feeding arteries and tumors. Excess feeding vessels were depicted in a HCC in one patient. This error might be the result of high sensitivity with rich enhancement of huge HCCs. In one patient, 3D tracking navigation imaging failed to detect the inferior phrenic artery feeding the HCC. Finally, selective angiography could correct false-positive detection of the feeders with the software. In studies of vessel identification software use, aberrant path formation during the software extraction process was found to be caused by crossed tumor feeders, feeder vessels with hairpin turns, artifacts, and arteroportal shunts, among other complicating factors.

It is anticipated that tracking navigation imaging software using cone-beam CT will reduce radiation exposure, shorten the overall procedure time, and cut the amount of contrast material used because the feedback that it provides will facilitate efficient angiographic procedures. However, to minimize radiation exposure, we should refrain from unnecessary an-

giography or cone-beam CT examination. Radiation exposure ranges from 15 to 20 mSv for an abdominal angiogram, and the effective dose is 4–5 mSv for a cone-beam CT abdominal scan [35, 36]. The need for clinical imaging information must be balanced against the potential negative effects of radiation.

The principal limitation of this study was its retrospective design, which inherently decreased the statistical strength. The second was that this study could suffer from selection bias because the patients were enrolled according to the operators' subjective judgment. However, tracking navigation imaging could assist therapeutic angiography and contribute to the effectiveness of TACE for HCC despite the inclusion of patients with complicated feeding vessels. The third limitation was the preliminary nature of this study with a relatively small number of patients. Further studies of this technique with a larger number of patients are warranted.

In summary, tracking navigation imaging with 3D cone-beam CT angiography can provide immediate feedback on the angiographic procedure and could easily identify HCC tumor feeders. Thereafter, these feeders could be catheterized quickly with the patient receiving low contrast/radiation doses. This new 3D tracking navigation imaging software can inspire greater confidence and should be useful for TACE in HCC patients with complicated feeding arteries.

Author Contributions

Yasunori Minami was responsible for the acquisition of clinical data and the writing of the manuscript. Takamichi Murakami helped develop the new tracking navigation imaging system and edited the manuscript. Yukinobu Yagyu provided technical instruction on 3D cone-beam CT angiography. Masatoshi Kudo reviewed and approved the final version of the manuscript.

Conflict of Interest

Y.M. Financial activities related to the present article: none to disclose. Financial activities not related to the present article: none to disclose. Other relationships: none to disclose. M.K. Financial activities related to the present article: none to disclose. Financial activities not related to the present article: none to disclose. Other relationships: none to disclose. Y.Y. Financial activities related to the present article: none to disclose. Financial activities not related to the present article: none to disclose. Other relationships: none to disclose. T.M. Financial activities related to the present article: none to disclose. Financial activities not related to the present article: none to disclose. Other relationships: none to disclose.

References

▶1 Nakamura H, Hashimoto T, Oi H, Sawada S: Transcatheter oily chemoembolization of hepatocellular carcinoma. Radiology 1989;170:783–786.
▶2 Matsui O, Kadoya M, Yoshikawa J, Gabata T, Arai K, Demachi H, Miyayama S, Takashima T, Unoura M, Kogayashi K: Small hepatocellular carcinoma: treatment with subsegmental transcatheter arterial embolization. Radiology 1993;188:79–83.
▶3 Takayasu K, Arii S, Ikai I, Omata M, Okita K, Ichida T, Matsuyama Y, Nakanuma Y, Kojiro M, Makuuchi M, Yamaoka Y, Liver Cancer Study Group of Japan: Prospective cohort study of transarterial chemoembolization for unresectable hepatocellular carcinoma in 8510 patients. Gastroenterology 2006;131:461–469.
▶4 Llovet JM, Real MI, Montaña X, Planas R, Coll S, Aponte J, Ayuso C, Sala M, Muchart J, Solà R, Rodés J, Bruix J, Barcelona Liver Cancer Group: Arterial embolisation or chemoembolisation versus symptomatic treatment in patients with unresectable hepatocellular carcinoma: a randomised controlled trial. Lancet 2002;359:1734–1739.

5 Sergio A, Cristofori C, Cardin R, Pivetta G, Ragazzi R, Baldan A, Girardi L, Cillo U, Burra P, Giacomin A, Farinati F: Transcatheter arterial chemoembolization (TACE) in hepatocellular carcinoma (HCC): the role of angiogenesis and invasiveness. Am J Gastroenterol 2008;103:914–921.
6 Imai Y, Chikayama T, Nakazawa M, Watanabe K, Ando S, Mizuno Y, Yoshino K, Sugawara K, Hamaoka K, Fujimori K, Inao M, Nakayama N, Oka M, Nagoshi S, Mochida S: Usefulness of miriplatin as an anticancer agent for transcatheter arterial chemoembolization in patients with unresectable hepatocellular carcinoma. J Gastroenterol 2011;47:179–186.
7 Lencioni R: Chemoembolization in patients with hepatocellular carcinoma. Liver Cancer 2012;1:41–50.
8 Ricke J, Seidensticker M, Mohnike K: Noninvasive diagnosis of hepatocellular carcinoma in cirrhotic liver: current guidelines and future prospects for radiological imaging. Liver Cancer 2012;1:51–58.
9 Lewandowski RJ, Geschwind JF, Liapi E, Salem R: Transcatheter intraarterial therapies: rationale and overview. Radiology 2011;259:641–657.
10 Lencioni R, Crocetti L: Local-regional treatment of hepatocellular carcinoma. Radiology 2012;262:43–58.
11 Bouvier A, Ozenne V, Aubé C, Boursier J, Vullierme MP, Thouveny F, Farges O, Vilgrain V: Transarterial chemoembolisation: effect of selectivity on tolerance, tumour response and survival. Eur Radiol 2011;21:1719–1726.
12 Gaba RC: Chemoembolization practice patterns and technical methods among interventional radiologists: results of an online survey. AJR Am J Roentgenol 2012;198:692–699.
13 Nelson RC, Chezmar JL, Sugarbaker PH, Bernardino ME: Hepatic tumors: comparison of CT during arterial portography, delayed CT, and MR imaging for preoperative evaluation. Radiology 1989;172:27–34.
14 Kanematsu M, Hoshi H, Imaeda T, Murakami T, Inaba Y, Yokoyama R, Nakamura H: Detection and characterization of hepatic tumors: value of combined helical CT hepatic arteriography and CT during arterial portography. AJR Am J Roentgenol 1997;168:1193–1198.
15 Murakami T, Oi H, Hori M, Kim T, Takahashi S, Tomoda K, Narumi Y, Nakamura H: Helical CT during arterial portography and hepatic arteriography for detecting hypervascular hepatocellular carcinoma. AJR Am J Roentgenol 1997;169:131–135.
16 Takayasu K, Muramatsu Y, Maeda T, Iwata R, Furukawa H, Muramatsu Y, Moriyama N, Okusaka T, Okada S, Ueno H: Targeted transarterial oily chemoembolization for small foci of hepatocellular carcinoma using a unified helical CT and angiography system: analysis of factors affecting local recurrence and survival rates. AJR Am J Roentgenol 2001;176:681–688.
17 Toyoda H, Kumada T, Sone Y: Impact of a unified CT angiography system on outcome of patients with hepatocellular carcinoma. AJR Am J Roentgenol 2009;192:766–774.
18 Lee JM, Yoon JH, Joo I, Woo HS: Recent advances in CT and MR imaging for evaluation of hepatocellular carcinoma. Liver Cancer 2012;1:22–40.
19 Hirota S, Nakao N, Yamamoto S, Kobayashi K, Maeda H, Ishikura R, Miura K, Sakamoto K, Ueda K, Baba R: Cone-beam CT with flat-panel-detector digital angiography system: early experience in abdominal interventional procedures. Cardiovasc Intervent Radiol 2006;29:1034–1038.
20 Kakeda S, Korogi Y, Ohnari N, Moriya J, Oda N, Nishino K, Miyamoto W: Usefulness of cone-beam volume CT with flat panel detectors in conjunction with catheter angiography for transcatheter arterial embolization. J Vasc Interv Radiol 2007;18:1508–1516.
21 Loffroy R, Lin M, Rao P, Bhagat N, Noordhoek N, Radaelli A, Blijd J, Geschwind JF: Comparing the detectability of hepatocellular carcinoma by C-arm dual-phase cone-beam computed tomography during hepatic arteriography with conventional contrast-enhanced magnetic resonance imaging. Cardiovasc Intervent Radiol 2012;35:97–104.
22 Miyayama S, Yamashiro M, Hashimoto M, Hashimoto N, Ikuno M, Okumura K, Yoshida M, Matsui O: Blood supply of the main bile duct from the caudate artery and medial subsegmental artery of the hepatic artery: Evaluation using images obtained during transcatheter arterial chemoembolization for hepatocellular carcinoma. Hepatol Res 2013. [Epub ahead of print].
23 Miyayama S, Yamashiro M, Okuda M, Yoshie Y, Sugimori N, Igarashi S, Nakashima Y, Matsui O: Usefulness of cone-beam computed tomography during ultraselective transcatheter arterial chemoembolization for small hepatocellular carcinomas that cannot be demonstrated on angiography. Cardiovasc Intervent Radiol 2009;32:255–264.
24 Miyayama S, Yamashiro M, Hattori Y, Orito N, Matsui K, Tsuji K, Yoshida M, Matsui O: Efficacy of cone-beam computed tomography during transcatheter arterial chemoembolization for hepatocellular carcinoma. Jpn J Radiol 2011;29:371–377.
25 Higashihara H, Osuga K, Onishi H, Nakamoto A, Tsuboyama T, Maeda N, Hori M, Kim T, Tomiyama N: Diagnostic accuracy of C-arm CT during selective transcatheter angiography for hepatocellular carcinoma: comparison with intravenous contrast-enhanced, biphasic, dynamic MDCT. Eur Radiol 2012;22:872–879.
26 Deschamps F, Solomon SB, Thornton RH, Rao P, Hakime A, Kuoch V, de Baere T: Computed analysis of three-dimensional cone-beam computed tomography angiography for determination of tumor-feeding vessels during chemoembolization of liver tumor: a pilot study. Cardiovasc Intervent Radiol 2010. [Epub ahead of print].
27 Lencioni R, Llovet JM: Modified RECIST (mRECIST) assessment for hepatocellular carcinoma. Semin Liver Dis 2010;30:52–60.
28 Landis JT, Koch GG: The measurement of observer agreement for categorical data.Biometrics 1977;13:159–174.
29 Calhoun PS, Kuszyk BS, Heath DG, Carley JC, Fishman EK: Three-dimensional volume rendering of spiral CT data: theory and method. Radiographics 1999;19:745–764.

30 Dalrymple NC, Prasad SR, Freckleton MW, Chintapalli KN: Informatics in radiology (infoRAD): introduction to the language of three-dimensional imaging with multidetector CT. Radiographics 2005;25:1409–1428.
31 Fishman EK, Ney DR, Heath DG, Corl FM, Horton KM, Johnson PT: Volume rendering versus maximum intensity projection in CT angiography: what works best, when, and why. Radiographics 2006;26:905–922.
32 Wang X, Shah RP, Maybody M, Brown KT, Getrajdman GI, Stevenson C, Petre EN, Solomon SB: Cystic artery localization with a three-dimensional angiography vessel tracking system compared with conventional two-dimensional angiography. J Vasc Interv Radiol 2011;22:1414–1419.
33 Miyayama S, Yamashiro M, Hashimoto M, Hashimoto N, Ikuno M, Okumura K, Yoshida M, Matsui O: Identification of small hepatocellular carcinoma and tumor-feeding branches with cone-beam CT guidance technology during transcatheter arterial chemoembolization. J Vasc Interv Radiol 2013;24:501–508.
34 Iwazawa J, Ohue S, Hashimoto N, Muramoto O, Mitani T: Clinical utility and limitations of tumor-feeder detection software for liver cancer embolization. Eur J Radiol 2013;82:1665–1671.
35 Koyama S, Aoyama T, Oda N, Yamauchi-Kawaura C: Radiation dose evaluation in tomosynthesis and C-arm cone-beam CT examinations with an anthropomorphic phantom. Med Phys 2010;37:4298–4306.
36 Verdun FR, Bochud F, Gundinchet F, Aroua A, Schnyder P, Meuli R: Quality initiatives* radiation risk: what you should know to tell your patient. Radiographics 2008;28:1807–1816.

World Journal of Gastroenterology

Online Submissions: http://www.wjgnet.com/esps/
bpgoffice@wjgnet.com
doi:10.3748/wjg.v20.i15.4160

World J Gastroenterol 2014 April 21; 20(15): 4160-4166
ISSN 1007-9327 (print) ISSN 2219-2840 (online)

TOPIC HIGHLIGHT

WJG 20th Anniversary Special Issues (1): Hepatocellular carcinoma

Therapeutic response assessment of RFA for HCC: Contrast-enhanced US, CT and MRI

Yasunori Minami, Naoshi Nishida, Masatoshi Kudo

Yasunori Minami, Naoshi Nishida, Masatoshi Kudo, Department of Gastroenterology and Hepatology, Kinki University Faculty of Medicine, Osaka 589-8511, Japan
Author contributions: Minami Y drafted the manuscript and wrote the final version of the manuscript; Nishida N reviewed the manuscript; Kudo M approved the final version of the manuscript.
Correspondence to: Masatoshi Kudo, MD, PhD, Department of Gastroenterology and Hepatology, Kinki University Faculty of Medicine, 377-2 Ohno-Higashi Osaka-Sayama, Osaka 589-8511, Japan. m-kudo@med.kindai.ac.jp
Telephone: +81-72-3660221-3525 Fax: +81-72-3672880
Received: October 12, 2013 Revised: January 22, 2014
Accepted: February 26, 2014
Published online: April 21, 2014

Abstract

Radiofrequency ablation (RFA) is commonly applied for the treatment of hepatocellular carcinoma (HCC) because of the facile procedure, and the safety and effectiveness for the treatment of this type of tumor. On the other hand, it is believed that HCC cells should spread predominantly through the blood flow of the portal vein, which could lead to the formation of intrahepatic micrometastases. Therefore, monitoring tumor response after the treatment is quite important and accurate assessment of treatment response is critical to obtain the most favorable outcome after the RFA. Indeed, several reports suggested that even small HCCs of ≤ 3 cm in diameter might carry intrahepatic micrometastases and/or microvascular invasion. From this point of view, for preventing local recurrences, RFA should be performed ablating a main tumor as well as its surrounding non-tumorous liver tissue where micrometastases and microvascular invasion might exist. Recent advancement of imaging modalities such as contrast-enhanced ultrasonic, computed tomography, and magnetic resonance imaging are playing an important role on assessing the therapeutic effects of RFA. The local recurrence rate tends to be low in HCC patients who were proven to have adequate ablation margin after RFA; namely, not only disappearance of vascular enhancement of main tumor, but also an adequate ablation margin. Therefore, contrast enhancement gives important findings for the diagnosis of recurrent HCCs on each imaging. However, hyperemia of non-tumorous liver surrounding the ablated lesion, which could be attributed to an inflammation after RFA, may well obscure the findings of local recurrence of HCCs after RFA. Therefore, we need to carefully address to these imaging findings given the fact that diagnostic difficulties of local recurrence of HCC. Here, we give an overview of the current status of the imaging assessment of HCC response to RFA.

Key words: Hepatocellular carcinoma; Micrometastasis; Microvascular invasion; Radiofrequency ablation; Safety margin

Core tip: Radiofrequency ablation (RFA) therapy is needed to ablate wider range of region than targeted tumor, including surrounding liver tissues that involve micrometastases and microvascular invasion. The local recurrence rate tends to be lower in hepatocellular carcinoma patients with an adequate ablation margin, and thus, it is essential to assess safety margin accurately to reduce local recurrence. From this point of view, we need to focus on the achievement of a sufficient ablation margin as well the lack of tumor vascular enhancement for the assessment of successful RFA. However, inflammatory hyperemia due to RFA which often appears as peripheral rim enhancement, and non-typical imaging features of tumor recurrence sometimes lead to the inappropriate diagnosis.

Minami Y, Nishida N, Kudo M. Therapeutic response assessment of RFA for HCC: Contrast-enhanced US, CT and MRI. *World J Gastroenterol* 2014; 20(15): 4160-4166 Available from: URL: http://www.wjgnet.com/1007-9327/full/v20/i15/4160.htm DOI: http://dx.doi.org/10.3748/wjg.v20.i15.4160

INTRODUCTION

Surgical resection is the first treatment of choice for hepatocellular carcinoma (HCC). Unfortunately, the majority of HCC patients are not suitable for curative resection at the time of diagnosis because of large tumor size, multifocal disease, vascular involvement, extrahepatic spread, poor liver function, *etc.*[1-6]. Therefore, there is a need to develop a simple and effective technique to treat unresectable HCC. Several local, minimally invasive hepatic therapies [percutaneous ethanol injection (PEI), acetic acid injection, microwave coagulation therapy, and radiofrequency ablation (RFA)] have been developed to prolong survival in unresectable HCC patients over the past few decades[7-13]. Especially, RFA is currently performed widely due to its ease of use, safety and effectiveness for managing HCC in patients with cirrhosis[14-17], while its high repeatability makes it particularly valuable for controlling intrahepatic recurrences[18].

Monitoring tumor response to therapy is an important part of the clinical management of cancer patients, and accurate assessment of tumor response is essential for favorable outcomes. Imaging techniques such as contrast-enhanced ultrasound (US), computed tomography (CT) and magnetic resonance imaging (MRI) are generally used to diagnose HCC or assess therapeutic effects[19-21]. However, these techniques naturally use different principles to generate images, and the type and dose of contrast agents are different. Contrast enhancement is an important finding on imaging; however, enhancement does not necessarily depict the same phenomenon between US, CT and MRI. Therefore, we need to be familiar with the findings on each modality after ablation to evaluate the success of treatment, detect residual or recurrent tumors, and diagnose new lesions.

In this review, we focus our discussion on the imaging assessment of HCC response to RFA.

CLINICOPATHOLOGICAL FEATURES OF HCC FOR ABLATION

HCC cells spread mainly *via* the portal system and form intrahepatic micrometastases[22,23]. Among risk factors for recurrences, tumor size, portal vein invasion, and intrahepatic metastasis are generally considered the major causes of intrahepatic HCC recurrence after treatment. A previous pathologic study showed that intrahepatic metastasis occurs in 10% of cases even in early HCC (lesions < 2 cm in diameter)[22]. Okusaka *et al*[24] reported that 19% of HCC nodules of 3.0 cm or less in diameter had satellite lesions that were not detected during pretreatment evaluation. Nakashima *et al*[25] revealed that 59.1% of small HCC of ≤ 3.0 cm in diameter had micrometastases within 5 mm of each micrometastatic lesion and its primary HCC. Especially, among single nodular type HCC, micrometastases were shown in 77.8% within 5 mm.

Several studies address the relation between microvascular invasion of HCC cells and tumor size. Kojiro *et al*[22] reported that the tumor invades the portal vein in 27% of cases even in early HCC (lesions < 2 cm in dimension). Esnaola *et al*[26] found the frequency of microvascular invasion to be 25% and 31% for tumors < 2 cm and 2-4 cm in the greatest dimension, respectively. On the other hand, microvascular invasion was shown in 17% of patients with tumors < 2 cm and 20% of patients with tumors 2-3 cm[24]. The reported frequency of microvascular invasion in patients with an HCC tumor of 2-3 cm ranges from approximately 20%-30%. Thus, it has reported that the risk factors for early local tumor recurrence were larger tumor size, poor pathologic differentiation of tumor cells and advanced tumor staging[27,28].

PRINCIPLE OF TUMOR RESPONSE ASSESSMENT TO RFA FOR HCC

Efficacy of treatment is usually monitored radiologically. Effective treatment is indicated by not only lack of vascular enhancement of HCC, but also the safety margin. The safety margin is ablated peritumoral liver tissue that is located between a necrotic tumor and unablated liver tissue (Figure 1). For the RFA procedure to be considered technically successful, the tumor and at least a 5 mm safety margin must be included in the ablation zone[29]. The local recurrence rate differs markedly depending on whether or not a 5 mm safety margin is secured. Kudo *et al*[14] reported that the local recurrence rate was 2.6% in HCC patients with a ≥ 5 mm safety margin at 2 years after RFA, whereas it was 20.8% in HCC patients without safety margin ($P = 0.01$). Another report indicated that the significant risk factors for local recurrence of RFA were a tumor with a diameter ≥ 2.3 cm, an insufficient safety margin, and a multinodular tumor[30]. In addition, the safety margin has one more important role as security in avoiding limitations on CT assessment due to a partial volume effect.

Alpha-fetoprotein (AFP), lens culinaris agglutinin-reactive fraction of AFP (AFP-L3), and des-γ-carboxy prothrombin (DCP) have been used as tumor markers for HCC[31-34]. Levels of tumor markers often fall to within the normal range after effective treatment and rise before tumor relapse is detected by imaging studies. However, sensitivity and specificity of tumor markers are insufficient to detect HCC in all patient samples, and the monitoring of tumor marker levels after therapy does not replace imaging[35].

Recurrence of tumors in the treated area or elsewhere is defined as re-appearance of vascular enhancement. The ideal imaging interval is unknown, but initially

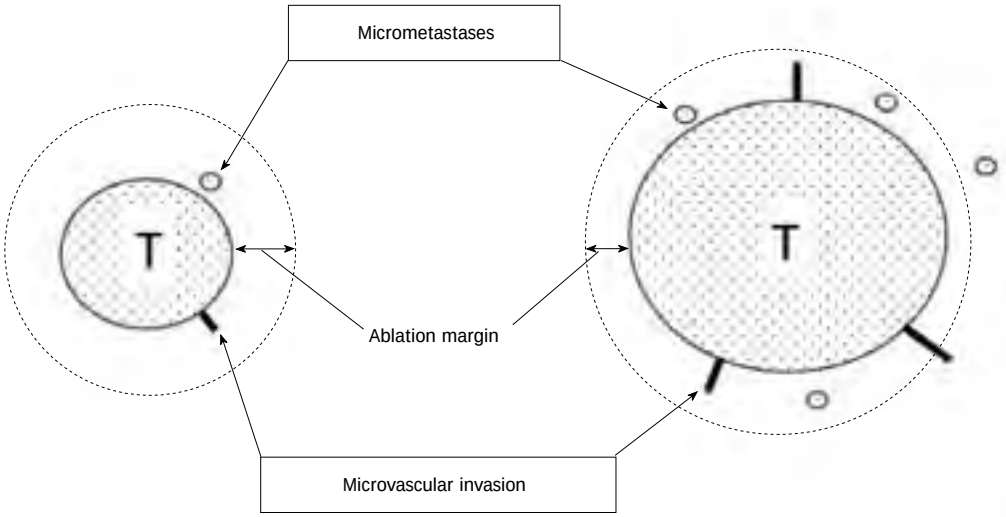

Figure 1 Ablation margin and micrometastases/microvascular invasion. Radiofrequency ablation (RFA) therapy is required to ablate the main tumor and its surrounding liver tissues involving micrometastases and microvascular invasion. However, as the tumor get bigger, micrometastases and microcascular invasion frequently occur. Unablated lesions lead to local recurrences after RFA. T: Tumor.

a 3-4 mo interval is commonly used to monitor HCC lesions after initial treatment. After about 2 years of recurrence-free survival, the interval of follow-up imaging examinations can be at less frequent intervals[35].

Imaging

CT: Contrast-enhanced CT has been most widely used for the evaluation of treatment response after RFA because of the advantages of CT: the rapid acquisition of images, clear and specific information, and the referring of a wide range of the abdomen including the liver. After a bolus dispense of contrast agent, tissue contrast enhancement depends on arterial blood flow, capillary permeability, rate of diffusion, and extravascular extracellular space volume. In clinical practice, evaluation of successful treatment was based on a visual comparison of the pre- and post-RFA CT images by referring specific landmarks such as hepatic vessels and the liver surface[14,36,37]. If the non-enhancing ablation zone included the original tumor and an adequate safety margin in all directions, the RFA should be regarded as technically successful[38]. Sala *et al*[39] revealed that the independent predictors of survival were Child-Pugh class ($P = 0.0001$) and initial complete response to percutaneous ablation ($P = 0.006$). Among patients classified as Child-Pugh grade A, a 20% difference of survival rate was achieved at 5 years (42% in responders *vs* 18% in non-responders), while among patients classified as Child-Pugh grade B, the difference of survival rate was observed at 3 years (42% in responders *vs* 16% in non-responders).

Compared with RFA alone, the combination of RFA and transcatheter arterial chemoembolization (TACE) markedly increased the extent of induced coagulation of RFA[40]. Combined TACE and RFA have several advantages over RFA treatment alone. Theoretically, embolization along with the chemotherapy is synergic to thermal ablation by lowering the convection by vascular flow, decreasing the impedance in the tumor and facilitating heat distribution within the tumor. Moreover, satellite nodules, which are found more commonly around large HCCs can be depicted by Lipiodol spots. Thus, RFA combined with TACE has been reported to be promising for local control of medium-size of tumors[41-44]. In addition, Lipiodol-TACE could offer another advantage for assessment of following RFA procedure. When the ablated area could cover the whole HCC with a sufficient margin, the ablative margin can be shown as the boundary between the high density area as Lipiodol accumulation in HCC and the enhancing area as surrounding normal liver parenchyma. As the area of Lipiodol deposition is an ideal landmark of the tumor margin, the successful safety margin can be easily evaluated only by post-RFA dynamic CT images in HCC patients treated by RFA combined with TACE, without a comparison of the pre- and post-RFA CT images (Figure 2)[45].

Hyperemia in tissue surrounding the ablated lesion can represent an inflammatory reaction due to thermal injury. Peripheral rim enhancement resulting from reactive hyperemia is usually uniform in thickness and envelops the ablated lesion (Figure 2), whereas residual HCC demonstrates focal and irregular peripheral enhancement[46,47]. However, differentiation of reactive hyperemia from residual HCCs is sometimes difficult. Moreover, typical imaging features (arterial enhancement followed by delayed washout on dynamic contrast-enhanced CT) are not usually depicted for the diagnosis of recurrent HCCs. Mikami *et al*[48] reported that 17.5% of patients were diagnosed as local recurrent HCC with typical enhancement pattern, while 40.6% had arterial hypervascularity without washout in the portal venous phase and 11.9% showed washout in portal venous phase without arterial hypervascularity. A non-typical enhancement pattern of local HCC recurrence may reflect the fact that insufficient RFA therapy could lead to further malignant

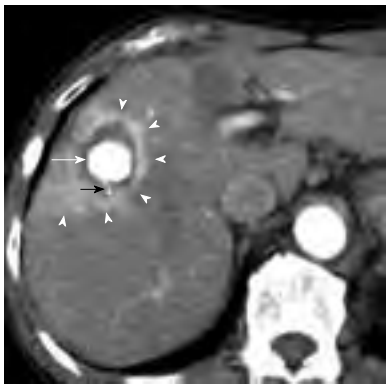

Figure 2 A 80-year-old woman with 2.5 cm hepatocellular carcinoma after radiofrequency ablation combined with transcatheter arterial chemoembolization. Early-phase dynamic computed tomography shows a high-density center indicating Lipiodol deposition in hepatocellular carcinoma (white arrow) and a surrounding low-density zone indicating radiofrequency ablation-induced coagulation necrosis of the liver. A microsatellite (black arrow) was depicted as a high-density spot in the low-density zone. Therefore, this ablation therapy achieved complete necrosis of chief tumor and micrometastasis. Moreover, hyperemia surrounding the ablated lesion is depicted as peripheral rim enhancement (arrowheads).

transformation of HCC[49]. Therefore, careful comparison with imaging before ablation and close follow-up are necessary in in patients who showed unusual pattern of enhancement in the liver after RFA.

US: US contrast agents consist of gas-cored microbubbles that are encapsulated by a shell constructed of a lipid monolayer or cross-linked albumin. Each bubble acts as a harmonic oscillator and contrast-enhanced echo signals contain significant energy components at higher harmonics, while tissue echoes do not. With the use of a contrast agent, contrast harmonic imaging possesses not only a very high sensitivity to contrast agents but also a high spatial resolution, and can depict signals from microbubbles with a very slow flow. Several researchers have reported that contrast-enhanced US is a useful tool for assessing the vascularity of local recurrence of HCCs[50-54]. The detectability of viable HCCs was 83.5% in B-mode US and increased to 93.2% in contrast-enhanced US, using contrast-enhanced CT was used as the reference standard[55]. As reported by Kim *et al*[56], the diagnostic concordance between the contrast-enhanced US just after the RFA and the CT after the 1-mo follow-up was 99% in terms of the assessment of the therapeutic response to RFA. The sensitivity, specificity, and diagnostic accuracy of contrast-enhanced US were 95.3%, 100%, and 98.1%, respectively[57]. Consequently, contrast-enhanced US may provide an alternative approach that shows high diagnostic concordance with dynamic CT in assessing the therapeutic response of RFA in hypervascular HCC (Figure 3). However, it is often difficult to identify the safety margin on US in the some cases. Zhou *et al*[58] found that contrast-enhanced US could not evaluate safety margin in 34.8% of HCC nodules because the tumor boundary could not be identified clearly by US after RFA. Therefore, contrast-enhanced US and contrast-enhanced CT should carry a complementary role for the evaluation of the treatment response after RFA.

Perfluorocarbon microbubbles (Sonazoid) is classified as second-generation US-contrast agents. Unlike others, perfluorocarbon microbubbles are not trapped by Kupffer cells. A double contrast US technique using Sonazoid reinjection has been developed on the basis of two specific characteristics of Sonazoid: real-time blood flow images with low acoustic power and robust Kupffer images tolerable for repeated scanning in the Kupffer phase[59-61]. According to contrast-enhanced US using Sonazoid, peripheral hyperemia areas show hyper-echogenicity during the early vascular phase and iso-echogenicity as adjacent liver parenchyma during the Kupffer phase. On the other hand, residual HCC demonstrates a focal defect during the Kupffer phase and represents hypervascular enhancement by the reinjection of Sonazoid. Therefore, differentiation of reactive hyperemia from residual HCCs is not difficult. Dynamic contrast-enhanced US guidance in ablation therapy for locally recurrent HCCs should be an efficient approach[61].

MRI: MRI provides better contrast between the different soft tissues and higher spatial resolution with sensitivity than CT. Recent advances in MRI allow imaging of the liver with a high spatial resolution during a single breathhold. Khankan *et al*[62] reported that a hyperintense zone on non-enhanced T1-weighted MRI within 2 d after RFA reflected the extent of the ablated region. Evaluation of the safety margin also needs comparisons of the pre- and post-RFA images because of the blurriness of tumor boundary on non-enhanced MRI after RFA.

Hepatocyte-specific MRI contrast agents were developed for detection and characterization of focal liver lesions. Gadolinium-ethoxybenzyl-diethylenetriamine pentaacetic acid (Gd-EOB-DTPA) is a contrast agent with combined properties of a conventional non-specific extracellular and hepatocyte-specific contrast agent[63]. It is recognized that hepatocyte phase images help to distinguish vascular pseudolesions (*e.g.*, those due to arterioportal shunting, portal venule obstruction, nonportal splanchnic veins, or rib compression) from hypervascular tumors[64]. Meanwhile, a recent study[65] reported that more than 10% of vascular pseudolesions showed hypointensity on hepatocyte-phase images and that those pseudolesions occasionally mimicked the configurations and signal intensities of HCCs. Watanabe *et al*[66] analyzed the image of HCC tumors using the area under the receiver operating characteristic (ROC) curve, and concluded that the incorporation of hepatocyte phase images did not improve the diagnostic accuracy of Gd-EOB-DTPA-enhanced MRI for locally recurrent HCCs after RFA. On the other hand, Koda *et al*[67] reported the ablative margin grading assessment using superparamagnetic iron oxide (SPIO)-enhanced MRI. They intravenously injected ferucarbotran (0.016 mL/kg body weight) 20-60 min before RFA, and performed MRI at 7 d after RFA. Because SPIO remained in ablated hepatic parenchyma,

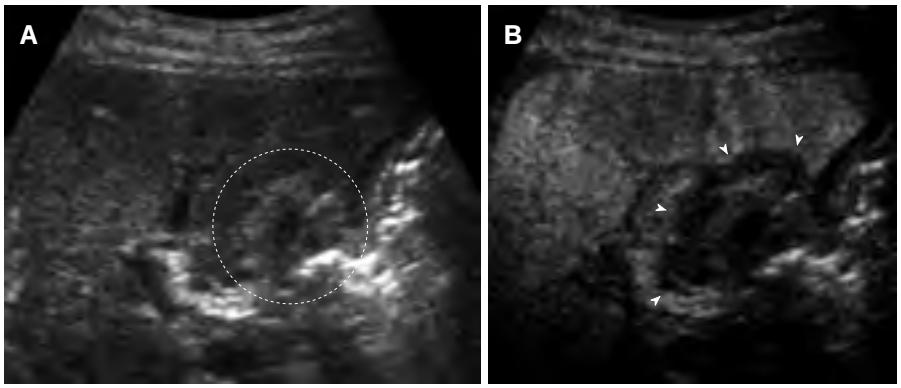

Figure 3 A 70-year-old man with 1.5 cm hepatocellular carcinoma after radiofrequency ablation. A: The ablated tumor is depicted as hyper echoic lesion (circle) on B-mode ultrasound (US). However, the boundary between ablated area and unablated liver tissue could not be identified clearly; B: Contrast-enhanced US using Sonazoid shows the defect (arrows) in the Kupffer phase. The ablation margin is shown as low echoic zone surrounding the ablated tumor.

post-ablation MRI showed a high-intensity area of HCC surrounding by low-intensity area of ablative margin.

CONCLUSION

The prognosis of patients with small HCC is still unsatisfactory because of frequent recurrence even after complete ablation. The high recurrence rate may be attributed to the undefined satellite lesions or microvascular invasion before treatment, which are too small to be detected with the current imaging modality. For the procedure of local ablation therapies including RFA, we need to ablate wider range of region than targeted tumor, including surrounding non-tumorous liver tissues that could involve micrometastases and microvascular invasion. The local recurrence rate tends to be lower in HCC patients with an adequate ablation margin, and thus, it is essential to assess safety margin accurately to reduce local recurrence. From this point of view, we need to focus on the achievement of a sufficient ablation margin as well the lack of tumor vascular enhancement for the assessment of successful RFA. However, inflammatory hyperemia due to RFA which often appears as peripheral rim enhancement, and non-typical imaging features of tumor recurrence sometimes lead to the inappropriate diagnosis. Therefore, we need to be careful for the imaging findings given the fact that the diagnostic difficulties for local recurrence of HCC. Careful comparison of imaging before ablation and close follow-up are critical in HCC patients treated with RFA.

REFERENCES

1 **Minagawa M**, Makuuchi M, Takayama T, Kokudo N. Selection criteria for repeat hepatectomy in patients with recurrent hepatocellular carcinoma. *Ann Surg* 2003; **238**: 703-710 [PMID: 14578733 DOI: 10.1097/01.sla.0000094549.11754.e6]
2 **Capussotti L**, Muratore A, Massucco P, Ferrero A, Polastri R, Bouzari H. Major liver resections for hepatocellular carcinoma on cirrhosis: early and long-term outcomes. *Liver Transpl* 2004; **10**: S64-S68 [PMID: 14762842 DOI: 10.1002/lt.20035]
3 **Poon RT**, Fan ST. Hepatectomy for hepatocellular carcinoma: patient selection and postoperative outcome. *Liver Transpl* 2004; **10**: S39-S45 [PMID: 14762838 DOI: 10.1002/lt.20040]
4 **Song TJ**, Ip EW, Fong Y. Hepatocellular carcinoma: current surgical management. *Gastroenterology* 2004; **127**: S248-S260 [PMID: 15508091 DOI: 10.1053/j.gastro.2004.09.039]
5 **Llovet JM**, Schwartz M, Mazzaferro V. Resection and liver transplantation for hepatocellular carcinoma. *Semin Liver Dis* 2005; **25**: 181-200 [PMID: 15918147 DOI: 10.1055/s-2005-871198]
6 **Lin S**, Hoffmann K, Schemmer P. Treatment of Hepatocellular Carcinoma: A Systematic Review. *Liver Cancer* 2012; **1**: 144-158 [PMID: 24159579 DOI: 10.1159/000343828]
7 **Shiina S**, Tagawa K, Unuma T, Takanashi R, Yoshiura K, Komatsu Y, Hata Y, Niwa Y, Shiratori Y, Terano A. Percutaneous ethanol injection therapy for hepatocellular carcinoma. A histopathologic study. *Cancer* 1991; **68**: 1524-1530 [PMID: 1654196]
8 **Livraghi T**, Bolondi L, Lazzaroni S, Marin G, Morabito A, Rapaccini GL, Salmi A, Torzilli G. Percutaneous ethanol injection in the treatment of hepatocellular carcinoma in cirrhosis. A study on 207 patients. *Cancer* 1992; **69**: 925-929 [PMID: 1310435]
9 **Seki T**, Wakabayashi M, Nakagawa T, Itho T, Shiro T, Kunieda K, Sato M, Uchiyama S, Inoue K. Ultrasonically guided percutaneous microwave coagulation therapy for small hepatocellular carcinoma. *Cancer* 1994; **74**: 817-825 [PMID: 8039109]
10 **Seki T**, Wakabayashi M, Nakagawa T, Imamura M, Tamai T, Nishimura A, Yamashiki N, Okamura A, Inoue K. Percutaneous microwave coagulation therapy for patients with small hepatocellular carcinoma: comparison with percutaneous ethanol injection therapy. *Cancer* 1999; **85**: 1694-1702 [PMID: 10223562]
11 **Ohnishi K**, Yoshioka H, Ito S, Fujiwara K. Prospective randomized controlled trial comparing percutaneous acetic acid injection and percutaneous ethanol injection for small hepatocellular carcinoma. *Hepatology* 1998; **27**: 67-72 [PMID: 9425919 DOI: 10.1002/hep.510270112]
12 **Rossi S**, Di Stasi M, Buscarini E, Cavanna L, Quaretti P, Squassante E, Garbagnati F, Buscarini L. Percutaneous radiofrequency interstitial thermal ablation in the treatment of small hepatocellular carcinoma. *Cancer J Sci Am* 1995; **1**: 73-81 [PMID: 9166457]
13 **Curley SA**, Izzo F, Ellis LM, Nicolas Vauthey J, Vallone P. Radiofrequency ablation of hepatocellular cancer in 110 patients with cirrhosis. *Ann Surg* 2000; **232**: 381-391 [PMID: 10973388]
14 **Kudo M**. Local ablation therapy for hepatocellular carcinoma: current status and future perspectives. *J Gastroenterol* 2004; **39**: 205-214 [PMID: 15064996 DOI: 10.1007/s00535-003-1280-y]
15 **Shiina S**, Teratani T, Obi S, Sato S, Tateishi R, Fujishima T, Ishikawa T, Koike Y, Yoshida H, Kawabe T, Omata M. A randomized controlled trial of radiofrequency ablation with ethanol injection for small hepatocellular carcinoma. *Gastroenterology* 2005; **129**: 122-130 [PMID: 16012942 DOI: 10.1053/j.gastro.2005.04.009]

16 **Llovet JM**, Bruix J. Novel advancements in the management of hepatocellular carcinoma in 2008. *J Hepatol* 2008; **48** Suppl 1: S20-S37 [PMID: 18304676]

17 **Lencioni R**, Crocetti L. Local-regional treatment of hepatocellular carcinoma. *Radiology* 2012; **262**: 43-58 [PMID: 22190656 DOI: 10.1148/radiol.11110144]

18 **Rossi S**, Ravetta V, Rosa L, Ghittoni G, Viera FT, Garbagnati F, Silini EM, Dionigi P, Calliada F, Quaretti P, Tinelli C. Repeated radiofrequency ablation for management of patients with cirrhosis with small hepatocellular carcinomas: a long-term cohort study. *Hepatology* 2011; **53**: 136-147 [PMID: 20967759 DOI: 10.1002/hep.23965]

19 **Lee JM**, Yoon JH, Joo I, Woo HS. Recent Advances in CT and MR Imaging for Evaluation of Hepatocellular Carcinoma. *Liver Cancer* 2012; **1**: 22-40 [PMID: 24159569 DOI: 10.1159/000339018]

20 **Minami Y**, Kudo M. Therapeutic response assessment of transcatheter arterial chemoembolization for hepatocellular carcinoma: ultrasonography, CT and MR imaging. *Oncology* 2013; **84** Suppl 1: 58-63 [PMID: 23428860]

21 **Minami Y**, Kitai S, Kudo M. Treatment response assessment of radiofrequency ablation for hepatocellular carcinoma: usefulness of virtual CT sonography with magnetic navigation. *Eur J Radiol* 2012; **81**: e277-e280 [PMID: 21392916]

22 **Kojiro M**. Pathology of early hepatocellular carcinoma: progression from early to advanced. *Hepatogastroenterology* 1998; **45** Suppl 3: 1203-1205 [PMID: 9730375]

23 **Sasaki A**, Kai S, Iwashita Y, Hirano S, Ohta M, Kitano S. Microsatellite distribution and indication for locoregional therapy in small hepatocellular carcinoma. *Cancer* 2005; **103**: 299-306 [PMID: 15578688 DOI: 10.1002/cncr.20798]

24 **Okusaka T**, Okada S, Ueno H, Ikeda M, Shimada K, Yamamoto J, Kosuge T, Yamasaki S, Fukushima N, Sakamoto M. Satellite lesions in patients with small hepatocellular carcinoma with reference to clinicopathologic features. *Cancer* 2002; **95**: 1931-1937 [PMID: 12404287 DOI: 10.1002/cncr.10892]

25 **Nakashima Y**, Nakashima O, Tanaka M, Okuda K, Nakashima M, Kojiro M. Portal vein invasion and intrahepatic micrometastasis in small hepatocellular carcinoma by gross type. *Hepatol Res* 2003; **26**: 142-147 [PMID: 12809942 DOI: 10.1016/S1386-6346(03)00007-X]

26 **Esnaola NF**, Lauwers GY, Mirza NQ, Nagorney DM, Doherty D, Ikai I, Yamaoka Y, Regimbeau JM, Belghiti J, Curley SA, Ellis LM, Vauthey JN. Predictors of microvascular invasion in patients with hepatocellular carcinoma who are candidates for orthotopic liver transplantation. *J Gastrointest Surg* 2002; **6**: 224-232; discussion 232 [PMID: 11992808 DOI: 10.1016/S1091-255X(01)00015-4]

27 **Lin SM**, Lin CJ, Lin CC, Hsu CW, Chen YC. Randomised controlled trial comparing percutaneous radiofrequency thermal ablation, percutaneous ethanol injection, and percutaneous acetic acid injection to treat hepatocellular carcinoma of 3 cm or less. *Gut* 2005; **54**: 1151-1156 [PMID: 16009687 DOI: 10.1136/gut.2004.045203]

28 **Yu HC**, Cheng JS, Lai KH, Lin CP, Lo GH, Lin CK, Hsu PI, Chan HH, Lo CC, Tsai WL, Chen WC. Factors for early tumor recurrence of single small hepatocellular carcinoma after percutaneous radiofrequency ablation therapy. *World J Gastroenterol* 2005; **11**: 1439-1444 [PMID: 15770718]

29 **Goldberg SN**, Grassi CJ, Cardella JF, Charboneau JW, Dodd GD, Dupuy DE, Gervais D, Gillams AR, Kane RA, Lee FT, Livraghi T, McGahan J, Phillips DA, Rhim H, Silverman SG. Image-guided tumor ablation: standardization of terminology and reporting criteria. *J Vasc Interv Radiol* 2005; **16**: 765-778 [PMID: 15947040 DOI: 10.1097/01.RVI.0000170858.46668.65]

30 **Zytoon AA**, Ishii H, Murakami K, El-Kholy MR, Furuse J, El-Dorry A, El-Malah A. Recurrence-free survival after radiofrequency ablation of hepatocellular carcinoma. A registry report of the impact of risk factors on outcome. *Jpn J Clin Oncol* 2007; **37**: 658-672 [PMID: 17766723 DOI: 10.1093/jjco/hym086]

31 **Marrero JA**, Feng Z, Wang Y, Nguyen MH, Befeler AS, Roberts LR, Reddy KR, Harnois D, Llovet JM, Normolle D, Dalhgren J, Chia D, Lok AS, Wagner PD, Srivastava S, Schwartz M. Alpha-fetoprotein, des-gamma carboxyprothrombin, and lectin-bound alpha-fetoprotein in early hepatocellular carcinoma. *Gastroenterology* 2009; **137**: 110-118 [PMID: 19362088 DOI: 10.1053/j.gastro.2009.04.005]

32 **Yamamoto K**, Imamura H, Matsuyama Y, Kume Y, Ikeda H, Norman GL, Shums Z, Aoki T, Hasegawa K, Beck Y, Sugawara Y, Kokudo N. AFP, AFP-L3, DCP, and GP73 as markers for monitoring treatment response and recurrence and as surrogate markers of clinicopathological variables of HCC. *J Gastroenterol* 2010; **45**: 1272-1282 [PMID: 20625772 DOI: 10.1007/s00535-010-0278-5]

33 **Toyoda H**, Kumada T, Tada T, Niinomi T, Ito T, Kaneoka Y, Maeda A. Prognostic significance of a combination of pre- and post-treatment tumor markers for hepatocellular carcinoma curatively treated with hepatectomy. *J Hepatol* 2012; **57**: 1251-1257 [PMID: 22824818 DOI: 10.1016/j.jhep.2012.07.018]

34 **Song P**, Gao J, Inagaki Y, Kokudo N, Hasegawa K, Sugawara Y, Tang W. Biomarkers: Evaluation of Screening for and Early Diagnosis of Hepatocellular Carcinoma in Japan and China. *Liver Cancer* 2013; **2**: 31-39 [PMID: 24159594 DOI: 10.1159/000346220]

35 **Bruix J**, Sherman M. Management of hepatocellular carcinoma: an update. *Hepatology* 2011; **53**: 1020-1022 [PMID: 21374666 DOI: 10.1002/hep.24199]

36 **Okuwaki Y**, Nakazawa T, Shibuya A, Ono K, Hidaka H, Watanabe M, Kokubu S, Saigenji K. Intrahepatic distant recurrence after radiofrequency ablation for a single small hepatocellular carcinoma: risk factors and patterns. *J Gastroenterol* 2008; **43**: 71-78 [PMID: 18297439 DOI: 10.1007/s00535-007-2123-z]

37 **Tateishi R**, Shiina S, Ohki T, Sato T, Masuzaki R, Imamura J, Goto E, Goto T, Yoshida H, Obi S, Sato S, Kanai F, Yoshida H, Omata M. Treatment strategy for hepatocellular carcinoma: expanding the indications for radiofrequency ablation. *J Gastroenterol* 2009; **44** Suppl 19: 142-146 [PMID: 19148809]

38 **Kim KW**, Lee JM, Klotz E, Kim SJ, Kim SH, Kim JY, Han JK, Choi BI. Safety margin assessment after radiofrequency ablation of the liver using registration of preprocedure and postprocedure CT images. *AJR Am J Roentgenol* 2011; **196**: W565-W572 [PMID: 21512046]

39 **Sala M**, Llovet JM, Vilana R, Bianchi L, Solé M, Ayuso C, Brú C, Bruix J. Initial response to percutaneous ablation predicts survival in patients with hepatocellular carcinoma. *Hepatology* 2004; **40**: 1352-1360 [PMID: 15565564]

40 **Kitamoto M**, Imagawa M, Yamada H, Watanabe C, Sumioka M, Satoh O, Shimamoto M, Kodama M, Kimura S, Kishimoto K, Okamoto Y, Fukuda Y, Dohi K. Radiofrequency ablation in the treatment of small hepatocellular carcinomas: comparison of the radiofrequency effect with and without chemoembolization. *AJR Am J Roentgenol* 2003; **181**: 997-1003 [PMID: 14500217 DOI: 10.2214/ajr.181.4.1810997]

41 **Kagawa T**, Koizumi J, Kojima S, Nagata N, Numata M, Watanabe N, Watanabe T, Mine T; Tokai RFA Study Group. Transcatheter arterial chemoembolization plus radiofrequency ablation therapy for early stage hepatocellular carcinoma: comparison with surgical resection. *Cancer* 2010; **116**: 3638-3644 [PMID: 20564097 DOI: 10.1002/cncr.25142]

42 **Peng ZW**, Zhang YJ, Liang HH, Lin XJ, Guo RP, Chen MS. Recurrent hepatocellular carcinoma treated with sequential transcatheter arterial chemoembolization and RF ablation versus RF ablation alone: a prospective randomized trial. *Radiology* 2012; **262**: 689-700 [PMID: 22157201 DOI: 10.1148/radiol.11110637]

43 **Lu Z**, Wen F, Guo Q, Liang H, Mao X, Sun H. Radiofrequency ablation plus chemoembolization versus radiofrequency ablation alone for hepatocellular carcinoma: a meta-analysis of randomized-controlled trials. *Eur J Gastroenterol Hepatol* 2013; **25**: 187-194 [PMID: 23134976 DOI: 10.1097/MEG.0b013e32835a0a07]

44 **Peng ZW**, Zhang YJ, Chen MS, Xu L, Liang HH, Lin XJ,

Guo RP, Zhang YQ, Lau WY. Radiofrequency ablation with or without transcatheter arterial chemoembolization in the treatment of hepatocellular carcinoma: a prospective randomized trial. *J Clin Oncol* 2013; **31**: 426-432 [PMID: 23269991 DOI: 10.1200/JCO.2012.42.9936]

45 **Nishikawa H**, Inuzuka T, Takeda H, Nakajima J, Sakamoto A, Henmi S, Matsuda F, Eso Y, Ishikawa T, Saito S, Kita R, Kimura T, Osaki Y. Percutaneous radiofrequency ablation therapy for hepatocellular carcinoma: a proposed new grading system for the ablative margin and prediction of local tumor progression and its validation. *J Gastroenterol* 2011; **46**: 1418-1426 [PMID: 21845378 DOI: 10.1007/s00535-011-0452-4]

46 **Limanond P**, Zimmerman P, Raman SS, Kadell BM, Lu DS. Interpretation of CT and MRI after radiofrequency ablation of hepatic malignancies. *AJR Am J Roentgenol* 2003; **181**: 1635-1640 [PMID: 14627588 DOI: 10.2214/ajr.181.6.1811635]

47 **Kim SK**, Lim HK, Kim YH, Lee WJ, Lee SJ, Kim SH, Lim JH, Kim SA. Hepatocellular carcinoma treated with radio-frequency ablation: spectrum of imaging findings. *Radiographics* 2003; **23**: 107-121 [PMID: 12533646 DOI: 10.1148/rg.231025055]

48 **Mikami S**, Tateishi R, Akahane M, Asaoka Y, Kondo Y, Goto T, Shiina S, Yoshida H, Koike K. Computed tomography follow-up for the detection of hepatocellular carcinoma recurrence after initial radiofrequency ablation: a single-center experience. *J Vasc Interv Radiol* 2012; **23**: 1269-1275 [PMID: 22999746 DOI: 10.1016/j.jvir.2012.06.032]

49 **Obara K**, Matsumoto N, Okamoto M, Kobayashi M, Ikeda H, Takahashi H, Katakura Y, Matsunaga K, Ishii T, Okuse C, Suzuki M, Itoh F. Insufficient radiofrequency ablation therapy may induce further malignant transformation of hepatocellular carcinoma. *Hepatol Int* 2008; **2**: 116-123 [PMID: 19669287 DOI: 10.1007/s12072-007-9040-3]

50 **Meloni MF**, Goldberg SN, Livraghi T, Calliada F, Ricci P, Rossi M, Pallavicini D, Campani R. Hepatocellular carcinoma treated with radiofrequency ablation: comparison of pulse inversion contrast-enhanced harmonic sonography, contrast-enhanced power Doppler sonography, and helical CT. *AJR Am J Roentgenol* 2001; **177**: 375-380 [PMID: 11461867 DOI: 10.2214/ajr.177.2.1770375]

51 **Vilana R1**, Bianchi L, Varela M, Nicolau C, Sánchez M, Ayuso C, García M, Sala M, Llovet JM, Bruix J, Bru C; BCLC Group. Is microbubble-enhanced ultrasonography sufficient for assessment of response to percutaneous treatment in patients with early hepatocellular carcinoma? *Eur Radiol* 2006; **16**: 2454-2462 [PMID: 16710666 DOI: 10.1007/s00330-006-0264-8]

52 **Minami Y**, Kudo M. Review of dynamic contrast-enhanced ultrasound guidance in ablation therapy for hepatocellular carcinoma. *World J Gastroenterol* 2011; **17**: 4952-4959 [PMID: 22174544 DOI: 10.3748/wjg.v17.i45.4952]

53 **Inoue T**, Kudo M, Hatanaka K, Arizumi T, Takita M, Kitai S, Yada N, Hagiwara S, Minami Y, Sakurai T, Ueshima K, Nishida N. Usefulness of contrast-enhanced ultrasonography to evaluate the post-treatment responses of radiofrequency ablation for hepatocellular carcinoma: comparison with dynamic CT. *Oncology* 2013; **84** Suppl 1: 51-57 [PMID: 23428859 DOI: 10.1159/000345890]

54 **Salvatore V**, Bolondi L. Clinical Impact of Ultrasound-Related Techniques on the Diagnosis of Focal Liver Lesions. *Liver Cancer* 2012; **1**: 238-246 [PMID: 24159588 DOI: 10.1159/000343838]

55 **Masuzaki R**, Shiina S, Tateishi R, Yoshida H, Goto E, Sugioka Y, Kondo Y, Goto T, Ikeda H, Omata M, Koike K. Utility of contrast-enhanced ultrasonography with Sonazoid in radiofrequency ablation for hepatocellular carcinoma. *J Gastroenterol Hepatol* 2011; **26**: 759-764 [PMID: 21054516 DOI: 10.1111/j.1440-1746.2010.06559.x]

56 **Kim CK**, Choi D, Lim HK, Kim SH, Lee WJ, Kim MJ, Lee JY, Jeon YH, Lee J, Lee SJ, Lim JH. Therapeutic response assessment of percutaneous radiofrequency ablation for hepatocellular carcinoma: utility of contrast-enhanced agent detection imaging. *Eur J Radiol* 2005; **56**: 66-73 [PMID: 15913940 DOI: 10.1016/j.ejrad.2005.03.023]

57 **Wen YL**, Kudo M, Zheng RQ, Minami Y, Chung H, Suetomi Y, Onda H, Kitano M, Kawasaki T, Maekawa K. Radiofrequency ablation of hepatocellular carcinoma: therapeutic response using contrast-enhanced coded phase-inversion harmonic sonography. *AJR Am J Roentgenol* 2003; **181**: 57-63 [PMID: 12818830 DOI: 10.2214/ajr.181.1.1810057]

58 **Zhou P**, Kudo M, Minami Y, Chung H, Inoue T, Fukunaga T, Maekawa K. What is the best time to evaluate treatment response after radiofrequency ablation of hepatocellular carcinoma using contrast-enhanced sonography? *Oncology* 2007; **72** Suppl 1: 92-97 [PMID: 18087188 DOI: 10.1159/000111713]

59 **Kudo M**. New sonographic techniques for the diagnosis and treatment of hepatocellular carcinoma. *Hepatol Res* 2007; **37** Suppl 2: S193-S199 [PMID: 17877482 DOI: 10.1111/j.1872-034X.2007.00184.x]

60 **Kudo M**, Hatanaka K, Maekawa K. Newly developed novel ultrasound technique, defect reperfusion ultrasound imaging, using sonazoid in the management of hepatocellular carcinoma. *Oncology* 2010; **78** Suppl 1: 40-45 [PMID: 20616583 DOI: 10.1159/000315229]

61 **Kudo M**, Hatanaka K, Kumada T, Toyoda H, Tada T. Double-contrast ultrasound: a novel surveillance tool for hepatocellular carcinoma. *Am J Gastroenterol* 2011; **106**: 368-370 [PMID: 21301463 DOI: 10.1038/ajg.2010.432]

62 **Khankan AA**, Murakami T, Onishi H, Matsushita M, Iannaccone R, Aoki Y, Tono T, Kim T, Hori M, Osuga K, Passariello R, Nakamura H. Hepatocellular carcinoma treated with radio frequency ablation: an early evaluation with magnetic resonance imaging. *J Magn Reson Imaging* 2008; **27**: 546-551 [PMID: 18183580 DOI: 10.1002/jmri.21050]

63 **Campos JT**, Sirlin CB, Choi JY. Focal hepatic lesions in Gd-EOB-DTPA enhanced MRI: the atlas. *Insights Imaging* 2012; **3**: 451-474 [PMID: 22700119 DOI: 10.1007/s13244-012-0179-7]

64 **Yoon JH**, Lee EJ, Cha SS, Han SS, Choi SJ, Juhn JR, Kim MH, Lee YJ, Park SJ. Comparison of gadoxetic acid-enhanced MR imaging versus four-phase multi-detector row computed tomography in assessing tumor regression after radiofrequency ablation in subjects with hepatocellular carcinomas. *J Vasc Interv Radiol* 2010; **21**: 348-356 [PMID: 20116285 DOI: 10.1016/j.jvir.2009.11.014]

65 **Motosugi U**, Ichikawa T, Sou H, Sano K, Tominaga L, Muhi A, Araki T. Distinguishing hypervascular pseudolesions of the liver from hypervascular hepatocellular carcinomas with gadoxetic acid-enhanced MR imaging. *Radiology* 2010; **256**: 151-158 [PMID: 20574092 DOI: 10.1148/radiol.10091885]

66 **Watanabe H**, Kanematsu M, Goshima S, Yoshida M, Kawada H, Kondo H, Moriyama N. Is gadoxetate disodium-enhanced MRI useful for detecting local recurrence of hepatocellular carcinoma after radiofrequency ablation therapy? *AJR Am J Roentgenol* 2012; **198**: 589-595 [PMID: 22357997 DOI: 10.2214/AJR.11.6844]

67 **Koda M**, Tokunaga S, Miyoshi K, Kishina M, Fujise Y, Kato J, Matono T, Murawaki Y, Kakite S, Yamashita E. Ablative margin states by magnetic resonance imaging with ferucarbotran in radiofrequency ablation for hepatocellular carcinoma can predict local tumor progression. *J Gastroenterol* 2013; **48**: 1283-1292 [PMID: 23338488 DOI: 10.1007/s00535-012-0747-0]

P- Reviewers: Beierle EA, Nagai H, Tanaka K
S- Editor: Wen LL **L- Editor**: A **E- Editor**: Liu XM

百世登
Baishideng®

Published by **Baishideng Publishing Group Co., Limited**
Flat C, 23/F., Lucky Plaza,
315-321 Lockhart Road, Wan Chai, Hong Kong, China
Fax: +852-65557188
Telephone: +852-31779906
E-mail: bpgoffice@wjgnet.com
http://www.wjgnet.com

ISSN 1007-9327
15>

J Gastroenterol (2014) 49:492–501
DOI 10.1007/s00535-013-0785-2

ORIGINAL ARTICLE—LIVER, PANCREAS, AND BILIARY TRACT

Relevance of the Core 70 and IL-28B polymorphism and response-guided therapy of peginterferon alfa-2a ± ribavirin for chronic hepatitis C of Genotype 1b: a multicenter randomized trial, ReGIT-J study

Shuhei Nishiguchi · Hirayuki Enomoto · Nobuhiro Aizawa · Hiroki Nishikawa · Yukio Osaki · Yasuhiro Tsuda · Kazuhide Higuchi · Kazuichi Okazaki · Toshihito Seki · Soo Ryang Kim · Yasushi Hongo · Hisato Jyomura · Naoshi Nishida · Masatoshi Kudo

Received: 20 January 2013 / Accepted: 19 February 2013 / Published online: 30 March 2013

Abstract
Background We conducted a multicenter randomized clinical trial to determine the optimal treatment strategy against chronic hepatitis C virus (HCV) with genotype 1b and a high viral load (G1b/high).
Methods The study subjects included 153 patients with G1b/high. Patients were initially treated with PEG-IFNα-2a alone and then randomly assigned to receive different treatment regimens. Ribavirin (RBV) was administered to all patients with HCV RNA at week 4. Patients negative for HCV RNA at week 4 were randomly assigned to receive PEG-IFNα-2a (group A) or PEG-IFNα-2a/RBV (group B). Patients who showed HCV RNA at week 4 but were negative at week 12 were randomly assigned to receive weekly PEG-IFNα-2a (group C) or biweekly therapy (group D). Patients who showed HCV RNA at week 12 but were negative at week 24 were randomly assigned to receive PEG-IFNα-2a/RBV (group E) or PEG-IFNα-2a/RBV/fluvastatin (group F).
Results Overall, the rate of sustained virological response (SVR) was 46 % (70/153). The total SVR rate in the group (A, D, and F) of response-guided therapy was significantly higher than that in the group (B, C, and E) of conventional therapy [70 % (38/54) versus 52 % (32/61), $p = 0.049$]. Although IL28-B polymorphism and Core 70 mutation were significantly associated with efficacy, patients with rapid virological response (RVR) and complete early virological response (cEVR) achieved high SVR rates regardless of their status of IL-28B polymorphism and Core 70 mutation.
Conclusion In addition to knowing the IL-28B polymorphism and Core 70 mutation status, understanding the likelihood of virological response during treatment is critical in determining the appropriate treatment strategy.

Keywords Chronic hepatitis C · IL-28B · Peginterferon alfa-2a · Ribavirin · Response-guided therapy

S. Nishiguchi (✉) · H. Enomoto · N. Aizawa
Division of Hepatobiliary and Pancreatic Disease, Department of Internal Medicine, Hyogo College of Medicine, 1-1 Mukogawa-cho, Nishinomiya, Hyogo 663-8501, Japan
e-mail: nishiguc@hyo-med.ac.jp

H. Nishikawa · Y. Osaki
Department of Gastroenterology and Hepatology, Osaka Red Cross Hospital, Osaka, Japan

Y. Tsuda · K. Higuchi
Second Department of Internal Medicine, Osaka Medical College, Osaka, Japan

K. Okazaki · T. Seki
Department of Gastroenterology and Hepatology, Kansai Medical University, Osaka, Japan

S. R. Kim
Department of Internal Medicine, Kobe Asahi Hospital, Hyogo, Japan

Y. Hongo
Department of Gastroenterology and Hepatology, Hirakata City Hospital, Osaka, Japan

H. Jyomura
Wakakoukai Medical Clinic, Osaka, Japan

N. Nishida · M. Kudo
Department of Gastroenterology and Hepatology, Kinki University School of Medicine, Osaka, Japan

Introduction

The introduction of combined treatment with peginterferon (PEG-IFN) and ribavirin (RBV) has dramatically increased the rate of sustained virological response (SVR) in patients with genotype 1 high virus titer chronic hepatitis C (HCV RNA titer ≥ 5 Log IU/mL), a disease generally considered intractable, to approximately 50 % [1–4]. Currently, a protease inhibitor, telaprevir, can be used for the treatment of chronic hepatitis C, further increasing the SVR rate to approximately 70 % after initial treatment; however, adverse events such as severe anemia, dermatopathy, and renal dysfunction due to increased creatinine level have been reported [5, 6].

RBV is also associated with adverse events, such as anemia, dermatopathy and taste disturbance, and these events can be accentuated in elderly patients or patients with renal dysfunction or anemia. In Japan, there are many elderly patients with chronic hepatitis C and they often cannot tolerate a treatment combination involving RBV [7]. For such patients, PEG-IFN monotherapy could be a treatment option. It has been reported that patients with genotype 1 high virus titer chronic hepatitis C are more likely to achieve SVR if their HCV RNA becomes negative within 4 weeks after initiation of PEG-IFN monotherapy (Rapid Virological Response: RVR) [8].

Patients receiving the PEG-IFNα-2a/RBV combination therapy can also achieve an excellent SVR rate if their HCV RNA becomes negative within 12 weeks after initiation of treatment, whereas the rate is known to decrease with a delay in the timing of HCV RNA-negative conversion [3]. Based on these findings, we propose the use of "response-guided therapy", in which a treatment regimen is modified according to viral kinetics. For the treatment of genotype 1 chronic hepatitis C, proposed treatment strategies include shortening of treatment period in patients with RVR and extension of treatment period in patients with a delayed response to the initial treatment as judged at week 12 [9–17]. For the treatment of genotype 1 high virus titer chronic hepatitis C, shortening of the treatment period may not be recommended even if RVR is achieved because of a possible reduction in the SVR rate, whereas extension of the treatment period to 72 weeks has been reported to increase the SVR rate in patients showing a delayed response to the initial treatment [12, 14–18]. In addition, combined use of HMG-CoA reductase inhibitors and IFN has been shown to enhance the antiviral effects in a synergistic manner [19]. Addition of fluvastatin (FLV), an HMG-CoA reductase inhibitor reported to exhibit the highest antiproliferative activity against hepatitis C virus, to PEG-IFNα-2a/RBV combination therapy has improved the SVR rate [20–22].

Factors affecting the efficacy of PEG-IFN/RBV combination therapy can be divided into viral and host factors. The viral factors include virus titer, genotype, amino acid substitution at position 70 of the core protein (Core 70) and mutations in the interferon sensitivity-determining region (ISDR) in the HCV NS5A region [23–27]. The host factors include age, sex, the degree of liver fibrosis, and a single nucleotide polymorphism (SNP) close to the IL-28B gene [28–33].

We therefore conducted a randomized trial to explore the optimal treatment strategy for patients with genotype 1 high virus titer chronic hepatitis C by comparing several treatment regimens modified according to the concept of "response-guided therapy" in consideration of tolerability (PEG-IFNα-2a monotherapy, PEG-IFNα-2a weekly or biweekly/RBV combination, and PEG-IFNα-2a/RBV/FLV combination therapy). We also evaluated the relations of IL-28B polymorphism and Core 70 mutation to the rate of HCV-RNA-negative conversion and SVR.

Patients and methods

Patients

The study subjects included 153 patients with genotype 1b high virus titer chronic hepatitis C (HCV RNA ≥ 5 Log IU/mL) who visited 17 institutions from April 2007 to December 2010 and met the following inclusion criteria: laboratory data before study treatment of white blood cell count ≥ 3,000/mm^3, neutrophil count ≥ 1,500/mm^3, platelet count ≥ 90,000/mm^3, and hemoglobin ≥ 12 g/dL. Before the study treatments were carried out, all patients gave written informed consent after receiving a sufficient explanation of the therapy. All patients had genotype 1b chronic hepatitis C with a mean HCV RNA titer of 6.4 Log IU/mL. There were 63 male and 90 female patients with a mean age of 56.5 years. Sixty patients had received prior treatment with IFN, though it was ineffective in 30 of these patients (Table 1).

Treatment protocol

The study design is shown in Fig. 1. After a lead-in therapy with PEG-IFNα-2a 180 μg/week alone (for 4 weeks), RBV was added to the treatment for patients without HCV RNA-negative conversion (according to their weight; ≤ 60 kg, 600 mg/day; 60–80 kg, 800 mg/day; and >80 kg, 1,000 mg/day). Patients with negative HCV RNA (TaqMan < 1.2 Log IU/mL) at week 4 (rapid virological response, RVR) were randomly assigned to receive PEG-IFNα-2a alone (group A) or PEG-IFNα-2a/RBV combination (group B). Patients with negative HCV RNA

Table 1 Baseline characteristics of patients ($n = 153$)

Age (years)	56.5 ± 11.1
Gender (male/female)	63/90
HCV RNA (Log IU/mL)	6.4 ± 0.7
BMI (kg/m^2)	22.8 ± 3.3
ALT (IU/L)	60.5 ± 41.3
AST (IU/L)	51.7 ± 31.5
Previous IFN (no/yes)	93/60 (non-responder for 30)
Fibrosis (F0-2/F3-4)	72/32 (unknown for 49)
Activity (A0-1/A2-3)	49/56 (unknown for 48)
Core 70 (wild/mutant)	54/38 (unknown for 61)
IL-28B, rs8099917 (TT/non-TT)	43/26 (unknown for 84)

Values are mean ± standard deviation (SD)

BMI body mass index, *ALT* alanine aminotransferase, *AST* aspartate aminotransferase

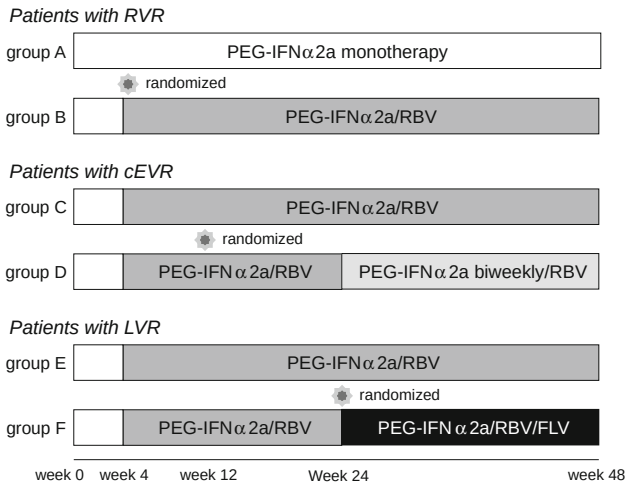

Fig. 1 Study design. After a lead-in therapy with PEG-IFNα-2a for 4 weeks, patients with negative HCV RNA at week 4 (RVR) were randomly assigned to receive PEG-IFNα-2a alone (group A) or PEG-IFNα-2a/RBV combination (group B). Patients with negative HCV RNA at week 12 (cEVR) were randomly assigned to receive weekly PEG-IFNα-2a/RBV combination (group C) or biweekly PEG-IFNα-2a/RBV combination (group D). Patients with negative HCV RNA at week 24 (LVR) were randomly assigned to receive PEG-IFNα-2a/RBV combination (group E) or PEG-IFNα-2a/RBV/fluvastatin (FLV) combination (group F)

at week 12 (complete early virological response, cEVR) were randomly assigned to receive weekly PEG-IFNα-2a/RBV combination (group C) or biweekly PEG-IFNα-2a/RBV combination (group D). Patients with negative HCV RNA at week 24 (late virological response, LVR) were randomly assigned to receive PEG-IFNα-2a/RBV combination (group E) or PEG-IFNα-2a/RBV/fluvastatin (FLV) combination (group F). For assignment, we used Microsoft Access to generate random numbers.

Cases with RVR: evaluation of necessity of RBV (PEG-IFNα-2a monotherapy versus PEG-IFNα-2a/RBV combination therapy)

Patients with negative HCV RNA at week 4 after the introduction of lead-in therapy with PEG-IFNα-2a alone (RVR) were randomly assigned to receive PEG-IFNα-2a alone (group A) or PEG-IFNα-2a/RBV combination (group B) to compare the efficacy and safety between the treatment groups and to evaluate the significance of addition of RBV in RVR cases.

Cases with cEVR: evaluation of dosage interval of PEG-IFNα-2a (weekly versus biweekly PEG-IFNα-2a in combination of RBV)

Patients positive for HCV RNA at week 4 but negative at week 12 (cEVR) were randomly assigned to receive weekly PEG-IFNα-2a/RBV combination (group C) or biweekly PEG-IFNα-2a/RBV combination (group D) after week 24, to compare the efficacy and safety between the treatment groups and to evaluate the dosage interval of PEG-IFNα-2a.

Cases with LVR: evaluation of clinical significance of addition of fluvastatin (PEG-IFNα-2a/RBV combination therapy versus PEG-IFNα-2a/RBV/FLV combination therapy)

Patients with positive HCV RNA at week 4 and 12 but negative HCV RNA at week 24 (LVR) were randomly assigned to a treatment group of PEG-IFNα-2a/RBV (group E) or PEG-IFNα-2a/RBV/FLV (group F) to compare the efficacy and safety between the treatment groups and to evaluate the significance of adding FLV. The dosage of FLV was set to 20 mg/day.

The primary efficacy endpoint was SVR. We also investigated correlations of IL-28B polymorphism (rs8099917) and Core 70 mutation with the rate of HCV RNA-negative conversion and SVR. The IL-28B polymorphism and Core 70 mutation were measured only in patients who wished to have this done. The genetic testing (IL-28B) was performed only in patients who gave written informed consent after obtaining the approval from the ethical committee. This study was a multicenter trial, and the numbers of patients with available HCV-RNA data were different for the week-4, -12, and -24 responses, because not all of the participating institutions completed all of these time points. Therefore, the numbers of patients with regard to IL28B and Core 70 mutation did not completely match at each time point.

If a decrease in the neutrophil count, platelet count, or Hb level reached a critical level or other adverse events

occurred, dose reduction or discontinuation of PEG-IFNα-2a or RBV was performed.

Statistical analysis

All statistical analyses were done using JMP version 9 (SAS). We used the *t* test, Chi-square test, and Fisher's exact test for univariate analysis. To identify factors affecting the SVR rate, we used the logistic regression test. A *p* value of less than 0.05 was considered statistically significant.

Results

Flowchart of the study

A flowchart of the study is shown in Fig. 2. PEG-IFNα-2a monotherapy was initiated in 153 patients, out of which 15 patients necessitated treatment discontinuation due to the patient's hope of recovery or adverse events. The timing of treatment discontinuation was within 4 weeks in three patients, between 5 and 12 weeks in nine patients, and between 13 and 24 weeks in three patients. RVR, cEVR, and LVR were achieved in 18, 70, and 27 patients, respectively, and these 115 patients were randomly assigned to treatment groups according to the response-guided therapy. However, 23 patients remained positive for HCV RNA (non-virological response, NVR) at week 24 and were finally judged as non-SVR.

Of 18 patients with RVR, 10 were assigned to group A (PEG-IFNα-2a monotherapy) and eight to group B (PEG-IFNα-2a/RBV combination); of 70 patients with cEVR, 39 were assigned to group C (weekly PEG-IFNα-2/RBV combination) and 31 to group D (biweekly PEG-IFNα-2/RBV combination); and of 27 patients with LVR, 14 were assigned to group E (PEG-IFNα-2a/RBV combination) and 13 to group F (PEG-IFNα-2a/RBV/FLV combination).

PEG-IFNα-2a monotherapy versus PEG-IFNα-2a/RBV combination therapy in cases with RVR (group A versus group B)

The SVR rate in 18 patients with negative HCV RNA at week 4 after initiation of PEG-IFNα-2a monotherapy (RVR) was 100 % (10/10) in group A (PEG-IFNα-2a monotherapy) and 87.5 % (7/8) in group B (PEG-IFNα-2a/RBV combination), showing no significant difference between the two groups ($p = 0.444$). The rate of treatment discontinuation was 0 % (0/10) in group A. However, treatment discontinuation was required in one patient (12.5 %) in group B due to hemolytic anemia caused by RBV, resulting in non-SVR. Although the rate of RVR by PEG-IFNα-2a monotherapy was only 12 % (18/153), once

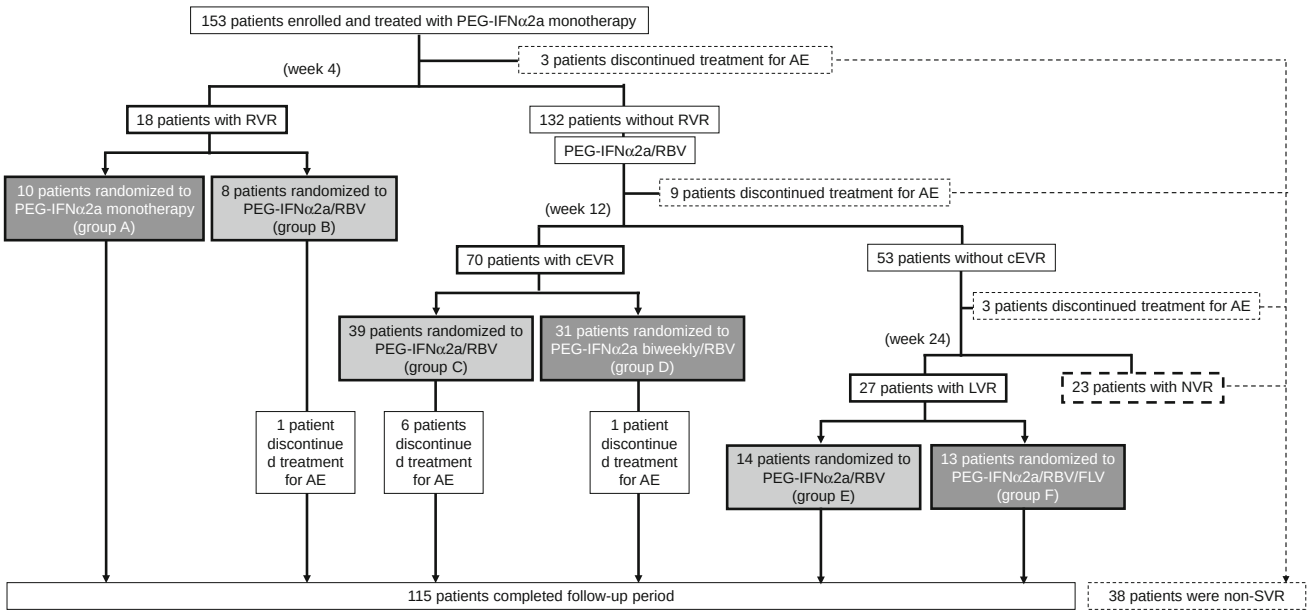

Fig. 2 Flowchart of the study. PEG-IFNα-2a monotherapy was initiated in 153 patients, of whom 15 patients necessitated treatment discontinuation. A total of 115 patients with RVR, cEVR, or LVR were randomly assigned to treatment groups, while 23 patients remained positive for HCV RNA (non-virological response, NVR) at week 24 and were finally judged as non-SVR. Of 18 patients with RVR, 10 were assigned to group A (PEG-IFNα-2a monotherapy) and eight to group B (PEG-IFNα-2a/RBV combination); of 70 patients with cEVR, 39 were assigned to group C (weekly PEG-IFNα-2/RBV combination) and 31 to group D (biweekly PEG-IFNα-2/RBV combination); and of 27 patients with LVR, 14 were assigned to group E (PEG-IFNα-2a/RBV combination) and 13 to group F (PEG-IFNα-2a/RBV/FLV combination)

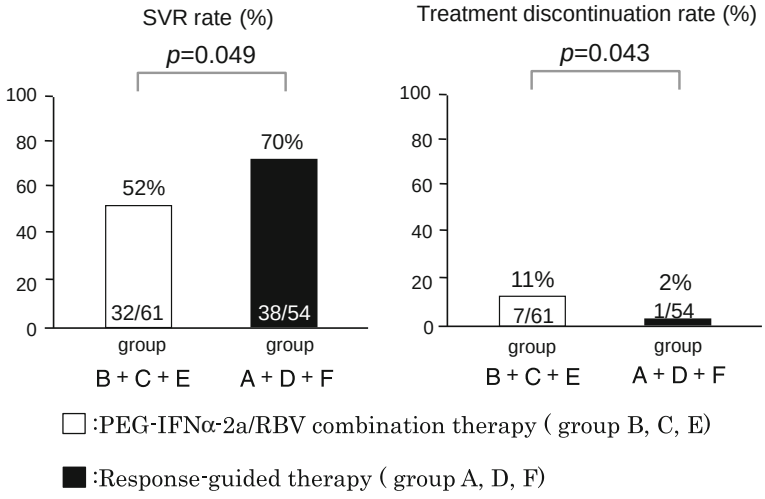

Fig. 3 The SVR and treatment discontinuation rate in the group (A + D + F) of treatment regimens modified according to response-guided therapy and in the group (B + C + E) of PEG-IFNα-2a/RBV combination therapy

RVR is achieved, PEG-IFNα-2a monotherapy without addition of RBV can induce SVR at a high rate with a high tolerability.

Weekly PEG-IFNα-2/RBV combination versus biweekly PEG-IFNα-2/RBV combination therapy in patients with cEVR (group C versus group D)

The SVR rate in 70 patients with cEVR was 54 % (21/39) in group C (weekly PEG-IFNα-2/RBV combination) and 65 % (20/31) in group D (biweekly PEG-IFNα-2/RBV combination). Adverse events leading to treatment discontinuation occurred in six patients (15 %) in group C (a decrease in Hb level, chest pain, fatigue, dizziness, a sense of feeling bad, and a suspicion of HCC) but in only one patient (3 %) in group D (depression), suggesting that the rate of treatment discontinuation tended to be higher in group C than in group D ($p = 0.123$). The difference in the SVR rates between groups C and D may reflect the difference in the rate of treatment discontinuation between the groups.

PEG-IFNα-2a/RBV combination versus PEG-IFNα-2a/RBV/FLV combination therapy in patients with LVR (group E versus group F)

The SVR rate in 27 patients with LVR was 29 % (4/14) in group E (PEG-IFNα-2a/RBV combination therapy) and 62 % (7/13) in group F (PEG-IFNα-2a/RBV/FLV combination therapy), suggesting that the rate tended to be higher in group F than in group E ($p = 0.085$). Thus, addition of an HMG-CoA inhibitor, FLV, increased the SVR rate even in patients with LVR showing delayed negative conversion of HCV RNA. There were no adverse events leading to treatment discontinuation in both groups, and FLV did not augment the adverse events in group F.

Group with PEG-IFNα-2a/RBV combination therapy versus group with response-guided therapy (groups B + C + E versus groups A + D + F)

We then divided all of these groups into two groups according to treatment regimens, a group (A + D + F) in which treatment regimen was modified according to response-guided therapy and a group (B + C + E) of PEG-IFNα-2a/RBV combination therapy. The SVR rate in the response-guided therapy group was significantly higher than in the PEG-IFNα-2a/RBV combination therapy group [70 % (38/54) versus 52 % (32/61), $p = 0.049$].

The rate of treatment discontinuation due to adverse events was significantly lower in the response-guided therapy group than in the PEG-IFNα-2a/RBV combination therapy group [11 % (7/61) versus 2 % (1/54), $p = 0.043$] (Fig. 3).

Factors influencing negative conversion of HCV RNA at week 4, 12, and 24

Factors influencing negative conversion of HCV RNA at week 4 were analyzed in 18 patients with negative HCV RNA and 132 patients with positive HCV RNA. Factors identified as significantly different between the negative and positive groups were age and HCV RNA titer before study treatment, but IL-28B polymorphism and Core 70 mutation were not associated with negative conversion at this time point. Comparison between 88 negative and 53 positive HCV RNA patients at week 12 and that between 115 negative and 23 positive HCV RNA patients at week 24 identified IL-28B polymorphism and Core 70 mutation as factors, showing differences with a statistical significance (Table 2).

Table 2 Characteristics of HCV RNA-negative or positive patients at week 4, 12, and 24

At week 4	Negative ($n = 18$)	Positive ($n = 132$)	p value
Age (years)	49.5 ± 14.6	57.6 ± 10.3	0.003
HCV RNA (Log IU/mL)	6.0 ± 0.7	6.4 ± 0.7	0.009
At week 12	Negative ($n = 88$)	Positive ($n = 53$)	p value
Core 70 substitution (wild/mutant)	39/14	13/22	<0.001
IL-28B, rs8099917 (TT/non-TT)	31/8	10/18	<0.001
At week 24	Negative ($n = 115$)	Positive ($n = 23$)	p value
Core 70 substitution (wild/mutant)	48/23	4/11	0.003
IL-28B, rs8099917 (TT/non-TT)	38/14	3/10	0.003

Value are mean ± standard deviation (SD)

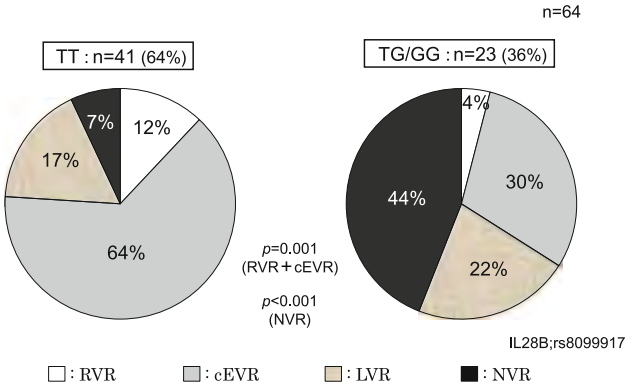

Fig. 4 Treatment response to PEG-IFNα-2a with or without RBV according to the IL-28B single nucleotide polymorphisms (TT versus TG/GG genotype)

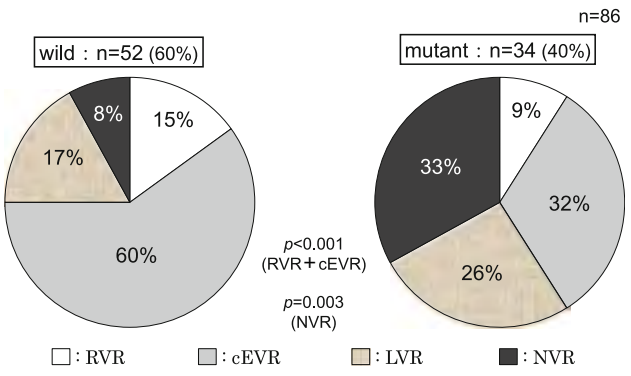

Fig. 5 Treatment response to PEG-IFNα-2a with or without RBV according to the Core 70 mutation (wild-type versus mutant Core 70)

We also investigated the correlation between IL-28B polymorphism and HCV RNA-negative conversion within 12 weeks (RVR + cEVR) in 64 patients in whom IL-28B polymorphism was examined. Negative HCV RNA was achieved within 12 weeks in 76 % of 41 patients with IL-28B TT genotype (major) and in 34 % of 23 patients with IL-28B TG or GG genotype (minor), showing a significant difference between them ($p = 0.001$). Especially in cases with NVR, negative HCV RNA was achieved in 7 % of patients with IL-28B major genotype and in 44 % of patients with IL-28B minor genotype ($p < 0.001$), suggesting that IL-28B polymorphism is strongly associated with treatment response (Fig. 4). Similarly, in 86 patients with determined Core 70 mutation status, negative HCV RNA was achieved within 12 weeks in 75 % of 52 patients with wild-type Core 70 and 41 % of 34 patients with mutant Core 70, showing a significant difference between them ($p < 0.001$). In patients with NVR, the rate of becoming HCV RNA-negative within 12 weeks was 8 % in patients with wild-type Core 70 and 33 % in those with mutant Core 70 ($p = 0.003$) (Fig. 5).

The SVR rates at different time points of HCV RNA-negative conversion by IL-28B polymorphism and Core 70 mutation

The SVR rates were investigated in patients with different time points of HCV RNA-negative conversion (RVR in six patients, cEVR in 33, LVR in 13, and NVR in 13) according to the IL-28B genotypes. The SVR rate was 100 % (5/5) in patients with RVR, 65 % (17/26) in patients with cEVR, 57 % (4/7) in patients with LVR, and 0 % (0/3) in patients with NVR with IL-28B major genotype; whereas the rate was 100 % (1/1) in patients with RVR, 43 % (3/7) in patients with cEVR, 83 % (5/6) in patients with LVR, and 0 % (0/10) in patients with NVR with IL-28B minor genotype. Similarly, the SVR rates were investigated in patients with different time points of HCV RNA-negative conversion (RVR in 11 patients, cEVR in 42, LVR in 18, and NVR in 15) according to the Core 70

Table 3 Characteristics of sustained virological response (SVR) and non-SVR patients

	SVR ($n = 70$)	Non-SVR ($n = 83$)	p value
Age (years)	53.1 ± 12.7	59.4 ± 8.7	<0.001
Gender (male/female)	29/41	34/49	0.954
HCV RNA (Log IU/mL)	6.4 ± 0.7	6.4 ± 0.7	0.782
BMI (kg/m^2)	22.7 ± 3.9	22.9 ± 2.8	0.815
Previous IFN (no/yes)	49/21	44/39	0.032
Fibrosis (F0-2/F3-4)	41/9	31/23	0.007
Activity (A0-1/A2-3)	24/27	25/29	0.938
NS5A mutation, *n* (0-1/2-)	31/10	47/3	0.013
Core 70 substitution (wild/mutant)	30/11	24/27	0.012
IL-28B, rs8099917 (TT/non-TT)	26/9	17/18	0.027
HCV RNA-negative at week 12 (yes/no)	58/12	30/41	<0.001
Treatment group (B,C,E/A,D,F)	32/38	29/16	0.049

Values are mean ± standard deviation (SD)

BMI body mass index

Table 4 Associated factors with sustained virological response (SVR) by multivariate logistic regression analysis

Factor	Odds ratio	95 % CI	p value
Age (per 1 year)	0.94	0.89–0.98	0.005
Previous IFN (no/yes)	1.62	0.62–4.27	0.323
Fibrosis (F0-2/F3-4)	3.38	1.15–10.8	0.026
NS5A mutation, *n* (2-/0-1)	7.18	1.32–61.0	0.021
Core 70 substitution (wild/mutant)	2.49	1.51–8.28	0.044
IL-28B, rs8099917 (TT/non-TT)	1.85	0.85-8.61	0.563
HCV RNA-negative at week 12 (yes/no)	7.89	2.92–24.0	<0.001

mutation status. The SVR rate was 100 % (RVR), 58 % (cEVR), 44 % (LVR), and 0 % (NVR) in patients with wild-type Core 70; whereas the rate was 67 % (RVR), 55 % (cEVR), 33 % (LVR), and 0 % (NVR) in patients with mutant Core 70. Thus, when the SVR rates were investigated according to the different time points of HCV RNA-negative conversion, there was no association of IL-28B polymorphism or Core 70 mutation with the SVR rates.

Factors affecting the SVR rate

An univariate analysis in 70 SVR patients and 83 non-SVR patients identified age, previous IFN treatment, fibrosis, NS5A mutation, Core 70 mutation, EVR, IL-28B, and treatment group as factors affecting the SVR rate (Table 3). In this analysis, we examined 83 non-SVR patients: 45 non-SVR patients are presented in Fig. 3, and 38 non-SVR patients (23 patients with NVR and 15 patients who discontinued the Peg-IFN-RBV treatment prior to the enrollment of the randomized trial) are presented in Fig. 2. Multivariate analysis using a logistic regression analysis revealed age (younger), fibrosis (mild), NS5A mutation (two or more mutations), Core 70 status (wild-type), and EVR (RVR + cEVR), to be independent factors affecting the SVR rate, and among them EVR was the most significant factor (odds ratio, 7.89; $p < 0.001$) (Table 4). Therefore, even in patients considered intractable based on the IL-28B genotype or Core 70 mutation status, SVR is expected to be achieved once RVR or cEVR is reached during treatment.

Discussion

The introduction of combined treatment with PEG-IFN and RBV has increased the SVR rate to approximately 40–50 % even in intractable cases with genotype 1b high virus titer chronic hepatitis C after a standard treatment course of 48 weeks [1–4]. In an attempt to further improve the SVR rate, we propose a concept of "response-guided therapy", in which the treatment regimen (such as an extension of a treatment period) is determined according to the viral response to the initial treatment [7–15]. In cases with positive HCV RNA at week 4 or 12, extension of the treatment period from 48 to 72 weeks has been reported to prevent the recurrence and improve the SVR rate [12–14]. Recently, Miyase et al. [34] showed that PEG-IFNα-2a/ribavirin combination therapy resulted in better SVR rates than PEG-IFNα-2b/ribavirin combination therapy in female, older or low-weight patients. In addition, Minami et al. [35] reported that the rate of severe adverse events was not negligible in PEG-IFN/ribavirin combination therapy, and the rate was affected by treatment regimens. Therefore, it is important to establish a treatment regimen of PEG-IFN/RBV combination therapy that has a high efficacy with minimal adverse events. We herein investigated the treatment regimens based on the concept of response-guided therapy to minimize the rate of treatment discontinuation, without changing the treatment period, in consideration of aged patients in Japan.

Factors influencing SVR have been evaluated in many studies that reported IL-28B (a host factor) and Core 70 mutation (a viral factor) as factors predicting the treatment outcome [23, 24, 36–38]. Our present study also demonstrate that the SVR rate was lower in patients with IL-28B minor genotype and those with mutant Core 70, suggesting that IL-28B polymorphism and Core 70 mutation represent factors largely influencing the negative conversion of HCV RNA. Regarding the correlation between treatment response and SVR, Thompson et al. [38] reported that RVR and cEVR rates were lower in patients with the IL-28B minor genotype than in those with the major genotype but the SVR rate was not affected by the IL-28B genotype in patients with RVR or cEVR. In recent studies published after recognition of IL-28B polymorphism, virological response at week 4 and 12 was highly associated with SVR [39, 40]. In our present results, if RVR or EVR is achieved, a high SVR rate can be obtained regardless of the IL-28B polymorphism or Core 70 mutation status.

If RVR is achieved, PEG-IFNα-2a monotherapy exhibits a treatment effect equivalent to that of PEG-IFNα-2a/RBV combination therapy. Conversely, one patient receiving PEG-IFNα-2a/RBV combination therapy developed anemia caused by RBV, resulting in treatment discontinuation and non-SVR. In a phase III clinical trial in Japanese patients, the SVR rate in patients with RVR was 100 % (14/14) in control patients receiving PEG-IFNα-2a monotherapy but was 78 % (18/23) in those receiving PEG-IFNα-2a/RBV combination therapy [41]. Therefore, in terms of preventing treatment discontinuation due to adverse events of RBV, PEG-IFNα-2a monotherapy is recommended in cases with RVR.

In cases with cEVR, the SVR rate in patients who received biweekly PEG-IFNα-2/RBV combination therapy was comparable or even higher as compared to those who received weekly PEG-IFNα-2/RBV combination therapy. This means that biweekly PEG-IFNα-2a in a later treatment period did not reduce the antiviral effects in a subset of cases achieving a good antiviral effect (cEVR). This is partly because the half-life of PEG-IFNα2a is longer than that of PEG-IFNα2b [42–44], thus enabling the maintenance of antiviral effects. Therefore, this biweekly regimen appears possible only with PEG-IFNα2a. Regarding treatment discontinuation, the rate of treatment discontinuation was 3 % (1/31) in patients receiving biweekly PEG-IFNα-2 and 15 % (6/39) in those receiving weekly PEG-IFNα-2, suggesting that the reduced rate of adverse events and subsequent treatment discontinuation by biweekly administration may lead to the increased SVR rate.

Ikeda et al. [19] reported that one of the HMG-CoA reductase inhibitors, FLV, exhibits inhibitory effects on HCV RNA replication in a system of HCV RNA replication clone. In the clinical setting, Sezaki et al. and Rao and Pandya [20–22] reported that combined use of FLV from the treatment initiation period improved the SVR rate [21]. The HCV RNA is replicated using the lipid droplet in hepatocytes [45, 46], and HMG-CoA reductase inhibitors are reported to inhibit the proliferation of HCV RNA by suppressing the synthesis of mevalonic acid through geranylgeranylation [47].

We investigated whether the SVR rate is improved by the addition of FLV only in cases with LVR, because a high SVR rate is expected in patients showing rapid negative conversion of HCV RNA (such as RVR and cEVR cases) without the combined use of FLV. Our results showed that combined use of FLV yielded a higher SVR rate (62 %) as compared to the rate (29 %) obtained without the use of FLV, suggesting that the difference in the recurrence rate may reflect the difference in the SVR rate in patients negative for HCV RNA. Thus, because we used FLV in patients with LVR at high risk of recurrence, but not in those with RVR or cEVR at low risk of recurrence, the difference in anti-HCV activities by FLV was more pronounced. It has been reported that treatment with HMG-CoA reductase inhibitors does not increase the risk of severe hepatotoxicity in patients with chronic hepatitis C [48], which is consistent with our present results showing no adverse events associated with the addition of FLV.

In summary, the SVR rate was 52 % (32/61) in the group receiving PEG-IFNα-2a/RBV combination therapy and 70 % (38/54) in the group receiving modified treatment regimens according to response-guided therapy, showing a significant increase in the latter group. This result may be attributed to the difference in the rate of treatment discontinuation, which was significantly lower in the response-guided therapy group [2 % (1/54)] than in the PEG-IFNα-2a/RBV combination group [11 % (7/61)]. In addition, anti-HCV effects of FLV in patients with LVR at high risk of recurrence may contribute to the improved SVR in the response-guided therapy group. Our results demonstrated the safety and efficacy of PEG-IFNα-2a monotherapy in patients with RVR, biweekly PEG-IFNα-2a/RBV combination therapy in those with cEVR, and PEG-IFNα-2a/RBV/FLV combination therapy in those with LVR.

In conclusion, for the treatment of genotype 1b high virus titer chronic hepatitis C, the selection of an optimal response-guided therapy option, taking into consideration the viral response to initial treatment, the IL-28B polymorphism and Core 70 mutation status, and the safety of individual patients, can improve the SVR rate.

Acknowledgments We thank Ms. R. Nakatani for her assistance with data collection. We also thank Ms. N. Kanazawa for her excellent lab work on IL28B SNPs and Core 70 substitution in this study.

Conflict of interest Shuhei Nishiguchi received financial support from Chugai pharmaceutical, MSD, Dainippon Sumitomo Pharma,

Ajinomoto Pharma, and Otsuka pharmaceutical. The remaining authors declare no conflict of interest.

References

1. Manns MP, McHutchison JG, Gordon SC, et al. Peginterferon alfa-2b plus ribavirin compared with interferon alfa-2b plus ribavirin for initial treatment of chronic hepatitis C: a randomized trial. Lancet. 2001;358:958–65.
2. Fried MW, Shiffman ML, Reddy KR, et al. Peginterferon alfa-2a plus ribavirin for chronic hepatitis C virus infection. N Engl J Med. 2002;347:975–82.
3. Kuboki M, Iino S, Okuno T, Omata M, et al. Peginterferon a-2a (40 KD) plus ribavirin for the treatment of chronic hepatitis C in Japanese patients. J Gastroenterol Hepatol. 2007;22:645–52.
4. Yamada G, Iino S, Okuno T, et al. Virological Response in patients with hepatitis C virus genotype 1b and a high viral load impact of peginterferon-α-2a plus ribavirin dose reductions and host-related factors. Clin Drug Invest. 2008;28(1):9–16.
5. Kumada H, Toyota J, Okanoue T, Chayama K, Tsubouchi H, Hayashi N. Telaprevir with peginterferon and ribavirin for treatment-naive patients chronically infected with HCV of genotype 1 in Japan. J Hepatol. 2012;56:78–84.
6. Hayashi N, Okanoue T, Tsubouchi H, Toyota J, Chayama K, Kumada H. Efficacy and safety of telaprevir, a new protease inhibitor, for difficult-to-treat patients with genotype 1 chronic hepatitis C. J Viral Hepatol. 2012;19:e134–42.
7. Imai Y, Tamura S, Tanaka H, et al. Reduced risk of hepatocellular carcinoma after interferon therapy in aged patients with chronic hepatitis C is limited to sustained virological responders. J Viral Hepatol. 2010;17:185–91.
8. Tanaka T, Shakado S, Morihara D et al. The prognostic factors of sustained virologic response among patients of chronic hepatitis C treated with peg-interferon alpha 2a monotherapy. Kanzo 2008;49:417–25.
9. Berg T, von Wagner M, Nasser S, et al. Extended treatment duration for hepatitis C virus type 1: comparing 48 versus 72 weeks of peginterferon-alfa-2a plus ribavirin. Gastroenterology. 2006;130:1086–97.
10. Sanchez-Tapias JM, Diago M, Escartin P, et al. Peginterferon-alfa2a plus ribavirin for 48 versus 72 weeks in patients with detectable hepatitis C virus RNA at week 4 of treatment. Gastroenterology. 2006;131:451–60.
11. Ferenci P, Laferl H, Scherzer TM, et al. Peginterferon alfa-2a/ribavirin for 48 or 72 weeks in hepatitis C genotypes 1 and 4 patients with slow virologic response. Gastroenterology. 2010; 138:503–12.
12. Pearlman BL, Ehleben C, Saifee S. Treatment extension to 72 weeks of peginterferon and ribavirin in hepatitis c genotype 1-infected slow responders. Hepatology. 2007;46:1688–94.
13. Nabci C Teoh et al. Individualisation of antiviral therapy for chronic hepatitis C. J Gastroenterol Hepatol. 2010; 25:1206–16.
14. Reddy KR, Lin F, Zoulim F. Response-guided and -unguided treatment of chronic hepatitis C. Liver Int. 2012;32:64–73.
15. Di Martino V, et al. Response-guided peg-interferon plus ribavirin treatment duration in chronic hepatitis C: meta-analyses of randomized, controlled trials and implications for the future. Hepatology. 2011;54:789–800.
16. Zeuzem S, et al. Pegylated-interferon plus ribavirin therapy in the treatment of CHC: individualization of treatment duration according to on-treatment virologic response. Curr Med Res Opin. 2010;26:1733–43.
17. Franik H, et al. Meta-analysis shows extended therapy improves response of patients with chronic hepatitis C virus genotype 1 infection. Clin Gastroenterol Hepatol. 2010;8:884–90.
18. Yu ML, Dai CY, Huang JF, et al. Rapid virological response and treatment duration for chronic hepatitis C genotype 1 patients: a randomized trial. Hepatology. 2008;47:1884–93.
19. Ikeda M, Abe K, Yamada M, et al. Different anti HCV profiles of statins and their potential for combination therapy with interferon. Hepatology. 2006;44:117–25.
20. Sezaki H,Suzuki F,Akuta N et al. Influence of HMG-CoA reductase inhibitor to virological response of peginterferon/ribavirin combination therapy in chronic hepatitis C. Kanzo 2008: 49;22–4.
21. Sezaki H, Suzuki F, Akuta N, et al. An open pilot study exploring the efficacy of fluvastatin, pegylated interferon and ribavirin in patients with hepatitis C virus genotype 1b in high viral loads. Intervirology. 2009;52:43–8.
22. Rao GA, Pandya PK. Statin therapy improves sustained virologic response among diabetic patients with chronic hepatitis C. Gastroenterology. 2011;140:144–52.
23. Akuta N, Suzuki F, Kawamura Y, et al. Predictive factors of early and sustained responses to peginterferon plus ribavirin combination therapy in Japanese patients infected with hepatitis C virus genotype 1b: amino acid substitutions in the core region and low-density lipoprotein cholesterol levels. J Hepatol. 2007;46:403–10.
24. Akuta N, Suzuki F, Sezaki H, et al. Association of amino acid substitution pattern in core protein of hepatitis C virus genotype 1b high viral load and non-virological response to interferon-ribavirin combination therapy. Intervirology. 2005;48:372–80.
25. Enomoto N, Sakuma I, Asahina Y, et al. Comparison of full-length sequences of interferon-sensitive and resistant hepatitis C virus 1b. Sensitivity to interferon is conferred by amino acid substitutions in the NS5A region. J Clin Invest. 1995;96:224–30.
26. Enomoto N, Sakuma I, Asahina Y, et al. Mutations in the non-structural protein 5A gene and response to interferon in patients with chronic hepatitis C virus 1b infection. N Engl J Med. 1996;334:77–81.
27. Shirakawa H, Matsumoto A, Joshita S, et al. Pretreatment prediction of virological response to peginterferon plus ribavirin therapy in chronic hepatitis C patients using viral and host factors. Hepatology. 2008;48:1753–60.
28. Oze T, Hiramatsu N, Yakushijin T, et al. Indications and limitations for aged patients with chronic hepatitis C in pegylated interferon alfa-2b plus ribavirin combination therapy. J Hepatol. 2011;54:604–11.
29. Kogure T, Ueno Y, Fukushima K, et al. Pegylated interferon plus ribavirin for genotype Ib chronic hepatitis C in Japan. World J Gastroenterol. 2008;14:7225–30.
30. Sezaki H, Suzuki F, Kawamura Y, et al. Poor response to pegylated interferon and ribavirin in older women infected with hepatitis C virus of genotype 1b in high viral loads. Dig Dis Sci. 2009;54:1317–24.
31. Ge D, Fellay J, Thompson AJ, et al. Genetic variation in IL28B predicts hepatitis C treatment-induced viral clearance. Nature. 2009;461:399–401.
32. Suppiah V, Moldovan M, Ahlenstiel G, et al. IL28B is associated with response to chronic hepatitis C interferon alpha and ribavirin therapy. Nat Genet. 2009;41:1100–4.
33. Tanaka Y, Nishida N, Sugiyama M, et al. Genome-wide association of IL28B with response to pegylated interferon alpha and ribavirin therapy for chronic hepatitis C. Nat Genet. 2009;41: 1105–9.

34. Miyase S, Haraoka K, Ouchida Y, et al. Randomized trial of peginterferon α-2a plus ribavirin versus peginterferon α-2b plus ribavirin for chronic hepatitis C in Japanese patients. J Gastroenterol. 2012;47:1014–21.
35. Minami T, Kishikawa T, Sato M et al. Meta-analysis: mortality and serious adverse events of peginterferon plus ribavirin therapy for chronic hepatitis C. J Gastroenterol. 2012. [Epub ahead of print].
36. Kobayashi M, Suzuki F, Akuta N et al. Relationship between SNPs in the *IL28B* region and amino acid substitutions in HCV core region in Japanese patients with chronic hepatitis C. Kanzo 2010;51:322–3.
37. Kurosaki M, Tanaka Y, Nishida N, et al. Pre-treatment prediction of response to pegylated -interferon plus ribavirin for chronic hepatitis C using genetic polymorphism in IL28B and viral factors. J Hepatol. 2011;54:439–48.
38. Thompson AJ, Muir AJ, Sulkowski MS, et al. Interleukin-28b polymorphism improves viral kinetics and is the strongest pretreatment predictor of sustained virologic response in genotype 1 hepatitis C virus. Gastroenterology. 2010;139:120–9.
39. Toyoda H, Kumada T, Tada T, et al. Predictive value of early viral dynamics during peginterferon and ribavirin combination therapy based on genetic polymorphisms near the IL28B gene in patients infected with HCV genotype 1b. J Med Virol. 2012; 84:61–70.
40. Marcellin P, Reau N, Ferenci P, et al. Refined prediction of week 12 response and SVR based on week 4 response in HCV genotype 1 patients treated with peginterferon alfa-2a (40KD) and ribavirin. J Hepatol. 2012;56:1276–82.
41. Sakai T.[PEG-interferonα-2a/ribavirin therapy for chronic hepatitis type 1b.] Kan Tan Sui 2006; 52:75–84. (in Japanese).
42. Perry CM, Jarvis B. Peginterferon-alpha-2a (40 kD): a review of its use in the management of chronic hepatitis C. Drugs. 2001; 61(15):2263–88.
43. Glue P, Fang JW, Rouzier-Panis R, Raffanel C, Sabo R, Gupta SK, et al. Pegylated interferon-alpha2b: pharmacokinetics, pharmacodynamics, safety, and preliminary efficacy data. Hepatitis C Intervention Therapy Group. Clin Pharmacol Ther. 2000;68(5): 556–67.
44. Formann E, Jessner W, Bennett L, et al. Twice-weekly administration of peginterferon-α-2b improves viral kinetics in patients with chronic hepatitis C genotype 1. J Viral Hepat. 2003;10: 271–6.
45. Aizaki H, Lee KJ, Sung VM, et al. Characterization of the hepatitis C virus RNA replication complex associated with lipid rafts. Virology. 2004;324:450–61.
46. Miyanari Y, Atsuzawa K, Usuda N, et al. The lipid droplet is an important organelle for hepatitis C virus production. Nat Cell Biol. 2007;9:1089–97.
47. Goldstein JL, Brown MS. Regulation of the mevalonate pathway. Nature. 1990;343:425–30.
48. Khorashadi S, Hasson NK, Cheung RC. Incidence of statin hepatotoxicity in patients with hepatitis C. Clin Gastroenterol Hepatol. 2006;4:902–7.

The Gross Classification of Hepatocellular Carcinoma: Usefulness of Contrast-enhanced US

Kinuyo Hatanaka, MD, PhD,[1] Yasunori Minami, MD, PhD,[1] Masatoshi Kudo, MD, PhD,[1] Tatsuo Inoue, MD, PhD,[1] Hobyung Chung, MD, PhD,[1] Seiji Haji, MD, PhD[2]

[1] Department of Gastroenterology and Hepatology, Kinki University Faculty of Medicine, 377-2 Ohno-Higashi, Osaka-Sayama, Osaka 589–8511, Japan
[2] Department of Surgery, Kinki University Faculty of Medicine, 377-2 Ohno-Higashi, Osaka-Sayama, Osaka 589–8511, Japan

Received 17 February 2012; accepted 26 June 2013

ABSTRACT: *Background.* This study investigated the usefulness of postvascular images of contrast-enhanced ultrasonography (CE-US) in the gross classification of hepatocellular carcinoma (HCC) in comparison with contrast-enhanced CT (CE-CT) findings.

Methods. This is a prospective study with consecutive HCC patients who had both CE-US and CE-CT prior to surgical resection. Fifty-one patients (32 men, 19 women; mean age, 68.9 years) with 61 HCCs were enrolled. The maximal diameters of all tumors ranged from 1.0 to 5.0 cm (mean ± SD, 2.5 cm ± 1.1). Weighted kappa statistics were used to assess the agreement of the sonographic or CT findings versus the results of macroscopic configurations.

Results. Thirty-nine tumors were macroscopically diagnosed as simple nodule type; 19 tumors were macroscopically diagnosed as simple nodular type with extranodular growth, and 3 were macroscopically diagnosed as confluent multinodular type from the resected specimen. The diagnostic accuracy was 86.9% (53/61) for CE-US and 65.6% (40/61) for CE-CT. The differences in accuracy between CE-US and CE-CT were statistically significant (McNemar; $p = 0.007$). Agreement analysis between gross classification using CE-US and final macroscopic results gave a kappa value of 0.74 (95% CI: 0.65–0.82), which was considered a good agreement. On the other hand, kappa coefficient value was 0.38 (95% CI: 0.28–0.48) between gross classification using CE-CT and final macroscopic results.

Conclusions. CE-US is a more reliable tool than CE-CT to evaluate the gross type of HCC than CE-CT. Accurate gross classification using imaging is considered to be essential for the determination of the correct treatment strategy and the estimates of the patients' prognosis. © 2013 Wiley Periodicals, Inc. *J Clin Ultrasound* **42**:1–8, 2014; Published online in Wiley Online Library (wileyonlinelibrary.com). DOI: 10.1002/jcu.22080

Keywords: hepatocellular carcinoma; contrast-enhanced US

Based on an analysis of surgically resected hepatocellular carcinomas (HCCs), Kanai et al have proposed a gross classification in which Eggel's nodular type is subclassified into simple nodular type, simple nodular type with extranodular growth, and confluent multinodular type.[1,2] With the progress of nodular subclassification from simple nodular type to confluent multinodular type, HCC nodules were at risk to develop a higher rate of malignancy from moderate to poor differentiation on pathology. The macroscopic type of HCC has been reported to be a significant prognostic factor for HCC patients undergoing hepatectomy.[3,4] Therefore, accurate classification of the nodular type of HCC would change its management.

Gray-scale ultrasonography (US) is the most widely used modality for HCC screening and surveillance. However, HCC nodules often show unclear borders partly due to innumerable large regenerating nodules in the cirrhotic liver.[5] In recent years, contrast-enhanced US (CE-US) has been able to demonstrate tumor vascularity

Correspondence to: Y. Minami

with higher sensitivity and accuracy due to developments in US instruments and contrast agents.[6–8] Perfluorocarbon microbubbles (Sonazoid; Daiichi Sankyo, Tokyo, Japan), a second-generation US contrast agent, are phagocytosed by Kupffer cells unlike other second-generation contrast agents and accumulate in the liver parenchyma over time.[9] This contrast agent can provide a functional imaging with high contrast in the postvascular phase.[10–12] Thus, Kupffer imaging easily shows the tumor contours on CE-US using Sonazoid according to the shape of defects.[13–16] However, no study has investigated the value of the gross classification on CE-US in patients with HCC in comparison with other modalities. The aim of this study was to compare the gross classification of HCC on CE-US and contrast-enhanced CT (CE-CT) with the gold standard of pathologic findings.

TABLE 1
Characteristics of 51 Patients with 61 HCCs

Age (years)	68.9 ± 6.7 (52–79)
Male/female	32/19
Etiology (HBV/HCV/HBV + HCV/NBNC)	8/34/3/6
Child-Pugh classification (A/B/C)	46/5/0
Platelet count ($\times 10^4/\mu l$)	14.1 ± 7.5 (3.4–46.9)
ICG R^{15} (%)	18.1 ± 8.8 (5–54)
AFP (ng/ml)	741 (4–4,571)
AFP L_3 (%)	25.8 (0–83.7)
DCP (AU/ml)	741 (9–27333)
Tumor size (cm)	2.5 ± 1.1 (1.0–5.0)
Differentiation of HCC (%) (well/moderate/poor)	10/41/10
Fibrosis (F0–1/2–3/4)	13/9/30
Operative procedures	
Lobectomy	2
Segmentectomy	5
Anatomical subsegmentectomy	8
Nonanatomical minor hepatectomy	36

Abbreviations: DCP, des-r-carboxyprothrombin; HBV, hepatitis B virus; HCV, hepatitis C virus; NBNC, patients negative for both HBs antigen and HCV antibody; ICG R^{15}, indocyanine green retention rate at 15 minutes.

PATIENTS AND METHODS

Patients

The Ethics Committee of our institution approved the study protocol. Written consent was obtained from each patient or a family member at enrollment. This is a prospective study with 51 consecutive HCC patients who underwent surgical resection who had both CE-US and CE-CT prior to surgery. Between June 2007 and July 2010, 51 patients (32 men, 19 women; age range, 52–79 years; mean age ± SD, 68.9 years ± 6.7) with 61 HCCs underwent hepatic resection at Kinki University Faculty of Medicine (Table 1). The underlying liver diseases, diagnosed using a combination of serum biomarkers and pathologic findings, were as follows: HCV-related cirrhosis (n = 22), HCV-related chronic hepatitis (n = 12), HBV-related cirrhosis (n = 6), HBV-related chronic hepatitis (n = 2), HCV- and HBV-related chronic hepatitis (n = 3), cirrhosis of unknown causes (n = 3), and hepatitis of unknown causes (n = 3). The maximal diameters of all tumors ranged from 1.0 to 5.0 cm (mean ± SD, 2.5 cm ± 1.1). The surgical procedures applied were partial hepatectomy in 36 patients, sebsegmentectomy in 8 patients, segmentectomy in 5 patients, and lobectomy in 2 patients.

HCCs were diagnosed based on three-phase CE-CT findings such as hyperenhancement in the arterial phase and washout in the equilibrium phase in patients with chronic liver disease. Unresectable disease was defined as the presence of extrahepatic metastases; severe cirrhosis of the proposed liver remnant precluding resection; or extensive disease without the possibility of leaving a sufficient liver remnant precluding radical resection. Therefore, the number of lesions was not an absolute exclusion criterion for resection.

CE-US

Gray-scale sonograms and the coded phase-inversion images were obtained using a LOGIQ 7 scanner (GE Healthcare, Milwaukee, WI). The convex-arrayed transducer of LOGIQ 7 was used at a frequency of 4 or 6.5 MHz. The acoustic power of contrast harmonic US was set at the default setting with a mechanical index of 0.2; the dynamic range was fixed at 60–70 decibels. The focus point was just under the bottom of the lesion. The images were stored as a cine clip with GE exclusive raw-data format files in the LOGIQ 7 computer.

The US contrast agent was Sonazoid with a median diameter of the microbubbles of 2–3 μm. The anticipated clinical dose for the imaging of liver lesions is 0.01 ml encapsulated gas per kilogram of body weight, and this contrast agent was administered as a quick bolus and flushed with 10 ml saline at approximately 1 ml/s via a 22-gauge cannula placed in the antecubital vein.

Tumor enhancement was depicted in the vascular phase (from 10 seconds to 5–7 minutes after injection of the contrast agent), whereas parenchymal uptake of contrast agent was evaluated in the postvascular phase (from approximately

10 minutes after injection of the contrast agent). Two sonologists, one with 12 years of US imaging experience and the other with 15 years of US imaging experience who were blinded to the CT and pathologic findings, reviewed the arterial vascular images and the postvascular images known as Kupffer images.

CE-CT

A multidetector CT (LightSpeed VCT; GE Healthcare) was used for diagnosis. Triple-phase CE-CT scans were performed with a 5.0-mm slice thickness at 30, 60, and 180 seconds after initiating the injection of contrast media to obtain hepatic arterial, portal venous, and equilibrium phase images, respectively. A total of 100 ml of nonionic contrast material containing 300 mg of iodine per milliliter (Iomeprol; Eisai Co., Tokyo, Japan) was injected intravenously at a rate of 3 mL/s using an automatic power injector.

Two experienced radiologists reviewed the hyperenhancement in the arterial phase and washout in the equilibrium phase on CE-CT. These reviewers were blinded to any other information regarding the patients, and then the reviewers discussed all the patients until they reached consensus on the diagnosis.

Imaging assessment of HCC gross type

HCC of nodular type was defined as tumors characterized by a clear border between tumor and surrounding parenchyma. All HCCs were subclassified by imaging into the following three gross types before surgical resection: single nodular (SN) type, defined as those tumors showing a clear round shape; single nodular with extranodular growth (SNEG), defined as those tumors with one or more perinodular tumor growths; and confluent multinodular (CM) type, defined as those tumors forming a cluster of small and confluent nodules (Figures 1 and 2).

Macroscopic configurations of HCC

The resected specimens were cut into 5-mm sections in the transverse plane. The gross classification of HCC was assessed under all sections of tumors by an experienced surgeon (S.H.). In accordance with the classification proposed by the Liver Cancer Study Group of Japan, macroscopic configurations of nodular HCCs were divided into three types.[2]

Statistical analysis

Data are expressed as mean ± SD. The χ^2 test and Mann-Whitney *U* test for statistical analysis were used to compare the clinicopathologic features of patients. A p value of less than 0.05 was considered statistically significant. Significant differences in accuracy were calculated using the McNemar test. The 95% confidence intervals were calculated according to the binomial distribution. The agreement of the US or CT findings versus the results of macroscopic configurations was measured using the kappa coefficient (Tables 3 and 4). Data were analyzed using statistical software (SPSS 11.5; SPSS, Chicago, IL). A kappa statistic of 0.41–0.60 was considered to indicate moderate agreement; a weighted kappa statistic of 0.61–0.80 was considered to indicate good agreement, and a weighted kappa statistic of 0.81–1.00 was considered to indicate excellent agreement.[17]

RESULTS

Among 61 HCC nodules, 39 tumors (63.9%) were classified into SN type, 19 (31.2%) tumors into SNEG type, and 3 (4.9%) tumors into CM type from the resected specimen. HCCs of SNEG type and CM type could be lumped as non-SN type because they have higher malignant potential. Table 2 summarizes the comparison of characteristics between SN type and non-SN type. Five patients with multiple HCCs had two various HCC types of the gross classification. Non-SN-type HCCs were bigger and had a higher frequency of capsule invasion, respectively ($p = 0.0066$ and $p = 0.011$, respectively). All HCCs of the non-SN type were diagnosed as moderate or poorly differentiated tumors. In contrast, 25.6% (10/39) of HCCs of SN type were diagnosed as well-differentiated HCC. There was no statistical difference in hepatic fibrosis between the groups.

The diagnostic accuracy was 86.9% (53/61) for CE-US and 65.6% (40/61) for CE-CT (Tables 3 and 4). The differences in accuracy between CE-US and CE-CT were statistically significant (McNemar; $p = 0.007$). On CE-US, 50 HCCs were shown as clear defects. The seven HCCs shown as defects with unclear boundaries were diagnosed as being associated with severe liver cirrhosis in the resected specimens, and the four HCCs shown as **lower contrast defects** with clear boundaries were histologically diagnosed as well-differentiated HCC. Kappa coefficient showed a value of 0.74 (95% CI: 0.65–0.82), which is considered to be a good agreement between gross classification using CE-US and macroscopic final results (Table 3). Overclassification occurred in four nodules (6.6%), and underclassification

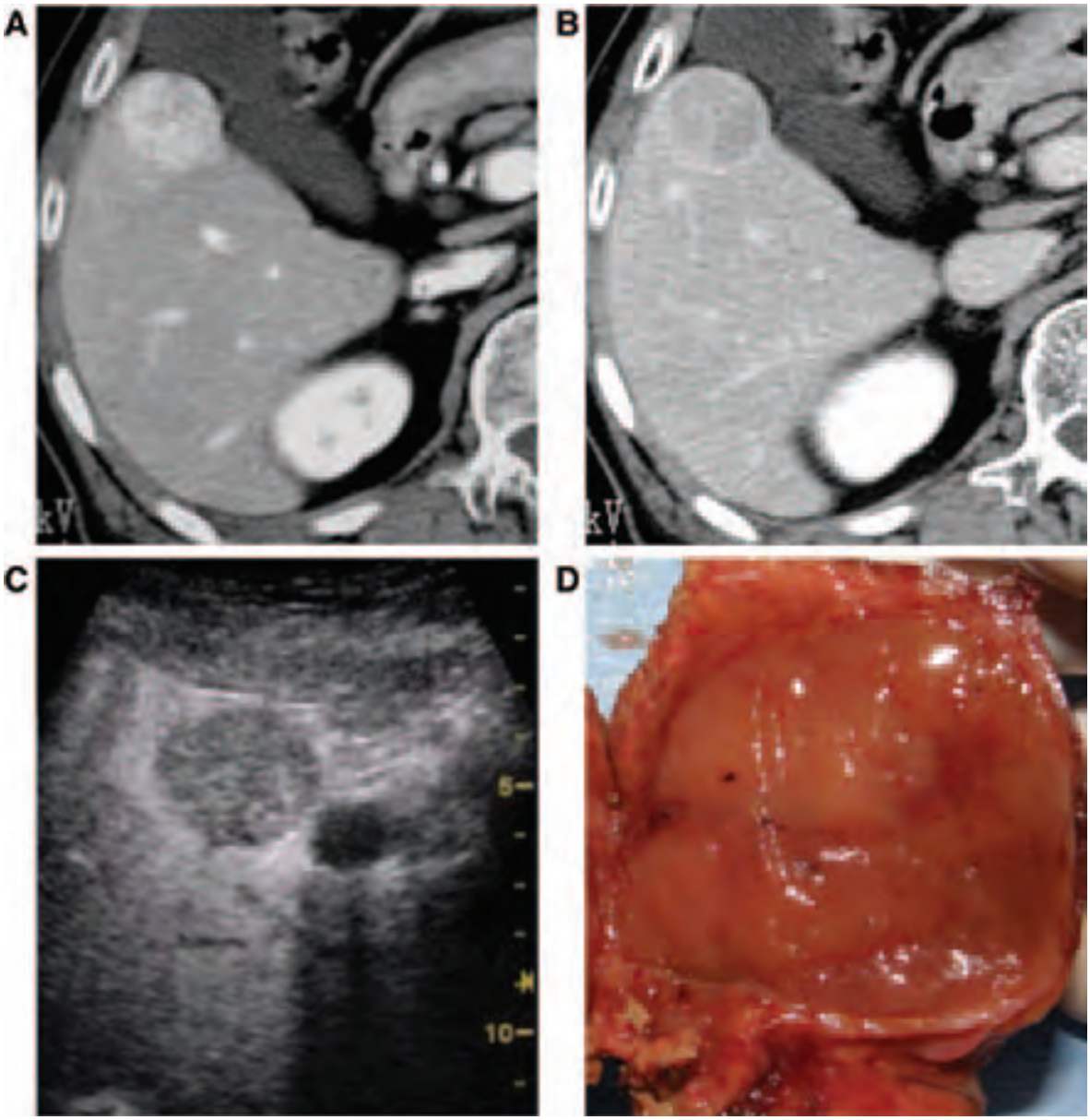

FIGURE 1. A 61-year-old man pathologically diagnosed with moderately differentiated HCC measuring 2.5 cm in diameter in segment VI of the liver. (**A, B**) HCC was depicted as a tumor with elliptical contour. CE-CT showed hyperenhancement in the arterial phase **(A)** and washout in the equilibrium phase **(B)**. (**C**) CE-US images in the postvascular phase indicate a single well-circumscribed nodule. (**D**) The gross surgical specimen was also diagnosed as a single nodular type.

occurred in four nodules (6.6%) for CE-US. On the other hand, kappa coefficient showed a value of 0.38 (95% CI: 0.28–0.48), which is considered a poor degree of agreement between gross classification using CE-CT and macroscopic final results (Table 4). Overclassification occurred in 13 nodules (21.3%), and underclassification occurred in 7 nodules (11.5%) for CE-CT.

DISCUSSION

The classification of HCC is based on gross patterns of tumor growth and spread. Some researchers have reported that moderate differentiated HCC is the majority in SN type, and the percentage of poorly differentiated HCC increase in SNEG type and more in CM type.[18–21] In short, the macroscopic classification can be useful to estimate prognosis in HCC patients because the histologic grade of malignancy is shown to be strongly related to survival after treatment. However, the gross classification is conventionally defined by the resected specimens of HCC. Before treatment, including surgical resection, radiofrequency ablation, or transcatheter arterial chemoembolization, accurate gross classification by

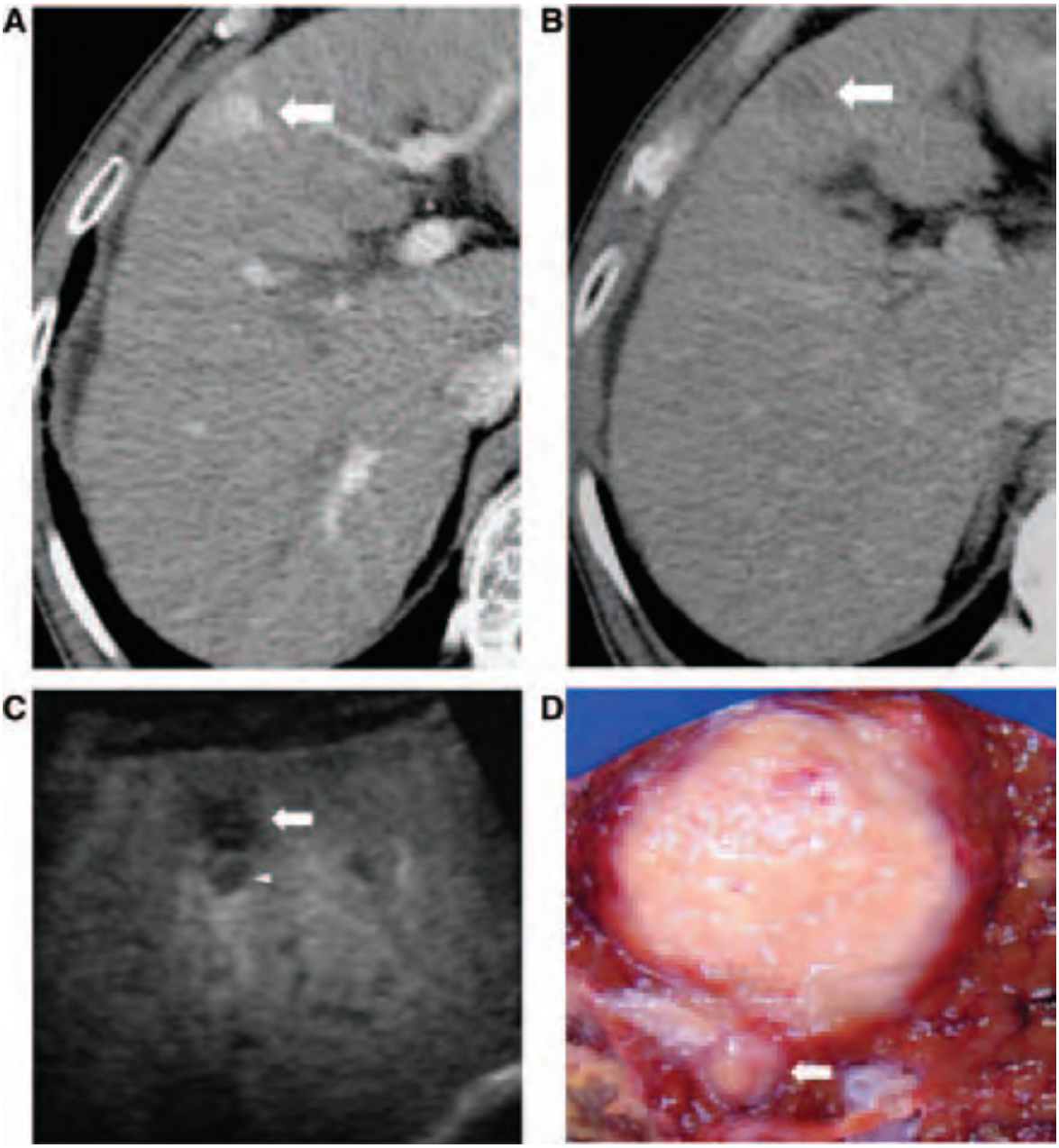

FIGURE 2. A 65-year-old man pathologically diagnosed with moderately differentiated HCC measuring 1.6 cm in diameter in segment V of the liver. **(A, B)** CE-CT shows tumor with an elliptical tumor contour (arrow) in the arterial phase **(A)** and the equilibrium phase **(B)**. **(C)** CE-US in the postvascular phase demonstrates an extragrowth (arrowhead) next to the primary tumor (arrow). This lesion was not depicted on CE-CT. **(D)** Gross evaluation of the surgical specimen, diagnosed as a single nodular type with an extranodular growth. The arrow indicates an extranodular growth of HCC.

TABLE 2
Characteristics in HCC Patients with SN Type and Non-SN Type

Variables	SN Type (39 HCCs)	Non-SN Type (SNEG + CM type) (22 HCCs)	*p* Value
Capsule invasion	23.1% (9/39)	59.0% (13/22)	0.011
Positive vascular invasion	7.7% (3/39)	13.6% (3/22)	0.66
Differentiation of HCC (well/moderate/poor)	10/22/7	0/19/3	0.059

Abbreviations: CM, confluent multinodular; HCC, hepatocellular carcinoma; SN, single nodular; SNEG, single nodular with extranodular growth.

TABLE 3
Comparison of CE-US and Resected Specimen in the Gross Type of HCC

	CE-US			
Pathologic Findings	SN type	SNEG type	CM type	
SN type (n = 39)	35	3	1	39
SNEG type (n = 19)	3	16	0	19
CM type (n = 3)	0	1	2	3
	38	20	3	61

Abbreviations: CE-US, contrast-enhanced ultrasonography; CM, confluent multinodular; HCC, hepatocellular carcinoma; SN, single nodular; SNEG, single nodular with extranodular growth.

TABLE 4
Comparison of CE-CT and Resected Specimen in the Gross Type of HCC

	CE-CT			
Pathologic Findings	SN type	SNEG type	CM type	
SN type (n = 39)	30	6	3	39
SNEG type (n = 19)	6	9	4	19
CM type (n = 3)	1	0	2	3
	37	15	9	61

Abbreviations: CE-CT, contrast-enhanced CT; CM, confluent multinodular; HCC, hepatocellular carcinoma; SN, single nodular; SNEG, single nodular with extranodular growth.

imaging could be key to successful management of HCC patients.

In this study, the diagnostic accuracy was significantly better for CE-US compared with CE-CT (86.9% versus 65.6% respectively; $p = 0.036$). Agreement analysis between gross classification using CE-US and macroscopic final results gave a kappa value of 0.74, which was considered a good agreement. On the other hand, kappa coefficient showed a value of 0.38 between gross classification using CE-CT and macroscopic final results. The advantages of CE-US are high spatial resolution, temporal resolution, and contrast resolution. The contrast agent can provide detailed insight into the perfusion features of the tumoral microvascular bed in the vascular phase. For example, small extranodular growth of HCC could be depicted as a projection of hyperenhanced tumor in the vascular phase. In addition, Sonazoid microbubbles act as functional imaging agents. The postvascular image represents the function of the reticuloendothelial system, which is mainly determined by the number and function of Kupffer cells.[22–24] During the postvascular phase, low mechanical index real-time US allows repeated sweep scanning for obtaining defects images and could markedly improve the characterization of nodular HCCs in comparison with CE-CT.

However, some small HCC nodules were misclassified on CE-US or CE-CT due to the tumor size. The mean tumor size of CE-US misclassified nodules was smaller than that of CE-CT misclassified nodules (2.3 ± 0.7 cm versus 2.6 ± 1.0 cm, respectively). Of the seven misclassified nodules on CE-US, five nodules were diagnosed as simple nodule type and the remaining two nodules were diagnosed as simple nodular type with extranodular growth. Because all misclassified nodules on CE-US had septum formation, it was difficult to evaluate the shapes of nodules by the difference in perfusion defect. The mean tumor size of SNEG-type HCCs misclassified on CE-US was 1.7 ± 0.2 (range, 1.5–1.8 cm). Despite the classification of SNEG type, the mean tumor size was smaller. In the 16 CE-CT misclassified nodules, it was difficult to evaluate the shapes of nodules on CE-CT because of the partial volume effect.

Table 2 showed that the gross HCC type was associated with histologic cellular differentiation and clinical malignancies. Minagawa et al reported that one of the independent prognostic factors was gross classification in a nationwide cohort study of Japanese patients with resected HCCs.[25] Therefore, it might be also useful to assess gross type of HCC for decision of treatment strategies. Radiofrequency ablation, a local ablative technique, has been performed widely because of difficulties in surgical resection related to the size, site, and number of tumors, vascular and extrahepatic involvement, as well as liver function of HCC patients.[26–30] The main goal of radiofrequency ablation is complete thermal coagulation of the tumor, leaving no viable malignant tissue.[31] Histologic evidence directly validates radiofrequency ablation as an effective treatment of small (<3 cm) HCC.[32] For patients with small HCC of nonSN type, it would be more effective to receive surgical resection that has more curability than radiofrequency ablation. On the other hand, in patients with HCC of simple nodular type that are not small, it would be more effective to receive the less invasive therapy radiofrequency ablation rather than surgical resection. In deciding to administer HCC therapy, it is essential to obtain the imaging information of gross patterns.

The principal limitation of this study was the lack of independence of data, as some patients contributed more than one tumor to the analysis. Another limitation is the relatively small number of patients. Further studies of this

technique with a larger number of patients are warranted.

In conclusion, CE-US is a more reliable tool to evaluate the gross type of HCC than CE-CT. In particular, postvascular phase imaging using Sonazoid could show the clear contours of tumor. Accurate gross classification by imaging is considered to be essential for the determination of treatment strategy and the estimates of the patients' prognosis.

REFERENCES

1. Kanai T, Hirohashi S, Upton MP, et al. Pathology of small hepatocellular carcinoma: a proposal for a new gross classification. Cancer 1987;60:81.
2. Liver Cancer Study Group of Japan. The general rules for the clinical and pathological study of primary liver cancer. 1989;19:98.
3. Hui AM, Takayama T, Sano K, et al. Predictive value of gross classification of hepatocellular carcinoma on recurrence and survival after hepatectomy. J Hepatol 2000;33:975.
4. Shirabe K, Aishima S, Taketomi A, et al. Prognostic importance of the gross classification of hepatocellular carcinoma in living donor-related liver transplantation. Br J Surg 2011;98:261.
5. Minami Y, Kudo M, Chung H, et al. Contrast harmonic sonography-guided radiofrequency ablation therapy versus B-mode sonography in hepatocellular carcinoma: prospective randomized controlled trial. AJR Am J Roentgenol 2007;188:489.
6. Solbiati L, Tonolini M, Cova L, et al. The role of contrast-enhanced ultrasound in the detection of focal liver lesions. Eur Radiol 2001;11:E15.
7. Konopke R, Bunk A, Kersting S. The role of contrast-enhanced ultrasound for focal liver lesion detection: an overview. Ultrasound Med Biol 2007; 33:1515.
8. Furuse J, Nagase M, Ishii H, et al. Contrast enhancement patterns of hepatic tumours during the vascular phase using coded harmonic imaging and Levovist to differentiate hepatocellular carcinoma from other focal lesions. Br J Radiol 2003;76:385.
9. Yanagisawa K, Moriyasu F, Miyahara T, et al. Phagocytosis of ultrasound contrast agent microbubbles by Kupffer cells. Ultrasound Med Biol 2007;33:318.
10. Sontum PC, Ostensen J, Dvrstad K, et al. Acoustic properties of NC100100 and their relation with the microbubble size distribution. Invest Radiol 1999; 34:268.
11. Ramnarine KV, Kyriakopoulou K, Gordon P, et al. Improved characterisation of focal liver tumours: dynamic power Doppler imaging using NC100100 echo-enhancer. Eur J Ultrasound 2000;11:95.
12. Korenaga K, Korenaga M, Furukawa M, et al. Usefulness of Sonazoid contrast-enhanced ultrasonography for hepatocellular carcinoma: comparison with pathological diagnosis and superparamagnetic iron oxide magnetic resonance images. J Gastroenterol 2009;44:733.
13. Kudo M, Hatanaka K, Maekawa K. Defect reperfusion imaging, a newly developed novel technology using Sonazoid in treatment of hepatocellular carcinoma. J Med Ultrasound 2008;16:169.
14. Hatanaka K, Kudo M, Minami Y, et al. Differential diagnosis of hepatic tumors: value of contrast-enhanced harmonic sonography using the newly developed contrast agent, Sonazoid. Intervirology 2008;51:61.
15. Hatanaka K, Kudo M, Minami Y, et al. Sonazoid-enhanced ultrasonography for diagnosis of hepatic malignancies: comparison with contrast-enhanced CT. Oncology 2008;75:42.
16. Minami Y, Kudo M, Hatanaka K, et al. Radiofrequency ablation guided by contrast harmonic sonography using perfluorocarbon microbubbles (Sonazoid) for hepatic malignancies: an initial experience. Liver Int 2010;30:759.
17. Cohen J. A coefficient of agreement for nominal scales. Educ Psychol Meas 1960;20:37.
18. Nakashima Y, Nakashima O, Tanaka M, et al. Portal vein invasion and intrahepatic micrometastasis in small hepatocellular carcinoma by gross type. Hepatol Res 2003;26:142.
19. Shimada M, Rikimaru T, Hamatsu T, et al. The role of macroscopic classification in nodular-type hepatocellular carcinoma. Am J Surg 2001;182:177.
20. Komatsu S, Murakami M, Fukumoto T, et al. Risk factors for survival and local recurrence after particle radiotherapy for single small hepatocellular carcinoma. Br J Surg 2011;98:558.
21. Roayaie S, Blume IN, Thung SN, et al. A system of classifying microvascular invasion to predict outcome after resection in patients with hepatocellular carcinoma. Gastroenterology 2009;137:850.
22. Inoue T, Kudo M, Watai R, et al. Differential diagnosis of nodular lesions in cirrhotic liver by postvascular phase contrast-enhanced US with Levovist: comparison with superparamagnetic iron oxide magnetic resonance images. J Gastroenterol 2005; 40:1139.
23. Inoue T, Kudo M, Maenishi O, et al. Value of liver parenchymal phase contrast-enhanced sonography to diagnose premalignant and borderline lesions and overt hepatocellular carcinoma. AJR Am J Roentgenol 2009;192:698.
24. Tanaka M, Nakashima O, Wada Y, et al. Pathomorphological study of Kupffer cells in hepatocellular carcinoma and hyperplastic nodular lesions in the liver. Hepatology 1996;24:807.
25. Minagawa M, Ikai I, Matsuyama Y, et al. Staging of hepatocellular carcinoma: assessment of the Japanese TNM and AJCC/UICC TNM systems in a cohort of 13,772 patients in Japan. Ann Surg 2007;245:909.
26. Kudo M. Radiofrequency ablation for hepatocellular carcinoma: updated review in 2010. Oncology 2010;78:S113.

27. Shiozawa K, Watanabe M, Takayama R, et al. Evaluation of local recurrence after treatment for hepatocellular carcinoma by contrast-enhanced ultrasonography using Sonazoid: comparison with dynamic computed tomography. J Clin Ultrasound 2010;38:182.
28. Chen MS, Li JQ, Zheng Y, et al. A prospective randomized trial comparing percutaneous local ablative therapy and partial hepatectomy for small hepatocellular carcinoma. Ann Surg 2006;243:321.
29. Huang J, Yan L, Cheng Z, et al. A randomized trial comparing radiofrequency ablation and surgical resection for HCC conforming to the Milan criteria. Ann Surg 2010;252:903.
30. Rossi S, Di Stasi M, Buscarini E, et al. Percutaneous radiofrequency interstitial thermal ablation in the treatment of small hepatocellular carcinoma. Cancer J Sci Am 1995;1:73.
31. Kim YS, Lee WJ, Rhim H, et al. The minimal ablative margin of radiofrequency ablation of hepatocellular carcinoma (> 2 and < 5 cm) needed to prevent local tumor progression: 3D quantitative assessment using CT image fusion. AJR Am J Roentgenol 2010;195:758.
32. Lu DS, Yu NC, Raman SS, et al. Radiofrequency ablation of hepatocellular carcinoma: treatment success as defined by histologic examination of the explanted liver. Radiology 2005;234:954.

ORIGINAL PAPER

THE INTERNATIONAL JOURNAL OF CLINICAL PRACTICE

GIDEON (Global Investigation of therapeutic DEcisions in hepatocellular carcinoma and Of its treatment with sorafeNib): second interim analysis

R. Lencioni,[1] M. Kudo,[2] S.-L. Ye,[3] J.-P. Bronowicki,[4] X.-P. Chen,[5] L. Dagher,[6] J. Furuse,[7] J. F. Geschwind,[8] L. Ladrón de Guevara,[9] C. Papandreou,[10] T. Takayama,[11] S. K. Yoon,[12] K. Nakajima,[13] R. Lehr,[14] S. Heldner,[15] A. J. Sanyal[16]

SUMMARY

Background: GIDEON (Global Investigation of therapeutic DEcisions in hepatocellular carcinoma [HCC] and Of its treatment with sorafeNib) is a global, prospective, non-interventional study undertaken to evaluate the safety of sorafenib in patients with unresectable HCC in real-life practice, including Child-Pugh B patients who were excluded from clinical trials. **Methods:** Patients with unresectable HCC, for whom the decision to treat with sorafenib, based on the approved label and prescribing guidelines, had been taken by their physician, were eligible for inclusion. Demographic data and disease/medical history were recorded at entry. Sorafenib dosing and adverse events (AEs) were collected at follow-up visits. The second interim analysis was undertaken when ~1500 treated patients were followed up for ≥ 4 months. **Results:** Of the 1571 patients evaluable for safety, 61% had Child-Pugh A status and 23% Child-Pugh B. The majority of patients (74%) received the approved 800 mg initial sorafenib dose, regardless of Child-Pugh status; however, median duration of therapy was shorter in Child-Pugh B patients. The majority of drug-related AEs were grade 1 or 2, and the most commonly reported were consistent with previous reports. The incidence and nature of drug-related AEs were broadly similar across Child-Pugh, Barcelona Clinic Liver Cancer (BCLC) and initial dosing subgroups, and consistent with the overall population. **Conclusions:** Consistent with the first interim analysis, overall safety profile and dosing strategy are similar across Child-Pugh subgroups. Safety findings also appear comparable irrespective of initial sorafenib dose or BCLC stage. Final analyses in > 3000 patients are ongoing.

What's known

- The oral multikinase inhibitor sorafenib significantly improves overall survival in patients with uHCC. However, pivotal studies generally included only patients with preserved liver function; therefore, investigation of sorafenib in wider patient groups is needed.
- GIDEON is a global, non-interventional study evaluating uHCC patients treated with sorafenib in clinical practice, thereby allowing a broad evaluation of patient subgroups, including those with advanced liver dysfunction.

What's new

- The second interim analysis of the GIDEON study has now been completed in > 1500 uHCC patients treated with sorafenib in clinical practice.
- Consistent with the first interim analysis conducted in ~500 patients, these data highlight that the safety profile of sorafenib appears to be comparable across Child-Pugh and BCLC subgroups in real-life practice.
- Safety findings also appear to be similar, irrespective of the initial sorafenib dose.

Background

Hepatocellular carcinoma (HCC) is now the third leading cause of cancer-related death and the fifth most common malignancy in men; the seventh in women (1,2). The major risk factors for HCC include chronic hepatitis C and hepatitis B viral infections, as well as alcohol consumption, non-alcoholic steatohepatitis and diabetes (3,4). The vast majority (70–90%) of HCC cases occur in the context of liver cirrhosis (5), and consequently many patients present with hepatic dysfunction and experience a high rate of comorbidity. HCC is therefore a heterogeneous disease in terms of aetiology as well as clinical presentation and behaviour, thus presenting challenges for disease management (6).

Most patients with HCC present with unresectable disease (uHCC) that cannot be managed by surgery. Non-surgical locoregional treatment options, such as image-guided ablation and transarterial chemoembolisation, are not suitable for all patients and are associated with high rates of recurrence (7–9). At present, there is no global standardisation of treatment for uHCC, although systemic therapies may offer a new alternative in the treatment of uHCC.

Sorafenib is a multikinase inhibitor used for the treatment of uHCC (10). Two Phase III studies (SHARP and Asia-Pacific) demonstrated significant improvements in overall survival in uHCC patients, the majority of whom had Child-Pugh A (11,12), and sorafenib is suggested as first-line therapy in HCC patients with advanced-stage disease (13).

[1]Division of Diagnostic Imaging and Intervention, Pisa University Hospital and School of Medicine, Pisa, Italy
[2]Department of Gastroenterology and Hepatology, Kinki University School of Medicine, Osaka, Japan
[3]Liver Cancer Institute and Zhongshan Hospital, Fudan University, Shanghai, China
[4]Department of Gastroenterology and Hepatology, INSERM U954, University Hospital, University of Lorraine, Nancy, France
[5]Hepatic Surgery Center, Tongji Hospital, Tongji Medical College, Huazhong University of Science and Technology, Wuhan, China
[6]Policlínica Metropolitana, Caracas, Venezuela
[7]Kyorin University School of Medicine, Mitaka, Tokyo, Japan
[8]Vascular and Interventional Radiology, Johns Hopkins University School of Medicine, Baltimore, MD, USA
[9]Hospital Angeles Clínica Londres, Mexico City, Mexico
[10]University Hospital of Larissa, Larissa, Greece
[11]Department of Digestive Surgery, Nihon University School of Medicine, Tokyo, Japan
[12]The Catholic University of Korea, Seoul, Korea
[13]Global Medical Affairs, Bayer HealthCare Pharmaceuticals, Montville, NJ, USA
[14]Clinical Statistics, Bayer HealthCare Pharmaceuticals, Montville, NJ, USA
[15]Global Medical Affairs and Pharmacovigilance, Bayer HealthCare Pharmaceuticals, Berlin, Germany
[16]Virginia Commonwealth University Medical Center, Richmond, VA, USA

Int J Clin Pract, May 2014, **68**, 5, 609–617. doi: 10.1111/ijcp.12352

Correspondence to:
Professor Riccardo Lencioni, Division of Diagnostic Imaging and Intervention, Pisa University Hospital and School of Medicine, Pisa, Italy
Tel.: +39 050 997 321
Fax: +39 050 996 561
Email: riccardo.lencioni@med.unipi.it

ClinicalTrials.gov identifier: NCT00812175

Disclosures
Riccardo Lencioni has participated in a speaker bureau with Bayer; Jean-Pierre Bronowicki has a consulting role with Bayer; Junji Furuse has a consulting role with Bayer, has participated in a speaker bureau with Bayer and has received a research grant from Bayer; Jeff F. Geschwind has a consulting role with Bayer and has received a research grant from Bayer; Laura Ladrón de Guevara has a consulting role with Bayer; Christos Papandreou has a consulting role with Bayer and has received a travel grant from Bayer; Keiko Nakajima is an employee of Bayer and has stock ownership with Bayer; Robert Lehr and Stephanie Heldner are employees of Bayer; Masatoshi Kudo, Sheng-Long Ye, Xiao-Ping Chen, Lucy Dagher, Tadatoshi Takayama, Seung Kew Yoon and Arun J. Sanyal have no financial interests to disclose.

GIDEON (Global Investigation of therapeutic DEcisions in HCC and Of its treatment with sorafeNib) is a prospective, non-interventional study undertaken to fulfil postapproval commitments to licensing agencies (14). The primary objective of GIDEON is to evaluate the safety of sorafenib in uHCC patients under real-life clinical practice conditions and to gather more comprehensive data on the use of sorafenib in patients with Child-Pugh B liver function, who were excluded from the randomised clinical trials (11,12). In general, clinical trials in HCC include only patients with preserved liver function (15), as severe liver dysfunction associated with Child-Pugh B or Child-Pugh C status represents a competing cause of death and may confound results (11).

GIDEON is one of the largest studies undertaken in patients with uHCC, allowing for a broad evaluation of patient subgroups. Multiple predefined subanalyses were therefore undertaken, focusing on potentially predictive or prognostic factors, including Child-Pugh score, Barcelona Clinic Liver Cancer (BCLC) stage and aetiology.

The first interim analysis of GIDEON was performed per protocol when ~500 patients had been enrolled; 479 patients were evaluated (16). Recently published findings of this preliminary analysis highlighted regional variations in patient characteristics, underlying disease aetiology and sorafenib dosing patterns, as well as consistent safety findings across Child-Pugh patients (16).

The second interim analysis of GIDEON was performed per protocol once ~1500 patients had been treated and followed up for ≥ 4 months. Here, we present clinically relevant findings of this analysis, including safety findings across Child-Pugh, BCLC and initial sorafenib dose subgroups (17–19).

Methods

Study design and objectives

GIDEON includes patients who are candidates for systemic therapy and in whom the decision to treat with sorafenib has been made under real-life practice conditions, including patients with Child-Pugh B liver function. Full details of the study design have been previously published (14).

Two interim analyses were preplanned, the first when 500 patients had been followed up for ≥ 4 months, and the second when 1500 patients had reached this point. The final analysis is scheduled at 12-month follow-up following the enrolment of 3000 sorafenib-treated patients (14).

Patients

Eligible patients are those diagnosed histologically, cytologically or radiographically with uHCC, who have a life expectancy of > 8 weeks and in whom the decision to treat with sorafenib has been made by their physician (14). Further inclusion criteria are outlined in the previously published study design report (14). Exclusion criteria are based on the local product information for sorafenib (14). All patients provided informed and signed consent, and the study is being conducted according to established recommendations and regulations relating to non-interventional and postauthorisation safety studies (20) and according to Good Clinical Practice. Documented approval from appropriate ethics committees and institutional review boards was obtained in accordance with local laws, regulations and organisations.

Data collection and analyses

All data were collected using case report forms as previously outlined (14). All adverse events (AEs) were graded according to the National Cancer Institute Common Terminology Criteria for Adverse Events version 3.0. Patients who received at least one dose of sorafenib and underwent at least one follow-up assessment were evaluable for safety.

Target enrolment was based on an overall sample of 3000 patients, the number determined sufficient for comprehensive evaluation of safety for the overall population, as well as specified subgroups (14). All baseline and safety data are summarised with descriptive statistics (14).

Results

Patient demographics and disease characteristics at study entry

In the second interim analysis, 1571 patients were eligible for safety analysis. The study population included patients across all BCLC stages and Child-Pugh status groups. The majority of patients (61%) had Child-Pugh A, with 23% having Child-Pugh B, and most had BCLC stage C (54%). The median age of the study population was 62, and the majority of patients were men (82%) (Table 1).

Patient demographics and disease characteristics were generally similar between patients receiving an initial sorafenib dose of 400 or 800 mg. Disease characteristics were also broadly comparable across Child-Pugh and BCLC subgroups (Table 1). There was some variation in prior treatment across Child-Pugh subgroups, as a greater proportion of Child-Pugh A patients had received prior locoregional treatment compared with Child-Pugh B (61% vs. 45%). Transarterial chemoembolisation was the most common locoregional treatment in both Child-Pugh A and Child-Pugh B patients and across all BCLC stages (Table 1).

Table 1 Patient demographics, disease characteristics and prior treatment by initial sorafenib dose, Child-Pugh status and BCLC stage

		Initial sorafenib dose*		Child-Pugh status†,‡			BCLC stage†,§			
	Total	400 mg	800 mg	A (< 7)	B (7–9)	C (> 9)	A	B	C	D
Patients, n (% of total)	1571 (100)	347 (22)	1161 (74)	957 (61)	367 (23)	35 (2)	115 (7)	298 (19)	851 (54)	92 (6)
Median age, years (range)	62 (18–98)	63 (19–89)	62 (18–98)	64 (18–94)	61 (23–86)	58 (39–82)	67 (33–87)	66 (25–98)	60 (18–89)	61 (33–82)
Gender, n (%)										
Men	1285 (82)	279 (80)	963 (83)	790 (83)	297 (81)	29 (83)	76 (66)	238 (80)	724 (85)	72 (78)
Women	286 (18)	68 (20)	198 (17)	167 (17)	70 (19)	6 (17)	39 (34)	60 (20)	127 (15)	20 (22)
ECOG PS, n (%)†,¶										
0	627 (40)	106 (31)	499 (43)	478 (50)	96 (26)	5 (14)	65 (57)	178 (60)	302 (36)	23 (25)
1	670 (43)	170 (49)	472 (41)	370 (39)	171 (47)	19 (54)	43 (37)	98 (33)	412 (48)	29 (32)
≥ 2	183 (12)	44 (13)	133 (11)	68 (7)	75 (20)	10 (29)	4 (4)	19 (6)	94 (11)	40 (44)
TNM status, n (%)†,**										
I	105 (7)	28 (8)	62 (5)	67 (7)	25 (7)	4 (11)	63 (55)	27 (9)	7 (1)	3 (3)
II	177 (11)	43 (12)	124 (11)	128 (13)	34 (9)	3 (9)	30 (26)	101 (34)	27 (3)	4 (4)
III	534 (34)	109 (31)	417 (36)	327 (34)	142 (39)	12 (34)	14 (12)	139 (47)	322 (38)	27 (29)
IV	561 (36)	129 (37)	411 (35)	352 (37)	113 (31)	12 (34)	5 (4)	13 (4)	440 (52)	52 (57)
Extrahepatic spread, n (%)†	612 (39)	141 (41)	453 (39)	382 (40)	127 (35)	11 (31)	1 (1)	5 (2)	503 (59)	50 (54)
Prior surgery, n (%)	294 (19)	66 (19)	221 (19)	218 (23)	34 (9)	1 (3)	13 (11)	59 (20)	168 (20)	7 (8)
Prior LRT, n (%)††	871 (55)	221 (64)	610 (53)	585 (61)	166 (45)	9 (26)	76 (66)	178 (60)	466 (55)	36 (39)
Prior TACE, n (%)	722 (46)	183 (53)	511 (44)	485 (51)	140 (38)	7 (20)	58 (50)	151 (51)	388 (46)	29 (32)

BCLC, Barcelona Clinic Liver Cancer; ECOG PS, Eastern Cooperative Oncology Group performance status; LRT, locoregional treatment; TACE, transarterial chemoembolisation; TNM, tumour node metastasis. *Data missing for eight patients; data not shown for 55 patients (4%) who received an initial dose of 100, 200 or 600 mg sorafenib. †Recorded at study entry (which is defined as start of therapy and is indicated by the initial visit). ‡Child-Pugh status unknown for five patients; 207 patients not evaluable and not tabulated. §Data missing for 13 patients; 202 patients not evaluable and not tabulated. ¶Data missing for 91 patients. **Data missing for 14 patients; 180 patients not evaluable and not tabulated. ††Patients may have received more than one prior treatment. Other LRT received included radiofrequency ablation (15%), hepatic arterial infusion (5%), percutaneous ethanol injection (4%) and other (9%).

Sorafenib administration

Table 2 summarises sorafenib administration for the overall study population and by initial dose and Child-Pugh and BCLC subgroups. Overall, the majority of patients received the approved initial dose of 800 mg (74%). The median daily dose across all patients was 693 mg.

A slightly higher percentage of patients who received an initial sorafenib dose of 400 mg had treatment duration of ≤ 4 weeks compared with those who initially received 800 mg (20% vs. 16%). Patients with an initial dose of 400 mg also had lower median treatment duration (9.7 weeks) compared with those with an initial dose of 800 mg (12.3 weeks).

A similar proportion of patients across Child-Pugh subgroups received the recommended 800 mg initial dose, although the median daily dose was slightly higher in Child-Pugh B (721 mg) compared with Child-Pugh A patients (680 mg). However, median duration of sorafenib therapy was less in Child-Pugh B (8.6 weeks) than in Child-Pugh A patients (13.7 weeks) and shorter with increasing Child-Pugh B scores: B7 (9.0 weeks), B8 (8.5 weeks) and B9 (6.7 weeks).

Initial sorafenib dose and median daily dose were broadly consistent across BCLC stages. However, patients with BCLC stage C tended to have a shorter duration of treatment (10.1 weeks) than patients with BCLC stage B (16.3 weeks) and BCLC stage A (19.6 weeks) (Table 2).

Safety assessments

Safety data from the overall population are presented in Tables 3–5. Overall, 83% of patients experienced a treatment-emergent AE, with 64% in total reporting a drug-related AE. The majority of drug-related AEs were grade 1 or 2, and only 9% of patients experienced a drug-related serious AE (SAE) (Table 3). The most commonly observed drug-related AEs across all patients were diarrhoea, hand-foot skin reaction and fatigue (Table 5).

The incidence of AEs and drug-related AEs was comparable between Child-Pugh A and Child-Pugh B patients (Table 3). The majority of drug-related AEs were grade 1 or 2 in both Child-Pugh A and Child-Pugh B patients. However, there was a higher percentage of SAEs and drug-related SAEs, and a higher rate of

Table 2 Summary of sorafenib administration by initial sorafenib dose, Child-Pugh status and BCLC stage

Sorafenib administration	Total (n = 1571)	Initial sorafenib dose		Child-Pugh status*,†					BCLC stage*,‡			
		400 mg (n = 347)	800 mg (n = 1161)	A (< 7) (n = 957)	B (7) (n =196)	B (8) (n = 96)	B (9) (n = 69)	B (7–9) (n = 367)	C (> 9) (n = 35)	A (n = 115)	B (n = 298)	C (n = 851)	D (n = 92)
Duration of treatment ≤ 4 weeks, n (%)§,¶	265 (17)	69 (20)	183 (16)	120 (13)	43 (22)	21 (22)	20 (29)	86 (23)	16 (46)	15 (13)	26 (9)	150 (18)	27 (29)
Median treatment duration, weeks	11.7	9.7	12.3	13.7	9.0	8.5	6.7	8.6	4.1	19.6	16.3	10.1	7.2
Median daily dose, mg**,††	693.0	400.0	800.0	680.0	718.0	729.0	749.0	721.0	679.5	696.5	669.0	718.0	800.0
Initial dose of 800 mg/day, n (%)‡‡	1161 (74)	NA	1161 (100)	733 (77)	143 (73)	66 (69)	46 (67)	260 (71)	24 (69)	77 (67)	227 (76)	659 (77)	67 (73)

BCLC, Barcelona Clinic Liver Cancer; NA, not available. *At start of therapy. †Child-Pugh status unknown for five patients; 207 patients not evaluable and not tabulated; six patients documented as having Child-Pugh B but specific score not recorded. ‡Data missing for 13 patients; 202 patients not evaluable and not tabulated. §Time in weeks from initial visit to last dosing date (for ongoing patients to last visit date) +1. ¶1283 patients received > 4 weeks of sorafenib treatment and data missing for 23 patients. **Determined within patient based on actual days on study drug (interruptions excluded). ††Based on 1243 patients. ‡‡402 patients received ≤ 600 mg/day and data missing for eight patients.

treatment discontinuation because of AEs, in Child-Pugh B compared with Child-Pugh A patients.

The most frequent drug-related AEs across Child-Pugh subgroups were consistent with findings in the overall population and comparable across Child-Pugh subgroups (Table 5). Diarrhoea, hand-foot skin reaction and fatigue were the most frequently observed drug-related AEs in both Child-Pugh A and Child-Pugh B patients. However, a lower incidence of skin toxicity was observed in Child-Pugh B patients compared with Child-Pugh A patients (15% vs. 29%). No unexpected AEs were observed in patients with more severe liver dysfunction.

Neither the incidence nor the severity of drug-related AEs was notably different across BCLC subgroups. SAEs were more frequent in advanced disease but the incidence of drug-related SAEs was similar regardless of BCLC stage (Table 3). The nature of the most frequent drug-related AEs was consistent across all BCLC stages and with the overall population (Table 5).

Safety profiles appeared to be similar regardless of initial dose. The number of drug-related AEs and SAEs, and the number of patients in whom treatment was discontinued because of AEs, were similar across dosing subgroups (Table 4). The type and incidence of the most commonly reported drug-related AEs were also comparable for patients receiving an initial sorafenib dose of either 400 or 800 mg; diarrhoea (26% vs. 25%), hand-foot skin reaction (23% vs. 25%) and fatigue (17% vs. 14%) (Table 5).

Overall, the incidence of AEs, drug-related AEs and SAEs was similar in both older (≥ 65 years) and younger patients (Table 4). Across Eastern Cooperative Oncology Group (ECOG) subgroups, the incidence of SAEs was higher in patients with a greater ECOG score at baseline; however, the incidence of drug-related SAEs was similar (Table 3).

Nearly half of all deaths were HCC-related (40%), with 14% of deaths determined as liver-related and 11% both HCC- and liver-related (Table 6). Generally, the causes of death were similar between Child-Pugh A and Child-Pugh B patients, with HCC-related the most common cause of death.

Discussion

GIDEON is a Phase IV non-interventional study undertaken to evaluate the safety of sorafenib in clinical practice. The GIDEON study population is therefore a heterogeneous one, and multiple subgroup analyses, based on predictive and prognostic factors, were preplanned. The second interim analysis allowed for assessment of overall safety findings in the larger population of > 1500 patients and for

Table 3 Treatment-emergent adverse events by ECOG PS, Child-Pugh status and BCLC stage

		ECOG PS		Child-Pugh status*,†			BCLC stage*,‡			
Treatment-emergent adverse events, n (%)	**Total (n = 1571)**	**≤ 1 (n = 1297)**	**2 (n = 143)**	**A (< 7) (n = 957)**	**B (7–9) (n = 367)**	**C (> 9) (n = 35)**	**A (n = 115)**	**B (n = 298)**	**C (n = 851)**	**D (n = 92)**
AEs (all grades)	1307 (83)	1066 (82)	121 (85)	780 (82)	326 (89)	30 (86)	82 (71)	244 (82)	718 (84)	76 (83)
AEs (grade 3 or 4)	472 (30)	391 (30)	42 (29)	278 (29)	115 (31)	12 (34)	34 (30)	101 (34)	243 (29)	25 (27)
Drug-related AEs (all grades)	1010 (64)	850 (66)	79 (55)	639 (67)	230 (63)	16 (46)	70 (61)	206 (69)	562 (66)	45 (49)
Drug-related AEs (grade 3 or 4)	366 (23)	315 (24)	26 (18)	228 (24)	80 (22)	8 (23)	29 (25)	84 (28)	187 (22)	19 (21)
SAEs§ (all grades)	587 (37)	435 (34)	83 (58)	278 (29)	206 (56)	22 (63)	27 (24)	94 (32)	324 (38)	51 (55)
Drug-related SAEs§ (all grades)	142 (9)	123 (9)	11 (8)	72 (8)	54 (15)	2 (6)	10 (9)	35 (12)	75 (9)	6 (7)
AEs resulting in permanent discontinuation of sorafenib¶	434 (28)	336 (26)	56 (39)	225 (24)	141 (38)	18 (51)	28 (24)	76 (26)	226 (27)	40 (44)
Deaths**	343 (22)	250 (19)	49 (34)	154 (16)	125 (34)	13 (37)	14 (12)	48 (16)	196 (23)	34 (37)

AE, adverse event; BCLC, Barcelona Clinic Liver Cancer; ECOG PS, Eastern Cooperative Oncology Group performance status; SAE, serious adverse event. *At start of therapy. †Child-Pugh status unknown for five patients; 207 patients not evaluable and not tabulated. ‡Data missing for 13 patients; 202 patients not evaluable and not tabulated. §An SAE is defined as any AE occurring at any dose that results in any of the following outcomes: death; life-threatening; hospitalisation or prolongation of existing hospitalisation; persistent or significant disability/incapacity; congenital anomaly/birth defect; medically important event. ¶Any AE. **Deaths while on treatment and up to 30 days after last study medication dose.

Table 4 Treatment-emergent adverse events by initial sorafenib dose and age

Treatment-emergent adverse events, n (%)	Total (n = 1571)	Initial sorafenib dose		Age	
		400 mg (n = 347)	800 mg (n = 1161)	< 65 years (n = 883)	≥ 65 years (n = 688)
AEs (all grades)	1307 (83)	318 (92)	940 (81)	713 (81)	594 (86)
AEs (grade 3 or 4)	472 (30)	123 (35)	334 (29)	233 (26)	239 (35)
Drug-related AEs (all grades)	1010 (64)	237 (68)	740 (64)	530 (60)	480 (70)
Drug-related AEs (grade 3 or 4)	366 (23)	84 (24)	274 (24)	172 (20)	194 (28)
SAEs* (all grades)	587 (37)	152 (44)	412 (36)	329 (37)	258 (38)
Drug-related SAEs* (all grades)	142 (9)	33 (10)	101 (9)	60 (7)	82 (12)
AEs resulting in permanent discontinuation of sorafenib†	434 (28)	109 (31)	309 (27)	219 (25)	215 (31)
Deaths‡	343 (22)	84 (24)	248 (21)	199 (23)	144 (21)

AE, adverse event; BCLC, Barcelona Clinic Liver Cancer; SAE, serious adverse event. *An SAE is defined as any AE occurring at any dose that results in any of the following outcomes: death; life-threatening; hospitalisation or prolongation of existing hospitalisation; persistent or significant disability/incapacity; congenital anomaly/birth defect; medically important event. †Any AE. ‡Deaths while on treatment and up to 30 days after last study medication dose.

further evaluation across key clinical subgroups, including initial sorafenib dose, Child-Pugh status and BCLC stage. The final GIDEON analysis, in > 3000 patients, is currently being undertaken and will report data from final analyses across all subgroups.

Results of this second interim analysis, in 1571 patients, are consistent with observations reported in the first interim analysis in 479 patients (16). As previously observed, patient demographics in GIDEON are in line with previous HCC epidemiological reports in terms of age, gender, Child-Pugh status and prior treatment (21,22).

Consistent with the first interim analysis, the majority of patients received the recommended initial dose of sorafenib (800 mg), and had Child-Pugh A status and BCLC stage C. Patients across all BCLC stages and Child-Pugh status subgroups were treated with sorafenib. Nearly 25% of patients had Child-Pugh B status, and based on initial and median dose there was no evidence that the dosing strategy differs between Child-Pugh A and Child-Pugh B patients. However, duration of treatment tended to be less for patients with Child-Pugh B and was increasingly shorter with higher Child-Pugh B scores. Therefore, the dosing patterns observed in the larger patient population of the second interim analysis reflect those previously reported in the first interim analysis.

As reported in the first interim analysis, sorafenib was generally well tolerated in the clinical setting. In line with the SHARP and Asia-Pacific Phase III trials, the majority of drug-related AEs were grade 1 or 2 in nature (11,12). Similarly, the nature of the AEs was consistent with the Phase III trials, with diarrhoea, hand-foot skin reactions, fatigue and rash/desquamation being the most commonly reported drug-related AEs in the GIDEON, SHARP and Asia-Pacific studies, respectively (11,12).

The most commonly reported drug-related AEs across Child-Pugh subgroups were comparable in both type and incidence and were consistent with the overall population, although there was a lower incidence of skin toxicity in Child-Pugh B compared with Child-Pugh A patients.

Generally, drug-related safety findings appeared similar in both younger and older patients and in patients with lower and higher ECOG performance status at baseline. Also, the safety profile of sorafenib did not appear to differ across BCLC stages. Importantly, BCLC represents one of several staging systems used in HCC patients (23), and final analyses from the GIDEON study will allow for further exploration of findings across other staging systems and prognostic variables.

The safety profile of sorafenib appeared to be similar irrespective of initial dose; however, the lower initial dose of 400 mg was associated with a slightly shorter duration of treatment. Interestingly, this is in contrast to a recent Italian observational study in which a lower sorafenib dose was associated with a longer duration of treatment and improved outcomes (24). However, the outcome findings need to be interpreted with caution as the analysis did not account for the notable difference in treatment duration between the lower and higher dosing groups.

In this second interim analysis, study treatment duration findings must be considered preliminary.

Table 5 Treatment-emergent drug-related adverse events (any grade) in ≥ 5% of the total study population stratified by initial sorafenib dose, Child-Pugh status and BCLC stage at start of therapy

	Total	Initial sorafenib dose		Child-Pugh status			BCLC stage			
n (%)	Any grade (n = 1571)	400 mg (n = 347)	800 mg (n = 1161)	A (< 7) (n = 957)	B (7–9) (n = 367)	C (> 9) (n = 35)	A (n = 115)	B (n = 298)	C (n = 851)	D (n = 92)
Any adverse event	1010 (64)	237 (68)	740 (64)	639 (67)	230 (63)	16 (46)	70 (61)	206 (69)	562 (66)	45 (49)
Diarrhoea	387 (25)	90 (26)	289 (25)	248 (26)	86 (23)	3 (9)	26 (23)	95 (32)	217 (26)	13 (14)
Hand-foot skin reaction	380 (24)	79 (23)	293 (25)	278 (29)	54 (15)	1 (3)	22 (19)	91 (31)	213 (25)	14 (15)
Fatigue	222 (14)	60 (17)	157 (14)	139 (15)	41 (11)	6 (17)	18 (16)	41 (14)	122 (14)	10 (11)
Rash/desquamation	190 (12)	47 (14)	140 (12)	123 (13)	36 (10)	2 (6)	14 (12)	41 (14)	96 (11)	9 (10)
Anorexia	141 (9)	31 (9)	108 (9)	93 (10)	30 (8)	1 (3)	12 (10)	24 (8)	84 (10)	6 (7)
Hypertension	104 (7)	25 (7)	78 (7)	85 (9)	11 (3)	0	5 (4)	23 (8)	66 (8)	2 (2)
Alopecia	102 (7)	19 (6)	82 (7)	79 (8)	11 (3)	1 (3)	8 (7)	21 (7)	63 (7)	3 (3)
Nausea	93 (6)	26 (8)	65 (6)	51 (5)	18 (5)	2 (6)	10 (9)	6 (2)	44 (5)	9 (10)
Weight loss	74 (5)	14 (4)	60 (5)	45 (5)	15 (4)	1 (3)	11 (10)	18 (6)	34 (4)	3 (3)

BCLC, Barcelona Clinic Liver Cancer.

Table 6 Cause of death*,† while on sorafenib therapy or within 30 days of discontinuing therapy, by Child-Pugh status at study entry

		Child-Pugh status		
Deaths, n (%)	**Total‡ (n = 343)**	**A§ (< 7) (n = 154)**	**B§ (7–9) (n = 125)**	**C (> 9) (n = 13)**
HCC-related	138 (40)	61 (40)	50 (40)	4 (31)
HCC- and liver-related	38 (11)	15 (10)	15 (12)	3 (23)
HCC- and liver-related and MOF	9 (3)	4 (3)	2 (2)	1 (8)
Liver-related	49 (14)	22 (14)	18 (14)	2 (15)
HCC-related and MOF	15 (4)	8 (5)	4 (3)	0
MOF	22 (6)	10 (7)	8 (6)	1 (8)

HCC, hepatocellular carcinoma; MOF, multi-organ system failure. *Incidence > 2% in total population. †Patients may be included in more than one cause of death category. ‡Child-Pugh status missing for one patient. §Data missing for seven Child-Pugh A and seven Child-Pugh B patients.

Final data are needed to fully evaluate duration of treatment, and final outcome analyses will adjust for duration of treatment.

Conclusions

This updated analysis of the GIDEON study confirms the findings from earlier reports. Sorafenib is well tolerated in the clinical setting and safety findings are as anticipated. The safety profile of sorafenib appears to be similar irrespective of Child-Pugh status, BCLC stage or initial sorafenib dose.

The GIDEON study is an observational study and thus is limited by the lack of either a control arm or a randomised study population. However, a non-interventional study provides an opportunity to observe treatment patterns in clinical practice and allows the assessment of a wider patient population than in randomised clinical trials. Thus, while GIDEON is a non-controlled, non-interventional study, the opportunity to evaluate > 3000 patients with uHCC in clinical practice, including patients with a greater degree of liver dysfunction, is of considerable clinical interest and relevance.

The GIDEON study is ongoing, with final analyses planned for 12 months following the recruitment of 3000 treated patients (14). Therefore, reports from interim analyses need to be considered preliminary and results interpreted with caution. Final reports will include updated analysis of safety, both overall and across subgroups, reports on duration of treatment and evaluation of treatment outcomes.

Acknowledgements

The authors would like to thank all participating clinical sites that are contributing to the GIDEON study. All data management-related activities for the GIDEON study are coordinated and overseen by Anja Laske at Bayer HealthCare Pharmaceuticals. The contract research organisation Kantar Health GmbH (Munich, Germany) is responsible for the data management system, data capture, quality review, statistical analysis and report writing. Kieran Davey, PhD, at Complete HealthVizion provided assistance in the preparation and revision of the draft manuscript, funded by Bayer HealthCare Pharmaceuticals. The authors take full responsibility for the scope, direction and content of the manuscript.

The GIDEON study is funded by Bayer HealthCare Pharmaceuticals and Onyx Pharmaceuticals.

Author contributions

Riccardo Lencioni, Masatoshi Kudo and Sheng-Long Ye are members of the GIDEON Global Steering Committee and were involved in the GIDEON study design and data interpretation; Keiko Nakajima is the study sponsor physician and contributed to data analysis and interpretation; Riccardo Lencioni, Masatoshi Kudo, Sheng-Long Ye, Jean-Pierre Bronowicki, Xiao-Ping Chen, Lucy Dagher, Junji Furuse, Jeff F. Geschwind, Laura Ladrón de Guevara, Christos Papandreou, Tadatoshi Takayama, Seung Kew Yoon and Arun J. Sanyal were responsible for the provision of patients/data acquisition; Stephanie Heldner supervised the set-up and conduct of the study; Robert Lehr was responsible for statistical analysis; Riccardo Lencioni was responsible for the concept and design of the manuscript. All authors critically reviewed the manuscript and approved the final version for publication.

References

1 Maillard E. [Epidemiology, natural history and pathogenesis of hepatocellular carcinoma]. *Cancer Radiother* 2011; **15**: 3–6. (in French).

2 El-Serag HB. Epidemiology of viral hepatitis and hepatocellular carcinoma. *Gastroenterology* 2012; **142**: 1264–73.e1.

3 El-Serag HB, Hampel H, Javadi F. The association between diabetes and hepatocellular carcinoma: a systematic review of epidemiologic evidence. *Clin Gastroenterol Hepatol* 2006; **4**: 369–80.

4 Gao J, Xie L, Yang WS et al. Risk factors of hepatocellular carcinoma – current status and perspectives. *Asian Pac J Cancer Prev* 2012; **13**: 743–52.

5 Okuda H. Hepatocellular carcinoma development in cirrhosis. *Best Pract Res Clin Gastroenterol* 2007; **21**: 161–73.

6 Thomas MB, Zhu AX. Hepatocellular carcinoma: the need for progress. *J Clin Oncol* 2005; **23**: 2892–9.

7 Bruix J, Sala M, Llovet JM. Chemoembolization for hepatocellular carcinoma. *Gastroenterology* 2004; **127**(Suppl 1): S179–S188.

8 Bruix J, Sherman M. Practice Guidelines Committee American Association for the Study of Liver Diseases. Management of hepatocellular carcinoma. *Hepatology* 2005; **42**: 1208–36.

9 Llovet JM, Burroughs A, Bruix J. Hepatocellular carcinoma. *Lancet* 2003; **362**: 1907–17.

10 National Comprehensive Cancer Network. NCCN Clinical Practice Guidelines in Oncology: Hepatobiliary Cancers (Version 2.2013). http://www.nccn.org/professionals/physician_gls/pdf/hepatobiliary.pdf. 2012 (accessed June 2013).

11 Cheng AL, Kang YK, Chen Z et al. Efficacy and safety of sorafenib in patients in the Asia-Pacific region with advanced hepatocellular carcinoma: a phase III randomised, double-blind, placebo-controlled trial. *Lancet Oncol* 2009; **10**: 25–34.

12 Llovet JM, Ricci S, Mazzaferro V et al. Sorafenib in advanced hepatocellular carcinoma. *N Engl J Med* 2008; **359**: 378–90.

13 Bruix J, Sherman M. Management of hepatocellular carcinoma: an update. *Hepatology* 2011; **53**: 1020–2.

14 Lencioni R, Marrero J, Venook A, Ye SL, Kudo M. Design and rationale for the non-interventional Global Investigation of therapeutic DEcisions in hepatocellular carcinoma and Of its treatment with sorafeNib (GIDEON) study. *Int J Clin Pract* 2010; **64**: 1034–41.

15 Ozenne V, Paradis V, Pernot S et al. Tolerance and outcome of patients with unresectable hepatocellular carcinoma treated with sorafenib. *Eur J Gastroenterol Hepatol* 2010; **22**: 1106–10.

16 Lencioni R, Kudo M, Ye SL et al. First interim analysis of the GIDEON (Global Investigation of therapeutic DEcisions in hepatocellular carcinoma and Of its treatment with sorafeNib) non-interventional study. *Int J Clin Pract* 2012; **66**: 675–83.

17 Marrero J, Venook A, Kudo M et al. Second interim analysis of GIDEON (Global Investigation of therapeutic DEcisions in unresectable hepatocellular carcinoma and Of its treatment with sorafeNib): subgroup analysis by initial sorafenib dose. Abstract 2192 presented at the Liver Meeting 2011 – The 62nd Annual Meeting of the American Association for the Study of Liver Diseases, San Francisco, CA, USA, 4–8 November 2011.

18 Marrero JA, Lencioni R, Kudo M et al. Global Investigation of therapeutic DEcisions in hepatocellular carcinoma and Of its treatment with sorafeNib (GIDEON) second interim analysis in more than 1,500 patients: clinical findings in patients with liver dysfunction. *J Clin Oncol* (*Meeting Abstracts*) 2011; **29**: abs 4001.

19 Lencioni R, Venook A, Marrero J et al. Second interim results of the GIDEON (Global Investigation of therapeutic DEcisions in HCC and Of its treatment with sorafeNib) study: Barcelona Clinic Liver Cancer (BCLC) stage subgroup analysis. Abstract 6500 presented at the ECCO-ESMO, Stockholm, Sweden, 23–27 September 2011.

20 European Medicines Agency. EUDRALEX: the rules governing medicinal products in the European Union. http://ec.europa.eu/enterprise/newsroom/cf/itemdetail.cfm?&item_id=897. 2013 (accessed June 2013).

21 Farinati F, Rinaldi M, Gianni S, Naccarato R. How should patients with hepatocellular carcinoma be staged? Validation of a new prognostic system. *Cancer* 2000; **89**: 2266–73.

22 Tandon P, Garcia-Tsao G. Prognostic indicators in hepatocellular carcinoma: a systematic review of 72 studies. *Liver Int* 2009; **29**: 502–10.

23 Pons F, Varela M, Llovet JM. Staging systems in hepatocellular carcinoma. *HPB (Oxford)* 2005; **7**: 35–41.

24 Iavarone M, Cabibbo G, Piscaglia F et al. Field-practice study of sorafenib therapy for hepatocellular carcinoma: a prospective multicenter study in Italy. *Hepatology* 2011; **54**: 2055–63.

Paper received July 2013, accepted October 2013

subgroup analysis was limited, by our calculations rs12979860-CC genotype was significantly associated with treatment response in each arm of the trial ($P = 0.04$, Fisher's exact test; Fig. 1).

It appears, therefore, that a very high proportion of patients with a favorable host genotype who meet the selection criteria for this trial will achieve SVR with 24 weeks of peg-interferon-α/ribavirin alone. Otherwise similar patients with an unfavorable host genotype are less likely to respond to that regimen. Additional data, ideally based on genotype for *IFNL4*-ΔG, are needed to provide more precise estimates in that group.

Patients who are very likely to respond to a shortened course of peg-interferon-α/ribavirin may be more willing to undergo such treatment now rather than await development of interferon-free regimens. The authors assert host genotype has no role in identifying such patients once the HCV RNA level and RVR are considered.[1] Their data, however, indicate otherwise.

Acknowledgment: Supported by the Intramural Research Program of the National Institutes of Health (National Cancer Institute, Division of Cancer Epidemiology and Genetics). The content of this publication does not necessarily reflect the views or policies of the Department of Health and Human Services, nor does mention of trade names, commercial products, or organizations imply endorsement by the U.S. Government.

Alan S. Wang, B.A.[1]
Ruth M. Pfeiffer, Ph.D.[2]
Timothy R. Morgan, M.D.[3]
Thomas R. O'Brien, M.D., MPH[1]
[1]*Infections and Immunoepidemiology Branch, Division of Cancer Epidemiology and Genetics, National Cancer Institute, Bethesda, MD*
[2]*Biostatistics Branch, Division of Cancer Epidemiology and Genetics, National Cancer Institute, Bethesda, MD*
[3]*Gastroenterology Service, VA Long Beach Healthcare System, Long Beach, CA, Division of Gastroenterology, University of California - Irvine, Irvine, CA*

References

1. Pearlman BL, Ehleben C. Hepatitis C genotype 1 virus with low viral load and rapid virologic response to peginterferon/ribavirin obviates a protease inhibitor. Hepatology 2014;59:71-77.
2. Balagopal A, Thomas DL, Thio CL. IL28B and the control of hepatitis C virus infection. Gastroenterology 2010;139:1865-1876.
3. Prokunina-Olsson L, Muchmore B, Tang W, Pfeiffer RM, Park H, Dickensheets H, et al. A variant upstream of IFNL3 (IL28B) creating a new interferon gene IFNL4 is associated with impaired clearance of hepatitis C virus. Nat Genet 2013;45:164-171.

View this article online at wileyonlinelibrary.com.
DOI 10.1002/hep.26771
Potential conflict of interest: Dr. O'Brien is an inventor on patent applications filed by the National Cancer Institute for the IFNL4-Δ*G (ss469415590) genotype-based test and for the IFNL4 protein. Dr. Morgan received grants from Bristol-Myers Squibb, Genentech, Gilead, Vertex, and Merck.*

Reply:

We appreciate Dahari and Cotler's interest in our findings. We agree that viral kinetics during the lead-in phase with peg-interferon-α/ribavirin (PEG/RBV) may enable individualization and prediction of a minimum therapy duration to effect a sustained virological response (SVR); we likewise agree that further studies would be necessary to confirm this approach.

We believe that Wang, Pfeiffer, and Morgan missed the point of our analysis regarding the interleukin (IL)−28B genotype. We do not dispute that relative to the non-CC subtype, CC conferred an advantage in terms of higher SVR rates (CC 97% and 97% versus non-CC 78% and 76% in double and triple therapy arms, respectively); however, in genotype 1-infected patients with low viral load at baseline who achieve aviremia at week 4 with PEG/RBV, there was no benefit in adding boceprevir, regardless of a patient's IL28B subtype. Although patients with the unfavorable subtype respond less well to therapy, for those patients with low viral load and RVR after lead-in with PEG/RBV there is still no advantage of adding a protease inhibitor.

Brian L. Pearlman, M.D.[1]
Carole M. Ehleben, Ph.D.[2]
[1]*Center for Hepatitis C, Atlanta Medical Center*
Medical College of Georgia
Emory School of Medicine
Atlanta, GA
[2]*Department of Graduate Medical Education*
Atlanta Medical Center
Atlanta, GA

View this article online at wileyonlinelibrary.com.
DOI 10.1002/hep.26777
Potential conflict of interest: Nothing to report.

Assessment for Retreatment (ART) Score for Repeated Transarterial Chemoembolization in Patients With Hepatocellular Carcinoma

To the Editor:

We read with great interest the article by Sieghart et al. published in Hepatology.[1] The authors developed a point scoring system, the Assessment for Retreatment (ART) with Transarterial Chemoembolization (TACE), to assist in decision making whether retreating hepatocellular carcinoma (HCC) patients with TACE. Patients with HCC who received at least two TACE sessions within 90 days were the subjects of their study. The ART score differentiated patients into two groups (0-1.5 points; ≥2.5 points) with distinct prognosis (median overall survival [OS]: 23.7 versus 6.6 months; $P < 0.001$). These results were confirmed in an external validation cohort (median OS: 27.6 versus 8.1 months; $P < 0.001$). They concluded that an ART score ≥2.5 prior to second TACE can be used to identify patients with a dismal prognosis who may not benefit from further TACE sessions. Provided that this objective scoring system is universally reproducible, it will be an epoch-making development in the differentiation of patients into those who will benefit from repeated TACE and those who will not.

Repeated TACE is more frequently performed in patients with HCC in Japan than in other regions. In addition, we sense that few patients in Japan receive a second TACE within 3 months. Therefore, we attempted a validation study in Japanese patients.

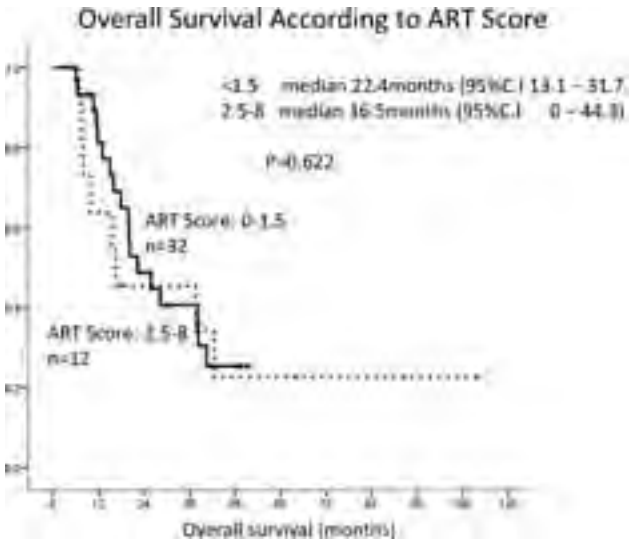

Fig. 1. Overall survival according to ART score. No significant difference was noted in overall survival between patients with an ART score of 0-1.5 points and those with an ART score of 2.5-8 ($P = 0.622$).

From 2004 to 2011, 513 patients with HCC underwent >2 TACE sessions. Among them, only 49 (9.6%) had two TACE sessions within 90 days. This is a marked difference from the Sieghart et al. report[1] (204 of 231 patients [88%] in Vienna and 224 of 252 patients [89%] in Innsbruck). More surprisingly, the ART score in 49 patients did not have any predictive impact on survival (Fig. 1).

Several possible explanations exist for the discrepancy between the Austrian and Japanese results. First, patients with intermediate-stage HCC constitute a heterogeneous population. For example, due to the established nationwide surveillance, Japanese patients who undergo TACE usually have fewer and smaller nodules than patients in other regions of the world. Second, superselective TACE, which leads to a complete response, is routinely performed in Japan. Third, in Sieghart et al.'s study,[1] the second TACE was performed 13-90 days after the first TACE. Performing a second TACE only 13 days after the first TACE suggests that the second TACE is already considered necessary after completion of the first TACE. This implies that their HCC patients had huge or bilobar advanced tumors. In Japan, such HCC cases are seldom encountered.

In conclusion, the ART score could be applied to only <10% of Japanese patients and then did not have any prognostic predictive impact on survival in these patients. Therefore, the ART score should not be considered a universal point-scoring system.

Masatoshi Kudo, M.D., Ph.D.
Tadaaki Arizumi, M.D.
Kazuomi Ueshima, M.D.
Department of Gastroenterology and Hepatology
Kinki University School of Medicine
Osaka-Sayama, Osaka, Japan

Reference

1. Sieghart W, Hucke F, Pinter M, Graziadei I, Vogel W, Muller C, et al. The ART of decision making: retreatment with transarterial chemoembolization in patients with hepatocellular carcinoma. Hepatology 2013;57:2261-2273.

View this article online at wileyonlinelibrary.com.
DOI 10.1002/hep.26760
Potential conflict of interest: Nothing to report.

Reply:

We read with interest the letter of Kudo et al. from one of the large Japanese series of patients undergoing transarterial chemoembolization (TACE), who tried to validate the Assessment for Retreatment (ART) score[1] in their patient sample. When the authors applied the same selection criteria to their 513 patients treated with >2 TACE procedures, only 49 patients were eligible for ART score-based analysis for having received two TACE procedures within 90 days (all others had longer intervals between TACE sessions) and the ART score was not able to differentiate between two prognostic groups.

Looking at the two ART score groups in the Japanese patient sample more closely, it is quite obvious that the Japanese low ART score group was very similar to our own European cohort (median survival 22.4 versus 23.7/27.6 months), while the big difference was in the high ART score group between Kudo et al.'s and our cohorts (median survival 16.5 versus 6.6/8.1 months). In trying to understand this, one would have to take a closer look at the patient characteristics in both cohorts.

First of all, the ART score does yield two groups with different survival in the Japanese patients as well, but the difference is much less pronounced than in the European patients and did not reach statistical significance. This could well be due to the small patient number in this analysis, which was only performed in 44 of the 49 patients (see fig. 1 of Kudo et al.). Regarding the overall small sample size (n = 49), the unexplained exclusion of 10% of patients may have had a significant impact on survival analysis.

Besides that, and as pointed out by the authors, there are obvious differences in the patient and procedural characteristics between European and Japanese centers. In particular, Japanese patients usually present with smaller tumors due to nationwide screening programs and the TACE procedure is often carried out more meticulously than in European centers, allowing for less frequent TACE procedures and supposedly longer survival in patients undergoing TACE in Japan.[2] This could potentially introduce a special selection bias, as indicated by the fact that less than 10% of Kudo et al.'s cohort was eligible for ART score calculation compared to almost 90% in the Austrian cohorts. But for a universally applicable score, these differences should be taken care of by diverting a different fraction of patients into the appropriate prognostic group. Surprisingly, this was not the case as much as we would expect: despite presumably smaller tumors and a more selective TACE procedure, still 27.3% of the Japanese patients retreated with TACE within 3 months presented with a high ART score before TACE 2, not so different from the 38% in the Austrian cohort.

Considering that overall survival in TACE patients seems to be longer in Japan compared to Europe,[2] it is not so much the longer survival in the Japanese high ART score group but the surprisingly low survival in the Japanese low ART score group that is hard to explain. Since we do not have any data on the BCLC-staging, Child-Pugh scores, which type of Child-Pugh score was applied, the differences in etiology of liver disease, the reason for performing a second TACE within 3 months, causes of death, total number of TACE cycles applied, etc., in the Japanese patients, it is impossible to reach any firm conclusions from the data presented by Kudo et al. In particular, BCLC-stage A could be much more prevalent in Japan, where cadaveric liver transplantation is very rare and living donors will likely not be able to fill in the demand, leaving more BCLC-A patients for TACE compared to Europe.

With such a small patient number, it is conceivable that there was a significant imbalance between baseline variables in the Japanese cohort, e.g., BCLC-stage A in high ART score versus B in low ART score, which would have a major impact on survival.

Liver Cancer

Liver Cancer 2014;3:68–70
DOI: 10.1159/000343862
Published online: May 8, 2014

2235-1795/14/0032-0068$39.50/0
www.karger.com/lic

Editorial

Recent Advances in Bioinformatics Reveal the Molecular Heterogeneity of Hepatocellular Carcinoma

Prof. M. Kudo

Editor *Liver Cancer*

Bioinformatics is an academic field that manages information about materials and substances essential for the biological activities of genes, proteins, and RNA. Bioinformatics enables vast amounts of biological data to be made available for statistical analysis to improve our understanding, diagnosis, and treatment of diseases. In recent years, genome-wide association studies (GWAS) and next-generation DNA sequencing technology have made it possible to generate large amounts of data very quickly. Consequently, the biggest challenge today is to extract clinically useful data from overwhelmingly large datasets, and this challenge has become a major research objective in the field of bioinformatics. A key example is that these techniques made it possible to achieve the long-held goal of molecular classification of hepatocellular carcinoma (HCC) [1, 2](fig. 1).

In 2011, the National Cancer Center of Japan achieved a world first by the whole-genome sequencing of HCC using next-generation sequencers [3], and this was successively followed by reports of whole-genome and exome sequencing of HCC by both Japanese and overseas research groups [4–8]. However, in contrast to the well-known high-frequency mutations of epidermal growth factor receptor genes and the anaplastic-lymphoma-kinase fusion gene in lung adenocarcinoma, the whole-genome sequence of HCC revealed the presence of low-frequency mutations in various genes but no single driver mutation, thereby practically ruling out the possibility that HCC is caused by a single driver mutation. However, since such vast amounts of bioinformatic data are now readily available to clinicians, we believe that if the correct approaches are taken, it is only a matter of time before a paradigm-shattering concept buried deep in bioinformatic data will be found that will revolutionize medical care.

In the field of bioinformatics, a very wide range of applications is possible; for example, it can be used to predict tumor malignancy, optimal treatments, and prognosis. Also, GWAS data are useful for predicting drug sensitivity and adverse effects. This is truly the dawn of the era of individualized medicine, and the application of bioinformatics in the field of oncology is already forging a path to this goal.

KARGER

Liver Cancer 2014;3:68–70
DOI: 10.1159/000343862
Published online: May 8, 2014

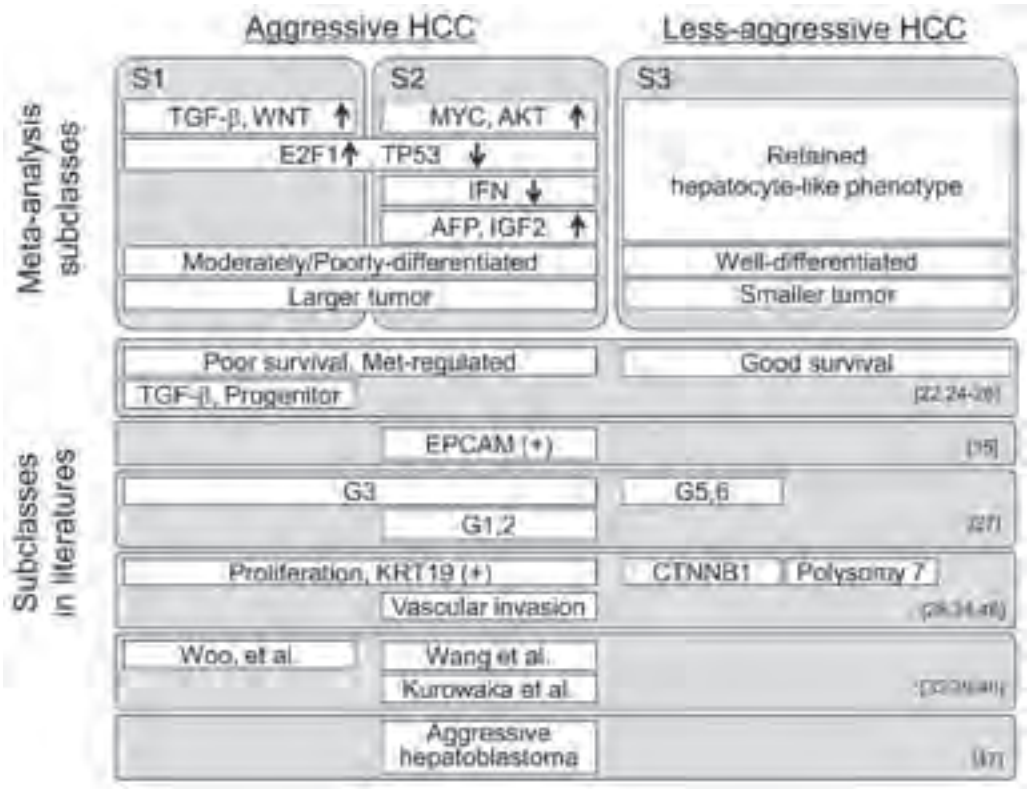

Fig.1. Molecular Classification of Hepatocellular Carcinoma. Reproduced with permission from Hoshida et al.[2].

Work on cancer stem cells continues to attract great attention [9]. It has been reported that approximately 40–50% of HCC cases exhibit stem cell-like features. Similar to colorectal cancer, a small population of so-called well-differentiated liver cancers may even possess stem cell-like characteristics. On the other hand, several studies have shown that prognosis is poor for HCC expressing Sal-like protein 4 (SALL4) [10–12], a transcription factor and stem-cell marker. Interestingly, knock-down of this single gene transforms the gene expression pattern of HCC cell lines from a stem cell-like pattern to a mature parenchymal cell-like pattern [11]. Some groups have started to report the clinical efficacy of DNA methylation and histone deacetylation inhibitors in SALL4-positive HCC [13]. Is it possible, then, to treat a large population of HCC cells by rewriting genetic information in the epigenome even if no single driver mutation is found? Since the study of SALL4 has just begun, we look forward to future developments in this area.

The field of bioinformatics is still at an early stage of development, and more studies are needed to establish its importance and significance; nonetheless, it clearly has the potential to revolutionize medical care.

References

▶1 Hoshida Y, Nijman SM, Kobayashi M, Chan JA, Brunet JP, Chiang DY, Villanueva A, Newell P, Ikeda K, Hashimoto M, Watanabe G, Gabriel S, Friedman SL, Kumada H, Llovet JM, Golub TR: Integrative transcriptome analysis reveals common molecular subclasses of human hepatocellular carcinoma. Cancer Res 2009;69:7385–7392.

Liver Cancer 2014;3:68–70
DOI: 10.1159/000343862
Published online: May 8, 2014

2 Hoshida Y, Toffanin S, Lachenmayer A, Villanueva A, Minguez B, Llovet JM: Molecular classification and novel targets in hepatocellular carcinoma: recent advancements. Semin Liver Dis 2010;30:35–51.
3 Totoki Y, Tatsuno K, Yamamoto S, Arai Y, Hosoda F, Ishikawa S, Tsutsumi S, Sonoda K, Totsuka H, Shirakihara T, Sakamoto H, Wang L, Ojima H, Shimada K, Kosuge T, Okusaka T, Kato K, Kusuda J, Yoshida T, Aburatani H, Shibata T: High-resolution characterization of a hepatocellular carcinoma genome. Nat Genet 2011;43:464–469.
4 Huang J, Deng Q, Wang Q, Li KY, Dai JH, Li N, Zhu ZD, Zhou B, Liu XY, Liu RF, Fei QL, Chen H, Cai B, Zhou B, Xiao HS, Qin LX, Han ZG: Exome sequencing of hepatitis B virus-associated hepatocellular carcinoma. Nat Genet 2012;44:1117–1121.
5 Sung WK, Zheng H, Li S, Chen R, Liu X, Li Y, Lee NP, Lee WH, Ariyaratne PN, Tennakoon C, Mulawadi FH, Wong KF, Liu AM, Poon RT, Fan ST, Chan KL, Gong Z, Hu Y, Lin Z, Wang G, Zhang Q, Barber TD, Chou WC, Aggarwal A, Hao K, Zhou W, Zhang C, Hardwick J, Buser C, Xu J, Kan Z, Dai H, Mao M, Reinhard C, Wang J, Luk JM: Genome-wide survey of recurrent HBV integration in hepatocellular carcinoma. Nat Genet 2012;44:765–769.
6 Guichard C, Amaddeo G, Imbeaud S, Ladeiro Y, Pelletier L, Maad IB, Calderaro J, Bioulac-Sage P, Letexier M, Degos F, Clément B, Balabaud C, Chevet E, Laurent A, Couchy G, Letouzé E, Calvo F, Zucman-Rossi J: Integrated analysis of somatic mutations and focal copy-number changes identifies key genes and pathways in hepatocellular carcinoma. Nat Genet 2012;44:694–698.
7 Li M, Zhao H, Zhang X, Wood LD, Anders RA, Choti MA, Pawlik TM, Daniel HD, Kannangai R, Offerhaus GJ, Velculescu VE, Wang L, Zhou S, Vogelstein B, Hruban RH, Papadopoulos N, Cai J, Torbenson MS, Kinzler KW: Inactivating mutations of the chromatin remodeling gene ARID2 in hepatocellular carcinoma. Nat Genet 2011;43:828–829.
8 Fujimoto A, Totoki Y, Abe T, Boroevich KA, Hosoda F, Nguyen HH, Aoki M, Hosono N, Kubo M, Miya F, Arai Y, Takahashi H, Shirakihara T, Nagasaki M, Shibuya T, Nakano K, Watanabe-Makino K, Tanaka H, Nakamura H, Kusuda J, Ojima H, Shimada K, Okusaka T, Ueno M, Shigekawa Y, Kawakami Y, Arihiro K, Ohdan H, Gotoh K, Ishikawa O, Ariizumi S, Yamamoto M, Yamada T, Chayama K, Kosuge T, Yamaue H, Kamatani N, Miyano S, Nakagama H, Nakamura Y, Tsunoda T, Shibata T, Nakagawa H: Whole-genome sequencing of liver cancers identifies etiological influences on mutation patterns and recurrent mutations in chromatin regulators. Nat Genet 2012;44:760–764.
9 Yamashita T, Ji J, Budhu A, Forgues M, Yang W, Wang HY, Jia H, Ye Q, Qin LX, Wauthier E, Reid LM, Minato H, Honda M, Kaneko S, Tang ZY, Wang XW: EpCAM-positive hepatocellular carcinoma cells are tumor-initiating cells with stem/progenitor cell features. Gastroenterology 2009;136:1012–1024.
10 Oikawa T, Kamiya A, Kakinuma S, Zeniya M, Nishinakamura R, Tajiri H, Nakauchi H: Sall4 regulates cell fate decision in fetal hepatic stem/progenitor cells. Gastroenterology 2009;136:1000–1011.
11 Oikawa T, Kamiya A, Zeniya M, Chikada H, Hyuck AD, Yamazaki Y, Wauthier E, Tajiri H, Miller LD, Wang XW, Reid LM, Nakauchi H: Sal-like protein 4 (SALL4), a stem cell biomarker in liver cancers. Hepatology 2013;57:1469–1483.
12 Yong KJ, Gao C, Lim JS, Yan B, Yang H, Dimitrov T, Kawasaki A, Ong CW, Wong KF, Lee S, Ravikumar S, Srivastava S, Tian X, Poon RT, Fan ST, Luk JM, Dan YY, Salto-Tellez M, Chai L, Tenen DG: Oncofetal gene SALL4 in aggressive hepatocellular carcinoma. N Engl J Med 2013;368:2266–2276.
13 Zeng SS, Yamashita T, Kondo M, Nio K, Hayashi T, Hara Y, Nomura Y, Yoshida M, Hayashi T, Oishi N, Ikeda H, Honda M, Kaneko S: The transcription factor SALL4 regulates stemness of EpCAM-positive hepatocellular carcinoma. J Hepatol 2014;60:127–134.

MOLECULAR CANCER

RESEARCH Open Access

Homozygous deletion of the activin A receptor, type IB gene is associated with an aggressive cancer phenotype in pancreatic cancer

Yosuke Togashi[1], Hiroki Sakamoto[2], Hidetoshi Hayashi[1], Masato Terashima[1], Marco A de Velasco[1], Yoshihiko Fujita[1], Yasuo Kodera[1], Kazuko Sakai[1], Shuta Tomida[1], Masayuki Kitano[2], Akihiko Ito[3], Masatoshi Kudo[2] and Kazuto Nishio[1*]

Abstract

Background: Transforming growth factor, beta (TGFB) signal is considered to be a tumor suppressive pathway based on the frequent genomic deletion of the *SMAD4* gene in pancreatic cancer (PC); however; the role of the activin signal, which also belongs to the TGFB superfamily, remains largely unclear.

Methods and results: We found a homozygous deletion of the activin A receptor, type IB (*ACVR1B*) gene in 2 out of 8 PC cell lines using array-comparative genomic hybridization, and the absence of *ACVR1B* mRNA and protein expression was confirmed in these 2 cell lines. Activin A stimulation inhibited cellular growth and increased the phosphorylation level of SMAD2 and the expression level of $p21^{CIP1/WAF1}$ in the Sui66 cell line (wild-type *ACVR1B* and *SMAD4* genes) but not in the Sui68 cell line (homozygous deletion *of ACVR1B* gene). Stable *ACVR1B*-knockdown using short hairpin RNA cancelled the effects of activin A on the cellular growth of the PC cell lines. In addition, *ACVR1B*-knockdown significantly enhanced the cellular growth and colony formation abilities, compared with controls. In a xenograft study, *ACVR1B*-knockdown resulted in a significantly elevated level of tumorigenesis and a larger tumor volume, compared with the control. Furthermore, in clinical samples, 6 of the 29 PC samples (20.7%) carried a deletion of the *ACVR1B* gene, while 10 of the 29 samples (34.5%) carried a deletion of the *SMAD4* gene. Of note, 5 of the 6 samples with a deletion of the *ACVR1B* gene also had a deletion of the *SMAD4* gene.

Conclusion: We identified a homozygous deletion of the *ACVR1B* gene in PC cell lines and clinical samples and proposed that the deletion of the *ACVR1B* gene may mediate an aggressive cancer phenotype in PC. Our findings provide novel insight into the role of the activin signal in PC.

Keywords: Pancreatic cancer, Activin signal, Activin A receptor, Type IB, SMAD4

Background

Pancreatic cancer (PC) is a devastating disease. Gemcitabine has been the standard therapy for experimental regimens in patients with advanced PC for over a decade, but recently, the overall survival has been significantly prolonged using combination therapies, such as gemcitabine plus erlotinib or a combination of oxaliplatin, irinotecan, fluorouracil and leucovorin (FOLFIRINOX) [1-3]. Despite some recent progress, however, the overall survival rate of patients with PC is still less than 5% [4]. The model explaining the progression of PC is influenced by multiple genetic alterations. During early genetic events, such as activating point mutations in the *K-ras* oncogene and the overexpression of the *HER-2/neu* gene, pancreatic duct lesions show minimal cytological and architectural atypia. The inactivation of the *p16* tumor suppressor gene appears to occur at a later stage, followed by the loss of the *p53*, *SMAD4*, and *BRCA2* tumor suppressor genes [5-8]. For instance, the *HER-2/neu* gene is not expressed in the epithelium lining of normal pancreatic duct, but it is highly expressed in pancreatic intraepithelial neoplasia [9]. However, two clinical trials assessing anit-HER2 trastuzumab

* Correspondence: knishio@med.kindai.ac.jp
[1]Department of Genome Biology, Kinki University Faculty of Medicine, 377-2 Ohno-higashi, Osaka-Sayama, Osaka 589-8511, Japan
Full list of author information is available at the end of the article

therapy in patients with PC overexpressing HER2 have produced disappointing results [10,11]. Although such recent breakthroughs in the molecular biology of PC have assisted in translational research, creating hope for individualized therapy and better disease management, the inhibition of epidermal growth factor receptor using erlotinib is, to date, the only targeted approach that has been demonstrated to result in a survival [1]. Therefore, further understanding of the molecular biology of PC is needed.

The transforming growth factor, beta (TGFB) receptor II (*TGFBR2*) and *SMAD4* genes are commonly inactivated in several types of cancer, providing evidence that the TGFB signal functions as a tumor suppressor [12,13]. Thirty percent of colorectal cancers are thought to contain a mutation in the *TGFBR2* gene. The human locus 18q21, which encodes the *SMAD2* and *SMAD4* genes, is often mutated or lost completely in several cancers. The loss of the *SMAD4* gene eliminates the classic SMAD2/3/4 heteromeric complexes that have been implicated in a large number of TGFB-dependent transcriptional regulatory complexes. As a result, TGFB-mediated growth inhibition is lost. The *SMAD4* gene is inactivated in 55% of PC tumors, and numerous studies on TGFB signal in PC have been reported. The loss of the *SMAD4* gene is correlated with both a poor prognosis and the development of widespread metastases in patients. The *TGFBR2* gene is also altered in a smaller subset of PC tumors [5-7,14,15]. In addition, pancreatic-specific *TGFBR2* or *SMAD4*-knockout mice with active *K-ras* expression developed PC [16,17]. However, the roles of defects other than those in the *SMAD4* and *TGFBR2* genes in PC remain unclear, and few studies regarding the activin signal, which also belongs to the TGFB superfamily, have been reported [18-20]. Defects in several genes involved in the activin signal pathway have been characterized in several cancers. For instance, two 8-bp polyadenine tracts in the activin A receptor, type IIA (*ACVR2A*) gene were reported to be targets for frameshift mutations in gastrointestinal cancers with microsatellite instability [21]. Similarly, the activin signal induces growth inhibition and apoptosis mainly through SMAD-dependent pathways in many other cancers [22-27]. Thus, the dysregulation of the activin signal is directly involved in carcinogenesis. In contrast, however, a recent study has demonstrated that Nodal/Activin signal is associated with self-renewal and the tumorigenicity of PC stem cells [20]; thus, the role of activin signal in pancreatic carcinogenesis remains controversial. In the present study, we identified a homozygous deletion of the activin A receptor, type IB (*ACVR1B*) gene in PC cell lines using array-comparative genomic hybridization (array-CGH). Furthermore, we investigated the role of this homozygous deletion in PC cell lines and the status of the *ACVR1B* gene in clinical samples of PC.

Results

Identification of homozygous deletion of *ACVR1B* gene in PC cell lines

The results of an array-CGH demonstrated the homozygous deletion of the *ACVR1B* gene in the Sui65 and Sui68 cell lines (chromosome 12) and the homozygous deletion of the *SMAD4* gene in the Sui65, Sui70, and Sui71 cell lines (chromosome 18) (Figure 1A and B). No deletions of other SMAD genes or other main TGFB and activin receptors, including the *TGFBR1, TGFBR2, ACVR2A, ACVR2B, SMAD2* genes, were found. To examine the *ACVR1B* and *SMAD4* gene copy numbers in the PC cell lines, we used a real-time PCR-based detection method, the TaqMan Copy Number Assay, and the experiment was performed in triplicate. The copy number results are summarized in Table 1. The copy number of the *ACVR1B* gene in the Sui68 cell line was 0 and that in the Sui65 cell line was nearly 0 (0.115 ± 0.025). The copy numbers of the *SMAD4* gene in the Sui65, Sui70, and Sui71 cell lines were all 0. These results were similar to those of the array-CGH.

mRNA and protein expressions of ACVR1B and SMAD4 in PC cell lines

To examine the mRNA expressions of the *ACVR1B* and *SMAD4* genes, we performed real-time reverse transcription PCR (RT-PCR) using samples of normal pancreatic tissue from Clontech and PC cell lines. *ACVR1B* mRNA was scarcely expressed in the Sui65 and Sui68 cell lines, and *SMAD4* mRNA was also scarcely expressed in the Sui65, Sui70, and Sui71 cell lines (Figure 2A). These results were similar to those for the array-CGH and copy number assay (Table 1). Western blot analyses were performed and showed that ACVR1B was scarcely expressed in the Sui65 and Sui68 cell lines and that SMAD4 was scarcely expressed in the Sui65, Sui70, and Sui71 cell lines. The protein expressions of ACVR1B and SMAD4 reflected the mRNA expression levels (Figure 2B).

Influence of activin A on cellular growth and cell cycle in PC cell lines

To examine the influence of ligands in the PC cell lines, we performed cellular growth assays using the Sui65 (homozygous deletion of *ACVR1B* and *SMAD4* genes), Sui66, Sui73 (wild-type *ACVR1B* and *SMAD4* genes), Sui68 (homozygous deletion of *ACVR1B* gene and wild-type *SMAD4* gene), and Sui70 (wild-type *ACVR1B* and homozygous deletion of *SMAD4* gene) cell lines in the presence of ligands. Based on numerous previous studies and our data on cellular growth inhibition [22,28], we used concentrations of 0.1, 1, or 10 ng/mL of TGFB1 or 1, 10, or 100 ng/mL of activin A. TGFB1 inhibited cellular growth in the Sui66, Sui68, and Sui73 cell lines (Figure 3B, C, and D). Activin A did not influence cellular

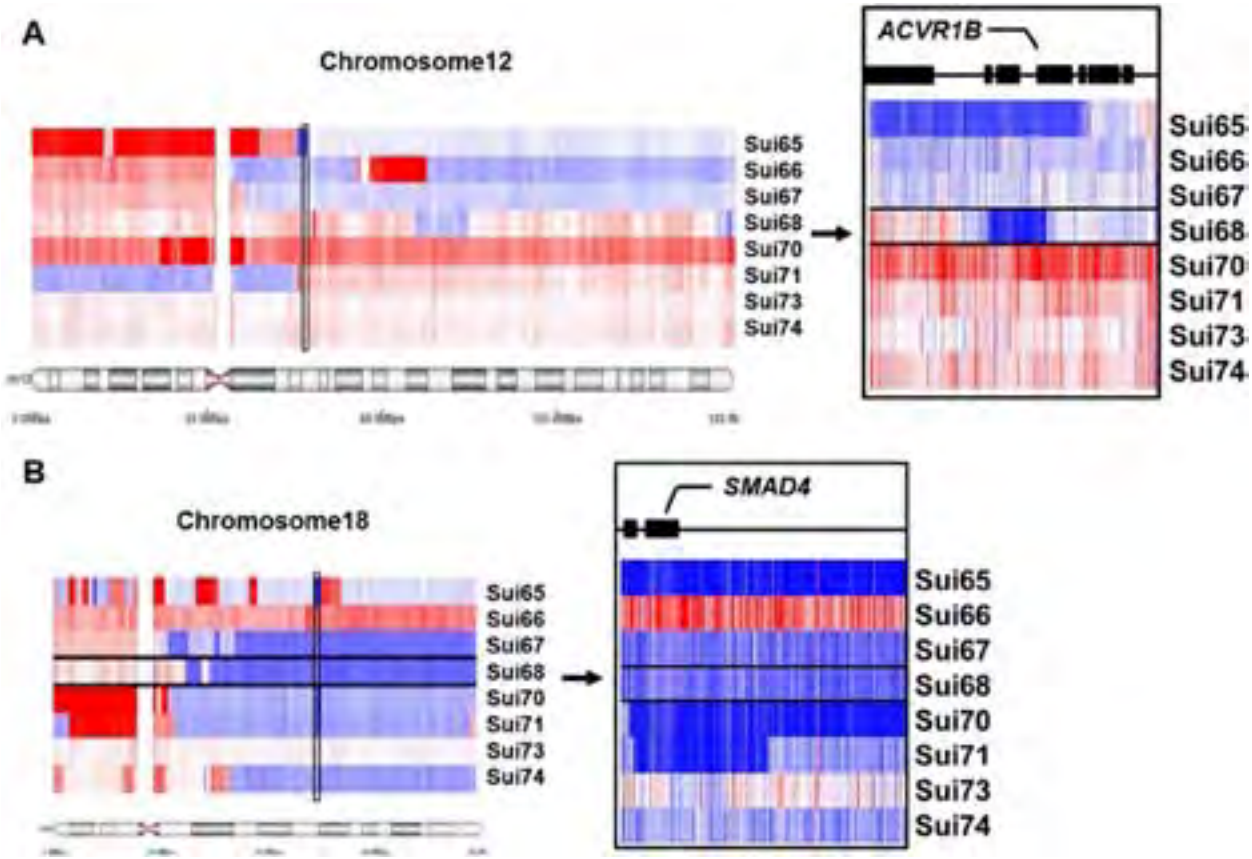

Figure 1 Array-CGH of PC cell lines. A gain (>4 copies, red) and a deletion (<0.5 copies, blue) of genomic copy number are shown. **(A)** Array-CGH of chromosome 12. The homozygous deletion of the *ACVR1B* gene was found in the Sui65 and Sui68 cell lines. **(B)** Array-CGH of chromosome 18. The homozygous deletion of the *SMAD4* gene was found in the Sui65, Sui70, and Sui71 cell lines.

Table 1 Cell line characteristics and the status of ACVR1B and SMAD4

Cell lines	Source	Histology	ACVR1B		SMAD4	
			CN	Expression	CN	Expression
Sui65	Peritoneum	Tubular	0	-	0	-
Sui66	Pancreas	Tubular	1	+	2	++
Sui67	Pancreas	Tubular	1	-	1	+
Sui68	Pancreas	Ad	0	-	1	+
Sui70	Pancreas	Ad	2	+	0	-
Sui71	Liver	Ad	1	+	0	-
Sui73	Pancreas	Tubular	2	+	2	+
Sui74	Pancreas	Tubular	1	+	1	-

ACVR1B, activin receptor A, type IB; Tubular, tubular adenocarcinoma; Ad, adenocarcinoma; CN, gene copy number.
Legend: The copy numbers of the *ACVR1B* gene in the Sui65 and Sui68 cell line was 0, and the copy numbers of the *SMAD4* gene in the Sui65, Sui70, and Sui71 cell lines were all 0. *ACVR1B* mRNA was scarcely expressed in the Sui65 and Sui68 cell lines, and *SMAD4* mRNA was also scarcely expressed in the Sui65, Sui70, and Sui71 cell lines. These results were similar to those for the copy number assay.

growth in the Sui65 and Sui68 cell lines (Figure 3A and C), although it inhibited cellular growth in the Sui66 and Sui73 cell lines (Figure 3B and D). In addition, the Sui70 cell line was not influenced by either TGFB1 or activin A (Additional file 1A).

Next, cell cycle distribution analyses were also performed. Both TGFB1 and activin A increased the proportion of cells in the G0/G1 phase and decreased the proportion of cells in the S phase in the Sui66 and Sui73 cell line (Figure 4B and D). In the Sui68 cell line, however, TGFB1 increased the proportion of cells in the G0/G1 phase and decreased the proportion of cells in the S phase, while activin A did not affect the cell cycle distribution (Figure 4C). In the Sui65 cell line, activin A did not affect the cell cycle distribution, either (Figure 4A). These results indicate that activin A inhibits cellular growth and induces G1 phase cell arrest in PC cell lines with wild-type *ACVR1B*, while activin A does not inhibit cellular growth and does not influence the cell cycle in cell lines with a homozygous deletion of the *ACVR1B* gene.

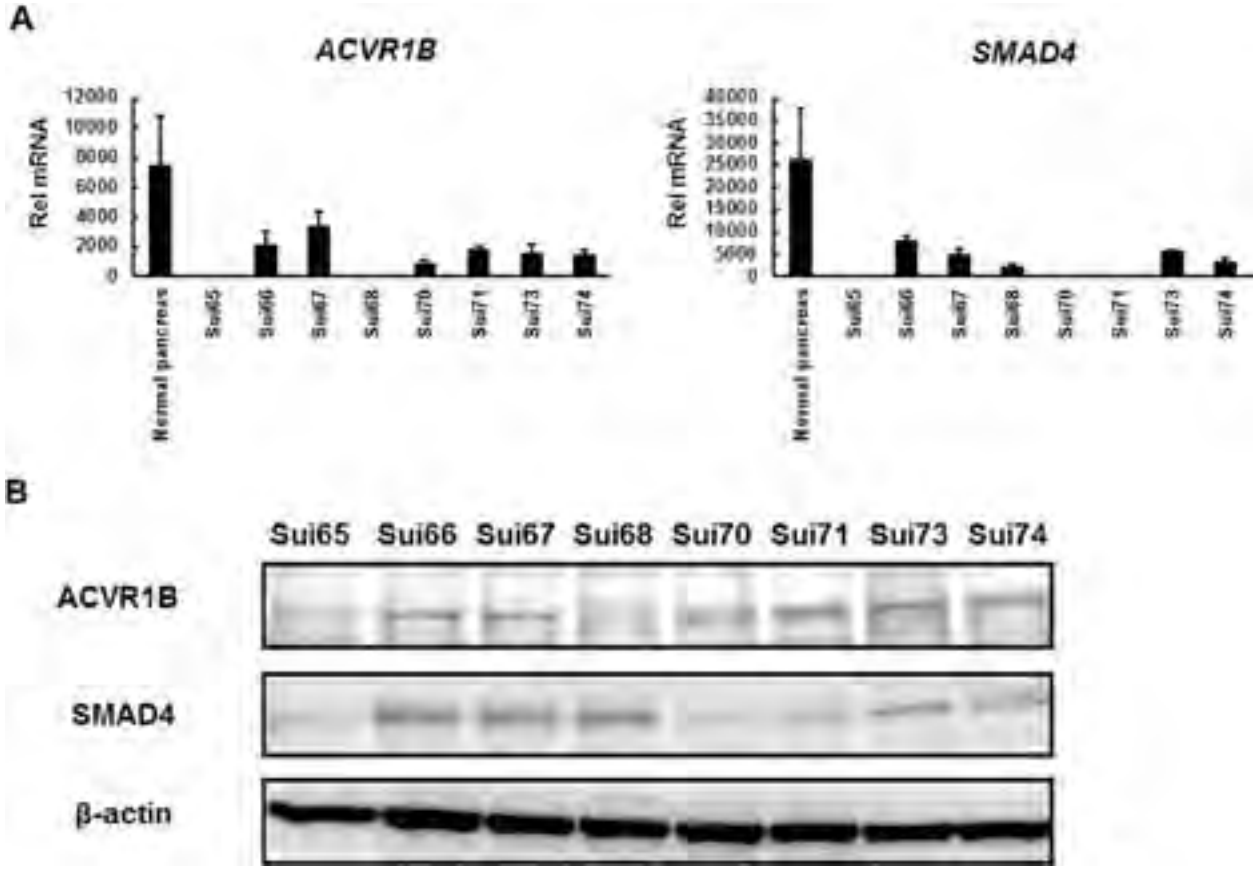

Figure 2 Expression of *ACVR1B* and *SMAD4* in PC cell lines. (A) mRNA expression levels of the *ACVR1B* and *SMAD4* genes in normal pancreatic tissue (RNA from Clontech) and PC cell lines. The expressions were analyzed using real-time RT-PCR. *ACVR1B* mRNA was scarcely expressed in the Sui65 and Sui68 cell lines, and *SMAD4* mRNA was also scarcely expressed in the Sui65, Sui70, and Sui71 cell lines. Rel mRNA, normalized mRNA expression levels (*ACVR1B* or *SMAD4*/*GAPD* × 10^6); Columns, mean of independent triplicate experiments; Bars, SD. **(B)** Western blot analysis of ACVR1B and SMAD4 in PC cell lines. ACVR1B was scarcely expressed in the Sui65 and Sui68 cell lines. SMAD4 was scarcely expressed in the Sui65, Sui70, and Sui71 cell lines. The findings confirmed the array-comparative genomic hybridization results. β-actin was used as an internal control.

Effect of activin A on SMAD2 phosphorylation and p21 induction in PC cell lines

Activin A inhibited the cellular growth of cell lines with wild-type *ACVR1B* and *SMAD4* genes; therefore, we examined the downstream signal under TGFB1 or activin A stimulation. Based on numerous previous studies and our data on cellular growth inhibition [22,28], we used 1 ng/mL of TGFB1 or 10 ng/mL of activin A. The time points were also decided based on the previous studies [22,28]. In the Sui66 cell line (wild-type *ACVR1B* and *SMAD4* genes), both TGFB1 and activin A increased the phosphorylation levels of SMAD2 (Figure 5A); these effects were cancelled by the ACVR1B/TGFBR1/ACVR1C-specific inhibitor SB431542 (Figure 5C). In the Sui68 cell line (homozygous deletion of *ACVR1B* gene and wild-type *SMAD4* gene), TGFB1, but not activin A, increased the phosphorylation levels of SMAD2 (Figure 5A); these effects were cancelled by SB431542 (Figure 5C). These results suggest that activin A activates the SMAD signal in a manner similar to TGFB1 in PC cell lines with the wild-type *ACVR1B* gene, but does not activate in PC cell lines with the homozygous deletion of the *ACVR1B* gene.

Next, we evaluated the expression levels of $p21^{CIP1/WAF1}$. $p21^{CIP1/WAF1}$ is a major cdk inhibitor and is a hallmark of the cytostatic role of the TGFB signal pathway [29]. TGFB and activin A are known to increase p21 expression [22,28]. The expression of p21 was evaluated in whole-cell lysates. p21 expression was increased by both TGFB1 and activin A in the Sui66 cell line. In the Sui68 cell line, however, its expression was increased only by TGFB1 (Figure 5B). Therefore, we speculated that p21 may have a role in activin A-mediated growth inhibition and cell-cycle progression.

To evaluate the effect of activin A on SMAD4-independent pathways, the phosphorylation of ERK1/2 and AKT, which are representative signals of SMAD4-independent pathways, was investigated in the Sui70 cell line (wild-type *ACVR1B* and homozygous deletion of *SMAD4* genes).

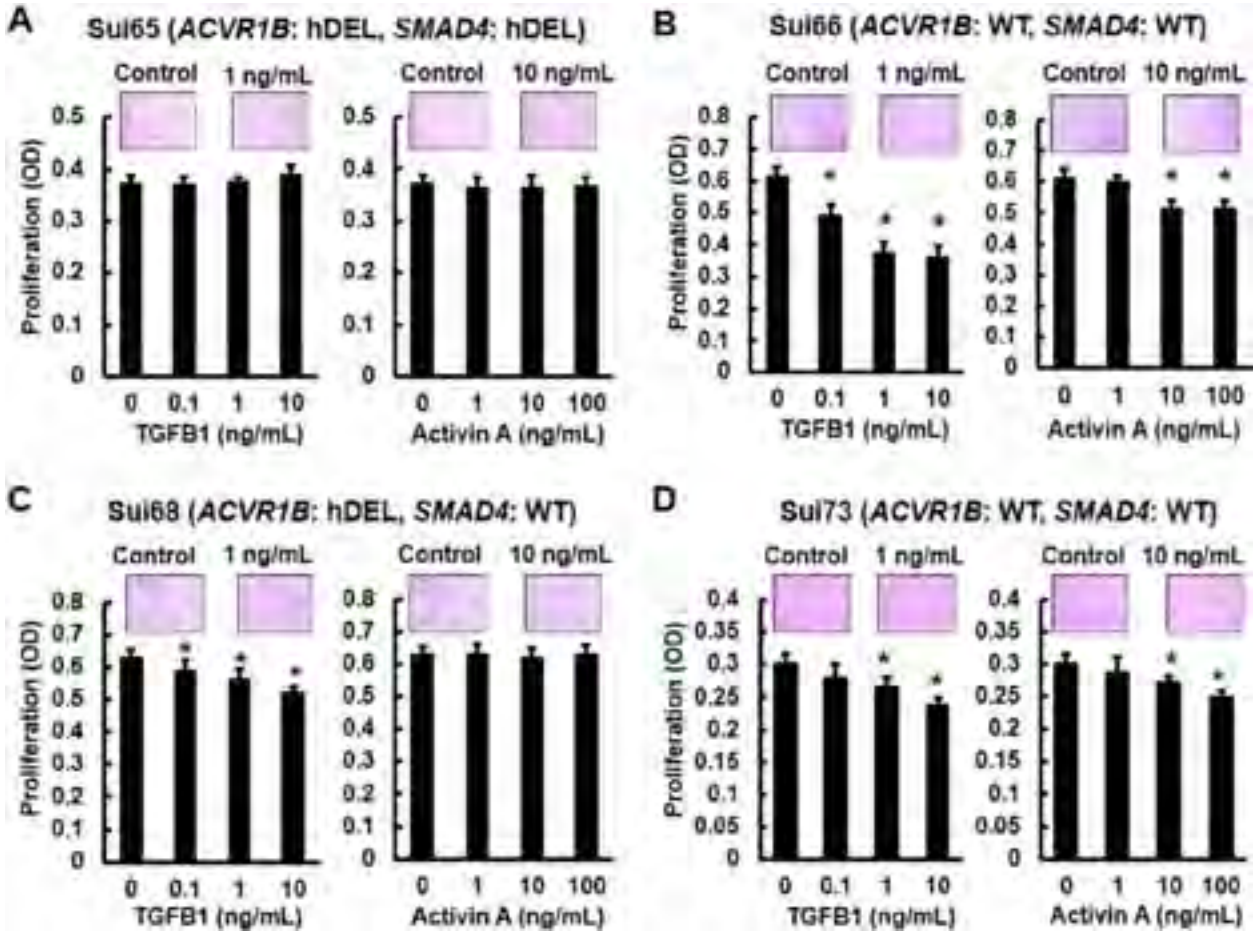

Figure 3 Influence of TGFB1 and activin A on cellular growth. The cells were stimulated with the indicated doses of TGFB1 or activin A for 72 hours. Cell proliferation was assayed using an MTT assay. **(A)** Cellular growth of Sui65 cell line (homozygous deletion of *ACVR1B* and *SMAD4* genes). Both TGFB1 (0.1 ng/mL, $P = 0.56$; 1 ng/mL, $P = 0.51$; 10 ng/mL, $P = 0.69$) and activin A (1 ng/mL, $P = 0.51$; 10 ng/mL, $P = 0.71$; 100 ng/mL, $P = 0.65$) did not influence the cellular growth. **(B)** Cellular growth of Sui66 cell line (wild-type *ACVR1B* and *SMAD4* genes). Both TGFB1 (0.1 ng/mL, $P = 0.0049$*; 1 ng/mL, $P = 0.0028$*; 10 ng/mL, $P = 0.0016$*) and activin A (1 ng/mL, $P = 0.051$; 10 ng/mL, $P = 0.010$*; 100 ng/mL, $P = 0.0081$*) inhibited cellular growth. **(C)** Cellular growth of Sui68 cell line (homozygous deletion of the *ACVR1B* gene and wild-type *SMAD4* gene). TGFB1 inhibited cellular growth (0.1 ng/mL, $P = 0.011$*; 1 ng/mL, $P = 0.013$*; 10 ng/mL, $P = 0.0039$*), but activin A did not influence the cellular growth (1 ng/mL, $P = 0.65$; 10 ng/mL, $P = 0.93$; 100 ng/mL, $P = 0.82$). **(D)** Cellular growth of Sui73 cell line (wild-type *ACVR1B* and *SMAD4* genes). As is seen in the Sui66 cell line, both TGFB1 (0.1 ng/mL, $P = 0.072$; 1 ng/mL, $P = 0.0087$*; 10 ng/mL, $P = 0.0066$*) and activin A (1 ng/mL, $P = 0.21$; 10 ng/mL, $P = 0.0018$*; 100 ng/mL, $P = 0.028$*) inhibited cellular growth. hDEL, homozygous deletion; WT, wild-type; Columns, mean of independent triplicate experiments; Bars, SD; *$P < 0.05$.

The phosphorylation was not changed by activin A (Additional file 1B). Particularly, both AKT and ERK1/2 were phosphorylated before the stimulations. The expression of p21 also remained unchanged.

Enhanced cellular growth and colony formation, but no response to activin A, of Sui66/shACVR1B and Sui73/shACVR1B cell lines

To evaluate the role of the *ACVR1B* gene, we examined the colony formation and the cellular growth of stable *ACVR1B*-knockdown cell lines (Sui66/shACVR1B-1, Sui66/shACVR1B-2, Sui73/shACVR1B-1, and Sui73/shACVR1B-2) or control cell lines (Sui66/shScr-1, Sui66/shScr-2, Sui73/shScr-1, and Sui73/shScr-2) (Figure 6A). Activin A did not increase the phosphorylation level of SMAD2 in the Sui66/shACVR1B-1, Sui66/shACVR1B-2, Sui73/shACVR1B-1, or Sui73/shACVR1B-2 cell lines (Figure 6A). Although activin A inhibited the cellular growth of the Sui66/shScr-1, Sui66/shScr-2, Sui73/shScr-1, and Sui73/shScr-2 cell lines, it did not influence the cellular growth of the Sui66/shACVR1B-1, Sui66/shACVR1B-2, Sui73/shACVR1B-1, or Sui73/shACVR1B-2 cell lines (Figure 6B). The colony formation and cellular growth of the Sui66/shACVR1B-1, Sui66/shACVR1B-2, Sui73/shACVR1B-1, and Sui73/shACVR1B-2 cell lines were also enhanced, compared with the controls (Figure 6C and D).

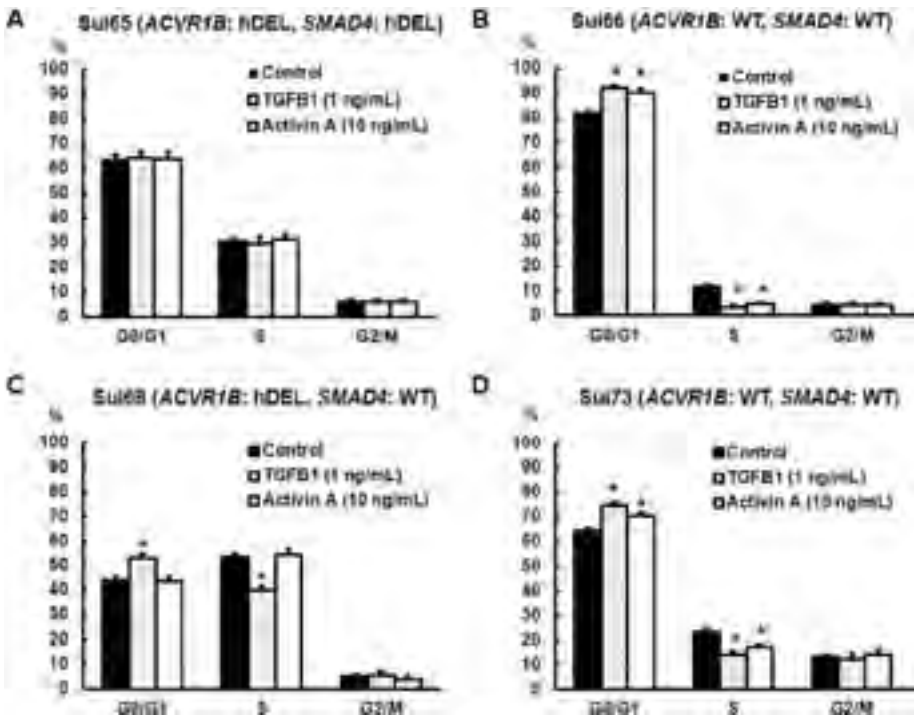

Figure 4 Influence of TGFB1 and activin A on the cell cycle. The cell lines were exposed to the ligands (TGFB1, 1 ng/mL; activin A, 10 ng/mL) for 48 hours. The cells were then stained using propidium iodide/RNase Staining Buffer and were analyzed using a flow cytometer. **(A)** Cell cycle distribution of Sui65 cell line (homozygous deletion of *ACVR1B* and *SMAD4* genes). Both TGFB1 and activin A did not influence the cell cycle distribution. **(B)** Cell cycle distribution of Sui66 cell line (wild-type *ACVR1B* and *SMAD4* genes). Both TGFB1 and activin A increased the proportion of cells in G0/G1 phase ($P = 0.0039$* and 0.031*, respectively) and decreased the proportion of cells in S phase ($P = 0.0043$* and 0.039*, respectively). **(C)** Cell cycle distribution of Sui68 cell line (homozygous deletion of the *ACVR1B* gene and wild-type *SMAD4* gene). TGFB1 increased the proportion of cells in G0/G1 phase ($P = 0.0016$*) and decreased the proportion of cells in S phase ($P = 0.019$*), while activin A did not influence the cell cycle distribution. **(D)** Cell cycle distribution of Sui73 cell line (wild-type *ACVR1B* and *SMAD4* genes). As is seen in the Sui66 cell line, both TGFB1 and activin A increased the proportion of cells in G0/G1 phase ($P = 0.014$* and 0.039*, respectively) and decreased the proportion of cells in S phase ($P = 0.0034$* and 0.0021*, respectively). hDEL, homozygous deletion; WT, wild-type; Columns, mean of independent triplicate experiments; Bars, SD; *$P < 0.05$.

These results indicate that the *ACVR1B* gene is involved in tumorigenicity and cellular growth.

Enhanced *in vivo* tumorigenicity and tumor growth of stable *ACVR1B*-knockdown cell lines

We evaluated the *in vivo* tumorigenicity of Sui66-transfectant cell lines and the tumor growth of Sui73-transfectant cell lines. Sui66/shACVR1B exhibited a significantly elevated level of tumorigenesis (Sui66/shScr-1 1/14 vs. Sui66/shACVR1B-1 8/14, $P = 0.013$ and Scr-2 2/14 vs. ACVR1B-2 10/14, $P = 0.0063$*), and Sui73/shACVR1B exhibited a larger tumor volume than Sui73/shScr (Sui73/Scr-1, 167.7 ± 59.1 mm^3 vs. Sui73/ACVR1B-1, 275.0 ± 56.3 mm^3; $P = 0.018$* on day 36 and Sui73Scr-2, 105.7 ± 27.2 mm^3 vs. Sui73/ACVR1B-2, 217.3 ± 81.8 mm^3; $P = 0.020$* on day 29, respectively). (Figure 7A and B). There was no significant difference in body weight (Sui73/Scr-1, 24.3 ± 1.0 g vs. Sui73/ACVR1B-1, 23.24 ± 1.5 g; $P = 0.22$ on day 36 and Sui73/Scr-2, 21.6 ± 1.3 g vs. Sui73/ACVR1B-2, 21.1 ± 1.8 g; $P = 0.61$ on day 29, respectively). According to western blot analyses of the tumors and immunostaining, the expressions of p21 were clearly elevated in the cancer cells in the shScr-inoculated tumors, compared with the expression levels in the shACVR1B cells (Figure 7C). In addition, the expressions of Ki67 were clearly elevated in the cancer cells in the shACVR1B-inoculated tumors (Figure 7C). These results indicate that the *ACVR1B* gene is involved in tumorigenicity and tumor growth and that it downregulated the expression level of p21 in cancer cells *in vivo*, similar to its effect *in vitro*.

Suppressed *in vitro* cellular growth and colony formation, and *in vivo* tumorigenicity of p21-overexpressed Sui68 cell line

To determine whether p21 expression reverses the phenotype of the *ACVR1B* gene homozygous deletion, we created a p21-overexpressed Sui68 cell line (homozygous deletion of *ACVR1B* gene and wild-type *SMAD4* gene) (Figure 8A). The colony formation and cellular growth of

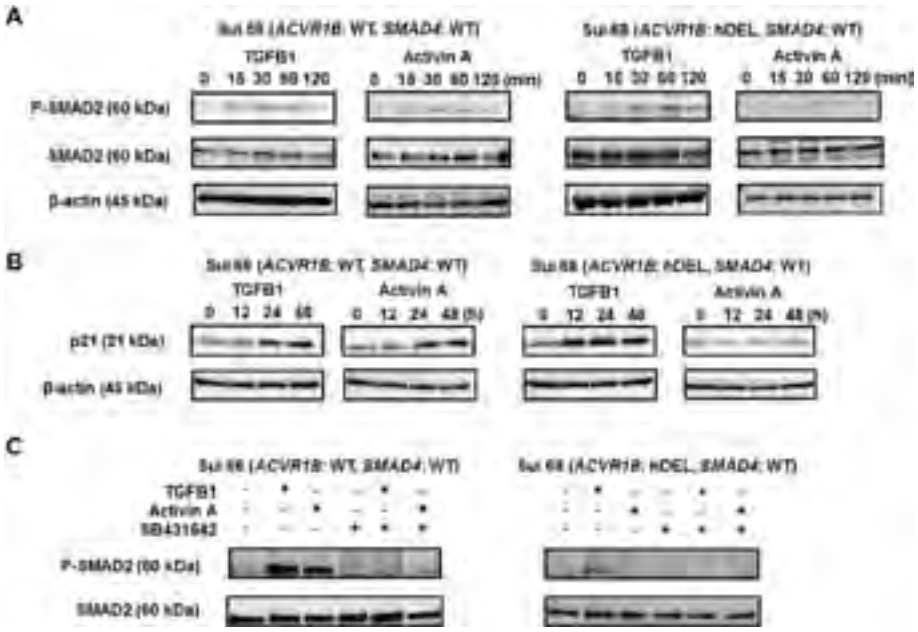

Figure 5 Western blot analyses using Sui66 and Sui68 cell lines. The cell lines were treated with or without 2 μM of SB431542 for 30 min, then stimulated with TGFB1 (1 ng/mL) or activin A (10 ng/mL). β-actin was used as an internal control. **(A)** Phosphorylation of SMAD2 in Sui66 (wild-type *ACVR1B* and *SMAD4* genes) and Sui68 (homozygous deletion of the *ACVR1B* gene and wild-type *SMAD4* gene) cell lines without SB431542. Both TGFB1 and activin A increased the phosphorylation levels of SMAD2 in Sui66 cell line. TGFB1 increased the phosphorylation level of SMAD2, but activin A did not influence phosphorylation in Sui68 cell line. **(B)** Expression of p21 in Sui66 and Sui68 cell lines without SB431542. The expression of p21 was evaluated in whole-cell lysates. Although p21 expression was increased by both TGFB1 and activin A in Sui66 cell line, its expression was increased only by TGFB1 in Sui68 cell line. **(C)** Phosphorylation of SMAD2 in Sui66 and Sui68 cell lines with or without SB431542. The cell line was stimulated by TGFB1 or activin A for 1 hour. The phosphorylation levels of SMAD2 increased in response to both TGFB1 and activin A but were cancelled by SB431542 in Sui66 cell line. The phosphorylation level of SMAD2 increased only in response to TGFB1 and was cancelled by SB431542 in Sui68 cell line.

the Sui68/p21 cell line were greatly suppressed, compared with the controls (Figure 8B and C). In addition, Sui68/EGFP exhibited a significantly elevated level of tumorigenesis (Sui68/EGFP 14/14 vs. Sui68/p21 8/14, $P = 0.016$), and Sui68/EGFP exhibited a larger tumor volume than Sui68/p21 on day 15 (Sui68/EGFP, 507.0 ± 83.5 mm^3 vs. Sui68/p21, 276.5 ± 95.0 mm^3; $P = 0.0036$*) (Figure 8D). No significant difference in body weight was seen on day 15 (Sui68/EGFP, 20.3 ± 0.8 g vs. Sui68/p21, 20.2 ± 1.5 g; $P = 0.94$). These results suggest that p21 expression reverses the phenotype arising from the homozygous deletion of the *ACVR1B* gene.

ACVR1B and SMAD4 gene copy numbers in clinical samples of PC

To examine the *ACVR1B* and *SMAD4* gene copy numbers in PC clinical samples, we performed a TaqMan Copy Number Assay. The *ACVR1B* gene copy numbers in 6 samples (6/29, 20.7%) were less than 0.5 (Figure 9A), while the *SMAD4* gene copy numbers in 10 samples (10/29, 34.5%) were less than 0.5 (Figure 9A). The association between the patient characteristics and the *ACVR1B* gene status is summarized in Table 2. Interestingly, 5 of the 6 samples with a deletion of the *ACVR1B* gene also had a deletion of the *SMAD4* gene ($P = 0.011$), but no significant differences in the other patient characteristics were observed between the two groups. According to the immunostaining results, the expressions of p21 were clearly elevated in the cancer cells of patients with wild-type *ACVR1B* and *SMAD4* genes, compared with the expression levels in patients with the homozygous deletion of the *ACVR1B* gene (Figure 9B). Twenty-one patients with a good performance status received chemotherapy (gemcitabine, n = 12; gemcitabine/S1, n = 5; S1, n = 4) at Kinki University Hospital. These regimens were commonly used in Japan before the availability of erlotinib or FOLFIRINOX. Among these patients, no significant differences in progression-free survival (PFS) or overall survival (OS) were seen between the two groups (Figure 9C and Table 2).

Discussion

In this study, we identified a homozygous deletion of the *ACVR1B* gene in PC cell lines and clinical samples. Activin A inhibited cellular growth in the cell lines with wild-type *ACVR1B* and *SMAD4* genes, and *ACVR1B*-knockdown enhanced cellular growth and colony formation *in vitro* as well as tumor growth and tumorigenicity

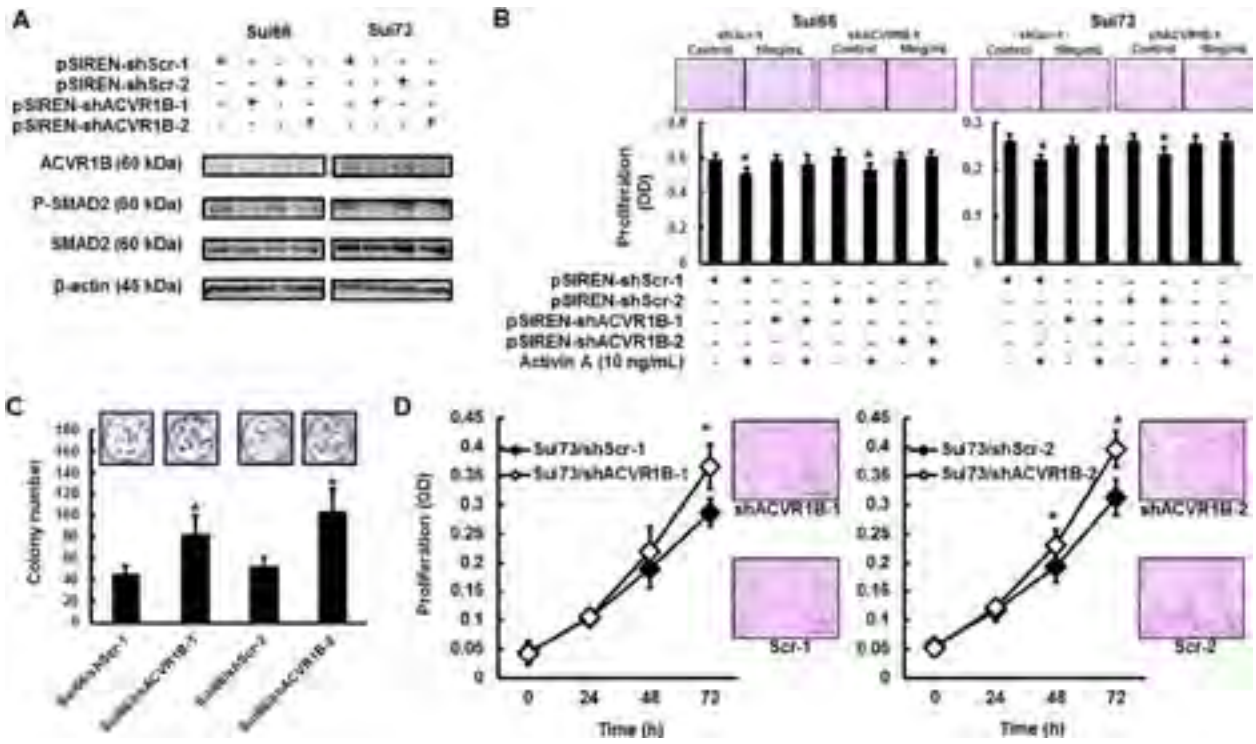

Figure 6 Role of *ACVR1B* gene in colony formation and cellular growth. To evaluate the role of the *ACVR1B* gene, we used stable *ACVR1B*-knockdown cell lines (shACVR1B) or control (shScr). **(A)** Western blot analyses after activin A stimulation (10 ng/mL). In contrast to Sui66/shScr and Sui73/shScr cell lines, ACVR1B was not expressed in Sui66/shACVR1B and Sui73/shACVR1B cell lines. SMAD2 was not phosphorylated by activin A in Sui66/shACVR1B and Sui73/shACVR1B cell lines. β-actin was used as an internal control. **(B)** Influence of activin A on cellular growth. The cell lines were stimulated with or without activin A (10 ng/mL) for 72 hours. Cell proliferation was assayed using an MTT assay. Although activin A inhibited cellular growth in Sui66/shScr and Sui73/shScr cell lines (Sui66/shScr-1; $P = 0.0014$*, Sui66/shScr-2; $P = 0.0032$*, Sui73/shScr-1; $P = 0.0085$*, and Sui73/shScr-2, $P = 0.0053$*, respectively), it did not influence the cellular growth in Sui66/shACVR1B and Sui73/shACVR1B cell lines (Sui66/shACVR1B-1; $P = 0.81$, Sui66/shACVR1B-2; $P = 0.73$, Sui73/shACVR1B-1; $P = 0.90$, and Sui73/shACVR1B-2; $P = 0.87$, respectively). **(C)** Colony formation of Sui66-transfectant cell lines. The colony formations in Sui66/shACVR1B cell lines were enhanced, compared with that in the control cell lines (Scr-1, 46.11 ± 8.00 vs. ACVR1B-1, 83.00 ± 16.75, $P = 0.026$* and Scr-2, 52.55 ± 9.24 vs. ACVR1B-2, 103.70 ± 21.00, $P = 0.017$*). **(D)** Cellular growth of Sui73-transfectant cell lines. The cellular growth was evaluated using an MTT assay. The cellular growths in Sui73/shACVR1B cell lines were enhanced, compared with Sui73/shScr (shScr-1 vs. shACVR1B-1, 0 h, $P = 081$; 24 h, $P = 0.88$; 48 h, $P = 0.063$; 72 h, $P = 0.013$*, and shScr-2 vs. shACVR1B-2, 0 h, $P = 040$; 24 h, $P = 0.45$; 48 h, $P = 0.040$*; 72 h, $P = 0.014$*). Columns, mean of independent triplicate experiments; Lines, mean of independent triplicate experiments; Bars, SD; *$P < 0.05$.

in vivo. These results suggest that the activin signal has a tumor suppressive role in PC and that the deletion of the *ACVR1B* gene mediates an aggressive cancer phenotype relative to PC carrying the wild-type *ACVR1B* gene.

Similar to our study, several articles have shown an anti-tumorigenic effect of the activin signal. Activin A induces growth inhibition and apoptosis mainly through SMAD-dependent pathways in many other cancers, such as gall bladder cancer, prostate cancer, neuroblastoma, breast cancer, ovarian cancer, and colon cancer [22-27]. In our study, activin A inhibited cellular growth and induced G1 phase cell arrest in a PC cell line with wild-type *ACVR1B* and *SMAD4* genes via the phosphorylation of SMAD2 and the expression of p21, while the cellular growth of a cell line with the homozygous deletion of the *ACVR1B* gene was not inhibited by activin A. In addition, the cellular inhibitory effect of activin A and the activin-induced phosphorylation of SMAD2 were cancelled by *ACVR1B*-knockdown in cell lines with wild-type *ACVR1B* and *SMAD4* genes. *In vivo*, *ACVR1B*-knockdown also enhanced the tumorigenicity and tumor growth. The Sui68 cell line (homozygous deletion of the *ACVR1B* gene and the wild-type *SMAD4* gene) was capable of generating sufficient tumors, suggesting that the deletion of the *ACVR1B* gene contributes to tumorigenicity even in the presence of the wild-type *SMAD4* gene. In addition, the *in vitro* colony formation and cellular growth and the *in vivo* tumorigenicity of the Sui68 cell line were greatly inhibited by *p21*-overexpression. Thus, the anti-tumorigenic effect of the activin signal via the SMAD pathways and p21 was lost by *ACVR1B*-knockdown, which was related to an aggressive phenotype of PC.

Interestingly, another article and the present study both demonstrated that the inactivation of the *ACVR1B*

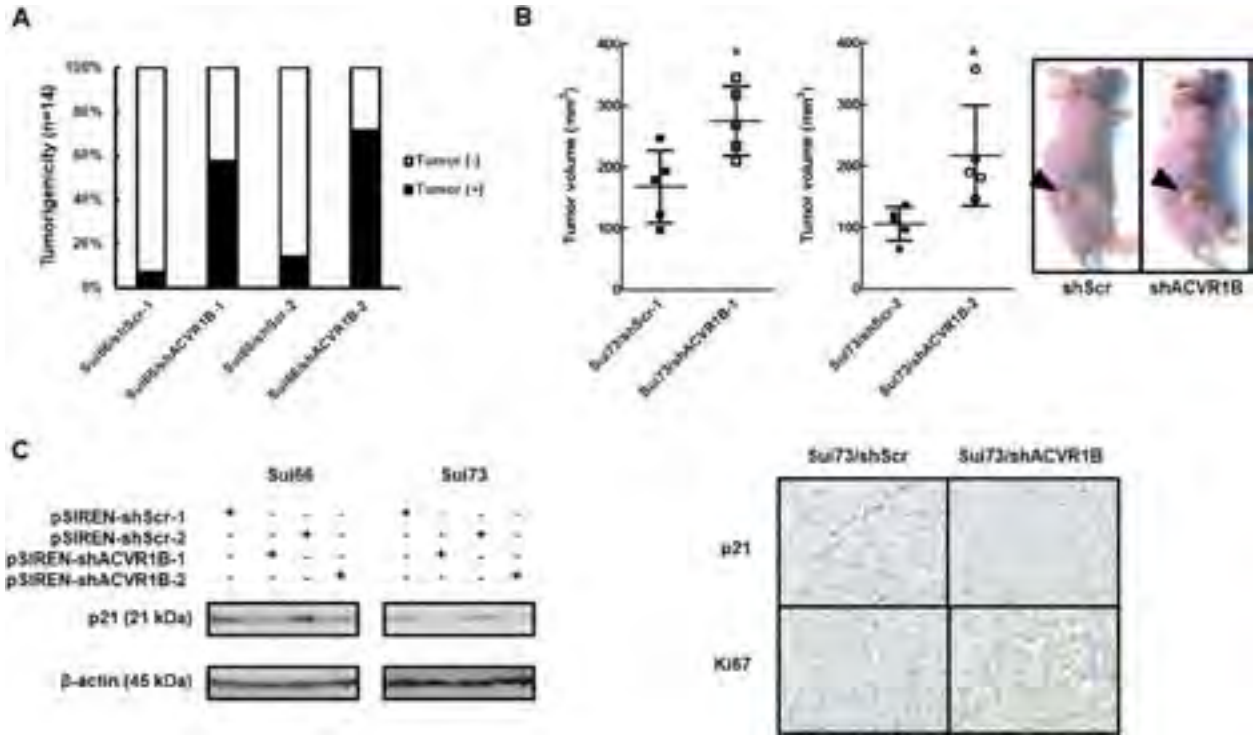

Figure 7 Xenograft study in Sui66- and Sui73-transfectant cell lines. (A) Tumorigenesis *in vivo*. To evaluate tumorigenicity *in vivo*, a suspension of 5×10^6 Sui66-transfectant cells (in 50 μL PBS) were subcutaneously inoculated into both flanks of nude mice (n = 7). Tumor formation was assessed every 2 or 3 days. Sui66/sh-ACVR1B exhibited a significantly elevated level of tumorigenesis *in vivo* (Scr-1 1/14 vs. ACVR1B-1 8/14, $P = 0.013$* and Scr-2 2/14 vs. ACVR1B-2 10/14, $P = 0.0063$*). **(B)** Tumor growth *in vivo*. To assess the tumor growth *in vivo*, a suspension of 5×10^6 Sui73-transfectant cell lines (in 50 μL PBS) with 50 μL of Matrigel were subcutaneously inoculated into the right flank of nude mice (n = 5). The tumor volume was assessed every 2 or 3 days. Sui73/shACVR1B exhibited a significantly elevated tumor volume (Sui73/Scr-1, 167.7 ± 59.1 mm^3 vs. Sui73/ACVR1B-1, 275.0 ± 56.3 mm^3; $P = 0.018$* on day 36 and Sui73Scr-2, 105.7 ± 27.2 mm^3 vs. Sui73/ACVR1B-2, 217.3 ± 81.8 mm^3; $P = 0.020$* on day 29, respectively). Lines, mean of 5 tumors; Error bars, SD; *$P < 0.05$. **(C)** Western blot analyses of the tumors and immunostaining. The expressions of p21 were clearly elevated in cancer cells in shScr-inoculated tumors, compared with the expression levels in shACVR1B cells. The expressions of Ki67 were also clearly elevated in the cancer cells in the shACVR1B-inculated tumors. β-actin was used as an internal control.

gene is frequently complicated by the inactivation of the *SMAD4* gene [19]. The TGFB and activin signals have non-SMAD pathways, and the ERK/MAPK signal and the PI3K/AKT signal are representative signals that are associated with cellular growth and survival [30]. In the Sui70 cell line (wild-type *ACVR1B* gene and the homozygous deletion of the *SMAD4* gene), however, activin A did not influence the cellular growth, and neither the phosphorylation of ERK1/2 nor that of AKT was enhanced. Approximately 95% of PC, including the Sui70 cell line has a *K-ras* mutation [5-8], and both ERK1/2 and AKT are phosphorylated in the Sui70 cell line because of this mutation [31]. Therefore, non-SMAD pathways may have little effect on the aggressiveness of PC carrying the wild-type *ACVR1B* gene and a homozygous deletion of the *SMAD4* gene. In addition, some other reports have suggested that the inactivation of a TGFB receptor is not mutually exclusive with that of the *SMAD4* gene, since both members are known to be genetically inactivated in some tumors [32,33]. Therefore, these findings would fit with a combined input model, which could explain the observed coexistence of the genetic inactivations of these genes.

Pancreatic-specific *TGFBR2* or *SMAD4*-knockout mice with active *K-ras* expression reportedly developed PC [16,17]. However, systemic *ACVR1B*-knockout mice do not survive beyond embryonic day 9.5 [34], and pancreatic-specific *ACVR1B*-knockout mice have not been previously studied. Considering the tumor suppressive role of the *ACVR1B* gene, the development of PC in pancreatic-specific *ACVR1B*-knockout mice seems reasonable. In contrast to our results, however, a recent study has demonstrated that Nodal/Activin signal is associated with self-renewal and the tumorigenicity of PC stem cells [20]. Therefore, to investigate these findings, further research is required.

Since the clinical DNA samples were obtained using needle biopsies, the inclusion of some normal pancreas tissue was unavoidable. Thus, the copy number data does not exactly reflect that for cancer tissue. In addition, the

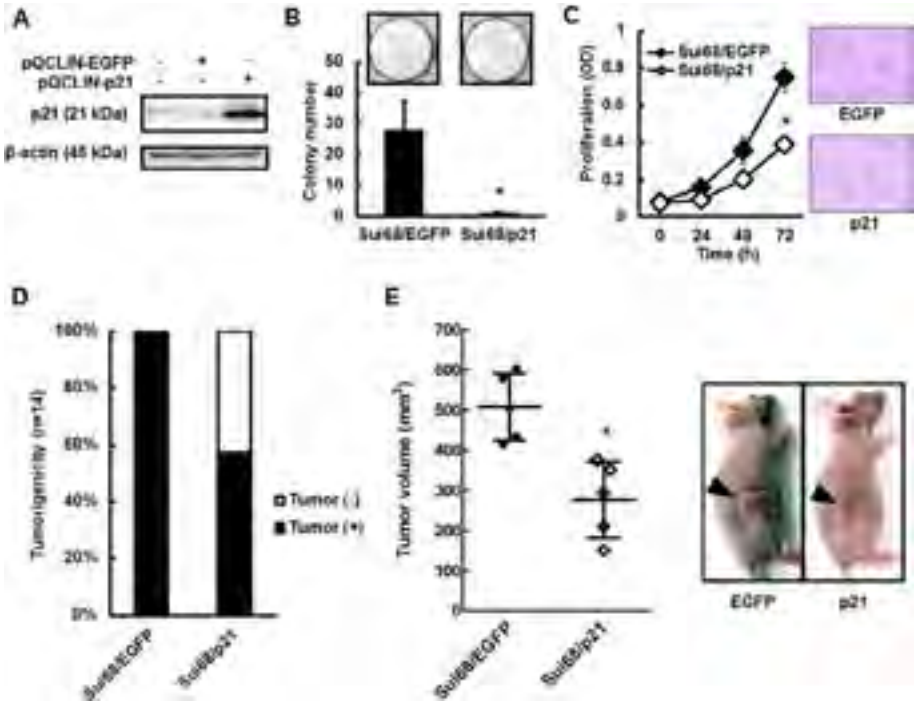

Figure 8 Role of *p21* gene in colony formation and cellular growth *in vitro* and tumorigenicity *in vivo*. To see if p21 expression reverses the phenotype for *ACVR1B* gene homozygous deletion, we created a *p21*-overexpressed Sui68 cell line (homozygous deletion of *ACVR1B* gene and wild-type *SMAD4* gene). **(A)** Western blot analyses. The overexpression of p21 was confirmed using western blot analyses in the Sui68/p21 cell line. β-actin was used as an internal control. **(B)** Colony formation of Sui68-transfectant cell lines. The colony formation in the Sui68/p21 cell line was suppressed, compared with that in the control cell line (EGFP, 28.0 ± 9.17 vs. p21, 0.89 ± 0.19, $P = 0.035$*). Columns, mean of independent triplicate experiments; Bars, SD; *$P < 0.05$. **(C)** Cellular growth of Sui68-transfectant cell lines. The cellular growth was evaluated using an MTT assay. Cellular growth in the Sui68/p21 cell line was suppressed, compared with Sui68/EGFP (0 h, $P = 065$; 24 h, $P = 0.074$; 48 h, $P = 0.053$; 72 h, $P = 0.030$*). Lines, mean of independent triplicate experiments; Bars, SD; *$P < 0.05$. **(D)** Tumorigenesis *in vivo*. To evaluate tumorigenicity *in vivo*, a suspension of 5×10^6 Sui68-transfectant cells (in 50 μL PBS) were subcutaneously inoculated into both flanks of nude mice (n = 7). Sui68/EGFP exhibited a significantly elevated level of tumorigenesis (Sui68/EGFP 14/14 vs. Sui68/p21 8/14, $P = 0.016$). **(E)** Tumor growth *in vivo*. To evaluate the tumor growth, a suspension of 5×10^6 Sui68-transfectant cells (in 50 μL PBS) with 50 μL of Matrigel were subcutaneously inoculated into the right flanks of nude mice (n = 5). Sui68/EGFP exhibited a larger tumor volume than Sui68/p21 on day 15 (Sui68/EGFP, 507.0 ± 83.5 mm^3 vs. Sui68/p21, 276.5 ± 95.0 mm^3; $P = 0.0036$*). Lines, mean of five tumors; Bars, SD; *$P < 0.05$.

number of clinical samples was very small. Therefore, this cohort has many limitations. No significant differences in the PFS or OS were observed between the patients with *ACVR1B* gene deletions and those without. To confirm the clinical importance of the *ACVR1B* gene deletion, larger studies including more precise genome evaluations are needed.

Conclusion

We identified the homozygous deletion of the *ACVR1B* gene in PC cell lines and clinical samples. Our experimental findings indicate that the activin signal has a tumor suppressive role and that the deletion of the *ACVR1B* gene may mediate an aggressive cancer phenotype in PC.

Materials and methods

Cell culture, ligands, and reagents

Human PC cell lines (Sui65, Sui66, Sui67, Sui68, Sui70, Sui71, Sui73, and Sui74) were maintained in RPMI-1640 medium (Sigma-Aldrich, St. Louis, MO) with 10% FBS (GIBCO BRL, Grand Island, NY) (Table 1) [31]. The cell lines were maintained in a 5% CO_2-humidified atmosphere at 37˚C.

TGFB1 and activin A were both purchased from R&D Systems (Minneapolis, MN). The ACVR1B/TGFBR1/ACVR1C-specific inhibitor SB431542 was purchased from Sigma-Aldrich.

Array-based comparative genomic hybridization

The Genome-wide Human SNP Array 6.0 (Affymetrix, Santa Clara, CA) was used to perform array-CGH on genomic DNA from each of the PC cell lines as described previously [35]. The GeneChip Human Mapping 250 K Nsp Array (Affymetrix) was used to perform array-CGH on genomic DNA from each of the cell lines. A total of 250 ng of genomic DNA was digested with Nsp I (250 K) or both Nsp I and Sty I in independent parallel reactions (SNP6.0), subjected to restriction enzymes, ligated to the

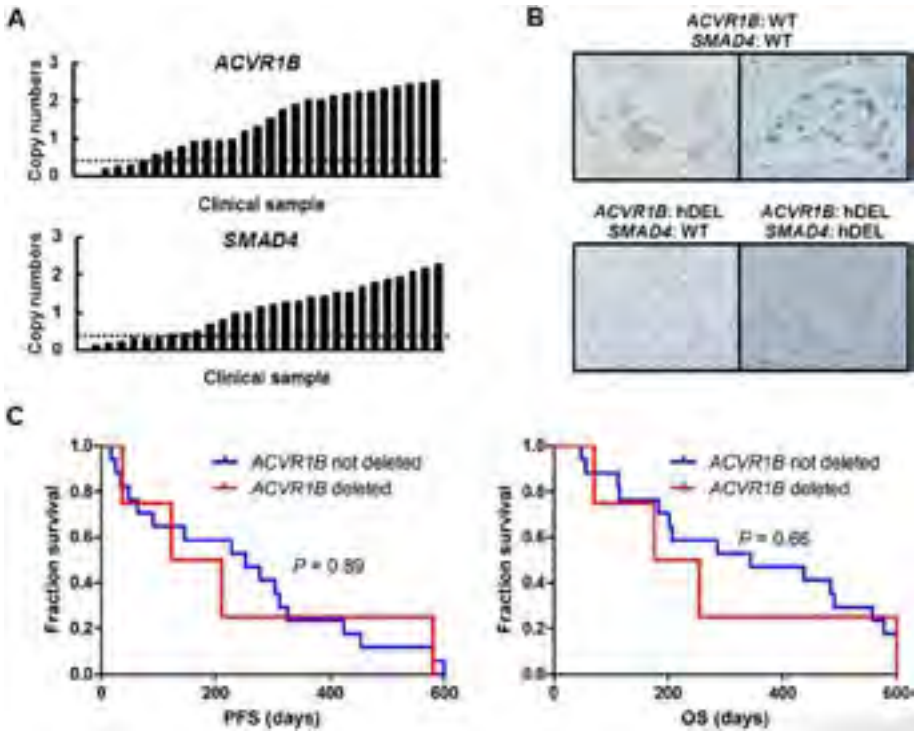

Figure 9 Copy numbers of *ACVR1B* and *SMAD4* genes, immunostaining of p21, and Kaplan-Meier curves for PFS and OS in PC clinical samples. (A) The copy numbers were analyzed using TaqMan copy number assays. Copy number of the *ACVR1B* gene. Six samples (6/29, 20.7%) had a copy number of less than 0.5 (deletion). Copy number of the *SMAD4* gene. Ten samples (10/29, 34.5%) had a copy number of less than 0.5 (deletion). **(B)** Immunostaining of p21. The expressions of p21 were clearly elevated in the cancer cells of patients with wild-type *ACVR1B* and *SMAD4* genes, compared with the expression levels in those of patients with a homozygous deletion of the *ACVR1B* gene. WT, wild-type; hDEL, homozygous deletion. **(C)** Kaplan-Meier curves for PFS and OS. Among 21 patients who received chemotherapy, no significant differences in PFS or OS were seen between the patients without a homozygous deletion of the *ACVR1B* gene and those with such a deletion (median PFS, 252 days vs. 167 days, P = 0.89, and median OS, 344 days vs. 215 days, P = 0.66, respectively).

adaptor, and amplified using PCR with a universal primer and TITANIUM Taq DNA Polymerase (Clontech, Palo Alto, CA). The PCR products were then quantified, fragmented, end-labeled, and hybridized onto a GeneChip Human Mapping 250 K Nsp Array or a Genome-wide Human SNP6.0 Array. After washing and staining in Fluidics Station 450 (Affymetrix), the arrays were scanned to generate CEL files using the GeneChip Scanner 3000 and GeneChip Operating Software, ver.1.4.

Copy number assay for ACVR1B and SMAD4 genes

The copy numbers for *ACVR1B* and *SMAD4* genes were determined using commercially available and pre-designed TaqMan Copy Number Assays (Applied Biosystems, Foster City, CA) as described previously [36]. The primer IDs used for the *ACVR1B* and *SMAD4* genes were Hs06931689_cn (intron 1) and Hs07120826_cn (intron 1), respectively. The *TERT* locus was used for the internal reference copy number. Human Genomic DNA (TaKaRa) was used as a normal control. Real-time genomic PCR was performed in a total volume of 20 μL in each well, which contained 10 μL of TaqMan genotyping master mix and 20 ng of genomic DNA and each primer. The PCR conditions were 95°C for 10 min and 40 cycles of 95°C for 15 sec and 60°C for 1 min; the resulting products were detected using the ABI PRISM 7900 HT Sequence Detection System (Applied Biosystems). Data were analyzed using SDS 2.2 software and CopyCaller software (Applied Biosystems). Samples with a gene copy number of less than 0.5 were defined as having a copy number of 0 (deletion of the gene), while those with a gene copy number of 0.5 or more but less than 1.5 were defined as having a copy number of 1 and those with a gene copy number of 1.5 or more but less than 2.5 were defined as having a copy number of 2.

Real-time RT-PCR

One microgram of total RNA from each of the PC cell lines and normal pancreas tissue purchased from Clontech were converted to cDNA using the GeneAmp RNA-PCR kit (Applied Biosystems). Real-time PCR was performed using the Applied Biosystems 7900 HT Fast Real-time PCR System (Applied Biosystems), as described previously [28] under the following conditions:

Table 2 Patient characteristics and the association with *ACVR1B* gene status

Patients characteristics	*ACVR1B* gene		*P*
	Not deletion (n = 23)	Deletion (n = 6)	
Age			
<70 years	15	3	0.65
≥ 70 years	8	3	
Gender			
Male	12	3	1.00
Female	11	3	
Primary size			
<2 cm	18	5	1.00
≥2 cm	5	1	
Lymph node metastasis			
Negative	4	0	0.55
Positive	19	6	
Distant metastasis			
Negative	10	4	0.39
Positive	13	2	
SMAD4 gene status			
Not deletion	18	1	0.011*
Deletion	5	5	
Treatment			
Best supportive care	4	2	0.59
Chemotherapy	17	4	
Unknown	2	0	
Response to chemotherapy			
PR	7	1	1.00
SD or PD	10	3	
Median PFS (days)	252	167	0.89
Median OS (days)	344	215	0.66

ACVR1B, activin receptor A, type IB; PR, partial response; SD, stable disease; PD, progressive disease; PFS, progression-free survival; OS, overall survival. PFS and OS were analyzed by log-rank test and the others by Fisher exact test.
Legend: Six patients (6/29, 20.7%) had a deletion of *ACVR1B* gene, 10 patients (10/29, 34.5%) had a deletion of *SMAD4* gene. Five of the 6 patients with a deletion of the *ACVR1B* gene also had a deletion of the *SMAD4* gene ($P = 0.011$), but no significant differences in the other patient characteristics were observed between the two groups. Among 21 patients who received chemotherapy, no significant differences in PFS or OS were seen between the two groups.

95°C for 5 min, 50 cycles of 95°C for 10 sec, and 60°C for 1 min. Glyceraldehyde 3 phosphate dehydrogenase (*GAPD*, NM_002046) was used to normalize the expression levels in subsequent quantitative analyses. To amplify the target genes, the following primers were used: *ACVR1B*-F, CAGCAGAACCTTGGCGGTTTA; *ACVR1B*-R, GTTGGCAGATCCCAGAGGCTAC; *SMAD4*-F, CAG CTATGCCAGAAGCCAGA; *SMAD4*-R, GAACTCCTGG GACTTTCAACTGAC; *GAPD*-F, GCACCGTCAAGGCT GAGAAC; *GAPD*-R, ATGGTGGTGAAGACGCCAGT. The experiment was performed in triplicate.

Plasmid construction, viral production, and stable transfectants

A short hairpin RNA (shRNA)-targeting *ACVR1B* gene was constructed using oligonucleotides encoding small interfering RNA directed against the *ACVR1B* gene and a non-specific target as follows: GAATTGCTCATCGA-GACTT and GGCTTGTTTCTGACTATCA for ACVR1B shRNA (shRNA ACVR1B-1 and shRNA ACVR1B-2, respectively), and ACTTGGTTCGCGTATCAAA and CCA TATTGCGCGTTGATTT for control shRNA (shRNA scramble-1 and shRNA scramble-2, respectively). The method was described previously [28]. Briefly, the oligonucleotides were cloned into an RNAi-Ready pSIREN-RetroQZsGreen vector (Clontech). A pVSV-G vector (Clontech) for the constitution of the viral envelope and the RNAi-Ready pSIREN-RetroQZsGreen constructs were cotransfected into gpIRES-293 cells using FuGENE6 transfection reagent (Roche Diagnostics, Basel, Switzerland). After 48 hours of transfection, the culture medium was collected and the viral particles were concentrated by centrifugation at 15,000 × *g* for 3 hours at 4°C. The viral pellet was then resuspended in fresh RPMI-1640 medium. The titer of the viral vector was calculated by counting the green-positive cells that were infected by serial dilutions of virus-containing media, and the multiplicity of infection was then determined. The viral vectors were designated as pSIREN-shACVR1B-1, pSIREN-shACVR1B-2, pSIREN-shScr-1, and pSIREN-shScr-2. The stable transfectants expressing shRNA ACVR1B-1, shRNA ACVR1B-2, shRNA scramble-1 or shRNA scramble-2 in the Sui66 and Sui73 cell lines were designated as Sui66/shACVR1B (Sui66/shACVR1B-1 and Sui66/shACVR1B-2), Sui66/shScr (Sui66/shScr-1 and Sui66/shScr-2), Sui73/shACVR1B (Sui73/shACVR1B-1 and Sui73/shACVR1B-2), and Sui73/shScr (Sui73/shScr-1 and Sui73/shScr-2), respectively.

A full-length cDNA fragment encoding the human *p21* gene was introduced into a pQCLIN retroviral vector (Clontech) together with enhanced green fluorescent protein (EGFP) following the internal ribosome entry site sequence (IRES) to monitor the expression of the inserts indirectly. The methods used for viral production and the stable transfectant were described above. The vectors and stable viral transfectant Sui68 cell line was designated as pQCLIN-EGFP, pQLCIN-p21, Sui68/EGFP and Sui68/p21, respectively.

Antibody

A goat antibody specific for ACVR1B was obtained from R&D Systems. Rabbit antibodies specific for SMAD2, phospho-SMAD2, SMAD4, AKT, phospho-AKT, ERK1/

2, phospho-ERK1/2, p21, and β-actin were obtained from Cell Signaling (Beverly, MA).

Western blot analysis

A western blot analysis was performed as described previously [28]. Briefly, subconfluent cells were washed with cold phosphate-buffered saline (PBS) and harvested with Lysis A buffer containing 1% Triton X-100, 20 mM Tris–HCl (pH7.0), 5 mM EDTA, 50 mM sodium chloride, 10 mM sodium pyrophosphate, 50 mM sodium fluoride, 1 mM sodium orthovanadate, and a protease inhibitor mix, Complete™ (Roche Diagnostics). Whole-cell lysates were separated using a 5%-20% SDS-PAGE and were blotted onto a polyvinylidene fluoride membrane. After blocking with 3% bovine serum albumin in a TBS buffer (pH8.0) with 0.1% Tween-20, the membrane was probed with primary antibody. After rinsing twice with TBS buffer, the membrane was incubated with horseradish peroxidase-conjugated secondary antibody and washed, followed by visualization using an ECL detection system (GE Healthcare, Buckinghamshire, United Kingdom) and LAS-3000 (Fujifilm, Tokyo, Japan). When the influence of the ligands was evaluated, the cultured medium was replaced with 1% FBS medium 6 hours before exposure to the ligands.

Cellular growth assay

The Sui66-, Sui68-, and Sui73-transfectant cell lines were incubated on 96-well plates at a density of 2,000/well with 200 μL of cultured medium at 37°C in 5% CO_2. After 24, 48, or 72 hours of incubation, 20 μL of MTT [3-(4, 5-dimethyl-thiazoyl-2-yl)2,5-diphenyltetrazolium bromide] solution (Sigma-Aldrich) was added and the culture medium was discarded; the wells were then filled with DMSO. The absorbance of the cultures at 570 nm was measured using VERSAmax (Japan Molecular Devices, Tokyo, Japan). To evaluate growth in the presence of ligands, we also used an MTT assay. The cell lines (2,000/well) were transferred to 96-well plates and cultured using 1% FBS medium for 24 hours at 37°C. Then, the ligands (TGFB1: 0, 0.1, 1, and 10 ng/mL; activin A: 0, 1, 10, and 100 ng/mL) were added and the incubation was further continued for 72 hours at 37°C using 1% FBS medium. The average O.D. values of the 6 wells were used for a single experiment, and the experiment was performed in triplicate.

Colony formation assay

Sui66- and Sui73-transfectant cell lines were seeded into 6-well plates at a density of 200 cells/well, and Sui68-transfectant cell lines were seeded into 6-well plates at a density of 500 cells/well. After 2 weeks, the cells were washed with PBS and fixed with 4% paraformaldehyde for 10 min and then stained with 0.1% crystal violet for 15 min; the colonies were then counted under a light microscope. The experiment was performed in triplicate.

Cell cycle distribution analysis

The cell cycle analyses were performed as described previously [37]. Briefly, cell lines were seeded into 6-cm dishes of 2×10^5 cells and cultured using 1% FBS medium for 24 hours at 37°C. Then, the ligands (TGFB1, 1 ng/mL; activin A, 10 ng/mL) were added, and the incubation was further continued for 48 hours at 37°C using 1% FBS medium. Cells were harvested by trypsinization, washed twice with PBS, and fixed with cold 70% ethanol at 4°C for 30 min. Then, the cells were washed twice with PBS and stained using propidium iodide/RNase Staining Buffer (BD Biosciences, San Jose, CA) at room temperature for 15 min. The cells were analyzed using a flow cytometer (BD FACSCalibur™, BD Biosciences), and the cell cycle analysis was performed using ModFit LT software. The experiment was performed in triplicate.

Xenograft studies

Nude mice (BALB/c nu/nu; 6-week-old females; CLEA Japan, Tokyo, Japan) were used for the *in vivo* studies and were cared for in accordance with the recommendations for the Handling of Laboratory Animals for Biomedical Research compiled by the Committee on Safety and Ethical Handling Regulations for Laboratory Animals Experiments, Kinki University. The ethical procedures followed and met the requirements of the United Kingdom Coordinating Committee on Cancer Research guidelines. To evaluate tumorigenicity, a suspension of 5×10^6 Sui66- and Sui68-transfectant cells (in 50 μL PBS) were subcutaneously inoculated into both flanks of nude mice (n = 7). To evaluate the tumor growth, a suspension of 5×10^6 Sui68- and Sui73-transfectant cells (in 50 μL PBS) with 50 μL of Matrigel were subcutaneously inoculated into the right flanks of nude mice (n = 5). The tumor volume was calculated as the length × width^2 × 0.5. The tumor formation and volume were assessed every 2 to 3 days. At the end of the experiment, the mice were sacrificed and the xenografts were resected, fixed in 10% buffered formalin for 6 to 10 hours, and processed for histologic analysis. The method was described previously [38].

Patients and samples

A total of 29 patients who had been diagnosed as having unresectable PC based on the results of an endoscopic biopsy performed at Kinki University Hospital between April 2007 and March 2008 were enrolled. This study was retrospectively performed and was approved by the institutional review board of the Kinki University Faculty of Medicine. The staging of the PC was determined according to the TNM classification. Among those who

had a good performance status and received chemotherapy, the PFS was defined as the time from the initiation of chemotherapy until the first observation of disease progression or death from any cause, OS was defined as the time from the initiation of chemotherapy until death from any cause. The response to chemotherapy was evaluated at one month after the start of therapy and every 2 months thereafter using computed tomography according to the Response Evaluation Criteria in Solid Tumors.

DNA extraction

The endoscopic biopsy samples were immediately stored at −80°C. Other biopsy samples obtained from the same location were reviewed by a pathologist to confirm the presence of tumor cells. The DNA was extracted using a QIAamp DNA Micro kit (Qiagen, Hilden, Germany) as described previously [36]. The DNA concentration was determined using the NanoDrop2000 (Thermo Fisher Scientific, Waltham, MA).

Statistical analysis

Continuous variables were analyzed using the Student *t*-test, and the results were expressed as the average and standard deviations (SD). Dichotomous variables were analyzed using the Fisher exact test. PFS and OS were analyzed using the Kaplan-Meier method and were compared among groups using the log-rank test. The statistical analyses were two-tailed and were performed using Microsoft Excel (Microsoft, Redmond, WA). A *P*-value of less than 0.05 was considered statistically significant.

Additional file

Additional file 1: Effects of ligands on the Sui70 cell line (wild-type *ACVR1B* gene and homozygous deletion of *SMAD4* gene). A. Influence of TGFB1 and activin A on cellular growth in the Sui70 cell line. Both TGFB1 (0.1 ng/mL, $P = 0.42$; 1 ng/mL, $P = 0.65$; 10 ng/mL, $P = 0.30$) and activin A (1 ng/mL, $P = 0.38$; 10 ng/mL, $P = 0.47$; 100 ng/mL, $P = 0.35$) did not influence the cellular growth. hDEL, homozygous deletion; WT, wild-type. B. Western blot analyses for non-SMAD pathway and p21. Both AKT and ERK1/2 had already been phosphorylated, and the phosphorylation was not enhanced by activin A. The expression of p21 was not changed by activin A.

Abbreviations

ACVR: Activin A receptor; CGH: Comparative genomic hybridization; OS: Overall survival; PBS: Phosphate-buffered saline; PC: Pancreatic cancer; PFS: Progression-free survival; RT-PCR: Reverse-transcription PCR; Scr: Scramble; SD: Standard deviations; sh: Short hairpin; TGFB: Transforming growth factor beta; TGFBR: Transforming growth factor beta receptor.

Competing interests

The authors declare that they have no competing interests.

Authors' contributions

YT designed and participated in the experiments and drafted the manuscript. HS and MK collected clinical samples. HH and MT carried out the experiments with cells. VM and YF carried out the *in vivo* experiments. YK and KS carried out the clinical sample analyses. AI reviewed the histology. ST performed the statistical analysis. MK and KN conceived the study, participated in its design and coordination, and helped to draft the manuscript. All the authors have read and approved the final manuscript.

Acknowledgment

We thank Mr. Shinji Kurashimo, Mr. Yoshihiro Mine, Ms. Eiko Honda, Ms. Tomoko Kitayama, and Ms. Ayaka Kurumatani for their technical assistance. This work was supported in part by the Third-Term Comprehensive 10-Year Strategy for Cancer Control and Grant-in Aid for Japan Society for Promotion of Science Fellows.

Author details

[1]Department of Genome Biology, Kinki University Faculty of Medicine, 377-2 Ohno-higashi, Osaka-Sayama, Osaka 589-8511, Japan. [2]Department of Gastroenterology and Hepatology, Kinki University Faculty of Medicine, Osaka-Sayama, Osaka, Japan. [3]Department of Pathology, Kinki University Faculty of Medicine, Osaka-Sayama, Osaka, Japan.

Received: 13 November 2013 Accepted: 20 May 2014
Published: 27 May 2014

References

1. Moore MJ, Goldstein D, Hamm J, Figer A, Hecht JR, Gallinger S, Au HJ, Murawa P, Walde D, Wolff RA, Campos D, Lim R, Ding K, Clark G, Voskoglou-Nomikos T, Ptasynski M, Parulekar W, National Cancer Institute of Canada Clinical Trials Group: **Erlotinib plus gemcitabine compared with gemcitabine alone in patients with advanced pancreatic cancer: a phase III trial of the National Cancer Institute of Canada Clinical Trials Group.** *J Clin Oncol* 2007, **25:**1960–1966.
2. Conroy T, Desseigne F, Ychou M, Bouché O, Guimbaud R, Bécouarn Y, Adenis A, Raoul JL, Gourgou-Bourgade S, de la Fouchardière C, Bennouna J, Bachet JB, Khemissa-Akouz F, Péré-Vergé D, Delbaldo C, Assenat E, Chauffert B, Michel P, Montoto-Grillot C, Ducreux M, Groupe Tumeurs Digestives of Unicancer; PRODIGE Intergroup: **FOLFIRINOX versus gemcitabine for metastatic pancreatic cancer.** *N Engl J Med* 2011, **364:**1817–1825.
3. Von Hoff DD, Ervin T, Arena FP, Chiorean EG, Infante J, Moore M, Seay T, Tjulandin SA, Ma WW, Saleh MN, Harris M, Reni M, Dowden S, Laheru D, Bahary N, Ramanathan RK, Tabernero J, Hidalgo M, Goldstein D, Van Cutsem E, Wei X, Iglesias J, Renschler MF: **Increased survival in pancreatic cancer with nab-paclitaxel plus gemcitabine.** *N Engl J Med* 2013, **369:**1691–1703.
4. Siegel R, Naishadham D, Jemal A: **Cancer statistics, 2013.** *CA Cancer J Clin* 2013, **63:**11–30.
5. Bardeesy N, DePinho RA: **Pancreatic cancer biology and genetics.** *Nat Rev Cancer* 2002, **2:**897–909.
6. Singh P, Srinivasan R, Wig JD: **Major molecular markers in pancreatic ductal adenocarcinoma and their roles in screening, diagnosis, prognosis, and treatment.** *Pancreas* 2011, **40:**644–652.
7. Macgregor-Das AM, Iacobuzio-Donahue CA: **Molecular pathways in pancreatic carcinogenesis.** *J Surg Oncol* 2013, **107:**8–14.
8. Baker CH, Solorzano CC, Fidler IJ: **Blockade of vascular endothelial growth factor receptor and epidermal growth factor receptor signaling for therapy of metastatic human pancreatic cancer.** *Cancer Res* 2002, **62:**1996–2003.
9. Day JD, Digiuseppe JA, Yeo C, Lai-Goldman M, Anderson SM, Goodman SN, Kern SE, Hruban RH: **Immunohistochemical evaluation of HER-2/neu expression in pancreatic adenocarcinoma and pancreatic intraepithelial neoplasms.** *Hum Pathol* 1996, **27:**119–124.
10. Safran H, Iannitti D, Ramanathan R, Schwartz JD, Steinhoff M, Nauman C, Hesketh P, Rathore R, Wolff R, Tantravahi U, Hughes TM, Maia C, Pasquariello T, Goldstein L, King T, Tsai JY, Kennedy T: **Herceptin and gemcitabine for metastatic pancreatic cancers that overexpress HER-2/neu.** *Cancer Invest* 2004, **22:**706–712.
11. Harder J, Ihorst G, Heinemann V, Hofheinz R, Moehler M, Buechler P, Kloeppel G, Röcken C, Bitzer M, Boeck S, Endlicher E, Reinacher-Schick A, Schmoor C, Geissler M: **Multicentre phase II trial of trastuzumab and capecitabine in patients with HER2 overexpressing metastatic pancreatic cancer.** *Br J Cancer* 2012, **106:**1033–1038.
12. Ikushima H, Miyazono K: **TGFbeta signalling: a complex web in cancer progression.** *Nat Rev Cancer* 2010, **10:**415–424.
13. Akhurst RJ, Hata A: **Targeting the TGFβ signalling pathway in disease.** *Nat Rev Drug Discov* 2012, **11:**790–811.

14. Hilbig A, Oettle H: **Transforming growth factor beta in pancreatic cancer.** *Curr Pharm Biotechnol* 2011, **12:**2158–2164.
15. Birnbaum DJ, Mamessier E, Birnbaum D: **The emerging role of the TGFβ tumor suppressor pathway in pancreatic cancer.** *Cell Cycle* 2012, **11:**683–686.
16. Ijichi H, Chytil A, Gorska AE, Aakre ME, Fujitani Y, Fujitani S, Wright CV, Moses HL: **Aggressive pancreatic ductal adenocarcinoma in mice caused by pancreas-specific blockade of transforming growth factor-beta signaling in cooperation with active Kras expression.** *Genes Dev* 2006, **20:**3147–3160.
17. Izeradjene K, Combs C, Best M, Gopinathan A, Wagner A, Grady WM, Deng CX, Hruban RH, Adsay NV, Tuveson DA, Hingorani SR: **Kras(G12D) and Smad4/Dpc4 haploinsufficiency cooperate to induce mucinous cystic neoplasms and invasive adenocarcinoma of the pancreas.** *Cancer Cell* 2007, **11:**229–243.
18. Kleeff J, Ishiwata T, Friess H, Büchler MW, Korc M: **Concomitant over-expression of activin/inhibin beta subunits and their receptors in human pancreatic cancer.** *Int J Cancer* 1998, **77:**860–868.
19. Su GH, Bansal R, Murphy KM, Montgomery E, Yeo CJ, Hruban RH, Kern SE: **ACVR1B (ALK4, activin receptor type 1B) gene mutations in pancreatic carcinoma.** *Proc Natl Acad Sci U S A* 2001, **98:**3254–3257.
20. Lonardo E, Hermann PC, Mueller MT, Huber S, Balic A, Miranda-Lorenzo I, Zagorac S, Alcala S, Rodriguez-Arabaolaza I, Ramirez JC, Torres-Ruíz R, Garcia E, Hidalgo M, Cebrián DÁ, Heuchel R, Lour M, Berger F, Bartenstein P, Aicher A, Heeschen C: **Nodal/Activin signaling drives self-renewal and tumorigenicity of pancreatic cancer stem cells and provides a target for combined drug therapy.** *Cell Stem Cell* 2011, **9:**433–446.
21. Hempen PM, Zhang L, Bansal RK, Iacobuzio-Donahue CA, Murphy KM, Maitra A, Vogelstein B, Whitehead RH, Markowitz SD, Willson JK, Yeo CJ, Hruban RH, Kern SE: **Evidence of selection for clones having genetic inactivation of the activin A type II receptor (ACVR2) gene in gastrointestinal cancers.** *Cancer Res* 2003, **63:**994–999.
22. Bauer J, Sporn JC, Cabral J, Gomez J, Jung B: **Effects of activin and TGFβ on p21 in colon cancer.** *PLoS One* 2012, **7:**e39381.
23. McPherson SJ, Mellor SL, Wang H, Evans LW, Groome NP, Risbridger GP: **Expression of activin A and follistatin core proteins by human prostate tumor cell lines.** *Endocrinology* 1999, **140:**5303–5309.
24. Yokomuro S, Tsuji H, Lunz JG 3rd, Sakamoto T, Ezure T, Murase N, Demetris AJ: **Growth control of human biliary epithelial cells by interleukin 6, hepatocyte growth factor, transforming growth factor beta1, and activin A: comparison of a cholangiocarcinoma cell line with primary cultures of non-neoplastic biliary epithelial cells.** *Hepatology* 2000, **32:**26–35.
25. Panopoulou E, Murphy C, Rasmussen H, Bagli E, Rofstad EK, Fotsis T: **Activin A suppresses neuroblastoma xenograft tumor growth via antimitotic and antiangiogenic mechanisms.** *Cancer Res* 2005, **65:**1877–1886.
26. Burdette JE, Jeruss JS, Kurley SJ, Lee EJ, Woodruff TK: **Activin A mediates growth inhibition and cell cycle arrest through Smads in human breast cancer cells.** *Cancer Res* 2005, **65:**7968–7975.
27. Ramachandran A, Marshall ES, Love DR, Baguley BC, Shelling AN: **Activin is a potent growth suppressor of epithelial ovarian cancer cells.** *Cancer Lett* 2009, **285:**157–165.
28. Kaneda H, Arao T, Matsumoto K, De Velasco MA, Tamura D, Aomatsu K, Kudo K, Sakai K, Nagai T, Fujita Y, Tanaka K, Yanagihara K, Yamada Y, Okamoto I, Nakagawa K, Nishio K: **Activin A inhibits vascular endothelial cell growth and suppresses tumour angiogenesis in gastric cancer.** *Br J Cancer* 2011, **105:**1210–1217.
29. Weiss RH: **p21Waf1/Cip1 as a therapeutic target in breast and other cancers.** *Cancer Cell* 2003, **4:**425–429.
30. Mu Y, Gudey SK, Landström M: **Non-Smad signaling pathways.** *Cell Tissue Res* 2012, **347:**11–20.
31. Yanagihara K, Takigahira M, Tanaka H, Arao T, Aoyagi Y, Oda T, Ochiai A, Nishio K: **Establishment and molecular profiling of a novel human pancreatic cancer panel for 5-FU.** *Cancer Sci* 2008, **99:**1859–1864.
32. Goggins M, Shekher M, Turnacioglu K, Yeo CJ, Hruban RH, Kern SE: **Genetic alterations of the transforming growth factor beta receptor genes in pancreatic and biliary adenocarcinomas.** *Cancer Res* 1998, **58:**5329–5332.
33. Grady WM, Myeroff LL, Swinler SE, Rajput A, Thiagalingam S, Lutterbaugh JD, Neumann A, Brattain MG, Chang J, Kim SJ, Kinzler KW, Vogelstein B, Willson JK, Markowitz S: **Mutational inactivation of transforming growth factor beta receptor type II in microsatellite stable colon cancers.** *Cancer Res* 1999, **59:**320–324.
34. Gu Z, Nomura M, Simpson BB, Lei H, Feijen A, van den Eijnden-van RJ, Donahoe PK, Li E: **The type I activin receptor ActRIB is required for egg cylinder organization and gastrulation in the mouse.** *Genes Dev* 1998, **12:**844–857.
35. Furuta K, Arao T, Sakai K, Kimura H, Nagai T, Tamura D, Aomatsu K, Kudo K, Kaneda H, Fujita Y, Matsumoto K, Yamada Y, Yanagihara K, Sekijima M, Nishio K: **Integrated analysis of whole genome exon array and array-comparative genomic hybridization in gastric and colorectal cancer cells.** *Cancer Sci* 2012, **103:**221–227.
36. Matsumoto K, Arao T, Hamaguchi T, Shimada Y, Kato K, Oda I, Taniguchi H, Koizumi F, Yanagihara K, Sasaki H, Nishio K, Yamada Y: **FGFR2 gene amplification and clinicopathological features in gastric cancer.** *Br J Cancer* 2012, **106:**727–732.
37. Tamura D, Arao T, Tanaka K, Kaneda H, Matsumoto K, Kudo K, Aomatsu K, Fujita Y, Watanabe T, Saijo N, Kotani Y, Nishimura Y, Nishio K: **Bortezomib potentially inhibits cellular growth of vascular endothelial cells through suppression of G2/M transition.** *Cancer Sci* 2010, **101:**1403–1408.
38. Kaneda H, Arao T, Tanaka K, Tamura D, Aomatsu K, Kudo K, Sakai K, De Velasco MA, Matsumoto K, Fujita Y, Yamada Y, Tsurutani J, Okamoto I, Nakagawa K, Nishio K: **FOXQ1 is overexpressed in colorectal cancer and enhances tumorigenicity and tumor growth.** *Cancer Res* 2010, **70:**2053–2063.

doi:10.1186/1476-4598-13-126
Cite this article as: Togashi *et al.*: Homozygous deletion of the activin A receptor, type IB gene is associated with an aggressive cancer phenotype in pancreatic cancer. *Molecular Cancer* 2014 **13**:126.

Original Investigation

Effect of Everolimus on Survival in Advanced Hepatocellular Carcinoma After Failure of Sorafenib
The EVOLVE-1 Randomized Clinical Trial

Andrew X. Zhu, MD, PhD; Masatoshi Kudo, MD, PhD; Eric Assenat, MD, PhD; Stéphane Cattan, MD; Yoon-Koo Kang, MD, PhD; Ho Yeong Lim, MD, PhD; Ronnie T. P. Poon, MD, PhD; Jean-Frederic Blanc, MD, PhD; Arndt Vogel, MD; Chao-Long Chen, MD, PhD; Etienne Dorval, MD; Markus Peck-Radosavljevic, MD; Armando Santoro, MD; Bruno Daniele, MD, PhD; Junji Furuse, MD, PhD; Annette Jappe, RN; Kevin Perraud, MS; Oezlem Anak, MD; Dalila B. Sellami, MD; Li-Tzong Chen, MD, PhD

IMPORTANCE Aside from the multikinase inhibitor sorafenib, there are no effective systemic therapies for the treatment of advanced hepatocellular carcinoma.

OBJECTIVE To assess the efficacy of everolimus in patients with advanced hepatocellular carcinoma for whom sorafenib treatment failed.

DESIGN, SETTING, AND PARTICIPANTS EVOLVE-1 was a randomized, double-blind, phase 3 study conducted among 546 adults with Barcelona Clinic Liver Cancer stage B or C hepatocellular carcinoma and Child-Pugh A liver function whose disease progressed during or after sorafenib or who were intolerant of sorafenib. Patients were enrolled from 17 countries between May 2010 and March 2012. Randomization was stratified by region (Asia vs rest of world) and macrovascular invasion (present vs absent).

INTERVENTIONS Everolimus, 7.5 mg/d, or matching placebo, both given in combination with best supportive care and continued until disease progression or intolerable toxicity. Per the 2:1 randomization scheme, 362 patients were randomized to the everolimus group and 184 patients to the placebo group.

MAIN OUTCOMES AND MEASURES The primary end point was overall survival. Secondary end points included time to progression and the disease control rate (the percentage of patients with a best overall response of complete or partial response or stable disease).

RESULTS No significant difference in overall survival was seen between treatment groups, with 303 deaths (83.7%) in the everolimus group and 151 deaths (82.1%) in the placebo group (hazard ratio [HR], 1.05; 95% CI, 0.86-1.27; $P = .68$; median overall survival, 7.6 months with everolimus, 7.3 months with placebo). Median time to progression with everolimus and placebo was 3.0 months and 2.6 months, respectively (HR, 0.93; 95% CI, 0.75-1.15), and disease control rate was 56.1% and 45.1%, respectively ($P = .01$). The most common grade 3/4 adverse events for everolimus vs placebo were anemia (7.8% vs 3.3%, respectively), asthenia (7.8% vs 5.5%, respectively), and decreased appetite (6.1% vs 0.5%, respectively). No patients experienced hepatitis C viral flare. Based on central laboratory results, hepatitis B viral reactivation was experienced by 39 patients (29 everolimus, 10 placebo); all cases were asymptomatic, but 3 everolimus recipients discontinued therapy.

CONCLUSIONS AND RELEVANCE Everolimus did not improve overall survival in patients with advanced hepatocellular carcinoma whose disease progressed during or after receiving sorafenib or who were intolerant of sorafenib.

TRIAL REGISTRATION clinicaltrials.gov Identifier: NCT01035229

JAMA. 2014;312(1):57-67. doi:10.1001/jama.2014.7189

Supplemental content at jama.com

Author Affiliations: Author affiliations are listed at the end of this article.

Corresponding Author: Andrew X. Zhu, MD, PhD, Massachusetts General Hospital Cancer Center, Harvard Medical School, PO Box 232, 55 Fruit St, Boston, MA 02114 (azhu@mgh.harvard.edu).

Patients with advanced hepatocellular carcinoma (HCC) have a median overall survival of less than 1 year, largely because of the absence of effective therapies.[1] The multikinase inhibitor sorafenib is the only systemic therapy shown to significantly improve overall survival in advanced HCC.[2,3] However, sorafenib benefits are mostly transient and modest, and disease eventually progresses. As many as 28.9% of patients with Child-Pugh A liver cirrhosis discontinue sorafenib because of adverse events (AEs),[4] and there is no approved alternative in this setting. Effective therapies are needed for patients who experience progression during or after receiving sorafenib or who have sorafenib intolerance.

The phosphatidylinositol 3-kinase/Akt/mammalian target of rapamycin (mTOR) pathway, a key regulator of cellular growth, proliferation, angiogenesis, and survival,[5] is a novel therapeutic target for HCC. The mTOR pathway is implicated in hepatocarcinogenesis,[6,7] with activation occurring in up to 45% of HCC[6] and associated with less differentiated tumors, early recurrence, and poor prognosis.[7,8] In preclinical models, mTOR inhibition with everolimus and other rapamycin analogues prevented tumor progression and improved survival, and mTOR activation was associated with HCC recurrence.[7,9,10] In transgenic mice, mTOR activation caused by liver-specific *Tsc1* knockout was sufficient for HCC development,[11] and in *Pten*-deficient mice with constitutive mTOR activation, steatohepatitis and HCC development were induced.[12] In early-phase clinical studies, everolimus demonstrated manageable safety and clinical activity.[13,14] In a phase 1 study conducted in Taiwan, the maximum tolerated dose was 7.5 mg/d with a 71% disease control rate across daily doses.[13] In a phase 1/2 study conducted in the United States, the disease control rate was 44% at 10 mg/d, the maximum dose tested.[14]

The first Everolimus for Liver Cancer Evaluation (EVOLVE-1) study compared the efficacy and safety of everolimus, 7.5 mg/d, with matching placebo, both given with best supportive care, in patients with advanced HCC who were refractory to or intolerant of sorafenib.

Methods

EVOLVE-1 was an international, double-blind, placebo-controlled, phase 3 study. Adults aged 18 years and older with Barcelona Clinic Liver Cancer stage B or C advanced HCC[15] and radiologically confirmed disease progression during or after sorafenib therapy or sorafenib intolerance were eligible. Prior local and hormonal therapy and 0 or 1 systemic chemotherapy regimen before sorafenib were allowed. Additional inclusion criteria included current cirrhotic status of Child-Pugh class A (5-6 points) without encephalopathy (calculated based on clinical findings and laboratory results during the screening period), Eastern Cooperative Oncology Group (ECOG) performance status 2 or lower, adequate organ function, and alcohol intake less than 80 g/d. Previous organ transplantation requiring immunosuppression, long-term immunosuppressive therapy, known history of HIV seropositivity, clinically significant third-space fluid accumulation, acute or chronic infectious disorders except for chronic hepatitis B (HBV) and hepatitis C (HCV) virus infection, or other severe or uncontrolled medical condition resulted in exclusion from the study.

The protocol was approved by the appropriate ethics body at each participating center. The study was performed per the protocol, Good Clinical Practice guidelines, local regulations, and the ethical principles of the Declaration of Helsinki. All patients provided written informed consent.

Randomization and Masking

Patients were assigned unique identification numbers at enrollment and registered using an interactive voice- or web-response system that randomly allocated patients 2:1 to receive everolimus or placebo. Randomization was stratified by region (Asia [China, South Korea, Taiwan, and Thailand] vs rest of the world [Australia, Austria, Belgium, Canada, France, Germany, Greece, Hungary, Israel, Italy, Japan, Spain, and the United States]) and macrovascular invasion (yes vs no). Based on possible differences in treatment patterns and disease etiology, Australia and Japan were grouped with rest of the world. A validated system randomly assigned patient numbers to randomization numbers linked to the treatment groups and medication numbers. The medication randomization list was produced by Novartis Drug Supply Management using a validated system that automated the random assignment of medication numbers to study drug packs. If necessary, emergency treatment unblinding was performed using the interactive response system.

Procedures

Patients received everolimus, 7.5 mg, once daily or matching placebo, both with best supportive care (anything believed to be in the patient's best interest, excluding other antineoplastic treatments, delivered per normal local practice). Treatment continued until progression, intolerable toxicity, or another reason. For patients unable to tolerate the protocol-specified dosing scheme, dose adjustments and interruptions per a protocol-specified algorithm were permitted. The chosen everolimus dose was based on the results of the phase 1 study of everolimus for HCC conducted in Taiwan.[13] Results of a pharmacokinetic study suggest everolimus, 7.5 mg, in patients with Child-Pugh class A liver function provides similar exposure to 10 mg given to patients with normal liver function.[16]

Per US Food and Drug Administration guidance on the collection of race and ethnicity data in clinical trials[17] and their potential prognostic value, race/ethnicity information was recorded on the baseline clinical report form. The clinical report form included categories of Caucasian, Black, Asian, Native American, Pacific Islander, and other for race and Hispanic/Latino, Chinese, Indian (Indian subcontinent), Japanese, mixed ethnicity (specify), and other. Study sites were not given specific instruction regarding the collection of this information. Therefore, it is possible that for some patients, race/ethnicity information was determined by the site without input from the patient.

During screening, all patients were evaluated for HBV and HCV infection (eMethods in the Supplement). To reduce viral

reactivation risk, at-risk patients received prophylactic antiviral therapy (eTable 1 in the Supplement). Definitions of HBV reactivation and HCV flare are provided in the eMethods in the Supplement.

Primary end point was overall survival, defined as time from randomization to date of death of any cause. The key secondary end point was time to progression, defined as time from randomization to date of radiologically confirmed disease progression. Other secondary end points included disease control rate, defined as percentage of patients who achieved complete or partial response or stable disease per RECIST (Response Evaluation Criteria in Solid Tumors) version 1.0, time to definitive 5% deterioration in the global quality-of-life and physical functioning scales of the European Organisation for the Research and Treatment of Cancer 30-item Quality of Life Questionnaire (EORTC QLQ-C30), and safety.

Tumors were measured by computed tomography or magnetic resonance imaging with contrast of the chest, abdomen, and pelvis at baseline, every 6 weeks until disease progression, and at study end or early discontinuation. Complete or partial responses required confirmation at least 4 weeks after initial response observation. After disease progression or start of new anticancer therapy, patients were followed up for survival every 4 weeks until the number of deaths required for final analysis was observed. Safety assessments included incidences of AEs and serious AEs and changes in vital signs and laboratory results. Adverse events were assessed according to the Common Terminology Criteria for Adverse Events version 3.0 and coded using the *Medical Dictionary for Regulatory Activities*.

Statistical Analysis

Sample size estimation was based on the ability to detect a 28.6% reduction in risk of death (hazard ratio [HR] for overall survival, 0.714), corresponding to a 40% prolongation in median overall survival from 5 months with placebo to 7 months with everolimus. In the absence of definitive data, the anticipated overall survival for placebo was estimated based on the difference between time to progression and overall survival observed in phase 3 studies of sorafenib for advanced HCC.[2,3] An overall survival of 7 months for everolimus was considered reasonable based on preliminary survival observed in early-phase studies of everolimus for HCC (final data published as Shiah et al[13] and Zhu et al[14]). Given the 2:1 randomization scheme and 2 interim analyses planned after occurrence of the first 135 and 270 deaths, it was estimated that 449 deaths would provide 90% power to detect a clinically meaningful overall survival improvement with the use of a group sequential log-rank test with a 2.5% cumulative 1-sided significance level. Assuming uniform patient accrual, 531 patients were needed to observe the required number of deaths. When the Lan-DeMets procedure[18] with an O'Brien-Fleming stopping boundary was used to account for the 2 interim analyses in light of the 454 overall survival events at final analysis, the significance boundary for final analysis was $P \leq .023573$.

All randomly assigned patients who received 1 or more doses of study drug and had 1 or more postbaseline assessments were evaluated for safety. All enrolled patients were assessed for efficacy. Overall survival, time to progression, and deterioration in quality of life were analyzed by Kaplan-Meier methods. Study groups were compared using a stratified log-rank test (1-sided 2.5% significance level). Hazard ratios and 95% confidence intervals were estimated using a stratified Cox proportional hazards model. For analysis of overall survival, patients without a known date of death at the time of analysis were censored at the date of last contact. For analysis of time to progression, patients without radiologically confirmed disease progression at the time of analysis or receipt of further antineoplastic therapy were censored at the time of the last adequate tumor assessment before the analysis cutoff date or start date of further antineoplastic therapy. For analysis of time to definitive deterioration in quality of life, patients receiving further antineoplastic therapy before definitive worsening were censored at the date of last assessment before start of therapy; patients without worsening were censored at the date of last assessment before cutoff. Effects of potential prognostic factors on overall survival were investigated using a stratified Cox regression model including ECOG performance status, extrahepatic spread, age, sorafenib status, and baseline alpha-fetoprotein level. Time to progression was compared between treatment groups only if the overall survival difference was statistically significant. Disease control rate was compared between groups using the Cochran-Mantel-Haenszel test, with adjustment for stratification factors. All statistical analyses were performed using SAS version 9.2 (SAS Institute).

Results

Between May 27, 2010, and March 21, 2012, 546 patients from 111 centers in 17 countries with advanced HCC whose disease progressed during or after sorafenib or who were sorafenib intolerant were randomly assigned to receive treatment with everolimus (n = 362) or placebo (n = 184) and were included in the full analysis population (**Figure 1**). One patient in the everolimus group and 2 in the placebo group did not receive study treatment and were excluded from the safety population.

At the time of analysis (June 14, 2013), 303 deaths (83.7%) in the everolimus group and 151 (82.1%) in the placebo group had occurred, and treatment was ongoing for 0.8% of everolimus and 3.3% of placebo recipients (Figure 1). The most common reasons for treatment discontinuation in the everolimus and placebo groups were disease progression (72.1% and 81.0%, respectively), AEs (16.9% and 7.6%, respectively), and consent withdrawal (5.5% and 3.8%, respectively).

Baseline demographics and disease characteristics were well balanced between treatment groups (**Table 1**). In the total population, most patients were enrolled from the rest of the world (83.3%); did not have macrovascular invasion (67.2%); and had ECOG performance status 0 to 1 (95.4%), Barcelona Clinic Liver Cancer stage C disease (86.3%), and extrahepatic disease (74.0%). The most common disease etiologies were HBV (26.2%), HCV (25.1%), and alcohol abuse (20.0%). Before sorafenib, 15.9% of patients received another antineoplastic

Figure 1. Disposition and Analysis Population for Patients Enrolled in the EVOLVE-1 Trial

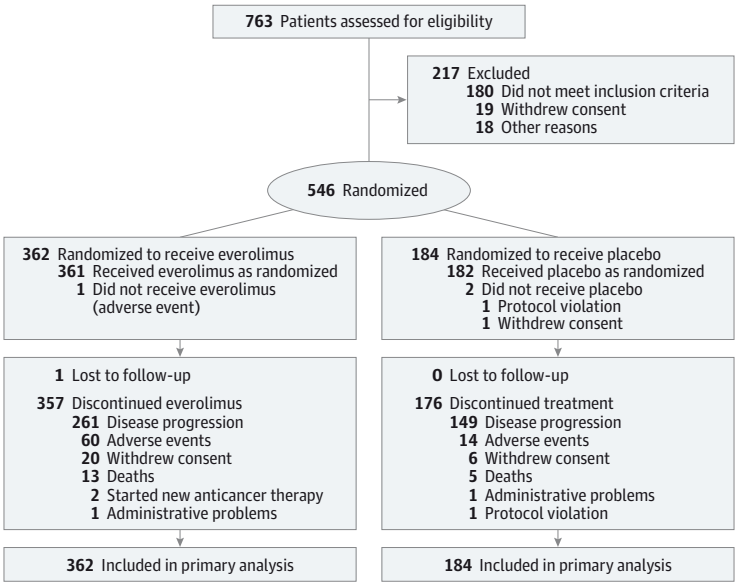

Note that only those deaths that occurred during study treatment (ie, were the direct cause of study treatment discontinuation) are shown.

medication, most commonly chemotherapy (10.3%). Previous sorafenib was discontinued for progression in 80.8% and for intolerance in 19.0%; 1 patient in the everolimus group discontinued sorafenib for planned surgery for inguinal hernia.

Median follow-up duration from randomization to the cutoff date was 24.6 months (range, 14.8-36.6). Median duration of exposure to everolimus and placebo was 9.43 weeks (range, 0.1-120.0) and 8.93 weeks (range, 0.4-136.3), respectively. Median relative dose intensity was 100% (range, 27%-100%) and 100% (range, 58%-105%), respectively. After study treatment discontinuation, 38.1% of everolimus and 41.3% of placebo recipients received further antineoplastic therapy, most commonly chemotherapy (19.6% and 18.5%, respectively).

No difference in the risk of death was noted between everolimus and placebo (HR, 1.05; 95% CI, 0.86-1.27; P = .68) (**Figure 2**A). Median overall survival was 7.6 months (95% CI, 6.7-8.7) and 7.3 months (95% CI, 6.3-8.7), respectively. Overall, 91.4% of deaths in the everolimus group and 94.7% of deaths in the placebo group were the result of disease progression. Estimated overall survival rates in the everolimus and placebo groups were 67.0% and 65.6%, respectively, at 5 months, and 53.4% and 51.4%, respectively, at 7 months. Adjustment for prognostic factors did not affect the risk of death between treatment groups (HR, 1.11; 95% CI, 0.91-1.36). Prespecified subgroup analyses revealed similar results in most subgroups (**Figure 3**). The exception was HCC etiology; patients with HBV appeared to have prolonged overall survival with everolimus (HR, 0.64; 95% CI, 0.45-0.93), whereas patients with an etiology other than HBV or HCV appeared to have a shorter overall survival with everolimus (HR, 1.35; 95% CI, 1.01-1.80).

There was no apparent difference between treatment groups in time to progression (HR, 0.93; 95% CI, 0.75-1.15) (Figure 2B). Per the prespecified analysis plan, the statistical significance of this difference was not formally tested. At the time of analysis, 252 progression events (69.6%) in the everolimus group and 133 (72.3%) in the placebo group had occurred. Median time to progression was 3.0 months (95% CI, 2.8-4.0) and 2.6 months (95% CI, 1.5-2.8), respectively.

The disease control rate was 56.1% (95% CI, 50.8%-61.3%) and 45.1% (95% CI, 37.8%-52.6%) in the everolimus and placebo groups, respectively (P = .01) (**Table 2**). There were no complete responses. A greater proportion of placebo recipients experienced progressive disease. No significant difference in time to definitive deterioration in the EORTC QLQ-C30 global quality-of-life scale was observed (P = .47); time to definitive deterioration in physical functioning was significantly shorter with everolimus (P = .01) (eTable 2 in the Supplement).

Adverse events of any grade, regardless of relationship with study drug, were experienced by 99.2% of everolimus and 94.0% of placebo recipients (**Table 3**). Grade 3/4 AEs and serious AEs were more frequent with everolimus (70.9% vs 52.2% and 47.4% vs 35.2%, respectively). Adverse events led to treatment discontinuation in 16.6% of everolimus and 7.7% of placebo recipients and dose interruptions or reductions in 55.7% and 29.1%, respectively. Grade 3/4 AEs with incidence 5% or greater in the everolimus group (everolimus vs placebo) were asthenia (7.8% vs 5.5%, respectively), anemia (7.8% vs 3.3%, respectively), decreased appetite (6.1% vs 0.5%, respectively), HBV (as reported on AE forms) (6.1% vs 4.4%, respectively), ascites (5.6% vs 8.7%, respectively), and thrombocytopenia (5.6% vs 0.5%, respectively) (Table 3).

On baseline screening, 73 patients (20.2%) in the everolimus and 44 (24.2%) in the placebo group were positive for HBV-DNA or surface antigen (HBsAg). Despite antiviral prophylaxis, HBV reactivation based on central laboratory results was experienced by 27 (37.0%) everolimus and 10 (22.7%) placebo recipients. An additional 69 (19.1%) and 29 (15.9%), respectively, were negative for HBV-DNA or HBsAg but positive for

Table 1. Baseline Demographic and Disease Characteristics (Full Analysis Population)

	Everolimus and Best Supportive Care (n = 362)	Placebo and Best Supportive Care (n = 184)
Age, median (range), y	67.0 (21-86)	64.0 (34-87)
Male, No. (%)	303 (83.7)	160 (87.0)
Geographical region, No. (%)		
Asia[a]	59 (16.3)	32 (17.4)
Rest of the world[b]	303 (83.7)	152 (82.6)
Race, No. (%)		
Caucasian	192 (53.0)	110 (59.8)
Black	6 (1.7)	3 (1.6)
Asian	137 (37.8)	58 (31.5)
Pacific Islander	0	1 (0.5)
Other	27 (7.5)	12 (6.5)
ECOG performance status, No. (%)[c]		
0	214 (59.1)	104 (56.5)
1	129 (35.6)	74 (40.2)
2	19 (5.2)	6 (3.3)
Reason for discontinuation of sorafenib, No. (%)		
Disease progression	294 (81.2)	147 (79.9)
Intolerance	67 (18.5)	37 (20.1)
Other	1 (0.3)	0
Macroscopic vascular invasion, No. (%)		
No	243 (67.1)	124 (67.4)
Yes	119 (32.9)	60 (32.6)
Extrahepatic disease, No. (%)		
No	93 (25.7)	49 (26.6)
Yes	269 (74.3)	135 (73.4)
Metastatic sites, No. (%)		
Visceral[d]	194 (53.6)	103 (56.0)
Lung	155 (42.8)	73 (39.7)
Lymph nodes	78 (21.5)	32 (17.4)
Bone	37 (10.2)	17 (9.2)
Bone only	13 (3.6)	6 (3.3)
Central nervous system	4 (1.1)	2 (1.1)
Other	76 (21.0)	43 (23.4)
Current Barcelona Clinic Liver Cancer stage, No. (%)[e]		
B	49 (13.5)	26 (14.1)
C	313 (86.5)	158 (85.9)
Lesion type, No. (%)		
Target only	71 (19.6)	45 (24.5)
Nontarget only	14 (3.9)	8 (4.3)
Target and nontarget	276 (76.2)	131 (71.2)
None	1 (0.3)	0
HCC etiology, No. (%)		
Hepatitis B	91 (25.1)	52 (28.3)
Hepatitis C	94 (26.0)	43 (23.4)
Alcohol	64 (17.7)	45 (24.5)
Nonalcoholic steatohepatitis	14 (3.9)	6 (3.3)
Unknown	78 (21.5)	25 (13.6)
Other	21 (5.8)	13 (7.1)
Child-Pugh score, No. (%)[f]		
A	354 (97.8)	182 (98.9)
B	8 (2.2)	2 (1.1)
Baseline alpha-fetoprotein level, No. (%)		
<200 ng/mL	179 (49.4)	88 (47.8)
≥200 ng/mL	171 (47.2)	88 (47.8)
Missing	12 (3.3)	8 (4.3)
Any prior antineoplastic therapy, No. (%)[g]	298 (82.3)	149 (81.0)
Any prior radiotherapy	51 (14.1)	27 (14.7)
Any prior surgery	142 (39.2)	71 (38.6)
Any prior local therapy	277 (76.5)	138 (75.0)
Any prior medication	59 (16.3)	28 (15.2)
Chemotherapy	41 (11.3)	15 (8.2)
Hormonal therapy	1 (0.3)	1 (0.5)
Immunotherapy	3 (0.8)	1 (0.5)
Targeted therapy	11 (3.0)	11 (6.0)
Other	4 (1.1)	1 (0.5)

(continued)

Table 1. Baseline Demographic and Disease Characteristics (Full Analysis Population) (continued)

Abbreviations: ECOG, Eastern Cooperative Oncology Group; HCC, hepatocellular carcinoma.

[a] Asia includes China, South Korea, Taiwan, and Thailand.

[b] Rest of the world includes Australia, Austria, Belgium, Canada, France, Germany, Greece, Hungary, Israel, Italy, Japan, Spain, and the United States.

[c] Status of 0 indicates patient is fully active; 1, patient is restricted in physically strenuous activity but ambulatory and able to carry out tasks of a light or sedentary nature; 2, patient is ambulatory and capable of all self-care but unable to carry out any work activities.

[d] Includes pleura, pleural effusion (malignant), lung, pericardial effusion (malignant), spleen, pancreas, gallbladder, bile duct, omentum, esophagus, stomach, small bowel, appendix, colon, rectum, peritoneum, ascites (malignant), uterus, cervix, ovary, testis, prostate, adrenal, kidney, ureter, bladder, thyroid, neck, and salivary glands.

[e] Barcelona Clinic Liver Cancer stage B disease is defined as Child-Pugh classification of A or B, an ECOG performance status of 0, and a multinodular tumor. Stage C disease is defined as Child-Pugh classification of A or B, an ECOG performance status of 1 or 2, and portal invasion or disease that has spread to the regional lymph nodes or distant organs.

[f] Child-Pugh score is calculated by assessing ascites (1 point for none, 2 points for slight, and 3 points for moderate), serum bilirubin level (1 point for <2.0 mg/dL, 2 points for 2.0-3.0 mg/dL, and 3 points for >3.0 mg/dL), serum albumin level (1 point for >3.5 mg/dL, 2 points for 2.8-3.5 mg/dL, and 3 points for <2.8 mg/dL), prolongation of prothrombin time (1 point for <4 seconds, 2 points for 4-6 seconds, and 3 points for >6 seconds), and encephalopathy (1 point for none, 2 points for grade 1 or 2, and 3 points for grade 3 or 4). Child-Pugh class A is a total score of 5 or 6 points, and class B is a total score of 7-9 points.

[g] Any prior antineoplastic therapy includes patients who have had medication, radiotherapy, surgery (excluding biopsy), or local therapy for HCC. Patients could have received ≥1 prior antineoplastic therapy, although only 1 prior systemic therapy, before sorafenib.

hepatitis B surface or core antibody (HBsAb or HBcAb) and, per protocol, did not receive antiviral prophylaxis. Two of these patients, both in the everolimus group, experienced HBV reactivation. All reactivation cases were asymptomatic, although 3 everolimus recipients discontinued therapy because of reactivation. None of the 79 patients in the everolimus group or 39 in the placebo group with detectable HCV-RNA or

Figure 2. Overall Survival and Time to Progression in the Full Analysis Population

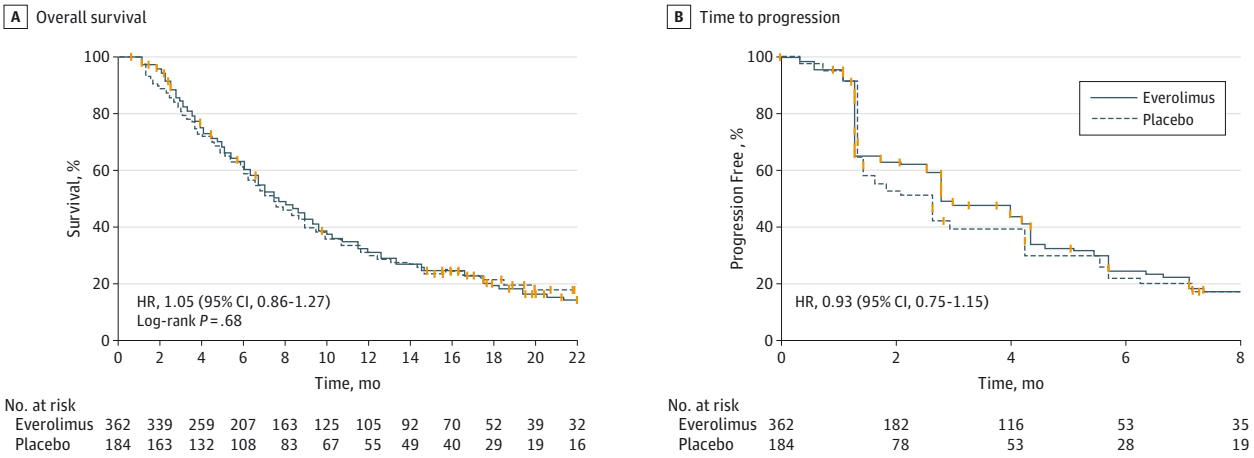

Kaplan-Meier estimates of overall survival (A) and time to progression (B). The curves were truncated when the percentage of patients remaining at risk was approximately 10%. Vertical ticks on the curves indicate censoring events.

known history of HCV infection without detectable HCV-RNA experienced HCV flare. Incidence of other AEs of clinical interest for everolimus is shown in eTable 3 in the Supplement.

Seventy-five patients (13.8%) died during treatment or within the 28 days after discontinuation, with 47 deaths (13.0%) in the everolimus and 28 (15.4%) in the placebo group. Progressive disease was the primary cause of death in 36 (10.0%) everolimus and 24 (13.2%) placebo recipients. Adverse events led to death in 11 (3.0%) everolimus recipients (2 cases each of death of unknown cause and renal failure and 1 case each of cerebrovascular accident, gastrointestinal hemorrhage, interstitial lung disease, peritonitis, pneumonitis, respiratory failure, and upper gastrointestinal hemorrhage) and 4 (2.2%) placebo recipients (1 case each of cardiac arrest, gastrointestinal hemorrhage, hepatic cirrhosis, and multiorgan failure).

Discussion

No systemic therapies have been established for patients with advanced HCC for whom sorafenib fails or who cannot tolerate sorafenib, highlighting the unmet need in this setting. Since sorafenib was approved for HCC, interest in developing molecularly targeted agents in this disease has been renewed. Although most phase 3 efforts have focused on vascular endothelial growth factor-targeted agents, everolimus inhibits mTOR, another critical target implicated in hepatocarcinogenesis.

Despite the strong scientific rationale[6-8,11,12,19-22] and preclinical data,[7,9,10,23] everolimus plus best supportive care failed to improve survival over placebo plus best supportive care in patients with advanced HCC that progressed during or after receiving sorafenib or who were sorafenib intolerant in the EVOLVE-1 study. The known prognostic factors, including ECOG performance status and the presence of macrovascular invasion or extrahepatic disease, were well balanced between treatment groups, and adjustment for these factors did not improve the risk of death between groups. A comprehensive, prespecified subgroup analysis revealed similar outcomes in most groups. Patients with HBV appeared to have prolonged overall survival with everolimus. Whether this finding truly represents a benefit in this subgroup or rather reflects an imbalance of prognostic factors between populations requires further investigation. In EVOLVE-1, improvements in secondary outcomes, including time to progression and overall response rate, were not observed. Although the disease control rate favored everolimus, this finding should be considered exploratory given the primary end point was not met. Furthermore, any benefit could be counterbalanced by the higher AE rate observed with everolimus. Despite the negative results from the EVOLVE-1 trial, given the immunosuppressive and antitumor effects of mTOR inhibitors, the potential benefits of this class of agents in the adjuvant setting are being assessed in a phase 3 trial of sirolimus for patients with HCC after liver transplantation (NCT00355862).

The AE profile observed for everolimus in this study was mostly consistent with the known safety profile of everolimus in other cancers. Hepatitis B virus reactivation, a known complication of immunosuppressive therapy, has been reported in other everolimus trials[13,24] and in published case reports.[25-27] In the phase 1 trial of everolimus for advanced HCC, routine antiviral prophylaxis was not given, and HBV reactivation with hepatitis flare was reported in 4 of 27 patients (15%) who were HBsAg-positive.[13] In all 4 patients, reactivation resolved within 4 to 8 weeks of everolimus withdrawal and initiation of antiviral therapy. Despite preemptive antiviral therapy in EVOLVE-1, HBV reactivation based on central laboratory findings occurred in 37.0% of everolimus and 22.7% of placebo recipients who were HBV-DNA or HBsAg-positive (or both) at baseline. An additional 2.9% of everolimus recipients who were HBsAg-negative but HBsAb- or HBcAb-positive experienced HBV reactivation. Of note, all cases were asymptomatic. Our study represents the largest prospective

experience with HBV reactivation in patients receiving everolimus with antiviral prophylaxis and, to the best of our knowledge, is the first report describing events in patients with past HBV infection receiving everolimus. These results suggest antiviral prophylaxis and close monitoring may be important for everolimus recipients with underlying HBV infection. The mecha-

Figure 3. Subgroup Analysis of Overall Survival

	Everolimus		Placebo		
	No. of Events	No. of Patients	No. of Events	No. of Patients	HR (95% CI)
All	303	362	151	184	1.05 (0.86-1.27)
Region					
Asia	54	59	29	32	0.97 (0.61-1.52)
Rest of world	249	303	122	152	1.04 (0.84-1.29)
Macrovascular invasion					
Present	111	118	54	61	1.21 (0.87-1.68)
Absent	192	244	97	123	0.96 (0.75-1.22)
Age					
<65 y	130	155	78	93	0.95 (0.72-1.26)
≥65 y	173	207	73	91	1.10 (0.84-1.45)
ECOG performance status					
0	169	214	83	104	1.02 (0.79-1.33)
≥1	134	148	68	80	1.03 (0.77-1.39)
Sorafenib status					
Progressor	248	294	123	147	0.94 (0.76-1.17)
Intolerant	54	67	28	37	1.44 (0.91-2.30)
Tumor size at baseline					
≤10 cm	107	143	56	75	0.95 (0.68-1.31)
>10 cm	185	204	91	101	1.05 (0.81-1.35)
Prior local treatment for HCC					
Yes	230	277	113	138	0.97 (0.78-1.22)
No	73	85	38	46	1.22 (0.83-1.81)
BCLC stage					
B	37	49	22	26	0.94 (0.55-1.60)
C	266	313	129	158	1.04 (0.84-1.29)
Extrahepatic spread					
Yes	228	269	112	135	1.02 (0.81-1.27)
No	75	93	39	49	1.05 (0.71-1.54)
Macrovascular invasion or extrahepatic spread or both					
Yes	258	301	124	150	1.05 (0.85-1.31)
No	45	61	27	34	0.87 (0.54-1.14)
Etiology					
Hepatitis B	75	91	47	52	0.64 (0.45-0.93)
Hepatitis C	78	94	36	43	0.96 (0.65-1.43)
Other	150	177	68	89	1.35 (1.01-1.80)
Alpha-fetoprotein					
<200 ng/mL	138	179	65	88	0.98 (0.73-1.32)
≥200 ng/mL	156	171	78	88	1.20 (0.91-1.57)

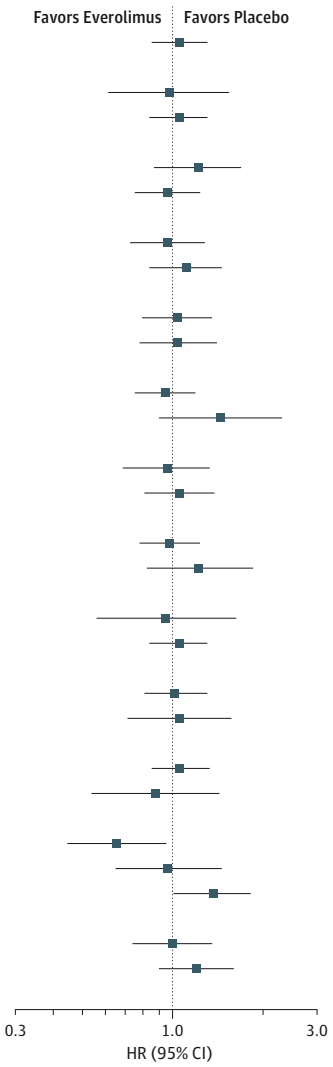

Hazard ratios (HRs) and 95% CIs were calculated using a stratified Cox proportional hazards model for all patients and an unstratified Cox proportional hazards model for subgroup analyses. BCLC indicates Barcelona Clinical Liver Cancer; ECOG, Eastern Cooperative Oncology Group; HCC, hepatocellular carcinoma.

Table 2. Best Overall Response and Disease Control Rate per RECIST (Full Analysis Population)

	Everolimus and Best Supportive Care (n = 362)	Placebo and Best Supportive Care (n = 184)	*P* Value
Best overall response, No. (%)			
Complete response	0	0	
Partial response	8 (2.2)	3 (1.6)	
Stable disease	195 (53.9)	80 (43.5)	
Progressive disease	115 (31.8)	73 (39.7)	
Unknown	44 (12.2)	28 (15.2)	
Disease control rate, % (95% CI)[a]	56.1 (50.8-61.3)	45.1 (37.8-52.6)	.01

[a] Proportion of patients whose best overall response is complete response, partial response, or stable disease according to RECIST (Response Evaluation Criteria in Solid Tumors).

nism and clinical significance of subclinical HBV reactivation in HBsAg-positive placebo recipients require elucidation.

The results from EVOLVE-1 extend the list of failed phase 3 studies in advanced HCC, highlighting the challenge of developing effective therapies for this cancer. In the first-line setting, 3 multikinase inhibitors—sunitinib, brivanib, and linifanib—have been compared with sorafenib, and all failed to achieve their primary end point.[28-30] Another first-line trial failed to demonstrate a survival benefit for erlotinib plus sorafenib over sorafenib alone.[31] In the phase 3 BRISK-PS study of patients with advanced HCC who progressed during or after sorafenib or who were sorafenib intolerant, brivanib failed to improve overall survival compared with placebo, despite improvements in time to progression and objective response rate.[32] Similar to BRISK-PS, median overall survival in the EVOLVE-1 control group was longer than expected, likely reflecting patient selection and improved supportive management of this population. The shorter median overall survival in the placebo group of EVOLVE-1 compared with that of BRISK-PS (7.3 vs 8.2 months) could reflect enrollment of a higher percentage of patients with poor prognostic factors in EVOLVE-1 (eg, macrovascular invasion, 32.8% vs 18%). The natural history of patients for whom sorafenib treatment failed remains to be explored.

EVOLVE-1 and the other failed phase 3 studies have provided several important lessons. First, it is difficult to assess efficacy signals from phase 2 trials. For everolimus, the initial modest efficacy signal was obtained from 2 phase 1/2

Table 3. Adverse Events of Any Cause With Incidence 5% or Greater in the Everolimus Group (Safety Population)

	No. (%)					
	Everolimus and Best Supportive Care (n = 361)			Placebo and Best Supportive Care (n = 182)		
	All Grades	Grade 3	Grade 4	All Grades	Grade 3	Grade 4
Any preferred term	358 (99.2)	188 (52.1)	68 (18.8)	171 (94.0)	62 (34.1)	33 (18.1)
Stomatitis	143 (39.6)	10 (2.8)	0	9 (4.9)	1 (0.5)	0
Decreased appetite	117 (32.4)	21 (5.8)	1 (0.3)	27 (14.8)	1 (0.5)	0
Edema peripheral	103 (28.5)	6 (1.7)	0	27 (14.8)	1 (0.5)	0
Diarrhea	94 (26.0)	5 (1.4)	0	25 (13.7)	2 (1.1)	0
Pyrexia	92 (25.5)	4 (1.1)	0	13 (7.1)	0	0
Fatigue	91 (25.2)	15 (4.2)	1 (0.3)	30 (16.5)	6 (3.3)	1 (0.5)
Epistaxis	85 (23.5)	4 (1.1)	0	5 (2.7)	0	0
Cough	79 (21.9)	3 (0.8)	0	24 (13.2)	1 (0.5)	0
Rash	76 (21.1)	3 (0.8)	0	16 (8.8)	0	0
Asthenia	66 (18.3)	27 (7.5)	1 (0.3)	34 (18.7)	8 (4.4)	2 (1.1)
Pruritus	65 (18.0)	1 (0.3)	0	29 (15.9)	0	0
Abdominal pain	62 (17.2)	12 (3.3)	0	33 (18.1)	8 (4.4)	1 (0.5)
Nausea	60 (16.6)	5 (1.4)	0	24 (13.2)	0	0
Anemia	59 (16.3)	24 (6.6)	4 (1.1)	14 (7.7)	4 (2.2)	2 (1.1)
Ascites	57 (15.8)	18 (5.0)	2 (0.6)	29 (15.9)	15 (8.2)	1 (0.5)
Vomiting	57 (15.8)	3 (0.8)	0	19 (10.4)	1 (0.5)	0
Dyspnea	51 (14.1)	10 (2.8)	0	25 (13.7)	6 (3.3)	1 (0.5)
Thrombocytopenia	44 (12.2)	15 (4.2)	5 (1.4)	2 (1.1)	1 (0.5)	0
Insomnia	37 (10.2)	0	0	15 (8.2)	0	0
Weight decreased	36 (10.0)	0	0	8 (4.4)	0	0
Abdominal pain upper	31 (8.6)	5 (1.4)	0	17 (9.3)	3 (1.6)	0
Constipation	31 (8.6)	1 (0.3)	0	24 (13.2)	1 (0.5)	0
Dysgeusia	31 (8.6)	1 (0.3)	0	4 (2.2)	0	0
Pneumonia	27 (7.5)	10 (2.8)	3 (0.8)	2 (1.1)	1 (0.5)	0
Headache	26 (7.2)	1 (0.3)	0	9 (4.9)	0	0
Hepatitis B	25 (6.9)	22 (6.1)	0	8 (4.4)	8 (4.4)	0
Back pain	25 (6.9)	1 (0.3)	0	13 (7.1)	1 (0.5)	0
Aspartate aminotransferase increased	24 (6.6)	15 (4.2)	1 (0.3)	19 (10.4)	10 (5.5)	0
Dry skin	24 (6.6)	0	0	6 (3.3)	0	0
Dry mouth	23 (6.4)	0	0	5 (2.7)	0	0
Platelet count decreased	21 (5.8)	9 (2.5)	0	0	0	0
Pain in extremity	20 (5.5)	4 (1.1)	0	9 (4.9)	1 (0.5)	0
Hypokalemia	20 (5.5)	13 (3.6)	2 (0.6)	1 (0.5)	0	0
Hyperglycemia	20 (5.5)	13 (3.6)	0	3 (1.6)	3 (1.6)	0
γ-Glutamyltransferase increased	18 (5.0)	11 (3.0)	1 (0.3)	12 (6.6)	9 (4.9)	1 (0.5)

studies.[13,14] As has been recommended,[15] assessing efficacy in a randomized phase 2 study should be considered before proceeding to phase 3 testing. Second, surrogate end points such as time to progression, progression-free survival, and response rate inconsistently predict overall survival in phase 3 trials. Third, clinical and biologic heterogeneity likely affects the performance of targeted therapies in HCC. In the absence of well-characterized and validated predictive biomarkers, targeted agents will likely continue to have a high risk of failure if phase 3 trials are conducted in unselected populations. Relevant biomarkers that may predict clinical outcome in patients receiving everolimus are being assessed in the EVOLVE-1 population. Future studies of targeted agents for HCC should aim to enrich patient populations based on molecular classification and predictive biomarkers. A limitation of EVOLVE-1 was that it was not designed to identify a molecularly or clinically selected population that may have benefited from everolimus.

Conclusions

Everolimus did not improve overall survival in patients with advanced hepatocellular carcinoma whose disease progressed during or after taking sorafenib or who were intolerant of sorafenib.

ARTICLE INFORMATION

Author Affiliations: Massachusetts General Hospital Cancer Center, Harvard Medical School, Boston (Zhu); Kinki University School of Medicine, Osaka, Japan (Kudo); ICM Val d'Aurelle, Montpellier, France (Assenat); University Nord De France, Lille, France (Cattan); Asan Medical Center, University of Ulsan College of Medicine, Seoul, Republic of Korea (Kang); Samsung Medical Center, Sungkyunkwan University School of Medicine, Seoul, Republic of Korea (Lim); University of Hong Kong, Queen Mary Hospital, Hong Kong, China (Poon); Hôpital Saint André, Bordeaux, France (Blanc); Medical School Hannover, Hannover, Germany (Vogel); Kaohsiung Chang Gung Memorial Hospital, Taiwan (C.-L. Chen); CHRU de Tours, Tours, France (Dorval); Medical University of Vienna, Vienna, Austria (Peck-Radosavljevic); Humanitas Cancer Center, Istituto Clinico Humanitas, Rozzano, Italy (Santoro); G Rummo Hospital, Benevento, Italy (Daniele); Kyorin University School of Medicine, Tokyo, Japan (Furuse); Novartis Pharma, Basel, Switzerland (Jappe, Perraud, Anak); Novartis Pharmaceuticals, East Hanover, New Jersey (Sellami); National Institute of Cancer Research, National Health Research Institutes, Tainan, Taiwan (L.-T. Chen); National Cheng Kung University Hospital, Tainan, Taiwan (L.-T. Chen); Kaohsiung Medical University Hospital, Kaohsiung Medical University, Kaohsiung, Taiwan (L.-T. Chen).

Author Contributions: Dr Zhu had full access to all of the data in the study and takes responsibility for the integrity of the data and the accuracy of the data analysis.
Study concept and design: Zhu, Poon, C.-L. Chen, Furuse, Anak, L.-T. Chen.
Acquisition, analysis, or interpretation of data: Zhu, Kudo, Assenat, Cattan, Kang, Lim, Poon, Blanc, Vogel, Dorval, Peck-Radosavljevic, Santoro, Daniele, Furuse, Jappe, Perraud, Anak, Sellami, L.-T. Chen.
Drafting of the manuscript: Zhu, Lim, C.-L. Chen, Jappe, Perraud, Anak, Sellami.
Critical revision of the manuscript for important intellectual content: Zhu, Kudo, Assenat, Cattan, Kang, Poon, Blanc, Vogel, Dorval, Peck-Radosavljevic, Santoro, Daniele, Furuse, Perraud, Anak, Sellami, L.-T. Chen.
Statistical analysis: Jappe, Perraud, Anak.
Administrative, technical, or material support: Zhu, Kang, Vogel, C.-L. Chen, Santoro, Furuse, Jappe.
Study supervision: Zhu, Kudo, Lim, Peck-Radosavljevic, Anak, Sellami, L.-T. Chen.

Conflict of Interest Disclosures: All authors have completed and submitted the ICMJE Form for Disclosure of Potential Conflicts of Interest. Dr Zhu reports consultancy for sanofi-aventis, Exelixis, Eisai, and Daiichi Sankyo. Dr Kudo reports having received a grant, consulting fee or honorarium, and support for travel to meetings for the study or other purposes and consultancy for Novartis. Dr Cattan reports receiving support for travel to meetings for the study or other purposes from Novartis and consultancy for Novartis. Dr Kang reports board membership, consultancy, and grants or grants pending for Novartis. Dr Vogel reports consultancy, payment for lectures, and payment for manuscript preparation from Bayer, Celgene, and Roche; consultancy and payment for lectures from Amgen; and payment for lectures from Dr Falk Pharma. Dr Peck-Radosavljevic reports consulting fee or honorarium and support for travel to meetings for the study or other purposes from Novartis; board membership for BioAlliance Pharma; consultancy for Bayer, Gilead, Merck Sharpe Dohme, Jansen, Roche, AbbVie, Bristol-Myers Squibb, and Boehringer Ingelheim; grants or grants pending for Bayer, Abbott, and Gilead; payments for lectures including service on speakers' bureaus for Bayer, Merck Sharpe Dohme, Roche, Eli Lilly, Bristol-Myers Squibb, and Jansen; payment for manuscript preparation for Bayer; and payment for development of educational presentation for Bayer and Gilead. Dr Daniele reports board membership for Bayer and Daiichi Sankyo, consultancy for Bayer, and payments for lectures including service on speakers' bureaus for Bayer, Daiichi Sankyo, and Novartis. Dr Furuse reports consulting fee or honorarium from Novartis; fees for participation in review activities such as data monitoring boards, statistical analysis, end point committees, and the like from Novartis; board membership for Chugai Pharmaceutical, Taiho Pharmaceutical, Bayer Pharmaceutical, Zeria Pharmaceutical, GlaxoSmithKline, and Yakult; consultancy for GlaxoSmithKline, Zeria Pharmaceutical, Ono Pharmaceutical, and Boehringer Ingelheim; grants or grants pending from Taiho Pharmaceutical, Chugai Pharmaceutical, Pfizer, Bayer Pharmaceutical, GlaxoSmithKline, Takeda BioDevelopment Center Limited, Eli Lilly Japan, Yakult, Ono Pharmaceutical, Onco Therapy Science, and Takeda Pharmaceutical; payment for lectures including service on speakers' bureaus for Chugai Pharmaceutical, Taiho Pharmaceutical, Bayer Pharmaceutical, Eli Lilly Japan, and Pfizer. Ms Jappe reports employment and stock/stock options for Novartis Pharma AG. Mr Perraud reports employment for Novartis Pharma AG. Dr Anak reports employment and stock/stock options for Novartis Pharma AG. Dr Sellami reports employment and stock/stock options for Novartis Pharmaceuticals Corporation. Dr L.-T. Chen reports support for travel to meetings for the study or other purposes, consultancy, grants/grants pending, and payment for lectures including service on speakers' bureaus for Novartis. No other disclosures were reported.

Funding/Support: This study was sponsored by Novartis Pharmaceuticals. Medical writing and editorial support in the preparation of the manuscript was provided by Melanie Leiby, PhD, and Dolores Matthews, MEd, of ApotheCom (Yardley, Pennsylvania) and was supported by Novartis Pharmaceuticals.

Role of the Sponsor: Representatives of the study sponsor contributed to the design of the trial. Data were collected through the sponsor's data management system and were analyzed by their statistical team. An independent data monitoring committee reviewed interim efficacy analyses and oversaw safety data. As authors of the manuscript, representatives of the sponsor contributed to data interpretation and writing, reviewing, and amending the manuscript and participated in the decision to submit the manuscript for publication.

Previous Presentation: These data were presented in part at the 2014 Gastrointestinal Cancers Symposium; January 16-18, 2014; San Francisco, California.

Study Steering Committee: *Co-chairs:* Zhu, L.-T. Chen (senior author). *Members:* Kang, Lim, Poon, Vogel, Daniele, Furuse, Perraud, Anak, Sellami.

Additional Contributions: We thank Ghassan Abou-Alfa, MD (Memorial Sloan-Kettering Cancer Center, New York, New York), Hironobu Minami, MD (Kobe University Hospital, Kobe, Japan), Richard S. Finn, MD (University of California, Los Angeles), and Lee-Jen Wei, PhD (Harvard School of Public Health, Boston, Massachusetts) for serving on the independent data monitoring committee (chaired by Dr Abou-Alfa) that reviewed interim efficacy analyses and oversaw safety data. These individuals were compensated. We thank the following investigators for enrolling patients in the EVOLVE-1 study: *Australia:* Jonathan Cebon (Ludwig Institute for Cancer Research, Heidelburg), Jacob George (Westmead Hospital, Westmead), Simone Strasser (Royal Prince Alfred Hospital, Camperdown), Amany Zekry (St George Hospital Clinical School, University of New South Wales, Sydney). *Austria:* Rudolf Stauber (LKH Graz Med. Universität Klinik, Graz), Wolfgang Vogel (Univ

Klinik fur Innere Medizin Innsbruck, Innsbruck). *Belgium:* Ivan Borbath (Cliniques Universitaires Saint-Luc, Brussels), Marc Peeters (UZ Antwerpen, Edegem), Jean-Luc Van Laethem (CHU Erasme, Brussels), Chris Verslype (Gasthuisberg University Hospital, Leuven). *Canada:* Yoo-Joung Ko (Sunnybrook Health Sciences Center, Toronto), Walter Kocha (London Regional Cancer Cantre, London), Richard Létourneau (CHUM–Campus St Luc, Montreal), Peter Metrakos (MUHC–Royal Victoria Hospital, Montreal). *China:* Minshan Chen (Sun Yat-sen University Cancer Center, Guangzhou), Guohong Han (Xijing Hospital, Fourth Military Medical University, Xi'an), Hongming Pan (Sir Run Run Shaw Hospital and Zhejiang University Medical College, Zhejiang), Shukui Qin (PLA No. 81 Hospital, Nanjing), Jianming Xu (307 Hospital of the PLA, Beijing), Lvnan Yan (West China Hospital of Sichuan and University Chengdu, Sichuan). *France:* Sandrine Faivre (Hôpital Beaujon, Clichy), Armand Abergel (CHU de Clermont-Ferrand–Hôpital d'Estaing, Clermont Ferrand), Michel Doffoel (HUS–Nouvel Hôpital Civil, Strasbourg), Cyrille Féray (Hôtel-Dieu Hospital, Nantes), René Gerolami Santandrea (AP-HP Hôpital de la Conception, Marseille), Alexandra Heurgué-Berlot (Hôpital Robert Debré, Reims), Come Lepage (CHU–Hôpital du Bocage, Dijon), Phillipe Merle (Hôpital de la Croix Rousse, Lyon), Pierre Michel (CHU de Rouen, Rouen), Laurent Mineur (Institut Sainte Catherine, Avignon), Eric Nguyen-Khac (CHU d'Amiens–Hôpital Nord, Amiens), Isabelle Ollivier (CHU d'Amiens–Hôpital Côte de Nacre, Caen), Jean Marc Phelip (CHU de Saint Etienne–Hôpital Nord, Saint Priest en Jarez), Albert Tran (Hôpital de l'Archet 2, Nice). *Germany:* Christoph Antoni (University Medical Centre Mannheim, University of Heidelberg, Mannheim), Thomas Berg (Univ. Klinikum Leipzig, Leipzig), Michael Geissler (Städt Kliniken Esslingen, Esslingen), Frank Kolligs (Klinikum der Univ. München–Grosshadern, Munich), Michael Scheurlen (Klinik der Universität Würzburg, Würzburg), Eckart Schott (Charité Berlin Campus Vircho-Klinikum, Berlin), Joerg Schlaak (University Hospital Essen, Essen), Cameron Silke (Universitätskliniken Göttingen, Göttingen), Jörg Trojan (Universitätsklinikum Frankfurt, Frankfurt), Henning Wege (Universitätsklinikum Hamburg-Eppendorf, Hamburg). *Greece:* Christos Papandreou (University General Hospital of Larisa, Larisa), Amanda Psyrri (Attikon University General Hospital of Athens, Athens), Nikolaos Touroutoglou (Interbalkan Medical Center, Thessaloniki). *Hungary:* András Csejtei (Markusovszky Korhaz, Szombathely), István Láng (Orszagos Onkologiai Intezet, Budapest), János Szántó (Institute of Oncology, Medical and Health Science Center, University of Debrecen, Debrecen), László Thurzó (SZOTE Onkoterapias Klinika Szeged). *Israel:* Dan Aderka (Chaim Sheba Medical Center, Ramat Gan), Salomon Stemmer (Rabin Medical Center, Petah-Tiqva). *Italy:* Raffaele Addeo (Osp. Presidio Ospedaliero S. Giovanni di Dio, Frattamaggiore), Carlo Barone (Policlinico Univ A Gemelli–Univ Cattolica del Sacro Cuore, Rome), Antonio Bernardo (Fondzione Salvatore Maugeri IRCCS–1st Scientifico Pavia, Pavia), Luigi Bolondi (Az Osp. di Bologna Policl. S. Orsola-Malpighi, Bologna), Ignazio Carrea (Az Osp. Univ. Policlinico P. Giaccone Università Studi Palermo, Palermo), Francesco Cognetti (Istituti Fisioterapici Ospitalieri–Polo Onco. Regine Elena, Rome), Massimo Colombo (Fond. IRCCS Cà Granda Osp. Maggiore Policlinico, Milan), Camillo Porta (Fodazione IRCCS Policlinico S. Matteo, Univ. degli Studi Pavia, Pavia), Fabio Farinati (Azienda Ospedaliera–Università di Padova, Univer. Degli Studi, Padova), Sergio Frustaci (Centro di Riferimento Oncologico IRCCS, Aviano), Rosario Vincenzo Iaffaioli (IRCCS Fondazione G Pascale, Napoli), Gabriele Luppi (A.O. Univ Policl de Modena, Univ. Studi Modena e R. Emilia, Modena), Sante Romito (AO Universitaria OO.RR Foggia–Presidio Osp Riuniti Foggia, Foggia). *Japan:* Masayuki Furukawa (National Kyushu Cancer Center, Fukuoka), Masafumi Ikeda (National Cancer Center Hospital East, Kashiwa), Yoshitaka Inaba (Aichi Cancer Center Hospital, Aichi), Takao Iwasaki (Tohoku University Hospital, Sendai), Akihide Masumoto (Iizuka Hospital, Iizuka), Seijin Nadano (National Hospital Organization, Shikoku Cancer Center, Matsuyama), Yoichi Nishigaki (Gifu Municipal Hospital, Gifu), Kazushi Numata (Yokohama City University Medical Center, Yokohama), Takuji Okusaka (National Cancer Center Hospital Chuoku, Tokyo), Hideki Saitsu (NHO Kyushu Medical Center Fukuoka, Fukuoka), Yutaka Sasaki (Kumamoto University Hospital, Kumamoto), Takuma Teratani (Kanto Medical Center NTT EC, Shinagawa-ku), Hidenori Toyoda (Ogaki Municipal Hospital, Ogaki), Tatsuya Yamashita (Kanazawa University Hospital, Kanazawa), Osamu Yokosuka (Chiba University Hospital, Chiba). *Korea:* Hyun Cheol Chung (Severance Hospital, Seoul), Tae-You Kim (Seoul National University Hospital, Seoul). *Spain:* Jordi Bruix (Hospital Clinic I Provincial de Barcelona, Barcelona), Meritxell Casas Rodrigo (Consorci Hospitalari Parc Tauli, Barcelona), Lluis Castells Fuste (Hospital Vall D'Hebron, Barcelona), Enrique Grande Pulido (Hospital Ramon y Cajal Madrid, Madrid), Jose Montero Alvarez (Hospital Universitario Reina Sofia, Córdoba), Bruno Sangro Gomez Acebo (Clinica Universitaria de Navarra, Pamplona). *Taiwan:* Yee Chao (Taipei Veterans General Hospital, Taipei), Long-Bin Jeng (China Medical University Hospital, Taichung), Cheng-Yao Lin (Chi Mei Foundation Hospital–Liouying, Liouying Township), Deng-Yn Lin (Chang-Gung Memorial Hospital-Lino, Lin-Ko), Ying-Chun Shen (National Taiwan University Hospital, Taipei). *Thailand:* Touch Ativitavas (Ramathibodi Hospital, Bangkok), Vichien Srimuninnimit (Siriraj Hospital, Bangkok). *United States:* Jared Acoba (Queen's Medical Center, Honolulu, Hawaii), Sanjiv Agarwala (St Luke's Hospital and Health Network, Bethlehem, Pennsylvania), Ari Baron (California Pacific Medical Center, San Francisco), J. Thaddeus Beck (Highlands Oncology Group, Fayetteville, Arkansas), Allen Cohn (Rocky Mountain Cancer Centers, Denver, Colorado), David Cosgrove (Sidney Kimmel Cancer Center at Johns Hopkins Hospital, Baltimore, Maryland), Bradley Freilich (Midwest Cancer Care Physicians, Kansas City, Missouri), William Harris (Fred Hutchinson Cancer Research Center/Seattle Cancer Care Alliance, Seattle, Washington), Aram Hezel (University of Rochester Medical Center, Rochester, New York), Haresh Jhangiani (Compassionate Cancer Care Medical Group, Fountain Valley, Fountain Valley, California), Roy MacKintosh (VA Sierra Nevada Health Care System, Reno), Anthony Reid (University of California, San Diego, La Jolla), Spencer Shao (Northwest Cancer Specialists, Portland, Oregon), Carlos Taboada (Methodist Charlton Cancer Center, Dallas, Texas), Udit Verma (University of Texas Southwestern Medical Center, Dallas).

REFERENCES

1. Frenette C, Gish R. Targeted systemic therapies for hepatocellular carcinoma: clinical perspectives, challenges and implications. *World J Gastroenterol*. 2012;18(6):498-506.

2. Llovet JM, Ricci S, Mazzaferro V, et al; SHARP Investigators Study Group. Sorafenib in advanced hepatocellular carcinoma. *N Engl J Med*. 2008;359 (4):378-390.

3. Cheng AL, Kang YK, Chen Z, et al. Efficacy and safety of sorafenib in patients in the Asia-Pacific region with advanced hepatocellular carcinoma: a phase III randomised, double-blind, placebo-controlled trial. *Lancet Oncol*. 2009;10(1):25-34.

4. Marerro JA, Lencioni R, Ye SL, et al. Final analysis of GIDEON (Global Investigation of Therapeutic Decisions in Hepatocellular Carcinoma [HCC] and of its Treatment with Sorafenib [Sor]) in >3000 Sor-treated patients (pts): clinical findings in pts with liver dysfunction. *J Clin Oncol*. 2013;31(15 suppl):A4126.

5. Meric-Bernstam F, Gonzalez-Angulo AM. Targeting the mTOR signaling network for cancer therapy. *J Clin Oncol*. 2009;27(13):2278-2287.

6. Sahin F, Kannangai R, Adegbola O, Wang J, Su G, Torbenson M. mTOR and P70 S6 kinase expression in primary liver neoplasms. *Clin Cancer Res*. 2004; 10(24):8421-8425.

7. Villanueva A, Chiang DY, Newell P, et al. Pivotal role of mTOR signaling in hepatocellular carcinoma. *Gastroenterology*. 2008;135(6):1972-1983.

8. Zhou L, Huang Y, Li J, Wang Z. The mTOR pathway is associated with the poor prognosis of human hepatocellular carcinoma. *Med Oncol*. 2010; 27(2):255-261.

9. Semela D, Piguet AC, Kolev M, et al. Vascular remodeling and antitumoral effects of mTOR inhibition in a rat model of hepatocellular carcinoma. *J Hepatol*. 2007;46(5):840-848.

10. Huynh H, Chow KH, Soo KC, et al. RAD001 (everolimus) inhibits tumour growth in xenograft models of human hepatocellular carcinoma. *J Cell Mol Med*. 2009;13(7):1371-1380.

11. Menon S, Yecies JL, Zhang HH, et al. Chronic activation of mTOR complex 1 is sufficient to cause hepatocellular carcinoma in mice. *Sci Signal*. 2012;5 (217):ra24.

12. Horie Y, Suzuki A, Kataoka E, et al. Hepatocyte-specific Pten deficiency results in steatohepatitis and hepatocellular carcinomas. *J Clin Invest*. 2004;113(12):1774-1783.

13. Shiah HS, Chen CY, Dai CY, et al. Randomised clinical trial: comparison of two everolimus dosing schedules in patients with advanced hepatocellular carcinoma. *Aliment Pharmacol Ther*. 2013;37(1):62-73.

14. Zhu AX, Abrams TA, Miksad R, et al. Phase 1/2 study of everolimus in advanced hepatocellular carcinoma. *Cancer*. 2011;117(22):5094-5102.

15. Llovet JM, Di Bisceglie AM, Bruix J, et al; Panel of Experts in HCC-Design Clinical Trials. Design and endpoints of clinical trials in hepatocellular carcinoma. *J Natl Cancer Inst*. 2008;100(10):698-711.

16. Peveling-Oberhag J, Zeuzem S, Yong WP, et al. Effects of hepatic impairment on the pharmacokinetics of everolimus: a single-dose, open-label, parallel-group study. *Clin Ther*. 2013;35 (3):215-225.

17. Guidance for industry: collection of race and ethnicity data in clinical trials. US Food and Drug Administration. http://www.fda.gov/downloads/RegulatoryInformation/Guidances/ucm126396.pdf. Accessed June 4, 2014.

18. Lan KKG, DeMets DL. Discrete sequential boundaries for clinical trials. *Biometrika*. 1983;70(3):659-663.

19. Sieghart W, Fuereder T, Schmid K, et al. Mammalian target of rapamycin pathway activity in hepatocellular carcinomas of patients undergoing liver transplantation. *Transplantation*. 2007;83(4):425-432.

20. Baba HA, Wohlschlaeger J, Cicinnati VR, et al. Phosphorylation of p70S6 kinase predicts overall survival in patients with clear margin-resected hepatocellular carcinoma. *Liver Int*. 2009;29(3):399-405.

21. Fornari F, Milazzo M, Chieco P, et al. MiR-199a-3p regulates mTOR and c-Met to influence the doxorubicin sensitivity of human hepatocarcinoma cells. *Cancer Res*. 2010;70(12):5184-5193.

22. Kenerson HL, Yeh MM, Kazami M, et al. Akt and mTORC1 have different roles during liver tumorigenesis in mice. *Gastroenterology*. 2013;144(5):1055-1065.

23. Buitrago-Molina LE, Pothiraju D, Lamlé J, et al. Rapamycin delays tumor development in murine livers by inhibiting proliferation of hepatocytes with DNA damage. *Hepatology*. 2009;50(2):500-509.

24. Yao JC, Shah MH, Ito T, et al; RAD001 in Advanced Neuroendocrine Tumors, Third Trial (RADIANT-3) Study Group. Everolimus for advanced pancreatic neuroendocrine tumors. *N Engl J Med*. 2011;364(6):514-523.

25. Sezgin Göksu S, Bilal S, Coşkun HS. Hepatitis B reactivation related to everolimus. *World J Hepatol*. 2013;5(1):43-45.

26. Teplinsky E, Cheung D, Weisberg I, et al. Fatal hepatitis B reactivation due to everolimus in metastatic breast cancer: case report and review of literature. *Breast Cancer Res Treat*. 2013;141(2):167-172.

27. Mizuno S, Yamagishi Y, Ebinuma H, et al. Progressive liver failure induced by everolimus for renal cell carcinoma in a 58-year-old male hepatitis B virus carrier. *Clin J Gastroenterol*. 2013;6(2):188-192.

28. Cainap C, Qin S, Huang WT, et al. Phase III trial of linifanib versus sorafenib in patients with advanced hepatocellular carcinoma (HCC). *J Clin Oncol*. 2013;31(4 suppl):A249.

29. Cheng AL, Kang YK, Lin DY, et al. Sunitinib versus sorafenib in advanced hepatocellular cancer: results of a randomized phase III trial. *J Clin Oncol*. 2013;31(32):4067-4075.

30. Johnson PJ, Qin S, Park JW, et al. Brivanib versus sorafenib as first-line therapy in patients with unresectable, advanced hepatocellular carcinoma: results from the randomized phase III BRISK-FL study. *J Clin Oncol*. 2013;31(28):3517-3524.

31. Zhu AX, Rosmorduc O, Evans J, et al. A phase III randomized, double-blind, placebo-controlled trial of sorafenib plus erlotinib in patients with hepatocellular carcinoma (HCC). Presented at: Congress of the European Society of Medical Oncology; Vienna, Austria; September28–October 2, 2012.

32. Llovet JM, Decaens T, Raoul JL, et al. Brivanib in patients with advanced hepatocellular carcinoma who were intolerant to sorafenib or for whom sorafenib failed: results from the randomized phase III BRISK-PS study. *J Clin Oncol*. 2013;31(28):3509-3516.

Hepatology Research

Hepatology Research 2014; 44: 829–836 doi: 10.1111/hepr.12184

Original Article

Nationwide survey in Japan regarding splenectomy/partial splenic embolization for interferon treatment targeting hepatitis C virus-related chronic liver disease in patients with low platelet count

Naoto Ikeda,[1] Hiroyasu Imanishi,[1] Nobuhiro Aizawa,[1] Hironori Tanaka,[1] Yoshinori Iwata,[1] Hirayuki Enomoto,[1] Masaki Saito,[1] Hiroko Iijima,[1] Yuji Iimuro,[2] Jiro Fujimoto,[2] Satoshi Yamamoto,[3] Shozo Hirota,[3] Masatoshi Kudo,[4] Shigeki Arii[5] and Shuhei Nishiguchi[1]

[1]*Division of Hepatobiliary and Pancreatic Disease, Department of Internal Medicine, Departments of* [2]*Surgery and* [3]*Radiology, Hyogo College of Medicine, Nishinomiya,* [4]*Department of Gastroenterology and Hepatology, Faculty of Medicine, Kinki University, Sayama, and* [5]*Department of Hepato-Biliary-Pancreatic Surgery, Tokyo Medical and Dental University, Tokyo, Japan*

Aim: In chronic liver disease associated with hepatitis C virus (HCV), a low platelet count is a major obstacle in carrying out interferon (IFN) treatment. We used a questionnaire to clarify the extent to which splenectomy/partial splenic embolization (PSE) is performed before IFN treatment, as well as the efficacy and complications thereof.

Methods: Two questionnaires were distributed to 413 medical institutes in Japan specializing in the treatment of liver diseases, and responses were obtained from 204 institutes. Furthermore, a more detailed questionnaire was completed by 10 institutes that experienced cases of death.

Results: In patients with HCV genotype 1b and a high viral load (HCV1b/High), the sustained viral response (SVR) rate was 28% for the splenectomy group and 22% for the PSE group, with no significant difference between these groups. In patients that were not HCV1b/High, the SVR rate was higher in those that underwent splenectomy (71%) compared to the PSE group (56%; $P = 0.025$). There were cases of death in seven of 799 splenectomy cases (0.89%) and four of 474 PSE cases (0.84%). Infectious diseases were involved in nine of 11 cases of death, with a peculiar patient background of Child–Pugh B (6/10) and an age of 60 years or greater (7/11).

Conclusion: The application of splenectomy/PSE before IFN treatment should be avoided in patients with poor residual hepatic function and/or elderly patients. In HCV1b/High patients, splenectomy/PSE should be performed only after selecting those in which IFN treatment should be highly effective.

Key words: chronic hepatitis C, interferon, low platelet count, partial splenic embolization, questionnaires, splenectomy

Correspondence: Professor Shuhei Nishiguchi, Division of Hepatobiliary and Pancreatic Disease, and Department of Internal Medicine, Hyogo College of Medicine, 1-1 Mukogawa-cho, Nishinomiya, Hyogo 663-8501, Japan. Email: nishiguc@hyo-med.ac.jp

Conflict of interest: Shuhei Nishiguchi received financial support from Chugai Pharmaceutical, MSD, Dainippon Sumitomo Pharma, Ajinomoto Pharma and Otsuka Pharmaceutical. Hiroko Iijima received financial support from Chugai Pharmaceutical. Hiroyasu Imanishi received financial support from Chugai Pharmaceutical. The remaining authors have no conflict of interest.

Received 29 March 2013; revision 4 June 2013; accepted 10 June 2013.

INTRODUCTION

IN JAPAN, MANY patients with hepatitis C virus (HCV)-related chronic liver disease (CLD) exhibit advanced aging and a long disease duration. These patients often have pancytopenia due to hypersplenism caused by advanced liver fibrosis, thus leading to difficulty in receiving a sufficient dose of interferon (IFN). Because low adherence to IFN often results in treatment failure, pancytopenia, including low platelet count, is a major challenge for IFN therapy in Japanese HCV-infected patients.

The rate of hepatocellular carcinoma (HCC) development increases with the progression of liver fibrosis, and the annual occurrence rate in HCV positive Japanese cirrhotic patients is high (~7–8%).[1] The incidence of HCC significantly decreases after viral eradication by IFN treatment (sustained viral response [SVR]) in patients with HCV-related CLD, even in patients with liver cirrhosis.[2–5] However, the SVR rate in cirrhotic patients with HCV genotype 1b is approximately 25%, that is significantly lower than that of chronic hepatitis patients (~50%). Hypersplenism due to portal hypertension is believed to be one of the causes of the low SVR rate of IFN treatment observed in cirrhotic patients.[6–9] In patients with hypersplenism, reducing the dose or discontinuing IFN is often required because of their thrombocytopenia and/or granulocytopenia. Furthermore, with the combined use of ribavirin (RBV), the adherence to treatment declines in association with the degree of anemia. Discontinuing or reducing the dose of antiviral agents (IFN and/or RBV) decreases the SVR rate,[10,11] and the presence of hypersplenism-related pancytopenia can be a major cause of this decrease. In particular, a low platelet count is the main factor that is linked to the discontinuation of IFN treatment. Therefore, in order to increase the platelet count and improve adherence to antiviral agents, splenectomy/partial splenic embolization (PSE) before the initiation of IFN therapy is considered a useful option for patients with hypersplenism-linked pancytopenia.[12–23]

In Japan, it is recommended that splenectomy/PSE be performed on patients with a low platelet count before IFN treatment, as specified in the Guidelines for Chronic Hepatitis C of 2008 and onwards.[24] However, neither splenectomy nor PSE is recommended in guidelines outside of Japan. Therefore, it is important and necessary to investigate whether these surgical or interventional treatments for anti-hypersplenism should be a standard precursor to IFN treatment for patients with a low platelet count. In addition, if splenectomy/PSE is indeed a valid therapeutic option, the patients that would most benefit from these treatments should be identified.[9,10,25–27]

In the present study, we investigated the current state of the treatment of splenectomy/PSE in HCV positive patients with low platelet count. We conducted a survey in the form of a questionnaire that probed the following topics with regard to splenectomy/PSE: the current status of implementation, associated complications, degree of increased platelets and its effect on IFN treatment.[15]

METHODS

Subjects

A SURVEY WAS conducted as a part of research by the "Standards and Clinical Research Aimed at Establishment of IFN Treatment Towards Cases with Low Platelet Counts" group from the scientific research grant from the Ministry of Health, Labor and Welfare in Japan. The sample included the 413 medical institutes to which the liver disease specialists (Japan Society of Hepatology, Board of Councilors of the Western and Eastern Association, Director of the Liver Cancer Study Group of Japan, and Councilor of The Japanese Society of Interventional Radiology) belong. Approval was obtained from the three associations (the Japan Society of Hepatology, the Liver Cancer Study Group of Japan and the Japanese Society of Interventional Radiology) prior to distributing this questionnaire. This study is a summary of the questionnaire responses, and ethical considerations toward patients were ensured by anonymizing personal information.

Questionnaires

Three types of questionnaires were prepared with internists, surgeons and radiologists as the subjects; each type of questionnaire was sent to 336, 46 and 31 institutes, respectively. As a general rule, one questionnaire was sent to one medical institute.

In this study, thrombocytopenia was defined as a platelet count of less than 100×10^9 platelets/L. A survey was conducted to determine whether splenectomy or PSE was performed to improve adherence to IFN treatment in patients with thrombocytopenia, and the selection criteria for splenectomy/PSE (including a platelet count and the liver function tests) were also queried in the first questionnaires (sent in September 2009 and collected on 22 December 2009). The state of the implementation of splenectomy/PSE was questioned again in the second questionnaire. The second questionnaire also focused on the appropriateness of performing splenectomy or PSE for IFN treatment in the patients, and investigated the aforementioned topics, including the efficacy of splenectomy/PSE, complications, and the prevalence of prophylactic administration of pneumococcal vaccine (sent in September 2010 and collected on 14 January 2011).[28] The third questionnaire (sent in November 2011 and collected on 6 December 2011) was performed as a detailed investigation of the 11 cases in which death was reported in the second questionnaire.

Statistical analysis

Data were expressed as mean ± standard deviation. A χ^2-test was used to compare splenectomy/PSE implementation cases, and Student's *t*-test and Mann–Whitney *U*-test were used for other comparisons. $P < 0.05$ indicated statistically significant difference.

RESULTS

FOR THE FIRST and second questionnaire, responses were obtained from internists, surgeons and radiologists (Table 1). For the third questionnaire, responses were obtained from all 10 institutes (11 patients died in 10 institutes: 100% recovery of the questionnaire sheets).

Standard platelet count required to initiate IFN treatment and the initial dose of IFN for patients with low platelet count

Eighty-nine percent (95/107) of institutes began IFN treatment even when the platelet count was less than 100×10^9 platelets/L. The adherence to IFN treatment of the patients was also answered. In the patients with a platelet count of 80×10^9 platelets/L or more before IFN treatment, 90% (72/80) of the institutions initiated therapy with a sufficient (≥80% of the normal dose) initial dose of IFN. However, among patients with a platelet count of less than 80×10^9 platelets/L, only 27% (25/93) started treatment with an insufficient (<80% of the normal dose) initial dose of IFN. Thus, many patients with a platelet count of less than 80×10^9 platelets/L prior to IFN introduction received a dose of IFN that was reduced to a level at which the IFN SVR rate was predicted to be low.

Implementation status of splenectomy/PSE prior to IFN treatment in patients with low platelet counts

The questionnaire results clarified that splenectomy and/or PSE were performed in 61% of the specialized institutes providing IFN therapy.

The platelet count that each institute considered when performing splenectomy/PSE before IFN treatment was $64 \times 10^9 \pm 18 \times 10^9$ platelets/L ($n = 25$) for splenectomy and $79 \times 10^9 \pm 14 \times 10^9$ platelets/L ($n = 24$) for PSE, with splenectomy having a significantly low value compared to PSE ($P = 0.002$).

Reasons for not performing splenectomy

In the questionnaire given to the internists (114 institutes), 60 institutes responded "splenectomy is not performed for IFN treatment".

In these 60 institutes, 28 described the possible severe complications as the reason for not carrying out splenectomy. Of these 28 institutes, four institutes that performed splenectomy for IFN treatment in the past experienced cases of portal thrombosis.

In the 26 institutes in which the surgeon-specific questionnaire was completed, 18 (69%) were performing splenectomy before IFN treatment; of these institutes, 59% experienced cases of portal thrombosis. In the questionnaire with internists and surgeons as subjects, the respondents strongly indicated complications as a reason for not performing splenectomy.

Reasons for not performing PSE

From the questionnaire that targeted internists (114 institutes), 70 institutes responded "PSE is not performed for IFN treatment".

In these 70 institutes, 36 described the possible severe complications as the reason for not performing splenectomy.

Of the 10 institutes in which questionnaires were completed by radiologists, one institute responded that PSE should not be performed for IFN treatment because of complication issues.

Platelet count transition and period before IFN treatment initiation following splenectomy/PSE

The changes in platelet count following splenectomy/PSE were investigated at each institute (Fig. 1), and a significantly increased platelet count was observed after carrying out splenectomy or PSE. However, this platelet count increase appeared to be higher and more sustained in patients who underwent splenectomy relative to those that underwent PSE. IFN administration was initiated within 1 – 3 months following PSE and within

Table 1 Questionnaire collection rates

	Internists	Surgeons	Radiologists
1st response	32% (107/336)	52% (24/46)	23% (7/31)
2nd response	34% (114/336)	57% (26/46)	32% (10/31)

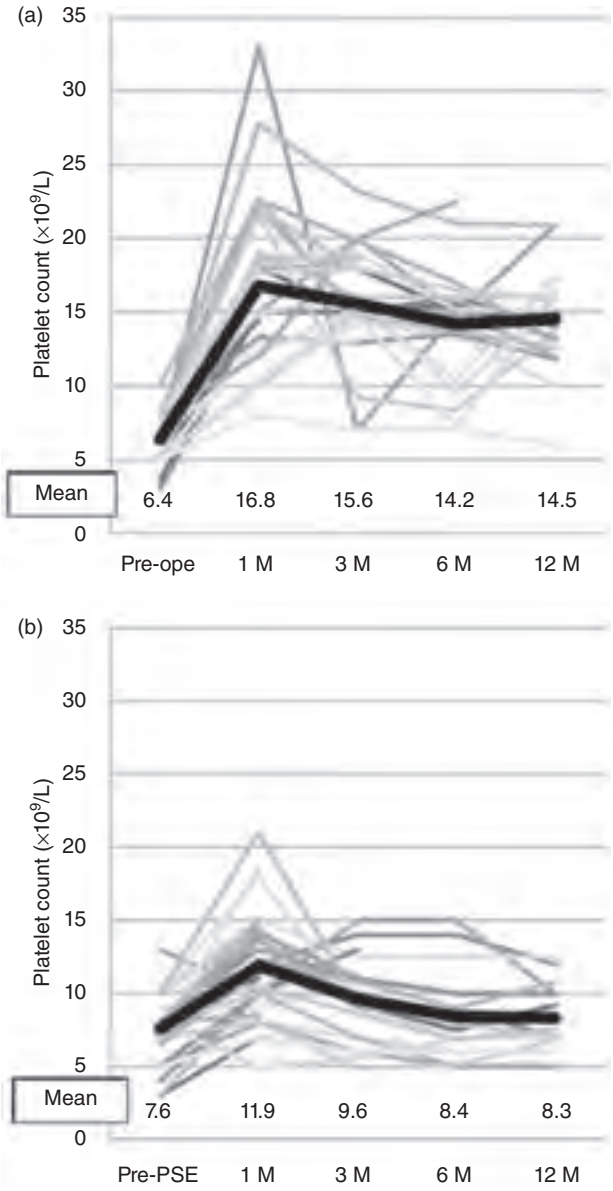

Figure 1 Platelet count transition of each institute following splenectomy/partial splenic embolization (PSE); average platelet count number of institutes. The bold line represents the transition of the mean platelet counts of each institute. (a) Splenectomy cases. (b) PSE cases.

3 – 6 months following splenectomy in the majority of cases (Table 2).

Complications following splenectomy/PSE

The splenectomy-associated complications experienced in each institute included portal thrombosis (28 of 63 institutes), postoperative infectious diseases (11 of 63 institutes) and ascites (12 of 62 institutes). However, the incidence of these complications varied depending on the institute.

In 64 institutes, fever ($n = 28$), thrombosis ($n = 22$), abscess ($n = 4$) and ascites ($n = 12$) were reported as frequent complications after PSE. However, the incidence of these complications also varied depending on the institute.

From 2005 to 2010, patient deaths were observed in seven of 788 (0.89%) cases of splenectomy, and in four of 474 (0.84%) cases of PSE. In nine of the 11 death cases, there appeared to be causal relationship between death and splenectomy as well as PSE (a causal relationship was indicated to exist by five of seven institutes for splenectomy and four of four institutes for PSE).

The age at the time of death ranged 46–70 years, with many patients older than 60 years. The sex included six male cases and five female cases, and there were two cases of chronic hepatitis and nine cases of liver cirrhosis (Child–Pugh classification grade A, two cases; B, six cases; and unknown, one case). The cirrhotic patients that died tended to have higher Child–Pugh scores and poor residual hepatic function. Pneumococcal vaccine inoculation was only performed in one splenectomy patient, and the other 10 patients were not inoculated. The cause of death was related to infectious diseases in nine cases (there was one patient with an apparent pneumococcal infection who was not inoculated with a pneumococcal vaccine). In most cases, death occurred within 3 months after treatment (splenectomy or PSE), although it also occurred over 3 months after treatment. Three patients died during IFN treatment (two cases after splenectomy, one case after PSE). Two patients died within 3 months after IFN treatment (two cases after splenectomy) (Table 3).

SVR rate of cases in which IFN treatment was performed following splenectomy or PSE

Among patients with low platelet count, IFN treatment was introduced in 92% (236/257) of the cases in which

Table 2 Period from splenectomy/PSE to initiation of IFN treatment

	Splenectomy ($n = 64$)	PSE ($n = 56$)
Within 1 month	6 (9%)	23 (42%)
>1 to 3 months	26 (41%)	23 (42%)
>3 to 6 months	17 (27%)	6 (10%)
>6 to 12 months	8 (12%)	3 (5%)
>12 months	7 (11%)	1 (1%)

IFN, interferon; PSE, partial splenic embolization.

Table 3 Period from splenectomy/PSE to death

	Splenectomy (7 cases of death)	PSE (4 cases of death)
Within 3 months	3 §Postoperative bleeding (hemophilia) §Pancreatic fistula, local infection §Intra-abdominal abscess (MRSA)	3 §Thrombocytopenia, cerebral hemorrhage §Pneumonia, ARDS, sepsis (MRSA) §Peritonitis
Within 6 months	0	1 †Spondylodiscitis, sepsis
Within 1 year	2 †SAH, bacteremia (MRSA) ‡Sepsis	0
Within 2 years	1 ‡Liver failure, suspect of SBP	0
Over 2 years	1 †Pneumococcal infection	0

†Death occurred during IFN treatment.
‡Death occurred within 3 months after IFN treatment.
§Death except † and ‡.
ARDS, acute respiratory distress syndrome; MRSA, methicillin-resistant *Staphylococcus aureus*; PSE, partial splenic embolization; SAH, subarachnoid hemorrhage; SBP, spontaneous bacterial peritonitis.

splenectomy was performed for IFN, 94% (295/314) of the cases in which PSE was performed for IFN, and 84% (241/285) of cases in which such pretreatment (splenectomy or PSE) was not performed before the introduction of IFN. Discontinuation of IFN occurred in 22% of cases of splenectomy, 28% of cases of PSE and 33% of those without pretreatment. Due to the pretreatment, the IFN introduction rates were increased ($P < 0.001$) and discontinuation rate declined ($P = 0.02$).

The pretreatment platelet count was $64 \times 10^9 \pm 17 \times 10^9$ platelets/L in splenectomy cases and $76 \times 10^9 \pm 21 \times 10^9$ platelets/L in PSE cases, while that of cases without pretreatment was $85 \times 10^9 \pm 16 \times 10^9$ platelets/L. In patients with a platelet count of 80×10^9 platelets/L or more, the majority of IFN treatments were without pretreatment to increase the platelet count.

The tabulation of the IFN treatment effects of cases in each institute is shown in Table 4. The SVR rate of cases of HCV genotype 1b and high viral load was 42 of 228 (22%) for the PSE group and 63 of 228 (28%) for the splenectomy group, with an odds ratio of 0.78 ($P = 0.19$). The SVR rate of so-called "others" (patients other than those with genotype 1b and high viral load) was 62 of 110 (56%) for the PSE group and 84 of 119 (71%) for the splenectomy group, with an odds ratio of 0.54 ($P = 0.025$). Additionally, in the "others" group, the SVR rate following IFN treatment was higher in patients who underwent splenectomy compared to that of patients who underwent PSE.

DISCUSSION

THE PRESENT STUDY was conducted to clarify the current conditions of splenectomy/PSE performed for the purpose of IFN treatment. This was the first national questionnaire conducted in Japan, and no similar studies have been reported previously. The results of these questionnaires revealed that the lower limit of the platelet count achieved prior to IFN administration varied widely depending on the institute in

Table 4 SVR rate of IFN treatment following splenectomy/PSE

	Splenectomy	PSE	*P* (odds ratio)
1b-high	28% (63/228)	22% (42/190)	0.19 (0.74)
Others	71% (84/119)	56% (62/110)	0.025 (0.54)

A difference in SVR rate was observed between splenectomy and PSE groups. In patients with hepatitis C virus genotype 1b and a high viral load, there was no significant difference in the low SVR rate. The SVR rate was high in cases other than those of a 1b genotype/high viral load, with splenectomy having a significantly higher SVR rate compared to PSE.
IFN, interferon; PSE, partial splenic embolization; SVR, sustained virological response.

Japan. Currently, for pegylated (PEG) IFN-α-2a/RBV treatment of liver cirrhosis, Japanese insurance considers a platelet count of 75×10^9 platelets/L or more as the standard count for treatment initiation and less than 50×10^9 platelets/L as that for discontinuation. However, it is now clear that half of the specialized institutes surveyed were initiating IFN therapy even in patients with platelet counts below the recommended value, and 9% of institutes were administrating IFN even in patients with platelet counts below the standard discontinuation value. Moreover, there was disproportionate selection and application of splenectomy and/or PSE, perhaps because each institute tended to select its experienced method. Therefore, in order to obtain consensus in the future, it is necessary to investigate the actual situation of splenectomy/PSE treatment in HCV positive patients with a low platelet count through the collection of clinical data.

Beneficial information regarding the effects of splenectomy and/or PSE on IFN treatment for the patients was also obtained from this questionnaire. The platelet counts increased after splenectomy and/or PSE, thus resulting in the improvement of adherence to IFN treatment. However, an increased SVR rate was not prominent in patients with HCV genotype 1b and a high viral load. It was presumed that if the viral factor shows IFN-resistant characteristics and liver cirrhosis exists as an intractable factor on the patient side, only a small number of patients will achieve a SVR with PEG IFN/RBV treatment, despite increased platelet counts and IFN adherence following splenectomy and/or PSE. However, in the case of "others", a relatively high SVR rate was observed (Table 4). Interestingly, the SVR rate of the "others" splenectomy group was significantly higher than that of the "others" PSE group, despite the pretreatment platelet count being lower in the splenectomy group than that of the PSE group. If the platelet count is less than 80×10^9 platelets/L in cases of "others," anti-hypersplenism treatment should be performed to increase the platelet count, and we suggest that splenectomy should be selected because of its strong effect on the increase of the platelet count.

Many complications regarding patients' safety were observed in both splenectomy and PSE groups, and it should be noted that slightly less than 1% cases resulted in death. Most patients had liver cirrhosis. These patients typically have several medical problems that can become severe if they are not receiving anti-HCV therapy, including decompensated cirrhosis and/or the development of HCC. However, the high mortality rate reported in the present study should not be overlooked. We recommend that the application of splenectomy/PSE prior to IFN treatment should be chosen with careful consideration.

At present, splenectomy/PSE is also mentioned in the Guidelines for IFN Treatments in Liver Cirrhosis C in Japan as treatments for patients with low platelet counts, although the risk of death due to splenectomy/PSE for the purpose of IFN treatment has not been studied previously. Death was related to infections in many cases, but the rate of pneumococcal vaccine inoculation was low in cases of death. According to the questionnaire results, within institutes administrating pneumococcal vaccines when performing splenectomy, the vaccination rate was 80% or more in the department of internal medicine and 60% or more in the surgical department; however, this rate was only approximately 20% for PSE. The pneumococcal vaccine is inoculated at a high rate for splenectomy based on the recommendations from the insurance guidelines[29] and infection prevention guidelines.[30–32] In contrast, there is no evidence indicating the usefulness of pneumococcal vaccine inoculation when performing PSE, in which splenic function is preserved. Therefore, this vaccine was not given to patients undergoing PSE in many cases. However, considering the fact that most causes of death were related to infections, pneumococcal vaccine inoculation should also be necessary when carrying out PSE. Moreover, vaccinations against bacteria other than *Streptococcus pneumoniae* such as *Haemophilus influenzae* type b (Hib) and *Neisseria meningitidis*, which mainly exhibit immune reactions in the spleen, may be important to administrate before splenectomy and/or PSE.[33–36]

Deaths were primarily observed in Child–Pugh B or C cirrhotic patients and those aged above 60 years. Therefore, splenectomy/PSE must be applied with care in patients with poor residual hepatic function and elderly patients.[37,38]

As a result of this questionnaire, we determined that adherence to IFN treatment was increased by splenectomy and/or PSE; however, in patients with HCV genotype 1b and a high viral load, the rate of SVR was not improved. Therefore, splenectomy and/or PSE must be limited to the cases in which IFN is likely to be effective. In addition, it is essential to predict the sensitivity of IFN treatment by evaluating the IFN sensitivity-determining region of HCV, core domain amino acid 70 of HCV and interleukin-28B, as well as hepatic functional reserves and age before splenectomy and/or PSE. In the future, treatment by various oral therapeutic agents (direct antiviral agents) may be selected without administrating IFN for patients with low platelet counts.[39,40]

ACKNOWLEDGMENTS

THIS STUDY WAS conducted with the support of a scientific research grant from the Ministry of Health, Labor and Welfare (Research Project for Emergency Measures to Overcome Hepatitis; H21/hepatitis/general/007). We would like to thank all of the members of the "Standards and Clinical Research Aimed for Establishment of IFN Treatment Towards Cases with Low Platelet Counts" group. We would like to express our appreciation to the Japan Society of Hepatology, the Liver Cancer Study Group of Japan, and the Japanese Society of Interventional Radiology who approved these questionnaires, as well as members of the institutions that responded.

REFERENCES

1 Oka H, Kurioka N, Kim K *et al*. Prospective study of early detection of hepatocellular carcinoma in patients with cirrhosis. *Hepatology* 1990; **12:** 680–7.
2 Nishiguchi S, Kuroki T, Nakatani S *et al*. Randomised trial of effects of interferon-alpha on incidence of hepatocellular carcinoma in chronic active hepatitis C with cirrhosis. *Lancet* 1995; **346:** 1051–5.
3 Camma C, Giunta M, Andreone P, Craxi A. Interferon and prevention of hepatocellular carcinoma in viral cirrhosis: an evidence-based approach. *J Hepatol* 2001; **34:** 593–602.
4 Singal AK, Freeman DH, Jr, Anand BS. Meta-analysis: interferon improves outcomes following ablation or resection of hepatocellular carcinoma. *Aliment Pharmacol Ther* 2010; **32:** 851–8.
5 Kudo M, Sakaguchi Y, Chung H *et al*. Long-term interferon maintenance therapy improves survival in patients with HCV-related hepatocellular carcinoma after curative radiofrequency ablation. A matched case-control study. *Oncology* 2007; **72** (Suppl 1)**:** 132–8.
6 Roffi L, Colloredo G, Pioltelli P *et al*. Pegylated interferon-alpha2b plus ribavirin: an efficacious and well-tolerated treatment regimen for patients with hepatitis C virus related histologically proven cirrhosis. *Antivir Ther* 2008; **13:** 663–73.
7 Marrache F, Consigny Y, Ripault MP *et al*. Safety and efficacy of peginterferon plus ribavirin in patients with chronic hepatitis C and bridging fibrosis or cirrhosis. *J Viral Hepat* 2005; **12:** 421–8.
8 Everson GT. Management of cirrhosis due to chronic hepatitis C. *J Hepatol* 2005; **42** (Suppl)**:** S65–74.
9 Yee HS, Currie SL, Darling JM, Wright TL. Management and treatment of hepatitis C viral infection: recommendations from the Department of Veterans Affairs Hepatitis C Resource Center program and the National Hepatitis C Program office. *Am J Gastroenterol* 2006; **101:** 2360–78.
10 Craxi A. EASL Clinical Practice Guidelines: management of hepatitis C virus infection. *J Hepatol* 2011; **55:** 245–64.
11 Ohkoshi S, Yamagiwa S, Yano M *et al*. Very-low-dose pegylated interferon a2a plus ribavirin therapy for advanced liver cirrhosis type C: a possible therapeutic alternative without splenic intervention. *Case Rep Gastroenterol* 2010; **4:** 261–6.
12 Ikezawa K, Naito M, Yumiba T *et al*. Splenectomy and antiviral treatment for thrombocytopenic patients with chronic hepatitis C virus infection. *J Viral Hepat* 2010; **17:** 488–92.
13 Akahoshi T, Tomikawa M, Korenaga D, Ikejiri K, Saku M, Takenaka K. Laparoscopic splenectomy with peginterferon and ribavirin therapy for patients with hepatitis C virus cirrhosis and hypersplenism. *Surg Endosc* 2010; **24:** 680–5.
14 Hayashi PH, Mehia C, Joachim Reimers H, Solomon HS, Bacon BR. Splenectomy for thrombocytopenia in patients with hepatitis C cirrhosis. *J Clin Gastroenterol* 2006; **40:** 740–4.
15 Okamura S, Sakai T, Yoshikai H *et al*. [Case of overwhelming postsplenectomy infection (OPSI) with chronic hepatitis type C during peginterferon/ribavirin combination therapy]. *Nippon Shokakibyo Gakkai Zasshi* 2009; **106:** 411–7.
16 Kercher KW, Carbonell AM, Heniford BT, Matthews BD, Cunningham DM, Reindollar RW. Laparoscopic splenectomy reverses thrombocytopenia in patients with hepatitis C cirrhosis and portal hypertension. *J Gastrointest Surg* 2004; **8:** 120–6.
17 Shigekawa Y, Uchiyama K, Takifuji K *et al*. A laparoscopic splenectomy allows the induction of antiviral therapy for patients with cirrhosis associated with hepatitis C virus. *Am Surg* 2011; **77:** 174–9.
18 Foruny JR, Blazquez J, Moreno A *et al*. Safe use of pegylated interferon/ribavirin in hepatitis C virus cirrhotic patients with hypersplenism after partial splenic embolization. *Eur J Gastroenterol Hepatol* 2005; **17:** 1157–64.
19 Miyake Y, Ando M, Kaji E, Toyokawa T, Nakatsu M, Hirohata M. Partial splenic embolization prior to combination therapy of interferon and ribavirin in chronic hepatitis C patients with thrombocytopenia. *Hepatol Res* 2008; **38:** 980–6.
20 Barcena R, Moreno A, Foruny JR *et al*. Partial splenic embolization and peg-IFN plus RBV in liver transplanted patients with hepatitis C recurrence: safety, efficacy and long-term outcome. *Clin Transplant* 2010; **24:** 366–74.
21 Annicchiarico BE, Siciliano M, Di Stasi C, Bombardieri G. Proximal splenic artery embolization allows pegylated interferon and ribavirin combination therapy in chronic hepatitis C virus-infected patients with severe cytopenia. *Eur J Gastroenterol Hepatol* 2006; **18:** 119–21.
22 Moreno A, Barcena R, Blazquez J *et al*. Partial splenic embolization for the treatment of hypersplenism in cirrhotic HIV/HCV patients prior to pegylated interferon and ribavirin. *Antivir Ther* 2004; **9:** 1027–30.

23 Tahara H, Takagi H, Sato K *et al*. A retrospective cohort study of partial splenic embolization for antiviral therapy in chronic hepatitis C with thrombocytopenia. *J Gastroenterol* 2011; **46:** 1010–9.
24 Kumada H, Okanoue T, Onji M *et al*. Guidelines for the treatment of chronic hepatitis and cirrhosis due to hepatitis C virus infection for the fiscal year 2008 in Japan. *Hepatol Res* 2010; **40:** 8–13.
25 de Bruijne J, Buster EH, Gelderblom HC *et al*. Treatment of chronic hepatitis C virus infection – Dutch national guidelines. *Neth J Med* 2008; **66:** 311–22.
26 Booth JC, O'Grady J, Neuberger J. Clinical guidelines on the management of hepatitis C. *Gut* 2001; **49** (Suppl 1)**:** I1–21.
27 Ghany MG, Strader DB, Thomas DL, Seeff LB. Diagnosis, management, and treatment of hepatitis C: an update. *Hepatology* 2009; **49:** 1335–74.
28 Hadem J, Cornberg M, Hauptmann C, Suttmann U, Manns MP, Wedemeyer H. Pneumococcal meningitis during antiviral treatment with interferon and ribavirin in a splenectomized patient with chronic hepatitis C – do not miss vaccination before starting therapy. *Z Gastroenterol* 2008; **46:** 880–2.
29 Prevention of pneumococcal disease: recommendations of the Advisory Committee on Immunization Practices (ACIP). *MMWR Recomm Rep* 1997; **46:** 1–24.
30 Konradsen HB, Pedersen FK, Henrichsen J. Pneumococcal revaccination of splenectomized children. *Pediatr Infect Dis J* 1990; **9:** 258–63.
31 Shatz DV, Schinsky MF, Pais LB, Romero-Steiner S, Kirton OC, Carlone GM. Immune responses of splenectomized trauma patients to the 23-valent pneumococcal polysaccharide vaccine at 1 versus 7 versus 14 days after splenectomy. *J Trauma* 1998; **44:** 760–5; discussion 765–6.
32 Shatz DV, Romero-Steiner S, Elie CM, Holder PF, Carlone GM. Antibody responses in postsplenectomy trauma patients receiving the 23-valent pneumococcal polysaccharide vaccine at 14 versus 28 days postoperatively. *J Trauma* 2002; **53:** 1037–42.
33 Mourtzoukou EG, Pappas G, Peppas G, Falagas ME. Vaccination of asplenic or hyposplenic adults. *Br J Surg* 2008; **95:** 273–80.
34 Landgren O, Bjorkholm M, Konradsen HB *et al*. A prospective study on antibody response to repeated vaccinations with pneumococcal capsular polysaccharide in splenectomized individuals with special reference to Hodgkin's lymphoma. *J Intern Med* 2004; **255:** 664–73.
35 Cherif H, Landgren O, Konradsen HB, Kalin M, Bjorkholm M. Poor antibody response to pneumococcal polysaccharide vaccination suggests increased susceptibility to pneumococcal infection in splenectomized patients with hematological diseases. *Vaccine* 2006; **24:** 75–81.
36 Ejstrud P, Kristensen B, Hansen JB, Madsen KM, Schonheyder HC, Sorensen HT. Risk and patterns of bacteraemia after splenectomy: a population-based study. *Scand J Infect Dis* 2000; **32:** 521–5.
37 Jackson SC, Beck P, Buret AG *et al*. Long term platelet responses to Helicobacter pylori eradication in Canadian patients with immune thrombocytopenic purpura. *Int J Hematol* 2008; **88:** 212–8.
38 McHutchison JG, Dusheiko G, Shiffman ML *et al*. Eltrombopag for thrombocytopenia in patients with cirrhosis associated with hepatitis C. *N Engl J Med* 2007; **357:** 2227–36.
39 Gane EJ, Roberts SK, Stedman CA *et al*. Oral combination therapy with a nucleoside polymerase inhibitor (RG7128) and danoprevir for chronic hepatitis C genotype 1 infection (INFORM-1): a randomised, double-blind, placebo-controlled, dose-escalation trial. *Lancet* 2010; **376:** 1467–75.
40 Suzuki F, Suzuki Y, Akuta N *et al*. Sustained virological response in a patient with chronic hepatitis C treated by monotherapy with the NS3-4A protease inhibitor telaprevir. *J Clin Virol* 2010; **47:** 76–8.

Hepatology Research

Hepatology Research 2014; **44**: 584–590 doi: 10.1111/hepr.12145

Case Report

Serum amyloid A and C-reactive protein positive nodule in alcoholic liver cirrhosis, hard to make definite diagnosis

Soo Ryang Kim,[1] Fukuo Kondo,[3] Yumi Otono,[1] Susumu Imoto,[1] Kenji Ando,[1] Makoto Hirakawa,[1] Katsumi Fukuda,[1] Madoka Sasaki,[1] Soo Ki Kim,[4] Takamitsu Komaki,[5] Shinobu Tsuchida,[2] Sawako Kobayashi,[6] Toshiyuki Matsuoka[7] and Masatoshi Kudo[8]

[1]*Department of Gastroenterology, Kobe Asahi Hospital,* [2]*Department of Surgery, Kobe University Hospital, Kobe,* [3]*Department of Pathology, Teikyo University, Tokyo,* [4]*Department of Gastroenterology, Kyoto University, Kyoto,* [5]*Department of Internal Medicine, Saiseikai-Tondabayashi Hospital,* [6]*Department of Hepatology, Osaka City University Graduate School of Medicine,* [7]*Department of Radiology, Osaka City University Graduate School of Medicine, Osaka, and* [8]*Department of Gastroenterology and Hepatology, Kinki University School of Medicine, Osaka-Sayama, Japan*

We describe a case of serum amyloid A (SAA) and C-reactive protein (CRP) positive nodule detected by immunohistochemical analysis in a 37-year-old woman with alcohol-related cirrhosis. Imaging studies at first admission pointed to hepatocellular carcinoma (HCC), a dysplastic nodule, an inflammatory pseudotumor or focal nodular hyperplasia (FNH). Ultrasonography-guided biopsy in Segment 2 showed minimal atypical changes, except for a slight increase in cell density and micronodular cirrhosis in the non-nodular portion. gadolinium-ethoxybenzyl-diethylenetriamine pentaacetic acid-enhanced magnetic resonance imaging carried out after a year and a half revealed hypervascularity in the arterial phase and isointensity in the hepatobiliary phase. Three years thereafter, however, the imaging displayed a change from isointensity to a defect in the hepatobiliary phase, and the nodule demonstrated minimal histological atypia. Immunohistochemical staining of the nodule was positive for SAA, CRP, liver fatty acid-binding protein and glutamine synthetase, but negative for β-catenin, heat shock protein 70 and Glypican 3. Organic anion transporter (OATP)8 staining was weaker in the nodule than in the non-nodular portion of the alcohol-related micronodular cirrhosis. The nodule was diagnosed as an SAA and CRP positive nodule, and HCC was ruled out. Despite the change from isointensity to a defect in the hepatobiliary phase, no evidence of HCC was found in the biopsy specimen. The change may be explained more by the weak OATP8 staining compared with that of alcohol-related liver cirrhosis than by malignant transformation into HCC.

Key words: alcohol-related liver cirrhosis, defect in the hepatobiliary phase, focal nodular hyperplasia, gadolinium-ethoxybenzyl-diethylenetriamine pentaacetic acid-enhanced magnetic resonance imaging, hepatocellular carcinoma, inflammatory hepatocellular adenoma

INTRODUCTION

THE CLASSIFICATION AND nomenclature of benign hepatocytic nodules is largely based on a document written by the International Working Party in 1995.[1] Several important advances since, have necessitated the updating of the classification, especially with regard to hepatocellular adenoma (HCA) and focal nodular hyperplasia (FNH). HCA is a benign neoplastic lesion and FNH a non-neoplastic hyperplastic lesion. The risk of malignant transformation and hemorrhage is higher in HCA than in FNH, therefore clinical differentiation of the two lesions is very important.

Alcohol abuse in some cases gives rise to hyperplastic nodules such as FNH-like nodules that are usually associated with hypervascularity.[2,3] The nodules show hypervascularity and/or a tumor stain on angiography resembling the imaging findings of hepatocellular carcinoma (HCC). Development of the newly intro-

Correspondence: Dr Soo Ryang Kim, Department of Gastroenterology, Kobe Asahi Hospital, 3-5-25 Bououji-cho, Nagata-ku, Kobe 653-0801 Hyogo, Japan. Email: asahi-hp@arion.ocn.ne.jp

Conflict interest: None of the authors have any conflict of interest.
Financial support: None of the authors received any financial support.
Received 2 April 2012; revision 16 April 2013; accepted 17 April 2013.

duced diagnostic imaging technique, gadolinium-ethoxybenzyl-diethylenetriamine pentaacetic acid (Gd-EOB-DTPA)-enhanced magnetic resonance imaging (MRI), has provided higher rates in the detection of small HCC and other intrahepatic nodular lesions. Gd-EOB-DTPA has unique pharmacodynamics of being taken up by hepatocytes and then excreted into bile ducts; it shows considerable potential as a new imaging method for differentiating benign nodules such as HCA and FNH from malignant ones such as HCC.

Here, we describe the case of serum amyloid A (SAA) and C-reactive protein (CRP) positive nodule detected through immunohistochemical studies and differentiated from HCC in a 37-year-old woman with alcohol-related liver cirrhosis, characterized by hypervascularity in the arterial phase and defect in the hepatobiliary phase, as determined through Gd-EOB-DTPA-enhanced MRI.

CASE REPORT

A 37-YEAR-OLD JAPANESE woman was admitted to our hospital in 2006 for further examination of a 22-mm hypoechoic nodule in the liver. The patient's alcohol consumption over the previous 10 years was 120 g/day; she had no past history of taking oral contraception; she was 161 cm tall, weighed 57 kg and her body mass index (BMI) was 22. A physical examination on admission showed moderate splenomegaly and palmar erythema but no other remarkable abnormalities. The serum was negative for hepatitis C virus antibody, hepatitis B surface antigen and hepatitis B core antibody. Laboratory data on admission disclosed the following abnormal values: platelets, $3.6 \times 10^4/\mu L$ (normal, 13.4–34.9); aspartate aminotransferase, 198 U/L (normal, 10–40); alanine aminotransferase, 49 U/L (normal, 5–40); alkaline phosphokinase, 409 U/L (normal, 115–359); thymol turbidity, 19.3 U (normal, ≤4.0); zinc surface turbidity, 29.4 U (normal, 2.0–12.0); indocyanine green retention rate at 15 min, 57% (normal, <10); γ-globulin, 37.6% (normal, 10.8–19.6); and CRP, 1.37 mg/dL (normal, ≤0.30). The levels of tumor markers were as follows: α-fetoprotein (AFP), 15.3 ng/mL (normal, ≤10); *Lens culinaris* agglutinin-reactive fraction of AFP (AFP-L3), 4.3% (normal, <10.0); and protein-induced vitamin K absence (PIVKA-II), 33 mAU/mL (normal, <40).

B-mode ultrasonography (US) disclosed several hypoechoic nodules (<20 mm in both lobes) and a 22-mm hypoechoic nodule in segment two (S2). Those hypoechoic nodules less than 20 mm in both lobes were hypervascular nodules without venous washout, and histologically, they were diagnosed as alcoholic-related cirrhosis without HCC. We focused on the 22-mm nodule because of its size of over 20 mm and characteristic imaging features. Imaging studies revealed the following: Sonazoid (GE Healthcare, Amersham, Buckinghamshire, UK) contrast-enhanced US disclosed hypervascularity in the arterial phase and a defect in the Kupffer phase; contrast-enhanced computed tomography (CT) revealed enhancement in the arterial phase and washout in the equilibrium phase; CT during hepatic arteriography revealed hyperattenuation; however, CT during arterial portography failed to generate images of blood flow because of collateral formations; MRI revealed high intensity and isointensity on T_1- and T_2-weighted sequences, respectively; Gd-contrast-enhanced MRI revealed hypervascularity in the arterial phase and washout in the equilibrium phase; super paramagnetic iron oxide (SPIO)-MRI revealed isointensity.

Ultrasonography-guided biopsy in S2 showed micronodular cirrhosis in the non-nodular portion. Histologically, the nodular lesion showed minimal atypical changes except for a slight increase in cell density in the parenchymal tissue (Fig. 1a). An abnormally thick artery was observed in the portal tract within the nodule (Fig. 1b). In the interstitial components, some portal tracts showed inflammatory cell infiltration and ductular reaction (Fig. 1c). Also, the nodule was positive for Berlin blue staining. Nonetheless, these findings were not sufficient to differentiate between FNH and HCA. Histological analysis of HE staining revealed no specific findings of FNH, HCA, HCC or of other pathologies such as hemangioma, hemangioendothelioma, inflammatory pseudotumor, pseudolymphoma or metastatic liver cancer. Immunohistochemical staining of the nodule was positive for SAA and CRP, leading to suspicion of inflammatory HCA. Negative β-catenin and weakly positive glutamine synthetase (GS) around veins were not indicative of β-catenin-activated HCA. Liver fatty acid-binding protein (L-FABP) was positive for, but not indicative of, hepatocyte nuclear factor (HNF)1α-inactivated HCA. Heat shock protein (HSP)70 and Glypican (GPC)3 were negative, but not indicative of very well-differentiated HCC. The weak staining of the nodule by organic anion transporter (OATP)8 compared with that of the non-nodular lesion was compatible with the imaging findings of Gd-EOB-DTPA-enhanced MRI (Table 1). The lesion was kept under careful observation without any treatment.

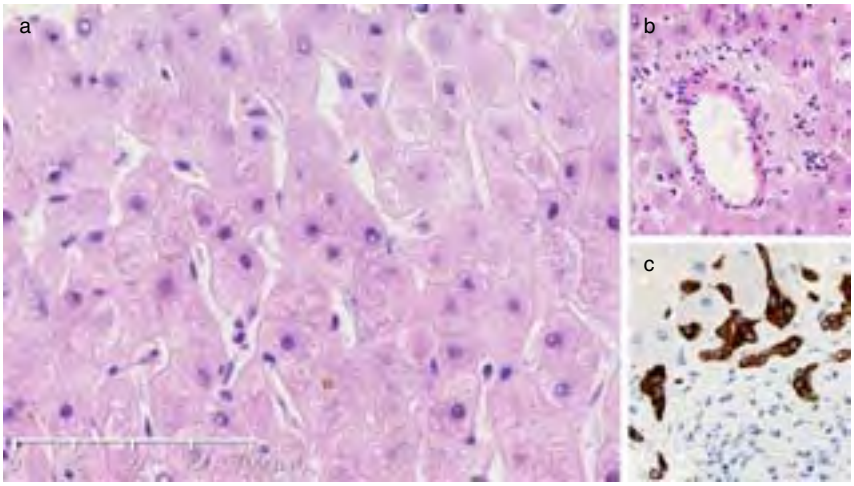

Figure 1 Histopathological findings of the biopsied specimen of the nodule in S2. The nodular lesion tissue shows minimal atypical changes except for a slight increase in cell density (hematoxylin–eosin [HE]) (a). An abnormally thick artery is seen in the portal tract within the nodule (HE stain) (b). A serial section of the specimen shows a bile duct, proving this figure is a portal tract. Within and around another portal tract, inflammatory cell infiltration and ductular reaction are observed (immunohistochemical staining with cytokeratin 7) (c).

Follow-up imaging examinations were carried out at the patient's readmission in 2008. Gd-EOB-DTPA-enhanced MRI revealed hypervascularity in the arterial phase and isointensity (Fig. 2a), but no defect, in the hepatobiliary phase.

In 2011, imaging examinations were carried out. B-mode US revealed several hypoechoic nodules in both lobes and a 22-mm hypoechoic one in S2 (Fig. 2b). CT and CT arterioportal angiography disclosed the same imaging findings as in 2006. Gd-EOB-DTPA-enhanced MRI, however, revealed hypervascularity in the arterial phase (Fig. 2c) but, this time, a defect in the hepatobiliary phase (Fig. 2d). Tumor markers including AFP, AFP-L3 and PIVKA-II demonstrated no change. Biopsy was carried out, and histopathological findings including immunohistological staining of SAA (Fig. 3a), CRP, HSP70, GPC3, L-FABP, β-catenin, GS and OATP8 (Fig. 3b,c) were the same as those in 2006, irrespective of the change from isointensity to a defect in the hepatobiliary phase determined by Gd-EOB-DTPA-enhanced MRI (Table 1).

DISCUSSION

VARIOUS BENIGN NODULAR lesions, as well as HCC, are routinely detected in the clinical setting. Among such benign hepatocellular nodular lesions, FNH and HCA are sometimes very difficult to differentiate from each other through both imaging modalities and biopsy analyses. FNH has been reported in 0.6–3% of the general population[4] and is 10-times more frequently observed than HCA in referral centers.[4] In approximately two-thirds of such cases, FNH is solitary. Most cases of FNH are diagnosed by chance, but some are symptomatic. FNH is associated with vascular abnormalities including hepatic hemangioma, which supports the concept of a vascular component in the pathogenesis of this lesion.[5,6]

Hepatocellular adenoma is a rare tumor observed in various clinical settings or by chance. It is important to stress that, at present, HCA cannot be identified conclusively by any currently available imaging technique. Hemangioma, hemangioendothelioma, inflammatory pseudotumor, pseudolymphoma and metastatic liver cancer need to be differentiated. HCA can, at best, only be strongly suspected, which may lead to liver biopsy or even surgical resection when the diagnosis is refuted.

Studies that correlate lesional genotypes with phenotypes form the basis of a new histological/molecular classification of HCA.[7] Based on two molecular criteria (HNF1α mutations and β-catenin mutations) and an additional histological criterion (the presence/absence of inflammation), subgroups of HCA[7] can be defined and distinguished from FNH.[8] Although there are several nomenclatures of HCA subclassification, HCA can now, according to a new World Health Organization (WHO) classification edited in 2010,[9] be subclassified into four categories: (i) HNF1α-inactivated HCA (tumors with HNF1α mutation with steatosis, lack of cytological abnormalities, no inflammatory infiltrate and negative liver fatty acid protein expression); (ii) β-catenin-activated HCA (tumors with β-catenin mutation with frequent cytological abnormalities and pseudoglandular formation); (iii) inflammatory HCA (telangiectatic/inflammatory HCA without HNF1α or β-catenin activation with cytological abnormalities,

Table 1 Summary of the imaging findings and immunohistochemical findings

			November 2006	June 2008	September 2011
Imaging findings	US	B-mode	Hypoechoic	Hypoechoic	Hypoechoic
		Sonazoid			
		(arterial phase)	Hypervascularity		Hypervascularity
		(Kupffer phase)	Defect		Defect
	CT	Contrast-enhanced			
		(arterial phase)	Enhancement		Enhancement
		(equilibrium phase)	Washout		Washout
	MRI	T_1	High intensity	High intensity	High intensity
		T_2	Isointensity	Isointensity	Isointensity
		SPIO	Isointensity		
		Gd-enhanced			
		(arterial phase)	Hypervascularity		
		(equilibrium phase)	Washout		
		Gd-EOB-DTPA-enhanced			
		(arterial phase)		Hypervascularity	Hypervascularity
		(hepatobiliary phase)		Isointensity	Defect
	CT arterioportal angiography	CTHA	Hyperattenuation		Hyperattenuation
		CTAP	Undeterminable		Undeterminable
Immunohistochemical findings of biopsied specimen		SAA	(+)		(+)
		CRP	(+)		(+)
		β-Catenin	(–)		(–)
		L-FABP	(+)		(+)
		GS	Weakly (+) around veins, non-map-like pattern		Weakly (+) around veins, non-map-like pattern
			(–)		(–)
		HSP70	(–)		(–)
		GPC3	(–)		(–)
		OATP8	Weakly (+)		Weakly (+)

CRP, C-reactive protein; CT, computed tomography; CTAP, CT during arterial portography; CTHA, CT during hepatic arteriography; Gd-EOB-DTPA, gadolinium-ethoxybenzyl-diethylenetriamine pentaacetic acid; GPC3, Glypican 3; GS, glutamine synthetase; HSP70, heat shock protein 70; L-FABP, liver fatty acid-binding protein; MRI, magnetic resonance imaging; OATP8, organic anion transporter 8; SAA, serum amyloid A; US, ultrasonography.

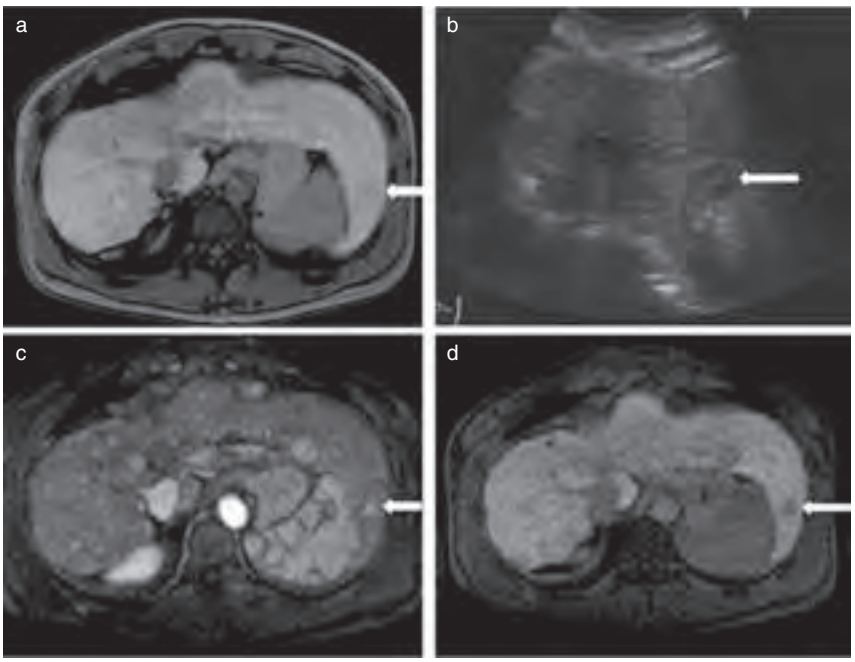

Figure 2 Imaging findings of the nodule in S2. gadolinium-ethoxybenzyl-diethylenetriamine pentaacetic acid (Gd-EOB-DTPA)-enhanced magnetic resonance imaging (MRI) in 2008 shows the nodule as isointensive in the hepatobiliary phase (arrow) (a). In 2011, B-mode ultrasonography reveals a hypoechoic nodule (arrow) (b); Gd-EOB-DTPA-enhanced MRI reveals a hypervascular nodule in the arterial phase (arrow) (c), but a defect in the hepatobiliary phase (arrow) (d).

ductular reaction, inflammatory infiltrates and frequent gp130 mutation); and (iv) unclassified HCA (tumors without any mutation/activation and no inflammatory infiltrate).[5,7]

Recently, unique hypervascular nodule mimicry and FNH-like lesions in alcohol-related liver cirrhosis have been clinicopathologically discussed intensely because their imaging and pathological findings are similar to those of HCC;[2] also, they appear hypervascular, resembling HCC. Moreover, their biopsy specimens usually display histological features similar to well-differentiated HCC. Unless clinicians and pathologists are aware of the aspects of this disease, they tend to misdiagnose it as HCC. The lesion is characteristically an FNH-like one, simply found in the liver of heavy drinkers.[3]

In the current case, hypervascularity in the arterial phase and a defect in the Kupffer phase were observed on Sonazoid contrast-enhanced US; hypervascularity in the early phase and venous washout in the late phase

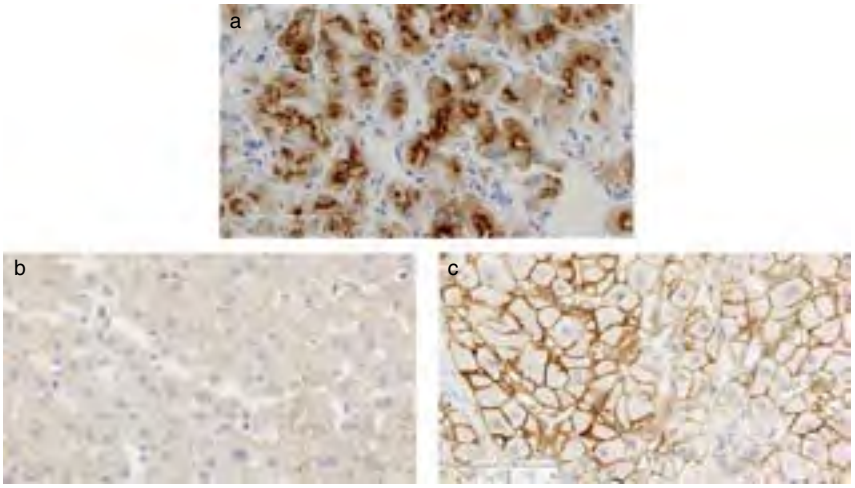

Figure 3 Immunohistochemical staining of serum amyloid A is positive (a). Organic anion transporter 8 staining is weaker in the nodule (b) than in the non-nodular lesion (c).

were observed on contrast-enhanced CT and MRI. MRI findings for each type of HCA have already been reported.[10] The telangiectatic/inflammatory HCA subtype is characterized by a -intensity signal on T_2-weighted sequences; however, the current case did not show similar findings on MRI (Table 1). Thus, although the nodule was compatible with the diagnosis of HCC from imaging studies, no histological evidence of HCC was confirmed by immunohistochemical staining with HSP70 and GPC3. Accordingly, at first, the nodule was diagnosed as an FNH-like lesion in alcohol-related liver cirrhosis without evidence of HCC.[11] Typical histopathological features of classic FNH include clear, well-delimited, but non-encapsulated, lesions composed of hepatocellular nodules, a central scar and radiating fibrous cords. The fibrous regions typically contain large dystrophic arteries and ductular reaction, and frequently lymphocytic infiltration is observed. FNH may be diagnosed by needle liver biopsies. Nonetheless, diagnosing FNH may be difficult if one or several major signs are absent or weak (central scar, ductular reaction), if FNH is steatotic, if the nodules are small or if FNH occurs uncharacteristically (i.e. in men, or in another tumoral context such as adenomatosis, primary malignant tumors), justifying the use of several immunostains, such as cytokeratin 7 and 19, CD34 and more recently L-FABP and SAA, used in identifying HCA subtypes. In all such difficult cases, GS immunostaining could be very useful for establishing a proper diagnosis, with no overexpression of inflammatory proteins such as SAA and CRP that characterize inflammatory HCA.[12] In the current case, GS immunostaining appeared weakly positive around veins without map-like patterns that characterize FNH. Recently, nodules previously termed "telangiectatic FNH", because of their display of abnormal arteries often associated with a ductular reaction, have with the use of genotypic and phenotypic markers been demonstrated as inflammatory/telangiectatic HCA.[8] In the current case, precise immunohistochemical findings including SAA and CRP were compatible with inflammatory HCA. The elevated level of serum CRP supported the diagnosis of inflammatory HCA clinically, especially that in 50% of cases serum levels of CRP are elevated in inflammatory HCA.[13] Inflammatory HCA frequently develops in patients with a high BMI and excessive alcohol consumption, suggesting that alcohol consumption and obesity play a direct role in the initiation of tumorigenesis in inflammatory HCA.[13] In the current case, alcohol abuse, but no obesity, was observed.

In this case, differentiating the nodule between FNH and HCA was difficult. A differential diagnosis of this nodule remains controversial, however. According to WHO classification, positivity of SAA and CRP by immunohistochemical analysis is compatible with HCA. Nonetheless, liver cirrhosis seen in this case has not been reported as a background of HCA;[7] however, a new type of SAA positive tumor in alcoholic patients has been recently reported.[14]

Moreover, an abnormally thick artery in the portal tract and Fe deposition observed by Berlin blue staining in this nodule are compatible with FNH-like lesions in alcoholic cirrhosis. We suppose that there is no proof that FNH does not show immunohistological staining like HCA. As a matter of fact, inflammatory HCA lesions were formerly called telangiectatic FNH because of histological features of FNH with telangiectasia.[8] Consequently, the nodule was diagnosed as an SAA and CRP positive one in alcoholic liver cirrhosis by immunohistochemical studies. Further case accumulation and precise study is needed to obtain a definite diagnosis of such nodules.

A risk of malignant transformation in telangiectatic/inflammatory HCA without β-catenin mutation may be markedly low;[5] however, no long-term studies on the transformation of HCA into HCC have been made. Malignancy has recently been described only in adenomas larger than 4 cm, occurring more often in men than in women.[15] Imaging criteria to detect malignant transformation are often disappointing except when signs of invasion, such as vascular invasion, are present. A change in the size of a lesion in cirrhotic patients with dysplastic nodules has proved informative, but this has not yet been adequately evaluated in adenomas.

A newly introduced contrast agent, Gd-EOB-DTPA, approved in Japan in 2008, is a hepatocyte-specific MRI contrast medium with a different mechanism that utilizes neither dynamic nor Kupffer cell imaging. It is useful in cases difficult to diagnose by techniques such as dynamic MRI or SPIO-MRI. In typical HCC, Gd-EOB-DTPA shows high intensity in the arterial-dominant phase and low intensity in the portal-dominant phase and thereafter. Moreover, the imaging diagnosis of HCC can be made approximately 10–20 min after the injection of Gd-EOB-DTPA. In other words, a defect in the hepatobiliary phase is pivotal in the diagnosis of small HCC. The diagnostic sensitivity of Gd-EOB-DTPA-enhanced MRI in HCC less than 2 cm is 76.5% in all nodules and 75.0% in moderately differentiated HCC.[16]

In the current case, the change from isointensity (2008) to a defect (2011) in the hepatobiliary phase, detected through Gd-EOB-DTPA-enhanced MRI imaging, was observed irrespective of no change in size. From the viewpoint of imaging studies, this could be interpreted as malignant transformation into HCC. As evaluated by histopathology and immunohistochemistry, malignant transformation into HCC was not observed. The change from isointensity to a defect through Gd-EOB-DTPA-enhanced MRI imaging may be explained more by the weak OATP8 staining compared with that of the non-nodular lesion than by malignant transformation into HCC. Recently, an FNH-like nodule with reduced expression of OATP8 in alcoholic liver cirrhosis has been presented,[17] although the reason is not clear. The authors emphasized that the weak OATP8 staining does not mean the occurrence of HCC in such cases. That was compatible with our case. In addition, weak OATP8 staining is sometimes observed in dysplastic nodules without malignant transformation, although the reason is also not clear.[18] In fact, weak OATP8 staining was observed in the biopsy specimens obtained in 2006 and 2011. Further follow up of the current case is needed to observe the occurrence of malignant transformation into HCC and to characterize nodules located in other segments.

ACKNOWLEDGMENT

WE ARE INDEBTED to Ms Yoshiko Kawamura of Kobe Asahi Hospital for assistance in the preparation of the manuscript.

REFERENCES

1 International Working Party. Terminology of nodular hepatocellular lesions. *Hepatology* 1995; **22:** 983–93.
2 Nakashima O, Kurogi M, Yamaguchi R *et al*. Unique hypervascular nodules in alcoholic liver cirrhosis: identical to focal nodular hyperplasia-like nodules? *J Hepatol* 2004; **41:** 992–8.
3 Kondo F. Focal nodular hyperplasia-like lesions in heavy drinkers. *Intern Med* 2009; **48:** 1117–23.
4 Vilgrain V, Uzan F, Brancatelli G, Federle MP, Zappa M, Menu Y. Prevalence of hepatic hemangioma in patients with focal nodular hyperplasia: MR imaging analysis. *Radiology* 2003; **229:** 75–9.
5 Bioulac-Sage P, Balabaud C, Bedossa P *et al*. Pathological diagnosis of liver cell adenoma and focal nodular hyperplasia: Bordeaux update. *J Hepatol* 2007; **46:** 521–7.
6 Kondo F, Koshima Y, Ebara M. Nodular lesions associated with abnormal liver circulation. *Intervirology* 2004; **47:** 277–87.
7 Zucman-Rossi J, Jeannot E, Tran Van Nhieu J *et al*. Genotype-phenotype correlation in hepatocellular adenoma: new classification and relationship with HCC. *Hepatology* 2006; **43:** 515–24.
8 Bioulac-Sage P, Rebouissou S, Sa Cunha A *et al*. Clinical, morphological and molecular features defining so called telangiectatic focal nodular hyperplasias of the liver. *Gastroenterology* 2005; **128:** 1211–8.
9 Bosman FT, Carneiro F, Ralph H *et al*. *WHO Classification of Tumours of the Digestive System*. Geneva: WHO Press, 2010.
10 Ronot M, Bahrami S, Calderaro J *et al*. Hepatocellular adenomas: accuracy of magnetic resonance imaging and liver biopsy in subtype classification. *Hepatology* 2011; **53:** 1182–91.
11 Kim SR, Imoto S, Ikawa H *et al*. Focal nodular hyperplasia-like lesion with venous washout in alcoholic liver cirrhosis. *Intern Med* 2008; **47:** 1899–903.
12 Bioulac-Sage P, Laumonier H, Rullier A *et al*. Overexpression of glutamine synthetase in focal nodular hyperplasia: a novel easy diagnostic tool in surgical pathology. *Liver Int* 2009; **29:** 459–65.
13 Bioulac-Sage P, Laumonier H, Couchy G *et al*. Hepatocellular adenoma management and phenotypic classification: the Bordeaux Experience. *Hepatology* 2009; **50:** 481–9.
14 Sasaki M, Yoneda N, Kitamura S, Sato Y, Nakanuma Y. A serum amyloid A-positive hepatocellular neoplasm arising in alcoholic cirrhosis: a previously unrecognized type of inflammatory hepatocellular tumor. *Mod Pathol* 2012; **25:** 1584–93.
15 Belghiti J, Dokmak S, Paradis V, Vilgrain V, Durand F, Valla D. Specific management for multiple liver cell adenoma: is it justified? *Hepatology* 2005; **42** (Suppl):297A.
16 Mita K, Kim SR, Kudo M *et al*. Diagnostic sensitivity of imaging modalities for hepatocellular carcinoma smaller than 2 cm. *World J Gastroenterol* 2010; **16:** 4187–92.
17 Doi N, Tomiyama Y, Kawase T *et al*. Focal nodular hyperplasia-like nodule with reduced expression of organic anion transporter 1B3 in alcoholic liver cirrhosis. *Intern Med* 2011; **50:** 1193–9.
18 Kitao A, Matsui O, Yoneda N *et al*. The uptake transporter OATP8 expression decreases during multistep hepatocarcinogenesis: correlation with gadoxetic acid enhanced MR imaging. *Eur Radiol* 2011; **21:** 2056–66.

Prognostic Impact of Spontaneous Tumor Rupture in Patients With Hepatocellular Carcinoma

An Analysis of 1160 Cases From a Nationwide Survey

Taku Aoki, MD, PhD, Norihiro Kokudo, MD, PhD,* Yutaka Matsuyama, PhD,† Namiki Izumi, MD, PhD,‡ Takafumi Ichida, MD, PhD,§ Masatoshi Kudo, MD, PhD,¶ Yonson Ku, MD, PhD,|| Michiie Sakamoto, MD, PhD,** Osamu Nakashima, MD, PhD,†† Osamu Matsui, MD, PhD,‡‡ and Masatoshi Makuuchi, MD, PhD§§; for the Liver Cancer Study Group of Japan*

Objective: The aim of the present study was to investigate the background characteriscs of ruptured hepatocellular carcinoma (HCC) and to clarify the true impact of tumor rupture on patient prognosis in a large patient cohort.

Background: Spontaneous tumor rupture of HCC has been associated with a very poor patient prognosis and the current TNM staging systems classify ruptured HCC as T4 based on insufficient evidence.

Methods: In total, 1106 patients with ruptured HCC were extracted from the database of a nationwide survey conducted in Japan from 2000 to 2005. The clinicopathological parameters associated with HCC rupture were investigated using univariate and multivariate logistic regression models. The survival curves for ruptured and nonruptured HCC were generated and compared to evaluate the impact of the event (rupture) itself on patient prognosis and the TNM staging systems.

Results: The multivariate analyses showed that tumor rupture was associated with both a poor liver functional reserve and an advanced tumor status. Analyses of the survival curves stratified according to the baseline TNM staging showed that tumor rupture had an additional impact on the baseline survival curves without rupture, and the impact corresponded to the addition of 0.5 to 2 stages to the baseline tumor staging.

Conclusions: The present study suggested that tumor rupture itself had a negative impact on patient survival. However, its impact was not strong enough to cancel the effects of the other tumor-related parameters. Therefore, it may be appropriate to give additional stages to the baseline tumor staging in cases of ruptured HCC.

Keywords: Hepatocellular carcinoma, nationwide survey, patient outcome, spontaneous tumor rupture, TNM staging system

(*Ann Surg* 2013;00: 1–11)

From the *Hepato-Biliary-Pancreatic Surgery Division, Artificial Organ and Transplantation Division, Department of Surgery, Graduate School of Medicine, University of Tokyo, Tokyo, Japan; †Department of Biostatistics, Graduate School of Medicine, University of Tokyo, Tokyo, Japan; ‡Department of Gastroenterology and Hepatology, Musashino Red-Cross Hospital, Musashino, Japan; §Department of Hepatology and Gastroenterology, Juntendo Shizuoka Hospital, Izunokuni, Japan; ¶Department of Gastroenterology and Hepatology, Kinki University School of Medicine, Osaka Sayama, Japan; ||Department of Surgery, Kobe University Graduate School of Medicine, Kobe, Japan; **Department of Pathology, Keio University School of Medicine, Tokyo, Japan; ††Department of Clinical Laboratory Medicine, Kurume University Hospital, Kurume, Japan; ‡‡Department of Radiology, Kanazawa University Graduate School of Medical Science, Kanazawa, Japan; and §§Surgery, Japanese Red Cross Medical Center, Tokyo, Japan.

Disclosure: The authors declare no conflicts of interest.

Reprints: Norihiro Kokudo, MD, PhD, Hepato-Biliary-Pancreatic Surgery Division, Artificial Organ and Transplantation Division, Department of Surgery, Graduate School of Medicine, University of Tokyo, 7-3-1 Hongo, Bunkyo-ku, Tokyo, Japan 113-8655. E-mail: kokudo-2su@h.u-tokyo.ac.jp.

ISSN: 0003-4932/13/00000-0001
DOI: 10.1097/SLA.0b013e31828846de

The spontaneous rupture of hepatocellular carcinoma (HCC) is a life-threatening presentation of this disease. The incidence of spontaneous tumor rupture has been reported to be 10% of deaths from HCC in Japan,[1] but this figure decreased to 6.4% in a recent report,[2] probably in response to advances in imaging modalities and the development of a surveillance system for patients infected with hepatitis B virus (HBV) or hepatitis C virus (HCV). However, some primary cases are still found as a result of such catastrophic events. Previous studies have reported that the prognosis of ruptured HCC is dismal, and that spontaneous tumor rupture occurs at an adavanced tumor stage in patients with a poor liver functional reserve, although the mechanism of spontaneous tumor rupture remains unclear.[3] The 1-month mortality rate ranged from 34% to 71%, with a median survival period of 7 to 21 weeks in previous series.[1,4–17] As a result, the current TNM staging systems for HCC, including the fifth edition of the Liver Cancer Study Group of Japan (LCSGJ) classification[18] and the seventh edition of the AJCC/UICC (American Joint Committee on Cancer/Union for International Cancer Control) classification,[19] assign all ruptured HCC tumors to T4 (Tables 1 and 2). However, the true impact of tumor rupture itself on patient survival has not been clarified because of the small number of patients, especially patients in relatively early stages, enrolled in previous studies, and the significance of tumor rupture in the tumor staging system has been provisional.

In the present study, we used the LCSGJ database containing information from nationwide surveys in Japan and collected data for over 1000 patients with ruptured HCC. The aim of the present study was to identify the clinicopathological parameters associated with the spontaneous tumor rupture of HCC and to assess the true impact of tumor rupture on patient survival as well as on the current TNM staging systems.

METHODS

Japanese Nationwide Survey of HCC Patients

The LCSGJ has conducted biannual nationwide surveys of patients with HCC since 1970 and has updated the survival data of the enrolled patients. Eight hundred institutions in Japan have participated in the surveys and have answered more than 180 questionnaires regarding patient characteristics, diagnostic findings, treatment selection, treatment findings, and patient outcome. Since the 16th survey (2000–2001), questions regarding spontaneous tumor rupture have been added to conduct this cohort study. In the first step, the physicians at the participating institutions completed the questionnaire and checked the accuracy of the data. In the second step, the nationwide survey committee checked the data, and whenever there were unusual data, the participating institution was requested to confirm the data to ensure the accuracy of the data.

Patients

We used data collected from the 16th, 17th, and 18th LCSGJ nationwide surveys (2000–2005). During the study period, 57,444 new patients with HCC were registered and were prospectively followed up. Among the 57,444 patients, information concerning the status of spontaneous tumor rupture and the patient outcome was available for 49,708 patients; these patients comprised the study cohort of the present analyses. Spontaneous tumor rupture was observed in 1160 patients (2.3%, ruptured HCC group) and was not observed in 48,548 patients (97.7%, nonruptured HCC group). Tumor rupture was suspected in 315 patients, but these patients were excluded from the analyses. The patients were followed up until the end of 2005, and the patients who were alive at the end of the study period were censored.

Parameters

The parameters extracted from the database were as follows: (a) 2 patient demographic parameters (age, sex), (b) 13 background clinical data parameters [chronic hepatitis, liver cirrhosis, hepatitis B antigen (HBsAg), anti-hepatitis C antibody (HCVAb), alcohol abuse, encephalopathy, ascites, prothrombin time, platelet count, indocyanine green retention ratio at 15 minutes (ICGR15), liver damage according to the LCSGJ classification,[20] Child-Pugh grade,[21] and gastroesophageal varices], (c) 9 tumor-related parameters [presence of spontaneous tumor rupture, number of tumors, maximum tumor diameter, tumor distribution, the Eggel gross classification,[22] portal venous invasion, hepatic venous invasion, bile duct invasion, serum level of alpha-fetoprotein (AFP), and plasma level of des-gamma-carboxy prothrombin (DCP)], (d) main treatment method, and (e) patient outcome. The tumor-related variables were extracted from the pathological findings in the surgically resected cases, and from the radiological findings in the other cases. A tumor stage was assigned to each patient, excluding the parameter associated with spontaneous tumor rupture, according to both the LCSGJ classification (fifth edition) and the UICC classification (seventh edition).

TABLE 1. LCSGJ Classification (5th Edition)

T – Primary tumor					
Criteria	1. Solitary tumor				
	2. Diameter < 2 cm				
	3. No vascular or bile duct invasion				
T1	All 3 criteria are fullfilled				
T2	Two of the 3 criteria are fulfilled.				
T3	One of the 3 criteria are fulfilled.				
T4	None of the 3 criteria are fulfilled *or* **ruptured HCC**				
N – Lymph node metastasis					
N0	No lymph node metastasis				
N1	Lymph node metastasis				
M – Distant metastasis					
M0	No distant metastasis				
M1	Distant metastasis				
	Japanese TNM staging				
		T1	T2	T3	T4
	N0 and M0	I	II	III	IVA
	N1 and M0	IVA	IVA	IVA	IVA
	Any N and M1	IVB	IVB	IVB	IVB

Statistical Analysis

Each parameter was compared between the ruptured HCC group and the nonruptured HCC group using chi-square tests. Thereafter, a multivariate logistic regression analysis was performed to identify the parameters that were independently associated with spontaneous HCC tumor rupture. In the multivariate logistic regression analysis, parameters for which the values were missing for over 20% of the study population were excluded. Additional multivariate logistic regression analyses were conducted for subgroups stratified according to HBsAg and HCVAb status.

The patient survival curves were generated using the Kaplan-Meier method for each tumor stage, excluding the spontaneous tumor rupture parameter, according to the LCSGJ classification (fifth edition) and the UICC classification (seventh edition) separately for both the ruptured HCC group and the nonruptured HCC group. The differences among the curves were examined using the Cox proportional hazards analysis. Kaplan-Meier curves were also generated according to the main treatment methods and were compared. The analyses were conducted using SAS, Version 9.2. Differences were considered significant when the *P* value was less than 0.05.

TABLE 2. UICC Classification (7th Edition)

T – Primary tumor						
TX	Primary tumor cannot be assessed.					
T0	No evidence of primary tumor.					
T1	Solitary tumor without vascular invasion.					
T2	Solitary tumor with vascular invasion *or* multiple tumors, none more than 5 cm in greatest dimension.					
T3	Multiple tumors any more than 5 cm *or* tumor involving a major branch of the portal or hepatic vein(s).					
	T3a: Multiple tumors any more than 5 cm.					
	T3b: Tumors involving a major branch of the portal or hepatic vein(s).					
T4	Tumor(s) with direct invasion of adjacent organs other than the gallbladder *or* **with perforation of visceral peritoneum**.					
N – Regional lymph nodes						
NX	Regional lymph nodes cannot be assessed.					
N0	No regional lymph node metastasis.					
N1	Regional lymph node metastasis.					
M – Distant metastasis						
M0	No distant metastasis.					
M1	Distant metastasis.					
UICC TNM staging						
		T1	T2	T3a	T3b	T4
	N0 and M0	I	II	IIIA	IIIB	IIIC
	N1 and M0	IVA	IVA	IVA	IVA	IVA
	Any N and M1	IVB	IVB	IVB	IVB	IVB

TABLE 3. Patient Demographics and Basic Clinical Data

Parameter	Ruptured (n = 1,160) Non-ruptured (n = 48,548)	P value (Chi-square)
Age (<60/≥60)	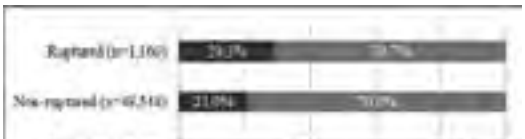	<0.0001
Sex (male/female)		0.0037
Chronic hepatitis (no/suspected/yes)		<0.0001
Liver cirrhosis (no/suspected/yes)	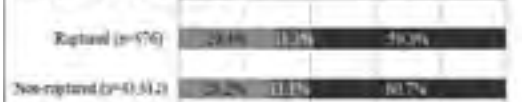	0.3632
HBsAg (negative/ positive)	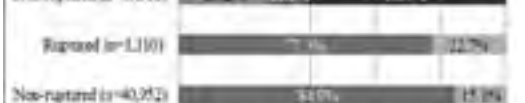	<0.0001
HCVAb (negative/ positive)	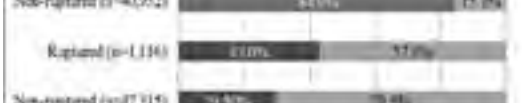	<0.0001
Alcohol (no/yes)	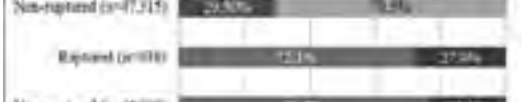	0.0010
Encephalopathy (none/minimal/ moderate)	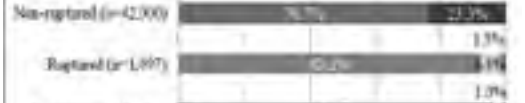	<0.0001
Ascites (no/controllable/ intractable)		<0.0001
Prothrombin time (%: <40/40-70/≥70)	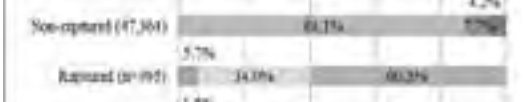	<0.0001
Platelet count (x10^3: <50/50-100/≥100)	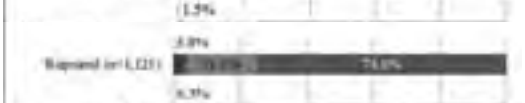	<0.0001
ICG R15 (<10%/ 10-20%/20-40%/ 40%-)		<0.0001
Liver damage (A/B/C)		<0.0001
Child-Pugh (A/B/C)	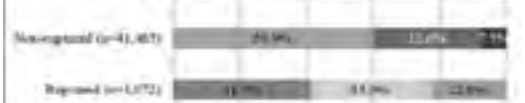	<0.0001
Gastroesophageal varices (none/ present/ruptured)		<0.0001

RESULTS

Parameters Associated With Spontaneous Tumor Rupture (Univariate Analyses)

The comparisons between the ruptured HCC group and the nonruptured HCC group showed that the following patient demographic and basic clinical data parameters were associated with spontaneous tumor rupture according to a univariate analysis: age, chronic hepatitis, HBsAg, HCVAb, alcohol, encephalopathy, ascites, prothrombin time, platelet count, ICGR15 value, liver damage, Child-Pugh grade, and gastroesophageal varices (Table 3). In other words, spontaneous tumor rupture was more frequently observed in patients with a younger age, positive HBsAg, greater alcohol intake, and a poorer liver functional reserve. On the other hand, spontaneous tumor rupture was also more frequently observed in patients with negative HCVAb, the absence of chronic hepatitis, a higher platelet count, and a better ICGR15 value.

The same analysis showed that the following tumor-related parameters were significantly associated with spontaneous tumor rupture according to a univariate analysis: the number of tumors, maximum tumor diameter, tumor distribution, the Eggel gross classification, portal invasion, venous invasion, bile duct invasion, serum AFP value, and plasma DCP value (Table 4). Namely, spontaneous tumor rupture occurred more frequently among patients with a more advanced tumor stage.

Parameters Associated With Spontaneous Tumor Rupture (Multivariate Analyses)

A multivariate analysis using logistic regression identified the following parameters as being independently associated with spontaneous tumor rupture: maximum tumor diameter [odds ratio (OR): 16.34 (>5 cm vs. ≤2 cm); 4.66 (2–5 cm vs. ≤2 cm); 3.50 (>5 cm vs. 2–5 cm)], Child-Pugh grade (OR: 2.57), plasma DCP value (OR: 1.66), platelet count (OR: 1.60), age (OR: 0.71), and the Eggel gross classification (OR: 1.42) (Table 5). The risk of spontaneous tumor rupture increased linearly with the increase in tumor size, and there were no clearcut thresholds. The model selected contained 25,404 cases.

Additional multiple logistic regression analyses were conducted for subgroups stratified according to HBsAg and HCVAb status: ie, an HBsAg(+) and HCVAB(–) group ($n = 6220$), an HBsAg(–) and HCVAb(+) group ($n = 32,097$), and an HBsAg(–) and HCVAb(–) group ($n = 8028$). As the number of patients who were positive for both HBsAg and HCVAb was relatively small compared with the other groups ($n = 894$), these patients were excluded from the subanalyses. The tumor size and Child-Pugh grade were independent significant parameters in all 3 subgroups. In the HBsAg(+) and HCVAb(–) group, the plasma DCP value was also associated with spontaneous tumor rupture; in the HBsAg(–) and HCVAb(+) group, tumor-related parameters (plasma DCP value, number of tumors, and

TABLE 4. Tumor-Related Data

Parameter	Ruptured (n = 1,160) Non-ruptured (n = 48,548)	P value (Chi-square)
Number of tumors (1/2/3 or more)	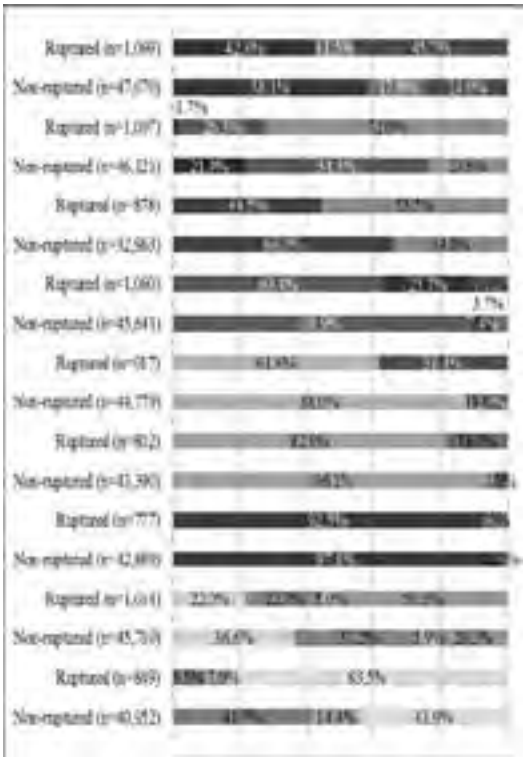	<0.0001
Maximum tumor Diameter (cm: <2/2-5/≥5)		<0.0001
Tumor distribution(unilobar/bilobar)		<0.0001
Eggel's classification (nodular/massive/ diffuse)		<0.0001
Portal invasion (negative/positive)		<0.0001
Venous invasion (negative/positive)		<0.0001
Bile duct invasion (negative/positive)		<0.0001
AFP* (ng/mL: <15/15-200/200-400/≥400)		<0.0001
DCP† (mAU/mL: <40/40-100/≥100)		<0.0001

*Alpha-fetoprotein.
†Des-gamma-carboxy prothrombin.

TABLE 5. Predictive Variables for Spontaneous Tumor Rupture by Multivariate Analysis Using Logistic Regression Model ($n = 25,404$)

Parameter		Odds Ratio	95% CI	*P*
Maximum tumor diameter	>5 cm vs. ≤2 cm	16.34	7.05–37.87	<0.001
Maximum tumor diameter	2–5 cm vs. ≤2 cm	4.66	2.03–10.7	<0.001
Child-Pugh classification	A/B/C	2.57	2.16–3.05	<0.001
DCP*	mAU/mL	1.66	1.39–1.99	<0.001
Platelet count	$\times 10^4/\mu$L	1.60	1.27–2.03	<0.001
Age	≥60 vs. <60	0.71	0.54–0.93	0.012
Eggel classification	Massive vs. nodular	1.42	1.05–1.92	0.023

*Des-gamma-carboxy prothrombin.
Maximum tumor diameter >5 cm versus 2–5 cm: odds ratio = 3.50 (95% CI: 2.66–4.61), $P < 0.001$.

portal invasion) were identified as additional significant parameters; in the HBsAg(–) and HCVAB(–) group, only patient age (other than the tumor size and Child-Pugh grade) was marginally associated with tumor rupture (Table 6).

Impact of Spontaneous Tumor Rupture on Patient Survival and TNM Staging

The overall survival of the ruptured HCC group was significantly poorer, compared with that of the nonruptured HCC group [hazard ratio (HR): 2.10; 95% confidence interval (CI): 2.03–2.18; $P < 0.001$, Fig. 1]. The 6-month, 1-year, 3-year, and 5-year overall survival rates were 54.4%, 41.4%, 21.1%, and 13.3%, respectively, in the ruptured HCC group, and 90.2%, 84.1%, 63.0%, and 45.8%, respectively, in the nonruptured HCC group. The median survival time in the ruptured HCC group was 228 days (95% CI: 196–273 days).

As spontaneous tumor rupture occurred more frequently in patients with advanced stages of HCC in the abovementioned analyses, the survival curves were depicted according to the LCSGJ classification and the AJCC/UICC classification, excluding tumor rupture from the staging. The divided curves according to the LCSGJ classification and a verification of the differences among the curves are shown in Figure 2. The depicted survival curves of the ruptured stage II, ruptured stage III, ruptured stage IV-A, and ruptured stage IV-B patients were significantly separated. Only 7 patients had ruptured stage I disease, making this group unsuitable for inclusion in the statistical analyses. The survival curve for ruptured stage II HCC (ie, when stage II HCC ruptures) was situated in between the curves for nonruptured stage III HCC and nonruptured stage IV-A HCC, and was significantly different from these 2 curves (HR: 1.60 and $P < 0.001$ vs. nonruptured stage III; HR: 0.56 and $P < 0.001$ vs. nonruptured stage IV-A). The survival curve of ruptured stage III HCC was not different from that of nonruptured stage IV-A HCC (HR: 0.93, $P = 0.493$). The survival curve of ruptured stage IV-A HCC was situated between the curves for nonruptured stage IV-A HCC and nonruptured stage IV-B HCC and was significantly different from the 2 curves (HR: 1.59 and $P < 0.001$ vs. nonruptured stage IV-A; HR: 0.72 and $P = 0.016$ vs. nonruptured stage IV-B). The survival of patients with ruptured stage IV-B HCC was poorer than that of patients with nonruptured stage IV-B HCC, with a difference that was borderline significant (HR: 1.21, $P = 0.081$).

Similar analyses were conducted according to the AJCC/UICC classification (Fig. 3). However, the survival curves for ruptured stage II HCC and for ruptured stage III-A HCC were similar ($P = 0.826$), whereas the survival curves for ruptured stages III-B and IV-A were similar ($P = 0.192$). The survival curve for ruptured stage I HCC was situated between the curves for nonruptured stage II HCC and those for nonruptured stage III-A HCC, and was different from the 2 curves (HR: 1.61 and $P < 0.001$ vs. nonruptured stage II; HR: 0.81 and $P = 0.05$ vs. nonruptured stage III-A). The survival curves for ruptured stage II and stage III-A HCC were situated between the curves for nonruptured stage III-A HCC and those for nonruptured stage III-B HCC, and were not different from that for nonruptured stage III-B. The survival curves for ruptured stage III-B and IV-A HCC were poorer than that for nonruptured stage IV-B HCC, and the survival curve for ruptured stage IV-B HCC was much poorer than those for ruptured stage III-B and stage IV-A HCC.

Patient Survival Stratified According to Treatment Modalities

The survival of patients with ruptured HCC was estimated after stratification according to the main treatment modalities. The prognosis of patients who underwent a liver resection ($n = 298$) or local ablative therapy ($n = 32$) was better than that of the patients who received transcatheter arterial chemoembolization (TACE; $n = 489$), chemotherapy ($n = 65$), or best supportive care ($n = 275$) ($P < 0.001$), although the number of patients receiving local ablative therapy was relatively small (Fig. 4). The 1-, 3-, and 5-year overall survival rates after hepatic resection were 76.0%, 48.6%, and 33.9%, respectively, and the 1-, 3-, and 5-year overall survival rates after TACE were 39.7%, 14.1%, and 6.0%, respectively.

DISCUSSION

Previous studies have documented the clinical course as well as the treatment results of spontaneously ruptured HCC.[1–17] However, the largest series to date consisted of 172 cases,[1] mainly because spontaneous tumor rupture is a relatively rare event. As a result, it has been difficult to assess the true impact of tumor rupture on patient survival, and ruptured HCC has been assigned to T4 in the present TNM staging systems based on insufficient evidence. Therefore, to settle these problems, the LCSGJ started to gather information regarding the presence of spontaneous tumor rupture, beginning in 2000, and patients with spontaneous tumor rupture have been prospectively followed up. In the present study, we have collected data from 1106 HCC cases of spontaneous tumor rupture followed up for a maximum of 6 years. The maximum follow-up period of 6 years may be relatively short; however, because the outcome of ruptured HCC was generally poor, almost all the events occurred within 6 years (only 10 patients were at risk at 6 years). We therefore think that the clinical outcome of ruptured HCC is adequately represented by the data we obtained. It is true that the present study population was limited to Japanese patients and the dominant etiologies of the liver disease were HCV and HBV; nevertheless, we believe that our results are of significant value, and that they can be applied to HCC patients in epidemic areas of HBV and/or HCV infection and serve a fundamental reference data to study the behavior of HCC.

TABLE 6. Parameters Associated With Spontaneous Tumor Rupture Stratified by HBV and HCV Infection Status

		HBsAg (+) and HCVAb (–) ($n = 6220$)			HBsAg (–) and HCVAb (+) ($n = 32,097$)			HBsAg (–) and HCVAb (–) ($n = 8028$)		
Parameter	**Reference**	**Odds Ratio**	**95% CI**	***P***	**Odds Ratio**	**95% CI**	***P***	**Odds Ratio**	**95% CI**	***P***
Age (≥60)	Age (<60)	0.72	0.44–1.17	0.19	0.67	0.36–1.25	0.21	0.54	0.28–1.04	0.064
Sex (female)	Sex (male)	0.82	0.50–1.33	0.424	0.46	0.17–1.21	0.114	0.88	0.37–2.07	0.765
Chronic hepatitis (yes)	Chronic hepatitis (no)	1.04	0.80–1.36	0.755	0.82	0.58–1.15	0.24	0.94	0.68–1.29	0.694
Alcohol (yes)	Alcohol (no)	0.98	0.61–1.56	0.923	0.55	0.25–1.20	0.133	1.43	0.73–2.77	0.295
Platelet count ($\times 10^3$)		1.05	0.75–1.48	0.776	1.89	0.90–3.97	0.094	1.41	0.65–3.07	0.387
Child-Pugh (A/B/C)		2.63	1.93–3.58	<0.001	2.20	1.26–3.85	0.006	2.14	1.24–3.71	0.006
AFP* (ng/mL)		1.12	0.94–1.34	0.199	1.07	0.83–1.37	0.608	1.19	0.92–1.53	0.187
DCP† (mAU/mL)		1.90	1.40–2.58	<0.001	1.85	1.08–3.17	0.025	1.15	0.72–1.84	0.549
Maximum tumor diameter (cm)		2.77	1.87–4.11	<0.001	5.54	2.61–11.73	<0.001	6.01	2.67–13.56	<0.001
Number of tumors		0.93	0.69–1.24	0.608	1.60	1.04–2.45	0.032	1.21	0.78–1.89	0.39
Portal invasion (positive)	Portal invasion (negative)	1.01	0.83–1.23	0.903	0.73	0.54–0.97	0.029	1.11	0.84–1.45	0.468
Venous invasion (positive)	Venous invasion (negative)	1.08	0.77–1.52	0.65	0.94	0.58–1.54	0.809	0.41	0.13–3.34	0.625
Bile duct invasion (positive)	Bile duct invasion (negative)	0.52	0.23–1.16	0.109	1.29	0.77–2.16	0.342	0.67	0.13–3.34	0.625
Eggel classification (massive)	Eggel classification (nodular)	1.68	0.98–2.90	0.06	1.06	0.52–2.16	0.881	1.54	0.73–3.28	0.26
Eggel classification (diffuse)	Eggel classification (nodular)	1.78	0.78–4.06	0.173	1.30	0.42–4.03	0.645	0.66	0.13–3.30	0.614
Gastroesophageal varices (none/present/ruptured)		1.03	0.81–1.32	0.792	0.82	0.52–1.28	0.373	0.90	0.57–1.42	0.646
Tumor distribution (bilobar)	Tumor distribution (unilobar)	0.80	0.48–1.35	0.405	1.22	0.60–2.48	0.586	0.74	0.33–1.68	0.47

*Alpha-fetoprotein.
†Des-gamma-carboxy prothrombin.

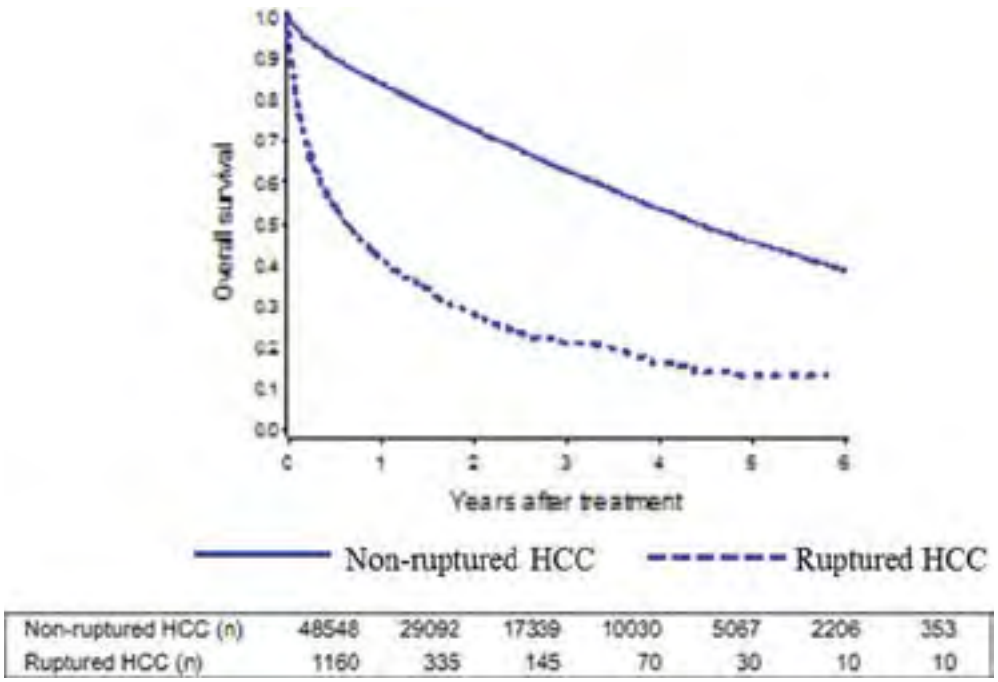

Non-ruptured HCC (n)	48548	29092	17339	10030	5067	2206	353
Ruptured HCC (n)	1160	335	145	70	30	10	10

FIGURE 1. Overall survival curves in the ruptured HCC group (dotted blue line) and the nonruptured HCC group (solid blue line) ($P < 0.001$).

A comparison between ruptured HCC and nonruptured HCC revealed that spontaneous tumor rupture was more frequent among patients with a poor liver functional reserve, as reflected by the Child-Pugh grade and liver damage classification. On the other hand, spontaneous tumor rupture was more frequently observed among younger patients, and in HBV-infected livers, rather than chronically hepatitic or cirrhotic livers or HCV-infected livers. Furthermore, in the ruptured HCC patients, the platelet count was higher and the ICGR15 value was better, although the ICGR15 value was mainly estimated in patients undergoing liver resections. These results suggested that spontaneous tumor rupture occurred in a heterogeneous population of patients, and subsequent subanalyses showed that the clinicopathological parameters associated with tumor rupture differed among the subgroups when stratified according to the infectious status for HBV and/or HCV.

The analyses of tumor-related parameters showed that ruptured HCC represented a more advanced tumor stage, as reflected by the tumor size, tumor number, vascular invasion, and tumor marker values. These results are consistent with those in previous reports. A previous report indicated that tumors in contact with or protruding from the liver surface ruptured more frequently,[12] but the present surveys could not assess this issue, as detailed information regarding the location and shape of the ruptured tumors was not collected. Data collection regarding the shape of the HCC were not planned because a definition of "extrahepatically protruding HCC" had not been established at the time of study planning. A subsequent multivariate analysis showed that parameters related to both liver function and tumor status were identified as independent parameters associated with spontaneous tumor rupture. The HR was highest for the tumor size and was second highest for the Child-Pugh grade. Again, the liver functional data in the ruptured HCC group were obtained at the time of disease presentation, and thus, may differ from the baseline data obtained prior to rupture.

Similar to the previous reports, the outcome for ruptured HCC patients was poor compared with that for nonruptured HCC patients; to evaluate the true impact of the tumor rupture itself, we performed subsequent subgroup analyses stratified according to the TNM staging. The results stratified according to the LCSGJ TNM classification suggested that the tumor rupture itself had an additional negative impact on patient survival, and the impact was equivalent to an additional 0.5 to 1.5 stages added to the baseline TNM stage. Although the tumor rupture itself worsened the patient prognosis, the impact was not decisively strong so as to cancel the effect of other tumor-related parameters. In other words, when an HCC tumor in an earlier stage ruptures, a better survival can be expected as compared with that in an advanced-stage rupture. Therefore, assigning all the ruptured HCC to T4 may result in an overestimation of severity; rather, in cases of ruptured HCC, it may be adequate to add (0.5 in the case of stage IV-A, 1 in the case of stage III, or 1.5 in case of the stage II) additional stages to the baseline TNM stage, determined according to the tumor size, tumor number, vascular invasion, lymph node metastasis, and distant metastasis. Meanwhile, the survival curves of patients with tumor rupture were poorly stratified according to the AJCC/UICC TNM staging system. The survival curves for ruptured stage II HCC and for ruptured stage III-A HCC were similar, whereas those for ruptured stage III-B and stage IV-A HCC were similar. According to the present AJCC/UICC TNM staging system, ruptured HCC is assigned to stage III-C if no lymph node or distant metastases are present. However, the present analysis showed that it may not be appropriate to assign the same stage to all ruptured cases, but rather to add an additional 0.5 to 2 stages to the baseline TNM stage.

An overall survival analysis stratified according to the main treatment modality showed that liver resection and local ablative therapy could benefit patients, although the number of patients receiving local ablative therapy was still small ($n = 32$), possibly because of the large tumor size and the tumor location. As only data

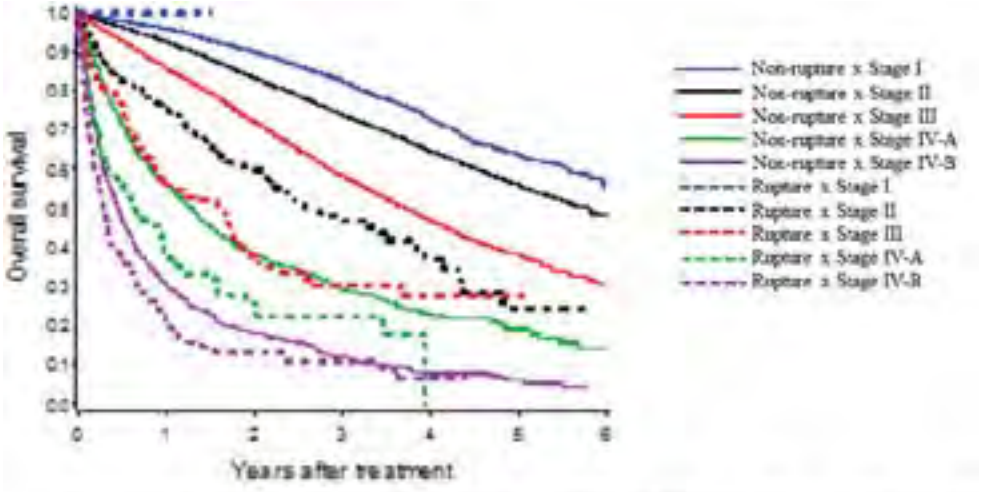

Non-rupture x Stage I (n)	6845	4549	2980	1832	981	440	63
Non-rupture x Stage II (n)	19783	13337	8250	4901	2528	1100	150
Non-rupture x Stage III (n)	10981	6720	3859	2120	996	405	59
Non-rupture x Stage IV-A (n)	1706	640	208	131	53	26	2
Non-rupture x Stage IV-B (n)	1353	267	97	42	21	6	2
Rupture x Stage I (n)	6	1	0	0	0	0	0
Rupture x Stage II (n)	267	145	73	36	14	4	0
Rupture x Stage III (n)	185	71	28	13	8	2	0
Rupture x Stage IV-A (n)	88	21	13	7	0	0	0
Rupture x Stage IV-B (n)	119	19	6	4	2	2	2

	Reference	Hazard ratio	95% C.I.	*P* value
Rupture x Stage II	Rupture x Stage I*	*	*	*
Rupture x Stage III	Rupture x Stage II	1.66	1.25-2.2	<.001
Rupture x Stage IV-A	Rupture x Stage III	1.72	1.24-2.38	0.001
Rupture x Stage IV-B	Rupture x Stage IV-A	1.67	1.21-2.31	0.002
Rupture x Stage II	Non-rupture x Stage III	1.60	1.31-1.94	<.001
	Non-rupture x Stage IV-A	0.56	0.46-0.68	<.001
Rupture x Stage III	Non-rupture x Stage III	2.65	2.15-3.26	<.001
	Non-rupture x Stage IV-A	0.93	0.75-1.15	0.493
	Non-rupture x Stage IV-B	0.42	0.34-0.52	<.001
Rupture x Stage IV-A	Non-rupture x Stage IV-A	1.59	1.22-2.07	<.001
	Non-rupture x Stage IV-B	0.72	0.56-0.94	0.016
Rupture x Stage IV-B	Non-rupture x Stage IV-B	1.21	0.98-1.49	0.081

* No event was observed in the Rupture x Stage I subgroup.

FIGURE 2. (Upper component) Overall survival curves stratified according to the presence of tumor rupture, in combination with the baseline LCSGJ classification staging (stage I, II, III, IV-A, and IV-B). (Lower component) The differences among the survival curves examined using a Cox proportional hazards analysis.

regarding the main treatment modality were available, the results of combination therapies, such as TACE plus liver resection, could not be assessed in the present series. Recent reports have shown that primary hemostasis using TACE followed by liver resection achieved the best treatment results;[17,23,24] indeed, in clinical settings in Japan, emergent TACE followed by hepatic resection is now the treatment of choice, if the general condition and liver function of the patient recovers after TACE.[25] A report on the latest nationwide survey in Japan documented that the 1-, 3-, and 5-year survival rates for all patients undergoing hepatic resection for HCC were 87.8%, 69.2%, and 53.4%, respectively.[2] The outcome of ruptured cases was somewhat poorer than that for all the resected cases; however, our results also suggested that, in selected cases, long-term survival can be expected if the patient's condition is tolerable to the curative treatment, ie, liver resection or local ablative therapy for the ruptured tumor.

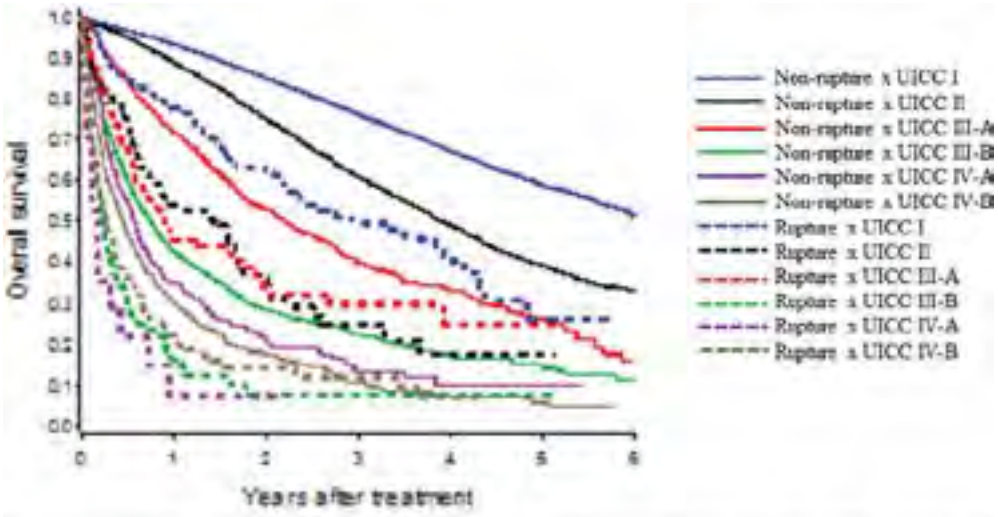

Non-rupture x UICC I (n)	22062	14895	9365	5188	2859	1269	165
Non-rupture x UICC II (n)	12487	8045	4587	2517	1239	499	72
Non-rupture x UICC III-A (n)	2285	1102	537	269	129	47	4
Non-rupture x UICC III-B (n)	1497	816	176	97	41	22	2
Non-rupture x UICC IV-A (n)	381	82	36	11	4	4	0
Non-rupture x UICC IV-B (n)	1256	244	84	34	16	4	1
Rupture x UICC I (n)	228	128	65	32	15	4	0
Rupture x UICC II (n)	113	48	20	6	3	1	0
Rupture x UICC III-A (n)	129	35	16	9	4	4	0
Rupture x UICC III-B (n)	87	8	2	1	1	1	0
Rupture x UICC IV-A (n)	17	17	17	0	0	0	0
Rupture x UICC IV-B (n)	110	18	6	4	2	2	2

	Reference	Hazard ratio	95% C.I.	P value
Rupture x Stage II	Rupture x Stage I	2.13	1.55-2.93	<.001
Rupture x Stage III-A	Rupture x Stage II	1.04	0.74-1.47	0.820
Rupture x Stage III-B	Rupture x Stage III-A	3.26	2.32-4.58	<.001
Rupture x Stage IV-A	Rupture x Stage III-B	1.45	0.83-2.53	0.192
Rupture x Stage IV-B	Rupture x Stage III-B	0.71	0.52-0.98	0.035
	Rupture x Stage IV-A	0.49	0.28-0.85	0.011
Rupture x Stage I	Non-rupture x Stage II	1.61	1.3-1.99	<.001
	Non-rupture x Stage III-A	0.81	0.65-1.01	0.057
Rupture x Stage II	Non-rupture x Stage III-A	1.72	1.34-2.2	<.001
	Non-rupture x Stage III-B	0.78	0.61-1	0.051
Rupture x Stage III-A	Non-rupture x Stage III-A	1.79	1.38-2.3	<.001
	Non-rupture x Stage III-B	0.81	0.63-1.05	0.109
	Non-rupture x Stage IV-A	0.59	0.45-0.78	<.001
Rupture x Stage III-B	Non-rupture x Stage IV-B	1.60	1.25-2.04	<.001
Rupture x Stage IV-A	Non-rupture x Stage IV-B	2.32	1.39-3.87	0.001
Rupture x Stage IV-B	Non-rupture x Stage IV-B	1.14	0.92-1.42	0.236

FIGURE 3. (Upper component) Overall survival curves stratified according to the presence of tumor rupture, in combination with the baseline AJCC/UICC classification staging (Stage I, II, III-A, III-B, IV-A, and IV-B). (Lower component) The differences among the survival curves examined using a Cox proportional hazards analysis.

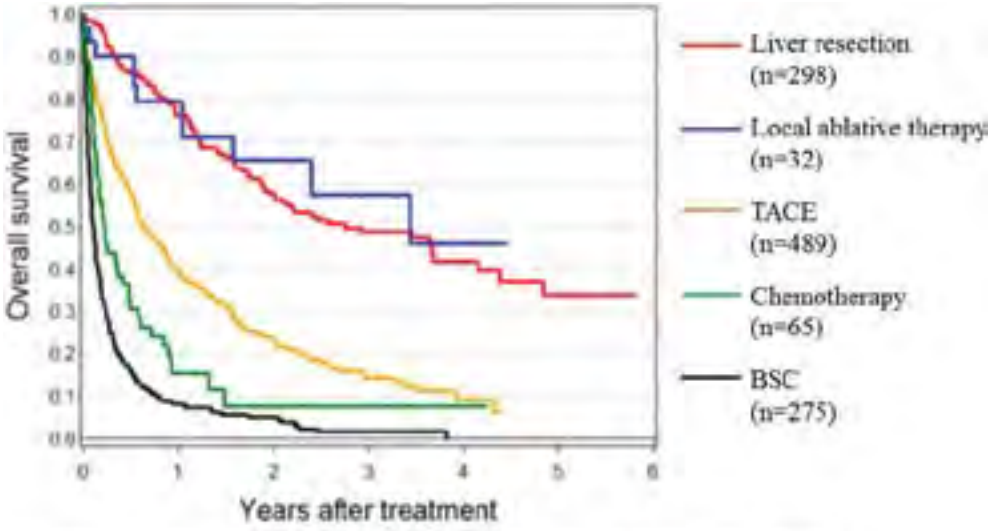

	Hazard ratio	95% C.I.	P value
BSC vs. liver resection	8.99	7.11-11.37	<0.001
Local ablative therapy vs. liver resection	0.87	0.47-1.63	0.671
TACE vs. liver resection	2.53	2.15-3.01	<0.001
Chemotherapy vs. liver resection	5.38	3.84-7.53	<0.001

BSC: best supportive care, TACE: transcatheter arterial chemoembolization

FIGURE 4. (Upper component) Overall survival curves stratified according to the main treatment modality. (Lower component) The differences among the survival curves examined using a Cox proportional hazards analysis.

CONCLUSIONS

In conclusion, we have investigated the parameters associated with spontaneous HCC rupture and have assessed the impact of tumor rupture on patient survival using information from a database containing nationwide survey data in Japan. Spontaneous tumor rupture had an additional negative impact on the baseline tumor status, and this impact corresponded to an additional 0.5 to 2.0 TNM stages. Our results provide important basic information for the next revision of the TNM staging system for HCC.

ACKNOWLEDGMENTS

The authors thank all their colleagues who participated in the nationwide survey of HCC in Japan. The authors also thank Mr Tomohiro Shinozaki, Department of Biostatistics, Graduate School of Medicine, University of Tokyo, for his assistance with the statistical analyses.

REFERENCES

1. Miyamoto M, Sudo T, Kuyama T. Spontaneous rupture of hepatocellular carcinoma: a review of 172 Japanese cases. *Am J Gastroenterol*. 1991;86:67–71.
2. Ikai I, Arii S, Okazaki M, et al. Report of the 17th nationwide follow-up survey of primary liver cancer in Japan. *Hepatol Res*. 2007;37:676–691.
3. Zhu LX, Wang GS, Fan ST. Spontaneous rupture of hepatocellular carcinoma. *Br J Surg*. 1996;83:602–607.
4. Ong GB, Chu EPH, Yu FYK, et al. Spontaneous rupture of hepatocellular carcinoma. *Br J Surg*. 1965;52:123–129.
5. Ong GB, Taw JL. Spontaneous rupture of hepatocellular carcinoma. *BMJ*. 1972;4:146–149.
6. Nagasue N, Inokuchi K. Spontaneous and traumatic rupture of hepatoma. *Br J Surg*. 1979;66:248–250.
7. Chearanai O, Plengvanit U, Asavanich C, et al. Spontaneous rupture of primary hepatoma: report of 63 cases with particular reference to the pathogenesis and rationale of treatment by hepatic artery ligation. *Cancer*. 1983;51:1532–1536.
8. Chen MF, Hwang TL, Jeng LB, et al. Surgical treatment for spontaneous rupture of hepatocellular carcinoma. *Surg Gynecol Obstet*. 1988;167:99–102.
9. Lai ECS, Wu KM, Choi TK, et al. Spontaneous ruptured hepatocellular carcinoma: an appraisal of surgical treatment. *Ann Surg*. 1989;210:24–28.
10. Dewar GA, Griffin SM, Ku KW, et al. Management of bleeding liver tumours in Hong Kong. *Br J Surg*. 1991;78:463–466.
11. Cherqui D, Panis Y, Rotman N, et al. Emergency liver resection for spontaneous rupture of hepatocellular carcinoma complicating cirrhosis. *Br J Surg*. 1993;80:747–749.
12. Chen CY, Lin XZ, Shin JS, et al. Spontaneous rupture of hepatocellular carcinoma: a review of 141 Taiwanese cases and comparison with nonrupture cases. *J Clin Gastroenterol*. 1995;21:238–242.
13. Leung KL, Lau WY, Lai PBS, et al. Spontaneous rupture of hepatocellular carcinoma: conservative management and selective intervention. *Arch Surg*. 1999;134:1103–1107.
14. Vergara V, Muratore A, Bouzari H, et al. Spontaneous rupture of hepatocellular carcinoma: surgical resection and long-term survival. *Eur J Surg Oncol*. 2000;26:770–772.
15. Liu CL, Fan ST, Lo CM, et al. Management of spontaneous rupture of hepatocellular carcinoma: single-center experience. *J Clin Oncol*. 2001;19:3725–3732.
16. Yeh CN, Lee WC, Jeng LB, et al. Spontaneous tumour rupture and prognosis in patients with hepatocellular carcinoma. *Br J Surg*. 2002;89:1125–1129.
17. Lai ECH, Lau WY. Spontaneous rupture of hepatocellular carcinoma. *Arch Surg*. 2006;141:191–198.
18. Liver Cancer Study Group of Japan. General Rules for the Clinical and Pathological Study of Primary Liver Cancer, 5th Japanese edition. Tokyo: Kanehara; 2008.
19. American Joint Committee on Cancer (AJCC). *Cancer Staging Manual*. 7th ed. New York: Springer; 2009.
20. Liver Cancer Study Group of Japan. *General Rules for the Clinical and Pathological Study of Primary Liver Cancer, 2nd English Edition*. Tokyo: Kanehara; 2003.

21. Pugh RNH, Murray-Lyon IM, Dawson JL, et al. Transection of the oesophagus for bleeding oesophagus varices. *Br J Surg*. 1973;6:646–649.
22. Eggel H. Ueber das Primare Carcinoma der Leber. *Beitr z Path Anat u z allgem Pathol.* 1901;30:506–604.
23. Nouchi T, Nishimura M, Maeda M, et al. Transcatheter arterial embolization of ruptured hepatocellular carcinoma associated with liver cirrhosis. *Did Dis Sci*. 1984;29:1137–1141.
24. Buczkowski AK, Kim PTW, Ho SG, et al. Multidisciplinary management of ruptured hepatocellular carcinoma. *J Gastrointest Surg*. 2006;10:379–386.
25. Shimada R, Imamura H, Makuuchi M, et al. Staged hepatectomy after emergency transcatheter arterial embolization for ruptured hepatocellular carcinoma. *Surgery*. 1998;124:526–535.

Digestive Endoscopy 2014; **26**: 636–637

Editorial

Endoscopic ultrasonography-guided gallbladder drainage procedures: Is the glass half-full or half-empty?

THE CURVILINEAR (CONVEX) echoendoscope enables real-time sonographic observation of the needle when accessing a target lesion either for tissue sampling or intervention. Endoscopic ultrasonography (EUS)-guided drainage was first reported for the treatment of pancreatic pseudocysts.[1] Its application has now expanded to include drainage of obstructive pancreatic and biliary ductal systems not accessible by endoscopic retrograde cholangiopancreatography (ERCP).[2,3] More recently, the range of its applications has been widened to include gallbladder drainage in poor-risk surgical candidates with gallbladder disease.[4,5] This is particularly relevant for patients in whom transpapillary and percutaneous approaches to gallbladder drainage has failed or is technically difficult. In this edition of the Journal, Widmer and colleagues conducted a review of the literature of patients who underwent EUS-guided gallbladder drainage and reported a technical success rate of 96.6% in 90 patients.[5] Patients in whom the procedure was technically successful also had equivalent treatment success rates.[5] Complications occurred in 12.2%.[5] These outcomes appear comparable to EUS-guided biliary drainage (technical success rate: 94–96%, complication rate: 15–18%) and certainly superior to pancreatic ductal drainage (technical success rate: 77–92%, complication rate: 64%).[2–5]

EUS-guided drainage involves four intricate steps.[1–5] The first step is to identify an appropriate route. The second step is to puncture the drainage target with a needle. The third step is dilation of the transmural tract. The fourth step is insertion of drainage tubes to facilitate drainage. In general, for EUS-guided gallbladder drainage, the transgastric route provides access to the body of the gallbladder and the transduodenal route to the neck of the gallbladder.[5] Although the procedural outcomes can possibly be improved further by determining the ideal route for drainage, no comparative studies to this effect have been undertaken so far.[1–5]

The procedural technique as outlined earlier involves multiple steps. A one-step device that enables puncture, transmural dilation and stent deployment would minimize the risk of guidewire dislodgement and potential complications such as bile leak.[3–5] Recently, there is a growing advocacy for the placement of self-expandable metal stents (SEMS) in patients undergoing EUS-guided drainage. This is mainly because of the premise that SEMS seals the 'gap' better between the stent and fistula thereby minimizing the chances for leak and pneumoperitoneum.[3–5] Also, the wider lumen of the covered SEMS (CSEMS) facilitates other interventions such as gallstone removal in patients not undergoing a cholecystectomy. Several prototypes with flanges and flares are currently in development to minimize the possibility of stent migration and preliminary reports appear promising.

While the review by Widmer *et al*. focuses mainly on clinical outcomes, there is a serious paucity of data on how EUS-guided gallbladder drainage compares with percutaneous drainage. In the only randomized trial conducted to date, EUS-guided gallbladder drainage was comparable to percutaneous techniques in terms of technical feasibility, efficacy and safety.[4] It is also very likely that EUS-guided gallbladder drainage, unlike percutaneous catheters, by virtue of being internal, is unlikely to dislodge, is not associated with skin infections, and provides for better quality of life. However, this crucial assumption has not been investigated so far. The glass unfortunately is half empty.

Although technological innovations and technical refinements have steadily improved the rates of procedural success and decreased complications associated with EUS-guided drainage procedures, much more needs to be done. While it is important to conduct well-designed, prospective, randomized trials comparing the different procedural techniques and devices under development for this indication, multidisciplinary studies comparing EUS to percutaneous techniques and/or surgery is essential to move the discipline forward. These studies should not only focus on the technical and treatment outcomes but also on quality of life and cost. Right now, the glass is only half-full.

Masayuki Kitano, Ken Kamata and Masatoshi Kudo
Department of Gastroenterology and Hepatology, Kinki University Faculty of Medicine, Osaka, Japan
doi: 10.1111/den.12327

REFERENCES

1 Grimm H, Binmoeller KF, Soehendra N. Endosonography-guided drainage of a pancreatic pseudocyst. *Gastrointest. Endosc.* 1992; **38**: 170–71.
2 Itoi T, Kasuya K, Sofuni A *et al*. Endoscopic ultrasonography-guided pancreatic duct access: Techniques and literature review

of pancreatography, transmural drainage and rendezvous techniques. *Dig. Endosc*. 2013; **25**: 241–52.
3 Yamao K, Hara K, Mizuno N *et al*. EUS-guided biliary drainage. *Gut Liver* 2010; **4** (Suppl 1): S67–75.
4 Jang JW, Lee SS, Song TJ *et al*. Endoscopic ultrasound-guided transmural and percutaneous transhepatic gallbladder drainage are comparable for acute cholecystitis. *Gastroenterology* 2012; **142**: 805–11.
5 Widmer J, Singhal S, Gaidhane M, Kahaleh M. Endoscopic ultrasound (EUS) guided endoluminal drainage of gallbladder. *Dig. Endosc*. 2014; **26**: 525–31.

Hepatology Research

Hepatology Research 2014; **44**: 1110–1118 doi: 10.1111/hepr.12286

Original Article

Current treatment status of polycystic liver disease in Japan

Koichi Ogawa,[1] Kiyoshi Fukunaga,[1] Tomoyo Takeuchi,[2] Naoki Kawagishi,[3] Yoshifumi Ubara,[4] Masatoshi Kudo[5] and Nobuhiro Ohkohchi[1]

[1]*Department of Surgery, Doctoral Program in Clinical Science, Graduate School of Comprehensive Human Sciences,* [2]*Institute of Clinical Medicine, Graduate School of Comprehensive Human Sciences, University of Tsukuba, Ibaraki,* [3]*Division of Organ Transplantation, Tohoku University Hospital, Miyagi,* [4]*Nephrology Center, Toranomon Hospital, Tokyo, and* [5]*Department of Gastroenterology and Hepatology, Kinki University School of Medicine, Osaka, Japan*

Aim: Polycystic liver disease (PLD) is a genetic disorder characterized by the progressive development of multiple liver cysts. No standardized criteria for the selection of treatment exist because PLD is a rare condition and most patients are asymptomatic. We here aimed to clarify the status of treatment and to present a therapeutic strategy for PLD in Japan.

Methods: From 1 June 2011 to 20 December 2011, we administered a questionnaire to 202 PLD patients from 86 medical institutions nationwide.

Results: The patients included 45 men and 155 women, and the median age was 63 years. Two hundred and eighty-one treatments were performed for these patients, as follows: cyst aspiration sclerotherapy (AS) in 152 cases, cyst fenestration (FN) in 53, liver resection (LR) in 44, liver transplantation (LT) in 13 and other treatments in 19. For cases of type I PLD (mild form) according to Gigot's classification, the therapeutic effects of AS, FN and LR were similar. For type II (moderate form), LT demonstrated the best therapeutic effects, followed by LR and FN. For type III (severe form), the effects of LT were the best. The incidences of complications were 23.0% in AS, 28.4% in FN, 31.8% in LR and 61.5% in LT.

Conclusion: Considering the therapeutic effects and complications, AS, LR and LT showed good results for type I, type II and type III PLD, respectively. However, LT for PLD was performed in a small number of patients. In Japan, the transplantation therapy is expected to be common in the future.

Key words: aspiration-sclerotherapy, cyst fenestration, liver resection, liver transplantation, polycystic liver disease

INTRODUCTION

POLYCYSTIC LIVER DISEASE (PLD) is a genetic disorder characterized by the progressive development of multiple liver cysts. PLD includes two different diseases: (i) autosomal dominant polycystic liver disease (ADPLD), which presents multiple cysts in only the liver; and (ii) autosomal dominant polycystic kidney disease (ADPKD), which is associated with multiple renal cysts.[1] Although ADPLD and ADPKD are distinct at the genetic level, the clinical symptoms of both are similar.[2] Most patients with PLD do not require treatment because liver function is maintained during all the stages of the disease. However, some patients with PLD present abdominal distension, abdominal pain and chest compression by extensive hepatomegaly due to an increase in the number of liver cysts and their expansion, which affect performance status (PS) and quality of life.[3,4] In addition, PLD may induce other serious conditions, such as obstructive jaundice or Budd-Chiari syndrome.[3] The purpose of treatment for PLD is to decrease liver volume and alleviate or remove the symptoms caused by hepatomegaly. Common treatments for PLD include cyst aspiration sclerotherapy (AS), cyst fenestration (FN), liver resection (LR) and liver transplantation (LT). However, no consensus on the selection of treatments has been reached. Because PLD is a rare disease and no large cohort study has been performed,

Correspondence: Professor Nobuhiro Ohkohchi, Department of Surgery, Doctoral Program in Clinical Science, Graduate School of Comprehensive Human Sciences, University of Tsukuba, 1-1-1 Tennodai, Tsukuba 305-8575, Japan. Email: nokochi3@md.tsukuba.ac.jp

Received 3 September 2013; revision 28 November 2013; accepted 2 December 2013.

the long-term outcome after treatment for PLD is poorly understood.[5] In this study, we administered a questionnaire to medical institutions nationwide with experience treating PLD. The aim of the present study was to clarify the current status of treatment and to present a therapeutic strategy for PLD in Japan.

METHODS

Subjects and data collection

THE SUBJECTS WERE PLD patients who had been treated in Japan. The questionnaire was sent to 102 medical institutions that belong to the Liver Cancer Study Group of Japan. The survey was conducted from 1 June 2011 to 20 December 2011. The information collected was as follows: patient age and gender, disease type by diagnostic imaging, presence or absence of polycystic kidney disease (PKD), renal function before treatment, Eastern Cooperative Oncology Group PS before treatment, indication for treatment, method of treatment, sclerosing agent used in AS, treatment-related complications and duration of treatment effect. PLD was classified into three types based on Gigot's classification.[6] Type I (mild form) included patients with a limited number (<10) of large cysts (>10 cm). Type II (moderate form) was represented by patients with diffuse involvement of the liver parenchyma by multiple medium-sized cysts with remaining large areas of non-cystic liver parenchyma. Type III (severe form) patients had extremely high numbers of diffuse cysts that were small to medium in size with little area of liver parenchyma between cysts.[6] The treatment indication was divided into two groups: patients with only subjective symptoms and those with objective symptoms. Subjective symptoms included abdominal pain, appetite loss, dyspnea, movement limitation, fever, leg edema and abdominal discomfort. Objective symptoms included cyst infection, liver dysfunction, compression inferior vena cava, intracavitary hemorrhage, malnutrition, and ascites. Duration of treatment effect was defined as the length of time between treatment and symptom recurrence or next therapy. The patients were censored at the time of loss to follow up.

Statistical analysis

Statistical analyses were performed using the χ^2-test and the log–rank test. Duration of treatment effect was calculated using Kaplan–Meier estimates. All analyses were performed utilizing GraphPad Prism version 5. Differences at $P < 0.05$ were considered statistically significant.

RESULTS

QUESTIONNAIRES WERE RETURNED by 86 of 102 institutions (collection rate, 84.3%), and 202 PLD patients were included in the analysis. The patients included 45 men (22.2%) and 155 women (76.7%), with a median age of 63 years (range, 39–91 years). Of the 202 patients with PLD, 92 patients (45.5%) had concomitant PKD. Renal insufficiency, namely, abnormal serum creatinine level or hemodialysis, was observed in 34 (16.8%) patients. The type of disease according to Gigot's classification was as follows: type I, 102 patients (50.5%); type II, 67 patients (33.2%); type III, 27 patients (13.4%); unknown, six patients (3.0%). A total of 281 treatments were performed for the 202 PLD patients.

Of the 281 treatments, 152 were AS (54.1%), 53 were FN (18.9%), 44 were LR (15.7%), 13 were LT (4.6%) and 19 were others (6.8%) (Table 1). The most common type of disease for each treatment was type I for AS and FN (57.9% and 45.3%, respectively), type II for LR (52.3%) and type III for LT (61.5%). The PS before treatment was two or less in many of the patients who underwent AS, FN and LR. However, the PS was 3 or more in many of the patients who underwent LT. Moreover, the proportion of patients with renal dysfunction before treatment was high in the LT (53.9%) group compared with the other treatments. Regarding the treatment indication, the frequency of objective symptoms was 25.7% for AS, 28.3% for FN, 45.5% for LR and 76.9% for LT. Treatment-related complications were reported in 23.0% of AS procedures, 28.3% of FN procedures, 31.8% of LR procedures and 61.5% of LT procedures. Severe complications of Clavien–Dindo classification grade IIIb or more were observed more frequently in LT cases (15.4%) compared with any other procedures. The most common complications were fever and abdominal pain for AS, a large amount of ascites for FN, and bile leakage and a large amount of ascites for LR. For LT, cases of death due to early transplant-specific complications such as hepatic necrosis and graft failure were observed. Moreover, various complications, including bile leakage, extensive ascites and renal failure, were reported following LT. Treatment-related death occurred following AS due to sepsis in one case; two cases of treatment-related death were also reported for LT.

Table 1 Characteristics and results according to each treatment

	AS	FN	LR	LT
No. of cases (%)	152 (54.1)	53 (18.9)	44 (15.7)	13 (4.6)
Gigot's classification, *n* (%)				
Type I	88 (57.9)	24 (45.3)	17 (38.6)	0
Type II	45 (29.6)	22 (41.5)	23 (52.3)	3 (23.1)
Type III	15 (9.9)	5 (9.4)	3 (6.8)	8 (61.5)
Performance status, *n* (%)				
≤2	143 (94.1)	48 (90.6)	42 (95.5)	5 (38.5)*†§
≥3	5 (3.3)	0	1 (2.3)	7 (53.8)*†§
Renal insufficiency, *n* (%)	21 (11.2)	8 (15.1)	7 (15.9)	7 (53.9)*†§
Abnormal serum creatinine	14 (9.2)	6 (11.3)	7 (15.9)	3 (23.1)
Hemodialysis	3 (2.0)	2 (3.8)	0	4 (30.8)*†§
Indication for treatment, *n* (%)				
With objective symptoms	39 (25.7)	15 (28.3)	20 (45.5)*	10 (76.9)*†§§
Only subjective symptoms	107 (70.4)	38 (71.7)	23 (52.2)**	2 (15.4)*†§
Complications, *n* (%)	35 (23.0)	15 (28.3)	14 (31.8)	8 (61.5)*††
Clavien–Dindo grade ≤IIIa	33 (21.7)	14 (26.4)	10 (22.7)	6 (46.2)**
Clavien–Dindo grade ≥ IIIb	2 (1.3)	1 (1.9)	4 (9.1)**	2 (15.4)**††
Mortality	1 (0.7)	0	0	2 (15.4)*†§§

*$P < 0.01$ vs AS, **$P < 0.05$ vs AS, †$P < 0.01$ vs FN, ††$P < 0.05$ vs FN, §$P < 0.01$ vs LR, §§$P < 0.05$ vs LR.
AS, aspiration sclerotherapy, FN, cyst fenestration, LR, liver resection, LT, liver transplantation.

The procedures of LR according to Gigot's classification are showed in Table 2. Lobectomy was performed in approximately half of type I and II PLD patients. The details of LT cases are demonstrated in Table 3. Twelve cases for living donor transplantation and one for domino transplantation were included. The indications for LT were progression of PLD in 10 cases and coexisting hepatocellular carcinoma in three cases. Although nine cases were associated with PKD, there was no case of kidney transplantation performed simultaneously. Seven donors were patients' relatives, and no donor was affected with PLD (data not shown).

The duration of treatment effect was analyzed according to the type of disease. The median follow-up period for all treatments was 16 months (range, 0–215). In the treatment of type I PLD, the 5-year efficacy rates for LR, FN and AS were 77.8%, 78.9% and 56.6%, respectively, but there were no significant differences between these procedures (Fig. 1). For type I patients, the AS procedures were analyzed according to the sclerosing agent used, which included ethanol in 48 cases (31.6%), ethanolamine oleate (EO) in 38 cases (25.0%), minocycline in 34 cases (22.4%) and no drug in 22 cases (14.5%). Regarding the duration of treatment effect, EO was better than the other reported drugs and had a therapeutic effect comparable to LR (Fig. 2). For type II patients, surgical treatments (i.e. FN, LR and LT) had a significantly better effect than AS. The 5-year efficacy rate was 79.1% for FN, 90.2% for LR and 100% for LT; there was no significant difference among these surgical treatments (Fig. 3). For type III patients, the surgical treatments also had a significantly better effect than AS. The 5-year efficacy rate of LT was 75%, which was significantly better than FN. However, there was no significant difference between FN and LR (Fig. 4).

Table 2 Procedures of liver resection

	Lobectomy	Segmentectomy	Partial resection	Total
Type I	9	5	3	17
Type II	10	7	6	23
Type III	1	1	2	4
Total	20	13	11	44

Table 3 Detail data of liver transplantation cases

Case no.	Sex/age(y)	Type	PKD	HD	Indication for LT	Donor state	Donor relationship	Liver graft	Postoperative complication	Prognosis (months)/ outcome
1	F/56	III	+	+	Abdominal pain	Living	Son	Right lobe	Ascites	84/alive
2	F/70	III	–	–	Liver failure	Living	Daughter	Right lobe	None	71/alive
3	M/51	III	–	–	Liver dysfunction, dyspnea	Living	Wife	Right lobe	Liver failure, graft failure	0/death†
4	F/60	ND	+	–	Malnutrition, abdominal pain	Living	Husband	Right lobe	Acute rejection	108/death‡
5	F/66	ND	+	+	Infection and rapture of cysts	Living	Son	Right lobe	Bile fistula, abdominal abscess	147/alive
6	M/70	II	–	–	Comorbidity (HCC)	Living	Nephew	Right lobe	Drain site hemorrhage	108/alive
7	F/61	III	+	–	Abdominal, low back pain	Living	Husband	Right lobe	None	102/alive
8	F/72	II	+	–	Comorbidity (HCC)	Living	Son	Right lobe	None	91/alive
9	F/51	III	+	–	Liver dysfunction, malnutrition, dyspnea	Living	Husband	Right lobe	MOF, graft necrosis	0/death†
10	F/54	II	+	+	Budd–Chiari syndrome	Living	Husband	Left lobe	Ascites, peritonitis	12/alive
11	M/63	III	+	+	IVC compression, malnutrition, dyspnea	Living (domino)	Domino	Whole liver	None	105/alive
12	F/63	III	+	+	IVC compression, malnutrition, cyst infection, dyspnea	Living	Daughter	Right lobe	Renal failure	101/alive
13	M/64	III	–	+	Comorbidity (HCC)	Living	Son	Right lobe	Renal dysfunction	12/alive

†Treatment-related death.
‡Death due to subarachnoid hemorrhage.
HCC, hepatocellular carcinoma; HD, hemodialysis; IVC, inferior vena cava; LT, liver transplantation; MOF, multiple organ failure; ND, not described; PKD, polycystic kidney disease; Type, disease type of PLD according to Gigot's classification.

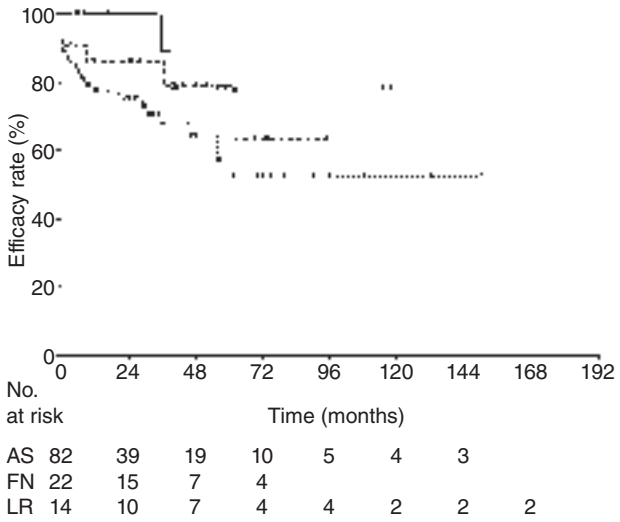

Figure 1 Duration of treatment effect in type I polycystic liver disease (PLD). There was no significant difference between treatments. However, there was the tendency toward a good effect for liver resection (LR), cyst fenestration (FN) and aspiration sclerotherapy (AS). ····, AS ($n = 88$); ·····, FN ($n = 24$); ——, LR ($n = 17$).

DISCUSSION

THE CHOICE OF treatment is difficult for PLD. LT is currently the only radical therapy for patients with PLD.[7,8] However, careful consideration of the indication for LT is needed because liver function is maintained even in the patient with symptomatic PLD.[3,9] Additionally, organ donation is limited, particularly in Japan. Instead, AS, FN and LR are generally performed to treat symptomatic PLD. The goals of treatment for PLD are to alleviate the abdominal symptoms and prevent symptom recurrence by decreasing liver volume.[3] These treatments do not change the natural course of the disease, and therefore, the symptoms usually recur due to the growth of new cysts or the re-growth of treated cysts. Hence, it is important to choose an appropriate treatment according to the condition of each patient. When classifying the form of PLD, the system proposed by Gigot *et al*. is often used.[6] This classification system is based on the number and size of the liver cysts and the amount of remaining liver parenchyma. It reflects the severity of the disease and is useful when choosing treatment options. Recently, some reports regarding PLD treatment have recommended AS, FN and LR for type I or II PLD and LT for type III PLD; even so, no standardized criteria for the selection of treatment exist.[1,3,5,10–12] In the present study, we clarified the treatment status for PLD in Japan by conducting a nationwide survey and evaluated the therapeutic effect of each treatment and its associated complications according to disease types.

Several reports have recommended FN for the treatment of type I PLD.[6,13] FN, namely, surgical de-roofing of the cyst, is a minimally invasive surgical treatment,[13,14] but, the recurrence rate has been reported to be 20–72%, with a large difference among reports.[15–18] The most common postoperative complication reported by the hospitals was ascites, and its incidence was relatively high at 33–69%. AS involves cyst aspiration followed by injection of a sclerosing agent that destroys the epithelial cells lining the cyst cavity, inhibiting cystic fluid production, and it is also performed primarily for type I PLD.[19,20] The most commonly used sclerosing agent is ethanol, although minocycline and tetracycline are also used. Only mild treatment-related complications were reported for AS with these agents, but AS is impractical because of the high associated recurrence rate, which exceeds 75%.[21] In the present study, the 5-year efficacy rate of AS for type I PLD was only approximately 50%. However, examining the rate according to the sclerosing agent used demonstrated that EO provided an excellent outcome when compared

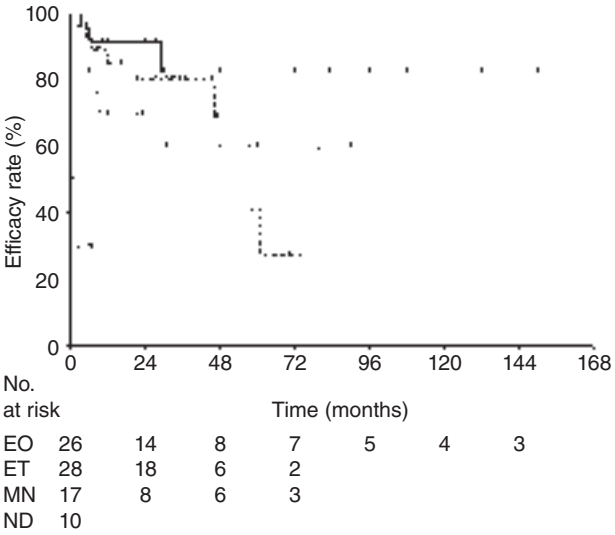

Figure 2 Duration of aspiration sclerotherapy (AS) effect according to the sclerosing agent used for type I polycystic liver disease (PLD). AS with any agent showed a significantly greater effect when compared with no drug (ND) ($P < 0.01$). Ethanolamine oleate (EO) tended to be better than the other evaluated drugs, although there was no significant difference. MN, minocycline. ——, EO ($n = 28$); ·····, ET ($n = 29$); ····, MN ($n = 18$); – · · ·, ND ($n = 11$).

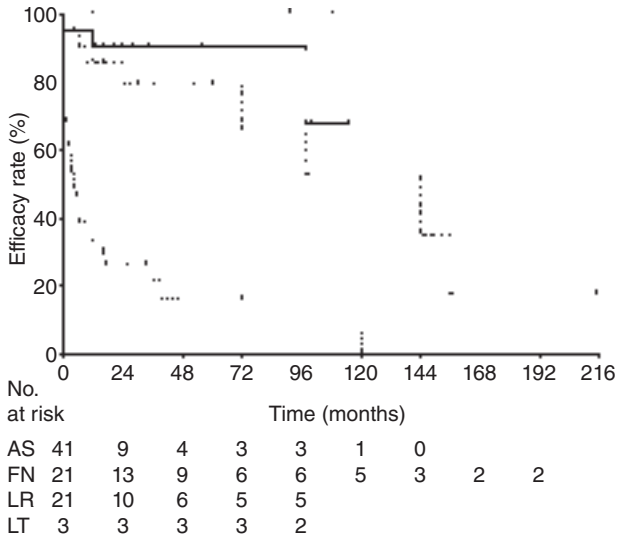

Figure 3 Duration of treatment effect in type II polycystic liver disease (PLD). All surgical treatments showed significantly greater effects compared with aspiration sclerotherapy (AS) ($P < 0.01$; cyst fenestration [FN] and liver resection [LR] vs AS, $P < 0.05$; liver transplantation [LT] vs AS). There was no significant difference between surgical treatments. ·····, AS ($n = 45$); - - - -, FN ($n = 23$); ——, LR ($n = 22$); – · –, LT ($n = 3$).

with the other drugs, with a result comparable to LR and FN. EO has been used with immense success in sclerotherapy for esophageal varices.[22] Nakaoka *et al*. reported that AS with EO for PLD had a 93.3% success rate with no recurrence during the observation period.[23] They used 5% EO and injected a volume of sclerosant equivalent to 10% of the volume of aspirated cystic fluid. However, there is no consensus on the appropriate concentration and volume of EO for PLD. Considering the therapeutic effects and complications, AS with EO is appropriate as an initial treatment for type I PLD.

Liver resection for type II PLD has been recommended by some reports, and one report noted that LR should be performed even for type III PLD.[11] The recurrence rate following LR has been reported to be 3–33%.[5,24,25] In type II or III PLD, the intrahepatic vasculature and biliary system are severely altered by cysts and the accurate preoperative definition of these structures remains difficult, even with current imaging modalities.[26] Therefore, the postoperative complication rate is high, at 20–83%, and includes ascites, pleural effusion, biliary leakage, hemorrhage and wound infection.[5,11,13,24,25] The present study demonstrated that the postoperative complications of LR include ascites, bile leakage and intra-abdominal abscess, with an incidence of 31.8%. However, the duration of treatment effect for type II PLD was more satisfactory following LR and LT than AS or FN. LT provides a desirable cure as the therapeutic effect is permanent. However, considering the high morbidity associated with LT and the limited number of donated organs in Japan, LR is recommended as the initial treatment for type II PLD.

In previous reports, LT was commonly recommended for type III PLD,[6,27–29] but one report proposed an extended indication of LR to type III.[11] However, LR for type III PLD is associated with difficulty determining the LR line and liver dysfunction caused by the small amount of remnant liver. In addition, most type III patients have a poor PS or renal dysfunction due to coexisting polycystic kidneys. Therefore, it would appear that the use of LR for type III PLD should be prudent. LT is the only radical treatment option for PLD.[8] Although LT carries increased risks of postoperative morbidity and mortality,[5,10,11,13] it has an excellent curative effect if these problems are overcome.[30–32] The outcome of LT for PLD is comparable to that for other liver diseases.[10,27] Therefore, LT appears to be a more appropriate treatment in type III PLD patients in Western countries in which cadaveric donor transplantation is common. However,

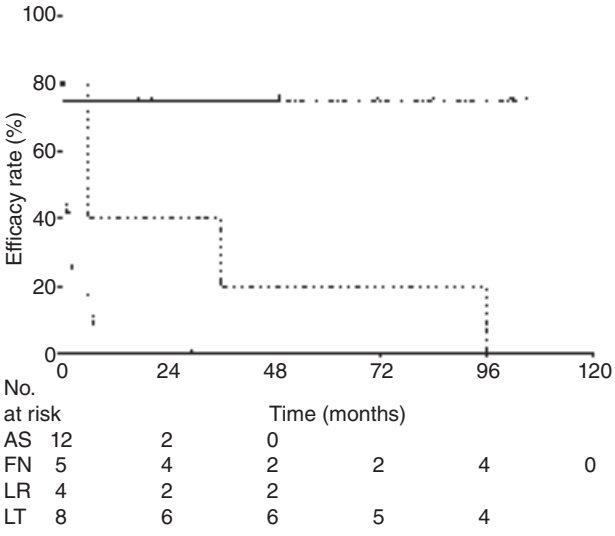

Figure 4 Duration of treatment effect in type III polycystic liver disease (PLD). All surgical treatments showed significantly greater effects compared with aspiration sclerotherapy (AS) ($P < 0.01$; liver transplantation [LT] vs AS, $P < 0.05$; cyst fenestration [FN] and liver resection [LR] vs AS). LT showed a markedly greater effect than FN ($P < 0.05$). There was no significant difference between LR and LT. ·····, AS ($n = 15$); - - - -, FN ($n = 5$); ——, LR ($n = 3$); – · –, LT ($n = 8$).

only 13 patients underwent LT in the present study. These results indicate that LT for PLD is not common in Japan. Organ shortage is a serious problem in Japan, in addition, the priority of PLD patients as recipient is low, and liver transplants from cadaveric donors are not expected. Therefore, it is not easy to recommend LT as initiation therapy for type III PLD in the present situation in Japan, and accumulation of experiences and discussion are necessary sequentially. On the other hand, the duration of treatment effect following LT for type III PLD was long compared with the other treatments in this study. In Japan, the number of cadaveric transplantation cases increased after revision of the Organ Transplant Law enforced in 2010, thereby increase in LT for PLD is expected. Living donor liver transplantation from a patient's relative may be a restricted treatment option, as PLD is an autosomal dominant disease. In the present study, almost all (12/13) of LT were living donor liver transplantation, of whom seven donors were relatives and five were spouses. The relative donors were four sons, two daughters and one nephew, and none was affected with PLD. Most relative donors were male, which might have been affected by the fact that three-quarters of PLD patients were female. Furthermore, it is possible to perform simultaneous liver and kidney transplantation (SLK) in patients with PKD. A meta-analysis by Drenth *et al*. reported that 42% of patients undergoing LT for PLD underwent SLK.[10] In the present study, there was no case that underwent SLK for PKD. Additionally, the first case of successful SLK was reported in 2013 in Japan.[33] In the current Japanese status, it is difficult to perform SLK even with renal failure, because most transplantation cases are dependent on a living donor. On the other hand, Simpson *et al*. reported that SLK has an immunological advantage over serial transplantation in terms of avoiding the risk of pre-sensitization, when recipients require liver and kidney transplantation.[34] In the future, increase in cadaveric donors would enable PLD patients with PKD to undergo SLK.

Other treatments for PLD include percutaneous transcatheter hepatic artery embolization (TAE). Ubara *et al*. reported that TAE reduced the cyst volume following the selective embolization of the hepatic artery because the blood flow in the liver cysts caused by PLD is predominantly supplied by the hepatic artery.[35] By performing TAE super-selectively, targeting hepatic arterial branches supplying localized hepatic regions replaced by multiple cysts with neither an intact portal vein nor intact hepatic parenchyma, they sought to minimize damage to remaining intact liver. Selection of embolized hepatic regions followed the same judgment process as for LR.[36] Takei *et al*. also noted that TAE decreased the liver volume by approximately 23% and the cyst volume by approximately 30% and that it could be performed for patients with poor general condition who are not candidates for surgical treatment.[36] We were unable to compare TAE with the other treatments in the present study because of the small number of included TAE cases and their short observation periods. Recently, somatostatin analogs were reported as a new treatment option for PLD.[37–39] Somatostatin inhibits fluid secretion and proliferation by reducing cyclic adenosine monophosphate in the cholangiocytes within PLD cysts.[40,41] Previous reports have demonstrated that somatostatin analogs can decrease the liver volume by 3–5% and provide 6–12 months of therapeutic effect. Moreover, it is less invasive than other treatments and can be used for all types of PLD.[26,38,42] Although the accumulation of experience with somatostatin analogs in Japan is required, they are expected to be a treatment option in the future.

In conclusion, considering the therapeutic effects and complications, AS, LR, and LT are good treatments for type I, type II and type III PLD, respectively. However, LT for PLD was performed in a small number of patients. In Japan, the transplantation therapy is expected to be common in the future. In addition, in the clinical setting, it is particularly important that treatment selection should be tailored to a patient's clinical status and that patients are informed that treatments other than LT are not radical treatment options.

ACKNOWLEDGMENTS

THIS WORK WAS supported in part by a Health Labor Sciences Research Grant (Tokyo, Japan) (H23-Nanchi-Ippan-081).

REFERENCES

1 Chandok N. Polycystic liver disease: a clinical review. *Ann Hepatol* 2012; **11:** 819–26.
2 Hoevenaren IA, Wester R, Schrier RW *et al*. Polycystic liver: clinical characteristics of patients with isolated polycystic liver disease compared with patients with polycystic liver and autosomal dominant polycystic kidney disease. *Liver Int* 2008; **28:** 264–70.
3 Temmerman F, Missiaen L, Bammens B *et al*. Systematic review: the pathophysiology and management of polycystic liver disease. *Aliment Pharmacol Ther* 2011; **34:** 702–13.

4 Arnold HL, Harrison SA. New advances in evaluation and management of patients with polycystic liver disease. *Am J Gastroenterol* 2005; **100:** 2569–82.
5 Schnelldorfer T, Torres VE, Zakaria S, Rosen CB, Nagorney DM. Polycystic liver disease: a critical appraisal of hepatic resection, cyst fenestration, and liver transplantation. *Ann Surg* 2009; **250:** 112–8.
6 Gigot JF, Jadoul P, Que F *et al*. Adult polycystic liver disease: is fenestration the most adequate operation for long-term management? *Ann Surg* 1997; **225:** 286–94.
7 Everson GT, Taylor MR, Doctor RB. Polycystic disease of the liver. *Hepatology* 2004; **40:** 774–82.
8 Pirenne J, Aerts R, Yoong K *et al*. Liver transplantation for polycystic liver disease. *Liver Transpl* 2001; **7:** 238–45.
9 Que F, Nagorney DM, Gross JB, Jr, Torres VE. Liver resection and cyst fenestration in the treatment of severe polycystic liver disease. *Gastroenterology* 1995; **108:** 487–94.
10 Drenth JP, Chrispijn M, Nagorney DM, Kamath PS, Torres VE. Medical and surgical treatment options for polycystic liver disease. *Hepatology* 2010; **52:** 2223–30.
11 Aussilhou B, Doufle G, Hubert C *et al*. Extended liver resection for polycystic liver disease can challenge liver transplantation. *Ann Surg* 2010; **252:** 735–43.
12 Gigot JF, Hubert C, Banice R, Kendrick ML. Laparoscopic management of benign liver diseases: where are we? *HPB* 2004; **6:** 197–212.
13 Russell RT, Pinson CW. Surgical management of polycystic liver disease. *World J Gastroenterol* 2007; **13:** 5052–9.
14 van Keimpema L, Ruurda JP, Ernst MF, van Geffen HJ, Drenth JP. Laparoscopic fenestration of liver cysts in polycystic liver disease results in a median volume reduction of 12.5%. *J Gastrointest Surg* 2008; **12:** 477–82.
15 Martin IJ, McKinley AJ, Currie EJ, Holmes P, Garden OJ. Tailoring the management of nonparasitic liver cysts. *Ann Surg* 1998; **228:** 167–72.
16 Koperna T, Vogl S, Satzinger U, Schulz F. Nonparasitic cysts of the liver: results and options of surgical treatment. *World J Surg* 1997; **21:** 850–4.
17 Kabbej M, Sauvanet A, Chauveau D, Farges O, Belghiti J. Laparoscopic fenestration in polycystic liver disease. *Br J Surg* 1996; **83:** 1697–701.
18 Farges O, Bismuth H. Fenestration in the management of polycystic liver disease. *World J Surg* 1995; **19:** 25–30.
19 Bean WJ, Rodan BA. Hepatic cysts: treatment with alcohol. *AJR Am J Roentgenol* 1985; **144:** 237–41.
20 Saini S, Mueller PR, Ferrucci JT, Jr, Simeone JF, Wittenberg J, Butch RJ. Percutaneous aspiration of hepatic cysts does not provide definitive therapy. *AJR Am J Roentgenol* 1983; **141:** 559–60.
21 Erdogan D, van Delden OM, Rauws EA *et al*. Results of percutaneous sclerotherapy and surgical treatment in patients with symptomatic simple liver cysts and polycystic liver disease. *World J Gastroenterol* 2007; **13:** 3095–100.
22 Iso Y, Kitano S, Iwanaga T, Koyanagi N, Sugimachi K. A prospective randomized study comparing the effects of large and small volumes of the sclerosant 5% ethanolamine oleate injected into esophageal varices. *Endoscopy* 1988; **20:** 285–8.
23 Nakaoka R, Das K, Kudo M, Chung H, Innoue T. Percutaneous aspiration and ethanolamine oleate sclerotherapy for sustained resolution of symptomatic polycystic liver disease: an initial experience. *AJR Am J Roentgenol* 2009; **193:** 1540–5.
24 Vons C, Chauveau D, Martinod E *et al*. Liver resection in patients with polycystic liver disease. *Gastroenterol Clin Biol* 1998; **22:** 50–4.
25 Soravia C, Mentha G, Giostra E, Morel P, Rohner A. Surgery for adult polycystic liver disease. *Surgery* 1995; **117:** 272–5.
26 Hogan MC, Masyuk TV, Page LJ *et al*. Randomized clinical trial of long-acting somatostatin for autosomal dominant polycystic kidney and liver disease. *J Am Soc Nephrol* 2010; **21:** 1052–61.
27 van Keimpema L, Nevens F, Adam R *et al*. Excellent survival after liver transplantation for isolated polycystic liver disease: an European Liver Transplant Registry study. *Transpl Int* 2011; **24:** 1239–45.
28 Mekeel KL, Moss AA, Reddy KS *et al*. Living donor liver transplantation in polycystic liver disease. *Liver Transpl* 2008; **14:** 680–3.
29 Kirchner GI, Rifai K, Cantz T *et al*. Outcome and quality of life in patients with polycystic liver disease after liver or combined liver-kidney transplantation. *Liver Transpl* 2006; **12:** 1268–77.
30 Alves RC, Fonseca EA, Mattos CA, Abdalla S, Goncalves JE, Waisberg J. Predictive factors of early graft loss in living donor liver transplantation. *Arq Gastroenterol* 2012; **49:** 157–61.
31 Jeon GS, Won JH, Wang HJ, Kim BW, Lee BM. Endovascular treatment of acute arterial complications after living-donor liver transplantation. *Clin Radiol* 2008; **63:** 1099–105.
32 Jain A, Reyes J, Kashyap R *et al*. Long-term survival after liver transplantation in 4,000 consecutive patients at a single center. *Ann Surg* 2000; **232:** 490–500.
33 Yagi T, Nobuoka D, Shinoura S *et al*. First successful case of simultaneous liver and kidney transplantation for patients with chronic liver and renal failure in Japan. *Hepatol Res* 2013. doi: 10.1111/hepr.12122
34 Simpson N, Cho YW, Cicciarelli JC, Selby RR, Fong TL. Comparison of renal allograft outcomes in combined liver-kidney transplantation versus subsequent kidney transplantation in liver transplant recipients: analysis of UNOS Database. *Transplantation* 2006; **82:** 1298–303.
35 Ubara Y, Takei R, Hoshino J *et al*. Intravascular embolization therapy in a patient with an enlarged polycystic liver. *Am J Kidney Dis* 2004; **43:** 733–8.
36 Takei R, Ubara Y, Hoshino J *et al*. Percutaneous transcatheter hepatic artery embolization for liver cysts in autosomal dominant polycystic kidney disease. *Am J Kidney Dis* 2007; **49:** 744–52.

37 van Keimpema L, Drenth JP. Effect of octreotide on polycystic liver volume. *Liver Int* 2010; **30:** 633–4.
38 van Keimpema L, Nevens F, Vanslembrouck R *et al*. Lanreotide reduces the volume of polycystic liver: a randomized, double-blind, placebo-controlled trial. *Gastroenterology* 2009; **137:** 1661-8 e1–2.
39 van Keimpema L, de Man RA, Drenth JP. Somatostatin analogues reduce liver volume in polycystic liver disease. *Gut* 2008; **57:** 1338–9.
40 Banales JM, Masyuk TV, Gradilone SA, Masyuk AI, Medina JF, LaRusso NF. The cAMP effectors Epac and protein kinase a (PKA) are involved in the hepatic cystogenesis of an animal model of autosomal recessive polycystic kidney disease (ARPKD). *Hepatology* 2009; **49:** 160–74.
41 Gong AY, Tietz PS, Muff MA *et al*. Somatostatin stimulates ductal bile absorption and inhibits ductal bile secretion in mice via SSTR2 on cholangiocytes. *Am J Physiol Cell Physiol* 2003; **284:** C1205–14.
42 Caroli A, Antiga L, Cafaro M *et al*. Reducing polycystic liver volume in ADPKD: effects of somatostatin analogue octreotide. *Clin J Am Soc Nephrol* 2010; **5:** 783–9.

Liver Cancer

Liver Cancer 2014;3:399–404
DOI: 10.1159/000343870
Published online: August 8, 2014

2235-1795/14/0034-0399$39.50/0
www.karger.com/lic

Editorial

Biomarkers and Personalized Sorafenib Therapy

Prof. M. Kudo

Editor *Liver Cancer*

Compared with other types of cancer, hepatocellular carcinoma (HCC) is highly heterogeneous because of the intrinsic diversity in its pathogenesis, molecular heterogeneity, its multicentric occurrence, and its etiology, among others. Until now, locoregional therapies such as resection, ablation, and transarterial chemoembolization (TACE) have been performed extensively to treat HCC because the application of systemic chemotherapy using cytotoxic anticancer drugs is limited by the presence of pancytopenia and hepatic dysfunction caused by the cirrhosis that usually accompanies HCC. Since its approval in 2007 as a systemic chemotherapeutic agent that improves the survival of patients with unresectable advanced HCC, sorafenib has been widely used as a novel treatment option in patients with advanced HCCs with extrahepatic spread and/or vascular invasion.

Need for Personalized Sorafenib Therapy

Sorafenib is the only anticancer drug with proven prognostic efficacy in HCC [1, 2]; however, it should be administered with care because of various adverse effects, including hand–foot skin reaction, hypertension, diarrhea, and liver dysfunction. Moreover, because cases of ineffective and incomplete response to sorafenib have been reported, and because the drug is extremely expensive, the development of prognostic factors and biomarkers for predicting adverse events are eagerly awaited. The ability to predict treatment outcome and adverse events would make it possible to avoid administering sorafenib to patients who would not benefit from it and to exclude patients likely to develop serious side effects. This would not only increase safety but also markedly improve the medico-economic situation. Consequently, studies are currently underway to develop biomarkers for predicting treatment outcome and adverse events, and some biomarkers for novel molecularly targeted drugs have already been identified in the early phase of clinical trials and subsequently evaluated in phase III trials.

Liver Cancer 2014;3:399–404
DOI: 10.1159/000343870
Published online: August 8, 2014

Signals Triggering Proliferation of Hepatocellular Carcinoma

Mutations of specific genes that play an important role in cancer proliferation (oncogene addiction), such as the BRAF V600E mutation in malignant melanoma [3] and the ALK fusion gene mutation in lung cancer [4], are perfect targets for molecularly targeted drugs. However, with regard to HCC, no study has reported a specific gene mutation that causes oncogene addiction, despite various proliferation-related signal transduction pathways being activated, such as those of MAP kinase [5], PI3K/Akt/mTOR [6], c-MET [7], IGF [8], Wnt-beta-catenin [9, 10], hedgehog [11], vascular endothelial growth factor (VEGF) receptor, and platelet-derived growth factor (PDGF) receptor [12]. It is therefore difficult to use gene mutations as biomarkers in HCC. The multikinase inhibitor sorafenib suppresses the proliferation of vascular endothelial cells and pericytes by inhibiting the activity of tyrosine kinase in the cytosolic domain of the VEGF and PDGF receptors. It also suppresses the proliferation of tumor cells by inhibiting the activity of Raf serine/threonine kinase in the MAP kinase cascade responsible for such proliferation. Sorafenib, therefore, exerts a multifaceted anticancer effect by inhibiting various kinases and appears to work well in HCC. In other words, the difficulty in identifying a specific biomarker in sorafenib therapy for HCC may be caused by the presence of multiple molecular targets. Despite previous reports of potential biomarkers, no definitive biomarker for sorafenib has been reported (Table 1 [13–24]).

FGF3/4 Gene Amplification

The SHARP [1] and Asia Pacific [2] trials revealed extremely low response rates in patients treated with sorafenib: the overall response was as low as a few percent, with almost no tumor response. In general, a drug's inhibitory action on tumor proliferation improves patient survival. In Japan, there has been a stream of super responders (i.e., complete responders and partial responders) to sorafenib since its approval in 2009, suggesting a common, yet unknown response factor in Japanese people [25]. In fact, when we gathered biopsy specimens from sorafenib super responders across Japan and performed genome analysis, the results revealed a high expression level of FGF3/4, lung metastasis, and poorly differentiated HCC as common factors [24], suggesting that each of these factors could serve as biomarkers. Although high expression of FGF3/4 may be a good marker because of its affinity for various molecular targets, it is difficult to use high levels of FGF3/4 expression as a general purpose marker because the FGF3/4 mutation has been observed in only a few percent of all HCC patients.

c-Jun N-Terminal Kinase

In addition, c-Jun N-terminal kinase (JNK), which acts as an intracellular signaling protein, is highly upregulated in patients with no response to sorafenib. Because JNK activation is closely related to CD133 expression, CD133 and JNK expression may serve as a biomarker for no tumor response to sorafenib [23].

Liver Cancer

Liver Cancer 2014;3:399–404
DOI: 10.1159/000343870
Published online: August 8, 2014

Table 1. Potential biomarkers for predicting treatment outcome and adverse events of sorafenib treatment in HCC

Biomarker	Author	Year	Reference
Symtoms and signs			
Dermal toxicity	Vincenzi B	2010	13
Hypertension	Estfan B	2013	14
Lung metastasis	Yau T	2009	21
Serum markers			
AFP decrease after 6 weeks (>20%)	Yau T	2011	15
AFP decrease in the early phase (comparing AFP after 2 and 4 weeks)	Kuzuya T	2011	16
DCP increase after 2 weeks	Ueshima K	2011	17
NX-DCP and DCP	Miyahara K	2013	18
Serum VEGF decrease after 8 weeks	Tsuchiya K	2014	19
Angiopoietin-2, G-CSF, HGF, leptin	Miyahara K	2011	20
Genes and proteins			
pERK	Zhang Z	2009	22
JNK activity	Hagiwara S	2012	23
FGF3/FGF4 amplification	Arao T	2013	24

AFP = alpha-fetoprotein; DCP = des-γ-carboxyprothrombin; G-CSF = granulocyte colony-stimulating factor; HGF = hepatocyte growth factor; pERK = phosphorylated extracellular-signal-regulated kinases.

Cytokine Biomarkers

Miyahara et al. measured changes in the levels of several serum angiogenesis markers before and after sorafenib treatment and showed that the number of HCC patients with progressive disease was high among HCC patients with high levels of serum angiogenesis markers before the treatment [20]. In addition, Tsuchiya et al. reported that chronological changes in serum VEGF levels can serve as a useful prognostic indicator [19]. As shown in these studies, changes in the levels of serum markers during drug therapy can be used to predict treatment outcome to a certain extent.

Although the aim is to use biomarkers to predict treatment outcome and adverse events before drug treatment, this is difficult to do at present. We await the results of genome-wide association studies currently underway. Another way to predict adverse events is to monitor laboratory test values and hemodynamics throughout drug therapy.

Liver Cancer 2014;3:399–404
DOI: 10.1159/000343870
Published online: August 8, 2014

Proteins Induced by Vitamin K Absence

Proteins induced by vitamin K absence (PIVKA)-II are markers for HCC. In hepatic cells, γ-glutamyl carboxylase and vitamin K are coenzymes responsible for the carboxylation of ten glutamic acid residues in the Gla domain located at the N-terminus of the prothrombin precursor, thereby converting the precursor to prothrombin, which possesses coagulation activity and is secreted into the bloodstream. However, when vitamin K is deficient, prothrombin is released into the circulation without complete carboxylation. PIVKA-II proteins are the non-functional precursors that accumulate in the circulation. Because sorafenib administration rapidly increases PIVKA-II levels in many cases, we retrospectively investigated the relationship between tumor progression and increases in PIVKA-II levels. The results showed that time to progression (TTP) was significantly prolonged in patients whose PIVKA-II level had been upregulated two-fold 2 weeks after sorafenib administration [17]. We believe that prolonged TTP is a reflection of ischemia in HCC caused by the anti-angiogenic effect of sorafenib. Such ischemia alters the actin molecules making up the cytoskeleton of HCC cells, thereby impairing the endocytosis of vitamin K. This subsequently leads to vitamin K deficiency and an increase in PIVKA-II levels, and means that PIVKA-II has potential as a surrogate marker for cellular ischemia as well as a monitoring marker for the anti-angiogenic effect of sorafenib.

Comparison of Images Taken Before and after Treatment

Because tumors develop ischemic conditions when sorafenib exerts its anti-angiogenic effect, the monitoring of hemodynamics by computed tomography or magnetic resonance imaging may provide useful evaluation criteria on whether to continue drug administration. Our investigation showed that survival was significantly prolonged in HCC patients with necrosis or decreased blood flow, even if only partial, compared with that in HCC patients with no change in blood flow [26].

In conclusion, it is not currently possible to predict treatment outcome or the likelihood of adverse effects of sorafenib treatment before administering the drug. Despite the discovery of genes that are potential biomarkers, such as FGF3/4, these genes have not been put to practical use: current clinical practice consists of starting sorafenib administration and monitoring patients individually to determine the treatment effects. In particular, we need to monitor the radiological response and response of tumor markers (AFP and PIVKA-II) carefully during the initial phase of drug administration (approximately 4 weeks.) At the time of evaluating the treatment effect (after 8 weeks), it may be considered to discontinue administration in patients who have not responded to sorafenib since the likely result will be progressive disease. However, in the real world clinical practice in those patients with slow growing HCCs (long stable diseases), administration of sorafenib even beyond progressive diseases should be continued since there is no second line targeted agents available at the present and maybe sorafenib is beneficial for prolonging survival of such patient population.

Liver Cancer 2014;3:399–404
DOI: 10.1159/000343870
Published online: August 8, 2014

References

1 Llovet JM, Ricci S, Mazzaferro V, Hilgard P, Gane E, Blanc JF, de Oliveira AC, Santoro A, Raoul JL, Forner A, Schwartz M, Porta C, Zeuzem S, Bolondi L, Greten TF, Galle PR, Seitz JF, Borbath I, Häussinger D, Giannaris T, Shan M, Moscovici M, Voliotis D, Bruix J, SHARP Investigators Study Group: Sorafenib in advanced hepatocellular carcinoma. N Engl J Med 2008;359:378–390.

2 Cheng AL, Kang YK, Chen Z, Tsao CJ, Qin S, Kim JS, Luo R, Feng J, Ye S, Yang TS, Xu J, Sun Y, Liang H, Liu J, Wang J, Tak WY, Pan H, Burock K, Zou J, Voliotis D, Guan Z: Efficacy and safety of sorafenib in patients in the Asia-Pacific region with advanced hepatocellular carcinoma: a phase III randomised, double-blind, placebo-controlled trial. Lancet Oncol 2009;10:25–34.

3 Chapman PB, Hauschild A, Robert C, Haanen JB, Ascierto P, Larkin J, Dummer R, Garbe C, Testori A, Maio M, Hogg D, Lorigan P, Lebbe C, Jouary T, Schadendorf D, Ribas A, O'Day SJ, Sosman JA, Kirkwood JM, Eggermont AM, Dreno B, Nolop K, Li J, Nelson B, Hou J, Lee RJ, Flaherty KT, McArthur GA, BRIM-3 Study Group: Improved survival with vemurafenib in melanoma with BRAF V600E mutation. N Engl J Med 2011;364:2507–2516.

4 Soda M, Choi YL, Enomoto M, Takada S, Yamashita Y, Ishikawa S, Fujiwara S, Watanabe H, Kurashina K, Hatanaka H, Bando M, Ohno S, Ishikawa Y, Aburatani H, Niki T, Sohara Y, Sugiyama Y, Mano H: Identification of the transforming EML4-ALK fusion gene in non-small-cell lung cancer. Nature 2007;448:561–566.

5 Schmidt CM, McKillop IH, Cahill PA, Sitzmann JV: Increased MAPK expression and activity in primary human hepatocellular carcinoma. Biochem Biophys Res Commun 1997;236:54–58.

6 Sahin F, Kannangai R, Adegbola O, Wang J, Su G, Torbenson M: mTOR and P70 S6 kinase expression in primary liver neoplasms. Clin Cancer Res 2004;10:8421–8425.

7 Boix L, Rosa JL, Ventura F, Castells A, Bruix J, Rodés J, Bartrons R: c-met mRNA overexpression in human hepatocellular carcinoma. Hepatology 1994;19:88–91.

8 Scharf JG, Braulke T: The role of the IGF axis in hepatocarcinogenesis. Horm Metab Res 2003;35:685–693.

9 de La Coste A, Romagnolo B, Billuart P, Renard CA, Buendia MA, Soubrane O, Fabre M, Chelly J, Beldjord C, Kahn A, Perret C: Somatic mutations of the beta-catenin gene are frequent in mouse and human hepatocellular carcinomas. Proc Natl Acad Sci USA 1998;95:8847–8851.

10 Klaus A, Birchmeier W: Wnt signalling and its impact on development and cancer. Nat Rev Cancer 2008;8:387–398.

11 Patil MA, Zhang J, Ho C, Cheung ST, Fan ST, Chen X: Hedgehog signaling in human hepatocellular carcinoma. Cancer Biol Ther 2006;5:111–117.

12 Poon RT, Ng IO, Lau C, Zhu LX, Yu WC, Lo CM, Fan ST, Wong J: Serum vascular endothelial growth factor predicts venous invasion in hepatocellular carcinoma: a prospective study. Ann Surg 2001;233:227–235.

13 Vincenzi B, Santini D, Russo A, Addeo R, Giuliani F, Montella L, Rizzo S, Venditti O, Frezza AM, Caraglia M, Colucci G, Del Prete S, Tonini G: Early skin toxicity as a predictive factor for tumor control in hepatocellular carcinoma patients treated with sorafenib. Oncologist 2010;15:85–92.

14 Estfan B, Byrne M, Kim R: Sorafenib in advanced hepatocellular carcinoma: hypertension as a potential surrogate marker for efficacy. Am J Clin Oncol 2013;36:319–324.

15 Yau T, Yao TJ, Chan P, Wong H, Pang R, Fan ST, Poon RT: The significance of early alpha-fetoprotein level changes in predicting clinical and survival benefits in advanced hepatocellular carcinoma patients receiving sorafenib. Oncologist 2011;16:1270–1279.

16 Kuzuya T, Asahina Y, Tsuchiya K, Tanaka K, Suzuki Y, Hoshioka T, Tamaki S, Kato T, Yasui Y, Hosokawa T, Ueda K, Nakanishi H, Itakura J, Takahashi Y, Kurosaki M, Izumi N: Early decrease in α-fetoprotein, but not des-γ-carboxy prothrombin, predicts sorafenib efficacy in patients with advanced hepatocellular carcinoma. Oncology 2011;81:251–258.

17 Ueshima K, Kudo M, Takita M, Nagai T, Tatsumi C, Ueda T, Kitai S, Ishikawa E, Yada N, Inoue T, Hagiwara S, Minami Y, Chung H, Sakurai T: Des-γ-carboxyprothrombin may be a promising biomarker to determine the therapeutic efficacy of sorafenib for hepatocellular carcinoma. Dig Dis 2011;29:321–325.

18 Miyahara K, Nouso K, Morimoto Y, Tomoda T, Kobayashi S, Takeuchi Y, Hagihara H, Kuwaki K, Ohnishi H, Ikeda F, Miyake Y, Nakamura S, Shiraha H, Takaki A, Yamamoto K, Okayama Liver Cancer Group: Evaluation of the effect of sorafenib using serum NX-des-γ-carboxyprothrombin in patients with hepatocellular carcinoma. Hepatol Res 2013;43:1064–1070.

19 Tsuchiya K, Asahina Y, Matsuda S, Muraoka M, Nakata T, Suzuki Y, Tamaki N, Yasui Y, Suzuki S, Hosokawa T, Nishimura T, Ueda K, Kuzuya T, Nakanishi H, Itakura J, Takahashi Y, Kurosaki M, Enomoto N, Izumi N: Changes in plasma vascular endothelial growth factor at 8 weeks after sorafenib administration as predictors of survival for advanced hepatocellular carcinoma. Cancer 2014;120:229–237.

20 Miyahara K, Nouso K, Tomoda T, Kobayashi S, Hagihara H, Kuwaki K, Toshimori J, Onishi H, Ikeda F, Miyake Y, Nakamura S, Shiraha H, Takaki A, Yamamoto K: Predicting the treatment effect of sorafenib using serum angiogenesis markers in patients with hepatocellular carcinoma. J Gastroenterol Hepatol 2011;26:1604–1611.

21 Yau T, Chan P, Ng KK, Chok SH, Cheung TT, Fan ST, Poon RT: Phase 2 open-label study of single-agent sorafenib in treating advanced hepatocellular carcinoma in a hepatitis B-endemic Asian population: presence of lung metastasis predicts poor response. Cancer 2009;115:428–436.

22 Zhang Z, Zhou X, Shen H, Wang D, Wang Y: Phosphorylated ERK is a potential predictor of sensitivity to sorafenib when treating hepatocellular carcinoma: evidence from an in vitro study. BMC Med 2009;7:41-52.

Liver Cancer 2014;3:399–404
DOI: 10.1159/000343870
Published online: August 8, 2014

23 Hagiwara S, Kudo M, Nagai T, Inoue T, Ueshima K, Nishida N, Watanabe T, Sakurai T: Activation of JNK and high expression level of CD133 predict a poor response to sorafenib in hepatocellular carcinoma. Br J Cancer 2012;106:1997–2003.
24 Arao T, Ueshima K, Matsumoto K, Nagai T, Kimura H, Hagiwara S, Sakurai T, Haji S, Kanazawa A, Hidaka H, Iso Y, Kubota K, Shimada M, Utsunomiya T, Hirooka M, Hiasa Y, Toyoki Y, Hakamada K, Yasui K, Kumada T, Toyoda H, Sato S, Hisai H, Kuzuya T, Tsuchiya K, Izumi N, Arii S, Nishio K, Kudo M: FGF3/FGF4 amplification and multiple lung metastases in responders to sorafenib in hepatocellular carcinoma. Hepatology 2013;57:1407–1415.
25 Kudo M, Ueshima K: Positioning of a molecular-targeted agent, sorafenib, in the treatment algorithm for hepatocellular carcinoma and implication of many complete remission cases in Japan. Oncology 2010;78(Suppl 1):154–166.
26 Arizumi T, Ueshima K, Takeda H, Osaki Y, Takita M, Inoue T, Kitai S, Yada N, Hagiwara S, Minami Y, Sakurai T, Nishida N, Kudo M: Comparison of systems for assessment of post-therapeutic response to sorafenib for hepatocellular carcinoma. J Gastroenterol 2014; epub ahead of print.

Liver Cancer

Liver Cancer 2014;3:417–427
DOI: 10.1159/000343860
Published online: August 8, 2014

2235-1795/14/0034-0417$39.50/0
www.karger.com/lic

Review

Alteration of Epigenetic Profile in Human Hepatocellular Carcinoma and Its Clinical Implications

Naoshi Nishida Masatoshi Kudo

Department of Gastroenterology and Hepatology, Kinki University Faculty of Medicine, Osaka, Japan

Key Words
DNA methylation · Etiology · Hepatocellular carcinoma · Transcription

Abstract
Hepatocellular carcinoma (HCC) is a common cancer worldwide and develops against a background of chronic liver damage. A variety of HCC-related genes are known to be altered by genetic and epigenetic mechanisms. Therefore, information regarding alteration of the genetic and epigenetic profiles in HCC is essential for understanding the biology of this type of tumor. Methylation at CpG sites in gene promoters is known to affect the transcription of the corresponding genes. Abnormal regional hypermethylation is observed in the 5′ region of several tumor suppressor genes (TSGs) in HCC, and this hypermethylation may promote carcinogenesis through the transcriptional inactivation of downstream TSGs. The DNA damage induced by oxidation is a trigger of abnormal DNA methylation and inactivation of TSGs through recruitment of the polycomb repressive complex to the promoter sequence. Thus, oxidative stress may be responsible for the emergence of HCC from chronic hepatitis and liver cirrhosis through the epigenetic alteration of TSGs. There have been several attempts to apply epigenetic information to the diagnosis and treatment of HCC. The predictive value of selected methylation events on survival in HCC patients has been reported, and the methylation profile of background liver could be associated with recurrence-free survival of HCC patients who have undergone hepatectomy. Another study detected methylated DNA from HCC cells in serum, and the circulating tumor DNA was regarded as a potential tumor marker. In addition, several trials of HCC therapy have targeted the epigenetic machinery and were based upon comprehensive analyses of DNA methylation of this type of tumor. Here, we present an overview of research regarding DNA methylation status in human HCC and describe the clinical application of epigenetic information to HCC.

Naoshi Nishida, MD, PhD

Department of Gastroenterology and Hepatology,
Kinki University Faculty of Medicine
337-2 Ohno-higashi, Osaka-sayama, Osaka 589-8511 (Japan)
Tel. +81 72 366 0221, E-Mail naoshi@med.kindai.ac.jp

KARGER

Introduction

The methylation status at CpG sites in gene promoters, which are generally located within CpG islands, is closely associated with transcription of the corresponding genes. In cancerous tissues, abnormal regional hypermethylation observed in the 5′ region of several tumor suppressor genes (TSGs) is thought to promote carcinogenesis through the transcriptional inactivation of downstream TSGs. On the other hand, global DNA hypomethylation is another characteristic of cancer and is thought to induce activation of transposons, oncogenes, and chromosomal alterations, thereby contributing to carcinogenesis [1, 2].

In human hepatocellular carcinoma (HCC), a variety of TSGs have shown abnormal hypermethylation in their promoter regions and down-regulation of their transcripts, suggesting the potential role of inactivation of these TSGs in hepatocarcinogenesis [3]. A relationship between the extent of abnormal chromosomal regions and the degree of DNA hypomethylation at repetitive DNA sequences has also been reported. This evidence supports the idea that global DNA hypomethylation could induce chromosomal instability and contribute to hepatocarcinogenesis [4]. Results from another study involving human HCC samples revealed an association between down-regulation of microRNA (miR) and abnormal methylation of the host gene [5]. This review gives a synopsis of comprehensive analyses of DNA methylation in human HCC and further focuses on the clinical application of epigenetic information, such as alteration of the histone code or DNA methylations in HCC.

Origin of Epigenetic Alteration in Human HCC

Although the methylation levels in TSG promoters are much higher in HCC than in non-cancerous liver, abnormal methylation has also been observed in the promoters of TSGs in non-cancerous liver of HCC patients. Additionally, several studies have confirmed that the methylation levels of non-cancerous liver show a progression from chronic hepatitis to liver cirrhosis, in parallel with the increase in risk for the development of HCC. Viral infection, chronic inflammation, and oxidative stress can induce abnormal DNA methylation in affected hepatocytes. Thus, chronic hepatitis and liver cirrhosis may be the background conditions that lead to HCC emergence via abnormal methylation patterns that result in transcriptional inactivation of TSGs.

Several studies have reported a mechanistic link between epigenetic instability and the oxidative stress induced by inflammation. HCC cells are known to frequently carry abnormally methylated *E-cadherin* genes. Lim et al. reported that reactive oxygen species (ROS) could induce the expression of Snail, a repressive transcription factor of E-cadherin, through activation of the PI3K-Akt pathway and induce hypermethylation of the *E-cadherin* promoter by recruiting histone deacetylase 1 (HDAC1) and DNA methyltransferase 1 (DNMT1) [6]. They also showed a correlation between ROS induction, E-cadherin down-regulation, Snail up-regulation, and the *E-cadherin* promoter methylation in HCC tissues.

O'Hagan et al. demonstrated that inducing cellular oxidative stress in a colorectal cancer cell line using hydrogen peroxide (H_2O_2) treatment recruits DNMT1 to damaged chromatin and causes relocalization of DNMTs and other members of the polycomb repressive complex 4 from non-GC-rich to GC-rich areas [7]. They also showed an increase in repressive histone modification, such as the trimethylation of lysine 27 of histone H3 (H3K27), and a decrease in active histone modification, such as the trimethylation of H3K4 and the acetylation of H4K16, on DNA sites showing oxidative damage. Using an HCC cell line and fetal liver cells, we also demonstrated that H_2O_2 treatment increases oxidative DNA damage on the promoters of multiple cancer-related genes that are known to show abnormal DNA methylation in

many types of cancers. We confirmed that H_2O_2 treatment alters histone modifications on these promoters from active to repressive patterns predominantly at damaged DNA sites [8].

Furthermore, using mice with humanized livers, Okamoto et al. reported that hepatitis B virus (HBV) or hepatitis C virus (HCV) infection could induce genome-wide, time-dependent changes in DNA methylation. Inhibition of natural killer cells or administration of neutralizing antibody of interferon-γ could inhibit methylation changes in the infected mice [9]. These results strongly support the idea that chronic inflammation and viral infection can cause a disturbance in DNA methylation status through the immune response as well as by the induction of ROS.

Increasing evidence suggests that non-alcoholic fatty liver disease (NAFLD) may be a risk factor for the emergence of HCC, and oxidative stress is believed to be a causal factor in NAFLD progression. From this observation, more methylation changes are likely to accumulate in the liver of patients with advanced NAFLD than in those with mild NAFLD. A recent report described many differently methylated CpGs between liver samples from patients with advanced and mild NAFLD, suggesting that epigenetic alteration also plays a role in NAFLD-related HCC emergence [10]. In that study, methylation levels were compared between mild and advanced NAFLD for more than 450,000 CpG sites, and about 70,000 CpG sites revealed methylation differences. Methylation correlated with gene transcript levels for 7% of differentially methylated CpG sites, indicating that these methylations affect expression of the corresponding genes. Tissue repair genes were hypomethylated and overexpressed, whereas genes in certain metabolic pathways were hypermethylated and underexpressed in advanced NAFLD [10].

Methylation Events Drive Hepatocarcinogenesis

Alteration of DNA methylation takes place in various promoters, gene bodies, intragenic regions, and repetitive DNA sequences. However, the importance of individual methylation changes to carcinogenesis is mostly unknown. Gao et al. determined and classified the pattern of methylation progression in 6,458 CpG sites in normal liver, non-cancerous liver of HCC patients, and HCC tissues. Some methylation events were observed in HCC tissues but were not found in non-cancerous liver and normal liver [11], suggesting the importance of this type of methylation in hepatocarcinogenesis. To determine the methylation events that might contribute to the emergence of HCC, we analyzed the methylation profiles of early HCC (eHCC), which is defined as HCC with hypovascular tumors < 2 cm, and compared them with those of non-cancerous liver and progressive HCC.

We also successfully classified methylation events into three patterns: methylation events showing prominent differences between non-cancerous liver and eHCC, methylation events showing gradual increase according to tumor progression, and methylation that could be detected in advanced tumors only [12]. It is noteworthy that the elevated levels of methylation detected in eHCC were also observed in non-cancerous liver, although the levels were much lower than those in HCC tissue [13]. Interestingly, the number of methylated TSGs in livers infected with chronic hepatitis C was significantly associated with the time taken for HCC to occur in patients with no history of HCC [12].

Therefore, we concluded that these methylation events might act as a driver that could accelerate hepatocarcinogenesis. On the other hand, although a number of methylation events were observed in advanced HCC, the majority of them were quantitatively low level and might be “passive” methylation events that emerge as a consequence of carcinogenesis, rather than being the drivers of carcinogenesis. In addition, we observed methylation events in normal

livers among the elderly [13]. It is conceivable that ROS induced by normal metabolic processes might cause abnormal DNA methylation in hepatocytes in an age-dependent manner, thereby promoting HCC emergence in livers without severe fibrosis. Recently, HCC has been observed in livers without advanced fibrosis, especially in elderly patients. This evidence also supports the idea that methylation events that are responsible for hepatocarcinogenesis exist in normal livers among the elderly as well as in livers infected with chronic hepatitis.

Differently Methylated Regions between HCC and Background Liver

As described above, in normal cells, the cytosine of CpG sites within TSG promoters and CpG-rich regions are generally unmethylated, whereas in other DNA regions, such as repetitive DNA sequences, these sites are densely methylated. However, TSG promoters showed regional hypermethylation in cancer cells. Irizarry et al. showed that, in colon cancer, most cancer related-alterations of DNA methylation did not take place in CpG islands, but in sequences up to 2 kb away; such regions were termed “CpG island shores” [14]. It was also reported that regions showing different methylation patterns between cancer and normal epithelial cells [cancer-specific differentially methylated regions (C-DMRs)] showed considerable overlap with those showing different methylation patterns among different tissues [tissue-specific differentially methylated regions]. Therefore, it is possible that the majority of methylation alterations found in cancer occur at CpG sites where epigenetic changes take place during tissue differentiation, and that some epigenetic alterations found in cancer might cause stem cell-like phenotypes, such as pluripotency. On the other hand, Ammerpohl et al. reported that several genes that showed abnormal methylation in human HCC were the targets of polycomb repressive complex 2 in embryonic stem cells [15, 16]. Polycomb- and trithorax-group proteins are known to participate in the modulation of histones and the alteration of gene expression patterns during cell differentiation [1]. Given that repressive histone modulation is associated with methylation of the corresponding genes, some methylation events could induce undifferentiated phenotypes through the transcriptional inactivation of genes necessary for cell differentiation.

Methylation Profile in HCC

Several studies have reported comprehensive analyses of the DNA methylation profile of HCC (table 1). A recent study analyzed more than 450,000 CpG sites and showed the methylation profile of HCC throughout the whole genome. According to the report, 60.1% of the CpGs that had undergone hypermethylation in HCC were located in CpG islands, 21.6% were in CpG shores, and 3.6% were in CpG shelves, which is defined as the region just outside CpG shores [17]. In contrast, the majority of hypomethylated CpGs in HCC were located away from CpG islands. Another group also reported that hypermethylated CpGs were mainly distributed close to transcription start sites, and the majority of hypomethylated CpGs were observed within 3′ regions of genes and intragenic regions [18].

Additionally, although hypomethylated CpGs were observed more frequently than hypermethylated TSGs were, the C-DMRs of HCC were observed more frequently in hypermethylated than in hypomethylated regions [17]. Because regional alteration of methylation may affect gene transcription more strongly than alteration of individual CpG methylation does, DNA hypermethylation may play a role in HCC emergence predominantly through the transcriptional inactivation of TSGs; however, DNA hypomethylation may contribute to car-

Table 1. Summary of comprehensive analyses of DNA methylation in human HCC

Year	Methods (CpG sites analyzed)	Number of cases analyzed	Results	Reference
2008	MCAMs (6,458 CpG islands) Pyrosequence	38 cases of HCC	Methylation events were classified into 4 groups according to the progression of methylation from normal liver to HCC	Gao et al. [11]
2009	BAMCA	25 cases of HCC 26 of normal liver	Methylation profile of HCC was associated with overall and recurrence-free survival after hepatectomy	Arai et al.[19]
2010	GoldenGate methylation assay[a] (1,505 CpG sites)	38 cases of HCC	Methylation status of 10 CpGs predicts survival of HCC patients	Hernandez-Vargas et al.[24]
2011	BAMCA Pyrosequence (203 CpG sites)	34 cases of HCC 45 of normal liver	Methylation status of background liver was associated with survival in patients who underwent liver resection	Nagashio et al.[25]
2011	HM27 BeadChip (27,578 CpG sites) COBRA (17 CpG sites)	13 cases of HCC	Methylation was analyzed in HCC cells isolated from HBV-related HCC tissues and 7 potential TSGs were identified	Tao et al.,[20]
2012	COBRA (27 genes or CpG sites)	177 cases of HCC 128 cases of hepatitis C	Methylation of 8 TSGs was identified as driver alterations for HCC through the analysis of early HCC and chronic hepatitis C without any history of HCC	Nishida et al.[12]
2012	HM27 BeadChip (27,578 CpGs) Pyrosequence (24 CpG sites)	62 cases of HCC	Five methylated genes were identified from the serum, which could constitute a potential tumor marker of HCC	Shen et al.[26]
2012	HM27 BeadChip (27,578 CpG sites)	62 cases of HCC	Several miRs showing abnormal methylation and their host genes were identified	Shen et al.[5]

Liver Cancer 2014;3:417–427
DOI: 10.1159/000343860
Published online: August 8, 2014

Year	Methods (CpG sites analyzed)	Number of cases analyzed	Results	Reference
2012	MeDIP-microarray (27,800 CpG islands)	162 cases of HCC	Eleven potential TSGs were reported through the MeDIP-microarray and pharmacological unmasking analyses. Functional analyses of MZB1 were performed	Matsumura et al.[22]
2012	HM27 BeadChip (27,578 CpG sites)	12 cases of HCC, 15 cases of liver cirrhosis	Methylation differences among HCC, liver cirrhosis, and normal liver were reported. In HCC, many methylated genes were identified as a target of PRC2 in embryonic stem cells	Ammerpohl et al.[15]
2012	HM27 BeadChip (27,578 CpG sites)	63 cases of HCC	Methylation, chromosomal alteration, and epigenetically silenced genes were analyzed comprehensively using BeadChip, array CGH, and expression arrays accompanied by pharmacological unmasking	Neumann et al.[16]
2013	HM450 BeadChip (485,577 CpG sites)	66 cases of HCC	Genome-wide analyses of hypermethylated and hypomethylated regions in HCC using HM450 BeadChip	Shen et al.[17]
2013	HM450 BeadChip (485,577 CpG sites)	45 cases of NAFLD	Methylation differences between mild and advanced NAFLD were reported	Murphy et al.[10]
2013	HM27 BeadChip (27,578 CpG sites)	71 cases of HCV-related HCC	Thirteen potential TSGs were reported using comprehensive methylation and expression analyses accompanied by pharmacological unmasking methods	Revill K et al.[23]
2013	HM450 BeadChip (485,577 CpG sites)	27 cases of HCC	Genome-wide analyses of hypermethylated and hypomethylated regions in HCC using HM450 BeadChip	Song et al.[18]

a=Illumina GoldenGate methylation assay using BeadArray technology. MCAMs=methylated CpG island amplification microarrays; BAMCA=bacterial artificial chromosome array-based methylated CpG island amplification; HM27=Illumina Bead Array, HumanMethylation27 BeadChip; CGH=comparative genomic hybridization; COBRA=combined bisulfite restriction analysis; MeDIP-microarray=methylated DNA immunoprecipitation-microarray analysis; HM450=Illumina Bead Array, HumanMethylation450 BeadChip.

Liver Cancer
Liver Cancer 2014;3:417–427
DOI: 10.1159/000343860
Published online: August 8, 2014

cinogenesis by additional mechanisms, such as induction of chromosomal instability. We also reported that the global DNA hypomethylation level was closely associated with the extent of the altered chromosomal region, and this association was independent of the tumor stage [4].

DNA Methylation and Etiology of HCC

Results from a previous study identified several methylation events that were associated with the etiology of HCC and background liver status: 75 CpGs showed differences in methylation patterns between livers of males and females, methylation at 228 CpGs was associated with HCV infection, and methylation at 17,207 CpGs showed different levels between cirrhotic and non-cirrhotic livers [17]. Among the 228 CpGs associated with HCV infection, methylation events at 56 CpGs also showed association with the presence of liver cirrhosis. The considerable overlap of HCV-associated and cirrhosis-associated methylation events suggested that HCC may be more commonly observed in livers that are infected with HCV and are cirrhotic. Additionally, methylation of TSG promoters was more prevalent in liver cirrhosis than in chronic hepatitis [11], and the methylation status of TSG promoters in background liver reflected the methylation profile of matched HCC tissues [19]. For example, HCV-related HCC, which frequently arises from cirrhotic liver, is known to carry many methylated TSGs, and methylation of TSG promoters is more prominent in HCV-positive than in HCV-negative liver tissues [13]. Therefore, it is possible that the duration of inflammation is related to the progression of liver fibrosis and to TSG methylation, which is more common in chronic hepatitis C.

Other studies analyzed the alteration of cancer-related pathways that might be affected by methylation-associated inactivation of TSGs. Shen et al. classified genes showing abnormal methylation and reported several pathways that involved genes showing increased or decreased methylation, such as G-protein, endothelin, PI3-K, interleukin, inflammatory cytokines, and insulin/growth factor signaling pathways [5]. Tao et al. analyzed DNA methylation in single isolated HCC cells, thereby eliminating the noise caused by the methylation of non-parenchymal cells, and reported that DNA methylation could lead to abnormal cellular function in gap junctions, calcium signaling, cell adhesion, and apoptosis [20]. However, because a variety of genes showed abnormal methylation in HCC, it was difficult to evaluate which methylation events might be responsible for carcinogenesis.

Newly Discovered TSGs Showed Abnormal Methylation and Transcriptional Inactivation

As described above, it is sometimes difficult to tell “driver” methylation events for HCC from “passive” methylation events that are merely consequences of carcinogenesis. Therefore, the effects of each methylation event need to be confirmed. A recent study isolated HBV-related HCC cells from cancerous tissues and performed comprehensive methylation analyses. Seven new genes were identified with abnormal methylation in HCC: *WNK2*, *EMILIN2*, *TRIM58*, *GRASP*, *TM6SF1*, *HIST1H4F*, and *TLX3* [20]. After treatment of these cancer cells with DNMT inhibitors, transcriptional reactivation was induced in these genes, suggesting that they were inactivated in HCC as a result of abnormal methylation. Gao et al. identified seven hypermethylated genes in HCC: *miR-219*, *MMP-14*, *RASSF1A*, *TBX4*, *GNA14*, *CDKN2A*, and *CCNA1*. They also confirmed re-expression by a pharmacological unmasking method in which an HCC cell line was treated with DNMT inhibitor 5-aza-deoxycytosine [11].

Neumann et al. conducted a study that involved the combination of comprehensive methylation and expression analyses before and after pharmacological unmasking. They determined the comprehensive methylation profile, chromosomal status, and epigenetically silenced genes of human HCC using HumanMethylation450 BeadArray (Illumina), array comparative genomic hybridization, and pharmacological unmasking expression array analysis. They reported three candidate TSGs (*PER3*, *PROZ*, and *IGFALS*) that showed abnormal methylation in HCC, loss of corresponding chromosomal regions, and re-expression after pharmacological unmasking [16]. Among these candidate TSGs, the functions of PER3 and IGFALS have already been reported, and they were shown to be potential TSGs of HCC [21]. Matsumura et al. also performed CpG island microarray analysis accompanied with pharmacological unmasking and reported *MZB1* as a new TSG of HCC [22]; the down-regulation of MZB1 was reportedly associated with survival of HCC patients. Revill et al. performed promoter methylation profiles using HumanMethylation27 BeadChip and expression array analysis combined with pharmacological unmasking and found 13 candidate TSGs [23]. That study showed that transfection of SMPD3 and NEFH led to growth inhibition in HCC cell lines, and knockdown of these genes by small interfering RNA induced tumor formation and invasiveness in nude mice, indicating that these were potential TSGs. The expression of SMPD3 was reportedly associated with recurrence-free survival after curative resection of HCC [23].

The transcription of non-coding RNA, such as miR and long non-coding RNA, is also known to be regulated by DNA methylation. The role of miR in carcinogenesis is particularly well recognized. Coding regions of miR are generally located within the intron of host genes, and abnormal methylation of host genes leads to transcriptional inactivation of miR. Several DNA methylations are reportedly related to the down-regulation of the corresponding miR. Recently, comprehensive methylation analyses identified hypermethylation of miR host genes, and the role of inactivation of each miR on hepatocarcinogenesis was analyzed [5]. The abnormal methylation of host gene HOXB4 was shown to induce activation of the NF-κB signaling pathway through transcriptional inactivation of miR-10a [5].

Epigenetic Information and Treatment of HCC

Because DNA methylation affects the phenotype mainly through expression of the corresponding genes, methylation profiles could reflect the biological characteristics of HCC if "passive methylation" could be eliminated appropriately. Several reports have shown the predictive value of selected methylation events on survival [19, 24]. The methylation profile of background liver may also be associated with the recurrence-free survival of HCC patients who undergo hepatectomy [25]. We also reported a prominent relationship between the number of methylated TSGs and the time to HCC occurrence by analyzing chronic hepatitis C patients without prior history of HCC [12]. Therefore, DNA methylation is crucial for HCC emergence and may be observed at high levels in livers infected with chronic hepatitis that have a high risk of hepatocarcinogenesis. Another study reported the presence of methylated DNA from HCC cells in serum and described the circulating tumor DNA as a potential tumor marker [26].

Recent HCC therapy trials have targeted the epigenetic machinery based on the comprehensive analyses of DNA methylation profiles of this type of tumor. Several novel molecular-targeted drugs have been developed using specific cancer mutation profiles [27]. However, the mutation profile of HCC is heterogeneous [28], and the frequencies of mutations in specific genes are relatively low. Therefore, it might be difficult to target individually altered genes for HCC therapy [3, 29].

On the other hand, a variety of TSGs showed abnormal DNA methylation in HCC [3] and altered epigenetic codes, including abnormal DNA methylation, could be reversed by using DNMT or HDAC inhibitors. For example, DNMT inhibitors induce the expression of inactivated TSGs through removal of promoter methylation, resulting in enhanced antitumor action. Two examples of this type of drug, 5-azacytidine and 5-aza-2'-deoxycytidine (decitabine), have already been approved for treatment of myelodysplastic syndrome and acute myelocytic leukemia [30, 31]. However, DNMT inhibitors have proven insufficient for the treatment of solid tumors in contrast to their encouraging activity against hematological malignancies [32]. Several kinds of cancers exhibit overexpression of HDACs, and transcriptional inactivation of growth-inhibitory and apoptosis-related genes have been observed through the abnormal deacetylation of histone tails. Several clinical trials involving the use of HDAC inhibitors, such as vorinostat for treatment of cutaneous T cell lymphoma, are currently ongoing [33].

Epigenetic therapy that modulates the epigenetic machinery could induce the alteration of cancer phenotypes through the rewriting of "abnormal" epigenetic codes; this would represent a distinctive type of therapy that is very different from conventional anti-cancer therapy. For example, cancer cells showing stem cell-like phenotypes are often resistant to conventional chemotherapy as well as to other molecular targeting agents [34]. However, rewriting the altered epigenetic code might induce differentiation in cancer cells, which could induce sensitivity to several types of chemotherapy. Additionally, because epigenetic therapy should be effective even after administration of the active agent has been discontinued, it could be effective in combination with other chemotherapeutic agents, either by administration at the beginning of, or before, the other chemotherapy. So far, no epigenetic therapy has proven effective against human HCC, although a recent report suggested the effectiveness of HDAC inhibitor panobinostat in a mouse xenograft model of HCC in combination with sorafenib [35]. Overexpression of HDAC has been reported in HCC [36]; thus, modulation of the epigenetic machinery should prove a promising approach for treating this type of malignancy.

Conclusion

Understanding the alteration of genetic and epigenetic codes is essential to predict the biological behavior and effectiveness of cancer therapy, because both codes represent important bioinformation regarding cancer [2]. The genetic code determines protein structure and quality, whereas the epigenetic code determines the quantity of protein produced. However, normal cells may have epigenetic codes that have been altered as a result of different physiological processes. As a result, it is more difficult to narrow down cancer-specific alterations in DNA methylation than those in gene mutation. Nonetheless, recent technological advancements such as BeadArray technology and next-generation sequencers allow us to perform comprehensive genome-wide analyses from a tiny amount of DNA. Therefore, it is possible to target a larger number of small, early stage lesions for comprehensive analyses [37]. It is anticipated that rapid technological progress and understanding of the alteration of the genetic and epigenetic codes will provide essential information for developing novel diagnostic approaches and therapies for HCC in the near feature.

References

▶1 Baylin SB, Jones PA: A decade of exploring the cancer epigenome – biological and translational implications. Nat Rev Cancer 2011;11:726–734.
▶2 You JS, Jones PA: Cancer genetics and epigenetics: two sides of the same coin? Cancer Cell 2012;22:9–20.

3 Nishida N, Goel A: Genetic and epigenetic signatures in human hepatocellular carcinoma: a systematic review. Curr Genomics 2011;12:130–137.
4 Nishida N, Kudo M, Nishimura T, Arizumi T, Takita M, Kitai S, Yada N, Hagiwara S, Inoue T, Minami Y, Ueshima K, Sakurai T, Yokomichi N, Nagasaka T, Goel A: Unique association between global DNA hypomethylation and chromosomal alterations in human hepatocellular carcinoma. PLoS ONE 2013;8:e72312.
5 Shen J, Wang S, Zhang YJ, Kappil MA, Chen Wu H, Kibriya MG, Wang Q, Jasmine F, Ahsan H, Lee PH, Yu MW, Chen CJ, Santella RM: Genome-wide aberrant DNA methylation of microRNA host genes in hepatocellular carcinoma. Epigenetics 2012;7:1230–1237.
6 Lim SO, Gu JM, Kim MS, Kim HS, Park YN, Park CK, Cho JW, Park YM, Jung G: Epigenetic changes induced by reactive oxygen species in hepatocellular carcinoma: methylation of the E-cadherin promoter. Gastroenterology 2008;135:2128–2140, e1–e8.
7 O'Hagan HM, Wang W, Sen S, Destefano Shields C, Lee SS, Zhang YW, Clements EG, Cai Y, Van Neste L, Easwaran H, Casero RA, Sears CL, Baylin SB: Oxidative damage targets complexes containing DNA methyltransferases, SIRT1, and polycomb members to promoter CpG Islands. Cancer Cell 2011;20:606–619.
8 Nishida N, Arizumi T, Takita M, Kitai S, Yada N, Hagiwara S, Inoue T, Minami Y, Ueshima K, Sakurai T, Kudo M: Reactive oxygen species induce epigenetic instability through the formation of 8-hydroxydeoxyguanosine in human hepatocarcinogenesis. Dig Dis 2013;31:459–466.
9 Okamoto Y, Shinjo K, Shimizu Y, Sano T, Yamao K, Gao W, Fujii M, Osada H, Sekido Y, Murakami S, Tanaka Y, Joh T, Sato S, Takahashi S, Wakita T, Zhu J, Issa JP, Kondo Y: Hepatitis virus infection affects DNA methylation in mice with humanized livers. Gastroenterology 2014;146:562–572.
10 Murphy SK, Yang H, Moylan CA, Pang H, Dellinger A, Abdelmalek MF, Garrett ME, Ashley-Koch A, Suzuki A, Tillmann HL, Hauser MA, Diehl AM: Relationship between methylome and transcriptome in patients with nonalcoholic fatty liver disease. Gastroenterology 2013;145:1076–1087.
11 Gao W, Kondo Y, Shen L, Shimizu Y, Sano T, Yamao K, Natsume A, Goto Y, Ito M, Murakami H, Osada H, Zhang J, Issa JP, Sekido Y: Variable DNA methylation patterns associated with progression of disease in hepatocellular carcinomas. Carcinogenesis 2008;29:1901–1910.
12 Nishida N, Kudo M, Nagasaka T, Ikai I, Goel A: Characteristic patterns of altered DNA methylation predict emergence of human hepatocellular carcinoma. Hepatology 2012;56:994–1003.
13 Nishida N, Nagasaka T, Nishimura T, Ikai I, Boland CR, Goel A: Aberrant methylation of multiple tumor suppressor genes in aging liver, chronic hepatitis, and hepatocellular carcinoma. Hepatology 2008;47:908–918.
14 Irizarry RA, Ladd-Acosta C, Wen B, Wu Z, Montano C, Onyango P, Cui H, Gabo K, Rongione M, Webster M, Ji H, Potash JB, Sabunciyan S, Feinberg AP: The human colon cancer methylome shows similar hypo- and hypermethylation at conserved tissue-specific CpG island shores. Nat Genet 2009;41:178–186.
15 Ammerpohl O, Pratschke J, Schafmayer C, Haake A, Faber W, von Kampen O, Brosch M, Sipos B, von Schönfels W, Balschun K, Röcken C, Arlt A, Schniewind B, Grauholm J, Kalthoff H, Neuhaus P, Stickel F, Schreiber S, Becker T, Siebert R, Hampe J: Distinct DNA methylation patterns in cirrhotic liver and hepatocellular carcinoma. Int J Cancer 2012;130:1319–1328.
16 Neumann O, Kesselmeier M, Geffers R, Pellegrino R, Radlwimmer B, Hoffmann K, Ehemann V, Schemmer P, Schirmacher P, Lorenzo Bermejo J, Longerich T: Methylome analysis and integrative profiling of human HCCs identify novel protumorigenic factors. Hepatology 2012;56:1817–1827.
17 Shen J, Wang S, Zhang YJ, Wu HC, Kibriya MG, Jasmine F, Ahsan H, Wu DP, Siegel AB, Remotti H, Santella RM: Exploring genome-wide DNA methylation profiles altered in hepatocellular carcinoma using Infinium HumanMethylation 450 BeadChips. Epigenetics 2013;8:34–43.
18 Song MA, Tiirikainen M, Kwee S, Okimoto G, Yu H, Wong LL: Elucidating the landscape of aberrant DNA methylation in hepatocellular carcinoma. PLoS ONE 2013;8:e55761.
19 Arai E, Ushijima S, Gotoh M, Ojima H, Kosuge T, Hosoda F, Shibata T, Kondo T, Yokoi S, Imoto I, Inazawa J, Hirohashi S, Kanai Y: Genome-wide DNA methylation profiles in liver tissue at the precancerous stage and in hepatocellular carcinoma. Int J Cancer 2009;125:2854–2862.
20 Tao R, Li J, Xin J, Wu J, Guo J, Zhang L, Jiang L, Zhang W, Yang Z, Li L: Methylation profile of single hepatocytes derived from hepatitis B virus-related hepatocellular carcinoma. PLoS ONE 2011;6:e19862.
21 Lin YM, Chang JH, Yeh KT, Yang MY, Liu TC, Lin SF, Su WW, Chang JG: Disturbance of circadian gene expression in hepatocellular carcinoma. Mol Carcinog 2008;47:925–933.
22 Matsumura S, Imoto I, Kozaki K, Matsui T, Muramatsu T, Furuta M, Tanaka S, Sakamoto M, Arii S, Inazawa J: Integrative array-based approach identifies MZB1 as a frequently methylated putative tumor suppressor in hepatocellular carcinoma. Clin Cancer Res 2012;18:3541–3551.
23 Revill K, Wang T, Lachenmayer A, Kojima K, Harrington A, Li J, Hoshida Y, Llovet JM, Powers S: Genome-wide methylation analysis and epigenetic unmasking identify tumor suppressor genes in hepatocellular carcinoma. Gastroenterology 2013;145:1424–1435, e1–e25.
24 Hernandez-Vargas H, Lambert MP, Le Calvez-Kelm F, Gouysse G, McKay-Chopin S, Tavtigian SV, Scoazec JY, Herceg Z: Hepatocellular carcinoma displays distinct DNA methylation signatures with potential as clinical predictors. PLoS ONE 2010;5:e9749.
25 Nagashio R, Arai E, Ojima H, Kosuge T, Kondo Y, Kanai Y: Carcinogenetic risk estimation based on quantification of DNA methylation levels in liver tissue at the precancerous stage. Int J Cancer 2011;129:1170–1179.
26 Shen J, Wang S, Zhang YJ, Kappil M, Wu HC, Kibriya MG, Wang Q, Jasmine F, Ahsan H, Lee PH, Yu MW, Chen CJ, Santella RM: Genome-wide DNA methylation profiles in hepatocellular carcinoma. Hepatology 2012;55:1799–1808.

27 Shen YC, Lin ZZ, Hsu CH, Hsu C, Shao YY, Cheng AL: Clinical trials in hepatocellular carcinoma: An update. Liver Cancer 2013;2:345–364.
28 Nishida N, Kudo M: Recent advancements in comprehensive genetic analyses for human hepatocellular carcinoma. Oncology 2013;84(Suppl 1):93–97.
29 Kudo M: Why does every hepatocellular carcinoma clinical trial using molecular targeted agents fail? Liver Cancer 2012;1:59–60.
30 Silverman LR, Demakos EP, Peterson BL, Kornblith AB, Holland JC, Odchimar-Reissig R, Stone RM, Nelson D, Powell BL, DeCastro CM, Ellerton J, Larson RA, Schiffer CA, Holland JF: Randomized controlled trial of azacitidine in patients with the myelodysplastic syndrome: a study of the cancer and leukemia group B. J Clin Oncol 2002;20:2429–2440.
31 Kantarjian H, Issa JP, Rosenfeld CS, Bennett JM, Albitar M, DiPersio J, Klimek V, Slack J, de Castro C, Ravandi F, Helmer R 3rd, Shen L, Nimer SD, Leavitt R, Raza A, Saba H: Decitabine improves patient outcomes in myelodysplastic syndromes: results of a phase III randomized study. Cancer 2006;106:1794–1803.
32 Goffin J, Eisenhauer E: DNA methyltransferase inhibitors – state of the art. Ann Oncol 2002;13:1699–1716.
33 Dokmanovic M, Clarke C, Marks PA: Histone deacetylase inhibitors: overview and perspectives. Mol Cancer Res 2007;5:981–989.
34 Snykers S, Henkens T, De Rop E, Vinken M, Fraczek J, De Kock J, De Prins E, Geerts A, Rogiers V, Vanhaecke T: Role of epigenetics in liver-specific gene transcription, hepatocyte differentiation and stem cell reprogrammation. J Hepatol 2009;51:187–211.
35 Lachenmayer A, Toffanin S, Cabellos L, Alsinet C, Hoshida Y, Villanueva A, Minguez B, Tsai HW, Ward SC, Thung S, Friedman SL, Llovet JM: Combination therapy for hepatocellular carcinoma: additive preclinical efficacy of the HDAC inhibitor panobinostat with sorafenib. J Hepatol 2012;56:1343–1350.
36 Wu LM, Yang Z, Zhou L, Zhang F, Xie HY, Feng XW, Wu J, Zheng SS: Identification of histone deacetylase 3 as a biomarker for tumor recurrence following liver transplantation in HBV-associated hepatocellular carcinoma. PLoS ONE 2010;5:e14460.
37 Song P, Gao J, Inagaki Y, Kokudo N, Hasegawa K, Sugawara Y, Tang W: Biomarkers: evaluation of screening for and early diagnosis of hepatocellular carcinoma in Japan and China. Liver Cancer 2013;2:31–39.

Liver Cancer

Liver Cancer 2014;3:458–468
DOI: 10.1159/000343875
Published online: October 13, 2014

2235-1795/14/0034-0458$39.50/0
www.karger.com/lic

Review

JSH Consensus-Based Clinical Practice Guidelines for the Management of Hepatocellular Carcinoma: 2014 Update by the Liver Cancer Study Group of Japan

Masatoshi Kudo[a] Osamu Matsui[b] Namiki Izumi[c] Hiroko Iijima[d] Masumi Kadoya[e] Yasuharu Imai[f] Takuji Okusaka[g] Shiro Miyayama[h] Kaoru Tsuchiya[c] Kazuomi Ueshima[a] Atsushi Hiraoka[i] Masafumi Ikeda[j] Sadahisa Ogasawara[k] Tatsuya Yamashita[l] Tetsuya Minami[m] Koichiro Yamakado[n] on behalf of the Liver Cancer Study Group of Japan

[a]Department of Gastroenterology and Hepatology, Kinki University School of Medicine, Osaka, [b]Department of Radiology, Kanazawa University Graduate School of Medical Science, Ishikawa, [c]Department of Gastroenterology and Hepatology, Musashino Red Cross Hospital, Tokyo, [d]Division of Hepatobiliary and Pancreatic Disease, Department of Internal Medicine, Hyogo College of Medicine, Hyogo, [e]Department of Radiology, Shinshu University School of Medicine, Nagano, [f]Department of Gastroenterology, Ikeda Municipal Hospital, Osaka, [g]Department of Hepatobiliary and Pancreatic Oncology, National Cancer Center Hospital, Tokyo, [h]Department of Diagnostic Radiology, Fukuiken Saiseikai Hospital, Fukui, [i]Department of Gastroenterology, Ehime Prefectural Central Hospital, Ehime, [j]Department of Hepatobiliary and Pancreatic Oncology, National Cancer Center Hospital East, Chiba, [k]Department of Gastroenterology and Nephrology, Graduate School of Medicine, Chiba University, Chiba, [l]Department of Gastroenterology and [m]Department of Radiology, Kanazawa University Hospital, Ishikawa, [n]Department of Interventional Radiology, Mie University School of Medicine, Mie, Japan

Key Words
Clinical practice guidelines · Definition of transarterial chemoembolization failure · Hepatocellular carcinoma· Japan Society of Hepatology · Liver Cancer Study Group of Japan

Abstract
The Clinical Practice Guidelines for the Management of Hepatocellular Carcinoma proposed by the Japan Society of Hepatology was updated in June 2014 at a consensus meeting of the

Masatoshi Kudo, MD, PhD
Department of Gastroenterology and Hepatology,
Kinki University School of Medicine
Ohno-Higashi, Osaka-Sayama, Osaka 589-8511 (Japan)
Tel. +81 72 366 0221, E-Mail m-kudo@med.kindai.ac.jp

KARGER

Liver Cancer

Liver Cancer 2014;3:458–468

DOI: 10.1159/000343875
Published online: October 13, 2014

Liver Cancer Study Group of Japan. Three important items have been updated: the surveillance and diagnostic algorithm, the treatment algorithm, and the definition of transarterial chemoembolization (TACE) failure/refractoriness. The most important update to the diagnostic algorithm is the inclusion of gadolinium-ethoxybenzyl-diethylenetriamine pentaacetic acid-enhanced magnetic resonance imaging as a first line surveillance/diagnostic tool. Another significant update concerns removal of the term "lipiodol" from the definition of TACE failure/refractoriness.

Introduction

Four years have passed since the 2010 version of the Consensus-Based Clinical Practice Guidelines proposed by the Japan Society of Hepatology (JSH) [1] was adopted, and recent efforts have been made to produce a revised, updated version. Most members of JSH who specialize in liver cancer also belong to the Liver Cancer Study Group of Japan (LCSGJ); consequently, a consensus meeting was held at the 50th Annual Meeting of the Liver Cancer Study Group of Japan (June 5–6, 2014, Kyoto) (Congress President: Prof. Masatoshi Kudo) to update these clinical practice guidelines as proposed by JSH. At the consensus meeting, members discussed revision of (1) the surveillance and diagnostic algorithm, (2) the treatment algorithm, and (3) the definition of transarterial chemoembolization (TACE) failure. Approximately 350 experts in the diagnosis and treatment of liver cancer participated in this consensus development session. Items that were approved by at least 67% of experts through a voting system were included in the final version of the consensus-based guidelines. The Surveillance and Diagnostic Algorithm, Treatment Algorithm, and Definition of TACE Failure sections of the consensus-based guidelines were subsequently presented at The 4th International Kyoto Liver Cancer Symposium (4th IKLS; June 7–8, 2014, Kyoto) (Congress President: Prof. Masatoshi Kudo), and more than two-thirds of participants at this international symposium agreed the 2014 update of the Clinical Practice Guidelines proposed by the JSH-LCSGJ. Thus, the new versions of the surveillance and diagnostic algorithm, the treatment algorithm, and the definition of TACE failure are also recognized internationally.

Surveillance and Diagnostic Algorithm

Major changes were made to this section of the guidelines compared to the 2010 version. Revisions were based on the surveillance and diagnostic algorithm created primarily by Prof. Osamu Matsui as part of a research project supported by the Japanese Ministry of Health, Labour and Welfare (Primary Investigator: Prof. Shigeki Arii) [2]. Various studies have verified the usefulness of gadolinium-ethoxybenzyl-diethylenetriamine pentaacetic acid (Gd-EOB-DTPA)-enhanced magnetic resonance imaging (Gd-EOB-DTPA-MRI) in the diagnosis of hepatocellular carcinoma (HCC) [2–89], although this method is not yet included in the guidelines of the American Association for the Study of Liver Diseases [90], the European Association for the Study of the Liver [91], or the Asian Pacific Association for the Study of the Liver [92] guidelines [93, 94]. Only the updated JSH-LCSGJ diagnostic algorithm includes Gd-EOB-DTPA-MRI as a first-line surveillance and diagnostic tool for HCC. While surveillance of patients at super-high risk for HCC (i.e., those with hepatitis B or C cirrhosis) and patients at high risk for HCC (i.e., those with chronic hepatitis B/C or cirrhosis of another etiology) is essentially performed using ultrasonography (US) or tumor markers

according to the JSH guideline [1, 95], it is recommended that super-high risk patients also undergo dynamic multidetector computed tomography (MDCT) or MRI every 6–12 months to pick up small HCC even when US shows no evidence of such a tumor [1, 95]. At institutions specializing in liver cancer in Japan, it is recommended that Gd-EOB-DTPA-MRI be used instead of dynamic MDCT even when no tumor is detected on US. If Gd-EOB-DTPA-MRI shows a hypervascular mass with venous washout, a definitive diagnosis of HCC can be made. If Gd-EOB-DTPA-MRI shows a hypervascular mass without venous washout, a diagnosis of HCC can be made if the mass shows hypointensity in the hepatobiliary phase of Gd-EOB-DTPA-MRI. Also, in this case, high-flow type hemangioma should be ruled out by using another modality because it can exhibit similar characteristics. If the mass is isointense or hyperintense in the hepatobiliary phase of Gd-EOB-DTPA-MRI, biopsy is necessary to confirm the diagnosis. Hypovascular masses on Gd-EOB-DTPA-MRI that are isointense or hyperintense in the hepatobiliary phase can enter the routine surveillance protocol. However, hypointense masses in the hepatobiliary phase have a high potential for malignant transformation [9, 11, 18, 22, 23, 37, 40, 41, 54, 55, 59, 86, 96–102], and therefore contrast-enhanced ultrasonography (CEUS*)* using Sonazoid (Sonazoid CEUS) is strongly recommended. HCC can be correctly diagnosed by Sonazoid CEUS if hypervascularity and/or a defect in the Kupffer phase [103] is observed. Even when a mass is hypovascular on CEUS and there is no defect in the Kupffer phase, hypointensity in the hepatobiliary phase of Gd-EOB-DTPA-MRI is highly suggestive of malignancy [7]. Accordingly, biopsy is recommended for small nodules of 1–1.5 cm or larger for differential diagnosis between early HCC [103] and a dysplastic nodule (DN). If a mass is diagnosed as a DN or a borderline lesion, intensive follow-up every 3 to 6 months with GD-EOB-DTPA-MRI (or dynamic MDCT) is recommended. The intensive follow-up is also recommended for small nodules of less than 1–1.5 cm (fig. 1).

Of course, institutions that cannot perform GD-EOB-DTPA-MRI every 6–12 months as the first-line modality may use dynamic MDCT as the first step of screening when no nodule is evident on US, but it is absolutely essential to perform GD-EOB-DTPA-MRI or Sonazoid CEUS when dynamic MDCT does not show hallmark of HCC (i.e., arterial enhancement with venous washout) in the mass detected by MDCT. This algorithm was approved by more than 90% of participants and is, therefore, now the new surveillance and diagnostic algorithm recommended by the JSH and LCSGJ (fig. 1).

Treatment Algorithm

No new treatments or molecular targeted agents have been developed for HCC since the 2010 JSH consensus-based treatment algorithm [1, 104] was adopted, so few changes were made to this section.

Decreased uptake in the Kupffer phase on CEUS was added to the third item of the annotations as an indicative finding in the diagnosis of early HCC [103]. In addition, although sorafenib is recommended for patients with minor portal vein invasion or portal invasion at the first portal branch (Vp1-3), the new algorithm reflects the consensus that it is not recommended for patients with portal invasion at the main portal branch (Vp4) due to the risk of hepatic failure. However, hepatic arterial infusion chemotherapy (HAIC) is still strongly recommended for patients with Vp4, and therefore recommendations regarding HAIC were left unchanged [105]. Moreover, because locoregional therapy for Child-Pugh C patients is now widely used and many studies have reported its survival benefits, it is now described as a “well accepted treatment” rather than an “experimental treatment” in the revised algorithm (fig. 2) [106–110].

Liver Cancer 2014;3:458–468
DOI: 10.1159/000343875
Published online: October 13, 2014

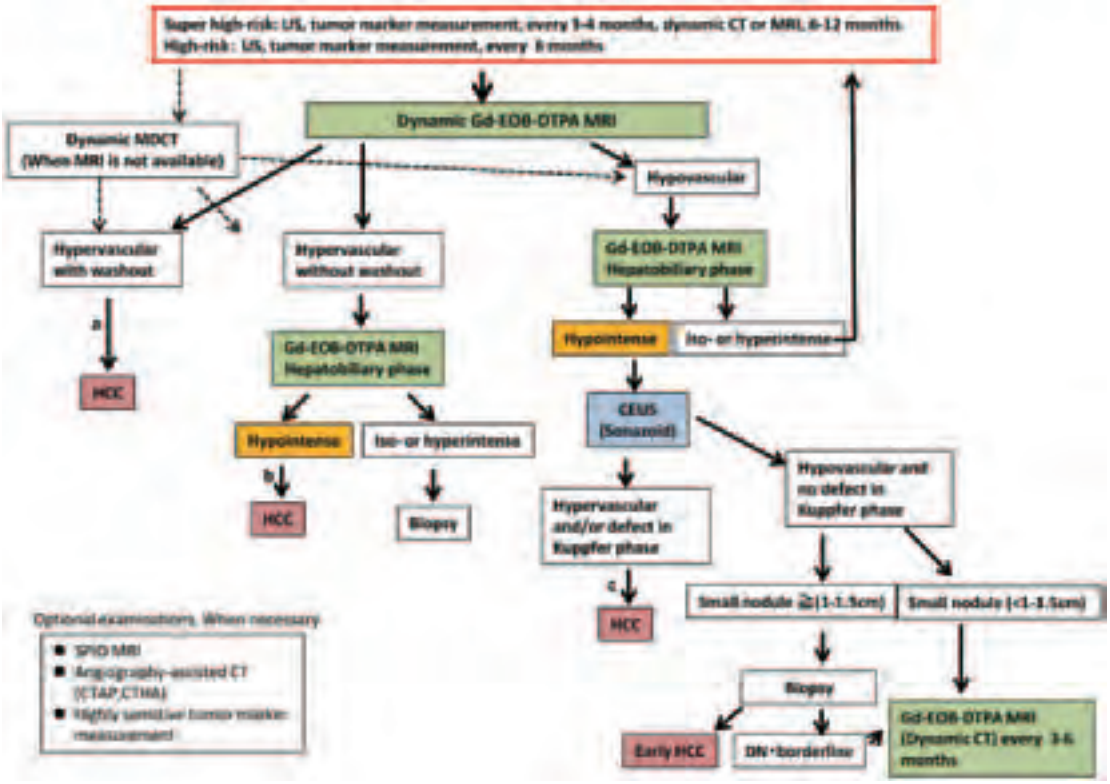

Fig. 1. Surveillance and Diagnostic Algorithm of HCC (Proposed by the Liver Cancer Study Group of Japan 2014). SPIO=superparamagnetic iron oxide; CTAP=computed tomographic arterial portography; CTHA=computed tomographic hepatic arteriography.
[a]Cavernous hemangioma may show hypointensity on equilibrium (transitional) phase of dynamic Gd-EOB-DTPA MRI (pseudo-washout). It should be excluded by other sequences of MRI and/or other imaging modalities. [b]Cavernous hemangioma usually shows hypointensity on hepatobiliary phase of Gd-EOB-DTPA MRI. It should be excluded by other sequences of MRI and/or other imaging modalities. [c]Biopsy may be considered for confirmation.

Definition of TACE Failure/Refractoriness

In the 2010 version of the JSH consensus-based treatment algorithm [1], TACE failure/refractoriness was defined assuming the use of superselective lipiodol TACE—which has been widely used worldwide and particularly in Japan—and areas with lipiodol deposition were considered to be necrotic. However, this concept is not well accepted internationally [111]. Furthermore, following the approval in Japan in February 2014 of emolic drug-eluting beads, an embolic material that does not use lipiodol, the phrase needed to be changed from "lipiodol deposition" to "necrotic lesion or viable lesion." Accordingly, the section was revised to define TACE failure as an ineffective response after two or more consecutive TACE procedures that is evident on response evaluation CT or MRI after 1–3 months, even after chemotherapeutic agents are changed and/or the feeding artery is reanalyzed. In addition, the appearance of more lesions in the liver than the number of lesions recorded at the previous TACE procedure (other than the nodule being treated) was added definition of TACE failure/refractoriness. Following discussion of the other issues concerning continuous elevation of tumor markers, vascular invasion, and extrahepatic spread, descriptions similar to those in the previous version were approved (table 1). The revision of these TACE failure definitions were approved by more than 85% of HCC experts.

Liver Cancer

Liver Cancer 2014;3:458–468
DOI: 10.1159/000343875
Published online: October 13, 2014

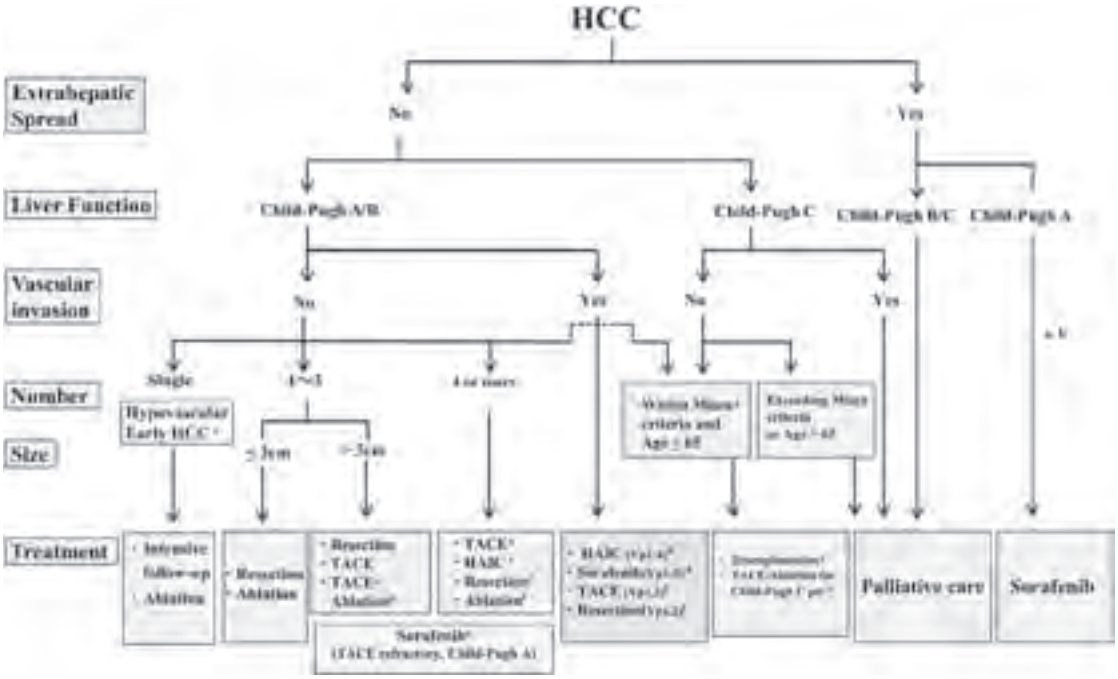

Fig. 2. JSH-LCSGJ Consensus-based Treatment Algorithm for Hepatocellular Carcinoma revised in 2014. [a]Treatment should be performed as if extrahepatic spread is negative when extrahepatic spread is not regarded as a prognostic factor. [b]Sorafenib is the first choice of treatment in this setting as a standard of care. [c]Intensive follow-up observation is recommended for hypovascular nodules by the Japanese Evidence-Based Clinical Practice Guidelines. However, local ablation therapy is frequently performed in the following cases: 1) when the nodule is diagnosed pathologically as early HCC, 2) when the nodules show decreased uptake on hepatobiliary phase Gd-EOB-DTPA-MRI, 3) when the nodules show decreased portal flow by CTAP or 4) decreased uptake is shown on Kupffer phase of Sonazoid enhanced US, since these nodules are known to frequently progress to the typical hypervascular HCC. [d]Even for HCC nodules exceeding 3 cm in diameter, combination therapy of TACE and ablation is frequently performed when resection is not indicated. [e]Transcatheter arterial chemoembolization (TACE) is the first choice of treatment in this setting. Hepatic arterial infusion chemotherapy (HAIC) using reservoir system is also recommended for TACE refractory patients. The regimen for this treatment is usually low-dose FP (5FU+CDDP) or 5FU infusion combined with systemic interferon therapy. Sorafenib is also a treatment of choice for TACE refractory patients with Child Pugh A liver function. [f]Resection is sometimes performed even when the number of nodules is greater than 4. Furthermore, ablation is sometimes performed in combination with TACE. [g]Milan criteria: Tumor size ≤ 3 cm and tumor number ≤ 3; or solitary tumor ≤ 5 cm. Even when liver function is good (Child-Pugh A/B), transplantation is sometimes considered for frequently recurring HCC patients. [h]Sorafenib and HAIC are recommended for HCC patients with Vp1,2 (minor portal vein invasion) or Vp3 (portal invasion at the 1st portal branch). Sorafenib is not recommended for HCC patients with Vp4 (portal invasion at the main portal branch), whereas HAIC is recommended for such patients with tumor thrombus in the main portal branch. [i]Resection and TACE is frequently performed when portal invasion is minor such as Vp1 (portal invasion at the 3rd or more peripheral portal branch) or Vp2 (portal invasion at the 2nd portal branch). [j]Even in Child-Pugh A/B patients, transplantation is sometimes performed for relatively younger patients with frequently or early recurring HCC after curative treatments. [k]Local ablation therapy or subsegmental TACE is performed even for Child-Pugh C patients (CP score 10 and 11) within Milan criteria when transplantation is not indicated. In the case, patients with no hepatic encephalopathy, no uncontrollable ascites, and a low bilirubin level (< 3.0mg/dl) are selected for treatment. Although these are well-accepted treatments in the routine clinical setting, there is no high-level evidence of its survival benefit in Child-Pugh C patients. A prospective study is necessary to clarify this issue.

Table 1. Definition of TACE Failure/Refractoriness (LCSGJ)

(1) Intrahepatic lesion
i. Two or more consecutive ineffective responses seen within the treated tumors (viable lesion >50%), even after changing the chemotherapeutic agents and/or reanalysis of feeding artery, on response evaluation CT/MRI after 1–3 months following adequately performed selective TACE
ii. Two or more consecutive progressions in the liver (including an increase in the number of tumors compared to that before the previous TACE procedure), even after changing the chemotherapeutic agents and/or reanalysis of feeding artery, on response evaluation CT/MRI after 1–3 months following adequately performed selective TACE
(2) Tumor marker
Continuous elevation of tumor markers right after TACE even though transient minor reduction is observed.
(3) Appearance of vascular invasion
(4) Appearance of extrahepatic spread

Conclusion

We report here the 2014 updated versions of the Surveillance and Diagnostic Algorithm, Treatment Algorithm, and Definition of TACE Failure/Refractoriness sections of the 2010 Consensus-Based Clinical Practice Guidelines proposed by JSH that were discussed and approved at the consensus meeting held at the 50th Annual Meeting of the Liver Cancer Study Group of Japan (June 5–6, 2014, Kyoto).

References

1 Kudo M, Izumi N, Kokudo N, Matsui O, Sakamoto M, Nakashima O, Kojiro M, Makuuchi M, HCC Expert Panel of Japan Society of Hepatology: Management of hepatocellular carcinoma in Japan: Consensus-Based Clinical Practice Guidelines proposed by the Japan Society of Hepatology (JSH) 2010 updated version. Dig Dis 2011;29:339–364.

2 Kudo M, Matsui O, Sakamoto M, Kitao A, Kim T, Ariizumi S, Ichikawa T, Kobayashi S, Imai Y, Izumi N, Fujinaga Y, Arii S: Role of gadolinium-ethoxybenzyl-diethylenetriamine pentaacetic acid-enhanced magnetic resonance imaging in the management of hepatocellular carcinoma: consensus at the Symposium of the 48th Annual Meeting of the Liver Cancer Study Group of Japan. Oncology 2013;84(Suppl 1):21–27.

3 Fujita N, Nishie A, Kubo Y, Asayama Y, Ushijima Y, Takayama Y, Moirta K, Shirabe K, Aishima S, Honda H: Hepatocellular carcinoma: clinical significance of signal heterogeneity in the hepatobiliary phase of gadoxetic acid-enhanced MR imaging. Eur Radiol 2014, Epub ahead of print.

4 Junqiang L, Yinzhong W, Li Z, Shunlin G, Xiaohui W, Yanan Z, Kehu Y: Gadoxetic acid disodium (Gd-EOBDTPA)-enhanced magnetic resonance imaging for the detection of hepatocellular carcinoma: a meta-analysis. J Magn Reson Imaging 2014;39:1079–1087.

5 Faletti R, Cassinis MC, Fonio P, Bergamasco L, Pavan LJ, Rapellino A, David E, Gandini G: Multiparametric Gd-EOB-DTPA magnetic resonance in diagnosis of HCC: dynamic study, hepatobiliary phase, and diffusion-weighted imaging compared to histology after orthotopic liver transplantation. Abdom Imaging 2014, Epub ahead of print.

6 Ueno A, Masugi Y, Yamazaki K, Komuta M, Effendi K, Tanami Y, Tsujikawa H, Tanimoto A, Okuda S, Itano O, Kitagawa Y, Kuribayashi S, Sakamoto M: OATP1B3 expression is strongly associated with Wnt/β-catenin signaling and represents the transporter of gadoxetic acid in hepatocellular carcinoma. J Hepatol 2014, Epub ahead of print.

7 Ichikawa T, Sano K, Morisaka H: Diagnosis of pathologically early HCC with EOB-MRI: experiences and current consensus. Liver Cancer 2014;3:97–107.

▶8 Chang WC, Chen RC, Chou CT, Lin CY, Yu CY, Liu CH, Chou JM, Hsu HH, Huang GS: Histological grade of hepatocellular carcinoma correlates with arterial enhancement on gadoxetic acid-enhanced and diffusion-weighted MR images. Abdom Imaging 2014, Epub ahead of print.
▶9 Matsuda M, Tsuda T, Yoshioka S, Murata S, Tanaka H, Hirooka M, Hiasa Y, Mochizuki T: Incidence for progression of hypervascular HCC in hypovascular hepatic nodules showing hyperintensity on gadoxetic acid-enhanced hepatobiliary phase in patients with chronic liver diseases. Jpn J Radiol 2014;32:405–413.
▶10 Shim JH, Han S, Shin YM, Lee YJ, Lee SG, Kim KM, Lim YS, Lee HC: Prognostic performance of preoperative gadoxetic acid-enhanced MRI in resectable hepatocellular carcinoma. J Magn Reson Imaging 2014, Epub ahead of print.
▶11 Jang KM, Kim SH, Kim YK, Choi D: Imaging features of subcentimeter hypointense nodules on gadoxetic acid-enhanced hepatobiliary phase MR imaging that progress to hypervascular hepatocellular carcinoma in patients with chronic liver disease. Acta Radiol 2014, Epub ahead of print.
▶12 Matsuda M, Ichikawa T, Amemiya H, et al: Preoperative gadoxetic acid-enhanced MRI and simultaneous treatment of early hepatocellular carcinoma prolonged recurrence-free survival of progressed hepatocellular carcinoma patients after hepatic resection. HPB Surg 2014;2014:641685, in press.
▶13 Yamashita T, Kitao A, Matsui O, Hayashi T, Nio K, Kondo M, Ohno N, Miyati T, Okada H, Yamashita T, Mizukoshi E, Honda M, Nakanuma Y, Takamura H, Ohta T, Nakamoto Y, Yamamoto M, Takayama T, Arii S, Wang XW, Kaneko S: Gd-EOB-DTPA-enhanced magnetic resonance imaging and alpha-fetoprotein predict prognosis of early-stage hepatocellular carcinoma. Hepatology 2014, Epub ahead of print.
▶14 Park VY, Choi JY, Chung YE, Kim H, Park MS, Lim JS, Kim KW, Kim MJ: Dynamic enhancement pattern of HCC smaller than 3 cm in diameter on gadoxetic acid-enhanced MRI: comparison with multiphasic MDCT. Liver Int 2014, Epub ahead of print.
▶15 Ishimaru H, Nakashima K, Sakugawa T, Sakamoto A, Matsuoka Y, Ashizawa K, Uetani M: Local recurrence after chemoembolization of hepatocellular carcinoma: uptake of gadoxetic acid as a new prognostic factor. AJR Am J Roentgenol 2014;202:744–751.
▶16 Yu MH, Kim JH, Yoon JH, Kim HC, Chung JW, Han JK, Choi BI: Small (≤1-cm) hepatocellular carcinoma: diagnostic performance and imaging features at gadoxetic acid-enhanced MR imaging. Radiology 2014;271:748–760.
▶17 Tada T, Kumada T, Toyoda H, Ito T, Sone Y, Okuda S, Ogawa S, Igura T, Imai Y: Diagnostic accuracy for macroscopic classification of nodular hepatocellular carcinoma: comparison of gadolinium ethoxybenzyl diethylenetriamine pentaacetic acid-enhanced magnetic resonance imaging and angiography-assisted computed tomography. J Gastroenterol 2014, Epub ahead of print.
▶18 Komatsu N, Motosugi U, Maekawa S, Shindo K, Sakamoto M, Sato M, Tatsumi A, Miura M, Amemiya F, Nakayama Y, Inoue T, Fukasawa M, Uetake T, Ohtaka M, Sato T, Asahina Y, Kurosaki M, Izumi N, Ichikawa T, Araki T, Enomoto N: Hepatocellular carcinoma risk assessment using gadoxetic acid-enhanced hepatocyte phase magnetic resonance imaging. Hepatol Res 2014, Epub ahead of print.
▶19 Kim KA, Kim MJ, Choi JY, Park MS, Lim JS, Chung YE, Kim KW: Detection of recurrent hepatocellular carcinoma on post-operative surveillance: comparison of MDCT and gadoxetic acid-enhanced MRI. Abdom Imaging 2014;39:291–299.
▶20 Phongkitkarun S, Limsamutpetch K, Tannaphai P, Jatchavala J: Added value of hepatobiliary phase gadoxetic acid-enhanced MRI for diagnosing hepatocellular carcinoma in high-risk patients. World J Gastroenterol 2013;19:8357–8365.
▶21 Zhao XT, Li WX, Chai WM, Chen KM: Detection of small hepatocellular carcinoma using gadoxetic acid-enhanced MRI: Is the addition of diffusion-weighted MRI at 3.0T beneficial? J Dig Dis 2014;15:137–145.
▶22 Iannicelli E, Di Pietropaolo M, Marignani M, Briani C, Federici GF, Delle Fave G, David V: Gadoxetic acid-enhanced MRI for hepatocellular carcinoma and hypointense nodule observed in the hepatobiliary phase. Radiol Med (Torino) 2014;119:367–376.
▶23 Inoue T, Hyodo T, Murakami T, Takayama Y, Nishie A, Higaki A, Korenaga K, Sakamoto A, Osaki Y, Aikata H, Chayama K, Suda T, Takano T, Miyoshi K, Koda M, Numata K, Tanaka H, Iijima H, Ochi H, Hirooka M, Imai Y, Kudo M: Hypovascular hepatic nodules showing hypointense on the hepatobiliary-phase image of Gd-EOB-DTPA-enhanced MRI to develop a hypervascular hepatocellular carcinoma: a nationwide retrospective study on their natural course and risk factors. Dig Dis 2013;31:472–479.
▶24 Park MJ, Kim YK, Park HJ, Hwang J, Lee WJ: Scirrhous hepatocellular carcinoma on gadoxetic acid-enhanced magnetic resonance imaging and diffusion-weighted imaging: emphasis on the differentiation of intrahepatic cholangiocarcinoma. J Comput Assist Tomogr 2013;37:872–881.
▶25 Kakihara D, Nishie A, Harada N, Shirabe K, Tajima T, Asayama Y, Ishigami K, Nakayama T, Takayama Y, Okamoto D, Fujita N, Kishimoto J, Honda H: Performance of gadoxetic acid-enhanced MRI for detecting hepatocellular carcinoma in recipients of living-related-liver-transplantation: Comparison with dynamic multidetector row computed tomography and angiography-assisted computed tomography. J Magn Reson Imaging 2013, Epub ahead of print.
▶26 Nishie A, Asayama Y, Ishigami K, Kakihara D, Nakayama T, Ushijima Y, Takayama Y, Shirabe K, Fujita N, Kubo Y, Hirakawa M, Honda H: Clinicopathological significance of the peritumoral decreased uptake area of gadolinium ethoxybenzyl diethylenetriamine pentaacetic acid in hepatocellular carcinoma. J Gastroenterol Hepatol 2014;29:561–567.
▶27 Hamada K, Saitoh S, Nishino N, Nakazawa T, Tobayashi K, Takano Y, Sakuma H: A liver tumor that progressed to hepatocellular carcinoma as observed on follow-up magnetic resonance images showing increased contrast medium uptake. Nippon Shokakibyo Gakkai Zasshi 2013;110:1976–1982.

28 Lim S, Kim YK, Park HJ, Lee WJ, Choi D, Park MJ: Infiltrative hepatocellular carcinoma on gadoxetic acid-enhanced and diffusion-weighted MRI at 3.0T. J Magn Reson Imaging 2014;39:1238–1245.
29 Cha DI, Lee MW, Kim YK, Kim SH, Park HJ, Rhim H, Lim HK: Assessing patients with hepatocellular carcinoma meeting the Milan criteria: Is liver 3 tesla MR with gadoxetic acid necessary in addition to liver CT? J Magn Reson Imaging 2014;39:842–852.
30 Liu X, Zou L, Liu F, Zhou Y, Song B: Gadoxetic acid disodium-enhanced magnetic resonance imaging for the detection of hepatocellular carcinoma: a meta-analysis. PLoS ONE 2013;8:e70896.
31 Wu LM, Xu JR, Gu HY, Hua J, Chen J, Zhu J, Zhang W, Hu J: Is liver-specific gadoxetic acid-enhanced magnetic resonance imaging a reliable tool for detection of hepatocellular carcinoma in patients with chronic liver disease? Dig Dis Sci 2013;58:3313–3325.
32 Kim JY, Lee SS, Byun JH, Kim SY, Park SH, Shin YM, Lee MG: Biologic factors affecting HCC conspicuity in hepatobiliary phase imaging with liver-specific contrast agents. AJR Am J Roentgenol 2013;201:322–331.
33 Baird AJ, Amos GJ, Saad NF, Benson MD: Retrospective audit to determine the diagnostic accuracy of Primovist-enhanced MRI in the detection of hepatocellular carcinoma in cirrhosis with explant histopathology correlation. J Med Imaging Radiat Oncol 2013;57:314–320.
34 Yamamoto A, Ito K, Tamada T, Higaki A, Kanki A, Sato T, Tanimoto D: Newly developed hypervascular hepatocellular carcinoma during follow-up periods in patients with chronic liver disease: observation in serial gadoxetic acid-enhanced MRI. AJR Am J Roentgenol 2013;200:1254–1260.
35 Park YS, Lee CH, Kim BH, Lee J, Choi JW, Kim KA, Ahn JH, Park CM: Using Gd-EOB-DTPA-enhanced 3-T MRI for the differentiation of infiltrative hepatocellular carcinoma and focal confluent fibrosis in liver cirrhosis. Magn Reson Imaging 2013;31:1137–1142.
36 Yoo SH, Choi JY, Jang JW, Bae SH, Yoon SK, Kim DG, Yoo YK, Rha SE, Lee YJ, Jung ES: Gd-EOB-DTPA-enhanced MRI is better than MDCT in decision making of curative treatment for hepatocellular carcinoma. Ann Surg Oncol 2013;20:2893–2900.
37 Ichikawa S, Ichikawa T, Motosugi U, Sano K, Morisaka H, Enomoto N, Matsuda M, Fujii H, Araki T: Presence of a hypovascular hepatic nodule showing hypointensity on hepatocyte-phase image is a risk factor for hypervascular hepatocellular carcinoma. J Magn Reson Imaging 2014;39:293–297.
38 Kim SH, Jeong WK, Kim Y, Kim MY, Kim J, Pyo JY, Oh YH: Hepatocellular carcinoma composed of two different histologic types: imaging features on gadoxetic acid-enhanced liver MRI. Clin Mol Hepatol 2013;19:92–96.
39 Choi JW, Lee JM, Kim SJ, Yoon JH, Baek JH, Han JK, Choi BI: Hepatocellular carcinoma: imaging patterns on gadoxetic acid-enhanced MR images and their value as an imaging biomarker. Radiology 2013;267:776–786.
40 Toyoda H, Kumada T, Tada T, Niinomi T, Ito T, Sone Y, Kaneoka Y, Maeda A: Non-hypervascular hypointense nodules detected by Gd-EOB-DTPA-enhanced MRI are a risk factor for recurrence of HCC after hepatectomy. J Hepatol 2013;58:1174–1180.
41 Hyodo T, Murakami T, Imai Y, Okada M, Hori M, Kagawa Y, Kogita S, Kumano S, Kudo M, Mochizuki T: Hypovascular nodules in patients with chronic liver disease: risk factors for development of hypervascular hepatocellular carcinoma. Radiology 2013;266:480–490.
42 Ooka Y, Kanai F, Okabe S, Ueda T, Shimofusa R, Ogasawara S, Chiba T, Sato Y, Yoshikawa M, Yokosuka O: Gadoxetic acid-enhanced MRI compared with CT during angiography in the diagnosis of hepatocellular carcinoma. Magn Reson Imaging 2013;31:748–754.
43 Granito A, Galassi M, Piscaglia F, Romanini L, Lucidi V, Renzulli M, Borghi A, Grazioli L, Golfieri R, Bolondi L: Impact of gadoxetic acid (Gd-EOB-DTPA)-enhanced magnetic resonance on the non-invasive diagnosis of small hepatocellular carcinoma: a prospective study. Aliment Pharmacol Ther 2013;37:355–363.
44 Kitao A, Matsui O, Yoneda N, Kozaka K, Kobayashi S, Koda W, Gabata T, Yamashita T, Kaneko S, Nakanuma Y, Kita R, Arii S: Hypervascular hepatocellular carcinoma: correlation between biologic features and signal intensity on gadoxetic acid-enhanced MR images. Radiology 2012;265:780–789.
45 Park MJ, Kim YK, Lee MH, Lee JH: Validation of diagnostic criteria using gadoxetic acid-enhanced and diffusion-weighted MR imaging for small hepatocellular carcinoma (<= 2.0 cm) in patients with hepatitis-induced liver cirrhosis. Acta Radiol 2013;54:127–136.
46 Jin YJ, Nah SY, Lee JW, Lee JI, Jeong S, Lee DH, Kim YS, Cho SG, Jeon YS: Utility of adding Primovist magnetic resonance imaging to analysis of hepatocellular carcinoma by liver dynamic computed tomography. Clin Gastroenterol Hepatol 2013;11:187–192.
47 An C, Park MS, Kim D, Kim YE, Chung WS, Rhee H, Kim MJ, Kim KW: Added value of subtraction imaging in detecting arterial enhancement in small (<3 cm) hepatic nodules on dynamic contrast-enhanced MRI in patients at high risk of hepatocellular carcinoma. Eur Radiol 2013;23:924–930.
48 Shinagawa Y, Sakamoto K, Fujimitsu R, Shimakura M, Kora S, Takano K, Yoshimitsu K: Pseudolesion of the liver on gadoxetate disodium-enhanced MR images obtained after transarterial chemoembolization for hepatocellular carcinoma: clinicoradiologic correlation. AJR Am J Roentgenol 2012;199:1010–1017.
49 Nakamura Y, Tashiro H, Nambu J, Ohdan H, Kakizawa H, Date S, Awai K: Detectability of hepatocellular carcinoma by gadoxetate disodium-enhanced hepatic MRI: tumor-by-tumor analysis in explant livers. J Magn Reson Imaging 2013;37:684–691.
50 Bashir MR, Gupta RT, Davenport MS, Allen BC, Jaffe TA, Ho LM, Boll DT, Merkle EM: Hepatocellular carcinoma in a North American population: does hepatobiliary MR imaging with Gd-EOB-DTPA improve sensitivity and confidence for diagnosis? J Magn Reson Imaging 2013;37:398–406.

51 Fujinaga Y, Kadoya M, Kozaka K, Shinmura R, Matsui O, Takayama T, Yamamoto M, Kokudo N, Kawasaki S, Arii S: Prediction of macroscopic findings of hepatocellular carcinoma on hepatobiliary phase of gadolinium-ethoxybenzyl-diethylenetriamine pentaacetic acid-enhanced magnetic resonance imaging: Correlation with pathology. Hepatol Res 2013;43:488–494.
52 Kim JY, Kim MJ, Kim KA, Jeong HT, Park YN: Hyperintense HCC on hepatobiliary phase images of gadoxetic acid-enhanced MRI: correlation with clinical and pathological features. Eur J Radiol 2012;81:3877–3882.
53 Kanata N, Yoshikawa T, Ohno Y, Kanda T, Uchida K, Izaki K, Fukumoto T, Ku Y, Itoh T, Kitajima K, Takahashi S, Sugimura K: HCC-to-liver contrast on arterial-dominant phase images of EOB-enhanced MRI: comparison with dynamic CT. Magn Reson Imaging 2013;31:17–22.
54 Kim YK, Lee WJ, Park MJ, Kim SH, Rhim H, Choi D: Hypovascular hypointense nodules on hepatobiliary phase gadoxetic acid-enhanced MR images in patients with cirrhosis: potential of DW imaging in predicting progression to hypervascular HCC. Radiology 2012;265:104–114.
55 Kobayashi S, Matsui O, Gabata T, Koda W, Minami T, Ryu Y, Kozaka K, Kitao A: Intranodular signal intensity analysis of hypovascular high-risk borderline lesions of HCC that illustrate multi-step hepatocarcinogenesis within the nodule on Gd-EOB-DTPA-enhanced MRI. Eur J Radiol 2012;81:3839–3845.
56 Kim AY, Kim YK, Lee MW, Park MJ, Hwang J, Lee MH, Lee JW: Detection of hepatocellular carcinoma in gadoxetic acid-enhanced MRI and diffusion-weighted MRI with respect to the severity of liver cirrhosis. Acta Radiol 2012;53:830–838.
57 Murakami T, Okada M, Hyodo T: CT versus MR imaging of hepatocellular carcinoma: toward improved treatment decisions. Magn Reson Med Sci 2012;11:75–81.
58 Kubota K, Tamura T, Aoyama N, Nogami M, Hamada N, Nishioka A, Ogawa Y: Correlation of liver parenchymal gadolinium-ethoxybenzyl diethylenetriaminepentaacetic acid enhancement and liver function in humans with hepatocellular carcinoma. Oncol Lett 2012;3:990–994.
59 Kobayashi S, Matsui O, Gabata T, Koda W, Minami T, Ryu Y, Kozaka K, Kitao A: Relationship between signal intensity on hepatobiliary phase of gadolinium ethoxybenzyl diethylenetriaminepentaacetic acid (Gd-EOB-DTPA)-enhanced MR imaging and prognosis of borderline lesions of hepatocellular carcinoma. Eur J Radiol 2012;81:3002–3009.
60 Lee JM, Yoon JH, Joo I, Woo HS: Recent advances in CT and MR imaging for evaluation of hepatocellular carcinoma. Liver Cancer 2012;1:22–40.
61 Rhee H, Kim MJ, Park MS, Kim KA: Differentiation of early hepatocellular carcinoma from benign hepatocellular nodules on gadoxetic acid-enhanced MRI. Br J Radiol 2012;85:e837–e844.
62 Inoue T, Kudo M, Komuta M, Hayaishi S, Ueda T, Takita M, Kitai S, Hatanaka K, Yada N, Hagiwara S, Chung H, Sakurai T, Ueshima K, Sakamoto M, Maenishi O, Hyodo T, Okada M, Kumano S, Murakami T: Assessment of Gd-EOB-DTPA-enhanced MRI for HCC and dysplastic nodules and comparison of detection sensitivity versus MDCT. J Gastroenterol 2012;47:1036–1047.
63 Sugimoto K, Moriyasu F, Saito K, Taira J, Saguchi T, Yoshimura N, Oshiro H, Imai Y, Shiraishi J: Comparison of Kupffer-phase Sonazoid-enhanced sonography and hepatobiliary-phase gadoxetic acid-enhanced magnetic resonance imaging of hepatocellular carcinoma and correlation with histologic grading. J Ultrasound Med 2012;31:529–538.
64 An C, Park MS, Jeon HM, Kim YE, Chung WS, Chung YE, Kim MJ, Kim KW: Prediction of the histopathological grade of hepatocellular carcinoma using qualitative diffusion-weighted, dynamic, and hepatobiliary phase MRI. Eur Radiol 2012;22:1701–1708.
65 Kim HY, Choi JY, Kim CW, Bae SH, Yoon SK, Lee YJ, Rha SE, You YK, Kim DG, Jung ES: Gadolinium ethoxybenzyl diethylenetriamine pentaacetic acid-enhanced magnetic resonance imaging predicts the histological grade of hepatocellular carcinoma only in patients with Child-Pugh class A cirrhosis. Liver Transpl 2012;18:850–857.
66 Watanabe H, Kanematsu M, Goshima S, Yoshida M, Kawada H, Kondo H, Moriyama N: Is gadoxetate disodium-enhanced MRI useful for detecting local recurrence of hepatocellular carcinoma after radiofrequency ablation therapy? AJR Am J Roentgenol 2012;198:589–595.
67 Kinner S, Umutlu L, Blex S, Maderwald S, Antoch G, Ertle J, Gerken G, Lauenstein TC: Diffusion weighted MR imaging in patients with HCC and liver cirrhosis after administration of different gadolinium contrast agents: is it still reliable? Eur J Radiol 2012;81:e625–e628.
68 Sugimoto K, Moriyasu F, Shiraishi J, Saito K, Taira J, Saguchi T, Imai Y: Assessment of arterial hypervascularity of hepatocellular carcinoma: comparison of contrast-enhanced US and gadoxetate disodium-enhanced MR imaging. Eur Radiol 2012;22:1205–1213.
69 Korkusuz H, Knau LL, Kromen W, Bihrer V, Keese D, Piiper A, Vogl TJ: Different signal intensity at Gd-EOB-DTPA compared with Gd-DTPA-enhanced MRI in hepatocellular carcinoma transgenic mouse model in delayed phase hepatobiliary imaging. J Magn Reson Imaging 2012;35:1397–1402.
70 Eso Y, Marusawa H, Osaki Y: Education and imaging. Hepatobiliary and Pancreatic: Detection of early hepatocellular carcinoma by enhanced magnetic resonance imaging. J Gastroenterol Hepatol 2012;27:416.
71 Alaboudy A, Inoue T, Hatanaka K, Chung H, Hyodo T, Kumano S, Murakami T, Moustafa EF, Kudo M: Usefulness of combination of imaging modalities in the diagnosis of hepatocellular carcinoma using Sonazoid®-enhanced ultrasound, gadolinium diethylene-triamine-pentaacetic acid-enhanced magnetic resonance imaging, and contrast-enhanced computed tomography. Oncology 2011;81(Suppl 1):66–72.
72 Hwang J, Kim SH, Lee MW, Lee JY: Small (≤ 2 cm) hepatocellular carcinoma in patients with chronic liver disease: comparison of gadoxetic acid-enhanced 3.0 T MRI and multiphasic 64-multirow detector CT. Br J Radiol 2012;85:e314–e322.

73 Nakamura Y, Toyota N, Date S, Oda S, Namimoto T, Yamashita Y, Beppu T, Awai K: Clinical significance of the transitional phase at gadoxetate disodium-enhanced hepatic MRI for the diagnosis of hepatocellular carcinoma: preliminary results. J Comput Assist Tomogr 2011;35:723–727.
74 Kim KA, Kim MJ, Jeon HM, Kim KS, Choi JS, Ahn SH, Cha SJ, Chung YE: Prediction of microvascular invasion of hepatocellular carcinoma: usefulness of peritumoral hypointensity seen on gadoxetate disodium-enhanced hepatobiliary phase images. J Magn Reson Imaging 2012;35:629–634.
75 Sano K, Ichikawa T, Motosugi U, Sou H, Muhi AM, Matsuda M, Nakano M, Sakamoto M, Nakazawa T, Asakawa M, Fujii H, Kitamura T, Enomoto N, Araki T: Imaging study of early hepatocellular carcinoma: usefulness of gadoxetic acid-enhanced MR imaging. Radiology 2011;261:834–844.
76 Chanyaputhipong J, Low SC, Chow PK. Gadoxetate acid-enhanced MR imaging for HCC: A review for clinicians. Int J Hepatol 2011;2011:489342.
77 Rhee H, Kim MJ, Park YN, Choi JS, Kim KS: Gadoxetic acid-enhanced MRI findings of early hepatocellular carcinoma as defined by new histologic criteria. J Magn Reson Imaging 2012;35:393–398.
78 Saito K, Moriyasu F, Sugimoto K, Nishio R, Saguchi T, Nagao T, Taira J, Akata S, Tokuuye K: Diagnostic efficacy of gadoxetic acid-enhanced MRI for hepatocellular carcinoma and dysplastic nodule. World J Gastroenterol 2011;17:3503–3509.
79 Baek CK, Choi JY, Kim KA, Park MS, Lim JS, Chung YE, Kim MJ, Kim KW: Hepatocellular carcinoma in patients with chronic liver disease: a comparison of gadoxetic acid-enhanced MRI and multiphasic MDCT. Clin Radiol 2012;67:148–156.
80 Chung J, Yu JS, Kim DJ, Chung JJ, Kim JH, Kim KW: Hypervascular hepatocellular carcinoma in the cirrhotic liver: diffusion-weighted imaging versus superparamagnetic iron oxide-enhanced MRI. Magn Reson Imaging 2011;29:1235–1243.
81 Choi JY, Kim MJ, Park YN, Lee JM, Yoo SK, Rha SY, Seok JY: Gadoxetate disodium-enhanced hepatobiliary phase MRI of hepatocellular carcinoma: correlation with histological characteristics. AJR Am J Roentgenol 2011;197:399–405.
82 Kim JE, Kim SH, Lee SJ, Rhim H: Hypervascular hepatocellular carcinoma 1 cm or smaller in patients with chronic liver disease: characterization with gadoxetic acid-enhanced MRI that includes diffusion-weighted imaging. AJR Am J Roentgenol 2011;196:W758-65.
83 Haradome H, Grazioli L, Tinti R, Morone M, Motosugi U, Sano K, Ichikawa T, Kwee TC, Colagrande S: Additional value of gadoxetic acid-DTPA-enhanced hepatobiliary phase MR imaging in the diagnosis of early-stage hepatocellular carcinoma: comparison with dynamic triple-phase multidetector CT imaging. J Magn Reson Imaging 2011;34:69–78.
84 Kim YK, Kim CS, Han YM, Yu HC, Choi D: Detection of small hepatocellular carcinoma: intraindividual comparison of gadoxetic acid-enhanced MRI at 3.0 and 1.5 T. Invest Radiol 2011;46:383–389.
85 Kagawa Y, Okada M, Kumano S, Katsube T, Imaoka I, Tanigawa N, Ishii K, Kudo M, Murakami T: Optimal scanning protocol of arterial dominant phase for hypervascular hepatocellular carcinoma with gadolinium-ethoxybenzyl-diethylenetriamine pentaacetic acid-enhanced MR. J Magn Reson Imaging 2011;33:864–872.
86 Kobayashi S, Matsui O, Gabata T, Koda W, Minami T, Ryu Y, Kawai K, Kozaka K: Gadolinium ethoxybenzyl diethylenetriamine pentaacetic acid-enhanced magnetic resonance imaging findings of borderline lesions at high risk for progression to hypervascular classic hepatocellular carcinoma. J Comput Assist Tomogr 2011;35:181–186.
87 Ariizumi S, Kitagawa K, Kotera Y, Takahashi Y, Katagiri S, Kuwatsuru R, Yamamoto M: A non-smooth tumor margin in the hepatobiliary phase of gadoxetic acid disodium (Gd-EOB-DTPA)-enhanced magnetic resonance imaging predicts microscopic portal vein invasion, intrahepatic metastasis, and early recurrence after hepatectomy in patients with hepatocellular carcinoma. J Hepatobiliary Pancreat Sci 2011;18:575–585.
88 Golfieri R, Renzulli M, Lucidi V, Corcioni B, Trevisani F, Bolondi L: Contribution of the hepatobiliary phase of Gd-EOB-DTPA-enhanced MRI to dynamic MRI in the detection of hypovascular small (≤ 2 cm) HCC in cirrhosis. Eur Radiol 2011;21:1233–1242.
89 Akai H, Kiryu S, Matsuda I, Satou J, Takao H, Tajima T, Watanabe Y, Imamura H, Kokudo N, Akahane M, Ohtomo K: Detection of hepatocellular carcinoma by Gd-EOB-DTPA-enhanced liver MRI: comparison with triple phase 64 detector row helical CT. Eur J Radiol 2011;80:310–315.
90 Bruix J, Sherman M American Association for the Study of Liver Diseases: Management of hepatocellular carcinoma: an update. Hepatology 2011;53:1020–1022.
91 European Association For The Study Of The Liver European Organisation For Research And Treatment Of Cancer: EASL-EORTC clinical practice guidelines: management of hepatocellular carcinoma. J Hepatol 2012;56:908–943.
92 Omata M, Lesmana LA, Tateishi R, Chen PJ, Lin SM, Yoshida H, Kudo M, Lee JM, Choi BI, Poon RT, Shiina S, Cheng AL, Jia JD, Obi S, Han KH, Jafri W, Chow P, Lim SG, Chawla YK, Budihusodo U, Gani RA, Lesmana CR, Putranto TA, Liaw YF, Sarin SK: Asian Pacific Association for the Study of the Liver consensus recommendations on hepatocellular carcinoma. Hepatol Int 2010;4:439–474.
93 Ricke J, Seidensticker M, Mohnike K: Noninvasive diagnosis of hepatocellular carcinoma in cirrhotic liver: current guidelines and future prospects for radiological imaging. Liver Cancer 2012;1:51–58.
94 Bota S, Piscaglia F, Marinelli S, Pecorelli A, Terzi E, Bolondi L: Comparison of international guidelines for noninvasive diagnosis of hepatocellular carcinoma. Liver Cancer 2012;1:190–200.
95 Kokudo N, Makuuchi M: Evidence-based clinical practice guidelines for hepatocellular carcinoma in Japan: the J-HCC guidelines. J Gastroenterol 2009;44(Suppl 19):119–121.

96 Joishi D, Ueno A, Tanimoto A, Okuda S, Masugi Y, Emoto K, Okuma K, Sakamoto M, Imai Y, Kuribayashi S: Natural course of hypovascular nodules detected on gadoxetic acid-enhanced MR imaging: presence of fat is a risk factor for hypervascularization. Magn Reson Med Sci 2013;12:281–287.
97 Motosugi U: Hypovascular hypointense nodules on hepatocyte phase gadoxetic acid-enhanced MR images: too early or too progressed to determine hypervascularity. Radiology 2013;267:317–318.
98 Takechi M, Tsuda T, Yoshioka S, Murata S, Tanaka H, Hirooka M, Mochizuki T: Risk of hypervascularization in small hypovascular hepatic nodules showing hypointense in the hepatobiliary phase of gadoxetic acid-enhanced MRI in patients with chronic liver disease. Jpn J Radiol 2012;30:743–751.
99 Takayama Y, Nishie A, Nakayama T, Asayama Y, Ishigami K, Kakihara D, Ushijima Y, Fujita N, Hirakawa M, Honda H: Hypovascular hepatic nodule showing hypointensity in the hepatobiliary phase of gadoxetic acid-enhanced MRI in patients with chronic liver disease: prediction of malignant transformation. Eur J Radiol 2012;81:3072–3078.
100 Akai H, Matsuda I, Kiryu S, Tajima T, Takao H, Watanabe Y, Imamura H, Kokudo N, Akahane M, Ohtomo K: Fate of hypointense lesions on Gd-EOB-DTPA-enhanced magnetic resonance imaging. Eur J Radiol 2012;81:2973–2977.
101 Motosugi U, Ichikawa T, Sano K, Sou H, Onohara K, Muhi A, Amemiya F, Enomoto N, Matsuda M, Fujii H, Araki T: Outcome of hypovascular hepatic nodules revealing no gadoxetic acid uptake in patients with chronic liver disease. J Magn Reson Imaging 2011;34:88–94.
102 Kumada T, Toyoda H, Tada T, Sone Y, Fujimori M, Ogawa S, Ishikawa T: Evolution of hypointense hepatocellular nodules observed only in the hepatobiliary phase of gadoxetate disodium-enhanced MRI. AJR Am J Roentgenol 2011;197:58–63.
103 Kudo M: Early hepatocellular carcinoma: definition and diagnosis. Liver Cancer 2013;2:69–72.
104 Arii S, Sata M, Sakamoto M, Shimada M, Kumada T, Shiina S, Yamashita T, Kokudo N, Tanaka M, Takayama T, Kudo M: Management of hepatocellular carcinoma: Report of Consensus Meeting in the 45th Annual Meeting of the Japan Society of Hepatology (2009). Hepatol Res 2010;40:667–685.
105 Kudo M: Treatment of advanced hepatocellular carcinoma with emphasis on hepatic arterial infusion chemotherapy and molecular targeted therapy. Liver Cancer 2012;1:62–70.
106 Kim YK, Kim CS, Chung GH, Han YM, Lee SY, Jin GY, Lee JM: Radiofrequency ablation of hepatocellular carcinoma in patients with decompensated cirrhosis: evaluation of therapeutic efficacy and safety. AJR Am J Roentgenol 2006;186(Suppl):S261–S268.
107 Kudo M, Osaki Y, Matsunaga T, Kasugai H, Oka H, Seki T: Hepatocellular carcinoma in Child-Pugh C cirrhosis: prognostic factors and survival benefit of nontransplant treatments. Dig Dis 2013;31:490–498.
108 Nishikawa H, Kita R, Kimura T, Ohara Y, Takeda H, Sakamoto A, Saito S, Nishijima N, Nasu A, Komekado H, Osaki Y: Clinical efficacy of non-transplant therapies in patients with hepatocellular carcinoma with Child-Pugh C liver cirrhosis. Anticancer Res 2014;34:3039–3044.
109 Nouso K, Ito Y, Kuwaki K, Kobayashi Y, Nakamura S, Ohashi Y, Yamamoto K: Prognostic factors and treatment effects for hepatocellular carcinoma in Child C cirrhosis. Br J Cancer 2008;98:1161–1165.
110 Wakuta A, Nouso K, Kariyama K, Nishimura M, Kishida M, Wada N, Mizushima T, Higashi T, Tanimoto M: Radiofrequency ablation for the treatment of hepatocellular carcinoma with decompensated cirrhosis. Oncology 2011;81:39–44.
111 Raoul JL, Gilabert M, Piana G: How to define transarterial chemoembolization failure or refractoriness: a European perspective. Liver Cancer 2014;3:119–124.

Preface

Digestive Diseases

Dig Dis 2014;32:655–657
DOI: 10.1159/000367981

Emerging Strategies for the Management of Hepatocellular Carcinoma

Masatoshi Kudo

Department of Gastroenterology and Hepatology, Kinki University School of Medicine, Osaka-Sayama, Japan

The 4th International Kyoto Liver Cancer Symposium (4th IKLS) was recently held in Kyoto. The event, attended by 350 participants, focused on the management of hepatocellular carcinoma (HCC) and was, like its predecessor meetings, a resounding success.

The IKLS has an auspicious history. It started in 2005 as a biannual event for discussing recent progress in the management of HCC. The 1st IKLS was held on Awaji Island, Kobe in 2005 in conjunction with the 4th Single Topic Conference sponsored by the Japan Society of Hepatology (JSH) and focused on 'Hepatocellular Carcinoma: International Consensus and Controversies'. Details of the session were published as a supplementary issue of *Hepatology Research* (vol. 37, 2007). The 2nd IKLS was held in Kobe in 2007. The main theme of this meeting was 'Recent Progress in Hepatocellular Carcinoma 2007' and details were published in *Oncology* (vol. 72, suppl. 1, 2007). The 3rd IKLS, held in 2009 in conjunction with the International Liver Cancer Association (ILCA) and the 45th Annual Conference of the JSH, had as its main theme 'From Prevention to Molecular Targeted Therapy', with a summary of the discussions published in *Oncology* (vol. 78, suppl. 1, 2010). Hepatologists, surgeons, radiologists, pathologists and basic researchers from all over the world who attended these IKLS meetings have helped make the meetings, with their unique topics, landmarks in HCC research and practice.

To continue the success of previous symposiums, the topic for the 4th IKLS was selected as 'Emerging Strategies to HCC', with attention being paid to the emerging topic of molecular targeted therapy in this field. This theme was chosen given that most of the world's HCC cases (80%) occur in Asian countries and there is an urgent need to create a global consensus for developing surveillance, diagnostic and treatment strategies in the region. The 4th IKLS was planned to disseminate the latest knowledge in HCC management among an international audience.

The 4th IKLS was held in Kyoto on June 7–8, 2014 (Congress President: Prof. Masatoshi Kudo) in conjunction with the 50th Liver Cancer Study Group of Japan (LCSGJ) Congress (Congress President: Prof. Masatoshi Kudo). Several HCC experts from around the world were invited to this academic meeting (table 1). On the first day of the event, during session I entitled 'Surveillance of HCC' [1, 2], attendees debated whether or not Sonazoid™ is also useful for surveillance during contrast ultrasound examination or whether tumor markers are required, and whether the surveillance period for patients with liver cirrhosis should be shortened. During session II entitled 'Diagnosis of Pathological Early HCC', the pathology in early HCC was discussed [3], with presenters from various countries explaining the clear usefulness of gadolinium-ethoxybenzyl-diethylenetriamine pentaacetic acid mag-

KARGER

E-Mail karger@karger.com
www.karger.com/ddi

0257–2753/14/0326–0655$39.50/0

Masatoshi Kudo, MD, PhD
Department of Gastroenterology and Hepatology
Kinki University School of Medicine
377-2, Ohno-Higashi, Osaka-Sayama, Osaka 589-8511 (Japan)
E-Mail m-kudo@med.kindai.ac.jp

Table 1. Invited speakers and chairs at the 4th IKLS

Western physicians	Non-Japanese Asian physicians	Japanese physicians	
1 Luigi Bolondi (Bologna)	1 Yee Chao (Taipei)	1 Yasuaki Arai (Tokyo)	30 Takamichi Murakami (Osaka)
2 Brian I. Carr (Bari)	2 Pei-Jer Chen (Taipei)	2 Shigeki Arii (Shizuoka)	31 Yasushi Nagata (Hiroshima)
3 Laura Crocetti (Pisa)	3 Jason Chia-Hsien Cheng (Seoul)	3 Shunichi Ariizumi (Tokyo)	32 Hiroaki Nagano (Osaka)
4 Richard S. Finn (Los Angeles)	4 Young-Hwa Chung (Seoul)	4 Junji Furuse (Tokyo)	33 Masayuki Nakano (Kanagawa)
5 Peter R. Galle (Mainz)	5 Byung Ihn Choi (Seoul)	5 Etsuro Hatano (Kyoto)	34 Osamu Nakashima (Fukuoka)
6 Rita Golfieri (Bologna)	6 Moon Seok Choi (Seoul)	6 Takafumi Ichida (Kanagawa)	35 Naoshi Nishida (Osaka)
7 Josep M. Llovet (Barcelona/ New York)	7 Pierce K.H. Chow (Singapore)	7 Tomoaki Ichikawa (Yamanashi)	36 Kazuto Nishio (Osaka)
8 Markus Peck-Radosavljevic (Vienna)	8 GuoHong Han (Xi'an)	8 Hiroko Iijima (Hyogo)	37 Kazushi Numata (Kanagawa)
9 Fabio Piscaglia (Bologna)	9 Kwang-Hyub Han (Seoul)	9 Kenji Ikeda (Tokyo)	38 Shuntaro Obi (Tokyo)
10 Jean-Luc Raoul (Marseille)	10 Shiu-Feng Huang (Zhunan)	10 Masafumi Ikeda (Chiba)	39 Hiroko Oka (Osaka)
11 Tania Roskams (Leuven)	11 Chih-Hung Hsu (Taipei)	11 Yasuharu Imai (Osaka)	40 Toshiyuki Okumura (Ibaraki)
12 Myron E. Schwartz (New York)	12 Shin Hwang (Seoul)	12 Hiroshi Imamura (Tokyo)	41 Takuji Okusaka (Tokyo)
13 Morris Sherman (Toronto)	13 Jae Young Jang (Seoul)	13 Satoru Imura (Tokushima)	42 Yukio Osaki (Osaka)
14 Andrew X. Zhu (Boston)	14 Do Young Kim (Seoul)	14 Tatsuo Inoue (Osaka)	43 Michiie Sakamoto (Tokyo)
	15 Jeong Min Lee (Seoul)	15 Namiki Izumi (Tokyo)	44 Toshiharu Sakurai (Osaka)
	16 Shi-Ming Lin (Taipei/Taoyuan)	16 Toshimi Kaido (Kyoto)	45 Yutaka Sasaki (Kumamoto)
	17 Ming-De Lu (Guangzhou/ Beijing)	17 Shuichi Kaneko (Ishikawa)	46 Shuichiro Shiina (Tokyo)
	18 Hee Chul Park (Seoul)	18 Seiji Kawasaki (Tokyo)	47 Ken Shirabe (Fukuoka)
	19 Young Nyun Park (Seoul)	19 Soo Ryang Kim (Hyogo)	48 Yasuhiko Sugawara (Tokyo)
	20 Mi-Suk Park (Seoul)	20 Tomomi Kogiso (Tokyo)	49 Hironori Tanaka (Hyogo)
	21 Joong-Won Park (Goyang)	21 Kazuhiko Koike (Tokyo)	50 Masatoshi Tanaka (Fukuoka)
	22 Ronnie T. Poon (Hong Kong)	22 Fukuo Kondo (Tokyo)	51 Shinji Tanaka (Tokyo)
	23 Jinsil Seong (Seoul)	23 Yonson Ku (Hyogo)	52 Ryosuke Tateishi (Tokyo)
	24 Sheng-Long Ye (Shanghai)	24 Shoji Kubo (Osaka)	53 Takuji Torimura (Fukuoka)
	25 Jung-Hwan Yoon (Seoul)	25 Takashi Kumada (Gifu)	54 Kaoru Tsuchiya (Tokyo)
	26 Seung Kew Yoon (Seoul)	26 Masayuki Kurosaki (Tokyo/ Yamanashi)	55 Shinji Uemoto (Kyoto)
		27 Koichi Matsuda (Tokyo)	56 Koichiro Yamakado (Mie)
		28 Osamu Matsui (Ishikawa)	57 Masakazu Yamamoto (Tokyo)
		29 Masashi Mizokami (Tokyo)	58 Taro Yamashita (Ishikawa)
			59 Hitoshi Yoshiji (Nara)

netic resonance imaging for the diagnosis of early HCC [4–7]. During session III entitled 'Diagnostic Algorithm of HCC' [8, 9], the topic for discussion was whether the American Association for the Study of Liver Diseases (AASLD) and the European Association for the Study of the Liver (EASL) guidelines should include contrast-enhanced ultrasonography. The Japanese diagnostic algorithm pertaining to hypervascular and hypovascular tumors in particular was then introduced. The South Korean diagnostic guideline was also explained. Discussion then moved to a new algorithm proposed by the JSH [10]. During session IV entitled 'Pathologic Diversity of HCC', the discussion topics were mixed pattern HCC and cancer stem cells [11, 12]. Subclasses in the classification of HCC were also discussed. Session V, 'Controversial Issues in Surgical Treatment', focused on controversial points during surgical techniques [13–16].

On the morning of the second day, four topics were discussed at the 'Early Morning Breakfast Workshop': (1) 'Surgical Treatment', (2) 'Liver Transplantation' [13, 17–20], (3) 'Carcinogenesis, Genomics, Pathways, and Targets', and (4) 'Radiation Therapy' [21, 22]. An intensive and extremely valuable discussion was conducted by specialists in the respective fields. Session VI focused on radiofrequency ablation (RFA). In this session, entitled 'Controversial Issues in RFA: How to Obtain a Sufficient Safety Margin?', differences between Japan and other countries in the technical aspects of RFA were discussed. In Japan, it is standard to perform RFA until 100% necrosis is achieved and a safety margin is obtained; in the United States and Europe, RFA is performed once and treatment effectiveness is evaluated 1 month later, so the necrosis rate is reported to be around 80%. Similar to Japan, extensive RFA procedures to obtain satisfactory safety margins are applied in Taiwan [23]. In addition, how a sufficient safety margin can be achieved with certainty was discussed in relation to the most recent fusion techniques from Japan. During session VII, on 'Treat-

ment Strategies for Intermediate Stage HCC', discussion focused on the heterogeneous nature of intermediate stage HCC and on the outcomes of treatments for intermediate stage HCC, namely the surgical treatments, superselective transcatheter arterial chemoembolization (TACE) with use of Lipiodol, and TACE using drug-eluting beads, molecular targeted agents and molecular targeted agents combined with TACE (SPACE trial). The discussion topics of session VIII included 'How to Define TACE Failure/Refractoriness?' and the EASL definition [24] and the Korean definition were introduced. The Assessment for Retreatment with TACE (ART) score, a discontinuation rule for TACE, was also introduced. The session ended with a presentation of the LCSGJ's updated version of the JSH TACE failure/refractoriness criteria, and finally participants voted using a voting system on the best definition of TACE failure/refractoriness [10]. The definition put forward by the LCSGJ was agreed to be the best. This result may have been influenced by the fact that 60% or more of the participants were Japanese.

Session IX, 'How to Manage Advanced HCC with Vascular Invasion?', involved a discussion of reports on various treatment modalities, including resection, radiation therapy, hepatic arterial infusion chemotherapy [25], intra-arterial radiotherapy and systemic therapy. In session X, 'Predictive Biomarkers of Molecular Targeted Therapy for HCC', biomarkers were presented and discussed [26]. In the final session, session XI entitled 'Emerging Strategies and Novel Trials for Advanced HCC', reports were presented on newly introduced molecular targeted agents and ongoing trials.

The 4th IKLS, therefore, covered a wide range of topics important to the surveillance, diagnosis and treatment of HCC, and contributions from experts from around the world helped make this another valuable event in the field of HCC management.

In this special issue of *Digestive Diseases*, discussions held at the 4th IKLS are summarized. We believe this will be a valuable compilation for readers who specialize in liver cancer management.

References

1 Kim DY, Han KH: Epidemiology and surveillance of hepatocellular carcinoma. Liver Cancer 2012;1:2–14.
2 Kudo M: Japan's successful model of nationwide hepatocellular carcinoma surveillance highlighting the urgent need for global surveillance. Liver Cancer 2012;1:141–143.
3 Kudo M: Early hepatocellular carcinoma: definition and diagnosis. Liver Cancer 2013;2:69–72.
4 Ichikawa T, Sano K, Morisaka H: Diagnosis of pathologically early HCC with EOB-MRI: experiences and current consensus. Liver Cancer 2014;3:97–107.
5 Lee JM, Yoon JH, Joo I, Woo HS: Recent advances in CT and MR imaging for evaluation of hepatocellular carcinoma. Liver Cancer 2012;1:22–40.
6 Joo I, Choi BI: New paradigm for management of hepatocellular carcinoma by imaging. Liver Cancer 2012;1:94–109.
7 Salvatore V, Bolondi L: Clinical impact of ultrasound-related techniques on the diagnosis of focal liver lesions. Liver Cancer 2012;1:238–246.
8 Ricke J, Seidensticker M, Mohnike K: Noninvasive diagnosis of hepatocellular carcinoma in cirrhotic liver: current guidelines and future prospects for radiological imaging. Liver Cancer 2012;1:51–58.
9 Bota S, Piscaglia F, Marinelli S, Pecorelli A, Terzi E, Bolondi L: Comparison of international guidelines for noninvasive diagnosis of hepatocellular carcinoma. Liver Cancer 2012;1:190–200.
10 Kudo M, Matsui O, Izumi N, Iijima H, Kadoya M, Imai Y, Okusaka T, Miyayama S, Tsuchiya K, Ueshima K, Hiraoka A, Ikeda M, Ogasawara S, Yamashita T, Minami T, Yamakado K; on behalf of the Liver Cancer Study Group of Japan: JSH Consensus-Based Clinical Practice Guideline for the Management of Hepatocellular Carcinoma: 2014 Update by the Liver Cancer Study Group of Japan. Liver Cancer 2014, in press.
11 Lo RC, Ng IO: Hepatic progenitor cells: their role and functional significance in the new classification of primary liver cancers. Liver Cancer 2013;2:84–92.
12 Oishi N, Yamashita T, Kaneko S: Molecular biology of liver cancer stem cells. Liver Cancer 2014;3:71–84.
13 Belghiti J, Fuks D: Liver resection and transplantation in hepatocellular carcinoma. Liver Cancer 2012;1:71–82.
14 Torzilli G, Donadon M, Cimino M: Are tumor exposure and anatomical resection antithetical during surgery for hepatocellular carcinoma? A critical review. Liver Cancer 2012;1:177–182.
15 Shindoh J, Kaseb A, Vauthey JN: Surgical strategy for liver cancers in the era of effective chemotherapy. Liver Cancer 2013;2:47–54.
16 Mise Y, Sakamoto Y, Ishizawa T, Kaneko J, Aoki T, Hasegawa K, Sugawara Y, Kokudo N: A worldwide survey of the current daily practice in liver surgery. Liver Cancer 2013;2:55–66.
17 Lee Cheah Y, Chow PKH: Liver transplantation for hepatocellular carcinoma: an appraisal of current controversies. Liver Cancer 2012;1:183–189.
18 Chan SC, Sharr WW, Chan AC, Chok KS, Lo CM: Rescue living-donor liver transplantation for liver failure following hepatectomy for hepatocellular carcinoma. Liver Cancer 2013;2:332–337.
19 Chan SC: Liver transplantation for hepatocellular carcinoma. Liver Cancer 2013;2:338–344.
20 Akamatsu N, Sugawara Y, Kokudo N: Living donor liver transplantation for patients with hepatocellular carcinoma. Liver Cancer 2014;3:108–118.
21 Jihye C, Jinsil S: Application of radiotherapeutic strategies in the BCLC-defined stages of hepatocellular carcinoma. Liver Cancer 2012;1:216–225.
22 Lee DS, Seong J: Radiotherapeutic options for hepatocellular carcinoma with portal vein tumor thrombosis. Liver Cancer 2014;3:18–30.
23 Lin SM: Local ablation for hepatocellular carcinoma in Taiwan. Liver Cancer 2013;2:73–83.
24 Raoul JL, Gilabert M, Piana G: How to define transarterial chemoembolization failure or refractoriness: a European perspective. Liver Cancer 2014;3:119–124.
25 Kudo M: Treatment of advanced hepatocellular carcinoma with emphasis on hepatic arterial infusion chemotherapy and molecular targeted therapy. Liver Cancer 2012;1:62–70.
26 Shao YY, Hsu CH, Cheng AL: Predictive biomarkers of antiangiogenic therapy for advanced hepatocellular carcinoma: where are we? Liver Cancer 2013;2:93–107.

Original Article

Digestive Diseases

Dig Dis 2014;32:658–663
DOI: 10.1159/000367982

Genome-Wide Profiling of DNA Methylation and Tumor Progression in Human Hepatocellular Carcinoma

Naoshi Nishida[a, c] Takafumi Nishimura[d] Takuya Nakai[b] Hirokazu Chishina[a] Tadaaki Arizumi[a] Masahiro Takita[a] Satoshi Kitai[a] Norihisa Yada[a] Satoru Hagiwara[a] Tatsuo Inoue[a] Yasunori Minami[a] Kazuomi Ueshima[a] Toshiharu Sakurai[a] Masatoshi Kudo[a]

Departments of [a]Gastroenterology and Hepatology and [b]Surgery, Kinki University Faculty of Medicine, Osaka-Sayama, and [c]Department of Gastroenterology and Hepatology, Kyoto University Graduate School of Medicine, and [d]Outpatient Oncology Unit, Kyoto University Hospital, Kyoto, Japan

Key Words
CpG sites · Cytosine residues · DNA methylation · Genome-wide profiling · Hypomethylation

Abstract
Objective: To clarify the progression pattern of abnormal DNA methylation during the development of hepatocellular carcinoma (HCC) using a comprehensive methylation assay. ***Methods:*** We used an Infinium HumanMethylation450 BeadChip array that can analyze >485,000 CpG sites distributed throughout the genome for a comprehensive methylation study of 117 liver tissues consisting of 59 HCC and 58 noncancerous livers. Altered DNA methylation patterns during tumor progression were also analyzed. ***Results:*** We identified 38,330 CpG sites with significant differences in methylation levels between HCCs and noncancerous livers (DM-CpGs) using strict criteria. Of the DM-CpGs, 92% were hypomethylated and only 3,051 CpGs (8%) were hypermethylated in HCC. The DM-CpGs were more prevalent within intergenic regions with isolated CpGs. In contrast, DM-CpGs that were hypermethylated in HCC were predominantly located within promoter regions and CpG islands ($p < 0.0001$). The association between methylation profiles of DM-CpGs and tumor size was statistically significant, especially in hepatitis C virus (HCV)-positive cases ($p = 0.0001$). ***Conclusions:*** We clarified the unique characteristics of DM-CpGs in human HCCs. The stepwise progression of alterations in DNA methylation was a common feature of HCV-related hepatocarcinogenesis.

Introduction

Hepatocellular carcinoma (HCC) is a common malignancy worldwide, and the at-risk population is still growing [1, 2]. Several reports have suggested that hepatocarcinogenesis involves multiple molecular pathways with the accumulation of genetic and epigenetic alterations, including point mutations and abnormal DNA methylation [3–6].

Methylation of cytosine residues at cytosine-guanine dinucleotides (CpG sites) is commonly found in eukary-

KARGER

E-Mail karger@karger.com
www.karger.com/ddi

0257–2753/14/0326–0658$39.50/0

Naoshi Nishida, MD
Department of Gastroenterology and Hepatology
Kinki University Faculty of Medicine
337-2 Ohno-Higashi, Osaka-Sayama, Osaka 589-8511 (Japan)
E-Mail naoshi@med.kindai.ac.jp

otic DNA, including human DNA, and carries important epigenetic information required for proper gene function [7]. For example, DNA methylation contributes to the regulation of gene transcription as well as the stabilization of chromosomes [8]. It is well known that the pattern of DNA methylation found in normal cells is handed down to the daughter cells during mature cell division. However, alterations in the DNA methylation profile of mature cells are frequently observed in many types of human cancers, including HCC [9]. The regional hypermethylation of a gene promoter is typically associated with transcriptional inactivation of corresponding tumor suppressor genes, while global hypomethylation can induce genomic instability, a process that can play an important role in carcinogenesis [3]. Therefore, it is necessary to identify differences in the DNA methylation status between HCCs and noncancerous livers to understand the contribution of epigenetic instability on the initiation and progression of HCC.

To clarify the genome-wide DNA methylation profiles in HCC, we used an Infinium HumanMethylation450 BeadChip array that can analyze >485,000 CpG sites distributed throughout the genome using a large number of human HCCs and noncancerous livers [10]. In addition, alterations in DNA methylation at each stage of tumor progression were also analyzed. We describe the unique distribution of CpG sites that had altered DNA methylation in HCC tissues, and describe the stepwise accumulation of abnormal DNA methylation during human hepatocarcinogenesis.

Materials and Methods

Patients

HCCs from 59 patients and 58 paired, noncancerous liver tissues were analyzed in this study. The tumors and paired noncancerous liver tissues were frozen immediately after surgical removal and stored at –80°C until DNA extraction. The clinical profiles of the patients are as follows: median age (25th–75th percentiles) was 65 years (59–72), 43 patients were male and 16 were female, 15 patients were positive for hepatitis B surface antigen (HBV positive), 23 were positive for hepatitis C virus (HCV) antibody (HCV positive), and 21 were negative for both HBV and HCV (virus negative). Four patients had liver fibrosis stage F0–F1, 7 had F2, 10 had F3, and 38 had F4. The median tumor size (25th–75th percentiles) was 3.0 cm (2.0–4.5). Written informed consent was obtained from all patients, and necessary approvals were obtained from the institutional review boards of the institution involved.

DNA Extraction/Bisulfite Treatment

Genomic DNA was extracted from frozen tissues using QIAamp DNA Mini Kits (Qiagen, Inc., Valencia, Calif., USA). Details of DNA extraction were described previously. After confirming DNA quality and concentration, 1 μg of genomic DNA was subjected to bisulfite treatment using the EZ DNA Methylation Kit (Zymo Research Corporation, Irvine, Calif., USA).

Methylation Analysis Using HumanMethylation450 BeadChip

Genome-wide DNA methylation profiles were assayed using a HumanMethylation450 BeadChip (Illumina, San Diego, Calif., USA) that contains probes covering >485,000 loci [10]. Whole genome amplification of DNA, enzymatic fragmentation, isopropanol precipitation and resuspension were performed followed by hybridization onto the BeadChips for 23 h. After washing away the unhybridized and nonspecific DNA and incorporation of the fluorescence-labeled oligonucleotide, images were obtained using the Illumina iScan SQ scanner (iScan Control v.3.2.45 software) and intensities of the images were extracted using GenomeStudio (v.2011.1) and Methylation Module (v.1.9.0) software. The obtained data were normalized with the background subtracted and to internal controls.

The methylation level was computed as a β value according to the normalized probe fluorescence intensity ratios between methylated and unmethylated signals: β value = signal intensity of the methylated allele/(sum of signal intensity of the unmethylated and methylated allele + 100). To evaluate the fidelity of the obtained β value and remove noise, each β value was accompanied by a detection p value indicating signals significantly greater than background. Probes containing single nucleotide polymorphisms or accompanied by single nucleotide polymorphisms within 10 bp from the 3′ end of the probe, and the probes on sex chromosomes were eliminated from the analysis to avoid methylation bias due to single nucleotide polymorphism and gender differences [11].

Extraction of Differentially Methylated CpGs and Statistics

Extraction of differentially methylated CpGs (DM-CpGs) from HCCs and surrounding noncancerous livers was performed as follows. First, we selected the CpG sites that had methylation differences between HCCs and noncancerous livers with a mean difference in the β value ≥0.15. Then, the Mann-Whitney U test and the false discovery rate control (Benjamini-Hochberg procedure) were applied for multiple comparisons. For the characterization of the DM-CpGs, we selected the 38,330 CpG sites showing a corrected value of $p < 1.0 \times 10^{-13}$. The Mann-Whitney U test was also performed to identify differences in the distribution between DM-CpGs and all CpGs on the BeadChip. For this purpose, the percentage of CpGs located within 1,500 bps of a transcription start site (TSS1500), 200 bp of a transcription start site (TSS200), 1st exon, 5′ untranslated region (UTR), body and 3′UTR were determined to identify differences in the distribution of CpGs in relation to gene structures. Similarly, to determine differences in the distribution in relation to CpG islands, the percentages of CpGs within a CpG island, CpG island shore (up to 2 kb away from islands), CpG island shelf (2–4 kb away from islands) and open sea (regions with isolated CpGs in the genome) were calculated. For the classification of tissues based on their methylation profile, we applied hierarchical clustering analysis using the β value of the top 1,000 DM-CpGs showing large methylation differences between HCCs and noncancerous livers. A principal component analysis (PCA) was also applied using the β value of these top 1,000 DM-CpGs. The χ^2 test was employed for comparisons of categorical variables. Student's t test was used for comparisons of two continuous variables.

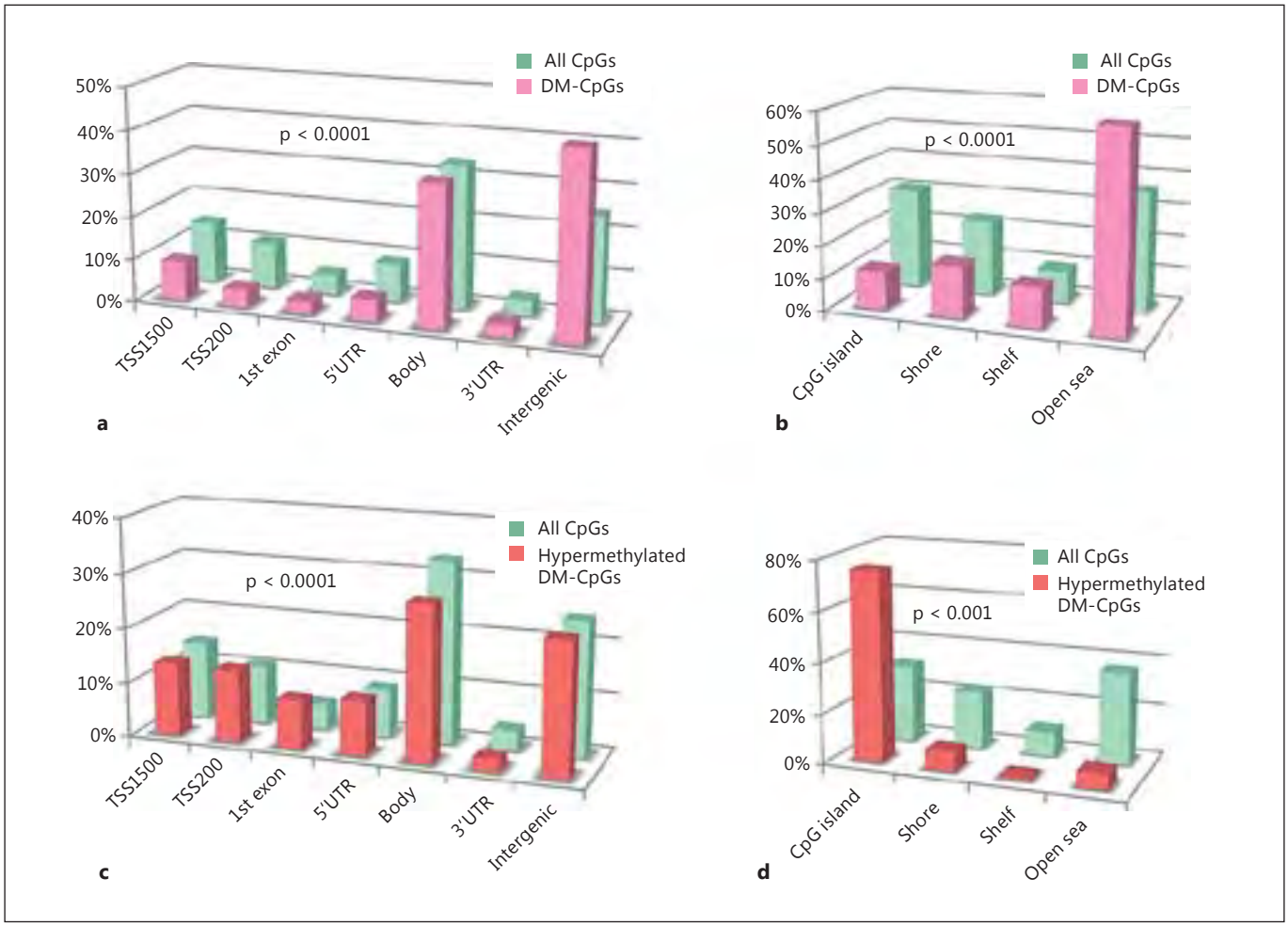

Color version available online

Fig. 1. Differences in the distribution of DM-CpGs and all CpGs on BeadChip arrays. DM-CpG and overall CpG distribution in relation to gene structure (**a**) and CpG islands (**b**). Hypermethylated DM-CpG and overall CpG distribution in relation to gene structure (**c**) and CpG islands (**d**). The bars indicate the distribution of DM-CpGs and all CpGs on the BeadChip (**a**, **b**) and the distribution of hypermethylated DM-CpGs and all CpGs (**c**, **d**). The y-axis shows the percentage of CpGs within each region among the CpGs analyzed. The p value was calculated using the Mann-Whitney U test for all comparisons. DM-CpGs were predominantly distributed within the intergenic regions (**a**) and open sea (**b**). On the other hand, hypermethylated DM-CpGs were distributed preferentially near the transcription start site (**c**) and within CpG islands (**d**).

All p values were two sided, and $p < 0.05$ was considered to be statistically significant. All statistical analyses were conducted using the R language (www.r-project.org) and JMP version 9.0 software (SAS Institute Inc., Cary, N.C., USA).

Results

Characteristics of DM-CpGs between HCCs and Noncancerous Livers

To determine differences in the methylation status between HCCs and noncancerous livers, we analyzed the distribution of 38,330 DM-CpGs. Among the 38,330 DM-CpGs, 35,279 (92%) showed decreased methylation in HCC tissues compared to the noncancerous liver tissues (hypomethylated DM-CpGs). Increased methylation in HCCs was observed at only 3,051 DM-CpGs (hypermethylated DM-CpGs: 8%). However, the absolute difference in the β value between HCCs and noncancerous livers was significantly larger at the hypermethylated DM-CpGs than the hypomethylated DM-CpGs (mean difference and 95% confidence interval, CI, were 0.285 and 0.283–0.287 for hypermethylated DM-CpGs, and 0.266 and 0.266–0.267 for hypomethylated DM-CpGs, respectively; $p < 0.0001$, Student's t test).

Figure 1a shows the distribution of the 38,330 DM-CpGs compared to all CpGs on the BeadChip. DM-CpGs occur more often in intergenic regions compared to all CpGs (16,507/38,330; 43% for DM-CpGs and 119,717/485,577; 24.7% for all CpGs). On the other hand, the proportion of DM-CpGs within the regions near the transcription start site is smaller than that for all CpGs (9.0, 4.0, 3.0 and 5.1% within TSS1500, TSS200, 1st exon and 5′UTR for DM-CpGs, and 14.2, 10.8, 4.7 and 8.8% within TSS1500, TSS200, 1st exon and 5′UTR for all CpGs, respectively). The difference in distributions between DM-CpGs and all CpGs on the BeadChip array was statistically significant ($p < 0.0001$, Mann-Whitney U test). Similarly, DM-CpGs were more often observed within open sea compared to all CpGs ($p < 0.0001$, Mann-Whitney U test; fig. 1b). When only the 3,051 hypermethylated DM-CpGs were considered, they were more often observed within regions near the transcription start site (13.3, 13.2, 8.8 and 10.0% within TSS1500, TSS200, 1st exon and 5′UTR, respectively) compared to all CpGs (14.2, 10.8, 4.7 and 8.8% within TSS1500, TSS200, 1st exon and 5′UTR, respectively; $p < 0.0001$, Mann-Whitney U test; fig. 1c). The distribution of hypermethylated DM-CpGs was also prominent within CpG islands and rare within open sea compared to all CpGs (75.2% within CpG islands and 6.5% within open sea for hypermethylated DM-CpGs vs. 30.9% within CpG islands and 36.3% within open sea for all CpGs; $p < 0.0001$, Mann-Whitney U test; fig. 1d).

Methylation Profile of DM-CpGs and Progression of HCC

We also determined the background factors of HCC that were associated with the methylation profile of the tumors. For this purpose, we selected the top 1,000 DM-CpGs showing large methylation differences between HCC and noncancerous liver tissues, and conducted a hierarchical clustering analysis using the β value of the top 1,000 DM-CpGs (fig. 2a). We examined the following clinical factors for this association: age (≥70 vs. <70 years), sex, etiology (HBV positive vs. HCV positive vs. virus negative), F-stage (F0–2 vs. F3–4), differentiation (well vs. moderately and poorly) and tumor size (>2.0 vs. ≤2.0 cm). Among them, tumor size had a significant association with the methylation profile of the selected 1,000 DM-CpGs, with tumors ≤2.0 cm associated with higher methylation levels ($p = 0.0028$, χ^2 test). Although not statistically significant, etiology classified by the presence of hepatitis virus also showed an association with the methylation-based classification ($p = 0.0540$, χ^2 test; data not shown). Therefore, we separated the HBV-positive, HCV-positive and virus-negative HCCs, and conducted PCA for each group using the β value of the top 1,000 DM-CpGs. Among the HCV-positive tumors, the first three principal components seemed to distinguish tumors ≤2.0 cm in size, which were distributed closer to noncancerous liver tissues, from tumors >2.0 cm. Figure 2b shows the 3D scatter diagram of PCA for HCV-positive liver tissues. However, the principal components failed to distinguish the tumors by their size in HBV-positive and virus-negative cases (data not shown). We further classified the HCV-positive liver tissues using a hierarchical clustering analysis (fig. 2c). HCV-positive liver tissues were clearly classified into two clusters with all HCCs in one cluster (cluster A) and all noncancerous liver tissue in the other cluster (cluster B). The HCC cluster could be further subdivided into A1 and A2. Interestingly, 4 of 5 HCCs (80.0%) in cluster A2 had a tumor size ≤2.0 cm. In contrast, only 3 of 18 HCCs (16.7%) in cluster A1 had a tumor size ≤2.0 cm. The association between methylation profile and tumor size was statistically significant for HCV-positive cases ($p = 0.0001$, χ^2 test; fig. 2d).

Discussion

It is well known that carcinogenesis is a multistep process involving mutation and subsequent clonal expansion of the mutated cells, and the accumulation of genetic and epigenetic alterations are hallmarks of the cancer genome, including HCC [3, 6]. In this study, we tried to clarify alterations in DNA methylation in HCC, one of the characteristics of epigenetic alterations, using the HumanMethylation450 BeadChip array. We clarified the characteristics of CpGs that showed differences in methylation levels between HCC and noncancerous liver tissues using a large number of samples. We also identified stepwise progression of DNA methylation changes during the development of HCC, especially in HCV-related hepatocarcinogenesis.

In this study, we comprehensively characterized CpGs that were differentially methylated between HCC and noncancerous liver tissues of HCC patients. As reported previously, >90% of DM-CpGs showed hypomethylation in cancer [12]. Our analyses also identified that the DM-CpGs were predominantly located within intergenic regions. In addition, DM-CpGs in the genome were prominent within the open sea, the region showing isolated CpGs. From this point of view, DNA hypomethylation in

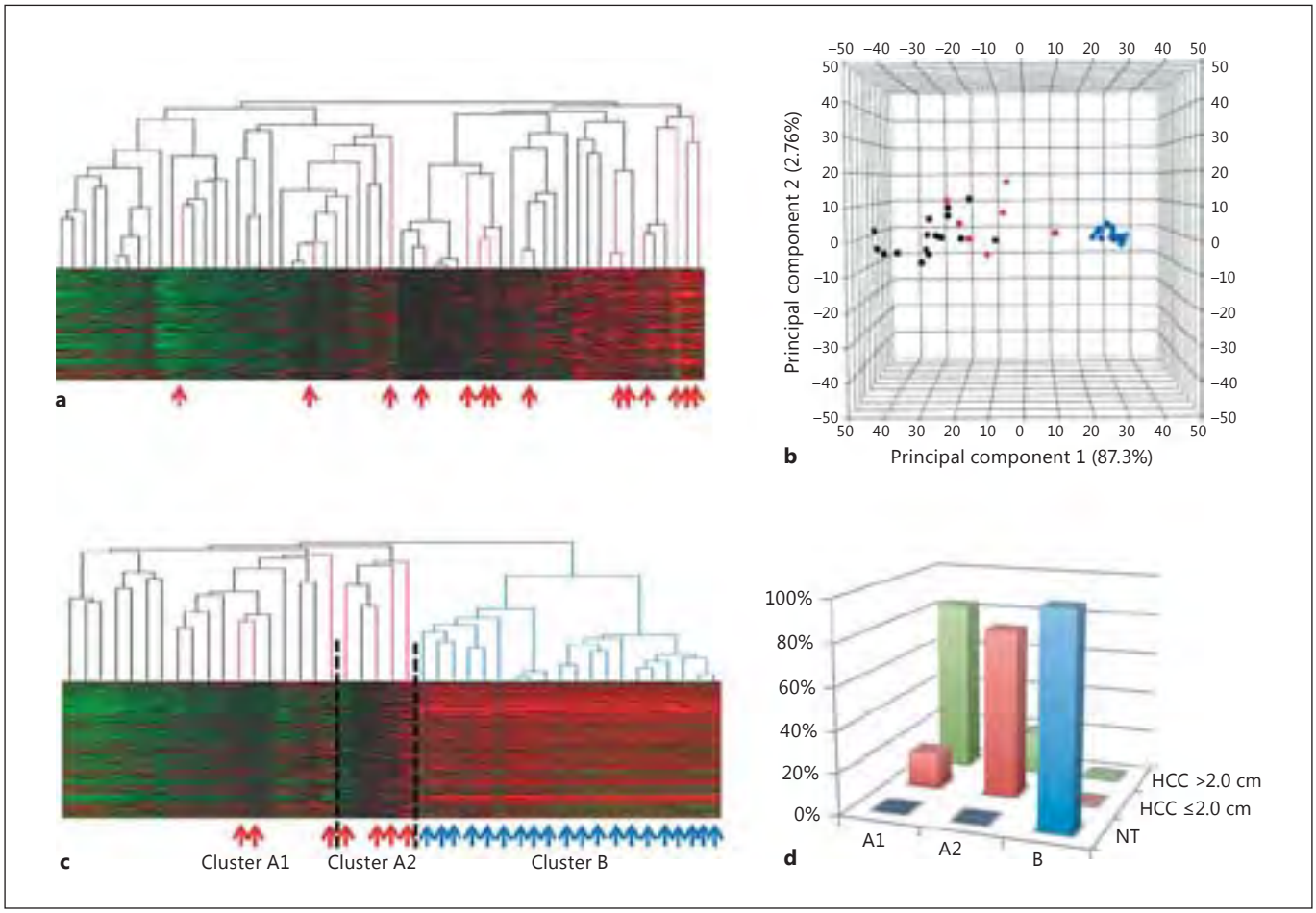

Color version available online

Fig. 2. Methylation profiles of noncancerous livers and HCCs classified by tumor size (colors are available in the only version only). **a**. Hierarchical clustering analysis of HCCs using the β value of the top 1,000 DM-CpGs. Tumors ≤2.0 cm were more frequent in the groups with higher methylation levels ($p = 0.0028$, χ^2 test). Heat map: green = decreased methylation density; red = increased methylation density; black = unchanged. Red arrows show HCCs ≤2.0 cm. **b** 3D scatter diagram of PCA for HCV-positive liver tissues using the β value of the top 1,000 DM-CpGs. Blue dots represent noncancerous livers, red dots HCCs ≤2.0 cm and black dots HCCs >2.0 cm. **c** Hierarchical clustering analysis for HCV-positive liver tissues. The clusters are divided into A1, A2 and B. Blue arrows show noncancerous livers and red arrows HCCs ≤2.0 cm. The samples without an arrow denote HCCs >2.0 cm. **d** Association between classifications based upon methylation profile and tumor size in HCV-positive liver tissues. A1, A2 and B correspond to the classification shown in **c**. Blue bars denote the distribution of noncancerous liver tissue (NT), red bars HCCs ≤2.0 cm and green bars HCCs >2.0 cm. $p < 0.0001$ (χ^2 test).

HCC might contribute to hepatocarcinogenesis through the activation of transcription in non-protein-coding regions, such as noncoding RNA and transposable elements [13]. We also found that global hypomethylation in HCC was associated with chromosomal instability [14], suggesting that the DNA hypomethylation could induce chromosomal fragility and play a role in human hepatocarcinogenesis. In contrast, hypermethylated DM-CpGs were mainly located within the region from TSS200 to the 1st exon, in close proximity to the gene promoter, and were predominantly observed within CpG islands. As the promoters within CpG islands generally regulate gene transcription by DNA methylation [9, 15], it is possible that hypermethylation of DNA could be responsible for HCC emergence mainly through the transcriptional inactivation of tumor suppressor genes.

DM-CpGs clearly discriminated HCCs from noncancerous livers by PCA and hierarchical clustering analysis. Interestingly, in HCC tissues, PCA and hierarchical clustering analysis using β values of DM-CpGs classified

HCCs into two subgroups according to tumor size (≤2.0 vs. >2.0 cm). The methylation profiles of smaller tumors were relatively similar to those of noncancerous livers compared to the methylation profiles of larger tumors. Therefore, stepwise progression of methylation alterations may take place during the development of HCC. Many studies have reported that DNA hypomethylation in tumors is associated with aggressive tumors showing rapid growth [16, 17]. We previously reported that the number of genes with hypermethylation increased with tumor progression [18]. From this point of view, accumulation of epigenetic alterations could be important for the progression of HCC, especially in HCV-positive cases [19]. However, we could not detect an association between methylation progression and tumor size in HBV-positive and virus-negative tumors. Further analyses using a large number of HCCs should clarify the accumulation of methylation events in HBV-positive and virus-negative hepatocarcinogenesis.

In this study, we clarified the characteristic feature of CpGs that had differences in methylation levels between HCCs and noncancerous livers. Furthermore, progressive alterations in DNA methylation were observed in HCV-related hepatocarcinogenesis. The comprehensive data on DNA methylation obtained here should be of importance to better understand the molecular mechanisms of multistep progression of epigenetic alterations during human hepatocarcinogenesis.

References

1 Kim do Y, Han KH: Epidemiology and surveillance of hepatocellular carcinoma. Liver Cancer 2012;1:2–14.
2 Kudo M: Prediction of hepatocellular carcinoma incidence risk by ultrasound elastography. Liver Cancer 2014;3:1–5.
3 Nishida N, Goel A: Genetic and epigenetic signatures in human hepatocellular carcinoma: a systematic review. Curr Genomics 2011; 12:130–137.
4 Moeini A, Cornella H, Villanueva A: Emerging signaling pathways in hepatocellular carcinoma. Liver Cancer 2012;1:83–93.
5 Ramakrishna G, Rastogi A, Trehanpati N, Sen B, Khosla R, Sarin SK: From cirrhosis to hepatocellular carcinoma: new molecular insights on inflammation and cellular senescence. Liver Cancer 2013;2:367–383.
6 Nishida N: Alteration of epigenetic profile in human hepatocellular carcinoma and its clinical implications. Liver Cancer, in press.
7 Esteller M: Epigenetics in cancer. N Engl J Med 2008;358:1148–1159.
8 Berdasco M, Esteller M: Aberrant epigenetic landscape in cancer: how cellular identity goes awry. Dev Cell 2010;19:698–711.
9 Herman JG, Baylin SB: Gene silencing in cancer in association with promoter hypermethylation. N Engl J Med 2003;349:2042–2054.
10 Marabita F, Almgren M, Lindholm ME, Ruhrmann S, Fagerstrom-Billai F, Jagodic M, Sundberg CJ, Ekstrom TJ, Teschendorff AE, Tegner J, Gomez-Cabrero D: An evaluation of analysis pipelines for DNA methylation profiling using the Illumina HumanMethylation450 BeadChip platform. Epigenetics 2013;8:333–346.
11 Shen J, Wang S, Zhang YJ, Wu HC, Kibriya MG, Jasmine F, Ahsan H, Wu DP, Siegel AB, Remotti H, Santella RM: Exploring genome-wide DNA methylation profiles altered in hepatocellular carcinoma using Infinium HumanMethylation 450 BeadChips. Epigenetics 2013;8:34–43.
12 Song MA, Tiirikainen M, Kwee S, Okimoto G, Yu H, Wong LL: Elucidating the landscape of aberrant DNA methylation in hepatocellular carcinoma. PLoS One 2013;8:e55761.
13 Kulis M, Queiros AC, Beekman R, Martin-Subero JI: Intragenic DNA methylation in transcriptional regulation, normal differentiation and cancer. Biochim Biophys Acta 2013; 1829:1161–1174.
14 Nishida N, Kudo M, Nishimura T, Arizumi T, Takita M, Kitai S, Yada N, Hagiwara S, Inoue T, Minami Y, Ueshima K, Sakurai T, Yokomichi N, Nagasaka T, Goel A: Unique association between global DNA hypomethylation and chromosomal alterations in human hepatocellular carcinoma. PLoS One 2013; 8:e72312.
15 Nishida N, Kudo M: Oxidative stress and epigenetic instability in human hepatocarcinogenesis. Dig Dis 2013;31:447–453.
16 Mudbhary R, Hoshida Y, Chernyavskaya Y, Jacob V, Villanueva A, Fiel MI, Chen X, Kojima K, Thung S, Bronson RT, Lachenmayer A, Revill K, Alsinet C, Sachidanandam R, Desai A, SenBanerjee S, Ukomadu C, Llovet JM, Sadler KC: UHRF1 overexpression drives DNA hypomethylation and hepatocellular carcinoma. Cancer Cell 2014;25:196–209.
17 Gao XD, Qu JH, Chang XJ, Lu YY, Bai WL, Wang H, Xu ZX, An LJ, Wang CP, Zeng Z, Yang YP: Hypomethylation of long interspersed nuclear element-1 promoter is associated with poor outcomes for curative resected hepatocellular carcinoma. Liver Int 2014;34: 136–146.
18 Nishida N, Kudo M, Nagasaka T, Ikai I, Goel A: Characteristic patterns of altered DNA methylation predict emergence of human hepatocellular carcinoma. Hepatology 2012;56: 994–1003.
19 Nishida N, Nagasaka T, Nishimura T, Ikai I, Boland CR, Goel A: Aberrant methylation of multiple tumor suppressor genes in aging liver, chronic hepatitis, and hepatocellular carcinoma. Hepatology 2008;47:908–918.

Original Article

Digestive Diseases

Dig Dis 2014;32:670–677
DOI: 10.1159/000367999

Radiofrequency Ablation for Hepatocellular Carcinoma Measuring 2 cm or Smaller: Results and Risk Factors for Local Recurrence

Masashi Kono[a] Tatsuo Inoue[a] Masatoshi Kudo[a] Hirokazu Chishina[a] Tadaaki Arizumi[a] Masahiro Takita[a] Satoshi Kitai[a] Norihisa Yada[a] Satoru Hagiwara[a] Yasunori Minami[a] Kazuomi Ueshima[a] Naoshi Nishida[a] Takamichi Murakami[b]

[a]Division of Gastroenterology and Hepatology, Department of Internal Medicine, and [b]Department of Radiology, Kinki University School of Medicine, Osaka-Sayama, Japan

Key Words
Hepatocellular carcinoma · Radiofrequency ablation · Local recurrence

Abstract
Objective: The purpose of this study was to evaluate the risk factors for local recurrence with radiofrequency ablation (RFA) for hepatocellular carcinoma (HCC) measuring ≤2 cm. ***Methods:*** This study involved 234 patients with 274 HCCs measuring ≤2 cm who had undergone RFA as the initial treatment. The mean tumor diameter was 1.478 cm. The median follow-up period was 829 days. We evaluated the post-RFA cumulative local recurrence rate and analyzed the risk factors contributing to clinical outcomes. ***Results:*** Cumulative local recurrence rates were 9, 19 and 19% at 1, 2 and 3 years, respectively. Among the 145 cases with a complete safety margin (SM) after RFA, only 4 developed local tumor recurrence and the cumulative rates of local tumor recurrence at 1, 2 and 3 years were 2, 3 and 3%, respectively. Among the 129 cases with incomplete SM, local tumor recurrence developed in 34 and the cumulative rates of local tumor progression at 1, 2 and 3 years were 14, 36 and 36%, respectively. In multivariate analysis, significant risk factors were tumor location (liver surface), irregular gross type and SM <5 mm. ***Conclusion:*** Even with HCC measuring ≤2 cm, location and gross type of tumor should be carefully evaluated before RFA is performed.

Introduction

Hepatocellular carcinoma (HCC) is one of the most common malignant tumors worldwide. Several local, minimally invasive hepatic therapies (percutaneous ethanol injection, acetic acid injection, microwave coagulation therapy and radiofrequency ablation [RFA]) have been developed to prolong survival in unresectable HCC patients over the past few decades [1–4].

In particular, RFA is commonly applied in the treatment of HCC because it is a relatively easy procedure to perform and has proven safety and efficacy in the treatment of this cancer. In randomized controlled trials comparing RFA with percutaneous ethanol injection therapy, RFA has shown better response and survival rates [5, 6].

KARGER

E-Mail karger@karger.com
www.karger.com/ddi

0257–2753/14/0326–0670$39.50/0

Masatoshi Kudo, MD, PhD
Division of Gastroenterology and Hepatology
Kinki University School of Medicine
377-2, Ohno-Higashi, Osaka-Sayama, Osaka 589-8511 (Japan)
E-Mail m-kudo@med.kindai.ac.jp

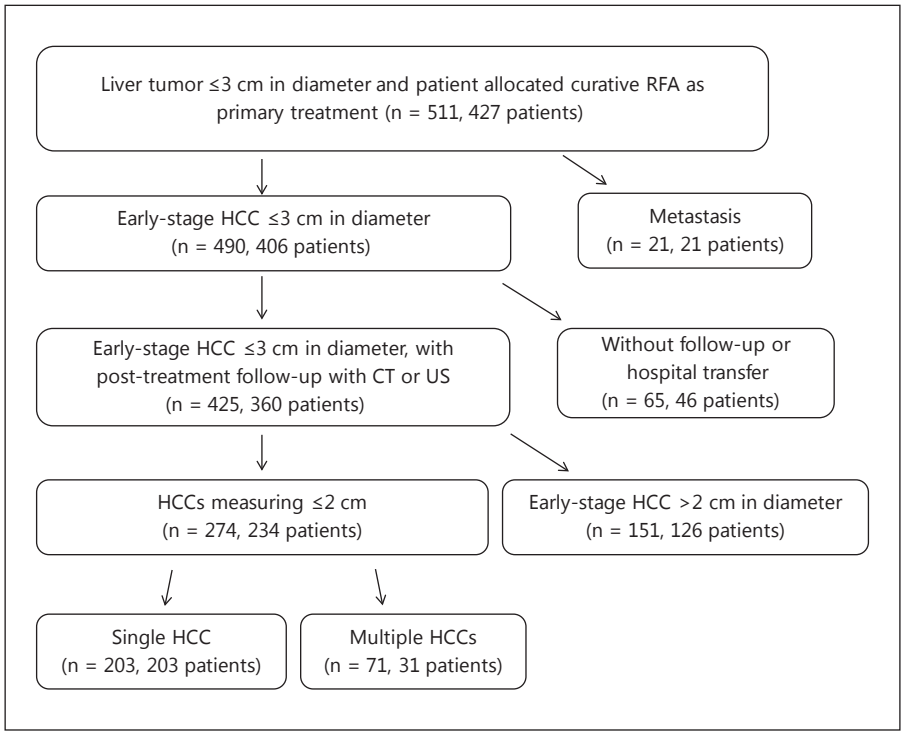

Fig. 1. Study design.

In addition, RFA is much less invasive and associated with lower mortality and shorter hospital stays than liver resection [7]. Small solitary HCC lesions <2 cm in diameter are referred to as 'early (stage A)' or 'very early (stage 0)' stages in the Barcelona Clinic Liver Cancer system [8]. Accordingly, surgical resection (SR) [9, 10] or RFA were considered as curative therapies for stage 0-A HCC if the patients also had good liver function [11]. Thus, RFA is a very important treatment in the management of HCC. However, tumor recurrence rates after curative therapy is a recognized issue [7, 12–14], and previous studies have reported cumulative tumor recurrence rates after RFA of 18–20.4, 37–43.4, 59.8 and 65.9% at 1, 2, 3 and 4 years, respectively [7]. Tumor size, Child-Pugh classification, alpha-fetoprotein (AFP) level, ablation margin and tumor number are generally considered the major causes of local recurrence after RFA [7, 11, 12, 14].

RFA therapy is often chosen as an initial treatment based on considerations of cost-effectiveness and the fact that it is less invasive for patients than SR. However, in terms of selecting a curative therapy, SR may be more reliable [15].

Recent reports have compared the efficacy of SR and percutaneous local ablative therapy in the treatment of HCC. Although some reports revealed no differences between the two therapies [16], others reported that SR was a more effective treatment compared with percutaneous local ablative therapy [15], although the cost-effectiveness of RFA in HCCs measuring ≤2 cm was superior to that of SR [17]. At present, whether SR is more effective than RFA in the treatment for HCCs measuring ≤2 cm remains controversial. However, it might be better to select SR, even for HCCs measuring ≤2 cm, in order to reduce local tumor recurrence, because an initial treatment response is essential for improving survival [11, 15, 18].

In this study, we first evaluated the outcome of RFA for HCCs measuring ≤2 cm and analyzed the predictive factors for local recurrence. Second, we analyzed which cases should be selected for SR as an initial treatment by evaluating their characteristics.

Patients and Methods

Between April 2007 and July 2014, 427 patients were admitted to Kinki University Hospital to receive treatment for HCC. Of these 427 patients, 21 were excluded because they had metastatic liver tumors and 46 were excluded because they were lost to follow-up or had been transferred to another hospital. A further 126 patients were excluded because the tumor was >2 cm; thus, we investigated 234 patients with 274 HCCs measuring ≤2 cm (fig. 1). Of these 274 HCCs, 227 received RFA alone, 41 received transcatheter arterial chemoembolization (TACE) and 6 received transcatheter arterial infusion before RFA.

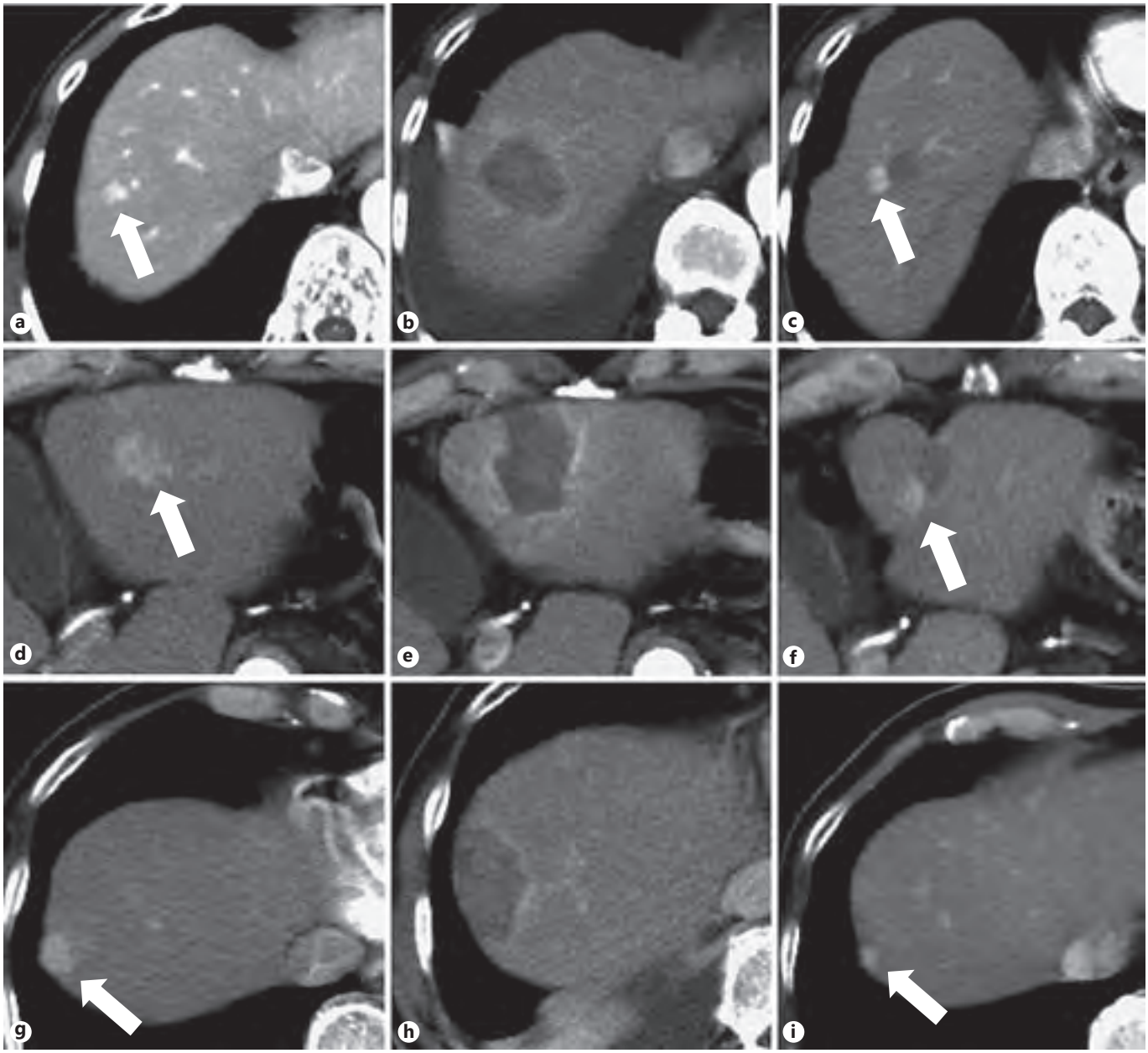

Fig. 2. Representative cases of local recurrence after RFA. **a** A 68-year-old woman diagnosed as SN type HCC by CECT. HCC location S8, not in the liver surface area (arrow). **b** After RFA, we assessed the treatment effect as SM-negative on CECT. Severe pain and high fever continued after RFA, so additional RFA was not performed. **c** Arterial phase of CECT, 9 months after RFA, showed local recurrence at the periphery of the ablation zone (arrow). **d** A 70-year-old man diagnosed as non-SN type HCC, not located in the liver surface area, on CECT (arrow). **e** Two days after ablation, we assessed the treatment effect as SM-negative on CECT. As the vessel was situated near the ablation area, we decided it would be too difficult to perform additional RFA. **f** Arterial phase of CECT, 11 months after RFA, showed local recurrence at the periphery of the ablation zone (arrow). **g** A 69-year-old man diagnosed as SN type HCC by CECT located on S7 liver surface area (arrow). **h** After ablation, we assessed the treatment effect as SM-positive on CECT. **i** Arterial phase of CECT, 7 months after RFA, showed local recurrence at the peripheral ablation zone (arrow).

Diagnosis of HCC

The diagnosis of HCC was based on the presence of typical tumor features on contrast-enhanced computed tomography (CECT), Sonazoid-enhanced ultrasonography (US) (Daiichi-Sankyo, Tokyo, Japan; GE Health Care, Oslo, Norway) and gadolinium-ethoxybenzyl-diethylenetriamine pentaacetic acid-enhanced magnetic resonance imaging (Gd-EOB-DTPA MRI) (Primovist; Bayer Schering Pharma, Berlin, Germany). The tumor was diagnosed as HCC if it showed typical appearance on at least one of these modalities: appearance of hyperattenuations in the arterial phase and hypoattenuations in the portal phase on CECT (Light Speed VCT; GE Medical Systems, Milwaukee, Wisc., USA); hyperenhancement in the early vascular phase followed by a defect in the Kupffer phase or defect in the Kupffer phase with a positive defect reperfusion by contrast-enhanced US using one of the following US units: GE LOGIQ 7, LOGIQ 9 (GE Medical Systems) or EUB 8500 (Hitachi, Tokyo, Japan) [19]; hyperintensity in the arterial dominant phase or washout of contrast material in the portal venous or low intensity area in the hepatobiliary phase on Gd-EOB-DTPA MRI [20–22] (Gyroscan Intera Nova [1.5 T] or an Achieva [3 T] series; Philips Medical System, Best, The Netherlands).

Definition of Safety Ablative Margin, Gross Type and HCC Location

Complete response was defined as the absence of enhanced tumoral areas reflecting complete tissue necrosis as assessed by follow-up imaging modalities within 1 week after RFA. We judged that a safety margin (SM) was positive if there was a complete circumferential ablative margin of ≥5 mm, based on a comparison of CT or MRI images obtained before and after RFA in a side-by-side manner. Conversely, a negative SM was a circumferential ablative margin of <5 mm [14]. All HCCs were subclassified by imaging into the following three gross types: single nodular (SN) type, single nodular type with extranodular growth (SNEG), and confluent multinodular (CM) type [23]. In this study, we divided the HCCs into two groups, SN type and non-SN type. In other words, SN was defined as SN type, whereas SNEG and CM were defined as non-SN type. For the diagnosis of gross type, we evaluated the imaging findings of CECT or Gd-EOB-DTPA MRI. Two experienced hepatologists reviewed the equilibrium phase on CECT or in the hepatocyte phase on Gd-EOB-DTPA MRI. These reviewers were blinded to any other information regarding the patients, and the reviewers discussed all the patients until they reached consensus on the diagnosis.

Regarding the determination of the location of HCC, tumors located at the edge of the liver or within 5 mm from the liver surface by imaging modalities were classified as liver surface HCCs. Otherwise, they were classified as non-liver surface HCCs (fig. 2).

RFA Technique

All RFAs were performed percutaneously by experienced hepatologists, each of whom had more than 5 years of experience in US-guided interventional procedures and RFA. The treatments were performed under local anesthesia and conscious sedation. Patients were treated with a cooled-tip needle RFA system (Cooltip, Covidien, Dublin, Ireland), which is a 480-kHz alternative current generator that can produce a maximum power of 180 W through a 17-gauge monopolar cooled-tip needle electrode. A single 2-cm exposed tip was selected for nodules <2 cm in diameter. CECT was performed 1–3 days after RFA to evaluate its effectiveness. We routinely performed additional RFA treatment until we had confirmed that the ablative margin surrounded the entire outer circumference of the tumor by more than 5 mm, provided that patient consent had been given. If we were not able to acquire consent from the patient or if the patient was judged to be at high risk if given additional treatment, no further RFA treatment was given. When applying RFA, fusion imaging was used in 32 patients with 42 HCCs [24, 25], Sonazoid-enhanced US in 21 patients with 27 HCCs [26, 27] and artificial pleural effusion in 12 patients with 13 HCCs [28].

Table 1. Baseline characteristics of RFA patients (n = 274, 234 patients)

Age, years	69 (41–89)
Sex, male/female	168/66
Location	
S1	3
S2	16
S3	18
S4	28
S5	46
S6	52
S7	35
S8	76
Etiology of liver disease	
Hepatitis C	173
Hepatitis B	21
Hepatitis C + hepatitis B	3
Others	37
Serum bilirubin, mg/dl	0.959 (0.2–3.7)
Serum albumin, g/dl	3.68 (1.9–5.2)
Prothrombin time	80.72 (46.5–120)
Platelet count ($\times 10^4/\mu l$)	11.43 (2.3–32.1)
AFP, ng/dl	64.94 (1–1,772)
AFP-L3, %	7.01 (0–274)
Des-γ-carboxyprothrombin, mAU/ml	133.02 (0.5–4,870)
Tumor size, cm	1.478 (0.5–2.0)
Observation period, days	829.1 (4–2,413)
SM-positive/SM-negative	145/129
Number of puncture times	1.4 (1–3)
Stage 0/A/B/C/D	177/57/0/0/0
Liver surface/non-liver surface	145/129
Child-Pugh classification A/B/C	203/31/0
SN type/non-SN type	267/7

Data are expressed as numbers or median values (range) unless specified otherwise.

Follow-Up Study and Assessment of Local Recurrence

After initial RFA therapy, each patient was followed up every 3 months with blood tests for liver function and tumor markers, as well as either CECT or Gd-EOB-DTPA MRI. When such modalities showed an enhancing area within or at the periphery of the ablated lesion, this was designated as local tumor recurrence [13] (fig. 2).

Table 2. Results of Cox regression analysis for local recurrence (n = 274, 234 patients)

Factors	Local recurrence rates	
	p, univariate analysis	p, multivariate analysis (RR, 95% CI)
Age	0.715	
Sex (male vs. female)	0.859	
Etiology of liver disease	0.585	
Serum bilirubin	0.863	
Serum albumin	0.849	
Prothrombin time	0.444	
Platelet count	0.171	
AFP	0.855	
AFP-L3	0.280	
Des-γ-carboxyprothrombin	0.789	
Tumor size	0.603	
SM	0.000	0.000 (10.24, 3.96–26.46)
Number of puncture times	0.516	
Liver surface	0.004	0.015 (2.77, 1.37–5.59)
Child-Pugh classification	0.522	0.252
Gross type	0.001	0.000 (6.18, 2.16–17.67)

Statistical Analysis

Cumulative local recurrence rates were calculated using the Kaplan-Meier method and assessed using the log-rank test. The Cox regression hazard model was used to examine the effect of the initial curative RFA treatment. Factors for analysis included age, sex, etiology of liver disease, serum bilirubin, serum albumin, prothrombin time, platelet counts, AFP, AFP-L3, des-γ-carboxyprothrombin, tumor size, local recurrence period, SM, number of puncture times, stage, tumor location (liver surface or non-liver surface), Child-Pugh classification and gross type. p values <0.05 were considered to be statistically significant. Statistical analysis was performed using SPSS software, version 11.5J (SPSS, Chicago, Ill., USA).

Results

Clinical Characteristics

The baseline patient characteristics are shown in table 1. No patient had major complications after RFA. The median tumor size and observation period were 1.478 cm and 829 days, respectively. 145 HCCs were located on the liver surface (53%) and 7 cases were classified as non-SN type (3%).

Assessment of Treatment Efficacy of RFA

In the present study, 145 HCCs (53%) were judged to be SM-positive and the remaining 129 HCCs as SM-negative.

Local Tumor Recurrence

The cumulative local tumor recurrence rate in all patients at 1, 2 and 3 years was 9, 19 and 19%, respectively (fig. 3a). Among the 145 patients with complete circumferential ablation (SM-positive), only 4 cases developed local tumor recurrence, and the cumulative rates of local tumor recurrence at 1, 2 and 3 years were 2, 3 and 3%, respectively (fig. 3b). In the 129 patients with incomplete circumferential ablation (SM-negative), 34 developed local tumor recurrence, and the cumulative rates of local tumor progression at 1, 2 and 3 years were 14, 36 and 36%, respectively. The local tumor progression rate was significantly lower in SM-positive versus SM-negative patients ($p < 0.001$).

Prognostic Factors of Local Recurrence by Univariate and Multivariate Analysis

Table 2 shows the results of univariate and multivariate analysis of the prognostic factors for local recurrence. Univariate analysis showed that SM-negative, liver surface, gross type (non-SN type) lesions were risk factors for local recurrence. Multivariate analysis showed that SM-negative (p = 0.000; relative risk [RR] 10.24; 95% confidence interval [CI] 3.96–26.46), liver surface (p = 0.015; RR 2.77; 95% CI 1.37–5.59), gross type (non-SN type; p = 0.000; RR 6.18; 95% CI 2.16–17.67) lesions were risk factors for local recurrence (fig. 3b–d).

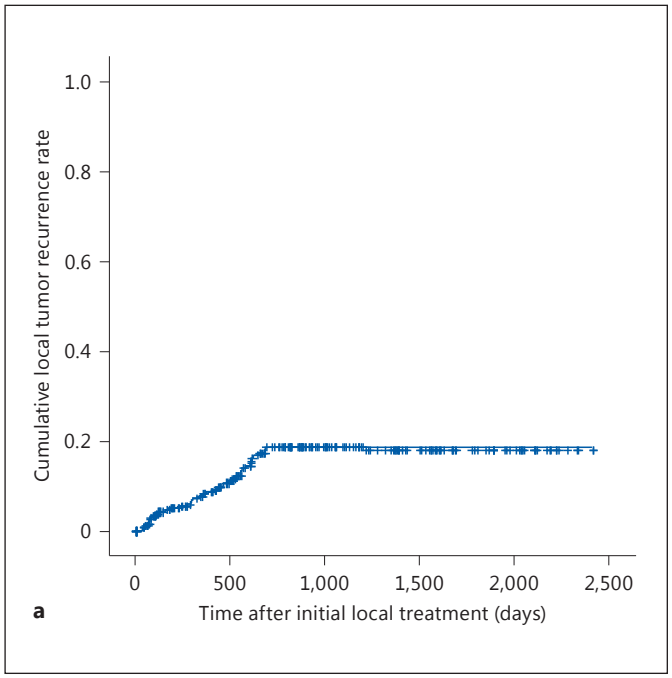

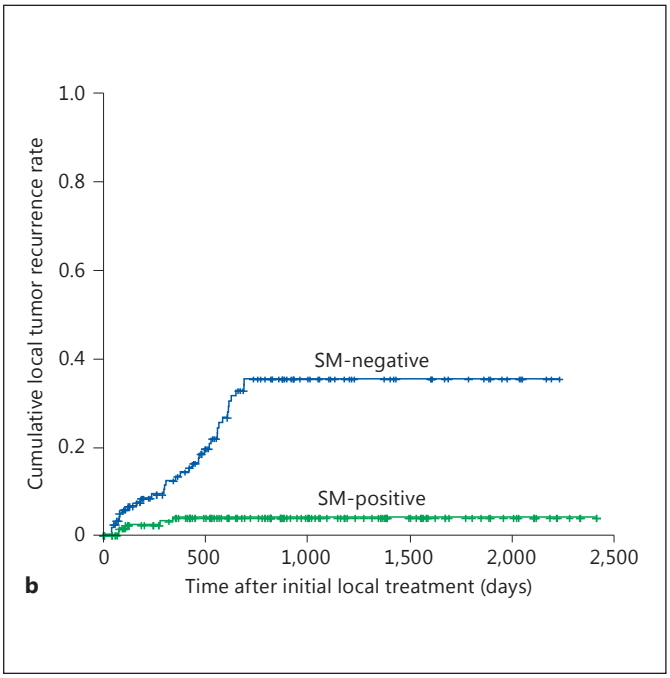

Color version available online

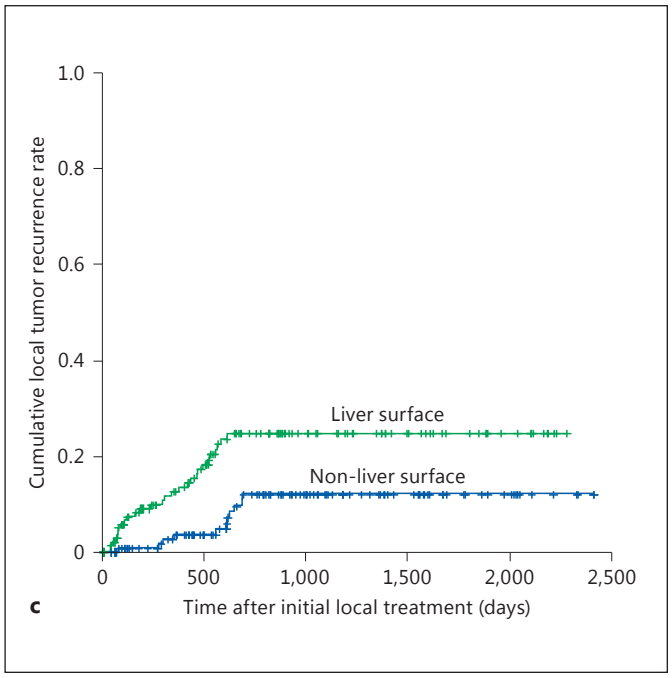

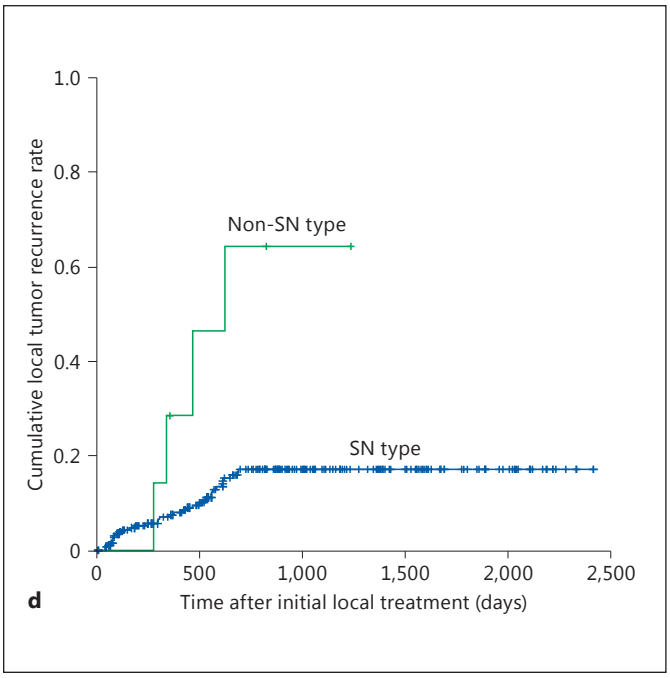

Fig. 3. a Overall cumulative local recurrence curve after RFA in all patients (Kaplan-Meier analysis). **b** Overall cumulative local recurrence curve by SM subgroups. The SM-negative group (blue line) was associated with a higher local recurrence rate than the SM-positive group (green line) (Kaplan-Meier analysis). **c** Cumulative local recurrence curves by tumor location subgroups. The liver surface group (green line) was associated with a higher local recurrence rate than the non-liver surface group (blue line) (Kaplan-Meier analysis). **d** Overall cumulative local recurrence curve by gross type subgroup. The non-SN type (green line) was associated with a higher local recurrence rate than the SN type (blue line) (Kaplan-Meier analysis). Colors in online version only.

Discussion

In the present study, we clarified the risk factors for local recurrence in patients with HCCs measuring ≤2 cm. The importance of achieving an adequate SM has already been reported as linked to the reduction in tumor recurrence, findings which were repeated in our study [14]. However, in the present study, local recurrence due to an inadequate SM occurred in 34 cases. Normally, these cases should have received additional RFA because a sufficient ablative margin was not obtained. The reasons we did not attempt to perform additional RFA, and the number of cases involved, were as follows: (1) the doctor decided it was too difficult to perform additional RFA at a location near a vessel (12 cases); (2) there was no space for performing additional RFA because the HCC was located at the liver surface (14 cases); (3) additional RFA was difficult to perform because HCC could not be identified by US or there was poor visibility owing to the patients' inability to hold their breath (3 cases); (4) complications such as high fever or continuing severe pain occurred (2 cases); (5) there was difficulty in judging reactive hyperemia in tissue surrounding the ablated lesion, iatrogenic arterioportal shunting or remaining small residual HCC at follow-up imaging using CECT (3 cases). For the 3 cases in reason 5, we could have achieved the SM by using fusion imaging of Sonazoid-enhanced US with CECT or virtual CT sonography with magnetic navigation [24, 25]. These two methods can evaluate the ablated area during the procedure, and if additional ablation is needed, RFA can be re-performed, which would result in sufficient ablation. Furthermore, additional TACE before RFA has been reported to increase the volume of coagulation diameter [29]. In addition, the good therapeutic effect of TACE, the improved overall survival and the ease in recognizing SM by evaluating the accumulation of iodized oil on CECT help us to arrive at the correct assessment of treatment effect [30].

In the present study, gross type (non-SN type) had a significantly higher local recurrence rate than SN type. Okusaka et al. [31] reported that small satellite nodules were found in the lesion within 0.5–1 cm of the main tumor and 12% of HCC nodules ≤3.0 cm in diameter had satellite lesions that were detected during pretreatment evaluation, and 19% of HCC nodules were not detected during pretreatment evaluation. They also concluded that macroscopic type and tumor differentiation were significantly associated with the prevalence of satellite lesions, even with small HCCs. Furthermore, Shimada et al. [23] and Roayaie et al. [32] reported that the percentage of poorly differentiated HCC increases in SNEG type and even more in CM type (non-SN type). A lower grade of tumor differentiation tended to be associated with invasion of the larger vascular and portal veins and was associated with a prevalence of satellite lesions and vascular invasion [32]. In this study, the non-SN type was associated with risk factors for local recurrence and the local recurrence rate was 71% (5/7). Taking this into account, the assessment of tumor gross type before treatment is important, even in small HCCs, and we should re-evaluate the indication of SR to get an adequate, sufficient margin [15, 31, 33]. In the present study, the HCCs located on the border to within 5 mm of the liver surface were a significant risk factor for local recurrence. Hori et al. [34] demonstrated that both tumor size and location relative to the liver surface affect local recurrence compared with tumors situated deep within the liver. They mentioned that it was difficult to insert the RFA electrode into a tumor located on the liver surface, and this was the main reason for the higher rate of local recurrence. Other speculations why location at or within 5 mm of the liver surface was associated with risk for local recurrence in the present study were as follows. (1) To evaluate the SM by comparing CT or MRI images obtained before and after RFA in a side-by-side manner was sometimes difficult, especially in the liver surface area, because there were no large vessels and bile ducts to compare on imaging modalities obtained before and after RFA, with the result that there was a lack of precision in the evaluation of treatment. (2) Hemodynamic change at the liver surface area might have influenced the increase in satellite nodules in this region [35].

The principal limitation of this study is its retrospective nature, which inherently decreases the statistical strength. Another limitation is its preliminary nature, leading to a relatively small number of patients and short follow-up time. Further prospective studies of this technique with a larger number of patients are warranted. In conclusion, even for HCCs measuring ≤2 cm, location on the liver surface and gross type (non-SN type) were significantly associated with local recurrence. For such HCCs, SR should be considered as the initial treatment.

References

1 Shiina S, Tagawa K, Unuma T, Takanashi R, Yoshiura K, Komatsu Y, Hata Y, Niwa Y, Shiratori Y, Terano A, et al: Percutaneous ethanol injection therapy for hepatocellular carcinoma. A histopathologic study. Cancer 1991; 68:1524–1530.

2 Seki T, Wakabayashi M, Nakagawa T, Imamura M, Tamai T, Nishimura A, Yamashiki N, Okamura A, Inoue K: Percutaneous microwave coagulation therapy for patients with small hepatocellular carcinoma: comparison with percutaneous ethanol injection therapy. Cancer 1999;85:1694–1702.

3 Lin S, Hoffmann K, Schemmer P: Treatment of hepatocellular carcinoma: a systematic review. Liver Cancer 2012;1:144–158.
4 Lin SM: Local ablation for hepatocellular carcinoma in Taiwan. Liver Cancer 2013;2:73–83.
5 Lencioni RA, Allgaier HP, Cioni D, Olschewski M, Deibert P, Crocetti L, Frings H, Laubenberger J, Zuber I, Blum HE, Bartolozzi C: Small hepatocellular carcinoma in cirrhosis: randomized comparison of radio-frequency thermal ablation versus percutaneous ethanol injection. Radiology 2003;228:235–240.
6 Shiina S, Teratani T, Obi S, Sato S, Tateishi R, Fujishima T, Ishikawa T, Koike Y, Yoshida H, Kawabe T, Omata M: A randomized controlled trial of radiofrequency ablation with ethanol injection for small hepatocellular carcinoma. Gastroenterology 2005;129:122–130.
7 Tateishi R, Shiina S, Teratani T, Obi S, Sato S, Koike Y, Fujishima T, Yoshida H, Kawabe T, Omata M: Percutaneous radiofrequency ablation for hepatocellular carcinoma. An analysis of 1000 cases. Cancer 2005;103:1201–1209.
8 Bruix J, Sherman M: Management of hepatocellular carcinoma: an update. Hepatology 2011;53:1020–1022.
9 Belghiti J, Fuks D: Liver resection and transplantation in hepatocellular carcinoma. Liver Cancer 2012;1:71–82.
10 Mise Y, Sakamoto Y, Ishizawa T, Kaneko J, Aoki T, Hasegawa K, Sugawara Y, Kokudo N: A worldwide survey of the current daily practice in liver surgery. Liver Cancer 2013;2:55–66.
11 Sala M, Llovet JM, Vilana R, Bianchi L, Sole M, Ayuso C, Bru C, Bruix J: Initial response to percutaneous ablation predicts survival in patients with hepatocellular carcinoma. Hepatology 2004;40:1352–1360.
12 Shiina S, Tateishi R, Arano T, Uchino K, Enooku K, Nakagawa H, Asaoka Y, Sato T, Masuzaki R, Kondo Y, Goto T, Yoshida H, Omata M, Koike K: Radiofrequency ablation for hepatocellular carcinoma: 10-year outcome and prognostic factors. Am J Gastroenterol 2012;107:569–577; quiz 578.
13 Komorizono Y, Oketani M, Sako K, Yamasaki N, Shibatou T, Maeda M, Kohara K, Shigenobu S, Ishibashi K, Arima T: Risk factors for local recurrence of small hepatocellular carcinoma tumors after a single session, single application of percutaneous radiofrequency ablation. Cancer 2003;97:1253–1262.
14 Nakazawa T, Kokubu S, Shibuya A, Ono K, Watanabe M, Hidaka H, Tsuchihashi T, Saigenji K: Radiofrequency ablation of hepatocellular carcinoma: correlation between local tumor progression after ablation and ablative margin. AJR Am J Roentgenol 2007;188:480–488.
15 Hasegawa K, Kokudo N, Makuuchi M, Izumi N, Ichida T, Kudo M, Ku Y, Sakamoto M, Nakashima O, Matsui O, Matsuyama Y: Comparison of resection and ablation for hepatocellular carcinoma: a cohort study based on a Japanese nationwide survey. J Hepatol 2013;58:724–729.
16 Chen MS, Li JQ, Zheng Y, Guo RP, Liang HH, Zhang YQ, Lin XJ, Lau WY: A prospective randomized trial comparing percutaneous local ablative therapy and partial hepatectomy for small hepatocellular carcinoma. Ann Surg 2006;243:321–328.
17 Ikeda K, Kobayashi M, Saitoh S, Someya T, Hosaka T, Sezaki H, Suzuki Y, Suzuki F, Akuta N, Arase Y, Kumada H, Matsuda M, Hashimoto M, Watanabe G: Cost-effectiveness of radiofrequency ablation and surgical therapy for small hepatocellular carcinoma of 3 cm or less in diameter. Hepatol Res 2005;33:241–249.
18 Takahashi S, Kudo M, Chung H, Inoue T, Ishikawa E, Kitai S, Tatsumi C, Ueda T, Minami Y, Ueshima K, Haji S: Initial treatment response is essential to improve survival in patients with hepatocellular carcinoma who underwent curative radiofrequency ablation therapy. Oncology 2007;72(suppl 1):98–103.
19 Kudo M, Hatanaka K, Maekawa K: Newly developed novel ultrasound technique, defect reperfusion ultrasound imaging, using sonazoid in the management of hepatocellular carcinoma. Oncology 2010;78(suppl 1):40–45.
20 Joo I, Choi BI: New paradigm for management of hepatocellular carcinoma by imaging. Liver Cancer 2012;1:94–109.
21 Lee JM, Yoon JH, Joo I, Woo HS: Recent advances in CT and MR imaging for evaluation of hepatocellular carcinoma. Liver Cancer 2012;1:22–40.
22 Ichikawa T, Sano K, Morisaka H: Diagnosis of pathologically early HCC with EOB-MRI: experiences and current consensus. Liver Cancer 2014;3:97–107.
23 Shimada M, Rikimaru T, Hamatsu T, Yamashita Y, Terashi T, Taguchi K, Tanaka S, Shirabe K, Sugimachi K: The role of macroscopic classification in nodular-type hepatocellular carcinoma. Am J Surg 2001;182:177–182.
24 Numata K, Fukuda H, Morimoto M, Kondo M, Nozaki A, Oshima T, Okada M, Takebayashi S, Maeda S, Tanaka K: Use of fusion imaging combining contrast-enhanced ultrasonography with a perflubutane-based contrast agent and contrast-enhanced computed tomography for the evaluation of percutaneous radiofrequency ablation of hypervascular hepatocellular carcinoma. Eur J Radiol 2012;81:2746–2753.
25 Minami Y, Kitai S, Kudo M: Treatment response assessment of radiofrequency ablation for hepatocellular carcinoma: usefulness of virtual CT sonography with magnetic navigation. Eur J Radiol 2012;81:e277–e280.
26 Inoue T, Minami Y, Chung H, Hayaishi S, Ueda T, Tatsumi C, Takita M, Kitai S, Hatanaka K, Ishikawa E, Yada N, Hagiwara S, Ueshima K, Kudo M: Radiofrequency ablation for hepatocellular carcinoma: assistant techniques for difficult cases. Oncology 2010;78(suppl 1):94–101.
27 Salvatore V, Bolondi L: Clinical impact of ultrasound-related techniques on the diagnosis of focal liver lesions. Liver Cancer 2012;1:238–246.
28 Minami Y, Kudo M, Kawasaki T, Chung H, Ogawa C, Shiozaki H: Percutaneous radiofrequency ablation guided by contrast-enhanced harmonic sonography with artificial pleural effusion for hepatocellular carcinoma in the hepatic dome. AJR Am J Roentgenol 2004;182:1224–1226.
29 Shibata T, Isoda H, Hirokawa Y, Arizono S, Shimada K, Togashi K: Small hepatocellular carcinoma: is radiofrequency ablation combined with transcatheter arterial chemoembolization more effective than radiofrequency ablation alone for treatment? Radiology 2009;252:905–913.
30 Nishikawa H, Osaki Y, Iguchi E, Takeda H, Matsuda F, Nakajima J, Sakamoto A, Hatamaru K, Saito S, Nasu A, Kita R, Kimura T: Radiofrequency ablation for hepatocellular carcinoma: the relationship between a new grading system for the ablative margin and clinical outcomes. J Gastroenterol 2013;48:951–965.
31 Okusaka T, Okada S, Ueno H, Ikeda M, Shimada K, Yamamoto J, Kosuge T, Yamasaki S, Fukushima N, Sakamoto M: Satellite lesions in patients with small hepatocellular carcinoma with reference to clinicopathologic features. Cancer 2002;95:1931–1937.
32 Roayaie S, Blume IN, Thung SN, Guido M, Fiel MI, Hiotis S, Labow DM, Llovet JM, Schwartz ME: A system of classifying microvascular invasion to predict outcome after resection in patients with hepatocellular carcinoma. Gastroenterology 2009;137:850–855.
33 Hasegawa K, Makuuchi M, Takayama T, Kokudo N, Arii S, Okazaki M, Okita K, Omata M, Kudo M, Kojiro M, Nakanuma Y, Takayasu K, Monden M, Matsuyama Y, Ikai I: Surgical resection vs. percutaneous ablation for hepatocellular carcinoma: a preliminary report of the Japanese nationwide survey. J Hepatol 2008;49:589–594.
34 Hori T, Nagata K, Hasuike S, Onaga M, Motoda M, Moriuchi A, Iwakiri H, Uto H, Kato J, Ido A, Hayashi K, Tsubouchi H: Risk factors for the local recurrence of hepatocellular carcinoma after a single session of percutaneous radiofrequency ablation. J Gastroenterol 2003;38:977–981.
35 Itai Y, Matsui O: Blood flow and liver imaging. Radiology 1997;202:306–314.

Review Article

Digestive Diseases

Dig Dis 2014;32:690–695
DOI: 10.1159/000368001

Ultrasound Fusion Imaging of Hepatocellular Carcinoma: A Review of Current Evidence

Yasunori Minami Masatoshi Kudo

Department of Gastroenterology and Hepatology, Kinki University Faculty of Medicine, Osaka-Sayama, Japan

Key Words
Hepatocellular carcinoma · Magnetic navigation · Multiplanar reconstruction images · Radiofrequency ablation · Ultrasound fusion imaging

Abstract
With advances in technology, imaging techniques that entail fusion of sonography and CT or MRI have been introduced in clinical practice. Ultrasound fusion imaging provides CT or MRI cross-sectional multiplanar images that correspond to the sonographic images, and fusion imaging of B-mode sonography and CT or MRI can be displayed simultaneously and in real time according to the angle of the transducer. Ultrasound fusion imaging helps us understand the three-dimensional relationship between the liver vasculature and tumors, and can detect small liver tumors with poor conspicuity. This fusion imaging is attracting the attention of operators who perform radiofrequency ablation (RFA) for the treatment of hepatic malignancies because this real-time, multimodality comparison can increase monitoring and targeting confidence during the procedure. When RFA with fusion imaging was performed on small hepatocellular carcinomas (HCCs) with poor conspicuity, it was reported that the rates of technical success and local tumor progression were 94.4–100% and 0–8.3%. However, there have been no studies comparing fusion imaging guidance and contrast-enhanced sonography, CT or MRI guidance in ablation. Fusion imaging-guided RFA has proved to be effective for HCCs that are poorly defined on not only conventional B-mode sonography but also contrast-enhanced sonography. In addition, fusion imaging could be useful to assess the treatment response of RFA because of three-dimensional information. Here, we give an overview of the current status of ultrasound fusion imaging for clinical application in the liver.

Introduction

Multiplanar reconstruction (MPR) is a method of displaying three-dimensional (3D) datasets and plays an important role in the interpretation of the 3D anatomical location or extent of disease. Multi-detector raw CT or thin-section MRI has facilitated better images with thinner slice thickness, which has allowed more MPR images to be evaluated in greater detail [1, 2]. Additionally, a fast and accurate magnetic position and orientation tracking method has been developed. By integrating special information between ultrasonic transducer and volume data, two-dimensional (2D) MPR images can display simulta-

KARGER

E-Mail karger@karger.com
www.karger.com/ddi

0257–2753/14/0326–0690$39.50/0

Masatoshi Kudo, MD, PhD
Department of Gastroenterology and Hepatology
Kinki University Faculty of Medicine
377-2 Ohno-Higashi, Osaka-Sayama, Osaka 589-8511 (Japan)
E-Mail m-kudo@med.kindai.ac.jp

neously in the same plane as sonography. Thus, ultrasound fusion imaging known as virtual sonography has emerged in radiology.

Percutaneous radiofrequency ablation (RFA) has been widely implemented in the management of small hepatocellular carcinomas (HCCs) [3–9]. The local efficacy of RFA for small HCCs (i.e. <2 cm) has been shown to be comparable to that of surgical outcomes [10–16]. However, multiple sessions of RFA therapy are required in difficult cases such as small HCCs with poor conspicuity [17–19]. Lee et al. [20] reported that the most common cause of mistargeting was confusion with cirrhotic nodules, followed by poor conspicuity, a poor sonic window, a poor electrode path and/or inaccurate electrode placement. Inconspicuous HCC on B-mode sonography accounted for 5.2–38.8% of the total nodules treated with percutaneous ablation [21–23]. Indeed, the primary success of percutaneous ablation therapies depends on correct targeting via an imaging technique, and local control is optimized by accurate electrode placement. Various techniques to overcome this problem, such as contrast-enhanced sonography [24] and ultrasound fusion imaging, are also powerful for the detection of hepatic nodules poorly defined with B-mode sonography. This article summarizes the principles, clinical applications and technique of ultrasound fusion imaging.

Background

The idea of virtual sonography was initiated by Oshio and Shinmoto in 1996 [25]. At that time, single-slice helical CT with a single detector was the only available modality. Obtaining CT images required a long time to scan the whole liver because helical CT allowed only one channel of image information to be recorded for each rotation of the gantry. Although MPR resembled sonographic images after reconstruction, it could not offer adequate CT image quality for clinical use because of low spatial resolution in the z direction. Multi-detector raw CT now offers rapid scanning of large longitudinal volumes and scan volumes over a large range within a short time with thin-slice images. Advances in volumetric image acquisition capabilities and computer graphics have permitted remarkable improvements in spatial resolution and interactive 3D image-processing techniques [26–28]. Cross-sectional MPR images of the liver from almost isovoxel volume data allow virtual sonographic visualization, and a powerful personal computer can perform the operations quickly [29–31].

Magnetic tracking techniques are based on accurate mapping of a 3D magnetic field. When using ultrasound fusion imaging, spatial information can be obtained from the relationship between the magnetic field generator and a magnetic sensor attached to a transducer. The low-frequency pulsed direct current fields are unaffected by body tissues and most non-ferrous metals.

Matrix Transformation on Fusion Imaging

The ultrasound fusion imaging system is mainly composed of the sonography machine with a built-in magnetic location detector unit, magnetic field generator and magnetic sensor. The field generator is set up beside the patient, and then the magnetic sensor is attached to the sonographic transducer connected to the magnetic location detector unit [32]. Generally, 3D special coordinates transformation can be calculated by a matrix transform as below:

$$\left[\mathrm{X'\ Y'\ Z'\ 1}\right] = \left[\mathrm{X\ Y\ Z\ 1}\right] \times \begin{vmatrix} r11 & r12 & r13 & 0 \\ r21 & r22 & r23 & 0 \\ r31 & r32 & r33 & 0 \\ Dx & Dy & Dz & 1 \end{vmatrix}$$

X, Y, Z represent the coordinate before transformation, X′, Y′, Z′ the coordinate after transformation, *r*11–*r*33 the rotating components, and *Dx*, *Dy*, *Dz* the parallel translation components.

The four coordinate systems of the CT volume, magnetic generator, magnetic sensor and ultrasonic transducer are needed to make calculations (fig. 1). In order to reconstruct the ultrasound fusion image, the following transformation matrixes are required: (i) transformation matrix US from the coordinates of the ultrasonic imaging plane to those of the magnetic sensor (US), (ii) transformation matrix SG from the coordinates of the magnetic sensor to those of the field generator (SG), and (iii) transformation matrix GC from the coordinates of the field generator to those of the CT volume data (GC).

The matrix (UC) that transforms the coordinates of the ultrasonography plane into those of the CT volume data can be expressed by the following equation:

$$\mathrm{UC} = \mathrm{US} \times \mathrm{SG} \times \mathrm{GC}$$

According to this equation, GC can be expressed as

$$\mathrm{GC} = \mathrm{SG}^{-1} \times \mathrm{US}^{-1} \times \mathrm{UC}$$

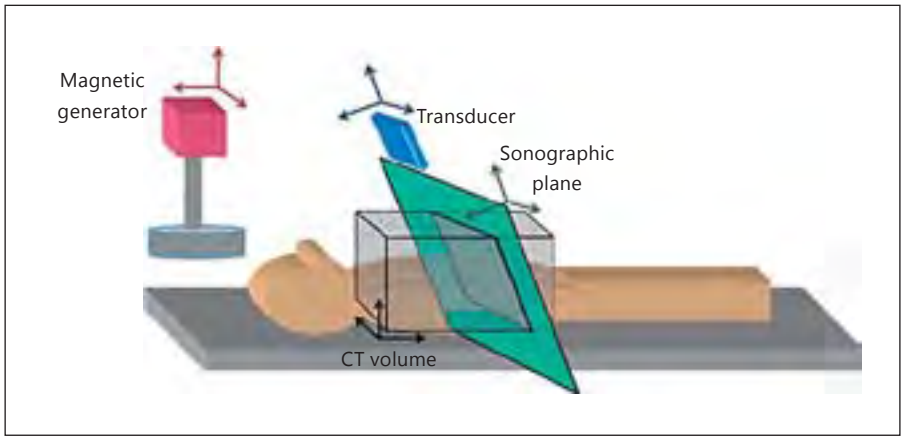

Color version available online

Fig. 1. 3D special coordinate transformations in ultrasound fusion imaging. The four coordinate systems of the CT volume (black), magnetic generator (red), magnetic sensor (blue) and ultrasonic probe (green) are shown (colors in online version). Ultrasound fusion imaging between sonography and MPR images are required the transformation matrixes in turn. Therefore, synchronous imaging can be demonstrated for each movement of the transducer.

Therefore, transformation matrix SG can be acquired from the magnetic sensor data, and transformation matrix US can be calculated from the geometrical position. Since the field generator will not be moved during a diagnosis with this system, transformation matrix GC can be treated as a constant matrix. Transformation matrix GC can thus be calculated if transformation matrix UC is evaluated by performing a calibration with a reference point set after the installation of the magnetic generator. Therefore, ultrasound fusion imaging can be synchronized by manually registering the live ultrasound image to the corresponding image area of the CT/MRI data.

Clinical Uses

Ultrasound Training

The training guidelines established by the American College of Radiology (ACR) and the American Institute of Ultrasound in Medicine (AIUM) for physicians who interpret diagnostic sonographic examinations require at least 3 months of sonographic training during the residency program and involvement in a minimum of 300–500 sonographic examinations during the training period. It is essential not only to demonstrate clear 2D images but also to understand the 3D relationship on abdominal sonographic examination. Sonographic images, which depend on the transducer angle and location, can be changed to produce various cross-sectional images according to the aiming of the operator. This is one of the advantages of sonography. Nevertheless, it is not easy to grasp the 3D vascular anatomy of the liver on sonography from contrast CT information with 2D transverse images [33, 34]. However, by using ultrasound fusion imaging, it is easy to compare the MPR images with B-mode images because the sonographic monitor shows them side-by-side. Okamoto et al. [35] reported that the sensitivity of detecting hepatic nodules on fusion imaging increased from 50.7 to 83.57% compared with using conventional B-mode sonography.

Guidance in RFA

Accurate localization and targeting of small HCCs with poor ultrasound conspicuity is critical to successful RFA. However, ultrasound-guided RFA is often difficult when a target lesion is sonographically obscure. Moreover, when there are regenerating or dysplastic nodules around a small HCC within a cirrhotic liver, incorrect targeting can occur when using ultrasound guidance due to the similarity in appearance of these nearby nodules on sonography. To overcome these limitations of ultrasound guidance, several alternatives such as CT or MRI guidance have been used. However, both imaging modalities have their own weaknesses: CT guidance takes longer and exposes the subject to radiation [30, 36], while MRI guidance is complicated by interference between MRI scanners and RFA systems [37, 38]. Contrast-enhanced sonography is another alternative, but the enhancement effect of commercially available ultrasound contrast agents is not of sufficient duration to clearly visualize an obscure target lesion throughout the RFA procedure [24, 39].

Fusion imaging-guided RFA has been used for HCCs with poor conspicuity on conventional sonography (fig. 2). This technique can increase operator confidence, the accuracy of the procedure and technical success. When RFA with fusion imaging was performed on small HCCs with poor conspicuity, the rates of technical success and local tumor progression were 94.4–100% and 0–8.3% [40–

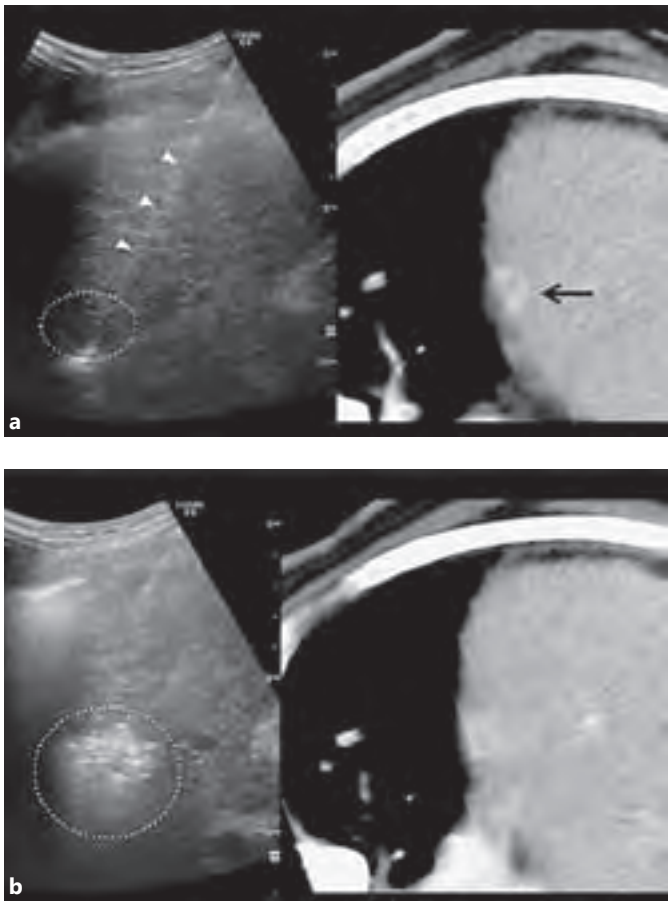

Fig. 2. A 64-year-old man with a 1.7-cm HCC in right hepatic dome. **a** The MPR image (right) corresponding to the sonographic image from intercostal view after synchronization shows a typical HCC nodule (arrow). B-mode sonography (left) shows the radiofrequency electrode needle (arrowheads) inserted into a low-echoic nodule of HCC (dotted circle). **b** During the percutaneous RFA procedure, air bubbles (dotted circle) obscured the HCC nodule on B-mode sonography (left).

44]. No studies have compared fusion imaging guidance and contrast-enhanced sonography guidance in ablation. However, fusion imaging-guided RFA has proved to be effective for HCCs that are poorly defined on not only conventional B-mode sonography but also contrast-enhanced sonography. In addition, it could be used for fusion imaging guidance comparing MPR images and contrast-enhanced sonography. On the other hand, it has been reported that fusion imaging occasionally could not show coincident images. This imaging incompatibility could be attributed to variance in the depth of breath-holding at CT and ultrasound examination, and may increase with the distance between the magnetic sensor attached to the ultrasonic transducer and the field generator. However, this imaging incompatibility has been reducing by enhanced performance of magnetic sensors.

Fusion imaging can be considered to have an acceptable registration error and to be an efficacious tool for overcoming the limitations of ultrasound-guided RFA, which include sonographically obscure nodule issues and confounding nodule issues.

Treatment Response Assessment

Axial images of CT/MRI are mainly used in the evaluation of the therapeutic response of HCCs after RFA [45–47]. However, some HCC patients showed local tumor progression a few months after first ablation because of residual tumors that went unnoticed on axial images. It used to be difficult to distinguish between small residual HCCs and hyperemia lesions because they both showed arterial enhancement. The problem of the partial volume effect cannot be resolved by using MPR. However, multi-angle images using MPR might be able to show the residual HCC as circular enhancement because the shape of enhanced lesions can help diagnose small residual HCC or hyperemia [48–50]. In addition, multi-angle images might be highly sensitive for assessing the 5-mm safety margin around the whole tumor. Assessment of RFA with 3D information could have higher accuracy than with 2D information [48].

Conclusion

Ultrasound fusion imaging has three important features for clinical application. The first is compatibility. The virtual sonographic images obtained using MPR can easily be compared with B-mode sonographic images because the monitor can show them side-by-side. The second is its swift response. With a powerful computer, the fusion imaging can be displayed smoothly for each movement of the transducer in real time. The third feature is synchronicity. This technique contributes to immediate feedback when identifying small hepatic nodules. Ultrasound fusion imaging can indicate the 3D relationship between the liver vasculature and tumors. Fusion imaging can be an efficacious tool in the management of HCCs that have poor ultrasound conspicuity.

Disclosure Statement

The authors have no conflicts of interest to disclose.

References

1 Lee JM, Yoon JH, Joo I, Woo HS: Recent advances in CT and MR imaging for evaluation of hepatocellular carcinoma. Liver Cancer 2012;1:22–40.
2 Murakami T, Tsurusaki M: Hypervascular benign and malignant liver tumors that require differentiation from hepatocellular carcinoma: key points of imaging diagnosis. Liver Cancer 2014;3:85–96.
3 Rossi S, Di Stasi M, Buscarini E, Cavanna L, Quaretti P, Squassante E, Garbagnati F, Buscarini L: Percutaneous radiofrequency interstitial thermal ablation in the treatment of small hepatocellular carcinoma. Cancer J Sci Am 1995;1:73–81.
4 Curley SA, Izzo F, Ellis LM, Nicolas Vauthey J, Vallone P: Radiofrequency ablation of hepatocellular cancer in 110 patients with cirrhosis. Ann Surg 2000;232:381–391.
5 Shiina S, Teratani T, Obi S, Sato S, Tateishi R, Fujishima T, Ishikawa T, Koike Y, Yoshida H, Kawabe T, Omata M: A randomized controlled trial of radiofrequency ablation with ethanol injection for small hepatocellular carcinoma. Gastroenterology 2005;129:122–130.
6 Lencioni R, Crocetti L: Local-regional treatment of hepatocellular carcinoma. Radiology 2012;262:43–58.
7 Lin S, Hoffmann K, Schemmer P: Treatment of hepatocellular carcinoma: a systematic review. Liver Cancer 2012;1:144–158.
8 Kudo M, Matsui O, Izumi N, Iijima H, Kadoya M, Imai Y, Okusaka T, Miyayama S, Tsuchiya K, Ueshima K, Hiraoka A, Ikeda M, Ogasawara S, Yamashita T, Minami T, Yamakado K; on behalf of the Liver Cancer Study Group of Japan: JSH consensus-based clinical practice guideline for the management of hepatocellular carcinoma: 2014 update by the Liver Cancer Study Group of Japan. Liver Cancer 2014, in press.
9 Lin SM: Local ablation for hepatocellular carcinoma in Taiwan. Liver Cancer 2013;2:73–83.
10 Chen MS, Li JQ, Zheng Y, Guo RP, Liang HH, Zhang YQ, Lin XJ, Lau WY: A prospective randomized trial comparing percutaneous local ablative therapy and partial hepatectomy for small hepatocellular carcinoma. Ann Surg 2006;243:321–328.
11 Takayama T, Makuuchi M, Hasegawa K: Single HCC smaller than 2 cm: surgery or ablation?: surgeon's perspective. J Hepatobiliary Pancreat Sci 2010;17:422–424.
12 Cho YK, Kim JK, Kim WT, Chung JW: Hepatic resection versus radiofrequency ablation for very early stage hepatocellular carcinoma: a Markov model analysis. Hepatology 2010;51:1284–1290.
13 Peng ZW, Lin XJ, Zhang YJ, Liang HH, Guo RP, Shi M, Chen MS: Radiofrequency ablation versus hepatic resection for the treatment of hepatocellular carcinomas 2 cm or smaller: a retrospective comparative study. Radiology 2012;262:1022–1033.
14 Feng K, Yan J, Li X, Xia F, Ma K, Wang S, Bie P, Dong J: A randomized controlled trial of radiofrequency ablation and surgical resection in the treatment of small hepatocellular carcinoma. J Hepatol 2012;57:794–802.
15 Mise Y, Sakamoto Y, Ishizawa T, Kaneko J, Aoki T, Hasegawa K, Sugawara Y, Kokudo N: A worldwide survey of the current daily practice in liver surgery. Liver Cancer 2013;2:55–56.
16 Belghiti J, Fuks D: Liver resection and transplantation in hepatocellular carcinoma. Liver Cancer 2012;1:71–82.
17 Minami Y, Kudo M, Chung H, Kawasaki T, Yagyu Y, Shimono T, Shiozaki H: Contrast harmonic sonography-guided radiofrequency ablation therapy versus B-mode sonography in hepatocellular carcinoma: prospective randomized controlled trial. AJR Am J Roentgenol 2007;188:489–494.
18 Minami Y, Kudo M, Hatanaka K, Kitai S, Inoue T, Hagiwara S, Chung H, Ueshima K: Radiofrequency ablation guided by contrast harmonic sonography using perfluorocarbon microbubbles (Sonazoid) for hepatic malignancies: an initial experience. Liver Int 2010;30:759–764.
19 Minami Y, Kudo M: Review of dynamic contrast-enhanced ultrasound guidance in ablation therapy for hepatocellular carcinoma. World J Gastroenterol 2011;17:4952–4959.
20 Lee MW, Lim HK, Kim YJ, Choi D, Kim YS, Lee WJ, Cha DI, Park MJ, Rhim H: Percutaneous sonographically guided radio frequency ablation of hepatocellular carcinoma: causes of mistargeting and factors affecting the feasibility of a second ablation session. J Ultrasound Med 2011;30:607–615.
21 Minami Y, Kudo M, Kawasaki T, Chung H, Ogawa C, Shiozaki H: Treatment of hepatocellular carcinoma with percutaneous radiofrequency ablation: usefulness of contrast harmonic sonography for lesions poorly defined with B-mode sonography. AJR Am J Roentgenol 2004;183:153–156.
22 Kim AY, Lee MW, Rhim H, Cha DI, Choi D, Kim YS, Lim HK, Cho SW: Pretreatment evaluation with contrast-enhanced ultrasonography for percutaneous radiofrequency ablation of hepatocellular carcinomas with poor conspicuity on conventional ultrasonography. Korean J Radiol 2013;14:754–763.
23 Rajesh S, Mukund A, Arora A, Jain D, Sarin SK: Contrast-enhanced US-guided radiofrequency ablation of hepatocellular carcinoma. J Vasc Interv Radiol 2013;24:1235–1240.
24 Salvatore V, Bolondi L: Clinical impact of ultrasound-related techniques on the diagnosis of focal liver lesions. Liver Cancer 2012;1:238–246.
25 Oshio K, Shinmoto H: Simulation of US imaging by using a 3D data. Radiology 1996;201(suppl):517.
26 Kawata S, Murakami T, Kim T, Hori M, Federle MP, Kumano S, Sugihara E, Makino S, Nakamura H, Kudo M: Multidetector CT: diagnostic impact of slice thickness on detection of hypervascular hepatocellular carcinoma. AJR Am J Roentgenol 2002;179:61–66.
27 Yagyu Y, Awai K, Inoue M, Watai R, Sano T, Hasegawa H, Nishimura Y: MDCT of hypervascular hepatocellular carcinomas: a prospective study using contrast materials with different iodine concentrations. AJR Am J Roentgenol 2005;184:1535–1540.
28 Onishi H, Kim T, Imai Y, Hori M, Nagano H, Nakaya Y, Tsuboyama T, Nakamoto A, Tatsumi M, Kumano S, Okada M, Takamura M, Wakasa K, Tomiyama N, Murakami T: Hypervascular hepatocellular carcinomas: detection with gadoxetate disodium-enhanced MR imaging and multiphasic multidetector CT. Eur Radiol 2012;22:845–854.
29 Hirooka M, Iuchi H, Kurose K, Kumagi T, Horiike N, Onji M: Abdominal virtual ultrasonographic images reconstructed by multidetector row helical computed tomography. Eur J Radiol 2005;53:312–317.
30 Hirooka M, Iuchi H, Kumagi T, Shigematsu S, Hiraoka A, Uehara T, Kurose K, Horiike N, Onji M: Virtual sonographic radiofrequency ablation of hepatocellular carcinoma visualized on CT but not on conventional sonography. AJR Am J Roentgenol 2006;186(suppl 5):S255–S260.
31 Kudo K, Moriyasu F, Mine Y, Miyata Y, Sugimoto K, Metoki R, Kamamoto H, Suzuki S, Shimizu M, Miyahara T, Yokoi M, Horibe T, Yamagata H: Preoperative RFA simulation for liver cancer using a CT virtual ultrasound system. Eur J Radiol 2007;61:324–331.
32 Minami Y, Kudo M, Chung H, Inoue T, Takahashi S, Hatanaka K, Ueda T, Hagiwara H, Kitai S, Ueshima K, Fukunaga T, Shiozaki H: Percutaneous radiofrequency ablation of sonographically unidentifiable liver tumors. Feasibility and usefulness of a novel guiding technique with an integrated system of computed tomography and sonographic images. Oncology 2007;72(suppl 1):111–116.
33 Hertzberg BS, Kliewer MA, Bowie JD, Carroll BA, DeLong DH, Gray L, Nelson RC: Physician training requirements in sonography: how many cases are needed for competence? AJR Am J Roentgenol 2000;174:1221–1227.
34 Sidhu HS, Olubaniyi BO, Bhatnagar G, Shuen V, Dubbins P: Role of simulation-based education in ultrasound practice training. J Ultrasound Med 2012;31:785–791.
35 Okamoto E, Sato S, Sanchez-Siles AA, Ishine J, Miyake T, Amano Y, Kinoshita Y: Evaluation of virtual CT sonography for enhanced detection of small hepatic nodules: a prospective pilot study. AJR Am J Roentgenol 2010;194:1272–1278.
36 Krücker J, Xu S, Glossop N, Viswanathan A, Borgert J, Schulz H, Wood BJ: Electromagnetic tracking for thermal ablation and biopsy guidance: clinical evaluation of spatial accuracy. J Vasc Interv Radiol 2007;18:1141–1150.

37 Clasen S, Boss A, Schmidt D, Schraml C, Fritz J, Schick F, Claussen CD, Pereira PL: MR-guided radiofrequency ablation in a 0.2-T open MR system: technical success and technique effectiveness in 100 liver tumors. J Magn Reson Imaging 2007;26:1043–1052.

38 Viallon M, Terraz S, Roland J, Dumont E, Becker CD, Salomir R: Observation and correction of transient cavitation-induced PRFS thermometry artifacts during radiofrequency ablation, using simultaneous ultrasound/MR imaging. Med Phys 2010;37:1491–1506.

39 Lee JY, Choi BI, Chung YE, Kim MW, Kim SH, Han JK: Clinical value of CT/MR-US fusion imaging for radiofrequency ablation of hepatic nodules. Eur J Radiol 2012;81:2281–2289.

40 Nakai M, Sato M, Sahara S, Takasaka I, Kawai N, Minamiguchi H, Tanihata H, Kimura M, Takeuchi N: Radiofrequency ablation assisted by real-time virtual sonography and CT for hepatocellular carcinoma undetectable by conventional sonography. Cardiovasc Intervent Radiol 2009;32:62–69.

41 Minami Y, Chung H, Kudo M, Kitai S, Takahashi S, Inoue T, Ueshima K, Shiozaki H: Radiofrequency ablation of hepatocellular carcinoma: value of virtual CT sonography with magnetic navigation. AJR Am J Roentgenol 2008;190:W335–W341.

42 Kitada T, Murakami T, Kuzushita N, Minamitani K, Nakajo K, Osuga K, Miyoshi E, Nakamura H, Kishino B, Tamura S, Hayashi N: Effectiveness of real-time virtual sonography-guided radiofrequency ablation treatment for patients with hepatocellular carcinomas. Hepatol Res 2008;38:565–571.

43 Kawasoe H, Eguchi Y, Mizuta T, Yasutake T, Ozaki I, Shimonishi T, Miyazaki K, Tamai T, Kato A, Kudo S, Fujimoto K: Radiofrequency ablation with the real-time virtual sonography system for treating hepatocellular carcinoma difficult to detect by ultrasonography. J Clin Biochem Nutr 2007;40:66–72.

44 Song KD, Lee MW, Rhim H, Cha DI, Chong Y, Lim HK: Fusion imaging-guided radiofrequency ablation for hepatocellular carcinomas not visible on conventional ultrasound. AJR Am J Roentgenol 2013;201:1141–1147.

45 Kim KW, Lee JM, Klotz E, Kim SJ, Kim SH, Kim JY, Han JK, Choi BI: Safety margin assessment after radiofrequency ablation of the liver using registration of preprocedure and postprocedure CT images. AJR Am J Roentgenol 2011;196:W565–W572.

46 Minami Y, Kudo M: Therapeutic response assessment of transcatheter arterial chemoembolization for hepatocellular carcinoma: ultrasonography, CT and MR imaging. Oncology 2013;84(suppl 1):58–63.

47 Joo I, Choi BI: New paradigm for management of hepatocellular carcinoma by imaging. Liver Cancer 2012;1:94–109.

48 Minami Y, Kitai S, Kudo M: Treatment response assessment of radiofrequency ablation for hepatocellular carcinoma: usefulness of virtual CT sonography with magnetic navigation. Eur J Radiol 2012;81:e277–e280.

49 Ross CJ, Rennert J, Schacherer D, Girlich C, Hoffstetter P, Heiss P, Jung W, Feuerbach S, Zorger N, Jung EM: Image fusion with volume navigation of contrast enhanced ultrasound (CEUS) with computed tomography (CT) or magnetic resonance imaging (MRI) for post-interventional follow-up after transcatheter arterial chemoembolization (TACE) of hepatocellular carcinomas (HCC): Preliminary results. Clin Hemorheol Microcirc 2010;46:101–115.

50 Ewertsen C, Săftoiu A, Gruionu LG, Karstrup S, Nielsen MB: Real-time image fusion involving diagnostic ultrasound. AJR Am J Roentgenol 2013;200:W249–W255.

Original Article

Digestive Diseases

Dig Dis 2014;32:705–710
DOI: 10.1159/000368006

Duration of Stable Disease Is Associated with Overall Survival in Patients with Advanced Hepatocellular Carcinoma Treated with Sorafenib

Tadaaki Arizumi Kazuomi Ueshima Hirokazu Chishina Masashi Kono Mashiro Takita Satoshi Kitai Tatsuo Inoue Norihisa Yada Satoru Hagiwara Yasunori Minami Toshiharu Sakurai Naoshi Nishida Masatoshi Kudo

Department of Gastroenterology and Hepatology, Kinki University Faculty of Medicine, Osaka-Sayama, Japan

Key Words
Hepatocellular carcinoma · mRECIST · Sorafenib · Stable disease

Abstract
Background: Sorafenib is a molecular-targeting agent showing improved overall survival (OS) for advanced hepatocellular carcinoma (HCC). Although tumor dormancy, characterized by stable tumor status or stable disease (SD) without tumor regression, is a unique feature of sorafenib treatment, the contribution of SD to OS remains debatable. This study aimed to clarify the correlation between SD periods and OS in patients with HCC treated with sorafenib. ***Methods:*** From May 2009 to January 2013, 269 patients with advanced-stage HCC were treated with sorafenib at the Kinki University Hospital. The antitumor response of sorafenib was evaluated in 158 patients using the modified Response Evaluation Criteria in Solid Tumors, and patients with SD were divided into two subgroups according to the median duration of SD: short SD (<3 months) and long SD (≥3 months). The relationship between the duration of SD and OS was analyzed among patients with complete (CR) and partial response (PR), and long and short SD using the Kaplan-Meier method. ***Results:*** The median OS was 5.7 months in the short SD, 20.8 months in the long SD and 17.9 months in the CR + PR group. Although the duration of OS was significantly longer in the long SD group than the short SD group, no difference in OS was detected between the patients with CR + PR and patients with long SD. The impact of long SD on OS could be as strong as that of CR + PR. ***Conclusion:*** Achievement of long SD is one of the important goals for improving survival in patients with HCC treated with sorafenib.

Introduction

Hepatocellular carcinoma (HCC) is the third most common cause of cancer death worldwide and causes significant public health problems, especially in association with chronic hepatitis B or C [1–3]. Because most patients are diagnosed with advanced disease, only 30% of patients receive potentially curative therapies, such as surgical resection [4, 5], transplantation [6, 7] or percutaneous ablation [8–10]. The majority of patients with unresectable HCC usually undergo palliative treatment, such as transarterial chemoembolization (TACE) [11], hepatic arterial infusion chemotherapy [12] and systemic chemotherapy, including molecular-targeting agents [12–17].

KARGER

E-Mail karger@karger.com
www.karger.com/ddi

0257–2753/14/0326–0705$39.50/0

Masatoshi Kudo, MD, PhD
Department of Gastroenterology and Hepatology, Kinki University Faculty of Medicine
377-2 Ohno-Higashi
Osaka-Sayama 589-8511 (Japan)
E-Mail m-kudo@med.kindai.ac.jp

Sorafenib is a multitarget tyrosine kinase inhibitor that suppresses tumor proliferation and angiogenesis. This agent carries a mild-to-moderate toxicity profile and exhibits antitumor activity against various solid tumors [18]. Administration of sorafenib is currently the only systemic, first-line therapy for patients with HCC who failed to respond to TACE [19] and present vascular invasion or extrahepatic spread [19–21]. In the Sorafenib HCC Assessment Randomized Protocol (SHARP) study, progression-free survival and overall survival (OS) were significantly longer with sorafenib than placebo, with a median OS of 10.7 months in the sorafenib group compared to 7.9 months in the placebo group [20]. Median time to progression (TTP) was also longer in the sorafenib group than the placebo group [20]. The improvement in median OS and TTP with sorafenib was also confirmed by another study from the Asian-Pacific region [21]. Interestingly, although both studies revealed improvements in OS and TTP, the response rate of HCC patients treated with sorafenib was quite low, with only 2.3 and 3.3% of patients achieving a partial response (PR) in the SHARP and the Asia-Pacific trials, respectively [20, 21]. Thus, it is conceivable to speculate that sorafenib may delay disease progression and contribute to an improvement in survival. To date, however, no reports have shown how achievement and maintenance of stable disease (SD) improve the OS of patients with HCC treated with this drug. Here, we addressed the unique association between the duration of SD and OS, and we clarified the importance of keeping tumor growth under control, even for cases of tumor regression, during sorafenib therapy.

Patients and Methods

Patients

Between May 2009 and November 2012, 269 patients with advanced HCC were treated with sorafenib at the Kinki University Hospital. Among these patients, 158 met the inclusion criteria listed below and were enrolled in the study. The diagnosis of HCC was made by histology or radiological findings using contrast-enhanced computed tomography (CE-CT) and/or dynamic magnetic resonance imaging (MRI). Informed consent was obtained from all patients, and the study was approved by the ethics review board of the institution involved.

Inclusion criteria for this study were: (1) HCC diagnosed by histological examination or typical radiological findings (early enhancement followed by late washout on CE-CT or dynamic MRI) and HCC refractory to radiofrequency ablation and TACE based on the indications for sorafenib, (2) continuous administration of sorafenib >1 month, (3) performance status of 0 or 1 and (4) Child-Pugh class A or B. Exclusion criteria were: (1) concomitant antineoplastic treatment, (2) TACE or radiofrequency ablation performed within 3 months of initiation of sorafenib and (3) lack of response evaluation using CE-CT or dynamic MRI during the follow-up period. Patient characteristics are summarized in online supplementary table 1 (for all online suppl. material, see www.karger.com/doi/10.1159/000368006).

Initial and Follow-Up Assessments

Liver function and tumor stage were evaluated before the initiation of sorafenib therapy using the Child-Pugh, Barcelona Clinic for Liver Cancer (BCLC) and Cancer of the Liver Italian Program classifications. CE-CT images were obtained during the arterial (40 s) and portal (70 s) phases using 120 ml of iomeprol at a flow rate of 3 ml/s. Dynamic MRI was performed using gadolinium-ethoxybenzyl-diethylenetriamine pentaacetic acid (Gd-EOB-DTPA) enhancement during the arterial (22–35 s after injection) and portal venous (70 s after injection) phases. A T1-weighted high-resolution sequence was obtained during a single breath hold. CE-CT and Gd-EOB-DTPA-MRI were reviewed by two independent radiologists. The response to sorafenib was assessed every 4–6 weeks using the modified Response Evaluation Criteria in Solid Tumors (mRECIST) according to the interval change in tumor size and vascularity after the initiation of treatment. Two experienced radiologists retrospectively reviewed each CE-CT and Gd-EOB-DTPA-MRI, and tumor response was evaluated in a nonblinded fashion [22]. For all patients, the target lesions were defined by two experienced hepatologists using the CT and/or MRI scans before treatment. Extrahepatic lesions were assessed as required by chest X-ray, bone scintigraphy or fluorodeoxyglucose positron emission tomography, and tumor markers were measured at 4- to 12-week intervals to assess the tumor status. The criteria for discontinuing sorafenib were (1) detection of progressive disease (PD), such as obvious tumor progression and/or onset of a new lesion (based on the mRECIST criteria); (2) grade 3 or higher adverse reactions that could not be well controlled by dose reduction or interruption (based on the Common Terminology Criteria for Adverse Events, version 4.0; http://ctep.cancer.gov/protocolDevelopment/electronic_applications/docs/ctcaev3.pdf), and (3) noncompliance to oral drug treatment and/or follow-up visits.

Definitions of Tumor Response

Complete response (CR) was defined as the disappearance of any arterial enhancement within all target lesions. PR was defined as ≥30% reduction in tumor size. Tumor size was determined by the sum of the diameters of target lesions, which were estimated using unidirectional measurement. PD was defined as ≥20% increase in tumor size determined by the sum of the maximal dimensions of the target lesions. mRECIST defines SD as the absence of either PR or PD; it defines response rate (PR) as the percentage of CR + PR among all cases, and disease control rate as the percentage of cases achieving CR, PR or SD. We further classified patients with SD into two subgroups: the long SD group was defined as continuous SD for ≥3 months, and the short SD group was defined as SD periods <3 months. The first estimation of response was performed 4–6 weeks after the initiation of sorafenib, and the second estimation was performed after 8–12 weeks. Therefore, we used the drug administration period of 3 months to separate patients into groups of short and long SD (fig. 1).

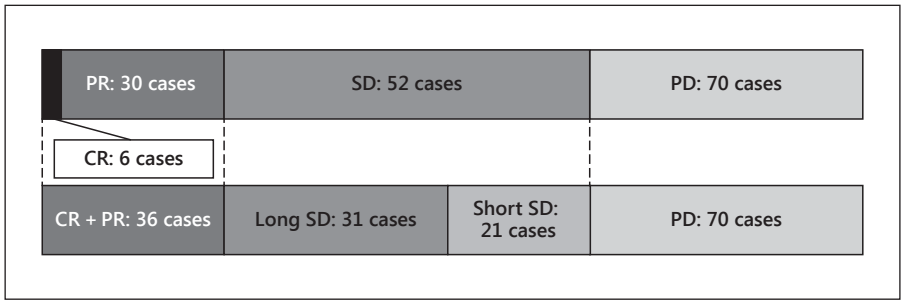

Fig. 1. Response evaluation by mRECIST criteria: OS was compared among the study groups with CR + PR, long and short SD, and PD.

Statistical Analysis

Survival curves were estimated using the Kaplan-Meier method with the primary endpoint of death for analysis of OS. Patients who did not meet the endpoint were censored at the time of the last follow-up visit. Survival rates were compared among the groups and differences were analyzed using the log-rank test; for categorical variables, the χ^2 test was used. For multiple comparisons, the Bonferroni correction was applied. A value of $p < 0.05$ was considered statistically significant. All analyses were performed using SAS statistical software (version 8.2; SAS Institute, Cary, N.C., USA) or the SPSS Medical Pack for Windows (version 10.0; SPSS, Inc., Chicago, Ill., USA).

Results

HCC Response to Sorafenib

Median OS of the entire cohort was 15.6 months (range, 9.9–21.3 months). According to mRECIST criteria, 6 patients had CR and 30 patients PR; these 36 patients with a decrease in tumor size comprised the CR + PR group. Similarly, according to estimates taken 1 month after the start of sorafenib, 52 and 70 cases were classified as having SD and PD, respectively. Response and disease control rates were 23.4 and 54.5%, respectively.

In the SD group, the median duration of SD was 4.6 months (range, 1.9–17.5 months). Among these patients, 26 (54.1%) were positive for anti-hepatitis C virus antibody, 9 (18.8%) were positive for hepatitis B virus surface antigen, and 17 (35.4%) were negative for both. The SD group was further subclassified into short and long SD subgroups according to the criteria described in the Materials and Methods. Representative patients with short and long SD are described in online supplementary figure 1. Among the four study groups (CR + PR, PD, short SD and long SD), there were statistically significant differences in BCLC stage, total dose of sorafenib, administration period, and serum levels of des-γ-carboxyprothrombin (DCP) and AST (online suppl. table 1).

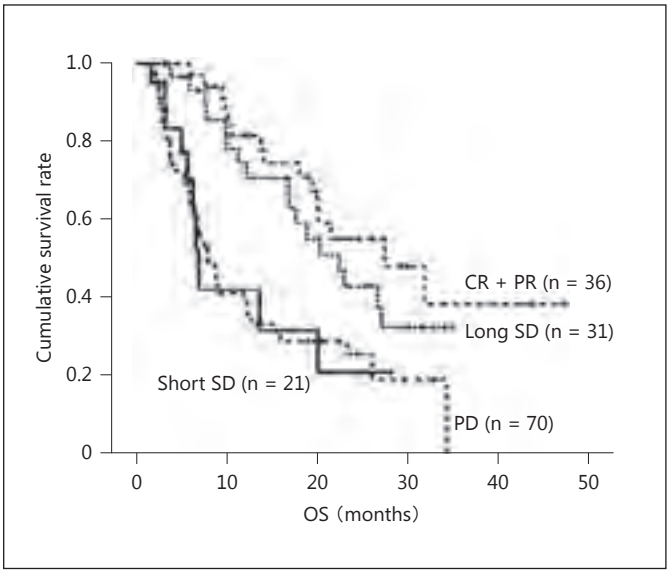

Fig. 2. Kaplan-Meier curves for OS of the 158 patients based on response to sorafenib therapy estimated by mRECIST criteria. The median OS of the patients classified as having CR + PR, long and short SD, and PD were 25.4 months (95% CI, 13.4–37.4), 20.8 months (95% CI, 14.5–27.0), 5.7 months (95% CI, 4.9–6.6) and 7.3 months (95% CI, 5.3–9.4), respectively ($p < 0.001$, log-rank test).

OS according to Response to Sorafenib

We compared OS among the CR + PR, long SD, short SD and PD groups using Kaplan-Meier estimates. Comparisons of the survival curves showed that the median OS was 25.4 months (95% confidence interval, CI, 13.4–37.4) in the CR + PR group, 20.8 months (95% CI, 14.5–27.0) in the long SD group, 6.3 months (95% CI, 5.5–7.1) in the short SD group and 7.3 months (95% CI, 5.3–9.4) in the PD group ($p < 0.001$; fig. 2). Pairwise comparisons verified a significantly longer OS in the CR + PR group than the short SD groups ($p < 0.001$, log-rank test). Similarly, OS was significantly longer in

Table 1. Uni- and multivariate analyses of prognostic factors in the 52 patients with HCC treated with sorafenib

Variable		n	OS, months		p value (log-rank)	Multivariate analysis		
			median	95% CI		HR	95% CI	p value
Gender	male	37	16.3	13.8–18.8				
	female	15	20.8	6.8–34.8	0.339			
Age	<73 years	18	16.3	4.8–27.8				
	≥73 years	34	17.4	5.1–29.7	0.812			
Child-Pugh stage	A	40	17.4	11.0–23.8				
	B	12	9.2	6.2–12.2	0.334			
Etiology	HCV	26	11.3	0.0–22.6				
	others	26	20.8	16.5–25.0	0.0285			
BCLC stage	A or B	21	18.8	7.5–30.1				
	C	31	9.2	5.0–13.4	0.124			
Serum AST	<54 mAU/ml	27	18.8	13.6–24.0				
	≥54 mAU/ml	25	10.3	5.7–14.9	0.234			
Serum ALT	<33 mAU/ml	25	20.8	13.1–28.4				
	≥33 mAU/ml	27	10.3	7.9–12.7	0.061			
Serum platelets	$<14 \times 10^4$ AU/ml	26	15.6	7.7–23.6				
	$\geq 14 \times 10^4$ AU/ml	26	18.8	4.1–33.5	0.971			
Serum AFP	<128 ng/ml	26	18.8	13.5–24.1				
	≥128 ng/ml	26	10.3	4.9–15.7	0.157			
Serum DCP	<389 mAU/ml	26	24.7	13.1–36.3		1		
	≥389 mAU/ml	26	9.1	1.4–16.9	0.018	1.281	0.458–3.580	0.637
Starting dose of sorafenib	≤400 mg	23	25.1	12.4–37.8		1		
	800 mg	29	11.3	0.0–23.4	0.027	1.738	0.751–4.021	0.196
Total dose of sorafenib	<71 g	26	18.6	0.0–38.4				
	≥71 g	26	16.3	13.7–18.9	0.863			
Administration period	<153 days	24	7.2	0.0–23.8				
	≥153 days	28	17.4	12.6–22.2	0.266			
Grade 3/4 of AE	yes	17	15.6	6.4–24.8				
	no	35	24.7	13.8–35.6	0.392			
SD period	long	31	20.8	14.5–27.0		1		
	short	21	5.7	4.9–6.6	0.002	3.244	1.46–7.18	0.004

AFP = α-Fetoprotein; HCV = hepatitis C virus.

the CR + PR group than the PD group ($p < 0.001$), significantly longer in the long SD group than the PD group ($p = 0.004$) and significantly longer in the long SD group than the short SD group ($p = 0.003$). In contrast, no significant differences in OS were detected between the CR + PR and long SD groups ($p = 0.44$) or between the short SD and PD groups ($p = 0.79$).

Prognostic Factors of SD Patients with HCC Treated with Sorafenib

We analyzed the baseline patient characteristics to identify factors that affect OS after sorafenib therapy. Univariate analysis revealed statistically significant differences in OS for the following variables: DCP level ($p = 0.018$), starting dose of sorafenib ($p = 0.027$) and

Dig Dis 2014;32:705–710
DOI: 10.1159/000368006

Table 2. Multivariate analysis of factors associated with long SD in patients with HCC treated with sorafenib

	p value	Hazard ratio	95% CI
α-Fetoprotein	0.403	1.927	0.414–8.958
DCP	0.006	9.609	1.944–47.506
Administration period of sorafenib	0.006	7.293	1.757–30.282

duration of SD (p = 0.002) at the initiation of sorafenib therapy. Multivariate analysis revealed that duration of SD was the only independent factor contributing to OS, with the long SD group having longer OS than the short SD group (odds ratio, 3.244; 95% CI, 1.46–7.18; p = 0.004; table 1).

Adverse Effects of Sorafenib and Duration of SD

Sorafenib was discontinued in 6 of the 21 patients in the short SD group due to sorafenib-related adverse events (AEs); 1 patient had hand-foot reaction, 1 patient had anorexia, 3 had hepatopathy, and 1 had hypertension. Discontinuation of sorafenib unrelated to AEs included 2 deaths due to ruptured HCC and 1 death from pneumonia. One patient refused treatment, and 12 patients discontinued treatment due to PD and received other therapies. Sorafenib was discontinued in 26 patients in the CR + PR group; 14 of these patients had PD, 10 died from HCC progression, and 2 withdrew from treatment. Sorafenib was discontinued in 28 of the 31 patients in the long SD group; 17 of these patients had PD, 4 patients died from HCC progression, 1 rejected continuation of treatment, and 6 had sorafenib-related AEs, including hand-foot reaction, diarrhea, hepatopathy, thrombocytopenia, hypoalbuminemia and interstitial pneumonia (online suppl. table 2). The median administration period of sorafenib for patients with therapy discontinuation due to sorafenib-related AEs was 70 days in the short SD group and 190 days in the long SD group (online suppl. table 3).

Characteristics of the Patients in the Long SD Group

Comparing characteristics between patients in the long and short SD groups, statistically significant differences between the two groups were found in the duration of treatment with sorafenib (p = 0.014) and α-fetoprotein (p = 0.020) and DCP levels (p = 0.001). Multivariate analysis revealed that the duration of sorafenib treatment and the level of DCP were important independent factors (odds ratio, 7.294; 95% CI, 1.757–30.282; p = 0.006, and odds ratio, 9.609; 95% CI, 1.944–47.506; p = 0.006, respectively; table 2).

Discussion

In this study, we demonstrated that in patients who achieved a long SD with sorafenib treatment OS was comparable to that of patients with a CR + PR, suggesting that achieving long SD may improve OS, even without tumor resolution and reduction.

The clinical utility of sorafenib has been demonstrated in the SHARP study [20] and in the Asia-Pacific study [21]. However, because the response rate for sorafenib treatment was low in both studies, it is conceivable to believe that sorafenib might induce tumor dormancy and thereby prolong the SD period.

In terms of the patients' clinical presentation, a significant difference was observed in treatment duration, but not in total dose, between the long and short SD groups. It is possible that patients in the long SD group receive longer treatment because of a longer SD duration. However, the increased treatment duration was not associated with an increased total dose of sorafenib, probably because treatment interruptions and/or sorafenib dose reductions were frequent in the long SD group; this may also account for the control of adverse drug reactions in the long SD group. In the short SD group, 6 patients discontinued treatment with sorafenib due to sorafenib-related AEs. It is possible that successful control of AEs leads to the long SD in patients with sorafenib-related AEs. Among the AEs of sorafenib observed in this study, hand-foot reaction, diarrhea, hypertension and anorexia were the major AEs, and these might be prevented with appropriate measures such as adjustment of the sorafenib dosage and additional medications. From this point of view, intensive care and early detection of AEs is critical to avoid the discontinuation of sorafenib and attain an adequate treatment period.

According to our analyses, the administration period of sorafenib and the serum DCP level could predict the achievement of long SD. Several reports have shown that the serum DCP level reflects aggressive tumor behavior, and this might be related to the refractory character of tumors resistant to antitumor agents [23, 24]. However, multivariate analysis failed to identify serum DCP as an independent factor associated with long SD. Further studies are required to confirm the role of DCP in predicting the effectiveness of sorafenib.

Our study showed an increase in OS compared to OS values observed in the SHARP and Asia-Pacific studies, and this increase is likely attributable to the establishment of effective control of AEs and the decrease in treatment discontinuation due to adverse drug reactions. Furthermore, patients developing PD during sorafenib treatment were managed actively with additional treatment, such as hepatic arterial infusion chemotherapy. These approaches may improve the OS of patients treated with sorafenib compared to the results of previous analyses.

Although the number of patients analyzed in this study was adequate, the retrospective design of the study might have led to bias in patient selection. To address these limitations and independently validate the results of this study, we are currently designing a prospective multicenter study investigating the significance of long SD in a larger patient cohort.

In conclusion, even in SD cases, prolonged sorafenib treatment improves OS to levels comparable to CR or PR. Therefore, achievement of long SD should be an important issue in the treatment of HCC with sorafenib.

References

1 El-Serag HB, Rudolph KL: Hepatocellular carcinoma: epidemiology and molecular carcinogenesis. Gastroenterology 2007;132:2557–2576.
2 Parkin DM: Global cancer statistics in the year 2000. Lancet Oncol 2001;2:533–543.
3 Kim DY, Han KH: Epidemiology and surveillance of hepatocellular carcinoma. Liver Cancer 2012;1:2–14.
4 Belghiti J, Fuks D: Liver resection and transplantation in hepatocellular carcinoma. Liver Cancer 2012;1:71–82.
5 Shindoh J, Kaseb A, Vauthey JN: Surgical strategy for liver cancers in the era of effective chemotherapy. Liver Cancer 2013;2:47–54.
6 Lee Cheah Y, Chow PKH: Liver transplantation for hepatocellular carcinoma: an appraisal of current controversies. Liver Cancer 2012;1:183–189.
7 Chan SC: Liver transplantation for hepatocellular carcinoma. Liver Cancer 2013;2:338–344.
8 Bruix J, Llovet JM: Prognostic prediction and treatment strategy in hepatocellular carcinoma. Hepatology 2002;35:519–524.
9 Park KW, Park JW, Choi JI, Kim TH, Kim SH, Park HS, Lee WJ, Park SJ, Hong EK, Kim CM: Survival analysis of 904 patients with hepatocellular carcinoma in a hepatitis B virus-endemic area. J Gastroenterol Hepatol 2008;23:467–473.
10 Lin SM: Local ablation for hepatocellular carcinoma in Taiwan. Liver Cancer 2013;2:73–83.
11 Lencioni R: Chemoembolization in patients with hepatocellular carcinoma. Liver Cancer 2012;1:41–50.
12 Kudo M: Treatment of advanced hepatocellular carcinoma with emphasis on hepatic arterial infusion chemotherapy and molecular targeted therapy. Liver Cancer 2012;1:62–70.
13 Ando E, Tanaka M, Yamashita F, Kuromatsu R, Yutani S, Fukumori K, Sumie S, Yano Y, Okuda K, Sata M: Hepatic arterial infusion chemotherapy for advanced hepatocellular carcinoma with portal vein tumor thrombosis: analysis of 48 cases. Cancer 2002;95:588–595.
14 Obi S, Yoshida H, Toune R, Unuma T, Kanda M, Sato S, Tateishi R, Teratani T, Shiina S, Omata M: Combination therapy of intraarterial 5-fluorouracil and systemic interferon-alpha for advanced hepatocellular carcinoma with portal venous invasion. Cancer 2006;106:1990–1997.
15 Lin S, Hoffmann K, Schemmer P: Treatment of hepatocellular carcinoma: a systematic review. Liver Cancer 2012;1:144–158.
16 Peck-Radosavljevic M: Drug therapy for advanced-stage liver cancer. Liver Cancer 2014;3:125–131.
17 Benson AB 3rd, Abrams TA, Ben-Josef E, Bloomston PM, Botha JF, Clary BM, Covey A, Curley SA, D'Angelica MI, Davila R, Ensminger WD, Gibbs JF, Laheru D, Malafa MP, Marrero J, Meranze SG, Mulvihill SJ, Park JO, Posey JA, Sachdev J, Salem R, Sigurdson ER, Sofocleous C, Vauthey JN, Venook AP, Goff LW, Yen Y, Zhu AX: NCCN clinical practice guidelines in oncology: hepatobiliary cancers. J Natl Compr Canc Netw 2009;7:350–391.
18 Strumberg D, Richly H, Hilger RA, Schleucher N, Korfee S, Tewes M, Faghih M, Brendel E, Voliotis D, Haase CG, Schwartz B, Awada A, Voigtmann R, Scheulen ME, Seeber S: Phase I clinical and pharmacokinetic study of the novel Raf kinase and vascular endothelial growth factor receptor inhibitor BAY 43-9006 in patients with advanced refractory solid tumors. J Clin Oncol 2005;23:965–972.
19 Raoul JL, Gilabert M, Piana G: How to define transarterial chemoembolization failure or refractoriness: a European perspective. Liver Cancer 2014;3:119–124.
20 Llovet JM, Ricci S, Mazzaferro V, Hilgard P, Gane E, Blanc JF, de Oliveira AC, Santoro A, Raoul JL, Forner A, Schwartz M, Porta C, Zeuzem S, Bolondi L, Greten TF, Galle PR, Seitz JF, Borbath I, Haussinger D, Giannaris T, Shan M, Moscovici M, Voliotis D, Bruix J: Sorafenib in advanced hepatocellular carcinoma. N Engl J Med 2008;359:378–390.
21 Cheng AL, Kang YK, Chen Z, Tsao CJ, Qin S, Kim JS, Luo R, Feng J, Ye S, Yang TS, Xu J, Sun Y, Liang H, Liu J, Wang J, Tak WY, Pan H, Burock K, Zou J, Voliotis D, Guan Z: Efficacy and safety of sorafenib in patients in the Asia-Pacific region with advanced hepatocellular carcinoma: a phase III randomised, double-blind, placebo-controlled trial. Lancet Oncol 2009;10:25–34.
22 Lencioni R, Llovet JM: Modified RECIST (mRECIST) assessment for hepatocellular carcinoma. Semin Liver Dis 2010;30:52–60.
23 Ueshima K, Kudo M, Takita M, Nagai T, Tatsumi C, Ueda T, Kitai S, Ishikawa E, Yada N, Inoue T, Hagiwara S, Minami Y, Chung H, Sakurai T: Des-gamma-carboxyprothrombin may be a promising biomarker to determine the therapeutic efficacy of sorafenib for hepatocellular carcinoma. Dig Dis 2011;29:321–325.
24 Nakazawa T, Hidaka H, Shibuya A, Koizumi W: Rapid regression of advanced hepatocellular carcinoma associated with elevation of des-gamma-carboxy prothrombin after short-term treatment with sorafenib – a report of two cases. Case Rep Oncol 2010;3:298–303.

Original Article

Digestive Diseases

Dig Dis 2014;32:717–724
DOI: 10.1159/000368008

Validation of Three Staging Systems for Hepatocellular Carcinoma (JIS Score, Biomarker-Combined JIS Score and BCLC System) in 4,649 Cases from a Japanese Nationwide Survey

Satoshi Kitai[a] Masatoshi Kudo[a] Namiki Izumi[b] Shuichi Kaneko[c] Yonson Ku[d] Norihiro Kokudo[e] Michiie Sakamoto[f] Tadatoshi Takayama[g] Osamu Nakashima[h] Masumi Kadoya[i] Yutaka Matsuyama[j] Takashi Matsunaga[k] for the Liver Cancer Study Group of Japan

[a]Department of Gastroenterology and Hepatology, Kinki University School of Medicine, Osaka-Sayama, [b]Department of Gastroenterology and Hepatology, Musashino Red Cross Hospital, Musashino, [c]Department of Gastroenterology, Kanazawa University Hospital, Kanazawa, [d]Department of Surgery, Kobe University Graduate School of Medicine, Kobe, [e]Hepato-Biliary-Pancreatic Surgery Division, Artificial Organ and Transplantation Division, Department of Surgery, and [f]Department of Pathology, Keio University School of Medicine, Tokyo, [g]Department of Digestive Surgery, Nihon University School Medicine, Tokyo, [h]Department of Clinical Laboratory Medicine, Kurume University Hospital, Kurume, [i]Department of Radiology, Shinshu University School of Medicine, Matsumoto, [j]Department of Biostatistics, School of Public Health, University of Tokyo, Tokyo, and [k]Clinical Laboratory and Medical Informatics, Osaka Medical Center for Cancer and Cardiovascular Diseases, Osaka, Japan

Key Words

Japan Integrated Staging score · Biomarker-combined Japan Integrated Staging score · Barcelona Clinic Liver Cancer staging system · *Lens culinaris* agglutinin-reactive alpha-fetoprotein fraction · Des-gamma-carboxyprothrombin

Abstract

Objective: Clinical staging is very important for optimal therapeutic strategy and prognostic prediction in patients with hepatocellular carcinoma (HCC). The Barcelona Clinic Liver Cancer (BCLC) staging system is the most widely used and best-validated method for HCC. Similarly, the conventional Japan Integrated Staging (c-JIS) score and the biomarker-combined JIS (bm-JIS) score have also been reported to effectively stratify HCC patients. The aim of this study was to evaluate the performance of these three staging systems for prognostic prediction. ***Methods:*** A total of 4,649 HCC patients were included in this study. A multivariate analysis identified the independent risk factors associated with overall survival. The stratification ability and the suitability as a prognostic model of the three staging systems were compared. ***Results:*** Multivariate analysis revealed that male sex, higher Child-Pugh score, tumor size >2.0 cm, multiple tumors, vascular invasion, higher alpha-fetoprotein (AFP) level, higher des-gamma-carboxyprothrombin level, higher *Lens culinaris* agglutinin-reactive AFP level, and a performance status of 3–4 were independent risk factors in HCC. The independent homogenizing ability and stratification value of the bm-JIS score were higher than those of the c-JIS score and the BCLC system (χ^2 = 972.7581, 758.1041 and

0257–2753/14/0326–0717$39.50/0

E-Mail karger@karger.com
www.karger.com/ddi

Masatoshi Kudo, MD, PhD
Department of Gastroenterology and Hepatology
Kinki University School of Medicine
377-2, Ohno-Higashi, Osaka-Sayama, Osaka 589-8511 (Japan)
E-Mail m-kudo@med.kindai.ac.jp

679.6832, respectively). Moreover, the bm-JIS score had the lowest Akaike Information Criteria value, followed by the c-JIS score and the BCLC system (9,844.278, 10,054.93 and 10,131.35, respectively). ***Conclusions:*** Our results suggest that the bm-JIS score offers good stratification ability and is a better prognostic predictor than the c-JIS score and the BCLC system.

Introduction

Hepatocellular carcinoma (HCC) is one of the most common malignancies worldwide and the second leading cause of cancer death [1, 2]. Clinical staging is very important for optimal therapeutic strategy selection and prognostic prediction. Especially in HCC patients, prognosis is defined by not only tumor status but also liver function. Therefore, it is essential to establish and validate the best clinical staging method for HCC. Several staging systems have been proposed for the classification and prognostic prediction of HCC patients [3–8]. They mainly consider liver function (i.e., Child-Pugh score, serum albumin, serum total bilirubin, ascites, etc.) and tumor status (i.e., tumor size, number of tumors, tumor-node-metastasis [TNM] stage, portal vein thrombosis, etc.).

Among these, the Barcelona Clinic Liver Cancer (BCLC) staging system has been validated and used worldwide. It is also well known as the best system for HCC treatment guidance [9]. However, the BCLC system strictly offers treatment selection staging instead of a prognostic predictive value, whereas it is necessary to consider patient prognosis when selecting the treatment strategy.

The Japan Integrated Staging (JIS) score [4] consists of the Child-Pugh score and TNM staging by the Liver Cancer Study Group of Japan (LCSGJ) [10]. The conventional JIS (c-JIS) score is widely used in Japan and Asian countries, and several reports have validated the effectiveness of the c-JIS score despite its simplicity [11–14].

The biomarker-combined JIS (bm-JIS) score [5] includes three tumor markers [15], alpha-fetoprotein (AFP), *Lens culinaris* agglutinin-reactive alpha-fetoprotein (AFP-L3) fraction [16] and des-gamma-carboxyprothrombin (DCP), specific for HCC. It has been shown to offer better stratification ability and prognostic predictive power than the c-JIS score, the Cancer of the Liver Italian Program (CLIP) score [6] and the BALAD score [17]. One of the reasons for such an advantage is that the bm-JIS score evaluates not only tumor morphology and liver function but also biological factors as it consists of TNM stage, the Child-Pugh score and three tumor markers (AFP, AFP-L3 and DCP). However, the bm-JIS score is used less often and has not been validated worldwide.

The aim of this study was to identify the independent prognostic predictors for overall survival (OS) in HCC and compare the stratification ability and suitability as a prognostic model of the c-JIS score, the bm-JIS score and the BCLC system by using data from a nationwide survey by the LCSGJ.

Table 1. Definitions of the c-JIS score and the bm-JIS score

Variable	Score				
	0	1	2	3	
Child-Pugh stage	A	B	C		c-JIS score
TNM stage by the LCSGJ[a]	I	II	III	IV	c-JIS score
Elevated tumor markers	0	1	2 or 3		c-JIS score

[a] Stage I: T1 (fulfilling 3 T factors) N0 M0. Stage II: T2 (fulfilling 2 T factors) N0 M0. Stage III: T3 (fulfilling 1 T factor) N0 M0. Stage IV: T4 (fulfilling 0 T factor) N0 M0 or any T N0–1 M1. T factor: I. single, II. <2 cm, III. no vascular involvement.

Patients and Methods

Patient Characteristics

Between January 2004 and December 2005, there were 19,499 patients registered in the database of a nationwide survey by the LCSGJ as newly diagnosed with HCC. Of these, 4,649 were eligible for this analysis owing to the availability of all required data (i.e., albumin, bilirubin, prothrombin time, hepatic encephalopathy, ascites, Child-Pugh score, AFP, AFP-L3, DCP, tumor size, number of tumors, metastasis, performance status and portal hypertension). All eligible patients were restaged according to the c-JIS score, the bm-JIS score and the BCLC system. Data collection and registration of the HCC patients included in this analysis were performed with the approval of each participating institution. Patients' informed consent was not required owing to the retrospective design of the study.

Definitions of c-JIS Score and bm-JIS Score

The c-JIS score was obtained via the summation of Child-Pugh score and TNM stage by the LCSGJ. The bm-JIS score was the summation of the c-JIS score and the levels of the three tumor markers using the following cut-off values: AFP 400 ng/ml, AFP-L3 15% and DCP 100 mAU/ml. Regarding these tumor markers, a score of 0 was allocated if none of the AFP, AFP-L3 and DCP markers were positive. Similarly, a score of 1 was assigned when any of the three tumor markers was positive and a score of 2 was given when any two of the three markers were positive. The definitions of c-JIS and bm-JIS scores are shown in table 1.

Table 2. Patient characteristics (n = 4,649)

Variable	n	%
Age, years		
Median ± SD	68.9±9.3	
Range	25.4–93.1	
Sex		
Male	3,224	69.3
Female	1,425	30.7
Cause of parenchymal disorder		
HCV	3,500	75.3
HBV	558	12.0
HCV + HBV	79	1.7
Non-B, non-C	512	11.0
Child-Pugh stage		
A	3,362	72.3
B	1,059	22.8
C	228	4.9
TNM stage by the LCSGJ		
I	870	18.7
II	1,398	30.1
III	1,421	30.6
IV	960	20.6
Initial treatment modality		
No	199	4.3
Yes		
Surgery	1,166	25.1
Percutaneous ablation therapy	1,829	39.3
TACE	1,184	25.5
Chemolipiodolization	260	5.6
Other	11	0.2
Positivity of tumor markers		
AFP (>400 ng/ml)	874	18.7
AFP-L3 (>15%)	1,338	28.7
DCP (>100 mAU/ml)	1,762	37.9

HBV = Hepatitis B virus; HCV = hepatitis C virus; SD = standard deviation; TACE = transcatheter arterial chemoembolization.

Table 3. Results of univariate and multivariate analysis

Variable	Univariate	Multivariate		
	p value	HR	95% CI	p value
Age, years				
≥60				
<60	0.001	0.938	0.782–1.124	0.487
Sex				
Female				
Male	<0.0001	1.31	1.088–1.577	0.004
Child-Pugh score				
C				
B		0.371	0.290–0.474	
A	<0.0001	0.163	0.128–0.206	<0.0001
Maximum tumor size, cm				
>2.0				
≤2.0	<0.0001	0.571	0.432–0.754	<0.0001
Number of tumors				
Multiple				
Solitary	<0.0001	0.772	0.649–0.917	0.003
Vascular invasion				
Positive				
Negative	<0.0001	0.318	0.265–0.382	<0.0001
AFP, ng/ml				
>400				
≤400	<0.0001	0.491	0.407–0.594	<0.0001
AFP-L3, %				
>15				
≤15	<0.0001	0.676	0.563–0.812	<0.0001
DCP, mAU/ml				
>100				
≤100	<0.0001	0.52	0.429–0.629	<0.0001
Performance status				
3–4				
0–2	<0.0001	0.348	0.230–0.527	<0.0001

CI = Confidence interval; HR = hazard ratio.

Statistical Analysis

To compare the OS of patients categorized according to each staging system, univariate survival curves were estimated using the Kaplan-Meier method, and intergroup differences in survival rates were compared using the log-rank test. OS was the only endpoint used in the analysis. Survival was defined as the time interval between HCC diagnosis and death or the last follow-up. Variables with a p value <0.05 on univariate analysis were subjected to multivariate analysis using the Cox proportional hazards regression model. The likelihood ratio test was calculated using the Cox regression model to evaluate the homogeneity of each staging system with small differences among the patients classified into the same group by each system. In addition, the test was employed to estimate gradient monotonicity, as the mean survival time of patients who are classified as having favorable prognosis by a system is always longer than that of patients with a less favorable prognosis. The Akaike Information Criteria (AIC) [18] were also used to evaluate the discriminatory ability of a given model. All analyses were performed using the statistical software program R version 2.13.0 (the Comprehensive R Archive Network) or the SPSS Medical Pack for Windows (version 19.0; SPSS Inc., Chicago, Ill., USA).

Results

Patient Characteristics

Table 2 shows the characteristics of the 4,649 enrolled patients. The median age was 68.9 years, and male was the dominant sex (69.3%). The most common cause of HCC

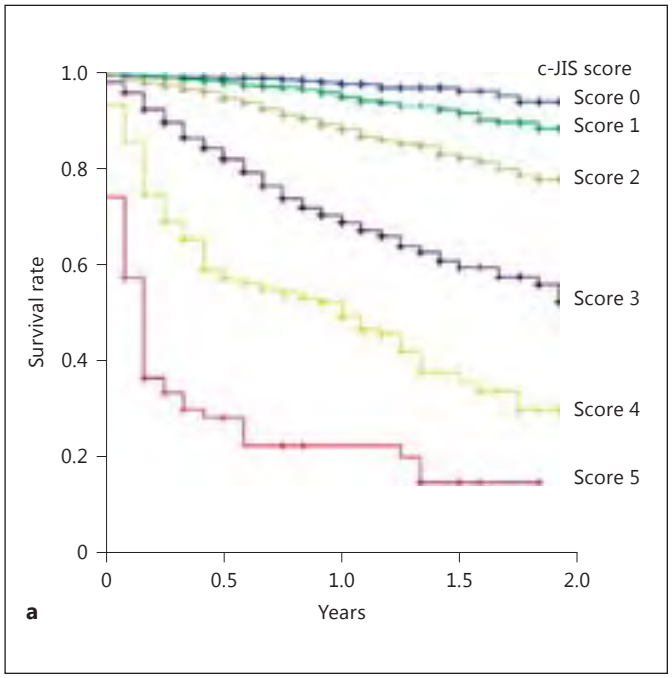

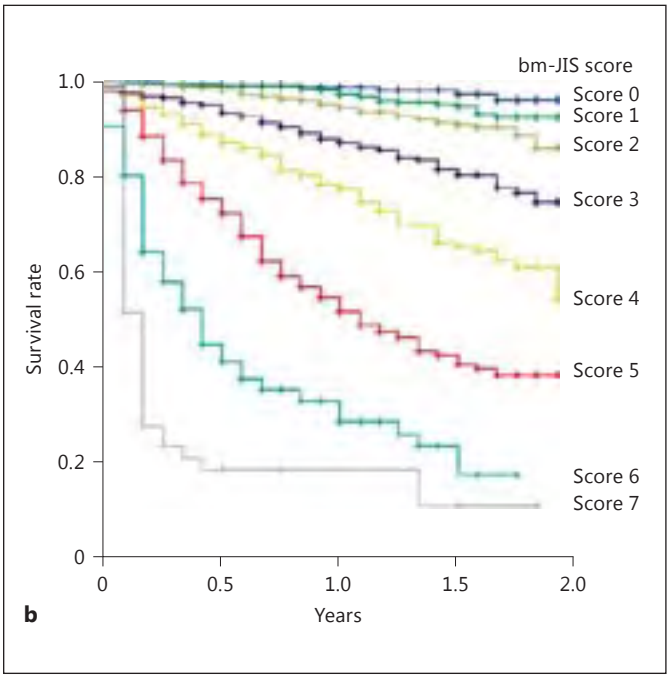

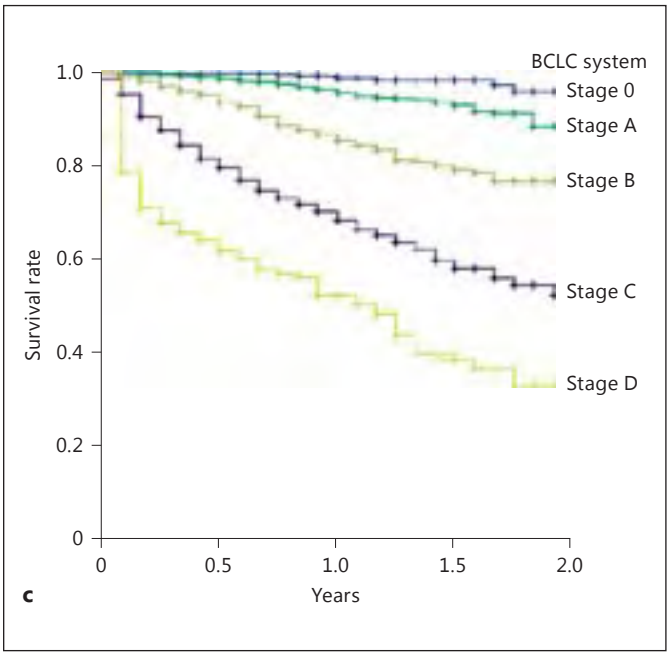

Color version available online

Fig. 1. OS rates according to the c-JIS score (**a**), the bm-JIS score (**b**) and the BCLC system (**c**) in 4,649 patients. Statistically significant differences in OS were observed among all c-JIS score groups ($p = 0.004$ for scores of 0–1 and $p < 0.0001$ for each score from 1 to 5). Similarly, HCC patients with different bm-JIS scores had significantly different OS ($p = 0.011$ for scores of 1–2 and $p < 0.0001$ for each score from 2 to 7), except for scores of 0–1 ($p = 0.076$). Furthermore, statistically significant differences in OS were observed among all BCLC stages ($p < 0.0001$).

was hepatitis C virus infection (75.3%). Approximately 72.3% of the patients were classified as Child-Pugh stage A. Most patients (95.6%) received some kind of treatment. In total, 874 patients (18.7%) were positive for AFP, 1,338 patients (28.7%) for AFP-L3, and 1,762 patients (37.9%) for DCP, with positivity being defined as a level above the cut-off value.

Clinical Factors Associated with Survival in HCC Patients

Univariate and multivariate analyses were performed to determine the factors contributing to an improved OS in HCC patients, and the results are shown in table 3. Multivariate analysis revealed that male sex, higher Child-Pugh score, tumor size >2.0 cm, multiple tumors, vascu-

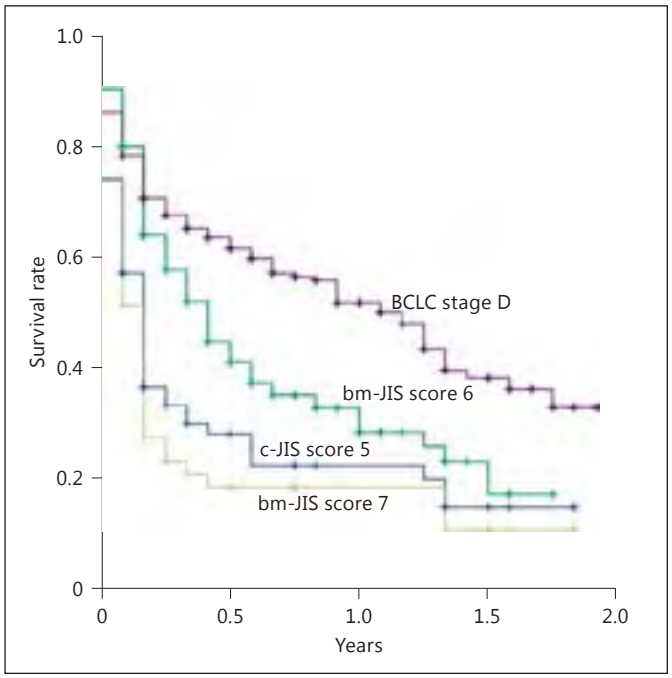

Fig. 2. When the Kaplan-Meier curves for the worst prognostic subgroups (i.e., c-JIS score of 5, bm-JIS score of 7 and BCLC stage D) were compared, there were significant differences between the bm-JIS score and the BCLC system as well as the c-JIS score and the BCLC system ($p < 0.0001$ for each comparison). Furthermore, when BCLC stage D was compared with the second worst bm-JIS score of 6, significant differences were also observed ($p < 0.0001$).

Color version available online

Table 4. Patient distribution, 2-year survival rate and mean survival time according to the bm-JIS score, the c-JIS score and the BCLC system (n = 4,649)

Staging system	n	%	2-year survival rate	Mean survival
bm-JIS score				
0	511	11.0	96.5%	22.7 months
1	871	18.8	92.8%	22.4 months
2	964	20.7	86.4%	21.9 months
3	839	18.0	75.0%	20.3 months
4	711	15.3	54.5%	18.1 months
5	517	11.1	38.6%	13.7 months
6	177	3.8	17.7%	8.2 months
7	59	1.3	11.4%	4.8 months
c-JIS score				
0	661	14.2	94.5%	22.6 months
1	1,222	26.3	88.9%	22.0 months
2	1,348	29.0	78.2%	20.6 months
3	1,038	22.3	52.7%	16.9 months
4	302	6.5	30.3%	12.1 months
5	79	1.7	15.3%	5.9 months
BCLC system				
0	601	13.0	96.1%	22.7 months
A	1,535	33.0	88.6%	22.1 months
B	916	19.7	76.9%	20.1 months
C	1,317	28.3	52.3%	16.5 months
D	280	6.0	33.4%	12.3 months

lar invasion, higher AFP level, higher DCP level, higher AFP-L3 level and a performance status of 3–4 were independent risk factors ($p = 0.004$ for sex, $p = 0.003$ for number of tumors and $p < 0.0001$ for all other variables).

Patient Distribution, Survival and Stratification Ability of the c-JIS Score, the bm-JIS Score and the BCLC System

Comparisons of OS according to the three staging systems are shown in figure 1. Statistically significant differences in OS were observed among all c-JIS score groups ($p = 0.004$ for scores of 0–1 and $p < 0.0001$ for each score from 1 to 5). Similarly, HCC patients with different bm-JIS scores had significantly different OS ($p = 0.011$ for scores of 1–2 and $p < 0.0001$ for each score from 2 to 7), except for scores of 0–1 ($p = 0.076$). Furthermore, statistically significant differences in OS were observed among all BCLC stages ($p < 0.0001$). These results indicated good stratification ability of the three staging systems and their effective predictive value of OS. However, when the Kaplan-Meier curves for the worst prognostic subgroups (i.e., c-JIS score of 5, bm-JIS score of 7 and BCLC stage D) were compared, there were significant differences between the bm-JIS score and the BCLC system as well as the c-JIS score and the BCLC system ($p < 0.0001$ for each comparison; fig. 2). Furthermore, when BCLC stage D was compared with the second worst bm-JIS score of 6, significant differences were also observed ($p < 0.0001$). Patient distribution, 2-year survival rate and median survival time according to the bm-JIS score, the c-JIS score and the BCLC system are shown in table 4. The median follow-up period was 9 months (range 1–24 months, from January 2004 to December 2005). The 2-year survival rates of the worst bm-JIS, c-JIS and BCLC subgroups were 11.4, 15.3 and 33.4%, respectively, whereas the corresponding median survival times were 4.8, 5.9 and 12.3 months, respectively.

Table 5 presents the independent homogenizing ability and stratification value of the c-JIS score, the bm-JIS score and the BCLC system as determined by the likeli-

Table 5. Evaluation of homogeneity and prognostic stratification according to the c-JIS score, the bm-JIS score and the BCLC system (all patients, n = 4,649)

Mode	Likelihood ratio (χ^2)	AIC
c-JIS score	972.7581	9,844.278
bm-JIS score	758.1041	10,054.93
BCLC system	679.6832	10,131.35

The model with a higher χ^2 value by the likelihood ratio test was considered the better model for discriminatory ability, homogeneity and monotonicity of gradients. Furthermore, lower values for AIC were considered better for discriminatory ability.

hood ratio test using the Cox proportional hazards regression model. The bm-JIS score had a higher χ^2 value (χ^2 = 972.7581) than the c-JIS score (χ^2 = 758.1041) and the BCLC system (χ^2 = 679.6832). Furthermore, a lower AIC value was obtained for the bm-JIS score (9,844.278) than for the c-JIS score (10,054.93) and the BCLC system (10,131.35), suggesting that the bm-JIS score was a better prognostic model than the c-JIS score and the BCLC system.

Discussion

In the prognostic assessment of HCC, the utilization of AFP, AFP-L3 and DCP for the detection and evaluation of tumor progression has been reported. AFP is a tumor marker that is routinely and most widely used for HCC surveillance and the evaluation of treatment efficacy [19–21]. On the other hand, AFP-L3 and DCP are well known to have an influence of malignancy grading. AFP-L3 production is largely related to the degree of biological malignancy of HCC [16, 22]. Moreover, a high level (>100 mAU/ml) of DCP is a risk factor for microvascular invasion [23]. The combination of AFP, AFP-L3 and DCP has also been proposed to be more useful than the use of each marker alone [15, 24]. In addition, positivity of these three tumor markers has clinical implications for advanced planning and appropriate management of HCC patients. Although several staging systems have been proposed to classify and estimate the prognosis of HCC patients, some of them, such as the Okuda classification, the BCLC system [3] and the c-JIS score [4], do not include tumor markers. Furthermore, the CLIP score [6], the GRETCH (Groupe d'Etude et de Traitement du Carcinome Hépatocellulaire) score [7] and the Chinese University Prognostic Index (CUPI) [8] only include AFP. These staging systems mainly combine liver function (i.e., Child-Pugh score: albumin, bilirubin, prothrombin time, hepatic encephalopathy and ascites), grade of cancer (i.e., tumor staging: number of tumors, tumor size, portal invasion, distant metastasis, tumor markers, etc.) and other factors (performance status, portal hypertension, etc.). In the present study, multivariate analysis revealed that higher AFP, AFP-L3 and DCP levels, besides others, were independent risk factors for OS. Such a result suggested that the measurement of these three tumor markers should be included in a staging system for HCC. Nonetheless, a possibly ideal system might need to consider not only the above-mentioned markers but also liver function as well as tumor status, as we previously reported [25].

In the worst subgroup analysis of this study, the bm-JIS score showed better stratification ability than the BCLC system. When the subgroups with bm-JIS scores of 6 and 7 were compared with that of BCLC stage D, significant differences were observed for each comparison. On the other hand, there were no significant differences between the subgroups with a bm-JIS score of 5 and BCLC stage D. Such a result indicated that the bm-JIS score evaluated patient prognosis more precisely than the BCLC system, especially in subgroups with poor prognosis. Likewise, the c-JIS score also evaluated patient prognosis more precisely than the BCLC system. We speculated that there might be two reasons for such findings. First, in the BCLC system, stage D was defined as the terminal stage (Child-Pugh score C or performance status of 3–4) regardless of tumor status. Therefore, patients classified into BCLC stage D were recommended the best supportive care. However, even in cases of very poor liver function, the utility of locoregional treatments (i.e., radiofrequency ablation and transcatheter arterial chemoembolization) has recently been reported from Japan [26, 27]. In fact, locoregional treatments for some HCC patients with decompensated cirrhosis were performed in Japan. The differences in treatment guidelines were part of the reason for such a result [28]. Second, several papers have reported difficulties to accurately diagnose minimal intrahepatic metastasis, microscopic portal invasion and distant metastasis by using imaging modalities [29, 30]. Therefore, the malignancy of a tumor might not be fully reflected on imaging findings alone. From this point of view, the bm-JIS score may stratify and predict the OS of HCC patients more accurately by evaluating three tumor markers as a useful index for malignancy grading.

In the present study, the c-JIS score, the bm-JIS score and the BCLC system showed good performance in accurately predicting patient survival. Moreover, the bm-JIS score also had better likelihood ratio test and AIC values, indicating its superior stratification ability and prognostic predictive power. Thus, our results suggest that the bm-JIS score was definitely the better staging model than the c-JIS score and the BCLC system.

However, there are some limitations in this study. First, the follow-up period was very short as this retrospective analysis used only data from the 18th annual nationwide survey. Therefore, it did not suffice to assess patients' OS especially in the early stage of the three staging systems. Second, there were inevitable selection biases owing to the retrospective nature of the study. Approximately three fourth of the available patients were excluded due to missing data (the variables needed for the bm-JIS score, the c-JIS score and the BCLC system staging). Further studies will be required to confirm our findings and validate them in different populations.

In conclusion, the bm-JIS score offered better stratification ability and prognostic predictive power than the c-JIS score and the BCLC system. Therefore, residual liver function, cancer grade and these three tumor markers should preferably be considered in a clinical staging system to more accurately predict the prognosis of HCC patients.

References

1 Jemal A, Bray F, Center MM, Ferlay J, Ward E, Forman D: Global cancer statistics. CA Cancer J Clin 2011;61:69–90.
2 Kim DY, Han KH: Epidemiology and surveillance of hepatocellular carcinoma. Liver Cancer 2012;1:2–14.
3 Llovet JM, Bru C, Bruix J: Prognosis of hepatocellular carcinoma: the BCLC staging classification. Semin Liver Dis 1999;19:329–338.
4 Kudo M, Chung H, Osaki Y: Prognostic staging system for hepatocellular carcinoma (CLIP score): its value and limitations, and a proposal for a new staging system, the Japan Integrated Staging Score (JIS score). J Gastroenterol 2003;38:207–215.
5 Kitai S, Kudo M, Minami Y, Ueshima K, Chung H, Hagiwara S, Inoue T, Ishikawa E, Takahashi S, Asakuma Y, Haji S, Osaki Y, Oka H, Seki T, Kasugai H, Sasaki Y, Matsunaga T: A new prognostic staging system for hepatocellular carcinoma: value of the biomarker combined Japan integrated staging score. Intervirology 2008;51(suppl 1):86–94.
6 A new prognostic system for hepatocellular carcinoma: a retrospective study of 435 patients: the Cancer of the Liver Italian Program (CLIP) investigators. Hepatology 1998;28:751–755.
7 Chevret S, Trinchet JC, Mathieu D, Rached AA, Beaugrand M, Chastang C: A new prognostic classification for predicting survival in patients with hepatocellular carcinoma. Groupe d'Etude et de Traitement du Carcinome Hépatocellulaire. J Hepatol 1999;31:133–141.
8 Forner A, Llovet JM, Bruix J: Hepatocellular carcinoma. Lancet 2012;379:1245–1255.
9 Leung TW, Tang AM, Zee B, Lau WY, Lai PB, Leung KL, Lau JT, Yu SC, Johnson PJ: Construction of the Chinese University Prognostic Index for hepatocellular carcinoma and comparison with the TNM staging system, the Okuda staging system, and the Cancer of the Liver Italian Program staging system: a study based on 926 patients. Cancer 2002;94:1760–1769.
10 The Liver Cancer Study Group of Japan: The General Rules for the Clinical and Pathological Study of Primary Liver Cancer (ed 5, revised, in Japanese). Tokyo, Kanehara, 2009.
11 Kudo M, Chung H, Haji S, Osaki Y, Oka H, Seki T, Kasugai H, Sasaki Y, Matsunaga T: Validation of a new prognostic staging system for hepatocellular carcinoma: the JIS score compared with the CLIP score. Hepatology 2004;40:1396–1405.
12 Toyoda H, Kumada T, Kiriyama S, Sone Y, Tanikawa M, Hisanaga Y, Yamaguchi A, Isogai M, Kaneoka Y, Washizu J: Comparison of the usefulness of three staging systems for hepatocellular carcinoma (CLIP, BCLC, and JIS) in Japan. Am J Gastroenterol 2005;100:1764–1771.
13 Kondo K, Chijiiwa K, Nagano M, Hiyoshi M, Kai M, Maehara N, Ohuchida J, Nakao H, Ohkuwa Y: Comparison of seven prognostic staging systems in patients who undergo hepatectomy for hepatocellular carcinoma. Hepatogastroenterology 2007;54:1534–1538.
14 Chung H, Kudo M, Takahashi S, Hagiwara S, Sakaguchi Y, Inoue T, Minami Y, Ueshima K, Fukunaga T, Matsunaga T: Comparison of three current staging systems for hepatocellular carcinoma: Japan integrated staging score, new Barcelona Clinic Liver Cancer staging classification, and Tokyo score. J Gastroenterol Hepatol 2008;23:445–452.
15 Song P, Gao J, Inagaki Y, Kokudo N, Hasegawa K, Sugawara Y, Tang W: Biomarkers: evaluation of screening for and early diagnosis of hepatocellular carcinoma in Japan and China. Liver Cancer 2013;2:31–39.
16 Kudo M: Alpha-fetoprotein-L3: useful or useless for hepatocellular carcinoma? Liver Cancer 2013;2:151–152.
17 Toyoda H, Kumada T, Osaki Y, Oka H, Urano F, Kudo M, Matsunaga T: Staging hepatocellular carcinoma by a novel scoring system (BALAD score) based on serum markers. Clin Gastroenterol Hepatol 2006;4:1528–1536.
18 Akaike H: A new look at statistical model identification. IEEE Trans Automat Contr 1974;19:716–722.
19 Oka H, Tamori A, Kuroki T, Kobayashi K, Yamamoto S: Prospective study of alpha-fetoprotein in cirrhotic patients monitored for development of hepatocellular carcinoma. Hepatology 1994;19:61–66.
20 Riaz A, Ryu RK, Kulik LM, Mulcahy MF, Lewandowski RJ, Minocha J, Ibrahim SM, Sato KT, Baker T, Miller FH, Newman S, Omary R, Abecassis M, Benson AB 3rd, Salem R: Alpha-fetoprotein response after locoregional therapy for hepatocellular carcinoma: oncologic marker of radiologic response, progression, and survival. J Clin Oncol 2009;27:5734–5742.
21 Shao YY, Hsu CH, Cheng AL: Predictive biomarkers of antiangiogenic therapy for advanced hepatocellular carcinoma: where are we? Liver Cancer 2013;2:93–107.
22 Tamura Y, Igarashi M, Suda T, Wakai T, Shirai Y, Umemura T, Tanaka E, Kakizaki S, Takagi H, Hiasa Y, Onji M, Aoyagi Y: Fucosylated fraction of alpha-fetoprotein as a predictor of prognosis in patients with hepatocellular carcinoma after curative treatment. Dig Dis Sci 2010;55:2095–2101.
23 Yamashita Y, Tsuijita E, Takeishi K, Fujiwara M, Kira S, Mori M, Aishima S, Taketomi A, Shirabe K, Ishida T, Maehara Y: Predictors for microinvasion of small hepatocellular carcinoma ≤ 2 cm. Ann Surg Oncol 2012;19:2027–2034.

24 Hamamura K, Shiratori Y, Shiina S, Imamura M, Obi S, Sato S, Yoshida H, Omata M: Unique clinical characteristics of patients with hepatocellular carcinoma who present with high plasma des-gamma-carboxy prothrombin and low serum alpha-fetoprotein. Cancer 2000;88:1557–1564.
25 Kitai S, Kudo M, Minami Y, Haji S, Osaki Y, Oka H, Seki T, Kasugai H, Sasaki Y, Matsunaga T: Validation of a new prognostic staging system for hepatocellular carcinoma: A comparison of the biomarker-combined Japan Integrated Staging Score, the conventional Japan Integrated Staging Score and the BALAD Score. Oncology 2008;75(suppl 1):83–90.
26 Nouso K, Ito Y, Kuwaki K, Kobayashi Y, Nakamura S, Ohashi Y, Yamamoto K: Prognostic factors and treatment effects for hepatocellular carcinoma in Child C cirrhosis. Br J Cancer 2008;98:1161–1165.
27 Kudo M, Osaki Y, Matsunaga T, Kasugai H, Oka H, Seki T: Hepatocellular carcinoma in Child-Pugh C cirrhosis: prognostic factors and survival benefit of nontransplant treatments. Dig Dis 2013;31:490–498.
28 Kudo M, Izumi N, Kokudo N, Matsui O, Sakamoto M, Nakashima O, Kojiro M, Makuuchi M: Management of hepatocellular carcinoma in Japan: Consensus-based clinical practice guidelines proposed by the Japan Society of Hepatology (JSH) 2010 updated version. Dig Dis 2011;29:339–364.
29 Yamashita F, Tanaka M, Satomura S, Tanikawa K: Prognostic significance of *Lens culinaris* agglutinin A-reactive alpha-fetoprotein in small hepatocellular carcinomas. Gastroenterology 1996;111:996–1001.
30 Koike Y, Shiratori Y, Sato S, Obi S, Teratani T, Imamura M, Yoshida H, Shiina S, Omata M: Des-gamma-carboxy prothrombin as a useful predisposing factor for the development of portal venous invasion in patients with hepatocellular carcinoma: a prospective analysis of 227 patients. Cancer 2001;91:561–569.

Original Article

Digestive Diseases

Dig Dis 2014;32:733–739
DOI: 10.1159/000368013

Decreased Blood Flow after Sorafenib Administration Is an Imaging Biomarker to Predict Overall Survival in Patients with Advanced Hepatocellular Carcinoma

Tadaaki Arizumi Kazuomi Ueshima Hirokazu Chishina Masashi Kono
Masahiro Takita Satoshi Kitai Tatsuo Inoue Norihisa Yada Satoru Hagiwara
Yasunori Minami Toshiharu Sakurai Naoshi Nishida Masatoshi Kudo

Department of Gastroenterology and Hepatology, Kinki University Faculty of Medicine, Osaka-Sayama, Japan

Key Words
Arterial blood flow · Hepatocellular carcinoma · Overall survival · Sorafenib · Tumor staining

Abstract
Background: Sorafenib is a multikinase inhibitor targeting Raf and protein tyrosine kinases, which are involved in cell growth and tumor angiogenesis. Sorafenib administration induces temporary inhibition of tumor growth and a decrease in arterial blood flow in a considerable number of hepatocellular carcinoma (HCC) patients. We retrospectively evaluated the association between decreased blood flow and the overall survival (OS) of HCC patients after the initiation of sorafenib therapy. ***Patients and Methods:*** Therapeutic responses of 158 advanced HCC patients with hypervascular tumors who had received sorafenib for more than 1 month were analyzed. To assess their therapeutic response, patients underwent radiological evaluation before and every 4–6 weeks after the initiation of sorafenib treatment. After the classification of patients into three groups based on the change in arterial enhancement during treatment (no change, decrease and disappearance), the OS of each group was compared using the Kaplan-Meier method. ***Results:*** Statistically significant differences in OS were observed among the three groups ($p < 0.001$). A decrease or disappearance of arterial enhancement was significantly associated with improved OS compared to patients with no change in arterial enhancement; the median OS was 19.9 months (95% confidence interval, CI, 16.4–24.5 months) and 6.0 months (95% CI, 4.0–8.8 months), respectively ($p < 0.001$). However, there was no difference in OS between the decrease and disappearance groups ($p = 0.88$). ***Conclusion:*** We conclude that decreased arterial enhancement during sorafenib treatment was associated with the longest OS and could therefore reflect an effective response.

Introduction

Hepatocellular carcinoma (HCC) is currently ranked as the fifth most common cancer and the third leading cause of cancer-related death worldwide [1, 2]. Because

KARGER

E-Mail karger@karger.com
www.karger.com/ddi

0257–2753/14/0326–0733$39.50/0

Masatoshi Kudo, MD, PhD
Department of Gastroenterology and Hepatology
Kinki University Faculty of Medicine
377-2 Ohno-Higashi, Osaka-Sayama 589-8511 (Japan)
E-Mail m-kudo@med.kindai.ac.jp

most patients are diagnosed at advanced stages, only about 30% of patients presenting with early-stage tumors undergo potentially curative therapies, such as surgical resection [3, 4], transplantation [5, 6] or percutaneous ablation [7–9]. In contrast, patients with unresectable HCC usually receive palliative treatments, such as transarterial chemoembolization (TACE) [10], radiotherapy [11, 12] or conventional chemotherapy [13], and some patients participate in clinical trials [10, 14–17]. Among these options, only TACE has been shown to lead to survival benefits [18, 19]. However, its application is often limited due to the presence of vascular invasion or extrahepatic spread [20–23].

Sorafenib, a small-molecule multikinase inhibitor [24], was the first systemic agent that was proven to prolong survival in patients with advanced HCC in two phase III trials [25, 26], and it is now the standard of care for systemically treated patients [13, 22, 27–30]. Sorafenib inhibits Raf protein kinase and receptor tyrosine kinases, including platelet-derived growth factor receptor and vascular endothelial growth factor receptor, which is involved in the neovascularization of HCC. In addition, sorafenib also inhibits Flt-3 and c-KIT, which are both involved in neovascularization and cellular growth [31–33]. However, because both trials were assessed using the Response Evaluation Criteria in Solid Tumors 1.1 (RECIST1.1), altered arterial enhancement and its association with overall survival (OS) in sorafenib-treated patients has not been evaluated thus far [34].

We reported that the modified RECIST (mRECIST) and the Response Evaluation Criteria in Cancer of the Liver (RECICL), which include the assessment of arterial tumor enhancement, are useful for evaluating therapeutic effects for HCC patients [35, 36]. Indeed, it has been reported that for patients treated with sorafenib, OS is better reflected by mRECIST than RECIST1.1 [37, 38], suggesting that a consequence of effective treatment may be the disappearance of tumor staining. Therefore, the association between decreased arterial enhancement and OS should be clarified.

In this study, we retrospectively examined the relationship between alterations in arterial enhancement determined by imaging and the survival of HCC patients who presented with hypervascular tumors and received sorafenib treatment. We demonstrated that patients with decreased tumor enhancement clearly demonstrated better OS than patients whose tumor staining remained unchanged. Therefore, a change in tumor enhancement should be a surrogate marker of tumor response after the initiation of sorafenib therapy.

Patients and Methods

Patients

Between May 2009 and November 2012, 269 patients with advanced HCC were treated with sorafenib at the Kinki University Hospital, and 158 patients who had received continuous sorafenib administration and met the inclusion criteria were selected for this retrospective study. Their response to sorafenib had been examined at least once using contrast-enhanced computed tomography (CE-CT) and/or dynamic magnetic resonance imaging (MRI).

The inclusion criteria for this study were: (1) a diagnosis of HCC based on histological examination or radiological findings showing early enhancement, followed by late washout on CE-CT or dynamic MRI in conjunction with HCC refractory to radiofrequency ablation and TACE based on the indications for sorafenib; (2) a performance status of 0 or 1, and (3) Child-Pugh class A or B. Exclusion criteria were: (1) concomitant antineoplastic treatment; (2) prior treatment with TACE or radiofrequency ablation less than 3 months before initiation of sorafenib treatment, and (3) lack of a response, which was assessed using CE-CT or dynamic MRI during the follow-up period.

Initial and Follow-Up Assessments

Liver function and tumor stage were evaluated using the Child-Pugh and Barcelona Clinic for Liver Cancer (BCLC) classifications. CE-CT images were obtained during the arterial (40 s) and portal (70 s) phases using 120 ml of iomeprol at a flow rate of 3 ml/s. Dynamic MRI scans were performed with gadolinium-ethoxybenzyl-diethylenetriamine pentaacetic acid (Gd-EOB-DTPA) enhancement during the arterial (22–35 s after injection) and portal venous (70 s after injection) phases using a T1-weighted high-resolution sequence in a single breath hold. The CE-CT and Gd-EOB-DTPA-MRI scans were reviewed by two independent radiologists, and the size and arterial enhancement of the tumors were evaluated every 4–6 weeks during and after treatment. Every CT and Gd-EOB-DTPA-MRI scan was reviewed retrospectively by two independent hepatologists. Responses after initiation of treatment were evaluated separately according to mRECIST in a non-blinded fashion (online suppl. table 1; for all online suppl. material, see www.karger.com/doi/10.1159/000368013) [35]. The target lesions were defined by both physicians for all patients on their CT and/or MRI scans before treatment. Extrahepatic lesions were assessed, as required, by chest radiography, bone scintigraphy or fluorodeoxyglucose positron emission tomography. Tumor markers were also measured every 4–6 weeks to assess tumor growth. OS analysis ended at the time of death or was censored at the time of the last follow-up visit. The criteria for sorafenib discontinuation were: (1) determination of progressive disease (PD) based on mRECIST, such as obvious tumor progression and/or onset of a new lesion; (2) grade 3 or greater adverse reactions that could not be controlled for by dose reduction or interruption based on the Common Terminology Criteria for Adverse Events, version 4.0 (http://ctep.cancer.gov/protocolDevelopment/electronic_applications/docs/ctcaev3.pdf), and (3) noncompliance with oral drug treatment and/or follow-up visits.

Tumor Classification Based on Arterial Enhancement

The lesions analyzed in this study were a maximum of five lesions when more than five intrahepatic lesions were present. For the classification based on alterations in arterial enhancement, the

Table 1. Comparison of characteristics of patients in the NC, DA and DEC groups

	NC group	DA group	DEC group	p value
Median age (25–75%), years	71 (64–77)	73 (65–77)	73 (68–77)	0.63
Gender				
Male	47	47	26	
Female	14	11	13	0.25
ECOG performance status				
0	60	58	38	
1	1	0	1	0.71
Child-Pugh class				
A	51	44	33	
B	10	14	6	0.24
Virus status[1]				
HBV	12	8	6	
HCV	30	37	18	
NBNC	19	13	15	0.52
BCLC stage				
A	6	12	10	
B	16	15	10	
C	39	31	19	0.15
Starting dose of sorafenib				
200 mg	3	1	1	
400 mg	25	20	18	
800 mg	33	37	20	0.38
Median serum AFP level (25–75%), ng/ml	324 (24–4,732)	99 (11–4,614)	131 (8–297)	0.52
Median serum DCP (25–75%), mAU/ml	1,703 (172–11,800)	859 (58–4,794)	579 (44–8,153)	0.52

ECOG = Eastern Cooperative Oncology Group; AFP = α-fetoprotein; DCP = des-γ-carboxyprothrombin. [1]Patients testing positive for HBV surface antigen were regarded as cases of HBV-related HCC and patients testing positive for HCV antibody were regarded as cases of HCV-related HCC.

decrease group (DEC) was defined as patients showing a clear decrease in part or the entire area of tumor staining after the administration of sorafenib, while the disappearance group (DA) comprised patients showing disappearance of tumor staining within a part of the tumor area or a complete disappearance of tumor staining in all phases (i.e. the arterial, portal and late phases). The DEC group was defined as a >15% decrease in tumor density in the early phase using CT. The no change (NC) group did not meet the criteria of the DEC and DA groups regarding tumor density on a CT scan. The NC group comprised patients with neither a clear decrease nor a disappearance of tumor staining after sorafenib administration. We compared OS among these three groups. The response group consists of patients showing DEC or DA. We compared OS among the previously mentioned three groups, as well as between the response and NC groups.

Statistical Analysis

Univariate survival curves were estimated using the Kaplan-Meier method. Survival rates among groups were compared using the log-rank test, and categorical variables were compared using the χ^2 test. For multiple comparisons, the Bonferroni correction was applied. The level of significance was set at $p < 0.05$. All analyses were performed using SAS statistical software (version 8.2; SAS Institute, Cary, N.C., USA) or the SPSS Medical Pack for Windows (version 10.0; SPSS, Inc., Chicago, Ill., USA).

Results

Characteristics of the Patients Enrolled in the Study

The median OS of the entire cohort was 16.7 months (95% confidence interval, CI, 10.6–22.8 months). The numbers of patients with a complete response (CR), partial response (PR), stable disease (SD) and PD were 6, 30, 52 and 70, respectively. The response rate and disease control rate (DCR) estimated by mRECIST were 23.4 and 54.5%, respectively. Eighty-five patients (53.8%) were positive for anti-hepatitis C virus (HCV) antibody and were thus considered to have HCV-related HCC, while 26 patients (16.5%) had tested positive for hepatitis B vi-

rus (HBV) surface antigen and 47 patients (29.7%) had tested negative for both HCV antibody and HBV surface antigen. One hundred fifty-six patients were asymptomatic (performance status 0) and 69 patients (43.7%) were classified as BCLC stage A or B. One hundred twenty-eight patients (81.0%) were Child-Pugh class A.

Classification of Patients according to Alterations in Tumor Staining after the Initiation of Sorafenib

Sixty-one patients showed no change in tumor staining (NC group), while 97 patients showed a decrease in the entire area or part of the area of tumor staining. Of these 97 patients, 58 showed a complete disappearance of tumor staining in the arterial, portal and late phases (DA group), while 39 patients showed decreased tumor staining in terms of staining intensity compared to the staining before sorafenib administration in the arterial phase (DEC group). The characteristics of the patients in the three groups are summarized in table 1. The NC group consisted of 47 men and 14 women with a median age of 71 years; 51 were Child-Pugh class A and 10 Child-Pugh class B. From the NC group, 12, 30 and 19 patients had HBV-, HCV- and non-B, non-C (NBNC)-related HCC, respectively. The DEC group consisted of 26 men and 13 women with a median age of 73 years; 33 patients had liver cirrhosis of Child-Pugh class A and 6 patients were Child-Pugh grade B. From the DEC group, 6, 18 and 15 patients had HBV-, HCV- and NBNC-related HCC, respectively. The DC group consisted of 47 men and 11 women with a median age of 73 years; 44 patients were Child-Pugh class A and 14 patients Child-Pugh class B, while 8, 37 and 13 patients had HBV-, HCV- and NBNC-related HCC, respectively. With regard to patient characteristics, there were no statistically significant differences among the three groups. Among the patients analyzed, tumor responses were classified using the mRECIST system and were as follows: CR = 0, PR = 4, SD = 20 and PD = 37 patients in the NC group; CR = 2, PR = 7, SD = 18 and PD = 12 patients in the DEC group, and CR = 4, PR = 19, SD = 14 and PD = 21 patients in the DA group. According to RECICL, tumor response was classified as CR in 0, PR in 4, SD in 19 and PD in 38 patients in the NC group; as CR in 2, PR in 7, SD in 17 and PD in 13 patients in the DEC group, and as CR in 4, PR in 22, SD in 14 and PD in 18 patients in the DA group. When evaluated by mRECIST and RECICL systems, both the DEC and the DA group were associated with a higher objective response rate (ORR) and DCR compared to the NC group. Among the three groups, the highest ORR was observed in the DA group (table 2).

Table 2. Classification of the response to sorafenib by mRECIST and RECICL

	CR	PR	SD	PD	Total	ORR, %	DCR, %
mRECIST							
DA	4	19	14	21	58	39.7	63.8
DEC	2	7	18	12	39	23.1	69.2
NC	0	4	20	37	61	6.6	39.3
Total	6	30	52	70	158	23.4	54.5
RECICL							
DA	4	22	14	18	58	44.8	69.0
DEC	2	7	17	13	39	23.1	66.7
NC	0	4	19	38	61	6.6	37.7
Total	6	33	50	69	158	24.7	56.3

The number of patients classified as CR, PR, SD and PD using each system are shown. ORR is the percentage of patients evaluated as CR or PR. DCR is the percentage of patients evaluated as CR, PR or SD.

Relationship between Disappearance/Decrease of Tumor Staining and OS

The median OS was 6 months (95% CI, 4.0–8.8 months) in the NC group, 20.8 months (95% CI, 11.8–29.8 months) in the DEC group and 18.8 months (95% CI, 14.8–22.8 months) in the DA group. These differences between the groups were statistically significant. Patients of the NC group showed significantly shorter OS than patients of the DA group ($p < 0.001$) and the DEC group ($p = 0.003$). No difference in OS was detected between patients of the DEC and DA groups ($p = 0.88$; fig. 1a).

To further clarify the impact of altered enhancement during sorafenib treatment, we combined the DEC and DA groups as the response group and compared the OS of this group with that of the NC group. The response group comprised 73 men and 24 women with a median age of 73 years; 76 patients were Child-Pugh class A and 20 were Child-Pugh class B; 14, 55 and 28 patients had HBV-, HCV- and NBNC-related HCC, respectively. There were no statistically significant differences in patient characteristics between the NC group and the response group (online suppl. table 2). According to the mRECIST system, 6 patients had CR, 26 patients had PR, 32 patients had SD and 33 patients had PD in the response group. Both ORR and DCR were increased in the response group compared to the NC group when evaluated by mRECIST and RECICL. OS of the response group was significantly different from that of the NC group ($p <$

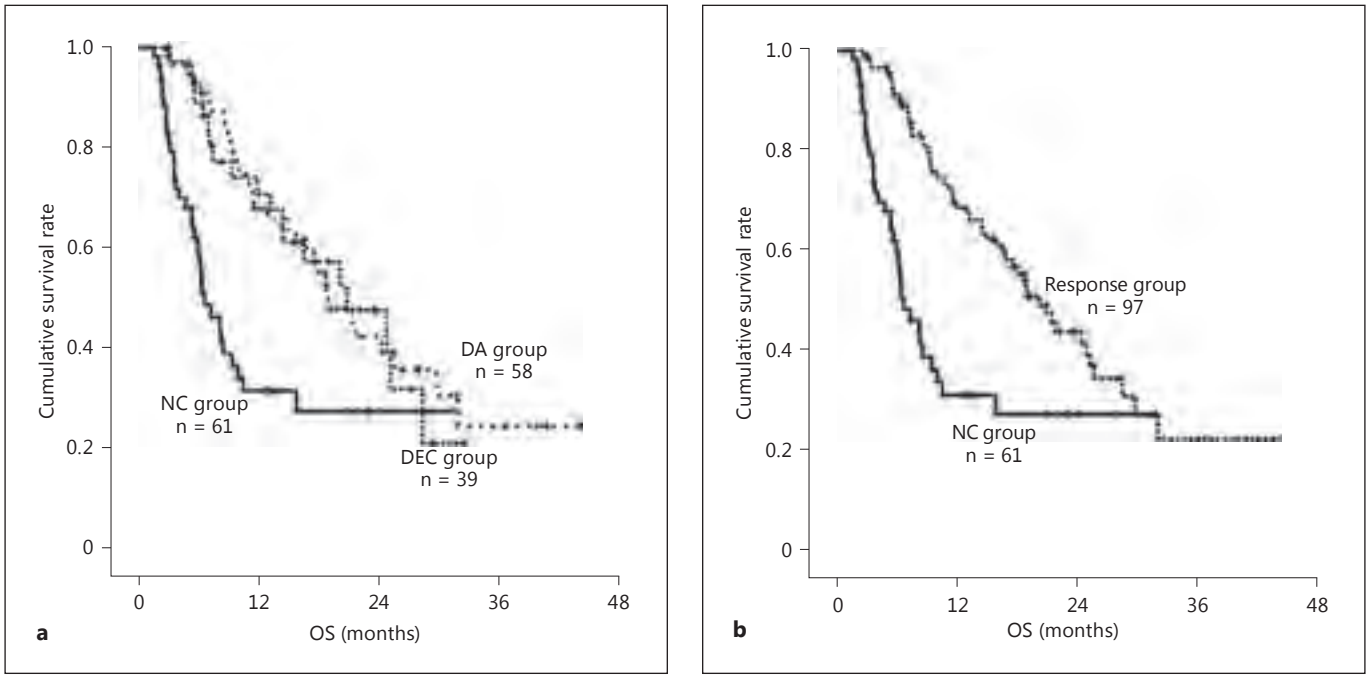

Fig. 1. **a** Kaplan-Meier curves of OS for 158 patients treated with sorafenib are shown for the DA, DEC and NC groups. The median OS of the DA, DEC and NC groups were 18.8 months (95% CI, 14.8–22.8 months), 20.8 months (95% CI, 11.8–29.8 months), and 6.0 months (95% CI, 4.0–8.8 months), respectively ($p < 0.001$). The differences between the NC group and both the DA and DEC groups were statistically significant ($p = 0.002$ and $p < 0.001$, respectively). The difference between the DA and DEC groups was nonsignificant ($p = 0.88$). **b** Kaplan-Meier curves of OS for 158 patients treated with sorafenib are shown for the response and NC groups. The median OS of the response group was 19.9 months (95% CI, 16.4–24.5 months). The difference in OS between the NC and response groups was statistically significant ($p < 0.001$).

0.001), with a median OS of 19.9 months (95% CI, 16.4–23.5 months) in the response group and 20.8 months (95% CI, 11.8–29.8 months) in the NC group (fig. 1b).

Relationship between Disappearance/Decrease of Tumor Staining and OS in Patients Evaluated as PD by mRECIST

According to mRECIST, tumor response was classified as CR in 6 and PR in 30 (objective response, OR), SD in 52 and PD in 70 patients. We further classified the patients with PD into two subgroups: the response PD was defined as patients with PD but a clear decrease or disappearance of tumor enhancement after sorafenib administration, while the no-response PD group consisted of patients without any change in tumor enhancement. Comparisons of the survival curves showed that the median OS was 25.4 months (95% CI, 13.4–37.4 months) in the tumor response group, 20.8 months (95% CI, 12.7–28.9 months) in the SD group, 11.4 months (95% CI, 8.1–14.7 months) in the response PD group and 5.4 months (95% CI, 4.3–6.5 months) in the no-response PD group. The no-response PD group showed significantly shorter OS than both the SD group ($p < 0.001$) and the response PD group ($p = 0.002$). Although the response PD group showed shorter OS than the SD group, OS was not significantly different between the two groups ($p = 0.050$; fig. 2).

Discussion

In this study, patients who showed complete disappearance of tumor staining, which reflects necrosis of HCC lesions, showed better OS than the patients of the NC group. In addition, a better OS was also observed in the DEC group compared to the NC group, suggesting that a decreased arterial blood flow could be a partial effect of sorafenib. On the other hand, OS did not differ between DA and DEC groups. Based on the results of the present analyses, a decrease in arterial blood flow could lead to partial treatment effects in terms of OS compared to patients with disappearance of enhancement, where tumor necrosis was expected.

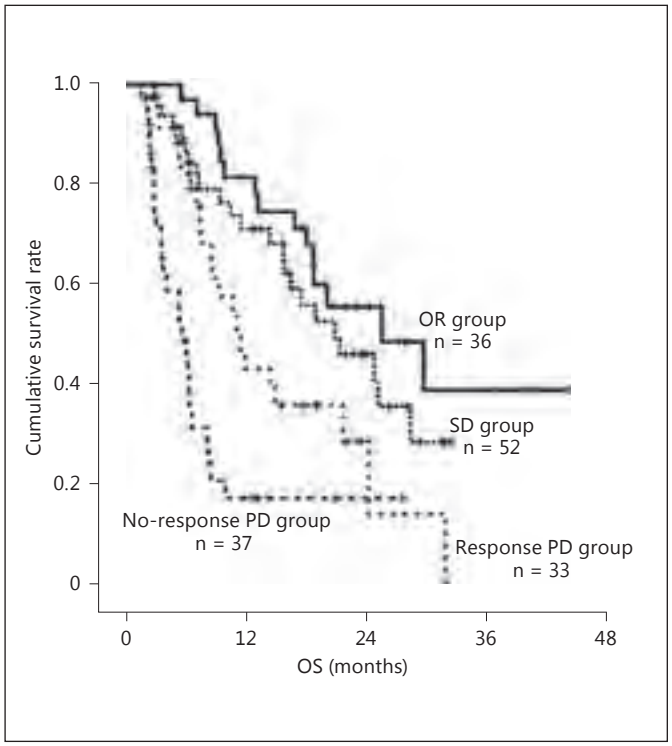

Fig. 2. Kaplan-Meier curves of OS for 158 patients treated with sorafenib are shown for the OR, SD, response PD and no-response PD groups. The median OS of the OR, SD, response PD and no-response PD groups were 25.4 months (95% CI, 13.4–37.4 months), 20.8 months (95% CI, 12.7–28.9 months), 11.4 months (95% CI, 8.1–14.7 months) and 5.4 months (95% CI, 4.3–6.5 months), respectively. Differences between the no-response PD group and both the SD and response PD groups were statistically significant ($p < 0.001$ and $p = 0.002$, respectively). Differences between the SD and response PD groups, and between the OR and SD groups were nonsignificant ($p = 0.050$ and 0.245, respectively).

Currently, RECIST1.1, mRECIST and RECICL are mainly used to evaluate tumor response during treatment of HCC. RECIST1.1 are the simplest criteria where tumor necrosis is not taken into consideration and only the largest tumor diameter is assessed. However, as OS was better in patients showing a disappearance or decrease of tumor blood flow, alterations in tumor enhancement apparently reflect tumor response in HCC treatment. As our results suggest that decreased blood flow is of prognostic significance, it is conceivable to speculate that applying the assessment of tumor enhancement is more important than evaluating the decrease in tumor size during sorafenib treatment.

When treating advanced HCC patients with sorafenib, complete disappearance of tumor staining is considered to reflect tumor necrosis, while decreased tumor staining may represent the presence of variable tumors due to the presence of blood flow. While the disappearance or lack of disappearance of blood flow is included in the evaluation criteria in mRECIST and RECICL, decreased blood flow is not taken into consideration among these criteria. In this study, OS was longer in patients of the response group in terms of tumor enhancement. The decrease in blood flow could induce temporary inhibition of tumor growth, thereby suppressing HCC progression. In addition, among patients showing PD, those with response PD had better OS than those with no-response PD. From this point of view, patients with response PD should not stop sorafenib treatment even if they were regarded as PD according to the conventional criteria.

In this study, we also encountered patients who showed decreased tumor staining with administration of sorafenib, but still showed tumor enlargement. Although improvement in OS was observed in the group showing a decrease or disappearance of tumor enhancement, some patients with decreased tumor blood flow still showed a short survival (<6 months). It is also known that poorly differentiated HCC can sometimes represent the decrease in arterial blood flow that reflects arterial abnormalities [39]. Because the decrease in tumor blood flow is sometimes associated with malignant transformation, the clinical course must be carefully followed even if patients display disappearance or decrease of enhancement during treatment.

This study has two major limitations that may reduce the generalizability of our results to other populations with advanced HCC. First, because the determination of tumor enhancement is not quantitative, it might reflect interphysician differences in terms of image interpretations. The measurement of tumor enhancement might also be affected by the timing of the imaging. Second, due to the retrospective nature of the study, there could be a bias regarding patient selection. To address these limitations and independently validate the results of this investigation, we are currently designing a prospective multicenter study in a larger patient cohort.

In conclusion, even if tumor blood flow has not completely disappeared, prolonged survival of patients with advanced HCC can be expected with sorafenib treatment if the tumor blood flow decreases, even when tumor necrosis is not achieved. This result should be of importance for the management of HCC patients receiving sorafenib treatment.

References

1 Jemal A, Siegel R, Ward E, Hao Y, Xu J, Murray T, Thun MJ: Cancer statistics, 2008. CA Cancer J Clin 2008;58:71–96.
2 Kim DY, Han KH: Epidemiology and surveillance of hepatocellular carcinoma. Liver Cancer 2012;1:2–14.
3 Belghiti J, Fuks D: Liver resection and transplantation in hepatocellular carcinoma. Liver Cancer 2012;1:71–82.
4 Mise Y, Sakamoto Y, Ishizawa T, Kaneko J, Aoki T, Hasegawa K, Sugawara Y, Kokudo N: A worldwide survey of the current daily practice in liver surgery. Liver Cancer 2013;2:55–66.
5 Lee Cheah Y, Chow PKH: Liver transplantation for hepatocellular carcinoma: an appraisal of current controversies. Liver Cancer 2012;1:183–189.
6 Chan SC: Liver transplantation for hepatocellular carcinoma. Liver Cancer 2013;2:338–344.
7 Bruix J, Llovet JM: Prognostic prediction and treatment strategy in hepatocellular carcinoma. Hepatology 2002;35:519–524.
8 Park KW, Park JW, Choi JI, Kim TH, Kim SH, Park HS, Lee WJ, Park SJ, Hong EK, Kim CM: Survival analysis of 904 patients with hepatocellular carcinoma in a hepatitis B virus-endemic area. J Gastroenterol Hepatol 2008;23:467–473.
9 Lin SM: Local ablation for hepatocellular carcinoma in Taiwan. Liver Cancer 2013;2:73–83.
10 Lencioni R: Chemoembolization in patients with hepatocellular carcinoma. Liver Cancer 2012;1:41–50.
11 Jihye C, Seong J: Application of radiotherapeutic strategies in the BCLC-defined stages of hepatocellular carcinoma. Liver Cancer 2012;1:216–225.
12 Lee DS, Seong J: Radiotherapeutic options for hepatocellular carcinoma with portal vein tumor thrombosis. Liver Cancer 2014;3:18–30.
13 Peck-Radosavljevic M: Drug therapy for advanced-stage liver cancer. Liver Cancer 2014;3:125–131.
14 Benson AB 3rd, Abrams TA, Ben-Josef E, Bloomston PM, Botha JF, Clary BM, Covey A, Curley SA, D'Angelica MI, Davila R, Ensminger WD, Gibbs JF, Laheru D, Malafa MP, Marrero J, Meranze SG, Mulvihill SJ, Park JO, Posey JA, Sachdev J, Salem R, Sigurdson ER, Sofocleous C, Vauthey JN, Venook AP, Goff LW, Yen Y, Zhu AX: NCCN clinical practice guidelines in oncology: hepatobiliary cancers. J Natl Compr Canc Netw 2009;7:350–391.
15 Lin S, Hoffmann K, Schemmer P: Treatment of hepatocellular carcinoma: a systematic review. Liver Cancer 2012;1:144–158.
16 Hsu C, Po Ching L, Morita S, Hu FC, Cheng AL: Perspectives on the design of clinical trials combining transarterial chemoembolization and molecular targeted therapy. Liver Cancer 2012;1:168–176.
17 Kim HY, Park JW: Clinical trials of combined molecular targeted therapy and locoregional therapy in hepatocellular carcinoma: past, present, and future. Liver Cancer 2014;3:9–17.
18 Llovet JM, Real MI, Montana X, Planas R, Coll S, Aponte J, Ayuso C, Sala M, Muchart J, Sola R, Rodes J, Bruix J: Arterial embolisation or chemoembolisation versus symptomatic treatment in patients with unresectable hepatocellular carcinoma: a randomised controlled trial. Lancet 2002;359:1734–1739.
19 Lo CM, Ngan H, Tso WK, Liu CL, Lam CM, Poon RT, Fan ST, Wong J: Randomized controlled trial of transarterial Lipiodol chemoembolization for unresectable hepatocellular carcinoma. Hepatology 2002;35:1164–1171.
20 Bruix J, Sherman M: Management of hepatocellular carcinoma. Hepatology 2005;42:1208–1236.
21 Lee HS: Management of patients with hepatocellular carcinoma and extrahepatic metastasis. Dig Dis 2011;29:333–338.
22 Kudo M: Treatment of advanced hepatocellular carcinoma with emphasis on hepatic arterial infusion chemotherapy and molecular targeted therapy. Liver Cancer 2012;1:62–70.
23 Han KH, Kudo M, Ye SL, Choi JY, Poon RT, Seong J, Park JW, Ichida T, Chung JW, Chow P, Cheng AL: Asian consensus workshop report: expert consensus guideline for the management of intermediate and advanced hepatocellular carcinoma in Asia. Oncology 2011;81(suppl 1):158–164.
24 Simpson D, Keating GM: Sorafenib: in hepatocellular carcinoma. Drugs 2008;68:251–258.
25 Llovet JM, Ricci S, Mazzaferro V, Hilgard P, Gane E, Blanc JF, de Oliveira AC, Santoro A, Raoul JL, Forner A, Schwartz M, Porta C, Zeuzem S, Bolondi L, Greten TF, Galle PR, Seitz JF, Borbath I, Haussinger D, Giannaris T, Shan M, Moscovici M, Voliotis D, Bruix J: Sorafenib in advanced hepatocellular carcinoma. N Engl J Med 2008;359:378–390.
26 Cheng AL, Kang YK, Chen Z, Tsao CJ, Qin S, Kim JS, Luo R, Feng J, Ye S, Yang TS, Xu J, Sun Y, Liang H, Liu J, Wang J, Tak WY, Pan H, Burock K, Zou J, Voliotis D, Guan Z: Efficacy and safety of sorafenib in patients in the Asia-Pacific region with advanced hepatocellular carcinoma: a phase III randomised, double-blind, placebo-controlled trial. Lancet Oncol 2009;10:25–34.
27 Keating GM, Santoro A: Sorafenib: a review of its use in advanced hepatocellular carcinoma. Drugs 2009;69:223–240.
28 Alves RC, Alves D, Guz B, Matos C, Viana M, Harriz M, Terrabuio D, Kondo M, Gampel O, Polletti P: Advanced hepatocellular carcinoma. Review of targeted molecular drugs. Ann Hepatol 2011;10:21–27.
29 Peck-Radosavljevic M, Greten TF, Lammer J, Rosmorduc O, Sangro B, Santoro A, Bolondi L: Consensus on the current use of sorafenib for the treatment of hepatocellular carcinoma. Eur J Gastroenterol Hepatol 2010;22:391–398.
30 Choi JY: Treatment algorithm for intermediate and advanced stage hepatocellular carcinoma: Korea. Oncology 2011;81(suppl 1):141–147.
31 Wilhelm SM, Carter C, Tang L, Wilkie D, McNabola A, Rong H, Chen C, Zhang X, Vincent P, McHugh M, Cao Y, Shujath J, Gawlak S, Eveleigh D, Rowley B, Liu L, Adnane L, Lynch M, Auclair D, Taylor I, Gedrich R, Voznesensky A, Riedl B, Post LE, Bollag G, Trail PA: BAY 43-9006 exhibits broad spectrum oral antitumor activity and targets the RAF/MEK/ERK pathway and receptor tyrosine kinases involved in tumor progression and angiogenesis. Cancer Res 2004;64:7099–7109.
32 Kano MR, Komuta Y, Iwata C, Oka M, Shirai YT, Morishita Y, Ouchi Y, Kataoka K, Miyazono K: Comparison of the effects of the kinase inhibitors imatinib, sorafenib, and transforming growth factor-beta receptor inhibitor on extravasation of nanoparticles from neovasculature. Cancer Sci 2009;100:173–180.
33 Tanaka S, Arii S: Molecular targeted therapy for hepatocellular carcinoma in the current and potential next strategies. J Gastroenterol 2011;46:289–296.
34 Therasse P, Arbuck SG, Eisenhauer EA, Wanders J, Kaplan RS, Rubinstein L, Verweij J, Van Glabbeke M, van Oosterom AT, Christian MC, Gwyther SG: New guidelines to evaluate the response to treatment in solid tumors. European Organization for Research and Treatment of Cancer, National Cancer Institute of the United States, National Cancer Institute of Canada. J Natl Cancer Inst 2000;92:205–216.
35 Lencioni R, Llovet JM: Modified RECIST (mRECIST) assessment for hepatocellular carcinoma. Semin Liver Dis 2010;30:52–60.
36 Kudo M, Kubo S, Takayasu K, Sakamoto M, Tanaka M, Ikai I, Furuse J, Nakamura K, Makuuchi M; Liver Cancer Study Group of Japan (Committee for Response Evaluation Criteria in Cancer of the Liver, Liver Cancer Study Group of Japan): Response Evaluation Criteria in Cancer of the Liver (RECICL) proposed by the Liver Cancer Study Group of Japan (2009 revised version). Hepatol Res 2010;40:686–692.
37 Edeline J, Boucher E, Rolland Y, Vauleon E, Pracht M, Perrin C, Le Roux C, Raoul JL: Comparison of tumor response by Response Evaluation Criteria in Solid Tumors (RECIST) and modified RECIST in patients treated with sorafenib for hepatocellular carcinoma. Cancer 2012;118:147–156.
38 Kawaoka T, Aikata H, Murakami E, Nakahara T, Naeshiro N, Tanaka M, Honda Y, Miyaki D, Nagaoki Y, Takaki S, Hiramatsu A, Waki K, Takahashi S, Chayama K: Evaluation of the mRECIST and alpha-fetoprotein ratio for stratification of the prognosis of advanced-hepatocellular-carcinoma patients treated with sorafenib. Oncology 2012;83:192–200.
39 Asayama Y, Yoshimitsu K, Nishihara Y, Irie H, Aishima S, Taketomi A, Honda H: Arterial blood supply of hepatocellular carcinoma and histologic grading: radiologic-pathologic correlation. AJR Am J Roentgenol 2008;190:W28–W34.

Original Article

Digestive Diseases

Dig Dis 2014;32:740–746
DOI: 10.1159/000368015

Identification of Epigenetically Inactivated Genes in Human Hepatocellular Carcinoma by Integrative Analyses of Methylation Profiling and Pharmacological Unmasking

Naoshi Nishida[a, b] Hirokazu Chishina[a] Tadaaki Arizumi[a] Masahiro Takita[a] Satoshi Kitai[a] Norihisa Yada[a] Satoru Hagiwara[a] Tatsuo Inoue[a] Yasunori Minami[a] Kazuomi Ueshima[a] Toshiharu Sakurai[a] Masatoshi Kudo[a]

[a]Department of Gastroenterology and Hepatology, Kinki University Faculty of Medicine, Osaka-Sayama, and
[b]Department of Gastroenterology and Hepatology, Kyoto University Graduate School of Medicine, Kyoto, Japan

Key Words
DNA methylation · Epigenetic alterations · Gene hypermethylation · Methylation profiling · Tumor suppressor genes

Abstract
Objectives: DNA methylation-dependent transcriptional inactivation of tumor suppressor genes (TSGs) is critical for the pathogenesis of hepatocellular carcinoma (HCC). This study identifies potential TSGs in HCCs using methylation profiling and pharmacological unmasking of methylated TSGs. ***Methods:*** Methylation profiling was performed on 22 pairs of HCCs and their corresponding noncancerous liver tissues using the Infinium HumanMethylation27 BeadChip. We also determined the gene reexpression after treatment with 5-aza-2′-deoxycytidine (5-Aza-dC) and trichostatin A (TSA) in 5 HCC cell lines. ***Results:*** We selected CpGs that exhibited a significant increase in methylation in HCC tissues compared with that of the noncancerous control group. Two hundred and thirteen CpGs on different gene promoters with a mean difference in the β value ≥0.15 and a value of $p < 0.05$ were selected. Of the 213 genes, 45 genes were upregulated in 3 or more HCC cell lines with multiplier value of differences ≥2.0 after 5-Aza-dC and TSA treatment. ***Conclusions:*** We identified several potential TSGs that participate in transcription inactivation through epigenetic interactions in HCC. The results of this study are important for the understanding of functionally important epigenetic alterations in HCC.

Introduction

Hepatocellular carcinoma (HCC) is the most common type of liver cancer [1]. Several risk factors contribute to the development of HCC, including chronic infection due to hepatitis virus, alcohol intake, nonalcoholic fatty liver disease, hemochromatosis, α_1-antitrypsin deficiency, Wilson's disease and aflatoxin exposure. Regardless of the etiology, chronic liver damage causes genetic and epigenetic alterations, which play an important role in hepatocarcinogenesis [2].

KARGER

E-Mail karger@karger.com
www.karger.com/ddi

0257–2753/14/0326–0740$39.50/0

Naoshi Nishida, MD
Department of Gastroenterology and Hepatology
Kinki University Faculty of Medicine
337-2 Ohno-Higashi, Osaka-Sayama, Osaka 589-8511 (Japan)
E-Mail naoshi@med.kindai.ac.jp

Recent technical advancement in genomic sequencing and comprehensive methylation analyses give us a profound insight into the molecular events that drive carcinogenesis, including HCC [3–8]. Several studies have noted abnormal DNA methylation in HCC; DNA methylation of specific sequences on the promoters of tumor suppressor genes (TSGs) is a key epigenetic alteration that marks HCC pathogenesis [2, 9]. Therefore, it is essential to determine unique methylation events that are linked to transcriptional inactivation and HCC pathology. Currently, the correlation between individual DNA methylation and transcription of its corresponding genes has not been fully clarified in HCC. Understanding this phenomenon will provide important insights into HCC pathology [10] and may provide a venue for novel therapeutics [11].

In this study, we have addressed this issue by performing a comprehensive analysis of hypermethylated genes within HCC promoters. To achieve this, we used the Infinium HumanMethylation27 BeadChip (Illumina, San Diego, Calif., USA) to target 27,578 CpGs within the promoters of 14,474 genes in patients with HCC, and compared the results with those of their corresponding noncancerous control group. Using pharmacological agents, we also determined the genes that were upregulated due to DNA demethylation and histone acetylation in HCC cell lines. Here, we report a systematic and integrative analysis of epigenetically inactivated genes in human HCC.

Materials and Methods

Patients

In this study, 22 pairs of HCCs and their corresponding noncancerous liver tissues were taken from 19 men and 3 women ranging in age from 53 to 79 years (median, 71 years). The patient cohort had different etiological profiles. Of the 22 study patients, 1 patient was positive for hepatitis B virus surface antigen, 9 were positive for hepatitis C virus antibody, and 12 patients were negative for both. Among these 12 patients, 4 patients consumed alcohol (>20 g/day). One, 5, 7 and 9 patients had stage F1, F2, F3 and F4 liver fibrosis, respectively. The median tumor size was 3.0 cm (25th–75th percentiles: 2.6–8.0 cm). The tumors were at different stages of differentiation. Of the 22 tumor samples, 9 tumors were well differentiated, 12 were moderately differentiated, and 1 was poorly differentiated. Written informed consent was obtained from all patients, and necessary approvals were obtained from the institutional review boards of the institution involved.

Methylation Analysis Using HumanMethylation27 BeadChip

Genomic DNA was extracted from frozen tissues as described previously [12]. After confirming the quality and concentration of DNA, 1 μg of genomic DNA was treated with bisulfite using the EZ DNA Methylation Kit (Zymo Research Corporation, Irvine, Calif., USA). Whole genome amplification of DNA, enzymatic fragmentation and isopropanol precipitation were performed according to the manufacturer's instructions (Infinium Methylation Assay, Manual Protocol, Rev.A). The DNA fragment was applied onto the HumanMethylation27 BeadChip array and hybridized overnight. Then, the array was scanned with the Illumina iScan SQ scanner (iScan Control software v.3.3.28) and the intensities of the images were captured using GenomeStudio (v.2011.1) and Methylation Module (v.1.9.0) software. The β value representing the methylation levels was calculated as the ratio of the signal intensity of the methylated allele divided by the sum of the signal intensity of the unmethylated and methylated allele + 100. Each β value was accompanied by a detection p value, which indicated statistical significance against the background. Only β values with a detection value of $p < 0.05$ were included in the data analysis. All samples showed a CpG coverage of >95% in this analysis.

Cell Culture and 5-Aza-2-Deoxycytidine and Trichostatin A Treatment

HCC, HLE, HLF, HepG2, Huh7 and PLC/PRF/5 cell lines were purchased from the Japanese Collection of Research Bioresources Bank at the National Institute of Biomedical Innovation (Osaka, Japan) and American Type Culture Collection (Manassas, Va., USA). To perform the pharmacological unmasking procedure, $1–5 \times 10^5$ cells were cultured in Dulbecco's modified Eagle's medium (Sigma-Aldrich, St. Louis, Mo., USA) with either 5 or 10% fetal bovine serum (Gibco, Life Sciences Technologies, St. Clara, Calif., USA) in 10-cm culture dishes for 24 h. The cell lines were then treated with 1 μM 5-aza-2′-deoxycytidine (5-Aza-dC; Sigma) for 72 h, followed by an additional 24-hour treatment with 100 nM trichostatin A (TSA; Wako, Osaka, Japan). Finally, the cells were harvested and studied for DNA methylation and RNA expression.

DNA and RNA Extraction, Combined Bisulfite Restriction Analysis and Array-Based Analysis of Reactivated Genes

DNA and RNA extraction was performed using the QIAamp DNA Mini Kit (Qiagen Inc., Valencia, Calif., USA) and RNeasy Mini Kit (Qiagen), respectively. To confirm DNA demethylation in response to 5-Aza-dC and TSA treatment, we performed COBRA (combined bisulfite restriction analysis) to determine the methylation status of the promoters on the *CDKN2A, GSTP1, HIC1, RIZ1, SOCS1* and *RASSF1A* genes [12, 13].

To elucidate the effects of DNA demethylation on transcription further, before and after 5-Aza-dC and TSA treatment, RNA samples were subjected to expression microarray analysis using Agilent SurePrint G3 human GE 8x60K v2 (Agilent Technology, St. Clara, Calif., USA). This system targets about 50,599 transcripts including 11,912 large intergenic noncoding RNAs and transcripts with uncertain coding potential. Data were analyzed with Agilent Feature Extraction software and the multiples of differentially expressed genes before and after treatment were calculated. Multiplier values of differences ≥2.0 were scored as upregulated genes, while those of differences ≤0.5 represented downregulated genes. The value between 0.5 and 2.0 was considered insignificant or unaltered gene expression.

Selection of Differentially Methylated and Reactivated Genes after 5-Aza-dC and TSA Treatment

Initially, we selected CpGs within promoters that showed increased methylation in HCC tissues compared with those in the

noncancerous livers, with the mean difference in a β value ≥0.15. The final data were analyzed with the Mann-Whitney U test with the false discovery rate controlled with the Benjamini-Hochberg procedure. The extracted CpGs in the hypermethylated promoters (corrected $p < 0.05$) were considered differentially methylated (hypermethylated DM-CpGs).

To determine the genes inactivated through DNA methylation, we performed pharmacological unmasking in HCC cell lines. Gene expression levels that increased over 2-fold in response to 5-Aza-dC and TSA treatment (multiplier value of differences ≥2.0) in at least 3 cell lines were considered as reactivated genes. Thus, genes with hypermethylated DM-CpGs that were transcriptionally reactivated through 5-Aza-dC and TSA treatment are candidates for genes that are inactivated through epigenetic mechanisms in human HCC.

All statistical analyses were conducted using the JMP version 9.0 software (SAS Institute Inc., Cary, N.C., USA). After calculating two-sided p values, $p < 0.05$ was considered statistically significant.

Results

Identification of Hypermethylated Genes That Were Reactivated after 5-Aza-dC and TSA Treatment in HCC

We selected hypermethylated CpGs based on the two criteria. First, CpGs must show increased methylation compared with noncancerous livers, with a difference in the β value ≥0.15. Second, the increase must be statistically significant (corrected $p < 0.05$) after the Mann-Whitney U test with the false discovery rate control. Overall, 213 CpGs in 213 different gene promoters met the above criteria. The mean distance of the location of the selected CpGs from the transcription start site was 269.5 bp (95% confidence interval 232.2–306.8 bp). We also performed an epigenetic unmasking procedure with 5-Aza-dC and TSA treatment, which induced DNA demethylation and histone acetylation in the 5 liver cancer cell lines. The optimal treatment conditions were determined by analyzing the demethylation status of 6 TSG promoters, *CDKN2A, GSTP1, HIC1, RIZ1, SOCS1* and *RASSF1A*, which were known to carry abnormal methylation in human HCC, after treatment (fig. 1) [12]. Then, we selected the transcripts that were upregulated (multiplier value of differences ≥2.0) after 5-Aza-dC and TSA treatment. In total, 2,412 transcripts were upregulated in at least 3 HCC cell lines. Of these, 317 transcripts were upregulated in all 5 cell lines, 711 transcripts were upregulated in 4 cell lines, and 1,384 transcripts were upregulated in 3 cell lines. Furthermore, among the 2,412 upregulated transcripts, 45 transcripts were derived from the genes carrying hypermethylated CpGs within the promoters in human HCC tissues. Detailed information regarding these 45 genes is listed in table 1.

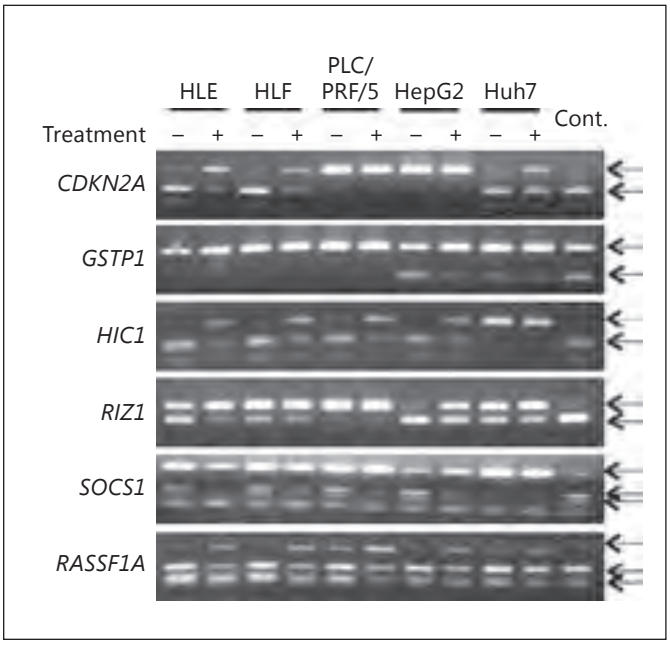

Fig. 1. DNA methylation status of 5 HCC cell lines before and after treatment with 5-Aza-dC and TSA by COBRA. – = Before treatment with 5-Aza-dC and TSA; + = after treatment with 5-Aza-dC and TSA; Cont. = a positive control of methylated DNA sample that was treated with CpG methylase (CpGenome™ universal methylated DNA; Chemicon International, Inc., Temecula, Calif., USA). The solid and dashed arrows indicate the methylated and unmethylated allele, respectively.

Discussion

TSG inactivation through DNA methylation is one of the most important mechanisms that drive human hepatocarcinogenesis [14]. In this study, we comprehensively analyzed alterations in promoter DNA methylation of human HCCs and integrated these results with those obtained from the pharmacological unmasking of 5 different HCC cell lines. We have successfully identified a set of genes that are strong candidates for epigenetically inactivated TSGs in HCCs.

At first, we obtained the methylation profile of HCCs and their corresponding noncancerous liver tissues with the Infinium HumanMethylation27 BeadChip array. Through this analysis, we selected the hypermethylated

Table 1. Candidate genes with transcriptional inactivation through DNA methylation in HCC

Ch.	Gene symbol	Annotation	Gene product	UCSC RefGene	β value difference
19	ZNF154	zinc ion binding; transcription factor	zinc finger protein 154	ZNF154	0.2910
19	TNFSF9	tumor necrosis factor receptor binding	tumor necrosis factor superfamily; member 9	TNFSF9	0.2239
13	EFNB2	ephrin receptor binding; cell differentiation; cell-cell signaling; nervous system development	ephrin B2	EFNB2	0.2146
11	FLJ33790		hypothetical protein LOC283212	KLHL35	0.2097
2	LOXL3	copper ion binding; oxidoreductase activity; scavenger receptor activity	lysyl oxidase-like 3 precursor	LOXL3	0.2053
11	OVOL1	putative transcription factor: zinc ion binding	OVO-like 1 binding protein	OVOL1	0.2031
10	NKX6-2	transcription factor activity	NK6 transcription factor related; locus 2	NKX6-2	0.2009
11	LRFN4	leucine-rich repeat and fibronectin type-III domain-containing 4 variant	leucine-rich repeat and fibronectin type-III domain-containing 4	LRFN4	0.2007
3	RBP1	retinol binding; vitamin A metabolism	retinol binding protein 1; cellular	RBP1	0.1994
X	FLJ14503	catalytic activity	hypothetical protein LOC256714	MAP7D2	0.1930
1	TRIM58	synonyms: BIA2; DKFZp434C091	tripartite motif-containing 58	TRIM58	0.1924
11	MAPK8IP1	mitogen-activated protein kinase scaffold activity; protein kinase inhibitor activity; regulation of the JNK cascade	mitogen-activated protein kinase 8-interacting protein 1	MAPK8IP1	0.1897
4	AFAP	actin filament-associated protein; 110 kDa	actin filament-associated protein	AFAP1	0.1866
5	APC	β-catenin binding; Wnt receptor signaling pathway	adenomatosis polyposis coli	APC	0.1842
2	FRZB	cell differentiation; negative regulation of Wnt receptor signaling pathway	frizzled-related protein	FRZB	0.1838
17	RND2	small GTPase-mediated signal transduction	Rho family GTPase 2	RND2	0.1807
2	TACSTD1	human epithelial glycoprotein-2; surface marker	tumor-associated calcium signal transducer 1 precursor	EPCAM	0.1789
6	BMP6	transforming growth factor-β; growth factor activity; cell differentiation	bone morphogenetic protein 6 precursor	BMP6	0.1784
14	SLC22A17	potent brain-type organic ion transporter	solute carrier family 22 (organic cation transporter); member 17 isoform a	SLC22A17	0.1748
11	UCP2	mitochondrial transport	uncoupling protein 2	UCP2	0.1726
X	SYN1	actin binding; transporter activity; go_process: neurotransmitter secretion	synapsin I isoform Ib	SYN1	0.1725
2	BOLL	RNA binding; spermatogenesis; cell differentiation; regulation of translation	boule isoform 2	BOLL	0.1710
19	ZNF177	negative regulation of transcription from RNA polymerase II promoter	zinc finger protein 177	ZNF177	0.1679
10	ALOX5	oxidoreductase activity; arachidonate 5-lipoxygenase activity; inflammatory response	arachidonate 5-lipoxygenase	ALOX5	0.1663
3	CLDN11	tight junction; calcium-independent cell-cell adhesion	claudin 11	CLDN11	0.1657
3	MCF2L2	synonyms: FLJ42509; KIAA0861	Rho family guanine-nucleotide exchange factor	MCF2L2	0.1640
7	AEBP1	transcription factor activity; cell adhesion; muscle development	adipocyte enhancer binding protein 1 precursor	AEBP1	0.1636

Table 1 (continued)

Ch.	Gene symbol	Annotation	Gene product	UCSC RefGene	β value difference
19	PBX4	embryonic development; regulation of transcription	pre-B cell leukemia transcription factor 4	PBX4	0.1631
16	SMPD3	sphingomyelin phosphodiesterase activity; cell cycle	sphingomyelin phosphodiesterase 3; neutral membrane	SMPD3	0.1624
11	THY1	T cell receptor signaling pathway; negative regulation of apoptosis, cell migration, protein kinase activity, T cell receptor signaling pathway	Thy-1 cell surface antigen	THY1	0.1621
7	FSCN1	cell proliferation; actin cytoskeleton organization	fascin 1	FSCN1	0.1617
8	RBM35A	nucleic acid binding	hypothetical protein LOC54845 isoform 1	ESRP1	0.1614
10	ADAM8	metalloendopeptidase activity	ADAM metallopeptidase domain 8 precursor	ADAM8	0.1613
2	NRP2	vascular endothelial growth factor receptor activity; cell adhesion; cell differentiation; nervous system development	neuropilin 2 isoform 2 precursor	NRP2	0.1611
12	WIF1	Wnt receptor signaling pathway	Wnt inhibitory factor-1 precursor	WIF1	0.1608
16	SOCS1	negative regulation of JAK-STAT cascade	suppressor of cytokine signaling 1	SOCS1	0.1589
14	CHGA	calcium ion binding; blood pressure regulation	chromogranin A precursor	CHGA	0.1579
1	KIF17	microtubule motor activity; microtubule-based movement	kinesin family member 17	KIF17	0.1575
11	CDKN1C	p57KIP2; Beckwith-Wiedemann syndrome; cyclin-dependent protein kinase inhibitor activity	cyclin-dependent kinase inhibitor 1C	CDKN1C	0.1574
20	C20orf100	regulation of transcription	chromosome 20 open reading frame 100	TOX2	0.1571
20	SALL4	sal *(Drosophila)*-like 4; zinc ion binding; go_function: metal ion binding; regulation of transcription	sal-like 4	SALL4	0.1568
20	GDAP1L1	synonyms: dJ881L22.1; DKFZp761K228; dJ995J12.1.1	ganglioside-induced differentiation-associated protein 1-like 1	GDAP1L1	0.1549
2	TFCP2L1	transcription factor activity; regulation of transcription from RNA polymerase II promoter	LBP-9	TFCP2L1	0.1533
9	CDKN2A	cyclin-dependent kinase 4 inhibitor p16-INK4; cyclin-dependent kinase inhibitor 2A; p14ARF	cyclin-dependent kinase inhibitor 2A isoform 3	CDKN2A	0.1513
X	TMSL8	thymosin β; cytoskeleton; actin binding	thymosin-like 8	TMSB15A	0.1504

The 45 genes that showed upregulation in 3 or more cell lines and hypermethylation on the promoters in human HCCs were listed. The β value difference denotes the difference in the mean β value between HCCs and noncancerous livers. Ch. = Chromosome; Annotation = the gene annotation provided by the National Center for Biotechnology Information (NCBI); Product = the name of the gene product by the NCBI; UCSC RefGene = the gene names by the University of California, Santa Cruz (UCSC) Genome Bioinformatics.

genes with a mean β value ≥1.5 in HCCs compared to that of noncancerous liver tissues. To obtain differentially methylated genes, the β values between the two groups were assessed with the Mann-Whitney U test with false discovery rate controlled using the Benjamini-Hochberg procedure. To confirm the reactivation of hypermethylated genes after pharmacological unmasking, we performed a comprehensive analysis of gene reactivation after 5-Aza-dC and TSA treatment in human HCC. In conclusion, the 45 hypermethylated genes that turned on transcription in 3 or more HCC cell lines were considered as key candidates for epigenetically inactivated genes during hepatocarcinogenesis.

Previously, we have reported that a set of 8 TSGs showed abnormal methylation in early HCC [15]. The number of these methylated TSGs in the hepatitis tissue correlated with the time to HCC occurrence in chronic hepatitis C patients. Among the 8 TSGs, the *APC*, *CDKN2A* and SOCS1 genes were also identified as transcriptionally inactivated TSGs by DNA methylation through the presented selection. In addition, a recent report identified *sphingomyelin phosphodiesterase 3* (*SMPD3*) as a TSG in HCC using HumanMethylation27 BeadChip and array-based reexpression profiling [16]. Another gene called the *Wnt inhibitory factor-1 precursor (WIF1)* also reportedly undergoes epigenetic silencing in HCC [17]. Notably, both of these genes were selected as epigenetically inactivated in HCC through our analysis. Together, these studies validate the robustness our data and methodology used to obtain the present data.

Interestingly, several potential TSGs, which were identified as epigenetically inactivated genes in this study, have not been reported in human HCCs but in other cancers. For example, the *frizzled-related protein (FRZB)* gene that regulates Wnt signaling shows hypermethylation in bladder cancer [18]. More importantly, our analysis identified *FRZB* as a potential TSG in HCC as indicated by its inactivation through DNA methylation. Another gene, *claudin 11 (CLDN11)* – an epigenetic biomarker of melanoma [19, 20] – was found having a hypermethylated promoter in our study. We have also identified the *cyclin-dependent kinase inhibitor 1C* (*CDKN1C)* as an epigenetically inactivated gene in HCCs. The loss of the *CDKN1C* gene product, p57(KIP2), correlates with a poor prognosis in HCC patients [21]. Therefore, it is possible that p57(KIP2) downregulation in HCCs may be due to an epigenetic interaction.

Our analyses have also revealed that increased methylation occurs in certain genes coding stem cell markers such as the *Sal-like protein 4 (SALL4)* and the *tumor-associated calcium signal transducer 1 (TACSTD1/EPCAM)* in a subset of HCCs. Studies have shown that increased expression of hepatic progenitor markers such as SALL4 and TACSTD1 are associated with a poor prognosis for cancer, including HCC [22, 23]. Until now, the biological implication of the hypermethylation of these progenitor cell markers in HCC was controversial owing to the reported lack of SALL4 expression in noncancerous liver [24]. However, we observed an increase in both SALL4 and TACSTD1 expression levels after the pharmacological unmasking procedure in HCC cell lines. Hypermethylated SALL4 reactivates in response to 5-Aza-dC treatment in the acute promyelocytic leukemia cell line and is responsible for aggressive tumors [25]. These studies indicate that further analyses of the epigenetic regulation of SALL4 and TACSTD1 in HCC should be required for the development of epigenetic-based therapies for HCC.

In this study, we identified several potential TSGs that are inactivated by epigenetic interactions in HCC. Since we analyzed a limited number of cell lines for pharmacological unmasking, many other epigenetically inactivated TSGs in HCC still need to be discovered [26, 27]. For example, the *GSTP1* and *RUNX3* genes, which have abnormal methylation in HCCs, were not listed because only 1–2 cell lines out of the 5 HCC cell lines analyzed showed abnormal methylation of these genes [15]. Nonetheless, the data presented here are important to understand what kinds of TSGs are inactivated through epigenetic mechanisms during HCC onset and progression.

Acknowledgments

This work was supported in part by a grant-in-aid for scientific research (KAKENHI: 24590997) from the Japanese Society for the Promotion of Science (N. Nishida) and a grant from the Smoking Research Foundation (N. Nishida).

References

1 Kim do Y, Han KH: Epidemiology and surveillance of hepatocellular carcinoma. Liver Cancer 2012;1:2–14.

2 Nishida N, Goel A: Genetic and epigenetic signatures in human hepatocellular carcinoma: a systematic review. Curr Genomics 2011; 12:130–137.

3 Esteller M: Epigenetics in cancer. N Engl J Med 2008;358:1148–1159.

4 Shen J, Wang S, Zhang YJ, Kappil M, Wu HC, Kibriya MG, Wang Q, Jasmine F, Ahsan H, Lee PH, Yu MW, Chen CJ, Santella RM: Genome-wide DNA methylation profiles in hepatocellular carcinoma. Hepatology 2012;55: 1799–1808.

5 Moeini A, Cornella H, Villanueva A: Emerging signaling pathways in hepatocellular carcinoma. Liver Cancer 2012;1:83–93.

6 Plass C, Pfister SM, Lindroth AM, Bogatyrova O, Claus R, Lichter P: Mutations in regulators of the epigenome and their connections to global chromatin patterns in cancer. Nat Rev Genet 2013;14:765–780.

7 Nishida N, Kudo M: Recent advancements in comprehensive genetic analyses for human hepatocellular carcinoma. Oncology 2013; 84(suppl 1):93–97.

8 Nishida N: Alteration of epigenetic profile in human hepatocellular carcinoma and its clinical implications. Liver Cancer, in press.
9 Nishida N, Kudo M: Oxidative stress and epigenetic instability in human hepatocarcinogenesis. Dig Dis 2013;31:447–453.
10 Ramakrishna G, Rastogi A, Trehanpati N, Sen B, Khosla R, Sarin SK: From cirrhosis to hepatocellular carcinoma: new molecular insights on inflammation and cellular senescence. Liver Cancer 2013;2:367–383.
11 Peck-Radosavljevic M: Drug therapy for advanced-stage liver cancer. Liver Cancer 2014; 3:125–131.
12 Nishida N, Nishimura T, Nagasaka T, Ikai I, Goel A, Boland CR: Extensive methylation is associated with beta-catenin mutations in hepatocellular carcinoma: evidence for two distinct pathways of human hepatocarcinogenesis. Cancer Res 2007;67:4586–4594.
13 Nishida N, Nagasaka T, Nishimura T, Ikai I, Boland CR, Goel A: Aberrant methylation of multiple tumor suppressor genes in aging liver, chronic hepatitis, and hepatocellular carcinoma. Hepatology 2008;47:908–918.
14 Nishida N: Impact of hepatitis virus and aging on DNA methylation in human hepatocarcinogenesis. Histol Histopathol 2010;25:647–654.
15 Nishida N, Kudo M, Nagasaka T, Ikai I, Goel A: Characteristic patterns of altered DNA methylation predict emergence of human hepatocellular carcinoma. Hepatology 2012;56: 994–1003.
16 Revill K, Wang T, Lachenmayer A, Kojima K, Harrington A, Li J, Hoshida Y, Llovet JM, Powers S: Genome-wide methylation analysis and epigenetic unmasking identify tumor suppressor genes in hepatocellular carcinoma. Gastroenterology 2013;145:1424.e25–1435.e25.
17 Ding Z, Qian YB, Zhu LX, Xiong QR: Promoter methylation and mRNA expression of DKK-3 and WIF-1 in hepatocellular carcinoma. World J Gastroenterol 2009;15:2595–2601.
18 Marsit CJ, Houseman EA, Christensen BC, Gagne L, Wrensch MR, Nelson HH, Wiemels J, Zheng S, Wiencke JK, Andrew AS, Schned AR, Karagas MR, Kelsey KT: Identification of methylated genes associated with aggressive bladder cancer. PLoS One 2010;5:e12334.
19 Izraely S, Sagi-Assif O, Klein A, Meshel T, Ben-Menachem S, Zaritsky A, Ehrlich M, Prieto VG, Bar-Eli M, Pirker C, Berger W, Nahmias C, Couraud PO, Hoon DS, Witz IP: The metastatic microenvironment: claudin-1 suppresses the malignant phenotype of melanoma brain metastasis. Int J Cancer 2014, DOI: 10.1002/ijc.29090.
20 Gao L, van den Hurk K, Moerkerk PT, Goeman JJ, Beck S, Gruis NA, van den Oord JJ, Winnepenninckx VJ, van Engeland M, van Doorn R: Promoter CpG island hypermethylation in dysplastic nevus and melanoma: CLDN11 as an epigenetic biomarker for malignancy. J Invest Dermatol 2014, DOI: 10.1038/jid.2014.270.
21 Nakai S, Masaki T, Shiratori Y, Ohgi T, Morishita A, Kurokohchi K, Watanabe S, Kuriyama S: Expression of p57(KIP2) in hepatocellular carcinoma: relationship between tumor differentiation and patient survival. Int J Oncol 2002;20:769–775.
22 Yamashita T, Ji J, Budhu A, Forgues M, Yang W, Wang HY, Jia H, Ye Q, Qin LX, Wauthier E, Reid LM, Minato H, Honda M, Kaneko S, Tang ZY, Wang XW: EpCAM-positive hepatocellular carcinoma cells are tumor-initiating cells with stem/progenitor cell features. Gastroenterology 2009;136:1012–1024.
23 Sugai T, Habano W, Endoh M, Konishi Y, Akasaka R, Toyota M, Yamano H, Koeda K, Wakabayashi G, Suzuki K: Molecular analysis of gastric differentiated-type intramucosal and submucosal cancers. Int J Cancer 2010; 127:2500–2509.
24 Yong KJ, Gao C, Lim JS, Yan B, Yang H, Dimitrov T, Kawasaki A, Ong CW, Wong KF, Lee S, Ravikumar S, Srivastava S, Tian X, Poon RT, Fan ST, Luk JM, Dan YY, Salto-Tellez M, Chai L, Tenen DG: Oncofetal gene SALL4 in aggressive hepatocellular carcinoma. N Engl J Med 2013;368:2266–2276.
25 Yang J, Corsello TR, Ma Y: Stem cell gene SALL4 suppresses transcription through recruitment of DNA methyltransferases. J Biol Chem 2012;287:1996–2005.
26 Neumann O, Kesselmeier M, Geffers R, Pellegrino R, Radlwimmer B, Hoffmann K, Ehemann V, Schemmer P, Schirmacher P, Lorenzo Bermejo J, Longerich T: Methylome analysis and integrative profiling of human HCCs identify novel protumorigenic factors. Hepatology 2012;56:1817–1827.
27 Matsumura S, Imoto I, Kozaki K, Matsui T, Muramatsu T, Furuta M, Tanaka S, Sakamoto M, Arii S, Inazawa J: Integrative array-based approach identifies MZB1 as a frequently methylated putative tumor suppressor in hepatocellular carcinoma. Clin Cancer Res 2012;18:3541–3551.

Review Article

Digestive Diseases

Dig Dis 2014;32:786–790
DOI: 10.1159/000368023

Clinical Features of Vascular Disorders Associated with Chronic Hepatitis Virus Infection

Naoshi Nishida Masatoshi Kudo

Department of Gastroenterology and Hepatology, Kinki University Faculty of Medicine, Osaka-Sayama, Japan

Key Words
Viral hepatitis · Polyarteritis nodosa · Cryoglobulinemia · Nephropathy · Vascular disorders

Abstract
Hepatitis virus infections can be accompanied by extrahepatic manifestations that may be caused by the host's immune reaction to the viral infection. Vascular involvement is one of these manifestations and is occasionally associated with life-threatening conditions due to systemic organ failure. The unique profile of hepatitis-related vascular involvement is associated with infection by different types of hepatitis viruses. For example, polyarteritis nodosa is more frequently reported in patients with chronic hepatitis B than those with chronic hepatitis C. Similarly, membranous nephropathy is a notable manifestation among hepatitis B virus-positive patients. In contrast, patients infected with hepatitis C virus are at risk for cryoglobulinemia and membranoproliferative glomerulonephritis. Antiviral therapy is necessary to control these kinds of vasculitis related to hepatitis virus infections; however, immunosuppressive agents may be required to treat severe cases. New antiviral drugs for viral hepatitis could improve the prognosis of vascular and renal involvement.

Introduction

Chronic infection with hepatitis B virus (HBV) and hepatitis C virus (HCV) is a life-threatening disease that causes progressive liver damage including liver cirrhosis and hepatocellular carcinoma [1, 2]. In addition, several extrahepatic manifestations may develop during the clinical course of chronic hepatitis [3, 4]. Among them, vasculitis is a significant complication of chronic HBV and HCV infection [5]. The onset of this condition is generally attributed to host immune response triggered by hepatitis virus infection [6]. However, the presence of the virus in immune and endothelial cells might also be associated with the pathogenesis of hepatitis virus-related vasculitis. Interestingly, the profile and condition of vasculitis differs between HBV- and HCV-related disease. For example, polyarteritis nodosa (PAN) is more frequently reported in patients with HBV infection than in those with HCV infection [7]. In contrast, cryoglobulinemia is one of the major extrahepatic manifestations of chronic HCV infection. Renal involvement and vasculitis can also be related to hepatitis virus infection. HCV is a known risk for membranoproliferative glomerulonephritis (MPGN), whereas HBV may cause membranous nephropathy (MN) [8]. In the present review, we focus on hepatitis virus-related vasculitis and the necessity for early diagnosis and treatment.

KARGER

E-Mail karger@karger.com
www.karger.com/ddi

0257–2753/14/0326–0786$39.50/0

Naoshi Nishida, MD
Department of Gastroenterology and Hepatology
Kinki University Faculty of Medicine
337-2 Ohno-Higashi, Osaka-Sayama, Osaka 589-8511 (Japan)
E-Mail naoshi@med.kindai.ac.jp

Cryoglobulinemia Associated with Hepatitis Virus Infection

Cryoglobulins are abnormal proteins, generally immunoglobulins, which precipitate from plasma at temperatures below 37°C and dissolve again if the blood is heated. These abnormal blood proteins are observed in several pathological conditions such as infection, autoimmune disease and malignant tumors. Cryoglobulins can cause organ damage through coagulation within peripheral vessels, which leads to vascular damage through immune reactions [9]. Cryoglobulinemia is classified by the types of immunoglobulin involved and the clonality. Type I is most commonly encountered in patients with plasma cell dyscrasia. The abnormal proteins involved are monoclonal IgM or IgG. Type II cryoglobulinemia is associated with monoclonal IgM and polyclonal IgG. The monoclonal IgM protein has rheumatoid factor activity and may react with the Fc region of IgG. Type III involves polyclonal IgM and IgG and is strongly associated with autoimmune disease such as systemic lupus erythematosus and rheumatoid arthritis. Types II and III carry both IgG and IgM components and are called mixed cryoglobulinemia (MC). The latter two types of cryoglobulinemia are associated with HCV infection, particularly with type II cryoglobulinemia [6]. However, HBV infection may also be involved in the pathogenesis of this complication [10], although the prevalence of HBV in MC patients is not as high [11]. A case of cryoglobulinemia onset after HBV vaccination has also been reported [12].

Onset of cryoglobulinemia may be asymptomatic or may lead to a MC syndrome or to a more severe vasculitis [13]. The frequency of cryoglobulinemia in HCV-positive patients is varied among the reports, which might be attributed to the duration of HCV infection and the stage of liver fibrosis [14]. The proportion of HCV-positive cases in MC patients ranges from 30 to 100% among studies. However, the occurrence of MC among HCV-positive patients was reported to be approximately 3% [9]. It has also been reported that the association of HCV envelope glycoprotein E2 with B cell CD81 receptors could trigger the monoclonal expansion of B cells and induce the production of monoclonal IgM [15]. This type of monoclonal protein could react with the HCV core protein and associate with IgG antibodies against several HCV-derived proteins [16]. These immune complexes may lead to vasculitis through the activation of the complement system.

Treatment of Hepatitis Virus-Related Cryoglobulinemia

Although the treatment of HCV-related MC depends on the severity of the disease, antiviral therapy against HCV is essential. Corticosteroids are used to control the acute phase of moderate to severe vasculitis [9]. Immunosuppressant therapy and plasma exchange might be required to remove cryoglobulins in life-threatening cases. Rituximab is also administered to suppress the expansion of B cells that could be a source of cryoglobulins. A combination therapy involving rituximab and antiviral agents against HCV has been reported to be more effective than antiviral therapy alone, and has shown a shorter mean time to clinical remission, better renal response rates and higher rates of cryoglobulin clearance [17].

In contrast to B cell proliferation, patients with HCV-related vasculitis reportedly present with reduction of regulatory T cells, and resolution of the HCV infection correlates with vasculitis resolution and recovery of regulatory T cell levels. Interestingly, administration of low-dose interleukin-2 led to restoration of regulatory T cells, reduction of cryoglobulinemia and concomitant clinical improvement in patients with HCV-induced vasculitis [6].

HBV Infection and PAN

The association between HBV infection and onset of PAN was first reported in the early 1970s [7]. This rare complication is reported more frequently in North America and Europe than in Asia [8]. According to previous reports, PAN was preceded by HBV infection [18]. Although the carrier rate of HBV among patients with all types of vasculitis was <1%, almost one-third of PAN cases yielded positive results for HBV markers [18]. However, the prevalence of PAN decreased with increased vaccination against HBV [19].

Generally, since the immune reaction responsible for PAN occurs within 6 months of infection by HBV, vasculitis may be symptomatic before the onset of hepatitis. Although the detailed mechanisms of HBV-related PAN are still controversial, the majority of HBV-related PAN cases carried wild-type HBV characterized by hepatitis B envelope (HBe) antigenemia and high HBV replication. This supports the theory that the deposition of viral antigen-antibody complexes, possibly involving HBeAg, might be responsible for the onset of PAN [18]. However, some HBV-related PAN cases showed a precore mutation, which abrogates the formation of HBeAg [20].

Dig Dis 2014;32:786–790
DOI: 10.1159/000368023

Therefore, it is also possible that an undefined circulating HBV-related protein is involved in the pathogenesis of PAN.

The activity of HBV-related PAN has been associated with the proliferation of HBV. On the other hand, serum levels of hepatitis B surface antigen (HBsAg) were not related to the activity of vasculitis, and remission of PAN was noted even in cases with high HBsAg titer.

The frequent complications reported in HBV-related PAN are gastrointestinal involvement followed by malignant hypertension, renal infarction, orchitis and epididymitis. The frequencies of these complications are similar to those of non-HBV PAN [18]. Generally, hepatic manifestations, such as elevated alanine and aspartate transaminase levels and icterus, are mild.

Treatment of HBV-Related PAN

PAN has generally been treated with corticosteroids and immunosuppressive agents [18]. This treatment combination might be effective in the active phase of PAN [21]; however, immunosuppression therapy may induce reactivation of HBV and lead to de novo HBV-related fulminant hepatitis, which is a serious condition with high mortality rates [22]. It is also known that the activity of HBV-related PAN decreases after seroconversion of HBeAg and reduction of serum HBV levels [21]. From this point of view, antiviral therapy using nucleotide analogs is necessary to treat HBV-related PAN. For severe cases of vasculitis, immunosuppression and removal of immune complexes using corticosteroids and plasma exchange are applied, followed by long-term suppression of HBV using nucleotide analogs [21].

Rare cases of PAN with HCV have also been reported; however, the association between HCV and PAN remains controversial [18].

Nephropathy Associated with Hepatitis Virus Infection

HBV-Related Nephropathy

Combes et al. [23] first reported nephropathy associated with HBV in 1971. Deposition of anti-HBV antibodies in immune complexes and complement in the glomerulus was observed in cases with HBV-related nephropathy.

MN is the most common condition with renal involvement among HBV-related nephropathy and more frequent in children than adults. However, MPGN and IgA nephropathy are sometimes observed in adults [8]. Plasma complement C3 and C4 in HBV-related MN patients were significantly lower than in idiopathic MN patients. In addition, segmental glomerular damage, mesangial cell proliferation and tubulointerstitial damage were more common in HBV-related MN than in idiopathic cases. Immunofluorescence staining of polyclonal immunoglobulin and polytypic complement immunoglobulin was frequently noted in HBV-related MN cases; however, no differences in prognosis between HBV-related MN and idiopathic cases were reported [24]. Deposits of IgG, complement 3 and HBeAg were observed in the glomerular capillary walls in the MN cases [25]. However, deposits of HBsAg were observed in the intraglomerular mesangial cell in cases of adult MPGN [8].

As described above, deposition of several HBV-related proteins and immunoglobulins is detected at the basement membrane of the capillary wall of the glomerulus in HBV-positive cases with renal involvement. The immune complex, with a molecular weight of <1,000 kDa, could reportedly trigger nephropathy; a positively charged immune complex of this size could pass through the capillary wall's basement membrane and deposit under the negatively charged glomerular epithelial cells. From this point of view, HBeAg could be a pivotal antigen responsible for HBV-related nephropathy [25]. The deposition of such an immune complex could lead to damage to the glomerulus through the activation of the complement system, platelet aggregation, infiltration of leucocytes, intraglomerular coagulation and fibrin deposition [26]. HBV DNA is also observed in renal tubules and mesangial cells and is associated with disease activity of nephropathy.

Treatment of HBV-Related Nephropathy

Corticosteroid and immunosuppressant therapy has been used for the treatment of MN. However, in HBV-related disease, immunosuppression should induce reactivation of HBV and cause severe hepatitis. In addition, since the response to corticosteroids might be insufficient in cases with HBV-related MN, they are not recommended for the treatment of this type of renal complication [26]. Reduction of viral protein using antiviral therapies, such as nucleotide analogs, is required for clinical remission. Lamivudine treatment has been reported to improve renal outcome in HBV carriers with MN [27]. However, dose adjustment of nucleotide analogs is required for cases with renal dysfunction [28].

Generally, HBV-related nephropathy could be improved after seroconversion and reduction of HBeAg levels. The prognosis of HBV-related nephropathy varies among geographic regions, probably due to the differ-

ences of the immune response and clinical course caused by different HBV genotypes. Renal failure should be possible, particularly in adult patients [8].

HCV-Related Nephropathy

MPGN is the most common nephropathy among HCV-positive cases [29]. One report noted that MPGN was present in 12 of 963 renal biopsies; 4 of these cases (4/12; 33%) were also positive for HCVAg [30]. HCV-related nephropathy is frequently accompanied by cryoglobulinemia, where IgG, IgM and complements are observed in mesangial cells and capillary walls [8]. A decrease in serum complement, particularly component 4, has been observed, and cryoglobulin-like structures are seen in glomerular epithelial cells using electron microscopy [8]. Antiviral therapy for HCV is administered to treat nephropathy and is effective for proteinuria. However, in cases with limited response, recurrence after antiviral therapy is possible. Recent advancement of antiviral therapy with or without interferon administration would lead to the complete elimination of HCV, which should also improve the extrahepatic manifestation of chronic hepatitis C, including nephropathy.

Conclusion

In this review, we describe several types of vascular involvement that may be triggered by hepatitis virus infection, and present accumulating evidence that antiviral therapy is critical to control this complication. Recent advances in antiviral therapy for hepatitis B and C have achieved considerable response rates for both HBV and HCV. These new therapeutic agents could improve the prognosis of vascular and renal involvement in cases with chronic viral hepatitis.

Acknowledgement

This work was supported in part by a grant from the Smoking Research Foundation to N. Nishida.

Disclosure Statement

The authors declare that there is no conflict of interest regarding the publication of this article.

References

1 Kim do Y, Han KH: Epidemiology and surveillance of hepatocellular carcinoma. Liver Cancer 2012;1:2–14.

2 Kawanaka M, Nishino K, Nakamura J, Oka T, Urata N, Goto D, Suehiro M, Kawamoto H, Kudo M, Yamada G: Quantitative levels of hepatitis B virus DNA and surface antigen and the risk of hepatocellular carcinoma in patients with hepatitis B receiving long-term nucleos(t)ide analogue therapy. Liver Cancer 2014;3:41–52.

3 Han SH: Extrahepatic manifestations of chronic hepatitis B. Clin Liver Dis 2004;8:403–418.

4 Himoto T, Masaki T: Extrahepatic manifestations and autoantibodies in patients with hepatitis C virus infection. Clin Dev Immunol 2012;2012:871401.

5 Nishida N: Vasculitis associated with hepatitis virus. J Clin Exp Med (Igaku no Ayumi) 2013;246:127–130.

6 Saadoun D, Rosenzwajg M, Joly F, Six A, Carrat F, Thibault V, Sene D, Cacoub P, Klatzmann D: Regulatory T-cell responses to low-dose interleukin-2 in HCV-induced vasculitis. N Engl J Med 2011;365:2067–2077.

7 Gocke DJ, Hsu K, Morgan C, Bombardieri S, Lockshin M, Christian CL: Association between polyarteritis and Australia antigen. Lancet 1970;2:1149–1153.

8 Pyrsopoulos NT, Reddy KR: Extrahepatic manifestations of chronic viral hepatitis. Curr Gastroenterol Rep 2001;3:71–78.

9 Ramos-Casals M, Stone JH, Cid MC, Bosch X: The cryoglobulinaemias. Lancet 2012;379:348–360.

10 Levo Y, Gorevic PD, Kassab HJ, Zucker-Franklin D, Franklin EC: Association between hepatitis B virus and essential mixed cryoglobulinemia. N Engl J Med 1977;296:1501–1504.

11 Trejo O, Ramos-Casals M, Garcia-Carrasco M, Yague J, Jimenez S, de la Red G, Cervera R, Font J, Ingelmo M: Cryoglobulinemia: study of etiologic factors and clinical and immunologic features in 443 patients from a single center. Medicine 2001;80:252–262.

12 Mathieu E, Fain O, Krivitzky A: Cryoglobulinemia after hepatitis B vaccination. N Engl J Med 1996;335:355.

13 Gorevic PD, Kassab HJ, Levo Y, Kohn R, Meltzer M, Prose P, Franklin EC: Mixed cryoglobulinemia: clinical aspects and long-term follow-up of 40 patients. Am J Med 1980;69:287–308.

14 Saadoun D, Asselah T, Resche-Rigon M, Charlotte F, Bedossa P, Valla D, Piette JC, Marcellin P, Cacoub P: Cryoglobulinemia is associated with steatosis and fibrosis in chronic hepatitis C. Hepatology 2006;43:1337–1345.

15 Rosa D, Saletti G, De Gregorio E, Zorat F, Comar C, D'Oro U, Nuti S, Houghton M, Barnaba V, Pozzato G, Abrignani S: Activation of naive B lymphocytes via CD81, a pathogenetic mechanism for hepatitis C virus-associated B lymphocyte disorders. Proc Natl Acad Sci USA 2005;102:18544–18549.

16 Knight GB, Gao L, Gragnani L, Elfahal MM, De Rosa FG, Gordon FD, Agnello V: Detection of WA B cells in hepatitis C virus infection: a potential prognostic marker for cryoglobulinemic vasculitis and B cell malignancies. Arthritis Rheum 2010;62:2152–2159.

17 Saadoun D, Resche Rigon M, Sene D, Terrier B, Karras A, Perard L, Schoindre Y, Coppere B, Blanc F, Musset L, Piette JC, Rosenzwajg M, Cacoub P: Rituximab plus Peg-interferon-alpha/ribavirin compared with Peg-interferon-alpha/ribavirin in hepatitis C-related mixed cryoglobulinemia. Blood 2010;116:326–334; quiz 504–505.

18 Trepo C, Guillevin L: Polyarteritis nodosa and extrahepatic manifestations of HBV infection: the case against autoimmune intervention in pathogenesis. J Autoimmun 2001;16:269–274.
19 Guillevin L, Lhote F, Cohen P, Sauvaget F, Jarrousse B, Lortholary O, Noel LH, Trepo C: Polyarteritis nodosa related to hepatitis B virus. A prospective study with long-term observation of 41 patients. Medicine 1995;74:238–253.
20 Wartelle-Bladou C, Lafon J, Trepo C, Pichoud C, Picon M, Pellissier JF, Zoulim F: Successful combination therapy of polyarteritis nodosa associated with a pre-core promoter mutant hepatitis B virus infection. J Hepatol 2001;34:774–779.
21 Guillevin L, Mahr A, Cohen P, Larroche C, Queyrel V, Loustaud-Ratti V, Imbert B, Hausfater P, Roudier J, Bielefeld P, Petitjean P, Smadja D: Short-term corticosteroids then lamivudine and plasma exchanges to treat hepatitis B virus-related polyarteritis nodosa. Arthritis Rheum 2004;51:482–487.
22 Locasciulli A, Testa M, Valsecchi MG, Bacigalupo A, Solinas S, Tomas JF, Ljungman P, Alberti A: The role of hepatitis C and B virus infections as risk factors for severe liver complications following allogeneic BMT: a prospective study by the Infectious Disease Working Party of the European Blood and Marrow Transplantation Group. Transplantation 1999;68:1486–1491.
23 Combes B, Shorey J, Barrera A, Stastny P, Eigenbrodt EH, Hull AR, Carter NW: Glomerulonephritis with deposition of Australia antigen-antibody complexes in glomerular basement membrane. Lancet 1971;2:234–237.
24 Li P, Wei RB, Tang L, Wu J, Zhang XG, Chen XM: Clinical and pathological analysis of hepatitis B virus-related membranous nephropathy and idiopathic membranous nephropathy. Clin Nephrol 2012;78:456–464.
25 Takekoshi Y, Tanaka M, Miyakawa Y, Yoshizawa H, Takahashi K, Mayumi M: Free 'small' and IgG-associated 'large' hepatitis B e antigen in the serum and glomerular capillary walls of two patients with membranous glomerulonephritis. N Engl J Med 1979;300:814–819.
26 Chadban SJ, Atkins RC: Glomerulonephritis. Lancet 2005;365:1797–1806.
27 Tang S, Lai FM, Lui YH, Tang CS, Kung NN, Ho YW, Chan KW, Leung JC, Lai KN: Lamivudine in hepatitis B-associated membranous nephropathy. Kidney Int 2005;68:1750–1758.
28 Lai CL, Yuen MF: Prevention of hepatitis B virus-related hepatocellular carcinoma with antiviral therapy. Hepatology 2013;57:399–408.
29 Manns MP, Rambusch EG: Autoimmunity and extrahepatic manifestations in hepatitis C virus infection. J Hepatol 1999;31(suppl 1):39–42.
30 Ohta S, Yokoyama H, Furuichi K, Segawa C, Hisada Y, Wada T, Takasawa K, Kobayashi K: Clinicopathologic features of glomerular lesions associated with hepatitis C virus infection in Japan. Clin Exp Nephrol 1997;1:216–224.

Original Article

Digestive Diseases

Dig Dis 2014;32:791–799
DOI: 10.1159/000368024

Accuracy of Real-Time Tissue Elastography for the Evaluation of Hepatic Fibrosis in Patients with Chronic Hepatitis B: A Prospective Multicenter Study

Tao Wu[a] Jie Ren[a] Shu-zhen Cong[b] Fan-kun Meng[c] Hong Yang[d] Yan Luo[e] Hong-jun Lin[f] Yan Sun[g] Xiu-yan Wang[h] Shu-Fang Pei[b] Ying Zheng[c] Yun He[d] Yang Chen[e] Yu Hu[f] Na Yang[g] Ping Li[h] Masatoshi Kudo[i] Rong-qin Zheng[a]

Departments of Ultrasound, [a]Third Affiliated Hospital, Sun Yat-sen University, [b]Guangdong General Hospital, Guangzhou, [c]Beijing Youan Hospital, Capital Medical University, Beijing, [d]First Affiliated Hospital, Guangxi Medical University, Nanning, [e]West China Hospital, Sichuan University, Chengdu, [f]Jiangsu Province Hospital, Nanjing, [g]Second Affiliated Hospital, Kunming Medical University, Kunming, and [h]Tongji Hospital, Tongji University, Shanghai, China; [i]Department of Gastroenterology and Hepatology, Kinki University School of Medicine, Osaka-Sayama, Japan

Key Words
Chronic hepatitis B · Hepatic fibrosis · Real-time tissue elastography

Abstract
Background: The prognosis and management of hepatic fibrosis are closely related to the stage of the disease. The limitations of liver biopsy, which is the gold standard for treatment, include its invasiveness and sampling error. Ultrasound elasticity might be the most promising imaging technology for the noninvasive and accurate assessment of hepatic fibrosis. Real-time tissue elastography (RTE) measures the relative stiffness of the tissue in the region of interest caused by the heartbeat. Many studies have verified that RTE is useful for the diagnosis of hepatic fibrosis in patients with chronic hepatitis C (CHC). ***Purpose:*** To determine the formula of the liver fibrosis index for chronic hepatitis B (BLFI) and to validate the diagnostic accuracy of the BLFI for hepatic fibrosis compared with the liver fibrosis index (LFI). ***Materials and Methods:*** RTE was performed in 747 prospectively enrolled patients with chronic hepatitis B (CHB) or cirrhosis from 8 centers in China; 375 patients were analyzed as the training set, and 372 patients were evaluated as the validation set. The fibrosis stage was diagnosed from pathological specimens obtained by ultrasound-guided liver biopsy. Nine image features were measured from strain images, and the new formula for the BLFI was obtained by combining the nine imaging features of the RTE images using multiple regression analysis of the training set. The BLFI and LFI were compared with the pathological fibrosis stage at diagnosis, and the diagnostic performances of the indexes were compared. ***Results:*** The Spearman correlation coefficient between the BLFI and hepatic fibrosis stages was significantly positive ($r = 0.711$, $p < 0.001$), and significant differences were present between all disease stages. The areas

Masatoshi Kudo, MD, PhD
Department of Gastroenterology and Hepatology
Kinki University School of Medicine
377-2 Ohno-Higashi, Osaka-Sayama, Osaka 589-8511 (Japan)
E-Mail m-kudo@med.kindai.ac.jp

Rong-qin Zheng, MD, PhD
Department of Ultrasound
Third Affiliated Hospital of Sun Yat-sen University
No. 600 Tianhe Road, Guangzhou 510630 (China)
E-Mail zhengrq@mail.sysu.edu.cn

0257–2753/14/0326–0791$39.50/0

E-Mail karger@karger.com
www.karger.com/ddi

under the receiver-operating characteristic (AUROC) curves of the BLFI and LFI for predicting significant fibrosis (S0–S1 vs. S2–S4) were 0.858 and 0.858, respectively. For cirrhosis (S0–S3 vs. S4), the AUROC curves of the BLFI and LFI were 0.868 and 0.862, respectively. ***Conclusion:*** The results of this large, multicenter study confirmed that RTE is valuable for the diagnosis of hepatic fibrosis in patients with CHB. However, the diagnostic efficiencies of the new BLFI and the original LFI, which were based on CHC, for the assessment of CHB hepatic fibrosis were similar; thus, the LFI has the potential to be used to directly evaluate the extent of hepatic fibrosis in patients with CHB.

Introduction

Chronic viral hepatitis infection increases liver fibrosis and stiffness and is an important cause of liver cirrhosis and hepatocellular carcinoma [1–6]. Liver biopsy remains the gold standard for the diagnosis of hepatic fibrosis; however, a biopsy is an invasive procedure associated with discomfort and adverse events [7]. Moreover, the evaluation of liver biopsies could be influenced by sampling errors and by intra- and interobserver variability [8, 9]. Thus, noninvasive diagnostic methods for the assessment of hepatic fibrosis are urgently needed. Ultrasound (US) elastography has been considered a promising noninvasive and accurate modality for the assessment of hepatic fibrosis in several studies; it includes many forms, such as sonographic transient elastography (FibroScan; EchoSens, London, UK) and acoustic radiation force impulse imaging. Results have shown that FibroScan measurements of the velocity of the shear wave correlated well with the stage of fibrosis [10, 11], and this method has been recommended for use by the European Association for the Study of the Liver [2, 12]. However, the FibroScan has its limitations, including the lack of 2D image guidance and difficulties in evaluating certain types of patients with thick, fat tissue under the skin and ascites [13, 14].

Real-time tissue elastography (RTE) belongs to the category of strain elastography, which is different from the FibroScan. RTE measures the relative stiffness of the tissue in the region of interest (ROI) caused by the heartbeat using a combined autocorrelation method [14–17]. RTE displays the stiffness by overlying the B-mode image in the ROI with a color; the colors range from blue to red and indicate the relative softness and hardness of the area, respectively. This method is less affected by the body mass index and ascites than the FibroScan [18]. Studies have demonstrated that RTE is useful for the diagnosis of hepatic fibrosis. However, evaluation indexes for the diagnosis of liver fibrosis in current reports are different, and some indexes are calculated manually and subjectively [16–22]. Recently, Fujimoto et al. [16] reported a novel image analysis method using RTE for the evaluation of hepatic fibrosis in patients with chronic hepatitis C (CHC). The authors extracted 9 image features to quantify the patchy pattern of the RTE images and used these features to characterize the image; the authors correlated these features with fibrosis staging. To improve the accuracy of estimating the extent of hepatic fibrosis and to make the method more convenient, they performed a multiple regression analysis that used the 9 image features. Thus, they obtained an index of the liver fibrosis index (LFI) from a multiple regression equation which correlated highly with the stages of hepatic fibrosis and also reflected the underlying hepatic fibrosis accurately [16].

However, published studies have demonstrated different results regarding liver stiffness in patients with CHC and chronic hepatitis B (CHB) [23–25]. A meta-analysis of FibroScan data indicated that different liver diseases influence the diagnostic performance of significant fibrosis [10]. The diagnostic performance of hepatic fibrosis assessment in patients with CHC and CHB might be different using this impressive and quantitative image analysis method. Estimates have indicated that there are more individuals with CHB (approx. 120 millions) than individuals with CHC in China; approximately 300,000 CHB patients die annually of liver cirrhosis and hepatocellular carcinoma [1]. Thus, the aims of this large, prospective, multicenter study in patients with CHB were (1) to obtain a new liver fibrosis index (BLFI), which is calculated from the image features of RTE images using a new multiple regression equation to examine the clinical data of our cases with CHB rather than CHC and (2) to explore the effectiveness of this new BLFI in the diagnosis of hepatic fibrosis and to compare these results with the LFI computed from the original multiple regression equation based on the data from CHC patients.

Patients and Methods

Patients

The study protocol was approved by the independent ethics committees of our institutions, and written informed consent was obtained from the participants. This prospective, multicenter, cross-sectional study was conducted at eight hospitals in China: the Third

Affiliated Hospital (Sun Yat-sen University), Guangdong General Hospital, Beijing Youan Hospital (Capital Medical University), First Affiliated Hospital (Guangxi Medical University), West China Hospital (Sichuan University), Jiangsu Province Hospital, Second Affiliated Hospital (Kunming Medical University) and Tongji Hospital (Tongji University). We selected 747 consecutive patients with CHB or cirrhosis who underwent percutaneous US-guided liver biopsy between June 2010 and July 2013 (table 1). In these patients, CHB was defined as the presence of hepatitis B surface antigen and the absence of anti-hepatitis C virus antibodies in the serum. Eighty-nine patients were excluded from the study. The 747 eligible patients were divided into two groups based on the included date and the stage of hepatic fibrosis. Three hundred seventy-five patients were studied in the training set to estimate the new multiple regression equation for the computation of the LFI for CHB; the remaining patients were included in the validation set (n = 372) to evaluate the effectiveness of the BLFI in the assessment of hepatic fibrosis and to compare the results between the BLFI and LFI.

Table 1. Clinical characteristics of and laboratory information on the study patients

Male/female ratio	472/275
Age, years	38.102±13.01
Range	18–72
Body mass index	21.787±2.820
AST, IU/l	60.502±77.747
ALT, IU/l	83.908±123.976
Albumin, g/dl	42.152±4.535
Total bilirubin, mg/dl	25.680±45.396
GGT, IU/l	137.757±249.299
ALP, IU/l	123.201±144.937
Platelet count, $\times 10^4$/l	197.538±63.414
Prothrombin time, %	103.393±15.464

Liver Histology Assessment

A US-guided percutaneous liver biopsy (1.2-mm-diameter and 160-mm-long needle, cutting technique) was performed within 1 week prior to the RTE examination. If the liver biopsy samples were less than 12 mm long, a second liver biopsy was performed to obtain longer samples in order to avoid sampling error in the identification of liver fibrosis [8]. The liver biopsy samples were fixed in formalin and embedded in paraffin. Slices (3 μm thick) were stained with hematoxylin-eosin and argyrophilic proteins. Fibrosis was staged by a single pathologist, who had more than 15 years of experience and was blinded to all patient characteristics.

Liver fibrosis was staged on a four-point scale from S0 to S4 according to the Scheuer scoring system as follows [26]: S0, no fibrosis; S1, enlarged, fibrotic portal tracts; S2, periportal or portal-portal septa, but intact architecture; S3, fibrosis with architectural distortion, but no obvious cirrhosis, and S4, probable or definite cirrhosis.

Measurement of Liver Stiffness

All study patients underwent RTE examinations using ultrasonography (HI-VISION Ascendus; Hitachi Aloka Medical, Tokyo, Japan) and the EUP-L52 linear probe (3–7 MHz; Hitachi Aloka Medical). The patients were examined in the supine position with the right arm elevated above the head to widen the intercostal space. The examinations were performed on the right lobe of the liver through the intercostal spaces while holding the transducer lightly against the skin without vibration to obtain RTE images that were displayed in the direction of the heart. The appropriate position was selected where the B-mode images were devoid of artifacts, and the position in which the hepatic parenchyma moves in a lateral direction as a result of cardiac motion was not appropriate for this study. While the patient was holding his breath, we ensured that the strain images were shown periodically by cardiac motion. The ROI of the strain image was 2.5 × 2.5 cm and was placed more than 1 cm below the surface of the liver. Additionally, to obtain accurate and reliable images, the ROI should avoid large vessels and attenuation by the lungs or ribs. Regions deep inside the liver are not suitable because they often appear blue because of poor US penetration. The best RTE images were selected for the final analysis. An average of the best 3–5 images for each patient was used in the multiple regression analysis and to calculate the BLFI [16]. In July 2012, we provided RTE education and training regarding the operation procedure, which was combined with previous experience. The RTE images that included horizontal slipping by cardiac movement, images that contained artifacts and images with poor penetration of the US were rejected; when the number of suitable RTE images for the patient was not sufficient, the patient was excluded.

We extracted the following 9 image features to quantify the variable pattern of the RTE images: mean relative strain value (MEAN); standard deviation of the relative strain value (SD); percentage of low strain area (percentage of blue color area: %AREA); complexity of low strain area (calculated as perimeter squared/area: COMP); skewness (SKEW); kurtosis (KURT); entropy (ENT); inverse difference moment (IDM) and angular second moment (ASM). A multiple regression analysis was performed to improve the diagnostic accuracy for hepatic fibrosis by combining these 9 image features rather than by a diagnosis using individual image features. The BLFI was assessed using these 9 image features as independent variables and the hepatic fibrosis stage as a dependent variable, and the multiple regression equation was estimated from the training set. The BLFI was applied to estimate the stage of hepatic fibrosis and to validate the diagnostic accuracy of the BLFI for hepatic fibrosis in the validation set. Moreover, the LFI was computed from the original multiple regression equation based on data from CHC patients as follows:

$$LFI = -0.009 \times MEAN - 0.005 \times SD + 0.023 \times \%AREA + 0.025 \times COMP + 0.775 \times SKEW - 0.281 \times KURT + 2.083 \times ENT + 3.042 \times IDM + 39.979 \times ASM - 5.542.$$

The effectiveness of the BLFI and LFI in the evaluation of fibrosis staging was compared.

Statistical Analysis

The BLFI equation was calculated using multiple regression analysis. The 9 image features comprised the independent variables, and the hepatic fibrosis stage comprised the dependent variable. For comparisons between included and excluded cases at the different times, the χ^2 test was employed. The stiffness measurements were not normally distributed. Therefore, the measurements were compared with the categories of the consensus fibrosis stage using the nonparametric Mann-Whitney U test. Correlations

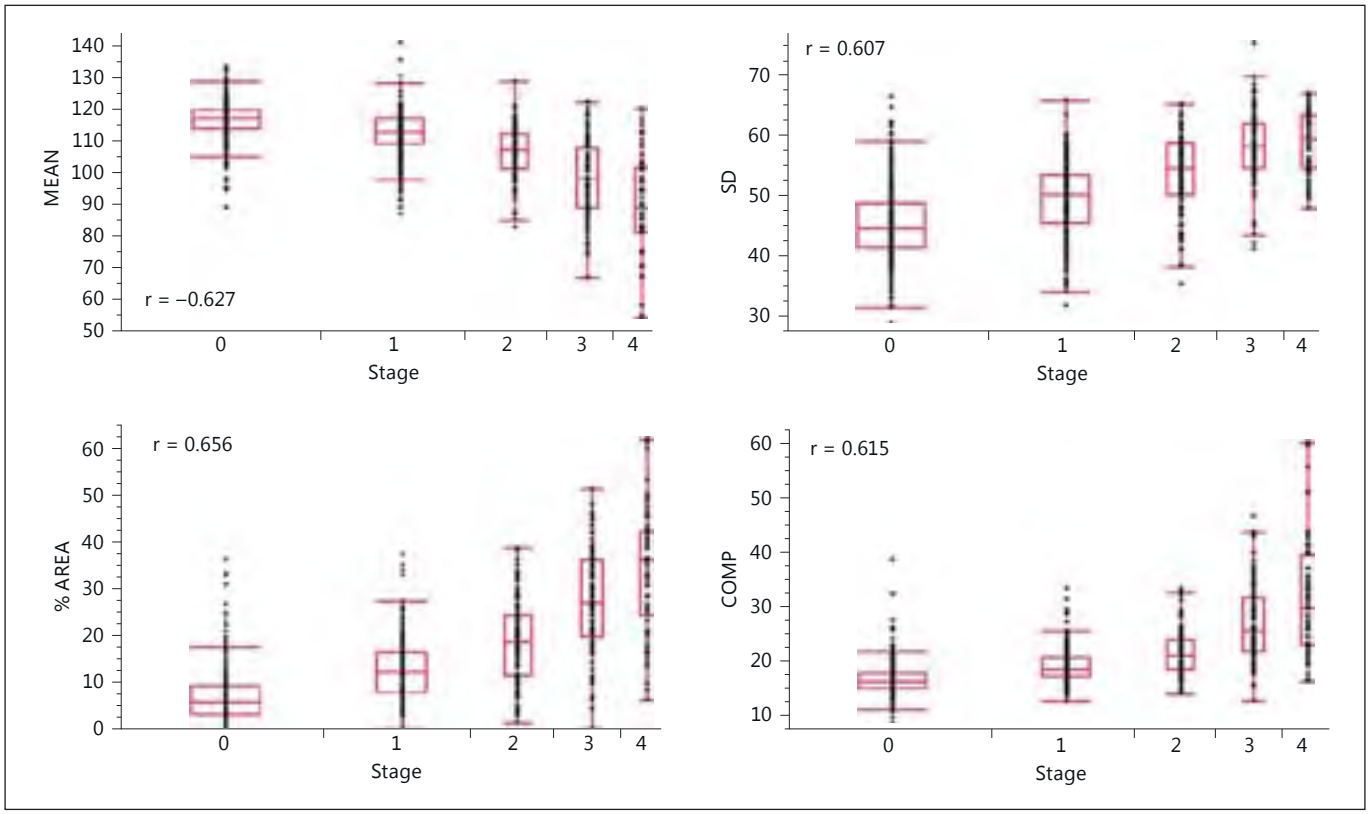

Fig. 1. Relationships between hepatic fibrosis stages and the MEAN, SD, %AREA and COMP in the combined data set. There was a high correlation between the MEAN, SD, %AREA and COMP and the stages of hepatic fibrosis.

Table 2. Number of cases recruited during the study

Study period	Eligible cases, n	Excluded cases, n	Total cases, n
June 2010 to July 2012	420	73 (14.8%)*	493
August 2012 to July 2013	327	16 (4.7%)*	343
Total	747	89 (10.6%)	836

* The 2 exclusion rates differed significantly ($p < 0.001$).

Table 3. Stages of hepatic fibrosis in the training and validation sets

Stage	Training set, n	Validation set, n	Total, n
S0	86 (23%)	85 (23%)	171 (23%)
S1	126 (34%)	126 (34%)	252 (34%)
S2	70 (19%)	69 (19%)	139 (19%)
S3	58 (15%)	57 (15%)	115 (15%)
S4	35 (9%)	35 (9%)	70 (9%)
Total	375 (100%)	372 (100%)	747 (100%)

between the measurements and the histologic fibrosis stage were analyzed by Spearman's correlation coefficients.

Receiver operating characteristic (ROC) curves were constructed, and the areas under the ROC (AUROC) curves were calculated using the trapezoidal rule. The optimal cutoff value for hepatic fibrosis was calculated according to the Youden index, which represents the best combination of sensitivity and specificity. The diagnostic performance for hepatic fibrosis was determined in terms of sensitivity, specificity and diagnostic accuracy using cutoff values obtained from the ROC curves. z scores were applied to compare AUROC curves between the BLFI and LFI [27].

$p < 0.05$ was considered statistically significant. Analyses were performed using SPSS Statistics 20 (IBM, Armonk, N.Y., USA) and MedCalc (version 12.7.0; MedCalc Software, Mariakerke, Belgium).

Results

Patients

We performed RTE in 836 patients between June 2010 and July 2013, and we excluded 89 patients from our study. The majority of the exclusions were related to the

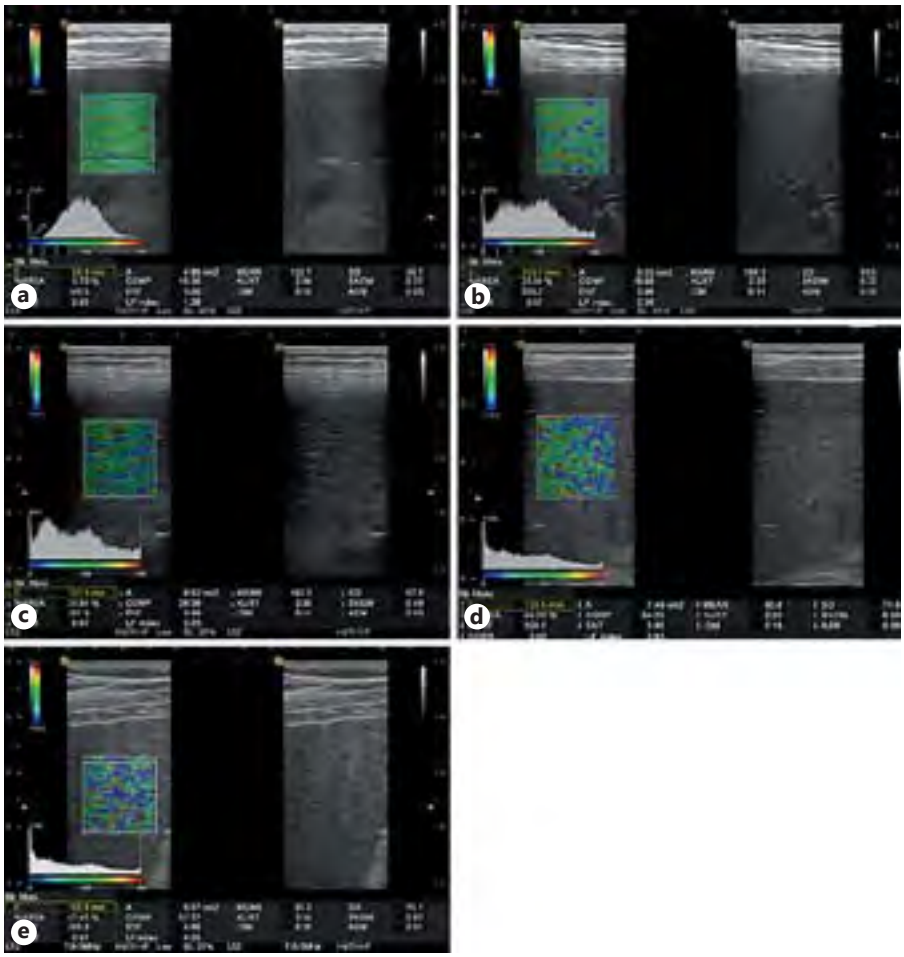

Color version available online

Fig. 2. RTE images for each fibrosis stage in patients with CHB. The blue areas (see online version for colors) of the RTE image gradually increased with the progression of liver fibrosis: stage 0 (**a**), stage 1 (**b**), stage 2 (**c**), stage 3 (**d**) and stage 4 (**e**).

inexperienced RTE skill level of the radiologists. The exclusion rate was significantly reduced from 14.8 to 4.7% ($p < 0.001$) after RTE education and training sessions were provided in July 2012 (table 2). The clinical characteristics of and laboratory information on the 747 patients are shown in table 1. The hepatic fibrosis stages of the cases, which were confirmed by liver histology assessment, are displayed in table 3.

Correlation between Features and Pathological Hepatic Fibrosis in All Sets

In our study, we extracted 9 image features and the LFI to quantify the RTE images. Correlation coefficients between the quantitative parameters of the RTE images, such as the MEAN, SD, %AREA, COMP, SKEW, KURT, ENT, IDM and ASM, and the hepatic fibrosis stage in all included patients were –0.627, 0.607, 0.656, 0.615, 0.482, –0.180, 0.278, 0.123 and 0.221, respectively (fig. 1). The MEAN, SD, %AREA and COMP were highly correlated with the stage of hepatic fibrosis. Characteristic RTE images for each fibrosis stage are shown in figure 2.

Equation for BLFI in the Training Set

The BLFI was estimated by combining the 9 image features using the multiple regression analysis of the training set. The multiple regression equation of BLFI was calculated using multiple regression analysis:

$$BLFI = -0.0475 \times MEAN + 0.0222 \times SD - 0.00555 \times AREA + 0.0151 \times COMP + 31.1 \times ASM + 4.27 \times ENT + 11 \times IDM - 0.0326 \times SKEW + 0.215 \times KURT - 12.9.$$

There were some differences compared with the original multiple regression equation for the LFI based on CHC patients described in the report of Fujimoto et al. [16].

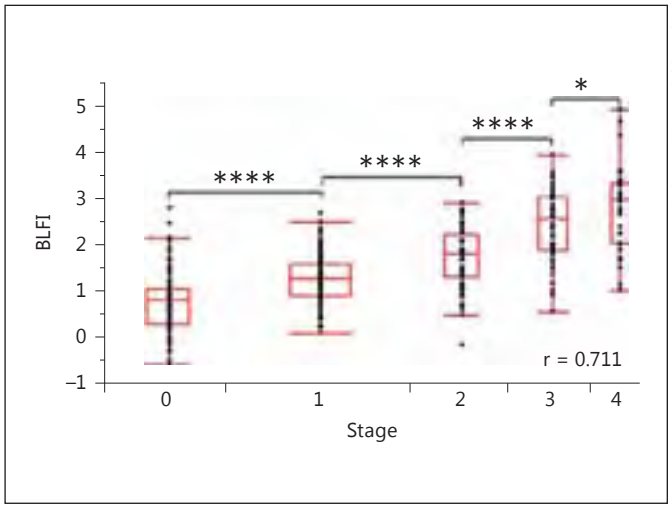

Color version available online

Fig. 3. Relationships between the hepatic fibrosis stages and the BLFI in the validation set. The graph shows the BLFI for each fibrosis stage. The bottom and top of each box represent the 25th and 75th percentiles, respectively. The horizontal line represents the median, and the vertical line represents the range. Significant differences were observed between the hepatic fibrosis stage and the BLFI (* $p < 0.05$, **** $p < 0.001$).

Diagnostic Performance of Fibrosis Staging by the BLFI in the Validation Set

Figure 3 shows the box-and-whisker plots for the BLFI in the validation set calculated from the 9 image features using the multiple regression analysis of the training set for each fibrosis stage. When the histologic liver fibrosis stages and the BLFI were compared, there was a high correlation between increased BLFI and increased hepatic fibrosis stages. The Spearman correlation coefficient between the BLFI and hepatic fibrosis stages was significantly positive ($r = 0.711$, $p < 0.001$), and significant differences existed between the different stages. The ROC curve analysis identified cutoff values of the BLFI as high as 1.603 for ≥stage 2 and 2.062 for stage 4 (fig. 4). The corresponding AUROC, sensitivity, specificity and accuracy data are shown in table 4.

Comparison of the BLFI and LFI in the Validation Set

In the validation set, assessments of diagnostic accuracy for each fibrosis stage were performed using the BLFI and LFI. Comparisons of the correlation coefficients of the BLFI and the LFI showed that there were no significant differences between the variables ($p > 0.05$). The AUROC curves of the BLFI and LFI for predicting significant fibrosis (S0–S1 vs. S2–S4) were 0.858 and 0.858, respectively. For cirrhosis (S0–S3 vs. S4), the AUROC curves of the BLFI and LFI were 0.868 and 0.862, respectively (table 4). Comparisons of the AUROC curves of the two index values indicated that there was no significant difference between the values (fig. 5; $p > 0.05$).

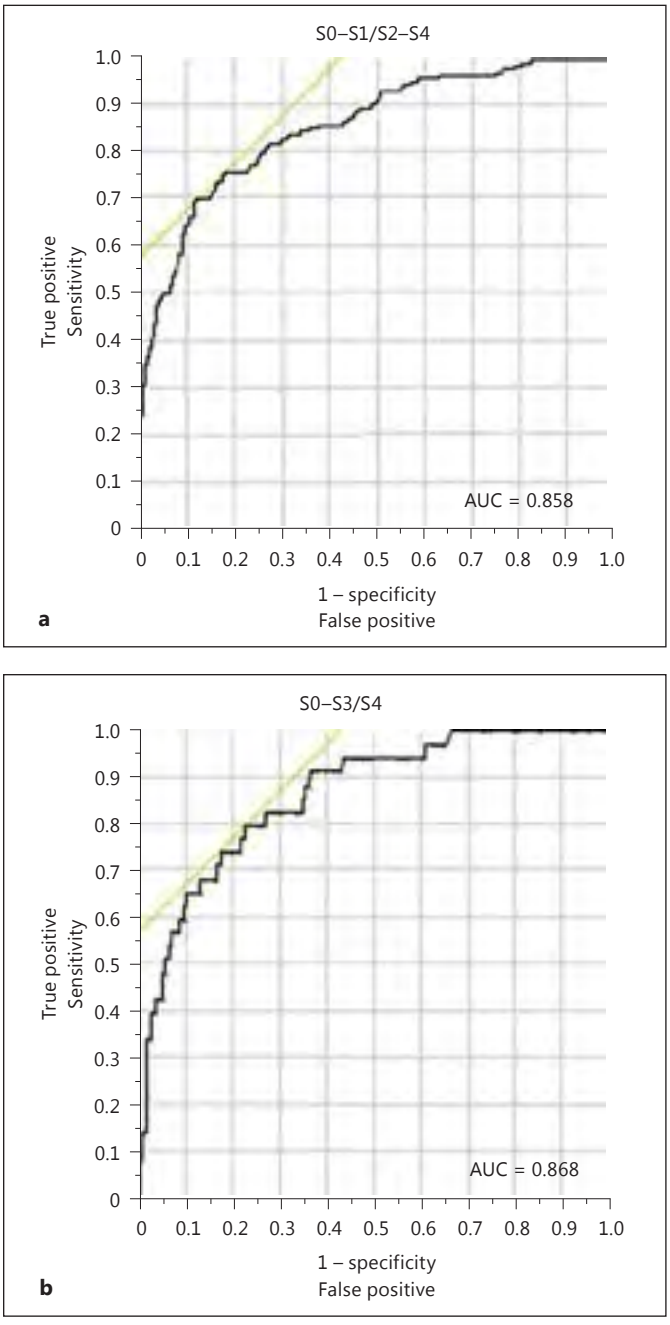

Color version available online

Fig. 4. ROC curves for the diagnosis of hepatic fibrosis with the BLFI in the validation set. ROC analysis differentiating S2–S4 from S0–S1 (**a**) and S4 from S0–S3 (**b**) using the BLFI.

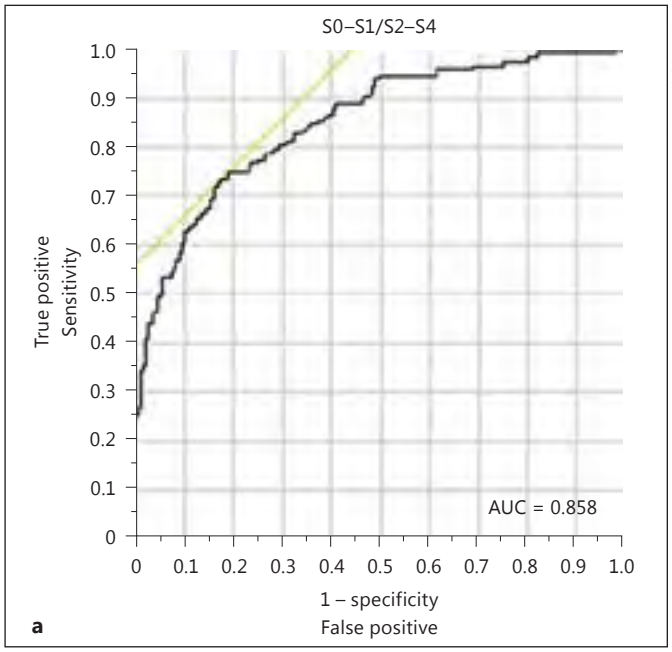

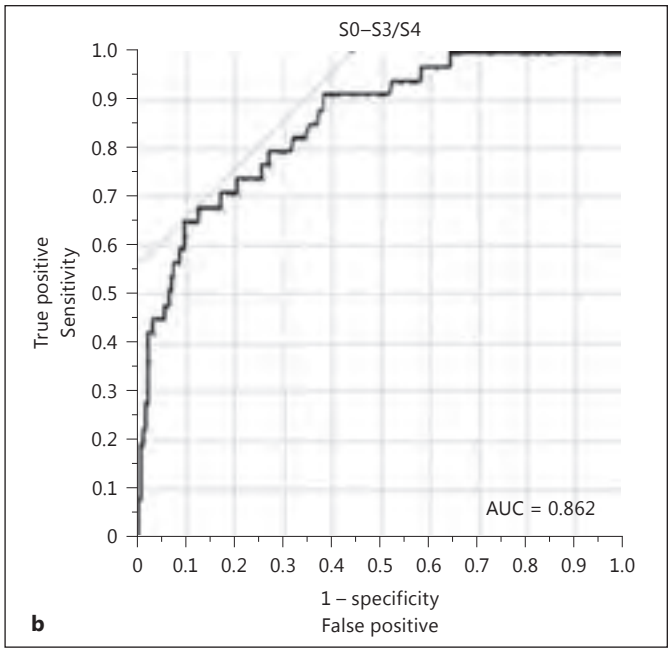

Fig. 5. ROC curves for the diagnosis of hepatic fibrosis with the LFI in the validation set. ROC analysis differentiating S2–S4 from S0–S1 (**a**) and S4 from S0–S3 (**b**) using the LFI.

Color version available online

Table 4. Diagnostic performance of the cutoff values of the BLFI and LFI for predicting significant fibrosis (S0–S1 vs. S2–S4) and cirrhosis (S0–S3 vs. S4)

	S0–S1/S2–S4		S0–S3/S4	
	BLFI	LFI	BLFI	LFI
AUROC	0.858	0.858	0.868	0.862
Cutoff value	1.603	2.099	2.062	2.511
Sensitivity, %	77.0	77.0	80.0	74.3
Specificity, %	77.3	76.8	77.4	79.8
Accuracy, %	77.2	76.9	77.7	79.3

There was no significant difference in the AUROC between the BLFI and LFI ($p > 0.05$).

Discussion

In our study, we showed that the parameters measured by RTE are useful predictive features for the determination of the hepatic fibrosis stage in patients with CHB. The MEAN, SD, %AREA and COMP showed a high correlation with the hepatic fibrosis stage; these results were similar to those of Fujimoto et al. [16]. The %AREA was the best indicator of the individual image features in all patients because the %AREA represents an area of low strain (blue) within the ROI; as hepatic fibrosis progresses, liver stiffness increases, with a corresponding increase in the area of low strain. Additionally, the BLFI is a comprehensive quantitative indicator of 9 image features that was developed using multiple regression analysis. It includes the most abundant information in the RTE images and highly correlates with the stages of hepatic fibrosis ($r = 0.711$, $p < 0.001$): significant differences in the BLFI were identified between each stage. Moreover, the AUROC and accuracy for predicting significant fibrosis and cirrhosis were as high as 0.858 and 0.770 and 0.868 and 0.800, respectively.

We compared the diagnostic performance of the new BLFI in the validation set with the LFI obtained from patients with CHC [16]. The AUROC and accuracy of the BLFI for the diagnosis of significant fibrosis and cirrhosis were similar to the LFI (table 4), and there was no significant difference between the values; this similarity might have been caused by the similar basic morphologic changes that occur during the pathology of CHB and CHC [26]. However, the epidemiology is different between CHB and CHC [1], and the necroinflammatory activity observed during HBV infection may differ with time, which makes patients with CHB prone to transaminase fluctuations [24]. Transient elastography is affected by inflammation, which might overestimate the degree of hepatic fibrosis. Studies have shown that the correlation coefficient between liver stiffness measured by transient

elastography and the stages of hepatic fibrosis in patients with CHC was higher compared with patients with CHB [10, 24]. However, our study showed that the diagnostic performances of the BLFI and LFI were similar, perhaps because the RTE might reflect the actual degree of hepatic fibrosis not affected by inflammation. The diagnostic performance of the BLFI for the assessment of hepatic fibrosis in CHB patients was not significantly better than the LFI; the BLFI did not achieve its expected purpose. Therefore, it might be possible to continue to use the LFI to evaluate hepatic fibrosis, as is done for CHB patients. The LFI is automatically calculated by the machine, which is convenient and widely accepted by clinicians.

In our study, we excluded 89 patients from our analysis, which accounted for 10.6% of the total cases; however, the exclusion rate was significantly reduced after completion of the RTE education and training sessions. The main reason for the exclusions was the examiners' lack of skill and experience, which might have an impact on the final outcome. It is necessary to further discuss the methodology of RTE in the future and to propose unified operational procedures for the training of examiners; these training procedures would be conducive to improving the acquisition rate and popularizing the applications of this technology.

Previous studies regarding RTE have shown that RTE is a useful and valuable tool for the assessment of hepatic fibrosis [16–22]. The subjects of these studies were primarily patients with CHC or chronic viral hepatitis, and there were only two reports regarding patients with CHB. Xie et al. [21] and Wang et al. [22] included patients with CHB; however, their evaluation indicators included the elastic strain ratio and elastic index, respectively. The LFI used in the study of Fujimoto et al. [16] contained abundant image information regarding the RTE, and the LFI was simple to use, which made it easier for clinicians to accept and further popularize and apply this technology. Our study was a large, multicenter prospective study of patients with CHB in China; we challenged a new index for evaluating hepatic fibrosis and explored whether this new index is suitable for patients suffering from CHB. Moreover, according to the diagnostic test method, we divided the patients into two groups: a training set for obtaining the new formula of the BLFI and a validation set for verifying the accuracy of the formula. This approach could make the results more convincing. Furthermore, we compared the results of the new BLFI with the LFI computed from the original multiple regression equation based on data from CHC patients, which has not been previously reported in any study.

We used the Scheuer scoring system as the gold standard of hepatic fibrosis in our study because this system has been generally applied and accepted, recommended by the Chinese Society of Hepatology and used in previous studies [21]. Furthermore, the staging criteria of the Scheuer scoring system are similar to the METAVIR System [26]. For these reasons, the Scheuer scoring system would not affect the judgment of our results. In our study, the number of CHB patients in S2–S4 was low and only accounted for 43% of the total cases (324/747), whereas in the study by Fujimoto et al. [16], CHC patients with F2–F4 accounted for 71% of the total cases (211/295), which had a more balanced distribution. To obtain a more accurate diagnostic threshold of hepatic fibrosis for patients with CHB, it is necessary to increase the number of S2–S4 cases to reduce the offset. Some of our study results were obtained only by comparisons with the previous literature [16]. The best method may be based on a comparison of two patient groups with different causes of fibrosis, which would increase the reliability of the results. Because the inflammation stage of some cases was missing during the data collection, we are unable to discuss the related research regarding inflammation in our study.

Conclusion

The results of this large, multicenter study confirmed that RTE is a valuable tool for the diagnosis of hepatic fibrosis in patients with CHB. However, the diagnostic efficiencies of the new BLFI and the original LFI, which was based on CHC patients, in assessing CHB hepatic fibrosis were similar. Thus, we might be able to use the LFI directly to evaluate the extent of hepatic fibrosis in patients with CHB.

Acknowledgments

We would like to thank Akiko Tonomura and Zhang Qi for their valuable contributions to this study.

References

1 Cui Y, Jia J: Update on epidemiology of hepatitis B and C in China. J Gastroenterol Hepatol 2013;28(suppl 1):7–10.
2 EASL clinical practice guidelines: management of hepatitis C virus infection. J Hepatol 2011;55:245–264.
3 Kudo M: Prediction of hepatocellular carcinoma incidence risk by ultrasound elastography. Liver Cancer 2014;3:1–5.

4 Kim do Y, Han KH: Epidemiology and surveillance of hepatocellular carcinoma. Liver Cancer 2012;1:2–14.
5 Kudo M: Japan's successful model of nationwide hepatocellular carcinoma surveillance highlighting the urgent need for global surveillance. Liver Cancer 2012;1:141–143.
6 Kawanaka M, Nishino K, Nakamura J, et al: Quantitative levels of hepatitis B virus DNA and surface antigen and the risk of hepatocellular carcinoma in patients with hepatitis B receiving long-term nucleos(t)ide analogue therapy. Liver Cancer 2014;3:41–52.
7 Cadranel JF, Rufat P, Degos F: Practices of liver biopsy in France: results of a prospective nationwide survey. For the Group of Epidemiology of the French Association for the Study of the Liver (AFEF). Hepatology 2000; 32:477–481.
8 Bedossa P, Dargere D, Paradis V: Sampling variability of liver fibrosis in chronic hepatitis C. Hepatology 2003;38:1449–1457.
9 Intraobserver and interobserver variations in liver biopsy interpretation in patients with chronic hepatitis C. The French METAVIR Cooperative Study Group. Hepatology 1994; 20:15–20.
10 Friedrich-Rust M, Ong MF, Martens S, et al: Performance of transient elastography for the staging of liver fibrosis: a meta-analysis. Gastroenterology 2008;134:960–974.
11 Fung J, Lai CL, But D, et al: Prevalence of fibrosis and cirrhosis in chronic hepatitis B: implications for treatment and management. Am J Gastroenterol 2008;103:1421–1426.
12 EASL clinical practice guidelines: management of chronic hepatitis B virus infection. J Hepatol 2012;57:167–185.
13 Bamber J, Cosgrove D, Dietrich CF, et al: EFSUMB guidelines and recommendations on the clinical use of ultrasound elastography. Part 1: basic principles and technology. Ultraschall Med 2013;34:169–184.
14 Cosgrove D, Piscaglia F, Bamber J, et al: EFSUMB guidelines and recommendations on the clinical use of ultrasound elastography. Part 2: clinical applications. Ultraschall Med 2013;34:238–253.
15 Kudo M, Shiina T, Moriyasu F, et al: JSUM ultrasound elastography practice guidelines: liver. J Med Ultrasonics 2013;40:325–357.
16 Fujimoto K, Kato M, Kudo M, et al: Novel image analysis method using ultrasound elastography for noninvasive evaluation of hepatic fibrosis in patients with chronic hepatitis C. Oncology 2013;84(suppl 1):3–12.
17 Yada N, Kudo M, Morikawa H, et al: Assessment of liver fibrosis with real-time tissue elastography in chronic viral hepatitis. Oncology 2013;84(suppl 1):13–20.
18 Koizumi Y, Hirooka M, Kisaka Y, et al: Liver fibrosis in patients with chronic hepatitis C: noninvasive diagnosis by means of real-time tissue elastography – establishment of the method for measurement. Radiology 2011; 258:610–617.
19 Lorenz A, Ermert H, Sommerfeld HJ, et al: Ultrasound elastography of the prostate. A new technique for tumor detection. Ultraschall Med 2000;21:8–15.
20 Fujimoto K, Wada S, Ohshita M, et al: Noninvasive evaluation of hepatic fibrosis in patients with chronic hepatitis C using elastography. Medix 2007;Suppl:24–27.
21 Xie L, Chen X, Guo Q, et al: Real-time elastography for diagnosis of liver fibrosis in chronic hepatitis B. J Ultrasound Med 2012;31:1053–1060.
22 Wang J, Guo L, Shi X, et al: Real-time elastography with a novel quantitative technology for assessment of liver fibrosis in chronic hepatitis B. Eur J Radiol 2012;81:e31–e36.
23 Ogawa E, Furusyo N, Toyoda K, et al: Transient elastography for patients with chronic hepatitis B and C virus infection: non-invasive, quantitative assessment of liver fibrosis. Hepatol Res 2007;37:1002–1010.
24 Sporea I, Sirli R, Deleanu A, et al: Liver stiffness measurements in patients with HBV vs HCV chronic hepatitis: a comparative study. World J Gastroenterol 2010;16:4832–4837.
25 Cardoso AC, Carvalho-Filho RJ, Stern C, et al: Direct comparison of diagnostic performance of transient elastography in patients with chronic hepatitis B and chronic hepatitis C. Liver Int 2012;32:612–621.
26 Fiel MI: Pathology of chronic hepatitis B and chronic hepatitis C. Clin Liver Dis 2010;14: 555–575.
27 Hinkle D, Wiersma W, Jurs S: Applied Statistics for the Behavioral Sciences, ed 2. Boston, Houghton Mifflin Company, 1988.

Oncology

Preface

Oncology 2014;87(suppl 1):1–6
DOI: 10.1159/000368140

Published online: November 22, 2014

Breakthroughs in the Management of Hepatocellular Carcinoma: Celebrating 50 Years of the Liver Cancer Study Group of Japan

Masatoshi Kudo

Department of Gastroenterology and Hepatology, Kinki University School of Medicine, Osaka-Sayama, Japan

The 50th Liver Cancer Study Group of Japan (LCSGJ) Congress (Congress President: Prof. Masatoshi Kudo) was held in Kyoto, Japan, on June 5–6, 2014. The LCSGJ is an academic society which was founded in 1967 by Dr. Ichio Honjo, Professor of the Department of Surgery at Kyoto University. On March 7, 1949, while working at Kokura Memorial Hospital, Prof. Honjo (fig. 1), at the young age of 35, became the first surgeon in the world to successfully perform an anatomical right lobectomy. Although the Japanese journal *Shujutsu* (*Operation)* published this breakthrough in 1950 [1], because it was not published in an English language journal until 1955 [2], there was a period in which articles cited the surgical technique performed by Lortat-Jacob [3] as the world's first anatomical right lobectomy. However, in the global history of liver surgery, Prof. Honjo is now well recognized as the pioneer who successfully completed the procedure first (fig. 2, 3) [4]. Prof. Honjo subsequently founded the LCSGJ and served as its first president in 1967. Largely due to the historical background, the LCSGJ maintained a head office at Kyoto University until 2008, when it moved to its current location, the Department of Gastroenterology and Hepatology at Kinki University (Head Office Representative: Prof. Masatoshi Kudo).

The theme of the 50th LCSGJ Congress was selected as 'Breakthroughs in the Management of Hepatocellular Carcinoma', to celebrate the breakthrough made by Prof. Honjo as well as the numerous breakthroughs in treatments for liver cancer made in the intervening 50 years. The congress program was packed with special features:

Fig. 1. Prof. Ichio Honjo (1913–1987), Professor Emeritus, Kyoto University School of Medicine (courtesy of Prof. Ryuji Mizumoto, Professor Emeritus, Mie University School of Medicine).

KARGER

E-Mail karger@karger.com
www.karger.com/ocl

0030–2414/14/0877–0001$39.50/0

Prof. Masatoshi Kudo
Department of Gastroenterology and Hepatology
Kinki University School of Medicine
377-2 Ohno-Higashi, Osaka-Sayama, Osaka 589-8511 (Japan)
E-Mail m-kudo@med.kindai.ac.jp

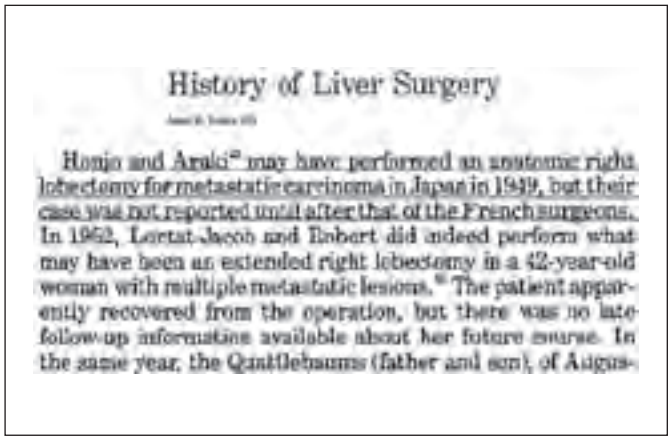

History of Liver Surgery

Honjo and Araki[2] may have performed an anatomic right lobectomy for metastatic carcinoma in Japan in 1949, but their case was not reported until after that of the French surgeons. In 1962, Lortat-Jacob and Robert did indeed perform what may have been an extended right lobectomy in a 42-year-old woman with multiple metastatic lesions.[3] The patient apparently recovered from the operation, but there was no late follow-up information available about her future course. In the same year, the Quattlebaums (father and son), of Augus-

Fig. 2. Extracted sentences from an article published in *Archives of Surgery* [4]. Dr. Foster clearly states that Prof. Honjo performed the world's first anatomic right hepatectomy in Japan in 1949.

two special lectures, one education lecture, one round-table-style commemorative session on the LCSGJ's history, three symposia, seven panel discussions, nine workshops, six video sessions, six difficult clinical case study sessions, and two consensus meetings (table 1).

In Symposium 1 entitled 'Basic Aspect, Diagnosis, Treatment, and Prognosis of Early Hepatocellular Carcinoma', discussions were held on next-generation sequencing analysis and diagnostic imaging for early hepatocellular carcinoma (HCC) [5], diagnosis by Sonazoid-enhanced ultrasonography and gadolinium ethoxybenzyl diethylenetriamine pentaacetic acid MRI, issues associated with pathological diagnosis, and the timing of treatment. Symposium 2 provided a forum for discussion in line with the session 'Treatment Strategies for Advanced and Large Liver Cancer' and particularly the attempts to

SOLID
LIVER
TUMORS

by
James H. Foster, M.D.

and
Martin M. Berman, M.D.

Volume XXII in the Series
MAJOR PROBLEMS IN CLINICAL SURGERY
PAUL A. EBERT, M.D.
Consulting Editor

a W. B. Saunders Company, Philadelphia, London, Toronto, 1977

Color version available online

Fig. 3. Extracts from the textbook by Dr. Foster and Dr. Berman (courtesy of Prof. Ryuji Mizumoto) [30]. **a** Cover picture of Solid Liver Tumors.

combine surgery and chemotherapy to treat vascular invasion, bile duct invasion, and large liver cancer. In Symposium 3, the heterogeneity of intermediate stage HCC, the attempt to subgroup heterogeneous intermediate stage HCC, the definition of transarterial chemoembolization (TACE) failure/refractoriness, and the treatment options for TACE failure/refractoriness cases were discussed under the title 'Treatment Strategies, Efficacy, and Prognosis of Intermediate Stage Liver Cancer'.

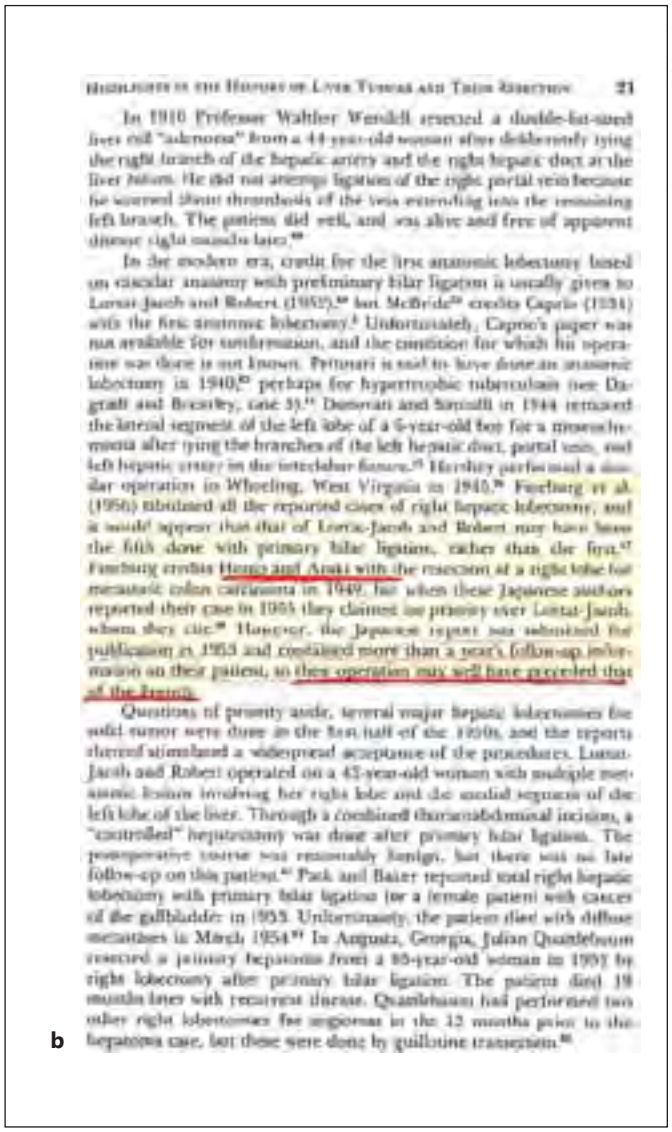

Color version available online

b

Fig. 3. Extracts from the textbook by Dr. Foster and Dr. Berman (courtesy of Prof. Ryuji Mizumoto) [30]. **b** Exracted sentences from the textbook. Dr. Foster clearly states 'Honjo and Araki's operation may well have preceeded that of the French'.

Latest diagnostic imaging modalities [6–9] were introduced in Panel Discussion 1, entitled 'Innovation in Diagnostic Imaging for Liver Cancer', while basic research approaches using, for example, oncogenes and methylation were discussed in Panel Discussion 2 on 'Future Prospects in Liver Cancer Treatment Based on Genome/Epigenome Data'. In Panel Discussion 3 on 'Future Perspectives on Molecular Targeted Therapy for Liver Cancer', discussions centered around the application of molecular targeted therapy, for which sorafenib is currently the only approved drug, the combination of sorafenib with conventional locoregional treatments [10–18], and other emerging targeted agents. In Panel Discussion 4, entitled 'Current Situation and Ongoing Challenges in Liver Transplantation for Patients with Hepatocellular Carcinoma', current issues associated with liver transplantation were addressed, while in Panel Discussion 5, 'Diagnosis and Pathology of Cystic Liver Tumor', new concepts such as intraductal papillary neoplasm of the intrahepatic bile duct and mucinous cystic neoplasm were reviewed. In Panel Discussion 6, pathological features were debated under the theme 'Pathology and Diagnosis of Combined Hepatocellular and Cholangiocellular Carcinoma'. Lastly, in Panel Discussion 7 on 'Various Issues Associated with Hepatocellular Adenoma and Focal Nodular Hyperplasia', the subgroups of hepatocellular adenomas, which have been attracting attention in recent years, and the imaging findings of focal nodular hyperplasia were reviewed.

Nine workshops were held at the congress. In Workshop 1 on 'Treatment for Child-Pugh C Liver Cancer', it was verified that locoregional therapy confers survival benefit to a specific subgroup of liver cancer patients with Child-Pugh C liver function. The discussions in Workshop 2 entitled 'Treatment Strategies for Recurrent Liver Cancer after Liver Transplantation' focused on recurrence, the most serious problem caused by liver transplantation [19–23]. In Workshop 3, the mechanism of and clinical approach to nonalcoholic steatohepatitis (NASH)-induced liver cancer were discussed under the theme of 'Basic and Clinical Aspects of NASH-Induced Liver Cancer: Including Diagnostic Criteria' [24]. Workshop 4 on 'Long-term Survival Cases (≥3 Years) of Advanced Hepatocellular Carcinoma after the Initiation of Molecular Targeted Therapy' focused on the characteristics of long-term survival cases after treatment with sorafenib. In Workshop 5 on 'Treatment Strategy for Intrahepatic Cholangiocarcinoma', surgical outcome of intrahepatic cholangiocarcinoma and the

Table 1. The 50th LCSGJ Congress: Special Programs

Special Lecture	1 Full Lifecycle Aquaculture of Bluefin Tuna: 32-Year Trajectory, by Prof. Hidemi Kumai 2 Management of Liver Cancer – Why We Do What We Do in Europe, by Prof. Markus Peck-Radosavljevic
Memorial Roundtable	Looking Back on the 50-Year History of the Liver Cancer Study Group of Japan
Education Lecture	Biomarkers in Molecular Targeted Therapy for Liver Cancer, by Prof. Kazuto Nishio
Symposium	1 Basic Aspect, Diagnosis, Treatment, and Prognosis of Early Hepatocellular Carcinoma 2 Treatment Strategies for Advanced and Large Liver Cancer 3 Treatment Strategies, Efficacy, and Prognosis of Intermediate Stage Liver Cancer
Panel Discussion	1 Innovation in Diagnostic Imaging for Liver Cancer 2 Future Prospects in Liver Cancer Treatment Based on Genome/Epigenome Data 3 Future Perspectives on Molecular Targeted Therapy for Liver Cancer 4 Current Situation and Ongoing Challenges in Liver Transplantation for Patients with Hepatocellular Carcinoma 5 Diagnosis and Pathology of Cystic Liver Tumor 6 Pathology and Diagnosis of Combined Hepatocellular and Cholangiocellular Carcinoma 7 Various Issues Associated with Hepatocellular Adenoma and Focal Nodular Hyperplasia
Consensus Meeting	1 A Diagnostic Algorithm for Liver Cancer 2 Updating the JSH Definition of TACE Failure/Refractoriness
Workshop	1 Treatment for Child-Pugh C Liver Cancer 2 Treatment Strategies for Recurrent Liver Cancer after Liver Transplantation 3 Basic and Clinical Aspects of NASH-Induced Liver Cancer: Including Diagnostic Criteria 4 Long-term Survival Cases (≥3 Years) of Advanced Hepatocellular Carcinoma after the Initiation of Molecular Targeted Therapy 5 Treatment Strategy for Intrahepatic Cholangiocarcinoma 6 Radiation Therapy for Hepatocellular Carcinoma 7 Treatment Strategy for Colorectal Liver Metastasis 8 Current Situation and Recent Advances in RFA 9 New Developments in TACE: How to Apply Beads TACE and cTACE Differently
Video Session	1 State-of-the-Art Contrast-Enhanced Ultrasonography 2 Advances in Simulation Imaging (Including 3- and 4-Dimensional Imaging) of Liver Cancer Treatment 3 Resection of Hepatocellular Carcinoma: Highly Technical Surgical Procedures 4 Technological Advances in TACE 5 The Frontline of Laparoscopic Therapy for Hepatocellular Carcinoma 6 Technological Advances in RFA Therapy (Including Fusion Imaging)
Difficult Clinical Case Study Sessions	1 Diagnosis 1 2 Diagnosis 2 3 Diagnosis 3 4 Treatment 1 5 Treatment 2 6 Treatment 3

characteristics of recurrence were discussed with a focus on hepatectomy. Workshop 6 focused on 'Radiation Therapy for Hepatocellular Carcinoma', and the participants discussed treatment directed solely at vascular invasion or the main lesion of HCC itself and proton and particle therapy [25, 26]. In addition, under the theme 'Treatment Strategy for Colorectal Liver Metastasis' in Workshop 7, the participants engaged in an active discussion of systemic chemotherapy, surgical approaches, microwave coagulation therapy, radiofrequency ablation (RFA), or particle therapy as locoreginal treatments. The main focus in Workshop 8, entitled 'Current Situation and Recent Advances in RFA' was bipolar RFA, and new RFA techniques including fusion image-guided RFA were also discussed [27]. Lastly, in Workshop 9 entitled 'New Developments in TACE: How to Apply Beads TACE and cTACE Differently', the participants discussed the differential application of conventional TACE [28] and beads (microsphere) TACE, the latter of which was introduced to Japan in January 2014.

In Video Session 1 entitled 'State-of-the-Art Contrast-Enhanced Ultrasonography', the significance of

this imaging modality for treatment guidance was discussed, as was its value in fusion imaging, in pretreatment diagnosis of malignant grade, in establishing treatment indications, and in selecting an appropriate treatment approach. Video Session 2 featured 'Advances in Simulation Imaging (Including 3- and 4-Dimensional Imaging) of Liver Cancer Treatment' and their applications. Extremely difficult surgical methods in liver resection were introduced and debated in Video Session 3 entitled 'Resection of Hepatocellular Carcinoma: Highly Technical Surgical Procedures', while 'Technological Advances in TACE' (e.g., beads TACE, balloon occluded-TACE, and FlightPlan) was the theme in Video Session 4. Video Session 5 on 'The Frontline of Laparoscopic Therapy for Hepatocellular Carcinoma' covered laparoscope-assisted treatment and robotic surgery with the da Vinci surgical system. Lastly, Video Session 6 entitled 'Technological Advances in RFA Therapy (Including Fusion Imaging)' introduced various recent advances in RFA. The six Difficult Clinical Case Study Sessions comprised three sessions on diagnosis and three on treatment, all of which were conducted with a moderator who was either a hepatologist, a surgeon, a pathologist, or a radiologist. In each session, a difficult case in terms of diagnosis or treatment was introduced, and the diagnosis or treatment approach in question was actively debated.

As a special program, a roundtable-style presentation was held under the title 'Looking Back on the 50-Year History of the Liver Cancer Study Group of Japan', and eight professors who had led the LCSGJ through the last 50 years introduced the history of the LCSGJ to the younger generation of LCSGJ members. This special program also provided a great opportunity to think about how we should develop the LCSGJ over the next 50 years.

In the Education Lecture, Prof. Kazuto Nishio gave a speech about 'Biomarkers in Molecular Targeted Therapy for Liver Cancer', which provided up-to-date information on biomarkers. In addition, Prof. Hidemi Kumai and Prof. Markus Peck presented highly relevant Special Lectures on 'Full Lifecycle Aquaculture of Bluefin Tuna: 32-Year Trajectory' and 'Management of Liver Cancer – Why We Do What We Do in Europe', respectively.

Two consensus meetings organized by the LCSGJ turned out to be the highlight of the 50th Congress. In Consensus Meeting 1 on 'A Diagnostic Algorithm for Liver Cancer', liver cancer experts used a voting system to decide on an updated version of the consensus-based diagnostic algorithm proposed by the Japan Society of Hepatology (JSH) [29]. In Consensus Meeting 2 on 'Updating the JSH Definition of TACE Failure/Refractoriness', experts decided to revise the definition [29].

The 50th LCSGJ Congress drew over 1,200 attendees over 2 days and was a great success. In this supplementary issue of *Oncology*, some of the articles discuss the sessions held at the congress, making it an extremely valuable special issue for readers specializing in liver cancer.

Disclosure Statement

The author declares that no financial or other conflicts of interest exist in relation to the content of this article.

References

1 Honjo I: Total resection of the right lobe of the liver (in Japanese). Shujutsu 1950;4:345–349.
2 Honjo I, Araki C: Total resection of the right lobe of the liver; report of a successful case. J Int Coll Surg 1955;23:23–28.
3 Lortat-Jacob JL, Robert HG: Well defined technic for right hepatectomy. Presse Med 1952;60:549–551.
4 Foster JH: History of liver surgery. Arch Surg 1991;126:381–387.
5 Kudo M: Early hepatocellular carcinoma: definition and diagnosis. Liver Cancer 2013;2:69–72.
6 Murakami T, Tsurusaki M: Hypervascular benign and malignant liver tumors that require differentiation from hepatocellular carcinoma: key points of imaging diagnosis. Liver Cancer 2014;3:85–96.
7 Lee JM, Yoon JH, Joo I, Woo HS: Recent advances in CT and MR imaging for evaluation of hepatocellular carcinoma. Liver Cancer 2012;1:22–40.
8 Joo I, Choi BI: New paradigm for management of hepatocellular carcinoma by imaging. Liver Cancer 2012;1:94–109.
9 Salvatore V, Bolondi L: Clinical impact of ultrasound-related techniques on the diagnosis of focal liver lesions. Liver Cancer 2012;1:238–246.
10 Kudo M: Treatment of advanced hepatocellular carcinoma with emphasis on hepatic arterial infusion chemotherapy and molecular targeted therapy. Liver Cancer 2012;1:62–70.
11 Kudo M: Why does every hepatocellular carcinoma clinical trial using molecular targeted agents fail? Liver Cancer 2012;1:59–60.
12 Hsu C, Po Ching L, Morita S, Hu FC, Cheng AL: Perspectives on the design of clinical trials combining transarterial chemoembolization and molecular targeted therapy. Liver Cancer 2012;1:168–176.
13 Liapi E, Geschwind JF: Combination of local transcatheter arterial chemoembolization and systemic anti-angiogenic therapy for unresectable hepatocellular carcinoma. Liver Cancer 2012;1:201–215.
14 Finn RS: Current and future treatment strategies for patients with advanced hepatocellular carcinoma: role of mTOR inhibition. Liver Cancer 2012;1:247–256.
15 Shindoh J, Kaseb A, Vauthey JN: Surgical strategy for liver cancers in the era of effective chemotherapy. Liver Cancer 2013;2:47–54.

16 Shao YY, Hsu CH, Cheng AL: Predictive biomarkers of antiangiogenic therapy for advanced hepatocellular carcinoma: where are we? Liver Cancer 2013;2:93–107.
17 Kim HY, Park JW: Clinical trials of combined molecular targeted therapy and locoregional therapy in hepatocellular carcinoma: past, present, and future. Liver Cancer 2014;3:9–17.
18 Peck-Radosavljevic M: Drug therapy for advanced-stage liver cancer. Liver Cancer 2014; 3:125–131.
19 Belghiti J, Fuks D: Liver resection and transplantation in hepatocellular carcinoma. Liver Cancer 2012;1:71–82.
20 Lee Cheah Y, K H Chow P: Liver transplantation for hepatocellular carcinoma: an appraisal of current controversies. Liver Cancer 2012; 1:183–189.
21 Chan SC, Sharr WW, Chan AC, Chok KS, Lo CM: Rescue living-donor liver transplantation for liver failure following hepatectomy for hepatocellular carcinoma. Liver Cancer 2013;2:332–337.
22 Chan SC: Liver transplantation for hepatocellular carcinoma. Liver Cancer 2013;2:338–344.
23 Akamatsu N, Sugawara Y, Kokudo N: Living donor liver transplantation for patients with hepatocellular carcinoma. Liver Cancer 2014; 3:108–118.
24 Kim DY, Han KH: Epidemiology and surveillance of hepatocellular carcinoma. Liver Cancer 2012;1:2–14.
25 Jihye C, Seong J: Application of radiotherapeutic strategies in the BCLC-defined stages of hepatocellular carcinoma. Liver Cancer 2012;1:216–225.
26 Lee DS, Seong J: Radiotherapeutic options for hepatocellular carcinoma with portal vein tumor thrombosis. Liver Cancer 2014;3:18–30.
27 Lin SM: Local ablation for hepatocellular carcinoma in Taiwan. Liver Cancer 2013;2:73–83.
28 Lencioni R: Chemoembolization in patients with hepatocellular carcinoma. Liver Cancer 2012;1:41–50.
29 Kudo M, Matsui O, Izumi N, et al: JSH consensus-based clinical practice guideline for the management of hepatocellular carcinoma: 2014 update by the Liver Cancer Study Group of Japan. Liver Cancer 2014;3:458–468.
30 Foster JM, Berman MM: Solid Liver Tumors. Philadelphia, WB Saunders, 1977.

Review

Oncology

Oncology 2014;87(suppl 1):7–21
DOI: 10.1159/000368141

Published online: November 22, 2014

Surveillance and Diagnostic Algorithm for Hepatocellular Carcinoma Proposed by the Liver Cancer Study Group of Japan: 2014 Update

Masatoshi Kudo[a] Osamu Matsui[b] Namiki Izumi[c] Hiroko Iijima[d]
Masumi Kadoya[e] Yasuharu Imai[f]
on behalf of the Liver Cancer Study Group of Japan

[a]Department of Gastroenterology and Hepatology, Kinki University School of Medicine, Osaka-Sayama, [b]Department of Radiology, Kanazawa University Graduate School of Medical Science, Kanazawa, [c]Department of Gastroenterology and Hepatology, Musashino Red Cross Hospital, Tokyo, [d]Division of Hepatobiliary and Pancreatic Disease, Department of Internal Medicine, Hyogo College of Medicine, Nishinomiya, [e]Department of Radiology, Shinshu University School of Medicine, Matsumoto, and [f]Department of Gastroenterology, Ikeda Municipal Hospital, Ikeda, Japan

Key Words
Hepatocellular carcinoma · Clinical practice guideline · Surveillance and diagnostic algorithm · Japan Society of Hepatology · Liver Cancer Study Group of Japan

Abstract
Surveillance and diagnostic algorithms for hepatocellular carcinoma (HCC) have already been described in guidelines published by the American Association for the Study of Liver Diseases (AASLD), the European Association for the Study of the Liver and the European Organisation for Research and Treatment of Cancer (EASL-EORTC), and the Japan Society of Hepatology (JSH), but the content of these algorithms differs slightly. The JSH algorithm mainly differs from the other two algorithms in that it is highly sophisticated and considers the functional imaging techniques of gadolinium ethoxybenzyl diethylenetriamine pentaacetic acid-enhanced MRI (EOB-MRI) and Sonazoid contrast-enhanced ultrasound (CEUS) to be very important diagnostic modalities. In contrast, the AASLD and EASL-EORTC algorithms are less advanced and suggest that a diagnosis be made based solely on hemodynamic findings using dynamic CT/MRI and biopsy findings. A consensus meeting regarding the JSH surveillance and diagnostic algorithm was held at the 50th Liver Cancer Study Group of Japan Congress, and a 2014 update of the algorithm was completed. The new algorithm reaffirms the very important role of EOB-MRI and Sonazoid CEUS in the surveillance and diagnosis of liver cancer and is more sophisticated than those currently used in the United States and Europe. This is now an optimized algorithm that can be used to diagnose early-stage to classical HCC easily and highly accurately.

Introduction

Unlike the surveillance and diagnostic algorithm in the guidelines by the American Association for the Study of Liver Diseases (AASLD) [1] and that in the guidelines by the European Association for the Study of the Liver and the European Organisation for Research and Treatment of Cancer (EASL-EORTC) [2], the Japan Society of

Prof. Masatoshi Kudo
Department of Gastroenterology and Hepatology
Kinki University School of Medicine
377-2 Ohno-Higashi, Osaka-Sayama, Osaka 589-8511 (Japan)
E-Mail m-kudo@med.kindai.ac.jp

Hepatology (JSH) algorithm in the JSH Consensus-Based Clinical Practice Guideline for hepatocellular carcinoma (HCC) is described in considerable detail [3]. The latter guideline recommends the following in relation to surveillance: super high-risk patients (with hepatitis B/C cirrhosis) should be screened by performing ultrasound (US) examinations and measuring the levels of 3 tumor markers (AFP, AFP L-3, and PIVKA-II) every 3–4 months and by performing dynamic CT/MRI every 6–12 months. High-risk patients (with chronic hepatitis B/C or cirrhosis of another origin) should be screened by performing US examinations and measuring the levels of the 3 tumor markers every 6 months [3–6].

The aforementioned diagnostic guidelines for HCC in the United States and Europe mention the diagnosis of HCC solely based on hemodynamic findings. However, the surveillance and diagnostic algorithms in the HCC guideline in Japan have traditionally included not only hemodynamic diagnostic methods, but also functional diagnostic methods such as superparamagnetic iron oxide MRI (SPIO-MRI), gadolinium ethoxybenzyl diethylenetriamine pentaacetic acid-enhanced MRI (EOB-MRI), and Sonazoid contrast-enhanced ultrasound (CEUS) [7, 8].

Recently, a consensus meeting has been held at the 50th Liver Cancer Study Group of Japan (LCSGJ) Congress (June 5–6, 2014, Kyoto) (Congress president: Prof. Masatoshi Kudo) to decide on an updated surveillance and diagnostic algorithm that incorporates the latest advances in the field [9]. The meeting began with a brief overview of the existing guidelines and debate over issues and was followed by a discussion of the roles and significance of EOB-MRI, dynamic CT, and Sonazoid CEUS in the diagnostic algorithm. The meeting concluded with members reaching a consensus and agreeing on an updated algorithm with the use of a voting system. The consensus process and the updated algorithm are described here.

Surveillance and Diagnostic Algorithm in the East and West

JSH Guidelines

Evidence-Based Surveillance and Diagnostic Algorithm

The surveillance and diagnostic algorithms for HCC proposed by the JSH are the surveillance and diagnostic algorithm introduced in the '2013 Scientific Evidence-Based Clinical Practice Guidelines for Liver Cancer' [5], which is an evidence-based algorithm, as well as the diagnostic algorithm for hypervascular and hypovascular hepatocellular nodules [3], which is a consensus-based algorithm.

The algorithm in the JSH guidelines separates patients into a high-risk group (patients with chronic hepatitis B/C or cirrhosis) and a super high-risk group (patients with hepatitis B/C cirrhosis). For the super high-risk group, it is recommended that dynamic CT/MRI be performed every 6–12 months. If a nodule is observed on routine US, dynamic CT/MRI should be performed and the nodule classified based on presence/absence of early contrast enhancement, presence/absence of late-phase washout, and tumor diameter. The tumor diameter cutoff that indicates whether more precise testing should be performed is 1 cm if there is early contrast enhancement but no late-phase washout on dynamic CT/MRI and 1.5 cm if there is no early contrast enhancement. Additionally, if the size exceeds the relevant cutoff value, then CEUS, tumor biopsy, CT during hepatic arteriography (CTHA), and CT during arterial portography (CTAP) are recommended as optional tests [5].

Consensus-Based Diagnostic Algorithm

In the consensus-based diagnostic algorithm, dynamic CT, dynamic MRI, and CEUS is performed after detecting a nodule on US, and a diagnosis is made according to the diagnostic algorithm for hypervascular nodules if contrast enhancement is observed in the early arterial phase. If it is not observed, the diagnostic algorithm for hypovascular nodules is applied. In the diagnostic algorithm for hypervascular nodules, a diagnosis of HCC can be made when washout is observed in the portal venous phase and the equilibrium phase. When washout is not observed, the presence/absence of uptake in the hepatobiliary phase of EOB-MRI or in the Kupffer phase of Sonazoid CEUS is assessed. In the diagnostic algorithm for hypovascular nodules, EOB-MRI/Sonazoid CEUS is performed and a diagnosis of well-differentiated HCC can be made if decreased uptake is observed with both modalities. However, when decreased uptake is observed on EOB-MRI only, a tumor biopsy is performed to diagnose the nodule as either well-differentiated HCC or a precancerous or borderline lesion if the tumor diameter corresponds to the ≥1.5 cm cutoff. If the tumor diameter is <1.5 cm, intensive follow-up is recommended. When decreased uptake is observed on Sonazoid CEUS only, regardless of the tumor diameter, a tumor biopsy is typically performed to diagnose the nodule as either well-differentiated HCC or a precancerous or borderline lesion. Furthermore, if uptake is seen on both modalities, the next workup is determined based on a tumor diameter cutoff of 1.5 cm. The algo-

rithms for hyper- and hypovascular nodules both suggest that for institutions capable of performing CTHA/CTAP, these should be selected as optional tests [3].

With the recent recognition that EOB-MRI is useful for diagnosing HCC, particularly hypovascular early HCC, the current HCC diagnostic algorithm needed to be updated in order to put slightly more emphasis on EOB-MRI, and thus this section was updated in the consensus meeting.

Diagnostic Algorithm in the AASLD Practice Guidelines

Diagnostic algorithms for HCC that have been proposed outside of Japan include the 'AASLD Practice Guidelines' [1] and the 'EASL-EORTC Clinical Practice Guidelines' [2].

The 2011 updated version of the AASLD diagnostic algorithm states that nodules found in cirrhotic patients should first be classified based on their diameter. If the nodule diameter is <1 cm, surveillance should be performed every 3 months because the diagnosis of such nodules is difficult. If the size does not change, surveillance every 3 months should be continued; if the diameter changes, the nodule should be diagnosed according to its size. If the diameter is ≥1 cm, a diagnosis of HCC is made when early enhancement is observed in the arterial phase and washout is observed in the portal venous phase on dynamic CT/MRI. If these findings are not observed, hemodynamics should be evaluated with a dynamic study that has not been used before, and a diagnosis of HCC is made if dynamic CT and dynamic MRI ultimately reveal these findings, whereas a biopsy is performed if they do not. As outlined above, this is a simple algorithm, which proposes that a diagnosis should be made based solely on hemodynamic information. Problems with this algorithm include that it does not mention functional diagnostic methods such as EOB-MRI or Sonazoid CEUS, that it requires biopsy more frequently, and that it would be difficult to make a diagnosis of early HCC by imaging [10].

Diagnostic Algorithm in the EASL-EORTC Clinical Practice Guidelines

The EASL-EORTC diagnostic algorithm proposes a fundamentally similar one to the AASLD algorithm for nodules <1 cm in diameter. However, it differs in that it proposes a different diagnostic flow for nodules ≥1 cm, namely, for nodules of 1–2 cm and >2 cm. If the nodule diameter is 1–2 cm, early enhancement in the arterial phase and washout in the portal venous phase must be seen on both dynamic CT and dynamic MRI (except if one imaging technique only is recommended in centers of excellence with high-end radiological equipment). If the nodule diameter is >2 cm, a diagnosis of HCC is made when these findings are seen on one of the two modalities. However, as it is actually still possible to diagnose a nodule as HCC if arterial enhancement with portal venous washout is observed on one modality even without high-end radiological equipment, the abovementioned annotation appears to have no meaning. This is a very simple algorithm because, as described above, it essentially considers radiologic hallmarks on one modality as an index that allows for a diagnosis of HCC to be made. Furthermore, neither the AASLD diagnostic algorithm nor the EASL-EORTC diagnostic algorithm is appropriate for diagnosing early HCC, and these algorithms are also problematic in that they do not actively promote the use of noninvasive diagnostic methods since they state that a biopsy must be performed for all nodules when early enhancement in the arterial phase and washout in the portal venous phase are not observed [2].

Diagnostic Algorithm for HCC Proposed by the Arii Research Group for the Japanese Ministry of Health, Labour and Welfare (2012 Updated Version)

The diagnostic algorithm for hepatocellular carcinoma proposed by the Arii Research Group as part of a research project funded by a 2008–2010 grant from the Japanese Ministry of Health, Labour and Welfare (principal investigator: Prof. Shigeki Arii) is an algorithm that was mainly compiled by Prof. Osamu Matsui as the group's final report. This is an easy-to-use algorithm centered on EOB-MRI [11, 12], which can detect and diagnose hyper- and hypovascular HCC with high performance, has strong diagnostic performance for differentiating between liver masses, and which has excellent objectivity and reproducibility. Minor updates were made to this algorithm at a consensus meeting held at the 48th LCSGJ Congress in 2012 [13].

Before the 2014 consensus meeting, HCC experts gathered to create an updated version of the diagnostic algorithm for HCC that was used to spark a discussion at the meeting. First, after surveillance with US and tumor markers, it is recommended that dynamic EOB-MRI should be performed (or dynamic CT for institutions unable to use MRI as the first-line modality) and that nodules are classified as 'hypervascular with washout', 'hypervascular without washout', or 'hypovascular'. Nodules that are hypervascular with washout are diagnosed as HCC. However, although cavernous hemangiomas usually do not exhibit washout in the equilibrium phase of dynamic CT, they can exhibit findings resembling washout (pseudo-washout) in

the equilibrium phase (transitional phase) of dynamic EOB-MRI. Thus, this possibility must be ruled out using another imaging modality or diagnostic method. Furthermore, nodules that are hypervascular without washout are diagnosed as HCC if they are hypointense in the hepatobiliary phase of EOB-MRI. However, the abovementioned issue with hemangiomas necessitates the cautionary notation that cavernous hemangiomas are usually hypointense in the hepatobiliary phase of EOB-MRI and thus should be ruled out using other sequences of MRI and/or other imaging modalities. Nodules that are hypovascular and hypointense in the hepatobiliary phase of EOB-MRI are further evaluated with Sonazoid CEUS and diagnosed as classical HCC if they are hypervascular on that modality. Furthermore, nodules that show a defect in the Kupffer phase of Sonazoid CEUS are diagnosed as early HCC. However, for nodules that are hypovascular with no defect in the Kupffer phase of Sonazoid CEUS, it is recommended that a biopsy be performed to differentiate between early HCC and dysplastic nodules (DN) or borderline lesions if the diameter is ≥1 cm, and that intensive follow-up with EOB-MRI be performed every 6 months if the diameter is <1 cm. During the 2014 consensus meeting, LCSGJ experts discussed the updated Arii Research Group algorithm to form a consensus for the new LCSGJ algorithm.

Diagnostic Algorithm

Role of Sonazoid CEUS

Sonazoid CEUS serves two roles in the diagnostic algorithm for HCC. First, it can be used to evaluate hypervascularity even in nodules that dynamic EOB-MRI or dynamic multidetector CT (MDCT) cannot determine to be hypervascular because CEUS can capture arterial blood flow within the nodule with high sensitivity without missing the timing of arterial blood flow due to its excellent real-time imaging capabilities. Therefore, CEUS should be performed to actively evaluate the arterial vascularity within the nodule, even for nodules determined to be hypovascular by dynamic EOB-MRI or dynamic MDCT. Second, it has been discovered that hypovascular nodules that are hypointense in the hepatobiliary phase of EOB-MRI and show decreased uptake in the Kupffer phase of Sonazoid CEUS are at high risk of malignancy and have a high rate of progression to hypervascular typical HCC. Therefore, hypovascular nodules that are hypointense in the hepatobiliary phase of EOB-MRI and hypoechoic in the Kupffer phase of Sonazoid CEUS can almost always be diagnosed as early HCC even without biopsy.

Role of Dynamic CT and CT Angiography

Findings of early enhancement in the arterial phase and washout in the portal venous phase on CT have been considered typical of HCC and have been widely used in its diagnosis [14]. However, some types of HCC such as 'moderately differentiated HCC with fat deposition' and 'highly malignant poorly differentiated HCC' do not show clear early enhancement in the arterial phase, and thus are considered difficult to diagnose with dynamic CT [14]. Furthermore, the lag in scan timing in the arterial phase of dynamic CT may decrease its ability to detect hypervascular lesions, and it is therefore necessary to either improve time resolution or strictly control scan timing. In addition, the enhancing effect of iodine contrast medium used in dynamic CT is weaker than that of gadolinium used in dynamic MRI, which means that it may not depict lesions detected by dynamic MRI.

However, dynamic CT has high spatial resolution and thus can also depict portal vein tumor thrombi that are not depicted in the hepatobiliary phase of EOB-MRI. In addition, EOB-MRI is actually more prone to artifacts with proper scan timing, whereas artifacts appear relatively infrequent on dynamic CT. Dynamic CT is also more reliable than EOB-MRI for differentiating HCC from hemangiomas. Therefore, dynamic CT plays a complementary role to EOB-MRI as it compensates for the shortcomings of EOB-MRI in diagnosing HCC.

The malignancy of hepatocellular nodules in multistep hepatocarcinogenesis has been shown to be correlated with the composition of arterial and portal vein blood flow, so an examination of that composition on CTAP and CTHA images has become the gold standard diagnostic method for estimating the malignancy grade [15, 16]. This diagnostic method can be used to evaluate the malignancy grade of hepatocellular nodules in the process of multistep hepatocarcinogenesis from DN to moderately differentiated HCC based on CTAP and CTHA findings.

In addition, although a nodule that shows enhancement in the early phase of CTHA could be an arterioportal (AP) shunt rather than HCC, HCC can be confirmed if corona enhancement is shown in the late phase [17]. Therefore, it is possible to differentiate HCC from AP shunts by taking late-phase CTHA images and determining whether there is corona enhancement.

These characteristics give CT angiography excellent diagnostic performance for HCC, and it can also reduce the risk of overlooking lesions when used to screen for hepatic lesions before surgery, making it a useful preoperative test as well. However, CT angiography is highly invasive as it requires arterial puncture and therefore is

categorized as an optional test in the JSH diagnostic algorithm for HCC. Actually, the need to perform diagnostic CTHA and CTAP in the routine clinical setting has decreased considerably since the emergence of EOB-MRI.

Role of EOB-MRI

Ability of EOB-MRI to Detect HCC

The sensitivity and Az values from alternative free-response receiver operating characteristic (AFROC) analysis of EOB-MRI for detecting HCC are significantly higher than those for MDCT, and the ability of EOB-MRI to detect small hypervascular HCC is particularly superior. It has actually become common to encounter cases where hypervascular HCC or nodule-in-nodule HCC that is undetectable by MDCT is detected in a routine screening by EOB-MRI because of early enhancement in the arterial phase or clear hypointensity in the hepatobiliary phase [11, 18–103]. Furthermore, studies comparing the diagnostic performance of EOB-MRI and MDCT for hypervascular HCC have shown that EOB-MRI is superior or, at the very least, that the two are equivalent.

EOB-MRI is also considered useful for diagnosing early HCC because hypovascular and well-differentiated HCC that cannot be detected by CTHA, CTAP, MDCT, or SPIO-MRI are depicted as hypointense in the hepatobiliary phase of EOB-MRI [10, 75, 76, 84, 89].

In a study of the diagnostic performance of various modalities for early HCC, Sano et al. [89] found that among the many findings with 100% specificity, the only finding with close to 100% sensitivity was hypointensity in the hepatobiliary phase of EOB-MRI (97%); this and other findings have now made it clear that the hepatobiliary phase of EOB-MRI is the superior modality for the diagnosis of early HCC [10, 21].

Moreover, when comparing the detection rates of progressed HCC, early HCC, and DN in the hepatobiliary phase of EOB-MRI with those in the Kupffer phase of Sonazoid CEUS, T1-, T2-, and diffusion-weighted images, the detection rate of progressed HCC with EOB-MRI was 93%; the remaining 7% were hyperintense typical HCC, so the actual detection rate was 100%. Furthermore, the detection rate of early HCC was also as high as 95%. In addition, 33% of DN were detected as faintly hypointense. The detection rate in the Kupffer phase of Sonazoid CEUS was 100% for progressed HCC but just 11% for early HCC, which indicates that the hepatobiliary phase of EOB-MRI is the superior modality for detecting early HCC. Furthermore, the EOB-MRI protocol also includes T1-, T2-, and diffusion-weighted images, so another advantage of EOB-MRI is that it can obtain these findings.

Risk Factors for Hypervascular Change of Hypovascular Nodules

In many Japanese studies that have discussed the risk of hypervascular change of hypovascular nodules that are hypointense in the hepatobiliary phase of EOB-MRI [23, 25, 32, 36, 37, 51, 55, 56, 69, 70, 74, 100, 104–110], tumor diameter and nodule growth speed have been reported as risk factors for hypervascularization; these characteristics are therefore important in predicting the hypervascularization of hypovascular nodules. It should be noted that the tumor diameter cutoff in these studies was often around 1 cm. Actually, intensive follow-up of hypovascular nodules that are hypointense in the hepatobiliary phase of EOB-MRI has shown that nodules with a higher growth speed are more prone to develop into hypervascular nodules [56], which suggests that nodule growth speed might be included in the algorithm as well. However, intensive follow-up by EOB-MRI should ensure that hypervascularization is detected at an early stage. In addition, the median tumor diameter of hypovascular nodules that are hypointense in the hepatobiliary phase of EOB-MRI but become hypervascular during the course of intensive follow-up is 1.2 cm, and many hypovascular nodules become hypervascular when they are ≤1 cm.

EOB-MRI has high diagnostic performance for both hypervascular HCC and early HCC compared with other modalities, so it should be considered the first choice for use after US screening in the HCC diagnostic algorithm.

Consensus Voting Results

A consensus meeting involving 350 liver cancer experts was held at the 50th LCSGJ Congress to discuss current issues concerning diagnostic algorithm for hepatocellular carcinoma. Participants' responses to each question were collected through a voting system, and the items which two-thirds (67%) of the participants agreed on were included in the new algorithm. These items are listed at the end of this paper as consensus statements. In addition, the items on which at least 50% of the participants agreed are also listed at the end of this paper as informative statements.

Participants' Backgrounds

The most common specialty of the physicians who participated in the consensus meeting was hepatology at 70%, followed by surgery at 12%, radiology at 7%, pathology at 4%, and medical oncology at 1%. In addition, 18%

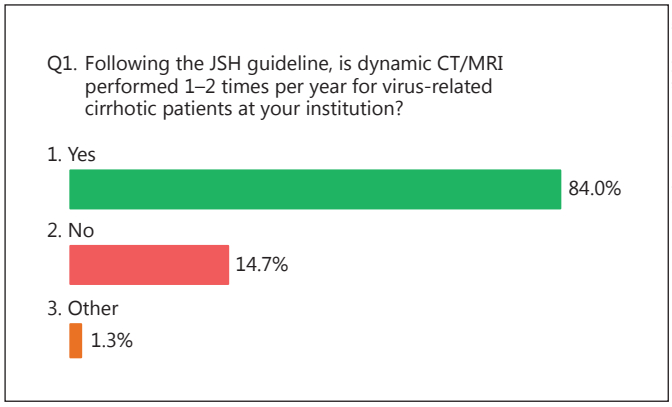

Fig. 1. Question 1 and answers on surveillance and diagnosis.

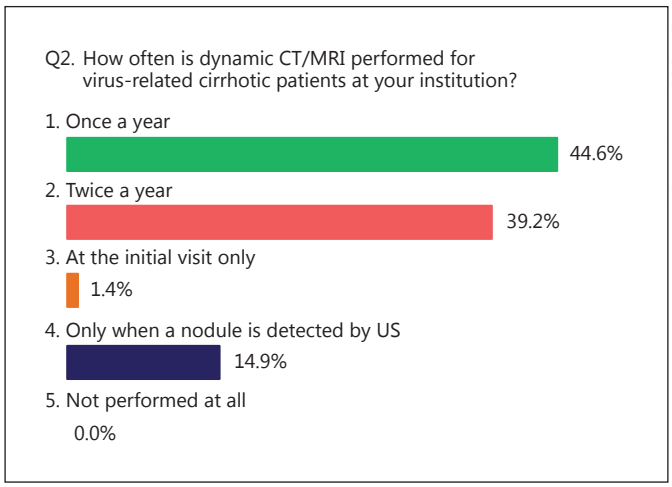

Fig. 2. Question 2 and answers on surveillance and diagnosis.

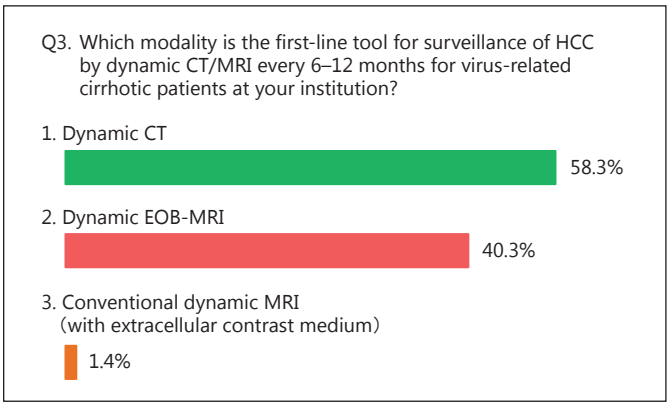

Fig. 3. Question 3 and answers on surveillance and diagnosis.

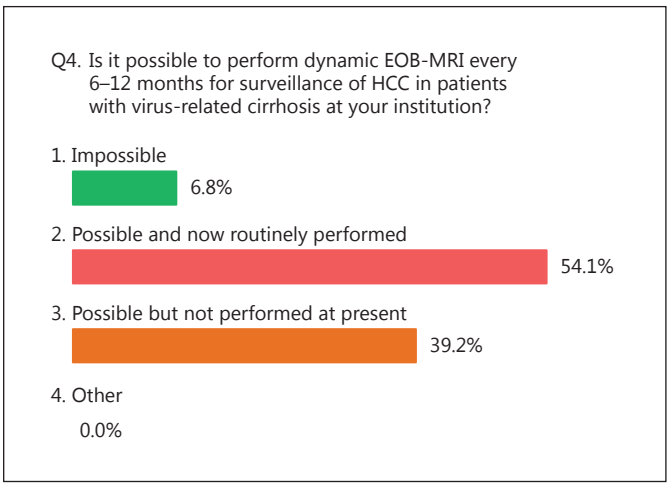

Fig. 4. Question 4 and answers on surveillance and diagnosis.

saw <5 patients per month, 44% saw 6–25 patients, 13% saw 26–50 patients, 14% saw 51–100 patients, and 11% saw ≥101 patients per month.

HCC Surveillance

The responses to questions regarding the use of imaging diagnostics for HCC were as follows: in answer to the question 'Following the JSH guideline, is dynamic CT/MRI performed 1–2 times per year for virus-related cirrhotic patients at your institution?', 84% responded affirmatively and 15% responded negatively, revealing that institutions are following the guideline and actively performing dynamic CT/MRI screening of super high-risk patients (fig. 1). When asked about the frequency of screening, 84% indicated that they performed screening 1–2 times a year (45% once a year and 39% twice a year; fig. 2).

When asked 'Which modality is the first-line tool for surveillance of HCC by dynamic CT/MRI every 6–12 months for virus-related cirrhotic patients at your institution?', 58% responded dynamic CT, 40% responded dynamic EOB-MRI, and 1% responded conventional dynamic MRI (with extracellular contrast medium) (fig. 3). Dynamic CT was the most common modality used, but it appears that dynamic EOB-MRI is becoming more commonly used as well. Next, when asked 'Is it possible to perform dynamic EOB-MRI every 6–12 months for surveillance of HCC in patients with virus-related cirrhosis at your institution?', 54% responded it was possible and now routinely performed, while 39% responded it was possible but not performed at present, indicating that the majority of institutions are currently capable of routinely performing EOB-MRI (fig. 4). In answer to the

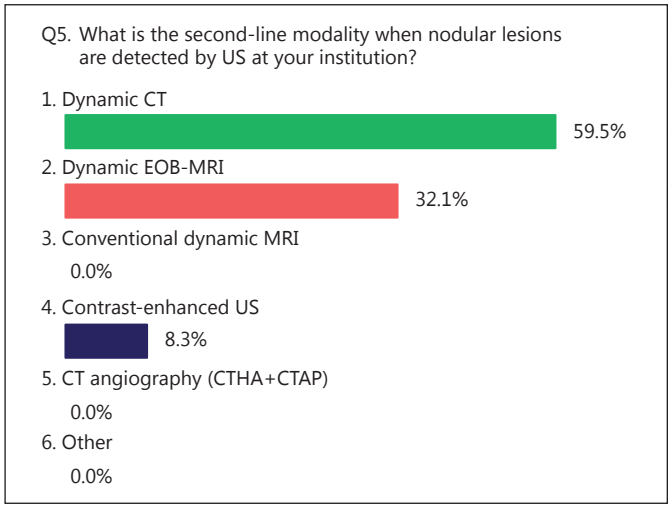

Fig. 5. Question 5 and answers on surveillance and diagnosis.

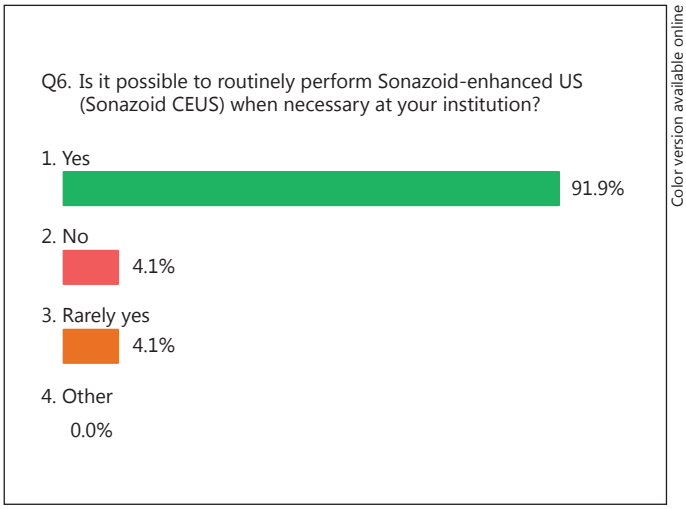

Fig. 6. Question 6 and answers on surveillance and diagnosis.

question 'What is the second-line modality when nodular lesions are detected by US at your institution?', 60% responded dynamic CT, 32% dynamic EOB-MRI, 8% CEUS, and 0% conventional dynamic MRI (with extracellular contrast medium) or CT angiography (CTHA + CTAP) (fig. 5). As expected, it appears that clinicians find dynamic CT to be an easier test than EOB-MRI to perform after US, due to throughput issues among other reasons. It was also confirmed that dynamic MRI with extracellular contrast medium has been completely replaced with dynamic EOB-MRI. When asked 'Is it possible to routinely perform Sonazoid-enhanced US (Sonazoid CEUS) when necessary at your institution?', 92% responded affirmatively, 4% responded negatively, and 4% responded 'rarely yes' (fig. 6). The respondents were all physician members of the LCSGJ, so it is likely that many of their institutions were actively engaged in the diagnosis and treatment of HCC. These findings reveal that institutions across Japan are becoming equipped to perform CEUS.

Role of CEUS and Need for Biopsy

The next item discussed at the consensus meeting was the '2014 Updated Diagnostic Algorithm for Hepatocellular Carcinoma' proposed by the LCSGJ. In this algorithm, hypovascular nodules that are hypointense in the hepatobiliary phase of EOB-MRI are evaluated with Sonazoid CEUS and those found to be hypervascular and/or those which show a defect in the Kupffer phase are diagnosed as HCC. However, it remains a point of contention whether nodules that are hypervascular and/or show a defect in the Kupffer phase of Sonazoid CEUS should be diagnosed as HCC without performing a biopsy.

Therefore, when asked 'Do you think Sonazoid CEUS should be performed if a nodule is not hypervascular in the arterial phase of EOB-MRI or on dynamic CT, especially when it is hypointense in the hepatobiliary phase of EOB-MRI, since Sonazoid CEUS is the most sensitive tool for depicting intranodular arterial vascularity?', the vast majority (75%) were of the opinion that CEUS should be performed (fig. 7). Next, participants were asked 'Is it possible to confirm a nodule is HCC without biopsy if the nodule is hypovascular, hypointense in the hepatobiliary phase of EOB-MRI, and shows a defect in the Kupffer phase of Sonazoid CEUS?'. The majority (58%) responded it is possible, but 27% responded that biopsy is mandatory (fig. 8). Although such nodules are uncommon, hypovascular nodules that are hypointense in the hepatobiliary phase of EOB-MRI and are hypervascular and/or show a defect in the Kupffer phase of Sonazoid CEUS may also be liver metastases or granulomatous nodules; thus, biopsy is considered necessary to rule out these possibilities. In addition, the current diagnostic algorithm for HCC recommends biopsy for nodules determined to be hypervascular without washout on dynamic EOB-MRI and isointense to hyperintense in the hepatobiliary phase of EOB-MRI. However, in clinical practice, most HCC that are hyperintense in the hepatobiliary phase of EOB-MRI have a capsule or mosaic structure and show radiologic hallmarks on dynamic CT, so biopsy is rarely necessary. This implicates that biopsy should be an optional test. At the same time, although it is possible to diagnose

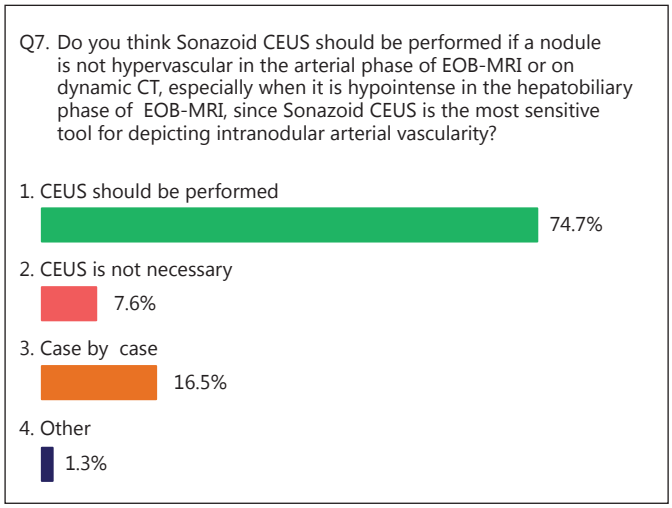

Fig. 7. Question and answers on the role of Sonazoid CEUS.

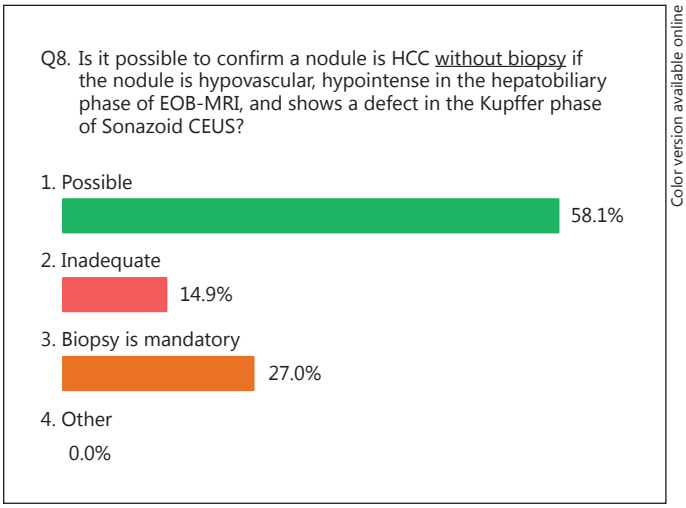

Fig. 8. Question and answers on the role of Sonazoid CEUS and biopsy.

hypovascular nodules that are hypointense in the hepatobiliary phase of EOB-MRI and hypervascular and/or show a defect in the Kupffer phase of Sonazoid CEUS as HCC with almost complete certainty based on their appearance (e.g., capsule or mosaic structure) and dynamic CT findings, the need for biopsy still cannot be denied. Therefore, the consensus was to recommend biopsy as an optional test on a case-by-case basis.

Tumor Diameter Cutoff Used to Determine Whether Biopsy Should Be Performed

The 2012 surveillance and diagnostic algorithm for hepatocellular carcinoma (updated version of the Arii Research Group algorithm) [13] states that hypovascular nodules that are hypointense in the hepatobiliary phase of EOB-MRI should be evaluated with Sonazoid CEUS and sets 1 cm as the tumor diameter cutoff that determines whether biopsy or intensive follow-up should be chosen when a nodule is not hypervascular and shows no defect in the Kupffer phase. The evidence for this is based on the data presented below.

When the data from the pathological diagnoses of 147 nonhypervascular nodules that were hypointense in the hepatobiliary phase of EOB-MRI were analyzed separately by tumor diameter, the percentage of HCC (early to poorly differentiated) was found to be 82% among nodules ≥1.5 cm and 87% among nodules <1.5 cm when using a cutoff size of 1.5 cm. When using a cutoff size of 1 cm, 86% of nodules ≥1 cm and 81% of nodules <1 cm were HCC. Essentially, over 80% of nonhypervascular nodules that were hypointense in the hepatobiliary phase of EOB-MRI were HCC, regardless of the tumor diameter. Therefore, a tumor diameter cutoff of 1 cm was chosen because the risk of HCC is high even when the tumor diameter is 1 cm and in consideration of data indicating that the tumor doubling time rapidly rises when the diameter is 1–1.5 cm.

The conventional morphological cutoff for malignancy, however, was 1.5 cm; thus, many members were opposed to the 1-cm cutoff in the 2012 surveillance and diagnostic algorithm for hepatocellular carcinoma (updated version of the Arii Research Group algorithm). This issue was therefore included as a topic for debate at the consensus meeting this year. When asked 'What size of nodule should be biopsied when it is hypovascular, hypointense in the hepatobiliary phase of EOB-MRI, and shows no defect in the Kupffer phase of Sonazoid CEUS?', 55% responded ≥1 cm, 35% responded ≥1.5 cm, 7% answered ≥2 cm, and 0% all nodules regardless of size (including <1 cm). The majority of participants responded ≥1 cm, but this was less than the 67% needed to reach a consensus (fig. 9).

The reason for supporting the tumor diameter cutoff of 1.5 cm was that it is difficult to accurately collect tissue from a 1-cm nodule by biopsy, and thus the possibility of sampling errors would increase if nodules ≥1 cm were considered candidates for biopsy. It was noted that neglecting intensive follow-up due to overlooking HCC that was too small to collect tissue from by biopsy would be more likely to delay diagnosis than if biopsy were only performed on nodules ≥1.5 cm. It was also suggested that different tumor diameter cutoffs should be set for hypo- and hypervascular

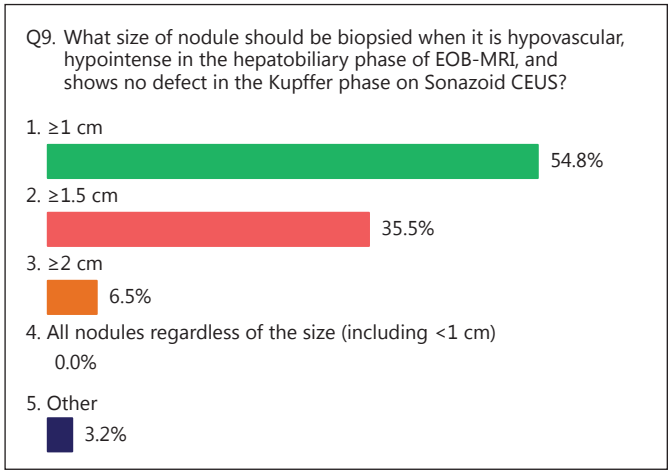

Fig. 9. Question and answers on the adequate nodular size for biopsy.

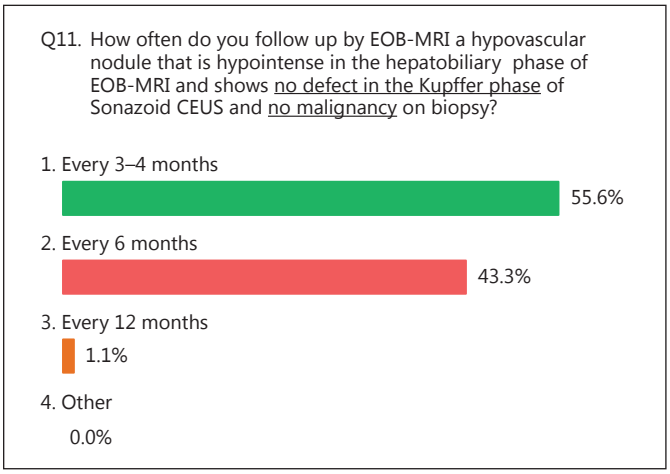

Fig. 11. Question and answers on intensive follow-up for a hypointense nodule in the hepatobiliary phase of EOB-MRI (2).

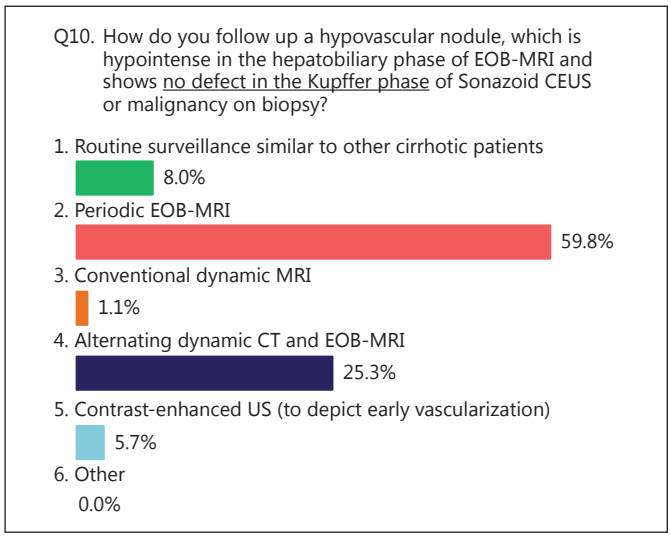

Fig. 10. Question and answers on intensive follow-up for a hypointense nodule in the hepatobiliary phase of EOB-MRI (1).

nodules because it is not as urgent to treat the former compared to the latter. As biopsy is invasive, its use should be carefully considered even when there is diagnostic evidence for choosing it. There is certainly a problem with tumor doubling time, but some members felt that this could probably be monitored by intensive follow-up to a certain extent. When using data collected by the LCSGJ for 6 years until 2005 to determine the percentage of hypo- and hypervascular nodules among single new nodules with ≤3-cm diameter divided into groups by diameter (at 5-mm intervals), it was found that the percentage of hypervascular nodules drastically increased around 1.5 cm. Furthermore, some members commented that a cutoff of 1.5 cm may not be appropriate as they had observed many hypovascular lesions ≤1.5 cm becoming hypervascular once they reached exactly 1.5 cm during follow-up. Therefore, since agreement with the cutoff points of ≥1 cm and ≥1.5 cm totaled over 90%, the cutoff of 'small nodules (1–1.5 cm)' was proposed to the members. Almost all members agreed by voting with a show of hands, so it was decided to adopt this cutoff size. Whether biopsy should actually be performed when nodules are in the 1–1.5 cm stage is left to the institutions themselves on a case-by-case basis.

Intensive Follow-Up

Participants were first asked 'How do you conduct follow-up for a hypovascular nodule that is hypointense in the hepatobiliary phase of EOB-MRI and shows no defect in the Kupffer phase of Sonazoid CEUS or malignancy on biopsy?'. The most frequent response was periodic EOB-MRI at 60%, followed by alternating dynamic CT and EOB-MRI at 25%, and routine surveillance similar to other cirrhotic patients at 6%. More than two-thirds of the respondents responded periodic EOB-MRI and alternating dynamic CT and EOB-MRI (fig. 10). Next, when asked about the frequency of follow-up with EOB-MRI for this type of nodule, 56% of participants answered every 3–4 months, 43% every 6 months, and 1% every 12 months. The majority answered every 3–4 months, but the percentage was lower than the 67% required to reach a consensus (fig. 11), and thus every 3–6 months was se-

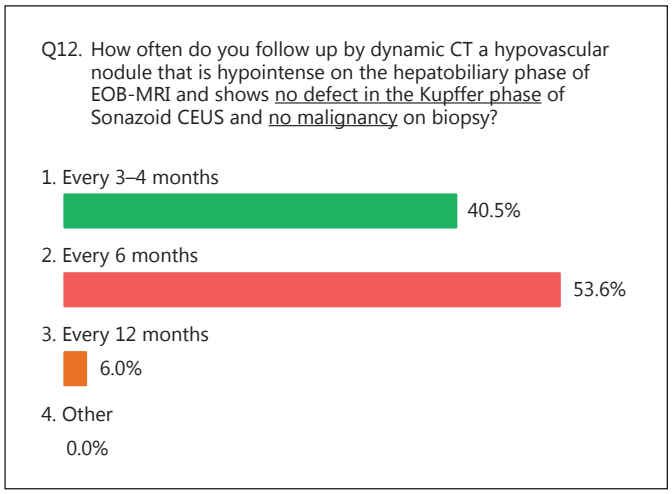

Fig. 12. Question and answers on intensive follow-up for a hypointense nodule in the hepatobiliary phase of EOB-MRI (3).

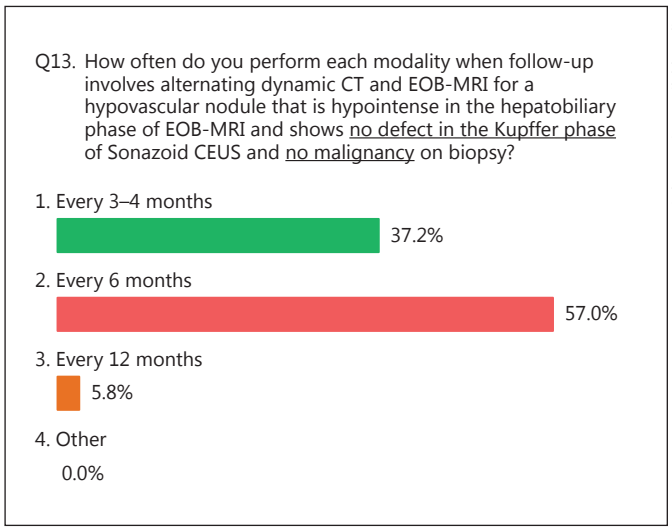

Fig. 13. Question and answers on intensive follow-up for a hypointense nodule in the hepatobiliary phase of EOB-MRI (4).

lected (99%). When asked about the frequency of follow-up with dynamic CT for this type of nodule, most respondents (54%) answered every 6 months, followed by every 3–4 months (41%) and every 12 months (6%) (fig. 12). In addition, when asked about the frequency of performing each modality when using alternating dynamic CT and EOB-MRI for follow-up of this type of nodule, most respondents (57%) again answered every 6 months, followed by every 3–4 months (37%) and every 12 months (6%) (fig. 13). Therefore, follow-up every 3–6 months was also recommended for this method (94%).

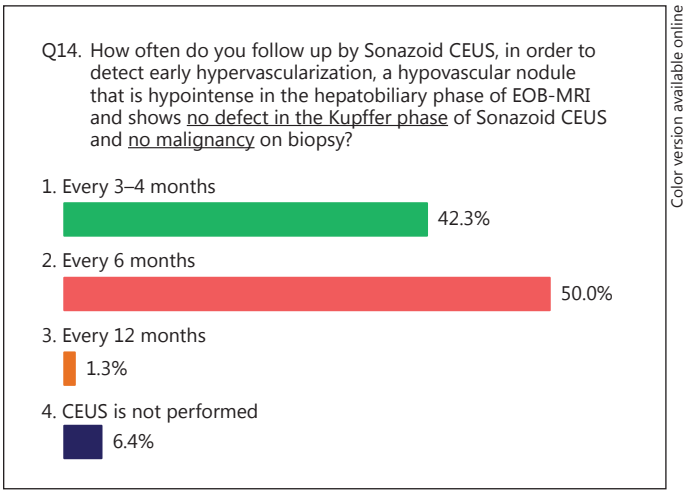

Fig. 14. Question and answers on intensive follow-up for a hypointense nodule in the hepatobiliary phase of EOB-MRI (5).

Finally, when asked how often this type of nodule was followed up by Sonazoid CEUS to evaluate hypervascularization in its early stages, most respondents (50%) again answered every 6 months, followed by every 3–4 months (42%), CEUS is not performed (6%), and every 12 months (1%) (fig. 14). In addition, almost all participants agreed that follow-up every 3–6 months with EOB-MRI or dynamic CT should be performed for hypovascular small nodules <1–1.5 cm that are hypointense in the hepatobiliary phase.

Summary

The following updates to the 2012 surveillance and diagnostic algorithm for hepatocellular carcinoma (updated version of the Arii Research Group algorithm)' [13] of the LCSGJ surveillance and diagnostic algorithm appear in the latest 2014 updated algorithm (fig. 15):

- The need for biopsy is mentioned as an optional test for hypovascular nodules that are hypointense in the hepatobiliary phase of EOB-MRI and are hypervascular and/or show a defect in the Kupffer phase of Sonazoid CEUS.
- 'Small nodules (1–1.5 cm)' is defined as the cutoff size that determines whether biopsy or intensive follow-up should be performed for hypovascular nodules that are hypointense in the hepatobiliary phase of EOB-MRI and are hypovascular with no defect in the Kupffer phase of Sonazoid CEUS.

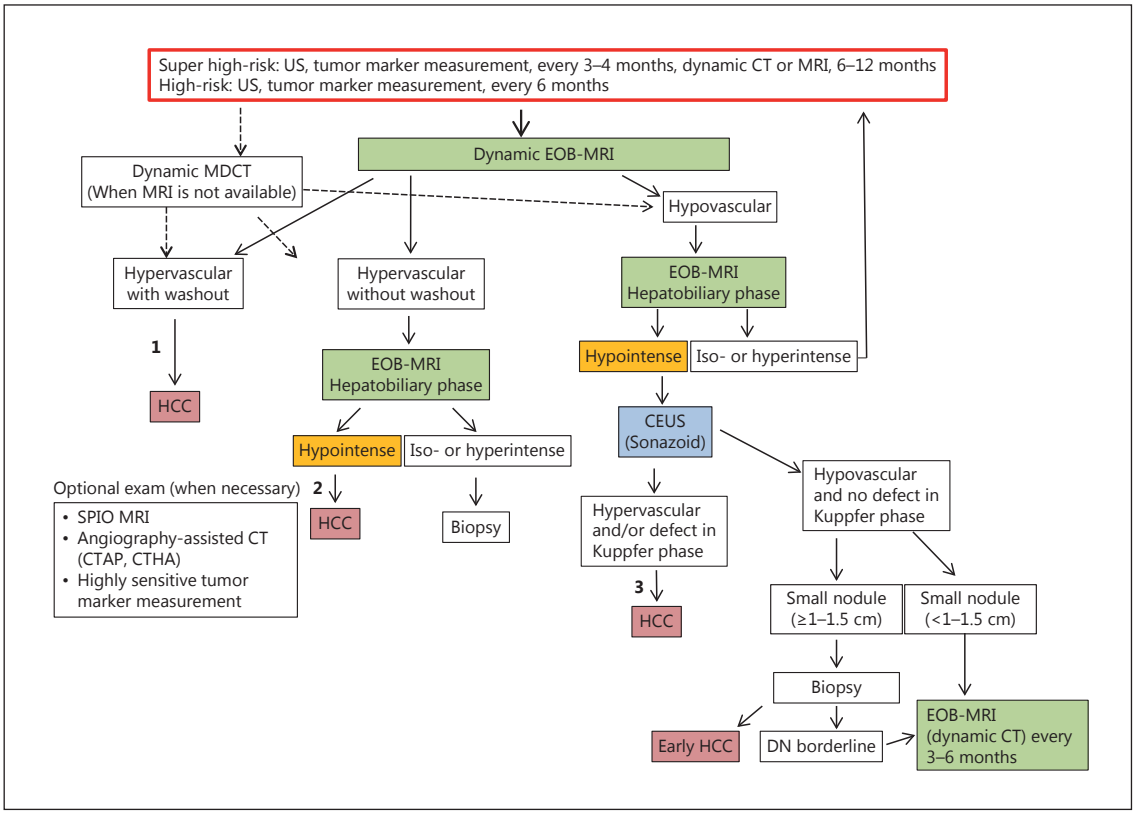

Fig. 15. Surveillance and Diagnostic Algorithm for HCC, proposed by the LCSGJ in 2014. 1 = Cavernous hemangioma may show hypointensity in the equilibrium (transitional) phase of dynamic EOB-MRI (pseudo-washout). It should be excluded by other sequences of MRI and/or other imaging modalities. 2 = Cavernous hemangioma usually shows hypointensity in the hepatobiliary phase of EOB-MRI. It should be excluded by other sequences of MRI and/or other imaging modalities. 3 = Biopsy may be considered for confirmation.

- Intensive follow-up 'every 3–6 months' with EOB-MRI (or dynamic CT) should be performed for hypovascular nodules that are hypointense in the hepatobiliary phase of EOB-MRI and show no defect in the Kupffer phase of Sonazoid CEUS when malignancy cannot be ruled out by biopsy.

Diagnostic Algorithm Updated by the Consensus Reached among the LCSGJ Members

Consensus Statements (≥67% Agreement)

(1) Dynamic CT or dynamic MRI is routinely performed 1–2 times per year for surveillance of HCC in patients with Child-Pugh A or B liver function in clinical settings in Japan (84%; percentages indicate the agreement ratio among 350 participants).

(2) Dynamic CT and dynamic EOB-MRI carried out 1–2 times per year are the most frequently performed modalities in the surveillance of HCC in patients with Child-Pugh A or B liver function (98%).

(3) Conventional dynamic MRI has been completely replaced by dynamic EOB-MRI for confirmation of HCC when nodules are detected by US (100%).

(4) Sonazoid CEUS can be performed whenever necessary in the majority of institutions in Japan (92%).

(5) When arterial hypervascularity is not depicted on dynamic EOB-MRI or dynamic CT, CEUS should be performed since the sensitivity of CEUS in detecting intranodular arterial vascularity is the highest among the existing imaging modalities (75%).

(6) In order to differentiate HCC from a dysplastic nodule, biopsy is mandatory for a small hypovascular nodule (≤1–1.5 cm) that is hypointense in the hepatobiliary phase of EOB-MRI and shows no defect in the Kupffer phase of Sonazoid CEUS (90%).

(7) Intensive follow-up by dynamic EOB-MRI (60%) or alternating dynamic EOB-MRI and dynamic CT (25%)

should be performed for a hypovascular nodule that is hypointense in the hepatobiliary phase of EOB-MRI and shows no defect in the Kupffer phase of Sonazoid CEUS or malignancy on biopsy (85%).

(8) The recommended interval of intensive follow-up by dynamic EOB-MRI for the nodule described in (7) is 3–6 months (3–4 months interval: 56%, 6 months interval: 43%; total: 99%).

(9) The recommended interval of intensive follow-up by alternating dynamic EOB-MRI and dynamic CT for the nodule described in (7) is recommended to be 3–6 months (99%).

Informative Statements (≥50% Agreement)

(1) Dynamic CT is more frequently performed as a first-line screening tool (58%; percentages indicate the agreement ratio among 350 participants) than dynamic EOB-MRI (40%).

(2) Dynamic CT is more frequently performed as a second-line diagnostic tool (60%) than dynamic EOB-MRI (32%) for confirming the diagnosis of a nodule detected by US.

(3) Diagnosis of HCC can be made without biopsy for a hypovascular nodule that is hypointense in the hepatobiliary phase of EOB-MRI and shows decreased uptake in the Kupffer phase of Sonazoid CEUS (58%). In such cases, biopsy is optional and determined on a case-by-case basis.

(4) The recommended interval of intensive follow-up by dynamic EOB-MRI of a hypovascular nodule that is hypointense in the hepatobiliary phase of EOB-MRI and shows no defect in the Kupffer phase of Sonazoid CEUS or malignancy on biopsy is 3–4 months (56%).

(5) The recommended interval of intensive follow-up by dynamic CT for the nodule described in (4) is 6 months (54%).

(6) The recommend interval of intensive follow-up by Sonazoid CEUS for the nodule described in (4) is 6 months (50%).

Conclusion

The 2014 updated version of the surveillance and diagnostic algorithm proposed by the LCSGJ was developed at a consensus meeting involving 350 experts in the diagnosis and treatment of liver cancer. This algorithm will be adopted shortly as part of the JSH Consensus-Based Clinical Practice Guideline.

Disclosure Statement

The authors declare that no financial or other conflicts of interest exist in relation to the content of this paper.

References

1 Bruix J, Sherman M: Management of hepatocellular carcinoma: an update. Hepatology 2011;53:1020–1022.
2 European Association for the Study of the Liver; European Organisation for Research and Treatment of Cancer: EASL-EORTC clinical practice guidelines: management of hepatocellular carcinoma. J Hepatol 2012;56:908–943.
3 Kudo M, Izumi N, Kokudo N, et al: Management of hepatocellular carcinoma in Japan: Consensus-Based Clinical Practice Guidelines proposed by the Japan Society of Hepatology (JSH) 2010 updated version. Dig Dis 2011;29:339–364.
4 Kudo M: Alpha-fetoprotein-L3: useful or useless for hepatocellular carcinoma? Liver Cancer 2013;2:151–152.
5 Kokudo N, Hasegawa K, Akahane M, et al: Evidence-based clinical practice guidelines for hepatocellular carcinoma – Japan Society of Hepatology 2013 update (3rd JSH-HCC Guideline). Hepatol Res 2015, in press.
6 Kokudo N: Recent progress in the treatment and diagnosis of hepatocellular carcinoma. Liver Cancer 2013;2:4.
7 Ricke J, Seidensticker M, Mohnike K: Noninvasive diagnosis of hepatocellular carcinoma in cirrhotic liver: current guidelines and future prospects for radiological imaging. Liver Cancer 2012;1:51–58.
8 Bota S, Piscaglia F, Marinelli S, et al: Comparison of international guidelines for noninvasive diagnosis of hepatocellular carcinoma. Liver Cancer 2012;1:190–200.
9 Kudo M, Matsui O, Izumi N, et al: JSH consensus-based clinical practice guideline for the management of hepatocellular carcinoma: 2014 update by the Liver Cancer Study Group of Japan. Liver Cancer 2014;3:458–468.
10 Kudo M: Early hepatocellular carcinoma: definition and diagnosis. Liver Cancer 2013;2:69–72.
11 Lee JM, Yoon JH, Joo I, et al: Recent advances in CT and MR imaging for evaluation of hepatocellular carcinoma. Liver Cancer 2012;1:22–40.
12 Joo I, Choi BI: New paradigm for management of hepatocellular carcinoma by imaging. Liver Cancer 2012;1:94–109.
13 Kudo M, Matsui O, Sakamoto M, et al: Role of gadolinium-ethoxybenzyl-diethylenetriamine pentaacetic acid-enhanced magnetic resonance imaging in the management of hepatocellular carcinoma: consensus at the Symposium of the 48th Annual Meeting of the Liver Cancer Study Group of Japan. Oncology 2013;84(suppl 1):21–27.
14 Murakami T, Tsurusaki M: Hypervascular benign and malignant liver tumors that require differentiation from hepatocellular carcinoma: key points of imaging diagnosis. Liver Cancer 2014;3:85–96.
15 Matsui O, Kadoya M, Kameyama T, et al: Benign and malignant nodules in cirrhotic livers: distinction based on blood supply. Radiology 1991;178:493–497.

16 Hayashi M, Matsui O, Ueda K, et al: Correlation between the blood supply and grade of malignancy of hepatocellular nodules associated with liver cirrhosis: evaluation by CT during intraarterial injection of contrast medium. AJR Am J Roentgenol 1999;172:969–976.
17 Ueda K, Matsui O, Kawamori Y, et al: Hypervascular hepatocellular carcinoma: evaluation of hemodynamic with dynamic CT during hepatic arteriography. Radiology 1998; 206:161–166.
18 Junqiang L, Yinzhong W, Li Z, et al: Gadoxetic acid disodium (Gd-EOBDTPA)-enhanced magnetic resonance imaging for the detection of hepatocellular carcinoma: a meta-analysis. J Magn Reson Imaging 2014;39: 1079–1087.
19 Faletti R, Cassinis MC, Fonio P, et al: Multiparametric Gd-EOB-DTPA magnetic resonance in diagnosis of HCC: dynamic study, hepatobiliary phase, and diffusion-weighted imaging compared to histology after orthotopic liver transplantation. Abdom Imaging 2014, Epub ahead of print.
20 Ueno A, Masugi Y, Yamazaki K, et al: OATP1B3 expression is strongly associated with Wnt/beta-catenin signaling and represents the transporter of gadoxetic acid in hepatocellular carcinoma. J Hepatol 2014, Epub ahead of print.
21 Ichikawa T, Sano K, Morisaka H: Diagnosis of pathologically early HCC with EOB-MRI: experiences and current consensus. Liver Cancer 2014;3:97–107.
22 Chang WC, Chen RC, Chou CT, et al: Histological grade of hepatocellular carcinoma correlates with arterial enhancement on gadoxetic acid-enhanced and diffusion-weighted MR images. Abdom Imaging 2014, Epub ahead of print.
23 Matsuda M, Tsuda T, Yoshioka S, et al: Incidence for progression of hypervascular HCC in hypovascular hepatic nodules showing hyperintensity on gadoxetic acid-enhanced hepatobiliary phase in patients with chronic liver diseases. Jpn J Radiol 2014;32:405–413.
24 Shim JH, Han S, Shin YM, et al: Prognostic performance of preoperative gadoxetic acid-enhanced MRI in resectable hepatocellular carcinoma. J Magn Reson Imaging 2014, Epub ahead of print.
25 Jang KM, Kim SH, Kim YK, et al: Imaging features of subcentimeter hypointense nodules on gadoxetic acid-enhanced hepatobiliary phase MR imaging that progress to hypervascular hepatocellular carcinoma in patients with chronic liver disease. Acta Radiol 2014, Epub ahead of print.
26 Matsuda M, Ichikawa T, Amemiya H, et al: Preoperative gadoxetic acid-enhanced MRI and simultaneous treatment of early hepatocellular carcinoma prolonged recurrence-free survival of progressed hepatocellular carcinoma patients after hepatic resection. HPB Surg 2014;2014:641685.
27 Yamashita T, Kitao A, Matsui O, et al: Gd-EOB-DTPA-enhanced magnetic resonance imaging and alpha-fetoprotein predict prognosis of early-stage hepatocellular carcinoma. Hepatology 2014, Epub ahead of print.
28 Park VY, Choi JY, Chung YE, et al: Dynamic enhancement pattern of HCC smaller than 3 cm in diameter on gadoxetic acid-enhanced MRI: comparison with multiphasic MDCT. Liver Int 2014, Epub ahead of print.
29 Ishimaru H, Nakashima K, Sakugawa T, et al: Local recurrence after chemoembolization of hepatocellular carcinoma: uptake of gadoxetic acid as a new prognostic factor. AJR Am J Roentgenol 2014;202:744–751.
30 Yu MH, Kim JH, Yoon JH, et al: Small (</= 1-cm) hepatocellular carcinoma: diagnostic performance and imaging features at gadoxetic acid-enhanced MR imaging. Radiology 2014;271:748–760.
31 Tada T, Kumada T, Toyoda H, et al: Diagnostic accuracy for macroscopic classification of nodular hepatocellular carcinoma: comparison of gadolinium ethoxybenzyl diethylenetriamine pentaacetic acid-enhanced magnetic resonance imaging and angiography-assisted computed tomography. J Gastroenterol 2014, Epub ahead of print.
32 Komatsu N, Motosugi U, Maekawa S, et al: Hepatocellular carcinoma risk assessment using gadoxetic acid-enhanced hepatocyte phase magnetic resonance imaging. Hepatol Res 2014, Epub ahead of print.
33 Kim KA, Kim MJ, Choi JY, et al: Detection of recurrent hepatocellular carcinoma on postoperative surveillance: comparison of MDCT and gadoxetic acid-enhanced MRI. Abdom Imaging 2014;39:291–299.
34 Phongkitkarun S, Limsamutpetch K, Tannaphai P, et al: Added value of hepatobiliary phase gadoxetic acid-enhanced MRI for diagnosing hepatocellular carcinoma in high-risk patients. World J Gastroenterol 2013;19: 8357–8365.
35 Zhao XT, Li WX, Chai WM, et al: Detection of small hepatocellular carcinoma using gadoxetic acid-enhanced MRI: Is the addition of diffusion-weighted MRI at 3.0T beneficial? J Dig Dis 2014;15:137–145.
36 Iannicelli E, Di Pietropaolo M, Marignani M, et al: Gadoxetic acid-enhanced MRI for hepatocellular carcinoma and hypointense nodule observed in the hepatobiliary phase. Radiol Med 2014;119:367–376.
37 Inoue T, Hyodo T, Murakami T, et al: Hypovascular hepatic nodules showing hypointense on the hepatobiliary-phase image of Gd-EOB-DTPA-enhanced MRI to develop a hypervascular hepatocellular carcinoma: a nationwide retrospective study on their natural course and risk factors. Dig Dis 2013;31: 472–479.
38 Park MJ, Kim YK, Park HJ, et al: Scirrhous hepatocellular carcinoma on gadoxetic acid-enhanced magnetic resonance imaging and diffusion-weighted imaging: emphasis on the differentiation of intrahepatic cholangiocarcinoma. J Comput Assist Tomogr 2013;37: 872–881.
39 Kakihara D, Nishie A, Harada N, et al: Performance of gadoxetic acid-enhanced MRI for detecting hepatocellular carcinoma in recipients of living-related-liver-transplantation: Comparison with dynamic multidetector row computed tomography and angiography-assisted computed tomography. J Magn Reson Imaging 2013, Epub ahead of print.
40 Nishie A, Asayama Y, Ishigami K, et al: Clinicopathological significance of the peritumoral decreased uptake area of gadolinium ethoxybenzyl diethylenetriamine pentaacetic acid in hepatocellular carcinoma. J Gastroenterol Hepatol 2014;29:561–567.
41 Hamada K, Saitoh S, Nishino N, et al: A liver tumor that progressed to hepatocellular carcinoma as observed on follow-up magnetic resonance images showing increased contrast medium uptake (in Japanese). Nihon Shokakibyo Gakkai Zasshi 2013;110:1976–1982.
42 Lim S, Kim YK, Park HJ, et al: Infiltrative hepatocellular carcinoma on gadoxetic acid-enhanced and diffusion-weighted MRI at 3.0T. J Magn Reson Imaging 2014;39:1238–1245.
43 Cha DI, Lee MW, Kim YK, et al: Assessing patients with hepatocellular carcinoma meeting the milan criteria: Is liver 3 tesla MR with gadoxetic acid necessary in addition to liver CT? J Magn Reson Imaging 2014;39:842–852.
44 Liu X, Zou L, Liu F, et al: Gadoxetic acid disodium-enhanced magnetic resonance imaging for the detection of hepatocellular carcinoma: a meta-analysis. PLoS One 2013;8:e70896.
45 Wu LM, Xu JR, Gu HY, et al: Is liver-specific gadoxetic acid-enhanced magnetic resonance imaging a reliable tool for detection of hepatocellular carcinoma in patients with chronic liver disease? Dig Dis Sci 2013;58:3313–3325.
46 Kim JY, Lee SS, Byun JH, et al: Biologic factors affecting HCC conspicuity in hepatobiliary phase imaging with liver-specific contrast agents. AJR Am J Roentgenol 2013;201:322–331.
47 Baird AJ, Amos GJ, Saad NF, et al: Retrospective audit to determine the diagnostic accuracy of Primovist-enhanced MRI in the detection of hepatocellular carcinoma in cirrhosis with explant histopathology correlation. J Med Imaging Radiat Oncol 2013;57:314–320.
48 Yamamoto A, Ito K, Tamada T, et al: Newly developed hypervascular hepatocellular carcinoma during follow-up periods in patients with chronic liver disease: observation in serial gadoxetic acid-enhanced MRI. AJR Am J Roentgenol 2013;200:1254–1260.
49 Park YS, Lee CH, Kim BH, et al: Using Gd-EOB-DTPA-enhanced 3-T MRI for the differentiation of infiltrative hepatocellular carcinoma and focal confluent fibrosis in liver cirrhosis. Magn Reson Imaging 2013;31: 1137–1142.
50 Yoo SH, Choi JY, Jang JW, et al: Gd-EOB-DTPA-enhanced MRI is better than MDCT in decision making of curative treatment for hepatocellular carcinoma. Ann Surg Oncol 2013;20:2893–2900.

51 Ichikawa S, Ichikawa T, Motosugi U, et al: Presence of a hypovascular hepatic nodule showing hypointensity on hepatocyte-phase image is a risk factor for hypervascular hepatocellular carcinoma. J Magn Reson Imaging 2014;39:293–297.
52 Kim SH, Jeong WK, Kim Y, et al: Hepatocellular carcinoma composed of two different histologic types: imaging features on gadoxetic acid-enhanced liver MRI. Clin Mol Hepatol 2013;19:92–96.
53 Fujita N, Nishie A, Kubo Y, et al: Hepatocellular carcinoma: clinical significance of signal heterogeneity in the hepatobiliary phase of gadoxetic acid-enhanced MR imaging. Eur Radiol 2014, Epub ahead of print.
54 Choi JW, Lee JM, Kim SJ, et al: Hepatocellular carcinoma: imaging patterns on gadoxetic acid-enhanced MR Images and their value as an imaging biomarker. Radiology 2013;267:776–786.
55 Toyoda H, Kumada T, Tada T, et al: Non-hypervascular hypointense nodules detected by Gd-EOB-DTPA-enhanced MRI are a risk factor for recurrence of HCC after hepatectomy. J Hepatol 2013;58:1174–1180.
56 Hyodo T, Murakami T, Imai Y, et al: Hypovascular nodules in patients with chronic liver disease: risk factors for development of hypervascular hepatocellular carcinoma. Radiology 2013;266:480–490.
57 Ooka Y, Kanai F, Okabe S, et al: Gadoxetic acid-enhanced MRI compared with CT during angiography in the diagnosis of hepatocellular carcinoma. Magn Reson Imaging 2013;31:748–754.
58 Granito A, Galassi M, Piscaglia F, et al: Impact of gadoxetic acid (Gd-EOB-DTPA)-enhanced magnetic resonance on the non-invasive diagnosis of small hepatocellular carcinoma: a prospective study. Aliment Pharmacol Ther 2013;37:355–363.
59 Kitao A, Matsui O, Yoneda N, et al: Hypervascular hepatocellular carcinoma: correlation between biologic features and signal intensity on gadoxetic acid-enhanced MR images. Radiology 2012;265:780–789.
60 Park MJ, Kim YK, Lee MH, et al: Validation of diagnostic criteria using gadoxetic acid-enhanced and diffusion-weighted MR imaging for small hepatocellular carcinoma (<= 2.0 cm) in patients with hepatitis-induced liver cirrhosis. Acta Radiol 2013;54:127–136.
61 Jin YJ, Nah SY, Lee JW, et al: Utility of adding Primovist magnetic resonance imaging to analysis of hepatocellular carcinoma by liver dynamic computed tomography. Clin Gastroenterol Hepatol 2013;11:187–192.
62 An C, Park MS, Kim D, et al: Added value of subtraction imaging in detecting arterial enhancement in small (<3 cm) hepatic nodules on dynamic contrast-enhanced MRI in patients at high risk of hepatocellular carcinoma. Eur Radiol 2013;23:924–930.
63 Shinagawa Y, Sakamoto K, Fujimitsu R, et al: Pseudolesion of the liver on gadoxetate disodium-enhanced MR images obtained after transarterial chemoembolization for hepatocellular carcinoma: clinicoradiologic correlation. AJR Am J Roentgenol 2012;199:1010–1017.
64 Nakamura Y, Tashiro H, Nambu J, et al: Detectability of hepatocellular carcinoma by gadoxetate disodium-enhanced hepatic MRI: tumor-by-tumor analysis in explant livers. J Magn Reson Imaging 2013;37:684–691.
65 Bashir MR, Gupta RT, Davenport MS, et al: Hepatocellular carcinoma in a North American population: does hepatobiliary MR imaging with Gd-EOB-DTPA improve sensitivity and confidence for diagnosis? J Magn Reson Imaging 2013;37:398–406.
66 Fujinaga Y, Kadoya M, Kozaka K, et al: Prediction of macroscopic findings of hepatocellular carcinoma on hepatobiliary phase of gadolinium-ethoxybenzyl-diethylenetriamine pentaacetic acid-enhanced magnetic resonance imaging: correlation with pathology. Hepatol Res 2013;43:488–494.
67 Kim JY, Kim MJ, Kim KA, et al: Hyperintense HCC on hepatobiliary phase images of gadoxetic acid-enhanced MRI: correlation with clinical and pathological features. Eur J Radiol 2012;81:3877–3882.
68 Kanata N, Yoshikawa T, Ohno Y, et al: HCC-to-liver contrast on arterial-dominant phase images of EOB-enhanced MRI: comparison with dynamic CT. Magn Reson Imaging 2013;31:17–22.
69 Kim YK, Lee WJ, Park MJ, et al: Hypovascular hypointense nodules on hepatobiliary phase gadoxetic acid-enhanced MR images in patients with cirrhosis: potential of DW imaging in predicting progression to hypervascular HCC. Radiology 2012;265:104–114.
70 Kobayashi S, Matsui O, Gabata T, et al: Intranodular signal intensity analysis of hypovascular high-risk borderline lesions of HCC that illustrate multi-step hepatocarcinogenesis within the nodule on Gd-EOB-DTPA-enhanced MRI. Eur J Radiol 2012;81:3839–3845.
71 Kim AY, Kim YK, Lee MW, et al: Detection of hepatocellular carcinoma in gadoxetic acid-enhanced MRI and diffusion-weighted MRI with respect to the severity of liver cirrhosis. Acta Radiol 2012;53:830–838.
72 Murakami T, Okada M, Hyodo T: CT versus MR imaging of hepatocellular carcinoma: toward improved treatment decisions. Magn Reson Med Sci 2012;11:75–81.
73 Kubota K, Tamura T, Aoyama N, et al: Correlation of liver parenchymal gadolinium-ethoxybenzyl diethylenetriaminepentaacetic acid enhancement and liver function in humans with hepatocellular carcinoma. Oncol Lett 2012;3:990–994.
74 Kobayashi S, Matsui O, Gabata T, et al: Relationship between signal intensity on hepatobiliary phase of gadolinium ethoxybenzyl diethylenetriaminepentaacetic acid (Gd-EOB-DTPA)-enhanced MR imaging and prognosis of borderline lesions of hepatocellular carcinoma. Eur J Radiol 2012;81:3002–3009.
75 Rhee H, Kim MJ, Park MS, et al: Differentiation of early hepatocellular carcinoma from benign hepatocellular nodules on gadoxetic acid-enhanced MRI. Br J Radiol 2012;85:e837–e844.
76 Inoue T, Kudo M, Komuta M, et al: Assessment of Gd-EOB-DTPA-enhanced MRI for HCC and dysplastic nodules and comparison of detection sensitivity versus MDCT. J Gastroenterol 2012;47:1036–1047.
77 Sugimoto K, Moriyasu F, Saito K, et al: Comparison of Kupffer-phase Sonazoid-enhanced sonography and hepatobiliary-phase gadoxetic acid-enhanced magnetic resonance imaging of hepatocellular carcinoma and correlation with histologic grading. J Ultrasound Med 2012;31:529–538.
78 An C, Park MS, Jeon HM, et al: Prediction of the histopathological grade of hepatocellular carcinoma using qualitative diffusion-weighted, dynamic, and hepatobiliary phase MRI. Eur Radiol 2012;22:1701–1708.
79 Kim HY, Choi JY, Kim CW, et al: Gadolinium ethoxybenzyl diethylenetriamine pentaacetic acid-enhanced magnetic resonance imaging predicts the histological grade of hepatocellular carcinoma only in patients with Child-Pugh class A cirrhosis. Liver Transpl 2012;18:850–857.
80 Watanabe H, Kanematsu M, Goshima S, et al: Is gadoxetate disodium-enhanced MRI useful for detecting local recurrence of hepatocellular carcinoma after radiofrequency ablation therapy? AJR Am J Roentgenol 2012;198:589–595.
81 Kinner S, Umutlu L, Blex S, et al: Diffusion weighted MR imaging in patients with HCC and liver cirrhosis after administration of different gadolinium contrast agents: is it still reliable? Eur J Radiol 2012;81:e625–e628.
82 Sugimoto K, Moriyasu F, Shiraishi J, et al: Assessment of arterial hypervascularity of hepatocellular carcinoma: comparison of contrast-enhanced US and gadoxetate disodium-enhanced MR imaging. Eur Radiol 2012;22:1205–1213.
83 Korkusuz H, Knau LL, Kromen W, et al: Different signal intensity at Gd-EOB-DTPA compared with Gd-DTPA-enhanced MRI in hepatocellular carcinoma transgenic mouse model in delayed phase hepatobiliary imaging. J Magn Reson Imaging 2012;35:1397–1402.
84 Eso Y, Marusawa H, Osaki Y: Education and imaging. Hepatobiliary and pancreatic: detection of early hepatocellular carcinoma by enhanced magnetic resonance imaging. J Gastroenterol Hepatol 2012;27:416.
85 Alaboudy A, Inoue T, Hatanaka K, et al: Usefulness of combination of imaging modalities in the diagnosis of hepatocellular carcinoma using Sonazoid®-enhanced ultrasound, gadolinium diethylene-triamine-pentaacetic acid-enhanced magnetic resonance imaging, and contrast-enhanced computed tomography. Oncology 2011;81(suppl 1):66–72.

86 Hwang J, Kim SH, Lee MW, et al: Small (</= 2 cm) hepatocellular carcinoma in patients with chronic liver disease: comparison of gadoxetic acid-enhanced 3.0 T MRI and multiphasic 64-multirow detector CT. Br J Radiol 2012;85:e314–e322.

87 Nakamura Y, Toyota N, Date S, et al: Clinical significance of the transitional phase at gadoxetate disodium-enhanced hepatic MRI for the diagnosis of hepatocellular carcinoma: preliminary results. J Comput Assist Tomogr 2011;35:723–727.

88 Kim KA, Kim MJ, Jeon HM, et al: Prediction of microvascular invasion of hepatocellular carcinoma: usefulness of peritumoral hypointensity seen on gadoxetate disodium-enhanced hepatobiliary phase images. J Magn Reson Imaging 2012;35:629–634.

89 Sano K, Ichikawa T, Motosugi U, et al: Imaging study of early hepatocellular carcinoma: usefulness of gadoxetic acid-enhanced MR imaging. Radiology 2011;261:834–844.

90 Chanyaputhipong J, Low SC, Chow PK: Gadoxetate acid-enhanced MR imaging for HCC: a review for clinicians. Int J Hepatol 2011;2011:489342.

91 Rhee H, Kim MJ, Park YN, et al: Gadoxetic acid-enhanced MRI findings of early hepatocellular carcinoma as defined by new histologic criteria. J Magn Reson Imaging 2012;35:393–398.

92 Saito K, Moriyasu F, Sugimoto K, et al: Diagnostic efficacy of gadoxetic acid-enhanced MRI for hepatocellular carcinoma and dysplastic nodule. World J Gastroenterol 2011;17:3503–3509.

93 Baek CK, Choi JY, Kim KA, et al: Hepatocellular carcinoma in patients with chronic liver disease: a comparison of gadoxetic acid-enhanced MRI and multiphasic MDCT. Clin Radiol 2012;67:148–156.

94 Chung J, Yu JS, Kim DJ, et al: Hypervascular hepatocellular carcinoma in the cirrhotic liver: diffusion-weighted imaging versus superparamagnetic iron oxide-enhanced MRI. Magn Reson Imaging 2011;29:1235–1243.

95 Choi JY, Kim MJ, Park YN, et al: Gadoxetate disodium-enhanced hepatobiliary phase MRI of hepatocellular carcinoma: correlation with histological characteristics. AJR Am J Roentgenol 2011;197:399–405.

96 Kim JE, Kim SH, Lee SJ, et al: Hypervascular hepatocellular carcinoma 1 cm or smaller in patients with chronic liver disease: characterization with gadoxetic acid-enhanced MRI that includes diffusion-weighted imaging. AJR Am J Roentgenol 2011;196:W758–W765.

97 Haradome H, Grazioli L, Tinti R, et al: Additional value of gadoxetic acid-DTPA-enhanced hepatobiliary phase MR imaging in the diagnosis of early-stage hepatocellular carcinoma: comparison with dynamic triple-phase multidetector CT imaging. J Magn Reson Imaging 2011;34:69–78.

98 Kim YK, Kim CS, Han YM, et al: Detection of small hepatocellular carcinoma: intraindividual comparison of gadoxetic acid-enhanced MRI at 3.0 and 1.5 T. Invest Radiol 2011;46:383–389.

99 Kagawa Y, Okada M, Kumano S, et al: Optimal scanning protocol of arterial dominant phase for hypervascular hepatocellular carcinoma with gadolinium-ethoxybenzyl-diethylenetriamine pentaacetic acid-enhanced MR. J Magn Reson Imaging 2011;33:864–872.

100 Kobayashi S, Matsui O, Gabata T, et al: Gadolinium ethoxybenzyl diethylenetriamine pentaacetic acid-enhanced magnetic resonance imaging findings of borderline lesions at high risk for progression to hypervascular classic hepatocellular carcinoma. J Comput Assist Tomogr 2011;35:181–186.

101 Ariizumi S, Kitagawa K, Kotera Y, et al: A non-smooth tumor margin in the hepatobiliary phase of gadoxetic acid disodium (Gd-EOB-DTPA)-enhanced magnetic resonance imaging predicts microscopic portal vein invasion, intrahepatic metastasis, and early recurrence after hepatectomy in patients with hepatocellular carcinoma. J Hepatobiliary Pancreat Sci 2011;18:575–585.

102 Golfieri R, Renzulli M, Lucidi V, et al: Contribution of the hepatobiliary phase of Gd-EOB-DTPA-enhanced MRI to Dynamic MRI in the detection of hypovascular small (</= 2 cm) HCC in cirrhosis. Eur Radiol 2011;21:1233–1242.

103 Akai H, Kiryu S, Matsuda I, et al: Detection of hepatocellular carcinoma by Gd-EOB-DTPA-enhanced liver MRI: comparison with triple phase 64 detector row helical CT. Eur J Radiol 2011;80:310–315.

104 Joishi D, Ueno A, Tanimoto A, et al: Natural course of hypovascular nodules detected on gadoxetic acid-enhanced MR imaging: presence of fat is a risk factor for hypervascularization. Magn Reson Med Sci 2013;12:281–287.

105 Motosugi U: Hypovascular hypointense nodules on hepatocyte phase gadoxetic acid-enhanced MR images: too early or too progressed to determine hypervascularity. Radiology 2013;267:317–318.

106 Takechi M, Tsuda T, Yoshioka S, et al: Risk of hypervascularization in small hypovascular hepatic nodules showing hypointense in the hepatobiliary phase of gadoxetic acid-enhanced MRI in patients with chronic liver disease. Jpn J Radiol 2012;30:743–751.

107 Takayama Y, Nishie A, Nakayama T, et al: Hypovascular hepatic nodule showing hypointensity in the hepatobiliary phase of gadoxetic acid-enhanced MRI in patients with chronic liver disease: prediction of malignant transformation. Eur J Radiol 2012;81:3072–3078.

108 Akai H, Matsuda I, Kiryu S, et al: Fate of hypointense lesions on Gd-EOB-DTPA-enhanced magnetic resonance imaging. Eur J Radiol 2012;81:2973–2977.

109 Motosugi U, Ichikawa T, Sano K, et al: Outcome of hypovascular hepatic nodules revealing no gadoxetic acid uptake in patients with chronic liver disease. J Magn Reson Imaging 2011;34:88–94.

110 Kumada T, Toyoda H, Tada T, et al: Evolution of hypointense hepatocellular nodules observed only in the hepatobiliary phase of gadoxetate disodium-enhanced MRI. AJR Am J Roentgenol 2011;197:58–63.

Review

Oncology

Oncology 2014;87(suppl 1):22–31
DOI: 10.1159/000368142

Published online: November 22, 2014

Transarterial Chemoembolization Failure/Refractoriness: JSH-LCSGJ Criteria 2014 Update

Masatoshi Kudo[a] Osamu Matsui[b] Namiki Izumi[c] Masumi Kadoya[d] Takuji Okusaka[e] Shiro Miyayama[f] Koichiro Yamakado[g] Kaoru Tsuchiya[c] Kazuomi Ueshima[a] Atsushi Hiraoka[h] Masafumi Ikeda[i] Sadahisa Ogasawara[j] Tatsuya Yamashita[k] Tetsuya Minami[l]

on behalf of the Liver Cancer Study Group of Japan

[a]Department of Gastroenterology and Hepatology, Kinki University School of Medicine, Osaka-Sayama, [b]Department of Radiology, Kanazawa University Graduate School of Medical Science, Kanazawa, [c]Department of Gastroenterology and Hepatology, Musashino Red Cross Hospital, Tokyo, [d]Department of Radiology, Shinshu University School of Medicine, Matsumoto, [e]Department of Hepatobiliary and Pancreatic Oncology, National Cancer Center Hospital, Tokyo, [f]Department of Diagnostic Radiology, Fukuiken Saiseikai Hospital, Fukui, [g]Department of Interventional Radiology, Mie University School of Medicine, Tsu, [h]Department of Gastroenterology, Ehime Prefectural Central Hospital, Matsuyama, [i]Department of Hepatobiliary and Pancreatic Oncology, National Cancer Center Hospital East, and [j]Department of Gastroenterology and Nephrology, Graduate School of Medicine, Chiba University, Chiba, and Departments of [k]Gastroenterology and [l]Radiology, Kanazawa University Hospital, Kanazawa, Japan

Key Words

Transarterial chemoembolization · Hepatocellular carcinoma · Criteria of transarterial chemoembolization failure

Abstract

In the 2010 version of the Japan Society of Hepatology (JSH) consensus-based treatment algorithm for the management of hepatocellular carcinoma (HCC), transarterial chemoembolization (TACE) failure/refractoriness was defined assuming the use of superselective lipiodol TACE, which has been widely used worldwide and particularly in Japan, and areas with lipiodol deposition were considered to be necrotic. However, this concept is not well accepted internationally. Furthermore, following the approval of microspheres, an embolic material that does not use lipiodol, in February 2014 in Japan, the phrase 'lipiodol deposition' needed to be changed to 'necrotic lesion or viable lesion'. Accordingly, the respective section in the JSH guidelines was revised to define TACE failure as an insufficient response after ≥2 consecutive TACE procedures that is evident on response evaluation computed tomography or magnetic resonance imaging after 1–3 months, even after chemotherapeutic agents have been changed and/or the feeding artery has been reanalyzed. In addition, the appearance of a higher number of lesions in the liver than that recorded at the previous TACE procedure (other than the nodule being treated) was added to the definition of TACE failure/refractoriness. Following the discussion of other issues concerning the continuous elevation of tumor markers, vascular invasion, and extrahepatic spread, descriptions similar to those in the previous version were approved. The revision of these TACE failure definitions was approved by over 85% of HCC experts.

KARGER

E-Mail karger@karger.com
www.karger.com/ocl

0030–2414/14/0877–0022$39.50/0

Prof. Masatoshi Kudo
Department of Gastroenterology and Hepatology
Kinki University School of Medicine
377-2 Ohno-Higashi, Osaka-Sayama, Osaka 589-8511 (Japan)
E-Mail m-kudo@med.kindai.ac.jp

Introduction

Transarterial chemoembolization (TACE) [1, 2] is the standard treatment for intermediate-stage hepatocellular carcinoma (HCC) and benefits patients in two ways: providing a treatment response and minimizing liver function damage (fig. 1). However, when repeated, TACE loses its efficacy at some point and patients enter the so-called state of TACE failure/refractoriness [3]. When this is the case, multifocal nodules are commonly seen scattered in both lobes or as a huge HCC mass, and the noncancerous liver tissue will have deteriorated due to the damage caused by TACE, resulting in a reduced survival time (fig. 2). As a result, it has become apparent in recent years that the treatment modality should be switched before patients enter this state. The concept of TACE refractoriness was first proposed in the clinical practice guidelines proposed by the Japan Society of Hepatology (JSH) [4] and then appeared in criteria published in Korea [5], criteria established by the European Association for the Study of the Liver (EASL) [3], and in the Assessment for Retreatment (ART) score system [6, 7], although the definition in the latter is slightly different from that for TACE refractoriness. In addition, other studies recommend the use of discontinuation rules or a scoring system, such as the Hepatoma Arterial-Embolisation Prognostic (HAP) score [8], to decide whether TACE should be continued. However, it should be noted that in Japan, HCC cases indicated for TACE generally involve only a limited number of small nodules because of a well-established nationwide surveillance program for HCC [9]. On the other hand, in the United States, Europe, and some Asian countries, patients already tend to have a huge tumor or multifocal bilobar intermediate-stage HCCs at the time of their first TACE treatment [10]. These patients should be further subclassified and treated as subgroups of individuals who would either respond or not respond favorably to TACE. To improve the prognosis of patients, the JSH criteria for TACE refractoriness recommend recognizing the time point of TACE refractoriness at the intermediate stage of the disease after having repeated TACE several times or even ≥10 times and having switched the treatment strategy to preserve residual liver function (fig. 2).

At the 50th Liver Cancer Study Group of Japan (LCSGJ) Congress (congress president: Prof. Masatoshi Kudo) held on June 5–6, 2014 in Kyoto, Japan, the definition of TACE refractoriness was updated by HCC experts, and a consensus meeting was convened to evaluate the proposed definition [11]. At this meeting, appropriate treatments for cases of TACE failure or refractoriness were also discussed. Moreover, during a session entitled 'The Definition of TACE Refractoriness' held at the 4th International Kyoto Liver Cancer Symposium (IKLS; congress president: Prof. Masatoshi Kudo) on June 7–8, 2014 in Kyoto, Japan, a voting system was used in a debate of the criteria. In this article, we report the updated JSH-LCSGJ criteria for TACE failure/refractoriness and the results of the meetings.

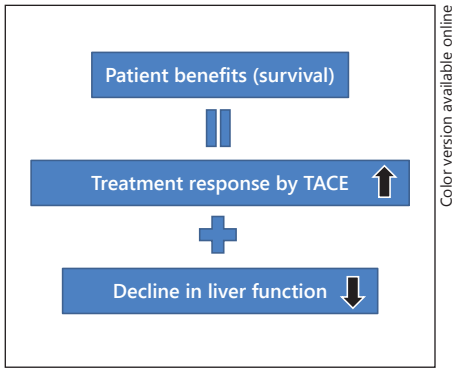

Fig. 1. Benefits of TACE for patients.

Consensus Meeting

Approximately 140 HCC experts, of which 51% were hepatologists, 6% surgeons, 6% oncologists, and 9% radiologists, used a voting system at the consensus meeting on TACE failure/refractoriness. The monthly number of cancer patients treated by the experts (proportion of experts) was as follows: <5 patients (16% of experts), 6–25 patients (46%), 26–50 patients (20%), 51–100 patients (9%), and ≥101 patients (9%). When asked which department performs TACE, 51% of experts answered internal medicine, 47% radiology, and 1% surgery. When asked about the number of patients they treated in a month, 30% of experts answered <5 patients, 11% 6–50 patients, and 4% answered ≥51 patients. Furthermore, when asked what primary embolic agent they used in TACE, 46% answered lipiodol, 35% porous gelatin sponge, 6% gelatin sponge, and 13% microspheres (beads). The primary anticancer agents used in TACE were, in descending order, epirubicin (44%), miriplatin (26%), cisplatin (24%), doxorubicin (4%), and mitomycin (3%). In addition, 56% of experts agreed and 17% disagreed with the question 'Do you think a scoring sys-

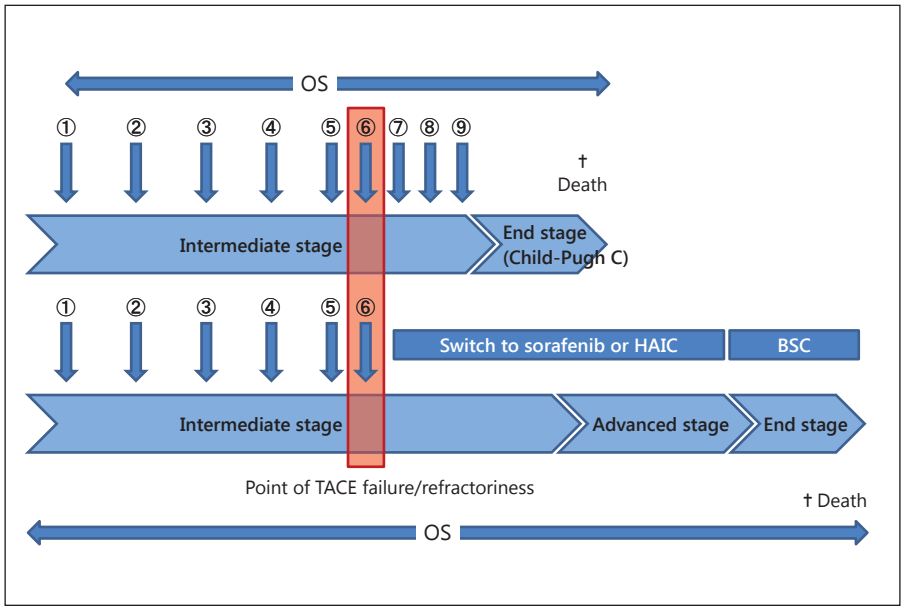

Fig. 2. Treatment strategy to prolong patient survival according to a TACE discontinuation and switching rule in patients with TACE failure/refractoriness. OS = Overall survival.

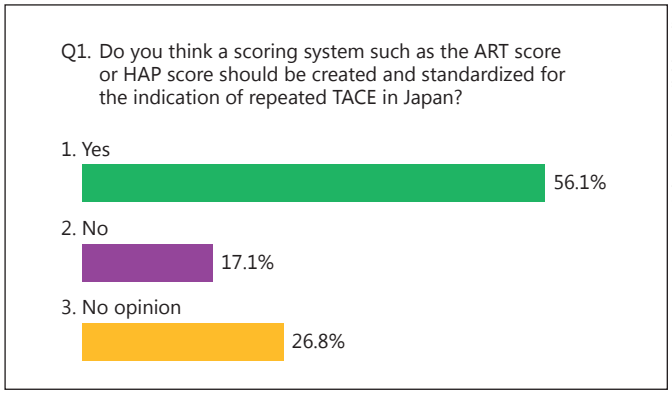

Fig. 3. Votes cast on the need for a scoring system for a TACE discontinuation rule.

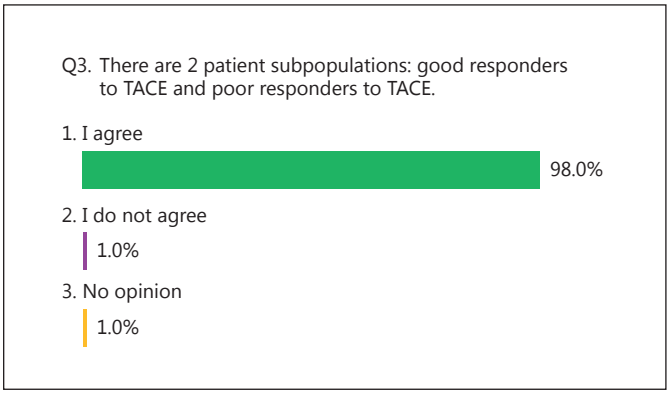

Fig. 5. Question and answers on whether there are two TACE responder subgroups.

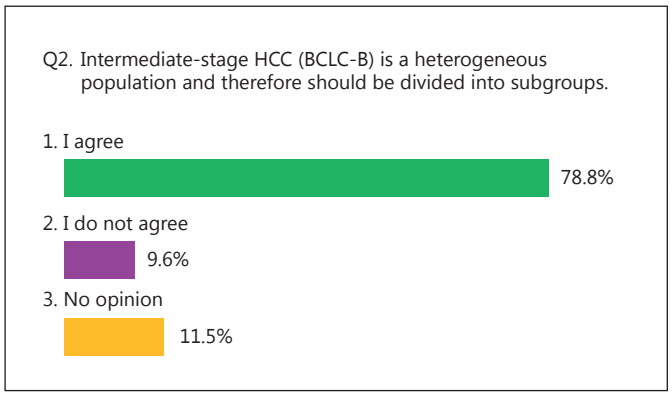

Fig. 4. Question and answers on intermediate-stage HCC.

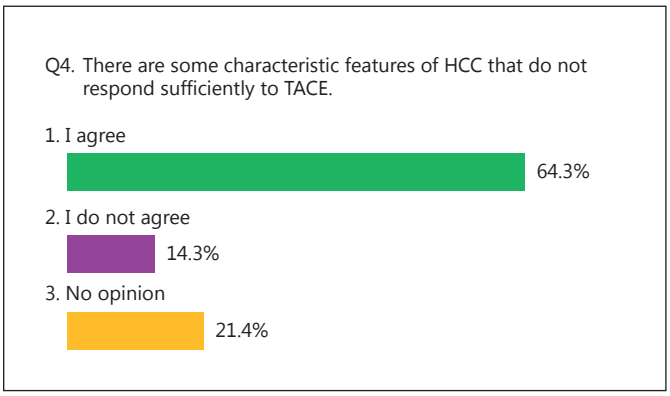

Fig. 6. Question and answers on whether there are some characteristic features in poor responders to TACE.

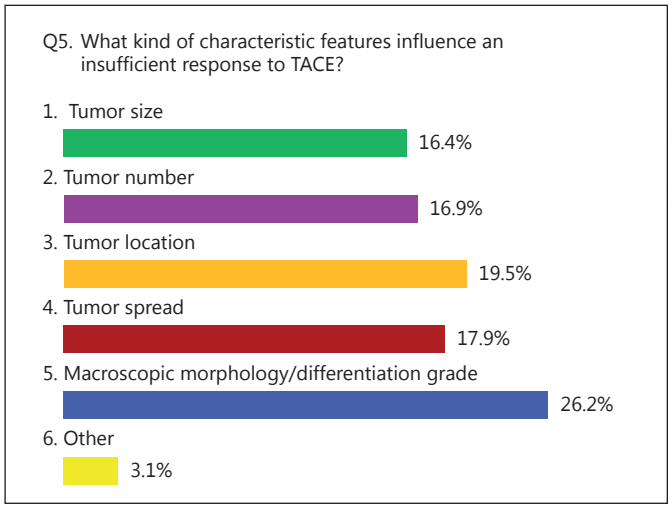

Fig. 7. Question and answers on the characteristic features of poor responders to TACE.

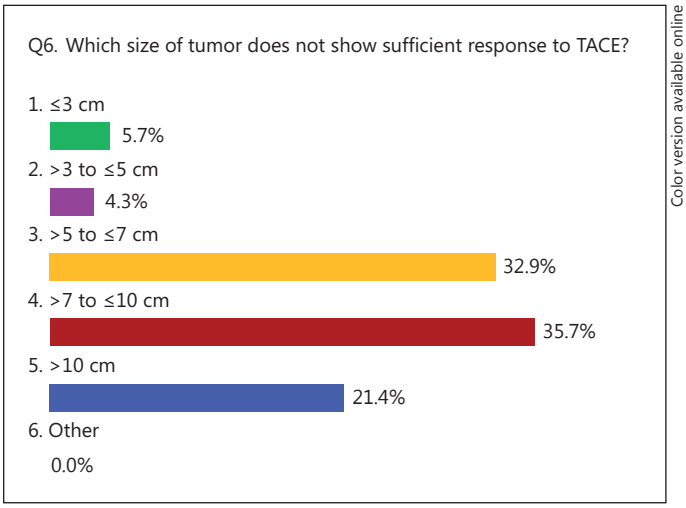

Fig. 8. Question and answers on the tumor size related to a poor response to TACE.

tem such as the ART score or HAP score should be created and standardized for the indication of repeated TACE in Japan?' (fig. 3).

Voting Results

Heterogeneity of Intermediate-Stage HCC

To the question asking if it is necessary on account of their heterogeneous nature to subgroup intermediate-stage HCCs (equivalent to stage B on the Barcelona Clinic Liver Cancer staging system), for which TACE is the standard treatment, 79% of experts agreed and 10% disagreed (fig. 4), suggesting that many experts are well aware of the extremely wide range of features of intermediate-stage HCCs, i.e. multifocal HCCs without vascular invasion or extrahepatic spread. In fact, 98% of experts agreed with the statement that some HCC cases respond well to TACE while others respond poorly to it (fig. 5). In addition, 64% of experts thought that HCCs which respond poorly to TACE exhibit specific features, indicating that many experts encounter such cases in clinical practice (fig. 6). When asked about the characteristic features of HCCs that respond poorly to TACE, experts mentioned equally the size, number, location, spread, and macroscopic morphology/pathological differentiation grade of HCCs (fig. 7). With regard to the size of HCC associated with a poor TACE efficacy, 5–7 cm was mentioned by 33% of experts, 7–10 cm by 36%, and ≥10 cm by 21%, suggesting that the efficacy of TACE decreases as the size of HCC increases (fig. 8). With regard to the number of HCC lesions associated with a poor TACE efficacy, 23, 42, and 32% of experts answered 4–6, 7–10, and ≥10, respectively (fig. 9). When asked about the extent of HCC that affects the TACE efficacy, 29 and 69% answered HCC spread over 'multiple segments' and 'both lobes', respectively (data not shown). As expected, 72% agreed that poorly differentiated HCCs respond poorly to TACE (fig. 10).

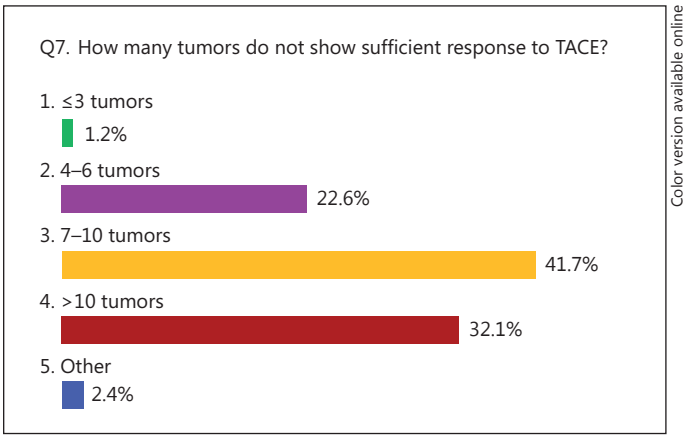

Fig. 9. Question and answers on the tumor number related to a poor response to TACE.

Contraindications of TACE

The following four contraindications for TACE are stated in the 2010 version of the JSH consensus-based

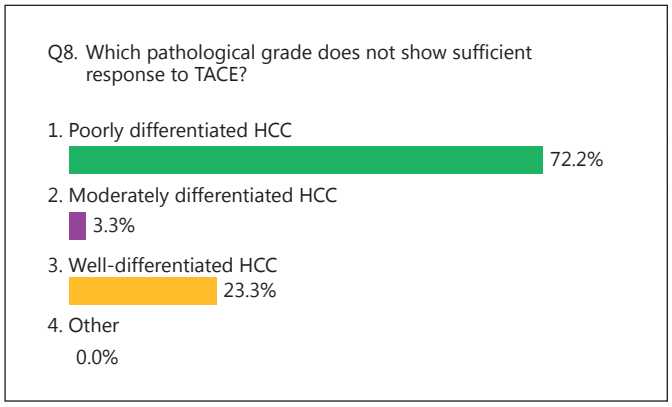

Fig. 10. Question and answers on the pathological grade related to a poor response to TACE.

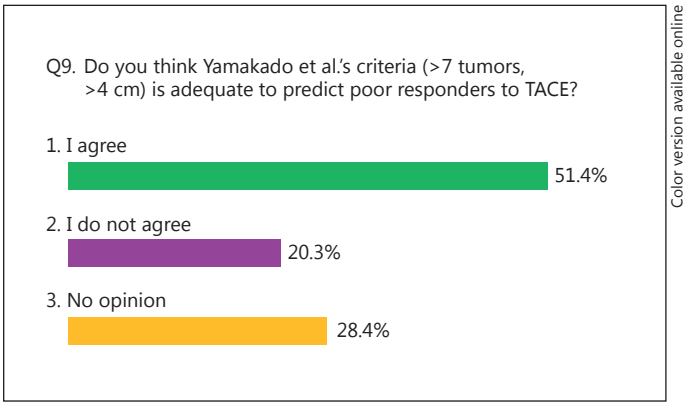

Fig. 11. Question and answers on Yamakado et al.'s [12] criteria.

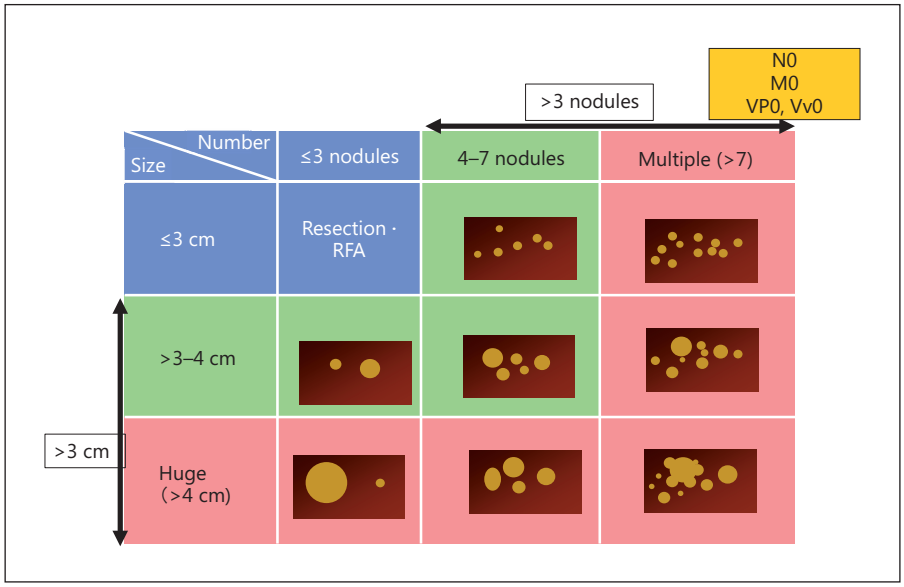

Fig. 12. Heterogeneity of intermediate-stage HCC. The green fields indicate good responders to TACE and the pink fields poor responders (colors refer to the online version only). RFA = Radiofrequency ablation.

practice guidelines [4], and no major amendments to these contraindications were made at the recent meeting.

- Blood vessels involved in treatment cannot be used and feeding vessels are unavailable for catheterization because of the damage caused by repeated TACE.
- Residual liver function graded as Child-Pugh C due to repeated treatment.
- HCC that has spread to the major branches of the portal vein (Vp3) or the portal trunk (Vp4).
- A large arterioportal shunt.

Poor Responders to TACE

In the question and answer session, experts agreed that >7 HCCs of >4 cm in size constitute an HCC subgroup that responds poorly to TACE. These criteria were adopted based on the findings of Yamakado et al. [12], stating that patients with tumors of >4 cm in size seldom benefit from TACE due to their poor response to the treatment and subsequent decline in residual liver function. Yamakado et al.'s criteria gained agreement from 51% of experts, indicating that >7 HCCs of >4 cm in size is essentially accepted as criterion defining a subgroup of patients responding poorly to TACE (fig. 11).

Good Responders to TACE

The meeting also revealed that a subgroup of patients with intermediate-stage HCCs who would benefit from TACE comprises individuals with 4–7 nodules of 3–4 cm

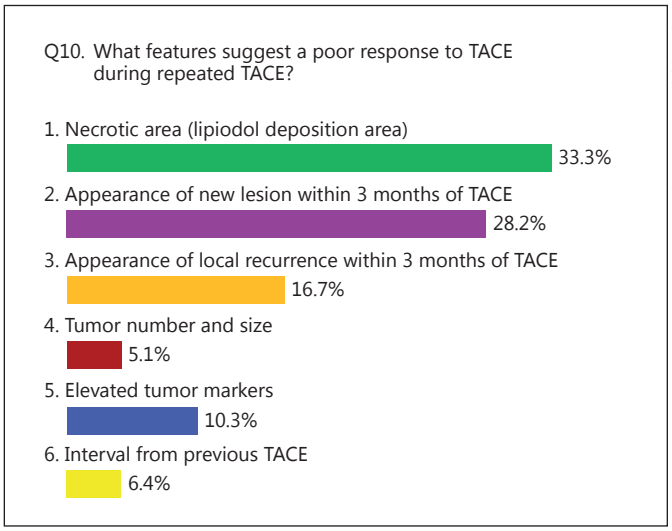

Fig. 13. Question and answers on factors related to a poor response to TACE.

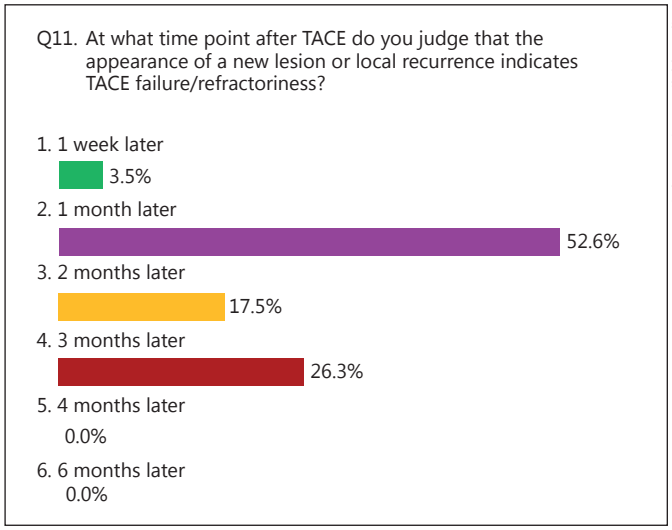

Fig. 14. Question and answers on the timing for evaluating TACE failure/refractoriness.

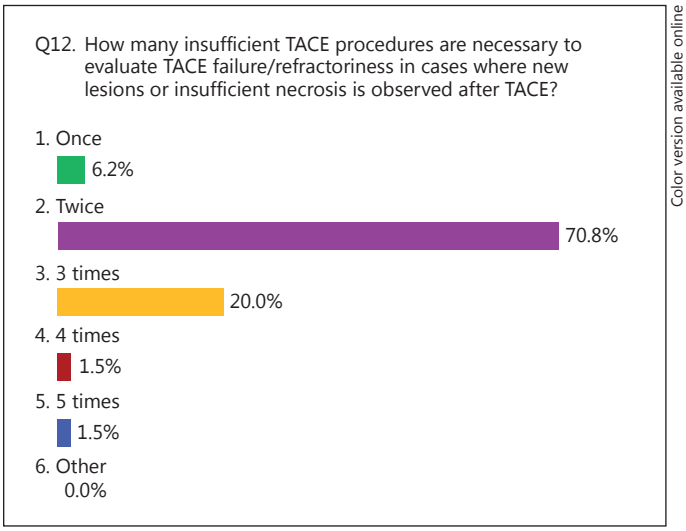

Fig. 15. Question and answers on the number of consecutive TACE procedures to evaluate TACE failure/refractoriness.

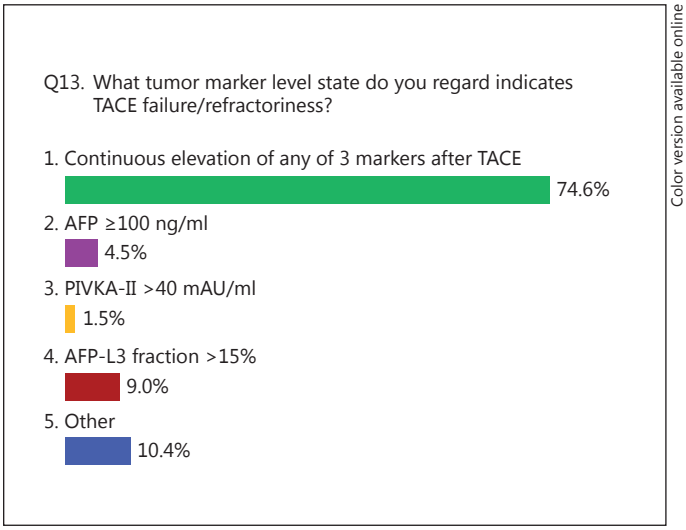

Fig. 16. Question and answers on the tumor marker levels related to TACE failure/refractoriness.

in size (fig. 12). When TACE has a high treatment efficacy and keeps the decline in residual liver function to a minimum, it is beneficial to HCC patients in this subgroup and makes long-term survival possible (fig. 1). Subsequently, even if HCC is still in the intermediate stage, it is extremely important to find out the time point of TACE failure as early as possible and switch the treatment strategy from that point on (fig. 2).

JSH TACE Failure/Refractoriness Criteria Updated by the LCSGJ in 2014

At the time of the consensus voting on TACE failure/refractoriness, when asked about the specific features of HCC cases that indicate a poor response to TACE even when repeated, 33% of experts answered insufficient necrosis (rate of lipiodol deposition), 28% answered the appearance of a new lesion within 3 months of TACE, and

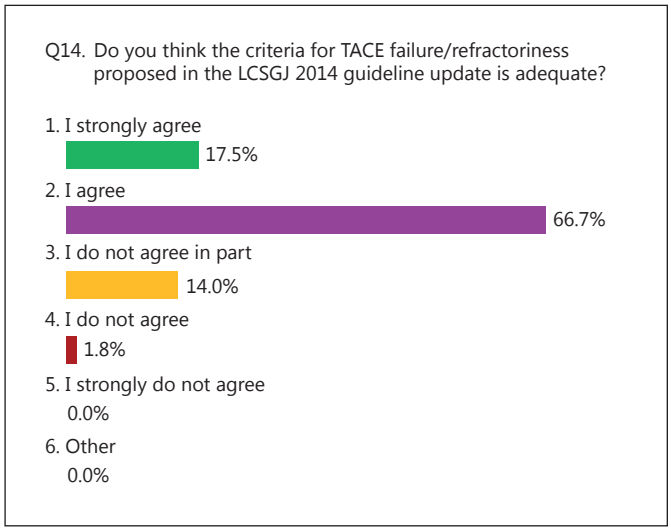

Fig. 17. The most important question asked, regarding whether the criteria for TACE failure/refractoriness updated in 2014 by the LCSGJ are adequate or not.

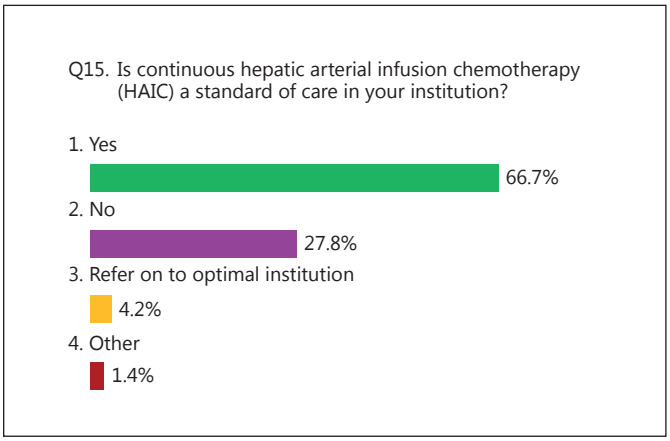

Fig. 18. Question and answers on continuous HAIC.

Table 1. Definition of TACE failure/refractoriness (LCSGJ)

(1)	Intrahepatic lesion	
	i	Two or more consecutive insufficient responses of the treated tumor (viable lesion >50%) even after changing the chemotherapeutic agents and/or reanalysis of the feeding artery seen on response evaluation CT/MRI at 1–3 months after having adequately performed selective TACE
	ii	Two or more consecutive progressions in the liver (tumor number increases as compared to tumor number before the previous TACE procedure) even after having changed the chemotherapeutic agents and/or reanalysis of the feeding artery seen on response evaluation CT/MRI at 1–3 months after having adequately performed selective TACE
(2)	Continuous elevation of tumor markers immediately after TACE even though slight transient decrease is observed	
(3)	Appearance of vascular invasion	
(4)	Appearance of extrahepatic spread	

17% answered local recurrence within 3 months of TACE (fig. 13). Furthermore, the largest proportion of experts (53%) answered '1 month' to the question on the interval between the previous TACE procedure and the appearance of a new lesion or local recurrence that indicates TACE failure/refractoriness (fig. 14). To the question asking at what point they consider TACE to be ineffective for HCC when observing the appearance of new lesions or no necrosis after TACE, 71% answered they would think it is ineffective when a similar treatment outcome occurs twice (fig. 15). About 75% of experts consider TACE failure/refractoriness to be the case when the level of any of 3 tumor markers continues to increase after TACE, even if they show a slight short-term decrease (fig. 16). Based on the answers to these questions, the definition of TACE failure/refractoriness after treatment was revised.

Table 1 shows the JSH criteria for TACE failure/refractoriness updated at the 50th LCSGJ Congress in 2014. Since 84% of experts agreed that the updated criteria are appropriate, they are now recommended for the assessment of TACE failure/refractoriness (fig. 17).

Treatment Options after TACE Failure/Refractoriness

Before the session on treatment options after TACE failure/refractoriness, 67% of experts reported that continuous hepatic arterial infusion chemotherapy (HAIC)

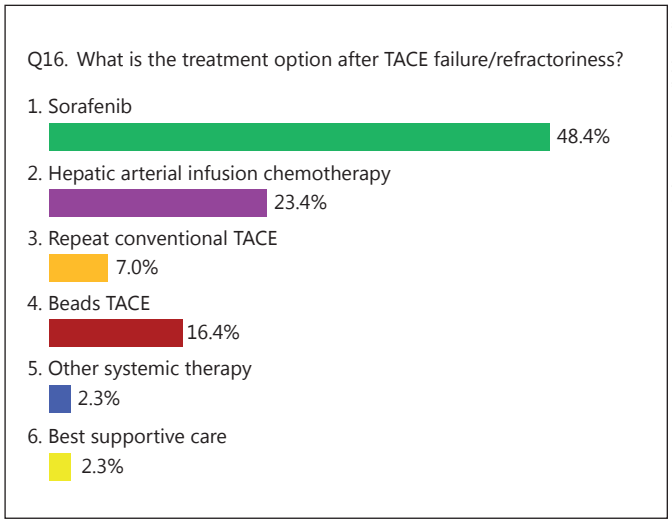

Fig. 19. Question and answers on the general treatment strategy after TACE failure/refractoriness.

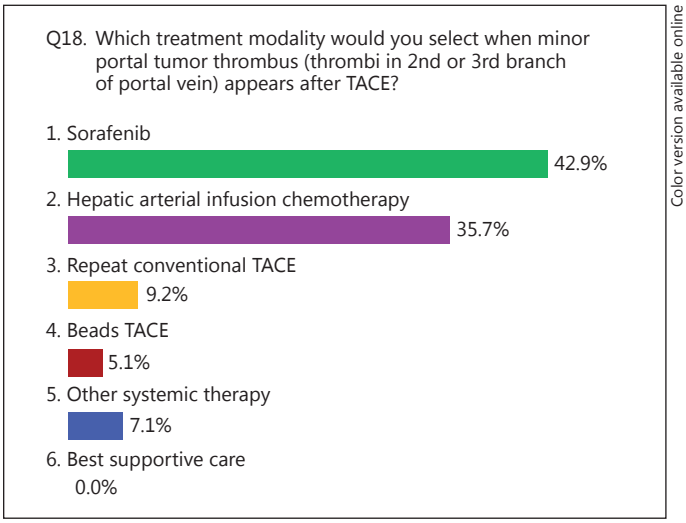

Fig. 21. Question and answers on the treatment strategy after TACE failure/refractoriness in patients with minor portal tumor thrombus.

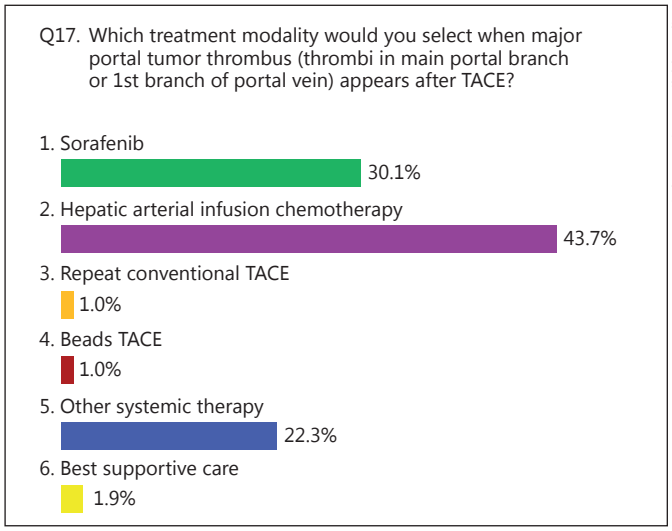

Fig. 20. Question and answers on the treatment strategy after TACE failure/refractoriness in patients with major portal tumor thrombus.

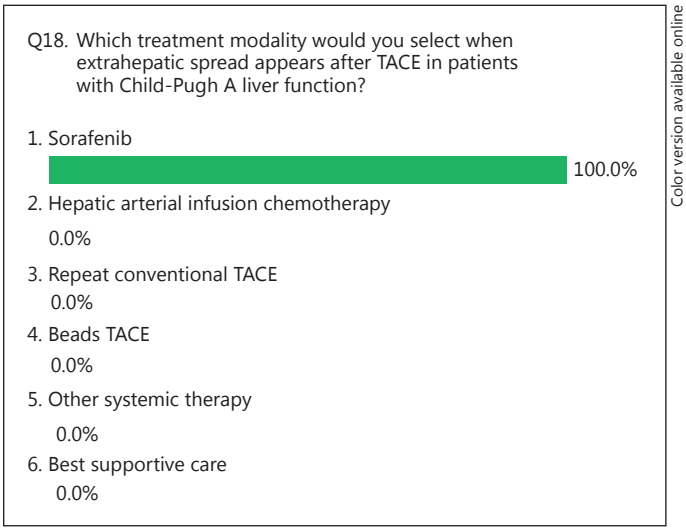

Fig. 22. Question and answers on the treatment strategy after TACE failure/refractoriness in patients with extrahepatic spread.

[13] is the routinely performed treatment modality at their institution, indicating its widespread use in Japan (fig. 18). When asked what their treatment of choice is in TACE failure/refractoriness cases (Q16), 48% of experts answered sorafenib and 23% answered HAIC (fig. 19). However, when asked what their treatment of choice is in cases of major portal vein thrombus after TACE (Q17), 30% answered sorafenib and 44% answered HAIC (fig. 20). On the contrary, for TACE failure/refractoriness cases with minor portal vein thrombus and Child-Pugh A liver function, 43 and 36% of experts stated that sorafenib and HAIC, respectively, was their treatment of choice (fig. 21). The difference in the answers to Q16 and Q17 reflects the potential risk that sorafenib administration can lead to liver failure in HCC cases with major portal vein thrombus. In contrast, HAIC is indicated even in cases of major portal tumor thrombus. Lastly, 100% of experts answered that sorafenib is their treat-

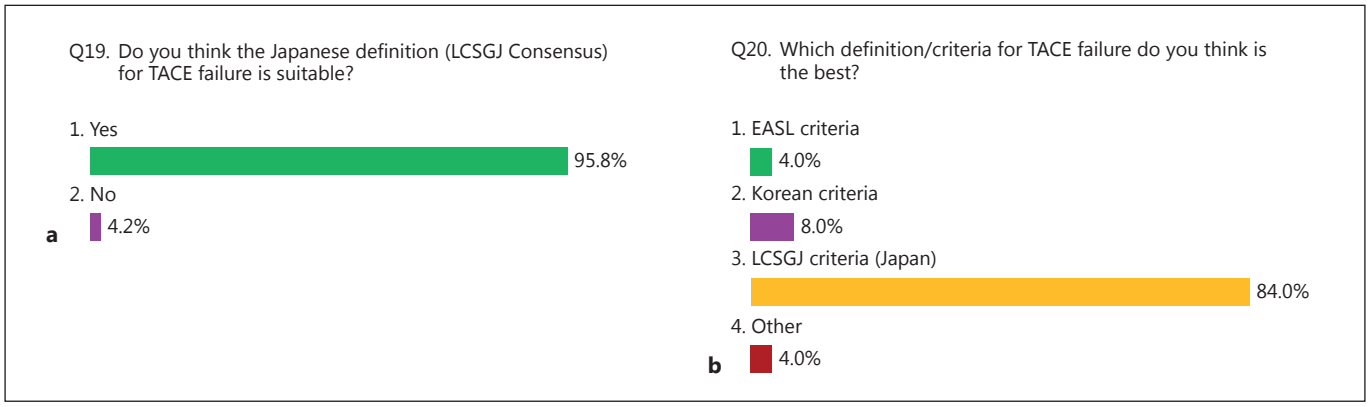

Fig. 23. Question and answers at the 4th IKLS on the suitability of the updated TACE failure/refractoriness criteria agreed upon at the LCSGJ consensus meeting (**a**) and on which definitions/criteria for TACE failure/refractoriness are the best (**b**). Of the experts present, 60% were from Japan, 20% from other Asian countries, and 20% from Europe and the USA.

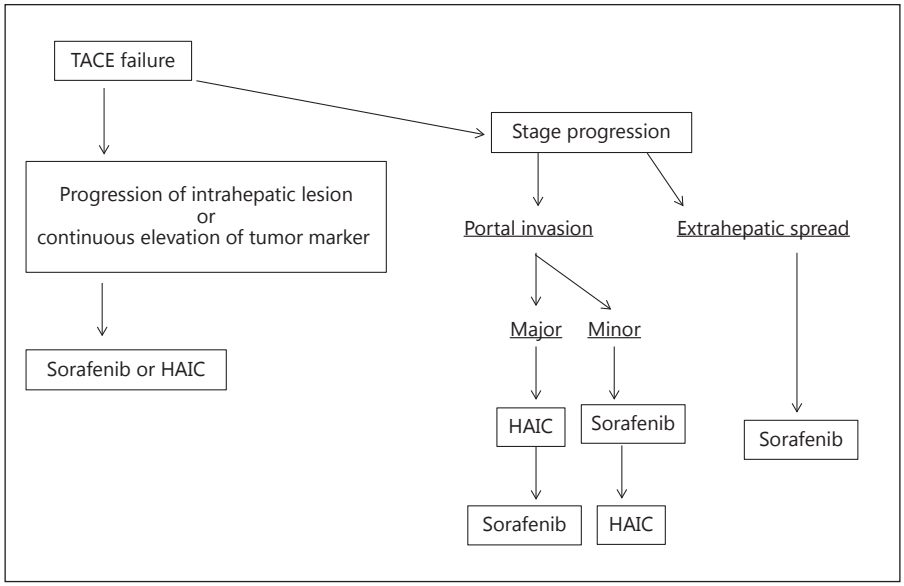

Fig. 24. Treatment strategy after TACE failure/refractoriness.

ment of choice for extrahepatic spread developed after TACE in HCC patients with Child-Pugh A liver function (fig. 22).

Also, at the 4th IKLS, 96% of HCC experts (60% from Japan, 20% from other Asian countries, and 20% from Europe or the USA) agreed that the criteria for TACE failure/refractoriness proposed at the 50th LCSGJ Congress were appropriate (table 1; fig. 23a). To the question on which definition/criteria for TACE failure/refractoriness the experts thought was the best, 84% answered the revised JSH criteria proposed by the LCSGJ (fig. 23b).

Conclusion

The definition of TACE failure in the JSH clinical practice guidelines has been updated based on agreement from 84% of HCC experts attending a consensus meeting held at the 50th LCSGJ Congress in 2014. The updated criteria also obtained 96% approval at the 4th IKLS.

To prolong the survival of HCC patients, it is important to switch treatment from TACE to, for example, sorafenib or HAIC as soon as the criteria for TACE failure/refractoriness are fulfilled, even if HCC is still in the intermediate stage. HAIC is the first treatment choice in

TACE failure/refractoriness cases with stage progression or major portal vein infiltration, whereas sorafenib is recommended in TACE failure/refractoriness cases with minor portal vein infiltration (fig. 24). Further studies are needed to determine the efficacy of microsphere TACE, such as drug-eluting beads TACE, in cases of TACE failure/refractoriness.

Consensus Statement (≥67% Agreement)

(1) Intermediate-stage HCC is a heterogeneous disease and therefore should be subgrouped (79%).

(2) There are 2 subgroups in the intermediate stage of HCC: good responders to TACE and poor responders to TACE (98%).

(3) Intrahepatic lesions not responding to TACE show insufficient necrosis (33%), the appearance of new lesions within 3 months (28%), or local recurrence within 3 months after TACE (17%) (total: 78%).

(4) Incomplete control of intrahepatic lesions within 1–3 months of TACE initiation should be included in the TACE failure criteria (96%).

(5) Timing of the judgment of TACE failure is after 1–3 months (96%).

(6) Two consecutive poor responses to TACE is an adequate criterion for TACE failure (71%).

(7) Continuous increase in any tumor marker should be included in the TACE failure criteria (75%).

(8) Continuous HAIC is widely performed in Japan (67%).

(9) When extrahepatic spread emerges during repeated TACE sessions, the treatment strategy should be changed to sorafenib (100%).

(10) The 2014 updated JSH criteria for TACE failure/refractoriness are adequate (84% at the 50th LCSGJ Congress and 96% at the 4th IKLS).

Informative Statement (≥50% Agreement)

(1) There are characteristic features of HCC that do not respond to TACE (64%).

(2) Yamakado et al.'s [12] criteria (HCC >4 cm and >7 nodules) are accepted as criteria for poor responders to TACE (51%).

Disclosure Statement

The authors declare that no financial or other conflicts of interest exist in relation to the content of this article.

References

1 Lencioni R: Chemoembolization in patients with hepatocellular carcinoma. Liver Cancer 2012;1:41–50.

2 Minami Y, Yagyu Y, Murakami T, et al: Tracking navigation imaging of transcatheter arterial chemoembolization for hepatocellular carcinoma using three-dimensional cone-beam CT angiography. Liver Cancer 2014;3:53–61.

3 Raoul JL, Gilabert M, Piana G: How to define transarterial chemoembolization failure or refractoriness: a European perspective. Liver Cancer 2014;3:119–124.

4 Kudo M, Izumi N, Kokudo N, et al: Management of hepatocellular carcinoma in Japan: Consensus-Based Clinical Practice Guidelines proposed by the Japan Society of Hepatology (JSH) 2010 updated version. Dig Dis 2011;29:339–364.

5 Park JW, Amarapurkar D, Chao Y, et al: Consensus recommendations and review by an International Expert Panel on Interventions in Hepatocellular Carcinoma (EPOIHCC). Liver Int 2013;33:327–337.

6 Sieghart W, Hucke F, Pinter M, et al: The ART of decision making: retreatment with transarterial chemoembolization in patients with hepatocellular carcinoma. Hepatology 2013;57:2261–2273.

7 Kudo M, Arizumi T, Ueshima K: Assessment for retreatment (ART) score for repeated transarterial chemoembolization in patients with hepatocellular carcinoma. Hepatology 2014;59:2424–2425.

8 Kadalayil L, Benini R, Pallan L, et al: A simple prognostic scoring system for patients receiving transarterial embolisation for hepatocellular cancer. Ann Oncol 2013;24:2565–2570.

9 Kudo M: Japan's successful model of nationwide hepatocellular carcinoma surveillance highlighting the urgent need for global surveillance. Liver Cancer 2012;1:141–143.

10 Kim DY, Han KH: Epidemiology and surveillance of hepatocellular carcinoma. Liver Cancer 2012;1:2–14.

11 Kudo M, Matsui O, Izumi N, et al: JSH consensus-based clinical practice guideline for the management of hepatocellular carcinoma: 2014 update by the Liver Cancer Study Group of Japan. Liver Cancer 2014;3:458–468.

12 Yamakado K, Miyayama S, Hirota S, et al: Subgrouping of intermediate-stage (BCLC stage B) hepatocellular carcinoma based on tumor number and size and Child-Pugh grade correlated with prognosis after transarterial chemoembolization. Jpn J Radiol 2014;32:260–265.

13 Kudo M: Treatment of advanced hepatocellular carcinoma with emphasis on hepatic arterial infusion chemotherapy and molecular targeted therapy. Liver Cancer 2012;1:62–70.

Clinical Study

Oncology

Oncology 2014;87(suppl 1):32–36
DOI: 10.1159/000368143

Published online: November 22, 2014

Validation of the Criteria of Transcatheter Arterial Chemoembolization Failure or Refractoriness in Patients with Advanced Hepatocellular Carcinoma Proposed by the LCSGJ

Tadaaki Arizumi Kazuomi Ueshima Hirokazu Chishina Masashi Kono Masahiro Takita Satoshi Kitai Tatsuo Inoue Norihisa Yada Satoru Hagiwara Yasunori Minami Toshiharu Sakurai Naoshi Nishida Masatoshi Kudo

Department of Gastroenterology and Hepatology, Kinki University School of Medicine, Osaka-Sayama, Japan

Key Words
Hepatocellular carcinoma · Transcatheter arterial chemoembolization failure · Sorafenib

Abstract

Background: Transcatheter arterial chemoembolization (TACE) failure or refractoriness is an indication for sorafenib therapy in patients with advanced hepatocellular carcinoma. The study evaluated the validity of the definition of TACE failure or refractoriness as proposed by the Liver Cancer Study Group of Japan (LCSGJ) through a retrospective analysis of sorafenib treatment. ***Methods:*** Out of 265 patients with advanced hepatocellular carcinoma who were treated with sorafenib at our hospital, 45 experienced TACE failure or refractoriness and were included in this study and retrospectively analyzed. ***Results:*** Multivariate analysis only identified the number of ineffective TACE procedures performed before starting sorafenib treatment as significant factors. Overall survival (OS) after starting sorafenib was statistically longer in patients treated with ≤2 consecutive ineffective TACE procedures before sorafenib administration than in patients treated with ≥3 consecutive ineffective TACE procedures ($p < 0.005$). This result matched the LCSGJ criteria. ***Conclusion:*** In patients treated with sorafenib, OS was extended with ≤2 consecutive ineffective TACE procedures compared to that with ≥3 consecutive ineffective TACE procedures. Thus, if tumors are uncontrolled, TACE should not be repeated. The result of this study supports the definition of TACE failure or refractoriness proposed by the LCSGJ.

Introduction

Hepatocellular carcinoma (HCC) is a leading cause of cancer-related deaths worldwide [1–4]. In Japan, HCC is currently the third leading cause of cancer-related deaths among both male and female patients, with a mortality rate of >33,000 patients per year [5]. HCC may develop at multiple sites on the liver and can give rise to numerous tumors with the potential to spread throughout the organ. Transcatheter arterial chemoembolization (TACE) is currently the standard of care for patients with multinodular HCC. TACE results in relatively preserved liver function without the risk of vascular invasion or extrahepatic spread [6–12]. Sorafenib, a molecular targeting agent, is presently the first-line agent for the treatment of unresectable HCC worldwide [13, 14]. Indications for the use of sorafenib in Japan include HCC with extrahepatic spread, vascular invasion, and TACE failure or refractoriness [15]. Accepted criteria for the classification of TACE failure or refractoriness are contentious in the field of hepatology. The Japan Society of Hepatology (JSH) and the Liver Cancer Study

KARGER

E-Mail karger@karger.com
www.karger.com/ocl

0030–2414/14/0877–0032$39.50/0

Prof. Masatoshi Kudo
Department of Gastroenterology and Hepatology
Kinki University School of Medicine
377-2 Ohno-Higashi, Osaka-Sayama, Osaka 589-8511 (Japan)
E-Mail m-kudo@med.kindai.ac.jp

Group of Japan (LCSGJ) have thus proposed a clear definition of TACE failure or refractoriness as described below.

The first criterion applies to intrahepatic lesions, where TACE failure is defined as ≥2 consecutive ineffective responses of treated tumors (viable lesions >50%) or ≥2 consecutive progressive increases in total tumor counts, despite a prior change in the choice of chemotherapeutic agent or reanalysis of the feeding artery. Ineffective responses are evaluated by computed tomography (CT)/magnetic resonance (MR) imaging 1–3 months after an adequately performed selective TACE procedure. Further criteria for the classification of TACE failure include the continuous elevation of tumor marker levels immediately after TACE (although a transient minor decrease may be observed) and the appearance of vascular invasion and extrahepatic spread [9, 16]. In other countries, ineffective TACE is considered a progressive disease based on the results of both the first and second TACE procedures. When the response is shown to be ineffective after 2 consecutive TACE procedures, sorafenib therapy is recommended [17, 18]. International opinions are divided as to whether the number of consecutive TACE failures should be defined as n = 2. In this study, we present a retrospective case analysis of sorafenib treatment outcomes and further examine the currently accepted definitions of TACE failure or refraction.

Materials and Methods

Patients

Between May 2009 and December 2012, 265 patients with advanced HCC were treated with sorafenib therapy at Kinki University Hospital, Osakasayama, Japan. Of these, 45 patients were treated with sorafenib monotherapy following the failure or refractoriness of TACE. This study did not require institutional approval or informed consent for the retrospective review of patient records or images. The research content was posted in our outpatient department and on our institution's website, and patients were given the right to refuse to participate in the study.

The study's inclusion criteria comprised the following: diagnosis of HCC based on histological results or radiological findings indicating early enhancement in conjunction with late wash-out with dynamic CT or dynamic MR imaging, a performance status of 0 or 1, a Child-Pugh score of 5–7 points indicating liver cirrhosis, and TACE failure or refractoriness where curability of intrahepatic lesions with locoregional therapy was not feasible. The exclusion criteria were defined as concomitant antineoplastic treatment as well as any other therapies undertaken during the period extending from the final TACE procedure up to the introduction of sorafenib.

Assessments

Contrast-enhanced CT (CECT) scans were obtained 4–8 weeks following the TACE procedure. If the tumor was well enhanced without lipiodol deposition, an additional TACE procedure was performed. If sufficient lipiodol deposition was observed with no evidence of tumor enhancement, CECT imaging was performed at the follow-up examination at intervals of approximately 8–12 weeks. TACE was performed as needed in the case of lipiodol wash-out or when new lesions appeared on the liver. If a patient exhibited a poor response to a previous TACE procedure, the subsequent procedure was performed within a 3-month period. In this study, ineffective TACE was defined as an interval of <3 months before the next procedure was performed.

Statistical Analysis

Univariate analysis was used to identify predictors of survival using the Kaplan-Meier method, and comparisons were performed using the log-rank test. Multivariate analysis was investigated using the Cox proportional hazard model. A p value of <0.05

Table 1. Characteristics of HCC patients treated with sorafenib

	Cases, n
Age	
Median (25–75%)	75 (68.5–78.5)*
Gender	
Male	38 (84.4)
Female	7 (15.6)
ECOG performance status	
0	45 (100)
1	0 (0)
Child-Pugh class	
A	37 (82.2)
B	8 (17.8)
Virus status†	
HBV	4 (8.9)
HCV	33 (73.3)
Both negative	8 (17.8)
Barcelona Clinic for Liver Cancer stage	
A	7 (15.6)
B	38 (84.4)
Starting dose of sorafenib, mg	
200	8 (17.8)
400	16 (35.5)
800	21 (46.7)
Serum AST level, ng/ml	
Median (25–75%)	57 (40–74.8)*
Serum ALT level, mAU/ml	
Median (25–75%)	39.5 (27.5–63.8)*
Serum AFP level, ng/ml	
Median (25–75%)	206.5 (17.5–1,738.8)*
Serum DCP level, mAU/ml	
Median (25–75%)	820 (51–4,840)*

Values in parentheses are percentages unless otherwise indicated. ECOG = Eastern Cooperative Oncology Group; AFP = alpha fetoprotein. * Dispersion variables are shown as median values (25–75%). † Cases positive for HBs-Ag were regarded as HBV-related HCC cases and cases positive for HCV Ab were regarded as HCV-related HCC cases.

Oncology 2014;87(suppl 1):32–36
DOI: 10.1159/000368143

Table 2. Univariate and multivariate analyses of the relationships between patient characteristics at the initiation of sorafenib therapy and OS after starting sorafenib therapy (n = 45)

	OS, months		p value[a]	Multivariate analysis		
	median	95% CI		HR	95% CI	p value
Gender						
Male (n = 38)	15.6	1.9–29.3				
Female (n = 7)	–	–	0.19			
Body mass index						
<25 (n = 34)	15.6	3.6–27.6				
≥25 (n = 11)	–	–	0.26			
Age, years						
<75 (n = 20)	15.6	–				
≥75 (n = 25)	21.6	6.4–36.8	0.74			
Child-Pugh stage						
A (n = 37)	21.6	–				
B (n = 8)	–	–	0.79			
Etiology						
HCV (n = 33)	21.6	–				
Others (n = 12)	20.8	–	0.65			
Barcelona Clinic for Liver Cancer stage						
A (n = 7)	21.6	0–43.4				
B (n = 38)	20.8	–	0.56			
AST, ng/ml						
<40 (n = 11)	–	–				
≥40 (n = 34)	11.4	3.8–18.9	0.027	4.6	0.87–24.53	0.072
ALT, mAU/ml						
<40 (n = 23)	–	–				
≥40 (n = 22)	9.6	6.2–13.1	0.036	2.2	0.49–10.08	0.30
AFP, ng/ml						
<400 (n = 27)	21.6	–				
≥400 (n = 18)	15.6	4.4–26.8	0.52			
DCP, mAU/ml						
<1,000 (n = 23)	–	–				
≥1,000 (n = 22)	9.6	4.1–15.2	0.041	1.6	0.48–5.67	0.43
Ineffective TACE procedures, n						
≤2 (n = 33)	–	–				
≥3 (n = 12)	8.0	5.7–10.4	0.005	4.4	1.11–17.37	0.035
Sorafenib starting dose, mg						
≤400 (n = 25)	–	–				
800 (n = 20)	15.6	4.6–26.6	0.33			

AFP = Alpha fetoprotein. [a] The p value was calculated with the log-rank test.

was considered statistically significant. All analyses were performed using the software package SPSS version 19.0 for Windows (IBM, New York, N.Y., USA).

Results

Baseline Characteristics

Patient characteristics are summarized and presented in table 1. Thirty-three patients (73.3%) tested positive for the anti-hepatitis C virus antibody (HCV Ab), 4 patients (8.9%) tested positive for the hepatitis B virus (HBV) surface antigen (HBs-Ag), and 8 patients (17.8%) tested negative for both HCV Ab and HBs-Ag. All patients were asymptomatic with a performance status of 0, and 38 patients (84.4%) were classified as Barcelona Clinic for Liver Cancer Stage B with TACE failure. Thirty-seven patients (82.2%) were classified as Child-Pugh class A.

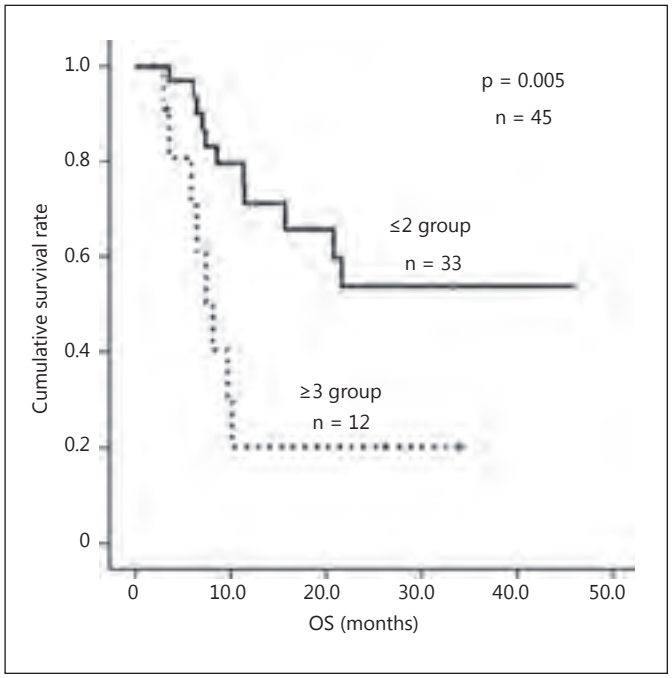

Fig. 1. Kaplan-Meier curves of OS in 45 patients treated with sorafenib classified by the number of ineffective TACE procedures performed. The median OS of the patients treated with ≥3 ineffective TACE procedures was 8.0 months (95% CI, 5.7–10.4; p = 0.005). The median OS of the patients treated with ≤2 ineffective TACE procedures was not calculated.

Overall Survival and Radiological Evaluation

In all patients, the median overall survival (OS) after starting sorafenib treatment was 20.7 months. The results of sorafenib therapy were as follows: 2 patients showed a clinically complete response, 5 patients showed a partial response, stable disease was observed in 7 patients, and progressive disease was observed in 12. Nine patients were not evaluated. Hypertension grade ≥3 was observed in 3 patients, and hand-foot skin reactions grade ≥3 in 4 patients. After the diagnosis of progressive disease, the 12 applicable patients underwent a subsequent TACE procedure, and 4 of them received hepatic arterial infusion chemotherapy. Eighteen patients were given best supportive care, and the remaining patients were on sorafenib therapy at the time of study completion.

Prognostic Factors

Baseline patient characteristics were analyzed in order to identify the factors influencing OS after treatment with sorafenib. Univariate analysis showed statistically significant differences in OS for the following variables: number of ineffective TACE (p = 0.005) and serum total bilirubin (p = 0.017), aspartate aminotransferase (AST; p = 0.027), alanine aminotransferase (ALT; p = 0.036), and des-gamma carboxyprothrombin (DCP; p = 0.041) at the initiation of sorafenib therapy. The number of ineffective TACE procedures performed was shown to be the only significant and independent factor by multivariate analysis [odds ratio, 4.396; 95% confidence interval (CI), 1.112–17.374; p = 0.035; table 2; fig. 1].

Discussion

TACE is widely used for the conventional intermediate-stage treatment of HCC. However, this course of therapy can be limited in terms of effectiveness as the tumor becomes refractory to TACE. Until the approval of sorafenib, ineffective TACE procedures were frequently repeated. In 2008, the first global phase III study successfully demonstrated the effectiveness of sorafenib as a treatment for advanced-stage HCC, and its publication led to the first established treatment method for advanced-stage HCC [13, 14]. An indication of sorafenib is unresectable HCC with distant metastases, vascular invasion, or TACE failure or refractoriness. In particular, the appropriate classification of TACE failure or refractoriness is a controversial topic. In 2010, the JSH proposed a standard definition of TACE failure or refractoriness [9], and this was subsequently revised in 2014 [16]. One of the JSH definitions of TACE failure or refractoriness concerns intrahepatic lesions, where ≥2 consecutive ineffective responses of treated tumors (viable lesions >50%) may be evaluated by CT/MRI imaging 1–3 months following an adequately performed selective TACE procedure, despite a prior change in the choice of chemotherapeutic agents or reanalysis of the feeding artery.

Thus, it is implied that ineffective TACE should not be performed repeatedly, and the patient should immediately be switched to an alternative therapy. In the present study, OS was prolonged in the group of patients not treated with ≥2 repeated ineffective TACE procedures. The definition of TACE failure or refractoriness, as proposed by the JSH, is thus considered reasonable, and the results of our multivariate analysis indicated that the number of ineffective TACE procedures performed prior to the initiation of sorafenib therapy was the sole determinant of OS. Short-term and frequently repeated TACE is known to worsen hepatic function. Ineffective TACE has a harmful and negative

effect without the benefit of increased OS and should not be repeated.

In conclusion, the OS of patients treated with sorafenib induced by TACE failure or refractoriness without extrahepatic spread or vascular invasion was prolonged in patients who received ≤2 consecutive ineffective TACE procedures compared to patients who received ≥3 consecutive ineffective TACE procedures. Thus, in the case of uncontrolled tumors, TACE should not be repeated and alternative treatments such as sorafenib are recommended. The results of this study support the definition of TACE failure or refractoriness as proposed by the LC-SGJ [16].

Disclosure Statement

The authors declare that no financial or other conflicts of interest exist in relation to the content of this article.

References

1 Altekruse SF, McGlynn KA, Reichman ME: Hepatocellular carcinoma incidence, mortality, and survival trends in the United States from 1975 to 2005. J Clin Oncol 2009;27:1485–1491.

2 El-Serag HB: Hepatocellular carcinoma. N Engl J Med 2011;365:1118–1127.

3 Kim do Y, Han KH: Epidemiology and surveillance of hepatocellular carcinoma. Liver Cancer 2012;1:2–14.

4 Parkin DM, Bray F, Ferlay J, Pisani P: Estimating the world cancer burden: Globocan 2000. I J Cancer 2001;94:153–156.

5 Moore MA, Sobue T: Cancer research and control activities in Japan: contributions to international efforts. Asian Pac J Cancer Prev 2009;10:183–200.

6 Bruix J, Sala M, Llovet JM: Chemoembolization for hepatocellular carcinoma. Gastroenterology 2004;127:S179–S188.

7 Bruix J, Sherman M; American Association for the Study of Liver Diseases: Management of hepatocellular carcinoma: an update. Hepatology 2011;53:1020–1022.

8 Llovet JM, Ducreux M, et al: EASL-EORTC clinical practice guidelines: management of hepatocellular carcinoma. J Hepatol 2012;56:908–943.

9 Kudo M, Izumi N, Kokudo N, Matsui O, Sakamoto M, Nakashima O, Kojiro M, Makuuchi M: Management of hepatocellular carcinoma in Japan: Consensus-Based Clinical Practice Guidelines proposed by the Japan Society of Hepatology (JSH) 2010 updated version. Dig Dis 2011;29:339–364.

10 Lencioni R: Chemoembolization for hepatocellular carcinoma. Semin Oncol 2012;39:503–509.

11 Lencioni R: Chemoembolization in patients with hepatocellular carcinoma. Liver Cancer 2012;1:41–50.

12 Lin S, Hoffmann K, Schemmer P: Treatment of hepatocellular carcinoma: a systematic review. Liver Cancer 2012;1:144–158.

13 Llovet JM, Ricci S, Mazzaferro V, Hilgard P, Gane E, Blanc JF, de Oliveira AC, Santoro A, Raoul JL, Forner A, Schwartz M, Porta C, Zeuzem S, Bolondi L, Greten TF, Galle PR, Seitz JF, Borbath I, Haussinger D, Giannaris T, Shan M, Moscovici M, Voliotis D, Bruix J: Sorafenib in advanced hepatocellular carcinoma. N Engl J Med 2008;359:378–390.

14 Cheng AL, Kang YK, Chen Z, Tsao CJ, Qin S, Kim JS, Luo R, Feng J, Ye S, Yang TS, Xu J, Sun Y, Liang H, Liu J, Wang J, Tak WY, Pan H, Burock K, Zou J, Voliotis D, Guan Z: Efficacy and safety of sorafenib in patients in the Asia-Pacific region with advanced hepatocellular carcinoma: a phase III randomised, double-blind, placebo-controlled trial. Lancet Oncol 2009;10:25–34.

15 Kudo M: Treatment of advanced hepatocellular carcinoma with emphasis on hepatic arterial infusion chemotherapy and molecular targeted therapy. Liver Cancer 2012;1:62–70.

16 Kudo M, Matsui O, Izumi N, Iijima H, Kadoya M, Imai Y, Okusaka T, Miyayama S, Tsuchiya K, Ueshima K, Hiraoka A, Ikeda M, Ogasawara S, Yamashita T, Minami T, Yamakado K; Liver Cancer Study Group of Japan: JSH consensus-based clinical practice guideline for the management of hepatocellular carcinoma: 2014 update by the Liver Cancer Study Group of Japan. Liver Cancer 2014;3:458–468.

17 Raoul JL, Sangro B, Forner A, Mazzaferro V, Piscaglia F, Bolondi L, Lencioni R: Evolving strategies for the management of intermediate-stage hepatocellular carcinoma: available evidence and expert opinion on the use of transarterial chemoembolization. Cancer Treat Rev 2011;37:212–220.

18 Raoul JL, Gilabert M, Piana G: How to define transarterial chemoembolization failure or refractoriness: a European perspective. Liver Cancer 2014;3:119–124.

Review

Oncology

Oncology 2014;87(suppl 1):37–49
DOI: 10.1159/000368144

Published online: November 22, 2014

Pathological Diagnosis of Benign Hepatocellular Nodular Lesions Based on the New World Health Organization Classification

Fukuo Kondo[a, b] Toshio Fukusato[b] Masatoshi Kudo[c]

Departments of Pathology at [a]Teikyo University Hospital and [b]Teikyo University School of Medicine, Tokyo, and [c]Department of Gastroenterology and Hepatology, Kinki University School of Medicine, Osaka-Sayama, Japan

Key Words

Benign hepatocellular nodule · New World Health Organization classification · Hepatocellular adenoma · Focal nodular hyperplasia · Nodular regenerative hyperplasia

Abstract

There are various types of benign hepatocellular nodular lesions, and their diagnostic criteria were formulated in detail. However, in 2010, the new World Health Organization (WHO) classification introduced immunohistochemical diagnostic criteria for hepatocellular adenoma (HCA) reflecting molecular pathological properties, and HCA was classified into 4 subtypes. These criteria were useful for its differential diagnosis from focal nodular hyperplasia (FNH). They were also useful for the diagnosis of HCA, its subtyping, and differentiation from FNH in Japan. However, the new WHO classification is based on principles that differ from those of conventional definitions of disease concepts and methods for the differential diagnosis. Therefore, it has caused disagreements in the diagnosis in some cases. Based on this background, we present a new perspective on the diagnosis of benign hepatocellular nodular lesions.

Introduction

There are various types of benign hepatocellular nodular lesions, and their diagnostic criteria were formulated in detail. However, in 2010, the new World Health Organization (WHO) classification introduced immunohistochemical diagnostic criteria for hepatocellular adenoma (HCA) reflecting molecular pathological properties, and HCA was classified into 4 subtypes. These criteria were truly useful for the diagnosis of HCA and its subtyping. They were also useful for the differentiation from focal nodular hyperplasia (FNH) in Japan. The introduction of this new diagnostic procedure is a great progress. However, the new WHO classification is based on principles that differ from those of conventional definitions. We sometimes encounter difficult cases that can be diagnosed as HCA or FNH depending on the different definitions. In order to solve this problem, we present a new perspective on the diagnosis of benign hepatocellular nodular lesions.

This article is a revision of a paper published in the Kanzo (in Japanese) 2013;54 807–818.

KARGER

E-Mail karger@karger.com
www.karger.com/ocl

0030–2414/14/0877–0037$39.50/0

Dr. Fukuo Kondo
Department of Pathology
Teikyo University Hospital
2-11-1, Kaga Itabashi-ku, Tokyo 173-8606 (Japan)
E-Mail fkondo55@med.teikyo-u.ac.jp

Table 1. Classification of various benign hepatocellular nodular lesions (cited from [13] with modification)

	HCA	FNH	NRH	PNT	IPH	LRN
Concept	Benign hepato-cellular neoplasm	Hyperplastic nodule with central scar	Regenerative/ hyperplastic nodules are formed diffusely in the liver. No fibrous septa are observed.	Hyperplastic nodules of the hilar region often accompanied by portal hypertension.	Noncirrhotic portal hypertension fulfilling detailed diagnostic criteria for IPH.	Varies in the definition. A large regenerative nodule observed in cirrhotic liver by the Japanese General Rules for Clinical and Pathological Studies of Liver Cancer. Noncirrhotic nodules are also included in the International Working Party Classification.
Sites of nodules	Anywhere in the liver	Anywhere in the liver, but frequently in the periphery	Diffusely present over the whole liver	Hilar region	Conceptually, a diffuse disease, but there are reports of nodule formation.	Anywhere in the liver
Number and size of nodules	Single/(multiple) A few centimeters	Single/(multiple) A few centimeters	Multiple Many are ≤1.5 cm	Single/(multiple) A few centimeters (occasionally occupies 2/3 of the liver)		Single/(multiple) From several millimeters to a few centimeters
Coexistence with portal hypertension	Rare	Infrequent	Frequent	Frequent	Always	Varies with definition
Coexistence with cirrhosis	None	None	None	None	None	Varies in the definition
Problems	– Not so often related to oral contraceptives in Japan as reported in Western countries. – Differentiation from FNH may pose a problem, particularly in patients showing central scar-like tissue. – A benign tumoral lesion but may be difficult to differentiate from hyperplasia.	– Although a hyperplastic lesion, it may be difficult to differentiate from HCA, a benign neoplastic lesion. – Extranodular areas are considered nearly normal, but there may be NRH-like or IPH-like lesions.	– There may be large coexisting nodules, which may be HCA- or FNH-like. – Areas without nodules resemble IPH.	– Considered to be an entity closely resembling IPH. The disease concept is questioned by some.	– Differentiation from NRH may pose a problem in patients showing marked nodule formation. – Some cases without clinical portal hypertension histologically resemble IPH.	– Definition differs between the Japanese General Rules and the IWP classification. – A large regenerative nodule in liver cirrhosis by the Japanese General Rules, but large regenerative nodules after extensive necrosis and FNH- or NRH-like regenerative nodules may also be included in the IWP classification.

Detailed disease concepts, definitions and methods for the differential diagnosis have been developed for various types of benign hepatocellular nodular lesions [1–16]. They have been applied effectively so far. Recently, however, the molecular pathological properties of HCA have been clarified, primarily by a French group, and immunohistochemical diagnostic methods reflecting these findings have been introduced [17–19]. They were truly excellent works. As a result, the 2010 WHO classification clearly described these diagnostic methods and disease types of HCA [20]. Thereafter, the diagnostic methods were also introduced to Japan. Attempts to diagnose benign hepatocellular nodular lesions and to discriminate them, particularly from FNH, have begun. However, the diagnoses based on these immunohistochemical criteria have not always agreed with those based on conventional diagnostic criteria for HCA or FNH. In addition, benign hepatocellular nodular lesions include not only HCA and FNH but also various other nodular lesions. Therefore, lesions that are difficult to diagnose definitively have increased, causing considerable difficulties in daily practice.

In this article, we describe conventional disease concepts and definitions of benign hepatocellular nodular lesions, diagnostic methods, and their changes. In addition, new diagnostic criteria are explained, and their new problems and measures to utilize them are discussed.

Conventional Classification and Diagnostic Criteria for Benign Hepatocellular Nodular Lesions

Benign hepatocellular nodular lesions have been classified in detail according to clinical data, state of the background liver, and gross and histological findings of the nodules (tables 1, 2; fig. 1) [1–16]. Among these lesions, HCA is a benign neoplastic lesion [1, 2], and the large regenerative nodule (LRN) is a large nodule observed in liver cirrhosis [10]. In the International Working Party (IWP) classification, various nontypical le-

Table 2. Differential diagnosis of HCA and FNH (cited from [15])

	FNH	HCA
Definition	Hyperplastic lesion caused by vascular malformation	Benign neoplastic lesion
Background liver	Normal	Normal
Gross characteristics	Central scar (+)	Central scar (–)
Histological characteristics	Anomalous blood vessels, anomalous portal tract	Portal tract (–)
Clinical characteristics	Associated with oral contraceptives (?)	Associations with oral contraceptives, anabolic steroid hormone, glycogen storage disease, etc.
	Malignant transformation (–), hemorrhage (–)	Malignant transformation (+), hemorrhage (+)

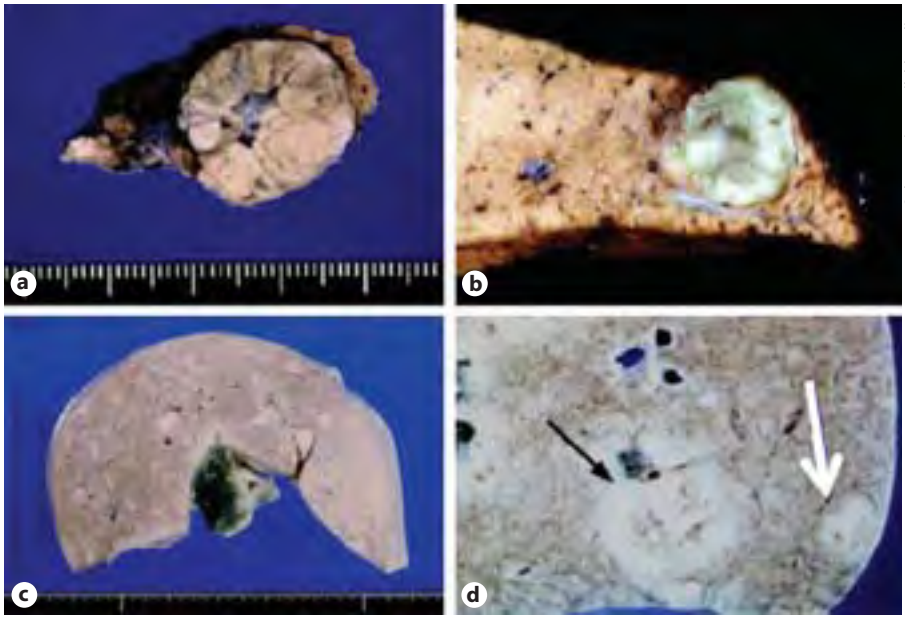

Color version available online

Fig. 1. Gross images of typical and nontypical benign hepatocellular nodular lesions (cited from [12, 13, 15] with modification). **a** FNH: a stellate central scar is clearly seen. **b** HCA: no central scar present. In both **a** and **b**, the background liver is normal. **c** NRH: while small nodules are distributed diffusely over the entire liver, no fibrous septa such as those in liver cirrhosis are noted. **d** A nontypical nodule is shown in this cross section of the liver shown in **c**. The background liver shows characteristics of NRH. The nodule indicated by the black arrow shows a clear central scar and closely resembles FNH. However, as the background liver is not normal, the lesion is not diagnosed as FNH according to the conventional definition. The nodule indicated by the white arrow cannot be definitively diagnosed because there is no central scar. Unlike FNH, the diameter is too large for NRH, and, while it resembles HCA, there is no history of the use of oral contraceptives.

sions of noncirrhotic benign hepatocellular nodules are also lumped together as LRN [10]. By the way, FNH [3, 4], nodular regenerative hyperplasia (NRH) [5, 6], partial nodular transformation (PNT) [7], and benign hepatocellular nodular lesions observed in idiopathic portal hypertension (IPH) [8, 9] are the lesions comprehensively called hepatocellular nodules caused by abnormal intrahepatic circulation. Presently, there are two concepts about FNH, NRH, PNT, and nodules in IPH. One is the conventional concept, namely, these are diseases caused by different etiological mechanisms: FNH is a hyperplastic lesion due to vascular malformation, NRH is characterized by small intrahepatic nodules formed by a compensatory regenerative mechanism induced primarily by secondary vascular disorders such as thrombosis and vasculitis, and IPH, the etiology of which remains unclear, is regarded as a lesion of a different entity [1–10]. According to the other concept, these lesions are different subtypes or variants of the same disease with transitional or intermediate types [11–13]. Their common cause is considered as vascular malformation [11–13].

The second concept was formulated to solve the various problems with the conventional concepts as shown in table 1. We encountered various difficult lesions when we used only the traditional concept. In the second concept, these lesions are considered analogous diseases forming the category of benign hepatocellular nodules caused by a common etiological mechanism, which is an anomaly of the components of the portal tract. Although the size and distribution of the nodular lesions are various, their interstitia, namely the portal tracts, show very similar features (fig. 2).

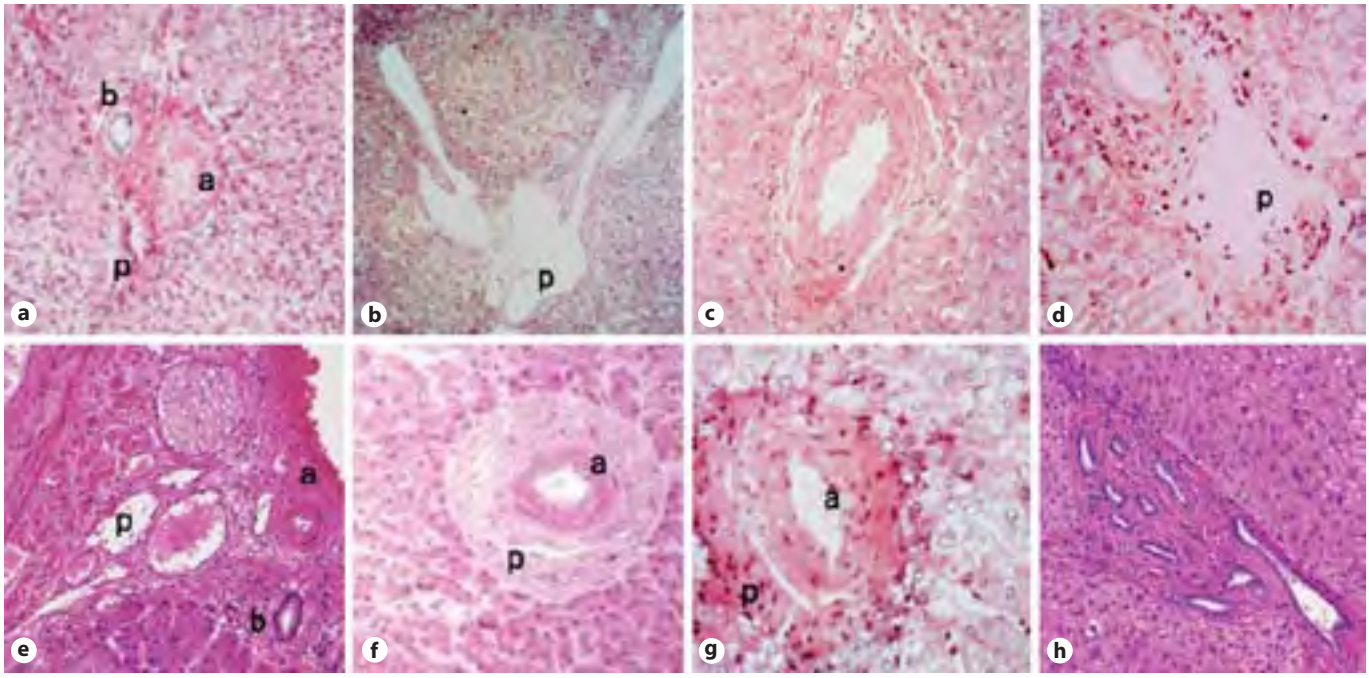

Color version available online

Fig. 2. Abnormalities of the portal tract observed in various nodular lesions and portal hypertension (cited from [13, 14]). **a**, **b** Intranodular area of FNH. In **a**, the artery (a) occupies an abnormally large proportion of the portal tract. The portal vein (p) is abnormally thin compared with the artery (a) or bile duct (b). In **b**, the portal vein (p) is abnormally dilated. **c**, **d** An extranodular area of FNH is shown. Abnormal findings such as an abnormally thick artery, portal vein (**c**), and a dilated portal vein (**d**) are noted outside as well as inside the nodule. In **e** a central scar in FNH is shown. This tissue is also considered to be an abnormal portal tract that has grown into giant dimensions due to malformation from the presence of the portal vein (p), artery (a), and bile duct (b). **f** NRH: a very thick artery (a) and a narrowed portal vein (p) are observed in the portal tract, and the presence of the bile duct is unclear. These findings are difficult to explain by thrombosis and suggest a congenital malformation. **g** IPH: a thick artery (a) that occupies a large portion of the portal tract and a narrowed portal vein (p) are observed, but the bile duct is unclear. The findings resemble those in the extranodular area of FNH (**c**) and NRH (**f**). **h** A congenital hepatic fibrosis is shown. The portal tract not only shows fibrosis but also contains a large number of bile ducts. The portal vein is narrowed, and this is considered the cause of portal hypertension. The presence of multiple bile ducts suggests malformation of this portal tract.

These lesions are called anomalous portal tract syndrome (fig. 3a) [12], and this concept is useful for the interpretation of various nontypical cases. It is also useful for the evaluation of their relationships with hemangiomas of the liver, portal hypertension, congenital hepatic fibrosis, and bile duct malformation (fig. 2, 3). Nontypical cases with hepatocellular hemangiomatous lesions can also be interpreted by this concept [21]. Although this concept alone may not be sufficient to explain the etiology of many lesions including IPH and NRH, it is recommended to consider this concept when we encounter various difficult cases [22]. Recently, the original concept (fig. 3a) has been revised (fig. 3b) owing to the development of the WHO classification. It is explained later in this study.

At any rate, benign hepatocellular nodular lesions were conventionally classified into benign neoplastic lesions, various nonneoplastic nodules associated with abnormal circulation, and regenerative nodules in liver cirrhosis (table 1).

Diagnosis of HCA Based on the New WHO Classification and Its Differentiation from FNH

Recently, however, the 2010 WHO Classification of the Tumours of the Digestive System has been published, and HCA was classified into 4 subtypes based on the genotype [20]: (1) hepatocyte nuclear factor 1α (HNF1α) inactivated type (H-HCA), (2) β-catenin activated type (b-

Oncology 2014;87(suppl 1):37–49
DOI: 10.1159/000368144

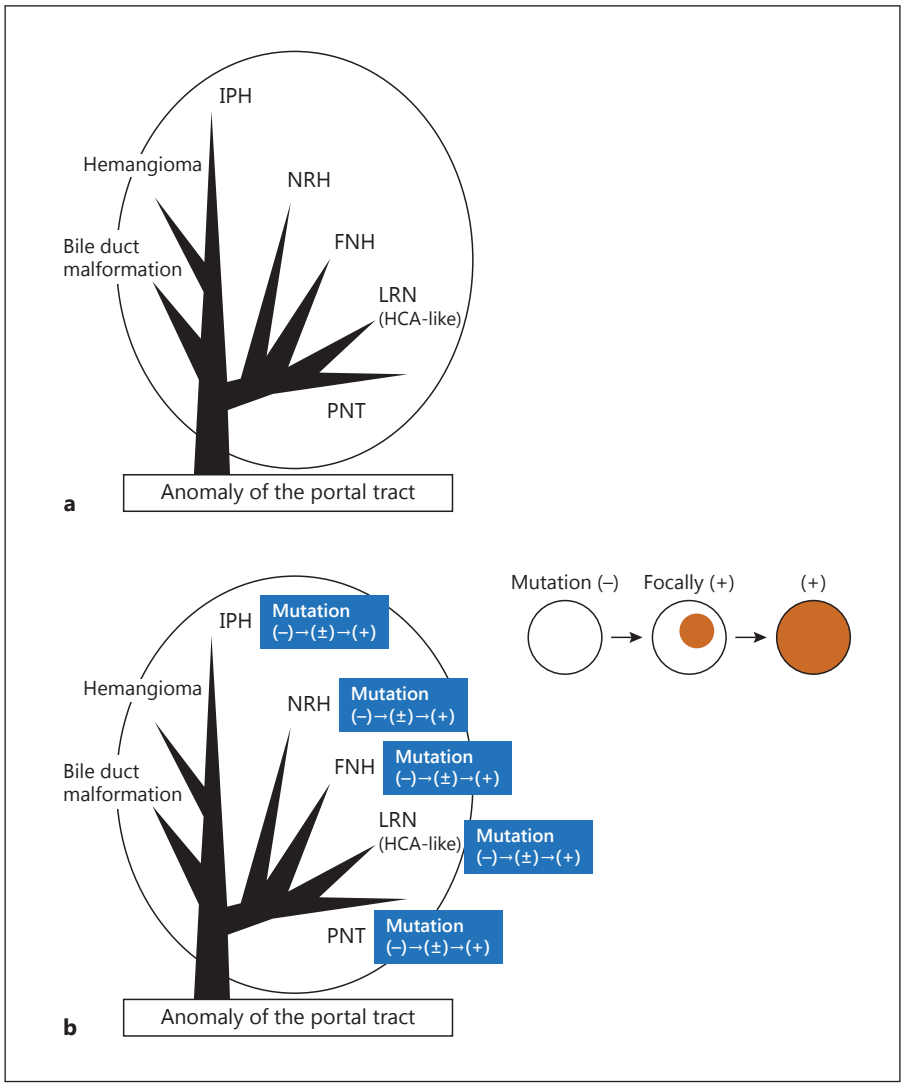

Color version available online

Fig. 3. Concept of anomalous portal tract syndrome (cited from [12, 13, 14] with modification). **a** The original concept is presented: various lesions are caused by congenital anomaly of the portal tract. Abnormal vasculature due to malformation causes various types of abnormal circulation, and in addition, it causes various types of hyperplastic hepatocellular nodular lesions. Hemangioma and various types of bile duct malformation sometimes coexist with these hepatocellular nodules because both blood vessels and bile ducts are components of the portal tract. **b** Revised concept after adjusting for the new WHO classification. The revised concept presumes the three stages in every lesion, i.e. nonmutated, focally mutated and entirely mutated stages.

HCA), (3) inflammatory HCA (I-HCA), and (4) the unclassifiable type (u-HCA). Points of differentiation from FNH were also specified (table 3, fig. 4). It is indeed a great advance in hepatology.

Concerning these 4 subtypes, the mutant gene, immunohistochemical findings reflecting the mutations, gender difference, histological characteristics, and characteristic clinical findings have been clarified: (1) H-HCA is characterized by inactivation of HNF1α, immunohistochemically, by a decrease in liver fatty acid-binding protein (L-FABP), a predominance in women, and, histologically, fatty degeneration (fig. 4a, b) and is suggested to be related to oral contraceptives. (2) b-HCA is characterized by activation of β-catenin, immunohistochemically, intranuclear accumulation of β-catenin or diffuse positivity for glutamine synthetase (GS), a predominance in women, and, histologically, cellular atypia and is associated with a high risk of carcinogenesis (however, nuclear atypia was rare in the Japanese cases reported) (fig. 4c–e). (3) I-HCA is characterized by mutations of genes such as gp130, STAT3, and GNAS, immunohistochemically, by positivity for serum amyloid A (SAA) and C-reactive protein, and, histologically, inflammatory cell infiltration, ductular reactions, and sinusoid dilation and is considered to be closely related to drinking and obesity (fig. 4f, g). (4) u-HCA lacks gene mutations or immunohistochemical findings, but is diagnosed as HCA from gross and histological findings. FNH shows no gene mutations or immunohistochemical characteristics described in (1) to (3), but is characterized immunohistochemically by a

Table 3. Characteristics of HCA subtypes and FNH (cited from [15])

	H-HCA	b-HCA	I-HCA	u-HCA	FNH
Gene mutations	HNF1α	β-catenin	gp130, STAT3, GNAS		
Immunostaining	attenuation of L-FABP	positive for GS, nucleus positive for β-catenin	positive for SAA positive for CRP		map-like GS distribution
Gender difference	predominant in women	predominant in women			
Histological features	fatty degeneration	cell atypia	inflammatory cell infiltration, ductular reaction, sinusoid dilation		central scar, abnormal vasculature, ductular reaction, sinusoid dilation
Characteristic clinical findings	oral contraceptives	oral contraceptives	drinking, obesity		central scar, abnormal vasculature demonstrated by imaging
Frequency in all adenoma patients	35 – 40%	10 – 15%	45 – 60%	10%	
Possibility of hemorrhage	(+)	(+)	(+)	(+)	(–)
Possibility of canceration	(+)?	(+) frequent?	(+)?	(+)?	(–)

map-like distribution of GS (fig. 4h). It is also reported to show a central scar, inflammatory cell infiltration, ductular reaction, and sinusoid dilation as characteristic features. However, as FNH occasionally shows no central scar, and as inflammatory cell infiltration, ductular reaction as well as sinusoid dilation are also observed in I-HCA, the map-like distribution of GS is useful for its diagnosis.

Results in Japan

The new diagnostic methods and histological and clinical findings observed above have been documented primarily by a French group [17–20]. Although they are excellent works, we had to examine whether or not these findings are directly applicable to Japanese patients. Race and clinical background are quite different between Japan and Europe. In Japan, there have been reports by Sasaki et al. [23, 24] and Soejima et al. [25].

Soejima et al. [25] evaluated 35 nodules of HCA in 26 patients (examined by surgery in 23, autopsy in 2, and biopsy in 1) consisting of 13 males and 13 females. None of them took oral contraceptives, and only 1 of them had glycogen storage disease. The clinical background of HCA in these Japanese patients markedly differed from that observed in reports from Western countries. However, 2 patients showed congenital absence of the portal vein, 1 showed IPH, 4 had complicating FNH, and a considerable number of patients showed abnormal intrahepatic circulation. These lesions have been conventionally classified as hyperplastic lesions caused by abnormal circulation or FNH-like lesions.

In addition, of the 35 HCA nodules, 11 (31%) were classified by immunostaining as H-HCA, 7 (20%) as b-HCA, 10 (29%) as I-HCA, and 7 (20%) as u-HCA. These percentages were similar to those in Western populations despite differences in clinical background. Their work did not include patients with alcoholic abuse or viral cirrhosis.

Moreover, the expression of OATP1B3 in various subtypes was analyzed by immunostaining. It was attenuated in 6 of 8 (75%) of the H-HCAs, 0 of 6 (0%) of the b-HCAs, 9 of 10 (90%) of the I-HCAs, and 4 of 6 (67%) of the u-HCAs, compared with nonnodular areas. Five nodules were excluded from the study because their stainability was difficult to evaluate. The expression was frequently attenuated in H-HCA and I-HCA, but not in b-HCA. In addition, the OATP1B3 expression was maintained or enhanced in all 8 nodules that showed intranuclear accumulation of β-catenin (6 nodules of b-HCA and 2 nodules of H-HCA). This indicates a close relationship between HCA subtypes (β-catenin gene mutation) and the OATP1B3 expression, as in hepatocellular carcinoma (HCC) [26].

Fig. 4. Histological and immunostaining findings of subtypes of HCA and FNH (cited from [15] with modification). **a** HE staining of H-HCA. T = Neoplastic area; NT = nonneoplastic area. Fatty degeneration is notable in the neoplastic area. **b** L-FABP immunostaining. The staining is clearly attenuated in the neoplastic area. **c** HE staining of the neoplastic area of b-HCA. No atypia as reported from Western countries was noted in our patients. **d** GS immunostaining. The neoplastic area (T) is diffusely and intensely positive. The nonneoplastic area (NT) shows a normal pattern, in which only the center of lobules is positive. **e** β-Catenin immunostaining shows that an intranuclear accumulation is evident. **f** HE staining of I-HCA shows that there are areas with marked inflammatory cell infiltration (**inset**). **g** SAA immunostaining shows that the neoplastic area is diffusely positive. **h** GS immunostaining of FNH. A map-like pattern is observed. Compared with the neoplastic area in **d**, the contrast between the negative and positive areas is clear.

(For figure see next page.)

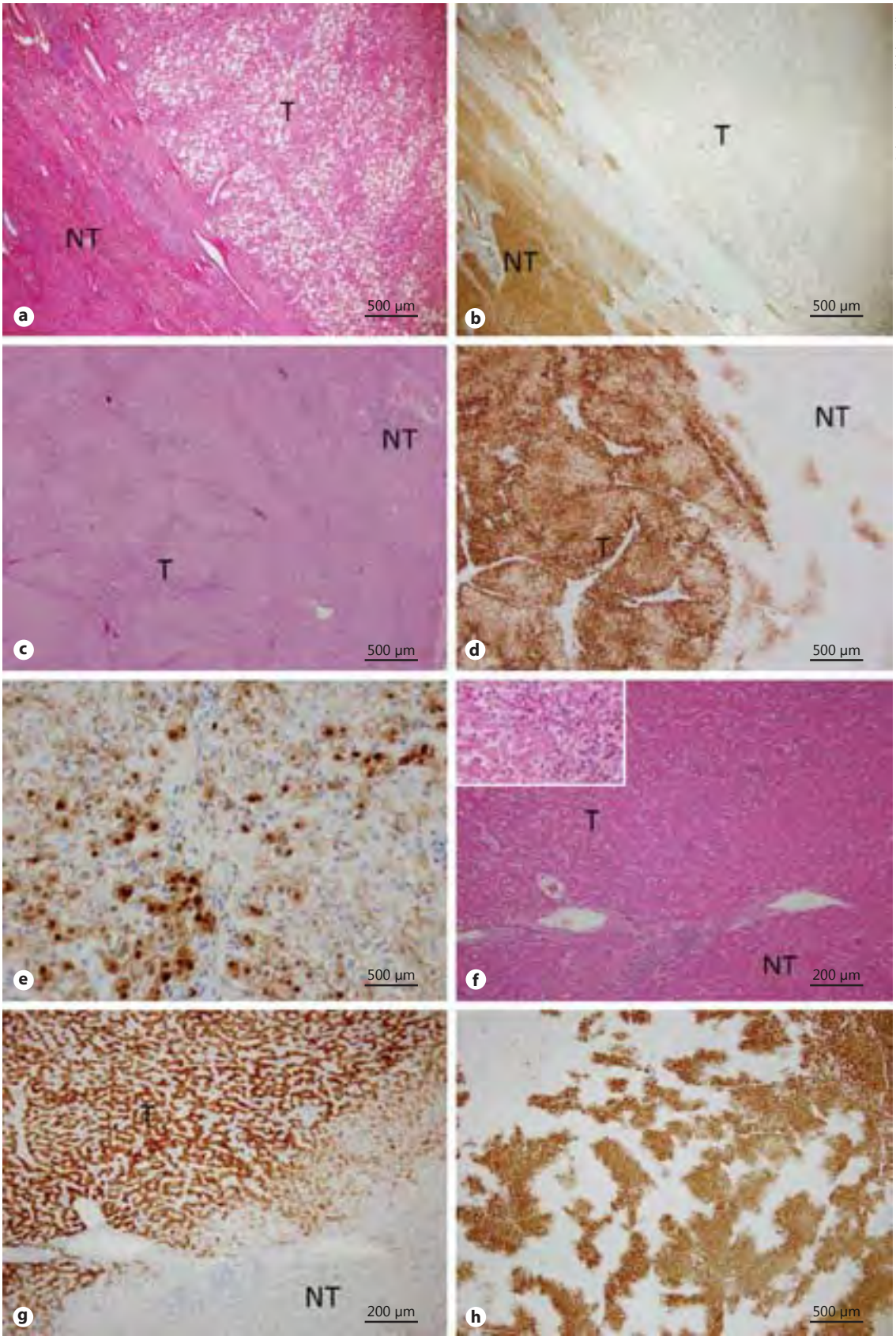

Color version available online

4

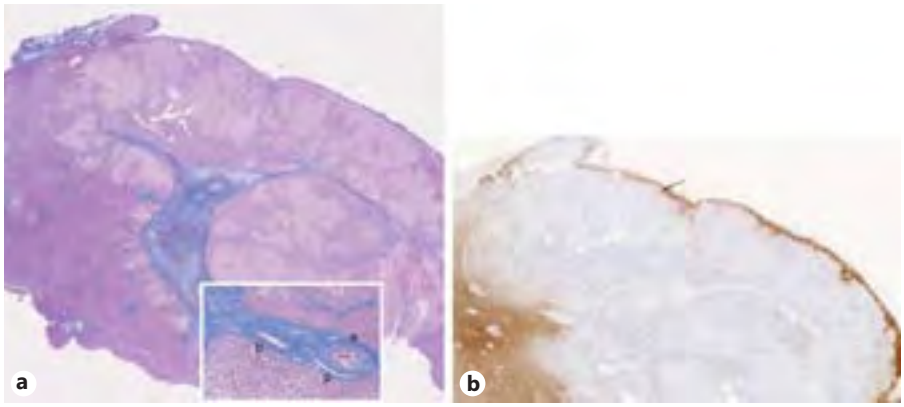

Fig. 5. Nodule of H-HCA that contains a thick portal tract and resembles FNH is shown. **a** A nodular lesion of 2.0 cm in diameter is shown. A very thick portal tract is present in the nodule. The **inset** is a high magnification view of the portal tract. The presence of the 3 components, namely, the artery (a), portal vein (p), and bile duct (b), is clear. Since this thick portal tract resembles the central scar of FNH, the nodule is difficult to diagnose as HCA morphologically (Masson's Trichrome staining). **b** On L-FABP immunostaining, the intensity of the staining is clearly attenuated in the nodule. This finding is consistent with H-HCA (cited from [28] with modification).

Color version available online

Furthermore, when correlations between OATP1B3 expression and gadolinium ethoxybenzyl diethylenetriamine pentaacetic acid MRI (EOB-MRI) findings [27, 28] were evaluated in 10 HCA nodules in 7 patients, the 8 nodules that showed attenuation of OATP1B3 expression were hypointense in the hepatocyte phase of EOB-MRI, and 1 nodule with intranuclear accumulation of β-catenin was isointense, showing a significant association in 9 (90%) of the 10 nodules. This suggests that HCA accompanied by intranuclear accumulation of β-catenin, such as b-HCA, which is reportedly at high risk of canceration [29], may be diagnosed by EOB-MRI. However, atypia was not significant in b-HCA in our patients, unlike in reports from Western countries. Additionally, the risk of malignant transformation of b-HCA needs to be evaluated further in a greater number of Japanese patients.

Usefulness and Problems of the New WHO Classification

The new WHO classification has reached an epoch-making progress. However, its usefulness and problems have to be precisely evaluated for further development.

Usefulness

When the new WHO classification incorporating knowledge about gene mutations and their immunohistochemical manifestations was applied to Japanese patients, it was confirmed to be very useful in the following respects. (1) The diagnosis of HCA was facilitated by evidence obtained by simple procedures of immunohistochemistry. (2) Each subtype was found to have characteristic histological features, genotype, and immunostaining findings, and they were useful for the imaging diagnosis and for predicting prognosis.

Problems

However, in interpreting the various lesions practically, the new WHO classification has the following problems. (i) There exist differences and contradictions compared with the conventional diagnostic criteria. (ii) Some patients with chronic liver diseases show positive immunohistochemical findings for HCA (HCA-like lesions with an abnormal background liver). (iii) Some lesions show immunohistochemically focal positive areas.

Differences and Contradictions Compared with the Conventional Diagnostic Criteria

Figure 5 shows a macroscopical FNH-like lesion that exhibited immunohistochemical findings of H-HCA [30]. A nodule of 2 cm in diameter was detected, which contained a thick portal tract and showed a structure resembling a central scar. In a high magnification view, the 3 elements of the portal tract, i.e., the artery (a), portal vein (p), and bile duct (b), are clearly observed. These findings widely deviate from the conventional diagnostic criteria for HCA. In addition, the patient showed abnormal intrahepatic circulation (i.e., congenital absence of the portal vein) in the background liver. The images suggested FNH rather than HCA. However, on L-FABP immunostaining, this nodule showed clear attenuation of staining compared with the background liver, and a diagnosis of H-HCA was made.

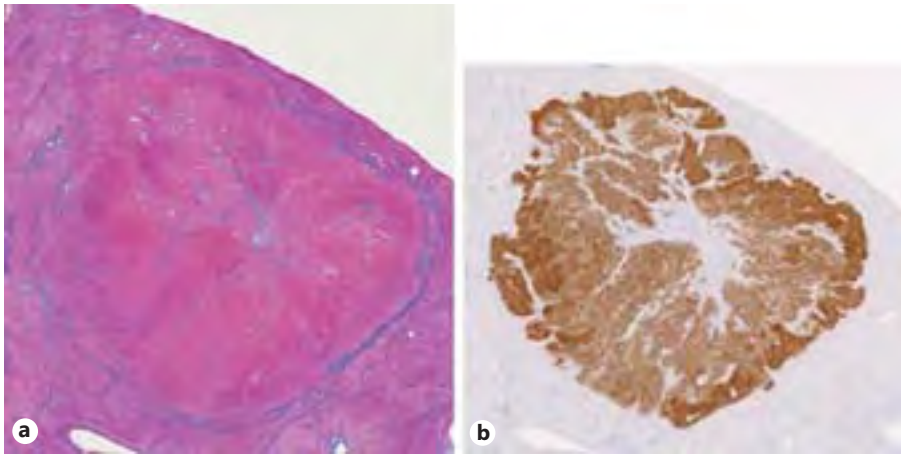

Fig. 6. An FNH-like SAA-positive nodule with a clear central scar (cited from [24] with modification). **a** A nodular lesion of 1.5 cm in diameter is shown. It contains a central scar and shows morphological features consistent with FNH. However, the background liver shows alcoholic cirrhosis and is not normal (Masson's Trichrome staining). **b** On SAA immunostaining, hepatic parenchymal cells in the entire nodule are diffusely positive. The findings are similar to those of H-HCA.

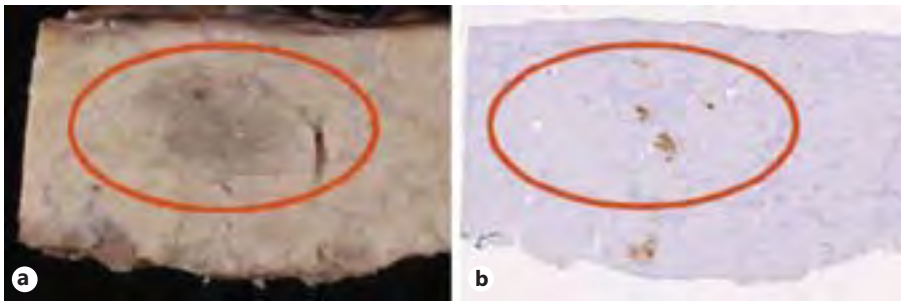

Fig. 7. Nodule showing focal SAA-positive areas (cited from [15] with modification). **a** Gross image of a nodular lesion measuring 8 × 5 mm. **b** SAA immunostaining. Focal positive areas are observed in the nodule.

HCA-Like Lesions with an Abnormal Background Liver

Figure 6 shows a nodular lesion of 1.5 cm in diameter detected in a patient with alcoholic liver cirrhosis [24]. In this nodule, the presence of a central scar suggestive of FNH is grossly clear. However, on immunostaining, SAA was clearly positive, and the lesion was diagnosed as a nodule with properties similar to those of I-HCA. However, according to the conventional diagnostic criteria, HCA is considered to occur in the normal liver. If these criteria are strictly applied, the lesion cannot be definitively diagnosed as I-HCA and is inevitably classified as an SAA-positive nodule present in a liver with alcoholic cirrhosis. In addition, nodular lesions in heavy drinkers have been reported to show characteristics resembling those of FNH [31, 32]. In this respect, the diagnosis as HCA in this lesion contradicts with the past reports [31, 32].

Presence of Focal Positive Areas

Figure 7a shows a macroscopic finding of a nodule with focal SAA-positive areas. Figure 7b is a panoramic view of the SAA immunostaining, showing foci of positive staining in the nodule. This lesion was found in the same patient as the one shown in figure 6 [24]. This patient had 7 benign hepatocellular lesions, of which 3 were diffusely SAA positive, 2 were partially SAA positive, and 2 were SAA negative. The coexistence of nodules that exhibit different staining properties in the same liver suggests that SAA-positive foci may appear in SAA-negative nodules and spread further to all nodules. It also poses a new question about how nodules showing focal SAA positivity should be definitively diagnosed. In our experience, it is not rare that SAA-positive foci are found in nodules. It has already been reported that SAA-positive microfoci are also present in the background liver [33]. Further evaluation is necessary to determine whether these focal SAA-positive areas are microfoci or evidence of the development of a neoplastic nodule (HCA) from a nonneoplastic nodule (FNH). A report has been published describing that HCA foci appeared in nodules of FNH [34]. We have also encountered another patient in whom SAA-positive and GS-attenuated I-HCA-like areas appeared in SAA-negative FNH-like nodules showing a map-like GS staining pattern [35].

Table 4. Characteristics and problems of the conventional diagnostic criteria for HCA and the new WHO classification

(A)	Conventional diagnostic criteria
	Characteristics
	Diagnosed by inferring a specific disease state, clinically, from HCA-related background factors (oral contraceptives, glycogen storage disease, etc.) and, pathologically, from characteristic gross and histological features.
	Problems
	(1) No molecular biological evidence for being a neoplasm.
	(2) Occasionally difficult to differentiate clearly from nonneoplastic lesions such as FNH and from well-differentiated HCC.
	(3) Nontypical cases increase if definitions are strictly applied.
(B)	Diagnostic criteria of the new WHO classification
	Characteristics
	Diagnosed based on gene mutations of hepatocytes or immunohistochemical findings, which are their indirect evidence.
	Problems
	(1) The diagnoses are not necessarily consistent with those based on the conventional criteria.
	(2) Gene mutation itself is not necessarily the definite evidence of the neoplastic nature.
	(3) Lesions showing multiple gene mutation patterns are difficult to subclassify.

Discussion on Difficult-to-Diagnose Lesions and Definitive Diagnosis of Individual Lesions

With the advent of the new WHO classification, the diagnosis of benign hepatocellular nodular lesions has entered a new era. However, the classification often contradicts the conventional diagnostic criteria, and considerable numbers of lesions are difficult to definitively diagnose. We should discuss how to cope with such difficult cases.

Characteristics and Problems of the Conventional Diagnostic Criteria and New WHO Classification

First, the characteristics of and problems with the conventional diagnostic criteria and new WHO classification are reviewed (table 4). According to the conventional diagnostic criteria, as shown in table 2, the diagnosis is made by inferring a specific disease from, clinically, background factors related to HCA and, pathologically, characteristic gross and histological features. Its problems include the following: (1) there are no molecular biological grounds for regarding lesions as neoplasms, (2) it is sometimes difficult to differentiate clearly from nonneoplastic lesions such as FNH and from well-differentiated HCC, and (3) nontypical lesions increase if the definition of HCA is strictly applied.

On the contrary, according to the new WHO criteria, diagnoses are made by demonstrating various gene mutations using molecular biological techniques or based on immunohistochemical findings, which are indirect evidence of such mutations. However, there are the following problems: (1) the diagnoses based on the new WHO classification are not necessarily consistent with those based on the conventional diagnostic criteria, (2) gene mutation itself is not necessarily the definite evidence of the neoplastic nature, and (3) lesions showing multiple gene mutation patterns are difficult to subclassify.

If the conventional diagnostic criteria and new WHO classification are summarized as in table 4, diagnostic inconsistency is easily explained by the differences of their diagnostic grounds.

Reevaluation of Disease Concepts

To solve such problems, adjustment between the conventional disease concepts and the new WHO classification is necessary. As mentioned above, some lesions showing HCA-related gene mutations and immunohistochemical findings appear to deviate considerably from the conventional disease concept of HCA. Lesions in males, those with no HCA-related clinical background, such as the use of oral contraceptives, nodules containing an abnormally thick portal tract, and those closely resembling FNH with a clear central scar are examples. The new WHO classification is considered to be a method to directly and indirectly demonstrate gene mutations of hepatocytes, rather than digging out latent HCA consistent with the conventional disease concept. In addition, HCA and FNH are not the only benign hepatocellular nodular lesions, which vary widely, as shown in table 1 and figure 3. Since there are also SAA-positive foci in the nonnodular background liver [33], theoretically, gene mutations may occur in each lesion presented in table 1. Indeed, the background liver had congenital absence of the portal vein in the patient shown in figure 5. This vascular anomaly suggested that the nodule was a hyperplastic nodule caused by circulatory abnormality (FNH-like lesion) ac-

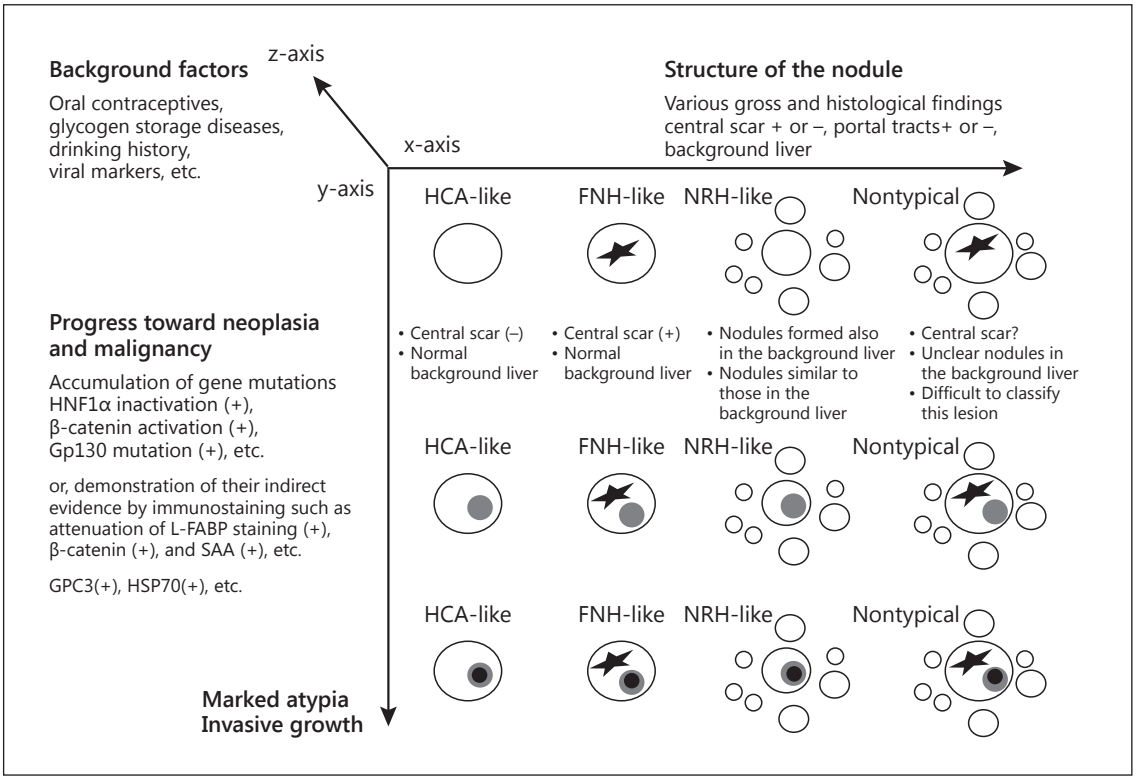

Fig. 8. Concept of the personalized diagnosis (three-dimensional diagnosis) (cited from [15] with modification). The x-axis shows various gross and histological findings. The y-axis shows the degree of progress toward neoplasia and malignancy. The z-axis shows various background factors.

cording to the conventional concepts. The background liver in the patients presented in figures 6 and 7 showed alcoholic cirrhosis. Therefore, the differential diagnoses of these nodules (particularly the nodule with no clear central scar shown in fig. 7) are considered to include LRN- as well as FNH-like lesions.

Reevaluation of the Classification of Disease Entities Based on Clinical Data and Histological Findings in the Background Liver

Classifying typical features of diseases in detail is useful to some extent for understanding the diseases and their differential diagnosis. However, if such a classification is applied with excessive rigidity, nontypical lesions increase, making the definitive diagnosis difficult. The definition that the background liver of HCA and FNH is normal can simply be a matter of probability. Chronic liver disease is not considered as the definite causative factor of HCA and FNH, while it is definitely related to hepatocarcinogenesis. There is no guarantee that patients with HCA or FNH are not infected by hepatitis virus or will not become heavy drinkers. In addition, not all patients with HCA have its risk factors.

Flexible thinking is important in the diagnosis and interpretation of the characteristics of each lesion.

Definitive Diagnosis of Each Lesion

Personalized Diagnosis

From the above viewpoints, a tentative proposal for the definitive diagnosis of individual patients including those with nontypical HCAs is presented (fig. 8; personalized diagnosis or the three-dimensional diagnosis).

The gross features of benign hepatocellular nodular lesions show a wide variation. They not only vary in the number of nodules, presence or absence of the capsule, and presence or absence of the central scar, but may also show incomplete patterns. In addition, in the background liver, there may be multiple clear nodules in some patients, but nodules are as obscure or difficult to recognize as nodules in others. The severity of the liver disorder also varies. Such morphological features are described in detail and mapped along the horizontal axis (x-axis). As a

result, they can be classified roughly into HCA-like, FNH-like, NRH-like, and nontypical.

The presence or absence of gene mutations such as HNF1α inactivation (+), β-catenin activation (+), and gp130 mutation (+) and their accumulation is mapped along the vertical axis (y-axis). Attenuation of L-FABP (+), β-catenin (+), and SAA (+), which is indirect evidence of the above mutations, may also be used. Thus, gene mutations occurring at 2 or more loci can also be automatically indicated. There is no need to force HCAs into 4 subtypes. If different gene mutations are discovered in the future, they can also be dealt with by this method. Moreover, independently of the x- and y-axes, clinical background factors such as the history of the use of oral contraceptives, infection with hepatitis virus, IPH, and heavy alcohol intake are mapped along the z-axis. By such a combination of morphological features, gene mutations, and clinical background factors, even nontypical lesions and lesions in which various factors are involved in a complex manner can be classified.

For example, the patient with the nodule shown in figure 6 was a heavy drinker. The gross and histological findings of the nodule were compatible with FNH, but the nodule was SAA positive. A more accurate diagnosis than this is impossible.

In addition, it is necessary to evaluate the degree of progress toward neoplasia and malignancy of the nodule. Conventionally, FNH and HCA were considered benign, but HCA has been reported to show malignant transformation. However, FNH has also been reported to be malignant in 2 of more than 800 cases [36]. Moreover, as HCC arising in the normal liver is encountered not infrequently, the occurrence of precancerous lesions, namely, accumulation of various gene mutations, in FNH and various benign nodular lesions is sufficiently possible. In diagnosing various benign hepatocellular nodular lesions, we immunohistochemically examine heat shock protein 70 (HSP70) and glypican 3 (GPC3) [37] to evaluate the possibility of well-differentiated HCC and precancerous conditions, in addition to the above HCA-related immunohistochemical examinations. The histological assessment of the presence or absence of stromal invasion is also important [37, 38]. The findings of the degree of malignancy are also mapped along the y-axis.

Figure 8 presents a conceptual diagram of this classification. By following this concept, various factors should be evaluated independently for the diagnosis of individual cases (personalized diagnosis or three-dimensional diagnosis). Thus, we can discuss whether the lesion is typical or nontypical.

Revised Concept of Anomalous Portal Tract Syndrome

We would like to reemphasize the usefulness of the revised concept of anomalous portal tract syndrome (fig. 3b). Although the original concept of anomalous portal tract syndrome was useful for the various nontypical lesions, it did not include the possibility of neoplastic change (fig. 3a). Owing to the development of the WHO classification, we added the three stages of mutation, i.e. nonmutated, focally mutated and entirely mutated, to each type of the nodule. The difficult cases such as those shown in the figures 5–8 are well interpreted by this revised concept. In Japanese cases, benign hepatocellular lesions accompany abnormal hepatic vasculature more frequently than oral contraceptives. They must have been caused by abnormal hepatic circulation rather than oral contraceptives. Especially for the interpretation of these Japanese cases, this revised concept is useful.

Closing Remarks

The new WHO classification is a very useful system that has clarified various gene mutations and immunostaining findings of benign hepatocellular nodular lesions. We truly respect former studies. However, the classification is not necessarily perfect and presents some problems. We sincerely hope that this article is helpful to solve these problems.

Disclosure Statement

The authors declare that no financial or other conflicts of interest exist in relation to the content of this article.

References

1 Rooks JB, Ory HW, Ishak KG, Strauss LT, Greenspan JR, Tyler CW Jr: The association between oral contraception and hepatocellular adenoma – a preliminary report. Int J Gynaecol Obstet 1977;15:143–144.

2 Ishak KG: Hepatic lesions caused by anabolic and contraceptive steroids. Semin Liver Dis 1981;1:116–128.

3 Wanless IR, Mawdsley C, Adams R: On the pathogenesis of focal nodular hyperplasia of the liver. Hepatology 1985;5:1194–1200.

4 Wanless IR, Albrecht S, Bilbao J, Frei JV, Heathcote EJ, Roberts EA, Chiasson D: Multiple focal nodular hyperplasia of the liver associated with vascular malformations of various organs and neoplasia of the brain: a new syndrome. Mod Pathol 1989;2:456–462.

5 Stromeyer FW, Ishak KG: Nodular transformation (nodular 'regenerative' hyperplasia) of the liver. A clinicopathologic study of 30 cases. Hum Pathol 1981;12:60–71.
6 Nguyen BN, Flejou JF, Terris B, Belghiti J, Degott C: Focal nodular hyperplasia of the liver: a comprehensive pathologic study of 305 lesions and recognition of new histologic forms. Am J Surg Pathol 1999;23:1441–1454.
7 Sherlock S, Feldman CA, Moran B, Scheuer PJ: Partial nodular transformation of the liver with portal hypertension. Am J Med 1966;40: 195–203.
8 Okuda K, Nakashima T, Okudaira M, Kage M, Aida Y, Omata M, Sugiura M, Kameda H, Inokuchi K, Bhusnurmath SR, Aikat BA: Liver pathology of idiopathic portal hypertension. Comparison with non-cirrhotic portal fibrosis of India. The Japan idiopathic portal hypertension study. Liver 1982;2: 176–192.
9 Nakanuma Y, Tsuneyama K, Ohbu M, Katayanagi K: Pathology and pathogenesis of idiopathic portal hypertension with an emphasis on the liver. Pathol Res Pract 2001;197:65–76.
10 International Working Party: Terminology of nodular hepatocellular lesions. Hepatology 1995;22:983–993.
11 Kondo F, Nagao T, Sato T, Tomizawa M, Kondo Y, Matsuzaki O, Wada K, Wakatsuki S, Nagao K, Tsubouchi H, Kobayashi H, Yasumi K, Tsukayama C, Suzuki M: Etiological analysis of focal nodular hyperplasia of the liver, with emphasis on similar abnormal vasculatures to nodular regenerative hyperplasia and idiopathic portal hypertension. Pathol Res Pract 1998;194:487–495.
12 Kondo F: Benign nodular hepatocellular lesions caused by abnormal hepatic circulation: etiological analysis and introduction of a new concept. J Gastroenterol Hepatol 2001;16: 1319–1328.
13 Kondo F, Koshima Y, Ebara M: Nodular lesions associated with abnormal liver circulation. Intervirology 2004;47:277–287.
14 Kondo F: Representative anomalies and hepatic lesions; in Nakanuma Y (ed): Textbook of Liver Pathology for Doctors. Tokyo, Nanko-do, 2013, pp 165–168.
15 Kondo F: Hepatocellular adenoma and focal nodular hyperplasia: new interpretation benign hepatocellular nodules based on the new WHO classification. Liver Cancer 2013;5: 174–183.
16 Kondo F: Pathological diagnosis of benign hepatocellular nodular lesions basesd on the new World Health Organization Classification. Kanzo 2013;54:807–818.
17 Bioulac-Sage P, Rebouissou S, Thomas C, Blanc JF, Saric J, Sa Cunha A, Rullier A, Cubel G, Couchy G, Imbeaud S, Balabaud C, Zucman-Rossi J: Hepatocellular adenoma subtype classification using molecular markers and immunohistochemistry. Hepatology 2007;46:740–748.
18 Bioulac-Sage P, Laumonier H, Couchy G, Le Bail B, Sa Cunha A, Rullier A, Laurent C, Blanc JF, Cubel G, Trillaud H, Zucman-Rossi J, Balabaud C, Saric J: Hepatocellular adenoma management and phenotypic classification: the Bordeaux experience. Hepatology 2009;50:481–489.
19 Bioulac-Sage P, Cubel G, Balabaud C, Zucman-Rossi J: Revisiting the pathology of resected benign hepatocellular nodules using new immunohistochemical markers. Semin Liver Dis 2011;31:91–103.
20 Bioulac-Sage P, Balabaud C, Wanless IR: Focal nodular hyperplasia and hepatocellular adenoma; in Bosman FT, Carneiro F, Hruban RH, Theise ND (eds): WHO Classification of Tumours of the Digestive System, ed 4. Lyon, IARC, 2010, pp 198–204.
21 Sasaki M, Ikeda T, Hatanaka KC, Nakanuma Y: Hyperplastic hepatocellular nodule with localized hemangiomatosis: a hither-to unrecognized type of hypervascular hepatic lesion. Hepatol Res 2014;44:E77–E83.
22 Ueda T, Starkey J, Mori K, Fukunaga K, Shimofusa R, Motoori K, Minami M, Kondo F: A pictorial review of benign hepatocellular nodular lesions: comprehensive radiological assessment incorporating the concept of anomalous portal tract syndrome. J Hepatobiliary Pancreat Sci 2011;18:386–396.
23 Sasaki M, Yoneda N, Kitamura S, Sato Y, Nakanuma Y: Characterization of hepatocellular adenoma based on the phenotypic classification: the Kanazawa experience. Hepatol Res 2011;41:982–988.
24 Sasaki M, Kondo F, Sawai Y, Imai Y, Kadowaki S, Sano K, Fukusato T, Matsui O, Nakanuma Y: Serum amyloid A-positive hepatocellular neoplasms in the resected livers from 3 patients with alcoholic cirrhosis. Histol Histopathol 2013;28:1499–1505.
25 Soejima Y, Kondo F, Inoue M, Takahashi Y, Sano K, Takikawa H, Fukusato T: Expression of OATP1B3 protein in subtypes of hepatocellular adenoma. Kanzo 2012;53:779–780.
26 Sekine S, Ogawa R, Ojima H, Kanai Y: Expression of SLCO1B3 is associated with intratumoral cholestasis and CTNNB1 mutations in hepatocellular carcinoma. Cancer Sci 2011; 102:1742–1747.
27 Murakami T, Tsurusaki M: Hypervascular benign and malignant liver tumors that require differentiation from hepatocellular carcinoma: key points of imaging diagnosis. Liver Cancer 2014;3:85–96.
28 Joo I, Choi BI: New paradigm for management of hepatocellular carcinoma by imaging. Liver Cancer 2012;1:94–109.
29 Zucman-Rossi J, Jeannot E, Nhieu JT, Scoazec JY, Guettier C, Rebouissou S, Bacq Y, Leteurtre E, Paradis V, Michalak S, Wendum D, Chiche L, Fabre M, Mellottee L, Laurent C, Partensky C, Castaing D, Zafrani ES, Laurent-Puig P, Balabaud C, Bioulac-Sage P: Genotype-phenotype correlation in hepatocellular adenoma: new classification and relationship with HCC. Hepatology 2006;43:515–524.
30 Tateishi Y, Furuya M, Kondo F, Torii I, Nojiri K, Tanaka Y, Umeda S, Okudela K, Inayama Y, Endo I, Ohashi K: Hepatocyte nuclear factor-1 alpha inactivated hepatocellular adenomas in patient with congenital absence of the portal vein: a case report. Pathol Int 2013; 63:358–363.
31 Nakashima O, Kurogi M, Yamaguchi R, Miyaaki H, Fujimoto M, Yano H, Kumabe T, Hayabuchi N, Hisatomi J, Sata M, Kojiro M: Unique hypervascular nodules in alcoholic liver cirrhosis: identical to focal nodular hyperplasia-like nodules? J Hepatol 2004;41: 992–998.
32 Kondo F: Focal nodular hyperplasia-like lesions in heavy drinkers. Intern Med 2009;48: 1117–1123.
33 Bioulac-Sage P, Laumonier H, Cubel G, Rossi JZ, Balabaud C: Hepatic resection for inflammatory hepatocellular adenomas: pathological identification of micronodules expressing inflammatory proteins. Liver Int 2010;30: 149–154.
34 Handra-Luca A, Paradis V, Vilgrain V, Dubois S, Durand F, Belghiti J, Valla D, Degott C: Multiple mixed adenoma-focal nodular hyperplasia of the liver associated with spontaneous intrahepatic porto-systemic shunt: a new type of vascular malformation associated with the multiple focal nodular hyperplasia syndrome? Histopathology 2006;48:309–311.
35 Sugimoto K, Kondo F, Furuichi Y, Oshiro H, Nagao T, Saito K, Yoshida H, Imai Y, Fukusato T, Moriyasu F: Focal nodular hyperplasia-like lesion of the liver with focal adenoma features associated with idiopathic portal hypertension. Hepatol Res 2014;44:E309–E315.
36 Ishak KG, Goodman ZD, Stocker JT: Benign hepatocellular tumors; in Ishak KG, Goodman ZD, Stocker JT (eds): Tumor of the Liver and Intrahepatic Bile Ducts. Atlas of Tumor Pathology, 3rd series. Washington, Armed Forces Institute of Pathology, 1999, pp 9–48.
37 The International Consensus Group for Hepatocellular Neoplasia: Pathologic diagnosis of early hepatocellular carcinoma: a report of the international consensus group for hepatocellular neoplasia. Hepatology 2009;49:658–664.
38 Kondo F: Assessment of stromal invasion for correct histological diagnosis of early hepatocellular carcinoma. Int J Hepatol 2011;2011: 241652.

Clinical Study

Oncology

Oncology 2014;87(suppl 1):50–54
DOI: 10.1159/000368145

Published online: November 22, 2014

Virtual Sonography for Novice Sonographers: Usefulness of SYNAPSE VINCENT® with Pre-Check Imaging of Tumor Location

Chikara Ogawa[a, b] Yasunori Minami[a] Yumiko Morioka[b] Akiyo Noda[b] Soichi Arasawa[b] Masako Izuta[b] Atsushi Kubo[b] Toshihiro Matsunaka[b] Noriyuki Tamaki[b] Mitsushige Shibatouge[b] Masatoshi Kudo[a]

[a]Department of Gastroenterology and Hepatology, Kinki University School of Medicine, Osaka-Sayama, and
[b]Department of Gastroenterology and Hepatology, Takamatsu Red Cross Hospital, Takamatsu, Japan

Key Words
SYNAPSE VINCENT® · Ultrasound beginners · Virtual sonography

Abstract
Purpose: To evaluate the usefulness of a virtual ultrasound (US) imaging device as a tool to assist novice sonographers. ***Materials and Methods:*** A prospective blinded pilot study was conducted involving patients with liver lesions. Two sonographers and 2 medical doctors with less than 5 years of experience performed US examinations. The time needed to detect liver lesions on US and the success rate for detecting liver lesions with and without using the virtual US imaging device SYNAPSE VINCENT® (Fujifilm Medical Co., Tokyo, Japan) before US examination were evaluated. ***Results:*** Thirty-two patients with the following 42 liver lesions were included: liver cyst (n = 24), hemangioma (n = 8), hepatocellular carcinoma (n = 6), and liver metastasis (n = 4). The maximal diameter of these lesions ranged from 0.3 to 1.5 cm (mean ± SD, 0.8 ± 0.4). The average time for detecting liver lesions on US was 47.8 s (range, 7–113) with VINCENT and 112.9 s (range, 14–313) without VINCENT before US examination. There were significant differences in the duration of US examination with and without VINCENT ($p = 0.0002$, Student's t test). The rates for accurately detecting liver lesions were 100 and 76.2% (16/21) in US beginners with and without VINCENT, respectively. Significantly higher detection rates were found in the US beginners who used VINCENT compared to those who did not use VINCENT ($p = 0.047$, Fisher's exact test). ***Conclusion:*** Before US examination, a reference with VINCENT could contribute to the successful detection of liver lesions and could be time-saving for US beginners.

Introduction

Multidetector CT has been in clinical use since the late 1990s, and 3D imaging technology has markedly advanced. At the beginning of its clinical application, CT image reconstruction focused on displaying organs in real time [1, 2]. Recently, 3D imaging analysis has diversified. The ease and speed of obtaining needed images from 3D volume data have become important for the treatment of liver tumors, especially radiofrequency ablation for hepatocellular carcinoma [3, 4]. Especially in the liver, diag-

KARGER

E-Mail karger@karger.com
www.karger.com/ocl

0030–2414/14/0877–0050$39.50/0

Prof. Masatoshi Kudo
Department of Gastroenterology and Hepatology
Kinki University School of Medicine
377-2 Ohno-Higashi, Osaka-Sayama, Osaka 589-8511 (Japan)
E-Mail m-kudo@med.kindai.ac.jp

nostic imaging offers diverse modalities, including noninvasive evaluations [5–14]. Many types of imaging softwares using multiplanar reconstruction (MPR) have become available for the diagnosis and/or treatment guidance for liver cancers [15–18].

Ultrasound (US) fusion imaging (Real-Time Virtual Sonography, HITACHI ALOKA Medical Systems, Tokyo, Japan; Fusion, GE Healthcare, Chalfont St. Giles, UK; Smart Fusion, Toshiba Medical Systems, Tokyo, Japan) is a new system using MPR, and fusion imaging of B-mode US and CT/MRI can be displayed simultaneously and in real time according to the angle of the transducer in the magnetic field [19–22]. Fusion imaging can help us understand the 3D relationship between the liver vasculature and tumors. However, this system only operates with high-end US machines, and the fusion process is somewhat complex.

The volume analyzer SYNAPSE VINCENT® (Fujifilm Medical Co., Tokyo, Japan) is a 3D image analysis system that enables quick and easy access to high-definition 3D images of organs and vessels using previously captured CT or MRI, while also providing highly practical analysis functions at the workstation [23]. In particular, this can also generate virtual sonographic images using MPR with a quick and easy operation. In this study, we evaluated the usefulness of SYNAPSE VINCENT, a virtual US imaging device,, as a tool to assist US beginners.

Materials and Methods

A prospective blinded pilot study was conducted involving patients with liver lesions. Two medical doctors and 2 sonographers with less than 5 years of experience performed US examinations. The primary objective was to compare the liver lesion detecting time on US and the success rate for detecting liver lesions with or without using the virtual US imaging device SYNAPSE VINCENT before US examination.

Equipment

The local area network system is connected to a computer with SYNAPSE (Fujifilm Medical Co.), a medical imaging and information management system, at the Takamatsu Red Cross Hospital. VINCENT is an application of imaging analyses using SYNAPSE and can display 2D MPR images as virtual sonography corresponding to the angle in the plane of 3D volume image data. This angle of the plane can be operated quickly and freely at the workstation for scanning in epigastric, subcostal, and intercostal positions.

B-mode sonographic scans were obtained using LOGIQ E9 (GE Healthcare) with a 2- to 5-MHz convex probe (C1–5D) and a 4- to 9-MHz linear probe (9LD), an Ascendas (HITACHI ALOKA Medical Systems) with a 1- to 5-MHz convex probe (EUP C715) and a 3- to 7-MHz linear probe (EUP L52), or a Xario XG (Toshiba Medical Systems) with a 3- to 6-MHz convex probe (PVT-375BT).

CT was performed using a 64-slice multidetector-row CT scanner (Aquilion 64, Toshiba Medical Systems) with the following scan parameters: reconstructed slice thickness = 1 mm; rotation time = 0.5 s; helical pitch = 23.0; pitch factor = 0.791; X-ray tube parameters = 120 kV, 300–400 mA. Triple-phase contrast-enhanced CT was performed at 40, 70, and 180 s after initiating the injection of contrast media to obtain hepatic arterial, portal venous, and equilibrium phase images, respectively. A total of 100 ml of nonionic contrast material containing 300 mg of iodine per milliliter (Iopamidol, Bayer Yakuhin, Osaka, Japan) was injected intravenously at a rate of 3 ml/s using an automatic power injector.

Evaluation

Patients with liver tumors who have previously been diagnosed by dynamic CT or MRI were selected for this study. US beginners were permitted to obtain imaging information of some patients using VINCENT, whereas information on previous imaging results of other patients was withheld.

The liver was examined first using a subcostal approach in sagittal and paraxial planes. As a rule, the right hepatic lobe was also examined with a lateral approach through the intercostal space. Sonographic reports and images were reviewed in conjunction with CT/MRI to determine whether a determinate lesion shown on CT/MRI could be detected sonographically and to confirm lesion correspondence. Thereby, the detection rates and duration of detecting liver lesions on US were evaluated.

Statistical Analysis

All values are expressed as the mean ± standard deviation (SD). Comparisons between the two groups were analyzed using Student's t test and Fisher's exact test. $p < 0.05$ was considered significant. Statistical analyses were performed using Microsoft Excel 2013 for Windows.

Results

This pilot study involved 32 patients undergoing routine US examinations. All patients with the following 42 liver lesions were included: liver cyst (n = 24), hemangioma (n = 8), hepatocellular carcinoma (n = 6), and liver metastasis (n = 4). The maximal diameter of these lesions ranged from 0.3 to 1.5 cm (mean ± SD, 0.8 ± 0.4) on CT.

The average time for detecting liver lesions on US was 47.8 s (range, 7–113) with VINCENT and 112.9 s (range, 14–313) without VINCENT before US examination. There were significant differences in the duration of US examination with and without VINCENT ($p = 0.0002$, Student's t test; fig. 1).

The rates for accurately detecting liver lesions were 100% (21/21) and 76.2% (16/21) in US beginners with

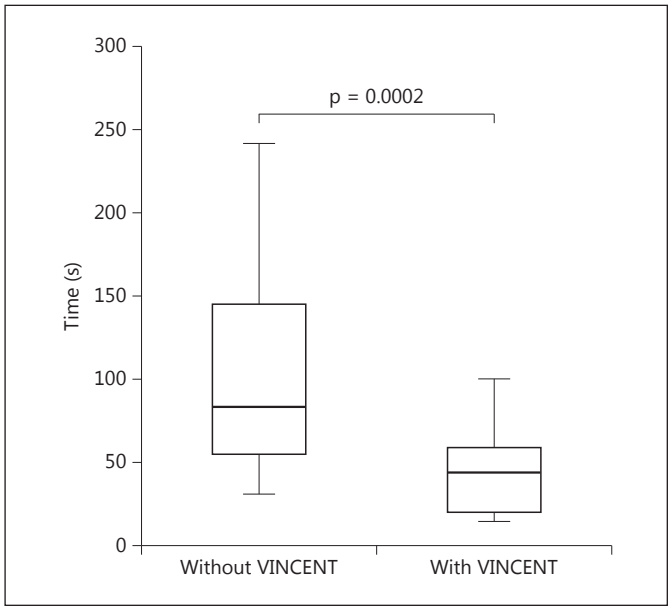

Fig. 1. The time needed to detect the liver lesions with and without VINCENT.

and without VINCENT, respectively. Significantly higher detection rates were found in the US beginners who used VINCENT compared to those who did not use VINCENT (p = 0.047, Fisher's exact test).

Discussion

Preparation is a necessary ingredient for success, and even more so for beginners. This study demonstrated that pre-check imaging by SYNAPSE VINCENT could contribute to the successful detection of liver lesions and could be time-saving on US examination for beginners. In general, axial imaging on CT is common in clinical use, whereas US shows cross-sectional images with various angles. In particular, an intercostal view of the liver on US provides quite a different image from usual CT images because the intercostal view is in a diagonal direction against the body trunk. Therefore, it is often difficult for US beginners to understand the 3D anatomy of the liver and display available images with an intercostal view. Moreover, US images may differ from a familiar view because the shape of the liver changes after surgical liver resection. This could also lead to wasting time on US examination. However, SYNAPSE VINCENT has the potential to resolve these problems. VINCENT can

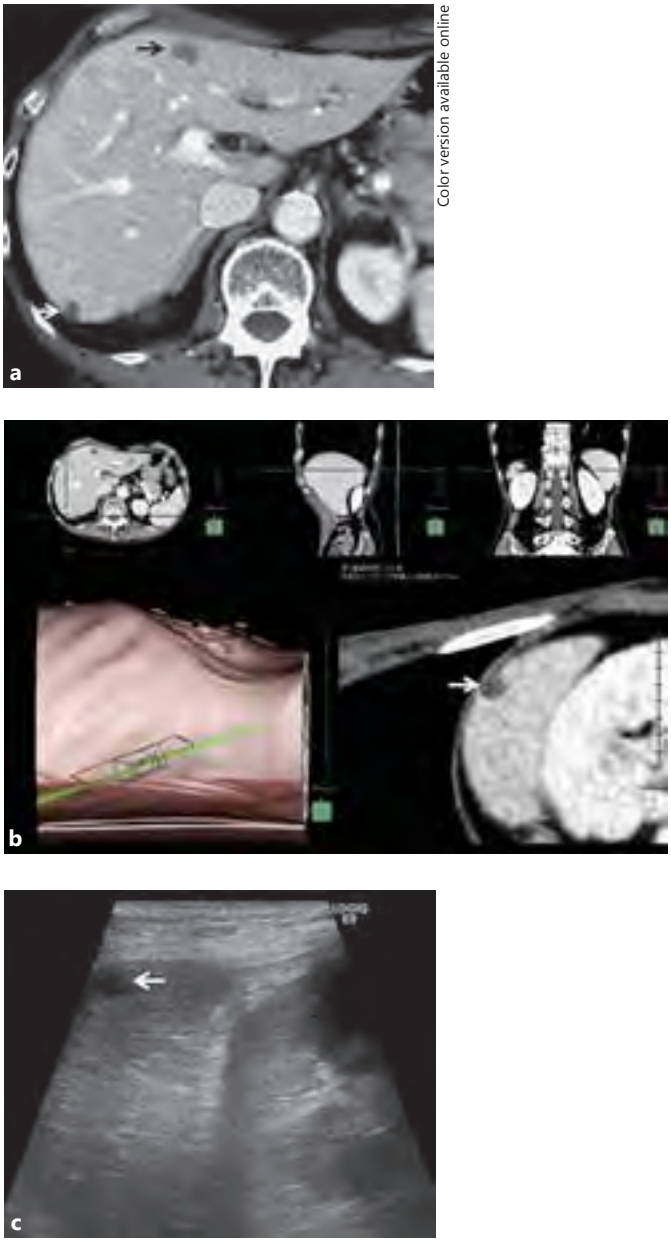

Fig. 2. Imaging of a 66-year-old man with liver cysts. **a** Transverse portal phase CT shows two cysts (arrows) in segment III and VI of the liver. **b** Screen shot shows setting windows for VINCENT. Upper images show the transverse, sagittal, and coronal views for the cyst in segment VI. The lower left image shows that the transducer angle in the plane of the body trunk indicates images obtained from the subcostal view. The lower right image displays the virtual US image and the cyst as low-density area. **c** B-mode US image corresponds to the virtual US image. The cyst is shown as low echoic area (arrow). Our US beginners missed this cyst without using VINCENT because the rib bone hid it.

simulate US examinations by virtual US imaging at a workstation [23]. Preparation using VINCENT could promote an efficient and successful US examination (fig. 2).

While the basic technical development depends on the frequency of US examination, successful experience would stimulate a US beginner's growth. This study gives powerful support for the effectiveness of training in early-phase US skill acquisition with the use of VINCENT. To perform US examination with competence, not only the sonographer, but also the medical doctor must have a good understanding of the abdominal anatomy. The use of various models and stimulators will help to understand the abdominal anatomy and shorten the learning curve. Therefore, a training program with the use of virtual US imaging would shorten the learning curve for US beginners.

However, virtual US devices such as VINCENT should provide reference images at a workstation. Virtual US images do not completely correspond to US images. This imaging incompatibility could be attributed to variations in the depth of breath holding on CT and US examination [20]. In addition, the liver is also rotated to varying degrees from the time when CT was previously captured.

The principal limitation of this study is that it could suffer from selection bias because patients with liver lesions were enrolled according to the senior doctors' subjective selections. Second, it is a preliminary study with a relatively small number of patients. Further studies of this technique with a larger number of patients are warranted.

In summary, SYNAPSE VINCENT could display virtual US images clearly and smoothly. Before US examination, a reference with VINCENT could contribute to the successful detection of liver lesions and could be time-saving for US beginners.

Disclosure Statement

The authors declare that no financial or other conflicts of interest exist in relation to the content of this article.

References

1 Lee KS, Yoon JH, Kim TK, Kim JS, Chung MP, Kwon OJ: Evaluation of tracheobronchial disease with helical CT with multiplanar and three-dimensional reconstruction: correlation with bronchoscopy. Radiographics 1997;17:555–567; discussion 568–570.

2 Lawler LP, Fishman EK: Multi-detector row CT of thoracic disease with emphasis on 3D volume rendering and CT angiography. Radiographics 2001;21:1257–1273.

3 Fishman EK, Ney DR, Heath DG, Corl FM, Horton KM, Johnson PT: Volume rendering versus maximum intensity projection in CT angiography: what works best, when, and why. Radiographics 2006;26:905–922.

4 Lin SM: Local ablation for hepatocellular carcinoma in Taiwan. Liver Cancer 2013;2:73–83.

5 Lee JM, Yoon JH, Joo I, Woo HS: Recent advances in CT and MR imaging for evaluation of hepatocellular carcinoma. Liver Cancer 2012;1:22–40.

6 Ricke J, Seidensticker M, Mohnike K: Noninvasive diagnosis of hepatocellular carcinoma in cirrhotic liver: current guidelines and future prospects for radiological imaging. Liver Cancer 2012;1:51–58.

7 Donati OF, Fischer MA, Chuck N, Hunziker R, Weishaupt D, Reiner CS: Accuracy and confidence of Gd-EOB-DTPA enhanced MRI and diffusion-weighted imaging alone and in combination for the diagnosis of liver metastases. Eur J Radiol 2013;82:822–828.

8 Forner A, Vilana R, Ayuso C, Bianchi L, Sole M, Ayuso JR, Boix L, Sala M, Varela M, Llovet JM, Bru C, Bruix J: Diagnosis of hepatic nodules 20 mm or smaller in cirrhosis: prospective validation of the noninvasive diagnostic criteria for hepatocellular carcinoma. Hepatology 2008;47:97–104.

9 Kudo M, Hatanaka K, Kumada T, Toyoda H, Tada T: Double-contrast ultrasound: a novel surveillance tool for hepatocellular carcinoma. Am J Gastroenterol 2011;106:368–370.

10 Bota S, Piscaglia F, Marinelli S, Pecorelli A, Terzi E, Bolondi L: Comparison of international guidelines for noninvasive diagnosis of hepatocellular carcinoma. Liver Cancer 2012;1:190–200.

11 Inoue T, Kudo M, Komuta M, Hayaishi S, Ueda T, Takita M, Kitai S, Hatanaka K, Yada N, Hagiwara S, Chung H, Sakurai T, Ueshima K, Sakamoto M, Maenishi O, Hyodo T, Okada M, Kumano S, Murakami T: Assessment of Gd-EOB-DTPA-enhanced MRI for HCC and dysplastic nodules and comparison of detection sensitivity versus MDCT. J Gastroenterol 2012;47:1036–1047.

12 Alzaraa A, Gravante G, Chung WY, Al-Leswas D, Morgan B, Dennison A, Lloyd D: Contrast-enhanced ultrasound in the preoperative, intraoperative and postoperative assessment of liver lesions. Hepatol Res 2013;43:809–819.

13 Joo I, Choi BI: New paradigm for management of hepatocellular carcinoma by imaging. Liver Cancer 2012;1:94–109.

14 Salvatore V, Bolondi L: Clinical impact of ultrasound-related techniques on the diagnosis of focal liver lesions. Liver Cancer 2012;1:238–246.

15 Lee SW, Shinohara H, Matsuki M, Okuda J, Nomura E, Mabuchi H, Nishiguchi K, Takaori K, Narabayashi I, Tanigawa N: Preoperative simulation of vascular anatomy by three-dimensional computed tomography imaging in laparoscopic gastric cancer surgery. J Am Coll Surg 2003;197:927–936.

16 Taketomi A, Takeishi K, Mano Y, Toshima T, Motomura T, Aishima S, Uchiyama H, Yoshizumi T, Shirabe K, Maehara Y: Total resection of the right hepatic vein drainage area with the aid of three-dimensional computed tomography. Surg Today 2012;42:46–51.

17 Minami Y, Kudo M, Chung H, Inoue T, Takahashi S, Hatanaka K, Ueda T, Hagiwara H, Kitai S, Ueshima K, Fukunaga T, Shiozaki H: Percutaneous radiofrequency ablation of sonographically unidentifiable liver tumors. Feasibility and usefulness of a novel guiding technique with an integrated system of computed tomography and sonographic images. Oncology 2007;72(suppl 1):111–116.
18 Fukuda H, Ito R, Ohto M, Sakamoto A, Otsuka M, Togawa A, Miyazaki M, Yamagata H: US-CT 3D dual imaging by mutual display of the same sections for depicting minor changes in hepatocellular carcinoma. Eur J Radiol 2012;81:2014–2019.
19 Hirooka M, Iuchi H, Kumagi T, Shigematsu S, Hiraoka A, Uehara T, Kurose K, Horiike N, Onji M: Virtual sonographic radiofrequency ablation of hepatocellular carcinoma visualized on CT but not on conventional sonography. AJR Am J Roentgenol 2006;186:S255–S260.
20 Minami Y, Chung H, Kudo M, Kitai S, Takahashi S, Inoue T, Ueshima K, Shiozaki H: Radiofrequency ablation of hepatocellular carcinoma: value of virtual CT sonography with magnetic navigation. AJR Am J Roentgenol 2008;190:W335–W341.
21 Okamoto E, Sato S, Sanchez-Siles AA, Ishine J, Miyake T, Amano Y, Kinoshita Y: Evaluation of virtual CT sonography for enhanced detection of small hepatic nodules: a prospective pilot study. AJR Am J Roentgenol 2010; 194:1272–1278.
22 Minami Y, Kitai S, Kudo M: Treatment response assessment of radiofrequency ablation for hepatocellular carcinoma: usefulness of virtual CT sonography with magnetic navigation. Eur J Radiol 2012;81:e277–e280.
23 Ohshima S: Volume analyzer SYNAPSE VINCENT for liver analysis. J Hepatobiliary Pancreat Sci 2014;21:235–238.

Clinical Study

Oncology

Oncology 2014;87(suppl 1):55–62
DOI: 10.1159/000368146

Published online: November 22, 2014

Combination Guidance of Contrast-Enhanced US and Fusion Imaging in Radiofrequency Ablation for Hepatocellular Carcinoma with Poor Conspicuity on Contrast-Enhanced US/Fusion Imaging

Tomohiro Minami Yasunori Minami Hirokazu Chishina Tadaaki Arizumi Masahiro Takita Satoshi Kitai Norihisa Yada Tatsuo Inoue Satoru Hagiwara Kazuomi Ueshima Naoshi Nishida Masatoshi Kudo

Department of Gastroenterology and Hepatology, Kinki University School of Medicine, Osaka-Sayama, Japan

Key Words

Contrast-enhanced US · Fusion imaging · Hepatocellular carcinoma · Poor conspicuity · Radiofrequency ablation · Sonazoid

Abstract

Purpose: The purpose of this study was to evaluate the usefulness of the combination guidance of contrast-enhanced US (CEUS) and fusion imaging in radiofrequency ablation (RFA) for hepatocellular carcinoma (HCC) with poor conspicuity on B-mode US and CEUS/fusion imaging. ***Materials and Methods:*** We conducted a retrospective cohort study, which included 356 patients with 556 HCCs that were inconspicuous on B-mode US. A total of 192 patients with 344 HCCs, 123 patients with 155 HCCs, and 37 patients with 57 HCCs underwent RFA under CEUS guidance, fusion imaging guidance, and the combination of CEUS and fusion imaging guidance. ***Results:*** The average number of treatment sessions was 1.1 (range: 1–2) in the CEUS guidance group, 1.1 (range: 1–2) in the fusion imaging guidance group, and 1.1 (range: 1–3) in the combination of CEUS and fusion imaging guidance group. Treatment analysis did not reveal significantly more RFA treatment sessions in the combination guidance group than in the other groups ($p = 0.97$, Student's t test). During the follow-up period (1.1–85.3 months, mean ± SD, 43.2 ± 59.5), the 3-year local tumor progression rates were 4.9, 7.2, and 5.9% in the CEUS guidance group, the fusion imaging guidance group, and the combination guidance group, respectively ($p = 0.84$, log-rank test). ***Conclusion:*** In spite of selection bias, session frequency and local tumor progression were not different under the combination guidance with CEUS and fusion imaging in RFA. The combination of fusion imaging and CEUS guidance in RFA therapy is an effective treatment for HCC with poor conspicuity on B-mode US and CEUS/fusion imaging.

Introduction

Radiofrequency ablation (RFA) is widely performed as a percutaneous local treatment for unresectable hepatocellular carcinoma (HCC). Extensive worldwide experience has supported the use of RFA as an excellent treatment option for small HCC (<3 cm), with 3-year disease control rates of up to 80–90% [1–3]. Some centers adopt RFA as first-line treatment for single HCC nodules <3.0 cm in diameter [4–7]. Percutaneous RFA is performed by advancing a specially designed electrode into the tumor under re-

KARGER

E-Mail karger@karger.com
www.karger.com/ocl

0030–2414/14/0877–0055$39.50/0

Prof. Masatoshi Kudo
Department of Gastroenterology and Hepatology
Kinki University School of Medicine
377-2 Ohno-Higashi, Osaka-Sayama, Osaka 589-8511 (Japan)
E-Mail m-kudo@med.kindai.ac.jp

al-time sonographic guidance. The technical effectiveness of RFA depends on correct targeting on US and adequate placement of the RFA needle. However, difficult situations are sometimes encountered in which B-mode US cannot adequately visualize HCCs. For example, viable HCC could not be differentiated from dysplastic nodules in cirrhotic liver or ablated liver tissue due to previous RFA [8, 9].

Contrast-enhanced US (CEUS) or fusion imaging of US with CT/MRI has been increasingly used for the detection, characterization and planning of therapeutic interventions for liver tumors [10, 11]. Especially, CEUS or fusion imaging has been reported to be useful for RFA guidance in difficult cases. CEUS is able to depict tumor vascularity sensitively and accurately [12–16]. In particular, when using only perfluorocarbon microbubbles (sonazoid), HCCs have been shown as defects during the Kupffer phase [10, 17–21]. These defect lesions could be used as targets for the insertion of a RFA needle [22–28]. Moreover, a definitive diagnosis of HCC can be made by tumor staining in defect lesions after injecting an additional new dose of sonazoid [21, 24]. On the contrary, a fusion imaging system enables the synchronized display of real-time US images and multiplanar reconstruction images of CT/MRI corresponding to the cross section of real-time US. The multiplanar reconstruction images are reconstructed based on CT/MR images and displayed as a reference with real-time US images side-by-side on the same monitor. Therefore, fusion imaging is also useful for the detection of HCC and safe RFA therapy of HCC [29–36]. Occasionally, however, there are HCC cases which are more difficult to be detected even when using CEUS or fusion imaging [37].

Incorrect targeting on imaging could cause inadequate placement of the RFA needle. This could lead to more treatment sessions or more frequent local recurrence after RFA. For those more difficult cases, we have attempted to conduct RFA under the combination of CEUS and fusion imaging guidance. The purpose of this study was to assess the value of the combination guidance of CEUS and fusion imaging in RFA for HCC with poor conspicuity on B-mode US and CEUS/fusion imaging.

Materials and Methods

Written informed consent to perform RFA was obtained from all patients before treatment. This cohort study was conducted as a retrospective analysis of a prospective database in a single institution in which RFAs are routinely performed.

The records of HCC patients with poor conspicuity on B-mode US, who received RFA guided by CEUS, fusion imaging, or the combination of CEUS and fusion imaging, were reviewed. Between January 2007 and October 2013, 352 patients with 556 HCCs were enrolled in this study. The first objective was to compare the numbers of treatment sessions for technical effectiveness of ablation between the three guidance groups in RFA. The second objective was to compare the incidences of local tumor progression after RFA. The third objective was to investigate the occurrences of postprocedural complications.

HCC was diagnosed based on three-phase contrast-enhanced CT findings such as positive enhancement in the arterial phase and washout in the equilibrium phase in patients with chronic liver disease. All patients met the following criteria for treatment with RFA: percutaneous accessibility of the tumors, absence of portal tumor thrombus and extrahepatic metastasis, prothrombin time ratio >50%, total bilirubin <4.0 mg/dl, and platelet count >30,000/μl.

Equipment

B-mode sonographic scans were obtained using a LOGIQ 7 or E9 (GE Healthcare, Chalfont St. Giles, UK) with a 1–5-MHz convex probe (4C). The acoustic power of contrast harmonic sonography was set at the default setting with a mechanical index of 0.2. A single focus point was set at the deepest point of the monitor. The sonographic contrast agent was perfluorocarbon microbubbles of NC100100 (Sonazoid; Daiichi-Sankyo, Tokyo, Japan; GE Healthcare) with a median diameter of 2–3 μm. This contrast agent was reconstituted for injection with 2 ml sterile water for injection. The anticipated clinical dose for imaging of liver lesions was 0.010 ml of encapsulated gas per kilogram of body weight.

Fusion imaging using the fusion system by GE Healthcare was composed of a main unit in the US machine, a corresponding probe sensor, and a magnetic field generator. Additionally, dedicated software must be installed on the US system. The probe sensor is detected by a magnetic positioning system, which calculates the exact position of the sensor in the room. Standard Digital Imaging and Communications in Medicine (DICOM) data sets of all cross-sectional modalities (CT or MRI) are used for image fusion. The DICOM data are loaded in the US system, after which registration of the datasets takes place. This registration can be performed based on a number of fixed reference points or by plane. After successful image fusion, the registered CT or MR images move simultaneously with the examined US imaging plane.

Patients were treated by RFA (Cool-Tip RF Ablation System; Covidien, Boulder, Colo., USA). 20-cm long, 17-gauge monopolar internally cooled electrodes with 3- or 2-cm long exposed metallic tips were used to deliver radiofrequency energy. A 200-Watt, 480-kHz monopolar radiofrequency generator regulated by impedance was used as the energy source.

RFA Procedure for HCC with Poor Conspicuity

We have used LOGIQ E9 for RFA treatment since September 2011 (before then LOGIQ 7 was used). Percutaneous RFA is mainly performed for clearly visualized HCC under B-mode US guidance in our hospital. If necessary, it can also be used under the guidance of CEUS or fusion imaging for HCC with poor conspicuity. The guidance selection in RFA is a complex decision involving many factors (fig. 1). Sonazoid-enhanced US guidance could be an option because of visualization or qualitative diagnosis of HCC (n = 196). On the contrary, the fusion imaging guidance in RFA could be an option because of the detection of HCC (n = 123). Moreover, in patients having poorly inconspicuous HCC on fusion imaging, additional CEUS using sonazoid was performed in order to accurately localize the tumor at the time of the RFA procedure

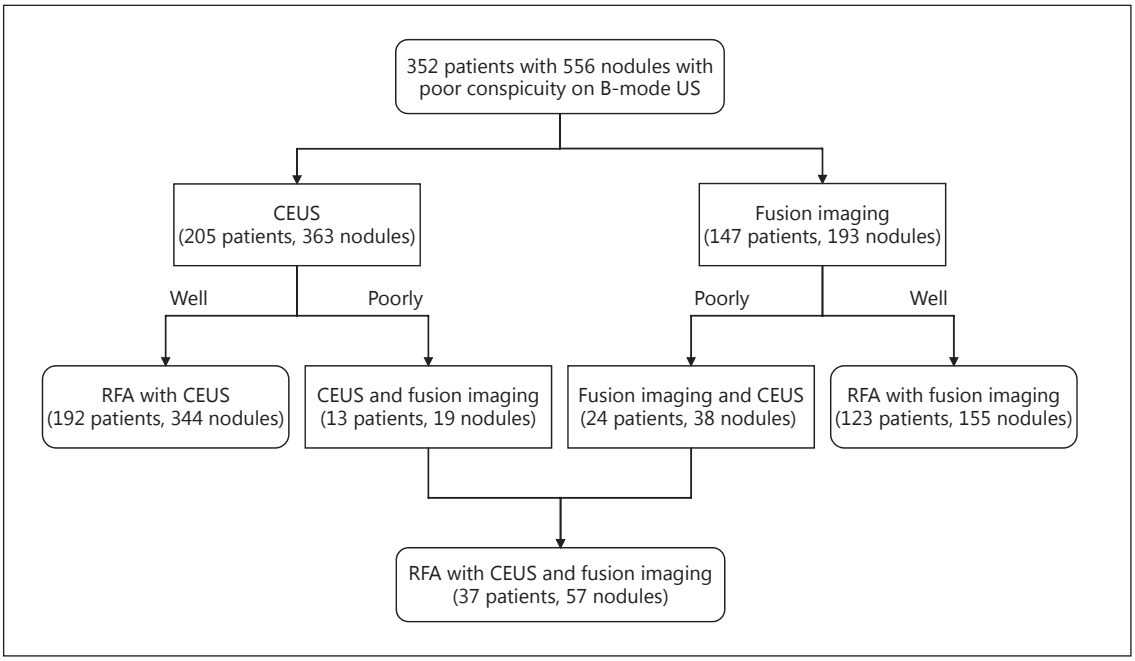

Fig. 1. Flow chart of the study.

(n = 24). The patients with poorly conspicuous HCC on CEUS underwent additional fusion imaging during the RFA procedure (n = 13).

In patients with the combination imaging guidance in RFA, HCCs were targeted on the Kupffer phase of the CEUS image, when the tumor was seen as a perfusion defect on CEUS at the corresponding site of the fused CT/MR image (fig. 2). After the RF electrode penetrated the HCC using a fixed-angle guide attachment, each ablation was performed for >8 min with >40 W at the beginning. Thereafter, the hyperechoic zone appeared and gradually increased at the ablated site. The ablation was continually monitored and was stopped when the HCC (including the safety margin) was completely covered by the zone of hyperechogenicity.

Assessment of Technical Effectiveness and Follow-Up

A few days after treatment, the technical effectiveness of ablation was assessed based on contrast-enhanced CT scan findings. A tumor was considered to have been successfully ablated when there were no longer any enhanced regions either within the entire tumor during the arterial phase or a >0.5-cm margin of apparently normal hepatic tissue surrounding the tumor during the portal phase [38]. Part of the tumor was diagnosed as remaining viable when images of the ablated area showed nodular peripheral enhancement. The residual portion was treated with additional RFA the next week. Any complications were recorded. If the follow-up CT images showed successful RFA and the absence of new tumors, three-phase dynamic CT scans were repeated at 3-month intervals.

Statistical Analysis

All values were expressed as means ± standard deviation (SD). Comparisons between the three groups were analyzed using the Student t test or Mann-Whitney U test. Local tumor progression rate curves of the three groups were compared by using a log-rank test. The χ^2 test was used to compare the rate of complications. $p < 0.05$ was considered statistically significant. Statistical analyses were performed using SPSS version 12.0 (SPSS, Chicago, Ill., USA).

Results

Patient Characteristics

During the study period, we detected 556 HCCs that were inconspicuous on B-mode US. The patient population included 252 men and 100 women (age range, 49–88 years; 65.8 ± 27.6 years). The maximal diameter of the tumors ranged from 0.5 to 6.0 cm (1.5 ± 0.9) on dynamic CT.

Table 1 shows the characteristics of the three groups. The distributions of sex, age, viral etiology, platelet count and tumor location were not different between these groups. A total of 29 (78.4%), 6 (16.2%) and 2 (5.4%) patients in the combination guidance group were classified as Child-Pugh classes A, B and C liver function, respectively. The proportions of patients with each Child-Pugh score and classification did not differ significantly. The mean tumor diameter was 1.5 ± 1.1 cm (range, 0.5–6.0) in the CEUS guidance group, 1.4 ± 0.6 cm (range, 0.5–4.0) in the fusion imaging guidance group and 1.3 ± 0.4 cm (range, 0.5–2.5) in the combination of CEUS and fusion imaging guidance group (p = 0.143).

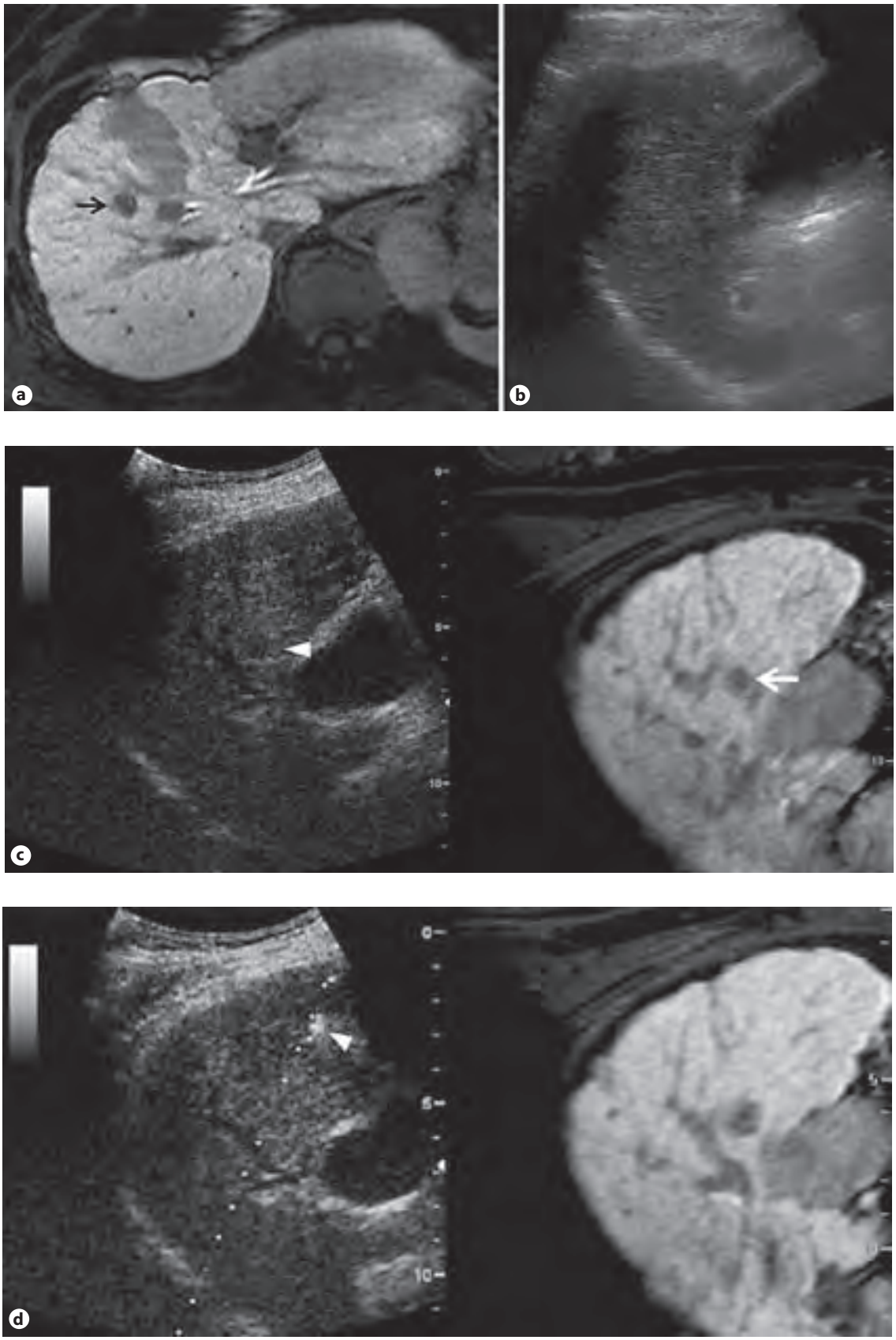

2

(For legend and figures 2e, f see next page.)

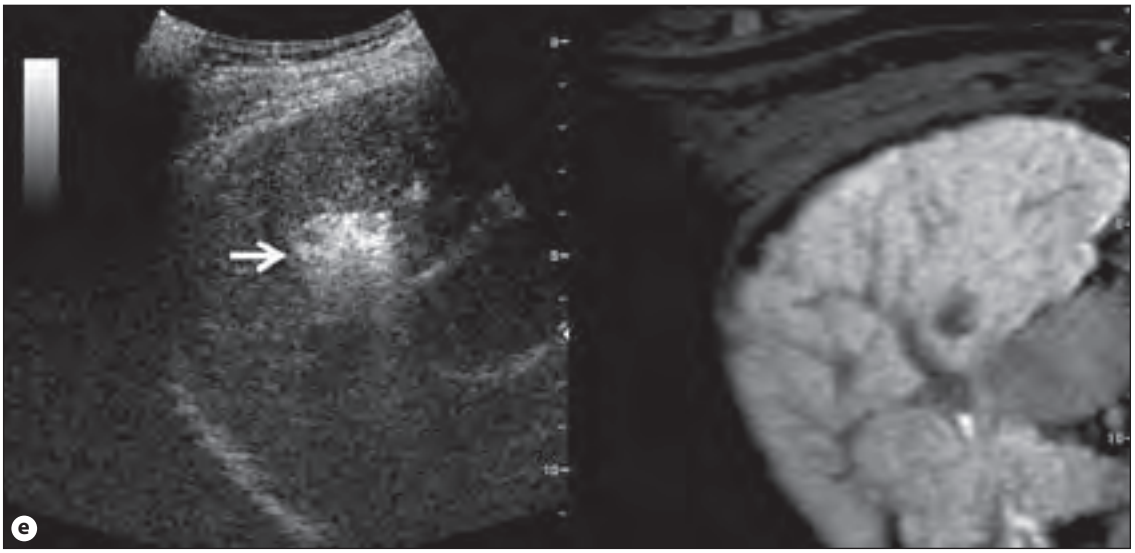

Fig. 2. Images of a 61-year-old man with a 1.2-cm local tumor progression of HCC after transcatheter arterial chemoembolization. **a** Local tumor progression of HCC as a defect lesion (arrow) in segment V of the liver is shown on a hepatobiliary phase image of gadolinium-ethoxybenzyl-diethylenetriamine pentaacetic acid-enhanced MRI. **b** B-mode US showing an area of segment V of the liver, but the HCC nodule cannot be clearly detected. **c** The right panel shows an oblique MR image with a HCC focus defect (arrow). The left panel shows a hypoechoic area (arrowhead) by CEUS using sonazoid. **d** A RFA needle (arrowhead) was inserted in the defect. **e** The hyperechoic area (arrow) covers the treated HCC after RFA. **f** An early-phase dynamic CT scan obtained 1 day after RFA therapy shows that the tumor and the surrounding area (arrow) are not enhanced.

Table 1. Patients' characteristics of the CEUS guidance group, the fusion imaging guidance group and the combination of fusion imaging and CEUS guidance group

	CEUS guidance (n = 192 with 344 HCCs)	Fusion imaging guidance (n = 123 with 155 HCCs)	Fusion imaging + CEUS guidance (n = 37 with 57 HCCs)	p value
Age, years	69.6±8.8	70.9±7.9	65.8±8.5	0.088
Sex (male/female), n	138/54	91/32	23/14	0.441
HBV/HCV/no HBV no HCV, n	25/150/21	20/86/17	7/28/2	0.475
Child-Pugh score	5.7±0.9	5.8±1.0	5.6±1.1	0.423
Platelet, $\times 10^5/\mu l$	11.3±5.6	11.4±5.7	12.2±5.5	0.475
Tumor size, cm	1.5±1.1	1.4±0.6	1.3±0.4	0.143
Location S1/lat/med/ant/post	3/54/46/144/97	2/15/25/64/49	0/4/7/22/24	0.110

HBV = Hepatic B virus; HCV = hepatic C virus; S1 = segment I; lat = lateral segment of the liver; med = medial segment of the liver; ant = anterior segment of the liver; post = posterior segment of the liver.

Table 2. Complications of RFA guided by CEUS, fusion imaging and the combination of CEUS and fusion imaging

	CEUS guidance, % (n = 192)	Fusion imaging guidance, % (n = 123)	Fusion imaging + CEUS guidance, % (n = 37)
Pleural effusion	6.8 (13/192)	7.3 (9/123)	0
Ascites	2.1 (4/192)	0.8 (1/123)	0
Hemothorax	1.6 (3/192)	1.6 (2/123)	0
Diaphragmatic injury	1.6 (3/192)	0.8 (1/123)	5.4 (2/37)
Pneumothorax	1.0 (2/192)	0	0
Hepatic infarction	0.5 (1/192)	0	0
Hemobilia	0.5 (1/192)	0	0

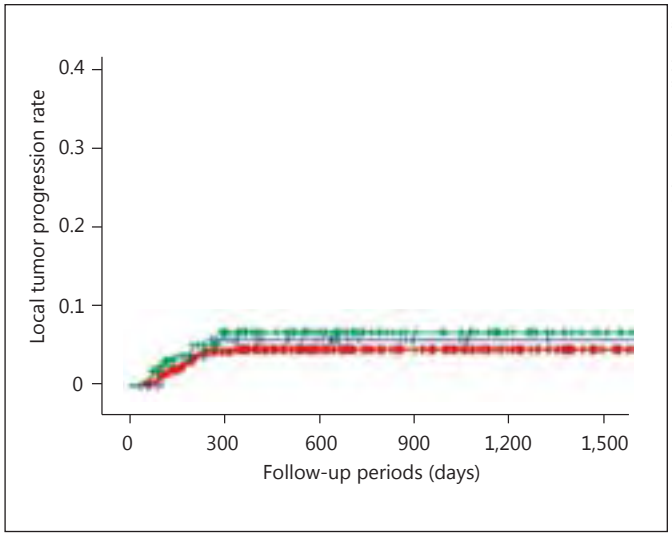

Color version available online

Fig. 3. A Kaplan-Meier curve of local tumor progression in HCC patients of the three imaging guidance groups undergoing RFA therapy is shown.

Technical Success of RFA Treatment

The technical success rates after a single session were 92.2% (177/199), 91.1% (112/123) and 89.2% (33/37) for the CEUS guidance group, the fusion imaging guidance group and the combination guidance group, respectively. The average number of treatment sessions was 1.1 ± 0.2 (range: 1–2) in the CEUS guidance group, 1.1 ± 0.3 (range: 1–2) in the fusion imaging guidance group, and 1.1 ± 0.4 (range: 1–3) in the combination of CEUS and fusion imaging guidance group. Treatment analysis revealed that the number of RFA treatment sessions in the combination guidance group was not significantly higher than in the other groups (p = 0.97, Student's t test).

Local Tumor Progression

Follow-up time ranged from 1.1 to 85.3 months (43.2 ± 59.5). During the follow-up period, the 3-year local tumor progression rates were 4.9, 7.2, and 5.9% in the CEUS guidance group, the fusion imaging guidance group, and the combination guidance group, respectively (p = 0.84, log-rank test)(fig. 3).

Complications

No major complications were encountered in any of the guidance groups, and the overall rates of minor complications were 15.1% (29/192) in the CEUS guidance group, 10.6% (13/123) in the fusion imaging guidance group, and 5.4% (2/37) in the combination of CEUS and fusion imaging guidance group (table 2). There were no significant differences in incidence between the imaging guidance groups (p = 0.31, χ^2 test).

Discussion

Small HCCs with poor sonographic conspicuity are difficult to localize for RFA therapy in patients with liver cirrhosis. These inconspicuous HCCs could be blindly ablated by placing an electrode into the expected area of the liver, but more frequent mistargeting or incomplete ablation would be induced. Patients with poor conspicuity on B-mode US and CEUS/fusion imaging receive RFA treatment under the most difficult conditions, and we expected that more frequent sessions of RFA and/or local tumor progression would occur. However, there were no significant differences in the technical success rates of RFA therapy and the incidence of local tumor progression between the imaging guidance groups.

By the combination guidance of CEUS and fusion imaging, we could place the RFA electrode close to incon-

spicuous HCC under the most difficult conditions. In addition, a larger ablation zone would preclude incomplete ablation. These might explain the absence of differences in the technical success of the combination guidance group.

In a strict and fair assessment of treatment response, a sufficient ablation margin can reduce the risk of local tumor progression after RFA. Our database is prospectively managed under the same criteria of treatment response assessment. Accordingly, it is unsurprising that there was no significant difference in the incidence of local tumor progression between the three imaging guidance groups. However, local tumor progression was observed in 3 patients with the combination of fusion imaging and CEUS guidance in RFA. In those patients, partial volume effects could have caused an underestimation of the tumor ablation margin.

There were several limitations in this study including its retrospective and single-center design. We are fully aware that this study suffered from selection bias because the imaging guidance method for RFA was chosen according to the RFA operator's subjectivity.

In summary, poor conspicuity on B-mode US and CEUS/fusion imaging represents the most difficult condition for percutaneous RFA. However, both increased frequency of RFA sessions and local tumor progression under the combination guidance with CEUS and fusion imaging in RFA did not occur in HCC patients with poor conspicuity on B-mode US and CEUS/fusion imaging. The combination of fusion imaging and CEUS guidance in RFA therapy is an effective treatment for poorly defined HCCs on B-mode US and CEUS/fusion imaging.

Disclosure Statement

The authors declare that no financial or other conflicts of interest exist in relation to the content of this article.

References

1 Lin SM, Lin CJ, Lin CC, et al: Radiofrequency ablation improves prognosis compared with ethanol injection for hepatocellular carcinoma < or=4 cm. Gastroenterology 2004;127:1714–1723.
2 Shiina S, Teratani T, Obi S, et al: A randomized controlled trial of radiofrequency ablation with ethanol injection for small hepatocellular carcinoma. Gastroenterology 2005;129:122–130.
3 Lu DS, Yu NC, Raman SS, et al: Radiofrequency ablation of hepatocellular carcinoma: treatment success as defined by histologic examination of the explanted liver. Radiology 2005;234:954–960.
4 Kudo M: Local ablation therapy for hepatocellular carcinoma: current status and future perspectives. J Gastroenterol 2004;39:205–214.
5 Livraghi T, Meloni F, Morabito A, Vettori C: Multimodal image-guided tailored therapy of early and intermediate hepatocellular carcinoma: long-term survival in the experience of a single radiologic referral center. Liver Transpl 2004;10(2 suppl 1):S98–S106.
6 Omata M, Tateishi R, Yoshida H, Shiina S: Treatment of hepatocellular carcinoma by percutaneous tumor ablation methods: ethanol injection therapy and radiofrequency ablation. Gastroenterology 2004;127(5 suppl 1):S159–S166.
7 Choi D, Lim HK, Rhim H, et al: Percutaneous radiofrequency ablation for early-stage hepatocellular carcinoma as a first-line treatment: long-term results and prognostic factors in a large single-institution series. Eur Radiol 2007;17:684–692.
8 Minami Y, Kudo M, Kawasaki T, et al: Treatment of hepatocellular carcinoma with percutaneous radiofrequency ablation: usefulness of contrast harmonic sonography for lesions poorly defined with B-mode sonography. AJR Am J Roentgenol 2004;183:153–156.
9 Minami Y, Kudo M, Chung H, et al: Contrast harmonic sonography-guided radiofrequency ablation therapy versus B-mode sonography in hepatocellular carcinoma: prospective randomized controlled trial. AJR Am J Roentgenol 2007;188:489–494.
10 Joo I, Choi BI: New paradigm for management of hepatocellular carcinoma by imaging. Liver Cancer 2012;1:94–109.
11 Salvatore V, Bolondi L: Clinical impact of ultrasound-related techniques on the diagnosis of focal liver lesions. Liver Cancer 2012;1:238–246.
12 Wilson SR, Burns PN, Muradali D, et al: Harmonic hepatic US with microbubble contrast agent: initial experience showing improved characterization of hemangioma, hepatocellular carcinoma, and metastasis. Radiology 2000;215:153–161.
13 Wen YL, Kudo M, Zheng RQ, et al: Characterization of hepatic tumors: value of contrast-enhanced coded phase-inversion harmonic angio. AJR Am J Roentgenol 2004;182:1019–1026.
14 Quaia E, Calliada F, Bertolotto M, et al: Characterization of focal liver lesions with contrast-specific US modes and a sulfur hexafluoride-filled microbubble contrast agent: diagnostic performance and confidence. Radiology 2004;232:420–430.
15 Inoue T, Kudo M, Maenishi O, et al: Value of liver parenchymal phase contrast-enhanced sonography to diagnose premalignant and borderline lesions and overt hepatocellular carcinoma. AJR Am J Roentgenol 2009;192:698–705.
16 Kudo M: Early hepatocellular carcinoma: definition and diagnosis. Liver Cancer 2013;2:69–72.
17 Hatanaka K, Kudo M, Minami Y, et al: Differential diagnosis of hepatic tumors: value of contrast-enhanced harmonic sonography using the newly developed contrast agent, Sonazoid. Intervirology 2008;51:S61–S69.
18 Hatanaka K, Chung H, Kudo M, et al: Usefulness of the post-vascular phase of contrast-enhanced ultrasonography with sonazoid in the evaluation of gross types of hepatocellular carcinoma. Oncology 2010;78(suppl 1):53–59.
19 Goto E, Masuzaki R, Tateishi R, et al: Value of post-vascular phase (Kupffer imaging) by contrast-enhanced ultrasonography using Sonazoid in the detection of hepatocellular carcinoma. J Gastroenterol 2012;47:477–485.
20 Alaboudy A, Inoue T, Hatanaka K, et al: Usefulness of combination of imaging modalities in the diagnosis of hepatocellular carcinoma using Sonazoid®-enhanced ultrasound, gadolinium diethylene-triamine-pentaacetic acid-enhanced magnetic resonance imaging, and contrast-enhanced computed tomography. Oncology 2011;81(suppl 1):66–72.

21 Kudo M, Hatanaka K, Kumada T, et al: Double-contrast ultrasound: a novel surveillance tool for hepatocellular carcinoma. Am J Gastroenterol 2011;106:368–370.
22 Numata K, Morimoto M, Ogura T, et al: Ablation therapy guided by contrast-enhanced sonography with Sonazoid for hepatocellular carcinoma lesions not detected by conventional sonography. J Ultrasound Med 2008; 27:395–406.
23 Maruyama H, Takahashi M, Ishibashi H, et al: Ultrasound-guided treatments under low acoustic power contrast harmonic imaging for hepatocellular carcinomas undetected by B-mode ultrasonography. Liver Int 2009;29: 708–714.
24 Minami Y, Kudo M, Hatanaka K, et al: Radiofrequency ablation guided by contrast harmonic sonography using perfluorocarbon microbubbles (Sonazoid) for hepatic malignancies: an initial experience. Liver Int 2010; 30:759–764.
25 Masuzaki R, Shiina S, Tateishi R, et al: Utility of contrast-enhanced ultrasonography with Sonazoid in radiofrequency ablation for hepatocellular carcinoma. J Gastroenterol Hepatol 2011;26:759–764.
26 Hiraoka A, Hiasa Y, Onji M, Michitaka K: New contrast enhanced ultrasonography agent: impact of Sonazoid on radiofrequency ablation. J Gastroenterol Hepatol 2011;26: 616–618.
27 Minami Y, Kudo M: Review of dynamic contrast-enhanced ultrasound guidance in ablation therapy for hepatocellular carcinoma. World J Gastroenterol 2011;17:4952–4959.
28 Kokudo N: Recent progress in the treatment and diagnosis of hepatocellular carcinoma. Liver Cancer 2013;2:4.
29 Hirooka M, Iuchi H, Kurose K, et al: Abdominal virtual ultrasonographic images reconstructed by multi-detector row helical computed tomography. Eur J Radiol 2005;53:312–317.
30 Hirooka M, Iuchi H, Kumagi T, et al: Virtual sonographic radiofrequency ablation of hepatocellular carcinoma visualized on CT but not on conventional sonography. AJR Am J Roentgenol 2006;186(5 suppl):S255–S260.
31 Minami Y, Chung H, Kudo M, et al: Radiofrequency ablation of hepatocellular carcinoma: value of virtual CT sonography with magnetic navigation. AJR Am J Roentgenol 2008; 190:W335–W341.
32 Minami Y, Kitai S, Kudo M: Treatment response assessment of radiofrequency ablation for hepatocellular carcinoma: usefulness of virtual CT sonography with magnetic navigation. Eur J Radiol 2012;81:e277–e280.
33 Numata K, Fukuda H, Morimoto M, et al: Use of fusion imaging combining contrast-enhanced ultrasonography with a perflubutane-based contrast agent and contrast-enhanced computed tomography for the evaluation of percutaneous radiofrequency ablation of hypervascular hepatocellular carcinoma. Eur J Radiol 2012;81:2746–2753.
34 Lee MW, Rhim H, Cha DI, et al: Percutaneous radiofrequency ablation of hepatocellular carcinoma: fusion imaging guidance for management of lesions with poor conspicuity at conventional sonography. AJR Am J Roentgenol 2012;198:1438–1444.
35 Song KD, Lee MW, Rhim H, et al: Fusion imaging-guided radiofrequency ablation for hepatocellular carcinomas not visible on conventional ultrasound. AJR Am J Roentgenol 2013;201:1141–1147.
36 Lin SM: Local ablation for hepatocellular carcinoma in Taiwan. Liver Cancer 2013;2:73–83.
37 Min JH, Lim HK, Lim S, et al: Radiofrequency ablation of very-early-stage hepatocellular carcinoma inconspicuous on fusion imaging with B-mode US: value of fusion imaging with contrast-enhanced US. Clin Mol Hepatol 2014;20:61–70.
38 Minami Y, Nishida N, Kudo M: Therapeutic response assessment of RFA for HCC: contrast-enhanced US, CT and MRI. World J Gastroenterol 2014;20:4160–4166.

Clinical Study

Oncology

Oncology 2014;87(suppl 1):63–72
DOI: 10.1159/000368147

Published online: November 22, 2014

Noninvasive Diagnosis of Liver Fibrosis: Utility of Data Mining of Both Ultrasound Elastography and Serological Findings to Construct a Decision Tree

Norihisa Yada[a] Masatoshi Kudo[a] Norifumi Kawada[b] Shuichi Sato[c] Yukio Osaki[d] Akihisa Ishikawa[e] Hisaaki Miyoshi[f] Michiie Sakamoto[g] Masayoshi Kage[h] Osamu Nakashima[i] Akiko Tonomura[j]

[a]Department of Gastroenterology and Hepatology, Kinki University School of Medicine, Osaka-Sayama, [b]Department of Hepatology, Graduate School of Medicine, Osaka City University, Osaka, [c]Department of Internal Medicine II, Shimane University School of Medicine, Shimane, [d]Department of Gastroenterology and Hepatology, Osaka Red Cross Hospital, Osaka, [e]Department of Internal Medicine, Hitachi General Hospital, Hitachi, [f]Department of Gastroenterology and Neurology, Faculty of Medicine, Kagawa University, Kagawa, [g]Department of Pathology, School of Medicine, Keio University, Tokyo, Departments of [h]Diagnostic Pathology and [i]Pathology, Kurume University School of Medicine, Kurume, and [j]Engineering R&D Department 1, Hitachi Aloka Medical, Ltd., Tokyo, Japan

Key Words

Data mining · Liver fibrosis · Liver fibrosis index · Real-time tissue elastography · Strain elastography

Abstract

Objective: Although liver biopsy is the gold standard for viral liver disease management, it is invasive and the sampling error rate is problematic. Real-time tissue elastography (RTE), a recently developed method of ultrasound elastography, can be used to assess liver fibrosis noninvasively but the overlap between fibrosis stages limits its ability to assess liver fibrosis adequately when used alone. ***Methods:*** A multicenter collaborative study involving 542 patients with chronic viral hepatitis and cirrhosis who were scheduled to undergo liver biopsy compared the image features obtained from RTE image analysis, the liver fibrosis index (LFI), and pathological diagnosis. RTE and a blood test were performed on the same day as the liver biopsy. Data mining was also performed to construct a decision tree, and its diagnostic performance for assessing liver fibrosis was evaluated. ***Results:*** The LFI was higher in patients with chronic hepatitis C (CHC) than in those with chronic hepatitis B (CHB). When a decision tree was constructed by data mining of RTE and serological findings, the diagnostic accuracy was very high for all fibrosis stages, with respective rates at F1, F2, F3, and F4 of 94.4, 54.1, 38.7, and 81.3% for patients with CHC and of 97.1, 50.0, 43.8, and 80.6% for patients with CHB. ***Conclusions:*** The variation in LFI values between the different etiologies appears to reflect the difference in the development style of liver fibrosis. The decision tree for assessing liver fibrosis constructed by data mining of both RTE and serological findings had a high diagnostic performance in assessing liver fibrosis and shows promising clinical utility.

KARGER

E-Mail karger@karger.com
www.karger.com/ocl

0030–2414/14/0877–0063$39.50/0

Prof. Masatoshi Kudo
Department of Gastroenterology and Hepatology
Kinki University School of Medicine
377-2 Ohno-Higashi, Osaka-Sayama, Osaka 589-8511 (Japan)
E-Mail m-kudo@med.kindai.ac.jp

Introduction

Spontaneous clearance of hepatitis C virus (HCV) almost never occurs once the infection has become chronic, so liver fibrosis progresses year after year and ultimately leads to cirrhosis in individuals with chronic hepatitis C (CHC) if they do not undergo antiviral therapy with agents such as interferons [1]. Viral hepatitis is a cause of hepatocarcinogenesis, and the incidence of liver cancer significantly increases as liver fibrosis progresses in CHC [2]. It is expected that the surveillance of liver cancer will improve detection rates of early-stage liver cancer and consequently improve prognosis through treatment, including local therapy, hepatectomy, and liver transplantation [3–9]. Liver fibrosis affects both the virus eradication rate and prognosis. Assessing liver fibrosis is therefore useful for determining the indication of treatment for viral hepatitis and predicting the risk of hepatocarcinogenesis, making it very important in clinical practice.

Liver biopsy is regarded as the gold standard for assessing liver fibrosis; however, it is an invasive technique that carries risks of bleeding and pain. Moreover, the biopsy sample evaluated is small, representing only 1/50,000 of the liver, so differences in assessment findings can arise depending on the site biopsied or the examining pathologist's judgment. One study that compared the pathological findings of liver biopsy with those of hepatectomy found a variation rate of approximately 30% [10].

Another useful assessment technique is ultrasound elastography, which noninvasively measures liver stiffness. Although liver stiffness is influenced by factors such as liver fibrosis and inflammation, it is correlated with the incidence of viral hepatocarcinogenesis, and studies have shown that the FibroScan is useful for the surveillance of liver cancer [5, 11–13]. Real-time tissue elastography (RTE), an ultrasound elastography with another measurement principle, noninvasively depicts the distortion in liver tissue caused by beating of the heart in real time; as liver fibrosis progresses, the percentage of blue low-strain areas and the textural disorganization increase [14, 15]. A verification study using a mechanical model of liver fibrosis suggested that changes in RTE images associated with the progression of liver fibrosis are seen because RTE is actually depicting liver fibrosis itself [16]. In addition, the liver fibrosis index (LFI), which is a multiple regression equation for assessing liver fibrosis using liver fibrosis estimates based on biopsy and RTE data obtained from patients with CHC and cirrhosis, is widely used as a technique for assessing liver fibrosis with RTE as it can be easily measured with RTE systems [17–20]. However, the LFI was developed based on data from patients with CHC and cirrhosis, and its usefulness for other etiologies has not been sufficiently discussed. Furthermore, the stage of fibrosis is often not completely clear when using the LFI in clinical practice, due to the large amount of overlap between the stages, so an assessment method with greater diagnostic accuracy is needed.

Against this background, in this study we examined differences between patients with CHC and chronic hepatitis B (CHB) by comparing image features from RTE image analysis, the LFI, and serological tests. We also constructed a decision tree by data mining both RTE and serological findings and evaluated its diagnostic performance for assessing liver fibrosis.

Patients and Methods

Patients

This was a multicenter collaborative study conducted at Kinki University Hospital, Osaka City University Hospital, Shimane University Hospital, Osaka Red Cross Hospital, Hitachi General Hospital, Kagawa University Hospital, Minami Wakayama Medical Center, Kumamoto Shinto General Hospital, Nagoya City University Hospital, Wakayama Medical University Hospital, Osaka Medical Center for Cancer and Cardiovascular Diseases, Ehime University Hospital, Takamatsu Red Cross Hospital, Tottori University Hospital, Yashiro General Hospital, Hyogo College of Medicine Hospital, and PL Hospital. Only patients chronically infected with either HCV or hepatitis B virus (HBV) were included (coinfected patients were excluded). The strain of hepatitis virus was determined based on whether a positive result was obtained when HCV-RNA and HBV-DNA were measured. Furthermore, patients who consumed ≥20 g of alcohol per day or had another type of chronic hepatitis such as primary biliary cirrhosis or autoimmune hepatitis were excluded. The study protocol conformed to the Declaration of Helsinki and was approved by the ethics committee of each participating institute. Informed consent to participate in the study was obtained from each patient.

Clinical and Laboratory Assessments

A blood test and RTE were performed on the same day as the liver biopsy. Aspartate aminotransferase (AST), alanine aminotransferase (ALT), gamma-glutamyl transpeptidase (GGT), total bilirubin (T-Bil), platelet count (PLT), prothrombin time (PT), international normalized ratio (INR), hyaluronic acid (HA), type IV collagen, type IV collagen 7S domain, type III procollagen N-peptide (P3P), and matrix metalloproteinase-3 (MMP3) were assessed using automated methods.

Histological Assessment

Percutaneous ultrasound-guided liver biopsy was performed on the right lobe with a Tru-Cut semiautomatic 16- or 18-gauge needle apparatus. The liver biopsy specimens were fixed in for-

malin, embedded in paraffin, and stained with hematoxylin and eosin, Masson's trichrome or Azan. All biopsy specimens were examined by 3 liver pathology experts who were blinded to the patient characteristics. Liver fibrosis was scored by the new Inuyama classification, the Japanese criteria for the histological assessment of chronic viral hepatitis [21]. The 3 pathologists assessed each case separately and differences in judgments were resolved by consensus. The stage of fibrosis was classified as follows: F0 = no fibrosis; F1 = fibrosis portal expansion; F2 = bridging fibrosis (portal-portal or portal-central linkage); F3 = bridging fibrosis with lobular distortion (disorganization), or F4 = cirrhosis.

Real-Time Tissue Elastography

The principle of RTE has been already reported by us [14, 15, 18–20, 22, 23]. Briefly, RTE was performed using ultrasonography (EUS-8500, HI-VISION 900, and HI-VISION Ascendus; Hitachi Aloka Medical, Tokyo, Japan) and the EUP-L52 linear probe (3–7 MHz; Hitachi Aloka Medical). Patients were examined in the spine position with the right arm in maximal abduction and were instructed to hold their breath. The examinations were performed on the right lobe through the intercostal spaces, with the transducer held firmly with no compression applied to the skin. The B-mode and static image superimposed on B-mode were both visualized in real time, enabling the optimal position to be easily selected. The region of interest of the strain image was 2.5 cm^2 and located about 1 cm below the surface of the liver. In addition, to obtain good images, scanning was performed to avoid large vessels and attenuation by the lungs and ribs. Videos comprising stable RTE images over ≥5 sequential heartbeats were saved 3 times. A reader blinded to patient characteristics selected 10 appropriate images from the saved videos using the electrocardiogram and strain graph as references and analyzed those images. As RTE is a technique for depicting relative strain, artifacts within the region of interest affect the results and therefore the reader selected images with few artifacts and then analyzed the areas without artifacts in these images. From each RTE image, 11 image features were extracted: mean relative strain value (MEAN); standard deviation of relative strain value (SD); percentage of low strain area (percentage of the blue colored area; %AREA); complexity of low strain area (calculated as square of perimeter divided by area; COM); skewness (SKEW); kurtosis (KURT); contrast (CON); entropy (ENT); textural complexity, inverse difference moment (IDM); angular second moment (ASM), and correlation (COR). LFI was calculated using a previously reported method [17–19].

Statistical Analysis

Descriptive statistics are shown as median and quartile, or percentage as appropriate. Differences in findings by etiology were evaluated using the nonparametric Mann-Whitney U test. Differences in findings by fibrosis stage were evaluated by multiple comparisons with Tukey's honestly significant difference test and trend analysis with the Jonckheere-Terpstra trend test. Differences were considered statistically significant at $p < 0.05$. The diagnostic performance for liver fibrosis was determined in terms of sensitivity, specificity, positive predictive value, negative predictive value, diagnostic accuracy, and area under the receiver operating characteristic curve (AUROC). All analyses were performed using SPSS Statistics 20 (IBM, Armonk, N.Y., USA).

Results

Demographics and Baseline Features

A total of 542 patients with good RTE images, good samples from liver biopsy, and with liver fibrosis were included in the analysis. The pathological diagnosis was HCV in 414 patients (F1: 179, F2: 98, F3: 62, and F4: 75) and HBV in 128 patients (F1: 69, F2: 12, F3: 16, and F4: 31).

Comparison of Serological Markers and Pathological Diagnosis

In the HCV-infected patients, as the stage of fibrosis progressed, a significant increasing trend was seen for AST, ALT, GGT, T-Bil, INR, HA, type IV collagen, type IV collagen 7S, and P3P ($p < 0.0001$), a significant decreasing trend was seen for PLT ($p < 0.0001$), and no significant trend was seen for MMP3 ($p = 0.565$). In the HBV-infected patients, as the stage of fibrosis progressed, a significant increasing trend was seen for GGT, INR, HA, type IV collagen, and type IV collagen 7S ($p < 0.0001$), a significant decreasing trend was seen for PLT ($p < 0.0001$), and no significant trend was seen for AST, ALT, T-Bil, P3P, and MMP3 ($p = 0.565$) (tables 1, 2).

Relationship between Liver Fibrosis Stage, RTE Image Features and LFI

As the stage of fibrosis progressed in the HCV-infected patients, a significant decreasing trend was seen for MEAN ($p < 0.0001$), a significant increasing trend was seen for SD, AREA, COM, CON, and SKEW ($p < 0.0001$), and no significant trend was seen for ASM, COR, ENT, IDM, and KURT. As the stage of fibrosis progressed in the HBV-infected patients, a significant decreasing trend was seen for MEAN ($p < 0.0001$), a significant increasing trend was seen for SD, AREA, COM, CON, and SKEW ($p < 0.0001$) as well as for KURT ($p = 0.001$), and no significant trend was seen for ASM, COR, ENT, and IDM.

A significant increasing trend was seen for the LFI in both HCV- and HBV-infected patients ($p < 0.0001$). Multiple comparisons between stages of fibrosis revealed a significant difference in the LFI between all stages of fibrosis in HCV-infected patients (F1 vs. F2, F1 vs. F3, F1 vs. F4, F2 vs. F3, F2 vs. F4, and F3 vs. F4). In HBV-infected patients, however, the only significant differences were between F1/F4 and F2/F4 (table 3).

Comparison of the LFI between HCV and HBV

When the LFI was compared between HCV- and HBV-infected patients at each stage of fibrosis, it was

Oncology 2014;87(suppl 1):63–72
DOI: 10.1159/000368147

Table 1. Comparison of serological markers and pathological fibrosis diagnosis

	HCV				p value	HBV				p value
	F1 (n = 179)	F2 (n = 98)	F3 (n = 62)	F4 (n = 75)		F1 (n = 69)	F2 (n = 12)	F3 (n = 16)	F4 (n = 31)	
Serum markers										
AST, IU/ml	33.0 (24.0, 51.0)	46.0 (30.0, 71.0)	66.5 (45.3, 111.0)	59.0 (44.0, 89.0)	<0.0001	33.0 (23.0, 58.5)	51.0 (21.0, 138.0)	43.5 (26.3, 80.0)	36.0 (25.3, 45.8)	0.619
ALT, IU/ml	38.0 (24.0, 56.0)	51.0 (29.0, 92.0)	66.5 (45.3, 117.0)	52.0 (32.0, 94.0)	<0.0001	34.0 (19.0, 110.0)	93.0 (23.0, 165.0)	58.5 (22.0, 74.3)	31.5 (17.8, 46.8)	0.315
GGT, IU/ml	29.0 (19.0, 57.0)	37.0 (22.0, 65.0)	43.5 (29.0, 69.5)	43.0 (25.0, 62.0)	<0.0001	26.0 (16.0, 46.5)	35.0 (18.0, 40.0)	57.0 (36.0, 89.8)	42.5 (26.5, 120.0)	<0.0001
T-Bil, mg/dl	0.70 (0.05, 0.90)	0.70 (0.50, 0.90)	0.75 (0.60, 1.08)	0.90 (0.70, 1.45)	<0.0001	0.60 (0.50, 0.85)	0.70 (0.60, 0.80)	0.70 (0.53, 0.98)	0.90 (0.60, 1.70)	0.005
PLT	19.4 (15.3, 22.2)	16.5 (12.3, 19.7)	12.8 (9.53, 16.2)	9.2 (6.6, 12.7)	<0.0001	20.4 (16.5, 26.9)	18.0 (15.1, 19.8)	15.6 (14.3, 19.8)	10.7 (7.8, 15.1)	<0.0001
INR	0.98 (0.94, 1.02)	1.02 (0.96, 1.06)	1.07 (1.01, 1.11)	1.14 (1.08, 1.23)	<0.0001	1.02 (0.99, 1.06)	1.06 (0.98, 1.10)	1.05 (0.99, 1.13)	1.10 (1.02, 1.14)	<0.0001
HA, ng/ml	38.0 (25.2, 75.8)	71.0 (41.0, 115.0)	233.2 (89.0, 413.0)	314.1 (170.8, 513.3)	<0.0001	26.8 (19.3, 45.1)	39.0 (25.0, 90.0)	87.1 (34.8, 148.0)	109.5 (83.2, 193.3)	<0.0001
Collagen type, ng/ml										
IV	116.0 (93.5, 145.5)	126.0 (96.5, 158.0)	181.0 (141.3, 232.0)	246.0 (174.0, 312.0)	<0.0001	104.0 (90.0, 125.5)	124.0 (79.3, 155.8)	153.5 (100.3, 224.8)	171.0 (119.0, 193.0)	<0.0001
IV 7S	4.4 (3.7, 5.2)	5.3 (4.4, 6.1)	7.2 (5.7, 8.9)	8.6 (7.0, 11.0)	<0.0001	4.0 (3.5, 4.9)	4.4 (3.8, 5.4)	5.7 (4.2, 6.7)	5.8 (5.0, 7.1)	<0.0001
P3P, U/ml	0.79 (0.66, 0.90)	0.80 (0.71, 1.00)	1.05 (0.83, 1.30)	1.10 (0.90, 1.30)	<0.0001	0.58 (0.50, 0.70)	0.84 (0.65, 0.94)	0.63 (0.48, 0.81)	0.63 (0.51, 0.77)	0.201
MMP3, ng/ml	37.7 (25.6, 58.1)	34.3 (27.0, 50.4)	40.2 (24.6, 52.7)	39.0 (32.5, 55.9)	0.565	36.7 (21.2, 46.0)	51.3 (28.0, 64.1)	62.9 (37.7, 80.7)	41.1 (28.5, 51.1)	0.152

Values are presented as median (first quartile, third quartile). The p values were calculated with the Jonckheere-Terpstra trend test.

Table 2. Comparison of serological markers and etiology

	F1		p value	F2		p value	F3		p value	F4		p value
	HCV (n = 179)	HBV (n = 69)		HCV (n = 98)	HBV (n = 12)		HCV (n = 62)	HBV (n = 16)		HCV (n = 75)	HBV (n = 31)	
Serum markers												
AST, IU/ml	33.0 (24.0, 51.0)	33.0 (23.0, 58.5)	0.941	46.0 (30.0, 71.0)	51.0 (21.0, 138.0)	0.767	66.5 (45.3, 111.0)	43.5 (26.3, 80.0)	0.049	59.0 (44.0, 89.0)	36.0 (25.3, 45.8)	0.000
ALT, IU/ml	38.0 (24.0, 56.0)	34.0 (19.0, 110.0)	0.776	51.0 (29.0, 92.0)	93.0 (23.0, 165.0)	0.497	66.5 (45.3, 117.0)	58.5 (22.0, 74.3)	0.202	52.0 (32.0, 94.0)	31.5 (17.8, 46.8)	0.000
GGT, IU/ml	29.0 (19.0, 57.0)	26.0 (16.0, 46.5)	0.110	37.0 (22.0, 65.0)	35.0 (18.0, 40.0)	0.431	43.5 (29.0, 69.5)	57.0 (36.0, 89.8)	0.263	43.0 (25.0, 62.0)	42.5 (26.5, 120.0)	0.394
T-Bil, mg/dl	0.70 (0.05, 0.90)	0.60 (0.50, 0.85)	0.694	0.70 (0.50, 0.90)	0.70 (0.60, 0.80)	0.991	0.75 (0.60, 1.08)	0.70 (0.53, 0.98)	0.891	0.90 (0.70, 1.45)	0.90 (0.60, 1.70)	0.832
PLT	19.4 (15.3, 22.2)	20.4 (16.5, 26.9)	0.030	16.5 (12.3, 19.7)	18.0 (15.1, 19.8)	0.380	12.8 (9.53, 16.2)	15.6 (14.3, 19.8)	0.056	9.2 (6.6, 12.7)	10.7 (7.8, 15.1)	0.078
INR	0.98 (0.94, 1.02)	1.02 (0.99, 1.06)	0.000	1.02 (0.96, 1.06)	1.06 (0.98, 1.10)	0.108	1.07 (1.01, 1.11)	1.05 (0.99, 1.13)	0.741	1.14 (1.08, 1.23)	1.10 (1.02, 1.14)	0.018
HA, ng/ml	38.0 (25.2, 75.8)	26.8 (19.3, 45.1)	0.002	71.0 (41.0, 115.0)	39.0 (25.0, 90.0)	0.091	233.2 (89.0, 413.0)	87.1 (34.8, 148.0)	0.016	314.1 (170.8, 513.3)	109.5 (83.2, 193.3)	0.000
Collagen type, ng/ml												
IV	116.0 (93.5, 145.5)	104.0 (90.0, 125.5)	0.136	126.0 (96.5, 158.0)	124.0 (79.3, 155.8)	0.879	181.0 (141.3, 232.0)	153.5 (100.3, 224.8)	0.331	246.0 (174.0, 312.0)	171.0 (119.0, 193.0)	0.002
IV 7S	4.4 (3.7, 5.2)	4.0 (3.5, 4.9)	0.035	5.3 (4.4, 6.1)	4.4 (3.8, 5.4)	0.123	7.2 (5.7, 8.9)	5.7 (4.2, 6.7)	0.020	8.6 (7.0, 11.0)	5.8 (5.0, 7.1)	0.000
P3P, U/ml	0.79 (0.66, 0.90)	0.58 (0.50, 0.70)	0.000	0.80 (0.71, 1.00)	0.84 (0.65, 0.94)	0.698	1.05 (0.83, 1.30)	0.63 (0.48, 0.81)	0.001	1.10 (0.90, 1.30)	0.63 (0.51, 0.77)	0.000
MMP3, ng/ml	37.7 (25.6, 58.1)	36.7 (21.2, 46.0)	0.217	34.3 (27.0, 50.4)	51.3 (28.0, 64.1)	0.177	40.2 (24.6, 52.7)	62.9 (37.7, 80.7)	0.030	39.0 (32.5, 55.9)	41.1 (28.5, 51.1)	0.542

Values are presented as median (first quartile, third quartile). The p values were calculated with the Mann-Whitney U test.

Table 3. Relationship between liver fibrosis stage, RTE image features and LFI

	HCV				p value	HBV				p value
	F1 (n = 179)	F2 (n = 98)	F3 (n = 62)	F4 (n = 75)		F1 (n = 69)	F2 (n = 12)	F3 (n = 16)	F4 (n = 31)	
RTE features										
MEAN	113.9 (107.2, 119.9)	109.6 (102.2, 115.1)	103.0 (94.8, 111.6)	93.4 (82.5, 105.0)	<0.0001	117.8 (107.4, 122.3)	119.0 (112.7, 121.8)	108.6 (103.1, 116.5)	101.4 (87.7, 109.7)	<0.0001
SD	52.3 (45.9, 58.7)	57.3 (50.6, 60.7)	59.6 (54.7, 63.4)	60.9 (57.6, 63.9)	<0.0001	49.1 (44.6, 56.9)	50.6 (44.6, 54.2)	57.3 (52.2, 61.5)	63.4 (56.9, 65.1)	<0.0001
AREA	14.2 (7.6, 20.8)	19.1 (11.8, 27.2)	25.2 (16.3, 33.7)	34.5 (22.5, 44.2)	<0.0001	11.2 (6.2, 19.2)	11.3 (6.2, 16.2)	20.6 (13.5, 27.7)	29.0 (19.8, 39.2)	<0.0001
COM	20.3 (18.5, 24.1)	22.8 (19.8, 26.2)	25.2 (21.3, 29.9)	31.3 (24.6, 40.2)	<0.0001	20.1 (18.5, 25.8)	20.7 (19.6, 21.8)	24.5 (21.3, 30.2)	28.9 (23.6, 34.5)	<0.0001
ASM	0.00025 (0.00019, 0.00035)	0.00020 (0.00017, 0.00032)	0.000212 (0.000178, 0.000315)	0.000294 (0.000190, 0.000453)	0.983	0.000209 (0.000183, 0.000268)	0.000196 (0.000170, 0.000220)	0.000177 (0.000175, 0.000188)	0.000213 (0.000177, 0.000285)	0.159
CON	229.6 (173.4, 268.6)	250.0 (206.9, 309.0)	261.2 (213.5, 324.0)	266.7 (233.8, 320.7)	<0.0001	221.7 (18.08, 285.2)	239.1 (198.4, 283.7)	272.2 (250.7, 279.0)	294.1 (249.1, 372.2)	<0.0001
COR	0.958 (0.947, 0.965)	0.958 (0.950, 0.966)	0.957 (0.950, 0.967)	0.962 (0.951, 0.966)	0.117	0.953 (0.944, 0.959)	0.946 (0.943, 0.955)	0.956 (0.947, 0.961)	0.954 (0.945, 0.968)	0.139
ENT	3.83 (3.76, 3.87)	3.85 (3.80, 3.89)	3.86 (3.81, 3.89)	3.84 (3.76, 3.88)	0.052	3.81 (3.74, 3.86)	3.80 (3.77, 3.86)	3.86 (3.84, 3.88)	3.84 (3.80, 3.89)	0.024
IDM	0.110 (0.095, 0.122)	0.101 (0.091, 0.117)	0.096 (0.091, 0.118)	0.108 (0.093, 0.122)	0.154	0.100 (0.091, 0.111)	0.092 (0.088, 0.100)	0.092 (0.089, 0.095)	0.100 (0.087, 0.106)	0.147
SKEW	0.199 (0.071, 0.300)	0.253 (0.122, 0.361)	0.332 (0.178, 0.461)	0.429 (0.321, 0.679)	<0.0001	0.116 (–0.517, 0.260)	0.124 (0.025, 0.219)	0.236 (0.178, 0.289)	0.376 (0.213, 0.540)	<0.0001
KURT	2.38 (2.24, 2.57)	2.34 (2.22, 2.48)	2.29 (2.20, 2.40)	2.34 (2.23, 2.64)	0.334	2.49 (2.31, 2.68)	2.48 (2.31, 2.63)	2.33 (2.29, 2.43)	2.33 (2.19, 2.47)	0.001
LFI	1.81 (1.41, 2.22)	2.10 (1.67, 2.56)	2.47 (1.97, 2.88)	2.97 (2.41, 3.45)	<0.0001	1.52 (1.16, 2.06)	1.61 (1.31, 1.84)	2.16 (1.66, 2.58)	2.66 (2.15, 3.13)	<0.0001

Values are presented as median (first quartile, third quartile). The p values were calculated with the Jonckheere-Terpstra trend test.

Oncology 2014;87(suppl 1):63–72
DOI: 10.1159/000368147

Table 4. Relationship between etiology, RTE image features and LFI

	F1		p value	F2		p value	F3		p value	F4		p value
	HCV (n = 179)	HBV (n = 69)		HCV (n = 98)	HBV (n = 12)		HCV (n = 62)	HBV (n = 16)		HCV (n = 75)	HBV (n = 31)	
RTE features												
MEAN	113.9 (107.2, 119.9)	117.8 (107.4, 122.3)	0.012	109.6 (102.2, 115.1)	119.0 (112.7, 121.8)	0.003	103.0 (94.8, 111.6)	108.6 (103.1, 116.5)	0.033	93.4 (82.5, 105.0)	101.4 (87.7, 109.7)	0.057
SD	52.3 (45.9, 58.7)	49.1 (44.6, 56.9)	0.091	57.3 (50.6, 60.7)	50.6 (44.6, 54.2)	0.006	59.6 (54.7, 63.4)	57.3 (52.2, 61.5)	0.162	60.9 (57.6, 63.9)	63.4 (56.9, 65.1)	0.395
AREA	14.2 (7.6, 20.8)	11.2 (6.2, 19.2)	0.121	19.1 (11.8, 27.2)	11.3 (6.2, 16.2)	0.010	25.2 (16.3, 33.7)	20.6 (13.5, 27.7)	0.055	34.5 (22.5, 44.2)	29.0 (19.8, 39.2)	0.109
COM	20.3 (18.5, 24.1)	20.1 (18.5, 25.8)	0.985	22.8 (19.8, 26.2)	20.7 (19.6, 21.8)	0.114	25.2 (21.3, 29.9)	24.5 (21.3, 30.2)	0.757	31.3 (24.6, 40.2)	28.9 (23.6, 34.5)	0.186
ASM	0.00025 (0.00019, 0.00035)	0.000209 (0.000183, 0.000268)	0.008	0.00020 (0.00017, 0.00032)	0.000196 (0.000170, 0.000220)	0.242	0.000212 (0.000178, 0.000315)	0.000177 (0.000175, 0.000188)	0.006	0.000294 (0.000190, 0.000453)	0.000213 (0.000177, 0.000285)	0.027
CON	229.6 (173.4, 268.6)	221.7 (18.08, 285.2)	0.484	250.0 (206.9, 309.0)	239.1 (198.4, 283.7)	0.673	261.2 (213.5, 324.0)	272.2 (250.7, 279.0)	0.488	266.7 (233.8, 320.7)	294.1 (249.1, 372.2)	0.117
COR	0.958 (0.947, 0.965)	0.953 (0.944, 0.959)	0.003	0.958 (0.950, 0.966)	0.946 (0.943, 0.955)	0.004	0.957 (0.950, 0.967)	0.956 (0.947, 0.961)	0.245	0.962 (0.951, 0.966)	0.954 (0.945, 0.968)	0.534
ENT	3.83 (3.76, 3.87)	3.81 (3.74, 3.86)	0.238	3.85 (3.80, 3.89)	3.80 (3.77, 3.86)	0.153	3.86 (3.81, 3.89)	3.86 (3.84, 3.88)	0.990	3.84 (3.76, 3.88)	3.84 (3.80, 3.89)	0.629
IDM	0.110 (0.095, 0.122)	0.100 (0.091, 0.111)	0.002	0.101 (0.091, 0.117)	0.092 (0.088, 0.100)	0.071	0.096 (0.091, 0.118)	0.092 (0.089, 0.095)	0.026	0.108 (0.093, 0.122)	0.100 (0.087, 0.106)	0.019
SKEW	0.199 (0.071, 0.300)	0.116 (–0.517, 0.260)	0.015	0.253 (0.122, 0.361)	0.124 (0.025, 0.219)	0.039	0.332 (0.178, 0.461)	0.236 (0.178, 0.289)	0.065	0.429 (0.321, 0.679)	0.376 (0.213, 0.540)	0.083
KURT	2.38 (2.24, 2.57)	2.49 (2.31, 2.68)	0.005	2.34 (2.22, 2.48)	2.48 (2.31, 2.63)	0.034	2.29 (2.20, 2.40)	2.33 (2.29, 2.43)	0.158	2.34 (2.23, 2.64)	2.33 (2.19, 2.47)	0.200
LFI	1.81 (1.41, 2.22)	1.52 (1.16, 2.06)	0.029	2.10 (1.67, 2.56)	1.61 (1.31, 1.84)	0.010	2.47 (1.97, 2.88)	2.16 (1.66, 2.58)	0.051	2.97 (2.41, 3.45)	2.66 (2.15, 3.13)	0.042

Values are presented as median (first quartile, third quartile). The p values were calculated with the Mann-Whitney U test.

Table 5. Diagnostic performance of the LFI for liver fibrosis assessment

	HCV			HBV		
	F4	>F3	>F2	F4	>F3	>F2
AUROC	0.803	0.774	0.73	0.821	0.806	0.744
Cutoff	2.45	2.42	2.31	2.07	1.94	1.91
Positive predictive value	37.8	58.2	58.7	80.6	78.7	66.1
Negative predictive value	92.9	81.6	79.9	71.1	75.3	72.5
Intensity	74.7	65	79.3	47.2	64.9	67.2
Specificity	72.9	76.9	59.6	92	85.9	71.4
Accuracy	73.2	72.2	67.9	73.4	76.6	69.5

found to be significantly higher in HCV-infected patients at stages F1, F2, and F4 (F1: HCV = 181, HBV = 1.52, p = 0.029; F2: HCV = 2.10, HBV = 1.61, p = 0.010; F4: HCV = 2.97, HBV = 2.66, p = 0.042) and marginally higher in HCV-infected patients at stage F3 (HCV = 2.47, HBV = 2.16, p = 0.051) (table 4).

AUROC Analysis

The LFI cutoff values for each stage of fibrosis were calculated by AUROC analysis to evaluate the diagnostic performance of the LFI for liver fibrosis assessment. In HCV-infected patients, the diagnostic accuracy was 73.2 at F4, 72.2 at ≥F3, and 67.9 at ≥F2. In HBV-infected patients, the diagnostic accuracy was 73.4 at F4, 76.6 at ≥F3, and 69.5 at ≥F2 (table 5).

Data Mining Analysis

The LFI is the numerical value calculated from HCV. Therefore, by using the LFI and the serological findings for HCV as well as the 11 feature values of RTE and the serological findings for HBV, the decision tree was calculated. The HCV decision tree, which comprises LFI, AST, ALT, GGT, T-Bil, PLT, HA, and type IV collagen, had a diagnostic accuracy of 94.4% for F1, 54.1% for F2, 38.7% for F3, and 81.3% for F4. The HBV decision tree, which comprises COM, CON, IDM, ALT, PLT, INR, and HA, had a diagnostic accuracy of 97.1% for F1, 50.0% for F2, 43.8% for F3, and 80.6% for F4 (fig. 1; table 6).

Discussion

The LFI, which is a multiple regression equation for assessing liver fibrosis using liver fibrosis estimates from biopsy and RTE image feature values obtained from patients with CHC or cirrhosis, is widely used as the primary diagnostic technique with RTE as it can easily be measured with RTE diagnostic equipment. However, few studies have examined differences in RTE images or the LFI due to differences in etiology, and the usefulness of the LFI for etiologies other than HCV has not been sufficiently discussed. In this study, we found that the LFI was significantly higher in HCV- than in HBV-infected patients with the same stage of fibrosis. This was likely influenced by differences in how fibrosis progresses in these etiologies. Specifically, HCV-infected patients develop micronodular cirrhosis, whereas HBV-infected patients develop macronodular cirrhosis. However, in criteria for evaluating pathological fibrosis in viral liver diseases (e.g., the new Inuyama classification), the stage of fibrosis is based on the area where fibrosis develops rather than the amount of fibrosis present. In essence, the amount of fibrosis per unit of area would be higher in HCV- than in HBV-infected patients with the same stage of fibrosis because the progression of HCV-related fibrosis is micronodular, thereby making the LFI higher as well. When using the LFI, the etiology of the patient must be confirmed before assessing the fibrosis stage.

Although evaluation using AUROC yields a somewhat high diagnostic accuracy for liver fibrosis assessment by the LFI, the stage of fibrosis when using LFI alone in clinical practice is often not exactly clear due to the large amount of overlap in the LFI between stages. Whereas AUROC can be used only to evaluate the diagnostic performance of assessment between two choices, namely ≥F2/F1, ≥F3/≤F2 or F4/≤F3, the decision tree can assess the exact stage of fibrosis (i.e., F1, F2, F3 or F4). Furthermore, the decision tree constructed in this study can be used to determine the specific stage of liver fibrosis based on etiology, serological findings, and RTE findings with very high diagnostic accuracy of each fibrosis stage, suggesting its utility in clinical practice as well. However, the sample size in the F2

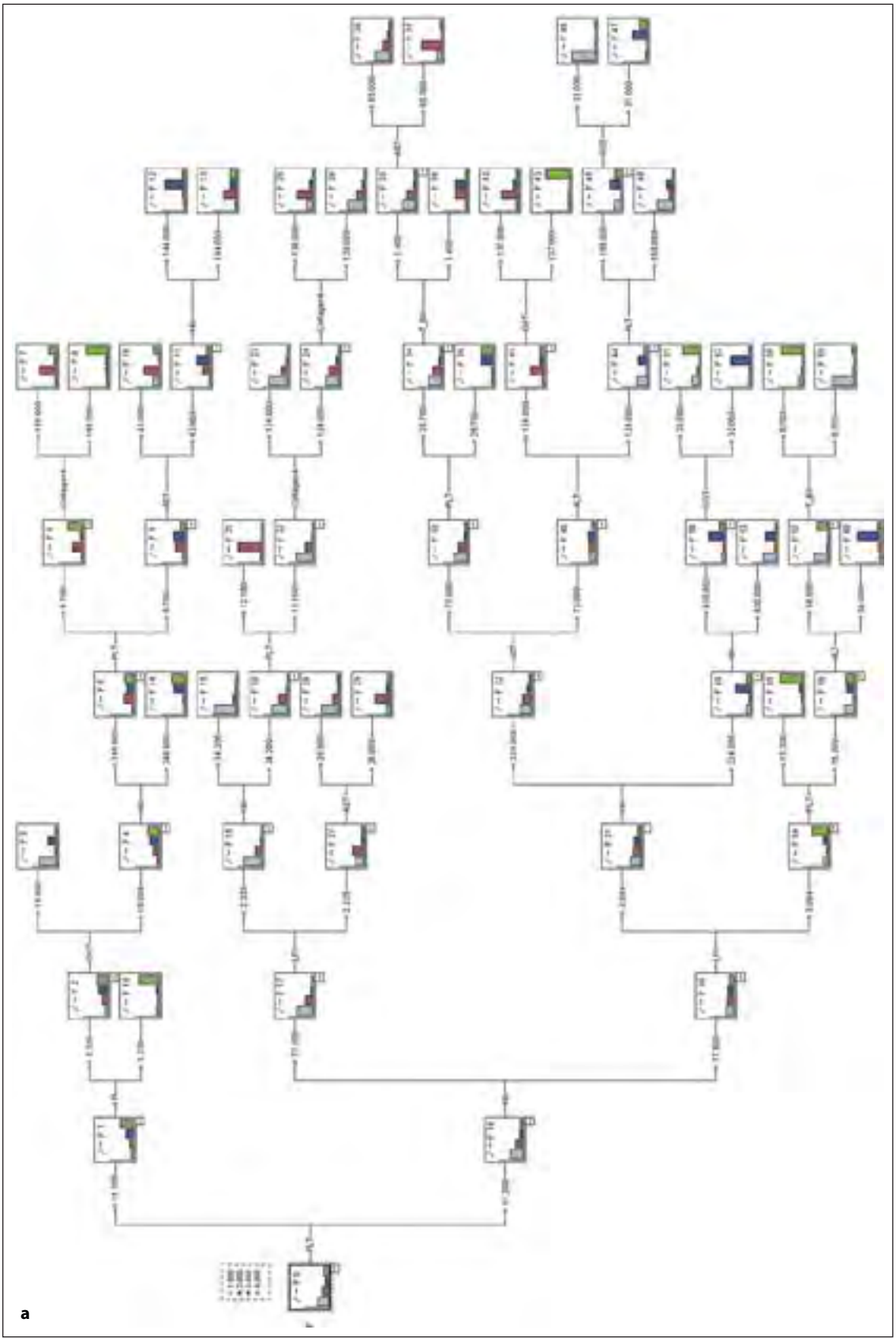

1 a

Color version available online

(For legend see next page.)

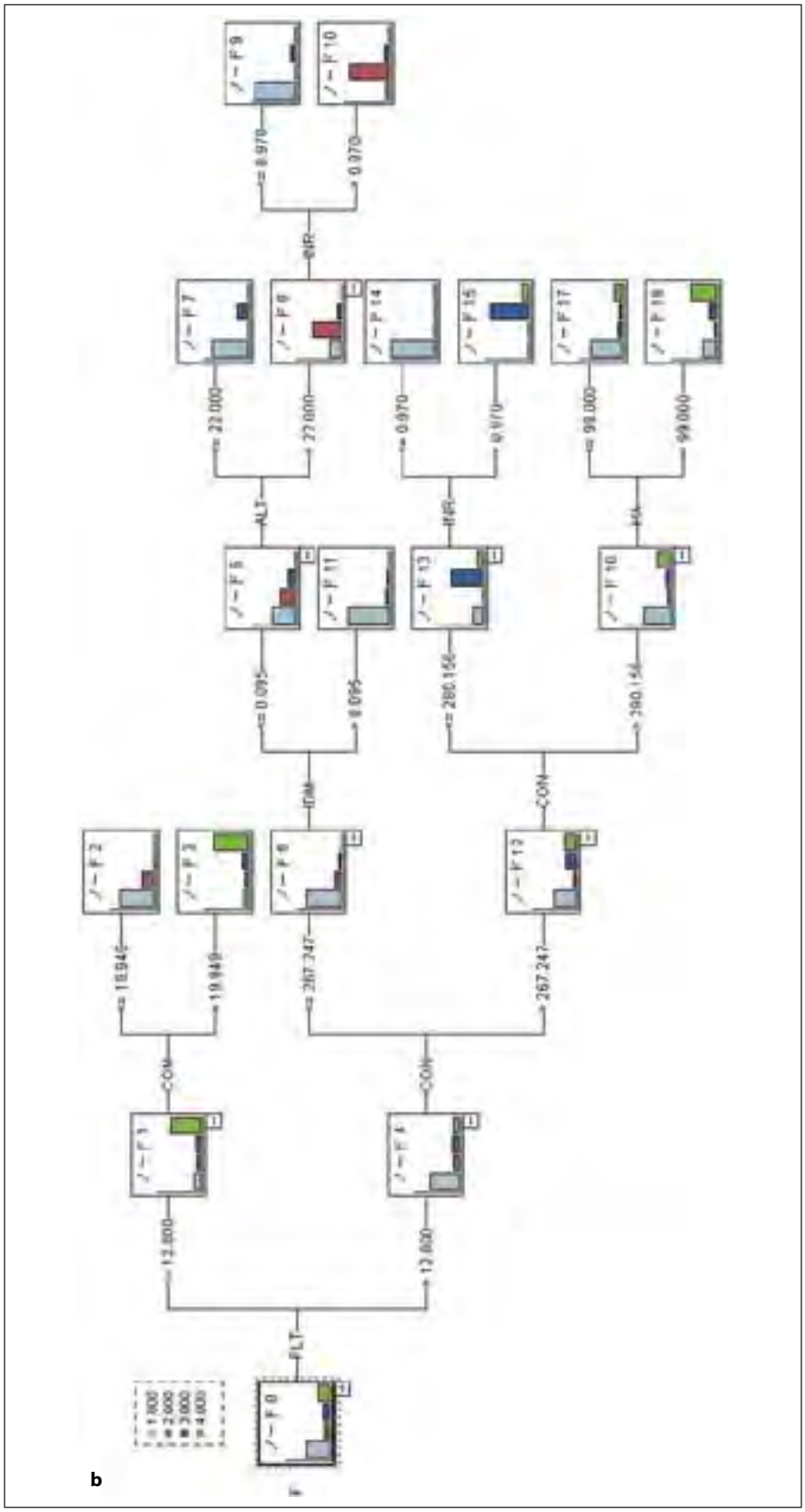

Color version available online

Fig. 1. Data mining for the diagnosis of the fibrosis stage in chronic viral hepatitis: fibrosis diagnosis of CHC (**a**) and CHB (**b**). Each bar graph shows the percentage of cases. The pale blue, red, blue, and green bars represent F1, F2, F3, and F4 fibrosis stage, respectively (colors refer to the online version only). T_Bil = Total bilirubin; Collagen4 = type IV collagen.

Table 6. Diagnostic performance of data mining with both ultrasound elastography and serological findings

	Data mining diagnosis							
	HCV				HBV			
	F1	F2	F3	F4	F1	F2	F3	F4
Pathological diagnosis								
F1	169 (94.4)	8 (4.5)	0	2 (1.1)	67 (97.1)	0	0	2 (2.9)
F2	42 (42.9)	53 (54.1)	1 (1.0)	2 (2.0)	5 (41.7)	6 (50)	0	1 (8.3)
F3	10 (16.1)	10 (16.1)	24 (38.7)	18 (29.0)	6 (37.5)	0	7 (43.8)	3 (18.8)
F4	3 (4.0)	6 (8.0)	5 (6.7)	61 (81.3)	5 (16.1)	0	1 (3.2)	25 (80.6)

Values are presented as n (%).

or F3 stage is too small both in HCV and HBV, which seems to be the reason of low accuracy of the F2 and F3 fibrosis stage.

In this study, we used the gold standard method of assessing liver fibrosis stage with samples obtained by liver biopsy, but, as mentioned previously, sampling error is more likely with an assessment by liver biopsy than with an assessment of hepatectomy specimens. Therefore, to construct a more accurate decision tree, it would be ideal to make the pathological diagnosis based on the hepatectomy specimens. Furthermore, it is also necessary to try to eliminate discrepancies in assessment between readers, for example, by adding computer-aided pathological diagnosis. In light of these issues, further research must be conducted to enable ultrasound elastography to be used as a tool for obtaining a more accurate diagnosis in clinical practice.

Acknowledgements

This study was supported by Health and Labour Sciences Research Grants for the Research on Hepatitis from the Japanese Ministry of Health, Labour and Welfare. The authors thank those who conducted the patient enrollment, namely Kenji Fujimoto (Division of Clinical Research and Department of Internal Medicine, Minami Wakakayama Medical Center, Tanabe, Japan), Shiho Miyase (Department of Gastroenterology and Hepatology, Kumamoto Shinto General Hospital, Kumamoto, Japan), Shunsuke Nojiri (Department of Gastroenterology and Metabolism, Nagoya City University Graduate School of Medical Sciences, Nagoya, Japan), Hideyuki Tamai (Second Department of Internal Medicine, Wakayama Medical University, Wakayama, Japan), Kazuho Imanaka (Department of Hepatobiliary and Pancreatic Oncology, Osaka Medical Center for Cancer and Cardiovascular Diseases, Osaka, Japan), Kazuyoshi Ohkawa (Department of Hepatobiliary and Pancreatic Oncology, Osaka Medical Center for Cancer and Cardiovascular Diseases, Osaka, Japan), Yoichi Hiasa (Department of Gastroenterology and Metabology, Ehime University Graduate School of Medicine, Toon, Japan), Chikara Ogawa (Department of Gastroenterology, Takamatsu Red Cross Hospital, Takamatsu, Japan), Masahiko Koda (Division of Medicine and Clinical Science, Department of Multidisciplinary Internal Medicine, Tottori University School of Medicine, Yonago, Japan), Shuichi Miyase (Department of Gastroenterology, Yatsushiro General Hospital, Yatsushiro, Japan), and Hiroko Iijima (Division of Hepatobiliary and Pancreatic Diseases, Department of Internal Medicine, Hyogo College of Medicine, Nishinomiya, Japan), and Katsuhiko Fukuda (Department of Gastroenterology, PL Hospital, Tondabayashi, Japan).

Disclosure Statement

The authors declare that no financial or other conflicts of interest exist in relation to the content of this article.

References

1 Shiratori Y, Imazeki F, Moriyama M, Yano M, Arakawa Y, Yokosuka O, Kuroki T, Nishiguchi S, Sata M, Yamada G, Fujiyama S, Yoshida H, Omata M: Histologic improvement of fibrosis in patients with hepatitis C who have sustained response to interferon therapy. Ann Intern Med 2000;132:517–524.

2 Yoshida H, Shiratori Y, Moriyama M, Arakawa Y, Ide T, Sata M, Inoue O, Yano M, Tanaka M, Fujiyama S, Nishiguchi S, Kuroki T, Imazeki F, Yokosuka O, Kinoyama S, Yamada G, Omata M: Interferon therapy reduces the risk for hepatocellular carcinoma: national surveillance program of cirrhotic and noncirrhotic patients with chronic hepatitis C in Japan. IHIT study group. Inhibition of Hepatocarcinogenesis by Interferon Therapy. Ann Intern Med 1999;131:174–181.

3 Kim DY, Han KH: Epidemiology and surveillance of hepatocellular carcinoma. Liver Cancer 2012;1:2–14.
4 Kudo M: Early hepatocellular carcinoma: definition and diagnosis. Liver Cancer 2013;2:69–72.
5 Kudo M: Prediction of hepatocellular carcinoma incidence risk by ultrasound elastography. Liver Cancer 2014;3:1–5.
6 Belghiti J, Fuks D: Liver resection and transplantation in hepatocellular carcinoma. Liver Cancer 2012;1:71–82.
7 Chan SC: Liver transplantation for hepatocellular carcinoma. Liver Cancer 2013;2:338–344.
8 Kudo M: Japan's successful model of nationwide hepatocellular carcinoma surveillance highlighting the urgent need for global surveillance. Liver Cancer 2012;1:141–143.
9 Lin SM: Local ablation for hepatocellular carcinoma in Taiwan. Liver Cancer 2013;2:73–83.
10 Bedossa P, Carrat F: Liver biopsy: the best, not the gold standard. J Hepatol 2009;50:1–3.
11 Masuzaki R, Tateishi R, Yoshida H, Yoshida H, Sato S, Kato N, Kanai F, Sugioka Y, Ikeda H, Shiina S, Kawabe T, Omata M: Risk assessment of hepatocellular carcinoma in chronic hepatitis C patients by transient elastography. J Clin Gastroenterol 2008;42:839–843.
12 Masuzaki R, Tateishi R, Yoshida H, Goto E, Sato T, Ohki T, Imamura J, Goto T, Kanai F, Kato N, Ikeda H, Shiina S, Kawabe T, Omata M: Prospective risk assessment for hepatocellular carcinoma development in patients with chronic hepatitis C by transient elastography. Hepatology 2009;49:1954–1961.
13 Jung KS, Kim SU, Ahn SH, Park YN, Kim do Y, Park JY, Chon CY, Choi EH, Han KH: Risk assessment of hepatitis B virus-related hepatocellular carcinoma development using liver stiffness measurement (fibroscan). Hepatology 2011;53:885–894.
14 Fujimoto K, Wada S, Oshita M, Kato M, Tonomura A, Mitake T: Non-invasive evaluation of hepatic fibrosis in patients with chronic hepatitis C using elastography. Medix 2007;(suppl):24–27.
15 Tatsumi C, Kudo M, Ueshima K, Kitai S, Takahashi S, Inoue T, Minami Y, Chung H, Maekawa K, Fujimoto K, Akiko T, Takeshi M: Noninvasive evaluation of hepatic fibrosis using serum fibrotic markers, transient elastography (FibroScan) and real-time tissue elastography. Intervirology 2008;51(suppl 1):27–33.
16 Shiina T, Maki T, Yamakawa M, Mitake T, Kudo M, Fujimoto K: Mechanical model analysis for quantitative evaluation of liver fibrosis based on ultrasound tissue elasticity imaging. Jpn J Appl Phys 2012;51:1–8.
17 Fujimoto K, Kato M, Tonomura A, Yada N, Tatsumi C, Oshita M, Wada S, Ueshima K, Ishida T, Furuta T, Yamasaki M, Tsujimoto M, Motoki M, Mitake T, Shiina T, Kudo M, Hayashi N: Non-invasive evaluation method of the liver fibrosis using real-time tissue elastography – usefulness of judgment liver fibrosis stage by liver fibrosis index (LF index) (in Japanese). Kanzo 2010;59:539–541.
18 Fujimoto K, Kato M, Kudo M, Yada N, Shiina T, Ueshima K, Yamada Y, Ishida T, Azuma M, Yamasaki M, Yamamoto K, Hayashi N, Takehara T: Novel image analysis method using ultrasound elastography for non-invasive evaluation of hepatic fibrosis in patients with chronic hepatitis C. Oncology 2013;84(suppl 1):3–12.
19 Yada N, Kudo M, Morikawa H, Fujimoto K, Kato M, Kawada N: Assessment of liver fibrosis with real-time tissue elastography in chronic viral hepatitis. Oncology 2013;84(suppl 1):13–20.
20 Kudo M, Shiina T, Moriyasu F, Iijima H, Tateishi R, Yada N, Fujimoto K, Morikawa H, Hirooka M, Sumino Y, Kumada T: JSUM ultrasound elastography practice guidelines: liver. J Med Ultrason 2013;40:325–357.
21 Ichida F, Tsuji T, Omata M, Ichida T, Inoue K, Kamimura T, Yamada G, Hino K, Yokosuka O, Suzuki H: New Inuyama classification; new criteria for histological assessment of chronic hepatitis. Int Hepatol Commun 1996;6:112–119.
22 Tatsumi C, Kudo M, Ueshima K, Kitai S, Ishikawa E, Yada N, Hagiwara S, Inoue T, Minami Y, Chung H, Maekawa K, Fujimoto K, Kato M, Tonomura A, Mitake T, Shiina T: Non-invasive evaluation of hepatic fibrosis for type C chronic hepatitis. Intervirology 2010;53:76–81.
23 Shiina T: JSUM ultrasound elastography practice guidelines: basics and terminology. J Med Ultrason 2013;40:309–323.

Review

Oncology

Oncology 2014;87(suppl 1):73–77
DOI: 10.1159/000368148

Published online: November 22, 2014

Recent Progress in Radiofrequency Ablation Therapy for Hepatocellular Carcinoma

Kenji Ikeda[a] Yukio Osaki[b] Hiroyuki Nakanishi[c] Akihiro Nasu[b] Yusuke Kawamura[a] Koji Jyoko[d] Takatomo Sano[e] Hajime Sunagozaka[f] Koji Uchino[g] Yasunori Minami[h] Yu Saito[i] Kazumasa Nagai[j] Ryosuke Inokuchi[k] Shigehiro Kokubu[l] Masatoshi Kudo[h]

[a]Department of Hepatology, Toranomon Hospital and Okinaka Memorial Institution of Medical Research, Tokyo, [b]Department of Gastroenterology, Osaka Red Cross Hospital, Osaka, [c]Department of Gastroenterology, Musashino Red Cross Hospital, Tokyo, [d]Department of Hepatobiliary and Pancreatic Disease, Matsuyama Red Cross Hospital, Matsuyama, [e]Department of Gastroenterology, Tokyo Medical University, Tokyo, [f]Department of Gastroenterology, Kanazawa University, Kanazawa, [g]Department of Gastroenterology, Tokyo University, Tokyo, [h]Department of Gastroenterology and Hepatology, Kinki University, Osaka-Sayama, [i]Department of Surgery, Tokushima University, Tokushima, [j]Department of Gastroenterology, Teine Keijinkai Hospital, Sapporo, [k]Department of Gastroenterology and Hepatology, Kansai Medical University, Osaka, and [l]Department of Hepatology, Shin-Yurigaoka General Hospital, Kawasaki, Japan

Key Words

Hepatocellular carcinoma · Radiofrequency ablation · Bipolar radiofrequency ablation · Dexmedetomidine · Sonazoid · Fusion imaging · Microwave · Surgery

Abstract

In order to attain better ablation and more effective management of hepatocellular carcinoma (HCC), new approaches and devices in radiofrequency ablation (RFA) therapy were presented and discussed in a workshop at the 50th Annual Meeting of the Liver Cancer Study Group of Japan. A novel bipolar RFA apparatus was introduced in Japan in January 2013. Hundreds of subjects with HCC were treated with multipolar RFA with varied devices and plans. Among these, no-touch ablation was one of the most useful procedures in the treatment of HCC with the apparatus. In RFA therapy, a few assisting devices and techniques were applied for convenience and improvement of the thermal ablation procedure. Contrast-enhanced ultrasonography and three-dimensional fusion imaging technique using volume data of CT or MRI could improve exact targeting and shorten the treatment time for RFA procedures under ultrasonographic guidance. A more complicated method using a workstation was also reported as being helpful in planning the ablated shape and volume in multineedle RFA. The effective use of sedatives and antianalgesics as well as a novel microwave apparatus with a cooled-tip electrode was also discussed.

KARGER

E-Mail karger@karger.com
www.karger.com/ocl

0030–2414/14/0877–0073$39.50/0

Dr. Kenji Ikeda
Department of Hepatology, Toranomon Hospital
Toranomon 2-2-2, Minato-ku
Tokyo 105-8470 (Japan)
E-Mail ikedakenji@tora.email.ne.jp

Introduction

Hepatocellular carcinoma (HCC) is one of the most common malignant tumors worldwide, with an annual incidence of one million new cases [1]. In about 90% of the patients, HCC is a late complication of cirrhosis. The 5-year incidence of HCC in patients with cirrhosis is 15–20%. The risk of developing HCC has been reported to be 0.5% per year for hepatitis B and 5% per year for hepatitis C patients. Consequently, HCC is now emerging as a major health concern for the next decades. Most patients develop few symptoms when the tumor is small and often present with multifocal disease only at a late stage. The natural course of HCC includes progressive tumor growth compromising the hepatic function, intrahepatic metastases and spread to distant sites. In general, HCC has a poor prognosis, with a median survival of 3–6 months after the onset of symptoms. Nowadays, an increasing number of HCCs is discovered at an early stage because of an increasing awareness and screening of asymptomatic patients with cirrhosis [2]. During the last decade, percutaneous locoregional therapy has become the predominant treatment for a small HCC associated with cirrhosis because of poor liver function reserve and a high recurrence rate after surgical resection.

Radiofrequency ablation (RFA) therapy [3] became available in 1999 in Japan, and turned into an indispensable procedure for the management of small-sized HCC. RFA therapy is especially useful for patients with recurrent tumors, bilobar tumors and tumors located deep in the liver. It is also effective in elderly patients and in patients with other concomitant diseases and cardiac, renal, lung or neurological complications. In the last 15 years, many devices and studies have been described in order to better manage the early stages of HCC.

At the 50th Annual Meeting of the Liver Cancer Study Group of Japan (congress president: Prof. Masatoshi Kudo), a workshop was conducted regarding the recent progress in RFA, which was presented and discussed by 11 hepatology experts (for a summary, see below).

Current Status of RFA

A complete tumor ablation rate of over 90% was achieved with RFA, and the remainder can usually be ablated with additional RFA therapy. Although the tumor recurrence rate or the residual tumor rate is significantly higher after RFA compared with surgical resection, overall survival is generally regarded as not significantly different between RFA and surgery.

Sunakozaka and colleagues compared the prognosis after surgical resection [4, 5] (n = 157) with that after RFA (n = 363) using propensity scores with the inverse probability of treatment weighting method. After selection bias regarding the treatment type (RFA or resection) was adjusted for to some extent, the survival rates between patients with RFA and resection were not different retrospectively. The odds ratio for survival of the propensity score was 1.15 (favoring surgical resection, 95% CI 0.56–2.28). These experts found that the survival period seemed prolonged when patients with decreased liver function received RFA therapy instead of surgery. A multicenter prospective randomized controlled trial (the SURF study) will show the real efficiency of RFA in recurrence-free survival and overall survival in the Japanese clinical setting.

Some surgeons have reported that recurrent or residual tumor tissue after RFA might have malignant characteristics in the pathology of resected HCCs. Saito and colleagues analyzed the clinicopathological features of 10 HCC patients who showed local recurrence after RFA therapy. They selected retrospective patient data as well as searched at the surgical department for biased data and compared them with data of 78 HCC patients without previous RFA intervention. The incidence of poorly differentiated histology (4/10 vs. 72/78, $p < 0.01$) and portal vein invasion (8/10 vs. 13/78, $p < 0.01$) was significantly higher in the HCC patients with previous RFA therapy than in the treatment-naïve HCC patients. The survival rate was significantly lower ($p = 0.03$) and the disease-free survival rate lower ($p = 0.01$) in the patients undergoing RFA therapy. The investigators also noticed a high incidence of extrahepatic metastases (3/10 vs. 6/78, $p < 0.05$) after surgical resection of recurrent HCC after RFA therapy. They analyzed angiogenesis markers (HIF-1, VEGF), cancer stem cell markers (EpCAM, CD44) [6, 7] and epithelial-mesenchymal transition (EMT) markers (TGF-β, twist, snail-1, vimentin) in RT-PCR of the patient serum and in immunohistochemistry of the resected specimen. Since almost all angiogenesis markers, stem cell markers and EMT markers increased to some extent in HCC with previous RFA therapy, the investigators supposed that insufficient thermal ablation led to a malignant transformation with EMT. Since treatment-naïve and treatment-resistant HCCs after the other modalities of therapy sometimes also show these malignant characteristics to some

extent, the analysis of the limited number of selected patients in the surgical department should be carefully interpreted considering the presence of significant data bias.

Monopolar and Bipolar Ablation

In Japan, monopolar RFA treatment (cooled-tip, LeVeen or RITA system) became available in 1999 and bipolar RFA treatment (CelonPOWER) in 2013. More than 50 institutions and hospitals currently use the bipolar system.

Kawamura and colleagues presented various advantages of the bipolar RFA system, especially the no-touch ablation procedure. Treatment benefit is mostly obtained in subcapsular tumors [8], tumor nodules just behind major vascular structure, potentially poorly differentiated tumors, and irregularly shaped nodules. Since other types of HCC nodules also showed a decreased dissemination risk with the treatment, 44 of 130 nodules (34%) were treated with no-touch ablation.

Joko and colleagues reported on 174 patients undergoing bipolar RFA. More than 70% of the treatments were performed using 3 electrodes, and more than half of the nodules were treated with no-touch ablation. These experts revealed that current bipolar apparatus could treat tumors as large as 3.5 cm in diameter with the no-touch system using 3 needles (6 electrodes) around the nodules. They proposed to extend the indication for RFA to cases where multipolar ablation is performed appropriately, except for small-sized HCC.

On the contrary, Nasu and colleagues studied the ideal use of single-needle ablation with the bipolar RFA system. They tried to obtain a small and round ablative area for a small HCC nodule using a single 20-mm applicator (T20) and compared two types of radiofrequency output programs: a conventional protocol with constant 20-Watt output to 10 kJ energy (n = 9) and a step-up protocol with increasing power from 10 W to 3 kJ, from 15 W to 6 kJ and from 20 W to 10 kJ (n = 6). The longitudinal length of the ablated area was the same in the two protocols; however, the transverse length was significantly longer in the step-up protocol ($p = 0.0015$). Although the step-up protocol required a longer treatment time, the revised manner of output control generated a more round and larger necrotic area. Nasu and colleagues therefore recommended the step-up control of output for a small-sized HCC using a 20-mm applicator.

Nakanishi and colleagues reported the usefulness of bipolar RFA in a patient with a cardiac pacemaker comparing monopolar and bipolar ablation. The patient showed a significant decrease in blood pressure with monopolar ablation but did not show any blood pressure change with the bipolar RFA procedure.

Application and Assisting Devices

When RFA is performed under ultrasonographic guidance, there are several reasons for the difficulty in targeting and inserting a needle to an exact point of an HCC nodule, e.g. a small lesion of less than 1 cm, invisible or vague nodules, concomitant confusing or misleading nodular lesions around the tumor and local tumor progression of a previously ablated lesion. When a small nodular lesion is detected on CT or MRI during the follow-up period after ablation therapy or surgical resection, ultrasonography sometimes cannot demarcate the lesion.

Uchino and colleagues studied patients with HCC tumors that are hard to visualize on B-mode ultrasonography. Sonazoid-enhanced ultrasonography was performed in 107 patients with 140 lesions that were vague and invisible on ordinary ultrasound. A total of 140 sessions of RFA therapy were performed under contrast-enhanced ultrasound, and an electrode was inserted in the Kupffer phase in 109 sessions (77.9%), in the arterial phase in 14 sessions (10.0%), and in the ordinary B-mode in the remaining 17 sessions (12.1%). In 114 cases (88.4%), an effective enhancement was achieved at the first session of RFA, and in these complete ablation was attained in 97.4%. Sonazoid-enhanced ultrasonography was useful in small-sized lesions, subcapsular lesions, lesions neighboring previous ablated areas and lesions requiring an additional ablation. On the contrary, sonazoid enhancement was often ineffective in obese patients and patients with a shrunk liver.

Minami and colleagues retrospectively analyzed difficult-to-visualize tumors on B-mode ultrasonography. They compared fusion imaging assistance, enhanced ultrasonography assistance and both fusion imaging plus enhanced ultrasonography assistance in the treatment of RFA. Enhanced ultrasonography was additionally performed when fusion imaging was ineffective in demarcating a tumor, and vice versa. Since the number of required treatment sessions, local tumor progression rate and incidence of adverse events were not different among the three treatment groups, fusion imaging and contrast-

enhanced ultrasonography are regarded as mutually complementary and useful assisting devices in RFA therapy. In addition, Nakanishi and colleagues stated that fusion imaging and sonazoid-enhanced ultrasonography in RFA are helpful and improve the certainty of the ablation procedure.

Sano and colleagues proposed various devices to improve RFA therapy with the bipolar system. The ablation area and shape after treatment were evaluated three-dimensionally using workstation software, and simulation techniques seemed helpful in an appropriate bipolar ablation procedure even after treatment. The ultrasonography function of the Virtu-TRAX™ (GE Healthcare) can indicate the exact depth of multiple inserted needles and helps to perform a sufficient and safe ablation.

Analgesic Agents

In the treatment of RFA, most Japanese doctors use morphine, pethidine, pentazocine or fentanyl as antianalgesics and midazolam or diazepam as sedatives instead of general anesthesia. The administration of these conventional analgesics is sometimes associated with insufficient analgesic effects, and sedatives may cause serious or life-threatening breathing problems such as shallow, slowed or temporarily stopped breathing. Since benzodiazepine derivatives often induce a drowsy and unconscious state followed by significant difficulty in 'awake ablation', following the operators' instructions is mandatory.

Nagai and colleagues used dexmedetomidine, an alpha-2 adrenergic receptor agonist highly specific to the central nervous system. Its indication has recently been expanded to include nonintubated patients requiring sedation for surgery or short-term procedures. It is also useful as an adjunct for sedation and general anesthesia in certain operations and invasive medical procedures such as colonoscopy. The investigators performed monopolar or bipolar RFA therapy in 23 patients with HCC. The sedative ability of dexmedetomidine was evaluated with six grades using the Ramsay sedation score. During the median ablation period of 14 min, all patients were successfully treated with (n = 18) or without (n = 5) additional analgesic agents. Although Nagai and colleagues added pentazocine or pethidine in some patients, they emphasized that dexmedetomidine was very safe during and after the procedure for elderly patients, and that its administration was easy to control.

Novel Microwave Ablation

Noguchi and colleagues introduced a novel microwave device, the cooled microwave antenna (CMA), which is already available in Western countries. The CMA system has been reported to ablate larger volumes of tissues than previous microwave devices without a tip-cooling system. The investigators compared the ablation ability of the cooled-tip RFA system with that of the CMA device using ex vivo bovine liver. The median size of the ablation area was 46.2 × 34.0 mm after 12 min with the cooled-tip system (n = 5), whereas it was 56.0 × 35.8 mm after 5 min and 69.0 × 48.6 mm after10 min with the CMA system (n = 5). The CMA system thus ablated a larger area in a shorter time, because high ablative power seemed to be provided to a wide range of liver tissues without heating the tip of the electrode. The experts emphasized that the use of the CMA system can result in both a shorter treatment time and a larger ablation volume in the treatment of HCC.

Future Perspective of RFA

The recent development of RFA has expanded the range of treatments of HCC. The main characteristic of RFA therapy is the localized tumor destruction in situ with maximal preservation of the noncancerous part of the liver parenchyma, in contrast to the significant liver damage caused by other interventional therapies such as transcatheter arterial chemoembolization and intra-arterial chemotherapeutic infusion [9].

Future studies from the technical viewpoint should focus on (1) the development of optimal ablation techniques for bipolar and multipolar systems that can generate optimal volumes and shapes of tissue destroyed, (2) varied efforts for reducing side effects (most favorable analgesic therapy, avoidance of biliary tree complication, and so on), (3) various attempts of image assistance to attain more effective RFA procedure, and (4) the assessment of efficacy of multimodal and combined treatments.

Disclosure Statement

The authors declare that no financial or other conflicts of interest exist in relation to the content of this article.

References

1 Kim DY, Han KH: Epidemiology and surveillance of hepatocellular carcinoma. Liver Cancer 2012;1:2–14.
2 Kudo M: Japan's successful model of nationwide hepatocellular carcinoma surveillance highlighting the urgent need for global surveillance. Liver Cancer 2012;1:141–143.
3 Lin SM: Local ablation for hepatocellular carcinoma in Taiwan. Liver Cancer 2013;2:73–83.
4 Mise Y, Sakamoto Y, Ishizawa T, et al: A worldwide survey of the current daily practice in liver surgery. Liver Cancer 2013;2:55–66.
5 Belghiti J, Fuks D: Liver resection and transplantation in hepatocellular carcinoma. Liver Cancer 2012;1:71–82.
6 Lo RC, Ng IO: Hepatic progenitor cells: their role and functional significance in the new classification of primary liver cancers. Liver Cancer 2013;2:84–92.
7 Oishi N, Yamashita T, Kaneko S: Molecular biology of liver cancer stem cells. Liver Cancer 2014;3:71–84.
8 Kawamura Y, Ikeda K, Fukushima T, et al: Potential of a no-touch pincer ablation procedure for small hepatocellular carcinoma that uses a multipolar radiofrequency ablation system: an experimental animal study. Hepatol Res 2013, DOI: 10.1111/hepr.12240.
9 Kudo M: Treatment of advanced hepatocellular carcinoma with emphasis on hepatic arterial infusion chemotherapy and molecular targeted therapy. Liver Cancer 2012;1:62–70.

Review

Oncology

Oncology 2014;87(suppl 1):78–81
DOI: 10.1159/000368149

Published online: November 22, 2014

Treatment Strategies of Intermediate-Stage Hepatocellular Carcinomas in Japan (Barcelona Clinic Liver Cancer Stage B)

Koichiro Yamakado[a] Masatoshi Kudo[b]

[a]Department of Interventional Radiology, School of Medicine, Tsu, and [b]Department of Gastroenterology and Hepatology, Kinki University School of Medicine, Osaka-Sayama, Japan

Key Words
Hepatocellular carcinoma · Intermediate stage · Chemoembolization · Child-Pugh score · Prognosis

Abstract
Hepatocellular carcinoma (HCC) is the fifth most common cancer in the world, and it shows increasing incidence worldwide. The Barcelona Clinic Liver Cancer (BCLC) staging system has become widely accepted in clinical practice, but in Japan, two clinical practice guidelines have been used for HCC: the Evidence-Based Clinical Practice Guidelines and the Consensus-Based Clinical Practice Guidelines. Although, in Japan, chemoembolization is the first-line treatment of intermediate-stage (stage B) HCC patients in the BCLC staging system, along with chemoembolization, locoregional treatments, such as resection and radiofrequency ablation, and hepatic arterial infusion chemotherapy are incorporated into the treatment algorithm based on the tumor number and size as well as on the liver profile.

Introduction

Hepatocellular carcinoma (HCC) is the fifth most common cancer in the world, and it shows increasing incidence worldwide [1, 2]. The Barcelona Clinic Liver Cancer (BCLC) staging system is accepted worldwide for clinical practice. The BCLC classification divides HCC patients into stages according to prognostic variables and allocates therapies according to treatment-related status [3]. For example, BCLC stage B is defined as intermediate stage. It includes extremely inhomogeneous patients. Chemoembolization is recommended as the standard treatment of intermediate-stage (BCLC stage B) HCC patients [3].

In contrast, two clinical practice guidelines for HCC have become common in Japan. One is the Evidence-Based Clinical Practice Guidelines created based on highly evidenced data [4]. The other is the Consensus-Based Clinical Practice Guidelines created by consensus among expert opinions [5]. In both guidelines, treatment algorithms have been fabricated based on liver function, extrahepatic lesions, vascular invasion, as well as tumor number and size. Although no definition of intermediate stage exists in these Japanese guidelines, not only chemoembolization [6], but also locoregional treatments, such as hepatic resection [7, 8], and radiofrequency ablation (RFA) [9], hepatic arterial infusion chemotherapy, and sorafenib [10] are incorporated into the treatment tactics in patients corresponding to intermediated-stage disease.

This study presents an explanation of the differences in the treatment strategies of intermediate-stage HCC patients by examining the Japanese guidelines and clarifying the BCLC staging system.

KARGER

E-Mail karger@karger.com
www.karger.com/ocl

0030–2414/14/0877–0078$39.50/0

Dr. Koichiro Yamakado
Department of Interventional Radiology
Mie University School of Medicine
2-174 Edobashi, Tsu, Mie 514-8507 (Japan)
E-Mail yama@clin.medic.mie-u.ac.jp

BCLC Staging System

The BCLC classification divides HCC patients according to 5 stages (0, A, B, C, and D) depending on tumor status-related variables (size, number, vascular invasion, N1, and M1), liver function (Child-Pugh class), and health status (ECOG) (fig. 1). Treatment allocation depends on variables that have been shown to influence therapeutic outcomes, e.g. bilirubin, portal hypertension, and the presence of symptoms. Actually, BCLC stage B, which is defined as intermediate stage, consists of patients having Child-Pugh class A and class B liver function with ≥4 tumors irrespective of size, or 2–3 tumors of >3 cm in maximal diameter, in the absence of cancer-related symptoms, macrovascular invasion, or extrahepatic spread.

Untreated patients at an intermediate stage (BCLC stage B) reportedly present a median survival of 16 months [11, 12] or 49% at 2 years [13]. Chemoembolization is recommended as the standard treatment, which is positioned as a palliative treatment, extending the survival of these patients to a median of up to 19–20 months according to randomized controlled trials and meta-analyses of pooled data [11].

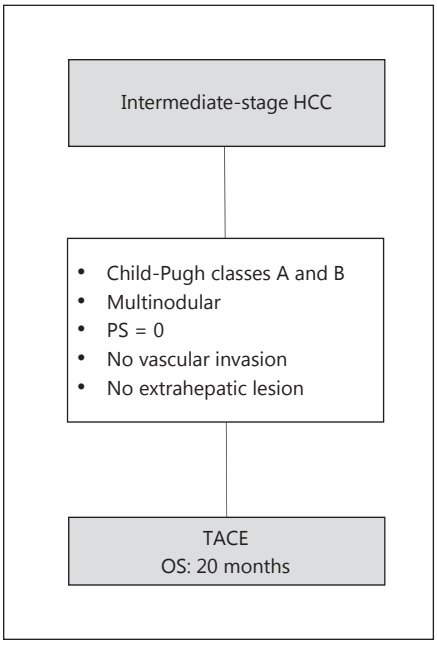

Fig. 1. Treatment strategy of intermediate-stage HCC patients (stage B) in the BCLC staging system. PS = Performance status; TACE = transarterial chemoembolization; OS = overall survival.

Evidence-Based Clinical Practice Guidelines in Japan

These guideline were first issued in 2005. They have been twice revised since, in 2009 and 2013. The treatment algorithm is based on liver function damage (or Child-Pugh class), tumor number and size, vascular invasion, and extrahepatic lesions [4]. Although no definition of intermediate stage exists, treatment strategies for patients corresponding to intermediate-stage disease consist of locoregional treatments, such as hepatectomy and RFA, hepatic arterial infusion chemotherapy, and sorafenib in addition to chemoembolization (fig. 2).

Many studies have demonstrated that tumor diameter is not a limitation of hepatectomy. The 5-year survival rates have been reported to be 20–30%, which are much better than natural history [13–16]. Although therapeutic results following hepatectomy worsen as the tumor number increases, these results are still better than those after other palliative treatments and supportive care [17, 18]. No evidence exists for tumor number that provides a survival benefit to patients undergoing surgical intervention, although a tumor number of ≥3 has been widely accepted as a good indication for locoregional treatments such as RFA. Therefore, hepatectomy is recommended when the tumor number is ≤3, irrespective of the tumor size. Recent studies also have demonstrated

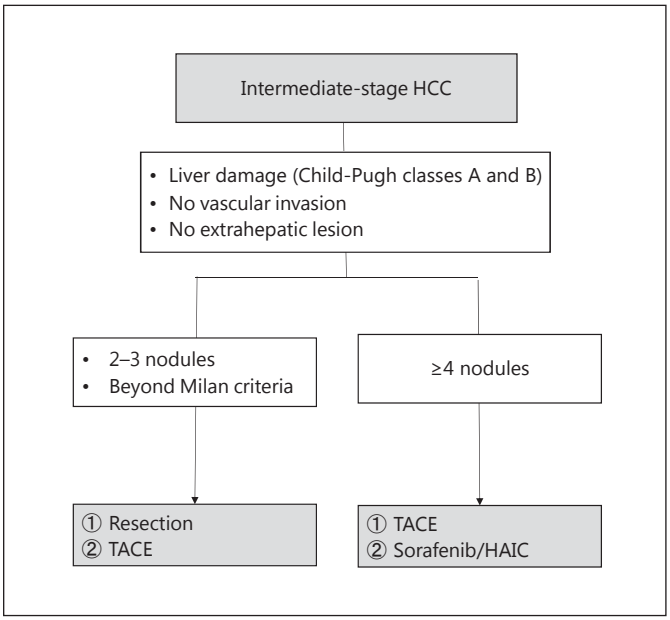

Fig. 2. Treatment strategy of intermediate-stage HCC patients in the Evidence-Based Clinical Practice Guidelines in Japan. TACE = Transarterial chemoembolization; HAIC = hepatic arterial infusion chemotherapy.

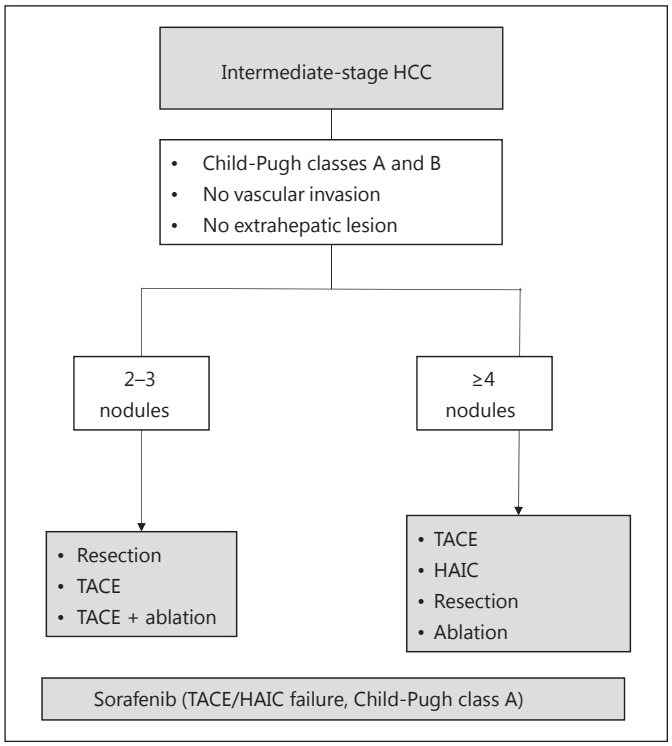

Fig. 3. Treatment strategy of intermediate-stage HCC patients in the Consensus-Based Clinical Practice Guidelines in Japan. TACE = Transarterial chemoembolization; HAIC = hepatic arterial infusion chemotherapy.

the utility of hepatectomy, even in intermediate-stage HCC patients [19].

When the tumor number is ≥4, chemoembolization is recommended as the first-line treatment. Sorafenib can be used after chemoembolization fails to control tumors in patients with Child-Pugh class A.

The literature provides little evidence that hepatic arterial infusion chemotherapy improves patient survival in HCC. However, many studies have proved a benefit to survival using this treatment instead of historical control [20]. Therefore, hepatic arterial infusion chemotherapy is listed in these guidelines.

Consensus-Based Clinical Practice Guidelines

This treatment algorithm, created based on experts' experiences, reflects clinical practices of managing HCC patients in Japan (fig. 3). When the tumor number is 2 or 3, in addition to chemoembolization, resection or combination of chemoembolization and RFA are considered for the therapeutic option. Combination therapy of chemoembolization and RFA is usually applied for the treatment of HCC lesions ≥3 cm [21].

When the tumor number is ≥4, chemoembolization is the first-line treatment. Hepatic arterial infusion chemotherapy is used when chemoembolization fails to control tumors. Even for patients having ≥4 tumors, resection and ablation are applicable if possible. Sorafenib is usually used when both chemoembolization and hepatic arterial infusion chemotherapy fail to control tumors and the patients' liver function is Child-Pugh class A.

Discussion

A great difference exists in the treatment strategy of HCC patients between the BCLC staging system and the Japanese treatment algorithms, as shown in this study.

In Japan, the BCLC staging system problem lies in its simplicity of recommending only chemoembolization, although the intermediate stage includes extremely inhomogeneous patients. Neither surgical intervention nor ablation therapy has been considered for intermediate-stage patients in the BCLC staging system, although both treatments are applied, particularly in Japanese patients with ≤3 HCC nodules.

Recently, some movements have been underway to stratify patients using some prognostic factors to identify patient groups showing a greater benefit from chemoembolization than other patient groups [22, 23]. Bolondi et al. [22] advocated the division of intermediate stage into 4 substages based on the up-to-7 criteria (in vs. out) and Child-Pugh scores (5–7 vs. 8–9). Recently, one study validated this substaging system and reported the difficulty in stratifying the patient group that benefits least from chemoembolization [23].

Aside from the up-to-7 criteria, the 4 tumors of the 7-cm criteria (4-of-7 cm) and Child-Pugh class A were identified as favorable prognostic factors in patients with intermediate-stage HCCs undergoing chemoembolization [24].

Sorafenib is usually used in Western countries after chemoembolization fails to control HCC lesions. The median survival times after sorafenib administration were 10.7 months in the SHARP trial and 6.5 months in the Asia-Pacific trial, although not all patients had chemoembolization-refractory HCC in these studies [25, 26]. In Japan, sorafenib is usually used after both chemoembolization and hepatic arterial infusion chemotherapy fail to control the disease, although there has been few data that hepatic arterial infusion chemotherapy is useful

in chemoembolization-refractory patients. One prospective report has described that hepatic arterial infusion chemotherapy using a fine-powder formulation of cisplatin appears to have only modest activity [27].

In conclusion, not only chemoembolization but also locoregional treatments, hepatic arterial infusion chemotherapy, and sorafenib are incorporated for the treatment algorithm of patients with intermediate-stage HCC depending on the tumor number and size. Liver function reserve in Japan, unlike chemoembolization, is the only standard treatment in BCLC staging. Since these differences in the treatment tactics are mostly attributable to the inhomogeneity of BCLC stage B patients, subclassification of BCLC stage B and its validation are necessary to allocate therapy appropriately in the new substaging system.

Disclosure Statement

The authors declare that no financial or other conflicts of interest exist in relation to the content of this article.

References

1 Llovet JM, Burroughs A, Bruix J: Hepatocellular carcinoma. Lancet 2003;362:1907–1917.
2 Kim DY, Han KH: Epidemiology and surveillance of hepatocellular carcinoma. Liver Cancer 2012;1:2–14.
3 Llovet JM, Ducreux M, et al: EASL-EORTC clinical practice guidelines: management of hepatocellular carcinoma. J Hepatol 2012;56:908–943.
4 Japan Society of Hepatology: Clinical Practice Guidelines for Hepatocellular Carcinoma (2013 Version). Kanehara, Tokyo, 2013.
5 Kudo M, Izumi N, Kokudo N, Matsui O, Sakamoto M, Nakashima O, Kojiro M, Makuuchi M: Management of hepatocellular carcinoma in Japan: Consensus-Based Clinical Practice Guidelines proposed by the Japan Society of Hepatology (JSH) 2010 updated version. Dig Dis 2011;29:339–364.
6 Lencioni R: Chemoembolization in patients with hepatocellular carcinoma. Liver Cancer 2012;1:41–50.
7 Belghiti J, Fuks D: Liver resection and transplantation in hepatocellular carcinoma. Liver Cancer 2012;1:71–82.
8 Mise Y, Sakamoto Y, Ishizawa T, Kaneko J, Aoki T, Hasegawa K, Sugawara Y, Kokudo N: A worldwide survey of the current daily practice in liver surgery. Liver Cancer 2013;2:55–66.
9 Lin SM: Local ablation for hepatocellular carcinoma in Taiwan. Liver Cancer 2013;2:73–83.
10 Kudo M: Treatment of advanced hepatocellular carcinoma with emphasis on hepatic arterial infusion chemotherapy and molecular targeted therapy. Liver Cancer 2012;1:62–70.
11 Llovet JM, Bruix J: Systematic review of randomized trials for unresectable hepatocellular carcinoma: chemoembolization improves survival. Hepatology 2003;37:429–442.
12 Llovet JM, Bruix J: Molecular targeted therapies in hepatocellular carcinoma. Hepatology 2008;48:1312–1327.
13 Cabibbo G, Enea M, Attanasio M, Bruix J, Craxi A, Camma C: A meta-analysis of survival rates of untreated patients in randomized clinical trials of hepatocellular carcinoma. Hepatology 2010;51:1274–1283.
14 Lee NH, Chau GY, Lui WY, King KL, Tsay SH, Wu CW: Surgical treatment and outcome in patients with a hepatocellular carcinoma greater than 10 cm in diameter. Br J Surg 1998;85:1654–1657.
15 Poon RT, Fan ST, Wong J: Selection criteria for hepatic resection in patients with large hepatocellular carcinoma larger than 10 cm in diameter. J Am Coll Surg 2002;194:592–602.
16 Liau KH, Ruo L, Shia J, Padela A, Gonen M, Jarnagin WR, Fong Y, D'Angelica MI, Blumgart LH, DeMatteo RP: Outcome of partial hepatectomy for large (>10 cm) hepatocellular carcinoma. Cancer 2005;104:1948–1955.
17 Ishizawa T, Hasegawa K, Aoki T, Takahashi M, Inoue Y, Sano K, Imamura H, Sugawara Y, Kokudo N, Makuuchi M: Neither multiple tumors nor portal hypertension are surgical contraindications for hepatocellular carcinoma. Gastroenterology 2008;134:1908–1916.
18 Ho MC, Huang GT, Tsang YM, Lee PH, Chen DS, Sheu JC, Chen CH: Liver resection improves the survival of patients with multiple hepatocellular carcinomas. Ann Surg Oncol 2009;16:848–855.
19 Zhong JH, Ke Y, Gong WF, Xiang BD, Ma L, Ye XP, Peng T, Xie GS, Li LQ: Hepatic resection associated with good survival for selected patients with intermediate and advanced-stage hepatocellular carcinoma. Ann Surg 2013, Epub ahead of print.
20 Obi S, Yoshida H, Toune R, Unuma T, Kanda M, Sato S, Tateishi R, Teratani T, Shiina S, Omata M: Combination therapy of intraarterial 5-fluorouracil and systemic interferon-alpha for advanced hepatocellular carcinoma with portal venous invasion. Cancer 2006;106:1990–1997.
21 Yamakado K, Nakatsuka A, Takaki H, Yokoi H, Usui M, Sakurai H, Isaji S, Shiraki K, Fuke H, Uemoto S, Takeda K: Early-stage hepatocellular carcinoma: radiofrequency ablation combined with chemoembolization versus hepatectomy. Radiology 2008;247:260–266.
22 Bolondi L, Burroughs A, Dufour JF, Galle PR, Mazzaferro V, Piscaglia F, Raoul JL, Sangro B: Heterogeneity of patients with intermediate (BCLC B) hepatocellular carcinoma: proposal for a subclassification to facilitate treatment decisions. Semin Liver Dis 2012;32:348–359.
23 Ha Y, Shim JH, Kim SO, Kim KM, Lim YS, Lee HC: Clinical appraisal of the recently proposed Barcelona Clinic Liver Cancer stage B subclassification by survival analysis. J Gastroenterol Hepatol 2014;29:787–793.
24 Yamakado K, Miyayama S, Hirota S, Mizunuma K, Nakamura K, Inaba Y, Maeda H, Matsuo K, Nishida N, Aramaki T, Anai H, Koura S, Oikawa S, Watanabe K, Yasumoto T, Furuichi K, Yamaguchi M: Subgrouping of intermediate-stage (BCLC stage B) hepatocellular carcinoma based on tumor number and size and Child-Pugh grade correlated with prognosis after transarterial chemoembolization. Jpn J Radiol 2014;32:260–265.
25 Llovet JM, Ricci S, Mazzaferro V, Hilgard P, Gane E, Blanc JF, de Oliveira AC, Santoro A, Raoul JL, Forner A, Schwartz M, Porta C, Zeuzem S, Bolondi L, Greten TF, Galle PR, Seitz JF, Borbath I, Haussinger D, Giannaris T, Shan M, Moscovici M, Voliotis D, Bruix J: Sorafenib in advanced hepatocellular carcinoma. N Engl J Med 2008;359:378–390.
26 Cheng AL, Kang YK, Chen Z, Tsao CJ, Qin S, Kim JS, Luo R, Feng J, Ye S, Yang TS, Xu J, Sun Y, Liang H, Liu J, Wang J, Tak WY, Pan H, Burock K, Zou J, Voliotis D, Guan Z: Efficacy and safety of sorafenib in patients in the Asia-Pacific region with advanced hepatocellular carcinoma: a phase III randomised, double-blind, placebo-controlled trial. Lancet Oncol 2009;10:25–34.
27 Iwasa S, Ikeda M, Okusaka T, Ueno H, Morizane C, Nakachi K, Mitsunaga S, Kondo S, Hagihara A, Shimizu S, Satake M, Arai Y: Transcatheter arterial infusion chemotherapy with a fine-powder formulation of cisplatin for advanced hepatocellular carcinoma refractory to transcatheter arterial chemoembolization. Jpn J Clin Oncol 2011;41:770–775.

Review

Oncology

Oncology 2014;87(suppl 1):99–103
DOI: 10.1159/000368152

Published online: November 22, 2014

Treatment of Hepatocellular Carcinoma with Child-Pugh C Cirrhosis

Kazuhiro Nouso[a] Norihiro Kokudo[b] Masatoshi Tanaka[c] Ryoko Kuromatsu[d] Hiroki Nishikawa[e] Hidenori Toyoda[f] Naoki Oishi[g] Kenji Kuwaki[h] Masashi Kusanaga[i] Takuki Sakaguchi[j] Zenichi Morise[k] Satoshi Kitai[l] Masatoshi Kudo[l]

[a]Department of Molecular Hepatology, Okayama University Graduate School of Medicine, Dentistry and Pharmaceutical Sciences, Okayama, [b]Hepato-Biliary-Pancreatic Surgery Division and Artificial Organ and Transplantation Division, Department of Surgery, Graduate School of Medicine, The University of Tokyo, Tokyo, [c]Yokokura Hospital, Fukuoka, [d]Division of Gastroenterology, Department of Medicine, Kurume University, Kurume, [e]Department of Gastroenterology and Hepatology, Osaka Red Cross Hospital, Osaka, [f]Department of Gastroenterology, Ogaki Municipal Hospital, Ogaki, [g]Department of Gastroenterology, Kanazawa University Hospital, Kanazawa, [h]Department of Gastroenterology and Hepatology, Okayama University Graduate School of Medicine, Dentistry and Pharmaceutical Sciences, Okayama, [i]Department of Gastroenterology, Yame General Hospital, Yame, [j]Department of Internal Medicine, Hiroshima City Hospital, Hiroshima, [k]Department of Surgery, Fujita Health University School of Medicine, Banbuntane Houtokukai Hospital, Nagoya, and [l]Department of Gastroenterology and Hepatology, Kinki University School of Medicine, Osaka-Sayama, Japan

Key Words
Hepatocellular carcinoma · Child-Pugh C cirrhosis · Liver transplantation

Abstract
Background: In most guidelines, no other interventional therapy but liver transplantation is recommended for the treatment of hepatocellular carcinoma (HCC) with Child-Pugh C cirrhosis (CP-C). However, in Japan, patients were sometimes treated with expectation of benefit. ***Summary:*** A workshop was conducted to explore the state of treatments for CP-C HCC in Japan. After the workshop, a questionnaire on therapies was given to the panelists. Clinical data of 769 patients with CP-C HCC from 8 hospitals as well as analyses of data collected by the Liver Cancer Study Group of Japan (LCSGJ) consisting of 1,344 CP-C HCC cases were presented. Patients who underwent liver transplantation were excluded. In total, 424 out of the 769 patients (55.1%) from the 8 hospitals and 537 out of 828 CP-C HCC cases (64.8%) from the LCSGJ data received interventional therapies, such as local ablation and transcatheter arterial chemoembolization. All panelists agreed that there was a subgroup of CP-C patients who benefitted from the locoregional therapies. The major goals for the therapies were to prevent HCC rupture and avoid obstruction of major vessels by tumor growth, which can lead to a sudden deterioration of the patients' condition. Patient liver function and tumor stage are both important factors for the decision to undergo treatment; however, the inclusion criteria for the treatments varied among the centers. ***Key Message:*** There exists a subgroup of CP-C patients who benefit from interventions for HCC.

KARGER

© 2014 S. Karger AG, Basel
0030–2414/14/0877–0099$39.50/0

E-Mail karger@karger.com
www.karger.com/ocl

Prof. Kazuhiro Nouso
Department of Molecular Hepatology Okayama University Graduate School of Medicine, Dentistry, and Pharmaceutical Sciences
2-5-1 Shikata-cho, Kita-ku, Okayama-City, Okayama 700-8558 (Japan)
E-Mail nouso@cc.okayama-u.ac.jp

Introduction

At the 50th Annual Meeting of the Liver Cancer Study Group of Japan (LCSGJ), which was held in Kyoto in 2014 (congress president: Prof. Masatoshi Kudo), a workshop on the subject 'treatment of hepatocellular carcinoma (HCC) with Child-Pugh C cirrhosis (CP-C)' was conducted. Recommended therapies for these patients include best supportive care from major treatment algorithms determined by the Japan Society of Hepatology [1], the American Association for the Study of Liver Diseases, and the European Association for the Study of the Liver [2, 3]. Liver transplantation [4–8] could be an alternative therapy when patients are younger than 65 years and the HCC is within the Milan criteria in the Japanese guidelines [9]. However, since the majority of HCC patients are older than 65 years and a shortage of donors has been a consistent problem in Japan, many patients instead receive locoregional therapies [10, 11] in clinical settings. At present, no concrete evidence exists for the recommendable treatment of CP-C HCC patients except for liver transplantation. However, we often experience cases in which treatment definitely prolongs survival, and there are several reports demonstrating the efficacy of treatments for CP-C HCC [12–19].

This workshop was conducted to elucidate the present status of treatments of CP-C HCC patients among Japanese high-volume centers and to identify subgroups of patients who might be able to receive a survival benefit with such locoregional treatments. After the congress, a questionnaire survey about CP-C HCC treatments was administered to the panelists.

Summary of the Workshop

Nine doctors from different institutes all over Japan, including the Kurume University, Osaka Red Cross Hospital, Ogaki Municipal Hospital, Kanazawa University, Okayama University, Yame General Hospital, Hiroshima City Hospital, Fujita Health University, and Kinki University, presented their research at this workshop. All panelists analyzed the cases of CP-C HCC at their own hospitals, except for the panelist from the Kinki University who used data collected by the LCSGJ from more than 800 medical institutions, consisting of a total of 58,886 patients with primary liver cancer.

Experiences in Individual Facilities

Clinical data of 769 CP-C HCC patients from 8 hospitals were presented. Although CP-C HCC patients might not be treated at community hospitals, 424 out of the 769 patients (55.1%) received interventional treatment [e.g., radiofrequency ablation, transcatheter arterial chemoembolization (TACE), etc.] at hospitals with which the panelists were associated.

In general, only low-risk patients were selected for the therapies; therefore, most presentations showed that the patients who received interventional treatments lived longer than the patients who did not undergo these treatments. Therefore, a considerable amount of bias existed for the beneficial effects of the treatments; however, several panelists conducted propensity score-matched analyses and multivariate analyses to compensate for potential bias. Data presented by the Osaka Red Cross Hospital (n = 265) indicated that, when conducting locoregional therapies, a low Child-Pugh score and low α-fetoprotein or des-gamma-carboxy prothrombin levels were indicators of a good prognosis. The investigators therefore concluded that the effects of the locoregional therapies were evident, especially in cases with a low Child-Pugh score and advanced HCC. Data from the Ogaki Municipal Hospital showed similar results, suggesting that bilirubin, tumor stage, and treatment type were prognostic factors.

Beneficial effects of branched-chain amino acids, short-term hepatic arterial infusion chemotherapy [20], and laparoscopic surgery [21, 22] for protruded HCC with a low Child-Pugh score were reported from the Hiroshima City Hospital, Yame General Hospital, and Fujita Health University, respectively. The importance of residual liver function for prolonged survival was reported from the Kurume, Kanazawa, and Okayama Universities. The possible improvement of liver function using nucleotide analogues in patients with hepatitis B virus infection was another topic of discussion.

Analysis of Data from the LCSGJ

Kitai and colleagues conducted a multivariate analysis and a propensity score-matched analysis of CP-C HCC patients enrolled in the database of the LCSGJ. There were 1,344 informative CP-C HCC cases, and the analysis was conducted with 1,236 cases after eliminating patients who underwent liver transplantation. As a result of the multivariate Cox proportional hazard analysis and propensity score-matched analysis, the investigators identified treat-

Table 1. Questionnaire results for the treatment of CP-C HCC patients

	Questions		Answers
Q1	Are there patients who benefit from interventional treatment?	A1	9 Yes (100%) 0 No
Q2	Interventional treatments should not always be applied to all patients.	A2	9 Agree (100%) 0 Disagree
Q3	Does treatment selection depend on the Milan criteria?	A3	6 Yes (66.7%) 3 No (33.3%)
Q4	What is the reason for your answer? (cause of death? please specify)	A4	Most of the answers revealed that liver function and tumor stage are factors influencing treatment choice
Q5	Which HCC stages are candidates for treatment? (I, II, III, IVa, IVb)	A5	Up to II (n = 1), up to III (n = 6), all stages (n = 1), II–IV (n = 1)
Q6	What is the maximum Child-Pugh score for treatment?	A6	Up to 10 (n = 1), up to 11 (n = 5), up to 12 (n = 2), up to 13 (n = 1)
Q7	What is the goal of the treatment? (please specify)	A7	Survival benefit (n = 9), satisfaction of the patients (n = 3)
Q8	What is the basis for the treatment? (please specify)	A8	Possible to cure HCC (n = 6), to prevent rupture (n = 9), to prevent vascular invasion (n = 5)
Q9	How do you treat these patients?	A9	Radiofrequency ablation (n = 7), percutaneous ethanol injection therapy (n = 5), TACE (n = 7), hepatic arterial chemotherapy (n = 4), continuous hepatic arterial chemotherapy (n = 4), laparoscopic hepatectomy (n = 1)

ment type, small tumor size, young age, and low Child-Pugh score (CP-10&11) as indicators of a good prognosis, revealing the beneficial effects of local ablation therapy and TACE in patients with a low Child-Pugh score.

Results of the Questionnaire Survey

The questionnaire consisted of 9 simple questions. A summary of the answers is shown in table 1. All panelists agreed that there was a certain subgroup of patients who benefitted from the treatment (A1). Approximately one half of the panelists considered that a treatment effect could be realized when the tumor stage was no more than III (A5). One reason for excluding stage IV HCC is that chemotherapies [23] are too invasive for patients with poor liver function. However, one panelist did not select patients with stage I HCC as candidates for treatment because early HCC takes time to progress to a life-threatening stage. In other words, this panelist does not treat stage I HCC because the deterioration of liver function, as a natural course of CP-C, is much faster than the cancer progression. While this idea appears logical, it must be proven by evidence.

In terms of liver function as a prognostic factor for treatment, one half of the panelists suggested that the upper Child-Pugh score limit should be 11 (A6). Although small differences in the limit score were observed, there was a consensus that patients with very poor liver function should be excluded from therapies because even a small deterioration of liver function as a consequence of these therapies might be life-threatening.

All panelists selected 'prolongation of patients' survival' as the reason to conduct active therapies, and 'satisfaction of the patients' was selected as a concomitant reason for treatment by 3 panelists (A7). All panelists felt that the prevention of HCC rupture by therapies leads to a prolongation of survival (A8). The prevention of vascular invasion that results in the immediate deterioration of liver function and control of tumor growth were the second most common reasons for the survival benefit. Bridging therapies to liver transplantation were another reason [14, 15]. Additional comments advocating that therapies should be selectively targeted and that the preservation of

Table 2. Summary of findings presented at the workshop

- Many patients with CP-C HCC receive interventional treatments in Japan.
- Some patients benefit from interventions for CP-C HCC.
- Most patients are treated for reasons of survival benefit but seldom for patient satisfaction alone.
- Prevention of HCC perforation and avoidance of major vessel obstruction are two major reasons to treat patients.
- Bridging therapy to liver transplantation is another reason.
- Patients with extremely poor liver function and/or advanced HCC are rarely treated.
- Note that antiviral therapies sometimes improve liver function to CP-B.

liver function by therapies as a minimum requirement were made by the panelists in the questionnaire.

In terms of treatment modalities, a wide variety of treatments, except for open surgery, were selected in the questionnaire. Unexpectedly, TACE was selected by 7 panelists, whereas only 1 panelist selected blunt embolization. The majority of panelists considered that the beneficial effects of anticancer drugs might exceed their damaging effects on liver function.

Future Directions

While the effects of interventional therapies for CP-C HCC were debated, the consensus obtained in this workshop was that there are certain patients who benefit from the interventions. However, all results were obtained via retrospective observations, and no clear evidence was presented. Recent developments in antiviral therapies that improve liver function are other important considerations. Although there are many uncertainties, this workshop revealed the present status of CP-C HCC treatments in Japan and provided a chance to reconsider treatment options for these difficult-to-treat patients. A summary of the workshop's findings is provided in table 2. Future prospective studies are mandatory to clarify optimal treatments for these patients.

Disclosure Statement

The authors declare that no financial or other conflicts of interest exist in relation to the content of this article.

References

1 Kudo M, Matsui O, Izumi N, Iijima H, Kadoya M, Imai Y, Okusaka T, Miyayama S, Tsuchiya K, Ueshima K, Hiraoka A, Ikeda M, Ogasawara S, Yamashita T, Minami T, Yamakado K; Liver Cancer Study Group of Japan: JSH consensus-based clinical practice guideline for the management of hepatocellular carcinoma: 2014 update by the Liver Cancer Study Group of Japan. Liver Cancer 2014;3:458–468.

2 Bruix J, Sherman M; American Association for the Study of Liver Diseases: Management of hepatocellular carcinoma: an update. Hepatology 2011;53:1020–1022.

3 European Association for the Study of the Liver; European Organisation for Research and Treatment of Cancer: EASL-EORTC clinical practice guidelines: management of hepatocellular carcinoma. J Hepat 2012;56:908–943.

4 Belghiti J, Fuks D: Liver resection and transplantation in hepatocellular carcinoma. Liver Cancer 2012;1:71–82.

5 YL Cheah, PK Chow: Liver transplantation for hepatocellular carcinoma: an appraisal of current controversies. Liver Cancer 2012;1:183–189.

6 Chan SC, Sharr WW, Chan AC, Chok KS, Lo CM: Rescue living-donor liver transplantation for liver failure following hepatectomy for hepatocellular carcinoma. Liver Cancer 2013;2:332–337.

7 Chan SC: Liver transplantation for hepatocellular carcinoma. Liver Cancer 2013;2:338–344.

8 Akamatsu N, Sugawara Y, Kokudo N: Living donor liver transplantation for patients with hepatocellular carcinoma. Liver Cancer 2014;3:108–118.

9 Kokudo N, Makuuchi M: Evidence-based clinical practice guidelines for hepatocellular carcinoma in Japan: the J-HCC guidelines. J Gastroenterol 2009;44(suppl 19):119–121.

10 Lin SM: Local ablation for hepatocellular carcinoma in Taiwan. Liver Cancer 2013;2:73–83.

11 Lencioni R: Chemoembolization in patients with hepatocellular carcinoma. Liver Cancer 2012;1:41–50.

12 Kim YK, Kim CS, Chung GH, Han YM, Lee SY, Jin GY, Lee JM: Radiofrequency ablation of hepatocellular carcinoma in patients with decompensated cirrhosis: evaluation of therapeutic efficacy and safety. AJR Am J Roentgenol 2006;186:S261–S268.

13 Kudo M, Osaki Y, Matsunaga T, Kasugai H, Oka H, Seki T: Hepatocellular carcinoma in Child-Pugh C cirrhosis: prognostic factors and survival benefit of nontransplant treatments. Dig Dis 2013;31:490–498.

14 Morise Z, Kawabe N, Kawase J, Tomishige H, Nagata H, Ohshima H, Arakawa S, Yoshida R, Isetani M: Pure laparoscopic hepatectomy for hepatocellular carcinoma with chronic liver disease. World J Hepatol 2013;5:487–495.

15 Morise Z, Kawabe N, Tomishige H, Nagata H, Kawase J, Arakawa S, Yoshida R, Isetani M: Recent advances in the surgical treatment of hepatocellular carcinoma. World J Gastroenterol 2014, in press.

16 Nakanishi S, Michitaka K, Miyake T, Hidaka S, Yoshino I, Konishi I, Iuchi H, Horiike N, Onji M: Decompensated hepatitis B virus-related cirrhosis successfully treated with lamivudine allowing surgery for hepatocellular carcinoma. Intern Med 2003;42:416–420.

17 Nishikawa H, Kita R, Kimura T, Ohara Y, Takeda H, Sakamoto A, Saito S, Nishijima N, Nasu A, Komekado H, Osaki Y: Clinical efficacy of non-transplant therapies in patients with hepatocellular carcinoma with Child-Pugh C liver cirrhosis. Anticancer Res 2014; 34:3039–3044.
18 Nouso K, Ito Y, Kuwaki K, Kobayashi Y, Nakamura S, Ohashi Y, Yamamoto K: Prognostic factors and treatment effects for hepatocellular carcinoma in Child C cirrhosis. Br J Cancer 2008;98:1161–1165.
19 Wakuta A, Nouso K, Kariyama K, Nishimura M, Kishida M, Wada N, Mizushima T, Higashi T, Tanimoto M: Radiofrequency ablation for the treatment of hepatocellular carcinoma with decompensated cirrhosis. Oncology 2011;81:39–44.
20 Kudo M: Treatment of advanced hepatocellular carcinoma with emphasis on hepatic arterial infusion chemotherapy and molecular targeted therapy. Liver Cancer 2012;1:62–70.
21 Gumbs AA, Gayet B: Adopting Gayet's techniques of totally laparoscopic liver surgery in the United States. Liver Cancer 2013;2:5–15.
22 Hwang DW, Han HS, Yoon YS, Cho JY: Laparoscopic liver resection for hepatocellular carcinoma: Korean experiences. Liver Cancer 2013;2:25–30.
23 Peck-Radosavljevic M: Drug therapy for advanced-stage liver cancer. Liver Cancer 2014; 3:125–131.

Review

Oncology

Oncology 2014;87(suppl 1):104–109
DOI: 10.1159/000368153

Published online: November 22, 2014

Characteristics of Long-Term Survivors following Sorafenib Treatment for Advanced Hepatocellular Carcinoma: Report of a Workshop at the 50th Annual Meeting of the Liver Cancer Study Group of Japan

Katsuaki Tanaka[a] Mitsuo Shimada[b] Masatoshi Kudo[c]

[a]Gastroenterological Center, Yokohama City University Medical Center, Yokohama, [b]Department of Surgery, The University of Tokushima, Tokushima, and [c]Department of Gastroenterology and Hepatology, Kinki University School of Medicine, Osaka-Sayama, Japan

Key Words

Hepatocellular carcinoma · Sorafenib · Long-term survival · Salvage treatment · Conversion surgery · Multidisciplinary therapy

Abstract

Background: Little data are available on the long-term survival of patients treated with sorafenib for advanced hepatocellular carcinoma (HCC). ***Summary:*** During a consensus workshop at the 50th annual meeting of the Liver Cancer Study Group of Japan held in Kyoto (June 5–6, 2014), experts met to discuss the characteristics of long-term (>3 years) survivors of advanced HCC following sorafenib treatment. A total of 70 long-term survivors following sorafenib treatment at eight institutions were included, and the long-term survival rate (>3 years) at each institution ranged from 2.6 to 6.9% (mean, 4.5). The long-term survival-related factors presented can be categorized as follows: (1) conversion options, including hepatic resection following successful sorafenib treatment, (2) additional salvage options when progressive disease is confirmed, (3) long-term sorafenib treatment, (4) effective post-sorafenib options to prolong postprogression survival, and (5) good pretreatment liver function. Sorafenib monotherapy exceeding 3 years is rare, and most of the patients receiving sorafenib required other treatment modalities in the form of multidisciplinary therapy. ***Conclusion:*** The overview obtained from the workshop reflects the pattern of management in practice for long-term survivors following sorafenib treatment for HCC in Japan and may also provide valuable information for other countries.

Introduction

Sorafenib is currently the standard systemic therapy approved for treatment of hepatocellular carcinoma (HCC) in patients with well-preserved liver function (Child-Pugh class A), advanced-stage HCC (Barcelona Clinic Liver Cancer-C), and progressive HCC after locoregional therapy [1–4]. Treatment with sorafenib is recommended based on its efficacy and safety, as reported by two international randomized controlled trials: the SHARP (Sorafenib HCC Assessment Randomized Protocol) and the Asia-Pacific trials [5, 6]. In addition, the efficacy and safety of the drug in clinical practice have been addressed by several field-practice experiences, including the multinational GIDEON (Global Investigation of therapeutic DEcisions in HCC and Of its treatment with

KARGER

E-Mail karger@karger.com
www.karger.com/ocl

0030–2414/14/0877–0104$39.50/0

Dr. Katsuaki Tanaka
Gastroenterological Center, Yokohama City University Medical Center
4-57, Urafune-cho, Minami-ku
Yokohama, Kanagawa 232-0024 (Japan)
E-Mail k_tanaka@yokohama-cu.ac.jp

Table 1. Profiles of long-term survivors following sorafenib treatment

Presenting group	Patients, n	Long-term survivors (male/female)	Etiology B/C/NBNC	TNM stage 3/4A/4B	Treatment response CR/PR/SD/PD	Conversion/salvage options (No. of patients)	Long-term survival-related factors
Imura[1]	–	4 (2/2)	4/0/0	–/–/3	–	Surgery (1), RFA (2)	Conversion surgery
Takeyama[2]	–	5 (5/0)	0/3/2	0/1/4	–	Surgery (3), TACE, RFA	Downstaging Multidisciplinary treatment
Wada[3]	131	9 (7/2)	–	–/3/2	2/1/6/0	Systemic chemotherapy (5), TACE (4)	Especially long SD Good liver function
Urata[4]	60	3 (2/1)	–	0/1/0	–	Combined with TACE (2)	–
Hattori[5]	147	7 (5/2)	2/3/2	–/–/3	2/1/4/0	Surgery (1), RFA (2), radiation (4)	VEGF/AFP response Multidisciplinary treatment
Morimoto[6]	337	15 (14/1)	0/10/5	5/2/6	3/4/4/4	TACE, RFA	Long PPS Good liver function
Ueshima[7]	222	15 (9/6)	6/6/3	9/1/5	4/5/6/0	Surgery (1), TACE, RFA, HAIC	Salvage options Good liver function
Nishijima[8]	465	12 (9/3)	3/4/5	6/0/6	2/3/7/0	TACE (3), chemotherapy (1)	Good liver function Low DCP, disease control

TNM = Tumor-node-metastasis; B/C/NBNC = HBV-positive/HCV-positive/negative for HBV and HCV, the so-called 'non-B non-C'.

[1] Department of Surgery, The University of Tokushima; [2] Department of Gastroenterological Surgery, Graduate School of Medical Sciences, Kumamoto University; [3] Department of Hepato-Biliary-Pancreatic Surgery, National Hospital Organization Kyushu Medical Center; [4] Department of Gastroenterology and Hepatology, Yamaguchi University Graduate School of Medicine; [5] Department of Gastroenterology and Hepatology, Musashino Red Cross Hospital; [6] Department of Hepatobiliary and Pancreatic Medical Oncology, Kanagawa Cancer Center; [7] Department of Gastroenterology and Hepatology, Kinki University School of Medicine; [8]Department of Gastroenterology and Hepatology, Osaka Red Cross Hospital.

sorafeNib) study [7]. In Japan, sorafenib has been administered in accordance with the consensus-based treatment algorithm for HCC proposed by the Japan Society of Hepatology [8]. Sorafenib is also recommended in cases with Child-Pugh class A where transcatheter arterial chemoembolization (TACE) [9] and hepatic arterial infusion chemotherapy (HAIC) are not indicated.

Recently, several case reports [10, 11] and a nationwide survey [12] have been published in which a complete response (CR) was obtained following sorafenib treatment. However, such cases are rare, and most long-term survivors following sorafenib treatment belong to the non-CR group and obtain a partial response (PR) or stable disease (SD). However, little data are available regarding long-term survivors following sorafenib treatment for advanced HCC. To address this issue, we held a workshop at the 50th annual meeting of the Liver Cancer Study Group of Japan, which took place from June 5 to 6, 2014 in Kyoto (congress president: Prof. Masatoshi Kudo). In this review, we present an overview of the factors influencing the management of long-term survivors following sorafenib treatment in Japan and discuss the potentially confounding effects associated with each factor as well as the possible interactions between the factors.

Summary of Presentations from Eight Institutions

The profiles of the long-term (>3 years) survivors following sorafenib treatment from eight institutions are shown in table 1. At the beginning of the workshop, Imura and colleagues (Department of Surgery, The University of Tokushima) presented a case of a 50-year-old man who developed a very large HCC with intrahepatic metastases in the right lobe of the liver (fig. 1a–c). He was administered sorafenib, and a subsequent treatment assessment revealed a PR (fig. 1d–f). Right hepatectomy as a conversion surgery was performed, and *FGF4* gene amplification was detected in the resected specimen [13]. This patient has remained alive with no sign of recurrence for 1.5 years following right hepatectomy. Imura and colleagues also presented 4 additional patients with HCC showing long-term survival after sorafenib treatment; 3 of these 4 patients underwent conversion/salvage treatment (locoregional therapy in 2 patients and surgical resection in 1 patient). All these patients have remained alive, and sorafenib therapy is ongoing for 2 patients.

Takeyama and colleagues (Department of Gastroenterological Surgery, Graduate School of Medical Sciences, Kumamoto University) presented 5 cases of HCC show-

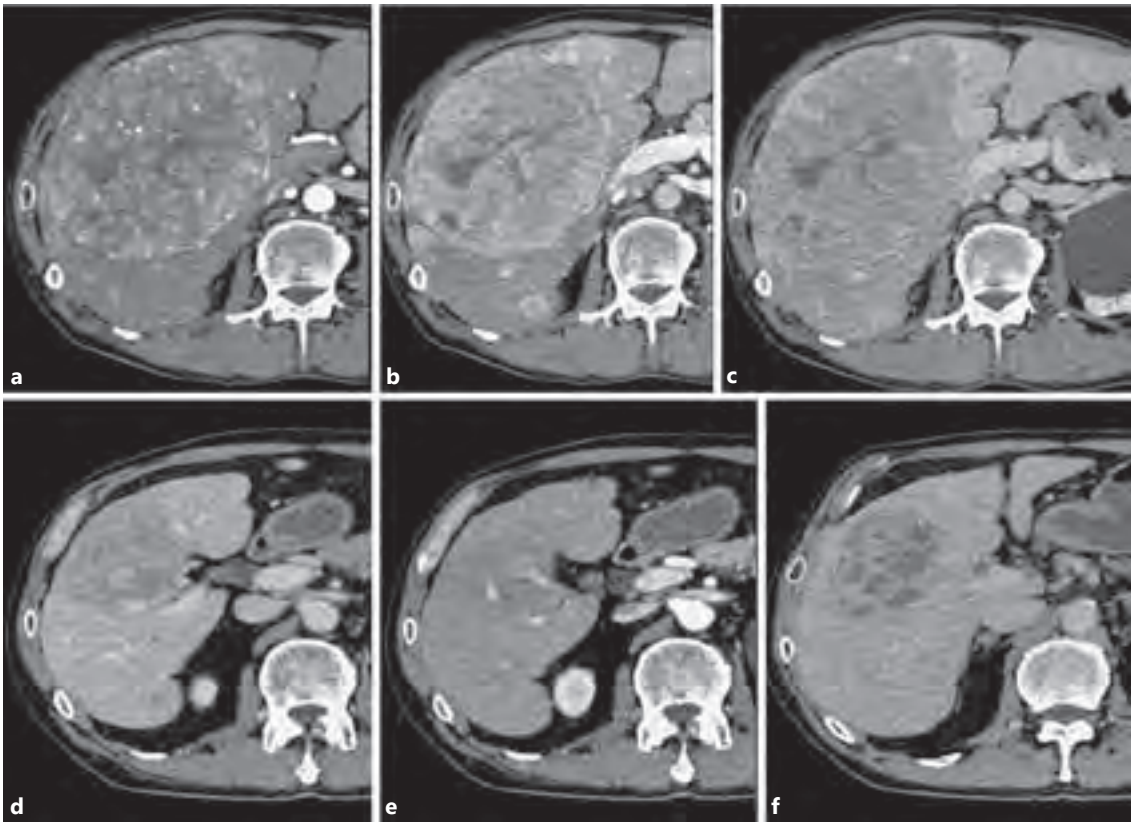

Fig. 1. A 50-year-old man with a very large HCC achieved a PR following sorafenib administration. **a–c** Computed tomography scan performed before sorafenib treatment showing a huge HCC with intrahepatic metastases in the right lobe. **a** Arterial phase. **b** Portal phase. **c** Delayed phase. **d–f** Following sorafenib treatment, the main tumor had shrunk and some of the intrahepatic metastases disappeared. **d** Arterial phase. **e** Portal phase. **f** Delayed phase.

ing long-term survival following sorafenib treatment. Of these, 3 patients underwent salvage hepatectomy with or without radiofrequency ablation (RFA) [14]. Furthermore, additional locoregional treatment (TACE or RFA) was carried out while sorafenib treatment continued. This group suggested that multidisciplinary treatment, including surgical treatment, might improve survival following sorafenib administration.

Wada and colleagues (Department of Hepato-Biliary-Pancreatic Surgery, National Hospital Organization, Kyushu Medical Center) presented 9 cases of long-term survivors (6.9%) out of 131 patients with HCC who started treatment with sorafenib monotherapy (mainly half-dose sorafenib) between 2009 and 2013. Of these, 2 patients achieved a CR, 1 had a PR, and the remaining 6 patients had SD. Sorafenib therapy exceeding 3 years of duration was administered only to 1 patient who achieved an especially long SD. Of the remaining 8 patients, 7 underwent post-sorafenib options, including systemic chemotherapy (n = 5) and/or TACE (n = 4).

Urata and colleagues (Department of Gastroenterology and Hepatology, Yamaguchi University Graduate School of Medicine) presented 3 cases of long-term survivors (5.0%) out of 60 patients treated with sorafenib for HCC. Two of the 3 long-term survivors received TACE combined with sorafenib.

Hattori and colleagues (Department of Gastroenterology and Hepatology, Musashino Red Cross Hospital) presented 7 cases of long-term survivors (4.8%) out of 147 patients with HCC who started sorafenib monotherapy between July 2009 and November 2013. Two patients initially received full-dose sorafenib, and the remaining 5 received a half-dose regimen. The median duration of sorafenib therapy was 980 days. Of these 7 patients, 2 achieved a CR, 1 had a PR, and the remaining 4 had SD. All of these long-term survivors underwent multidisci-

plinary treatment including conversion surgery (n = 1), RFA (n = 2), or radiation therapy (n = 4). Furthermore, Hattori and colleagues reported that a decreased plasma vascular endothelial growth factor (VEGF) concentration, 8 weeks after starting sorafenib treatment, may predict survival in patients with advanced HCC [15]. In univariate analysis, a decrease in VEGF and an early alpha-fetoprotein (AFP) response were significantly associated with survival following sorafenib treatment. All 4 patients who showed a decrease in VEGF and an objective response (CR or PR) survived during the observation period.

Morimoto and colleagues (Department of Hepatobiliary and Pancreatic Medical Oncology, Kanagawa Cancer Center) presented a multicenter study from the Kanagawa Liver Study Group, detailing the cases of 15 long-term survivors (4.5%) out of 337 patients with HCC who started treatment with sorafenib monotherapy between July 2009 and December 2013. The median duration of progression-free survival of the long-term survivors following sorafenib therapy was 12.7 months, and a significantly longer post-progression survival (PPS) was associated with the use of post-sorafenib salvage options. Good pretreatment liver function and low baseline levels of AFP and des-γ-carboxy prothrombin (DCP) were associated with longer survival. Furthermore, this group indicated that initial treatment with half-dose sorafenib led to fewer severe adverse events and a comparable survival benefit compared to the use of full-dose sorafenib in select patients with HCC, particularly those of advanced age [16].

Ueshima and colleagues (Department of Gastroenterology and Hepatology, Kinki University School of Medicine) presented the cases of 15 long-term survivors (6.8%) out of 222 patients with HCC who started treatment with sorafenib monotherapy between May 2009 and December 2013. Of these 15 long-term survivors, 9 patients were tumor-node-metastasis stage 3 (according to the Liver Cancer Study Group of Japan staging criteria), 1 patient was stage 4A, and 5 were stage 4B. Four patients achieved a CR, 5 had a PR, and the remaining 6 had SD. The 3 patients who achieved a CR have remained alive with or without sorafenib continuation [17], and a patient who achieved PR underwent conversion surgery with no sign of recurrence since the surgery. Of the remaining 10 patients who achieved a PR or SD, 6 patients underwent post-sorafenib salvage treatment (TACE, HAIC, or clinical trials), and 4 patients underwent additional locoregional therapy with sorafenib continuation.

Nishijima and colleagues (Department of Gastroenterology and Hepatology, Osaka Red Cross Hospital) presented a multicenter study from the Japanese Red Cross Liver Study Group, detailing the cases of 12 long-term survivors (2.6%) out of 465 patients with HCC who began sorafenib monotherapy between January 2008 and August 2013 [18]. Of these 12 long-term survivors, 2 patients achieved a CR, 3 had a PR, and the remaining 7 had SD. The median duration of sorafenib therapy in the cohort was 163 days, and 262 patients died within 1 year (short-term survivors). Subgroup analyses comparing long-term with short-term survivors showed that normal cholinesterase levels and lower baseline DCP levels, and disease control according to the modified Response Evaluation Criteria In Solid Tumors (RECIST) at an early stage of sorafenib treatment were significantly associated with long-term survival.

Long-Term Survival-Related Factors

An overview of long-term (>3 years) survival following sorafenib treatment was collated from eight Japanese institutions. A total of 70 cases of long-term survival following sorafenib treatment were presented and the long-term survival rate at each institution ranged from 2.6 to 6.9% (mean, 4.5). Clinically, sorafenib is characterized by a low objective tumor response rate but a relatively high disease control rate (2% PR rate and 40% SD rate) [5, 6]. Our expert panel demonstrated that, among 58 long-term survivors at five institutions, 13 patients achieved a CR (22.4%), 14 had a PR (24.1%), 27 had a SD (46.5%), and the remaining 4 had progressive disease (PD) (table 1). This shows that obtaining an objective response is of primary importance to long-term survival following sorafenib administration. Sorafenib monotherapy exceeding a 3-year duration is rare, and most of the patients receiving sorafenib require other treatment modalities in the form of a multidisciplinary therapy. Imura and colleagues emphasized conversion surgery for HCC that has been downstaged in patients who achieve PR. Takeyama and colleagues and Hattori and colleagues emphasized the use of salvage options for recurrent HCC during sorafenib treatment. Wada and colleagues, Morimoto and colleagues, and Ueshima and colleagues highlighted the importance of a continuation of sorafenib for as long as possible, and the latter two groups further reported the utility of post-sorafenib options to prolong PPS. Furthermore, good pretreatment liver function and low baseline levels of AFP and DCP have been reported as predictors of favorable long-term survival. Based on these reports, we categorized long-term survival-related factors as follows: (1) conversion options, including hepatic resection after successful sorafenib treatment, (2) additional salvage options with sorafenib continuation when PD is confirmed,

(3) long-term sorafenib treatment, (4) effective post-sorafenib options to prolong PPS, and (5) good pretreatment liver function. These categories appear to reflect the actual patterns of management in practice for long-term survivors following sorafenib treatment in Japan.

Sorafenib has been established as a standard therapy to prolong survival in patients with advanced HCC, but it provides only a small treatment response. A recent nationwide survey to examine the clinical characteristics of patients who obtained a CR following sorafenib use showed that only 18 patients (0.6%) obtained a CR out of 3,047 patients who were treated with sorafenib [12]. Predictive factors in the CR group were female sex, low body weight (<59 kg), early clinical stage, and small initial dose of sorafenib, implying that it is difficult to predict responders using baseline clinical characteristics of patients. Biomarkers that are able to predict patient prognosis or response to therapy may represent a major advancement towards a more personalized, tailored treatment for cancer patients [19, 20]. Arao et al. [13] reported that *FGF3/FGF4* gene amplification is frequently observed in tumors that respond to sorafenib. However, this amplification was only observed in around 2% of HCCs. HCC is a highly heterogeneous disease, and the identification of biomarkers is complex and has been poorly explored thus far. Llovet et al. [21] studied plasma biomarkers as predictors of outcome in patients with advanced HCC. They measured baseline levels of plasma biomarkers in 491 patients, and again after 12 weeks in 305 patients participating in a phase III randomized controlled trial (SHARP trial). They concluded that angiopoietin-2 and VEGF were independent predictors of survival in patients with advanced HCC, and that none of the biomarkers tested significantly predicted response to sorafenib.

With regard to on-treatment biomarkers, assessments of early AFP response [22] and a paradoxical increase in DCP [23] have been reported. Personeni et al. [24] have investigated the prognostic utility of serum AFP response, defined as a >20% decrease in AFP levels during 8 weeks of treatment with sorafenib, and concluded that the assessment of AFP response may be considered as an alternative to RECIST for monitoring sorafenib response in HCC. In the workshop, Hattori and colleagues reported on the utility of measuring decreases in VEGF, in addition to the assessment of AFP response. They reported that all patients who had both a VEGF decrease and an AFP response survived during the observation period (median, 19.7 months), and the triple combination of plasma VEGF decrease, AFP response, and modified RECIST is associated with an extremely favorable prognosis [15]. On-treatment biomarkers are important to identify patients who can expect long-term survival following sorafenib therapy, although their radiologic findings may not be categorized as objective responses.

To obtain a favorable outcome for HCC patients when locoregional therapy [9, 25] is not indicated, patients should immediately be treated with sorafenib, and should continue to be treated with the drug for as long as possible. If necessary, additional salvage options during sorafenib treatment or post-sorafenib therapy, such as second-line targeted therapy, may prolong survival. Although further research to optimize the use of sorafenib is ongoing, in particular to investigate potential laboratory and/or genetic biomarkers of response, the present consensus seems to accurately reflect the patterns of management of HCC currently practiced in Japan and also provides valuable information for other countries.

Disclosure Statement

The authors declare that no financial or other conflicts of interest exist in relation to the content of this article.

References

1 European Association for the Study of the Liver; European Organisation for Research and Treatment of Cancer: EASL-EORTC clinical practice guidelines: management of hepatocellular carcinoma. J Hepatol 2012;56:908–943.

2 Verslype C, Rosmorduc O, Rougier P; ESMO Guidelines Working Group: Hepatocellular carcinoma: ESMO-ESDO Clinical Practice Guidelines for diagnosis, treatment and follow-up. Ann Oncol 2012;23(suppl 7):vii41–vii48.

3 Kudo M: Treatment of advanced hepatocellular carcinoma with emphasis on hepatic arterial infusion chemotherapy and molecular targeted therapy. Liver Cancer 2012;1:62–70.

4 Kudo M, Matsui O, Izumi N, et al: JSH consensus-based clinical practice guideline for the management of hepatocellular carcinoma: 2014 update by the Liver Cancer Study Group of Japan. Liver Cancer 2014;3:458–468.

5 Llovet JM, Ricci S, Mazzaferro V, et al: Sorafenib in advanced hepatocellular carcinoma. N Engl J Med 2008;359:378–390.

6 Cheng AL, Kang YK, Chen Z, et al: Efficacy and safety of sorafenib in patients in the Asia-Pacific region with advanced hepatocellular carcinoma: a phase III randomised, double-blind, placebo-controlled trial. Lancet Oncol 2009;10:25–34.

7 Lencioni R, Kudo M, Ye SL, et al: GIDEON (Global Investigation of therapeutic DEcisions in hepatocellular carcinoma and Of its treatment with sorafeNib): second interim analysis. Int J Clin Pract 2014;68:609–617.
8 Kudo M, Izumi N, Kokudo N, et al: Management of hepatocellular carcinoma in Japan: Consensus-Based Clinical Practice Guidelines proposed by the Japan Society of Hepatology (JSH) 2010 updated version. Dig Dis 2011;29:339–364.
9 Lencioni R: Chemoembolization in patients with hepatocellular carcinoma. Liver Cancer 2012;1:41–50.
10 Inuzuka T, Nishikawa H, Sekikawa A, et al: Complete response of advanced hepatocellular carcinoma with multiple lung metastases treated with sorafenib: a case report. Oncology 2011;81(suppl 1):152–157.
11 Shiozawa K, Watanabe M, Ikehara T, et al: Sustained complete response of hepatocellular carcinoma with portal vein tumor thrombus following discontinuation of sorafenib: a case report. Oncol Lett 2014;7:50–52.
12 Shiba S, Okusaka T, Ikeda M, et al: Characteristics of 18 patients with hepatocellular carcinoma who obtained a complete response after treatment with sorafenib. Hepatol Res 2014, Epub ahead of print.
13 Arao T, Ueshima K, Matsumoto K, et al: FGF3/FGF4 amplification and multiple lung metastases in responders to sorafenib in hepatocellular carcinoma. Hepatology 2013;57:1407–1415.
14 Ishiko T, Beppu T, Chikamoto A, et al: The possible role of sorafenib as a part of the multimodal treatment for hepatocellular carcinoma (in Japanese). Gan To Kagaku Ryoho 2011;38:2499–2501.
15 Tsuchiya K, Asahina Y, Matsuda S, et al: Changes in plasma vascular endothelial growth factor at 8 weeks after sorafenib administration as predictors of survival for advanced hepatocellular carcinoma. Cancer 2014;120:229–237.
16 Morimoto M, Numata K, Kondo M, et al: Field practice study of half-dose sorafenib treatment on safety and efficacy for hepatocellular carcinoma: a propensity score analysis. Hepatol Res 2014, Epub ahead of print.
17 Kudo M, Ueshima K: Positioning of a molecular-targeted agent, sorafenib, in the treatment algorithm for hepatocellular carcinoma and implication of many complete remission cases in Japan. Oncology 2010;78(suppl 1):154–166.
18 Takeda H, Nishikawa H, Osaki Y, et al: Clinical features associated with radiological response to sorafenib in unresectable hepatocellular carcinoma: a large multicenter study in Japan. Liver Int 2014, Epub ahead of print.
19 Sawyers CL: The cancer biomarker problem. Nature 2008;452:548–552.
20 Shao YY, Hsu CH, Cheng AL: Predictive biomarkers of antiangiogenic therapy for advanced hepatocellular carcinoma: where are we? Liver Cancer 2013;2:93–107.
21 Llovet JM, Pena CE, Lathia CD, et al: Plasma biomarkers as predictors of outcome in patients with advanced hepatocellular carcinoma. Clin Cancer Res 2012;18:2290–2300.
22 Shao YY, Lin ZZ, Hsu C, et al: Early alpha-fetoprotein response predicts treatment efficacy of antiangiogenic systemic therapy in patients with advanced hepatocellular carcinoma. Cancer 2010;116:4590–4596.
23 Ueshima K, Kudo M, Takita M, et al: Des-gamma-carboxyprothrombin may be a promising biomarker to determine the therapeutic efficacy of sorafenib for hepatocellular carcinoma. Dig Dis 2011;29:321–325.
24 Personeni N, Bozzarelli S, Pressiani T, et al: Usefulness of alpha-fetoprotein response in patients treated with sorafenib for advanced hepatocellular carcinoma. J Hepatol 2012;57:101–107.
25 Lin SM. Local ablation for hepatocellular carcinoma in Taiwan. Liver Cancer 2013;2:73–83.

Clinical Study

Oncology

Oncology 2014;87(suppl 1):110–117
DOI: 10.1159/000368154

Published online: November 22, 2014

Efficacy and Safety of Telaprevir-Based Antiviral Treatment for Elderly Patients with Hepatitis C Virus

Masahiro Takita Satoru Hagiwara Masatoshi Kudo Masashi Kono
Hirokazu Chishina Tadaaki Arizumi Satoshi Kitai Norihisa Yada
Tatsuo Inoue Yasunori Minami Kazuomi Ueshima

Department of Gastroenterology and Hepatology, Kinki University School of Medicine, Osaka-Sayama, Japan

Key Words
Chronic hepatitis C · Telaprevir · Triple therapy

Abstract
Background: Telaprevir-based antiviral therapy has been the primary treatment for chronic hepatitis C genotype 1 at a high viral load since November 2011. On the other hand, a number of patients have been reported to require withdrawal from or reduced doses of drugs due to side effects, such as eruptions, anemia, and renal dysfunction. In addition, as hepatitis C patients are growing older, it is imperative to investigate the tolerability of triple combination therapy for elderly patients. ***Subjects and Methods:*** The study subjects comprised 35 patients who received telaprevir combination therapy after November 2011. They were divided into group A (age: <65 years; n = 21) and group B (age: ≥65 years; n = 14) in order to compare the treatment completion rate, sustained virological response at week 24 (SVR24), and adverse events between the groups. ***Results:*** The treatment completion rate was 82.8% (29/35) in all subjects, 90.4% (19/21) in group A, and 78.5% (11/14) in group B. The rate was lower in group B but without a significant difference between the groups (p = 0.804). The SVR24 rate was 88.5% (31/35) in all subjects, 90.4% (19/21) in group A, and 85.7% (12/14) in group B, without a significant difference between the groups (p = 0.161). ***Conclusion:*** Although the incidence of anemia was higher in group B, there was no significant difference in the treatment completion or SVR24 rate between the groups. Telaprevir combination therapy is suggested to be tolerable for elderly hepatitis C patients.

Introduction

Hepatocellular carcinoma causes the death of approximately 600,000–700,000 individuals annually worldwide and it is commonly due to chronic viral hepatitis [1]. In Japan, hepatocellular carcinoma is often caused by hepatitis C virus (HCV) [2–4], and patients with chronic hepatitis C (CHC) are growing older [5]. As elderly patients with CHC have been reported to show a higher incidence rate of carcinogenesis in noncirrhotic liver than younger adults, the treatment of elderly hepatitis C patients is important [6].

In 2004, the concomitant use of pegylated interferon (PEG-IFN) α-2b and ribavirin (RBV) for 48 weeks became available for patients with hepatitis C genotype 1 at a high viral load, and, as a result, it has become possible to achieve a sustained virological response (SVR) in approximately 50% of cases [7,8]. However, the treatment of CHC patients, particularly elderly adults, has been challenging due to se-

KARGER

E-Mail karger@karger.com
www.karger.com/ocl

0030–2414/14/0877–0110$39.50/0

Prof. Masatoshi Kudo
Department of Gastroenterology and Hepatology
Kinki University School of Medicine
377-2 Ohno-Higashi, Osaka-Sayama, Osaka 589-8511 (Japan)
E-Mail m-kudo@med.kindai.ac.jp

Table 1. Baseline patient characteristics

	Group A (aged <65 years; n = 21)	Group B (aged ≥65 years; n = 14)	p
Sex, male/female	11/10	9/5	0.482
Age, years	57 (35–64)	69 (65–77)	0.166
BMI	23.4 (12.2–36.8)	23.4 (17.32–30)	0.57
rs8099917 (TT/non-TT)	15/6	12/1	0.143
WBC, $\times 10^9$/l	5.7 (3.1–13.8)	5.2 (2.5–6.7)	0.261
Hb, g/dl	14.0 (11.7–17.3)	13.5 (11.9–15.3)	0.139
Platelets, $\times 10^{10}$/l	20.4 (7.9–35.7)	17.3 (9.2–23.9)	0.051
ALT, IU/l	35 (17–145)	34.55 (21–292)	0.44
γGTP, IU/l	31.5 (11–327)	30 (18–264)	0.733
Albumin, g/dl	4.3 (2.9–5.2)	4.4 (3.5–4.7)	0.46
Total cholesterol, mg/dl	169 (75–237)	164 (125–224)	0.837
Viral load	6.5 (1.8–7.4)	6.65 (4.3–7.7)	0.653
PEG-IFN α-2b, μg	90 (40–150)	80 (80–100)	0.867
PEG-IFN α-2b/kg/w, μg/kg/w	1.44 (0.80–1.81)	1.42 (0.71–1.73)	0.94
RBV, mg	600 (400–1,000)	600 (400–800)	0.34
RBV/kg/day, mg/kg/day	8.09 (3.4–12.69)	7.33 (4.01–10.52)	0.248
TBV, mg	2,250 (1,500–2,250)	2,250 (1,500–2,250)	0.627
TBV/kg/day, mg/kg/day	32.56 (18.75–45.91)	30.62 (15–40.17)	0.074
SVR24	19/2	12/2	0.161

For the categorical data, the number of patients in each category is shown. For the continuous data, the median and range are displayed. ALT = Alanine aminotransferase; BMI = body mass index; γGTP = γ-glutamyltranspeptidase; TBV = telaprevir; WBC = white blood cells.

vere side effects of PEG-IFN α-2b (e.g., anorexia, systemic lassitude, and cytopenia) and RBV (e.g., anemia) [9–11].

In 2011, the concomitant use of telaprevir, PEG-IFN, and RBV became available. Telaprevir strongly prevents viral multiplication by directly inhibiting HCV NS3/4A protease, which is a nonstructural protein [12]. It has been reported that this therapy achieves a higher SVR rate within a short period than when using the existing combination therapy with PEG-IFN and RBV [13–16]. However, the safety and beneficial effects of such a triple combination therapy for elderly patients have yet to be elucidated.

In the present study, we investigated older and younger adults who received telaprevir-based antiviral therapy at our hospital, in order to compare its safety and beneficial effects between the two groups.

Subjects and Methods

We conducted a retrospective study at Kinki University Hospital. The study subjects comprised 35 patients who received telaprevir-based antiviral therapy between November 2011 and March 2012. HCV-RNA levels were measured by the COBAS TaqMan HCV Test (Roche Diagnostics, Tokyo, Japan), and treatment-naive individuals were eligible when their HCV-RNA level was 5 log10 IU/ml or higher. Subcutaneous injections of PEG-IFN (Peg-Intron; Schering-Plough, Kenilworth, N.J., USA) were administered at a dose of 1.5 μg/kg once a week. RBV (Rebetol; Schering-Plough) was orally administered after a meal twice daily as follows: when the hemoglobin (Hb) level was ≥13 g/dl, 600, 800, and 1,000 mg for those weighing <60, 60–80, and >80 kg; and when the Hb level was <13 g/dl, 400, 600, and 800 mg for those weighing <60, 60–80, and >80 kg, respectively. Telaprevir (Telavic; Mitsubishi Tanabe Pharma, Osaka, Japan) was administered at a dose of 2,250 mg/day after a meal 3 times a day at 8-hour intervals, but the dose was reduced to 1,500 mg/day when the subject was female, aged ≥70 years, or weighed ≤50 kg.

The subjects received telaprevir-based antiviral therapy with telaprevir, PEG-IFN, and RBV for the first 12 weeks. After that, PEG-IFN and RBV were administered for 12 weeks if the subject showed an HCV-RNA level of <1.2 log10 IU/ml or was negative for HCV-RNA at week 4 and for the RNA at week 12. Individuals not meeting these criteria received response-guided therapy for 36 weeks from week 13.

Concerning skin disorders, localized lesions with areas accounting for ≤50% of the body surface were defined as grade 1; multifocal or diffuse lesions with areas accounting for ≤50% of the body surface along with a mucosal lesion not associated with ulcers or erosion were defined as grade 2, and systemic rashes with areas accounting for >50% of the body surface along with mucosal ulcers

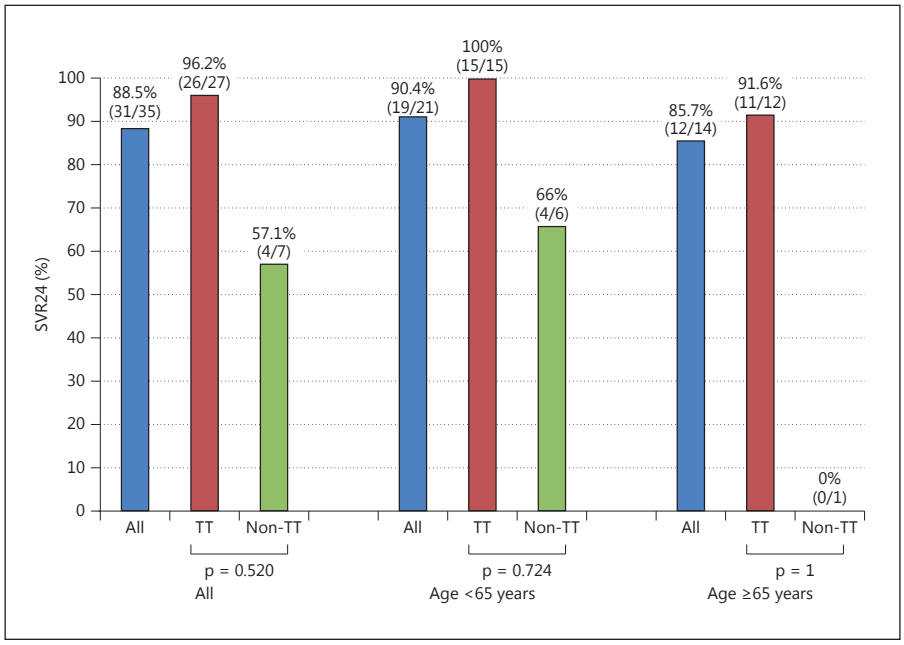

Fig. 1. Age-specific SVR rates according to the IL28 genotype in all subjects.

or erosion, eye lesions, epidermolysis, blisters, or purpura associated with infiltration were defined as grade 3. Regarding anemia, Hb levels of ≥9.5 and <11 g/dl, ≥8 and <9.5 g/dl, and <8 g/dl were defined as grade 1, 2, and 3, respectively.

The study subjects were divided into 23 individuals aged <65 years (group A) and 12 individuals aged ≥65 years (group B), and we compared the treatment completion rate, SVR at week 24 (SVR24), and adverse events between the groups.

Statistical Analysis

Data are expressed as median (range) values. Differences between groups were examined for significance using the t test and Fisher exact test where appropriate. A p value <0.05 was regarded as statistically significant in all analyses.

Results

Patient characteristics are shown in table 1. The number of treatment-naive patients and previously treated individuals in whom hepatitis had relapsed or for whom the administered drugs had been ineffective was 20 and 15 overall, 11 and 10 in group A, and 9 and 5 in group B, respectively. As a result of investigating rs8099917, which is an IL28B genotype, the number of patients with genotypes of TT and non-TT was 27 and 7 overall, 15 and 6 in group A, and 12 and 1 in group B, respectively. There was no significant difference in the BMI, IL28B SNPs, Hb, albumin, viral load, initial dose, or adherence to the regimen between the groups.

The SVR24 rate was 88.5% (31/35) in all subjects, 90.4% (19/21) in group A, and 85.7% (12/14) in group B. The rate showed a tendency to be lower in group B but without a significant difference between the groups (p = 0.161). We also investigated the SVR24 rate according to the IL28B genotype, which revealed that the rate was 96.2% (26/27) and 57.1% (4/7) overall (p = 0.520), 100% (15/15) and 66.6% (4/6) in group A (p = 0.720), and 91.6% (11/12) and 0% (0/1) in group B (p = 1) in patients with genotypes of TT and non-TT, respectively (fig. 1). According to the IL28B genotype among the treatment-naive patients, the SVR24 rate was 93.7% (15/16) and 50% (2/4) overall (p = 0.666), 100% (8/8) and 66.6% (2/3) in group A (p = 1), and 83.3% (7/8) and 0% (0/1) in group B (p = 1) in patients with TT and non-TT, respectively (fig. 2). We also investigated the SVR24 rate according to the IL28B genotype among the previously treated individuals in whom hepatitis had relapsed, which clarified that the rate was 100% (9/9) and 66.6% (2/3) overall (p = 1), 100% (6/6) and 66.6% (2/3) in group A (p = 1), and 100% (3/3) and 0% (0/0) in group B in patients with TT and non-TT, respectively (fig. 3). Among the previously treated individuals in whom the administered drugs had been ineffective, SVR was achieved both in group A (1 patient with TT) and in group B (1 patient with TT).

The SVR rate was compared to the initial dose of telaprevir, which revealed that among those receiving 1,500

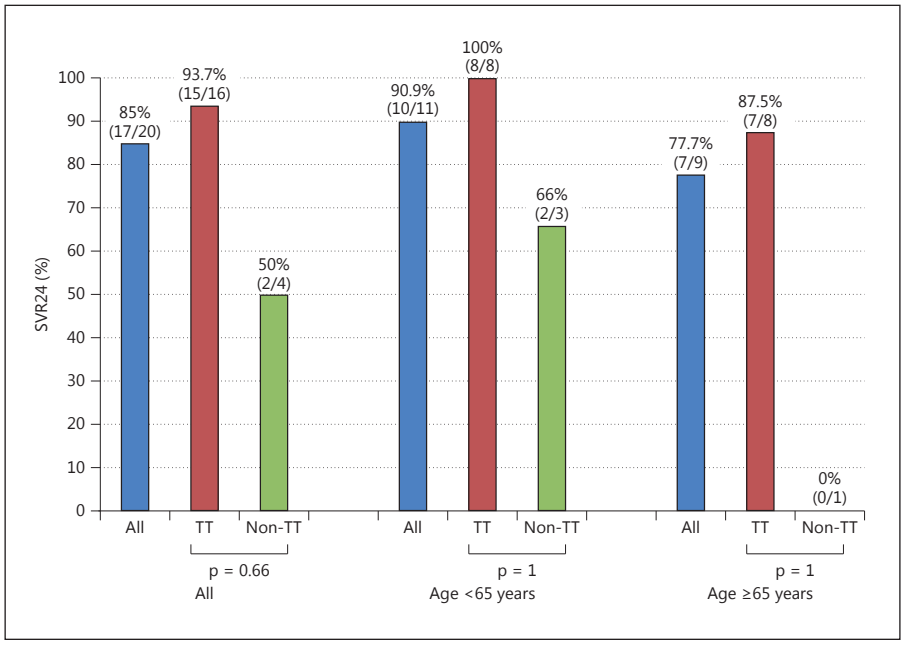

Fig. 2. Age-specific SVR rates according to the IL28 genotype among treatment-naive individuals.

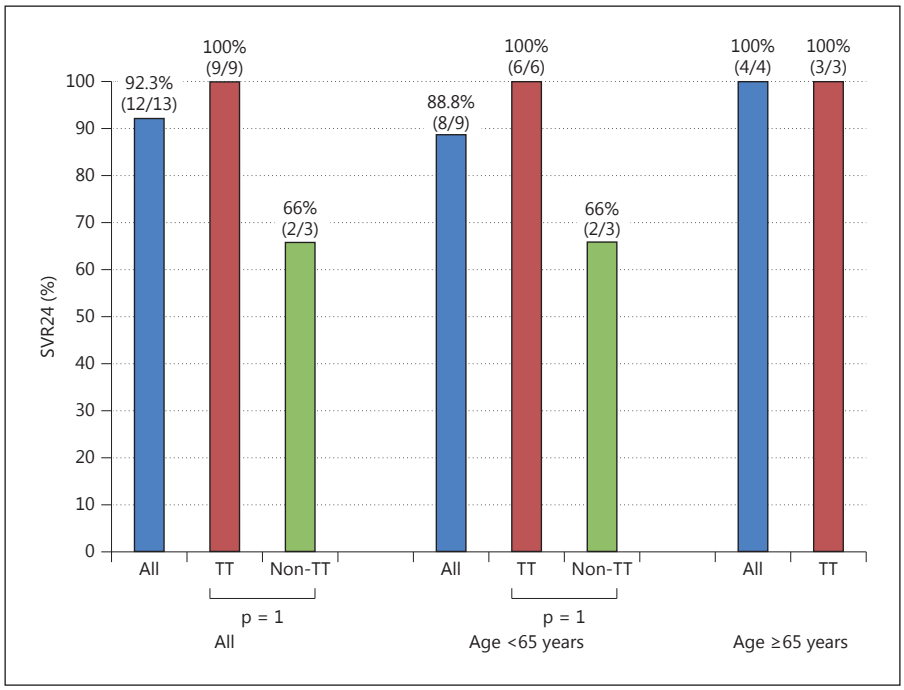

Fig. 3. Age-specific SVR rates according to the IL28 genotype among previously treated individuals in whom hepatitis C had relapsed.

mg of telaprevir, the SVR rate was 83.3% (5/6) and 80% (4/5) in group A and B, respectively (p = 1). Among those receiving 2,250 mg of telaprevir, the SVR rate was 93.3% (14/15) and 88.8% (8/9) in group A and B, respectively (p = 1; fig. 4).

The treatment completion rate was 82.8% (29/35) in all subjects, 90.4% (19/21) in group A, and 78.5% (11/14) in group B. The rate was lower in group B, but without a significant difference between the groups (p = 0.793). The reasons for treatment discontinuation were anemia

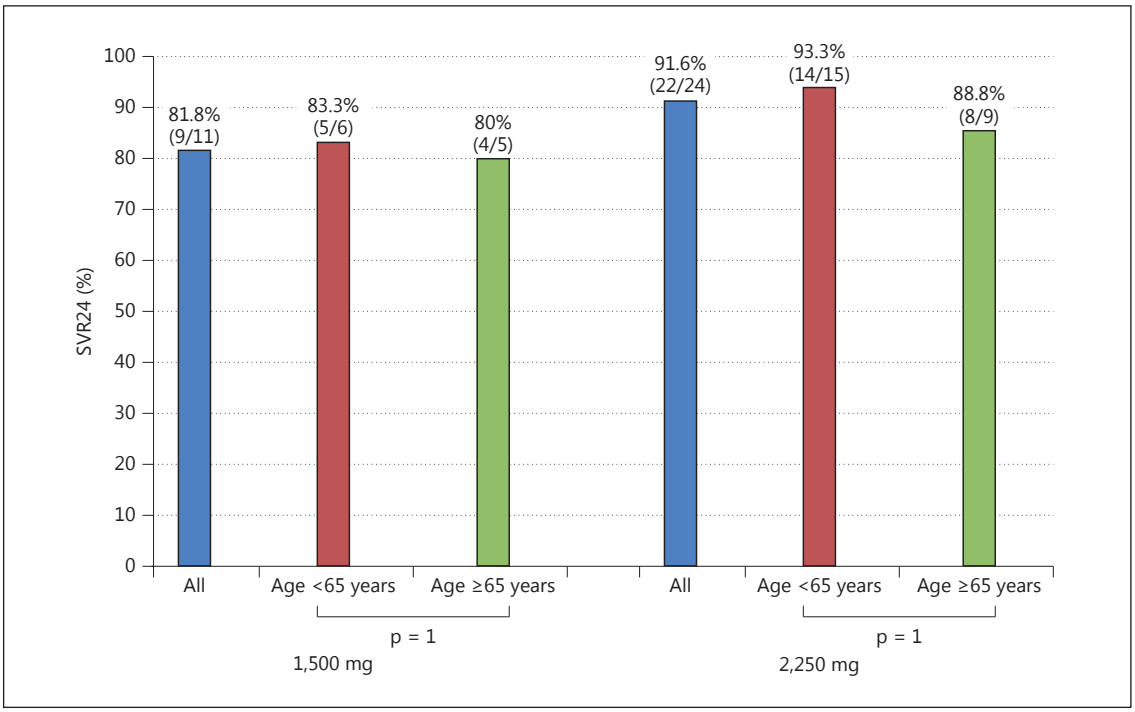

Fig. 4. Age-specific SVR rates according to the initial dose of telaprevir.

(n = 1) and skin disorders (n = 1) in group A and brain infarction (n = 1), systemic lassitude (n = 1), and infective endocarditis (n = 1) in group B.

Drug-induced skin disorders were identified in 76.1% (16/21) and 64.2% (9/14) of cases in group A and B, respectively. Severe (grade 3) side effects occurred in 9.5% (2/21) and 0% (0/14) of cases in group A and B, respectively, but without a significant difference (p = 0.156; fig. 5).

The incidence of anemia was significantly higher in group B than in group A: 71.4% (10/14) versus 52.3% (11/21) (p = 0.002; fig. 6).

Discussion

In this study, high SVR24 rates were achieved by elderly patients with hepatitis C receiving telaprevir-based antiviral therapy, and its safety among these patients was verified.

When conducting PEG-IFN/RBV therapy for elderly patients, it is often necessary to reduce their doses or discontinue the therapy when side effects occur, such as systemic lassitude, depression, anemia, or thrombocytopenia. According to a Japanese study involving 1,251 subjects, the treatment completion rate was 57 and 75% in older (aged ≥65 years) and younger adults, respectively [5]. In the present study, the treatment completion rate was 75% in the older subjects (group B), which was a relatively favorable result. This was probably because our triple combination therapy was shorter (24 weeks) than the typical PEG-IFN/RBV therapy (48 weeks). In our study, the SVR24 rate in the older subjects was also favorable (83.3%), possibly due to the potent inhibitory effects of telaprevir against viral multiplication [12]. The SVR rate achieved by the older group was slightly lower than that shown by the younger group, but the difference was not significant, and this finding was similar to that reported by Furusyo et al. [17]. Such a favorable SVR rate achieved by the older group was probably due to the maintained adherence to telaprevir and IFN [17].

According to Akuta et al. [18] and Chayama et al. [19], similarly to when using PEG-IFN/RBV therapy, subjects with an IL28B genotype of TT showed a high cure rate with telaprevir-based antiviral therapy. In the present study, the SVR rate achieved by subjects with an IL28B genotype of TT was high (96.2%) but not significantly different from that shown by those with non-TT (57.1%). As a result of investigating the SVR rate according to age among subjects

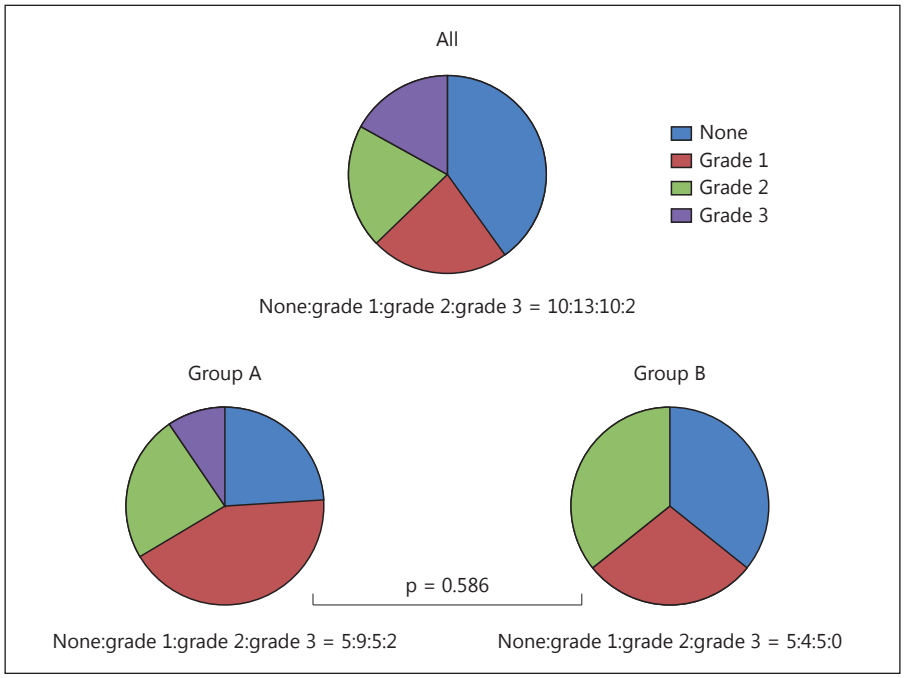

Fig. 5. Age-specific ratios of drug-induced skin disorders.

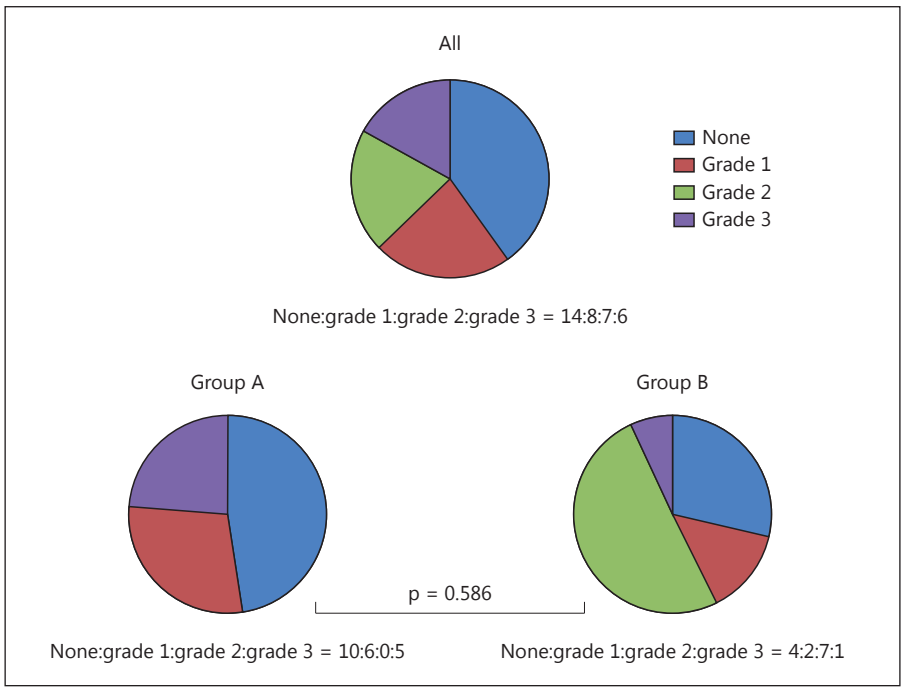

Fig. 6. Age-specific ratios of anemia: the incidence of anemia was significantly higher among those aged ≥65 years (group B).

with TT, those aged <65 years and those aged ≥65 showed SVR rates of 100 and 91.6%, respectively, which were favorable results. On the other hand, among subjects with non-TT, the rates were 66 and 0% in the former and latter group, respectively. However, as there was only 1 non-TT subject aged ≥65 years, the IL28B genotype was not investigated among a sufficient number of older adults (fig. 1).

Telaprevir-based antiviral therapy has been reported to be highly beneficial for treatment-naive patients and previously treated individuals in whom hepatitis had re-

lapsed [13–15]. In the present study, we investigated treatment-naive patients and those who had previously been treated but had a relapse, which clarified that the therapy was highly effective. Among the treatment-naive subjects, the SVR rates were 71.4 and 92.3% in the older (group B) and younger patients (group A), respectively. Among the previously treated subjects, the rates were 100 and 88.8% in group B and A, respectively (fig. 2, 3). The 2 previously treated subjects, in whom the drugs used had been ineffective, both achieved SVR. This was possibly because the therapy was more likely to be effective for those with an IL28B genotype of TT.

In this study, both the older (group B) and the younger subjects (group A) showed favorable SVR rates (80 and 83.3%, respectively) when using telaprevir at a dose of 1,500 mg/day (fig. 4). Marcellian et al. [20] conducted a randomized controlled trial in which the subjects were assigned to receive either 2,250 or 1,500 mg of telaprevir, and found that the SVR rate was not significantly different between the groups, and the safety of the two regimens was similarly verified. Hara et al. [21] reported that a decrease in Hb levels was significantly inhibited among a group receiving 1,500 mg of telaprevir. In our study, the incidence of anemia was significantly higher in the older subjects (group B; fig. 6). We suggest that a dose of 1,500 mg may be sufficient for elderly individuals, as Japanese patients receiving telaprevir are growing older and their body weight is commonly lower than that of patients in the US and Europe.

Drug-induced skin disorders occurred at a high rate in both the older (group B; 58.3%) and the younger (group A; 78.2%) patients. The incidence showed a tendency to be higher in the latter group, but without a significant difference (fig. 5). A previous study also reported a similar incidence rate of skin disorders between older and younger subjects [17].

Many studies have reported that antiviral therapy is useful as a radical treatment for hepatitis C, and hepatocarcinogenesis can be inhibited by achieving SVR [6, 22–24]. However, therapies involving IFN are sometimes challenging due to adverse events. In recent years, combination therapies with direct-acting antivirals, which do not involve IFN, have been developed. A phase 3 trial of combination therapy with asunaprevir and daclatasvir achieved a high SVR rate (84.7%). In this trial, the therapy was discontinued due to adverse events in 5% of cases, with a low incidence of severe adverse events (5.9%) [25]. Combination therapy with direct-acting antivirals will probably become the primary treatment for hepatitis C. However, the inhibitory effects of such therapy against carcinogenesis are unknown due to researchers' limited experience in this field.

The limitations of our study were that it was conducted in a retrospective manner and that it involved a small number of subjects. The treatment completion rate showed a tendency to be lower in the older group, but the SVR24 rate was equivalent between the two groups. Our findings suggest that telaprevir-based antiviral therapy may be tolerable for elderly hepatitis C patients.

Disclosure Statement

The authors declare that no financial or other conflicts of interest exist in relation to the content of this article.

References

1 Kawanaka M, Nishino K, Nakamura J, et al: Quantitative levels of hepatitis B virus DNA and surface antigen and the risk of hepatocellular carcinoma in patients with hepatitis B receiving long-term nucleos(t)ide analogue therapy. Liver Cancer 2014;3:41–52.

2 Kim D Y, Han KH: Epidemiology and surveillance of hepatocellular carcinoma. Liver Cancer 2012;1:2–14.

3 Ramakrishna G, Rastogi A, Trehanpati N, et al: From cirrhosis to hepatocellular carcinoma: new molecular insights on inflammation and cellular senescence. Liver Cancer 2013;2:367–383.

4 Sakurai T, Kudo M: Molecular Link between liver fibrosis and hepatocellular carcinoma. Liver Cancer 2013;2:365–366.

5 Kainuma M, Furusyo N, Kajiwara E, et al: Pegylated interferon α-2b plus ribavirin for older patients with chronic hepatitis C. World J Gastroenterol 2010;16:4400–4409.

6 Asahina Y, Tsuchiya K, Tamaki N, et al: Effect of aging on risk for hepatocellular carcinoma in chronic hepatitis C virus infection. Hepatology 2010;52:518–527.

7 Manns MP, McHutchison JG, Gordon SC, et al: Peginterferon alfa-2b plus ribavirin compared with interferon alfa-2b plus ribavirin for initial treatment of chronic hepatitis C: a randomised trial. Lancet 2001;358:958–965.

8 Fried MW, Shiffman ML, Reddy KR, et al: Peginterferon alfa-2a plus ribavirin for chronic hepatitis C virus infection. N Engl J Med 2002;347:975–982.

9 Nomura H, Tanimoto H, Kajiwara E, et al: Factors contributing to ribavirin-induced anemia. J Gastroenterol Hepatol 2004;19:1312–1317.

10 Hiramatsu N, Oze T, Tsuda N, et al: Should aged patients with chronic hepatitis C be treated with interferon and ribavirin combination therapy? Hepatol Res 2006;35:185–189.

11 Okanoue T, Sakamoto S, Itoh Y, et al: Side effects of high-dose interferon therapy for chronic hepatitis C. J Hepatol 1996;25:283–291.

12 Perni RB, Almquist SJ, Byrn RA, et al: Preclinical profile of VX-950, a potent, selective, and orally bioavailable inhibitor of hepatitis C virus NS3–4A serine protease. Antimicrob Agents Chemother 2006;50:899–909.

13 Hezode C, Forestier N, Dusheiko G, et al: Telaprevir and peginterferon with or without ribavirin for chronic HCV infection. N Engl J Med 2009;360:1839–1850.
14 McHutchison JG, Everson GT, Gordon SC, et al: Telaprevir with peginterferon and ribavirin for chronic HCV genotype 1 infection. N Engl J Med 2009;360:1827–1838.
15 McHutchison JG, Manns MP, Muir AJ, et al: Telaprevir for previously treated chronic HCV infection. N Engl J Med 2010;362:1292–1303.
16 Kumada H, Toyota J, Okanoue T, et al: Telaprevir with peginterferon and ribavirin for treatment-naive patients chronically infected with HCV of genotype 1 in Japan. J Hepatol 2012;56:78–84.
17 Furusyo N, Ogawa E, Nakamuta M, et al: Telaprevir can be successfully and safely used to treat older patients with genotype 1b chronic hepatitis C. J Hepatol 2013;59:205–212.
18 Akuta N, Suzuki F, Hirakawa M, et al: Amino acid substitution in hepatitis C virus core region and genetic variation near the interleukin 28B gene predict viral response to telaprevir with peginterferon and ribavirin. Hepatology 2010;52:421–429.
19 Chayama K, Hayes CN, Abe H, et al: IL28B but not ITPA polymorphism is predictive of response to pegylated interferon, ribavirin, and telaprevir triple therapy in patients with genotype 1 hepatitis C. J Infect Dis 2011;204:84–93.
20 Marcellin P, Forns X, Goeser T, et al: Telaprevir is effective given every 8 or 12 hours with ribavirin and peginterferon alfa-2a or -2b to patients with chronic hepatitis C. Gastroenterology 2011;140:459–468.e1, quiz e14.
21 Hara T, Akuta N, Fukushima T, et al: A pilot study of triple therapy with telaprevir 1500 mg, peginterferon and ribavirin for elderly HCV patients. Kanzo 2012;53:624–626.
22 Ikeda K, Arase Y, Saitoh S, et al: Anticarcinogenic impact of interferon on patients with chronic hepatitis C: a large-scale long-term study in a single center. Intervirology 2006;49:82–90.
23 Watanabe S, Enomoto N, Koike K, et al: Cancer preventive effect of pegylated interferon α-2b plus ribavirin in a real-life clinical setting in Japan: PERFECT interim analysis. Hepatol Res 2011;41:955–964.
24 Yu ML, Lin SM, Chuang WL, et al: A sustained virological response to interferon or interferon/ribavirin reduces hepatocellular carcinoma and improves survival in chronic hepatitis C: a nationwide, multicentre study in Taiwan. Antivir Ther 2006;11:985–994.
25 Kumada H, Suzuki Y, Ikeda K, et al: Daclatasvir plus asunaprevir for chronic HCV genotype 1b infection. Hepatology 2014;59:2083–2091.

Clinical Study

Oncology

Oncology 2014;87(suppl 1):118–123
DOI: 10.1159/000368155

Published online: November 22, 2014

Ultrasound Elastography Correlates Treatment Response by Antiviral Therapy in Patients with Chronic Hepatitis C

Norihisa Yada Toshiharu Sakurai Tomohiro Minami Tadaaki Arizumi Masahiro Takita Tatsuo Inoue Satoru Hagiwara Kazuomi Ueshima Naoshi Nishida Masatoshi Kudo

Department of Gastroenterology and Hepatology, Kinki University School of Medicine, Osaka-Sayama, Japan

Key Words

Antiviral therapy · Liver stiffness · Liver fibrosis · Liver fibrosis index · Strain elastography

Abstract

Objective: To investigate the relationship between tissue elasticity before and after antiviral therapy and shear wave as well as strain elastography. ***Methods:*** FibroScan and real-time tissue elastography were performed before and after antiviral therapy for chronic hepatitis C, and treatment efficacy and elastographic findings were comparatively analyzed. Elasticity was evaluated by measuring liver stiffness (LS) in kilopascals using FibroScan, and the liver fibrosis index (LFI) was assessed by real-time tissue elastography. ***Results:*** LS and LFI correlated well before and after therapy ($r = 0.567$, $p = 0.003$ and $r = 0.576$, $p = 0.002$, respectively). In the group without a sustained virological response (SVR), LS increased in 4 of 5 patients. Patients with an increase in both LS and LFI were all in the non-SVR group (3/3, 100%). In addition, LS increased in all patients except 1 in the non-SVR group (4/5, 80%). In the SVR group, both LS and LFI decreased in all patients except 1 (18/19, 94.7%). In the patient with an increase in LS despite achieving SVR, LS decreased quickly after alcohol cessation. ***Conclusions:*** With a few exceptions, SVR improved LS. All patients with an increase in LFI were in the non-SVR group, even though LFI decreased in 2 patients. Our findings suggest that an LFI increase indicates lack of treatment efficacy with antiviral therapy. LFI may be useful for the assessment of treatment efficacy in patients with worsening of LS despite achieving SVR with antiviral therapy.

Introduction

Chronic hepatitis patients have a high risk of developing cancer, and their prognosis depends largely on the early detection of liver cancer during routine medical screenings [1–3] because of the higher chance of receiving curative therapy [4–6]. Previous studies have shown that once a sustained virological response (SVR) with antiviral therapy has been achieved, liver fibrosis improves gradually, lowering the risk for liver cancer [3, 7, 8]. Despite its status as the gold standard for the diagnosis of liver fibrosis, liver biopsy is invasive and associated with sampling errors; therefore, a noninvasive diagnostic technique that utilizes, for example, serum markers or ultrasound (US) elastography for the assessment of liver fibrosis over time is desirable.

KARGER

E-Mail karger@karger.com
www.karger.com/ocl

0030–2414/14/0877–0118$39.50/0

Prof. Masatoshi Kudo
Department of Gastroenterology and Hepatology
Kinki University School of Medicine
377-2 Ohno-Higashi, Osaka-Sayama, Osaka 589-8511 (Japan)
E-Mail m-kudo@med.kindai.ac.jp

US elastography is broadly divided into shear wave elastography, in which an US device such as FibroScan generates shear waves and measures the velocity of waves propagating through the liver, and strain elastography, in which slight tissue deformation or strain caused by heartbeats is visualized in real-time tissue elastography (RTE) [9–11]. In shear wave elastography, the measurement of liver stiffness (LS) is affected greatly by the severity of inflammation, jaundice and congestion besides liver fibrosis [12–16]. In addition, LS is highly correlated with the risk of liver cancer in chronic hepatitis patients [17–19]. Although a study using shear wave elastography with the employment of FibroScan reported that LS was improved by interferon (IFN) therapy [20], the association between strain elastography and antiviral therapy has not been clarified. We therefore performed RTE and FibroScan measurement concurrently and investigated the association between the efficacy of IFN therapy and the differences in LS and liver fibrosis index (LFI) between pre- and posttreatment measurements.

Patients and Methods

Patients

The study included 26 patients with chronic hepatitis C who underwent US elastography before (pretreatment, PT) and 2 years after therapy initiation (after treatment, AT) at Kinki University Hospital between October 2010 and July 2013.

IFN Therapy

In accordance with the Japan Society of Hepatology Guidelines for the Management of Hepatitis C Virus (HCV) Infection, the treatment strategy was determined based on HCV serotype and the amount of HCV-RNA.

Patients with serotype 2 and <5 log IU/ml HCV-RNA underwent pegylated IFN alpha (PEG) monotherapy for 24 weeks. Patients with serotype 1 and <5 log IU/ml HCV-RNA as well as patients with serotype 2 and ≥5 log IU/ml HCV-RNA underwent PEG and ribavirin (RBV) combination therapy (PEG/RBV) for 24 weeks. In addition, patients with serotype 1 and ≥5 log IU/ml HCV-RNA underwent PEG/RBV therapy for 48 weeks or combination therapy with telaprevir (TVR), PEG, and RBV (TVR/PEG/RBV) for 24 weeks.

The IFN formulation was PEG 2a (Pegasys; Chugai Pharmaceutical Co., Ltd., Tokyo, Japan) in PEG monotherapy, and PEG 2a and RBV (Copegus; Chugai Pharmaceutical Co., Ltd.) or PEG 2b (Peg-Intron; Merck & Co., Inc., Whitehouse Station, N.J., USA) and RBV (Rebetol; Merck & Co., Inc.) in PEG/RBV therapy. In TVR/PEG/RBV therapy, TVR (Telavic; Mitsubishi Tanabe Pharma, Osaka, Japan), PEG, and RBV were used.

In each regimen, the initial dose of PEG 2a was 180 μg once a week. PEG 2b was administered at a dose of 1.5 μg/kg once a week. RBV was orally administered after meals twice daily, as follows: when the hemoglobin level was ≥13 g/dl, 600, 800, and 1,000 mg were administered to those weighing <60, 60–80, and >80 kg, respectively; when the hemoglobin level was <13 g/dl, 400, 600, and 800 mg were administered to those weighing <60, 60–80, and >80 kg, respectively.

TVR was administered at a dose of 2,250 mg/day after meals 3 times a day with doses separated by 8-hour intervals, but the dose was reduced to 1,500 mg/day when the subject was female, aged ≥70 years, or weighed <50 kg.

Chronic hepatitis C patients who had achieved SVR after completion of 24 weeks of therapy formed the SVR group (n = 21, 80.8%), while patients who did not achieve SVR were classified as the non-SVR group (n = 5, 19.2%).

Liver Fibrosis Index

RTE was performed before and after IFN therapy using US EUS-8500 and the linear probe EUP-L52 (3–7 MHz; Hitachi Aloka Medical, Ltd., Tokyo, Japan) to estimate the LFI. The probe was pressed against the right intercostal region of the patient in a supine position, and the strain of the liver caused by heartbeats was displayed on the screen in real time. An examiner who was unaware of the patients' background selected 10 high-quality images to estimate the median LFI value using a method that has been reported previously [21–23].

Liver Stiffness

FibroScan was used to perform abdominal US in patients in a supine position for the measurement of pre- and posttreatment LS. The convex probe was used to examine liver parenchyma at the right intercostal region, and after verifying the absence of a tumor, cyst or any lesion in the measurement area of the liver that might interfere with the examination, the measurement of the same area was repeated 10 times to calculate the median LS value and interquartile range. The measurements were normalized to the median values of 10 acquisitions with a success rate of ≥60% and an interquartile range of <30% of the median stiffness.

Statistical Analysis

Groups were compared using Wilcoxon's signed rank test and confirmed by the nonparametric Mann-Whitney U test. Correlation between data was tested using the Pearson correlation coefficient and the nonparametric Spearman rank correlation analysis. Differences were considered statistically significant if $p < 0.05$. Analysis was performed using SPSS Statistics 20 (IBM, Armonk, N.Y., USA).

Results

Demographics and Baseline Features

The number of patients who received PEG, PEG/RBV, and TVR/PEG/RBV therapy was 1, 12, and 13, respectively. The proportion of patients who achieved SVR with PEG, PEG/RBV, and TVR/PEG/RBV therapy was 100, 78, and 84.6%, respectively.

Relationship between Treatment Efficacy and LS or LFI before and after IFN Therapy

A significant positive correlation was observed both between pre- and posttreatment LS and LFI ($r = 0.567$, $p = 0.003$ and $r = 0.576$, $p = 0.002$, respectively).

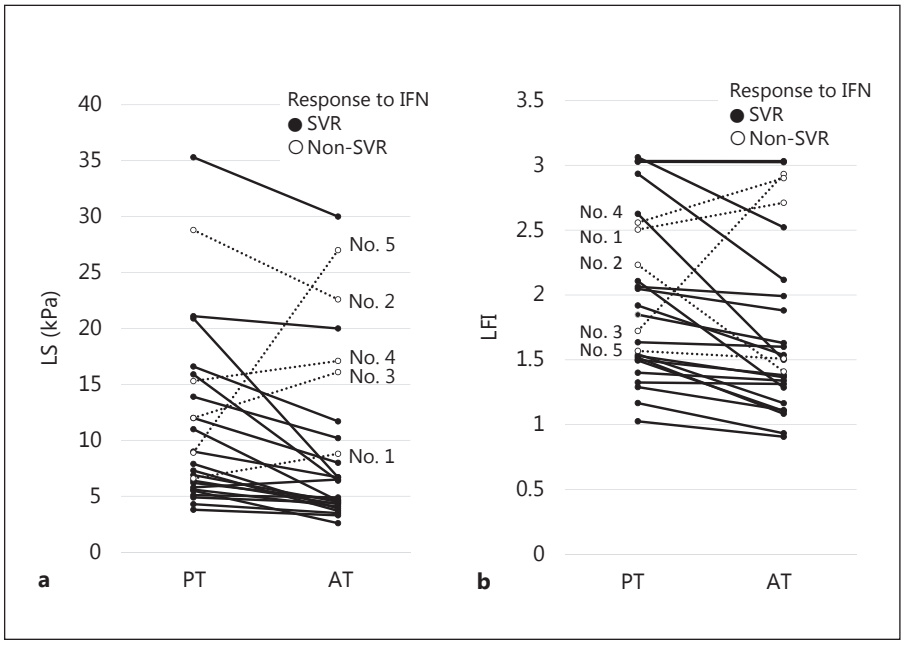

Fig. 1. LS and LFI before and after IFN therapy. Pre- and posttreatment LS (**a**) and LFI (**b**) are represented by solid and dotted lines for the SVR and non-SVR patients, respectively. Nos. 1–5 are the 5 patients in the non-SVR group.

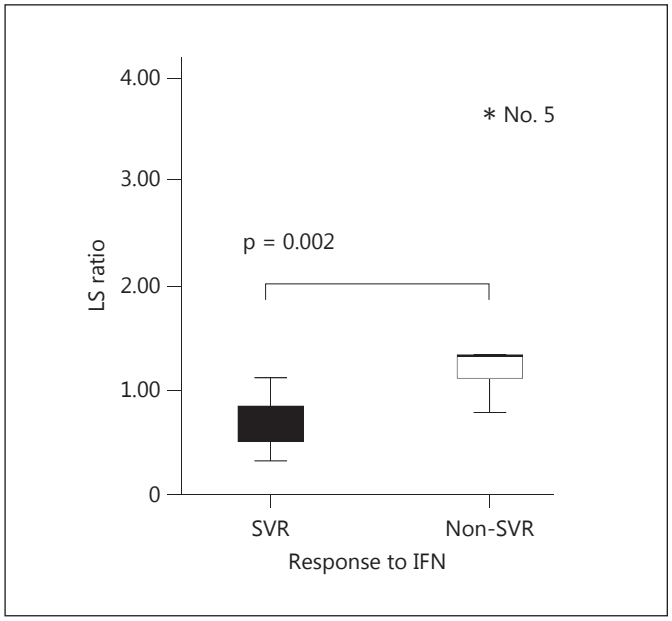

Fig. 2. Relationship between treatment efficacy and the LS ratio. The LS ratio was significantly lower in the SVR group than in the non-SVR group (p = 0.002). The asterisk is the extreme outlier with values more than 3 times the height of the boxes. No. 5 is a patient in the non-SVR group, numbered identical to figure 1.

While posttreatment LS was significantly lower in the SVR group (p = 0.003), no significant correlation was observed between posttreatment LFI and treatment efficacy (p = 0.079). After IFN therapy, LS mostly decreased in the SVR group, but increased in 4 (80%) of the 5 patients in the non-SVR group (fig. 1a, No. 1, 3–5). Overall, LFI decreased after therapy in the SVR group, but increased in 3 (60%) of the 5 patients in the non-SVR group (fig. 1b, No. 1, 3, 4).

Relationship between Treatment Efficacy and LS or LFI Ratios

LS (LFI at AT/LFI at PT) and LFI (LS at AT/LS at PT) ratios were calculated using the pre- and posttreatment values. While the LS ratio in the SVR group was significantly lower than in the non-SVR group (p = 0.002; fig. 2), the LFI ratio was slightly lower in the SVR group than in the non-SVR group (p = 0.067; fig. 3).

Investigation of the relationship between treatment efficacy and the LS or LFI ratios revealed that in the SVR group, the LS ratio was >1 in 1 patient, but other LFI ratios were all ≤1 (fig. 4). Both LS and LFI ratios were ≤1 in the majority of SVR patients (fig. 4).

In the non-SVR group, 4 of the 5 patients had a LS ratio >1. Patients with both LS and LFI ratios >1 all belonged to the non-SVR group (3/3, 100%). In addition, all patients but 1 with an LS ratio >1 belonged to the non-SVR group (4/5, 80%). On the other hand, all patients but 1 with both LS and LFI ratios <1 belonged to the SVR group (18/19, 94.7%).

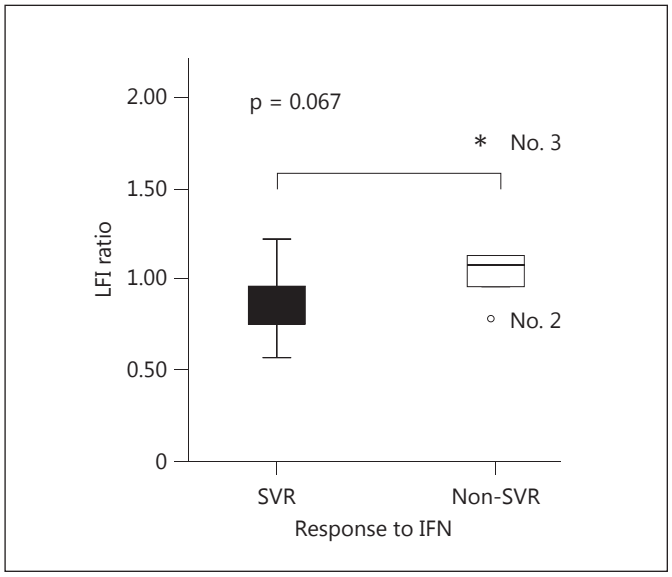

Fig. 3. Relationship between treatment efficacy and the LFI ratio. The LFI ratio tended to be low in the SVR group compared with the non-SVR group (p = 0.067). The open circle is the outlier, which is defined as values that do not fall in the inner fences. The asterisk is the extreme outlier with values more than 3 times the height of the boxes. Nos. 2 and 3 are the patients in the non-SVR group, numbered identical to figure 1.

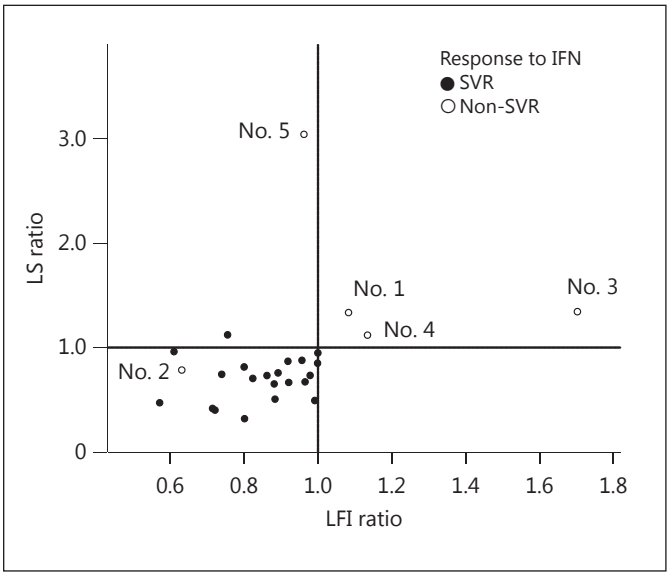

Fig. 4. Relationship between treatment efficacy and LS and LFI ratios. In the SVR group, all patients had a LFI ratio <1. Patients whose LS and LFI ratios were ≥1 all belonged to the non-SVR group. Nos. 1–5 are the 5 patients in the non-SVR group, numbered identical to figure 1.

Discussion

A previous study involving liver biopsies before and after antiviral therapy revealed that antiviral therapy improved fibrosis because of SVR [8]. Histological improvement also lowers the risk of liver cancer [7]. Therefore, even though the diagnosis of liver fibrosis is important and liver biopsy is the gold standard for its diagnosis, it is difficult to repeat liver biopsy because of its invasiveness and possible sampling errors [24]. A noninvasive diagnostic tool for liver fibrosis using hematological testing or ultrasonography is desirable. Shear wave elastography, using FibroScan for example, has become a popular method for the diagnosis of liver fibrosis and it measures LS or the propagation velocity of shear waves noninvasively [25]. However, shear wave elastography is also known to be affected by inflammation, jaundice, and congestion [12–16]. LS reportedly stays at low levels after antiviral therapy for HCV [20], but in addition to the improvement of liver fibrosis, the improvement of inflammation is thought to contribute greatly to the decline of LS values. However, because strain elastography represented by RTE visualizes slight deformations in the liver caused by heartbeats, this technology theoretically captures the changes in liver fibrosis without being affected by the presence of inflammation. Indeed, a study using an engineered model of liver fibrosis revealed that a blue area in RTE, which expands with the progression of liver fibrosis and represents an area with relatively low strain, was an area of collagen fibers that increases as the stage of liver fibrosis worsens [26]. This suggests that the influence of inflammation and fibrosis should be studied separately by concurrently performing and comparing the results of shear wave and strain elastography. In the present study, we therefore performed FibroScan and RTE concurrently before and after antiviral therapy (2 years after therapy initiation) and analyzed the correlation between the efficacy of antiviral therapy and changes in the measurement values.

A significant correlation was observed between treatment efficacy and LS or LFI. In particular, LFI was reduced in all SVR patients. Patients with a decrease in LS or LFI accounted for 96.2 and 100% of the patients who had achieved SVR, respectively. Patients with a decrease in both LS and LFI accounted for 100% of the SVR patients. Although LS increased in 1 of the SVR patients despite achieving SVR, it decreased quickly after alcohol cessation, indicating that the amount of alcohol consumption had increased greatly in this patient after viral clearance.

As reported previously, LS decreases in patients with successful antiviral therapy because of the improvement of liver fibrosis. However, LS is greatly affected by inflammation and tends to be higher in patients with alcoholic liver injury than in chronic hepatitis patients. Therefore, physicians should be aware that high LS values do not necessarily indicate ineffectiveness of antiviral therapy.

Theoretically, LFI is not affected by inflammation and simply reflects the severity of liver fibrosis. However, it was also reported that the levels of LFI vary between measurement sites or operators, suggesting that this might have been the cause of the decreased LFI in the non-SVR patients in this study. While the LFI decreased in some non-SVR patients, patients with an increased LFI all belonged to the non-SVR group. Therefore, an increased LFI may serve as a useful indicator of ineffective antiviral therapy. The LFI may also be useful for evaluating the efficacy of antiviral therapy in patients with an increase in LS despite achieving a SVR.

This study examined a small number of patients (21 SVR and 5 non-SVR patients), so further studies of a greater number of patients are needed to acquire more accurate results.

Acknowledgement

This study was supported by Health and Labour Sciences Research Grants for the Research on Hepatitis from the Japanese Ministry of Health, Labour and Welfare. The authors thank Akiko Tonomura (Engineering R&D Department 1, Hitachi Aloka Medical, Ltd.) who estimated the median LFI value.

Disclosure Statement

The authors declare that no financial or other conflicts of interest exist in relation to the content of this article.

References

1 Kudo M: Japan's successful model of nationwide hepatocellular carcinoma surveillance highlighting the urgent need for global surveillance. Liver Cancer 2012;1:141–143.
2 Kim DY, Han KH: Epidemiology and surveillance of hepatocellular carcinoma. Liver Cancer 2012;1:2–14.
3 Kudo M: Prediction of hepatocellular carcinoma incidence risk by ultrasound elastography. Liver Cancer 2014;3:1–5.
4 Lin SM: Local ablation for hepatocellular carcinoma in Taiwan. Liver Cancer 2013;2:73–83.
5 Belghiti J, Fuks D: Liver resection and transplantation in hepatocellular carcinoma. Liver Cancer 2012;1:71–82.
6 Mise Y, Sakamoto Y, Ishizawa T, Kaneko J, Aoki T, Hasegawa K, Sugawara Y, Kokudo N: A worldwide survey of the current daily practice in liver surgery. Liver Cancer 2013;2:55–66.
7 Yoshida H, Shiratori Y, Moriyama M, Arakawa Y, Ide T, Sata M, Inoue O, Yano M, Tanaka M, Fujiyama S, Nishiguchi S, Kuroki T, Imazeki F, Yokosuka O, Kinoyama S, Yamada G, Omata M: Interferon therapy reduces the risk for hepatocellular carcinoma: national surveillance program of cirrhotic and noncirrhotic patients with chronic hepatitis C in Japan. IHIT Study Group. Inhibition of hepatocarcinogenesis by interferon therapy. Ann Intern Med 1999;131:174–181.
8 Shiratori Y, Imazeki F, Moriyama M, Yano M, Arakawa Y, Yokosuka O, Kuroki T, Nishiguchi S, Sata M, Yamada G, Fujiyama S, Yoshida H, Omata M: Histologic improvement of fibrosis in patients with hepatitis C who have sustained response to interferon therapy. Ann Intern Med 2000;132:517–524.
9 Kudo M, Shiina T, Moriyasu F, Iijima H, Tateishi R, Yada N, Fujimoto K, Morikawa H, Hirooka M, Sumino Y, Kumada T: JSUM ultrasound elastography practice guidelines: liver. J Med Ultrason 2013;40:325–357.
10 Cosgrove D, Piscaglia F, Bamber J, Bojunga J, Correas JM, Gilja OH, Klauser AS, Sporea I, Calliada F, Cantisani V, D'Onofrio M, Drakonaki EE, Fink M, Friedrich-Rust M, Fromageau J, Havre RF, Jenssen C, Ohlinger R, Saftoiu A, Schaefer F, Dietrich CF; EFSUMB: EFSUMB guidelines and recommendations on the clinical use of ultrasound elastography. Part 2: clinical applications. Ultraschall Med 2013;34:238–253.
11 Bamber J, Cosgrove D, Dietrich CF, Fromageau J, Bojunga J, Calliada F, Cantisani V, Correas JM, D'Onofrio M, Drakonaki EE, Fink M, Friedrich-Rust M, Gilja OH, Havre RF, Jenssen C, Klauser AS, Ohlinger R, Saftoiu A, Schaefer F, Sporea I, Piscaglia F: EFSUMB guidelines and recommendations on the clinical use of ultrasound elastography. Part 1: basic principles and technology. Ultraschall Med 2013;34:169–184.
12 Arena U, Vizzutti F, Corti G, Ambu S, Stasi C, Bresci S, Moscarella S, Boddi V, Petrarca A, Laffi G, Marra F, Pinzani M: Acute viral hepatitis increases liver stiffness values measured by transient elastography. Hepatology 2008;47:380–384.
13 Sagir A, Erhardt A, Schmitt M, Haussinger D: Transient elastography is unreliable for detection of cirrhosis in patients with acute liver damage. Hepatology 2008;47:592–595.
14 Millonig G, Reimann FM, Friedrich S, Fonouni H, Mehrabi A, Buchler MW, Seitz HK, Mueller S: Extrahepatic cholestasis increases liver stiffness (fibroscan) irrespective of fibrosis. Hepatology 2008;48:1718–1723.
15 Colli A, Pozzoni P, Berzuini A, Gerosa A, Canovi C, Molteni EE, Barbarini M, Bonino F, Prati D: Decompensated chronic heart failure: increased liver stiffness measured by means of transient elastography. Radiology 2010;257:872–878.
16 Millonig G, Friedrich S, Adolf S, Fonouni H, Golriz M, Mehrabi A, Stiefel P, Poschl G, Buchler MW, Seitz HK, Mueller S: Liver stiffness is directly influenced by central venous pressure. J Hepatol 2010;52:206–210.
17 Masuzaki R, Tateishi R, Yoshida H, Yoshida H, Sato S, Kato N, Kanai F, Sugioka Y, Ikeda H, Shiina S, Kawabe T, Omata M: Risk assessment of hepatocellular carcinoma in chronic hepatitis C patients by transient elastography. J Clin Gastroenterol 2008;42:839–843.

18 Masuzaki R, Tateishi R, Yoshida H, Goto E, Sato T, Ohki T, Imamura J, Goto T, Kanai F, Kato N, Ikeda H, Shiina S, Kawabe T, Omata M: Prospective risk assessment for hepatocellular carcinoma development in patients with chronic hepatitis C by transient elastography. Hepatology 2009;49:1954–1961.
19 Jung KS, Kim SU, Ahn SH, Park YN, Kim do Y, Park JY, Chon CY, Choi EH, Han KH: Risk assessment of hepatitis B virus-related hepatocellular carcinoma development using liver stiffness measurement (fibroscan). Hepatology 2011;53:885–894.
20 Hezode C, Castera L, Roudot-Thoraval F, Bouvier-Alias M, Rosa I, Roulot D, Leroy V, Mallat A, Pawlotsky JM: Liver stiffness diminishes with antiviral response in chronic hepatitis C. Aliment Pharmacol Ther 2011;34:656–663.
21 Fujimoto K, Kato M, Tonomura A, Yada N, Tatsumi C, Oshita M, Wada S, Ueshima K, Ishida T, Furuta T, Yamasaki M, Tsujimoto M, Motoki M, Mitake T, Shiina T, Kudo M, Hayashi N: Non-invasive evaluation method of the liver fibrosis using real-time tissue elastograpy – usefulness of judgment liver fibrosis stage by liver fibrosis index (LF index). Kanzo 2010;59:539–541.
22 Fujimoto K, Kato M, Kudo M, Yada N, Shiina T, Ueshima K, Yamada Y, Ishida T, Azuma M, Yamasaki M, Yamamoto K, Hayashi N, Takehara T: Novel image analysis method using ultrasound elastography for non-invasive evaluation of hepatic fibrosis in patients with chronic hepatitis C. Oncology 2013;84 (suppl 1):3–12.
23 Yada N, Kudo M, Morikawa H, Fujimoto K, Kato M, Kawada N: Assessment of liver fibrosis with real-time tissue elastography in chronic viral hepatitis. Oncology 2013;84(suppl 1):13–20.
24 Bedossa P, Dargere D, Paradis V: Sampling variability of liver fibrosis in chronic hepatitis C. Hepatology 2003;38:1449–1457.
25 Ziol M, Handra-Luca A, Kettaneh A, Christidis C, Mal F, Kazemi F, de Ledinghen V, Marcellin P, Dhumeaux D, Trinchet JC, Beaugrand M: Noninvasive assessment of liver fibrosis by measurement of stiffness in patients with chronic hepatitis C. Hepatology 2005;41:48–54.
26 Shiina T, Maki T, Yamakawa M, Mitake T, Kudo M, Fujimoto K: Mechanical model analysis for quantitative evaluation of liver fibrosis based on ultrasound tissue elasticity imaging. Jpn J Appl Phys 2012;51:1–8.

HEPATOLOGY
Official Journal of the American Association for the Study of Liver Diseases

Brivanib as Adjuvant Therapy to Transarterial Chemoembolization in Patients With Hepatocellular Carcinoma: A Randomized Phase III Trial

Masatoshi Kudo,[1] Guohong Han,[2] Richard S. Finn,[3] Ronnie T.P. Poon,[4] Jean-Frederic Blanc,[5] Lunan Yan,[6] Jijin Yang,[7] Ligong Lu,[8] Won-Young Tak,[9] Xiaoping Yu,[10] Joon-Hyeok Lee,[11] Shi-Ming Lin,[12] Changping Wu,[13] Tawesak Tanwandee,[14] Guoliang Shao,[15] Ian B. Walters,[16] Christine Dela Cruz,[17] Valerie Poulart,[18] and Jian-Hua Wang[19]

Transarterial chemoembolization (TACE) is the current standard of treatment for unresectable intermediate-stage hepatocellular carcinoma (HCC). Brivanib, a selective dual inhibitor of vascular endothelial growth factor and fibroblast growth factor signaling, may improve the effectiveness of TACE when given as an adjuvant to TACE. In this multinational, randomized, double-blind, placebo-controlled, phase III study, 870 patients with TACE-eligible HCC were planned to be randomly assigned (1:1) after the first TACE to receive either brivanib 800 mg or placebo orally once-daily. The primary endpoint was overall survival (OS). Secondary endpoints included time to disease progression (TTDP; a composite endpoint based on development of extrahepatic spread or vascular invasion, deterioration of liver function or performance status, or death), time to extrahepatic spread or vascular invasion (TTES/VI), rate of TACE, and safety. Time to radiographic progression (TTP) and objective response rate were exploratory endpoints. The trial was terminated after randomization of 502 patients (brivanib, 249; placebo, 253) when two other phase III studies of brivanib in advanced HCC patients failed to meet OS objectives. At termination, median follow-up was approximately 16 months. Intention-to-treat analysis showed no improvement in OS with brivanib versus placebo (median, 26.4 [95% confidence interval {CI}: 19.1 to not reached] vs. 26.1 months [19.0-30.9]; hazard ratio [HR]: 0.90 [95% CI: 0.66-1.23]; log-rank $P = 0.5280$). Brivanib improved TTES/VI (HR, 0.64 [95% CI: 0.45-0.90]), TTP (0.61 [0.48-0.77]), and rate of TACE (0.72 [0.61-0.86]), but not TTDP (0.94 [0.72-1.22]) versus placebo. Most frequent grade 3-4 adverse events included hyponatremia (brivanib, 18% vs. placebo, 5%) and hypertension (13% vs. 3%). *Conclusions:* In this study, brivanib as adjuvant therapy to TACE did not improve OS. (HEPATOLOGY 2014;60:1697-1707)

Transarterial chemoembolization (TACE) is the most frequently used locoregional procedure for the management of unresectable hepatocellular carcinoma (HCC) confined to the liver.[1] This procedure blocks the principal arteries feeding the tumor while administering chemotherapy directly into the tumor for local disease control. TACE can prolong survival in selected patients.[2,3] However, the incidence of recurrence is high, and multiple TACE sessions are needed to eradicate residual tumors.[1]

Embolization induces hypoxia and the release of factors involved in tumorogenesis, angiogenesis, and fibrosis.[4,5] It is well documented that serum concentrations of vascular endothelial growth factor (VEGF)

Abbreviations: AE, adverse event; AFP, alpha-fetoprotein; ALT, alanine aminotransferase; AST, aspartate aminotransferase; BCLC, Barcelona Clinic Liver Cancer; CI, confidence interval; ECOG-PS, Eastern Cooperative Oncology Group performance status; GI, gastrointestinal; HCC, hepatocellular carcinoma; HR, hazard ratio; HTN, hypertension; ITT, intention to treat; IVRS, Interactive Voice Response System; mRECIST, Response Evaluation Criteria in Solid Tumors; OR, odds ratio; ORR, objective response rate; OS, overall survival; PES, postembolization syndrome; SAEs, serious adverse events; TACE, transarterial chemoembolization; TTDP, time to disease progression; TTES/VI, time to extrahepatic spread or vascular invasion; TTP, time to radiographic progression; TTUP, time to untreatable progression; VEGF, vascular endothelial growth factor.

and fibroblast growth factor (FGF), principal proangiogenic factors, increase after TACE.[6-10] These increases have been shown to be associated with increased risk of tumor growth, recurrence, metastasis, and poor survival.[6-10] Sorafenib, a multikinase inhibitor that targets multiple signaling pathways, including VEGF signaling, improves overall survival (OS) in advanced HCC patients.[11,12] These observations suggest that combining TACE with antiangiogenic agents has the potential to improve the effectiveness of TACE.

Brivanib (Bristol-Myers Squibb, Princeton, NJ), an oral selective dual inhibitor of VEGF and FGF receptor tyrosine kinases, exhibited both antiproliferative and -angiogenic activity in preclinical models and showed initial evidence of efficacy in a phase II trial of patients with advanced HCC.[13-18] Based on this activity profile of brivanib, we hypothesized that brivanib may potentially suppress the growth of microscopic lesions not treatable by TACE, shrink or stabilize tumors remaining after TACE, prevent tumors from spreading outside of the liver, and thereby improve OS. We tested this hypothesis in the present phase III trial that assessed the efficacy and safety of brivanib as adjuvant therapy to TACE in patients with unresectable HCC.

Patients and Methods

Patients. Men and women (age 18 or older) with unresectable HCC who were eligible for their first TACE therapy were enrolled. To be eligible for the first TACE, patients had to have specified histological, cytological, or radiological evidence of HCC. Patients with fewer than four lesions were to have at least one lesion measuring $\geq$5 cm in diameter and those with four or more lesions were to have at least one lesion measuring $\geq$2 cm in diameter. Other key inclusion criteria were Child-Pugh A or B liver function, an Eastern Cooperative Oncology Group performance status (ECOG-PS) score of 0 or 1, and adequate organ function. Key exclusion criteria included diffuse pattern of disease, presence of extrahepatic lesions, macroscopic vascular lesions, clinically significant ascites, previous TACE or transarterial embolization, and previous systemic treatment for HCC. A full list of inclusion and exclusion criteria for enrollment and randomization is provided in Supporting Table 1.

All patients provided written informed consent. The study was approved by the ethics committee/institutional review board at each center and was conducted according to good clinical practice guidelines and the Declaration of Helsinki. This study is registered with ClinicalTrials.gov (no.: NCT00908752).

Study Design. This was a randomized, double-blind, placebo-controlled, phase III study (acronym: BRISK-TA) in which 502 patients from 83 academic hospitals and community clinics across 12 countries were randomly assigned in a 1:1 ratio to receive either brivanib 800 mg or placebo once-daily orally. Randomization was performed after the first TACE

From the [1]Department of Gastroenterology and Hepatology, Kinki University School of Medicine, Osaka, Japan; [2]Xijing Hospital Fourth Military Medical University, Xi'an, Shaanxi, China; [3]Geffen School of Medicine at University of California Los Angeles, Los Angeles, CA; [4]Department of Hepatobiliary and Pancreatic Surgery, University of Hong Kong, Hong Kong S.A.R.; [5]Department of Hepato-Gastroenterology, Hospital Saint Andre and University Hospital of Bordeaux, Bordeaux, France; [6]Liver Transplantation Department, West China Hospital of Sichuan University, Chengdu, China; [7]Changhai Hospital, Shanghai, China; [8]Guangdong Provincial People's Hospital, Guangdong, China; [9]Department of Internal Medicine, Kyungpook National University Hospital, Daegu, Republic of Korea; [10]Hunan Provincial Tumor Hospital, Changsha, Hunan, China; [11]Division of Gastroenterology, Sungkyunkwan University School of Medicine, and Samsung Medical Center, Seoul, Republic of Korea; [12]Chang Gung Memorial Hospital, Linkou Branch, Kueishan Shiang, Taoyuan, Taiwan; [13]The First People's Hospital of Changzhou, Changzhou, China; [14]Faculty of Medicine, Siriraj Hospital, Mahidol University, Bangkok, Thailand; [15]Zhejiang Cancer Hospital, Hangzhou, China; [16]Bristol-Myers Squibb, Wallingford, CT; [17]Bristol-Myers Squibb, Singapore; [18]Bristol-Myers Squibb, Braine-l'Alleud, Belgium; and [19]Zhongshan Hospital, Shanghai, China.

Received November 15, 2013; accepted June 27, 2014.

The study was sponsored by Bristol-Myers Squibb Company (Princeton, NJ).

Kudo et al. Overall survival and safety of brivanib vs placebo as adjunctive therapy to Trans-Arterial Chemo-Embolization (TACE) in patients with unresectable hepatocellular carcinoma. This was presented orally at the International Liver Cancer Association 7th Annual Conference, Washington, DC, September 13-15, 2013.

Address reprint requests to: Masatoshi Kudo, M.D., Ph.D., Department of Gastroenterology and Hepatology, Kinki University School of Medicine, 377-2 Ohno Higashi, Osaka-Sayama City, Osaka 589-8511, Japan. E-mail: m-kudo@med.kindai.ac.jp; fax: +81-72-367-2880.

View this article online at wileyonlinelibrary.com.

DOI 10.1002/hep.27290

Potential conflict of interest: Dr. Kudo is on the speakers' bureau of and received grants from Bayer; he received grants from MSD and Chugai. Dr. Tak advises Bayer and Gilead; he received grants from Samil. Dr. Lee advises, is on the speakers' bureau of, and received grants from Bristol-Myers Squibb and Green Cross Cell; he advises and is on the speakers' bureau of Gilead. Dr. Walters is employed by and owns stock in Bristol-Myers Squibb. Dr. Dela Cruz is employed by and owns stock in Bristol-Myers Squibb. Dr. Poulart is employed by and owns stock in Bristol-Myers Squibb.

procedure to ensure the patient's ability to safely receive study drug. The interval between TACE and study drug administration was no less than 48 hours, but no longer than 21 days. This interval was dependent on the individual patient's recovery of liver function (defined as alanine aminotransferase [ALT] and aspartate aminotransferase [AST] concentrations of $\leq 5\times$ the upper limit of normal and serum total bilirubin concentrations <3 mg/dL) and resolution of any postembolization syndrome (fever, nausea, vomiting, and abdominal pain) to grade ≤ 1. Response to TACE was not a criterion for randomization. Treatment assignment was performed centrally through an Interactive Voice Response System (IVRS) using a computer-generated sequence of random digits. Randomization was stratified by Child-Pugh Class (A vs. B), ECOG-PS score (0 vs. 1), maximum tumor size (<10 vs. ≥ 10 cm), and study site and was dynamically balanced for stratification factors using the method of Pocock and Simon.[19] All investigators, patients, and personnel involved in study conduct, data collection, and data analysis were blinded to treatment allocations. To maintain blinding, brivanib or matching placebo as film-coated tablets was supplied in identical boxes. An independent data monitoring committee met four times throughout the trial to assess safety data. All meetings resulted in a recommendation that the trial be continued.

TACE was repeated if there was incomplete necrosis, tumor regrowth, or appearance of new lesions. To ensure safety, study drug was stopped 2 days before TACE and restarted between days 3 and 21 after repeat TACE depending on individual patient's recovery of liver function and resolution of any PESs (as defined above in this section).

Only one of two TACE approaches was allowed during initial or repeat TACE: either (1) injection of an emulsion of a single anticancer agent with lipiodol, followed by embolization of the feeding artery with an embolization agent, or (2) injection of drug-eluting beads preloaded with a single chemotherapy agent. Each study site was required to maintain consistency in the TACE procedure and the use of chemoembolization agent throughout the study duration.

Patients continued on study treatments until disease progression, defined by any of the following events: development of extrahepatic metastasis; development of vascular invasion; deterioration of liver function to Child-Pugh Class C; deterioration of ECOG-PS by 2 points if related to liver disease or if not related to liver disease; deterioration of ECOG-PS by 2 points that lasted longer than 2 weeks; or death. Treatment was allowed beyond disease progression if the investigator determined that the patient was benefiting from the blinded treatment.

Assessments. Assessments for Child-Pugh class, ECOG-PS, and tumor were performed at screening, 4 weeks after the first TACE procedure, and every 8 weeks thereafter. Tumor was assessed using dynamic contrast-enhanced spiral computed tomography/magnetic resonance imaging. Scans were evaluated by investigators using the Response Evaluation Criteria in Solid Tumors modified for the assessment of HCC tumors (mRECIST for HCC).[20]

Safety was assessed continuously. Adverse events (AEs) and serious AEs (SAEs) were graded according to the National Cancer Institute Common Terminology Criteria for Adverse Events version 3.0. Guidelines for dose reductions and discontinuation from therapy resulting from AEs are described in Supporting Table 2. In general, patients who experienced any drug-related grade 3 nonhematologic or hematologic AEs had their treatment interrupted until AEs decreased to grade ≤ 1. Study treatments were reinitiated at a lower dose level. Only two dose reductions (600 mg, then 400 mg) were allowed. If the same grade 3 nonhematologic or hematologic toxicity recurred despite two dose reductions, patients were discontinued from therapy. Once reduced, treatment continued at the lower dose and the dose was not re-escalated. Patients who experienced drug-related grade 4 nonhematologic toxicities (with the exception of increased ALT, increased AST, hyperbilirubinemia, and hyponatremia, where dose reductions were allowed for grade 4 events; see Supporting Table 2) or grade 4 hematologic toxicities were discontinued from study therapy. Guidelines for the management of specific AEs, such as increased ALT, increased AST, hyperbilirubinemia, hyponatremia, hypertension (HTN), and hypothyroidism were provided.

Endpoints. The primary endpoint was OS, defined as the time from randomization to death from any cause. Secondary efficacy endpoints included time to disease progression (TTDP), a new composite endpoint defined as the time from the first TACE to the date of disease progression (as defined above under Study Design). Other secondary endpoints were time to extrahepatic spread or vascular invasion (TTES/VI; time from the date of the first TACE to the date when extrahepatic spread or vascular invasion was documented), and the total number of TACE procedures between randomization and the occurrence of any TTDP event or censoring for TTDP, and safety. Exploratory endpoints included objective response rate

(ORR; the percentage of randomized patients whose best response was a complete or partial response) and time to radiographic progression (TTP; the time from the first TACE procedure to first radiographic tumor progression). Tumor response and tumor progression were assessed by investigators using mRECIST for HCC.[20]

Statistical Considerations. Sample size was calculated assuming an exponential distribution of survival time. A total of 520 deaths were required to detect an OS difference between the arms with ≥90% power using a stratified log-rank test at $\alpha = 0.05$, assuming that the true hazard ratio (HR) of brivanib to placebo was 0.75. This HR corresponded to a 6.0-month increase in the median OS for brivanib over placebo, assuming that the median OS for the placebo arm was 18 months. The number of patients needed to be randomized was estimated at 870. The study was terminated 2 years earlier than planned when the phase III BRISK-FL and BRISK-PS trials evaluating brivanib as first- and second-line treatment of advanced HCC failed to achieve their primary OS objectives.[23,24] At termination, at total of 502 patients were randomized.

All efficacy endpoints were assessed in all randomly assigned patients (intention-to-treat [ITT] population). Analyses for safety and treatment exposure were based on data from randomly assigned patients who received at least one dose of any study treatment. The primary endpoint of OS was compared between the treatment groups using a stratified log-rank test at $\alpha=0.05$, as were TTDP, TTES/VI, and TTP. The HR of brivanib versus placebo for each of these endpoints and associated 95% confidence intervals (CIs) were computed using a stratified Cox's proportional hazards model. A multivariate Cox's regression model was used to adjust the treatment effect on OS for the following baseline factors: age, risk factors (hepatitis B or C infection or alcohol use), alpha-fetoprotein (AFP) levels, tumor morphology, and previous locoregional treatment and to determine the association of OS with these factors. A Cox's proportional hazards model was used to analyze OS for subgroups based on baseline factors listed above for OS adjustment as well as race, region, Child-Pugh class, tumor size, gender, and age of female patients. Medians for OS, TTDP, TTES/VI, and TTP were estimated using Kaplan-Meier's methodology; 95% CIs for medians were computed.[21] No formal between-group comparison for the number of TACE procedures was performed. Rate functions of TACE procedure between randomization and TTDP events were compared between groups using a stratified semiparametric Andersen-Gill's model (Wald test at $\alpha = 0.05$). The ORR was compared between groups using a stratified Cochran-Mantel-Haenszel's test at $\alpha = 0.05$; associated odds ratio (OR) and its 95% CI were estimated. The 95% CI of ORR was computed.[22] The log-rank test, proportional hazards models, Anderson-Gill's model, and Cochran-Mantel-Haenszel's test were all stratified by three randomization factors: ECOG-PS score (0 vs. 1); maximum tumor size (<10 vs. ≥10 cm); and Child-Pugh class (A vs. B). All 95% CIs were two-sided. Secondary endpoints were to be tested hierarchically in the following order: TTDP, TTES/VI, and rate of TACE. The *P* values presented are for descriptive purposes only. All data analyses were performed using SAS software (version 9.2; SAS Institute Inc., Cary, NC).

Results

Patients. Two hundred forty-nine patients were randomly assigned to receive brivanib and 253 to receive placebo from August 25, 2009 until trial termination and unblinding on August 28, 2012 and constituted the ITT population for the analysis of primary and secondary efficacy endpoints (Fig. 1). Two hundred forty-six of two hundred forty-nine patients in the brivanib group and all 253 in the placebo group received at least one dose of either brivanib or placebo, respectively, and were used for the analysis of treatment exposure and safety. At study termination, all patients were given the option to discontinue the study. At the database lock on November 27, 2012, 57 (23%) patients in the brivanib group and 3 (1%) in the placebo group were still on treatment (Fig. 1). The primary reasons for study discontinuation were administrative reasons related to study termination (n = 12 [5%] in the brivanib group vs. n = 92 [36%] in the placebo group), disease progression (n = 45 [18%] vs. n = 91 [36%]), and drug toxicity (n = 65 [26%] vs. n = 6 [2%]).

Demographics and disease characteristics were balanced between the groups (Table 1). The majority of the randomly assigned patients were from Asia (n = 434 [86%]) and had hepatitis B infection (n = 326 [65%]). Whereas the majority of the patients had intermediate-stage HCC (Barcelona Clinic Liver Cancer [BCLC] stage B, n = 279 [57%]), there were 122 (24%) with early-stage HCC (BCLC stage A, single lesions measuring longer than 5 cm in diameter) and 98 (20%) with advanced-stage HCC (BCLC stage C).

Efficacy. At this analysis, the Kaplan-Meier's estimate of median follow-up was 16.6 months (95% CI: 14.8-17.6) in the brivanib group and 15.6 months

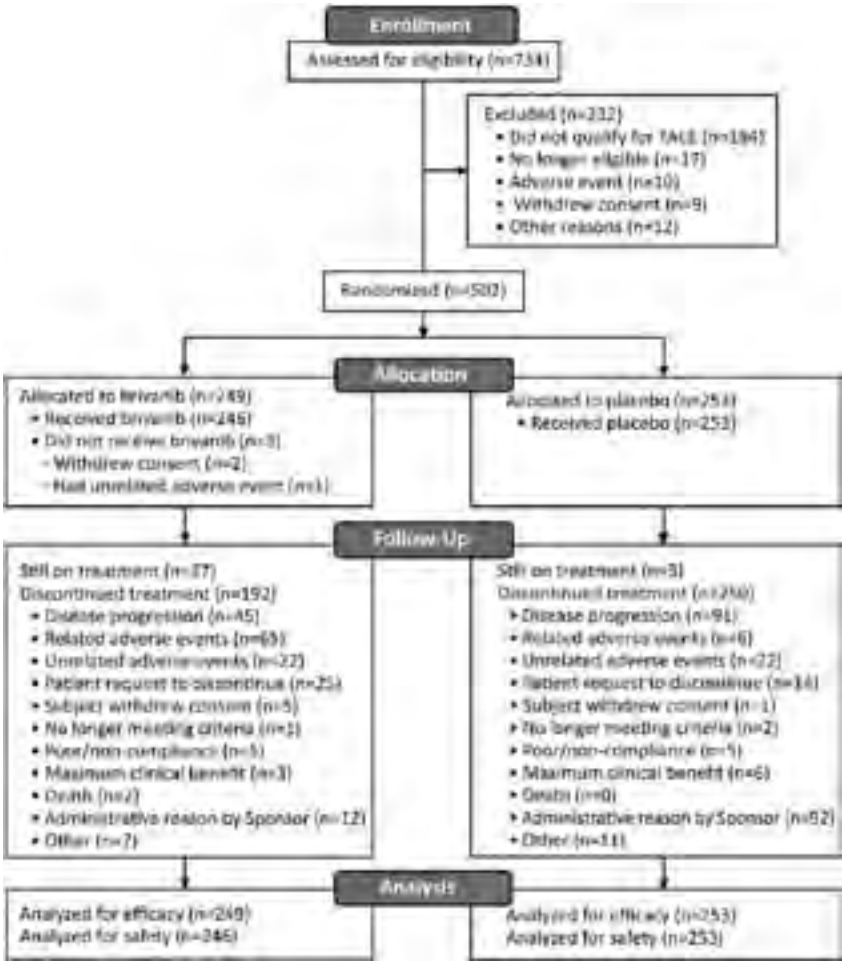

Fig. 1. Patient disposition. Ninety-one centers across 12 countries assessed 734 patients for eligibility. Eighty-three of these centers randomly assigned a total of 502 patients to treatment with either brivanib or placebo. The remaining eight centers assigned no patients to a study treatment. Countries (number of randomly assigned patients in parentheses) include: China (244), Japan (78), Korea (68), France (32), Taiwan (28), United States (18), Thailand (12), Spain (11), Hong Kong (4), Argentina (3), Canada (2), and Italy (2). A list of investigators who participated in the study is provided in Supporting Table 6.

(13.5-17.5) in the placebo group; 79 (32%) of 249 patients on brivanib and 85 (34%) of 253 on placebo had died, with the remaining being censored. The analysis showed no improvement in the primary endpoint of OS with brivanib versus placebo (HR, 0.90 [95% CI: 0.66-1.23]; $P = 0.5280$; Fig. 2). Median OS was 26.4 months (95% CI: 19.1 to not reached) in the brivanib group and 26.1 months (95% CI: 19.0-30.9) in the placebo group. Rates of OS in the brivanib group at 12 and 24 months were 74% (95% CI: 68-80) and 52% (43-61), respectively. Rates of OS in the placebo group at 12 and 24 months were 68% (61-75) and 54% (45-62), respectively. After adjusting for baseline factors, the effect of brivanib on OS versus placebo remained unchanged (HR, 0.92 [95% CI: 0.67-1.26]). Plasma AFP level at baseline (<100 vs. ≥ 100 ng/mL; $P < 0.0001$) was identified as a prognostic factor for OS in this study; other factors tested (age, risk factors, tumor morphologic feature, and previous locoregional therapy and/or surgery) were not prognostic. The OS results for selected subsets are presented in Fig. 3. Most HRs favored brivanib with a notable trend for a better OS in patients <65 years of age and in those with hepatitis B infection.

Thirty-six (14%) patients in the brivanib group and 53 (21%) in the placebo group received poststudy systemic therapies, with sorafenib being the most commonly used systemic therapy (n = 31 and n = 44, respectively). The number of patients who received poststudy nonsystemic therapies were 68 (27%) in the brivanib group and 54 (21%) in the placebo group, with TACE being the most commonly used nonsystemic therapy (n = 53 and n = 33, respectively).

There was no improvement in the composite endpoint of TTDP with brivanib versus placebo (median, 12.0 [95% CI: 9.5-15.3] vs. 10.9 [8.4-14.4] months; HR, 0.94 [0.72-1.22]; p = 0.6209; Fig. 4A), where death was the predominant event. TTES/IV was longer in the brivanib group than in the placebo group (median, not reached [95% CI: 17.6 to not reached] vs. 24.9 [13.8 to not reached] months; HR, 0.64 [0.45-0.90]; $P = 0.0096$; Fig. 4B). The median number of TACE procedures between randomization and disease progression and censoring was 0 (range, 0-13)

Table 1. Baseline Demographics and Disease Characteristics

Variable	Brivanib (N = 249)	Placebo (N = 253)
Age		
Median age (range), years	57 (21-85)	59 (25-85)
<65 years, n (%)	173 (70)	170 (67)
Male, n (%)	206 (83)	216 (85)
Region, n (%)		
Asia	216 (87)	218 (86)
Europe	22 (9)	23 (9)
Americas	11 (4)	12 (5)
ECOG-PS, n (%), per IVRS*		
0	201 (81)	203 (80)
1	48 (19)	50 (20)
ECOG-PS, n (%), per CRF†		
0	199 (80)	213 (84)
1	50 (20)	40 (16)
BCLC stage, n (%)		
A‡	65 (26)	57 (23)
B	129 (52)	150 (59)
C	54 (22)	44 (17)
D	1 (<1)	2 (1)
Child-Pugh Class, n (%)		
A	239 (96)	231 (91)
B	9 (4)	20 (8)
C	1 (<1)	2 (1)
Tumor morphology, n (%)		
Uninodular	91 (37)	83 (33)
Multinodular	158 (63)	170 (68)
Size of largest tumor nodule, n (%)		
≤10 cm	189 (76)	195 (77)
>10 cm	60 (24)	58 (23)
Risk factors, n (%)		
Any	222 (89)	228 (90)
Alcohol	40 (16)	38 (15)
Hepatitis B	158 (63)	168 (66)
Hepatitis C	49 (20)	42 (17)
Other	8 (3)	8 (3)
Serum AFP <100 ng/mL, n (%)	130 (52)	119 (47)
Previous nonsystemic treatment, n (%)		
Any	21 (8)	26 (10)
Liver resection	14 (6)	24 (9)
Radiofrequency ablation	10 (4)	4 (2)
Transcatheter arterial chemoembolization	3 (1)	2 (1)
Other	1 (<1)	2 (1)

*ECOG-PS was based on data from the IVRS and was used for stratification at randomization.

†ECOG-PS was based on Case Report Forms (CRFs) and was used for the calculation of the baseline BCLC stage.

‡Patients with single lesions measuring >5 cm in diameter.

in the brivanib group and 1 (range, 0-8) in the placebo group (Table 2). The rate of TACE was lower in the brivanib than in the placebo group (HR, 0.72 [95% CI: 0.61-0.86], $P = 0.0002$; Table 2). TTP was longer in the brivanib than in the placebo group (median, 8.4 [95% CI: 6.7-10.2] vs. 4.9 [4.7-6.5] months; HR, 0.61 [0.48-0.77]; $P < 0.0001$; Fig. 4C). The ORR was 48% in the brivanib group and 42% in the placebo group (Table 2). There were more complete responses (22% vs. 11%) and fewer documented disease progression events (9% vs. 18%) in the brivanib than in the placebo group. Disease control rate (the sum total of complete response, partial response, and stable disease) was 79% in both groups.

An exploratory posthoc subset analysis of OS and treatment duration by region was performed. The median OS values for brivanib versus placebo in Korea (n = 68), China (n = 244), Japan (n = 78), and the non-Asian region (North America, Europe, and Australia; n = 65) were 26.4 months versus not reached (HR, 0.55), 17.1 months versus not reached (HR, 0.80), not reached versus not reached (HR, 0.86), and 18.1 versus 17.5 months (HR, 1.41), respectively (Supporting Table 3). In the brivanib group, median treatment durations in Korea, China, and Japan were 10.1, 8.3, and 2.1 months, respectively (Supporting Table 4). In the placebo group, median treatment durations in Korea, China, and Japan were 10.6, 5.0, and 7.2 months, respectively. These results suggest regional variability in terms of OS and treatment duration.

Safety. At database lock, 79 (32%) patients in the brivanib group and 85 (34%) in the placebo group had died; disease was the primary cause (n = 61 and n = 75, respectively). Eighteen (7%) patients in the brivanib group and 12 (5%) in the placebo group had died within 30 days of the last dose; disease was the primary cause (n = 6 and n = 11, respectively). Four (2%) deaths in the brivanib group considered to be treatment related were the result of liver failure, bacterial peritonitis, intracranial bleeding, and pulmonary infection. One (<1%) death in the placebo group considered to be treatment related was the result of liver failure.

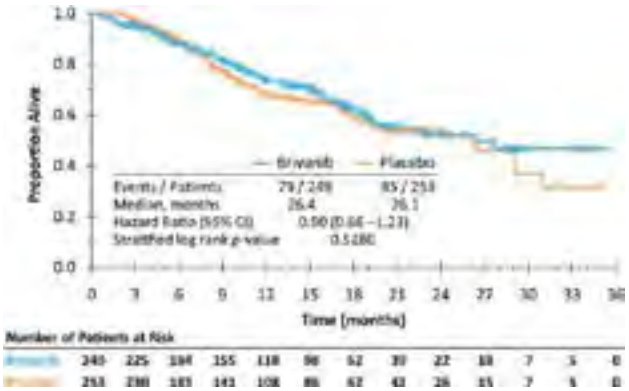

Fig. 2. Kaplan-Meier's curves for OS. OS was defined as the time from the date of randomization to the date of death from any cause. Patients who did not die were censored on the last dates known to have been alive or on the date the database was locked.

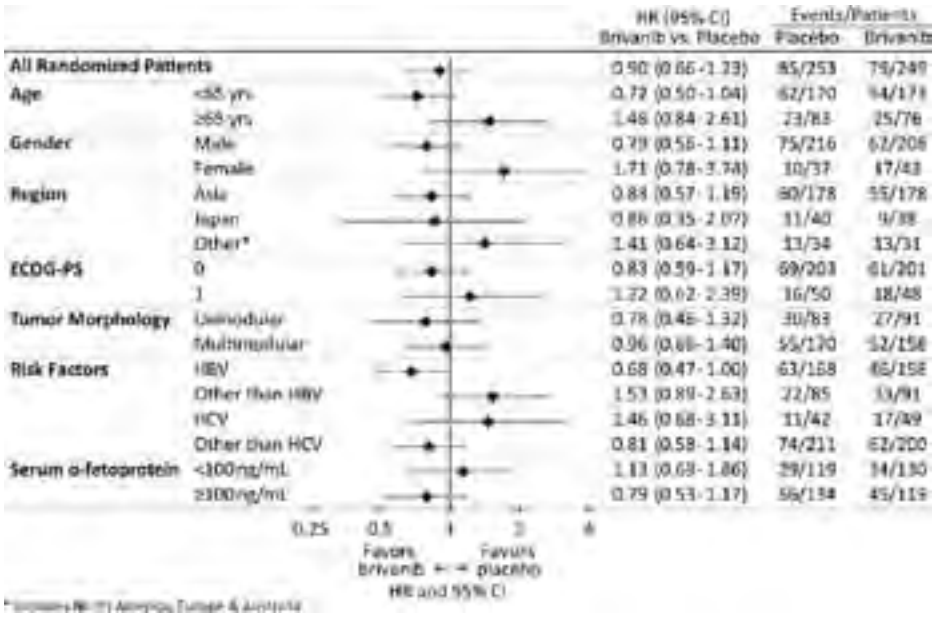

Fig. 3. OS in selected subsets.

One hundred eighteen (48%) patients in the brivanib group and 94 (37%) in the placebo group had one or more SAEs. The most frequent (≥2%) SAEs were malignant neoplasm progression (n = 15 in the brivanib group and n = 38 in the placebo group), ascites (n = 8 and n = 6), abdominal pain (n = 6 and n = 4), hepatic malignant neoplasm (n = 6 and n = 8), pyrexia (n = 6 and n = 5), decreased appetite (n = 5 and n = 2), hepatic encephalopathy (n = 5 and n = 2), and upper gastrointestinal (GI) hemorrhage (n = 5 and n = 2). SAEs reported in 2 or more patients are listed in Supporting Table 5.

The incidence of AEs was comparable between the brivanib and placebo groups (99% vs. 95%); however, incidence of grade 3-4 AEs was higher in the brivanib versus placebo group (69% vs. 43%; Table 3). The most frequently reported AEs (>20%, any grade) that occurred at a higher frequency (>10%) in the brivanib vs. the placebo group included HTN, decreased appetite, fatigue, diarrhea, hand-foot skin reaction, proteinuria, hyponatremia, and hypothyroidism (Table 3). Hepatic AEs of increased ALT, increased AST, and hyperbilirubinemia occurred at similar rates between the groups as did pyrexia, abdominal pain, and vomiting. Grade 3 AEs that occurred at a higher frequency in the brivanib (>5%) versus placebo group were hyponatremia, HTN, fatigue, diarrhea, and hand-foot skin reaction. Grade 4 AEs were infrequent.

One hundred twenty-one (49%) patients in the brivanib group and 16 (6%) in the placebo group had at least one dose reduction. Treatment-related AE was the primary cause of the first dose reduction (n = 68 [28%] in the brivanib group and n = 7 [3%] in the placebo group). Ninety-eight (40%) patients in the brivanib group and 46 (18%) in the placebo group discontinued treatment because of AEs. The most frequently reported AEs leading to discontinuation included malignant neoplasm (n = 13 in the brivanib group and n = 21 in the placebo group), HTN (n = 6 and n = 0), and proteinuria (n = 5 and n = 1). The Kaplan-Meier's estimate of median treatment duration was 6.0 months (95% CI: 4.7-7.7) in the brivanib group and 6.6 months (5.4-7.5) in the placebo group.

Discussion

This phase III randomized study showed no OS improvement with brivanib versus placebo (HR, 0.90; $P = 0.5280$) as adjuvant therapy to TACE in HCC patients. Adjusting the treatment effect for potential prognostic factors did not change the outcome (HR, 0.92). The median OS in the placebo group (26.1 months) of this study was longer than expected (18 months); this estimate is unreliable because of the early study termination and censoring. A potentially favorable OS outcome with brivanib in patients <65 years of age and in those with hepatitis B infection should be interpreted with caution because of the exploratory nature associated with subset analyses.

Although OS was similar between the brivanib and placebo groups, secondary and exploratory analyses of TTES/VI, TTP, and ORR suggested that brivanib in this setting may have slowed tumor growth and metastasis. Delayed TTES/VI is of particular interest, because

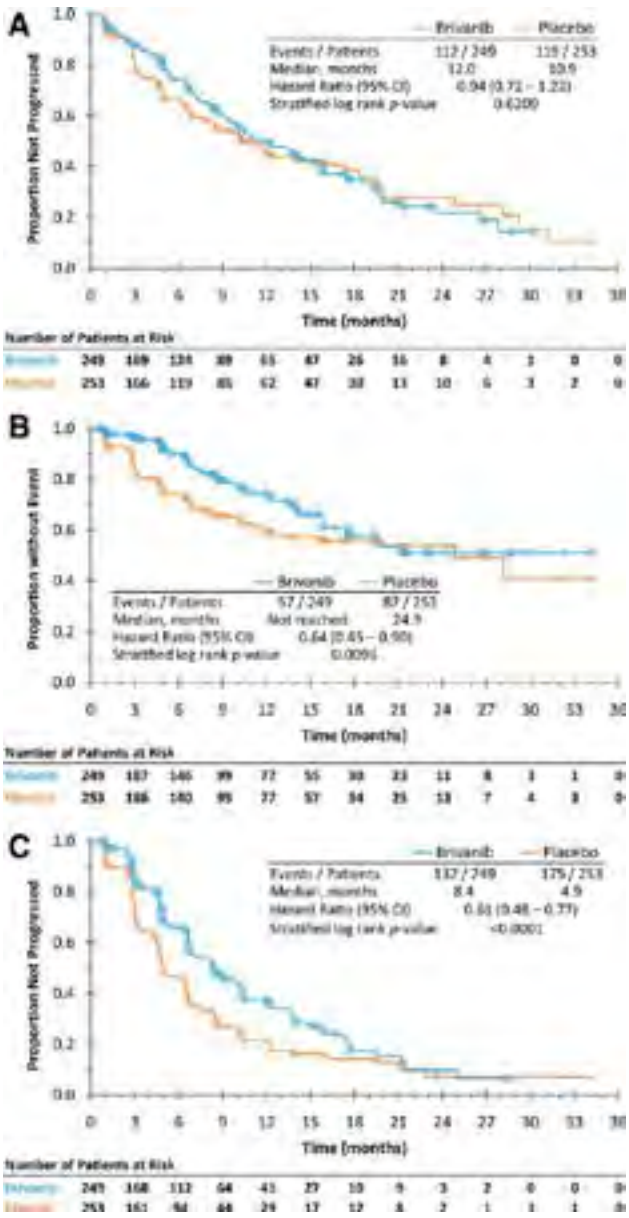

Fig. 4. Kaplan-Meier's curves for TTDP (A), TTES/VI (B), and TTP (C). (A) TTDP is a new composite endpoint defined as the time from the first TACE to the date of disease progression. Disease progression was defined as any of the following events: development of extrahepatic metastasis, development of vascular invasion, deterioration of liver function to Child-Pugh Class C, deterioration of ECOG-PS by 2 points if related to liver disease or if not related to liver disease, deterioration of ECOG-PS by 2 points that lasted for a period longer than 2 weeks, or death. Patients requiring alternative systemic therapy (e.g., sorafenib) before meeting the criteria for TTDP were censored at the time of their last assessment preceding alternative therapy where none of the events were observed. Patients without any of the events, and who did not receive alternative systemic therapy, were censored at their last assessment where none of the events were observed. (B) TTES/VI was defined as the time from the date of the first TACE to the date extrahepatic spread or vascular invasion was documented, whichever occurred first. Patients with no extrahepatic spread and no vascular invasion were censored at their last assessment where none of these events were observed. (C) TTP was defined as the time from the first TACE procedure to first radiographic tumor progression as assessed by investigators using mRECIST for HCC. Patients without radiographic tumor progression were censored at their last tumor assessment.

Table 2. Repeat TACE and Tumor Response

	Brivanib (N = 249)	Placebo (N = 253)
On-study repeat TACE		
Median number (range)	0.0 (0-13)	1.0 (0-8)
HR (95% CI)	0.72 (0.61-0.86)	
P value	0.0002	
ORR		
Events, n	120	106
ORR, % (95% CI)	48 (42-55)	42 (36-48)
OR (95% CI)	1.28 (0.90-1.83)	
Best response, n (%)		
Complete response	55 (22)	28 (11)
Partial response	65 (26)	78 (31)
Stable disease	76 (31)	93 (37)
Progressive disease	22 (9)	46 (18)
Unable to assess	31 (12)	6 (2)

The number of TACE was based on sessions between randomization and disease progression/censoring (i.e., excluding first TACE). The number of TACE and objective response rate were compared between arms using stratified Anderson-Gill's model and Cochran-Mantel-Haenszel's test, respectively. *P* values are for descriptive purposes only. Tumors were assessed by investigators using mRECIST for HCC.

this is an objective endpoint that may predict better prognosis when the disease is confined to the liver. Given the disease complexity characterized by the interplay between HCC and underlying liver disease, TTDP was introduced as another surrogate for OS. This composite endpoint was based on events (development of extrahepatic spread or vascular invasion, deterioration of liver function or ECOG-PS, or death) that would make patients ineligible for repeat TACE.[2,3] In the present study, TTDP was delayed only minimally with brivanib versus placebo (12.0 versus 10.9 months; HR, 0.94). This may be a result of death being the predominant TTDP event and non-tumor-related comorbidities being potential contributors to TTDP. The phase II SPACE trial comparing sorafenib/TACE combination with TACE alone in HCC patients used a different composite endpoint (time to untreatable progression; TTUP) based on ineligibility for further TACE and reported an HR for combination versus TACE alone of 1.586 for this endpoint.[25] Failure to achieve an objective response to treatment was the predominant event for TTUP. These results, including, in particular, the unexpected nature of factors that drove the composite endpoints, highlight the need for prospective studies to define relevant surrogate endpoints for OS.

In our study, there were fewer TACE sessions and a reduction in the risk of TACE in the brivanib group, compared to the placebo group. Fewer TACE sessions in the sorafenib group, compared to the placebo group, were also reported in the SPACE trial.[25] This lower rate of TACE could conceivably have been because the patient did not need further TACE as a

Table 3. Incidence of AEs

	Brivanib (N = 246)			Placebo (N = 253)		
AE, n (%)	Any Grade	Grade 3	Grade 4	Any Grade	Grade 3	Grade 4
Any	244 (99)	137 (56)	35 (14)	241 (95)	98 (39)	11 (4)
HTN	116 (47)	31 (13)	2 (1)	29 (11)	7 (3)	0
Pyrexia	93 (38)	2 (1)	0	115 (46)	1 (<1)	0
Decreased appetite	106 (43)	11 (4)	0	57 (23)	3 (1)	1 (<1)
Fatigue	101 (41)	22 (9)	0	59 (23)	6 (2)	0
Abdominal pain	90 (37)	10 (4)	0	101 (40)	10 (4)	2 (1)
AST increased	85 (35)	31 (13)	3 (1)	95 (38)	36 (14)	1 (<1)
ALT increased	88 (36)	22 (9)	2 (1)	84 (33)	26 (10)	0
Diarrhea	88 (36)	18 (7)	0	25 (10)	2 (1)	0
Hand-foot skin reaction	77 (31)	15 (6)	0	5 (2)	0	0
Proteinuria	71 (29)	12 (5)	0	24 (9)	2 (1)	0
Nausea	70 (28)	2 (1)	0	69 (27)	1 (<1)	0
Hyponatremia	68 (28)	42 (17)	2 (1)	27 (11)	11 (4)	2 (1)
Hypothyroidism	66 (27)	3 (1)	0	18 (7)	0	0
Vomiting	63 (26)	6 (2)	0	57 (23)	1 (<1)	0
Hyperbilirubinemia	60 (24)	14 (6)	5 (2)	57 (23)	5 (2)	2 (1)
Platelet count decreased	58 (24)	18 (7)	1 (<1)	42 (17)	10 (4)	0
Hypoalbuminemia	55 (22)	2 (1)	0	34 (13)	2 (1)	0
WBC count decreased	53 (22)	12 (5)	0	48 (19)	5 (2)	0
Dysphonia	45 (18)	3 (1)	0	5 (2)	0	0
Ascites	44 (18)	1 (<1)	0	18 (7)	6 (2)	1 (<1)
Upper abdominal pain	44 (18)	2 (1)	0	36 (14)	0	0
Peripheral edema	40 (16)	0	0	17 (7)	1 (<1)	0
Constipation	37 (15)	0	0	41 (16)	1 (<1)	0
Headache	39 (16)	1 (<1)	0	15 (6)	0	0
Abdominal distension	35 (14)	7 (3)	0	25 (10)	1 (<1)	0
Dizziness	34 (14)	3 (1)	0	8 (3)	0	0
Cough	31 (13)	0	0	19 (8)	0	0
GLT increased	32 (13)	5 (2)	0	34 (13)	8 (3)	2 (1)
PMN count increased	31 (13)	7 (3)	1 (<1)	29 (11)	8 (3)	0
Blood TSH increased	30 (12)	0	0	5 (2)	0	0
Insomnia	30 (12)	0	0	25 (10)	0	0
Blood ALP increased	23 (9)	1 (<1)	0	28 (11)	2 (1)	0
Rash	24 (10)	1 (<1)	0	13 (5)	0	0

Events listed are those (regardless of relationship to study treatment) occurring in at least 10% of the randomly assigned patients in either group who received at least one dose of any study treatment.

Abbreviations: WBC, white blood cell; GLT, λ-glutamyltransferase; PMN, peripheral blood neutrophil; TSH, thyroid-stimulating hormone; ALP, alkaline phosphatase.

result of either disease stabilization or drug toxicity. Though we cannot rule out the effect of drug toxicity (26% of patients came off for study drug toxicity in the brivanib arm vs. 2% in the placebo arm), the observed improvements in TTP and TTES/VI with brivanib suggest that disease stabilization by brivanib may have been a factor in reducing the number and risk of TACE with brivanib.

Optimal timing for drug administration, relative to TACE, has not been defined.[26] In our study, because of potential safety concerns, brivanib was stopped 2 days before a TACE session and restarted between days 3 and 21 after TACE. Because serum VEGF concentration peaks on day 1 after TACE,[9] brivanib may exert the greatest effects when administered immediately after or even before TACE. The ongoing ECOG E1208 phase III study (NCT01004978) will provide further insight on the time of the addition of sorafenib, relative to TACE, which may be useful for determining the timing of administration of other drugs in combination with TACE.

No unexpected safety findings for brivanib were identified in this study. Despite longer exposure to brivanib in this study (6.0 months), compared to BRISK-FL (3.2 months) and BRISK-PS (3.1 months) studies, AE profiles, rates of discontinuation (40%, 43%, and 42%, respectively) resulting from AEs, and rates of dose reduction (49%, 49%, and 54%, respectively) were comparable.[23,24] Rare treatment-related deaths were noted in all three studies, and the causes of these deaths were not unusual. As expected, AEs, including HTN, proteinuria, hyponatremia, and hypothyroidism, considered typical of brivanib, based on previous brivanib clinical studies,[23,24] were more frequent in the

brivanib group and were considered manageable. Hepatic AEs and certain GI AEs (e.g., abdominal pain and vomiting) occurred at higher rates in the placebo group, attesting to the seriousness of the underlying liver disease. Notably, these latter AEs appeared to be unaffected by brivanib administration. These data suggest that brivanib is reasonably well tolerated with an acceptable safety profile in patients with advanced or intermediate-stage HCC.

A major limitation of our study was its early closure. A sample size of 870 randomized patients with 520 death events for the primary OS analysis was planned. However, at final database lock, there were only 502 randomized patients and 164 death events (32% of the required events). Early closure thus compromised study power, warranting caution in interpreting the data. Furthermore, global studies aimed at evaluating TACE in combination with systemic agents are inherently challenging, given the heterogeneity in technique and interpretation of response.[1-3] In an attempt to manage these potential confounders, the study was designed not to assess the role of TACE in HCC, but the addition of brivanib by using a placebo control, requiring the use of standardized TACE procedures, standardizing response interpretation with mRECIST, using novel definition of disease progression, and stratifying by enrolling center (not just region or country), as well as using OS as the primary endpoint. Nevertheless, differences by region were still evident in a posthoc analysis of treatment duration and OS and may result, in part, from the regional differences in treatment practice. The present study underscores not only the need for rigorous definitions of trial design elements and assessments, but also the challenges such definitions may impose on trial execution.

In conclusion, brivanib as an adjuvant to TACE did not improve OS in this study. This study is the only phase III study using OS as the primary endpoint in the setting of combining TACE with an antiangiogenic agent. The only other published phase III trial evaluating the administration of sorafenib in patients who responded to TACE used TTP as the primary endpoint and OS as the secondary endpoint and showed improvement in neither TTP nor OS.[27] These results should be considered when planning future trials to evaluate the addition of antiangiogenic agents to TACE and point to the need for more rigorous preclinical and initial clinical investigations of combining antiangiogenic agents with TACE, innovative study design, and identification of predictive biomarkers for patient enrichment and relevant surrogate endpoints for survival. Better understanding of regional treatment practices and how they affect long-term outcomes are clearly needed.

Acknowledgment: The authors express their heartfelt thanks and gratitude to patients and their families. They also thank Motasim Billah of Bristol-Myers Squibb Company for providing professional medical writing assistance and the investigators for participating in the study. A full list of investigators is provided in Supporting Table 6.

References

1. Lencioni R. Chemoembolization for hepatocellular carcinoma. Semin Oncol 2012;39:503-509.
2. Llovet JM, Real MI, Montana X, Planas R, Coll S, Aponte J, et al. Arterial embolisation or chemoembolisation versus symptomatic treatment in patients with unresectable hepatocellular carcinoma: a randomised controlled trial. Lancet 2002;359:1734-1739.
3. Lo CM, Ngan H, Tso WK, Liu CL, Lam CM, Poon RT, et al. Randomized controlled trial of transarterial lipiodol chemoembolization for unresectable hepatocellular carcinoma. HEPATOLOGY 2002;35:1164-1171.
4. Rosmorduc O, Housset C. Hypoxia: a link between fibrogenesis, angiogenesis, and carcinogenesis in liver disease. Semin Liver Dis 2010;30:258-270.
5. Li X, Feng GS, Zheng CS, Zhuo CK, Liu X. Influence of transarterial chemoembolization on angiogenesis and expression of vascular endothelial growth factor and basic fibroblast growth factor in rat with Walker-256 transplanted hepatoma: an experimental study. World J Gastroenterol 2003;9:2445-2449.
6. Schoenleber SJ, Kurtz DM, Talwalkar JA, Roberts LR, Gores GJ. Prognostic role of vascular endothelial growth factor in hepatocellular carcinoma: systematic review and meta-analysis. Br J Cancer 2009;100:1385-1392.
7. Shim JH, Park JW, Kim JH, An M, Kong SY, Nam BH, et al. Association between increment of serum VEGF level and prognosis after transcatheter arterial chemoembolization in hepatocellular carcinoma patients. Cancer Sci 2008;99:2037-2044.
8. Sergio A, Cristofori C, Cardin R, Pivetta G, Ragazzi R, Baldan A, et al. Transcatheter arterial chemoembolization (TACE) in hepatocellular carcinoma (HCC): the role of angiogenesis and invasiveness. Am J Gastroenterol 2008;103:914-921.
9. Li X, Feng GS, Zheng CS, Zhuo CK, Liu X. Expression of plasma vascular endothelial growth factor in patients with hepatocellular carcinoma and effect of transcatheter arterial chemoembolization therapy on plasma vascular endothelial growth factor level. World J Gastroenterol 2004;10:2878-2882.
10. Poon RT, Ng IO, Lau C, Yu WC, Fan ST, Wong J. Correlation of serum basic fibroblast growth factor levels with clinicopathologic features and postoperative recurrence in hepatocellular carcinoma. Am J Surg 2001;182:298-304.
11. Llovet JM, Ricci S, Mazzaferro V, Hilgard P, Gane E, Blanc JF, et al. Sorafenib in advanced hepatocellular carcinoma. N Engl J Med 2008;359:378-390.
12. Cheng AL, Kang YK, Chen Z, Tsao CJ, Qin S, Kim JS, et al. Efficacy and safety of sorafenib in patients in the Asia-Pacific region with advanced hepatocellular carcinoma: a phase III randomised, double-blind, placebo-controlled trial. Lancet Oncol 2009;10:25-34.
13. Cai ZW, Zhang Y, Borzilleri RM, Qian L, Barbosa S, Wei D, et al. Discovery of brivanib alaninate ((S)-((R)-1-(4-(4-fluoro-2-methyl-1H-indol-5-yloxy)-5-methylpyrrolo[2,1-f][1,2,4] triazin-6-yloxy)propan-2-yl)2-aminopropanoate), a novel prodrug of dual vascular endothelial growth factor receptor-2 and fibroblast growth factor receptor-1 kinase inhibitor (BMS-540215). J Med Chem 2008;51:1976-1980.

14. Huynh H, Ngo VC, Fargnoli J, Ayers M, Soo KC, Koong HN, et al. Brivanib alaninate, a dual inhibitor of vascular endothelial growth factor receptor and fibroblast growth factor receptor tyrosine kinases, induces growth inhibition in mouse models of human hepatocellular carcinoma. Clin Cancer Res 2008;14:6146-6153.
15. Bhide RS, Lombardo LJ, Hunt JT, Cai ZW, Barrish JC, Galbraith S, et al. The antiangiogenic activity in xenograft models of brivanib, a dual inhibitor of vascular endothelial growth factor receptor-2 and fibroblast growth factor receptor-1 kinases. Mol Cancer Ther 2010;9: 369-378.
16. Allen E, Walters IB, Hanahan D. Brivanib, a dual FGF/VEGF inhibitor, is active both first and second line against mouse pancreatic neuroendocrine tumors developing adaptive/evasive resistance to VEGF inhibition. Clin Cancer Res 2011;17:5299-5310.
17. Finn RS, Kang YK, Mulcahy M, Polite BN, Lim HY, Walters I, et al. Phase II, open-label study of brivanib as second-line therapy in patients with advanced hepatocellular carcinoma. Clin Cancer Res 2012;18: 2090-2098.
18. Park JW, Finn RS, Kim JS, Karwal M, Li RK, Ismail F, et al. Phase II, open-label study of brivanib as first-line therapy in patients with advanced hepatocellular carcinoma. Clin Cancer Res 2011;17: 1973-1983.
19. Pocock SJ, Simon R. Sequential treatment assignment with balancing for prognostic factors in the controlled clinical trial. Biometrics 1975; 31:103-115.
20. Lencioni R, Llovet JM. Modified RECIST (mRECIST) assessment for hepatocellular carcinoma. Semin Liver Dis 2010;30:52-60.
21. Brookmeyer R, Crowley J. A confidence interval for the median survival time. Biometrics 1982;38:29-41.
22. Clopper CJ, Pearson ES. The use of confidence or fiducial limits illustrated in the case of the binomial. Biometrika 1934;26:404-413.
23. Johnson PJ, Qin S, Park JW, Poon RT, Raoul JL, Philip PA, et al. Brivanib versus sorafenib as first-line therapy in patients with unresectable, advanced hepatocellular carcinoma: results from the randomized phase III BRISK-FL study. J Clin Oncol 2013;31:3517-3524.
24. Llovet JM, Decaens T, Raoul JL, Boucher E, Kudo M, Chang C, et al. Brivanib in patients with advanced hepatocellular carcinoma who were intolerant to sorafenib or for whom sorafenib failed: results from the randomized phase III BRISK-PS study. J Clin Oncol 2013;31:3509-3516.
25. Lencioni M, Llovet JM, Han G, Tak WY, Yang J, Leberre MA, et al. Sorafenib or placebo in combination with transarterial chemoembolization (TACE) with doxorubicin-eluting beads (DEBDOX) for intermediate-stage hepatocellular carcinoma (HCC): phase II, randomized, double-blind SPACE trial. [Abstract]. J Clin Oncol 2012; 30(Suppl.);LBA154.
26. Strebel BM, Dufour JF. Combined approach to hepatocellular carcinoma: a new treatment concept for nonresectable disease. Expert Rev Anticancer Ther 2008;8:1743-1749.
27. Kudo M, Imanaka K, Chiba N, Nakachi K, Tak WT, Takayama T, et al. Phase III study of Sorafenib after transarterial chemoembolization in Japanese and Korean patients with unresectable hepatocellular carcinoma. Eur J Cancer 2011;47:2117-2127.

Supporting Information

Additional Supporting Information may be found in the online version of this article at the publisher's website.

98

Prospective Multicenter Randomized Controlled Trial of Histological Diagnostic Yield Comparing 25G EUS-FNA Needles With and Without a Core Trap in Patients With Solid Pancreatic Masses

Reiko Ashida*[1], Satoru Yasukawa[2], Akio Yanagisawa[2], Ken Kamata[3], Masatoshi Kudo[3], Takeshi Ogura[4], Kazuhide Higuchi[4], Nobuyasu Fukutake[1], Hiroko Nebiki[5], Satoru Hirose[6], Noriyuki Hoki[6], Masanori Asada[7], Shujiro Yazumi[7], Makoto Takaoka[8], Kazuichi Okazaki[8], Fumihiro Matsuda[9], Yoshihiro Okabe[9], Masayuki Kitano[3]

[1]Departments of Cancer Survey and Gastrointestinal Oncology, Osaka Medical Center for Cancer and Cardiovascular Diseases, Osaka, Japan; [2]Department of Surgical Pathology, Kyoto Prefectural University of Medicine, Kyoto, Japan; [3]Gastroenterology and Hepatology, Kinki University, Osaka-sayama, Japan; [4]The Second department of Internal Medicine, Osaka Medical College, Takatsuki, Japan; [5]Department of Gastroenterology, Osaka City General Hospital, Osaka, Japan; [6]Department of Gastroenterology, Bell Land General Hospital, Sakai, Japan; [7]Digestive Disease Center, Kitano Hospital, Osaka, Japan; [8]Gastroenterology and Hepatology, Dept.of Internal Medicine, Kansai Medical University, Hirakata, Japan; [9]Department of Gastroenterology and Hepatology, Osaka Red Cross Hospital, Osaka, Japan

Background: Endoscopic ultrasound (EUS)-guided fine needle aspiration (FNA) with 25G needles is safe and easy to handle but have been limited mainly to cytology. The newly developed core biopsy needles may overcome this limitation by providing core specimens for histological analysis. Aim: To compare the availability of histological diagnosis between the novel 25G EchoTip® ProCore™ (PrC) with a core trap and the standard 25G EchoTip® Ultra (Ult) (Cook Medical Inc. Bloomington, IN USA) for solid pancreatic masses. Patients and Methods: Consecutive patients with pancreatic solid masses presenting to 8 referral centers for EUS-FNA from April 2013 to Sept 2013 were prospectively recruited and randomized. The randomization was used to define which needle needed to be used by a random number generator. Regarding EUS-FNA, the stylet was slowly pulled out without suction while moving the needle to and fro 20 times (slow-pull technique). Only a single pass was performed for this study. The whole specimen was inserted into a formalin bottle and processed for histological analysis without rapid on-site evaluation. All tissue samples were brought to one facility where experienced pathologists (S.Y. and A.Y.) reviewed them independently. Both pathologists were blinded as to which needle was used. The final diagnosis of malignancy/benignancy was based on surgical histology or clinical follow up in non-surgical cases. Results: A total of 214 patients were enrolled. 112 males and 102 females (mean age=67.5yrs), with 106 patients in the PrC (49.5%) and 108 in the Ult (50.5%). The mean size of the pancreatic masses was 29.3 mm in the PrC and 27.9 mm in the Ult (ns). No procedure failures were observed with either needle. There were no procedure related complications. The tissue acquisition rate for histological analysis was significantly higher in the PrC than the Ult (96/106 cases (90.6%) vs. 86/108 cases (79.6%); p=0.025). The definite histological diagnosis achieved by the PrC was significantly higher than the Ult (86/106 cases (81.1%) vs. 75/108 cases (69.4%); p=0.048). All samples were divided into three groups based on quality (rich, moderate, and poor cellularity). The sample of the PrC showed significantly superior quality than the Ult (rich:moderate:poor = 38/106:29/106:39/106 cases in the PrC vs. 21/108:28/108:59/108 cases in the Ult; p=0.003). In the definitively diagnosable samples, sensitivity, specificity, and diagnostic accuracy of malignancy, at this interim analysis, were 89.5%, 100%, and 90.7%, respectively for the 25G PrC and 93.5%, 100%, and 94.7% for the 25G Ult (ns). Conclusions: This prospective multicenter randomized controlled trial indicated that the 25G ProCore needle with a single pass offers significantly better sample quality for histological diagnosis of solid pancreatic tumors compared with the 25G standard needle.

99

Prospective Randomized Blind Controlled Trial of Capillary EUS-FNA vs. Suction EUS-FNA for the Diagnosis of Solid Tumors

Ann M. Chen, Nirav C. Thosani*, Shai Friedland, Subhas Banerjee

Gastroenterology, Stanford University School of Medicine, Stanford, CA

Background: The diagnostic accuracy of endoscopic ultrasound guided fine needle aspiration (EUS-FNA) for solid lesions varies greatly from 39-93% with a median diagnostic rate of only 75%, even in expert hands. No standard technique has been established nor have different techniques been compared in randomized studies. Aim: To compare capillary vs. suction EUS-FNA on cellular adequacy during rapid-on-site cytologic evaluation (ROSE) and on final cytopathologic yield. Methods: A prospective randomized study was performed on patients at our institution undergoing EUS-FNA of solid lesions between January and November 2013. Two FNA techniques utilizing the 25G Echotip needle (Cook, Inc.) were compared: 1) Suction technique (ST), applying 10ml of syringe suction versus 2) Capillary technique (CT), slow stylet withdraw only without syringe. Patients were randomized to either ST or CT for the first pass then alternating techniques until adequate ROSE was achieved. Cytopathologists were blinded to the FNA technique. Results: A total of 65 patients with 80 biopsy sites were enrolled. 43 patients were randomized to initial CT and 37 to initial ST. Majority were carcinoma (n=63), neuroendocrine tumor (n=6), lymphoma (n=3), GIST (n=3). ROSE: ROSE was available for 132/143 (92%) CT samples and 121/131 (92%) of ST samples (Table 1). Immediate adequate cellularity was achieved in 99/132 (75%) of CT samples vs. 45/121 (37%) of ST samples, p<0.001. CT yielded significantly higher cellular adequacy for pancreas masses (57/78 vs. 24/71, p<0.001), liver lesions (14/15 vs. 4/13, p<0.001), and lymph nodes (21/28 vs. 10/26, p=0.01) than did ST samples. Cellular adequacy was achieved with a single CT pass in 57/80 sites compared to 28/80 with a single ST pass, p<0.001. Patients randomized to initial ST FNA required more passes to achieve adequate ROSE compared to the initial CT group, although this did not quite reach statistical significance (mean 3.7+1.2 vs. 3.2+1.0, p=0.06). Final Cytopathology: CT samples were superior to ST samples in cellular quality and more often rated higher in diagnostic yield by pathologists (50/80 cases vs. 12/80 cases, p<0.001; Table 2). Subanalysis indicated that CT FNA was significantly superior to ST FNA for pancreas masses (28/42 (67%) vs. 4/42 (10%), p<0.001) and liver lesions [8/11 (73%) vs. 0/11 (0%), p<0.001]. FNA method did not affect cytologic quality/yield for lymph nodes (11/20 CT vs. 6/20 ST samples, p=NS). Conclusions: Higher cytology quality is observed with capillary FNA, which may be a result of reduced tissue trauma and less bloody aspirate and is particularly important for sampling of highly vascular organs such as the pancreas and liver. Avascular lesions such as lymph nodes and submucosal nodules may be affected to a lesser extent by FNA technique. Optimizing FNA technique can improve efficiency and diagnostic accuracy.

Table 1. Rapid On-Site Evaluation of Cytology Adequacy Between Capillary and Suction FNA Samples by Biopsy Site

	Adequate			Scant			Blood Only		
	Capillary	Suction	p	Capillary	Suction	p	Capillary	Suction	p
Pancreas	57/78 (73%)	24/71 (34%)	<0.001	13/78 (17%)	18/71 (25%)	=0.23	8/78 (10%)	29/71 (41%)	<0.001
Liver	14/15 (93%)	4/13 (31%)	<0.001	0	4/13 (31%)	<0.03	1/15 (7%)	5/13 (38%)	=0.07
Lymph Node	21/28 (75%)	10/26 (38%)	<0.01	4/28 (14%)	10/26 (38%)	=0.06	3/28 (11%)	6/26 (23%)	=0.29
Submucosal/ Peri-luminal Mass	7/11 (64%)	7/11 (64%)	=1	3/11 (27%)	2/11 (18%)	=1	1/11 (9%)	2/11 (18%)	=1
Total	99/132 (75%)	45/121 (37%)	<0.001	20/132 (15%)	34/121 (28%)	<0.01	13/132 (10%)	42/121 (35%)	<0.001

Table 2. Comparison of Final Cytopathologic Diagnostic Yield and Cellular Superiority Between Capillary Versus Suction Samples by Blinded Pathologists

	Capillary >> Suction	Capillary > Suction	Capillary = Suction	Suction > Capillary	Suction >> Capillary	Sum of Diagnostic Yield Superiority, Capillary vs. Suction
Pancreas(n=42)	12 (29%)	16 (38%)	10 (24%)	4 (10%)	0	28 (67%) vs.4 (10%) p<0.001
Liver (n=11)	4 (36%)	4 (36%)	3 (27%)	0	0	8 (73%) vs. 0 p<0.001
Lymph nodes (n=20)	1 (5%)	10 (50%)	3 (15%)	5 (25%)	1 (5%)	11 (55%) vs. 6 (30%) p=0.2
Periluminal/ submucosal mass (n=7)	1 (14%)	2 (29%)	2 (29%)	2 (29%)	0	3 (43%) vs 2 (29%) p=1
Total (n=80)	18 (23%)	32 (40%)	18 (23%)	11 (14%)	1 (1%)	50 (63%) vs. 12 (15%) p<0.001

>>, Abundantly more cellular; >, moderately more cellular; =, equally cellular.

AP&T Alimentary Pharmacology and Therapeutics

Dynamic changes of the inflammation-based index predict mortality following chemoembolisation for hepatocellular carcinoma: a prospective study

D. J. Pinato*, G. Karamanakos*, T. Arizumi†, D. Adjogatse‡, Y. W. Kim§, J. Stebbing‡, M. Kudo†, J. W. Jang§ & R. Sharma*

*Division of Experimental Medicine, Imperial College London, Hammersmith Hospital, London, UK.
†Department of Gastroenterology and Hepatology, Kinki University School of Medicine, Osaka-Sayama, Osaka, Japan.
‡Department of Oncology, Imperial College London, Hammersmith Hospital, London, UK.
§Department of Internal Medicine, Incheon St. Mary's Hospital, The Catholic University of Korea, Seoul, Korea.

Correspondence to:
Dr R. Sharma, Imperial College London, Hammersmith Campus, Du Cane Road, London W12 0HS, UK.
E-mail: r.sharma@imperial.ac.uk

Publication data
Submitted 05 August 2014
First decision 27 August 2014
Resubmitted 27 September 2014
Resubmitted 28 September 2014
Accepted 28 September 2014
EV Pub Online 18 October 2014

This article was accepted for publication after full peer-review.

SUMMARY

Background
Transarterial chemoembolisation (TACE) is a standard treatment for unresectable, intermediate stage hepatocellular carcinoma (HCC). Survival after TACE, however, can be highly variable, with no suitable biomarker predicting therapeutic outcome. The inflammation-based index (IBI) has previously been shown to independently predict overall survival (OS) in all stages of HCC.

Aim
To explore the prognostic ability of IBI as a predictor of survival after TACE.

Methods
Baseline staging, biochemical and clinicopathological features including IBI were studied in a derivation set of 64 patients undergoing TACE for intermediate stage HCC. Dynamic changes in IBI before and after TACE were studied as predictors of survival using both a univariate and multivariate Cox regression model and further validated in two independent patient cohorts from Korea (n = 76) and Japan (n = 577).

Results
Pre-treatment IBI predicted for OS in the derivation set (P = 0.001). Other univariate predictors of OS included radiological response to TACE (P < 0.001), pre-TACE CLIP score (P < 0.01), tumour diameter >5 cm (P = 0.05) and AFP ≥400 (P < 0.001). Normalisation of IBI post-TACE was associated with radiological response by mRECIST criteria and improved OS (P < 0.001). Normalisation of IBI remained a significant multivariate predictor of OS in both the derivation and validation sets (P < 0.001).

Conclusions
Normalisation of IBI after TACE is shown to be an independent predictor of survival and may be integrated into the retreatment criteria for repeat TACE in intermediate stage HCC. IBI and its dynamic changes after treatment are validated as a biomarker allowing the stratification of patients with a significant survival advantage following initial TACE.

Aliment Pharmacol Ther 2014; **40**: 1270–1281

doi:10.1111/apt.12992

INTRODUCTION

Hepatocellular Carcinoma (HCC) is the commonest primary liver cancer and the third leading cause of cancer-related mortality worldwide.[1] The pathogenesis of HCC is inflammation-driven such that >80% of the incident cases arise in the context of liver cirrhosis.[2] Despite the introduction of active screening at least 60–70% of patients still present with inoperable disease and are ineligible for curative therapies.[3] In this context, the main focus of treatment is palliative, aimed at prolonging patient survival while maintaining quality of life.

Patients with liver-confined disease, preserved performance status (PS) and compensated liver functional reserve can be effectively offered transarterial chemoembolisation (TACE). TACE exploits the progressive arterialisation of the blood supply to the tumour to target the neoplastic tissue intra-arterially with focused chemotherapy administration followed by acute ischaemic damage with relative sparing of the surrounding tissue.[4] Evidence from randomised controlled trials highlights the efficacy of TACE in improving overall survival (OS) by slowing disease progression.[5]

International guidelines and consensus statements support the use of TACE for intermediate stage disease, identified by the Barcelona Clinic Liver Cancer (BCLC) staging system as BCLC-B stage.[6] However, there is uncertainty surrounding the optimal selection criteria for TACE as well as the ideal retreatment strategy.[7] Given the palliative intent of TACE, a careful and individualised risk-benefit assessment is necessary before proceeding with treatment. Several clinicopathological factors have been proven to predict outcome after TACE. It is accepted that within BCLC-B stage, patients with low alfa-fetoprotein (AFP) levels, limited tumour burden, preserved liver function and favourable radiological response after initial TACE will have significantly longer survival times.[8] Total bilirubin, PS $\geq$ 1 and total number of TACE sessions have also been identified as prognostic markers.[9] The developing experience in the administration of TACE and the relative safety of the procedure has prompted clinicians to expand its use beyond BCLC-B stage. A small but significant survival benefit has been reported in patient groups once precluded from TACE i.e. patients with extrahepatic disease or portal vein involvement.[10, 11] These studies highlight the acute and yet unmet need for objective clinical biomarkers to improve the accuracy of patient selection and predict clinical benefit from TACE in the individual patient. The non negligible rate of procedure-related morbidity and mortality further reinforces the importance of adequate patient selection, given the palliative intent of TACE.

Cancer-related inflammation is a pathogenic and prognostic domain with equal importance to angiogenesis and replicative immortality in cancer.[12] The presence of a systemic inflammatory reaction is a stage-independent prognostic factor in various malignancies,[13–15] including HCC.[16, 17] Systemic inflammation can be evaluated using widely accessible and objective markers such as C-reactive protein (CRP) and albumin levels.

We previously combined serum CRP and albumin to derive the inflammation-based index (IBI), a simple and validated measure of systemic inflammation that was shown to predict for OS in large, heterogeneous cohorts of patients with HCC, independent of BCLC stage.[16] We hypothesised whether the presence of an ongoing pro-inflammatory reaction may represent a predictor of outcome in HCC patients undergoing TACE and whether treatment-induced modulation of such systemic inflammatory response could exert an impact on patients' survival. We therefore designed this study to independently and prospectively validate the IBI as an objective prognostic marker in HCC patients undergoing TACE, and secondly to evaluate whether dynamic changes in the IBI following initial TACE can be used as a biomarker to predict survival advantage after treatment.

MATERIAL AND METHODS

Patient characteristics

The derivation dataset included 64 patients who had undergone TACE for intermediate stage HCC at Hammersmith Hospital, Imperial College London between 2001 and 2012. Our study included solely patients referred for palliative TACE, therefore excluding subjects undergoing TACE as bridging treatment prior to liver transplantation. All patients were diagnosed based on the American Association for the Study of the Liver guidelines. Clinicopathological variables including demographics, full blood count, albumin, C-reactive protein (CRP), alpha-fetoprotein (AFP), alanine aminotransferases (ALT), alkaline phosphatase (ALP), tumour staging (including number of focal lesions and maximum diameter of contrast enhancing disease), Child-Turcotte-Pugh class, Barcelona Clinic Liver Cancer (BCLC)[18] and Cancer of the Liver Italian Program (CLIP)[19] prognostic scores were collected at the time of referral to our unit, prior to treatment.

Transarterial chemoembolisation consisted of the intrarterial infusion of doxorubicin emulsified in lipiodol

followed by embolisation with gelatin sponge particles. Radiological response was assessed 6 weeks after the procedure using multiphase contrast-enhanced computed tomography (CT). Outcomes following treatment were reported by a senior radiologist blinded to clinical data as complete or partial response, stable or progressive disease according to mRECIST criteria.[20]

The IBI was calculated as previously described.[21] Briefly, patients with both a normal CRP of (<10 mg/L) and a normal albumin (>35 g/L) were allocated a score of 0. Those with only one abnormal measure were given a score of 1. Two points were allocated to patients with both abnormal CRP and albumin. The pre-TACE IBI was calculated using values obtained up to 48 h prior to the procedure. The post-TACE IBI was derived from values obtained at the first scheduled clinical reassessment, between 6 and 8 weeks following the first procedure depending on the institution. In the Japanese cohort, CRP levels were measured using a high sensitivity test (hsCRP) with a lower limit of detection of 3 mg/L. This value was chosen to reflect the local laboratory cut-off point, which is validated for cancer-related mortality.[22] Calculation of the IBI, in the sole Japanese validation cohort, was adjusted to hsCRP titres, with patients having levels >3 mg/L being allocated a score of 1. No changes were made to the cut-off point for albumin.

Dynamic changes in IBI were dichotomised as IBI normalisation vs. persistent abnormality of the score following treatment (Delta IBI). Normalisation of IBI included patients displaying any improvement of IBI score following treatment (i.e. changes from 2 to 1, 2 to 0 or 1 to 0) together with patients with a baseline IBI of 0 maintaining a normal score after treatment. Patients whose IBI had progressed by 1 or 2 points following treatment, or with a stable score of 1 or 2 despite treatment were considered together and classified as having a persistently abnormal IBI. OS (cancer specific) was calculated from the time of the first TACE to the time of death or last clinical follow-up.

Validation of prognostic scores

The first validation cohort consisted of 76 patients with newly diagnosed HCC referred to the Catholic University of Korea, St. Mary's Hospital, Seoul between 06/2011 and 07/2012. Data collection was performed prospectively. The TACE protocol agents used for the Korean patients consisted in the infusion of doxorubicin (50 mg) or combined epirubicin/cisplatin (50 + 60 mg) in a mixture of lipiodol followed by gelatin sponge embolisation.

The second validation cohort consisted of a retrospectively collected dataset of 557 consecutive patients with unresectable HCC treated with TACE at the Kinki University Faculty of Medicine (Japan) between 01/2004 and 08/2013. Chemoembolisation was performed using 20–50 mg of epirubicin or 50–100 mg of cisplatin emulsified with lipiodol and gelatin sponge particles. In both validation cohorts CT based mRECIST reassessment was conducted 6–8 weeks following TACE, in conjunction with reassessment of the IBI.

The study was approved by the local Research Ethics Committees. Prospective recruitment into the study followed written informed consent in accordance to the principles of the Declaration of Helsinki.

Statistical analysis

Pearson χ^2 test was employed to assess for any association between variables. Kaplan–Meier statistics and Log-rank test were used to study the impact of the different clinical factors associated with OS on univariate analysis, with significant variables ($P < 0.05$) being further tested on a multivariate stepwise backward Cox regression model. An entry threshold of 0.05 was used at each step of the multivariate analysis, whereas variables with a *P*-value >0.10 were removed from the model. Variables emerging as independent predictors of survival at the last step of the multivariate model were taken as significant if the correspondent *P*-value was <0.10. For all the other statistical tests, a *P*-value <0.05 was taken to be significant. All statistical analyses were performed using SPSS package version 11.5 5 (SPSS Inc., Chicago, IL, USA).

RESULTS

Demographics

The clinicopathological features of the derivation set are illustrated in Table 1. Median age was 64 years (range 33–83). The majority of patients (67%) were classified as intermediate stage HCC according to BCLC criteria, with preserved liver function (Child–Turcotte–Pugh class A, 83%). The most common aetiology of cirrhosis was alcohol excess (36%) followed by hepatitis C infection (30%). In total, 48% of patients received >1 TACE (range 1–5). Minimum follow-up time was 3 months or until date of death. At the time of analysis, 53% of patients had died. Median OS was 16.9 months (5.4–28.4 months). Restaging CT images were available in 95% of the patients. Of the three patients without post-procedure radiological assessment, two had died prior to restaging while for the remaining patient imaging was performed elsewhere.

Table 1 | Demographic and clinical characteristics of patients with HCC treated with TACE (Derivation and validation sets)

Baseline characteristic	Training set $n = 64$ (%) or median (range)	Validation Korea $n = 76$ (%) or median (range)	Validation Japan $n = 557$ (%) or median (range)
Age, years	64 (33–83)	58 (32–77)	73 (34–89)
Gender			
Male	49 (90)	56 (74)	392 (70)
Female	15 (10)	20 (26)	165 (30)
Aetiology of chronic liver disease*			
Hepatitis B virus	10 (15)	62 (81)	58 (20)
Hepatitis C virus	19 (30)	9 (11)	383 (60)
Alcohol consumption	23 (36)	16 (21)	99 (17)
Others	10 (15)	0 (0)	17 (3)
Unknown	8 (12)	4 (5)	0 (0)
Child–Turcotte–Pugh class			
A5	19 (30)	39 (50)	267 (48)
A6	34 (53)	15 (19)	147 (25)
B7	8 (13)	7 (9)	84 (15)
B8	2 (3)	8 (9)	37 (7)
B9	1 (1)	7 (9)	14 (3)
Missing	–	–	8 (1)
Maximum tumour diameter			
≤5 cm	26 (40)	41 (54)	477 (86)
>5 cm	38 (60)	35 (46)	80 (14)
Portal vein invasion			
Absent	60 (94)	57 (75)	525 (94)
Present	4 (6)	19 (25)	32 (6)
Albumin, g/L	33 (23–43)	36 (26–46)	36 (20–50)
Total bilirubin, μmol/L	12 (4–124)	31 (2–165)	14 (3–70)
ALT, IU/L	64 (10–348)	57 (11–392)	37 (4–197)
AST, IU/L	71 (22–365)	50 (19–450)	49 (6–303)
ALP, IU/L	120 (53–563)	232 (94–906)	346 (108–1901)
AFP, ng/mL	49 (2–130.000)	32 (2–699.520)	27 (1–974.819)
INR	1.1 (1.0–1.4)	1.2 (0.8–2.0)	1.0 (1.0–2.0)
Platelet Count, $\times 10^9$/L	152 (46–144)	110 (19–396)	115 (14–1653)
BCLC Stage			
A	11 (17)	30 (40)	199 (36)
B	43 (67)	27 (35)	307 (55)
C	10 (16)	19 (25)	51 (9)
CLIP score			
0–1	36 (58)	36 (48)	N.A.
≥2	28 (42)	40 (52)	
Inflammation-based index (IBI) at diagnosis			
0	18 (28)	35 (42)	258 (46)
1	24 (37)	30 (40)	236 (42)
2	20 (31)	11 (14)	63 (12)
Missing	2 (4)	–	–
Number of TACE procedures			
1	33 (52)	12 (16)	177 (31)
2	17 (26)	18 (24)	139 (25)
≥3	14 (22)	46 (60)	261 (44)
Prior treatments			
First line TACE	37 (58)	68 (90)	239 (43)
Resection	5 (8)	8 (10)	73 (13)
Transplantation	2 (3)	–	0 (0)
Radiofrequency ablation	10 (16)	–	221 (40)

Table 1 | (Continued)

Baseline characteristic	Training set $n = 64$ (%) or median (range)	Validation Korea $n = 76$ (%) or median (range)	Validation Japan $n = 557$ (%) or median (range)
Systemic treatment	12 (19)	–	24 (4)
Modified RECIST response following TACE			
Complete response	9 (14)	22 (30)	218 (40)
Partial response	17 (28)	15 (19)	95 (17)
Stable disease	16 (26)	27 (35)	56 (10)
Progressive disease	19 (31)	12 (16)	179 (32)
Missing	–		9 (2)
Overall survival, months	16.9 (5.4–28.4)	18.0 (14.4–21.6)	22.9 (1.1–102.5)

* Non cumulative percentages.

Inflammatory response and clinical outcomes

Baseline and post-TACE IBI scores were available in 62 and 54 patients, respectively. The IBI was computed based on the independent effect of hypoalbuminaemia (<35 g/L) and elevated CRP (>10 mg/L) on patient's OS.[21] Eighteen patients (29%) had a normal IBI score at baseline, while 24 patients (39%) were allocated a score of 1 (intermediate risk), and 20 (32%) a score of 2 (high risk).

Following TACE, no response to IBI was observed in 26/54 patients (47%): 11 maintained a score of 1 and 15 a score of 2. Worsening of IBI was noted in 16/54 patients, with 10 (17%) having a 1-point progression in their IBI score following treatment, while another 6 (12%) had a 2-points progression. Seven patients (13%) with an IBI of 0 retained normal levels of albumin and CRP following treatment. Four patients (7%) had a 1-point regression of their score, while another 2 (4%) had a 2-point regression. In total, 13 patients (24%) satisfied the criteria for IBI normalisation, while the remaining 41 (76%) were categorised as having a persistently abnormal score following treatment.

Univariate analysis of survival revealed that patients with an IBI of 1 or 2 at baseline had a median survival of 16.9 (95% CI 9.4–24.4) and 10.3 (95% CI 7.6–12.9) months, respectively, while for patients with an IBI score of 0 median survival was not achieved at the end of follow-up period (HR 4.2, 95% CI 2.1–8.3, $P < 0.001$) (Figure 1a). Patients having persistently abnormal IBI score after TACE had a median OS of 11.3 months (95% CI 9.8–12.8 months) while for patients achieving normalisation of the index, median OS was not reached (HR 12.1, 95% CI 2.7–53.3; $P < 0.001$) (Figure 1b). Other univariate predictors of survival included the extent of intrahepatic spread ($P < 0.001$), tumour size >5 cm ($P = 0.01$), AFP >400 ng/mL ($P = 0.002$), advanced CLIP score ($P = 0.001$), presence of portal vein thrombosis ($P = 0.05$) and radiological response following TACE ($P < 0.001$; Figure 1c).

On multivariate analysis, normalisation of IBI following TACE was confirmed as an independent predictor of OS ($P = 0.003$), together with radiological response ($P = 0.01$), tumour size ($P = 0.07$), and portal vein involvement ($P = 0.04$; Table 2). Normalisation of the IBI following TACE was associated with higher rates of radiological response to treatment according to mRECIST criteria ($P = 0.001$; Figure 2a).

Validation of prognostic models

Independent validation of the dynamic changes in the IBI following TACE. We assessed the prognostic ability of the dynamic changes of the IBI following TACE in an independently collected dataset of 76 consecutive patients considered for TACE at St. Mary's Hospital, Catholic University of Korea, whose baseline features are described elsewhere[23] and summarised in Table 1. Derivation and validation set were similar with regard to overall survival (median OS for the Korean cohort was 18.0 months, range 14.4–21.6 months) and baseline clinicopathological features but differed in terms of distribution of risk factors for underlying liver disease with hepatitis B virus (HBV) infection being most prevalent in the validation set ($n = 62$, 81%). Notably, the Korean dataset had a significantly higher prevalence of segmental portal vein invasion (25%), rendering a quarter of the patients stage BCLC-C.

With regard to inflammatory scores 35 patients (46%) had a normal IBI at baseline, while 30 had an IBI of 1 (40%) and 11 (14%) had an IBI of 2. Following treatment 34 patients (45%) achieved IBI normalisation, whereas 42 (55%) had a persistently abnormal IBI post-TACE.

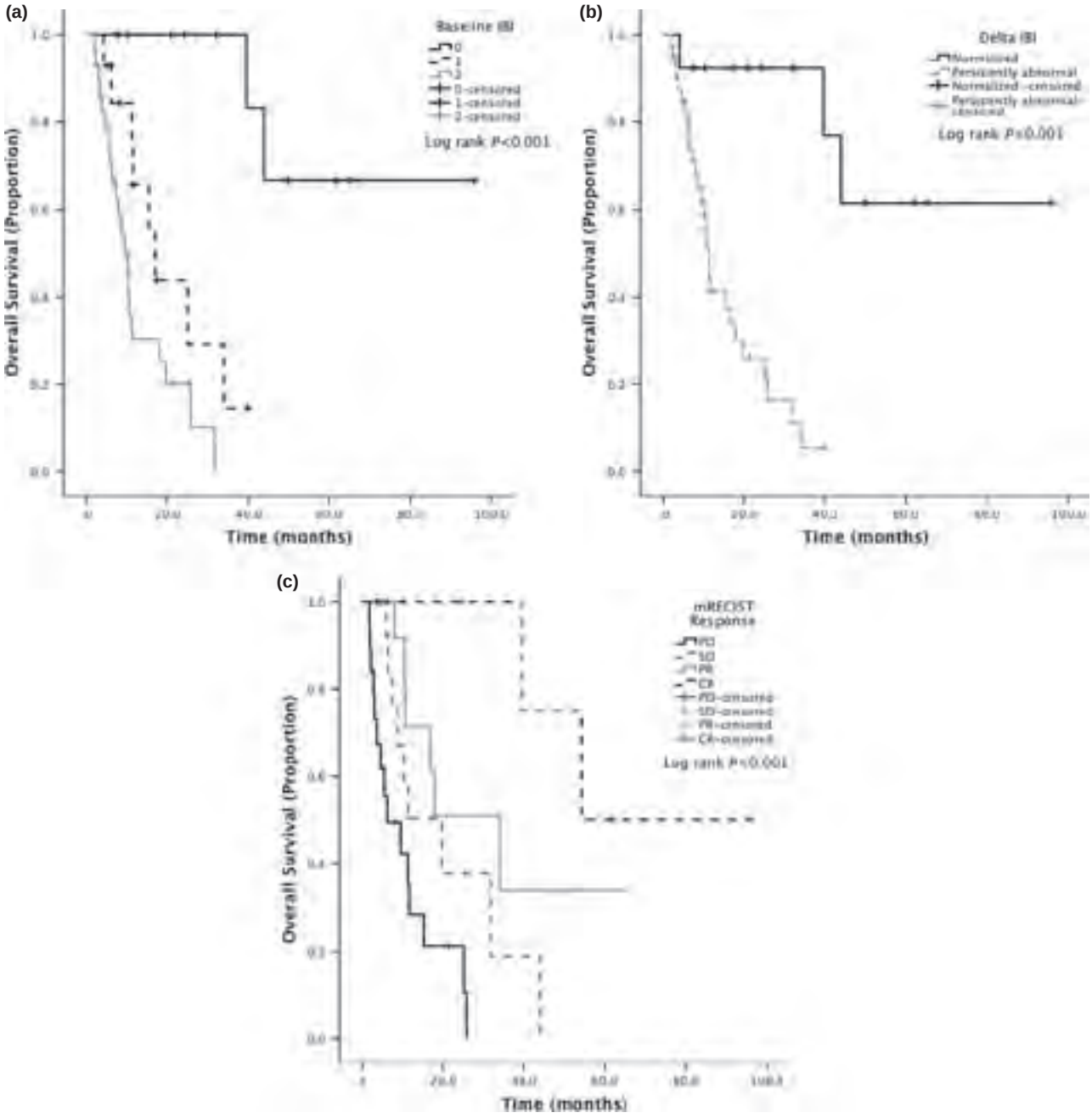

Figure 1 | Kaplan–Meier curve analysis showing the effect of baseline IBI (a), dynamic changes of the IBI post-TACE (Delta IBI, b) and modified RECIST based tumour response following TACE (c) as predictors of overall survival in HCC (Derivation Set).

Among the 42 patients showing evidence of a persistently abnormal IBI following treatment, 8 (20%) retained a score of 2, 17 (40%) maintained a score of 1 while 14 patients (33%) displayed a 1-point worsening and another 3 patients (7%) had a 2-point worsening from baseline. The 34 patients who had evidence of improved inflammatory scores post-TACE included 23 patients (29%) with a baseline IBI of 0 that remained unmodified post-TACE, and another 11 patients (14%) who achieved a 1-point regression from their baseline score: such regression was based on improvement in albumin concentration to ≥35 g/L in five patients and improved CRP concentration to <10 mg/L post-TACE in another 6.

Table 2 | Univariate and multivariate analysis of prognostic factors of overall survival (Derivation Set).

Univariate analysis				Multivariate analysis	
Variable	*N* = 64 (%)	Hazard ratio (95% CI)	*P*-value	Hazard ratio (95% CI)	*P*-value
Intrahepatic spread					
Uninodular <50%	23 (36)	2.3 (1.3–4.2)	<0.001*		
Multinodular <50%	28 (44)				
Massive ≥50%	13 (20)				
Maximum tumour diameter					
<5 cm	27 (43)	3.4 (1.6–7.3)	0.01*	2.3 (1.0–5.6)	0.07#
≥5 cm	37 (57)				
AFP, ng/mL					
<400	49 (77)	3.0 (1.5–6.3)	0.002*		
≥400	15 (23)				
CLIP score*					
0	16 (25)	2.3 (1.5–2.5)	0.001*		
1	20 (31)				
2	20 (31)				
3	5 (8)				
4–5	3 (5)				
Portal vein involvement					
Absent	60 (94)	2.7 (1.0–8.0)	0.05*	4.1 (1.0–16.5)	0.04#
Present	4 (6)				
Radiological response					
CR	9 (15)	0.4 (0.3–0.6)	<0.001*	0.5 (0.3–0.8)	0.01#
PR	17 (28)				
SD	16 (26)				
PD	19 (31)				
IBI post-TACE					
Normalised	13 (24)	12.1 (2.7–53.3)	<0.001*	3.6 (1.6–8.3)	0.003#
Persistently elevated	41 (76)				

AFP, alpha-fetoprotein; CLIP, Cancer of the Liver Italian Program Score; Radiological Response: CR, complete response; PR, partial response; SD, stable disease; PD, progressive disease.

For survival analysis, patients with CLIP score of 4 (n = 2) and 5 (n = 1) were considered together. Associations reaching statistical significance ($P < 0.05$) are marked with an asterisk (*).Variables emerging as independent predictors of survival at the last step of the stepwise regression Cox model were considered significant if the corresponding *P*-value was <0.10 and marked with an ash (#). The cut-off values for AFP and intrahepatic spread follow the CLIP prognostic scores.

Analysis of survival of the Korean cohort confirmed baseline IBI ($P < 0.001$), radiological response following TACE ($P < 0.001$) and normalisation of the IBI following TACE ($P < 0.001$) as validated predictors of OS. With regard to pre-treatment IBI, patients scoring 0 had a median survival of 33.0 months (95% CI 13.3–52.6 months) compared to 18.2 months (95% CI 8.8–27.6 months) of patients scoring 1 and 8.6 months (95% CI 4.9–12.2 months) of patients scoring 2 (HR 2.4 95% CI 1.6–3.6, $P < 0.001$) (Figure 3a). With regard to IBI changes following TACE, patients achieving normalisation of the score had a median OS of 33.0 months (95% CI 15–51 months), while patients with a persistently abnormal index despite treatment had a median OS of 11.0 months (6.7–15.3 months, HR 3.0 95% CI 1.7–5.5, $P < 0.001$) (Figure 3b). Patients achieving IBI normalisation post-TACE were more likely to have favourable radiological response to treatment ($P = 0.03$; Figure 2b).

The second validation cohort of 577 Japanese patients, whose features are listed in Table 1, had a median OS of 22.9 months (range 1.1–102.5 months) with 290 deaths (52%) recorded at the time of data analysis. HCV infection was the most prevalent recorded risk factor for HCC (n = 383, 60%), These patients were predominantly Child–Pugh A (73%) within BCLC-B stage (55%) with a limited proportion of patients exceeding intermediate stage criteria (9%). Measurement of the IBI at diagnosis, adjusted for the hsCRP cut-off value of 3 mg/L, showed 46% of the patients scoring 0, followed by 42% scoring 1 and 12% scoring 2. Both albumin <35 g/L ($P < 0.001$)

Aliment Pharmacol Ther 2014; 40: 1270-1281

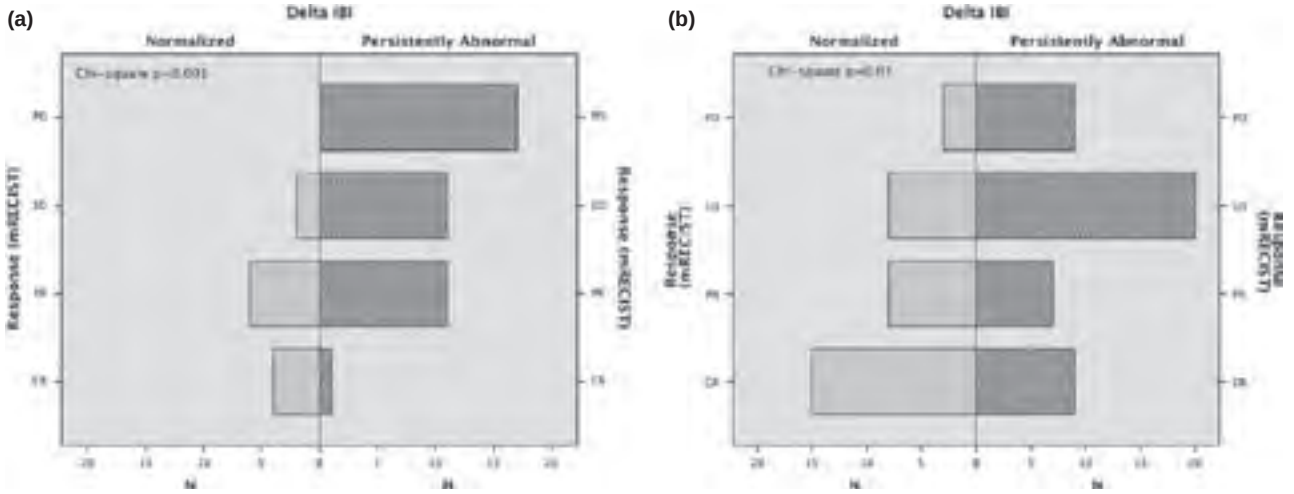

Figure 2 | Diagram illustrating the relationship between modified RECIST outcomes at 6 weeks post-TACE in the Derivation Set (a) and 8 weeks post-TACE in the Validation Set (Korea) (b).

and hsCRP >3 mg/L ($P < 0.001$) were preliminarily tested in this cohort and confirmed as prognostic markers in keeping with previously published work.[24, 25]

Reassessment of the IBI following TACE could be performed in 487 subjects: 215 clustered into the good prognosis category (44%), while 272 (56%) showed worsening of IBI. Of the 215 with improved IBI after TACE, 5 (2%) patients had an improvement in both albumin and hsCRP, 39 patients (18%) normalised their hsCRP while two patients (1%) normalised their albumin levels. The remaining 169 in the good prognostic group maintained persistently normal albumin and hsCRP following TACE (78%).

The 272 patients showing progressive IBI after TACE included 10 patients with a 2-point progression (4%), 50 (18%) with a worse hsCRP, 38 (14%) with a worse albumin while the remaining 174 (64%) patients demonstrated a stable, persistently deranged IBI score of either 1 or 2 post-TACE. Analysis of survival confirmed the baseline IBI as a strong predictor of survival: median OS for IBI 0 patient was 49.6 months (95% CI 45.7–53.4 months) compared with 35 months of IBI 1 patients (95% CI 28.8–41.3 months) and 20 months (95% CI 9.9–30.1 months) for IBI 2 patients (HR 1.6 95% CI 1.4–1.9, $P < 0.001$; Figure 3c). Similarly, IBI changes post-TACE predictor for a median OS of 46.4 months (95% CI 39.5–53.2 months) for patients achieving normalisation of the score, while patients with a persistently abnormal index despite treatment had a median OS of 31.5 months (23.4–39.5 months, HR 1.6 95% CI 1.2–2.0, $P < 0.001$; Figure 3d).

Using a stepwise backwards Cox regression model, an independent effect on patients' survival was confirmed for BCLC stage (HR 1.5, 95% CI 1.2–1.9, $P < 0.001$), mRECIST response (HR 1.6, 95% CI 1.5–1.8, $P < 0.001$) and either baseline IBI (HR 1.5, 95% CI 1.3–1.8 $P < 0.001$) or IBI changes post-TACE (HR 1.6, 95% CI 1.3–2.1, $P < 0.001$), tested alternatively in separate models to avoid colinearity bias.

DISCUSSION

Patient selection is a consolidated concept in oncology and governs the delicate balance between the administration of potentially toxic treatments with the expected benefits in terms of survival extension and symptomatic control. TACE is a relatively safe treatment for intermediate stage HCC. However, complications like post-embolisation syndrome can effect up to 50% of patients who may incur into acute liver failure, with an associated risk of post-procedure mortality.[26] There is a growing interest to discover novel biomarkers to predict treatment-induced survival benefit, with the expected intent of avoiding unjustifiable morbidity and mortality in an essentially palliative population.[27]

Following from our previous experience on the interplay between systemic inflammation and the prognosis of HCC, we hypothesised whether IBI could optimise the selection of patients undergoing TACE, a patient subgroup with varying tumour burden where predicted survival can be particularly variable.[28]

We have demonstrated that pre-treatment IBI is an independent prognostic marker in patients receiving

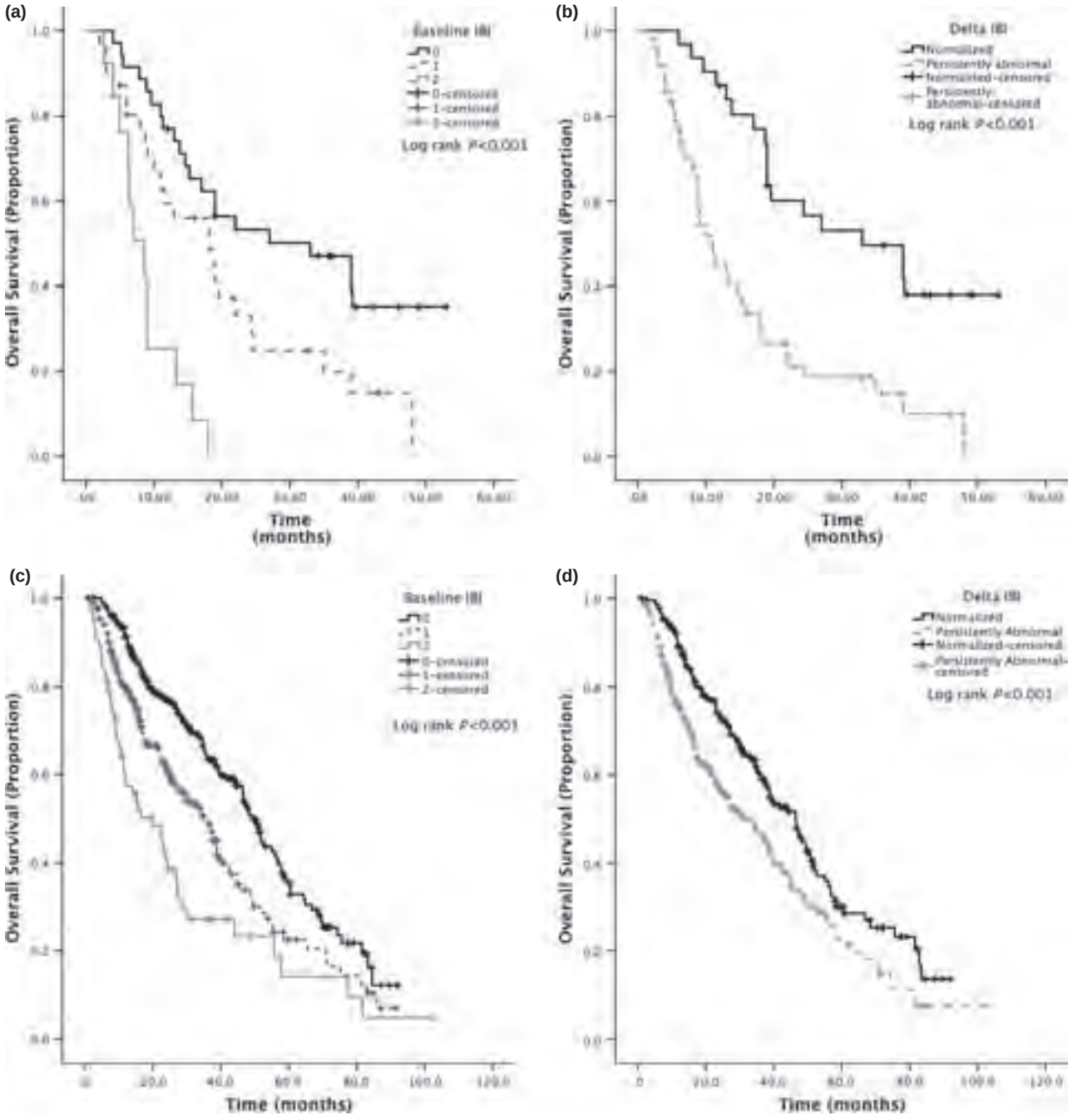

Figure 3 | Kaplan–Meier curve analysis showing the effect of baseline IBI (a), dynamic changes of the IBI post-TACE (Delta IBI, b) as predictors of overall survival in the Korean Validation Set. (c, d) the effect on overall survival of baseline IBI and its dynamic changes post-TACE respectively in the Japanese Validation Set.

TACE. This finding further validates systemic inflammation, as reflected by hypoalbuminaemia and elevated CRP, are prognostic across all stages of HCC, consistent with previous studies in early[29] and advanced stage disease.[30]

A growing body of evidence has demonstrated an association between a systemic inflammatory response with adverse clinical features such as cancer-related cachexia, a complex metabolic and nutritional derangement that correlates negatively with cancer patients' prognosis[31] including HCC.[25] However, a complete understanding of the molecular drivers involved in such reaction is yet to be fully elucidated. Genomic signature data suggest that systemic inflammation is sustained both by the tumour and its surrounding microenviron-

Aliment Pharmacol Ther 2014; 40: 1270-1281

ment,[32] where subtle changes in the immune response may confer survival advantage to the proliferating neoplastic clones through the activation of inflammatory pathways.[33] Similarly, modulation of the host's immune response may also be involved in facilitating tumour cell evasion from immunological clearance, therefore contributing to adverse outcomes.[34–36]

Recent studies have shown that systemic inflammation is not a static phenomenon in cancer, but can be potentially dampened through active treatment.[37–39] In our study, we found that normalisation of the IBI following initial TACE is significantly associated with objective tumour response and survival benefit. This is in keeping with previous studies showing that treatment-induced changes in the blood neutrophil to lymphocyte ratio (NLR), another biomarker of systemic inflammation, can predict survival after TACE.[40]

A number of studies have shown that TACE can directly modulate both innate and adaptive immunity, and some studies have linked the emergence of specific T-cell responses following TACE with improved clinical outcomes.[41] Interestingly, the systemic release of lymphocyte T-helper 2 cytokines such as interleukin 4, 5 and 10 which suppress anti-tumour response, is sustained after TACE and more prominent in larger tumours.[23] This data suggest an important link between the systemic release of pro-inflammatory cytokines and clinical outcome, which may provide further mechanistic insight into the prognostic significance we observed for IBI changes following treatment. Despite the established prognostic relationship between pro-inflammatory cytokines, systemic inflammation, angiogenesis and immune system dysfunction,[14, 42] further research is required to define distinct cytokine signalling pathways responsible for the inflammatory-driven deterioration in patients' prognosis, especially as it may yield a potential therapeutic strategy in HCC.

One of the crucial steps before a newly discovered prognostic biomarker is integrated into routine practice is the need for statistical validation. For this purpose, we opted to replicate our survival analysis across two independent patient cohorts with differing aetiologies and staging, with 25% of the Korean patients exceeding intermediate stage criteria. While the presence of extrahepatic spread generally discourages the use of locoregional treatments, the growing experience of delivering TACE in advanced disease has made it possible to achieve a significant, although smaller, survival benefit in BCLC-C patients.[43] Although technically feasible, the provision of TACE in patients exceeding BCLC-B criteria competes with other treatments like radioembolisation or sorafenib, lacking direct comparison in randomised controlled trials. Our study provides evidence for IBI changes as a reliable prognostic trait in patients that fulfil or exceed BCLC-B criteria.

Taken together, our findings reinforce the concept that the IBI is a validated prognostic model across both Eastern and Western populations where prognosis can be dissimilar as a result of differing risk factors, tumour phenotype and clinical management.[44] The relatively limited sample size stands as a limitation of our study, which we overcame by cross-validation. Given that the majority of patient data were collected retrospectively we could not accurately reconstruct whether patients were offered any anti-inflammatory agents either prior to or post-TACE. However, the fact that the IBI and its dynamic changes emerged as independent predictors of survival in different cohorts gives us no reason to suspect systematic bias. Similarly, the measurement of CRP was different across laboratories. However, we validated the prognostic impact of an hsCRP based IBI showing that normalisation of CRP and albumin persists as a highly significant predictor of survival in HCC regardless of the methodology used to test these analytes. The level of statistical significance achieved in all the tested datasets leaves in fact little doubt about the reliability and reproducibility of our findings.

To conclude, this is the first multi-institutional study to independently and prospectively validate the prognostic ability of the IBI and its dynamic changes following treatment in HCC patients being considered for TACE. Our study illustrates that the reversal of cancer-related inflammation, as measured by the IBI is associated with better response rates and improved survival, and can be used to select patients who may benefit from repeat TACE, protecting the others from unnecessary risks and adverse events. Sequential assessment of the IBI score may integrate the eligibility assessment for retreatment after initial TACE. IBI-based progression may in fact serve as a surrogate biomarker of chemoembolisation failure, prompting clinicians to consider switching to alternative treatments including sorafenib.

Unlike other clinical scores that are being developed as potential objective biomarkers to optimise the retreatment of patients with intermediate stage HCC,[45, 46] the IBI is much simpler to calculate, universally available, even in areas with limited healthcare resources, and its prognostic power is independent from imaging. Moreover, unlike some of the proposed scores,[24] the IBI is optimally conceived for sequential reassessment, with its

dynamic changes reflecting disease modifying effects following treatment. While provocative, our findings require validation in larger prospective cohorts.

AUTHORSHIP

Guarantor of the article: Rohini Sharma.

Author contributions: DJP, GK, RS: study concept and design. DJP, TA, DA, JWJ, GK, YWK, MK, MP: acquisition of data. DJP, JS, GK, DA, RS: analysis and interpretation of data. DJP, DA, RS: Drafting of the manuscript. DJP, RS: statistical analysis. JS, MK, JWJ: Administrative, technical or material support. DJP, JWJ, MK, JS, RS: study supervision. All authors contributed to critical revision of the manuscript for important intellectual content. All authors approved the final version of the manuscript.

ACKNOWLEDGEMENTS

The authors acknowledge Dr Paul Tait, consultant radiologist at the Hammersmith Hospital (Imperial College NHS Trust) for his help in reviewing mRECIST data.

Declaration of personal and funding interests: None.

REFERENCES

1. Parkin DM, Bray F, Ferlay J, Pisani P. Global cancer statistics, 2002. *CA Cancer J Clin* 2005; **55**: 74–108.
2. Berasain C, Castillo J, Perugorria MJ, Latasa MU, Prieto J, Avila MA. Inflammation and liver cancer: new molecular links. *Ann N Y Acad Sci* 2009; **1155**: 206–21.
3. Llovet JM, Bruix J. Novel advancements in the management of hepatocellular carcinoma in 2008. *J Hepatol* 2008; **48** (Suppl. 1): S20–37.
4. Llovet JM, Real MI, Montana X, *et al.* Arterial embolisation or chemoembolisation versus symptomatic treatment in patients with unresectable hepatocellular carcinoma: a randomised controlled trial. *Lancet* 2002; **359**: 1734–9.
5. Llovet JM, Bruix J. Systematic review of randomized trials for unresectable hepatocellular carcinoma: chemoembolization improves survival. *Hepatology* 2003; **37**: 429–42.
6. Raoul JL, Sangro B, Forner A, *et al.* Evolving strategies for the management of intermediate-stage hepatocellular carcinoma: available evidence and expert opinion on the use of transarterial chemoembolization. *Cancer Treat Rev* 2011; **37**: 212–20.
7. Camma C, Schepis F, Orlando A, *et al.* Transarterial chemoembolization for unresectable hepatocellular carcinoma: meta-analysis of randomized controlled trials. *Radiology* 2002; **224**: 47–54.
8. Heng-Jun G, Yao-Jun Z, Min-Shan C, *et al.* Rationality and effectiveness of transarterial chemoembolization as an initial treatment for BCLC B stage HBV-related hepatocellular carcinoma. *Liver Int* 2014; **34**: 612–20.
9. Cabibbo G, Genco C, Di Marco V, *et al.* Predicting survival in patients with hepatocellular carcinoma treated by transarterial chemoembolisation. *Aliment Pharmacol Ther* 2011; **34**: 196–204.
10. Zhao Y, Cai G, Zhou L, *et al.* Transarterial chemoembolization in hepatocellular carcinoma with vascular invasion or extrahepatic metastasis: a systematic review. *Asia Pac J Clin Oncol* 2013; **9**: 357–64.
11. Yoshidome H, Takeuchi D, Kimura F, *et al.* Treatment strategy for hepatocellular carcinoma with major portal vein or inferior vena cava invasion: a single institution experience. *J Am Coll Surg* 2011; **212**: 796–803.
12. Hanahan D, Weinberg RA. Hallmarks of cancer: the next generation. *Cell* 2011; **144**: 646–74.
13. Mohamed Z, Pinato DJ, Mauri FA, Chen KW, Chang PM, Sharma R. Inflammation as a validated prognostic determinant in carcinoma of unknown primary site. *Br J Cancer* 2014; **110**: 208–13.
14. Pinato DJ, Mauri FA, Ramakrishnan R, Wahab L, Lloyd T, Sharma R. Inflammation-based prognostic indices in malignant pleural mesothelioma. *J Thorac Oncol* 2012; **7**: 587–94.
15. Proctor MJ, Morrison DS, Talwar D, *et al.* An inflammation-based prognostic score (mGPS) predicts cancer survival independent of tumour site: a Glasgow Inflammation Outcome Study. *Br J Cancer* 2011; **104**: 726–34.
16. Pinato DJ, North BV, Sharma R. A novel, externally validated inflammation-based prognostic algorithm in hepatocellular carcinoma: the prognostic nutritional index (PNI). *Br J Cancer* 2012; **106**: 1439–45.
17. Kinoshita A, Onoda H, Imai N, *et al.* Comparison of the prognostic value of inflammation-based prognostic scores in patients with hepatocellular carcinoma. *Br J Cancer* 2012; **107**: 988–93.
18. Llovet JM, Bru C, Bruix J. Prognosis of hepatocellular carcinoma: the BCLC staging classification. *Semin Liver Dis* 1999; **19**: 329–38.
19. CLIP Investigators. A new prognostic system for hepatocellular carcinoma: a retrospective study of 435 patients: the Cancer of the Liver Italian Program (CLIP) investigators. *Hepatology* 1998; **28**: 751–5.
20. Lencioni R, Llovet JM. Modified RECIST (mRECIST) assessment for hepatocellular carcinoma. *Semin Liver Dis* 2010; **30**: 52–60.
21. Pinato DJ, Stebbing J, Ishizuka M, *et al.* A novel and validated prognostic index in hepatocellular carcinoma: the inflammation based index (IBI). *J Hepatol* 2012; **57**: 1013–20.
22. Ko YJ, Kwon YM, Kim KH, *et al.* High-sensitivity C-reactive protein levels and cancer mortality. *Cancer Epidemiol Biomarkers Prev* 2012; **21**: 2076–86.
23. Kim MJ, Jang JW, Oh BS, *et al.* Change in inflammatory cytokine profiles after transarterial chemotherapy in patients with hepatocellular carcinoma. *Cytokine* 2013; **64**: 516–22.
24. Kadalayil L, Benini R, Pallan L, *et al.* A simple prognostic scoring system for patients receiving transarterial embolisation for hepatocellular cancer. *Ann Oncol* 2013; **24**: 2565–70.
25. Sieghart W, Pinter M, Hucke F, *et al.* Single determination of C-reactive protein at the time of diagnosis predicts long-term outcome of patients with hepatocellular carcinoma. *Hepatology* 2013; **57**: 2224–34.
26. Lencioni R. Chemoembolization in Patients with Hepatocellular Carcinoma. *Liver Cancer* 2012; **1**: 41–50.
27. Lencioni R, Chen XP, Dagher L, Venook AP. Treatment of intermediate/

advanced hepatocellular carcinoma in the clinic: how can outcomes be improved? *Oncologist* 2010; **15**(Suppl 4): 42–52.
28. Dufour JF, Bargellini I, De Maria N, De Simone P, Goulis I, Marinho RT. Intermediate hepatocellular carcinoma: current treatments and future perspectives. *Ann Oncol* 2013; **24**(Suppl. 2): ii24–9.
29. Ishizuka M, Kubota K, Kita J, Shimoda M, Kato M, Sawada T. Impact of an inflammation-based prognostic system on patients undergoing surgery for hepatocellular carcinoma: a retrospective study of 398 Japanese patients. *Am J Surg* 2012; **203**: 101–6.
30. Morimoto M, Numata K, Moriya S, *et al.* Inflammation-based prognostic score for hepatocellular carcinoma patients on sorafenib treatment. *Anticancer Res* 2012; **32**: 619–23.
31. Argiles JM, Busquets S, Toledo M, Lopez-Soriano FJ. The role of cytokines in cancer cachexia. *Curr Opin Support Palliat Care* 2009; **3**: 263–8.
32. Hoshida Y, Moeini A, Alsinet C, Kojima K, Villanueva A. Gene signatures in the management of hepatocellular carcinoma. *Semin Oncol* 2012; **39**: 473–85.
33. Budhu A, Forgues M, Ye QH, *et al.* Prediction of venous metastases, recurrence, and prognosis in hepatocellular carcinoma based on a unique immune response signature of the liver microenvironment. *Cancer Cell* 2006; **10**: 99–111.
34. Korangy F, Ormandy LA, Bleck JS, *et al.* Spontaneous tumor-specific humoral and cellular immune responses to NY-ESO-1 in hepatocellular carcinoma. *Clin Cancer Res* 2004; **10**: 4332–41.
35. Fu J, Xu D, Liu Z, *et al.* Increased regulatory T cells correlate with CD8 T-cell impairment and poor survival in hepatocellular carcinoma patients. *Gastroenterology* 2007; **132**: 2328–39.
36. Gao Q, Qiu SJ, Fan J, *et al.* Intratumoral balance of regulatory and cytotoxic T cells is associated with prognosis of hepatocellular carcinoma after resection. *J Clin Oncol* 2007; **25**: 2586–93.
37. Pinato DJ, Stavraka C, Flynn MJ, *et al.* An inflammation based score can optimize the selection of patients with advanced cancer considered for early phase clinical trials. *PLoS ONE* 2014; **9**: e83279.
38. Chua W, Clarke SJ, Charles KA. Systemic inflammation and prediction of chemotherapy outcomes in patients receiving docetaxel for advanced cancer. *Support Care Cancer* 2012; **20**: 1869–74.
39. Kao SC, Pavlakis N, Harvie R, *et al.* High blood neutrophil-to-lymphocyte ratio is an indicator of poor prognosis in malignant mesothelioma patients undergoing systemic therapy. *Clin Cancer Res* 2010; **16**: 5805–13.
40. Pinato DJ, Sharma R. An inflammation-based prognostic index predicts survival advantage after transarterial chemoembolization in hepatocellular carcinoma. *Transl Res* 2012; **160**: 146–52.
41. Ayaru L, Pereira SP, Alisa A, *et al.* Unmasking of alpha-fetoprotein-specific CD4(+) T cell responses in hepatocellular carcinoma patients undergoing embolization. *J Immunol* 2007; **178**: 1914–22.
42. Canna K, McArdle PA, McMillan DC, *et al.* The relationship between tumour T-lymphocyte infiltration, the systemic inflammatory response and survival in patients undergoing curative resection for colorectal cancer. *Br J Cancer* 2005; **92**: 651–4.
43. Zhao Y, Cai G, Zhou L, *et al.* Transarterial chemoembolization in hepatocellular carcinoma with vascular invasion or extrahepatic metastasis: a systematic review. *Asia Pac J Clin Oncol* 2013; **9**: 357–64.
44. Hsu C, Shen YC, Cheng CC, Hu FC, Cheng AL. Geographic difference in survival outcome for advanced hepatocellular carcinoma: implications on future clinical trial design. *Contemp Clin Trials* 2010; **31**: 55–61.
45. Sieghart W, Hucke F, Pinter M, *et al.* The ART of decision making: retreatment with transarterial chemoembolization in patients with hepatocellular carcinoma. *Hepatology* 2013; **57**: 2261–73.
46. Hucke F, Sieghart W, Pinter M, *et al.* The ART-strategy: sequential assessment of the ART score predicts outcome of patients with hepatocellular carcinoma re-treated with TACE. *J Hepatol* 2014; **60**: 118–26.

Published OnlineFirst September 3, 2014; DOI: 10.1158/0008-5472.CAN-14-0471

Molecular and Cellular Pathobiology

Cancer Research

Stress Response Protein Cirp Links Inflammation and Tumorigenesis in Colitis-Associated Cancer

Toshiharu Sakurai[1], Hiroshi Kashida[1], Tomohiro Watanabe[2], Satoru Hagiwara[1], Tsunekazu Mizushima[3], Hideki Iijima[4], Naoshi Nishida[1], Hiroaki Higashitsuji[5], Jun Fujita[5], and Masatoshi Kudo[1]

Abstract

Colitis-associated cancer (CAC) is caused by chronic intestinal inflammation and is reported to be associated with refractory inflammatory bowel disease (IBD). Defective apoptosis of inflammatory cell populations seems to be a relevant pathogenetic mechanism in refractory IBD. We assessed the involvement of stress response protein cold-inducible RNA-binding protein (Cirp) in the development of intestinal inflammation and CAC. In the colonic mucosa of patients with ulcerative colitis, expression of Cirp correlated significantly with the expression of TNFα, IL23/IL17, antiapoptotic proteins Bcl-2 and Bcl-xL, and stem cell markers such as Sox2, Bmi1, and Lgr5. The expression of Cirp and Sox2 was enhanced in the colonic mucosae of refractory ulcerative colitis, suggesting that Cirp expression might be related to increased cancer risk. In human CAC specimens, inflammatory cells expressed Cirp protein. *Cirp*$^{-/-}$ mice given dextran sodium sulfate exhibited decreased susceptibility to colonic inflammation through decreased expression of TNFα, IL23, Bcl-2, and Bcl-xL in colonic lamina propria cells compared with similarly treated wild-type (WT) mice. In the murine CAC model, Cirp deficiency decreased the expression of TNFα, IL23/IL17, Bcl-2, Bcl-xL, and Sox2 and the number of Dclk1^{+} cells, leading to attenuated tumorigenic potential. Transplantation of *Cirp*$^{-/-}$ bone marrow into WT mice reduced tumorigenesis, indicating the importance of Cirp in hematopoietic cells. Cirp promotes the development of intestinal inflammation and colorectal tumors through regulating apoptosis and production of TNFα and IL23 in inflammatory cells. *Cancer Res; 74(21); 6119–28. ©2014 AACR.*

Introduction

The inflammatory bowel diseases (IBD)—ulcerative colitis and Crohn disease—are thought to result from aberrant activation of the intestinal mucosal immune system (1). Although the pathogenesis of IBD remains unclear, a number of studies have suggested the involvement of abnormal apoptosis in intestinal epithelial cells, resulting from increased production of cytokines, such as TNF, ILs, and IFNs (2). TNFα is a key mediator of inflammation in IBD and has been the primary target of biologic therapies (3). This cytokine induces inflammation by promoting the production of IL1β and IL6, expression of adhesion molecules, proliferation of fibroblasts, activation of procoagulant factors, and cytotoxicity of the acute phase response (4). The IL23/T_H17 (T-helper IL17–producing cell) pathway has been identified to play a critical role in IBD. IL23 has been shown to promote the expansion of a distinct lineage of T_H17 cells that are characterized by production of a number of specific cytokines not produced by T_H1 or T_H2 cells, including IL17A, IL17F, IL21, and IL22 (5). IL23/IL17 signaling enhances the immunosuppressive activity of regulatory T cells and reduces CD8^{+} cells in tumor, leading to enhanced tumor initiation and promotion (6, 7). Recently, a study has suggested that colorectal cancer tissue–derived Foxp3^{+} IL17^{+} cells have the capacity to induce cancer-initiating cells *in vitro* (8). The most conspicuous link between inflammation and colon cancer is seen in patients with IBD (9), and development of colorectal cancer is one of the most serious complications of IBD, which is also referred to as colitis-associated cancer (CAC; ref. 10). Thus, it is of great importance to improve our understanding of the molecular link between chronic inflammation and CAC to identify a target molecule with therapeutic potential for the treatment of IBD and prevention of CAC.

It is widely accepted that most tumors harbor cancer stem cells, which are crucial for a tumor's evolutionary capability. Cancer stem cells resemble normal stem cells in their capacity to self-renew and continuously replenish tumor progeny (11, 12). The G-protein–coupled receptor Lgr5 and the polycomb group protein Bmi1 are 2 recently described molecular markers of the self-renewing multipotent adult stem cell populations residing in intestinal crypts that mediate regeneration of the intestinal epithelium (13, 14). Pluripotency-

[1]Department of Gastroenterology and Hepatology, Kinki University Faculty of Medicine, Osaka-Sayama, Japan. [2]Center for Innovation in Immunoregulative Technology and Therapeutics, Graduate School of Medicine, Kyoto University, Kyoto, Japan. [3]Department of Surgery, Osaka University, Osaka, Japan. [4]Department of Gastroenterology and Hepatology, Osaka University, Osaka, Japan. [5]Department of Clinical Molecular Biology, Graduate School of Medicine, Kyoto University, Kyoto, Japan.

Note: Supplementary data for this article are available at Cancer Research Online (http://cancerres.aacrjournals.org/).

Corresponding Author: Toshiharu Sakurai, Department of Gastroenterology and Hepatology, Kinki University Faculty of Medicine, 377-2 Ohno-Higashi, Osaka-Sayama, Osaka 589-8511, Japan. Phone: 81-72-3660221, ext. 3525; Fax: 81-72-3672880; E-mail: sakurai@med.kindai.ac.jp

doi: 10.1158/0008-5472.CAN-14-0471

Published OnlineFirst September 3, 2014; DOI: 10.1158/0008-5472.CAN-14-0471

associated transcription factors like Sox2 are known to regulate cellular identity in embryonic stem cells. Sox2 expression specifically increased the numbers of stem cells and repressed Cdx2, a master regulator of endodermal identity. *In vivo* studies demonstrated that Sox21, another member of the SoxB gene family, was a specific, immediate, and cell-autonomous target of Sox2 in intestinal stem cells (15). Sox2 participates in the reprogramming of adult somatic cells to a pluripotent stem cell state and is implicated in tumorigenesis in various organs (16).

Cold-inducible RNA-binding protein (Cirp, also called Cirbp or hnRNP A18) was originally identified in the testis as the first mammalian cold shock protein (17) and is suggested to mediate the preservation of neural stem cells (18). Cirp is induced by cellular stresses such as UV irradiation and hypoxia (19–21). In response to the stress, Cirp, which migrates from the nucleus to the cytoplasm, affects posttranscription expression of its target mRNAs (22–24) and functions as a damage-associated molecular pattern molecule that promotes inflammatory responses when present extracellularly (25). Cirp also affects cell growth and cell death induced by TNFα or genotoxic stress (26, 27). However, the involvement of Cirp in colitis and CAC is not well understood.

Here, we examined whether Cirp plays a role in inflammatory immune responses and tumorigenesis in the gut by using a murine CAC model of Cirp-deficient ($Cirp^{-/-}$) mice and found that Cirp promoted colitis and colorectal tumorigenesis by inhibiting apoptosis and increasing TNFα and IL23 production in inflammatory cells. In patients with ulcerative colitis, refractory inflammation is associated with increased Cirp expression in the colonic mucosa, which would increase the risk for CAC. This study represents the first report of the functional link between Cirp and intestinal tumorigenesis.

Materials and Methods

Human tissue samples

In total, 236 colonic mucosa specimens were obtained by endoscopy or surgery from patients with ulcerative colitis, including 67 cases of refractory ulcerative colitis, 98 cases of nonrefractory active ulcerative colitis, and 20 cases in remission, as well as 21 colonic mucosa of patients with Crohn disease and 30 normal colonic mucosa specimens from controls without IBD. Refractory ulcerative colitis was defined according to endoscopic criteria and categorized as being active for more than 6 months. Active inflammation was defined as Mayo endoscopic score $\geq$2. CAC specimens were obtained from 10 patients who had undergone colorectal resection. The clinical study protocol conformed to the ethical guidelines of the 1975 Declaration of Helsinki and was approved by the relevant institutional review boards.

Mice and treatment

$Cirp^{-/-}$ mice showing neither gross abnormality nor colonic inflammation were used as a murine CAC model. The generation of $Cirp^{-/-}$ mice has been described previously (28). Sex- and age-matched C57BL/6 wild-type (WT) and $Cirp^{-/-}$ mice (8–12 weeks old) received 2.5% (w/v) dextran sodium sulfate (DSS; molecular weight, 36,000–50,000 kDa; MP Biomedicals) in drinking water. Mice were intrapertioneally injected with 20 mg/kg anti- TNFα antibody (#16-7423, eBioscience) or an IgG isotype control before DSS treatment.

Isolation of lamina propria cells was performed as described previously (29). The isolated cells were sorted using immunomagnetic beads coated with monoclonal antibodies against CD11b (MACS Beads, Miltenyi Biotec) with the help of a separation column and a magnetic separator from the same company in accordance with the manufacturer's recommendations for isolating murine macrophages.

As the protocol for the murine CAC model, mice were intraperitoneally injected with 12.5 mg/kg azoxymethane (AOM; Sigma-Aldrich). After 5 days, 2.0% DSS was included in the drinking water for 5 days, followed by 16 days of regular water. This cycle was repeated 3 times. Then, 1.5% DSS was included in the drinking water for 4 days, followed by 7 days of regular water. Upon sacrifice, the colon was excised from the ileocecal junction to the anus, cut open longitudinally, and prepared for histologic evaluation. Colons were assessed macroscopically for polyps under a dissecting microscope.

Bone marrow transplantation (BMT) experiments were performed as previously described, with slight modifications (30). Bone marrow from the tibia and femur was washed twice in Hank balanced salt solution, and 10^7 bone marrow cells were injected into the tail vein of lethally irradiated (11 Gy) recipient mice. Eight weeks posttransplantation, the mice were subjected to the murine CAC protocol. Bone marrow cells were grown in culture dishes in the presence of macrophage colony-stimulating factor (M-CSF; 10 ng/mL) and then differentiated to bone marrow–derived macrophages in 10 days. All animal procedures were performed according to approved protocols and in accordance with the recommendations for the proper care and use of laboratory animals. The animal study protocol was approved by the Medical Ethics Committee of Kinki University School of Medicine (Osaka-Sayama, Japan).

Colonic injury scoring

Excised colons were rolled up and fixed in 10% formaldehyde, embedded in paraffin, and stained with hematoxylin and eosin (H&E). The degree of colonic injury was assessed by histologic scoring as described previously (31), with minor modifications. The protocol is described in detail in Supplementary Materials and Methods.

Biochemical and immunochemical analyses

Real-time qPCR, immunoblotting, and immunohistochemistry were previously described (32). Primer sequences are given in Supplementary Materials and Methods. The following antibodies were used: anti-actin and anti-DCAMLK1 (Dclk1) from Sigma-Aldrich; anti-Bcl-2, anti-phospho-IκBα, anti-IκBα, anti-phospho-ERK, anti-ERK, anti-Sox2, anti-E-cadherin, anti-PCNA from Cell Signaling; and anti-F4/80 from eBioscience. Generation of anti-Cirp polyclonal antibody was previously described (28). Immunohistochemistry was performed using ImmPRESS reagents (Vector Laboratory) according to the manufacturer's recommendations. Immunofluorescent terminal deoxynucleotidyl transferase–mediated dUTP nick end labeling (TUNEL) staining was performed to measure

Published OnlineFirst September 3, 2014; DOI: 10.1158/0008-5472.CAN-14-0471

apoptosis in paraffin-embedded sections using the In Situ Apoptosis Detection Kit as described by the manufacturer (Takara). Nuclei were stained with 4,6′-diamidino-2-phenylindole to count the total cells per crypt. A minimum of 10 crypts were counted per section.

Statistical analysis

Differences were analyzed using the Student *t* test. To compare variables of more than 2 conditions, ANOVO with *post hoc* Tukey–Kramer honestly significant difference (HSD) multiple comparison was applied. The relationship between the expression of several genes was analyzed by Spearman rank correlation test. $P < 0.05$ was considered significant.

Results

Correlation of Cirp expression with TNFα, IL23/IL17, Bcl-2, and stem cell marker expression in patients with IBD

Cirp expression correlated weakly but significantly with TNFα with a linear coefficient of 0.26 in the colonic mucosa of patients with ulcerative colitis (Supplementary Fig. S1A). In patients with Crohn disease, Cirp expression did not significantly correlate with TNFα (data not shown) probably because the majority of patients with Crohn disease enrolled in this study had undergone anti-TNFα therapy. IL23p19 is the specific subunit of IL23, a positive regulator of T_H17 and other IL17-producing cells (5). A significant correlation was found between *Cirp* and *IL17A* or *IL23p19* mRNA expression in patients with ulcerative colitis (Supplementary Fig. S1B and S1C) and in patients with Crohn disease (Supplementary Fig. S2A).

Defective apoptosis of inflammatory cell populations regulated by Bcl-2 seems to be a relevant pathogenetic mechanism in IBD (33, 34). There was a significant correlation between Cirp and Bcl-2 expression with a linear coefficient of 0.76 in patients with ulcerative colitis and with a linear coefficient of 0.60 in patients with Crohn disease (Fig. 1A and Supplementary Fig. S2B). Expression of Bcl-xL, another antiapoptotic protein, was significantly correlated with that of Cirp with a linear coefficient of 0.60 in patients with ulcerative colitis (Supplementary Fig. S1D) and with a linear coefficient of 0.85 in patients with Crohn disease (Supplementary Fig. S2C).

Stem cells, characterized by their ability to self-renew indefinitely and produce progeny capable of repopulating tissue-specific lineages, are critical for maintaining normal tissue homeostasis (35). Cirp is suggested to mediate the preservation of neural stem cells (18). Cirp expression correlated with Sox2, Bmi1, Lgr5, and Dclk1 levels with linear coefficients of 0.62, 0.45, 0.42, and 0.25, respectively, in patients with ulcerative colitis (Fig. 1B–D and Supplementary Fig. S1E) and correlated with Sox2 with a linear coefficient of 0.63 in patients with Crohn disease (Supplementary Fig. S2D). Cirp might be involved in regulation of intestinal inflammation and homeostasis maintenance in patients with IBD.

Increased Cirp expression in the colonic mucosa of patients with refractory ulcerative colitis

We next explored whether an association exists between Cirp expression and the clinical status of patients with ulcerative colitis. Refractory and nonrefractory active ulcerative colitis could not be distinguished by endoscopic findings (Fig. 2A). Cirp expression levels were specifically increased in patients with refractory ulcerative colitis associated with long-term inflammation, whereas similar expression levels of Cirp were found between normal colonic mucosa and the mucosa of patients with nonrefractory active ulcerative colitis (Fig. 2B). Similarly, increased Sox2 expression levels were found in the colonic mucosa of patients with refractory IBD (Fig. 2C). Immunohistochemistry showed that Sox2 was expressed in the mesenchyme and Dclk1 was expressed in the crypt of patients with refractory ulcerative colitis (Supplementary Fig. S3A and S3D). In contrast, increased TNFα expression was found in the colonic mucosa of both refractory and nonrefractory active ulcerative colitis (Fig. 2D). Immunohistochemistry was performed to identify the cells expressing Cirp in the human intestine, and inflammatory cells were found to express more Cirp protein than epithelial cells, whose expression pattern was similar in controls and patients with ulcerative colitis. In chronically inflamed mucosa, Cirp expression was enhanced in inflammatory cells (Fig. 2E and Supplementary Fig. S3B). Inflammatory cells preferentially but not exclusively expressed Cirp protein also in human CAC cases (Supplementary Fig. S3C).

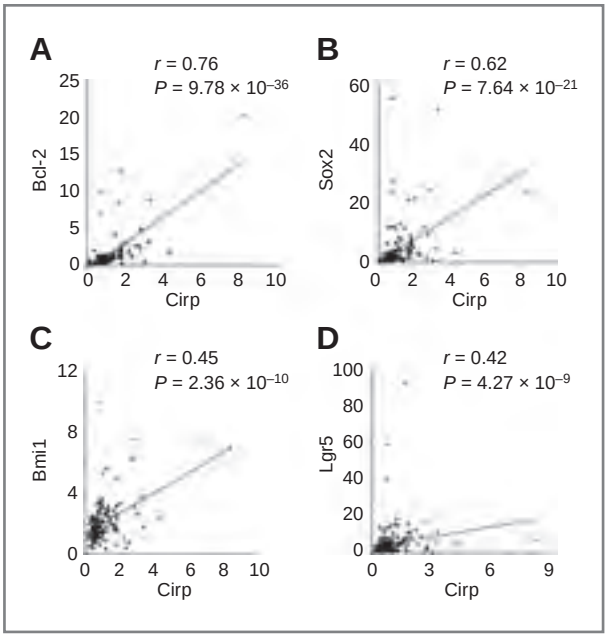

Figure 1. Association between Cirp and the expression of Bcl-2 and various stem cell markers in the colonic mucosa of patients with ulcerative colitis. Scatter plot of relative mRNA levels of Cirp and the respective genes (A, Bcl-2; B, Sox2; C, Bmi1; D, Lgr5) in human colonic mucosa.

Cirp$^{-/-}$ mice challenged with DSS have decreased susceptibility to inflammation

DSS-induced colitis is a murine model resembling human ulcerative colitis. Experimental colitis was induced by treating mice with 2.5% DSS. Histologic analysis revealed substantially less epithelial damage and disruption of crypt architecture in

Published OnlineFirst September 3, 2014; DOI: 10.1158/0008-5472.CAN-14-0471

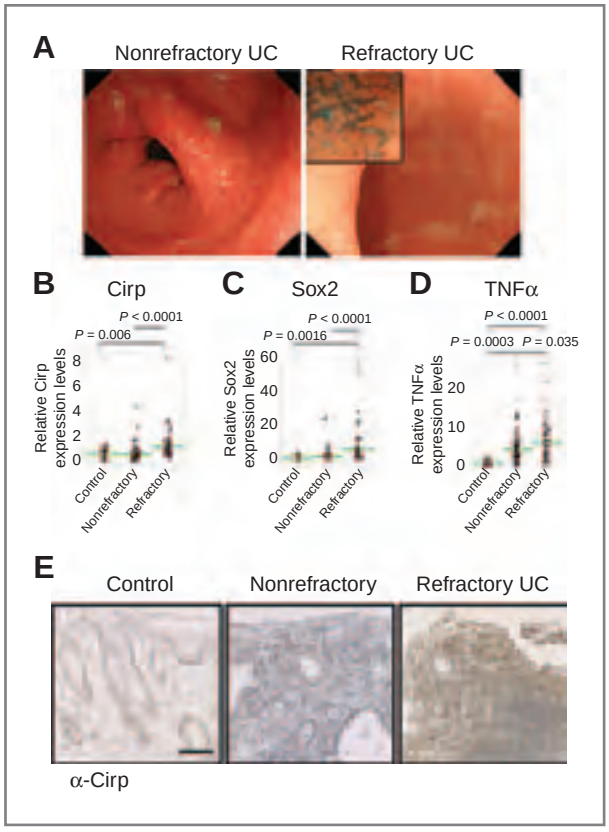

Figure 2. Cirp expression is increased in the colonic mucosa of patients with refractory ulcerative colitis (UC). A, endoscopic images of refractory and nonrefractory active ulcerative colitis specimens with a magnified inset. B–D, expression of Cirp (B), Sox2 (C), and TNFα (D) mRNA in normal colonic mucosa (control, $n = 30$), colonic mucosa of patients with nonrefractory active ulcerative colitis (nonrefractory, $n = 98$), and those with refractory ulcerative colitis (refractory, $n = 67$), as determined by quantitative real-time qPCR. *P* values were calculated by *post hoc* Tukey–Kramer HSD multiple comparison. The *F* and *P* values for the ANOVO test are as follows: F (2, 192) = 11.98; $P < 0.0001$ (B), F (2, 192) = 10.29; $P < 0.0001$ (C), and F (2, 192) = 13.70; $P < 0.0001$ (D). E, representative images of immunohistochemical findings in human colonic mucosa of patients without ulcerative colitis and those with nonrefractory and refractory ulcerative colitis. Scale bar, 50 μm.

Cirp$^{-/-}$ mice than in WT mice (Fig. 3A), and inflammatory cell infiltration into the colon was less in *Cirp*$^{-/-}$ mice (Fig. 3B). Immunohistochemically assessed macrophage infiltration was smaller in *Cirp*$^{-/-}$ than in WT mice after DSS administration (Fig. 3C), and the epithelial injury score was significantly smaller in the *Cirp*$^{-/-}$ mice than in the controls (Fig. 3D). Next, we compared apoptosis induction in DSS-treated WT and *Cirp*$^{-/-}$ mice. Apoptosis detected by TUNEL staining was observed in DSS-treated mice, primarily in the colonic crypts (Fig. 3E), but was blocked by 50% in the *Cirp*$^{-/-}$ mice (Fig. 3F). Examination of the colonic lysates from DSS-treated WT and *Cirp*$^{-/-}$ mice showed that the Cirp presence increased PCNA expression in the colon (Supplementary Fig. S4A).

The associated immune response was investigated by analyzing colonic cytokine levels. Colonic tissue from *Cirp*$^{-/-}$ mice showed a smaller immune response with lower levels of proinflammatory cytokine TNFα and IL23 than that of WT mice (Fig. 4A–C), which is consistent with the data in humans (Fig. 1 and Supplementary Fig. S1). TNFα expression was upregulated in nonrefractory active ulcerative colitis whereas Cirp expression was not in these patients (Fig. 2B and D). This is probably because TNFα is induced in both a Cirp-dependent and -independent manners in the colon. There was no significant difference in IL1β, IL10, and IL21 (Fig. 4B and Supplementary Fig. S4B). To explore the mechanisms of the effects of Cirp on TNFα production, we sought to confirm these findings *in vitro*. In lamina propria cells isolated from DSS-treated colons of Cirp-deficient mice, expression of TNFα and IL23 was decreased compared with those of WT mice (Fig. 4D). TNFα is produced chiefly by activated macrophages, although it can be produced by many other cell types as lymphocytes and natural killer cells (36), so we next isolated macrophages from DSS-treated colons. TNFα mRNA expression was significantly reduced in Cirp-deficient macrophages (Fig. 4E). Macrophages

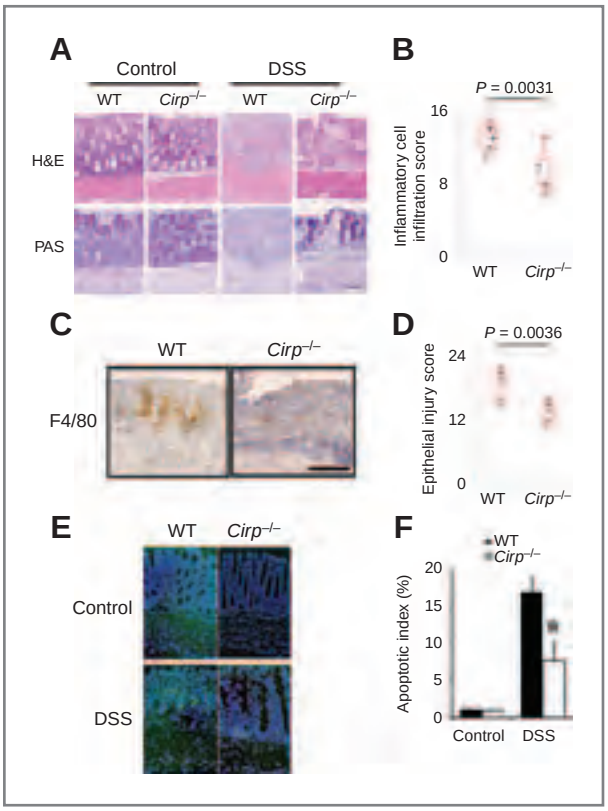

Figure 3. Susceptibility to inflammation is decreased in *Cirp*$^{-/-}$ mice challenged with DSS. A, representative photographs of H&E-stained and periodic acid—Schiff (PAS)-stained colons of WT and *Cirp*$^{-/-}$ mice 7 days after the initiation of DSS administration (original magnification, ×200). Scale bar, 50 μm. B, inflammatory cell infiltration into colonic tissues of WT and *Cirp*$^{-/-}$ mice 7 days after the initiation of DSS administration. Scoring was performed as described in Materials and Methods. $n = 6$ per group. C, representative images of immunohistochemical detection of F4/80, a marker for macrophages, in colonic tissue. Scale bar, 100 μm. D, histologic scoring of epithelial injury in colons. $n = 6$ per group. E, TUNEL staining of colonic tissues from DSS-treated mice (original magnification, ×200). F, the apoptotic index was measured by counting TUNEL signals in 100 randomly selected crypts. Results are expressed as means ± SEM ($n = 4$ per group). *, $P < 0.05$ compared with WT mice.

Published OnlineFirst September 3, 2014; DOI: 10.1158/0008-5472.CAN-14-0471

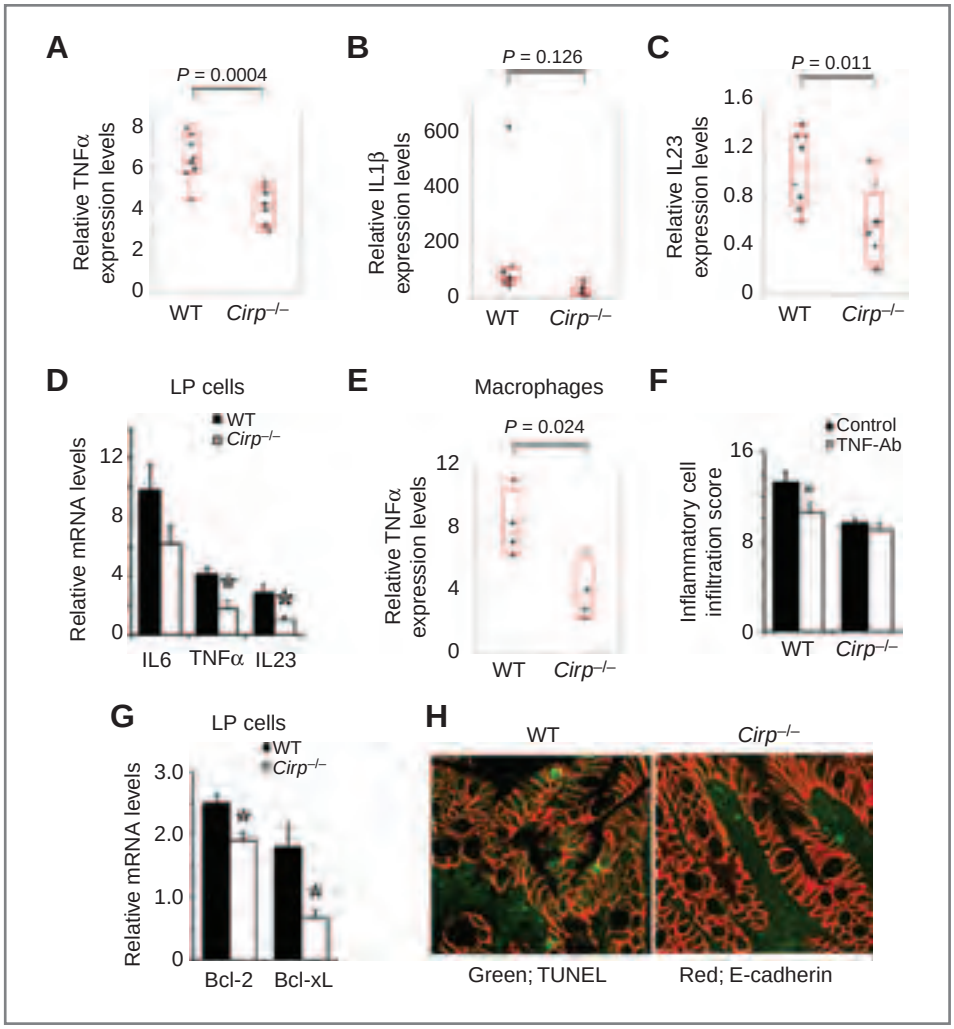

Figure 4. Cirp contributes to TNFα and IL23 production and Bcl-2 and Bcl-xL expression in inflammatory cells. A–C, relative levels of TNFα (A), IL1β (B), and IL23 (C) in colonic tissues from mice treated with DSS, as determined by real-time qPCR ($n = 8$ per group). Expression level in colonic tissues from nontreated WT mice was set as 1. D and E, effect of Cirp on gene expression in colonic lamina propria (LP) cells (D) and macrophages (E). Lamina propria cells and macrophages were isolated, and cytokine mRNA expression was analyzed by real-time qPCR. The mRNA expression levels in lamina propria cells or macrophages from nontreated WT mice were set as 1, respectively. Results are expressed as means ± SEM ($n = 4$ per group). *, $P < 0.05$ compared with WT mice. F, inflammatory cell infiltration into colonic tissues of WT and *Cirp*$^{-/-}$ mice 7 days after the initiation of DSS administration with or without anti-TNFα antibody treatment. Scoring was performed as described in Materials and Methods. $n = 3$ per group. *, $P < 0.05$ compared with control. G, effect of Cirp on gene expression in colonic lamina propria cells. Lamina propria cells were isolated, and cytokine mRNA expression was analyzed by real-time qPCR. The mRNA expression levels in lamina propria cells from nontreated WT mice were set as 1. *, $P < 0.05$ compared with WT LP cells. H, representative images of immunohistochemical detection of E-cadherin, a marker for epithelial cells, and TUNEL staining of colonic tissues from DSS-treated mice.

derived from WT bone marrow exhibited marked upregulation of TNFα mRNA relative to those derived from *Cirp*$^{-/-}$ bone marrow (Supplementary Fig. S4C). Cirp has been reported to activate NF-κB (25, 27). Consistently, the presence of Cirp increased IκBα phosphorylation in bone marrow–derived macrophages (Supplementary Fig. S4D). Treatment with anti-TNFα antibody reduced inflammatory cell infiltration in WT mice but not in *Cirp*$^{-/-}$ mice (Fig. 4F). These data indicate that Cirp in inflammatory cells augments the inflammatory response by producing cytokines such as TNFα and IL23. In addition, *Bcl-2* and *Bcl-xL* mRNA expression was significantly reduced in Cirp-deficient inflammatory cells (Fig. 4G), and more apoptosis was found in *Cirp*$^{-/-}$ immune cells than WT immune cells (Fig. 4H), which might at least partially contribute to the attenuated inflammatory responses by Cirp deficiency.

Cirp deficiency attenuated tumorigenesis in the murine CAC model

Chronic inflammation increases intestinal cancer risk in IBD (10). To investigate the precise pathogenic mechanisms underlying IBD-associated colorectal carcinogenesis, we used the AOM plus DSS mouse model to study the role of Cirp in CAC. In the AOM/DSS protocol, a significant decrease was noted in the number and maximum size of tumors in the *Cirp*$^{-/-}$ mice compared with WT mice (Fig. 5A and B). Histologic

Published OnlineFirst September 3, 2014; DOI: 10.1158/0008-5472.CAN-14-0471

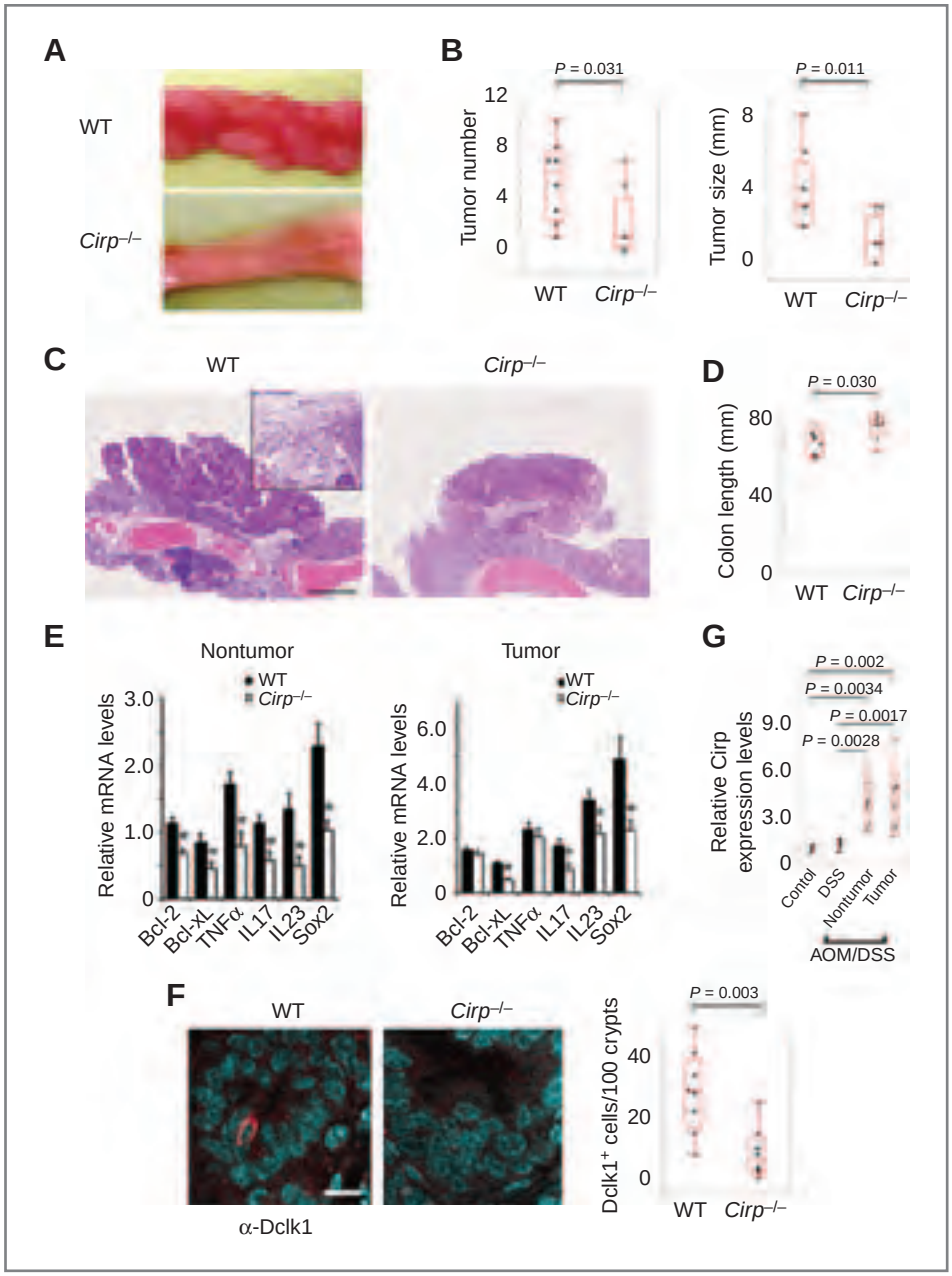

Figure 5. Cirp deficiency affects colonic tumorigenesis in a murine model of CAC. A, typical examples of macroscopic tumorigenesis in the CAC model. Colons were cut longitudinally. B, tumor number and maximum size (WT mice, $n = 8$; *Cirp*$^{-/-}$ mice, $n = 8$). C, typical examples of microscopic tumorigenesis in the CAC model with magnified insets. Scale bar, 500 μm. D, colon length after treatment with AOM and DSS. E, RNA was extracted from nontumorous colon and tumor tissues. Relative amounts of mRNA, as determined by real-time qPCR normalized to the amount of actin mRNA. The amount of each mRNA in the untreated colon was given an arbitrary value of 1.0. *, $P < 0.05$ compared with WT mice. F, immunohistochemical findings of colon sections of AOM/DSS-treated WT and *Cirp*$^{-/-}$ mice. The tumor bases stained with anti-Dclk1 antibody were identified by confocal microscopy. Scale bar, 15 μm. G, RNA was extracted from the colonic tissues of WT mice 7 days after the initiation of DSS administration (DSS, $n = 8$) and nontumorous colon and tumor tissues of WT mice after administration of AOM and DSS (DSS + AOM, $n = 6$). Relative amounts of mRNA as determined by real-time qPCR and normalized to the amount of actin mRNA. The mean value of mRNA in untreated colon (control, $n = 5$) was given an arbitrary value of 1.0. *P* values were calculated by *post hoc* Tukey–Kramer HSD multiple comparison.

examination of H&E-stained sections from the rolled-up colons revealed larger adenomas with a complex tumor growth pattern in WT tumors compared with *Cirp*$^{-/-}$ tumors (Fig. 5C). Extensive infiltration of inflammatory cells into the lamina propria and submucosal layer surrounding the tumors suggest the involvement of inflammatory responses in the tumorigenesis seen in the AOM/DSS-treated mice (Fig. 5C). Colon length was measured as one parameter to assess the severity of inflammation and was found to be significantly longer in *Cirp*$^{-/-}$ mice than in WT mice (Fig. 5D). The expression of TNFα was decreased in nontumorous tissue, but not in tumors, of *Cirp*$^{-/-}$ mice challenged with AOM and DSS (Fig. 5E). Tumor and nontumor cells would use different mechanisms to regulate gene expression. In tumor cells, expression of TNFα might be upregulated in a Cirp-independent manner. IL23 and IL17 inhibit antitumor immunity and promote tumorigenesis (6–8). Expression of IL23 and IL17 was decreased in *Cirp*$^{-/-}$ tumors and nontumor colons compared with WT counterparts (Fig. 5E). *Bcl-2* and *Bcl-xL* mRNA expression that is upregulated by Cirp in inflammatory cells (Fig. 4G) was significantly reduced in Cirp-deficient colons (Fig. 5E). Cirp deficiency decreased proliferating cell nuclear antigen (PCNA) expression in DSS-treated colons, whereas in established tumors, neither apoptosis nor PCNA expression was significantly affected by Cirp deletion (Supplementary Fig. S6). The expression of stemness factor Sox2 was decreased in Cirp-deficient colons

Published OnlineFirst September 3, 2014; DOI: 10.1158/0008-5472.CAN-14-0471

and tumors compared with WT tissues (Fig. 5E and Supplementary Fig. S5A). Dclk1 is a candidate tumor stem cell marker in the gut (37). Deletion of Cirp decreased the number of Dclk1$^+$ cells at the tumor base (Fig. 5F).

Cirp expression was increased in the colonic mucosa of tumor-harboring mice given DSS and AOM, whereas short-term inflammation induced by DSS administration for 7 days did not upregulate Cirp expression (Fig. 5G and Supplementary Fig. S5B). Coupled with the findings in humans (Fig. 2B and E), these results suggest that Cirp is induced by long-term intestinal inflammation.

Cirp promotes tumorigenesis through hematopoietic cell populations

To functionally characterize the contribution of different cell populations to colorectal tumorigenesis, we created Cirp chimeric mice using a combination of γ-irradiation and BMT. Nontransplanted controls survived less than 2 weeks after irradiation, indicating there was ablation of the endogenous marrow. Transplanted animals were allowed to recover for 2 months before placing them on the AOM/DSS protocol. WT mice rescued with *Cirp*$^{-/-}$ bone marrow had a significantly smaller tumor burden than those rescued with WT bone marrow (Fig. 6A and B). Both WT and *Cirp*$^{-/-}$ mice rescued with WT bone marrow had equivalent tumor sizes (Fig. 6B). Chimeras harboring *Cirp*$^{-/-}$ bone marrow diminished expression of TNFα (Fig. 6C), which indicates that Cirp in hematopoietic cells is involved in upregulation of TNFα. Cirp-chimeric mice with Cirp-deficient bone marrow showed a smaller number of Dclk1$^+$ and Sox2$^+$ cells in tumor than in the WT mice (Fig. 6D and E). Taken together, at least in this model, the absence of Cirp in hematopoietic cellular compartments protects against AOM/DSS-induced tumorigenesis.

Discussion

The association between IBD and colorectal cancer is well established; the cumulative risk of developing colorectal cancer after 20 years is 7% in ulcerative colitis and 8% in Crohn disease (10). Optimal IBD management would reduce the risk of CAC (35). While it is clear that chronic mucosal inflammation plays a causative role in the transition to adenocarcinoma, the molecular link between inflammation and cancer remains to be elucidated. AOM is a procarcinogen that is metabolically activated to a potent alkylating agent that forms O^6-methylguanine (38). Its oncogenic potential is markedly augmented in the setting of chronic inflammation, such as that induced by repeated cycles of DSS treatment (39). TNFα, a key mediator of inflammation in IBD (3), contributes to tumorigenesis by creating a tumor-supportive inflammatory microenvironment

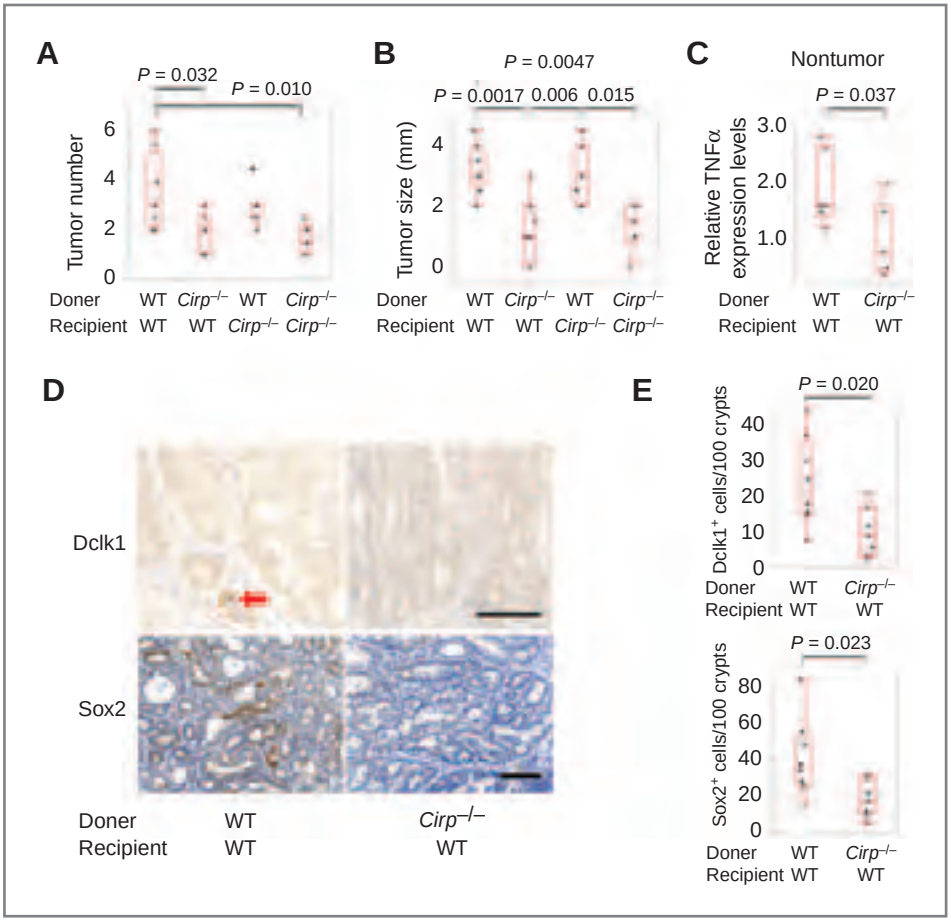

Figure 6. Cirp promotes tumorigenesis through hematopoietic cell populations. WT mice with WT or *Cirp*$^{-/-}$ bone marrow (BM) and *Cirp*$^{-/-}$ mice with WT or *Cirp*$^{-/-}$ bone marrow were generated by BMT. Number (A) and maximum size (B) of the tumors (WT-BM/WT mice, $n = 8$; *Cirp*$^{-/-}$-BM/WT mice, $n = 7$; WT-BM/*Cirp*$^{-/-}$ mice, $n = 7$; *Cirp*$^{-/-}$-BM/*Cirp*$^{-/-}$ mice, $n = 6$). *P* values were calculated by *post hoc* Tukey–Kramer HSD multiple comparison. C, RNA was extracted from nontumorous colon. Relative amounts of mRNA as determined by real-time qPCR normalized to the amount of actin mRNA. The amount of TNFα mRNA in the untreated colon was given an arbitrary value of 1.0. $n = 6$ per group. D, representative images of immunohistochemical detection of Dclk1 at the tumor base and Sox2 in tumors. Scale bar, 100 μm. E, the number of Dclk1$^+$ cells at the tumor base and Sox2$^+$ in tumors.

Published OnlineFirst September 3, 2014; DOI: 10.1158/0008-5472.CAN-14-0471

and through its direct effect on malignant cells (40). Interactions between tumor and immune cells regulate tumorigenesis. IL23/IL17 signaling has been correlated with promotion of tumor growth, as well as IBD pathogenesis. In the tumor microenvironment, IL23/IL17 signaling suppresses antitumorigenic immune response during tumor initiation, growth, and metastases (6–8). In the present study, Cirp deficiency decreased the production of TNFα and IL23 in inflammatory cells and attenuated DSS-induced colitis. In the murine CAC model, we found that TNFα, IL23, and IL17 expression were increased in Cirp-deficient mice and that Cirp was required for inflammation-associated colonic carcinogenesis. Cirp expression was positively associated with the levels of TNFα and IL23 in the colonic mucosa of patients with IBD. Increased Cirp expression, seen in refractory IBD, would promote tumorigenesis by enhancing TNFα and IL23 production. Given the contribution of Cirp in hematopoietic cells to tumor formation (Fig. 6), Cirp likely promotes tumorigenesis through its action in inflammatory cells.

Adult somatic stem cells of the colon sustain self-renewal and are targets for cancer initiation (41), and perturbation in stem cell dynamics is generally considered the first step toward colon tumorigenesis. High levels of stemness factor Sox2 expression are associated with poor prognosis and recurrence in patients with colorectal cancer (42). In patients with IBD, mucosal Cirp expression correlated with the expression of Sox2. We also showed that Cirp is important for sustained expression of Sox2 in the colonic mucosa during colorectal carcinogenesis. Cirp deficiency decreased the number of cells positive for an intestinal cancer stem cell marker Dclk1 at the tumor base. These data suggest a possible function of Cirp in influencing stem cell behavior.

Cancer stem cells, the microenvironment, and the immune system interact with each other through cytokines. In the context of chronic inflammation, cytokines, secreted by immune cells, activate the necessary pathways required by cancer stem cells (43). The number of $Sox2^+$ and $Dclk1^+$ cells in tumor was decreased upon Cirp deletion in the hematopoietic compartment (Fig. 6), suggesting that the absence of Cirp in inflammatory cells decreased production/secretion of these cytokines. There were statistically significant relationships between TNFα and Dclk1 expression and between IL23/IL17 and Sox2 expression in colonic mucosa of patients with ulcerative colitis (data not shown). Thus, Cirp-driven immune responses such as activation of TNFα and IL23/IL17 signaling would affect proliferation of stem cells and increase the expression of stem cell markers. It should be noted, however, that the direct causal link between Cirp and the stem cell markers has not been established in this study. In this regard, the reduced expression of the stem cell markers, such as Dclk1 and Sox2, seen in the absence of Cirp might be due to the secondary effects associated with reduced inflammation.

Apoptotic cell death has been implicated as a major homeostatic and pathogenic mechanism of the intestinal epithelium (2). The lower susceptibility to apoptosis observed in the $Cirp^{-/-}$ intestinal epithelial mucosa in our *in vivo* experiment was unexpected because a previous report showed that Cirp attenuates TNFα-mediated apoptosis by activating ERK and NF-κB in murine embryonic fibroblasts (27). However, expression of Cirp did not affect the sensitivity of murine embryonic fibroblasts to busulfan, and the numbers of apoptotic testicular cells was not different between $Cirp^{-/-}$ and WT mice after busulfan treatment (28). Thus, the role of Cirp may vary depending on cell type and kind of stimuli. In fact, in the DSS-treated colon, Cirp deficiency did not attenuate ERK activity (Supplementary Fig. S4A). In $Cirp^{-/-}$ mice, more inflammatory cells died because of decreased Bcl-2 and Bcl-xL expression than in WT mice (Fig. 4G and H), which would attenuate inflammatory response in $Cirp^{-/-}$ mice. Cell death and inflammation are intimately linked through a self-amplifying loop, making it difficult to distinguish between causes and effects. The attenuated mucosal immune activity due to augmented apoptosis of inflammatory cells likely contributed to the decreased apoptosis of epithelial cells in Cirp-deficient colon.

Bcl-2–mediated apoptosis resistance in inflammatory cells has been shown to attenuate therapeutic efficacy and exacerbate inflammation in IBD (33, 34). In chronically inflamed mucosa seen in refractory ulcerative colitis, Cirp expression is induced in inflammatory cells, which likely inhibits the apoptosis of inflammatory cells, augments proinflammatory cytokine production and treatment resistance via the upregulation of Bcl-2 and Bcl-xL expression. Thus, persistent inflammation resulting from insufficient treatment might further drive resistance to therapy through increased expression of Cirp and subsequent attenuated apoptosis in inflammatory cells. Hypoxia that is enhanced in chronic inflammatory diseases, including IBD, upregulates Cirp expression by a mechanism that involves neither hypoxia-inducible factor (HIF)1 nor mitochondria (20). This may be one explanation for Cirp induction by chronic inflammation. However, the exact mechanisms by which long-term inflammation upregulates Cirp expression remain to be elucidated.

It has been reported that Cirp released into the circulation stimulates the release of TNFα from macrophages via TLR4 and NF-κB activation and triggers an inflammatory response to hemorrhagic shock and sepsis (25). Here, we have shown that in bone marrow–derived macrophages, the presence of Cirp increased IκBα phosphorylation. NF-κB activation would be one of the mechanisms by which Cirp produces proinflammatory cytokines such as TNFα, IL17, and IL23 and upregulates expression of antiapoptotic genes such as Bcl-2 and Bcl-xL (Figs. 4 and 5). A recent study reported the involvement of Cirp in regulating expression of IL1β, another NF-κB target gene, in cultured fibroblasts (44). In bone marrow–derived macrophages, *IL1β* mRNA level was decreased in the absence of Cirp (data not shown). Although in DSS-induced colitis, Cirp protein was not detected in the blood (data not shown), it is conceivable that Cirp released from injured epithelial cells could function as damage-associated molecular pattern molecules *in situ* to activate NF-κB in immune cells of the colon. Furthermore, Cirp can bind the 3′untranslated region of specific transcripts to stabilize them and thus facilitate their transport to ribosomes for translation (22–24). Cirp might regulate the expression of cytokines and antiapoptotic genes posttranscriptionally as well.

Published OnlineFirst September 3, 2014; DOI: 10.1158/0008-5472.CAN-14-0471

Given the long-term impact of the natural history and treatment of IBD, cancer risk is a major lifelong concern for patients and gastroenterologists. Early detection of CAC/dysplasia is typically achieved by colonoscopic surveillance with multiple biopsies and alternatively by chromoendoscopy with targeted biopsies of all suspect areas. It has been reported that in patients with extensive colitis, surveillance should start after colonoscopy screening (8–10 years after disease onset) and be performed every 2 years for 20 years, then once or twice a year for the next 10 years of disease duration (45). However, such surveillance programs have a number of limitations such as low yield, high cost, invasiveness, incomplete patient enrollment, sampling variations, and poor agreement in histopathologic interpretation (46). If we can reliably predict an individual's risk of CAC so that surveillance strategies can be appropriately personalized, surveillance programs would make much progress. A number of molecular markers for predicting CAC have been reported (47–49) but are not feasible yet for the practical management of patients with IBD. Here, we showed significantly increased Cirp expression in mucosal specimens from patients with refractory IBD that is reported to be associated with increased cancer risk (9). Furthermore, in the murine CAC model, longstanding colonic inflammation increased Cirp expression, which led to enhanced AOM/DSS-induced colorectal tumorigenesis. Cirp expression reflects the presence of refractory inflammation and is therefore a potential marker for predicting the risk of CAC development. Analyzing the Cirp level in colonoscopy specimens may increase the identification rate of IBD patients with a high risk for developing CAC. A future large-scale study of Cirp in IBD patients with different duration and anatomical extent of the disease will be crucial for determining whether Cirp status can be used to predict the risk of cancer and prognosis of patients with IBD.

Taken together, Cirp, whose expression is upregulated by chronic inflammation in humans and mice, enhances the inflammatory response and tumorigenesis by increasing Bcl-2 and Bcl-xL expression and TNFα and IL23/IL17 production in inflammatory cells. Suppression and measurement of Cirp expression is a promising approach for advanced treatment and personalized management of patients with IBD.

Disclosure of Potential Conflicts of Interest

No potential conflicts of interest were disclosed.

Authors' Contributions

Conception and design: T. Sakurai
Development of methodology: T. Sakurai, J. Fujita
Acquisition of data (provided animals, acquired and managed patients, provided facilities, etc.): T. Sakurai, H. Kashida, T. Mizushima, H. Iijima, N. Nishida
Analysis and interpretation of data (e.g., statistical analysis, biostatistics, computational analysis): T. Sakurai, N. Nishida, J. Fujita, M. Kudo
Writing, review, and/or revision of the manuscript: T. Sakurai, H. Kashida, T. Watanabe, J. Fujita, M. Kudo
Administrative, technical, or material support (i.e., reporting or organizing data, constructing databases): T. Sakurai, S. Hagiwara
Study supervision: T. Sakurai, H. Kashida, H. Higashitsuji, M. Kudo

Grant Support

This research was supported by grants from the Takeda Science Foundation, the Japan Foundation for Research and Promotion of Endoscopy, and the Smoking Research Foundation of Japan, as well as a Grant-in-Aid for Scientific Research (26460979) and Health Labour Sciences Research Grant.

The costs of publication of this article were defrayed in part by the payment of page charges. This article must therefore be hereby marked *advertisement* in accordance with 18 U.S.C. Section 1734 solely to indicate this fact.

Received February 17, 2014; revised July 23, 2014; accepted August 19, 2014; published OnlineFirst September 3, 2014.

References

1. Xavier RJ, Podolsky DK. Unravelling the pathogenesis of inflammatory bowel disease. Nature 2007;448:427–34.
2. Edelblum KL, Yan F, Yamaoka T, Polk DB. Regulation of apoptosis during homeostasis and disease in the intestinal epithelium. Inflamm Bowel Dis 2006;12:413–24.
3. Perrier C, Rutgeerts P. Cytokine blockade in inflammatory bowel diseases. Immunotherapy 2011;3:1341–52.
4. Baumann B, Gauldie J. The acute phase response. Immunol Today 1994;15:74–80.
5. McKenzie BS, Kastelein RA, Cua DJ. Understanding the IL-23-IL-17 immune pathway. Trends Immunol 2006;27:17–23.
6. Kortylewski M, Xin H, Kujawski M, Lee H, Liu Y, Harris T, et al. Regulation of the IL-23 and IL-12 balance by Stat3 signaling in the tumor microenvironment. Cancer Cell 2009;15:114–23.
7. Wu D, Wu P, Huang Q, Liu Y, Ye J, Huang J. Interleukin-17: a promoter in colorectal cancer progression. Clin Dev Immunol 2013;2013:436307.
8. Yang S, Wang B, Guan C, Wu B, Cai C, Wang M, et al. Foxp3+IL-17+ T cells promote development of cancer-initiating cells in colorectal cancer. J Leukoc Biol 2011;89:85–91.
9. Itzkowitz SH, Yio X. Inflammation and cancer IV. Colorectal cancer in inflammatory bowel disease: the role of inflammation. Am J Physiol Gastrointest Liver Physiol 2004;287:G7–17.
10. Gillen CD, Walmsley RS, Prior P, Andrews HA, Allan RN. Ulcerative colitis and Crohn's disease: a comparison of the colorectal cancer risk in extensive colitis. Gut 1994;35:1590–2.
11. Clevers H. The cancer stem cell: premises, promises and challenges. Nat Med 2011;17:313–9.
12. Davies EJ, Marsh V, Clarke AR. Origin and maintenance of the intestinal cancer stem cell. Mol Carcinog 2011;50:254–63.
13. Barker N, van Es JH, Kuipers J, Kujala P, van den Born M, Cozijnsen M, et al. Identification of stem cells in small intestine and colon by marker gene Lgr5. Nature 2007;449:1003–1007.
14. Sangiorgi E, Capecchi MR. Bmi1 is expressed *in vivo* in intestinal stem cells. Nat Genet 2008;40:915–20.
15. Kuzmichev AN, Kim SK, D'Alessio AC, Chenoweth JG, Wittko IM, Campanati L, et al. Sox2 acts through Sox21 to regulate transcription in pluripotent and differentiated cells. Curr Biol 2012;22:1705–1710.
16. Lengerke C, Fehm T, Kurth R, Neubauer H, Scheble V, Müller F, et al. Expression of the embryonic stem cell marker SOX2 in early-stage breast carcinoma. BMC Cancer 2011;11:42.
17. Nishiyama H, Itoh K, Kaneko Y, Kishishita M, Yoshida O, Fujita J. A glycine-rich RNA-binding protein mediating cold-inducible suppression of mammalian cell growth. J Cell Biol 1997;137:899–908.
18. Saito K, Fukuda N, Matsumoto T, Iribe Y, Tsunemi A, Kazama T, et al. Moderate low temperature preserves the stemness of neural stem cells and suppresses apoptosis of the cells via activation of the cold-inducible RNA binding protein. Brain Res 2010;1358:20–9.
19. Fujita J. Cold shock response in mammalian cells. J Mol Microbiol Biotechnol 1999;1:243–55.
20. Wellmann S, Bührer C, Moderegger E, Zelmer A, Kirschner R, Koehne P, et al. Oxygen-regulated expression of the RNA-binding proteins RBM3 and CIRP by a HIF-1-independent mechanism. J Cell Sci 2004;117:1785–94.

Published OnlineFirst September 3, 2014; DOI: 10.1158/0008-5472.CAN-14-0471

21. Yang C, Carrier F. The UV-inducible RNA-binding protein A18 (A18 hnRNP) plays a protective role in the genotoxic stress response. J Biol Chem 2001;276:47277–84.
22. De Leeuw F, Zhang T, Wauquier C, Huez G, Kruys V, Gueydan C. The cold-inducible RNA-binding protein migrates from the nucleus to cytoplasmic stress granules by a methylation-dependent mechanism and acts as a translational repressor. Exp Cell Res 2007;313:4130–44.
23. Yang R, Weber DJ, Carrier F. Post-transcriptional regulation of thioredoxin by the stress inducible heterogenous ribonucleoprotein A18. Nucleic Acids Res 2006;34:1224–36.
24. Morf J, Rey G, Schneider K, Stratmann M, Fujita J, Naef F, et al. Cold-inducible RNA-binding protein modulates circadian gene expression posttranscriptionally. Science 2012;338:379–83.
25. Qiang X, Yang WL, Wu R, Zhou M, Jacob A, Dong W, et al. Cold-inducible RNA-binding protein (CIRP) triggers inflammatory responses in hemorrhagic shock and sepsis. Nat Med 2013;19:1489–95.
26. Artero-Castro A, Callejas FB, Castellvi J, Kondoh H, Carnero A, Fernández-Marcos PJ, et al. Cold-inducible RNA-binding protein bypasses replicative senescence in primary cells through extracellular signal-regulated kinase 1 and 2 activation. Mol Cell Biol 2009;29:1855–68.
27. Sakurai T, Itoh K, Higashitsuji H, Nonoguchi K, Liu Y, Watanabe H, et al. Cirp protects against tumor necrosis factor-alpha-induced apoptosis via activation of extracellular signal-regulated kinase. Biochim Biophys Acta 2006;1763:290–5.
28. Masuda T, Itoh K, Higashitsuji H, Higashitsuji H, Nakazawa N, Sakurai T, et al. Cold-inducible RNA-binding protein (Cirp) interacts with Dyrk1b/Mirk and promotes proliferation of immature male germ cells in mice. Proc Natl Acad Sci U S A 2012;109:10885–90.
29. Aranda R, Sydora BC, McAllister PL, Binder SW, Yang HY, Targan SR, et al. Analysis of intestinal lymphocytes in mouse colitis mediated by transfer of CD4+, CD45RBhigh T cells to SCID recipients. J Immunol 1997;158:3464–73.
30. Seki E, De Minicis S, Gwak GY, Kluwe J, Inokuchi S, Bursill CA, et al. CCR1 and CCR5 promote hepatic fibrosis in mice. J Clin Invest 2009;119:1858–70.
31. Araki A, Kanai T, Ishikura T, Makita S, Uraushihara K, Iiyama R, et al. MyD88-deficient mice develop severe intestinal inflammation in dextran sodium sulfate colitis. J Gastroenterol 2005;40:16–23.
32. Sakurai T, Kudo M, Umemura A, He G, Elsharkawy AM, Seki E, et al. p38α inhibits liver fibrogenesis and consequent hepatocarcinogenesis by curtailing accumulation of reactive oxygen species. Cancer Res 2013;73:215–24.
33. Catarzi S, Marcucci T, Papucci L, Favilli F, Donnini M, Tonelli F, et al. Apoptosis and Bax, Bcl-2, Mcl-1 expression in neutrophils of Crohn's disease patients. Inflamm Bowel Dis 2008;14:819–25.
34. Mudter J, Neurath MF. Apoptosis of T cells and the control of inflammatory bowel disease: therapeutic implications. Gut 2007, 56:293–303.
35. Reya T, Morrison SJ, Clarke MF, Weissman IL. Stem cells, cancer, and cancer stem cells. Nature 2001;414:105–11.
36. Olszewski MB, Groot AJ, Dastych J, Knol EF. TNF trafficking to human mast cell granules: mature chain-dependent endocytosis. J Immunol 2007;178:5701–9.
37. Nakanishi Y, Seno H, Fukuoka A, Ueo T, Yamaga Y, Maruno T, et al. Dclk1 distinguishes between tumor and normal stem cells in the intestine. Nat Genet 2013;45:98–103.
38. Pegg AE. Methylation of the O6 position of guanine in DNA is the most likely initiating event in carcinogenesis by methylating agents. Cancer Invest 1984;2:223–31.
39. Okayasu I, Ohkusa T, Kajiura K, Kanno J, Sakamoto S. Promotion of colorectal neoplasia in experimental murine ulcerative colitis. Gut 1996;39:87–92.
40. Grivennikov SI, Karin M. Inflammatory cytokines in cancer: tumour necrosis factor and interleukin 6 take the stage. Ann Rheum Dis 2011;70:i104–8.
41. McDonald SA, Preston SL, Lovell MJ, Wright NA, Jankowski JA. Mechanisms of disease: from stem cells to colorectal cancer. Nat Clin Pract Gastroenterol Hepatol 2006;3:267–74.
42. Saigusa S, Tanaka K, Toiyama Y, Yokoe T, Okugawa Y, Ioue Y, et al. Correlation of CD133, OCT4, and SOX2 in rectal cancer and their association with distant recurrence after chemoradiotherapy. Ann Surg Oncol 2009;16:3488–98.
43. Shigdar S, Li Y, Bhattacharya S, O'Connor M, Pu C, Lin J, et al. Inflammation and cancer stem cells. Cancer Lett 2014;345:271–8.
44. Brochu C, Cabrita MA, Melanson BD, Hamill JD, Lau R, Pratt MA, et al. NF-κB-dependent role for cold-inducible RNA binding protein in regulating interleukin 1β. PLoS One 2013;8:e57426
45. Rogler G. Inflammatory bowel disease cancer risk, detection and surveillance. Dig Dis 2012;30:48–54.
46. Gupta RB, Harpaz N, Itzkowitz S, Hossain S, Matula S, Kornbluth A, et al. Histologic inflammation is a risk factor for progression to colorectal neoplasia in ulcerative colitis: a cohort study. Gastroenterology 2007;133:1099–105.
47. Watanabe T, Kobunai T, Toda E, Kanazawa T, Kazama Y, Tanaka J, et al. Gene expression signature and the prediction of ulcerative colitis-associated colorectal cancer by DNA microarray. Clin Cancer Res 2007;13:415–20.
48. Fujii S, Tominaga K, Kitajima K, Takeda J, Kusaka T, Fujita M, et al. Methylation of the oestrogen receptor gene in non-neoplastic epithelium as a marker of colorectal neoplasia risk in longstanding and extensive ulcerative colitis. Gut 2005;54:1287–92.
49. Nishikawa M, Oshitani N, Matsumoto T, Nishigami T, Arakawa T, Inoue M. Accumulation of mitochondrial DNA mutation with colorectal carcinogenesis in ulcerative colitis. Br J Cancer 2005;93:331–7.

Published OnlineFirst September 3, 2014; DOI: 10.1158/0008-5472.CAN-14-0471

Cancer Research
The Journal of Cancer Research (1916–1930) | The American Journal of Cancer (1931–1940)
AACR

Stress Response Protein Cirp Links Inflammation and Tumorigenesis in Colitis-Associated Cancer

Toshiharu Sakurai, Hiroshi Kashida, Tomohiro Watanabe, et al.

Cancer Res 2014;74:6119-6128. Published OnlineFirst September 3, 2014.

Published in final edited form as:
Mucosal Immunol. 2014 November ; 7(6): 1312–1325. doi:10.1038/mi.2014.19.

NOD2 Down-Regulates Colonic Inflammation by IRF4-Mediated Inhibition of K63-Linked Polyubiquitination of RICK and TRAF6

Tomohiro Watanabe[1,2,3,*], **Naoki Asano**[2,4,*], **Guangxun Meng**[2], **Kouhei Yamashita**[5], **Yasuyuki Arai**[5], **Toshiharu Sakurai**[6], **Masatoshi Kudo**[6], **Ivan J Fuss**[2], **Atsushi Kitani**[2], **Tooru Shimosegawa**[4], **Tsutomu Chiba**[3], and **Warren Strober**[2]

[1]Center for Innovation in Immunoregulative Technology and Therapeutics, Kyoto University Graduate School of Medicine

[2]Mucosal Immunity Section, Laboratory of Host Defenses, National Institute of Allergy and Infectious Diseases, National Institutes of Health

[3]Department of Gastroenterology and Hepatology, Kyoto University Graduate School of Medicine

[4]Division of Gastroenterology, Tohoku University Graduate School of Medicine

[5]Department of Hematology and Oncology, Kyoto University Graduate School of Medicine

[6]Department of Gastroenterology and Hepatology, Kinki University School of Medicine

Abstract

It is well established that polymorphisms of the nucleotide-binding oligomerization domain 2 (NOD2) gene, a major risk factor in Crohn's disease (CD), lead to loss of NOD2 function. However, a molecular explanation of how such loss of function leads to increased susceptibility to CD has remained unclear. In a previous study exploring this question we reported that activation of NOD2 in human dendritic cells by its ligand, muramyl dipeptide (MDP) negatively regulates Toll-like receptor (TLR)-mediated inflammatory responses. Here we show that NOD2 activation results in increased interferon regulatory factor 4 (IRF4) expression and binding to TNF receptor associated factor 6 (TRAF6) and receptor interacting serine-threonine kinase (RICK). We then show that such binding leads to IRF4-mediated inhibition of Lys63-linked polyubiquitination of TRAF6 and RICK and thus to down-regulation of NF-κB activation. Finally, we demonstrate that protection of mice from the development of experimental colitis by MDP or IRF4 administration is accompanied by similar IRF4-mediated effects on polyubiquitination of TRAF6 and RICK in colonic lamina propria mononuclear cells. These findings thus define a mechanism of NOD2-mediated regulation of innate immune responses to intestinal microflora that could explain the relation of NOD2 polymorphisms and resultant NOD2 dysfunction to CD.

Correspondence to Tomohiro Watanabe MD, PhD or Warren Strober MD., Tomohiro Watanabe MD, PhD., Department of Gastroenterology and Hepatology, Kyoto University Graduate School of Medicine, 54 Shogoin Kawahara-cho, Sakyo-ku, Kyoto 606-8507, Japan. tmhrwtnb@kuhp.kyoto-u.ac.jp, Warren Strober MD., Mucosal Immunity Section, Laboratory of Host Defenses, National Institute of Allergy, and Infectious Diseases, National Institutes of Health, wstrober@niaid.nih.gov.
*These authors contributed equally to this work.

Conflicts of interest; none

The authors have no conflicting financial interests.

Introduction

Nucleotide-binding oligomerization domain 2 (NOD2) is a NLR family member that functions as an intracellular sensor of small peptides (such as muramyl dipeptide, MDP) derived from the peptidoglycan (PGN) component of the bacterial cell wall [1, 2]. Activation of NOD2 occurring upon sensing of its ligand through its leucine rich repeat domain is followed by NOD2 oligomerization and exposure of its caspase activation and recruitment domain (CARD). This enables a physical interaction between NOD2 and a downstream adaptor molecule, receptor interacting serine-threonine kinase (RICK) that then results in lysine 63 (K63)-linked polyubiquitination of RICK [1-3]. Ubiquitinated RICK then interacts with TGF-β-activated kinase 1 and TNF receptor associated factor 6 (TRAF6) to cause nuclear translocation of NF-κB subunits [4-8].

The functional importance of NOD2 is underscored by the fact that polymorphisms in the *CARD15* gene encoding NOD2 are associated with Crohn's disease and other immune disorders such as graft versus host disease [1, 2, 9]. However, despite extensive investigation, the molecular mechanisms by which such polymorphisms contribute to these diseases are not completely understood [1, 9]. A possible clue to the nature of these mechanisms comes from the fact that MDP activation of NOD2 can both positively and negatively regulate Toll-like receptor (TLR)-mediated inflammatory responses. For example, synergistic production of pro-inflammatory cytokine responses has been observed in human antigen-presenting cells (APCs) upon simultaneous stimulation of MDP and TLR ligands [10, 11]. This synergism could contribute to the control of the gastrointestinal commensal microflora that is necessary for the prevention of Crohn's disease [12].

However, the above described capacity of NOD2 activation to augment innate immune responses is accompanied by the fact that such activation also has a negative effect on TLR signaling. Thus, we and others have shown that pre-activation of NOD2 by MDP induces decreased pro-inflammatory cytokine responses in human APCs upon subsequent challenge with TLR ligands [13-17]. In addition, Hedl et al. have shown that such tolerogenic responses were not observed in human APCs from patients bearing Crohn's-disease-associated NOD2 mutations [15-17]. We have also found that systemic injection of MDP protects NOD2-intact mice from experimental colitis, but not NOD2-or RICK-deficient mice [6, 14, 18]. Collectively, these data support the idea that MDP activation of NOD2 down-regulates innate immune responses to intestinal microflora and thus suggest that the absence of such regulation leads to increased susceptibility to Crohn's disease.

In a previous study of the molecular mechanisms underlying NOD2 regulation of TLR response, we showed that MDP activation of NOD2 induces interferon regulatory factor 4 (IRF4) in human dendritic cells (DCs) and that such induction is necessary for the negative regulation of subsequent TLR-induced pro-inflammatory responses [14]. In this study, we report that following NOD2 activation, IRF4 interacts with myeloid differentiation factor 88 (MyD88), TRAF6, and RICK and down-regulates K63-linked polyubiquitinylation of RICK and TRAF6; this, in turn, disrupts NOD2- and TLR-MyD88-induced NF-κB activation pathways, respectively. Thus, IRF4 function initiated by NOD2 activation provides new

insight into how NOD2 influences colitis and why loss-of-function NOD2 polymorphisms serve as a risk factor in Crohn's disease.

Results

Physical interactions between IRF4 and MyD88, RICK, and TRAF6 in human DCs

In a previous study [14], we showed that NOD2 pre-stimulation of human DCs results in inhibition of subsequent TLR-induced cytokine responses and that such inhibition requires the up-regulation of IRF4. As for the mechanism of this IRF4 effect, we found in over-expression studies that NOD2 down-regulation of TLR-mediated NF-κB activation is associated with IRF4 interaction with MyD88, RICK, and TRAF6; thus it appeared that IRF4 was interfering with TLR signaling in some manner.

In the present study we addressed the molecular basis of this NOD2-IRF4 inhibitory mechanism by first assessing NOD2-induced IRF4 physical interaction with RICK, MyD88, and TRAF6 in human DCs under physiologic conditions. For this purpose, DCs derived from healthy control peripheral blood monocytes (obtained by culturing the latter in the presence of GM-CSF and IL-4) were pre-stimulated with MDP for 24 hours and then re-stimulated with MDP or lipopolysaccharide (LPS). As shown in Figure 1A, MDP pre-stimulation (designated in Figure 1 as 1st stimulation) up-regulated endogenous IRF4 expression in human DCs without altering their constitutive expression of RICK, MyD88, or TRAF6.

Accompanying studies in which immunoprecipitation (IP) followed by immuno-blotting (IB) was performed to assess signaling component interactions revealed that MDP pre-stimulation enhanced IRF4 binding to RICK, especially when it was accompanied by MDP re-stimulation. In addition, IRF4 binding to TRAF6 was barely seen in un-stimulated cells or cells stimulated with MDP or LPS without pre-stimulation, but was clearly evident in cells pre-stimulated with MDP especially when such pre-stimulation was followed by re-stimulation with MDP or LPS. Finally, IRF4 binding to MyD88 was increased in cells pre-stimulated with MDP and re-stimulated with LPS.

To verify the above IP-IB studies of interactions between IRF4 and various binding molecules in cells subjected to MDP stimulation we employed the Duolink assay which allows fluorescent visualization of interacting proteins [19]. As shown in Figure 1B, an IRF4-RICK complex was generated both in cells pre-stimulated with MDP and re-stimulated with MDP or LPS. In addition, IRF4-TRAF6 and IRF4-MyD88 complexes were generated in cells pre-stimulated with MDP and re-stimulated with either MDP or LPS, particularly the latter. Thus, both the IP-IB and Duo-link assays reveal enhanced interactions between IRF4 and RICK, MyD88, TRAF6 in human primary DCs pre-stimulated with MDP.

As also shown in Figure 1A, MDP pre-stimulation of cells was associated with reduced expression of phospho-IκBα and degradation of IκBα. Thus, the enhanced interaction between IRF4, RICK, and MyD88 in MDP pre-stimulated human DCs is associated with down-regulation of the NF-κB signaling pathway.

IRF4 with mutations at two known phosphorylation sites is capable of both RICK-IRF4 interaction and IRF4 negative regulation

Since RICK is a serine-threonine kinase, NOD2 activation of RICK could be regulating IRF4 function by enhancing RICK phosphorylation of IRF4. To investigate this possibility we first determined the ability of RICK mutated at K47 (K47A) and/or S176 (S176A), sites previously shown to be necessary for RICK kinase activity[20, 21]. As shown in Figure 2A, binding of IRF4 to RICK (in proportion to RICK expression) was observed in 293 cells after the transfection of FLAG-tagged IRF4 along with RICK mutants lacking kinase activity.

In related studies, we determined the ability of IRF4 mutated at both S447 (S447A) and S448 (S448A), potential serine phosphorylation sites previously shown to be necessary for IRF4 function in relation to IL-21 regulation, to bind to RICK [22]. As shown in Figure 2B, both wild type IRF4 and mutated IRF4 bound to RICK in 293 cells over-expressing V5-tagged RICK and FLAG-tagged IRF4. Thus, phospholylation of IRF4 at these two potential phosphorylation sites were not required for the interaction between RICK and IRF4.

Finally, to assess the capacity of IRF4 lacking two serine phosphorylation sites to regulate NF-κB activity we transfected plasmids expressing either wild type or mutated IRF4 into HT-29 cells (i.e., non-hematopoietic cells not likely to express endogenous IRF4 [23]) co-transfected with a RICK-expressing plasmid as well as an NF-κB luciferase reporter-expressing plasmid. As shown in Figure 2C, transfection with mutated IRF4 led to a significant reduction in RICK activation of NF-κB as compared to that of wild type (WT) IRF4. In complementary studies to address the same question in TLR-stimulated cells, we transfected either wild type or mutated IRF4 into human THP1 cells, which lack expression of IRF4 either before or after stimulation with MDP as shown in our previous study [14], and then cultured the cells with TLR2 ligand (Pam_3CSK4, PAM) or TLR4 ligand (LPS) to determine their capacity to produce NF-κB-dependent cytokines. As shown in Figure 2D, transfection of mutated IRF4 into THP1 cells led to a significant decrease in TLR2 induction of IL-12p40 as compared to that of WT IRF4. Thus, these data provide evidence that loss of potential serine phosphorylation sites enhances increased IRF4-mediated negative regulation of NF-κB activation and its down-stream effect on cytokine production.

IRF4 regulates Lys63-linked polyubiquitination of RICK

TLR and NLR activation of NF-κB requires Lysine 63 (K63)-polyubiquitination of signaling components such as RICK and TRAF6 [5-7, 24, 25]. It was therefore possible that IRF4 expression induced by NOD2 activation inhibits NF-κB activation by down-regulation of such polyubiquitination. To address this question we first investigated the effect of IRF4 on RICK polyubiquitination in 293 cells transfected with plasmids expressing HA-tagged ubiquitin (Ub), V5-tagged RICK, and FLAG-tagged IRF4 and then lysed to obtain cell lysates that were subjected to IP with anti-HA antibody (Ab) and IB with anti-V5 Ab.

As shown in Figure 3A, polyubiquitination of RICK was seen in 293 cells expressing HA-tagged wild type Ub and V5-tagged RICK alone but not in cells also expressing IRF4. Consistent with previous studies showing that the E3 ligases, TRAF6 and cellular inhibitors of apoptosis proteins (cIAPs) induce K63-linked polyubiquitination of RICK [6, 26], co-

transfection of plasmids expressing TRAF6 or cIAP1 or cIAP2 enhanced polyubiquitination of RICK; however, such enhanced polyubiquitination of RICK was markedly reduced in cells also expressing IRF4 (Figures 3A and 3B). In further studies to determine the linkage type of poly-Ub chains on RICK, 293 cells were transfected with plasmids expressing mutant forms of Ub that specifically ubiquitinate via either K48 or K63 linkages. As shown in Figure 3A (middle and right panels), 293 cells expressing IRF4 exhibited reduced K63-linked polyubiquitination of RICK, even in cells co-transfected with TRAF6 that expressed increased amounts of K63-polyubiquitinated RICK; however, IRF4 expression had little or no effect on the marginal amount of K48-linked polyubiquitination observed, even in the presence of TRAF6.

As shown in Figure 3B, enhanced K63-linked polyubiquitination of RICK induced by cIAP1 or cIAP2 (but not K48-linked polyubiquitination) was also inhibited in cells expressing IRF4 whereas K63-linked polyubiquitination of RICK by ITCH, another E3 ligase known to induce such polyubiquitination [25] was not reduced in cells expressing IRF4 (data not shown). In addition, as shown in Figure 3C, reduced RICK polyubiquitination was seen in cells expressing either wild type IRF4 or mutated IRF4 lacking its phosphorylation site, indicating that the inhibitory effect of IRF4 was not dependent on its phosphorylation status. Finally, as shown in Figure 3D, polyubiquitination of RICK induced by 30 min of stimulation with MDP in 293 cells stably expressing NOD2 was barely seen upon co-transfection of IRF4; thus the inhibitory effect of IRF4 also applies to RICK activated by NOD2.

In related studies we identified RICK domains that interact with IRF4 and that are necessary for IRF4 inhibition of polyubiquitination. RICK is composed of a kinase domain, an intermediate domain, and a CARD domain. We therefore transfected plasmids expressing V5-tagged RICK mutants lacking each of these domains as well as RICK fragments composed of each of these domains into 293 cells co-transfected with plasmids expressing FLAG-IRF4. As shown in Figure 4A, the interaction between RICK and IRF4 (defined by IP-IB studies) required the presence of the kinase and/or the intermediate RICK domains since the interaction could be detected in 293 cells over-expressing kinase and intermediate domain RICK mutants but not in cells expressing the CARD domain mutant. Thus, the interaction between RICK and IRF4 was mediated by the binding of IRF4 to either the kinase or the intermediate domain but not to the CARD domain. With this information in hand we next conducted ubiquitination studies of RICK domains in 293 cells transfected with plasmids expressing V5-RICK mutants or RICK fragments and co-transfected with plasmids expressing HA-Ub in the absence of IRF4 co-transfectlon. In previous studies, Hasegawa et al. showed that polyubiquitination of RICK at K209 in the kinase domain is essential for RICK-mediated NF-κB activation [7]. As shown in Figure 4B, consistent with this finding, 293 cells over-expressing mutant RICK lacking the kinase domain exhibited grossly defective polyubiquitination whereas those over-expressing RICK mutants lacking the intermediate or CARD domains still exhibited polyubiquitination, albeit less than that of WT RICK; in addition, as also shown in Figure 4B, whereas a kinase domain fragment of RICK was polyubiquitinated, an intermediate domain fragment of RICK was not. Thus, these studies demonstrate that the IRF4 inhibition of RICK polyubiquitination shown above

involves polyubiquitination of the kinase domain of RICK and this inhibition is facilitated by IRF4 binding to the kinase and/or intermediate domains of RICK.

IRF4 regulates polyubiquitination of TRAF6

Stimulation of the TLRs leads to the recruitment of MyD88 and TRAF6 to the receptor complex [27]. This process activates TRAF6 E3 ligase activity and TRAF6-mediated K63-linked polyubiquitination of downstream target proteins as well as TRAF6 itself [24]. Since IRF4 binds to TRAF6 following MDP pre-stimulation it seemed possible that as in the case of RICK polyubiquitination, TRAF6 polyubiquitination was regulated by IRF4. To address this question, 293 cells were transfected with HA-tagged TRAF6, His-tagged Ub, and FLAG-tagged IRF4 and subjected to IP-IB studies as described above. As shown in Figures 5A and 5B, cells expressing wild type or mutated IRF4 exhibited greatly reduced polyubiquitination of TRAF6 in the presence or absence of RICK. In addition, as shown in Figure 5C, robust TRAF6 polyubiquitination induced by 30 min of stimulation with LPS in 293 cells stably expressing TLR4, MD2, and CD14, was abolished in cells also expressing IRF4.

Taken together, these studies strongly suggest that IRF4 negatively regulates polyubiquitination of RICK and TRAF6 either in cells in which target proteins are being over-expressed and are being activated by NLR or TLR ligands, respectively.

Pre-stimulation of human DCs with MDP inhibits Lys63-linked polyubiquitination of RICK and TRAF6

To verify the results of the above over-expression studies of IRF4 under physiologic conditions we next investigated whether IRF4 expression induced by NOD2 inhibits K63-linked polyubiquitination of RICK and/or TRAF6 in human DCs. To this end, cell lysates prepared from human DCs that were pre-stimulated with MDP for 24 hours and then re-stimulated with MDP or LPS were subjected to IP with Abs specific to K63- or K48-ubiquitin and then IB with Abs specific for RICK or TRAF6.

As shown in Figure 6A, pre-stimulation of human DCs with MDP greatly reduced K63-linked, but not K48-linked polyubiquitination of RICK upon secondary stimulation with MDP of human DCs. Similarly, pre-stimulation with MDP greatly reduced K63-linked, but not K48-linked polyubiquitination of TRAF6 upon secondary stimulation with LPS. It should be noted that LPS stimulation did not induce K63-linked polyubiquitination of RICK and MDP stimulation did not induce K63-linked polyubiquitination of TRAF6; thus the possible effect of pre-stimulation of cells with MDP in these situations could not be evaluated.

To determine if the negative effect of MDP pre-stimulation on K63-linked polyubiquitination was in fact due to IRF4 we next conducted studies of cells in which IRF4 was down-regulated by IRF4-specific siRNA (Figure 6B). As shown in Figure 6C, whereas MDP pre-stimulation of cells again led to inhibition of MDP-stimulated RICK and LPS-stimulated TRAF6 K63-linked polyubiquitination, respectively, such inhibition was reversed in cells treated with IRF4 siRNA. These studies show that in physiologic human DCs MDP activation of NOD2 and generation of IRF4 result in subsequent inhibition of MDP-induced

RICK K63-linked polyubiquitination and LPS-induced TRAF6 K63-linked polyubiquitination. They thus fully corroborate the over-expression studies conducted with 293 cells.

Since K63-polyubiquitination of RICK and TRAF6 have been shown to be necessary for TLR-NLR activation of NF-κB [5, 24] we next asked if down-regulation of IRF4 expression by exposure to IRF4 siRNA also results in reversal of MDP pre-stimulation induced inhibition of NF-κB activation. As shown in Figure 6D, culture of DCs in the presence of IRF4 siRNA did in fact abolish the capacity of MDP pre-stimulation to inhibit either MDP or LPS induction of NF-κB activation as assessed by expression of phospho-IκBα whereas control siRNA had no effect on inhibition. These results strongly suggest that IRF4 inhibition of RICK and TRAF6 K63-linked polyubiquitination results in down-stream inhibition of NF-κB activation

Administration of MDP protects mice from trinitrobenzene sulfonic acid (TNBS) colitis via regulation of K63-linked polyubiquitination of RICK and TRAF6

The above results derived from *in vitro* studies of both 293 cells and human DCs suggest that MDP/NOD2-induced effects on K63-linked polyubiquitination in RICK and TRAF6 could explain our previous studies showing that MDP administration ameliorates experimental colitis [14]. To address this possibility we next determined the effect of MDP administration on K63-linked polyubiquitination in RICK and TRAF6 in mice with TNBS-colitis. As shown in Figures 7A, and 7B, and in the photomicrographs displayed in S1A, systemic administration of MDP protected mice from the induction of TNBS-colitis induced by intra-rectal instillation of TNBS and such protection was accompanied by reduced nuclear translocation of NF-κB subunits (p65, p50, and c-Rel) in colonic lamina propria mononuclear cells (LPMCs) [14].

Importantly, several IRF4-related effects accompanied this MDP-mediated protection from colitis. Thus, as shown in Figure 7C, MDP administration led to markedly enhanced IRF4 expression in colonic tissue of MDP-treated mice and, as shown in Figure 7D, Duolink assays revealed that such administration also caused enhanced interaction between IRF4 and RICK, MyD88 or TRAF6 in such colonic tissue. Furthermore, as shown in Figure 7E, MDP-administration led to reduced K63-linked polyubiquitination of RICK and TRAF6 in colonic LPMCs that was unaccompanied by reduced K48-linked polyubiquitination. These *in vivo* studies are therefore consistent with the *in vitro* studies described above in showing that MDP-induced IRF4 expression and inhibition of K63-linked polyubiquitination of RICK and TRAF6 is associated with a down-regulation of NF-κB; however, in this case they show that this IRF4 effect is also associated with greatly reduced colonic inflammation.

Prevention of TNBS-colitis by administration of IRF4-expressing plasmids

Whereas the above studies show that MDP-induced up-regulation of IRF4 and the latter's effect on K63-linked ubiquitination of RICK and TRAF6 is associated with down-regulation of NF-κB and colitis it remained possible that MDP inhibition of NF-κB activation was occurring through another mechanism that does not involved IRF4. To address this possibility we conducted further *in vivo* studies in which we explored the possibility that

exogenous IRF4 administration can directly prevent TNBS-colitis, thereby by-passing MDP stimulation. Accordingly, we administered a FLAG-tagged IRF4 plasmid as well as a control plasmid encapsulated in a Hemagglutinin Virus of Japan-Envelope (HVJ-E) viral coat to mice by intra-rectal instillation on each of the two days before and on the day of intra-rectal challenge with TNBS. This method of inducing *in vivo* protein expression following plasmid administration had proven to be highly efficient in previous studies [14] and, indeed, most of the colonic LPMCs expressing CD11b or CD11c were positive for the expression of FLAG-IRF4 in flow-cytometric analysis two days after the induction of TNBS-colitis (Figure S2). As shown in Figures 8A and S1B, intra-rectal administration of FLAG-tagged IRF4 plasmids prevented the development of TNBS-colitis as assessed by body weight loss and colonic pathology analysis. Thus, exogenous IRF4 administration, like MDP administration, is an effective inhibitor of TNBS-colitis.

In further studies, we investigated the interaction between the exogenously administered FLAG-tagged IRF4 and RICK, TRAF6 and MyD88 in the colonic mucosa of the mice subjected to intra-rectal TNBS challenge accompanied by IRF4 administration. To this end, whole protein extracts isolated from the colonic mucosa were subjected to IP with FLAG Ab and then IB with Abs specific for RICK, TRAF6 and MyD88. As shown in Figure 8B, administered FLAG-tagged IRF4 was bound to RICK, MyD88, and TRAF6. In a final set of studies we determined the effect of the exogenously administered IRF4 on NF-κB and MAP kinase expression as well as on down-stream pro-inflammatory cytokine expression. As shown in Figures 8C and 8D, exogenously administered IRF4 led to markedly reduced expression of phospho-κBa, phospho-p38, and phospho-ERK as well as reduced nuclear translocation of NF-κB subunits in the colonic mucosa of mice treated with intra-rectal administration of FLAG-tagged IRF4 plasmids as compared with treated those with control plasmid. In addition, evidence of reduced activation of NF-κB was associated with reduced pro-inflammatory cytokine responses by colonic LPMCs. Thus, as shown in Figures 8E and 8F, colonic LPMCs produced markedly less IL-12p40 and IFN-γ upon stimulation with MDP, Pam_3CSK4 (PAM, a TLR2 ligand), LPS, flagellin (a TLR5 ligand), CpG (a TLR9 ligand), and anti-CD3 Ab.

Taken together, these data show that IRF4 administration mimics the effect of MDP administration and increased NOD2 signaling during induction of TNBS-colitis as previously reported [14]. As such, they show that prevention of TNBS-colitis by MDP administration is most likely acting via the induction of IRF4.

Treatment of TNBS-colitis by administration of IRF4-expressing plasmids

The striking effect of IRF4-expressing plasmid administration on TNBS colitis shown above suggested that such administration could have therapeutic value. To address this possibility we determined if administration of IRF4-expressing plasmid could reverse previously established TNBS-colitis. Accordingly, mice were challenged with TNBS as described above but in this case they were administered FLAG-tagged IRF4 plasmid encapsulated in the HVJ-E vector three days after TNBS administration rather than at the time of TNBS administration. As shown in Figure 9A, expression of FLAG was again shown to be present in the colonic mucosa of mice following FLAG-tagged IRF4 plasmid administration. In

addition, as shown in Figures 9B and S1C, such mice promptly regained body weight and exhibited improved microscopic inflammation scores. Moreover, as shown in Figures 9C, 9D, and 9E, administration of IRF4 was followed by reduced nuclear translocation of NF-κB components in the colonic mucosa as well as greatly decreased production of pro-inflammatory cytokines by mesenteric lymph node (MLN) cells upon stimulation with TLR ligands and anti-CD3 mAb. These data thus provide further proof that MDP activation of NOD2 and generation of IRF4 leads to down-regulation of NF-κB activation and colonic inflammation. In addition, they suggest that IRF4 administration might have clinical value.

Discussion

In a previous study, we demonstrated that MDP activation of NOD2 has down-regulatory effects on multiple TLR signaling pathways [14]. We now provide a mechanism for such down-regulation by showing that MDP activation of NOD2 induces IRF4-mediated inhibition of molecular events essential to the activation of NF-κB, namely K63-linked polyubiquitination of RICK and TRAF6. The chain of evidence supporting this conclusion consisted first of the fact that MDP pre-stimulation of human DCs leads to binding of RICK to IRF4 and the binding of IRF4 to TRAF6 and MyD88. As shown in over-expression studies conducted in a cell line and more importantly in physiologic human DCs, these interactions set the stage for MDP/NOD2-induced IRF4 inhibition of K63-linked polyubiquitination of RICK and TRAF6; in addition, such inhibition could be linked to down-regulation of NF-κB activation by the demonstration that siRNA down-regulation of IRF4 reverses the negative effect by NOD2 signaling on K63-linked polyubiquitination and NF-κB activation. These *in vitro* studies were then supported by *in vivo* studies showing that protection from the development of TNBS-colitis by MDP administration is accompanied by greatly increased IRF4 expression and interaction with RICK, TRAF6 and MyD88 as well as inhibition of K63-linked polyubiquitination of RICK and TRAF6 in colonic cells and this, in turn, is associated with greatly reduced NF-κB activation. A final step in the chain of evidence consisted of studies showing that administration of an IRF4-expressing plasmid to mice both prevented TNBS-colitis and reversed already established TNBS-colitis. These latter studies established that MDP activation of NOD2 *in vivo* was in fact acting via IRF4 to inhibit NF-κB activity. Overall, these data provide a mechanistic explanation of how MDP-NOD2 stimulation of APCs negatively regulates inflammatory responses induced by TLR ligands and therefore explain how defective NOD2 function can lead to excessive TLR responses in the gut that contribute to the pathogenesis of Crohn's disease.

IRF4 has been shown in previous reports to function as a negative regulator of TLR signaling pathways in innate immune cells such as DCs [14, 28, 29]. As for the mechanisms accounting for such negative regulation, Negishi et al. provided evidence that IRF4 expression is up-regulated by activation of TLRs and then competes with IRF5 for binding to and activation of MyD88 [28]. While this mechanism of IRF4 inhibitory activity may be valid, it cannot be the only mechanism in play because we have shown previously as well in the present studies that MDP pre-stimulation acting through NOD2 inhibits LPS and other TLR ligand cytokine responses, including TLR responses that do not involve MyD88 [14]. It should be noted in this context that whereas NOD2 activation leads to RICK-IRF4 binding, LPS activation in the absence of MDP-induced NOD2 interaction does not have this effect

(Watanabe T, Asano N, Strober W, unpublished observation). Thus, it is possible that NOD2 activation leads to RICK-IRF4 complexes that have inhibitory functions not shared by IRF4 alone. In any case, we have shown that systemic administration of MDP to mice challenged with TNBS to induce TNBS-colitis leads to enhanced expression of IRF4 in colonic LPMCs and inhibition of inflammation due to reduced K63-linked polyubiquitination of TRAF6 and RICK in those cells. In addition, intra-rectal administration of an IRF4-expressing plasmid to mice challenged with TNBS had a similar anti-inflammatory effect. Thus, our study disclosed a molecular mechanism by which NOD2-induced IRF4 inhibits intestinal inflammation driven, at least in part, by activation of TLR signaling pathways that are not regulated by TLR-induced IRF4.

In the above studies of TNBS-colitis the development of colitis was inhibited either by systemic injection of MDP or intrarectal administration of IRF4 cDNA. These treatments were parallel in that administration of MDP resulted in enhanced interaction between IRF4 and RICK, TRAF6, and MyD88 and administration of IRF4 cDNA led to interaction of IRF4 with the same signaling molecules; moreover, reduction of NF-κB activation was seen in both treatments. Thus, it is likely that MDP activation of NOD2 prevents experimental colitis via induction of IRF4 expression. It should be noted that this conclusion leads to the assumption that activation of TLRs with the ability to induce the expression of IRF4 have the potential to inhibit experimental colitis via the same de-ubiquitination mechanism described here for NOD2. However, previous reports show that generation of tolerogenic responses by LPS depends upon the induction of IRAK-M rather than IRF4 [14, 29]. Thus, tolerogenic responses induced by MDP activation of NOD2 appear to be intrinsically different from those induced by LPS activation of TLR4 and while LPS administration may suppress colitis due to induction of LPS tolerance, such suppression will not by mediated by the de-ubiquitinization function of IRF4.

Of interest, IRF4 may be exerting inhibitory effects by a mechanism similar to that described here in other instances of pro-inflammatory responses. This includes IRF4-mediated suppression of TLR-induced cytokine responses leading to acute post-ischemic renal inflammation by IRF4 generated in renal DCs reacting to oxidative stress [30] and IRF4-mediated reduction of TLR-induced pro-inflammatory responses of liver plasmacytoid DCs by IRF4 generated in such cells by *in vivo* administration of MDP [13]. However, additional studies will be necessary to verify this possibility.

IRF4 is expressed in most types of cells in the lymphoid system and may have cell-specific functions [31]. This possibility is illustrated by the fact that, in contrast to the anti-inflammatory role of IRF4 in TNBS-colitis and post-ischemic renal inflammation described above, it has a pro-inflammatory role in experimental T cell-mediated autoimmune disorders [31]. The latter may be due to the fact that IRF4 has been shown to be a positive regulator of IL-17 and IL-21 responses in T cells and increased responsiveness to IL-21 in B cells [22, 31, 32]. Interestingly, there is evidence that this pro-inflammatory activity by IRF4 plays a critical role in a T cell-dependent colitis. Thus, Mudter et al. have shown that adoptive transfer of naive $CD4^+$ T cells from wild type mice, but not IRF4-deficient mice to immune-deficient mice resulted in severe colitis associated with increased production of IL-6 and Th17 cytokines [33, 34]. In our studies, intra-rectal delivery of a plasmid expressing

FLAG-tagged IRF4 was shown to lead to marked expression of FLAG-tagged IRF4 in colonic APCs rather than in colonic T cells. Thus, our data support the idea that whereas IRF4 expression in T cells may promote the development of colitis, its expression in APCs has the contrary effect. In this context, it should also be noted that the HVJ-E delivery of IRF4-expressing plasmid could have led to IRF4 expression in non-myeloid cells and thus we cannot rule out the possibility that the ability of exogenous IRF4 expression to affect colitis in these studies could have been mediated by effects on one or another non-myeloid cell.

As shown by the fact that intra-rectal administration of NF-κB decoy oligonucleotides that blocks activation of NF-κB target genes prevents and treats TNBS- or oxazolone-colitis, the pathogenic immune responses underlying experimental colitis depend on NF-κB transcriptional activity [35, 36]. In recent years evidence has accumulated that such NF-κB-mediated inflammation is tightly regulated by ubiquitination of various components of the NF-κB signaling cascade. This is well illustrated by the fact that the function of TRAF6, an essential component of the signaling cascade leading to NF-κB activation is dependent on its K63-linked polyubiquitination status. Thus, de-ubiquitination of TRAF6 by the de-ubiquitinating enzyme, A20, leads to inhibition of TLRs-induced NF-κB activation [24, 37] and A20 deficiency results in excessive NF-κB activation associated with the development of autoimmune disease or colitis due to stimulation by TLR ligands derived from the intestinal microflora [24, 38]. In this study, we show that down-regulation of K63-linked polyubiquitination of TRAF6 resulting from an inhibitory interaction with IRF4 also leads to decreased NF-κB activation. The mechanism of such IRF4 inhibition is presently unknown. However, given the fact that TRAF6 is an E3-ligase and can therefore facilitate both the polyubiquitination of down-stream signaling molecules as well as its own polyubiquitination, one possible mechanism is that IRF4 interferes with TRAF6 E3-ligase activity.

Despite the fact that *NOD2* polymorphisms associated with Crohn's disease are considered to be loss-of-function abnormalities that lead to decreased NOD2-mediated pro-inflammatory function, immune responses linked to Crohn's disease are characterized by production of pro-inflammatory cytokines driven by excessive NF-κB activation [39, 40]. One explanation of this paradox is that NOD2 signaling in epithelial cells is necessary for the elaboration of epithelial cell-derived cryptins that ordinarily control bacterial growth in the intestine; thus, loss of NOD2 function can lead to excessive bacterial growth that gives rise to colitis [41, 42]. It should be noted, however, that chronic NOD2 activation has been shown to mediate down-regulation of innate TLRs responses to microbial antigens in the intestine, a phenomenon known as cross-tolerance [14-17]. Therefore, an alternative explanation of how *NOD2* polymorphisms and loss of NOD2 function leads to intestinal disease is that NOD2 regulates innate responses to intestinal microflora by suppressing TLR responses in the healthy intestinal mucosa, whereas in the diseased Crohn's disease intestinal mucosa lack of NOD2 function leads to lack of cross-tolerance and excessive TLR responses. This study together with our previous study of NOD2 signaling shows that defective NOD2-induced IRF4 inhibitory function is likely to be the cause of the loss of cross-tolerance and thus the molecular basis for the role of loss of NOD2 function in Crohn's disease [14].

In conclusion, the present findings provide evidence that *CARD15* polymorphisms function as susceptibility factors in Crohn's disease by affecting the generation and activation of a factor, IRF4, that plays a key role in the regulation of TLR responses induced by the gut microflora. In addition, they show in studies of mice with experimental colitis that MDP administration leading to colonic IRF4 expression or intra-rectal delivery of an IRF4 expression plasmid have the potential to both prevent and treat such colitis and possibly Crohn's disease as well.

Methods

Reagents

Recombinant GM-CSF and IL-4 were from Peprotech. Unless otherwise described, the doses of TLR ligands and NOD2 ligands used for stimulation were as follows; Pam_3CSK4 (PAM, TLR2 ligand, 10 μg/ml, InvivoGen), LPS (TLR4 ligand, 1 μg/ml, Sigma), flagellin (TLR5 ligand, 1 μg/ml, InvivoGen), CpG (TLR9 ligand, 1 μM, InvivoGen), and MDP (NOD2 ligand, 10 μg/ml, InvivoGen).

Induction of colitis

TNBS-colitis was induced in C57BL10 mice obtained from Japan SLC as described previously [35]. On day -2, -1, and 0, mice received intra-peritoneal injection of MDP (100 μg) for a total of three times before intra-rectal administration of 3.75 mg of TNBS in 100 μl of 45 % ethanol. MLN cells and colon LPMCs were isolated at the indicated time points and cultured as described previously [14]. Cells were stimulated with anti-CD3 (1 μg/ml, BD Pharmingen) and TLR ligands as described above. Culture supernatants were collected at 24 hrs or 48 hrs and analyzed for cytokine production by ELISA. In some experiments, whole cell extracts were prepared from colon tissue or LPMCs for the immunoprecipitation and immunoblotting analysis. In the experiments in which mice received FLAG-tagged IRF4 vector [29] or control vector, plasmids were encapsulated in HVJ (GenomIdea) using protamine sulfate according to the manufacture's protocol. 75 μg/mouse of encapsulated plasmids were administered via the intra-rectal route on day -2, -1, and 0 for the evaluation of colitis prevention and on day 3 for the evaluation of colitis treatment. Colon was harvested at the indicated time points. Colon tissues were stained with hematoxylin and eosin (H&E) and used for the scoring of the inflammation as described previously [14]. Animal use adhered to Kyoto university animal care guidelines and protocols of animal experiments were approved by the review boards of Kyoto University.

Human monocyte-derived DCs

Monocytes were isolated from the peripheral blood of healthy donors by $CD14^+$ microbeads (Miltenybiotec) and were cultured in 6-well plates (1×10^6/ml) in 5 ml of complete medium (RPMI 1640 medium supplemented with 2 mM L-glutamine, and 10% fetal calf serum) supplemented with recombinant GM-CSF (20 ng/ml) and recombinant IL-4 (20 ng/ml). Ethical permission of this study was granted by the review boards of Kyoto University. After 3 days of culture, half of the medium in each well was exchanged for fresh medium. After 6 days of culture, cells (1×10^6/ml) were incubated with MDP or medium for 24 hrs in the absence of GM-CSF and IL-4, and then washed three times and stimulated with LPS or

MDP. In some experiments, cells were cultured with MG132 (10 μg/ml, Enzo Life Sciences). In siRNA-mediated gene silencing experiments, DCs were transfected with 100 nM of control siRNA or IRF4 siRNA (Hs IRF4 10 FlexiTube siRNA, Qiagen) by a human dendritic cell nucleofection kit (Lonza).

Immunoprecipitation and immunoblotting

HEK293 cells (ATCC) (1×10^6/cells) were transfected with 1 μg of FLAG-tagged human IRF4 vector [14], HA-tagged human MyD88, TRAF6 (InvivoGen), V5-tagged RICK [14], Myc-DDK-tagged cIAP1, Myc-DDK-tagged cIAP2 (Origene), HA-tagged wild type ubiquitin (Ub), K63 Ub, K48 Ub (kindly provided by Dr. J. Chen), and His-tagged Ub (kindly provided by Dr. H. Kondoh) by Lipofectamine 2000 (Invitrogen) or by Fugene 6 (Promega). Mutant plasmids expressing IRF4 S447A and S448A, RICK K47A and S176A, or RICK lacking the kinase domain, intermediate domain, or CARD were created by QuickChange site-directed mutagenesis kit (Stratagene). Whole cell lysates were prepared 24 or 48 hrs after the transfection and were incubated with anti-FLAG conjugated beads (Sigma), anti-V5 conjugated beads (Sigma), and anti-HA-conjugated beads (Sigma) overnight. In some experiments, whole cell lysates prepared from human DCs, colonic LPMCs, and colon tissue samples were incubated with anti-K63 Ub Ab, anti-K48 Ub Ab (MBL) or anti-IRF4 Ab (Santa Cruz Biotechnology) and protein A/G agarose (Santa Cruz Biotechnology). Anti-MyD88, anti-TRAF6, anti-IRF4, anti-κBα, anti-phospho-κBα, anti-phospho-p38 anti-p38, anti-phospho-ERK, anti-ERK, and anti-His Abs were obtained from Cell signaling technology (CST). Anti-actin Ab (Santa Cruz), anti-RICK Ab (Cayman Chemicals), anti-V5 Ab (Bethyl laboratories), anti-FLAG Ab (Sigma), anti-HA Ab (Sigma), and anti-Myc Ab (MBL) were used.

Immunofluorescence studies

Colon tissues were harvested and fixed in 10% formalin. Deparaffinized colon sections were then obtained and incubated with mouse anti-IRF4 Ab (Invitrogen) followed by Alexa546-conjugated anti-mouse IgG Ab (Invitrogen) by using Can Get Signal immunoreaction enhancer solution (Toyobo) as described previously [43]. For visualization of interaction between IRF4 and RICK, MyD88, TRAF6 in colon samples, a Duolink In Situ kit was used (Olink Bioscience). Goat anti-IRF4 Ab (Santa Cruz), rabbit anti-RICK Ab, rabbit anti-MyD88 Ab, and rabbit anti-TRAF6 Ab (Abcam) were used to visualize target protein interactions. For visualization of interaction between IRF4 and RICK, MyD88, TRAF6 in human DCs, cells were fixed in 4% paraformaldehyde and subjected to the protocols suggested by the Duolink In Situ kit.

Elisa

Protein concentrations of cytokines were determined by eBioscience ELISA kits for mouse IL-12p40, mouse IL-6, and mouse TNF-α. Concentration of IFN-γ was determined by BD Bioscience ELISA kit.

NF-κB activation studies

Nuclear extracts were prepared from colon tissues. Nuclear extracts was obtained with the use of a nuclear extraction kit (Active Motif). Binding activity of nuclear extract (5 μg) to NF-κB subunit (p50, p65, c-Rel) was measured using a Transam kit, obtained from Active Motif, as previously described [43].

Statistical analysis

Student's t test was used to evaluate the significance of the differences. Statistical analysis was performed with the Prism (Graphpad software). A value of $P < 0.05$ was regarded as statistically significant.

Supplementary Material

Refer to Web version on PubMed Central for supplementary material.

Acknowledgments

This work was supported by Grant-in-Aid for Scientific Research (25293172, 21229009, 24229005, and 24659363) from Japan Society for the Promotion of Science, the Japanese Society of Gastroenterology, and the Special Coordination Funds by the Ministry of Education, Culture, Sports, Science and Technology of Japan and Astellas Pharma Inc. in Creation of Innovation Centers for Advanced Interdisciplinary Research Areas Program, and by the Intramural Research Program of the National Institutes of Health. We thank Ms. M. Tosaka and Dr. H. Ezoe for their assistance.

References

1. Strober W, Watanabe T. NOD2, an intracellular innate immune sensor involved in host defense and Crohn's disease. Mucosal immunology. 2011; 4(5):484–495. [PubMed: 21750585]
2. Strober W, Murray PJ, Kitani A, Watanabe T. Signalling pathways and molecular interactions of NOD1 and NOD2. Nat Rev Immunol. 2006; 6(1):9–20. [PubMed: 16493424]
3. Inohara, Chamaillard, McDonald C, Nunez G. NOD-LRR proteins: role in host-microbial interactions and inflammatory disease. Annu Rev Biochem. 2005; 74:355–383. [PubMed: 15952891]
4. Abbott DW, Wilkins A, Asara JM, Cantley LC. The Crohn's disease protein, NOD2, requires RIP2 in order to induce ubiquitinylation of a novel site on NEMO. Curr Biol. 2004; 14(24):2217–2227. [PubMed: 15620648]
5. Abbott DW, Yang Y, Hutti JE, Madhavarapu S, Kelliher MA, Cantley LC. Coordinated regulation of Toll-like receptor and NOD2 signaling by K63-linked polyubiquitin chains. Molecular and cellular biology. 2007; 27(17):6012–6025. [PubMed: 17562858]
6. Bertrand MJ, Doiron K, Labbe K, Korneluk RG, Barker PA, Saleh M. Cellular Inhibitors of Apoptosis cIAP1 and cIAP2 Are Required for Innate Immunity Signaling by the Pattern Recognition Receptors NOD1 and NOD2. Immunity. 2009; 30(6):789–801. [PubMed: 19464198]
7. Hasegawa M, Fujimoto Y, Lucas PC, Nakano H, Fukase K, Nunez G, et al. A critical role of RICK/RIP2 polyubiquitination in Nod-induced NF-kappaB activation. The EMBO journal. 2008; 27(2):373–383. [PubMed: 18079694]
8. Kim YG, Park JH, Shaw MH, Franchi L, Inohara N, Nunez G. The cytosolic sensors Nod1 and Nod2 are critical for bacterial recognition and host defense after exposure to Toll-like receptor ligands. Immunity. 2008; 28(2):246–257. [PubMed: 18261938]
9. Cho JH. The genetics and immunopathogenesis of inflammatory bowel disease. Nat Rev Immunol. 2008; 8(6):458–466. [PubMed: 18500230]

10. Tada H, Aiba S, Shibata K, Ohteki T, Takada H. Synergistic effect of Nod1 and Nod2 agonists with toll-like receptor agonists on human dendritic cells to generate interleukin-12 and T helper type 1 cells. Infect Immun. 2005; 73(12):7967–7976. [PubMed: 16299289]
11. van Heel DA, Ghosh S, Butler M, Hunt KA, Lundberg AM, Ahmad T, et al. Muramyl dipeptide and toll-like receptor sensitivity in NOD2-associated Crohn's disease. Lancet. 2005; 365(9473): 1794–1796. [PubMed: 15910952]
12. Werts C, Rubino S, Ling A, Girardin SE, Philpott DJ. Nod-like receptors in intestinal homeostasis, inflammation, and cancer. Journal of leukocyte biology. 2011; 90(3):471–482. [PubMed: 21653239]
13. Castellaneta A, Sumpter TL, Chen L, Tokita D, Thomson AW. NOD2 ligation subverts IFN-alpha production by liver plasmacytoid dendritic cells and inhibits their T cell allostimulatory activity via B7-H1 up-regulation. J Immunol. 2009; 183(11):6922–6932. [PubMed: 19890047]
14. Watanabe T, Asano N, Murray PJ, Ozato K, Tailor P, Fuss IJ, et al. Muramyl dipeptide activation of nucleotide-binding oligomerization domain 2 protects mice from experimental colitis. The Journal of clinical investigation. 2008; 118(2):545–559. [PubMed: 18188453]
15. Hedl M, Li J, Cho JH, Abraham C. Chronic stimulation of Nod2 mediates tolerance to bacterial products. Proceedings of the National Academy of Sciences of the United States of America. 2007; 104(49):19440–19445. [PubMed: 18032608]
16. Hedl M, Abraham C. Secretory mediators regulate Nod2-induced tolerance in human macrophages. Gastroenterology. 2010; 140(1):231–241. [PubMed: 20854823]
17. Kullberg BJ, Ferwerda G, de Jong DJ, Drenth JP, Joosten LA, Van der Meer JW, et al. Crohn's disease patients homozygous for the 3020insC NOD2 mutation have a defective NOD2/TLR4 cross-tolerance to intestinal stimuli. Immunology. 2008; 123(4):600–605. [PubMed: 18028374]
18. Yeretssian G, Correa RG, Doiron K, Fitzgerald P, Dillon CP, Green DR, et al. Non-apoptotic role of BID in inflammation and innate immunity. Nature. 2011; 474(7349):96–99. [PubMed: 21552281]
19. Meinzer U, Barreau F, Esmiol-Welterlin S, Jung C, Villard C, Leger T, et al. Yersinia pseudotuberculosis effector YopJ subverts the Nod2/RICK/TAK1 pathway and activates caspase-1 to induce intestinal barrier dysfunction. Cell host & microbe. 2012; 11(4):337–351. [PubMed: 22520462]
20. Nembrini C, Kisielow J, Shamshiev AT, Tortola L, Coyle AJ, Kopf M, et al. The kinase activity of Rip2 determines its stability and consequently Nod1- and Nod2-mediated immune responses. The Journal of biological chemistry. 2009; 284(29):19183–19188. [PubMed: 19473975]
21. Dorsch M, Wang A, Cheng H, Lu C, Bielecki A, Charron K, et al. Identification of a regulatory autophosphorylation site in the serine-threonine kinase RIP2. Cellular signalling. 2006; 18(12): 2223–2229. [PubMed: 16824733]
22. Biswas PS, Gupta S, Chang E, Song L, Stirzaker RA, Liao JK, et al. Phosphorylation of IRF4 by ROCK2 regulates IL-17 and IL-21 production and the development of autoimmunity in mice. The Journal of clinical investigation. 2010; 120(9):3280–3295. [PubMed: 20697158]
23. Natkunam Y, Warnke RA, Montgomery K, Falini B, van De Rijn M. Analysis of MUM1/IRF4 protein expression using tissue microarrays and immunohistochemistry. Mod Pathol. 2001; 14(7): 686–694. [PubMed: 11455001]
24. Chen ZJ. Ubiquitin signalling in the NF-kappaB pathway. Nature cell biology. 2005; 7(8):758–765.
25. Tao M, Scacheri PC, Marinis JM, Harhaj EW, Matesic LE, Abbott DW. ITCH K63-ubiquitinates the NOD2 binding protein, RIP2, to influence inflammatory signaling pathways. Curr Biol. 2009; 19(15):1255–1263. [PubMed: 19592251]
26. Yang Y, Yin C, Pandey A, Abbott D, Sassetti C, Kelliher MA. NOD2 pathway activation by MDP or Mycobacterium tuberculosis infection involves the stable polyubiquitination of Rip2. The Journal of biological chemistry. 2007; 282(50):36223–36229. [PubMed: 17947236]
27. Akira S, Takeda K. Toll-like receptor signalling. Nat Rev Immunol. 2004; 4(7):499–511. [PubMed: 15229469]

28. Negishi H, Ohba Y, Yanai H, Takaoka A, Honma K, Yui K, et al. Negative regulation of Toll-like-receptor signaling by IRF-4. Proceedings of the National Academy of Sciences of the United States of America. 2005; 102(44):15989–15994. [PubMed: 16236719]
29. Honma K, Udono H, Kohno T, Yamamoto K, Ogawa A, Takemori T, et al. Interferon regulatory factor 4 negatively regulates the production of proinflammatory cytokines by macrophages in response to LPS. Proceedings of the National Academy of Sciences of the United States of America. 2005; 102(44):16001–16006. [PubMed: 16243976]
30. Lassen S, Lech M, Rommele C, Mittruecker HW, Mak TW, Anders HJ. Ischemia reperfusion induces IFN regulatory factor 4 in renal dendritic cells, which suppresses postischemic inflammation and prevents acute renal failure. J Immunol. 2010; 185(3):1976–1983. [PubMed: 20601597]
31. Xu WD, Pan HF, Ye DQ, Xu Y. Targeting IRF4 in autoimmune diseases. Autoimmunity reviews. 2012; 11(12):918–924. [PubMed: 23010632]
32. Biswas PS, Gupta S, Stirzaker RA, Kumar V, Jessberger R, Lu TT, et al. Dual regulation of IRF4 function in T and B cells is required for the coordination of T-B cell interactions and the prevention of autoimmunity. J Exp Med. 2012; 209(3):581–596. [PubMed: 22370718]
33. Mudter J, Amoussina L, Schenk M, Yu J, Brustle A, Weigmann B, et al. The transcription factor IFN regulatory factor-4 controls experimental colitis in mice via T cell-derived IL-6. The Journal of clinical investigation. 2008; 118(7):2415–2426. [PubMed: 18535667]
34. Mudter J, Yu J, Zufferey C, Brustle A, Wirtz S, Weigmann B, et al. IRF4 regulates IL-17A promoter activity and controls RORgammat-dependent Th17 colitis in vivo. Inflammatory bowel diseases. 2011; 17(6):1343–1358. [PubMed: 21305677]
35. Fichtner-Feigl S, Fuss IJ, Preiss JC, Strober W, Kitani A. Treatment of murine Th1- and Th2-mediated inflammatory bowel disease with NF-kappa B decoy oligonucleotides. The Journal of clinical investigation. 2005; 115(11):3057–3071. [PubMed: 16239967]
36. De Vry CG, Prasad S, Komuves L, Lorenzana C, Parham C, Le T, et al. Non-viral delivery of nuclear factor-kappaB decoy ameliorates murine inflammatory bowel disease and restores tissue homeostasis. Gut. 2007; 56(4):524–533. [PubMed: 16950831]
37. Ma A, Malynn BA. A20: linking a complex regulator of ubiquitylation to immunity and human disease. Nat Rev Immunol. 2012; 12(11):774–785. [PubMed: 23059429]
38. Hammer GE, Turer EE, Taylor KE, Fang CJ, Advincula R, Oshima S, et al. Expression of A20 by dendritic cells preserves immune homeostasis and prevents colitis and spondyloarthritis. Nat Immunol. 2011; 12(12):1184–1193. [PubMed: 22019834]
39. Strober W, Fuss I, Mannon P. The fundamental basis of inflammatory bowel disease. The Journal of clinical investigation. 2007; 117(3):514–521. [PubMed: 17332878]
40. Strober W, Fuss IJ. Proinflammatory cytokines in the pathogenesis of inflammatory bowel diseases. Gastroenterology. 2011; 140(6):1756–1767. e1751. [PubMed: 21530742]
41. Wehkamp J, Wang G, Kubler I, Nuding S, Gregorieff A, Schnabel A, et al. The Paneth cell alpha-defensin deficiency of ileal Crohn's disease is linked to Wnt/Tcf-4. J Immunol. 2007; 179(5): 3109–3118. [PubMed: 17709525]
42. Kobayashi KS, Chamaillard M, Ogura Y, Henegariu O, Inohara N, Nunez G, et al. Nod2-dependent regulation of innate and adaptive immunity in the intestinal tract. Science. 2005; 307(5710):731–734. [PubMed: 15692051]
43. Tsuji Y, Watanabe T, Kudo M, Arai H, Strober W, Chiba T. Sensing of commensal organisms by the intracellular sensor NOD1 mediates experimental pancreatitis. Immunity. 2012; 37(2):326–338. [PubMed: 22902233]

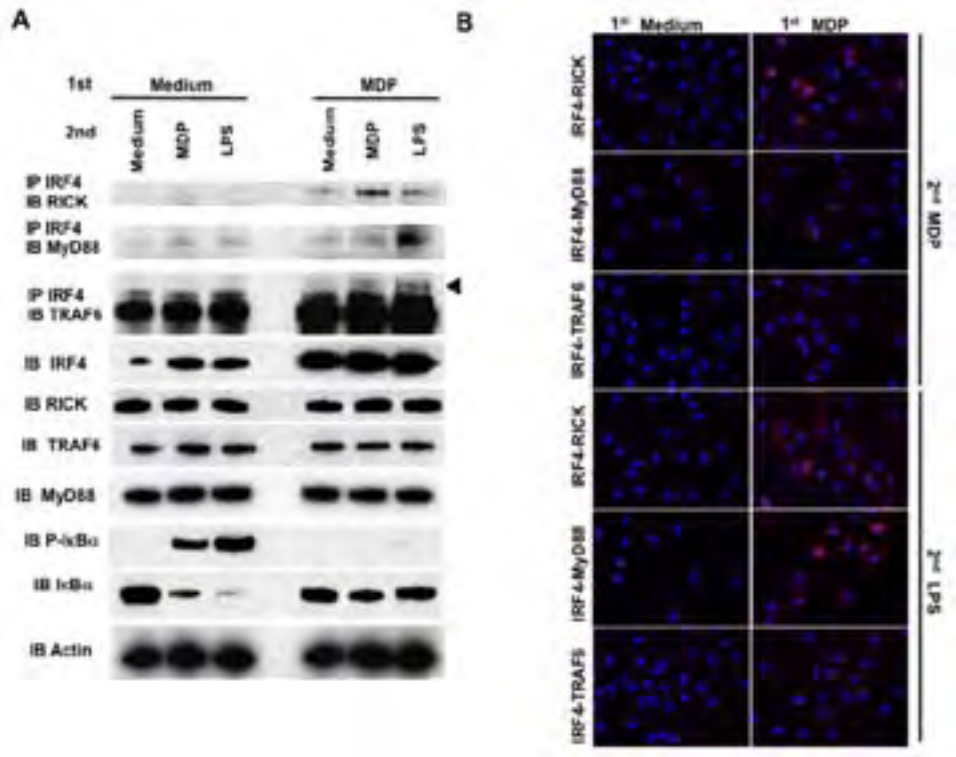

Figure 1. IRF4 expression induced by MDP activation of NOD2 and interaction between IRF4 and RICK, TRAF6, and MyD88

(A) Monocytes isolated from healthy individuals were cultured in the presence of GM-CSF and IL-4 for 6 days to generate monocyte-derived dendritic cells (DCs). DCs (1×10^6/ml) were pre-treated with MDP (10 μg/ml) for 24 hours followed by stimulation with MDP (10 μg/ml) or LPS (1 μg/ml) for 30 minutes; whole cell lysates were subjected to immunoprecipitation (IP) with the indicated Ab followed by immunoblotting (IB) with the indicated Ab. The arrow shows TRAF6-specific bands. (B) Human DCs were treated as described in (A). Interaction between IRF4 and RICK, TRAF6, and MyD88 was visualized in immunofluorescence microscopy by the Duolink assay. Magnification x800. Results shown are representative of at least two experiments.

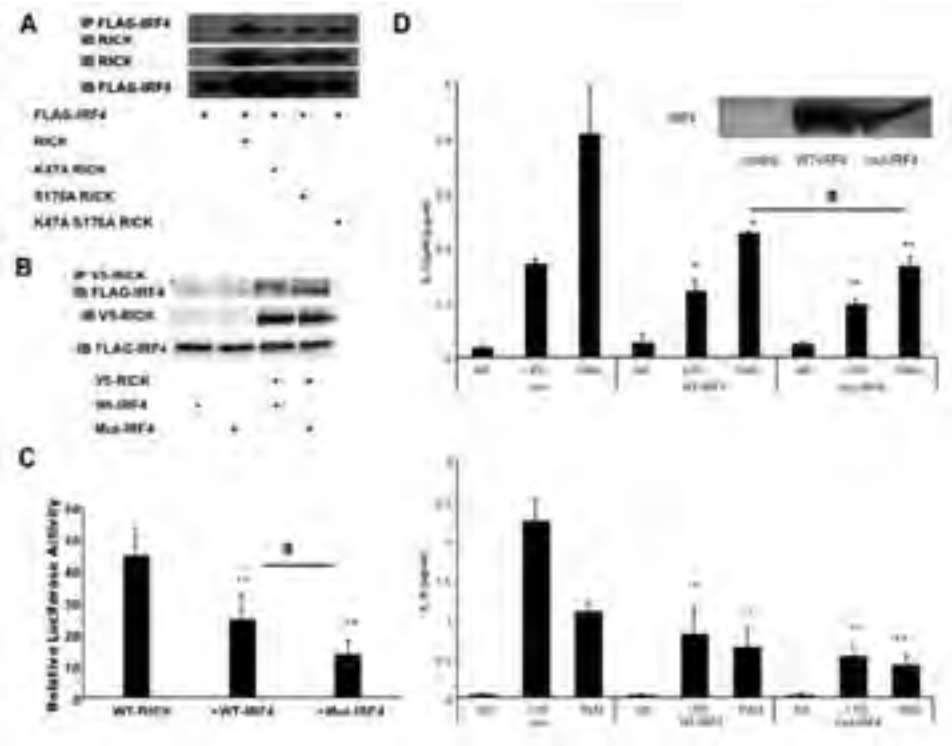

Figure 2. Phosphorylation of IRF4 is not necessary for its negative regulatory activity

(A) 293 cells were transfected with vectors expressing FLAG-tagged IRF4 and several forms of mutated RICK. Whole cell lysates were isolated 48 hours after the transfection and were subjected to immunoprecipitation (IP) with the indicated Ab followed by immunoblotting (IB) with the indicated Ab. (B) 293 cells were transfected with vectors expressing either wild type-IRF4 (Wt-IRF4) or Mutated-IRF4 (Mut-IRF4) in which serine residues at 447 and 448 are replaced with alanine; whole cell lysates were isolated 48 hours after transfection and were subjected to IP with anti-V5 Ab followed by IB with the indicated Ab. (C) HT29 cells were transfected with either empty control vector, Wt-IRF4 or Mut-IRF4 expressing vector together with RICK expressing vector, NF-κB luciferase reporter vector and pSV-β-galactosidase vector. The cells were then cultured for 24 hours after which relative luciferase activity values were calculated. Results are expressed as mean ± SD. **P<0.01, as compared with cells transfected with RICK vector alone. # P<0.01. (D) THP1 cells were transfected with either empty control (con) vector, wt-IRF4 or mut-IRF4 vector. The cells were then stimulated with LPS or Pam_3CSK4 (PAM) for 24 hours after which culture fluids were analyzed for cytokine concentration by ELISA. NS; no stimulation. Results were expressed as mean ± SD. *P<0.05, **P<0.01, as compared with control vector. # P<0.01. Results shown are representative of at least two experiments.

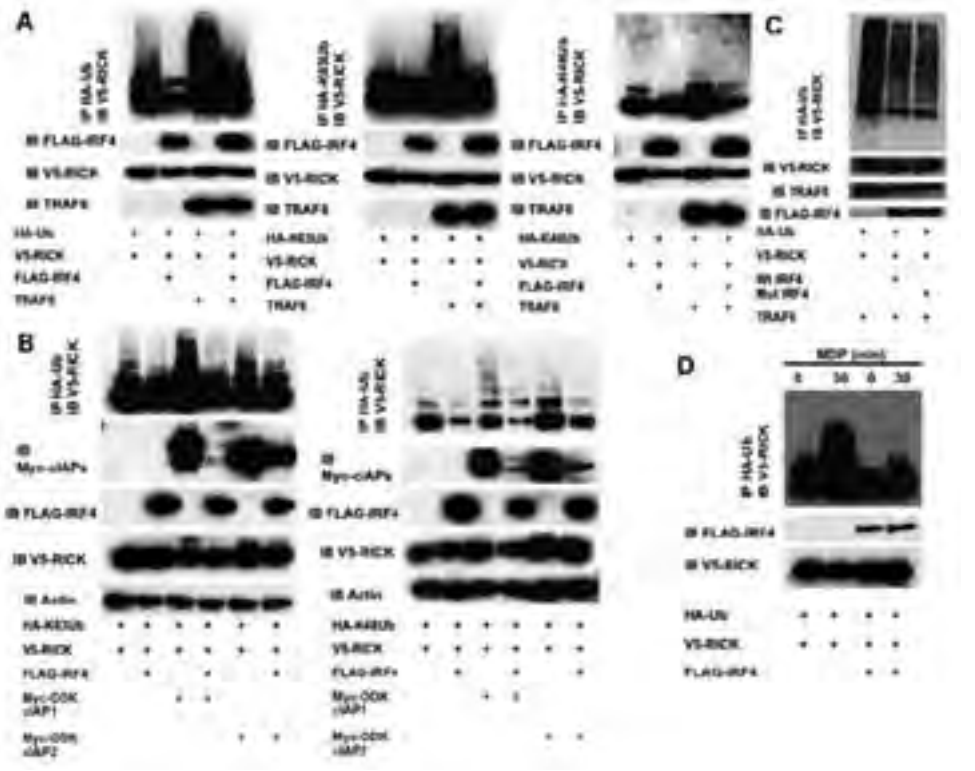

Figure 3. IRF4 regulates polyubiquitination of RICK

(A) 293 cells (1×10^6/6 well plate) were transfected with vectors (1 μg) expressing HA-tagged wild type ubiquitin (Ub), K48 Ub, K63 Ub, FLAG-tagged IRF4, V5-tagged RICK, and TRAF6; whole cell lysates were prepared 48 hours after the transfection and subjected to immunoprecipitation (IP) with the indicated Ab followed by immunoblotted (IB) with the indicated Ab. (B) 293 cells (1×10^6/6 well plate) were transfected with vectors (1 μg) expressing FLAG-tagged IRF4, Myc-DDK-tagged cIAP1, Myc-DDK-tagged cIAP2, V5-tagged RICK, and HA-tagged K48 or K63 Ub; whole cell lysates were subjected to IP with the indicated Ab followed by IB with the indicated Ab. (C) 293 cells (1×10^6/6 well plate) were transfected with vectors (1 μg) expressing HA-tagged wild type Ub, V5-tagged RICK, TRAF6, FLAG-tagged IRF4, FLAG-tagged mutated IRF4 (Mut IRF4) in which serine residues at 447 and 448 are replaced with alanine; whole cell lysates were prepared 48 hours after the transfection and subjected to IP with the indicated Ab followed by IB with the indicated Ab. (D) 293 cells stably expressing NOD2 (1×10^6/6 well plate) were transfected with vectors (1 μg) expressing HA-tagged wild type Ub, FLAG-tagged IRF4, and V5-tagged RICK. 48 hours after the transfection, cells were stimulated with MDP (10 μg/ml) for 30 min; whole cell lysates were subjected to IP with the indicated Ab followed by IB with the indicated Ab. Results shown are representative of two experiments.

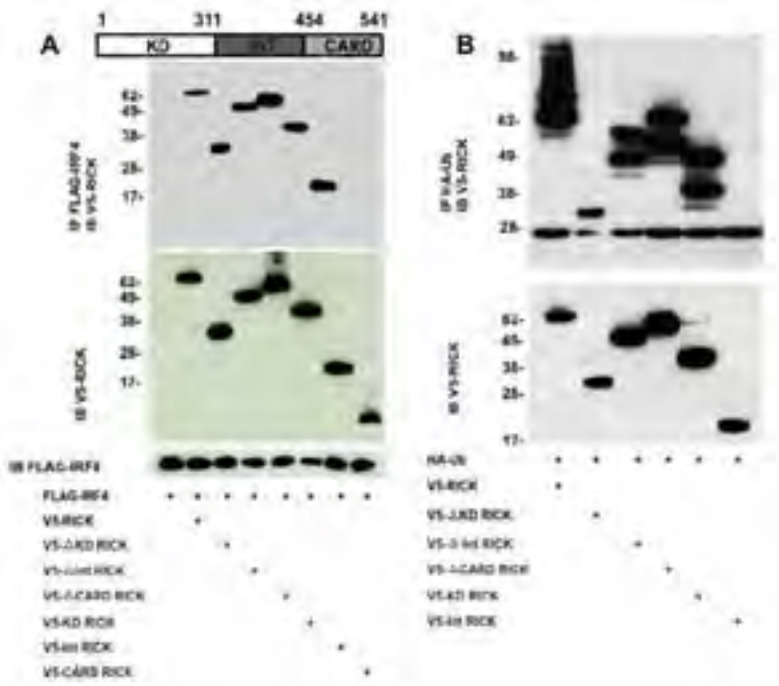

Figure 4. IRF4 inhibition of RICK polyubiquitination is facilitated by IRF4 binding to the kinase and/or intermediate domains of RICK

(A) 293 cells were transfected with vectors expressing FLAG-tagged IRF4 and various forms of V5-tagged mutated RICK; whole cell lysates were isolated 48 hours after the transfection and were then subjected to immunoprecipitation (IP) with the indicated Ab followed by immunoblotting (IB) with the indicated Ab. (B) 293 cells were transfected with vectors expressing various forms of V5-tagged mutated RICK and HA-tagged Ub; whole cell lysates were isolated 48 hours after the transfection and were subjected to IP with the indicated Ab followed by IB with the indicated Ab. Results shown are representative of two experiments.

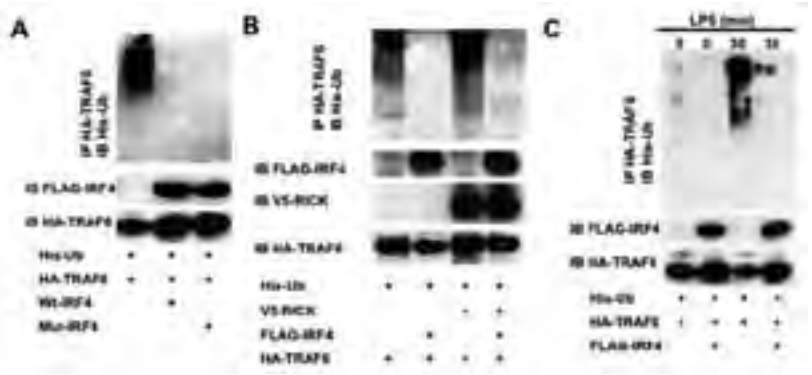

Figure 5. IRF4 regulates polyubiquitination of TRAF6

(A, B) 293 cells (1×10^6/6 well plate) were transfected with vectors (1 μg) expressing His-tagged wild type ubiquitin (Ub), FLAG-tagged IRF4, V5-tagged RICK and HA-tagged TRAF6; whole cell lysates were prepared 48 hours after the transfection and subjected to IP with the indicated Ab followed by IB with the indicated Ab. (C) 293 cells stably expressing TLR4 (1×10^6/6 well plate) were transfected with vectors (1 μg) expressing His-tagged wild type Ub, FLAG-tagged IRF4, and HA-tagged TRAF6. 48 hours after the transfection, cells were stimulated with LPS (1 μg/ml) for 30 min; whole cell lysates were subjected to IP with the indicated Ab followed by IB with the indicated Ab. Results shown are representative of two experiments.

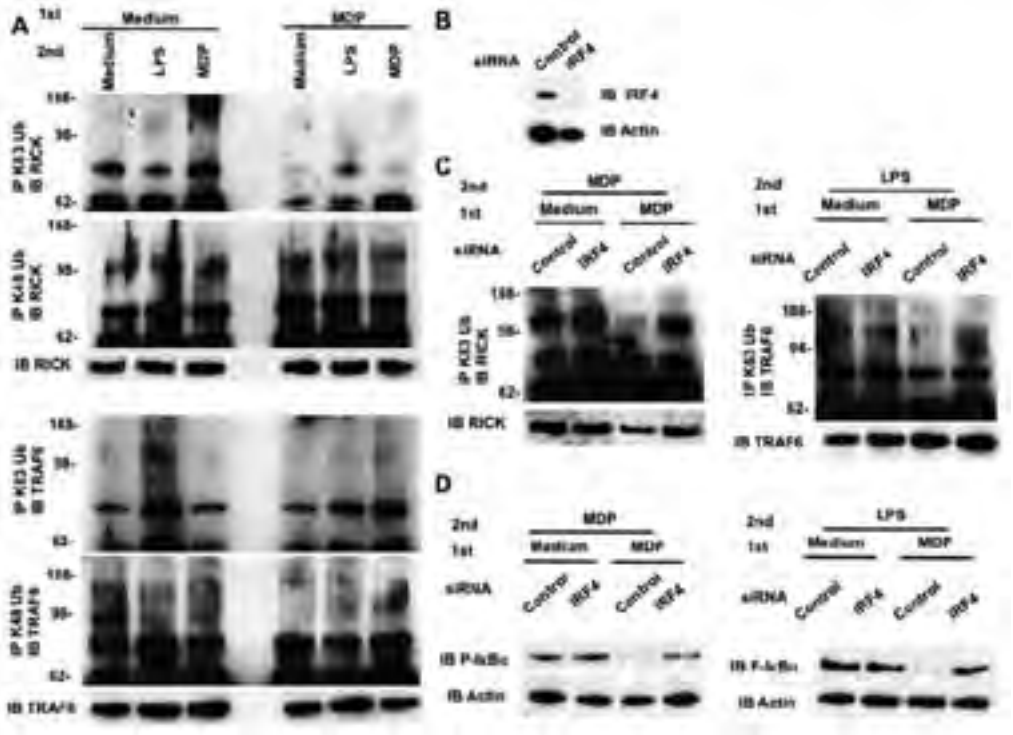

Figure 6. IRF4 expression induced by MDP activation of NOD2 inhibits K63-linked polyubiquitination of RICK and TRAF6

(A) Human monocyte-derived dendritic cells (DCs) were generated as described in Figure 1. DCs (1×10^6/ml) were pre-treated with MDP (10 μg/ml) for 24 hours followed by treatment with MG132 (10 μg/ml) for two hours and then were stimulated with MDP (10 μg/ml) or LPS (1 μg/ml) for 30 minutes. Whole cell lysates were subjected to immunoprecipitation (IP) with the indicated Ab followed by immunoblotted (IB) with the indicated Ab. (B) Human DCs were transfected with IRF4-specific siRNA or control siRNA (100 nM). One day after the transfection, DCs (1×10^6/ml) were treated with MDP (10 μg/ml) for 24 hours and then cell lysates were subjected to IB with the indicated Ab. (C) Human DCs were transfected with IRF4-specific siRNA or control siRNA (100 nM). One day after the transfection, DCs (1×10^6/ml) were pre-treated with MDP (10 μg/ml) for 24 hours followed by treatment with MG132 (10 μg/ml) for two hours and then were stimulated with MDP (10 μg/ml) or LPS (1 μg/ml) for 30 minutes; whole cell lysates were subjected to IP with the indicated Ab followed by IB with the indicated Ab. (D) Human DCs were transfected with IRF4-specific siRNA or control siRNA (100 nM). One day after the transfection, DCs (1×10^6/ml) were pre-treated with MDP (10 μg/ml) for 24 hours and then were stimulated with MDP (10 μg/ml) or LPS (1 μg/ml) for 30 minutes; whole cell lysates were subjected to IB with the indicated Ab. Results shown are representative of two experiments.

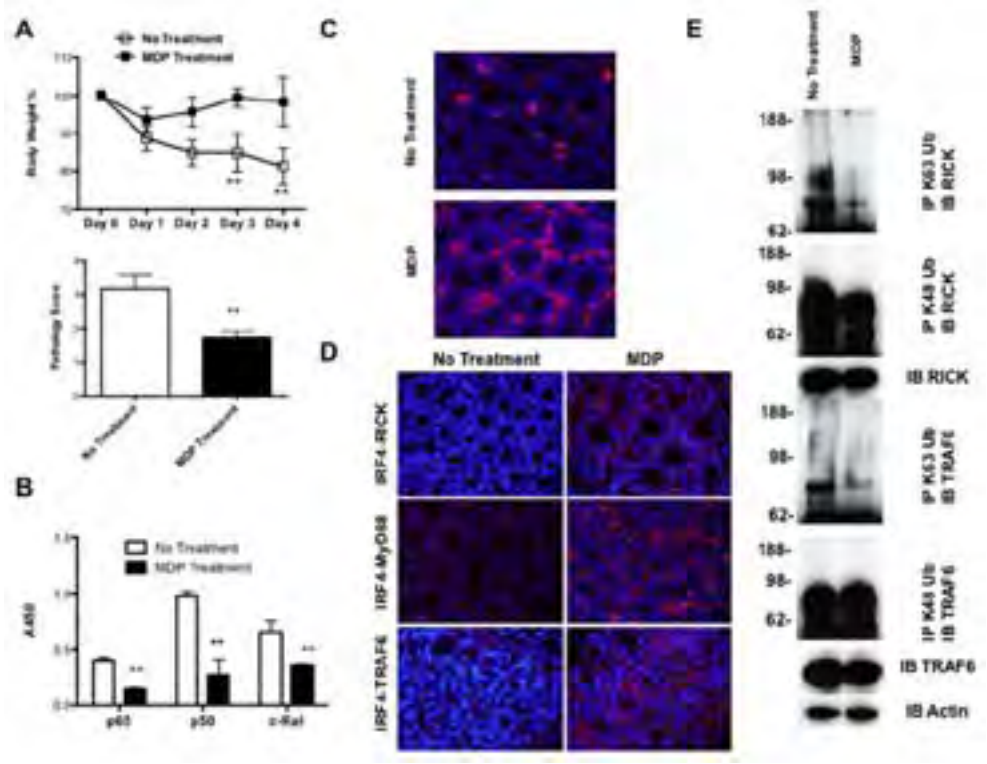

Figure 7. Administration of MDP protects mice from trinitrobenzene sulfonic acid (TNBS)-colitis via regulation of K63-linked polyubiquitination of RICK and TRAF6

C57BL/10 mice were administered MDP on days -2, -1, and 0 and then challenged with intra-rectal TNBS on day 0. (A) Upper panel: Changes in body weight of mice not-treated or treated with MDP (n=10) and challenged with intra-rectal administration of TNBS. Lower panel: Pathology scores of mice not-treated or treated with MDP on day 4. Results were expressed as means ± SD. ** $P<0.01$, as compared with untreated group. (B) NF-κB activation in colonic LPMCs in mice challenged with TNBS. Nuclear extracts were isolated from colonic LPMCs on day 1 and subjected to a Transfactor Binding Assay. Results are expressed as means ± SD. ** $P<0.01$, as compared with untreated group. (C) IRF4 expression in the colonic tissue of mice challenged with TNBS on day 1. (D) Interaction between IRF4 and RICK, MyD88, and TRAF6 in the colonic tissue of TNBS-challenged mice on day 1. Molecular interactions were visualized by Duolink assay (red color). (E) K48- or K63-linked polyubiquitination of RICK and TRAF6 in colonic LPMCs of TNBS-challenged mice. Whole cell lysates prepared from colonic LPMCs on day 1 were subjected to immunoprecipitation (IP) with the indicated Ab followed by immunoblotting (IB) with the indicated Ab.

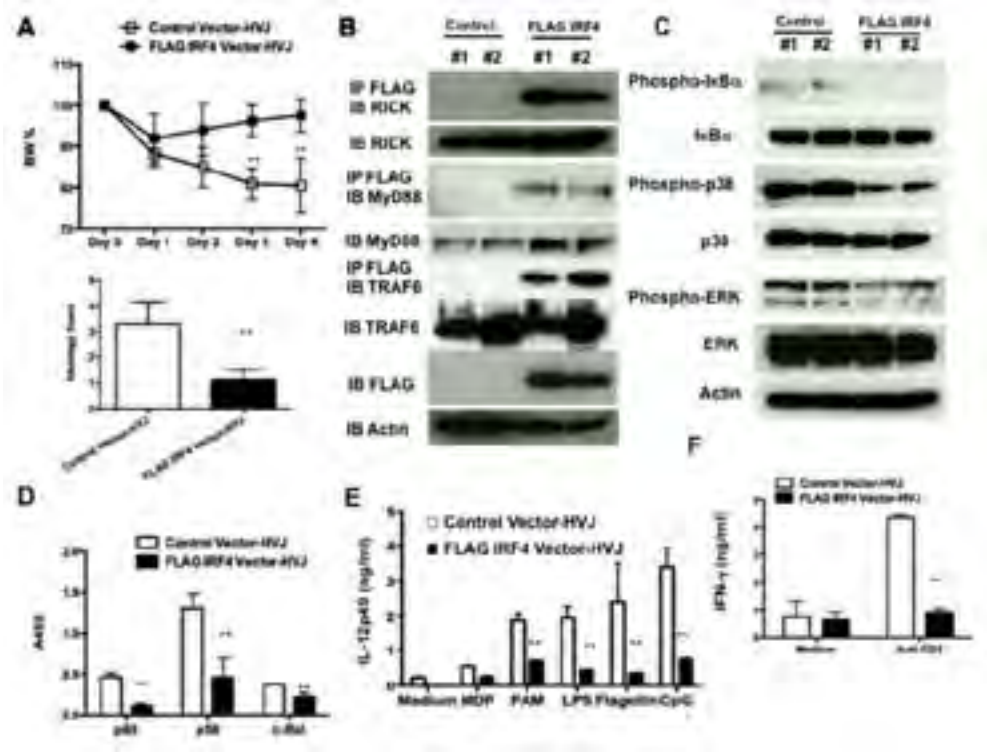

Figure 8. Prevention of TNBS-colitis by administration of an IRF4-expressing plasmid

C57BL/10 mice were administered HVJ-encapsulated FLAG-tagged IRF4 vector or control vector via the intra-rectal route on days -2, -1, and 0 and then challenged with intra-rectal TNBS on day 0. (A) Changes of body weight in mice (n=5; each group, top panel) and pathology scores of mice on day 4. Results were expressed as means ± SD. ** P<0.01, as compared with control vector group. (B) Interaction between FLAG-tagged IRF4 and RICK, MyD88, and TRAF6 in the colonic tissue of mice. Whole protein lysates were prepared from the colon tissues of TNBS-challenged mice on day 2 and were subjected to immunoprecipitation (IP) with the indicated Ab followed by immunoblotting (IB) with the indicated Ab. Two colon extracts from each group were used for the assay. (C) Activation of NF-κB and MAPK in the colon tissues of TNBS-challenged mice on day 2. Two colon extracts from each group were used for the immunoblotting. (D) NF-κB activation in colon tissues in mice challenged with TNBS. Nuclear extracts were isolated from colon tissues on day 2 and subjected to a Transfactor Binding Assay. Results were expressed as means ± SD. ** P<0.01, as compared with control vector group. (E, F) Production of IL-12p40 and IFN-γ by colon LPMCs isolated from TNBS-challenged mice on day 4. Colon LPMCs (1×10^6/ml) were stimulated with MDP, PAM, LPS, Flagellin, and CpG for 24 hours or with anti-CD3 Ab for 48 hours after which culture fluids were assayed for IL-12p40 or IFN-γ levels by ELISA, as indicated. Results were expressed as means ± SD. ** P<0.01, as compared with group administered control vector. Results shown are representative of two experiments.

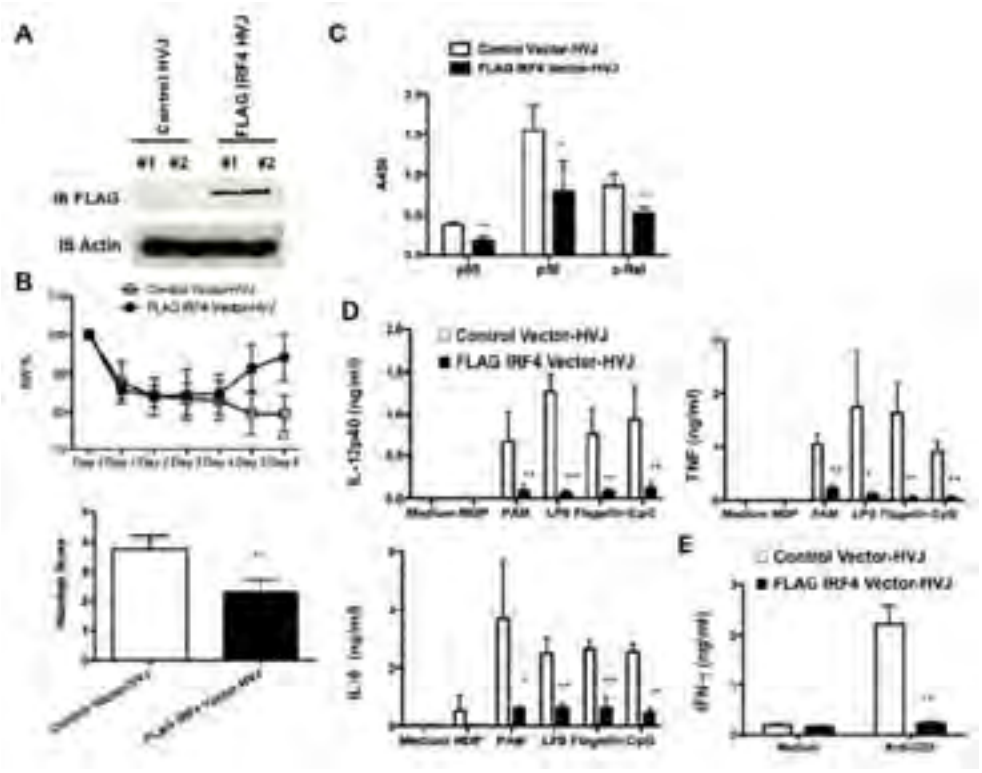

Figure 9. Treatment of TNBS-colitis by administration of an IRF4-expressing plasmid

C57BL/10 mice were administered HVJ-encapsulated FLAG-tagged IRF4 vector or control vector via the intra-rectal route on day 3 after challenge with TNBS on day 0. (A) Expression of FLAG-tagged IRF4 in the colonic tissues of mice. Whole protein lysates were prepared from the colonic tissues of TNBS-challenged mice on day 6 and were subjected to immunoblotting. Two colonic extracts from each group were used for the immunoblotting. (B) Changes of body weight in mice (n=7; each group, top panel) and pathology scores of mice on day 6. Results were expressed as means ± SD. Results shown are a pool of two independent experiments. **P<0.01, as compared with control vector group. (C) NF-κB activation in colon tissues in mice challenged with TNBS. Nuclear extracts were isolated from colon tissues on day 6 and subjected to Transfactor binding assay. Results were expressed as means ± SD. *P<0.05, **P<0.01, as compared with control vector group. (D, E) Production of IL-12p40, TNF, IL-6 and IFN-γ by mesenteric lymph node (MLN) cells isolated from TNBS-challenged mice on day 6. MLN cells (2×10^6/ml) were stimulated with MDP, PAM, LPS, Flagellin, and CpG for 24 hours to determine the protein levels of IL-12p40, TNF and IL-6. Cells were also stimulated with anti-CD3 Ab for 48 hours to determine the protein levels of IFN-γ. Results were expressed as means ± SD. *P<0.05, **P<0.01, as compared with control vector group.

J Gastroenterol (2014) 49:1578–1587
DOI 10.1007/s00535-014-0936-0

ORIGINAL ARTICLE—LIVER, PANCREAS, AND BILIARY TRACT

Comparison of systems for assessment of post-therapeutic response to sorafenib for hepatocellular carcinoma

Tadaaki Arizumi · Kazuomi Ueshima · Haruhiko Takeda · Yukio Osaki · Masahiro Takita · Tatsuo Inoue · Satoshi Kitai · Norihisa Yada · Satoru Hagiwara · Yasunori Minami · Toshiharu Sakurai · Naoshi Nishida · Masatoshi Kudo

Received: 23 August 2013 / Accepted: 9 January 2014 / Published online: 6 February 2014

Abstract
Background To test the hypothesis that use of the response evaluation criteria in cancer of the liver (RECICL), an improved evaluation system designed to address the limitations of the response evaluation criteria in solid tumors 1.1 (RECIST1.1) and modified RECIST (mRECIST), provides for more accurate evaluation of response of patients with hepatocellular carcinoma (HCC) to treatment with sorafenib, a molecularly targeted agent, as assessed by overall survival (OS).
Methods The therapeutic response of 156 patients with advanced HCC who had been treated with sorafenib therapy for more than 1 month was evaluated using the RECIST1.1, mRECIST, and RECICL. After categorization as showing progressive disease (PD), stable disease (SD), or objective response, the association between OS and categorization was examined using the Kaplan–Meier method to develop survival curves. The 141 cases categorized as PD or SD by the RECIST1.1, but objective response by the mRECIST and RECICL, were further analyzed for determination of the association between OS and categorization.
Results Only categorization using the RECICL was found to be significantly correlated with OS ($p = 0.0033$). Among the patients categorized as SD or PD by the RECIST1.1, reclassification by the RECICL but not the mRECIST was found to be significantly associated with OS and allowed for precise prediction of prognosis ($p = 0.0066$).
Conclusions Only the use of the RECICL allowed for identification of a subgroup of HCC patients treated with sorafenib with improved prognosis. The RECICL should, therefore, be considered a superior system for assessment of therapeutic response.

Keywords Hypervascular lesion · Liver cirrhosis · Response evaluation criteria in solid tumors · Response evaluation criteria in cancer of the liver · Tumor viability

Abbreviations

CE-CT	Contrast-enhanced computed tomography
CI	Confidence interval
CR	Complete response
DCR	Disease control rate
Gd-EOB-DTPA	Gadolinium ethoxybenzyl diethylenetriamine pentaacetic acid
HCC	Hepatocellular carcinoma
mRECIST	Modified RECIST
MRI	Magnetic resonance imaging
OR	Objective response
ORR	Objective response rate
OS	Overall survival
PD	Progressive disease
PR	Partial response

Electronic supplementary material The online version of this article (doi:10.1007/s00535-014-0936-0) contains supplementary material, which is available to authorized users.

T. Arizumi · K. Ueshima · M. Takita · T. Inoue · S. Kitai · N. Yada · S. Hagiwara · Y. Minami · T. Sakurai · N. Nishida · M. Kudo (✉)
Department of Gastroenterology and Hepatology, Kinki University Faculty of Medicine, 377-2 Ohno-higashi, Osaka-sayama, Osaka 589-8511, Japan
e-mail: m-kudo@med.kindai.ac.jp

H. Takeda · Y. Osaki
Department of Gastroenterology and Hepatology, Osaka Red Cross Hospital, 5-53 Fudegasaki-cho, Tennoji-ku, Osaka 543-8555, Japan

SD	Stable disease
RECICL	Response evaluation criteria in cancer of the liver
RECIST1.1	Response evaluation criteria in solid tumors 1.1
RFA	Radiofrequency ablation

Introduction

Hepatocellular carcinoma (HCC) is the third most common cause of cancer mortality worldwide [1], and a considerable number of patients continue to be diagnosed with advanced disease. Recently, sorafenib has been shown to improve the survival of patients with advanced-stage HCC [2]. The effectiveness is attributed to its unique antiproliferative and antiangiogenic mechanism [3–9].

Although the extent of tumor reduction observed with sorafenib therapy has been unsatisfactory, previous trials found that sorafenib significantly improved overall survival (OS) [2, 10]. Indeed, it has become well known that improvement in objective response (OR) without shrinkage of a tumor is a unique characteristic of this drug. As reduction in tumor vascularity appears to be direct effect of sorafenib, it is reasonable to speculate that the longer OS obtained with sorafenib can be attributed to its unique antiangiogenic mechanism, in addition to its antiproliferative effect on cancer cells. As increased tumor viability is typically accompanied by an increase in arterial vascularity, evaluation of arterial enhancement on imaging is critical in predicting OS. However, the response evaluation criteria in solid tumors 1.1 (RECIST1.1), the first set of criteria developed for assessment of response to treatment by HCC patients, focuses on assessment of tumor size and neglects consideration of changes in vascularity status.

In recognition that the vascularity of a lesion is important in evaluating response to HCC treatment, the modified-RECIST (mRECIST) requires assessment of tumor vascularity, which reflects the extent of tumor necrisis [11, 12]. However, use of the mRECIST still poses a difficulty in measuring irregularly shaped tumors, because it calls for unidirectional measurement of tumor size for overall evaluation of tumor burden. Therefore, use of the mRECIST, as well as the RECIST1.1, may not provide for completely adequate evaluation of tumor response in HCC patients.

To overcome the disadvantages of using the conventional criteria, we designed the response evaluation criteria in cancer of the liver (RECICL), a new evaluation system based on evaluation of change in tumor vascularity together with 2-directional assessment of tumor size. Due to the inclusion of these criteria, we hypothesized that use of the RECICL provides for more accurate evaluation of response to sorafenib therapy as assessed by OS than the RECIST1.1 or mRECIST. By testing this hypothesis, we attempted to fulfill 2 research aims in the present study. First, we endeavored to determine the means by which the therapeutic response of HCC patients, especially those presenting with hypervascular lesions and/or with lesions of irregular shape, should be estimated in the context of accurate prediction of OS. Second, we attempted to clarify the significance of and identify any problems with the use of the RECICL by retrospective comparison of its use with that of the RECIST1.1 and mRECIST criteria for evaluation of response among the same cohort of HCC patients.

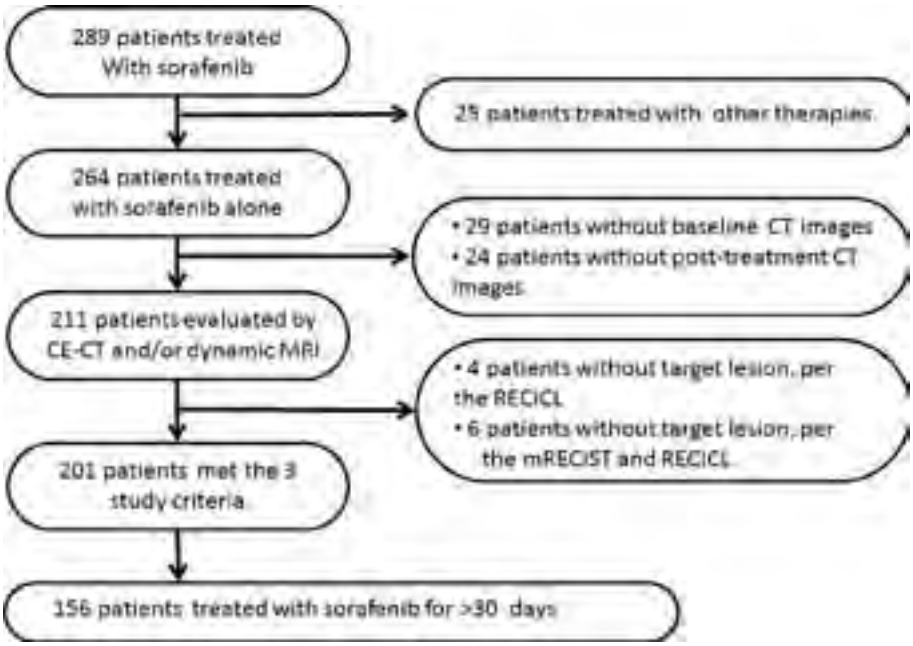

Fig. 1 Flow chart of patient selection process. After exclusion of patients who met the exclusion criteria or did not meet the inclusion criteria, 156 patients remained for analysis

Materials and methods

Patients

Between May 2009 and August 2011, 289 patients with advanced HCC had been treated with sorafenib therapy at Kinki University Hospital or Osaka Red Cross Hospital. From among these patients, 156 patients who had undergone continuous administration of sorafenib for more than 1 month and met the inclusion criteria were selected for study enrollment. The response of all patients to sorafenib had been examined at least once using contrast-enhanced computed tomography (CE-CT) and/or dynamic magnetic resonance imaging (MRI), both are imaging techniques (Fig. 1). Patients' characteristics are summarized in Table 1. Our institution did not require institution approval or informed consent for review of patient records and images in this retrospective study. We posted research content at outpatient areas and a website, and we gave patients the right to refusal for our study.

The inclusion criteria for this study were (1) diagnosis of HCC based on histological examination or radiologic findings showing early enhancement, followed by late wash-out on CE-CT or dynamic MRI, in conjunction with HCC refractory to radiofrequency ablation (RFA) and transarterial chemoembolization based on the indication of sorafenib; (2) performance status of 0 or 1; and (3) Child-Pugh class A or B liver cirrhosis. The exclusion criteria were (1) concomitant antineoplastic treatment; (2) transarterial chemoembolization or RFA performed less than 3 months before initiation of sorafenib; (3) lack of response evaluation using CE-CT or dynamic MRI during follow-up period; or (4) both the presence of extrahepatic lesions and the absence of intrahepatic lesions.

Initial and follow-up assessment

Liver function and tumor stage were evaluated using the Child-Pugh, Barcelona Clinic for Liver Cancer, and Cancer of the Liver Italian Program classifications. Two independent radiologists evaluated tumor size and vascularity every 4–6 weeks during and after treatment using the images of CE-CT and gadolinium ethoxybenzyl diethylenetriamine pentaacetic acid (Gd-EOB-DTPA)-MRI. In this study, we retrospectively determined the best response during the sorafenib treatment and adopted it as the overall response. The responses of all patients were evaluated using RECIST1.1, mRECIST, and RECICL criteria by evaluators who were not blind to the patients' diagnoses. The target lesions of each case were defined by 2 physicians by review of CE-CT and/or dynamic MRI images obtained during pretreatment. OS analysis was based on the length of time from initial treatment until time of death,

Table 1 Characteristics of hepatocellular carcinoma patients treated with sorafenib

	Number of cases (%)
Age	
Median (25–75 %)	73 (66–78)[a]
Gender	
Male	120 (76.9)
Female	36 (23.1)
ECOG PS	
0	150 (96.2)
1	5 (3.2)
2	1 (0.6)
Child-Pugh class	
A	129 (82.7)
B	27 (17.3)
Virus status[b]	
HBV	22 (14.1)
HCV	90 (57.7)
Virus negative	44 (28.2)
TNM stage	
I	5 (3.2)
II	34 (21.8)
IIIA	33 (21.2)
IIIB	4 (2.6)
IIIC	29 (18.6)
IV	51 (32.7)
CLIP score	
0	6 (3.8)
1	59 (37.8)
2	54 (28.9)
3	26 (16.7)
4	10 (6.4)
5	1 (0.6)
BCLC stage	
A	39 (25)
B	36 (23.1)
C	81 (51.9)
Starting dose of sorafenib (mg)	
200	4 (2.6)
400	83 (53.2)
800	69 (44.2)
Total dose of sorafenib (g)	
Median (25–75 %)	66.8 (38.8–135.6)[a]
Serum AFP level (ng/m)	
Median (25–75 %)	115 (12–2230)[a]
Serum DCP (mAU/ml)	
Median (25–75 %)	786 (46–4853)[a]

ECOG Eastern Cooperative Oncology Group, *PS* performance status, *AFP* alpha fetoprotein, *DCP* des-gamma carboxyprothrombin, *BCLC* Barcelona Clinic for Liver Cancer, *CLIP* Cancer of the Liver Italian Program, *HBV* hepatitis B virus, *HCV* hepatitis C virus

[a] Dispersion variables are shown as median values (25–75 %)

[b] Cases testing positive for hepatitis B virus surface antigen (HBsAg) were regarded as cases of HBV-related HCC and cases testing positive for hepatitis C antibody (HCV Ab) were regarded as cases of HCV-related HCC

and OS analysis of patients who were alive at the end of the observation was based on the length of time from initial treatment until time of the final hospital visit.

Response evaluation using the RECIST1.1, mRECIST, and RECICL

The differences among the RECIST1.1, mRECIST, and RECICL are summarized in Supplementary Table 1. Briefly, both the RECIST1.1 and mRECIST call for unidirectional measurement of tumors, but the RECIST1.1 does not require evaluation of tumor viability while the mRECIST requires evaluation of only those areas of the tumor showing arterial enhancement on CE-CT or dynamic MRI. In contrast, the RECICL requires 2-directional measurement of tumors showing arterial enhancement. Representative images of the cases evaluated by the RECIST1.1, mRECIST, and RECICL are shown in Supplementary Figure 1. As can be observed, use of the RECIST1.1 called for unidirectional measurement of both enhanced and necrotic lesions, which showed no change before and after treatment (Supplementary Figures 1A and 1B). On the other hand, use of the mRECIST and RECICL required evaluation of tumor enhancement, which revealed a response according to the mRECIST and RECICL criteria (Supplementary Figures 1C and 1D for mRECIST and Supplementary Figures 1E and 1F for RECICL). Unlike the mRECIST, which does not require evaluation of lesions that do not show enhancement, the RECICL considers tumors not showing enhancement to be viable if they increase in size after initiation of therapy, as demonstrated in Supplementary Figure 2.

Definition of terms

Complete response (CR) was defined as disappearance of all lesions by the RECIST1.1, as disappearance of any arterial enhancement within all target lesions by the mRECIST, and as either a 100 % tumor necrotizing effect or a 100 % reduction in tumor size accompanied by disappearance of all contrast enhancement at any phase by the RECICL. Partial response (PR) was defined as 30 % or greater decrease in tumor size as determined by evaluation of the sum of the diameters of the target lesions, whose size was estimated using unidirectional measurement, by both the RECIST1.1 and mRECIST, and as 50 % or greater reduction in tumor necrosis or size as determined by 2-directional measurement by the RECICL. Progressive disease (PD) was defined as 20 % or greater increase in tumor size as determined by evaluation of the sum of the maximal dimensions of the target lesions by both the RECIST1.1 and mRECIST and as either a 25 % or greater increase in tumor size or the appearance of 1 or more new lesions by the RECICL. The RECIST1.1, mRECIST, and the RECICL all defined stable disease (SD) as the absence of either PR or PD; OR as the sum of all cases showing CR and PR; objective response rate (ORR) as the percentage of OR among all cases; and disease control rate (DCR) as the percentage of cases showing CR, PR, or SD.

Statistical analysis

Univariate survival curves were estimated using the Kaplan–Meier method, comparison of survival rates among groups was conducted using the log-rank test, and comparison of categorical variables was performed using the Chi Square test. The level of significance was set at $p < 0.05$. All analyses were performed using SAS statistical software version 8.2 (SAS Institute, Cary, NC, USA) or the SPSS Medical Pack for Windows version 10.0 (SPSS, Inc., Chicago, IL, USA).

Results

Evaluation of response by the RECIST1.1, mRECIST, and RECICL

Of the 156 patients who had been successfully treated with sorafenib therapy for more than 30 days, the number of patients showing CR, PR, SD, and PD and the ORR and DCR as estimated by use of each system were, respectively, as follows: 3, 12, 71, and 70 cases and 9.6 % and 55.1 % according to the RECIST1.1; 6, 30, 55, and 65 cases and 23.1 % and 58.3 % according to the mRECIST; and 6, 29, 53, and 68 cases and 22.4 % and 56.4 % according to the RECICL (Tables 2, 3). Although no statistically significant difference was observed among the DCR estimated by the 3 systems, 20 patients (approximately 14 %) classified as SD by the RECIST1.1 were classified as OR by the mRECIST and RECICL.

Table 2 Classification of response to sorafenib by the RECIST1.1, mRECIST, and RECICL

	Number of patients				Percentage (%)	
	CR	PR	SD	PD	ORR	DCR
RECIST1.1	3	12	71	70	9.6	55.1
mRECIST	6	30	55	65	23.1	58.3
RECICL	6	29	53	68	22.4	56.4

The number of the patients classified as CR, PR, SD, and PD using each system are shown. Objective response rate (ORR) is the percentage of patients evaluated as CR or PR. Disease control rate (DCR) is the percentage of patients evaluated as CR, PR, or SD

Table 3 Comparisons of the response classification between RECIST1.1 and RECICL (A), and between mRECIST and RECICL (B)

	No. of patients (%)				
	RECICL				Total RECIST1.1 evaluation
	CR	PR	SD	PD	
(A) RECIST1.1					
CR	3 (1.9)				3 (1.9)
PR	2 (1.3)	10 (6.4)			12 (7.7)
SD	1 (0.6)	17 (10.9)	51 (32.7)	2 (1.3)	71 (45.5)
PD		2 (1.3)	2 (1.3)	66 (42.3)	70 (44.9)
Total RECICL evaluation	6 (3.8)	29 (18.6)	53 (34.0)	68 (43.6)	156
	No. of patients (%)				
	RECICL				Total mRECIST evaluation
	CR	PR	SD	PD	
(B) mRECIST					
CR	6 (3.8)				6 (3.8)
PR		28 (17.9)		2 (1.3)	30 (19.2)
SD		1 (0.6)	51 (32.7)	3 (1.9)	55 (35.3)
PD			2 (1.3)	63 (40.4)	65 (41.7)
Total RECICL evaluation	6 (3.8)	29 (18.6)	53 (34.0)	68 (43.6)	156

Comparison of Kaplan–Meier curves for OS as estimated by the RECIST1.1, mRECIST, and RECICL

Figure 2 shows the Kaplan–Meier curves for OS as estimated using the 3 systems (Fig. 2a as estimated by the RECIST1.1, Fig. 2b by the mRECIST, and Fig. 2c by the RECICL). The median OS of the patients classified as OR, SD, and PD, respectively, by the 3 systems was 19.9 months [95 % confidence interval (CI) 12.5–21.3 months], 19.2 months (95 % CI 15.1–23.3 months), and 14.3 months (95 % CI 9.7–18.8 months) by the RECIST1.1; 27.2 months (95 % CI 15.2–39.2), 16.8 months (95 % CI 13.8–19.7 months), and 14.3 months (95 % CI 10.5–18.0) by the mRECIST; and 27.2 months (95 % CI 9.6–44.8 months), 19.2 months (95 % CI 17.1–21.3 months), and 14.3 months (95 % CI 10.1–18.4 months) by the RECICL. As shown in Figs. 2a, b, use of both the RECIST1.1 and mRECIST failed to allow for stratification of OS, although classification of response by the mRECIST was found to be more strongly associated with OS than that by RECIST1.1 ($p = 0.0575$ and $p = 0.073$ by log-rank test, respectively). On the other hand, classification of response by RECICL was found to be significantly associated with OS, with the patients showing OR found to have the longest survival and those showing PD the shortest ($p = 0.0033$ by log-rank test; Fig. 2c; Table 4). Regarding the treatment response determined by RECICL, the OS was significantly higher in the group of OR than in PD patients ($p = 0.002$). However, we could not detect the significant association between SD and OR, and PD for OS, although there were the trends of higher OS in the better response groups (respectively, $p = 0.093$, $p = 0.069$).

Inconsistency among classification by the RECIST1.1, mRECIST, and RECICL

Figure 3 shows the differences in response classification obtained using the RECIST1.1, mRECIST, and RECICL. As can be observed, most patients classified as either PD or SD by RECIST1.1 were classified as either CR or PR (i.e., as OR) by both the mRECIST and RECICL, leading 28 of 156 patients to be classified differently by the RECIST1.1 compared to the mRECIST and RECICL. Specifically, of the 141 patients classified as either PD or SD by the RECIST1.1, 21 of the patients classified as PD and 20 classified as SD were classified as OR by the mRECIST and RECICL (Fig. 3). This finding suggested the possibility that patients classified as OR by the mRECIST and/or RECICL, even those classified as SD or PD by the RECIST1.1, showed better prognosis than those classified as non-OR. To examine this possibility, Kaplan–Meier survival analysis was performed of cases classified as SD or PD by the RECIST1.1 for comparison of their classification by the mRECIST, and RECICL. Among the 141 patients classified as PD or SD by the RECIST1.1, the number of cases of OR, SD, and PD and the ORR and DCR was estimated at 17 cases, 55 cases, and 69 cases and 12.1 %

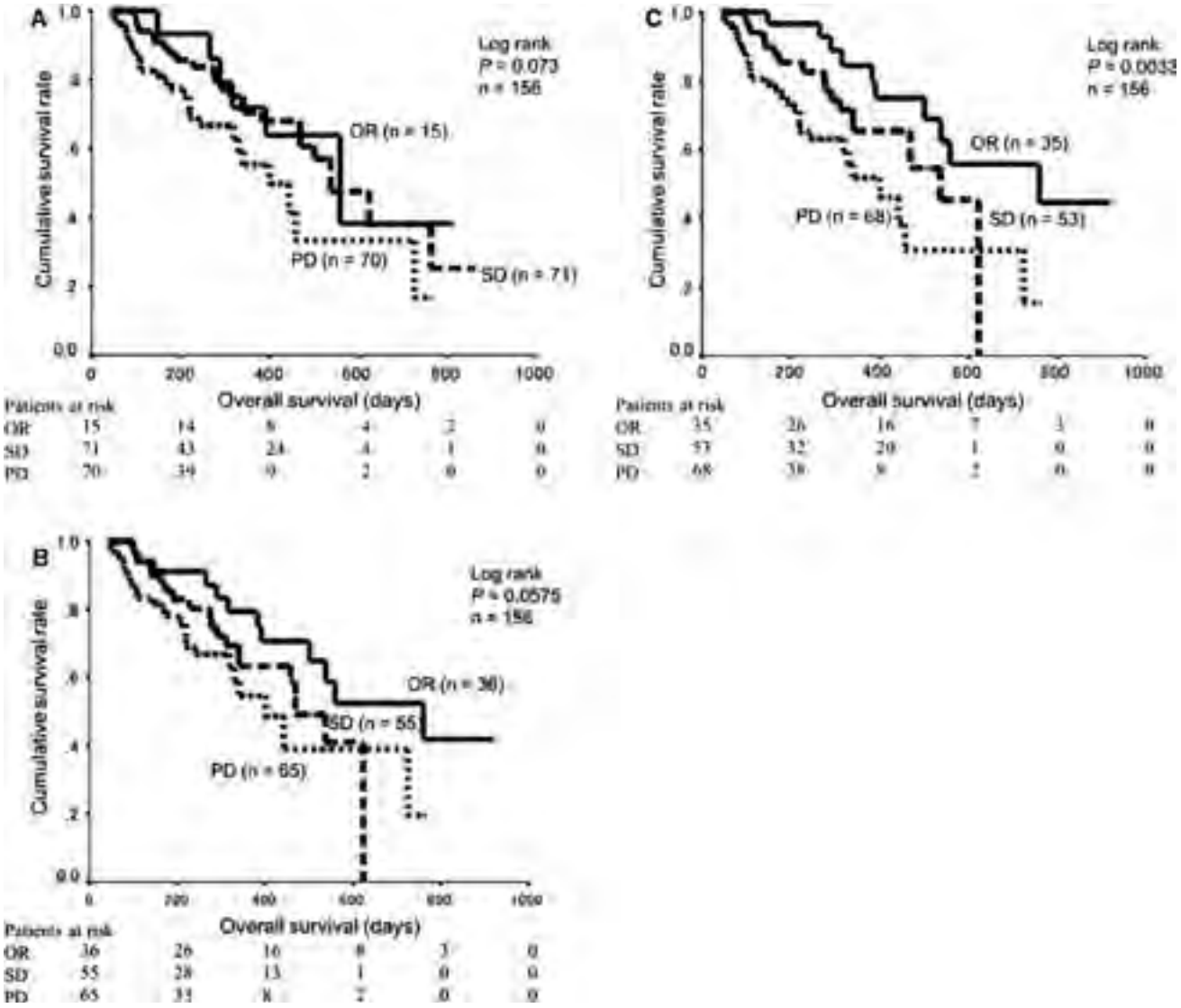

Fig. 2 Kaplan–Meier curves of overall survival based on response to treatment as estimated by the RECIST1.1, mRECIST, and RECICL. Kaplan–Meier curves of the overall survival of the 156 patients based on response to sorafenib therapy as estimated by the RECIST1.1 (**a**), mRECIST (**b**), and RECICL (**c**). The median OS of the patients classified as OR, SD, and PD, respectively, was 19.9 months, 19.2 months, and 14.3 months by the RECIST1.1 ($p = 0.073$ by log-rank test); 27.2 months, 16.8 months, and 14.3 months by the mRECIST ($p = 0.0575$); and 27.2 months, 19.2 months, and 14.3 months by the RECICL ($p = 0.0033$)

and 51.1 %, respectively, by the mRECIST and 15 cases, 56 cses, and 70 cases and 10.1 % and 50.3 %, respectively, by the RECICL.

Figure 4 shows the Kaplan–Meier curve for OS of these 141 patients as estimated by the mRECIST and RECICL. As can be observed, the median OS of patients classified as OR, SD, and PD was 27.2 months (95 % CI 11.7–42.7 months), 16.8 months (95 % CI 13.8–19.7 months), and 14.3 months (95 % CI 10.5–18.0 months), respectively, as estimated by the mRECIST and 27.2 months (95 % CI 11.9–42.5 months), 19.2 months (95 % CI 17.1–21.3 months), and 14.3 months (95 % CI 10.1–18.4 months), respectively, as estimated by the RECICL. Whereas classification of response by the mRECIST failed to allow for stratification of each type of response for OS ($p = 0.1124$; Fig. 4a), classification of response by RECICL was found to be significantly associated with OS, indicating that it allows for precise prediction of prognosis ($p = 0.0066$; Fig. 4b).

Discussion

For management of cancer chemotherapy, it is critical to have reliable tools to guide treatment planning in clinical practice. For this, OS should be considered as a critical

Table 4 Univariate and multivariate analyses for the contribution of clinical backgrounds and tumor response assessed by the three criteria on overall survivals

Variable	$N = 156$	Overall survival (days)		p value	Multivariate analysis		
		Median	95 % CI	Log rank	HR	95 % CI	p value
Age							
<73	77	399	292–505				
≥73	79	533	383–692	0.33			
Gender							
Male	120	409	308–5096				
Female	36	623	240–1005	0.45			
Child-Pugh stage							
A	129	457	359–554				
B	27	340	259–420	0.30			
Virus status†							
HBV	22	468	313–622				
Others	134	399	289–508	0.60			
HCV	90	361	243–478				
Others	66	468	349–586	0.49			
Negative	44	538	298–777				
Others	112	390	271–508	0.74			
TNM stage							
I, II, III	105	468	322–613				
IV	51	361	232–489	0.48			
CLIP score							
0, 1	65	538	–				
2, 3, 4, 5	91	341	238–443	0.004	1.475	0.76–2.86	0.25
0, 1, 2	119	500	418–581				
3, 4, 5	37	274	157–390	<0.001	2.139	1.07–4.24	**0.030**
BCLC stage							
A, B	75	538	338–737				
C	81	390	291–488	0.15			
A	39	–	–				
B, C	117	361	297–424	0.023	1.516	0.73–3.14	0.26
Starting dose of sorafenib (mg)							
200, 400	87	538	286–789				
800	69	409	282–535	0.85			
Total dose of sorafenib (g)							
<70	78	274	150–397				
≥70	78	538	435–640	<0.001	2.829	1.61–4.96	**<0.001**
AFP							
<100	79	500	435–564				
≥100	77	382	317–446	0.19			
DCP							
<800	77	538	453–622				
≥800	79	340	206–473	0.013	1.224	0.71–2.09	0.45
RECIST							
OR	15	–	–				
SD, PD	141	382	294–469	0.032	1.686	0.40–7.00	0.47
OR, SD	86	558	441–674				
PD	70	243	204–281	<0.001	1.284	0.24–6.87	0.77

Table 4 continued

Variable	$N = 156$	Overall survival (days)		p value	Multivariate analysis		
		Median	95 % CI	Log rank	HR	95 % CI	p value
mRECIST							
OR	36	558	337–778				
SD, PD	120	349	285–412	0.015	3.904	0.89–16.959	0.069
OR, SD	91	538	424–651				
PD	65	250	201–298	<0.001	1.274	0.438–3.704	0.65
RECICL							
OR	35	762	–				
SD, PD	121	341	276–405	<0.001	6.398	1.15–35.44	**0.034**
OR, SD	88	558	441–674				
PD	68	241	202–279	<0.001	1.915	0.40–9.10	0.41

The multivariate analysis revealed the CLIP score, a total dose of sorafenib and RECICL, as the independent factor contributing OS

HCV hepatitis C virus, *BCLC* Barcelona Clinic for Liver Cancer, *AST* aspartate aminotransferase, *ALT* alanine aminotransferase, *AFP* alpha fetoprotein, *DCP* des-gamma carboxyprothrombin

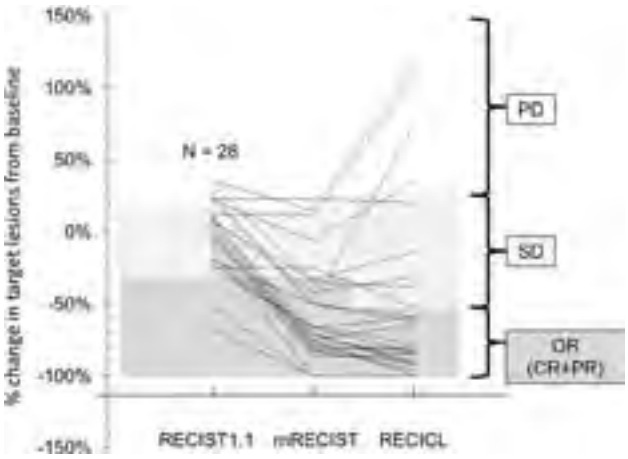

Fig. 3 Percentage change in tumor size of cases classified differently by the RECIST1.1, mRECIST, and RECICL. Percentage change in tumor size of 28 cases that were categorized differently by the RECIST1.1, mRECIST, and RECICL. The percentage change was calculated using the formula (tumor size post treatment – tumor size pretreatment)/tumor size pretreatment × 100 for estimation by the RECIST1.1 and mRECIST and the formula (tumor area post treatment—tumor area pretreatment/tumor area pretreatment × 100 for estimation by the RECICL. The *lower part* of the panel denotes the range of objective response (OR), the middle part of the panel the range of stable disease (SD), and the *upper part* the range of progressive disease (PD)

endpoint, although tumor response assessed by imaging was sometimes used as a surrogate endpoint so far. When the validity of the criteria in predicting OS in advanced HCC patients treated with sorafenib was compared, we found RECICL was the best criteria for the precise prediction of the prognosis of these patients compared to the RECIST1.1 and mRECIST.

In Western countries, World Health Organization criteria and the RECIST1.1 are commonly used for evaluation of treatment for liver cancer [13]. While their use has proven valuable in assessing response to conventional cytotoxic chemotherapy, there has been concern regarding their applicability to patients treated with recently developed molecularly targeted agents, such as sorafenib, which appear to have a "dormant" effect in that they initially appear to yield little response but ultimately lead to improvement in overall time to progression and OS [2, 10]. Sorafenib in particular has been a breakthrough agent in the treatment of advanced HCC, as demonstrated by the significant improvement in OS, despite the reporting of an ORR of only 2 % with its use [2, 10]. This observation of increased response to treatment has prompted use of imaging techniques, namely CE-CT and MRI, as an alternative method of assessing treatment response [14, 15]. While both mRECIST and RECICL incorporate vascularity as a factor in response assessment, the RECICL also calls for 2-directional measurement of tumor size and defines tumors that increase in size to be viable even if they do not show early enhancement upon imaging. The major advantage of use of the mRECIST and RECICL is that these call for evaluation of the contrast-enhancing portion of the tumor rather than evaluation of the entire tumor (Supplementary Figure 1) and consider tumor necrosis a sign of response. Such differences in criteria results in the ORR estimated using the mRECIST or RECICL to be approximately 2.5 times higher than that estimated using the RESICT1.1. Interestingly, the most significant association between tumor response and OS was found using the RECICL (Fig. 2c), although classification by mRECIST was found to be more strongly associated with

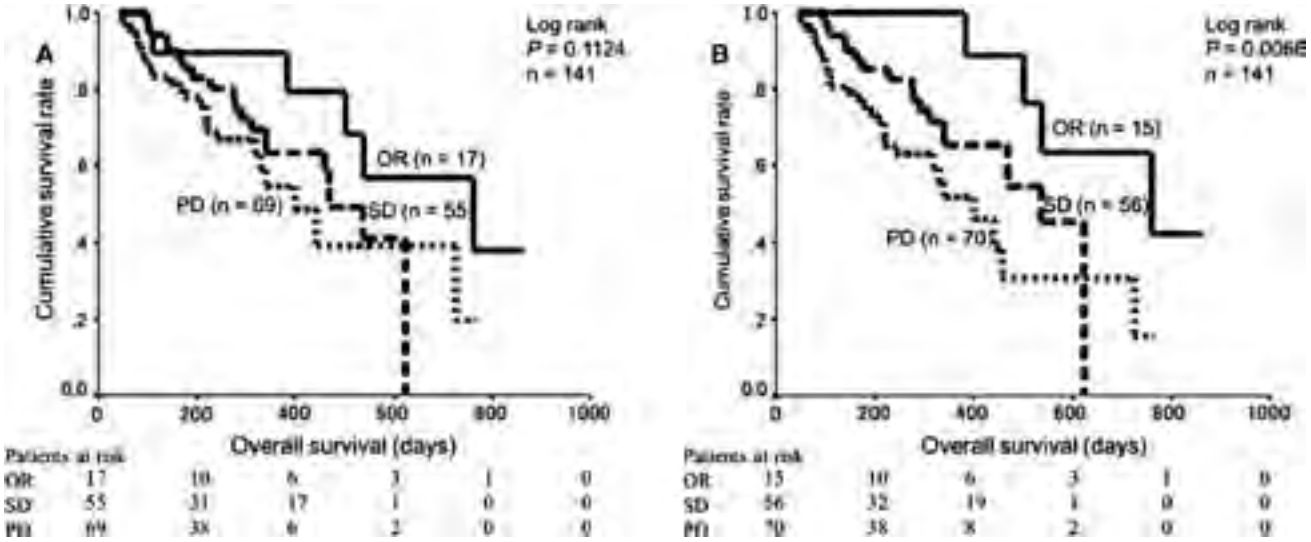

Fig. 4 Kaplan-Meier curves of overall survival of patients classified as SD or PD by the RECIST1.1 and as OR by the mRECIST and RECICL. Kaplan-Meier curves of 141 patients classified as SD or PD by the RECIST1.1 and as OR by the mRECIST (**a**) and RECICL. The median OS of patients classified as OR, SD, and PD was 27.2 months, 16.8 months, and 14.3 months, respectively, as estimated by the mRECIST ($p = 0.1124$ by log-rank test) and 27.2 months, 19.2 months, and 14.3 months, respectively, as estimated by the RECICL ($p = 0.0066$)

classification by RESICT1.1 (Fig. 2a, b). Therefore, it is reasonable to speculate that evaluation of tumor viability improves assessment of the antitumor activity of sorafenib by the mRECIST and RECICL but not by the RECIST1.1.

Another difference between the mRECIST and RECICL is that, while classification of response by the former is based on unidirectional measurement, that by the latter is based on 2-directional measurement. Moreover, while only the hypervascular area of the tumor is regarded as viable, and, thus, tumor viability is only estimated during the arterial phase, by the mRECIST, tumor viability is estimated at all phases by the RECICL. Supplementary Figs. 2 and 3 show examples of how use of the mRECIST and RECICL can lead to different classification of the same cases. In the case shown in Supplementary Fig. 3, marked reduction of tumor volume with enhancement was observed. Although the response was classified as SD by the mRECIST, it was classified as PR by the RECICL, as assessed by 2-directional measurement of size. Another advantage of using RECICL is that it calls for evaluation of non-enhanced areas of the target lesion, which are often found to have increased on post-therapeutic imaging. Indeed, some lesions that appear hypovascular on CE-CT are found to have increased in size and should, thus, be regarded as viable (Supplementary Figure 2). Therefore, patients classified as PR by the mRECIST would be classified as PD by the RECICL, indicating that use of the RECICL allows for more accurate categorization of response than the mRECIST for assessment of OS. Indeed, use of the RECICL was found to allow for successful discrimination of patients with tumor progression among the patients who had been classified as SD by the mRECIST.

There should be three limitations regarding the assessment by RECICL. First, the assessment of RECICL focus only on the measurable intrahepatic lesions without evaluating the portal vein thrombi and extrahepatic lesions. Second, a hypovascular HCC such as sarcomatoid HCC should be difficult for assessment by RECICL because the alteration of vascularity could not be determined. Evaluation of response for such lesions should be determined using another criteria. Third, the retrospective nature of the study might have led to bias in selection of the patients. To address the limitations and independently validate the results of this study, we are currently designing an investigation of the accuracy of use of the RECICL in the prediction of OS in a prospective multicenter patient cohort with a larger sample size.

In this comparison of the validity of use of the RECIST1.1, mRECIST, and RECICL, use of the RECICL was found to allow for much more precise identification of patients with better prognosis compared to the RECIST1.1 or mRECIST. This finding leads us to conclude that use of the RECICL is the best means of obtaining precise prognostic information at an early stage after treatment. Although further studies are required to confirm the superiority of RECICL in HCC with portal vein thrombi and extrahepatic lesions, the results of this study are of significance from a clinical viewpoint, especially in the selection of therapy. Given the robustness of the data

presented herein, we strongly assert that the RECICL should become the standard system used in the evaluation of response to chemotherapy, including molecularly targeted therapies, by HCC patients.

Acknowledgments This work was supported by a Health Labor Sciences Research Grant from the Ministry of Health Labour and Welfare of Japan (H22-Clinical Oncology-General-015).

Conflict of interest The authors declare that they have no conflict of interest.

References

1. El-Serag HB, Rudolph KL. Hepatocellular carcinoma: epidemiology and molecular carcinogenesis. Gastroenterology. 2007;132:2557–76.
2. Llovet JM, Ricci S, Mazzaferro V, et al. SHARP Investigators Study Group. Sorafenib in advanced hepatocellular carcinoma. N Engl J Med. 2008;359:378–90.
3. Sakurai T, Kudo M. Signaling pathways governing tumor angiogenesis. Oncology. 2011;81:24–9.
4. Wilhelm SM, Adnane L, Newell P, et al. Preclinical overview of sorafenib, a multikinase inhibitor that targets both RAF and VEGF and PDGF receptor tyrosine kinase signaling. Mol Cancer Ther. 2008;7:3129–40.
5. Rini BI. Sorafenib. Expert Opin Pharmacother. 2006;7:453–61.
6. Wu H, Huang C, Chang D. Anti-angiogenic therapeutic drugs for treatment of human cancer. J Cancer Mol. 2008;4:37–45.
7. Kano MR, Komuta Y, Iwata C, et al. Comparison of the effects of the kinase inhibitors imatinib, sorafenib, and transforming growth factor-beta receptor inhibitor on extravasation of nanoparticles from neovasculature. Cancer Sci. 2009;100:173–80.
8. Tanaka S, Arii S. Molecularly targeted therapy for hepatocellular carcinoma. Cancer Sci. 2009;100:1–8.
9. Llovet JM, Bruix J. Molecular targeted therapies in hepatocellular carcinoma. Hepatology. 2008;48:1312–27.
10. Cheng AL, Kang YK, Chen Z, et al. Efficacy and safety of sorafenib in patients in the Asia-Pacific region with advanced hepatocellular carcinoma: a phase III randomised, double-blind, placebo-controlled trial. Lancet Oncol. 2009;10:25–34.
11. Lencioni R, Llovet JM. Modified RECIST (mRECIST) assessment for hepatocellular carcinoma. Semin Liver Dis. 2010;30:52–60.
12. Llovet JM, Di Bisceglie AM, Bruix J, et al. Design and endpoints of clinical trials in hepatocellular carcinoma. J Natl Cancer Inst. 2008;100:698–711.
13. The Liver Cancer Study Group of Japan. General rules for the clinical and pathological study of primary liver cancer. 5th ed. Tokyo: Kanehara; 2009 (revised version).
14. Miller AB, Hogestraeten B, Staquet M, et al. Reporting results of cancer treatment. Cancer. 1981;47:207–14.
15. Ebied OM, Federle MP, Carr BI, et al. Evaluation of responses to chemoembolization in patients with unresectable hepatocellular carcinoma. Cancer. 2003;97:1042–50.

Stabilization Technique for Real-Time High-Resolution Vascular Ultrasound Using Frequency Domain Interferometry *

Hirofumi Taki, *Member, IEEE*, Kousuke Taki, Makoto Yamakawa, *Member, IEEE*, Tsuyoshi Shiina, *Member, IEEE*, Motoi Kudo, *Member, IEEE*, and Toru Sato, *Member, IEEE*

***Abstract*— We have proposed an ultrasound imaging method based on frequency domain interferometry (FDI) with an adaptive beamforming technique to depict real-time high-resolution images of human carotid artery. Our previous study has investigated the performance of the proposed imaging method under an ideal condition with a high signal-to-noise ratio (SNR). In the present study, we propose a technique that has the potential to improve accuracy in estimating echo intensity using the FDI imaging method. We investigated the performance of the proposed technique in a simulation study that two flat interfaces were located at depths of 15.0 and 15.2 mm and white noise was added. Because the –6 dB bandwidth of the signal used in this simulation study is 2.6 MHz, the conventional B-mode imaging method failed to depict the two interfaces. Both the conventional and proposed FDI imaging methods succeeded to depict the two interfaces when the SNR ranged from 15 to 30 dB. However, the average error of the estimated echo intensity at the interfaces using the conventional FDI imaging method ranged from 7.2 to 10.5 dB. In contrast, that using the FDI imaging method with the proposed technique ranged from 2.0 to 2.2 dB. The present study demonstrates the potential of the FDI imaging method in depicting robust and high-range-resolution ultrasound images of arterial wall, indicating the possibility to improve the diagnosis of atherosclerosis in early stages.**

I. Introduction

Cardiovascular disease remains a substantial cause of mortality [1]. Recent clinical issue is arterial plaque of which rupture or erosion lead to abrupt thrombosis. Urgent demand is how to establish a marker for vulnerable plaque [2]. Transcutaneous ultrasound B-mode imaging is widely used to detect plaque in carotid arteries [3]. Thus, improving the spatial resolution of the imaging would bring a major advance in identification of high-risk plaques.

*This work was partly supported by the Innovative Techno-Hub for Integrated Medical Bio-imaging Project of the Special Coordination Funds for Promoting Science and Technology, from the Ministry of Education, Culture, Sports, Science and Technology (MEXT), Japan and by MEXT/JSPS KAKENHI Grant Numbers 24592513 and 25870345.

H. Taki and T. Sato are with the Graduate School of Informatics, Kyoto University, Yoshida-honmachi, Sakyo-ku, Kyoto 606-8501, Japan (e-mail: htaki@i.kyoto-u.ac.jp; sato.toru.6e@kyoto-u.ac.jp).

K. Taki and M. Kudo are with the Department of Anatomy, Shiga University of Medical Science, Seta Tsukinowa-cho, Otsu City, Shiga 520-2192, Japan (e-mail: taki@belle.shiga-med.ac.jp; kudo@belle.shiga-med.ac.jp).

M. Yamakawa is with the Advanced Biomedical Engineering Research Unit, Kyoto University, Yoshida-honmachi, Sakyo-ku, Kyoto 606-8501, Japan (e-mail: yamakawa.makoto.6x@kyoto-u.ac.jp).

T. Shiina is with the Graduate School of Medicine, Kyoto University, Yoshida-honmachi, Sakyo-ku, Kyoto 606-8501, Japan (e-mail: shiina@hs.med.kyoto-u.ac.jp).

978-1-4244-7929-0/14/$26.00 ©2014 IEEE

Adaptive beamforming algorithms have been proposed to improve spatial resolution without using high transmit frequencies. One common technique is the use of a Capon beamformer, which uses a set of weights calculated by minimizing the output power, subject to the constraint that a desired signal gives a constant response [4]. Several groups have used the Capon method with spatial averaging to improve the lateral resolution in US [5], [6]. In our previous study, we have proposed an ultrasound imaging method based on frequency domain interferometry (FDI) with an adaptive beamforming algorithm that has high resolution in axial direction [7]−[10]. We have reported on the necessity of employing frequency averaging to suppress coherent interference under a simple simulation study without noise. We are currently working on the effect of the bandwidths used for frequency averaging and for imaging on the performance of the FDI imaging method in the condition with noise, and propose a technique that has the potential to acquire robust depiction of arterial interfaces when there is a thin layer close to the arterial wall.

II. Materials and Methods

The proposed technique is applied to the FDI imaging method with the Capon method, which is an adaptive beamforming algorithm. In this section, we briefly describe the FDI imaging method, and subsequently propose a technique that improves accuracy in estimating echo intensity using the FDI imaging method.

A. FDI Imaging Method Using Frequency Averaging

The FDI imaging method works under the condition where the echo at the desired depth and echoes at undesired depth have no correlation. Frequency averaging has been used to suppress the correlation between the echoes returned from different depths [7]. This technique is applied to the covariance matrix of the received signal in the frequency domain. The sub-matrices of the covariance matrix are averaged along the diagonal direction, as shown in Fig. 1. The covariance matrix after frequency averaging is given by

$$\mathbf{R}_{\mathrm{A}} = \frac{1}{M}\sum_{m=1}^{M}\mathbf{R}_m, \tag{1}$$

$$R_{mij} = X_{i+m-1}X^*_{j+m-1}, \tag{2}$$

where R_{mij} is the (i, j) element of the m-th submatrix $\mathbf{R}_m$, X_i is the i-th frequency components of the received RF signal after whitening, M is the number of submatrices, and $[]^*$ denotes the complex conjugate.

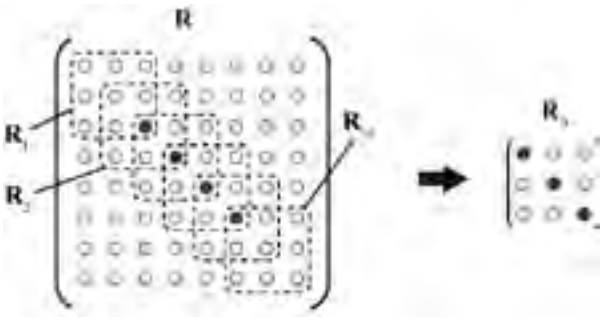

Figure 1. Schema of the frequency averaging technique. Gray diagonal elements of the covariance matrix **R** are distributed among the diagonal elements of the covariance matrix after frequency averaging $\mathbf{R}_{\mathrm{A}}$.

The FDI imaging method suppresses the contribution of echoes from targets at undesired depths, subject to a constant response at the desired depth. After applying frequency averaging to the covariance matrix, this problem expressed by the following formulae:

$$\begin{aligned} &\text{minimize} \quad P(r) = \mathbf{W}^{\mathrm{T}*}\mathbf{R}_{\mathrm{A}}\mathbf{W} \\ &\text{subject to} \quad \mathbf{C}^{\mathrm{T}*}\mathbf{W} = 1, \end{aligned} \tag{3}$$

$$\mathbf{C} = [\exp(\mathrm{j}k_1 r) \quad \exp(\mathrm{j}k_2 r) \quad \cdots \quad \exp(\mathrm{j}k_N r)]^{\mathrm{T}}, \tag{4}$$

Where $r/2$ is the desired depth, $P(r)$ is the output intensity at the desired depth, **W** is a weighting vector, k_n is the n-th wave number of frequency components of a received signal, N is the size of the correlation matrix $\mathbf{R}_{\mathrm{A}}$, and $[]^{\mathrm{T}}$ denotes the transpose [10].

The estimated intensity of the FDI imaging method employing an appropriate weighting vector is given by

$$P_{\mathrm{Cap}}(r) = \frac{1}{\mathbf{C}^{\mathrm{T}*}(\mathbf{R}_{\mathrm{A}} + \eta\mathbf{E})^{-1}\mathbf{C}}, \tag{5}$$

where $\eta\mathbf{E}$ is a diagonal loading matrix used to avoid the instability in calculating the inverse matrix $\mathbf{R}_{\mathrm{A}}^{-1}$ [7].

B. Stabilization Technique for the Improvement in Estimating Echo Intensity

When the bandwidth for frequency averaging is wider than that for imaging, i.e. the size of the sub-matrix L is smaller than the number of submatrices M, the output intensity of the FDI imaging method is rewritten as

$$\begin{aligned} P(r) &= \frac{1}{M}\sum_{m=1}^{M}\mathbf{W}^{\mathrm{T}*}\mathbf{R}_m\mathbf{W} = \frac{1}{M}\sum_{m=1}^{M}\left|\sum_{l=1}^{L}X^*_{l+m-1}W_l\right|^2 \\ &= \frac{1}{M}\sum_{m=1}^{M}\left|\sum_{l=1}^{L}X^*_{l+m-1}W_l\exp\{\mathrm{j}(m-1)\Delta kr\}\right|^2 \\ &\geq \frac{1}{M}\left|\sum_{m=1}^{M}\sum_{l=1}^{L}X^*_{i'}W_l\exp\{\mathrm{j}(i'-l)\Delta kr\}\right|^2 \\ &= \frac{1}{M}\left|\sum_{l=1}^{L}X^*_{\mathrm{B}l}W_l + \sum_{i'=L}^{M}X^*_{i'}\exp\mathrm{j}k_{i'}r\right|^2, \end{aligned} \tag{6}$$

$$\begin{aligned} X^*_{\mathrm{B}l} &= \sum_{i'=l}^{L-1}X^*_{i'}\exp\{\mathrm{j}(i'-l)\Delta kr\} \\ &\quad + \sum_{i'=M+1}^{M+l-1}X^*_{i'}\exp\{\mathrm{j}(i'-l)\Delta kr\}, \end{aligned} \tag{7}$$

where Δk is the wavenumber of the sampling frequency interval and $i' = l + m - 1$.

When we use a wider bandwidth for frequency averaging than that for imaging, the Capon beamformer with frequency averaging is similar to the combination of a simple phase-compensation beamformer for central frequency components and a Capon beamformer for peripheral frequency components. Under this condition, the intensity estimated by the FDI with the Capon method with frequency averaging would be larger than the summation of the intensities among the central frequency components from $L\Delta k$ to $M\Delta k$, i.e. the summation of the intensities of gray diagonal elements shown in Fig. 1. Therefore, the estimated intensity of the FDI imaging method is supposed to satisfy the following formulae:

$$I_{\mathrm{E}} \geq F_{\mathrm{S}} I_{\mathrm{True}}, \tag{8}$$

$$F_{\mathrm{S}} = (B_{\mathrm{A}} - B_{\mathrm{I}})/B_{\mathrm{A}}, \tag{9}$$

where B_{A} and B_{I} are the bandwidth used for frequency averaging and for imaging, respectively. We call F_{S} the stabilization factor. The employment of a sufficiently large value of F_{S} should suppress the underestimation of the echo intensity using the FDI imaging method with the Capon method at the cost of a little range resolution. When $F_{\mathrm{S}} = 1/3$, the estimated intensity is supposed to be larger than –4.77 dB relative to the true echo intensity.

III. Results

In the simulation study, we investigate the performance of the proposed technique when there were two horizontal interfaces in a ROI, where the waveform returned from each interface was the same as that of the reference signal. When

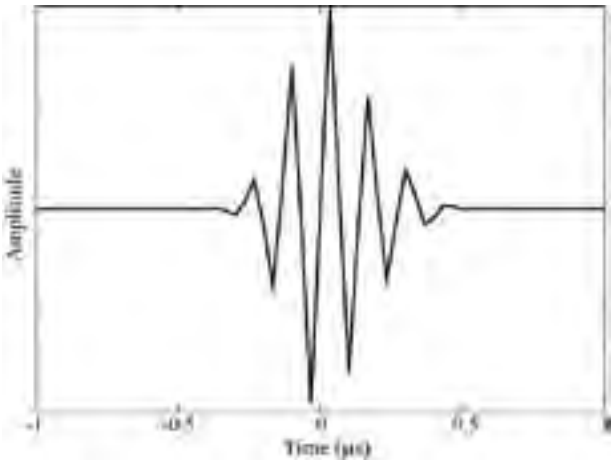

Figure 2. Echo waveform of a horizontal interface between 20% gelatin and 4% agar, where 10 echoes of different scan lines were coherently averaged to suppress noise.

the received signal includes no noise, the echo returned from two interfaces is given by

$$s(I_T, t) = s_R(t) + s_R(t - 2I_T / c), \quad (10)$$

where I_T is the target interval, $s_R(t)$ is the reference signal and c is the sound velocity. Fig. 2 shows the waveform used for the reference signal. The reference signal was the echo from the interface between the 20% gelatin and the 4% agar at a depth of 15 mm acquired by a Hitachi EUB-8500 (Hitachi Medical Co. Ltd., Tokyo, Japan) US device with a 7.5 MHz linear array, where 10 echoes of different scan lines were averaged. Before the averaging process, the center of each echo was adjusted to $t = 0$ to average coherently. The −6 dB bandwidth of the reference echo was 2.6 MHz. To investigate the effects of noise in the proposed method, we added white noise to the constructed received signal given by equation (10). The signal intensity was the average echo intensity in the −3 dB temporal width of a reference signal, and the noise intensity was the average echo intensity of the received signal in a 2 cm range that includes no echo signal.

Fig.3 shows the intensity at the target depth estimated by the conventional FDI imaging method under the condition of no noise, where there are two horizontal interfaces in the ROI and the true echo intensity at each target depth is adjusted to 0 dB. The imaging method used the band from 5.3 to 9.3 MHz, and the bandwidths for frequency averaging B_A were 3, 2, and 1 MHz. This result indicates that the employment of a wide bandwidth for frequency averaging improves the accuracy in estimating echo intensity under an ideal condition without noise.

Fig. 4 shows the intensity estimated using a conventional B-mode imaging method, the conventional FDI imaging method and the FDI imaging method with the proposed technique that employed a wider bandwidth for frequency averaging compared with that for imaging. The SNR ranged from 0 to 30 dB, there were two horizontal interfaces in a ROI and the target interval was 0.2 mm. The conventional FDI

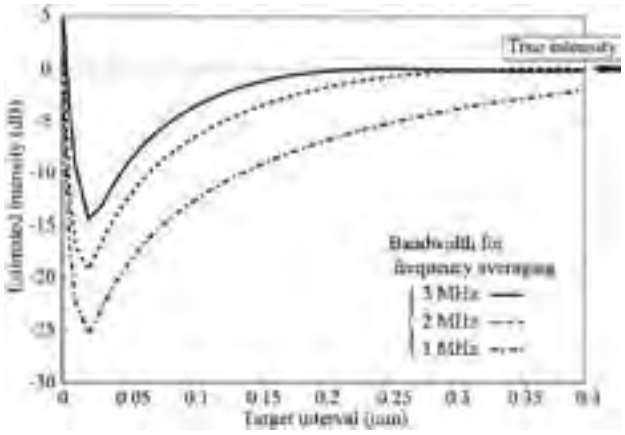

Figure 3. Estimated intensity at the target depth using the conventional FDI imaging method under the condition without noise, where two target interfaces are located in a ROI and the true echo intensity at the target depth is adjusted to 0 dB. The imaging method uses the band of the received data from 5.3 to 9.3 MHz, and the bandwidths for frequency averaging are 3, 2, and 1 MHz.

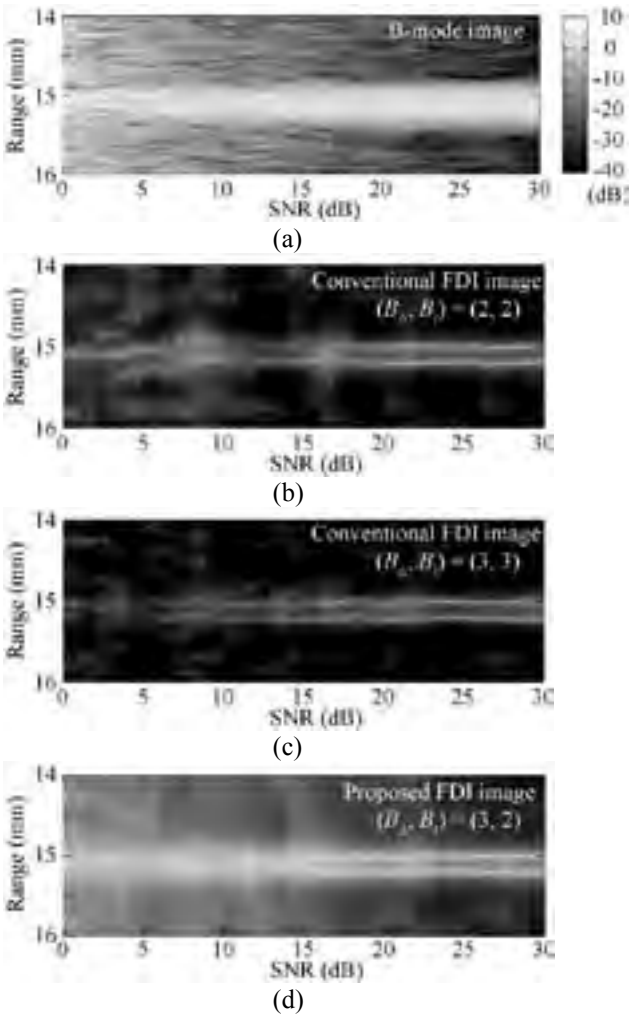

Figure 4. Estimated intensity as a function of the SNR from 0 to 30 dB when there are two interfaces at depths of 15.0 and 15.2 mm. The intensity profiles are estimated by (a) a conventional B-mode imaging method, (b) and (c) the conventional FDI imaging method, and (d) the FDI imaging method with the proposed technique. The bandwidth for frequency averaging (B_A) and that for imaging (B_I) are respectively (b) 2 and 2 MHz, (c) 3 and 3 MHz, and (d) 3 and 2 MHz, respectively.

imaging method allocates a half of the whole bandwidth for frequency averaging [7]. The FDI imaging method using the proposed technique employed the setting of (B_A, B_I) = (3 MHz, 2 MHz). Because the –6 dB bandwidth of the signal used in this simulation study is 2.6 MHz, the conventional B-mode imaging method has range resolution of about 0.3 mm and it failed to depict the two interfaces. The conventional FDI imaging method has higher range resolution than the B-mode imaging method under the condition where its SNR was higher than 20 dB. This result is consistent with our previous work [7]. Under the condition of low SNR less than 15 dB, in some cases the conventional FDI imaging succeeded to depict two interfaces. However, the estimated intensity at the interface position decreased severely, and the estimated depth of the interface varied. These two defects might have caused that some false images appeared in the conventional FDI images at the SNR of less than 10 dB. In contrast, the FDI imaging with the proposed technique succeeded to depict the interfaces reliably at the cost of little deterioration in range

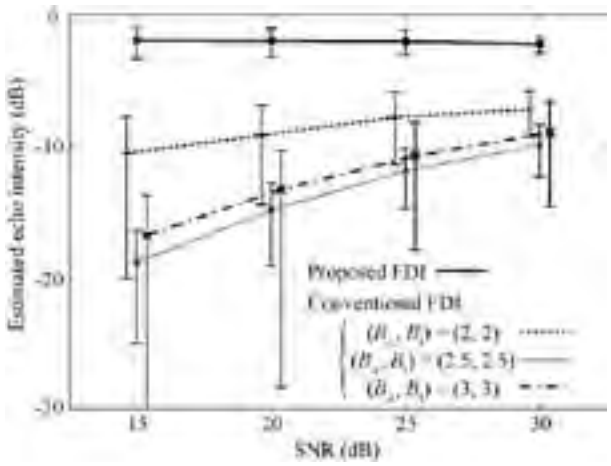

Figure 5. Estimated echo intensity of target interfaces calculated using the conventional FDI imaging method and the FDI imaging method with the proposed technique, where there are two target interfaces at depths of 15.0 and 15.2 mm and the true echo intensity is 0 dB. The FDI imaging method with the proposed method allocates bandwidths of 3 and 2 MHz for frequency averaging and imaging, respectively. The conventional FDI imaging method allocates half bandwidths for frequency averaging from total bandwidths of 4, 5 and 6 MHz. Each error bar denotes the standard deviation, where 10 simulation data with random white noise are used.

resolution. This result indicates the efficiency of the proposed setting that the bandwidth for frequency averaging is wider than that for imaging.

The above-mentioned defects of the conventional FDI imaging method cause uncertainty in selecting peak values as the estimated intensity at the interfaces. When SNR ranged from 15 to 30 dB, two peaks appeared clearly in both the conventional and proposed FDI imaging methods. We thus calculated the estimated echo intensity at the interfaces by averaging two peak values in each scan line under the condition that SNR ranged from 15 to 30 dB. Because the true echo intensity was 0 dB, we call the underestimation of the echo intensity at the interfaces as the estimation error. Fig. 5 shows the estimated echo intensity of the target interfaces calculated using the conventional FDI imaging method and using the FDI imaging method with the proposed technique. Using 3 MHz bandwidth for frequency averaging suppresses coherent interferences sufficiently when the target interval is 0.2 mm; however, using a wide bandwidth means using low SNR frequency components that makes the conventional FDI imaging method unreliable. Because the Capon method minimizes the output power, the conventional FDI imaging method underestimates the echo intensity with the average error ranged from 7.2 to 10.5 dB, and its unreliable performance results in large variations in estimated echo intensity. This should be one of the reasons why the conventional FDI imaging method has low continuity in the lateral direction [7]. In contrast, the FDI imaging method with the proposed setting succeeded in estimating the echo intensity with average estimation error ranged from 2.0 to 2.2 dB and with small variation. Under the condition of the FDI imaging method with the proposed technique, the stabilization factor F_S is equal to 1/3. In all cases, the normalized echo intensity estimated by the FDI imaging method with FAS is larger than –4.77 dB. This result is consistent with the results of the theoretical investigation shown in section II B. These results indicate that the proposed technique has high potential not only in estimating the echo intensity but also in improving continuity in the lateral direction.

IV. Conclusion

We proposed a high-range-resolution FDI imaging method employing a technique that improves robustness of the FDI imaging method in estimating echo intensity. We investigated the performance of the proposed technique in a simulation study under the condition. In a simulation study where the SNR ranged from 15 to 30 dB, the average error of the estimated echo intensity using the conventional FDI imaging method ranged from 7.2 to 10.5 dB. In contrast, that using the FDI imaging method with the proposed technique ranged from 2.0 to 2.2 dB. The present study demonstrates the potential of the FDI imaging method in depicting robust and high-range-resolution ultrasound image, indicating the possibility to improve the diagnosis of atherosclerosis in early stages.

References

[1] J. W. Levenson, P. J. Skerrett, P.J. and J. M. Gaziano, “Reducing the global burden of cardiovascular diseases: the role of risk factors,” *Prev. Cardiol*., vol. 5, pp. 188–199, 2002.

[2] M. Petretta, and A. Cuocolo, “In search of a marker of vulnerable carotid plaque: Is the key in the heart?,” *Atherosclerosis*, vol. 223, pp. 95–97, Jul. 2012.

[3] M. Rosenkranz, A. Russjan, E. Goebell, et al. "Carotid plaque surface irregularity predicts cerebral embolism during carotid artery stenting," *Cerebrovasc. Dis*. vol 32, pp. 163–169, 2011.

[4] J. Capon, “High resolution frequency-wavenumber spectrum analysis,” in *Proc. IEEE*, 1969, pp. 1408–1418.

[5] J. A. Mann and W. F. Walker, “A constrained adaptive beamformer for medical ultrasound: initial results,” in *Proc. IEEE Ultrason. Symp*., 2002, pp. 1807–1810.

[6] J.-F. Synnevåg, A. Austeng, and S. Holm, “Benefits of Minimum-Variance Beamforming in Medical Ultrasound Imaging,” *IEEE Trans. Ultrason. Ferroelectr. Freq. Control*, vol. 56, no. 9, pp. 1868–1879, Sep. 2009.

[7] H. Taki, K. Taki, T. Sakamoto, M. Yamakawa, T. Shiina, M. Kudo, and T. Sato, “High range resolution ultrasonographic vascular imaging using frequency domain interferometry with the Capon method,” *IEEE Trans. Med. Imaging*, Vol. 31, No. 2, pp. 417–429, Feb, 2012.

[8] H. Taki, T. Sakamoto, M. Yamakawa, T. Shiina, and T. Sato, “High Resolution Ultrasound Imaging Using Frequency Domain Interferometry―Suppression of Interference Using Adaptive Frequency Averaging,” *IEEJ Trans. Electron. Inf. Syst*., Vol. 132, No. 10, pp. 1552-1557, 2012.

[9] H. Taki, T. Sakamoto, K. Taki, M. Yamakawa, T. Shiina, M. Kudo, and T. Sato, “High range resolution ultrasound imaging of a human carotid artery using frequency domain interferometry,” in *Proc. IEEE Ultrasonics Symp*, 2011, pp. 2201–2204.

[10] H. Taki, T. Sakamoto, K. Taki, M. Yamakawa, T. Shiina, K. Kudo and T. Sato, “Real-time high-resolution vascular ultrasound using frequency domain interferometry with the ROI-division process, “ in *Proc. IEEE EMBS*, 2013, pp. 1398-1401.

Antegrade biopsy by using a trans-catheter technique through EUS-guided hepaticojejunostomy

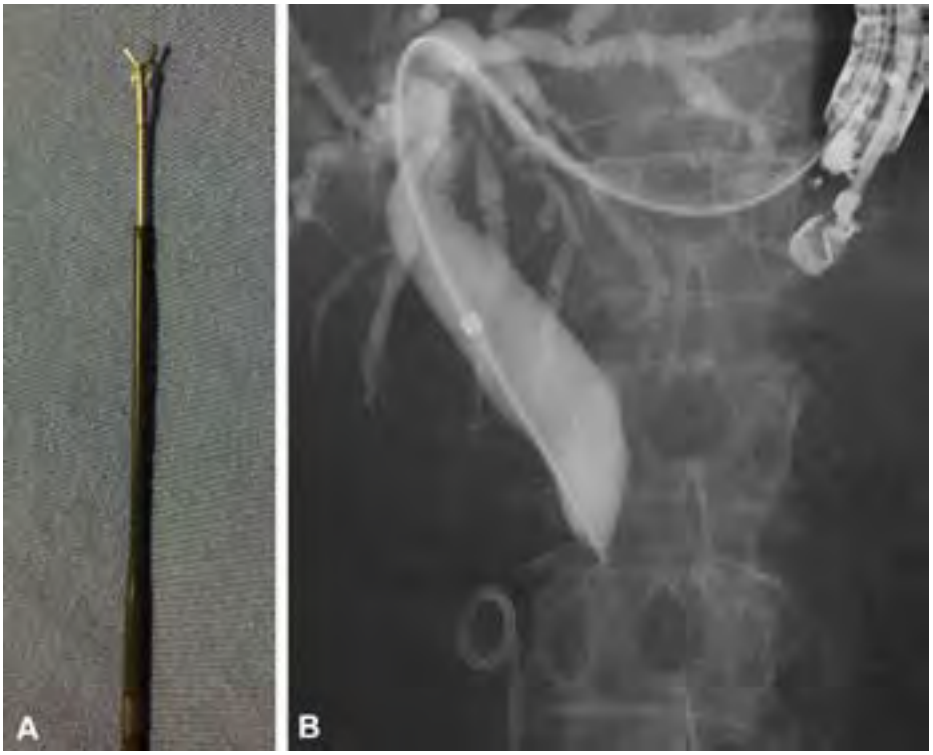

Figure 1. A, Image of the forceps biopsy trans-catheter technique. In this method, forceps biopsy is being performed through the dilator. **B,** Forceps biopsy by using the trans-catheter technique.

A 63-year-old woman who underwent total gastrectomy with Roux-en-Y anastomosis because of gastric cancer was admitted because of obstructive jaundice. Lymph node recurrence was suspected. As shown in Video 1 (available online at www.giejournal.org), after puncturing the intrahepatic bile duct by using a 19-gauge, FNA needle, we injected contrast medium. The lower bile duct was obstructed, and a guidewire was advanced into the common bile duct. Next, we inserted a dilator (SBDC-9; Soehendra Biliary Dilation Catheter, Cook Medical, Bloomington, Ind) to the site of bile duct obstruction. First, we inserted the biopsy device (Spy Bite Biopsy Forceps; Boston Scientific, Tokyo, Japan) through a dilator catheter and performed forceps biopsy (Fig. 1B). Next, we performed brush cytology. Recurrent gastric cancer was subsequently diagnosed.

This video can be viewed directly from the GIE website or by using the QR code and your mobile device. Download a free QR code scanner by searching "QR Scanner" in your mobile device's app store.

We perform antegrade biopsy and brushing cytology by using rapid, on-site evaluation by a cytopathologist, allowing determination of whether a lesion is malignant or benign during the procedure. If biopsy or cytology results show a benign lesion, we place a plastic stent across the stricture and the endoscopic nasal biliary drainage tube into the common bile duct to avoid bile leakage. After several days, we remove this tube. If the results show malignancy, we place a metal stent from the intrahepatic bile duct to the jejunum.

Devices for forceps biopsy or brush cytology should not be inserted into the bile duct through the GI wall because bile leakage may occur during insertion or removal. With our method, bile leakage does not occur after insertion of the dilator catheter. In addition, we were easily able to perform repeat biopsy or repeat brush cytology across the dilator. To the best of our knowledge, EUS-guided access has not been reported as a diagnostic modality, especially for obtaining cytologic or histologic evidence.

DISCLOSURE

All authors disclosed no financial relationships relevant to this article.

Takeshi Ogura, MD, PhD, Akira Imoto, MD, PhD, Daisuke Masuda, MD, PhD, Tatsushi Sano, MD, Saori Onda, MD, *Second Department of Internal Medicine,* **Kazuhiro Yamamoto, MD, PhD,** *Department of Radiology, Osaka Medical College, Osaka,* **Masayuki Kitano, MD, PhD,** *Department of Gastroenterology and Hepatology, Kinki University Faculty of Medicine, Osaka-Sayama,* **Toshihisa Takeuchi, MD, PhD, Takuya Inoue, MD, PhD, Kazuhide Higuchi, MD, PhD,** *Second Department of Internal Medicine, Osaka Medical College, Osaka, Japan*

http://dx.doi.org/10.1016/j.gie.2014.06.032

Single-session, transgastric ERCP using sutured gastropexy for treatment of pancreatic duct leak in a patient with Roux-en-Y gastric bypass anatomy and pancreatic divisum

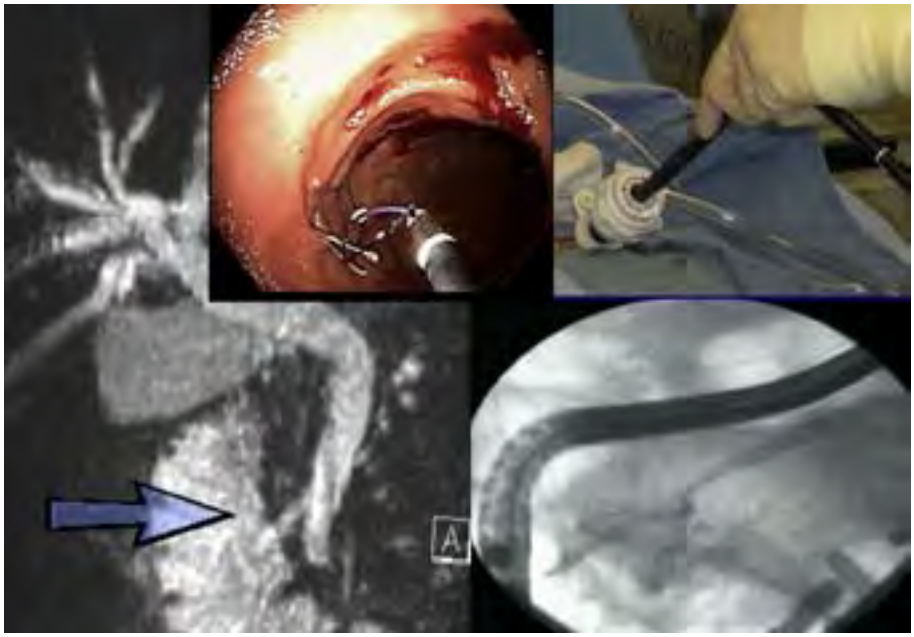

Figure 1. Pancreatic divisum on MRCP, sutured gastropexy, and transgastric ERCP.

A 56-year-old woman with a history of Roux-en-Y gastric bypass, admitted with necrotizing pancreatitis, experienced signs of sepsis 2 weeks after admission. A CT scan revealed a large fluid collection in the left upper quadrant and left pleural effusion. She was treated by percutaneous catheter placement. Over the next 4 days she had a persistently high output of fluid rich in amylase, suggesting ongoing pancreatic duct leak. An ERCP with deep enteroscopy revealed a pancreatic divisum and a severely dilated bile duct. A plastic stent was placed into the bile duct without performance of a sphincterotomy. Pancreatic divisum was later confirmed on MRI.

To perform transgastric ERCP, a secure gastrostomy was created by advancement of a pediatric colonoscope into the stomach in a retrograde manner. Sutured gastropexy was performed with a 2-mm suture passing needle. A 45F laparoscopic trocar was placed after dilating gastrostomy to allow passage of a duodenoscope. Dorsal duct cannulation and injection of contrast medium revealed 2 separate sites of pancreatic duct leak. A 7F plastic stent was placed

This video can be viewed directly from the GIE website or by using the QR code and your mobile device. Download a free QR code scanner by searching "QR Scanner" in your mobile device's app store.

同門会　名簿

名前	施設	卒業年度	出身大学
工藤　正俊	近畿大学医学部	昭和 53年	京都大学
樫田　博史	近畿大学医学部	昭和 58年	京都大学
汐見　幹夫	近畿大学医学部	昭和 55年	近畿大学
北野　雅之	近畿大学医学部	平成　2年	鳥取大学
西田　直生志	近畿大学医学部	昭和 60年	大阪医科大学
松井　繁長	近畿大学医学部	平成　3年	近畿大学
上嶋　一臣	近畿大学医学部	平成　7年	神戸大学
櫻井　俊治	近畿大学医学部	平成　7年	京都大学
依田　広	近畿大学医学部	平成　8年	京都大学
南　康範	近畿大学医学部	平成　9年	近畿大学
萩原　智	近畿大学医学部	平成 10年	近畿大学
矢田　典久	近畿大学医学部	平成 11年	滋賀医科大学
朝隈　豊	近畿大学医学部	平成 14年	近畿大学
田北　雅弘	近畿大学医学部	平成 15年	近畿大学
米田　賴晃	近畿大学医学部	平成 13年	北里大学
岡崎　能久	近畿大学医学部	平成 13年	大阪大学
永井　知行	近畿大学医学部	平成 16年	近畿大学
今井　元	近畿大学医学部	平成 17年	近畿大学
山雄　健太郎	近畿大学医学部	平成 18年	東京医科大学
山田　光成	近畿大学医学部	平成 18年	近畿大学
有住　忠晃	近畿大学医学部	平成 19年	近畿大学
鎌田　研	近畿大学医学部	平成 19年	近畿大学
峯　宏昌	近畿大学医学部	平成 19年	近畿大学
宮田　剛	近畿大学医学部	平成 19年	近畿大学
三長　孝輔	近畿大学医学部	平成 19年	京都大学
松田　友彦	近畿大学医学部	平成 19年	弘前大学
足立　哲平	近畿大学医学部	平成 21年	近畿大学
大本　俊介	近畿大学医学部	平成 21年	近畿大学
門阪　薫平	近畿大学医学部	平成 21年	近畿大学
田中　梨絵	近畿大学医学部	平成 22年	近畿大学
千品　寛和	近畿大学医学部	平成 22年	近畿大学
河野　匡志	近畿大学医学部	平成 22年	近畿大学
南　知宏	近畿大学医学部	平成 23年	近畿大学
岡元　寿樹	近畿大学医学部	平成 23年	近畿大学
岩西　美奈	近畿大学医学部	平成 25年	近畿大学
黒木　恵美(旧姓 石川)		平成 11年	近畿大学
岡田　無文	山本病院	平成 13年	近畿大学
柴田　千栄(旧姓 辰巳)		平成 15年	近畿大学
上田　泰輔		平成 15年	近畿大学

上硲　俊法	近畿大学医学部臨床検査学	昭和 60年	近畿大学
前川　清	近畿大学医学部超音波室		
辻　直子	近畿大学医学部堺病院	昭和 60年	京都府立医科大学
川崎　正憲	近畿大学医学部堺病院	平成 15年	近畿大学
谷池　聡子	近畿大学医学部堺病院	平成 7年	奈良県立医科大学
奥村　直己	近畿大学医学部堺病院		近畿大学
高場　雄久	近畿大学医学部堺病院		近畿大学

川崎　俊彦	近畿大学医学部奈良病院	昭和 58年	京都大学
岸谷　譲	近畿大学医学部奈良病院	昭和 62年	近畿大学
宮部　欽生	近畿大学医学部奈良病院	平成 14年	近畿大学
清水　昌子	近畿大学医学部奈良病院	平成 12年	近畿大学
茂山　朋広	近畿大学医学部奈良病院	平成 17年	近畿大学
奥田　英之	近畿大学医学部奈良病院	平成 19年	
木下　大輔	近畿大学医学部奈良病院	平成 20年	
秦　康倫	近畿大学医学部奈良病院	平成 21年	
水野　成人	近畿大学医学部奈良病院	昭和 61年	京都府立医科大学
高山　政樹	近畿大学医学部奈良病院	平成 19年	近畿大学
加藤　玲明	かとう内科眼科クリニック	平成11年	近畿大学
宮本　容子(旧姓 北口)		平成12年	近畿大学
林　道友	林内科クリニック		
梅原　康湖	JR大阪鉄道病院	平成 12年	近畿大学
山本　俊夫(ご逝去)		昭和 26年	京都大学
山本　健二	岡本クリニック		神戸大学
亀山　千晴	しあわせクリニック	平成　7年	近畿大学
南野　達夫	なんの医院	昭和 55年	近畿大学
中里　勝	上ヶ原病院		
鍋島　紀滋	三菱京都病院	昭和 61年	京都大学
由谷　逸朗	高石藤井病院	昭和 62年	近畿大学
遠田　弘一	慈温堂遠田医院	平成 7年	近畿大学
遠田　由紀			
川端　一史	川端内科クリニック	平成元年	近畿大学
米田　円	米田内科胃腸科	平成 元年	近畿大学
小川　力	高松赤十字病院	平成11年	近畿大学
渡邉　和彦	結核予防会大阪府支部相談診療所	平成　3年	近畿大学
森村　正嗣	森村医院	平成　3年	帝京大学
中岡　良介	山本病院	平成　8年	近畿大学
冨田　崇文	冨田病院	平成 14年	近畿大学
西尾　健		平成 14年	近畿大学
仲谷　達也	仲谷クリニック	平成　3年	近畿大学
福永　豊和	北野病院	平成　4年	京都大学
福田　信宏	朝日大学村上記念病院	平成 10年	近畿大学
坂口　康浩	坂口クリニック	平成 11年	近畿大学
永島　美樹	桃坂クリニック	平成 12年	近畿大学
坂本　康明	坂本クリニック	平成 15年	近畿大学
市川　勉	内海町いちかわ診療所	平成 12年	近畿大学
齊藤　佳寿(旧姓 野田)		平成 14年	近畿大学
高橋　俊介	堺市立総合医療センター	平成 14年	近畿大学
末冨　洋一郎	末冨内科クリニック	平成　8年	近畿大学
梅原　泰	辻腎太郎クリニック	平成 11年	近畿大学

鄭　浩柄	神戸市立医療センター中央市民病院	平成　8年	東京慈恵医科大学
小牧　孝充	富田林病院	平成　7年	近畿大学
畑中　絹世		平成 13年	川崎医科大学
早石　宗右	早石病院	平成 18年	近畿大学
乾　可苗	乾クリニック	平成 12年	近畿大学
山本　典雄	大阪市立大学医学部附属病院	平成 19年	近畿大学
井上　達夫	井上医院	平成 11年	近畿大学
坂本　洋城	葛城病院	平成 12年	近畿大学
永田　嘉昭	永田医院	平成 16年	近畿大学
北井　聡	北井整形外科	平成 14年	近畿大学
鄭　扶美	近畿大学医学部　元秘書		
木村　由佳	近畿大学医学部　元秘書		
川辺　仁美	近畿大学医学部　元秘書		
西川　由佳	近畿大学医学部　元秘書		
二見　佳央里	近畿大学医学部　元秘書		
井上　真由美	近畿大学医学部　元秘書		
坂上　浩美	近畿大学医学部　元秘書		
小田　智裕子	近畿大学医学部　元秘書		
土井　由香利	近畿大学医学部　元秘書		
上田　由未子	近畿大学医学部　元秘書		
林　直子	近畿大学医学部　元秘書		
垣井　麻莉	近畿大学医学部　元秘書		
東野　愛	近畿大学医学部　元秘書		
山本　有紀	近畿大学医学部　元秘書		
児玉　美由紀	近畿大学医学部　元CRC		
田中　真紀	近畿大学医学部　教授秘書		
村橋　亜季	近畿大学医学部　教授秘書		
本廣　佳香	近畿大学医学部　教授秘書		
和田　千尋	近畿大学医学部　教授秘書		
胡桃　由佳	近畿大学医学部　医局秘書		
朝隈　智	近畿大学医学部　医局秘書		
浦田　亜樹	近畿大学医学部　医局秘書		
田村　利恵	近畿大学医学部　肝癌研究会事務局		
前原　なつみ	近畿大学医学部　肝癌研究会事務局		
上妻　智子	近畿大学医学部　肝癌研究会事務局		
弓削　公子	近畿大学医学部　臨床研究補助員		
濱田　恵里	近畿大学医学部　臨床研究補助員		
鏡　郁子	近畿大学医学部　基礎研究補佐員(実験助手)		
久々　彩香	近畿大学医学部　基礎研究補佐員(実験助手)		

近畿大学消化器内科　同門会役員

会長　　工藤正俊

副会長　　北野雅之

幹事　　松井繁長

会計　　上嶋一臣

庶務　　西田直生志

同門会誌作製　秘書一同

近畿大学医学部消化器内科教室同門会会則

第一条　名称

本会は近畿大学医学部消化器内科教室同門会と称する。

第二条　目的

本会は会員相互の親睦及び教室の隆盛を図ることを目的とする。

第三条　会員

会員は消化器内科教室出身者、教室員及び同教室の発展に寄与するものをもって構成される。

第四条　役員

１．　本会の運営を円滑にするために幹事会を設ける。幹事会は代表幹事を長とし、代表幹事が指名する教室員をもって構成する。尚、幹事会は代表幹事が随時召集するものとする。その他、会計をおく。

２．　会長

①　会長は現職主任教授より選出される。

②　会長退任後は名誉会長となる。また、名誉会長は主任教授経験者からも選出できる。

３．　顧問

本会の発展に寄与したもので、幹事会が推戴する。

４．　役員の選出

①　幹事は役員より選出する。

②　代表幹事は医局長が兼任する。

５．　幹事の任期は２年とする。但し再任を妨げない。

第五条　会議

１．　総会は年１回の開催とする。

２．　幹事会において仮決議された条件の最終決定権は総会に委ねられる。

３．　決議は総会出席者の多数決により成立する。

第六条　会計

１．　本会の経費は会費をもって充てる。

２．　本会の会費は年額壱萬円とする。

３．　会計年度は４月１日から翌年３月 31 までとし、会計担当者は年１回会計報告を行う。

第七条

事務局は近畿大学医学部消化器内科教室内に置く。

第八条　会則の改正

会則の改正は幹事会の仮決議を経て総会で議決されるものとする。

附則　除名規定

本会の名誉を毀損したものや、その他本会に不適当と考えられるものは幹事会の動議により総会にて除名が議決される。

編集後記

2014 年版の annual report が完成しました。

消化器内科の秘書は、現在、胡桃さん、田中さん、朝隈さん、田村さん、前原さん、村橋さん、弓削さん、鏡さん、久々さん、本廣さん、和田さん、上妻さん、浦田さん、濱田さん（現在教授室 4 名、医局秘書 3 名、肝癌研究会事務局 3 名、臨床研究補助 2 名、実験助手 2 名）での 14 人体制となっております。

2014 年版年報も遅い発刊となってしまいましたが、2015 年版はもう少し早い機会に発刊できるよう頑張ります。

年報業務に加えまして、その他業務におきましても、今後とも何卒宜しく御願い申し上げます。

平成 28 年 2 月末

秘書一同